

Volume 7 Issue 12

December 2016



ISSN 2156-5570(Online)

ISSN 2158-107X(Print)



www.ijacsa.thesai.org

Editorial Preface

From the Desk of Managing Editor...

It may be difficult to imagine that almost half a century ago we used computers far less sophisticated than current home desktop computers to put a man on the moon. In that 50 year span, the field of computer science has exploded.

Computer science has opened new avenues for thought and experimentation. What began as a way to simplify the calculation process has given birth to technology once only imagined by the human mind. The ability to communicate and share ideas even though collaborators are half a world away and exploration of not just the stars above but the internal workings of the human genome are some of the ways that this field has moved at an exponential pace.

At the International Journal of Advanced Computer Science and Applications it is our mission to provide an outlet for quality research. We want to promote universal access and opportunities for the international scientific community to share and disseminate scientific and technical information.

We believe in spreading knowledge of computer science and its applications to all classes of audiences. That is why we deliver up-to-date, authoritative coverage and offer open access of all our articles. Our archives have served as a place to provoke philosophical, theoretical, and empirical ideas from some of the finest minds in the field.

We utilize the talents and experience of editor and reviewers working at Universities and Institutions from around the world. We would like to express our gratitude to all authors, whose research results have been published in our journal, as well as our referees for their in-depth evaluations. Our high standards are maintained through a double blind review process.

We hope that this edition of IJACSA inspires and entices you to submit your own contributions in upcoming issues. Thank you for sharing wisdom.

Thank you for Sharing Wisdom!

Managing Editor
IJACSA
Volume 7 Issue 12 December 2016
ISSN 2156-5570 (Online)
ISSN 2158-107X (Print)
©2013 The Science and Information (SAI) Organization

Editorial Board

Editor-in-Chief

Dr. Kohei Arai - Saga University

Domains of Research: Technology Trends, Computer Vision, Decision Making, Information Retrieval, Networking, Simulation

Associate Editors

Chao-Tung Yang

Department of Computer Science, Tunghai University, Taiwan

Domain of Research: Software Engineering and Quality, High Performance Computing, Parallel and Distributed Computing, Parallel Computing

Elena SCUTELNICU

"Dunarea de Jos" University of Galati, Romania

Domain of Research: e-Learning, e-Learning Tools, Simulation

Krassen Stefanov

Professor at Sofia University St. Kliment Ohridski, Bulgaria

Domains of Research: e-Learning, Agents and Multi-agent Systems, Artificial Intelligence, Big Data, Cloud Computing, Data Retrieval and Data Mining, Distributed Systems, e-Learning Organisational Issues, e-Learning Tools, Educational Systems Design, Human Computer Interaction, Internet Security, Knowledge Engineering and Mining, Knowledge Representation, Ontology Engineering, Social Computing, Web-based Learning Communities, Wireless/ Mobile Applications

Maria-Angeles Grado-Caffaro

Scientific Consultant, Italy

Domain of Research: Electronics, Sensing and Sensor Networks

Mohd Helmy Abd Wahab

Universiti Tun Hussein Onn Malaysia

Domain of Research: Intelligent Systems, Data Mining, Databases

T. V. Prasad

Lingaya's University, India

Domain of Research: Intelligent Systems, Bioinformatics, Image Processing, Knowledge Representation, Natural Language Processing, Robotics

Reviewer Board Members

- **Aamir Shaikh**
- **Abbas Al-Ghaili**
Mendeley
- **Abbas Karimi**
Islamic Azad University Arak Branch
- **Abdelghni Lakehal**
Université Abdelmalek Essaadi Faculté
Polydisciplinaire de Larache Route de Rabat, Km 2 -
Larache BP. 745 - Larache 92004. Maroc.
- **Abdul Razak**
- **Abdul Karim ABED**
- **Abdur Rashid Khan**
Gomal University
- **Abeer Elkorany**
Faculty of computers and information, Cairo
- **ADEMOLA ADESINA**
University of the Western Cape
- **Aderemi A. Atayero**
Covenant University
- **Adi Maaita**
ISRA UNIVERSITY
- **Adnan Ahmad**
- **Adrian Branga**
Department of Mathematics and Informatics,
Lucian Blaga University of Sibiu
- **agana Becejski-Vujaklija**
University of Belgrade, Faculty of organizational
- **Ahmad Saifan**
yarmouk university
- **Ahmed Boutejdar**
- **Ahmed AL-Jumaily**
Ahlia University
- **Ahmed Nabih Zaki Rashed**
Menoufia University
- **Ajantha Herath**
Stockton University Galloway
- **Akbar Hossain**
- **Akram Belghith**
University Of California, San Diego
- **Albert S**
Kongu Engineering College
- **Alcinia Zita Sampaio**
Technical University of Lisbon
- **Alexane Bouënard**
Sensopia
- **ALI ALWAN**
International Islamic University Malaysia
- **Ali Ismail Awad**
Luleå University of Technology
- **Alicia Valdez**
- **Amin Shaqrah**
Taibah University
- **Amirrudin Kamsin**
- **Amitava Biswas**
Cisco Systems
- **Anand Nayyar**
KCL Institute of Management and Technology,
Jalandhar
- **Andi Wahyu Rahardjo Emanuel**
Maranatha Christian University
- **Anews Samraj**
Mahendra Engineering College
- **Anirban Sarkar**
National Institute of Technology, Durgapur
- **Anthony Isizoh**
Nnamdi Azikiwe University, Awka, Nigeria
- **Antonio Formisano**
University of Naples Federico II
- **Anuj Gupta**
IKG Punjab Technical University
- **Anuranjan misra**
Bhagwant Institute of Technology, Ghaziabad, India
- **Appasami Govindasamy**
- **Arash Habibi Lashkari**
University Technology Malaysia(UTM)
- **Aree Mohammed**
Directorate of IT/ University of Sulaimani
- **ARINDAM SARKAR**
University of Kalyani, DST INSPIRE Fellow
- **Aris Skander**
Constantine 1 University
- **Ashok Matani**
Government College of Engg, Amravati
- **Ashraf Owis**
Cairo University
- **Asoke Nath**

St. Xaviers College(Autonomous), 30 Park Street,
Kolkata-700 016

- **Athanasios Koutras**
- **Ayad Ismaeel**
Department of Information Systems Engineering-
Technical Engineering College-Erbil Polytechnic
University, Erbil-Kurdistan Region- IRAQ
- **Ayman Shehata**
Department of Mathematics, Faculty of Science,
Assiut University, Assiut 71516, Egypt.
- **Ayman EL-SAYED**
Computer Science and Eng. Dept., Faculty of
Electronic Engineering, Menofia University
- **Babatunde Opeoluwa Akinkunmi**
University of Ibadan
- **Bae Bossoufi**
University of Liege
- **BALAMURUGAN RAJAMANICKAM**
Anna university
- **Balasubramanie Palanisamy**
- **BASANT VERMA**
RAJEEV GANDHI MEMORIAL COLLEGE, HYDERABAD
- **Basil Hamed**
Islamic University of Gaza
- **Basil Hamed**
Islamic University of Gaza
- **Bhanu Prasad Pinnamaneni**
Rajalakshmi Engineering College; Matrix Vision
GmbH
- **Bharti Waman Gawali**
Department of Computer Science & information T
- **Bilian Song**
LinkedIn
- **Binod Kumar**
JSPM's Jayawant Technical Campus, Pune, India
- **Bogdan Belean**
- **Bohumil Brtnik**
University of Pardubice, Department of Electrical
Engineering
- **Bouchaib CHERRADI**
CRMEF
- **Brahim Raouyane**
FSAC
- **Branko Karan**
- **Bright Keswani**
Department of Computer Applications, Suresh Gyan
Vihar University, Jaipur (Rajasthan) INDIA
- **Brij Gupta**

University of New Brunswick

- **C Venkateswarlu Sonagiri**
JNTU
- **Chanashekhhar Meshram**
Chhattisgarh Swami Vivekananda Technical
University
- **Chao Wang**
- **Chao-Tung Yang**
Department of Computer Science, Tunghai
University
- **Charlie Obimbo**
University of Guelph
- **Chee Hon Lew**
- **Chien-Peng Ho**
Information and Communications Research
Laboratories, Industrial Technology Research
Institute of Taiwan
- **Chun-Kit (Ben) Ngan**
The Pennsylvania State University
- **Ciprian Dobre**
University Politehnica of Bucharest
- **Constantin POPESCU**
Department of Mathematics and Computer
Science, University of Oradea
- **Constantin Filote**
Stefan cel Mare University of Suceava
- **CORNELIA AURORA Gyorödi**
University of Oradea
- **Cosmina Ivan**
- **Cristina Turcu**
- **Dana PETCU**
West University of Timisoara
- **Daniel Albuquerque**
- **Dariusz Jakóbczak**
Technical University of Koszalin
- **Deepak Garg**
Thapar University
- **Devena Prasad**
- **DHAYA R**
- **Dheyaa Kadhim**
University of Baghdad
- **Djilali IDOUGH**
University A.. Mira of Bejaia
- **Dong-Han Ham**
Chonnam National University
- **Dr. Arvind Sharma**

- Aryan College of Technology, Rajasthan Technology University, Kota
- **Duck Hee Lee**
Medical Engineering R&D Center/Asan Institute for Life Sciences/Asan Medical Center
 - **Elena SCUTELNICU**
"Dunarea de Jos" University of Galati
 - **Elena Camossi**
Joint Research Centre
 - **Eui Lee**
Sangmyung University
 - **Evgeny Nikulchev**
Moscow Technological Institute
 - **Ezekiel OKIKE**
UNIVERSITY OF BOTSWANA, GABORONE
 - **Fahim Akhter**
King Saud University
 - **FANGYONG HOU**
School of IT, Deakin University
 - **Faris Al-Salem**
GCET
 - **Firkhan Ali Hamid Ali**
UTHM
 - **Fokrul Alom Mazarbhuiya**
King Khalid University
 - **Frank Ibikunle**
Botswana Int'l University of Science & Technology (BIUST), Botswana
 - **Fu-Chien Kao**
Da-Y eh University
 - **Gamil Abdel Azim**
Suez Canal University
 - **Ganesh Sahoo**
RMRIMS
 - **Gaurav Kumar**
Manav Bharti University, Solan Himachal Pradesh
 - **George Pecherle**
University of Oradea
 - **George Mastorakis**
Technological Educational Institute of Crete
 - **Georgios Galatas**
The University of Texas at Arlington
 - **Gerard Dumancas**
Oklahoma Baptist University
 - **Ghalem Belalem**
University of Oran 1, Ahmed Ben Bella
 - **gherabi noreddine**
 - **Giacomo Veneri**
University of Siena
 - **Giri Babu**
Indian Space Research Organisation
 - **Govindarajulu Salendra**
 - **Grebenisan Gavril**
University of Oradea
 - **Gufan Ahmad Ansari**
Qassim University
 - **Gunaseelan Devaraj**
Jazan University, Kingdom of Saudi Arabia
 - **GYÖRÖDI ROBERT STEFAN**
University of Oradea
 - **Hadj Tadjine**
IAV GmbH
 - **Haewon Byeon**
Nambu University
 - **Haiguang Chen**
ShangHai Normal University
 - **Hamid Alinejad-Rokny**
The University of New South Wales
 - **Hamid AL-Asadi**
Department of Computer Science, Faculty of Education for Pure Science, Basra University
 - **Hamid Mukhtar**
National University of Sciences and Technology
 - **Hany Hassan**
EPF
 - **Harco Leslie Henic SPITS WARNARS**
Bina Nusantara University
 - **Hariharan Shanmugasundaram**
Associate Professor, SRM
 - **Harish Garg**
Thapar University Patiala
 - **Hazem I. El Shekh Ahmed**
Pure mathematics
 - **Hemalatha SenthilMahesh**
 - **Hesham Ibrahim**
Faculty of Marine Resources, Al-Mergheb University
 - **Himanshu Aggarwal**
Department of Computer Engineering
 - **Hongda Mao**
Hossam Faris
 - **Huda K. AL-Jobori**
Ahlia University
 - **Imed JABRI**

- **iss EL OUADGHIRI**
- **Iwan Setyawan**
Satya Wacana Christian University
- **Jacek M. Czerniak**
Casimir the Great University in Bydgoszcz
- **Jai Singh W**
- **JAMAIAH HAJI YAHAYA**
NORTHERN UNIVERSITY OF MALAYSIA (UUM)
- **James Coleman**
Edge Hill University
- **Jatinderkumar Saini**
Narmada College of Computer Application, Bharuch
- **Javed Sheikh**
University of Lahore, Pakistan
- **Jayaram A**
Siddaganga Institute of Technology
- **Ji Zhu**
University of Illinois at Urbana Champaign
- **Jia Uddin Jia**
Assistant Professor
- **Jim Wang**
The State University of New York at Buffalo,
Buffalo, NY
- **John Sahlin**
George Washington University
- **JOHN MANOHAR**
VTU, Belgaum
- **JOSE PASTRANA**
University of Malaga
- **Jui-Pin Yang**
Shih Chien University
- **Jyoti Chaudhary**
high performance computing research lab
- **K V.L.N.Acharyulu**
Bapatla Engineering college
- **Ka-Chun Wong**
- **Kamatchi R**
- **Kamran Kowsari**
The George Washington University
- **KANNADHASAN SURIYAN**
- **Kashif Nisar**
Universiti Utara Malaysia
- **Kato Mivule**
- **Kayhan Zrar Ghafoor**
University Technology Malaysia
- **Kennedy Okafor**
Federal University of Technology, Owerri
- **Khalid Mahmood**
IEEE
- **Khalid Sattar Abdul**
Assistant Professor
- **Khin Wee Lai**
Biomedical Engineering Department, University
Malaya
- **Khurram Khurshid**
Institute of Space Technology
- **KIRAN SREE POKKULURI**
Professor, Sri Vishnu Engineering College for
Women
- **KITIMAPORN CHOOCHOTE**
Prince of Songkla University, Phuket Campus
- **Krasimir Yordzhev**
South-West University, Faculty of Mathematics and
Natural Sciences, Blagoevgrad, Bulgaria
- **Krassen Stefanov**
Professor at Sofia University St. Kliment Ohridski
- **Labib Gergis**
Misr Academy for Engineering and Technology
- **LATHA RAJAGOPAL**
- **Lazar Stošić**
College for professional studies educators
Aleksinac, Serbia
- **Leanos Maglaras**
De Montfort University
- **Leon Abdillah**
Bina Darma University
- **Lijian Sun**
Chinese Academy of Surveying and
- **Ljubomir Jerinic**
University of Novi Sad, Faculty of Sciences,
Department of Mathematics and Computer Science
- **Lokesh Sharma**
Indian Council of Medical Research
- **Long Chen**
Qualcomm Incorporated
- **M. Reza Mashinchi**
Research Fellow
- **M. Tariq Banday**
University of Kashmir
- **madjid khalilian**
- **majzoob omer**
- **Mallikarjuna Doodipala**
Department of Engineering Mathematics, GITAM
University, Hyderabad Campus, Telangana, INDIA

- **Manas deep**
Masters in Cyber Law & Information Security
- **Manju Kaushik**
- **Manoharan P.S.**
Associate Professor
- **Manoj Wadhwa**
Echelon Institute of Technology Faridabad
- **Manpreet Manna**
Director, All India Council for Technical Education,
Ministry of HRD, Govt. of India
- **Manuj Darbari**
BBD University
- **Marcellin Julius Nkenlifack**
University of Dschang
- **Maria-Angeles Grado-Caffaro**
Scientific Consultant
- **Marwan Alseid**
Applied Science Private University
- **Mazin Al-Hakeem**
LFU (Lebanese French University) - Erbil, IRAQ
- **Md Islam**
sikkim manipal university
- **Md. Bhuiyan**
King Faisal University
- **Md. Zia Ur Rahman**
Narasaraopeta Engg. College, Narasaraopeta
- **Mehdi Bahrami**
University of California, Merced
- **Messaouda AZZOUZI**
Ziane AChour University of Djelfa
- **Milena Bogdanovic**
University of Nis, Teacher Training Faculty in Vranje
- **Miriampally Venkata Raghavendra**
Adama Science & Technology University, Ethiopia
- **Mirjana Popovic**
School of Electrical Engineering, Belgrade University
- **Miroslav Baca**
University of Zagreb, Faculty of organization and
informatics / Center for biometrics
- **Moeiz Miraoui**
University of Gafsa
- **Mohamed Eldosoky**
- **Mohamed Ali Mahjoub**
Preparatory Institute of Engineer of Monastir
- **Mohamed Kaloup**
- **Mohamed El-Sayed**
Faculty of Science, Fayoum University, Egypt
- **Mohamed Najeh LAKHOUA**
ESTI, University of Carthage
- **Mohammad Ali Badamchizadeh**
University of Tabriz
- **Mohammad Jannati**
- **Mohammad Alomari**
Applied Science University
- **Mohammad Haghighat**
University of Miami
- **Mohammad Azzeh**
Applied Science university
- **Mohammed Akour**
Yarmouk University
- **Mohammed Sadgal**
Cadi Ayyad University
- **Mohammed Al-shabi**
Associate Professor
- **Mohammed Hussein**
- **Mohammed Kaiser**
Institute of Information Technology
- **Mohammed Ali Hussain**
Sri Sai Madhavi Institute of Science & Technology
- **Mohd Helmy Abd Wahab**
University Tun Hussein Onn Malaysia
- **Mokhtar Beldjehem**
University of Ottawa
- **Mona Elshinawy**
Howard University
- **Mostafa Ezziyani**
FSTT
- **Mouhammd sharari alkasassbeh**
- **Mourad Amad**
Laboratory LAMOS, Bejaia University
- **Mueen Uddin**
University Malaysia Pahang
- **MUNTASIR AL-ASFOOR**
University of Al-Qadisiyah
- **Murphy Choy**
- **Murthy Dasika**
Geethanjali College of Engineering & Technology
- **Mustapha OUJAOURA**
Faculty of Science and Technology Béni-Mellal
- **MUTHUKUMAR SUBRAMANYAM**
DGCT, ANNA UNIVERSITY
- **N.Ch. Iyengar**
VIT University
- **Nagy Darwish**

Department of Computer and Information Sciences,
Institute of Statistical Studies and Researches, Cairo
University

- **Najib Kofahi**
Yarmouk University
- **Nan Wang**
LinkedIn
- **Natarajan Subramanyam**
PES Institute of Technology
- **Natheer Gharaibeh**
College of Computer Science & Engineering at
Yanbu - Taibah University
- **Nazeeh Ghatasheh**
The University of Jordan
- **Nazeeruddin Mohammad**
Prince Mohammad Bin Fahd University
- **NEERAJ SHUKLA**
ITM UNiversity, Gurgaon, (Haryana) Inida
- **Neeraj Tiwari**
- **Nestor Velasco-Bermeo**
UPFIM, Mexican Society of Artificial Intelligence
- **Nidhi Arora**
M.C.A. Institute, Ganpat University
- **Nilanjan Dey**
- **Ning Cai**
Northwest University for Nationalities
- **Nithyanandam Subramanian**
Professor & Dean
- **Noura Aknin**
University Abdelamlek Essaadi
- **Obaida Al-Hazaimeh**
Al- Balqa' Applied University (BAU)
- **Oliviu Matei**
Technical University of Cluj-Napoca
- **Om Sangwan**
- **Omaima Al-Allaf**
Asesstant Professor
- **Osama Omer**
Aswan University
- **Ouchtati Salim**
- **Ousmane THIARE**
Associate Professor University Gaston Berger of
Saint-Louis SENEGAL
- **Paresh V Virparia**
Sardar Patel University
- **Peng Xia**
Microsoft

- **Ping Zhang**
IBM
- **Poonam Garg**
Institute of Management Technology, Ghaziabad
- **Prabhat K Mahanti**
UNIVERSITY OF NEW BRUNSWICK
- **PROF DURGA SHARMA (PHD)**
AMUIT, MOEFDRE & External Consultant (IT) &
Technology Tansfer Research under ILO & UNDP,
Academic Ambassador for Cloud Offering IBM-USA
- **Purwanto Purwanto**
Faculty of Computer Science, Dian Nuswantoro
University
- **Qifeng Qiao**
University of Virginia
- **Rachid Saadane**
EE departement EHTP
- **Radwan Tahboub**
Palestine Polytechnic University
- **raed Kanaan**
Amman Arab University
- **Raghuraj Singh**
Harcourt Butler Technological Institute
- **Rahul Malik**
- **raja boddu**
LENORA COLLEGE OF ENGINEERNG
- **Raja Ramachandran**
- **Rajesh Kumar**
National University of Singapore
- **Rakesh Dr.**
Madan Mohan Malviya University of Technology
- **Rakesh Balabantaray**
IIIT Bhubaneswar
- **Ramani Kannan**
Universiti Teknologi PETRONAS, Bandar Seri
Iskandar, 31750, Tronoh, Perak, Malaysia
- **Rashad Al-Jawfi**
Ibb university
- **Rashid Sheikh**
Shri Aurobindo Institute of Technology, Indore
- **Ravi Prakash**
University of Mumbai
- **RAVINA CHANGALA**
- **Ravisankar Hari**
CENTRAL TOBACCO RESEARCH INSTITUE
- **Rawya Rizk**
Port Said University

- **Reshmy Krishnan**
Muscat College affiliated to Stirling University.U
- **Ricardo Vardasca**
Faculty of Engineering of University of Porto
- **Ritaban Dutta**
ISSL, CSIRO, Tasmania, Australia
- **Rowayda Sadek**
- **Ruchika Malhotra**
Delhi Technological University
- **Rutvij Jhaveri**
Gujarat
- **SAADI Slami**
University of Djelfa
- **Sachin Kumar Agrawal**
University of Limerick
- **Sagarmay Deb**
Central Queensland University, Australia
- **Said Ghoniemy**
Taif University
- **Sandeep Reddivari**
University of North Florida
- **Sanskriti Patel**
Charotar University of Science & Technology,
Changa, Gujarat, India
- **Santosh Kumar**
Graphic Era University, Dehradun (UK)
- **Sasan Adibi**
Research In Motion (RIM)
- **Satyena Singh**
Professor
- **Sebastian Marius Rosu**
Special Telecommunications Service
- **Seema Shah**
Vidyalankar Institute of Technology Mumbai
- **Seifedine Kadry**
American University of the Middle East
- **Selem Charfi**
HD Technology
- **SENGOTTUVELAN P**
Anna University, Chennai
- **Senol Piskin**
Istanbul Technical University, Informatics Institute
- **Sérgio Ferreira**
School of Education and Psychology, Portuguese
Catholic University
- **Seyed Hamidreza Mohades Kasaei**
University of Isfahan
- **Shafiqul Abidin**
HMR Institute of Technology & Management
(Affiliated to GGS Indraprastha University), Hamidpur, Delhi -
110036
- **Shahanawaj Ahamad**
The University of Al-Kharj
- **Shaidah Jusoh**
- **Shaiful Bakri Ismail**
- **Shakir Khan**
Al-Imam Muhammad Ibn Saud Islamic University
- **Shawki Al-Dubaei**
Assistant Professor
- **Sherif Hussein**
Mansoura University
- **Shriram Vasudevan**
Amrita University
- **Siddhartha Jonnalagadda**
Mayo Clinic
- **Sim-Hui Tee**
Multimedia University
- **Simon Ewedafe**
The University of the West Indies
- **Siniša Opic**
University of Zagreb, Faculty of Teacher Education
- **Sivakumar Poruran**
SKP ENGINEERING COLLEGE
- **Slim BEN SAOUD**
National Institute of Applied Sciences and
Technology
- **Sofien Mhatli**
- **sofyan Hayajneh**
- **Sohail Jabbar**
Bahria University
- **Sri Devi Ravana**
University of Malaya
- **Sudarson Jena**
GITAM University, Hyderabad
- **Suhail Sami Owais Owais**
- **Suhas J Manangi**
Microsoft
- **SUKUMAR SENTHILKUMAR**
Universiti Sains Malaysia
- **Süleyman Eken**
Kocaeli University
- **Sumazly Sulaiman**
Institute of Space Science (ANGKASA), Universiti
Kebangsaan Malaysia

- **Sumit Goyal**
National Dairy Research Institute
 - **Supareerk Janjarasjitt**
Ubon Ratchathani University
 - **Suresh Sankaranarayanan**
Institut Teknologi Brunei
 - **Susarla Sastry**
JNTUK, Kakinada
 - **Suseendran G**
Vels University, Chennai
 - **Suxing Liu**
Arkansas State University
 - **Syed Ali**
SMI University Karachi Pakistan
 - **T C.Manjunath**
HKBK College of Engg
 - **T V Narayana rao Rao**
SNIST
 - **T. V. Prasad**
Lingaya's University
 - **Taiwo Ayodele**
Infonetmedia/University of Portsmouth
 - **Talal Bonny**
Department of Electrical and Computer Engineering, Sharjah University, UAE
 - **Tamara Zhukabayeva**
 - **Tarek Gharib**
Ain Shams University
 - **thabet slimani**
College of Computer Science and Information Technology
 - **Totok Biyanto**
Engineering Physics, ITS Surabaya
 - **Touati Youcef**
Computer sce Lab LIASD - University of Paris 8
 - **Tran Sang**
IT Faculty - Vinh University - Vietnam
 - **Tsvetanka Georgieva-Trifonova**
University of Veliko Tarnovo
 - **Uchechukwu Awada**
Dalian University of Technology
 - **Udai Pratap Rao**
 - **Urmila Shrawankar**
GHRCE, Nagpur, India
 - **Vaka MOHAN**
TRR COLLEGE OF ENGINEERING
 - **VENKATESH JAGANATHAN**
- ANNA UNIVERSITY
 - **Vinayak Bairagi**
AISSMS Institute of Information Technology, Pune
 - **Vishnu Mishra**
SVNIT, Surat
 - **Vitus Lam**
The University of Hong Kong
 - **VUDA SREENIVASARAO**
PROFESSOR AND DEAN, St.Mary's Integrated Campus, Hyderabad
 - **Wali Mashwani**
Kohat University of Science & Technology (KUST)
 - **Wei Wei**
Xi'an Univ. of Tech.
 - **Wenbin Chen**
360Fly
 - **Xi Zhang**
illinois Institute of Technology
 - **Xiaojing Xiang**
AT&T Labs
 - **Xiaolong Wang**
University of Delaware
 - **Yanping Huang**
 - **Yao-Chin Wang**
 - **Yasser Albagory**
College of Computers and Information Technology, Taif University, Saudi Arabia
 - **Yasser Alginahi**
 - **Yi Fei Wang**
The University of British Columbia
 - **Yihong Yuan**
University of California Santa Barbara
 - **Yilun Shang**
Tongji University
 - **Yu Qi**
Mesh Capital LLC
 - **Zacchaeus Omogbadegun**
Covenant University
 - **Zairi Rizman**
Universiti Teknologi MARA
 - **Zarul Zaaba**
Universiti Sains Malaysia
 - **Zenzo Ncube**
North West University
 - **Zhao Zhang**
Deptment of EE, City University of Hong Kong
 - **Zhihan Lv**

Chinese Academy of Science

- **Zhixin Chen**
ILX Lightwave Corporation
- **Ziyue Xu**
National Institutes of Health, Bethesda, MD

- **Zlatko Stacic**
University of Zagreb, Faculty of Organization and
Informatics Varazdin
- **Zuraini Ismail**
Universiti Teknologi Malaysia

CONTENTS

Paper 1: Estimation Method of Ionospheric TEC Distribution using Single Frequency Measurements of GPS Signals

Authors: Win Zaw Hein, Yoshitaka Goto, Yoshiya Kasahara

PAGE 1 – 6

Paper 2: A New Mixed Signal Platform to Study the Accuracy/Complexity Trade-Off of DPD Algorithms

Authors: Hanan Thabet, Morgan Roger, Caroline Lelandais-Perrault

PAGE 7 – 10

Paper 3: A Universally Designed and Usable Data Visualization for A Mobile Application in the Context of Rheumatoid Arthritis

Authors: Suraj Shrestha, Pietro Murano

PAGE 11 – 23

Paper 4: Towards Development of Real-Time Handwritten Urdu Character to Speech Conversion System for Visually Impaired

Authors: Tajwar Sultana, Abdul Rehman Abbasi, Bilal Ahmed Usmani, Sadeem Khan, Wajeeha Ahmed, Naima Qaseem, Sidra

PAGE 24 – 30

Paper 5: Scheduling of Distributed Algorithms for Low Power Embedded Systems

Authors: Stanislaw Deniziak, Albert Dzitkowski

PAGE 31 – 38

Paper 6: RSECM: Robust Search Engine using Context-based Mining for Educational Big Data

Authors: D. Pratiba, G. Shobha

PAGE 39 – 51

Paper 7: A Heterogeneous Framework to Detect Intruder Attacks in Wireless Sensor Networks

Authors: Mustafa Al-Fayoumi, Yasir Ahmad, Usman Tariq

PAGE 52 – 58

Paper 8: Segmentation using Codebook Index Statistics for Vector Quantized Images

Authors: Hsuan T. Chang, Jian-Tein Su

PAGE 59 – 65

Paper 9: An Enhanced Partial Transmit Sequence Segmentation Schemes to Reduce the PAPR in OFDM Systems

Authors: Yasir Amer Al-Jawhar, Nor Shahida M. Shah, Montadar Abas Taher, Mustafa Sami Ahmed, Khairun N. Ramli

PAGE 66 – 75

Paper 10: Model and Criteria for the Automated Refactoring of the UML Class Diagrams

Authors: Evgeny Nikulchev, Olga Deryugina

PAGE 76 – 79

Paper 11: Improved Sliding Mode Nonlinear Extended State Observer based Active Disturbance Rejection Control for Uncertain Systems with Unknown Total Disturbance

Authors: Wameedh Riyadh Abdul-Adheem, Ibraheem Kasim Ibraheem

PAGE 80 – 93

Paper 12: Towards A Broader Adoption of Agile Software Development Methods

Authors: Abdallah Alashqur

PAGE 94 – 98

Paper 13: A Bayesian Approach to Predicting Water Supply and Rehabilitation of Water Distribution Networks

Authors: Abdelaziz Lakehal, Fares Laouacheria

PAGE 99 – 106

Paper 14: Reducing Energy Consumption in Wireless Sensor Networks using Ant Colony Algorithm and Autonomy Mechanisms

Authors: Javad Mozaffari, Mehdi EffatParvar

PAGE 107 – 112

Paper 15: Measuring the Data Openness for the Open Data in Saudi Arabia e-Government – A Case Study

Authors: Marwah W. AlRushaid, Abdul Khader Jilani Saudagar

PAGE 113 – 122

Paper 16: Automatic Fall Detection using Smartphone Acceleration Sensor

Authors: Tran Tri Dang, Hai Truong, Tran Khanh Dang

PAGE 123 – 129

Paper 17: All in Focus Image Generation based on New Focusing Measure Operators

Authors: Hossam Eldeen M. Shamardan

PAGE 130 – 134

Paper 18: Stemmer Impact on Quranic Mobile Information Retrieval Performance

Authors: Huda Omar Aljaloud, Mohammed Dahab, Mahmoud Kamal

PAGE 135 – 139

Paper 19: Internal Model Control of A Class of Continuous Linear Underactuated Systems

Authors: Asma Mezzi, Dhaou Soudani

PAGE 140 – 148

Paper 20: Comparison Study of Different Lossy Compression Techniques Applied on Digital Mammogram Images

Authors: Ayman AbuBaker, Mohammed Eshray, Maryam AkhoZahia

PAGE 149 – 155

Paper 21: Evaluating Confidentiality Impact in Security Risk Scoring Models

Authors: Eli Weintraub

PAGE 156 – 164

Paper 22: Formal Modeling and Verification of Smart Traffic Environment with Design Aided by UML

Authors: Umber Noureen Abbas, Nazir Ahmad Zafar, Farhan Ullah

PAGE 165 – 172

Paper 23: Response Prediction for Chronic HCV Genotype 4 Patients to DAAs

Authors: Mohammed A.Farahat, Khaled A.Bahnasy, A. Abdo, Sanaa M.Kamal, Samar K. Kassim, Ahmed Sharaf Eldin

PAGE 173 – 178

Paper 24: RAX System to Rank Arabic XML Documents

Authors: Hesham Elzentani, Mladen Veinović, Goran Šimić

PAGE 179 – 190

Paper 25: A Novel Method for Measuring the Performance of Software Project Managers

Authors: Jasem M. Alostad

PAGE 191 – 200

Paper 26: A Topic based Approach for Sentiment Analysis on Twitter Data

Authors: Pierre FICAMOS, Yan LIU

PAGE 201 – 205

Paper 27: An Improved Malicious Behaviour Detection Via k-Means and Decision Tree

Authors: Warusia Yassin, Sifi Rahayu, Faizal Abdollah, Hazlin Zin

PAGE 206 – 212

Paper 28: Integrated Approach to Conceptual Modeling

Authors: Lindita Nebiu Hyseni, Zamir Dika

PAGE 213 – 219

Paper 29: Low Complexity for Scalable Video Coding Extension of H.264 based on the Complexity of Video

Authors: Mayada Khairy, Amr Elsayed, Alaa Hamdy, Hesham Farouk Ali

PAGE 220 – 225

Paper 30: An M-Learning Framework in the Podcast Form (MPF) using Context-Aware Technology

Authors: Mohamed A. Amasha, Elsayed E. AbdElrazek

PAGE 226 – 234

Paper 31: An Inclusive Comparison in LAN Environment between Conventional and Hybrid Methods for Spectral Amplitude Coding Optical CDMA Systems

Authors: Hassan Yousif Ahmed, Nisar K.S, Z. M Gharseldien, S. A. Aljunid

PAGE 235 – 244

Paper 32: An Approach for Analyzing ISO / IEC 25010 Product Quality Requirements based on Fuzzy Logic and Likert Scale for Decision Support Systems

Authors: Hasnain Iqbal, Muhammad Babar

PAGE 245 – 260

Paper 33: Analysis of IPv4 vs IPv6 Traffic in US

Authors: Mahmood-ul-Hassan, Muhammad Amir Khan, Khalid Mahmood, Ansar Munir Shah

PAGE 261 – 267

Paper 34: Clustering-based Spam Image Filtering Considering Fuzziness of the Spam Image

Authors: Master Prince

PAGE 268 – 270

Paper 35: Overview of Technical Elements of Liver Segmentation

Authors: Nazish Khan, Imran Ahmed, Mehreen Kiran, Awais Adnan

PAGE 271 – 278

Paper 36: Automatic Cloud Resource Scaling Algorithm based on Long Short-Term Memory Recurrent Neural Network

Authors: Ashraf A. Shahin

PAGE 279 – 285

Paper 37: U Patch Antenna using Variable Substrates for Wireless Communication Systems

Authors: Saad Hassan Kiani, Khalid Mahmood, Umar Farooq Khattak, Burhan-Ud-Din, Mehre Munir

PAGE 286 – 291

Paper 38: Novel Causality in Consumer's Online Behavior: Ecommerce Success Model

Authors: Amna Khatoon, Shahid Nazir Bhatti, Atika Tabassum, Aneesa Rida, Sehrish Alam

PAGE 292 – 299

Paper 39: Role of Requirements Elicitation & Prioritization to Optimize Quality in Scrum Agile Development

Authors: Aneesa Rida Asghar, Shahid Nazir Bhatti, Atika Tabassum, Zainab Sultan, Rabiya Abbas

PAGE 300 – 306

Paper 40: Optimizing the Locations of Intermediate Rechlorination Stations in a Drinking Water Distribution Network

Authors: Amali Said, Mourchid Mohammed, EL Faddouli Nour-eddine, Zouhri Mohammed

PAGE 307 – 314

Paper 41: A Semantic Learning Object (SLO)Web-Editor based on Web Ontology Language (OWL) using a New OWL2XSLO Approach

Authors: Zouhair Rimale, EL Habib Benlahmar, Abderrahim Tragha

PAGE 315 – 320

Paper 42: Detection and Classification of Mu Rhythm using Phase Synchronization for a Brain Computer Interface

Authors: Oana Diana Eva

PAGE 321 – 328

Paper 43: Reducing the Electrical Consumption in the Humidity Control Process for Electric Cells using an Intelligent Fuzzy Logic Controller

Authors: Rafik Lasri, Larbi Choukri, Mohammed Bouhorma, Ignacio Rojas, Héctor Pomares

PAGE 329 – 336

Paper 44: Representing Job Scheduling for Volunteer Grid Environment using Online Container Stowage

Authors: Saddam Rubab, Mohd Fadzil Hassan, Ahmad Kamil Mahmood, Syed Nasir Mehmood Shah

PAGE 337 – 345

Paper 45: An Incident Management System for Debt Collection in Virtual Banking

Authors: Sareh Saberi, Seyyed Mohsen Hashemi

PAGE 346 – 355

Paper 46: Credibility Evaluation of Online Distance Education Websites

Authors: Khalid Al-Omar

PAGE 356 – 362

Paper 47: Implementation of Cooperative Spectrum Sensing Algorithm using Raspberry Pi

Authors: Ammar Ahmed Khan, Aamir Zeb Shaikh, Shabbar Naqvi, Talat Altaf

PAGE 363 – 367

Paper 48: A Centralized Reputation Management Scheme for Isolating Malicious Controller(s) in Distributed Software-Defined Networks

Authors: Bilal Karim Mughal, Sufian Hameed, Ghulam Muhammad Shaikh

PAGE 368 – 373

Paper 49: Crowd Mobility Analysis using WiFi Sniffers

Authors: Anas Basalamah

PAGE 374 – 378

Paper 50: Fault-Tolerant Resource Provisioning with Deadline-Driven Optimization in Hybrid Clouds

Authors: Emmanuel Ahene, Kingsley Nketia Acheampong, Heyang Xu

PAGE 379 – 389

Paper 51: Using Real-World Car Traffic Dataset in Vehicular Ad Hoc Network Performance Evaluation

Authors: Lucas Rivoirard, Martine Wahl, Patrick Sondi, Marion Berbineau, Dominique Gruyer

PAGE 390 – 398

Paper 52: Modeling and Solving the Open-End Bin Packing Problem

Authors: Maiza Mohamed, Tebbal Mohamed, Rabia Billal

PAGE 399 – 404

Paper 53: Performance Comparison between MAI and Noise Constrained LMS Algorithm for MIMO CDMA DFE and Linear Equalizers

Authors: Khalid Mahmood

PAGE 405 – 410

Paper 54: Software Defined Security Service Provisioning Framework for Internet of Things

Authors: Faraz Idris Khan, Sufian Hameed

PAGE 411 – 425

Paper 55: The Art of Crypto Currencies

Authors: Sufian Hameed, Sameef Farooq

PAGE 426 – 435

Paper 56: A New Approach of Graph Realization for Data Hiding using Human Encoding

Authors: Fatema Akhter, Md. Selim Al Mamun

PAGE 436 – 442

Estimation Method of Ionospheric TEC Distribution using Single Frequency Measurements of GPS Signals

Win Zaw Hein[#], Yoshitaka Goto[#], Yoshiya Kasahara[#]

[#]Division of Electrical Engineering and Computer Science,
Graduate School of Natural Science and Technology,
Kanazawa University
〒920-1192, Kakuma-machi, Kanazawa, Ishikawa, Japan

Abstract—The satellite-to-ground communications are influenced by ionospheric plasma which varies depending on solar and geomagnetic activities as well as regions and local times. With the expansion of use of the space, continuous monitoring of the ionospheric plasma has become an important issue. In Global Positioning System (GPS), the ionospheric delay, which is proportional to ionospheric total electron content (TEC) along the propagation path, is the largest error in signal propagation. The TEC has been observed from dual frequency GPS signals because only the ionospheric delay has frequency dependences. Costs of multi-frequency receivers are, however, much higher than those of single frequency ones. In the present study, an estimation method of TEC distribution map from single frequency GPS measurements was developed. The developed method was evaluated by comparing its results with those from dual frequency measurements. The method makes it possible to expand ionospheric TEC observation networks easily.

Keywords—Global Positioning System; GPS; Signal processing and propagation; Ionospheric Delay; Total Electron Content (TEC)

I. INTRODUCTION

The Earth's ionosphere consists of electrons and ions called plasma [1]. They are generated by ionization of neutral particles of the atmosphere by ultraviolet rays from the Sun. Our daily lives are based on a variety of satellite-to-ground communications and they are greatly influenced by the ionospheric plasma, such as delays and scintillations. Monitoring of the ionospheric plasma is getting more important with the expansion of use of the space.

The ionosphere is the dominant source of space plasma around the Earth. Plasma density and constituent in the ionosphere show complex dependences on solar and geomagnetic activities. Responses of the ionospheric plasma to such activities has usually been investigated by direct observations from spacecraft and radar observations from the ground. In these observations, there are restrictions and limitation in observational periods, regions or time continuity. These restrictions are essential problems in a view point of the monitoring of the ionospheric plasma.

Continuous monitoring of the total electron content (TEC), which denotes integration of electron density, using observational networks of GNSS (global navigation satellite

system) signals has recently become popular in many countries. The GNSS observation networks make it possible to reconstruct vertical TEC maps in wide regions in high spatial and temporal resolutions. The most widely distributed network service is provided by the International GNSS service (IGS). In Japan, more than 1,200 GNSS stations are installed all over the islands. This observational network is called GEONET and was originally built for land survey. This kind of observational network of GNSS signals are now an important tool to measure TEC and are used as an important information source of space weather forecast. Most of the networks are, however, built in mid latitude regions. It is important to expand them in lower latitudes regions where the effect of ionospheric plasma on radio waves for satellite-to-ground communications is the largest and the most complex.

In the GNSS observation stations, multi-frequency receivers are generally installed. They can accurately derive the ionospheric effects because only the ionospheric delay depends on the frequency among ranging errors. There are several reconstruction methods of TEC distribution map from each slant TEC measurement [2, 3, 4, 5, 6, 7, 8]. The global ionosphere maps (GIM) is provided by CODE using data from about 200 GNSS stations of the IGS and other stations [2]. The vertical TEC is modeled in a solar geomagnetic coordinate system using a spherical harmonics expansion. Global TEC maps are also provided by ESA/ESOC. The maps are also modelled by spherical harmonics in combination with a daily DCBs fitting using GPS and GLONASS data. Three shells are used in NASA/JPL ionospheric model from data obtained at 200 globally distributed stations [3, 4]. In this method, Kalman filter is used to smooth temporal variations. Most of the reconstruction methods are based on spherical harmonics.

The multi-frequency receivers used in the GNSS stations are, however, much more expensive than single frequency receivers which are widely distributed as consumer products. In the present study, an estimation method of ionospheric TEC map from single frequency measurements of GPS signals was developed. In the method, the TEC maps over a receiver are estimated under the condition that the receiver location is accurately known. The method can make it possible to build observation networks of ionospheric TEC at low cost.

II. IONOSPHERIC DELAY IN GPS SIGNAL AND TOTAL ELECTRON CONTENT, TEC

One of the most fundamental GPS observables is C/A code pseudorange which is generally used for standard positioning [9, 10]. The code pseudorange is measured from propagation time of the signal from i^{th} satellite to the receiver and is represented by

$$R^i = \rho^i + c(\delta t_r - \delta t_s^i) + \delta_{\text{ion}}^i + \delta_{\text{tro}}^i + \varepsilon, \quad (1)$$

where ρ^i is the geometric distance between satellite and receiver, c is the velocity of light, δt_s^i and δt_r are transmitting and receiving time errors, respectively, δ_{ion}^i and δ_{tro}^i are the ionospheric and tropospheric effects along the propagation path of the signal. ε denotes the other effect, such as multipath effect and receiver noise [11].

The ionospheric delay δ_{ion}^i is directly proportional to the total electron content (TEC) from the i^{th} satellite to the receiver. This TEC is called slant TEC and represented by I_{slant}^i as shown in the following formula,

$$\delta_{\text{ion}}^i = \frac{e^2}{8\pi^2 m \varepsilon_0 c f^2} I_{\text{slant}}^i \equiv \frac{I_{\text{slant}}^i}{\Lambda}, \quad (2)$$

where e , m , ε_0 and f are charge and mass of the electron, permittivity of free space and the signal frequency, respectively. For convenience, the coefficient of I_{slant}^i in the right term in equation (2) is defined as $1/\Lambda$. When δ_{ion}^i is represented as meter and I_{slant}^i as TECU (1 TECU = 10^{16} electrons/m²), $1/\Lambda$ is approximately equal to $40.3/f^2$, where $f = 1575.42$ MHz.

Since only the ionospheric effect depends on the signal frequency among the measurement errors in equation (1), I_{slant}^i is generally calculated from distance measurements by dual frequency signals as follows;

$$I_{\text{slant}}^i = \frac{\Lambda f_2^2}{(f_1^2 - f_2^2)} (R_2^i - R_1^i), \quad (3)$$

where subscripts 1 and 2 corresponds to L1 and L2 signals. In practical, this value is compensated by differential code biases of the satellites and the receiver.

In the present paper, a new method to estimate I_{slant}^i from single frequency measurement of GPS signals is proposed by adopting a spatial model for vertical TEC distribution in the ionosphere. Estimation accuracy of I_{slant}^i is discussed by comparing with that from dual frequency observations as represented by equation (3).

III. IONOSPHERIC TEC FROM SINGLE FREQUENCY MEASUREMENT

Precise satellite orbit, velocity and clock error can be calculated from precise ephemeris, which is provided by the international GNSS service (IGS) [7]. Since the precise ephemeris is composed from location and clock error of each satellite whose time interval is 5 minutes, they are interpolated with 9th order Lagrange polynomial function. Then, ρ^i and δt_s in equation (1) are obtained with an accuracy of few cm at any timing. In this calculation, relativistic effects are taken

into account. As for δ_{tro}^i , the Hopfield model whose accuracy is known to be less than 10 cm is adopted [12].

Under the condition that the receiver location is accurately known, the terms δ_{ion}^i and δt_r are undetermined in equation (1). While δt_r is common for all the satellite, δ_{ion}^i depends on the satellite locations. This is an essential feature to distinguish each effect. From equations (1) and (2), the slant TEC I_{slant}^i is represented by

$$I_{\text{slant}}^i = \Lambda(R^i - \rho^i + c\delta t_s^i - \delta_{\text{tro}}^i) - \Lambda c\delta t_r + \varepsilon', \quad (4)$$

The right side of the equation (4) can be separated into two parts, and defined $\kappa \equiv \Lambda(R^i - \rho^i + c\delta t_s^i - \delta_{\text{tro}}^i)$ as a known part and $\alpha \equiv \Lambda c\delta t_r$ as an unknown part.

Since the ionospheric TEC distribution is usually shown by vertical TEC map, the slant TEC is converted to vertical TEC by a slant factor. This conversion is important in the TEC map reconstruction from single frequency GPS data because the effects of slant TEC and the receiver clock error on propagation delays should be distinguished depending on the slant effects. In practical, the ionosphere can be assumed to be a thin layer and the ray path crosses the ionosphere at one point called the ionospheric pierce point (IPP) as shown in Fig. 1.

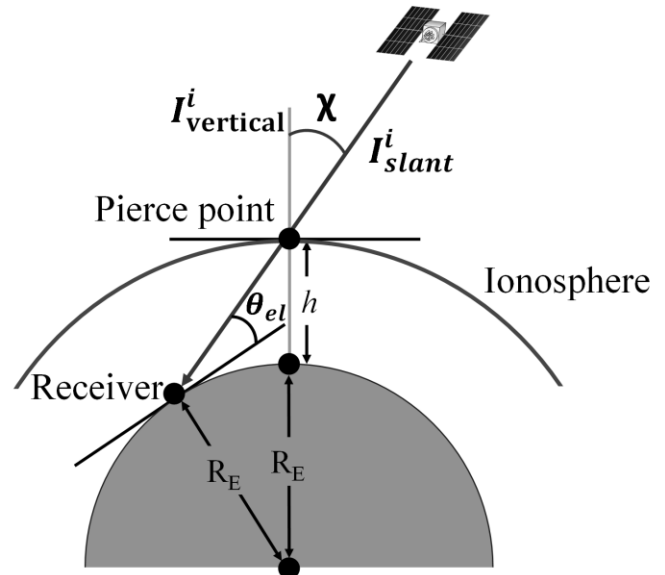


Fig. 1. Conversion model from slant TEC to vertical TEC in a thin layer assumption for the ionosphere

The conversion method from slant TEC I_{slant}^i to vertical TEC I_{vertical}^i can be used as follows;

$$I_{\text{slant}}^i = I_{\text{vertical}}^i \cdot \frac{1}{\cos \chi^i}, \quad (5)$$

where the angle χ between zenith direction and satellite direction from the IPP can be calculated as follows;

$$\chi^i = \sin^{-1} \left(\frac{R_E}{R_E + h} \cos \theta_{\text{el}}^i \right), \quad (6)$$

where R_E is Earth radius, h is the altitude of IPP which is assumed to be 350 km [13] and θ_{el}^i is elevation angle of the satellite at the receiver location.

From Eq. (4), (5) and (6), vertical TEC can be represented by,

$$I_{\text{vertical}}^i = (\kappa - \alpha) \cos \chi \equiv (\kappa - \alpha) F, \quad (7)$$

where $\cos \chi$ is defined as a slant factor F . This factor is used as a thin layer slant model for conversion of slant TEC to vertical TEC.

IV. SPATIAL DISTRIBUTION MODEL OF IONOSPHERIC TEC

There are some reconstruction methods of TEC distribution from dual frequency GPS data, as shown in Introduction. In the present study, TEC distribution is assumed to be represented by two dimensional (latitude-longitude) model with a first order function in each dimension because we deal with a small area within a few hundred kilometers squares. Vertical TEC distributions are represented as follows;

$$I_{\text{vertical}}^i = I_0 + \Delta I_x x + \Delta I_y y, \quad (8)$$

where x and y are normalized longitude (local time) and latitude. I_0 , ΔI_x , and ΔI_y are vertical TEC at the reference point (135 °E, 36 °N), gradients of vertical TEC for x and y directions. I_0 , ΔI_x , and ΔI_y are parameters which should be estimated from measurements.

From Equations (7) and (8), the following relation is obtained;

$$I_0 + \Delta I_x x + \Delta I_y y = (\kappa - \alpha) F, \quad (9)$$

where I_0 , ΔI_x , I_y and α are unknown parameters to be solved. At least four independent equations are required to solve the unknown parameters in Eq. (9), that is, the number of visible satellite from the receiver must be more than four. According to the GPS constellation, this condition is always satisfied. When n numbers of satellites are visible from the receiver location, the following matrix is obtained,

$$\begin{pmatrix} 1 & x_0 & y_0 & F_1 \\ 1 & x_1 & y_1 & F_2 \\ \vdots & \vdots & \vdots & \vdots \\ 1 & x_n & y_n & F_n \end{pmatrix} \begin{pmatrix} I_0 \\ \Delta I_x \\ \Delta I_y \\ \alpha \end{pmatrix} = \begin{pmatrix} \kappa \cdot F_1 \\ \kappa \cdot F_2 \\ \vdots \\ \kappa \cdot F_n \end{pmatrix}, \quad (10)$$

In this equation, (x_i, y_i) denotes location of the pierce point of i^{th} visible satellites and F_i is a slant factor of the i^{th} satellite. As described in Section III, these values are accurately obtained from the precise ephemeris and location of the receiver. When equation (10) is represented as $\mathbf{X}\mathbf{I} = \mathbf{m}$, unknown vector \mathbf{I} can be estimated using linear least square

method as follows;

$$\mathbf{I} = (\mathbf{X}^T \mathbf{X})^{-1} \mathbf{X}^T \mathbf{m}. \quad (11)$$

The estimated parameters are used in the reconstruction of the vertical TEC map.

V. EXAMPLE APPLICATION TO THE GEONET DATA

The developed method was applied to pseudorange data obtained by the GEONET which is the GPS observation network in Japan. The pseudorange data are open to the public through a FTP site. Actually, although dual frequency data are available, only L1 frequency pseudorange data are used for examination of the proposed method.

An example result of TEC map is shown for data obtained at Uchinada station (136°E, 36°N) in Japan on November 10, 2013. From the precise ephemeris on the day, locations of the pierce points and elevation angle factors are calculated for all visible satellites. Figure 2. (a) shows the TEC map at local time of 11 hour in JST (Japan Standard Time) that is 2 hour UT (Universal Time) on Nov. 10 which is reconstructed from the estimated parameter vector \mathbf{I} in Eq. (11). The map is shown from 125°E to 150°E in longitude and from 25°N to 47.5°N in latitude. The color bar at the right side of the figure shows the vertical TEC in TECU. The receiving station is shown as black circle in the figure. The pierce points are shown by blue triangle points. In this period, 9 satellites are visible from the receiving station. According to the satellite constellation, GPS satellites do not appear in north part of Japan.

The result shows the TEC above the receiver location is around 45 TECU and it is decreasing from 50-60 TECU to 30-40 TECU as the location moves from lower to higher latitudes. As for local time variation of the TEC, the maximum value is generally found in the early afternoon. Since data acquisition time is 11 hour JST and the JST is defined at 135°E, TEC in the east side of Japan should be larger than the west side. In the result, such longitudinal gradient is clearly found. The estimated values and their variations for latitude and longitude are typical.

The result is compared with the TEC map derived from dual frequency observations. The NASA Jet Propulsion Laboratory (JPL) provides global ionospheric map (GIM) with every 2 hours from data obtained at more than 400 GNSS stations all over the world. Figure 2. (b) shows the longitudinal and latitudinal TEC variation map around Japan from dual frequency measurement on the same period. The result shows almost the same tendency to the single frequency result in latitudinal and longitudinal variations while the TEC values of the single are a few TECU lower than those of the dual at same locations.

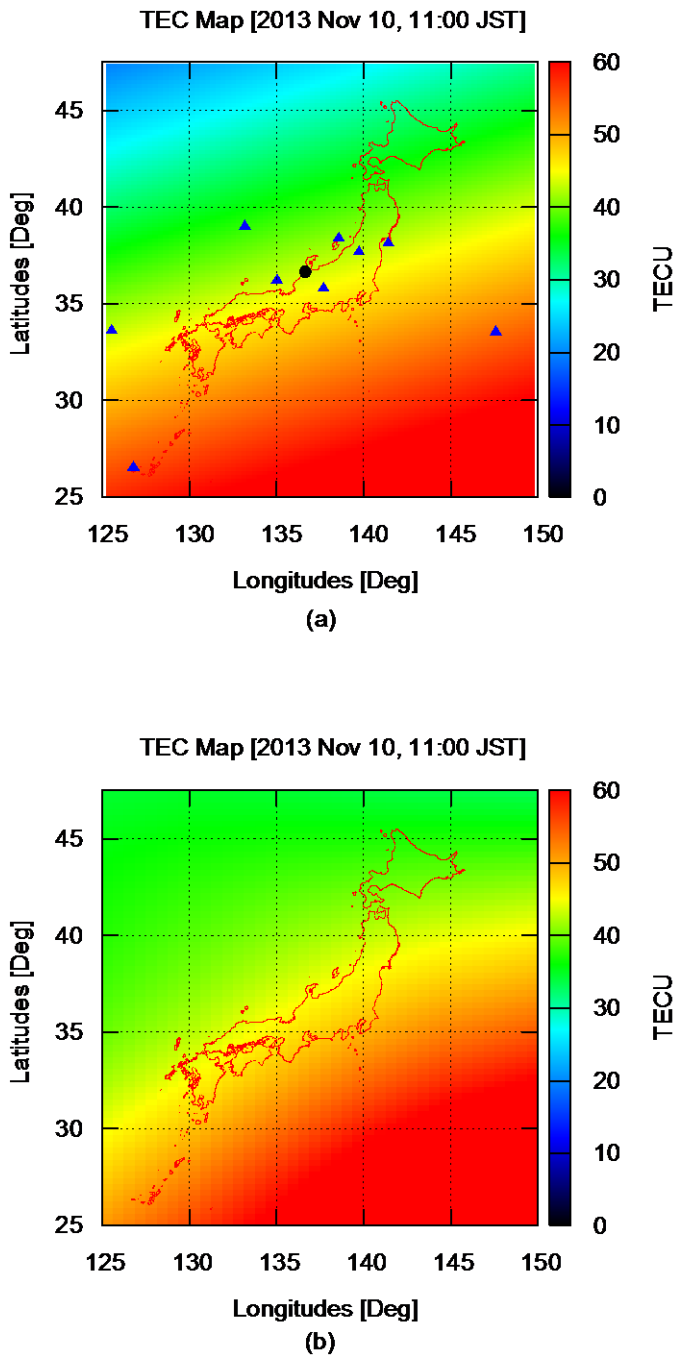


Fig. 2. (a) Latitudinal and longitudinal TEC map derived by single frequency measurement of proposed model. (b) Latitudinal and longitudinal TEC map derived by dual frequency measurements provided by IGS

VI. ANALYSIS OF ONE DAY VARIATION

One-day data analysis can make it possible to check the statistical validity of the proposed method to various kinds of TEC variations. The proposed method was applied to the whole data obtained at the Uchinada station on November 10, 2013. The data are provided every 30 seconds and thus there are 2880 data sets. The parameters I_0 , ΔI_x , ΔI_y and α are independently estimated for each data. The estimated parameters are evaluated by comparing with vertical TECs

converted from slant TECs that are measured by dual frequency signals at the same times.

Figure 3 shows results of estimated parameters of I_0 , ΔI_x , ΔI_y , and receiver clock error α and its residual error. In this figure, the horizontal axis shows local time in JST from 9 hour on Nov. 10 to 9 hour on Nov. 11, that is, 0 to 24 hour in UT on Nov. 11. In figures 3 (a), the vertical TECs estimated at the reference point I_0 is represented by a red dotted line and the vertical TEC at each pierce point by dual frequency signal is represented by black line. From this result, both the vertical TECs show around 40 TECU in daytimes from 9 to 15 hour of JST. It is decreasing from 40 TECU to 10 TECU in the evening from 15 to 19 hour. It becomes less than 10 TECU and there is no remarkable variation at night. In the morning, it increases again from 10 TECU to 30 TECU. There seems a good correspondence between I_0 and dual frequency measurement.

The longitudinal and latitudinal gradients of TEC ΔI_x and ΔI_y are represented by green and by blue lines, respectively, in figure 3 (b). The gradients are defined by TEC variations for 15 degrees in TECU. The longitudinal gradient is plus values before 13 hour. After that, it takes minus values until the next morning. Because longitudinal gradient mainly signifies local time gradient due to the Earth's rotation, it should take plus values from morning region to the noon. In the afternoon, it should be minus. Thus, the estimated gradient is consistent with the typical local time variation. As a comparison of the results from figure 3 (a) and (b), the local time gradient of vertical TEC I_0 and longitudinal TEC ΔI_x are reasonably same each other.

As for latitudinal gradient ΔI_y , it takes minus values except for after midnight. The value is largely fluctuated from around -5 to -40 TECU in the daytime. Since the latitudinal TEC gradient indicates TEC gradients from south to north, it is reasonable to take minus values in the daytime.

Figure 3 (c) shows the estimated receiver clock error α in meter by red dotted line and that derived from the dual frequency measurements by black solid line. Actually, there are two types of GPS receivers; one adjusts its receiver clock error successively and the other adjusts its clock error after it is accumulated to a certain extent, such as 1 ms. From the absolute values of the receiver clock error in figure 3 (c), it is noted that the receiver of the Uchinada station is former type.

From comparison of the two curves in figure 3 (c), the receiver clock error is well estimated by the proposed method. This means that the assumption of TEC model with 1st order gradients is appropriate during the day. There are small deviations at around local times of 13 hour, 15 hour and 21-26 hour. During these periods, there are also deviations on the estimated TEC in figure 3 (a). Since 1 TECU estimation error corresponds to 16 cm of receiver clock error, the receiver clock error should be estimated with much higher accuracy than its hourly variation to get ionospheric TEC.

Figure 3 (d) shows residual error of the least square method applied on equation (10). The error is shown in meter. From the result, the fitting error seems around 0.5 m which is equivalent to 3 TECU in average. There are a few peaks

during day time in the figure. During these periods, the residual errors are more than 1 meter, which means that the estimated TEC may include errors greater than 6 TECU. The TEC values are, however, large during these periods, and during night time when small TEC values are obtained, the fitting error is also small.

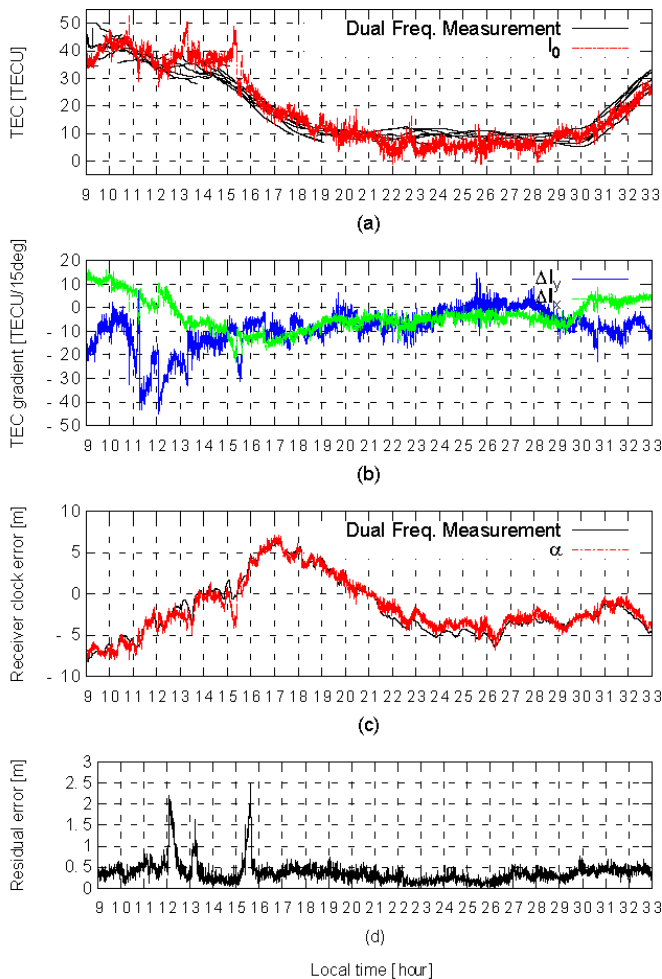


Fig. 3. (a) Comparison of estimated vertical TEC from single and dual frequency measurement, (b) Longitudinal and latitudinal TEC gradients, (c) comparison of estimated receiver clock error from single and dual frequency measurement, (d) estimation error of receiver clock error

The TEC errors estimated by the proposed method is discussed. Figure. 4 shows the histogram of the estimated TEC errors to those derived from the dual frequency measurements, that is differences between red and black lines in figure 3 (a). The horizontal axis shows the TEC errors in TECU and vertical axis does counts. The average of the TEC error is 0.87 TECU and the standard deviation is 8.52 TECU. There is no artificial bias of the estimated TEC.

The proposed method was applied to data obtained at other 680 GEONET stations and examined their TEC errors. Figure 5 shows spatial distribution of average of the TEC errors. In the figure, the average less than -3.16 TECU are shown by red pluses, between -3.16 TECU and 0 are by green crosses, between 0 and +3.16 TECU are as blue stars, and larger than +3.16 TECU are as magenta rectangles. From the figure, a

clear regional dependence of the average of TEC errors is found. As the location moves to south, large bias errors appear. In the east side, larger negative bias regions are also found, as shown by the red pluses.

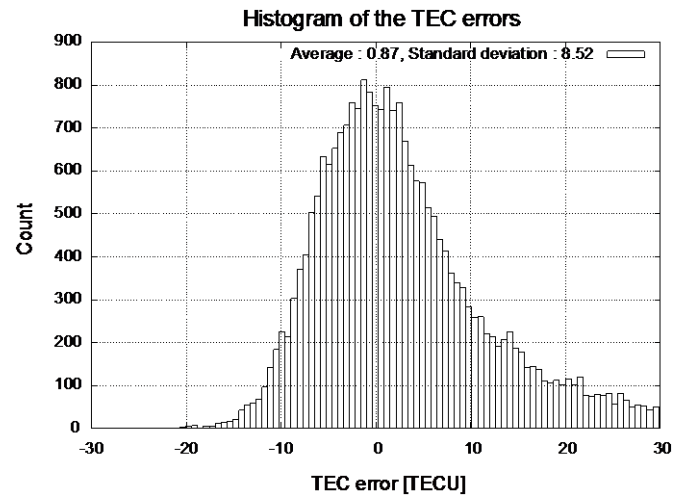


Fig. 4. Histogram of the TEC errors of the proposed method applied on Uchinada data on 2013 Nov. 10

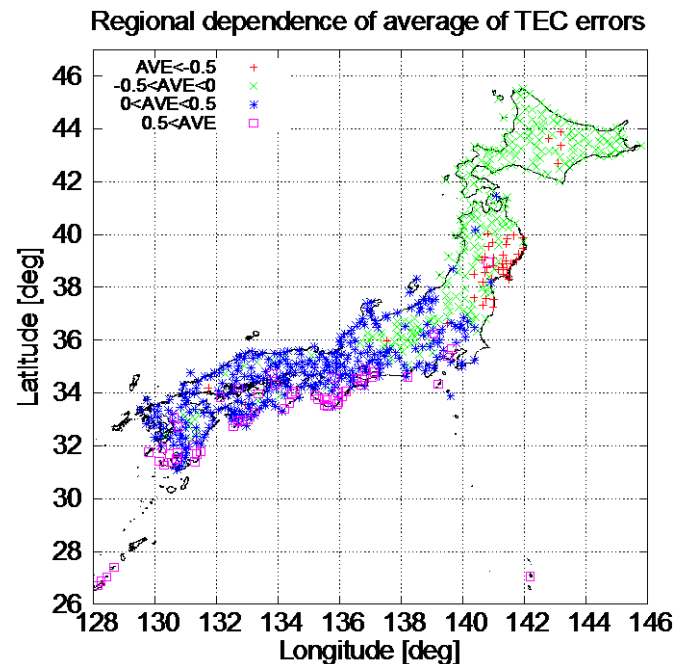


Fig. 5. Spatial distribution of average of the TEC errors

The regional dependences of the standard deviation of the TEC errors were also examined. The result is shown in Figure 6. In the figure, the standard deviation less than 9.2 are shown by red pluses, between 9.2 and 12.3 are by green crosses, between 12.3 and 18.5 are by blue stars, and larger than 18.5 are by magenta rectangles. The largest standard deviation is found at around (142°E, 38°N) and it becomes smaller as the location moves away from there.

From the regional dependences of the average and standard deviation of the estimated TECs, it is found that the accuracy of the proposed method deeply depends on the

assumption of the spatial distribution of the TEC. In the method, the TEC variation is assumed to be represented by 1st order gradient for both latitude and longitude. From the average distribution, however, when the receiver is located at lower latitudes where a large latitudinal TEC gradient exists in a typical daytime, accuracy of the TEC estimation becomes worse. This result implies that the latitudinal distribution cannot be represented by 1st order formula in such regions. To apply the method to data obtained at low latitude regions, higher order function should be required.

Another restriction of the method is found in the standard deviation map. There is no regional dependence of performance of the receivers in GEONET, and thus the large standard deviations found at (142°E, 38°N) is due to other effects. In the terms in equation (1), only δ_{ion}^i and δ_{tro}^i have regional dependences. Since the tropospheric delay δ_{tro}^i is much smaller than the ionospheric delay δ_{ion}^i , the large standard deviation is considered to be caused by complex TEC distributions which cannot be represented by the 1st order model. It should be noted that the proposed method cannot adapt such complex TEC structures.

Regional dependence of standard deviation of TEC errors

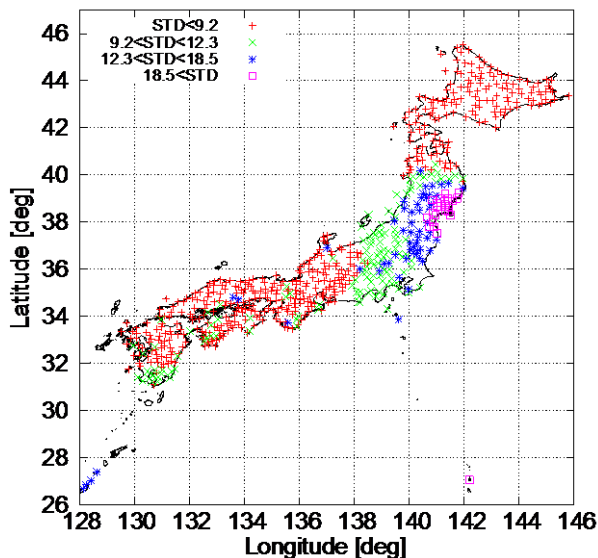


Fig. 6. Spatial distribution of standard deviation of the TEC errors

VII. CONCLUSION

In this paper, an estimation method of TEC distribution map from GPS signals was proposed. A remarkable point of the method is that it only uses single frequency measurements while the TEC observation has been conducted by dual frequency measurements. By this method, it becomes easy to construct TEC observation networks at low costs where the GPS networks are not yet installed.

In the developed method, the TEC distributions is assumed

to be represented by a 1st order gradient model for latitude and longitude. This assumption sometimes causes large TEC errors when the TEC distributions have unexpected structures. It was confirmed that TEC gradients from low to mid latitudes in a daytime cannot be represented by the model. To solve this problem, higher order formula, such as 2nd order polynomial function, is available. As higher order functions are adopted, the number of parameters to be solved increases. By using data from multiple receivers, several independent equations can be used while its receiver clock error should be estimated as an additional parameter. This modification remains to be solved in the future study. We are planning to build observation networks of ionospheric TEC distribution at lower latitude regions, where the networks are not yet installed, at low cost.

ACKNOWLEDGEMENTS

The code pseudorange data used in this study are provided by Geospatial Information Authority of Japan. The ionospheric vertical TEC map and the orbital data of the GPS satellites are provided by the International GNSS Service (IGS).

REFERENCES

- [1] T. Ondoh and K. Marubashi eds., Science of Space Environment, Ohmsha, IOS Press, 2001.
- [2] M. Hernández-Pajares, J. M. Juan, J. Sanz, R. Orus, A. Garcia-Rigo, J. A. Feltens, S. C. Komjathy, Schaer & Krankowski, A. (2009). The IGS VTEC maps: a reliable source of ionospheric information since 1998. *Journal of Geodesy*, Vol. 83 (3-4), pp. 263-275.
- [3] Feltens, J. Dow, J.M. Realized and planned improvements in ESA/ESOC ionosphere modelling, IGS Workshop 2006.
- [4] Zishen Li, Yunbin Yuan, Ningbo Wang, Manuel Hernandez-Pajares, Xingliang Huo (2015). SHPTS: towards a new method for generating precise global ionospheric TEC map based on spherical harmonic and generalized trigonometric series functions. *Journal of Geodesy*.
- [5] H. P. Zhang, W. Xu, M. Han, Ge and C. Shi, Eliminating negative VTEC in global ionosphere maps using inequality-constrained least squares, *Advances in Space Research* Vol. 51, No. 6, 2013, pp. 988-1000.
- [6] J. M. Dow, R. E. Neilan, and C. Rizos, The international GNSS service in a changing landscape of global navigation satellite systems, *Journal of Geodesy*, 83:191-198, DOI: 10.1007/s00190-008-0300-3, 2009.
- [7] International GNSS Service (IGS). Ionosphere Product. NASA CDDIS. Available from <ftp://cddis.gsfc.nasa.gov/gnss/products/ionex/>
- [8] S. Schaer, W. Gurtner, and J. Feltens, IONEX: The IONosphere Map Exchange Format Version 1, Proc. Of the IGS AC Workshop.
- [9] J. G. Grimes, GPS Standard Positioning Service (SPS) Performance Standard 4th Ed, 2008.
- [10] M. J. Dunn, Global Positioning Systems Directorate Systems Engineering and Integration, Interface Specification, IS-GPS-200H, 2013.
- [11] G. Xu, GPS Theory, Algorithms and Applications 2nd Ed, Springer, 2007.
- [12] P. Misra, P. Enge, Global Positioning System, Signals, Measurements, and Performance, Revised Second Edition, 2011.
- [13] J. A. Klobuchar, Ionospheric time-delay algorithm for single-frequency GPS users, *IEEE Trans. on Aero. and Elec. Sys.*, AES-23, 3, 1987.

A New Mixed Signal Platform to Study the Accuracy/Complexity Trade-Off of DPD Algorithms

Hanan Thabet

Department of Signal Processing &
Electronic Systems
Centrale Supélec
Gif Sur Yvette, FRANCE

Morgan Roger

Department of Signal Processing &
Electronic Systems
Centrale Supélec
Gif Sur Yvette, France

Caroline Lelandais-Perrault

Department of Signal Processing &
Electronic Systems
Centrale Supélec
Gif Sur Yvette, FRANCE

Abstract—The increase in bandwidth of Power Amplifier (PA) input signals has led to the development of more complex behavioral PA models. Most recent models such as the Generalized Memory Polynomial (1) or the Polyharmonic distortion modeling (2) can be used to design very performant but complex and thus very consuming Digital Predistortion algorithms (DPDs). On the other hand, with earlier simpler models, the precision of the DPD may not be enough. The model order is also the major factor influencing the requirements in terms of bandwidth and dynamic range of the digitized signal in the feedback loop of a typical Power amplification system architecture: the higher the order, the more information is needed for identification.

This paper describes a new mixed signal simulation platform developed to study the complexity vs. accuracy trade-off from the DPD point of view. The platform estimates the accuracy of the DPD and the power consumption (including the consumption of the DPD itself) of the whole feedback loop, by comparing various PA models with various DPDs algorithms. Contrary to older works, measuring the accuracy on the open loop without DPD and estimating the complexity in theoretical number of operations, our goal is to be able to estimate with precision the performances and the power consumption of the whole amplification system (PA + DPD + DAC + feedback loop) for optimization of DPD algorithms.

Keywords—LTE; DPD algorithms; Simulation Platform; Accuracy/Complexity; Power Consumption; Co-Simulation

I. INTRODUCTION

The increase of mobile services based on 4G LTE services across global markets, provides subscribers with the type of responsive Internet browsing experience that previously was only possible on wired broadband connections. In fact, LTE has a rapid uptake since LTE subscriptions are expected to exceed 1.3 billion by the end of 2018 (3), while they does not exceed more than 200 commercial LTE networks in operation as of August 2013 (3). Furthermore, with the exponential growth in network data traffic, the mobile industry must offers products with higher capabilities and performances with lower cost than existing wireless systems, including LTE (4). This strategy will enable new services, new applications and thus must be based on a combination of network topology innovations and new terminal capabilities. To address these requirements, wireless transmission systems, operating at higher frequencies, requires more bandwidth and increases the demands on the linearity of power amplifiers (PAs). Moreover,

with the growth of power consuming base stations' number, it is very important to develop power-efficient linear devices in radio base stations (5). Since for mobile devices the power is driven from limited battery supplies, the power consumption is the most critical parameter to optimize. As the RF power amplifiers (PAs) are the most power consuming building blocks in wireless transmitters, their design is highly constrained by trade-off between power efficiency and linearity. This is why, in recent years, the interest in PA modeling has increased. In this paper, the second session describes the state of the art and advancements of one of the most promising linearization techniques.

In Sections III, IV and V, we describe three platforms developed in order to study the complexity/efficiency trade-off for LTE base stations.

II. PA LINEARIZATION TECHNIQUES

A. PA characteristics

In fact, high efficiency operating PA induces unacceptable nonlinear distortions at the output of the PA. On the other hand, the price for linearity is a sharp drop in power efficiency (6). So, power efficiency and linearity present key parameters of amplification systems but they cannot be achieved simultaneously. This is why it is necessary to apply linearization techniques to a high-performance amplifier but not sufficient linear. Many techniques have been developed to achieve high efficiency linear operating modes of PAs, but the main drawback of such techniques comes from the fact that the generated waveforms are extremely vulnerable to imperfections in the transmission chain (shown in Figure 1). Some of these techniques were dedicated to improve efficiency behaviour and others to extend the linear behaviour into high efficiency regions of operation. The latter's are known as linearization techniques.

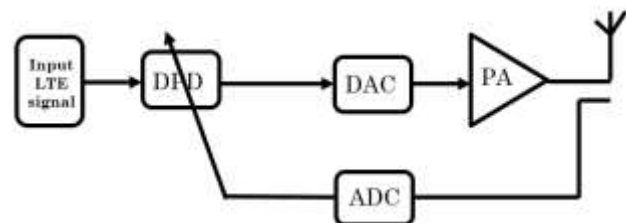


Fig. 1. Typical Power amplification system architecture

An amplifier is linear if its gain is constant throughout the range of the input signal. If this gain is not linear, the output signal is distorted by clipping. The DC bias point is the most important factor in determining the relationship between PA nonlinearity and efficiency. For a real amplifier, the gain and phase-shift are functions of the input signal. The complex transfer function is dependent on the amplifier input power. As a result, the gain decreases and phase-shift changes as the level of the input signal drives the amplifier into its saturation region. The PA output amplitude and phase characteristics are known as AM-AM (Amplitude-to-Amplitude) and AM-PM (Amplitude-to-Phase) characteristics, respectively (7). AM/AM and AM/PM are typical way to characterize the nonlinearity of a PA. An example of AM/AM and AM/PM characteristics is shown in Figure 2. Unfortunately, to model a real PA there is an important parameter to characterize which is the Power Added Efficiency (PAE) (Figure 3). At the base station, linearity in the PA is more important than efficiency (8).

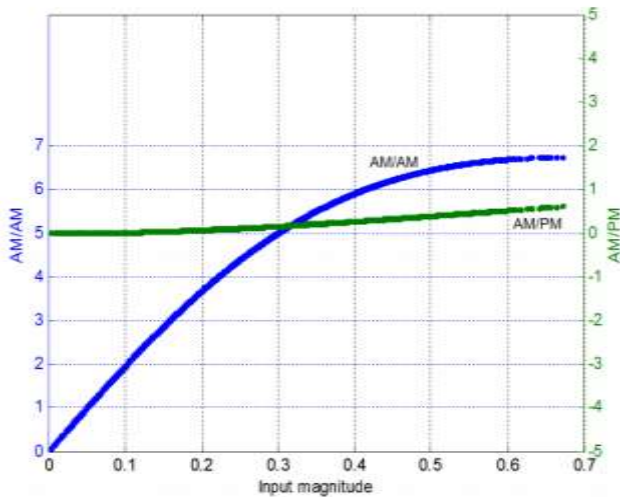


Fig. 2. AM/AM and AM/PM characteristics for a Typical PA

B. Digital Predistortion Technique

In fact, there are various linearization techniques which are classified according to their functionality, architecture, and application. Details of these schemes and their techniques are described in (8) and (10).

The digital predistortion technique (DPD) is considered as a key enabling technique for future radio transmitters. It is entirely implemented using digital processors and this offers re-configurability capabilities, one of the main features of future communication systems. This common technique provides an inexpensive solution in which a nonlinear circuit is inserted between the input signal and the PA. The nonlinear circuit generates IMD products inverse to that produced by the PA and thereby cancels the effect of the PA nonlinearity.

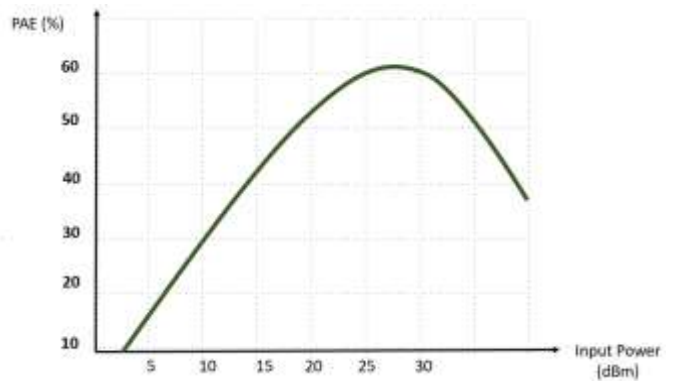


Fig. 3. PA Power Added Efficiency (PAE)

This can be viewed as the predistorter having characteristics inverse to the real PA AM-AM curve in Figure. 1. So DPD is a baseband signal processing technique that corrects impairments of RF PAs. These impairments cause out-of-band emissions, spectral regrowth and in-band distortion of Wideband signals with a high peak-to-average ratio. LTE/4G transmitters, are particularly susceptible to these unwanted effects. The Error Vector Magnitude (EVM) and Peak-to-Average Power Ratio (PAPR) metrics are measured to evaluate the power efficiency and the linearity of an amplification system (figure .1). As shown in Figure 4, DPD improves the adjacent channel power ratio (ACPR) caused by impairments already discussed.

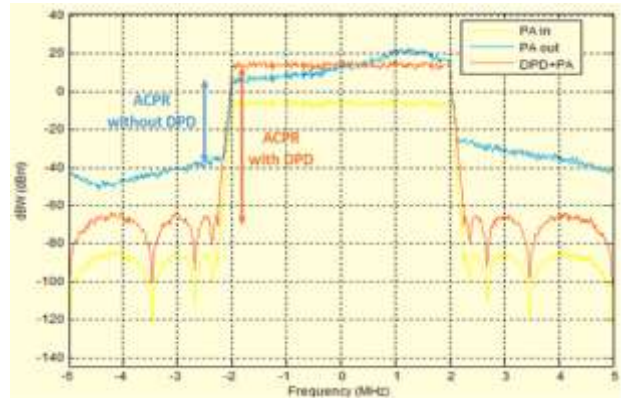


Fig. 4. Example of Adjacent channel power ratio (ACPR) improvement with DPD

III. MATLAB PLATFORM

To simplify the implementation of the platform developed and to solve various problems that may be encountered, we have chosen to divide the implementation into three dependent stages or steps. The first Matlab platform is developed in Matlab/Simulink to implement an adaptive DPD algorithm. This platform uses Simulink block circuits to model the chain

presented in Figure 1. The modeling, itself, was divided into three parts and is based on some simplifications to accelerate simulations. In fact, the PA is an analog circuit using a real pass-band signal while we use a base-band complex signal for a discrete time system. Furthermore, we do not include quantization effects due to the ADC and DAC and up/down conversion effects. First, we model the PA using a polynomial memoryless Saleh amplifier described in (12) followed by an asymmetrical complex filter. The PA simulation then extracts the system inputs and outputs that will be used later to find the expression of the DPD algorithm. Equation (1) describes a memory polynomial (11) form for a non-linear PA:

$$y_{MP}(n) = \sum_{k=0}^{K-1} \sum_{m=0}^{M-1} a_{km} x(n-m)^k \quad (1)$$

Where x is the PA complex input, y is the PA complex output, a_{km} are the PA polynomial complex coefficients, M is the PA memory depth, K is the degree of PA non-linearity and n is the time index. The next part consists on deriving DPD coefficients using matrix inverse algorithm by reversing the roles of x and y in equation (1) as the DPD is the inverse non-linear function. So we can derive DPD coefficients using this equation (2):

$$x_{MP}(n) = \sum_{k=0}^{K-1} \sum_{m=0}^{M-1} d_{km} u(n-m)^k \quad (2)$$

Where d_{km} are DPD coefficients used for implementing equation (2) in Matlab for a static DPD. The last part consists of extending the static DPD design to adaptive one based on Least Mean Square (LMS) algorithm in order to evaluate a functional validation of the amplification system and provide an estimation of the ACPR and the EVM. The LMS algorithm used an indirect learning architecture to implement an adaptive DPD with no matrix inverse. Figure 4. Shows an example of curve's Output spectrum using the platform Matlab/Simulink simulation for a system with $K=M=5$.

IV. MATLAB/CADENCE PLATFORM

This second Matlab/Cadence platform was developed to estimate with more accuracy ACPR, EVM and the analog part power consumption. So, the design of the analog part of the amplification system was done on Cadence using Verilog A language and modifying models of the PA, mixers, VCO, ADC and DAC available in Cadence library. This platform shown in Figure 5. Is based on a Matlab/Cadence co-simulation using couplers and saving the DPD algorithm already developed and presented in section III for the Matlab platform. Figure 6. Shows an example of simulation results of co-simulation using the AMS designer as Cadence simulator. In fact, the high level system concept is often specified in the early stages of design work. This process is well supported by both concept engineering and system-level simulation tools such as MATLAB/Simulink. Co-simulation using AMS designer and MATLAB/Simulink combines the best of system-level simulation with lower-level analog and RF simulation. Simulink provides large libraries of DSP algorithms for generating complicated signals and post processing while AMS supports transient and envelope analysis of RF and

communication circuits, such as mixers and oscillators both at the transistor and behavioral levels. Therefore, to run the co-simulation, Cadence recommends using specific software versions and some libraries and blocks must be installed for the two tools such as Couplers (13).

V. CADENCE ULTIMATE PLATFORM

The PA, in the previous platform, modeled in Verilog A does not include the AM/PM distortion, therefore, it was necessary to add a filter after the PA. Furthermore, the power consumption of the analog part does not be accurate estimated. So, we implement the third Cadence Platform with the RF analog part in Transistor Level and Digital part in VHDL to obtain accurate estimation of power consumption of digital part (DPD algorithm). But, by using the AMS designer simulator, Harmonic Balance simulation cannot be established to visualize spectrums and deduce ACPR, EVM and DPD parameters. As a solution, we develop Post processing in Matlab using Cadence simulation results. In fact, we need also to improve PA model by including memory effects and the recursive adaptive DPD algorithm in VHDL. So to design the RF analog part at transistor level, we use the 0.35 μm AMS CMOS standard technology.

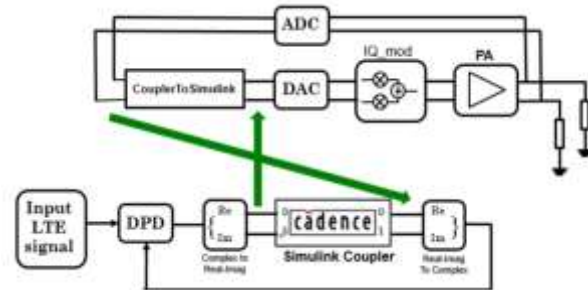


Fig. 5. Matlab/Cadence Platform prototype

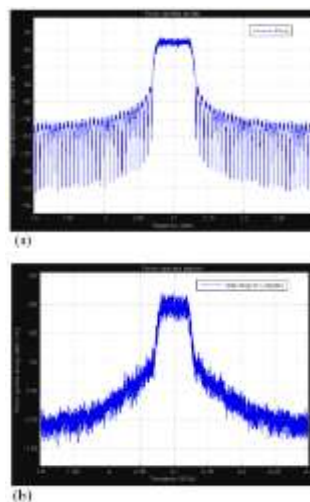


Fig. 6. Example simulation result of Matlab/Cadence Platform: (a) Input LTE Spectrum, (b) PA output Spectrum

VI. CONCLUSION

This paper demonstrated workflow for implementation of three mixed signal platforms developed for the study of the

accuracy/complexity trade-off of Digital Predistortion (DPD) algorithms and optimization of the power consumption for LTE base station applications. The project goal achieved was providing libraries in order to compare various PA models with various DPDs algorithms and be able to estimate with precision the performances and the power consumption of the whole amplification system. We used Co-simulation: MATLAB was used to model digital part, and Cadence used to model and design the RF analog part of the amplification system.

REFERENCES

- [1] D. E. Root, J. Verspecht, D. Sharrit, J. Wood and A. Cognata, "Broadband poly-harmonic distortion (PHD) behavioral models from fast automated simulations and large-signal vectorial network measurements", *IEEE Trans. Microwave Theory Tech.*, vol. 53, no. 11, pp. 3656-3664, 2005.
- [2] A. S. Tehrani, H. Cao, S. Afsardoost, T. Eriksson, M. Isaksson and C. Fager, "A comparative analysis of the complexity/accuracy tradeoff in power amplifier models", *IEEE Trans. Microwave Theory Tech.*, vol. 58, no.7, pp. 1510-1520, 2010.
- [3] Ericsson Mobility Report, "On the pulse of the networked society", November
- [4] B. Bangerter ; S. Talwar ; R. Arefi ; K. Stewart," Networks and devices for the 5G era", *IEEE Communications Magazine* , Volume:52 , Issue: 2 , February 2014, Page(s): 90 – 96.
- [5] Ali Soltani Tehrani, Haiying Cao, Sepideh Afsardoost, Thomas Eriksson, Magnus Isaksson and Christian Fager, "A Comparative Analysis of the Complexity/Accuracy Tradeoff in Power Amplifier Behavioral Models", *IEEE transactions on microwave theory and techniques*, vol. 58, no. 6, june 2010.
- [6] Mazen Abi Hussein, Olivier Venard, Bruno Feuvrie and Yide Wang, "Digital predistortion for RF power amplifiers: State of the art and advanced approaches", 11th International IEEE New Circuits and Systems Conference (NEWCAS), Paris, 16-19 June 2013.
- [7] Hsing-Hung Chen, Ching-Shyang Maa, Yeong-Cheng Wang, and Jiunn-Tsair Chen, "Joint polynomial and look-up-table power amplifierlinearization scheme," in 57th IEEE Semiannual Vehicular Tech. Conf. (VTC 2003), Jeju, Korea, April, 2003, vol. 2, pp. 1345-1349.
- [8] S. Cripps, *RF Power Amplifiers for Wireless Communications*, Boston, MA: Artech House Inc., Academic Publishers, 1999.
- [9] M. Hella and M. Ismail, *RF CMOS Power Amplifiers: Theory, Design, Implementation*. Norwell, MA: Kluwer Academic Publishers, 2002
- [10] S. Bruss, "Linearization Methods," Class Lecture, Dep. Elect. Comput. Eng., University of California, Davis, April 2003
- [11] Morgan, Ma, Kim, Zierdt, and Pastalan. "A Generalized Memory Polynomial Model for Digital Predistortion of RF Power Amplifiers". *IEEE Trans. on Signal Processing*, Vol. 54, No. 10, Oct. 2006
- [12] Saleh, A.A.M., "Frequency-independent and frequency-dependent nonlinear models of TWT amplifiers," *IEEE Trans. Communications*, vol. COM-29, pp.1715-1720, November 1981.
- [13] Cadence Design system, "Co-simulation with SpectreRF MATLAB/Simulink Tutorial", Product Version 6.1.1, November 2006.

A Universally Designed and Usable Data Visualization for A Mobile Application in the Context of Rheumatoid Arthritis

Suraj Shrestha¹

Department of Computer Science, The Universal Design of ICT Research Group, Oslo and Akershus University College of Applied Sciences
Oslo, Norway

Dr. Pietro Murano²

Department of Computer Science, The Universal Design of ICT Research Group, Oslo and Akershus University College of Applied Sciences
Oslo, Norway

Abstract—This paper discusses the design, development and evaluation of a data visualization prototype for a mobile application, for people with rheumatoid arthritis conditions. The visualizations concern ways of displaying graphically data for monitoring and evaluating the daily activities of rheumatoid arthritis sufferers. An initial visualization was developed and then a second was developed, aiming to be more usable and universally designed than the first version. An empirical experiment was used for evaluation and collection of quantitative data. Furthermore, semi-structured interviews were used for eliciting more qualitative data in terms of participant opinions. The overall results suggest that the second visualization was more usable and more universally designed than the first version. The paper concludes with some recommendations for future improvements.

Keywords—universal design; usability; evaluation; data visualization; mobile application; rheumatoid arthritis

I. INTRODUCTION

The use and interest in mobile apps has reached significant proportions in recent years. Statista [1] indicates that apps available from Google, Apple, Microsoft, Amazon and BlackBerry total approximately 5 700 000. Within these, there is also a group of apps developed for health related aspects such as monitoring certain body readings, e.g. heart rate etc.

Linked to this large increase in app availability, the use of mobile devices has steadily increased among all user groups. In 2016, it is estimated that there are about 4.61 billion mobile phone users around the world [2]. However, in 2014 there were only about 1.75 billion smartphone users globally [3]. Similarly, the use of mobile devices in the health sector is increasing sharply. This sharp increase is related to the affordability and availability of mobile devices and smartphones, which have higher processing capacities. Most healthcare information systems are designed for health professionals to enter, receive and exchange information about patients [4]. A term called mHealth [5] apps was coined, which is used to represent the increase of mobile health applications available on the market.

The research discussed in this paper is in the context of mobile health apps. The authors discuss designing and evaluating ways of displaying graphically data for monitoring

and evaluating daily activities of rheumatoid arthritis sufferers. The app's presentation of information is compared by means of an experiment and post-experiment interviews using two methods of visualization. The first method which lacked in universal design and usability was redesigned into a second version to be a more user friendly universally designed version.

In the first part of this paper, some relevant literature is discussed. In the second part, the two data visualizations are described in detail and linked with the principles of universal design. The third part describes the evaluation carried out for the two visualizations along with the results achieved. The fourth part consists of a discussion of the results in relation to the universal design principles. The paper then concludes with an overall conclusion and suggestions for improvement in this work.

Finally throughout this paper, the authors use the terms 'visualization' and 'prototype' interchangeably. The reason for this is that although the focus of the research is actually on the visualization aspects, in order to achieve these visualizations and subsequent evaluation, a working prototype had to be developed to facilitate these aspects.

II. RELEVANT LITERATURE

This literature review will indicate to readers what others have done in similar areas to the research presented later in this paper. It will also indicate by its absence that universal design is not mentioned or considered in these other works. Furthermore, it shows that the authors' research described later in this paper is original because of having considered more closely universal design and usability in a real world problem for visualizing several types of data together.

According to the World report on Disability, produced by WHO and World Bank, almost one billion people in the world are struggling with some form of disability [6]. Among these different disabilities, rheumatoid arthritis is the 31st leading cause of Years Lived with Disability (YLD) and almost one percent of the total population of the world suffers from rheumatoid arthritis [7]. Therefore techniques to visualize information such as data visualizations must be accessible in

design to include different groups of users despite impairments [8].

Some of the common challenges regarding data visualization with all types of mobile devices are designing visualizations, which are aesthetically pleasing and convey the intended information in an accurate manner. Another common problem is the difficulty to use data visualizations with small screens of mobile devices [9]. There has been little or no research specifically targeted towards data visualization for mobile devices [9]. Therefore, there needs to be more focused research on how to use universal design principles and standards to create accessible data visualizations for mobile devices [9-10].

There are many apps available for download which aim to help with various conditions, e.g. arthritis etc. Some examples of these are My Pain Diary®[11], TRACK + REACT® [12], Learn Arthritis Prevention® [13], MyRA® [14], RheumaTrack® [15] and RHEUMATOID ARTHRITIS® [16]. However to our knowledge there is no published information regarding formal aspects of usability and universal design for these apps. However from an informal examination of these apps, the visualization of the data could be difficult to understand for users. Furthermore the RHEUMATOID ARTHRITIS® app has no visualization of data for the user. Therefore the remaining discussion in this brief literature review will concentrate on works that have been published.

Several mHealth apps have already been developed targeting arthritis patients; one such app is called “Pain Information on the Go (PInGO)” [17]. It was developed in order to examine and assess muscle improvement in juvenile arthritis patients who were undergoing a training program for a period of 6 weeks [17]. The app consisted of a questionnaire for before and after exercise, which had to be completed by the patients. This provided valuable assessment of the exercises and their effects on patients, which in turn helped the medical professionals to generate an effective fitness regimen for their patients. “PInGO” is available as an android mobile app as well as a web-based version available via Google Chrome.

In [18], “MyWalk, a mobile app for gait asymmetry rehabilitation in the community” is discussed. This is relevant in the context of this study as it records real time data and analyzes it to provide a visualization of the data. However, “MyWalk” has some issues related to accuracy of data and visualization. Unlike “PInGO”, “MyWalk” consists of a data visualization feature. However, “MyWalk” uses a line chart to visualize the data, which has several issues. One of the issues is related to the size of the line charts and its correlation with accuracy. In terms of normal line charts, the optimal chart height was found to be 24 pixels (6.8 mm on 14.1” 1024 X 768 pixel display) [19]. This suggests that line charts are not suitable for mobile devices with smaller screen sizes due to loss of accuracy of information and interaction capabilities.

In another research paper, by Pereira and Moreira [20], it was suggested that in real time monitoring systems, there are issues surrounding simultaneous monitoring of multiple patients and storage of data in the database. Their solution

included a network of wireless sensors, which can be used to monitor the vital signs of patients. Data from the sensors are stored in a central repository, which can be accessed locally using Ethernet or Wi-Fi connections, and remotely through the use of the Internet. However, sensor-based networks generate large amounts of data and the authors suggested that complex visualization is not the best solution because of the processing requirements of the client system. The application must also be made scalable to cope with the increase of users for the future.

In one article, [21], it is suggested that medical decision-making is a complicated process where a large amount of data is stored in Electronic Health Record (EHR) systems. In this article the authors have surveyed and reviewed the data visualization and interaction techniques found in 14 EHR systems. The authors have attempted to divide the data types into categorical and numerical data, where they suggest that the most common method to visualize categorical data is by placing icons (for point events), and line segments (for events with duration) on a horizontal time line. This can be further differentiated using color codes. While numerical data can be visualized using line plots, use of point plots or bar charts is also accepted. However, in systems which visualize both categorical and numerical data, the dual visualization technique, such as “Web Based Information Visualization System (WBIVS)” [21] is used. This uses line charts for numerical data and a matrix view for categorical data. The authors have concluded that medical information is complex and difficult to interpret. This problem can be solved by using appropriate data visualization techniques.

The “Spatial OLAP Visualization and Analysis Tool (SOVAT)” [22] is another tool used to make community health decisions. This tool can be used to handle large amounts of data and visualize the information in numerical and spatial views. It consists of two technologies: 1. “Online Analytical Processing (OLAP)” and a “Geospatial Information System (GIS)” [22]. This article suggested that there is a need for a powerful multidimensional data storage and manipulation system especially concerning spatial data. “SOVAT” is an example of an application which combines “OLAP” and “GIS” and consists of abilities such as: storage of data sets, statistical analysis, exploration of data, visualization of data using charts and spatial objects and can perform spatial analysis. However, the system still lacked ease of use and the complexity of usage makes it difficult to adopt technologies like “SOVAT”. Therefore, specific concerns regarding usefulness and ease of use of systems must also be addressed during the development of such systems.

“HealthMap” is an event based monitoring system for infectious diseases. Data from various sources is collected through Rich Site Summary (RSS) at the backend, whereas at the front end Google Maps public API is used to create mappings [23]. “HealthMap” organizes and visualizes data according to three categories: date, location and disease. The developers allowed the system to adapt to the needs of the users where customization options were created to adapt the system to expert users as well as novice ones. The data showed in the visualization changed according to the selection of categories by the user. Users had the ability to zoom into

the specific maps of countries and track for any alerts for diseases that were ordered by reverse chronological order. Therefore, "HealthMap" allowed the users to visualize the data according to their selection of categories. However, due to the complexity of this application the front end still needs to improve to provide better user experience and automation capabilities.

More recently some other researchers have done work on a mobile app for rheumatoid arthritis [24, 25, 26]. In [24] the authors aimed to find out about requirements specifications for the app and the user group and desired features of the app. Then in [25] the researchers carried out an evaluation with the app and users. Overall they concluded from their data that the app was found to be 'easy and fun to use, and as providing sufficient physical activity (PA) support and information [25].' Further, about 20% of the user group seemed to be unsure about the 'feasibility of goal setting and PA planning'. However although this work is related to our work, they did not seem to concentrate on the actual visualization issues that we have specifically been designing and evaluating. Therefore this suggests that the work discussed in this paper is both important and novel.

This literature review has shown that some research has been carried out in terms of health apps, but not specifically like the research described later in this paper. The literature has also given some indications on what could be done, what could be avoided and that with some apps/prototypes there is room for improvement, e.g. "PInGO" does not provide a data visualization [17].

Also in [18] real time data recording is indicated to be beneficial, but there were problems with accuracy and using a line chart for data representation on a small screen.

Having considered some relevant literature the next section will describe the first and second main attempts for visualizing activity data for rheumatoid arthritis sufferers.

III. DESCRIPTION OF THE TWO VISUALIZATIONS

The first visualization and its features are described below:

A. Overview of the First Visualization

The app is a mobile application for rheumatoid arthritis sufferers, which records activities performed by the user for a definite period of time. Each activity consists of three attributes as listed below:

- a) Importance
- b) Energy
- c) Duty/Pleasure

Importance has two extremes (Important and Not Important). Energy has two extremes (Energy Giving or Energy Taking). Every activity must be categorized as Duty or Pleasure.

The user can select any of these two extremes by sliding a slider. The position of the slider before or after the middle point mark determines one of the two extremes. This information is then saved for review later on.

These categories are assessed using a continuous slider visualization, which allocates a decimal value between 0 and 1. This value is registered by the user of the application as per their experiences.

1) Explanation of Visualization

The visualization consists of an X-axis and a Y-axis, which intersect each other to form a cross section. The X and Y axes intersect to form four quadrants.

- a) Quadrant I: Activities which were desired and important
- b) Quadrant II: Unimportant activities that are required
- c) Quadrant III: Important required activities
- d) Quadrant IV: Unimportant, desired activities

Each quadrant consists of two axes as described above. The attributes provided by the user within each category for every activity by using the slider determine the position of the activity within these four quadrants. The user can tap on each of these quadrants to get detailed information about activities, which lie within respective quadrants (The explanation above consists of no images due to copyright issues).

As mentioned in the Introduction section of this paper, the first main attempt for visualization lacked somewhat in universal design. Therefore, the next section will discuss how the first main attempt of the app visualization was lacking in universal design.

2) Universal Design Issues in the Old Prototype

Universal design consists of seven principles [27]. These seven principles are considered to be fundamental for developing artifacts for all users. They were developed in 1997 by a team led by the late Ronald Mace in North Carolina State University:

- a) Principle 1: Equitable Use
- b) Principle 2: Flexibility in Use
- c) Principle 3: Simple and Intuitive Use
- d) Principle 4: Perceptible Information
- e) Principle 5: Tolerance for Error
- f) Principle 6: Low Physical Effort
- g) Principle 7: Size and Space for Approach and Use

Based on these principles the following principles and guidelines are specifically pertinent to the first visualization. (Note: The descriptors for each category and numbering scheme used below are directly extracted from the original universal design principles and guidelines as they appear in [27]).

Principle 2 - Flexibility in Use: This principle states that the design must accommodate a wide range of individual preferences and abilities, which are addressed through four guidelines [27]. However, for the purpose of our mobile application two particular guidelines are relevant:

2a. Provide choice in methods of use: The old data visualization prototype does not possess features to customize the data visualization according to the needs of the users. The data visualization as well as other features of the old prototype cannot be adjusted or changed.

2b. Accommodate right or left-handed access and use: Similarly, the old data visualization prototype is not suited for single-handed use. Single-handed access becomes difficult, as the user cannot reach all the “User Interface (UI)” elements on the screen. The icons and other UI elements are placed in inappropriate positions causing difficulty in access and accuracy.

Principle 3: Simple and Intuitive Use: This principle states that the use of design must be easy to understand, regardless of the user’s experience, knowledge, language skills, or current concentration level, which is addressed through four guidelines [27]. However, for the purpose of our mobile application two particular guidelines are relevant:

3a. Eliminate unnecessary complexity: The old data visualization prototype consists of four quadrants created by the intersection of X and Y axes. The activities are displayed in each of these four quadrants and are represented by small squares. It remains unclear as to how the activities are sorted within these four quadrants and the user needs to interact multiple times to get the details about each activity.

3c. Accommodate a wide range of literacy and language skills: The old data visualization does not consist of multiple language support.

Principle 4: Perceptible Information: The fourth principle states that the design must communicate necessary information effectively to the user, regardless of ambient conditions or the user’s sensory abilities [27] which is addressed through four guidelines. However, for the purpose of our prototype, only one particular guideline is relevant:

4d. Provide compatibility with a variety of techniques or devices used by people with sensory limitations: The old data visualization prototype does not provide multimodal means of presentation of information. It does not support screen-readers or other assistive technologies, which makes it difficult for users of different abilities to access the data visualization.

Principle 5: Tolerance for Error: The fifth principle states that the design must minimize hazards and the adverse consequences of accidental or unintended actions [28], which is addressed through four guidelines. However, for the purpose of our prototype, only one particular guideline is relevant:

5a. Arrange elements to minimize hazards and errors: most used elements, most accessible; hazardous elements eliminated, isolated, or shielded: The activities are represented by small square objects, which are scattered throughout the graph in the old data visualization prototype, which does not convey much information to the user. In order to gain further insight about a certain desired activity the user must go through the entire list of activities, which makes it tedious.

Principle 6: Low Physical Effort: The sixth principle states that the design must be able to accommodate efficient and comfortable use and with a minimum of fatigue [27], which is addressed through four guidelines. However, for the purpose of our prototype, two particular guidelines are relevant.

6c. Minimize repetitive actions: The old data visualization consists of complex and repetitive actions, which increase task

time and complexity. An example of a repetitive action involved tapping a quadrant which expanded that area of the visualization. Then further selections down a fairly deep nesting of options was required to access a specific item of information involving a daily activity’s details.

6d. Minimize sustained physical effort: As mentioned above the old data visualization prototype consists of complex and repetitive tasks which require a sequence of steps to complete simple tasks. This also causes fatigue more often and wears out the user faster. An example of a task was to find out the details of a particular activity such as gardening and/or work etc.

Having described the first main attempt for visualization along with its shortcomings in universal design, the next section will describe the second redesigned version for visualization.

B. Overview of the New Data Visualization

In this section an overview of the second visualization describing the new user interface and a new data visualization technique is presented. This overview will also show some of the steps users will use to interact with the prototype of the visualization.

The new data visualization was developed as a platform independent prototype, which could run on Apple and Android devices without change. Furthermore, the prototype was developed so as to be readable by screen readers.

The design of the new visualizations is shown graphically below. The reader will perceive that the use of axes and quadrants as described in Section III (A) above was replaced with a ‘bar graph’ type representation. This choice was made to try and make understanding and comparison of the various data easier for the user. Bar graphs are specialized for focusing attention on individual values and support comparison of one to another. They also emphasize the individual values of the thing being measured per categorical subdivision. A bar graph might be one of the easiest methods of data visualization. According to Meyer [29], whenever there is uncertainty regarding which graph to use to represent a particular set of data, the easiest answer is to use a bar graph. However, there is a limit to what kind of data can be represented using such graphs and how to make the best application of such graphs. For example use of 3D bar graphs to represent data might give ineffective results and provide false information due to distortion of data, which can cause data ambiguity and distraction from what the data might try to convey through that graph. Such graphs can cause cognitive overload for the reader in order to separate each section of the bar and then compare it against other bars [30]. The choice of colors to represent data in these graphs can be crucial as well as the text alignment and location can also play a vital role to convey the message. A flat bar graph conveys more accuracy of information than a three dimensional bar graph.

Therefore, for a simple comparison of categorical subdivisions of one or more measures in no particular order, a bar graph is suggested [31].



Fig. 1. Prototype Home Screen

Fig. 1, shows the first step. This figure shows the header which consists of Activity Overview as text and two flags which can be tapped by the user to change the language. Below the header is the sub-header which shows two buttons for activity overview and settings and below the buttons is the time period.

The sub-header is followed by the three drop-down boxes which represent the three categories of data: Importance, Energy and Motive.

Finally it shows the list of activities. The default list of activities is shown to the user at first.

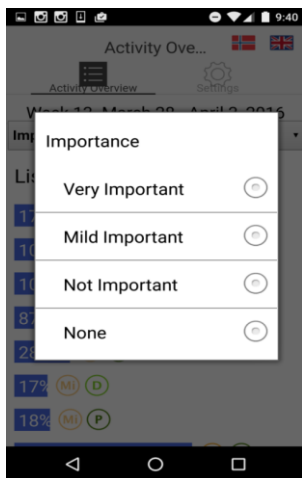


Fig. 2. Importance Drop Down Menu

Fig. 2, shows the second step. This prototype shows the drop down menu for a category called Importance. This drop down menu shows four variations of importance:

- 1) Very Important
- 2) Mild Important
- 3) Not Important
- 4) None

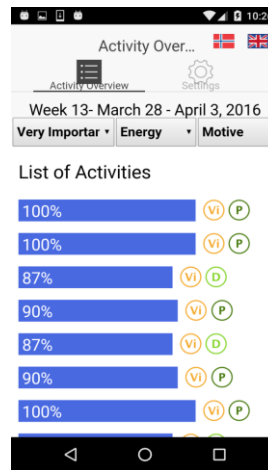


Fig. 3. Selection of Variation for First Category

Fig. 3, shows the third step. This step shows selection of the Very Important variation of the Importance category. The selection of Very Important from the drop down menu adds the first level of filter. Therefore, all the activities which have been entered as very important by the user are displayed.

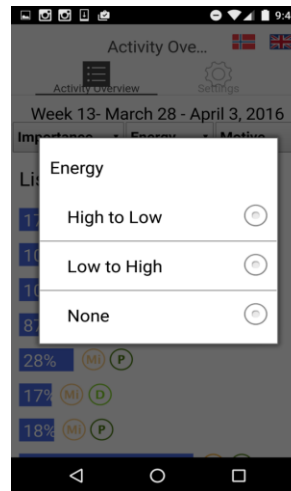


Fig. 4. Drop Down Menu for Energy

Fig. 4, shows the fourth step. When the user taps on the drop down menu for Energy the user is shown three variations of Energy category:

- 1) High to Low
- 2) Low to High
- 3) None

Once a user selects one of these variations the data is filtered according to the selection.



Fig. 5. Selection of Variation for Second Category

Fig. 5, shows the data which is sorted according to the selection of one of the options from the energy category. In this case, High to Low was selected and the data is sorted accordingly.



Fig. 7. Final View

Fig. 7, shows the seventh step. In this step, the user has selected all three variations for all three categories. In the first drop down menu, the user selected Very Important. In the second drop down menu, the user selected High to Low. In the third drop down menu, the user selected Duty.

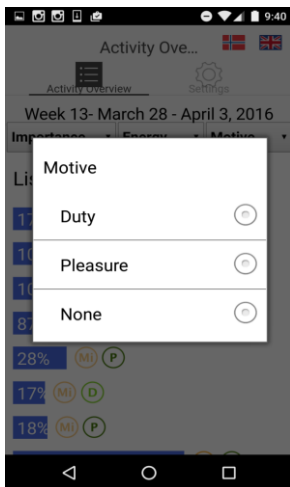


Fig. 6. Drop Down Menu for Motive

Fig. 6, shows the sixth step. In this step, the user can tap on the drop down menu for “Motive” and the menu shows three variations: Duty, Pleasure and None.

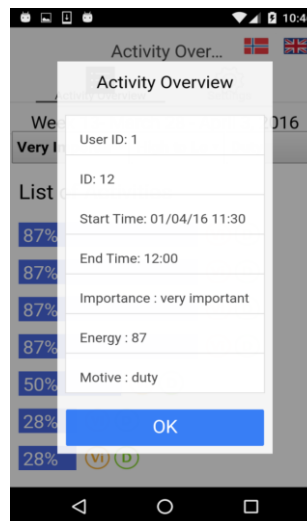


Fig. 8. Activity Details

Fig. 8, shows the details view. When the user taps on the bars which represent activities, the details of that activity are shown.

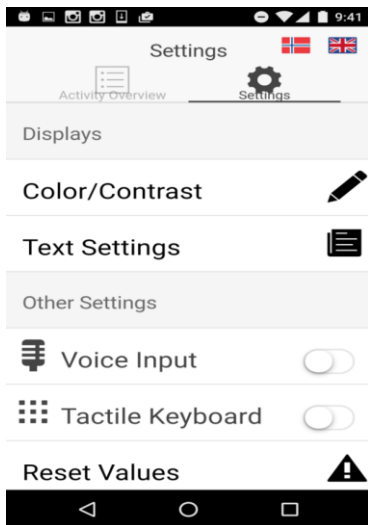


Fig. 9. Setting Home Button

Fig. 9, shows the different customization options consisting of two main categories.

1. Displays

Displays consist of two sub-categories:

- i. Color/ Contrast
- ii. Text Settings

2. Other Settings

Other settings consist of two sub-categories:

- i. Voice Over (The user can tap on the toggle button to turn on/off the voice over function.)
- ii. Tactile Keyboard (The user can turn on/off the tactile keyboard option by using the toggle button.)

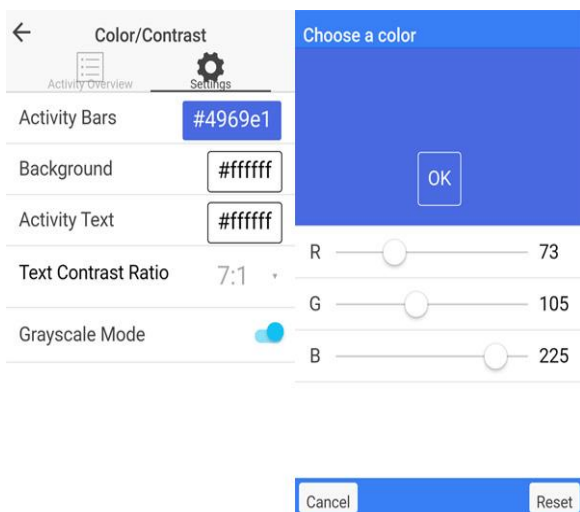


Fig. 10. Color/Contrast Settings

Figure 10 shows the color/contrast settings. The user can customize the colors of the Activity Bars, Background and Text. The grayscale option can be turned on and off using the toggle button. Colors can be selected by manipulating the

three RGB scale sliders which will then display the color chosen above the sliders (in this image blue is showing). The Ok button can be used to commit to the changes. Alternatively, the reset button can be used to reset the values.

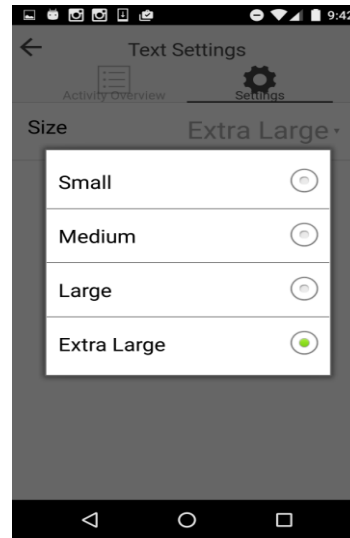


Fig. 11. Text Menu

Fig. 11, shows the Text Settings menu. The size of text can be changed by selecting any one of the four categories as listed:

- 1. Small
- 2. Medium
- 3. Large
- 4. Extra Large

C. Future Considerations

There are three categories in this application for data manipulation: Importance, Energy and Motive.

In future, if there is a need to add another category, then the application will automatically adjust its size to accommodate this feature. The screen will also automatically adjust the size of the area, which shows the list of activities represented using bars. These bars will automatically adjust in size and length in proportion to the area available for each bar respective to the entire space. However, the clickable area for each bar will remain similar to support flexibility of use.

Having produced a new design, the next stage was to formally evaluate the two designs. A quantitative experimental approach was used along with a more qualitative post-experiment interview of the participants, aiming to capture essential evaluation aspects not easily captured in a quantitative manner. These aspects are described in detail in the following section.

IV. DATA VISUALIZATION EXPERIMENT

An experiment consisting of 18 participants was conducted using a within users design. The main aim of the experiment was to try and obtain evidence to show that the new design of

the visualization interfaces was more usable and universally designed than the first main version.

A. Hypotheses

Two hypotheses were created for this experiment. These are detailed as follows:

H₁: The new visualization will be easier to use and more universally designed in terms of speed when compared with the old visualization.

H₀₁: There will be no difference between the two visualization methods in terms of speed and universal design.

H₂: Participants perceptions of the new visualization will be more positive than their perceptions for the old visualization.

H₀₂: There will be no difference between the two visualization methods in terms of participant perceptions.

A total of six tasks were performed on each data visualization separately. Tasks 1 to 5 were similar in nature with some small disparities. The sixth task was completely different for the two data visualizations therefore findings from this last task were not included as a comparative analysis.

B. Tasks

1) Tasks for the New Data Visualization

Task 1: Find out which activities are considered “Very Important” by selecting it from the “Importance” category.

Task 2: Find out which activities are considered “Duty” by selecting it from the “Motive” category.

Task 3: Find out which activities gained energy from looking at the data visualization.

Task 4: Tap on the bars which represent activities and find out details about at least three activities.

Task 5: Use a screen reader to use the app.

2) Tasks for the Old and Present Data Visualization

Task 1: Find out which activities are considered important from looking at the data visualization.

Task 2: Find out which activities are considered duty from looking at the data visualization.

Task 3: Find out which activities gained energy from looking at the data visualization.

Task 4: Tap on the small green squares which represent activities and find details for at least three activities.

Task 5: Use a screen reader to use the app.

3) Tasks Specific to New Data Visualization

Task 6: Change the font-size and color of text.

4) Tasks Specific to Old Data Visualization

Task 6: Tap on each quadrant to discover any further information.

C. Participants

As stated above, 18 participants (16 males and 2 females) were recruited for this experiment. The participants were all students of various international backgrounds. For this experiment, participants were expected to be experienced with mobile phones especially smartphones as well as laptops.

In the recruitment survey a range of questions investigating the familiarity of prospective participants with smartphones were asked. The survey asked questions regarding their experiences using various mobile devices, familiarity with smartphones in terms of years etc. Based on this, the participants who spent more than a year using smartphones were selected as it indicated familiarity with smartphones and various mobile applications. Participants were also asked about their familiarities with different kinds of smartphones and operating platforms. The highest number of participants used Android devices followed by Apple’s iPhone.

The authors had initially wanted to recruit participants with actual rheumatoid arthritis, for realism. However this was not pursued for two reasons. The first reason was that it was extremely difficult to obtain access to a good number of actual rheumatoid arthritis sufferers with specific problems in the hands and fingers (this experiment involved using a smartphone). The second reason was that arthritis is a condition that can affect different people in different ways and at different levels [32]. This could have made it difficult to control certain experimental variables. It was therefore decided that the use of simulation gloves (see Section IV(F) below) would provide a ‘standard’ type of impairment and therefore a factor that could be controlled in the experiment.

D. Design

A within users design was chosen for this experiment. This design was chosen to expose the participants to both data visualizations. Therefore, each participant was asked to complete a set of tasks for both data visualizations. Half of the participants carried out the tasks with the new visualization followed by the old visualization. The remaining half carried out the tasks in the opposite order. Participants were randomly assigned to each ordering described here.

E. Variables

The independent variables were the two prototypes (i.e. the old and new visualizations) and the tasks which were performed on the two different data visualization prototypes.

The dependent variables were performance, attitude and experiences. The dependent measures were the completion of the tasks (success/failure), time taken for an overall task, errors in terms of incorrect option selections and participants’ subjective opinions while interacting with the data visualizations and their features.

A semi-structured interview was conducted after the experiments for each participant. The interview consisted of questions relating to the comprehension of the data visualizations. The aim was to understand if the participants understood the information through the data visualizations and to ascertain their feelings and experiences.

F. Apparatus and Materials

The following materials were used in the experiment:

- Two smartphones: Android smart-phone running android version 6.0 (marshmallow) and Apple iPhone running iOS 9.3. For the experiment, Android was used for the new data visualization and iOS was used for the old data visualization. Both devices were approximately equivalent in terms of hardware specification and software sophistication.
- The old data visualization and the new visualization.
- A stopwatch to record the time for completion of tasks.
- A recruitment questionnaire and a consent form for participants before conducting the experiments.
- A sheet of instructions for participants to inform them about the details regarding the experiment in which they were involved.
- A post experiment semi-structured interview guide.
- One pair of Cambridge Simulation Gloves designed by the University of Cambridge [33], Engineering Design Center.

As the visualizations for the app were for use by rheumatoid arthritis sufferers, the Cambridge Simulation Gloves were used to simulate the obstruction of movement of hands and fingers. The main focus of the usage of the gloves in this experiment was to understand how reduction in mobility of hand and fingers affects the usage of the two prototypes for data visualizations. The usage of these gloves can simulate the affects arthritis might have on the hands and fingers of the participants, and the problems faced by them when using mobile devices and applications.

The Structural Design of the simulation gloves consisted of plastic strips, which limit the strength as well as the range of motion of the fingers and thumb [33]. Also the straps on the wrist can be adjusted according to need and the length of the straps can be adjusted for the plastic strips according to the size of the fingers of the participants.

Although the gloves help to simulate dexterity problems, they cannot help to simulate problems such as pain, tremors, problems of the wrist, loss of tactile sensitivity and deformities to the shape of the hand [33].

G. Procedure

Participant recruitment was first conducted through a survey via www.surveymonkey.com. The recruitment survey was used to understand the capabilities of the participants since participants were required to be familiar with smartphones. The recruitment survey lasted for three days. After the recruitment, the experiment was conducted for a period of one week. The experiments were conducted in a study room at the university. The participants and the experimenter were located in the same quiet room at the same time for the experiments. Overall each session with participants lasted for almost 30 minutes for the experiment

and the time varied from 10 to 15 minutes for the semi-structured interviews.

Each participant was allocated a time slot in advance. Social media such as Facebook and Messenger were used to keep in contact with the participants to confirm their schedules. Conventional communication mediums such as telephone calls and text messages were used for those participants who wished to share their contact details. However these details were not stored anywhere.

When the participant arrived he/she was greeted and asked to take a seat. They were introduced to the experiment and then the consent form was presented to them. The participants carefully read the consent form and signed it. The consent form informed the participants about the research and the ethical treatment of them and the data collected.

Participants were randomly assigned to use one of the two data visualizations. A brief explanation about both data visualizations was provided to familiarize participants. Participants were asked to complete a set of tasks for each data visualization in sequence. Each participant was asked to speak aloud while performing the tasks. Participants were specifically asked to say out loud what they intended to do next.

Further participants were observed for any effects that could arise concerning the use of the simulation gloves. Specifically aspects to do with interaction difficulties were observed.

At the end of the experiment, a semi-structured interview was conducted to gain further insight about their experiences, performance and features of data visualizations. The interview targeted the user experience, feature specific explanations, preference regarding the data visualizations and the comprehensibility of the data represented by the visualization models.

H. Results

The data that was collected from the experiment was explored through summary statistics. The data showed that for tasks 1, 2 and 3 in the new prototype, the values for skewness and kurtosis were high. However for the remaining tasks, the skewness and kurtosis values remained low. This suggested that a paired t-test could be used. This was also selected because of its robustness.

The overall mean time in seconds for the new visualization is 36.04 seconds (SD, 48.06) and the overall mean time for the old visualization is 51.88 seconds (SD, 40.30). The t-test result is $t = -3.40$, $p < 0.019$. This indicates an overall significant amount of difference in terms of time.

Paired t-tests were conducted individually for Tasks 1-5.

Task 1, asked participants to identify an activity or activities, which were considered as important. The means for time taken are 7.11 (SD, 6.69) seconds for the new data visualization and for the old data visualization 29.31 (SD, 26.63) seconds. The t-test result is $t = -3.60$, $p < 0.001$. Therefore, the new data visualization prototype was

significantly faster than the old data visualization prototype in terms of time taken to complete the task.

Task 2, asked participants to identify activities, which were considered as duty. The means for time taken are, 7.35 (SD, 8.43) seconds to complete the task with the new data visualization and 20.48 (SD, 15.45) seconds for the old data visualization. The t-test result is $t = -3.39$, $p < 0.0006$. Therefore, the new data visualization prototype was significantly faster than the old data visualization prototype in terms of time taken to complete the task.

Task 3, asked participants to identify activities, which were considered as less energy consuming, or giving energy. The means for time taken are 8.97 (SD, 9.96) seconds to complete the task with the new data visualization and for the old data visualization 35.25 (SD, 25.95) seconds. The t-test result is $t = -4.91$, $p < 0.00006$. Therefore, the new data visualization prototype was significantly faster than the old data visualization prototype in terms of time taken to complete the task.

Task 4, asked participants to find out details of at least three activities. The means for time taken are, 27.59 (SD, 16.66) seconds to complete the task with the new data visualization and for the old data visualization 35.97 (SD, 21.73) seconds. The t-test result is $t = -1.24$, $p < 0.11$. Therefore there is no significant difference between the two visualizations in terms of task time.

Task 5, asked participants to interact using a screen reader. The means for time taken are 131.34 (SD, 58.85) seconds to complete the task with the new data visualization and for the old data visualization 129.44 (SD, 59.21) seconds. The t-test result is $t = 0.08$, $p < 0.46$.

Therefore there is no significant difference between the two visualizations in terms of task time. However, in the interviews the participants clarified that the new visualization was significantly better when used with screen readers than the old visualization. However, there were still serious issues with the new prototype because certain screen elements could not be selected and some of the sliders were difficult to operate.

Task 6 was specific to each data visualization prototype. These tasks were not considered as a part of the paired t-test because the data is statistically irrelevant since the two tasks are not similar to each other and measure different things. Task 6 for the new data visualization asked participants to change the color and size of the text, whereas Task 6 for the old data visualization asked participants to discover further information about each quadrant in the XY-axis plane. The participants were asked to think aloud when they were performing these tasks. The reactions thus obtained from the participants were used as suggestions for improvement.

All participants completed all the tasks under both conditions and so there were no incorrect option selection errors during the tasks.

The results from the “speak-aloud” process used in the experiment did not reveal any new information, which could provide help with the issues of improving universal design and

usability in the new visualization. The aim of the “speak-aloud” process was to see if this could provide the authors with more information regarding design issues of the user interface.

The results from observing the participants interacting with the prototypes using the impairment simulation gloves suggested that the gloves caused mobility problems when tapping the icons, which were small in size for both visualizations. The gloves also affected two-handed use of the applications, as some participants were accustomed to use a mobile device with both hands. Further, all participants used their index fingers to tap and scroll on the screen rather than using their thumbs, which may suggest difficulty in using the thumbs. Lastly it was also observed that the very action of grasping the smartphone was difficult when wearing the simulation gloves.

1) Results From the Semi-Structured Interview

A semi-structured interview was conducted at the end of every experiment for all 18 participants of the experiment. Each participant was asked a total of nine questions. This interview was conducted to get opinions and discover impressions of the participants concerning the two prototypes. For the first question, which asked the participants about their experiences using smartphones, all the participants answered that they were familiar with them and everyone had used such devices for more than 1 year, which was the mandatory minimum that was set in the recruitment survey. All the users used various features of smartphones and they were familiar with different mobile applications such as the organizer and games, etc. The main purpose of using smartphones for all the users in most cases was social media.

For the second question, which asked users about their preference between the two prototypes, all 18 of the participants suggested they would prefer the new visualization because it was easier and more convenient to use. They said it was more understandable and the visualized data was more legible.

For the third and fourth questions, which asked about the meaning of icons in each prototype, the opinions were almost similar for both prototypes. For the old prototype all 18 participants replied that none of them were able to understand the meanings of icons until they were explained. For the new prototype, the icons were not even perceived as important since the data was sorted according to their selection. Some participants never even realized that there were icons in the new visualization and they were familiar with icons such as the Settings Icon, icon used for voice input, text-size and language options.

The fifth question asked the participants about the customization settings available in the new prototype. Almost all the participants were satisfied with the base design of the prototype and they did not feel it necessary to change it. However, they tried changing the colors of the user interface elements for exploration purposes and discovered it to be very useful.

The sixth and seventh questions asked the participants about whether they were able to obtain details about desired

activities for each prototype. For both of these questions, the answers were almost the same and they found it almost equally easy for both prototypes to navigate for finding the details of activities, since all 18 participants were able to complete the tasks. However, for the new data visualization the interaction time was found to be faster and easier as well as requiring less touch gestures for interaction.

The eighth and the ninth questions asked about their experiences while using the two prototypes with screen readers. For the old prototype, the participants were not satisfied since the data visualization lacked complete screen reader compatibility and therefore little could be read by the screen reader. However, for the new prototype there was a mixed reaction. Some users found it easy to use and understand with the screen reader while some wanted it to have further improvements. None of the participants were completely satisfied with the screen reader compatibility of the new prototype, but all of them appreciated that it was much more screen reader friendly than the old prototype.

Finally participants were asked about the use of the simulation gloves and their effects. The basic response from all participants was that they felt the new visualization was better.

V. DISCUSSION

The issues raised at the beginning of this paper and in Section III and their solutions provided in Section III including the new prototype developed are discussed further in this section.

Although the new prototype has not addressed all the issues raised at the beginning of this paper, it has tried to accommodate as many of them as possible.

Furthermore, the experiment was designed to provide evidence to support the solutions provided in the new data visualization that are actually effective in real-time use. The first issue that was raised in this paper was related to Principle 2, Guideline 2a, which was addressed in the new data visualization by providing customization options to customize user interface elements according to the needs of the users. The evidence suggested through the results of the semi-structured interviews that the customization settings were very useful. The new visualization also supports the increasing in size of on-screen icons and the font. This would appear to be useful as it was observed during the experiment that small icons were difficult to select with the simulation gloves.

The second issue was related to Principle 3, Guideline 3a, which was addressed in the new data visualization by providing drop-down lists of categories, which could be selected, and the data would automatically be sorted according to the selection. The experiment showed that the users took very little time to complete tasks 1, 2 and 3 in the new data visualization in comparison to the old data visualization. This evidence along with the results from the interviews suggests that the new data visualization prototype was easier to use and understand.

For Principle 3, Guideline 3c, the new data visualization consisted of dual language support for English and Norwegian, which could be selected as needed by the user.

For Principle 4, Guideline 4d, the new data visualization provided multi-modal communication through screen-readers. Also as stated above the prototype was developed to be platform independent and so could run on Apple and Android devices without change. The experiment showed that the old prototype did not support screen-reader interaction. The new prototype supported screen-reader interactions for Android and Apple devices. However, the participants were not completely satisfied with the performance. Therefore, there is still room for improvement in this context.

Principle 5, Guideline 5a was addressed in the new prototype by the use of drop-down categories. The users were allowed to select one item from each drop-down menu and each selection filtered the data. From the experiment, it was shown that the time taken to complete tasks 1, 2, 3 and 4 for the new data visualization prototype was significantly less than the time taken to complete the same tasks for the old data visualization prototype. The evidence from the experiment was strengthened by the results from the semi-structured interviews.

Principle 6, Guideline 6c and 6d were addressed in the new prototype by arranging user interface elements in drop-down menus using categories. Customization options were placed in appropriate categories for changing text, background and other user interface elements. The evidence from the experiment shows that the time taken to complete tasks for the new data visualization was shorter than the time taken to complete the same tasks for the old data visualization. In the semi-structured interviews the participants also stated that due to the short time taken to complete the tasks for the new prototype they felt less fatigue in their hands and arms in comparison to the old prototype.

Therefore as this discussion suggests that overall the new visualization was indeed more usable and universally designed, the authors accept both positive hypotheses stated earlier. These essentially postulated that the new visualization would be better in terms of usability, universal design and user preference.

VI. CONCLUSION

The main goal of this research was to design and develop a data visualization prototype adhering to the standards of Universal Design. Through a literature review it was discovered that there is a lack of use of Universal Design principles in design and development of "mHealth" applications. There are several national and international laws, which are created to enforce and encourage the use of Universal Design standards to provide equality for all. However, there seems to be a lack of strong motivation for adherence and enforcement of these laws.

The goal of designing a new prototype was to make it accessible for people with rheumatoid arthritis who had

REFERENCES

problems related to dexterity and movement of hands and fingers. Therefore, the new prototype consisted of various customization options, which could be used to customize it according to the needs of the users. Special considerations were also made for screen-reader users and the prototype was designed to be compliant with screen-reader technologies. Experiments were conducted with the built-in screen reader technologies in Android and Apple mobile phones to extract further information regarding improving the screen reader experiences. The findings suggested that although the new prototype had better screen reader support, it still needs further improvements.

Previous literature, as well as different Universal Design guidelines suggest that multi-modal means of communication should be established. Therefore, in future, the new prototype can consist of features containing multi-modal input like speech input and a tactile keyboard. These features can be beneficial for our user group. Another issue is related to the use of icons. Although this issue is not within the scope of this research, there are some issues regarding the usage of abbreviations in the place of icons in the new visualization. The icons used in the old data visualization model were discovered to be difficult to understand by the users; therefore these icons were replaced with new abbreviations of categories. Although this approach was found to be more relatable to categories when the English language was used for the prototype, it had no meaning when used with the Norwegian language. This suggests that abbreviations are language dependent and it becomes difficult to use abbreviations when multiple languages are used for mobile applications. Therefore, more research is required to understand the use of suitable icons, which can be universal in nature and translate across different languages. Furthermore, the new prototype used sliders with RGB values and displaying above the sliders the resulting selected color. While this option gives users more color choice, it may not be the best option. Therefore more research is needed on this aspect, but one option could be to use a color palette in place of manipulating sliders.

This evaluation could have been improved by having a larger sample of users. Another issue was regarding the use of an impairment simulation using the Cambridge Simulation gloves. A similar future experiment could be improved by perhaps using actual participants with rheumatoid arthritis in the hands/fingers to a certain level. The experiment has shown that the new prototype seems promising to solve some issues related to usability and universal design and with some improvements as mentioned above; it can be useful for different user groups besides the target population. A future experiment could also be expanded to include participants with cognitive impairments to test if the prototype is simple enough to be used by them.

ACKNOWLEDGMENTS

The authors would like to thank Kristin Skeide Fuglerud and Trenton Schulz at the Norwegian Computing Centre for their input, ideas and conception of the original (old) visualization method.

- [1] Statista, <http://www.statista.com/statistics/276623/number-of-apps-available-in-leading-app-stores/> Accessed August 2016, 2016.
- [2] Statista, <http://www.statista.com/statistics/274774/forecast-of-mobile-phone-users-worldwide/> Accessed September 2016, 2016.
- [3] eMarketer, Smartphone Users Worldwide Will Total 1.75 Billion in 2014. from <http://www.emarketer.com/Article/Smartphone-Users-Worldwide-Will-Total-175-Billion-2014/1010536>, . 2014.
- [4] A. Lorenz and R. Oppermann, "Mobile health monitoring for the elderly: Designing for diversity", *Pervasive and Mobile Computing*, 5(5), 2009, pp.478-495.
- [5] E. Jovanov, "Wireless technology and system integration in body area networks for m-health applications", Paper presented at the Engineering in Medicine and Biology Society, IEEE-EMBS 2005, 2005 [27th Annual International Conference of the IEEE Engineering in Medicine and Biology Society, Shanghai, China, 2006].
- [6] World Health Organization, "World report on disability 2011", http://www.who.int/disabilities/world_report/2011/report.pdf, Accessed September 2016, 2011.
- [7] D. Symmons, C. Mathers, and B. Pflieger, "The global burden of rheumatoid arthritis in the year 2000", Geneva: World Health Organization, 2003.
- [8] R. D. Jacobson, "Representing spatial information through multimodal interfaces. Paper presented at the Information Visualisation, 2002. Proceedings", Sixth International Conference on IEEE, 2002, pp.730-734.
- [9] L. Chittaro, "Visualizing information on mobile devices", *Computer*, 39(3), 2006, pp.40-45.
- [10] S. K. Kane, C. Jayant, J. O. Wobbrock, and R. E. Ladner, "Freedom to roam: a study of mobile device adoption and accessibility for people with visual and motor disabilities", Paper presented at the Proceedings of the 11th international ACM SIGACCESS conference on Computers and accessibility, 2009.
- [11] My Pain Diary, <http://chronicpainapp.com/>, Accessed October 2016, 2016.
- [12] Track and React, <http://www.arthritis.org/living-with-arthritis/tools-resources/track-and-react/>, Accessed October 2016, 2016.
- [13] Learn Arthritis Prevention, <http://www2.selectsoft.com/>, Accessed October 2016, 2016.
- [14] MyRA, <https://trackmyra.com/>, Accessed October 2016, 2016.
- [15] RheumaTrack, <http://www.rheumatrack.com/>, Accessed October 2016, 2016.
- [16] Rheumatoid Arthritis, <http://atpointofcare.com/>, Accessed October 2016, 2016.
- [17] R. Kazi and R. Deters, "A dissemination-based mobile web application framework for juvenile idiopathic arthritis patients", Paper presented at the Proceedings of the 2013 IEEE/ACM International Conference on Advances in Social Networks Analysis and Mining, 2013.
- [18] T.-V. How, J. Chee, E. Wan, and A. Mihailidis, "Mywalk: a mobile app for gait asymmetry rehabilitation in the community", Paper presented at the Proceedings of the 7th International Conference on Pervasive Computing Technologies for Healthcare, 2013.
- [19] J. Heer, N. Kong and M. Agrawala, "Sizing the horizon: the effects of chart size and layering on the graphical perception of time series visualizations", Paper presented at the Proceedings of the SIGCHI Conference on Human Factors in Computing Systems, 2009.
- [20] D. Pereira, A. Moreira and R. Simões, "Challenges on real-time monitoring of patients through the Internet", Paper presented at the Information Systems and Technologies (CISTD), 2010 5th Iberian Conference on Information Systems and Technologies IEEE, 2010, pp.1-5.
- [21] A. Rind, T. D. Wang, W. Aigner, S. Miksch, K. Wongsuphasawat, C. Plaisant and B. Shneiderman, "Interactive information visualization to explore and query electronic health records", *Foundations and Trends in Human-Computer Interaction*, 5(3), 2011, pp.207-298.
- [22] M. Scotch and B. Parmanto, "SOVAT: Spatial OLAP visualization and analysis tool", Paper presented at the System Sciences, 2005. HICSS'05.

- Proceedings of the 38th Annual Hawaii International Conference on System Sciences IEEE, 2005, pp.142b-142b.
- [23] C. C. Freifeld, K. D. Mandl, B. Y. Reis, and J. S. "Brownstein. HealthMap: global infectious disease monitoring through automated classification and visualization of Internet media reports", Journal of the American Medical Informatics Association, 15(2), 2008, pp.150-157.
- [24] Å. Revenäs, C. H. Opava, C. Martin, I. Demmelmaier, C. Keller, and P. Åsenlöf, "Development of a web-based and mobile app to support physical activity in individuals with rheumatoid arthritis: results from the second step of a co-design process", JMIR research protocols, 4(1), e22, 2015.
- [25] Å. Revenäs, C. H. Opava, H. Ahlén, M. Brusewitz, S. Pettersson, and P. Åsenlöf, "Mobile internet service for self-management of physical activity in people with rheumatoid arthritis: evaluation of a test version", RMD open, 2(1), e000214, 2016.
- [26] Å. Revenäs, C. H. Opava, and P. Åsenlöf, "Lead users' ideas on core features to support physical activity in rheumatoid arthritis: a first step in the development of an internet service using participatory design", BMC medical informatics and decision making, 14(1), 1, 2014.
- [27] M. F. Story, J. L. Mueller, and R. L. Mace, "The universal design file: Designing for people of all ages and abilities", 1998.
- [28] M. F. Story, "Maximizing usability: the principles of universal design", Assistive technology, 10(1), 4-12, 1998.
- [29] E. K. Meyer, "Designing infographics", Hayden Books, 1997.
- [30] S. Few, "Show me the numbers: "Designing tables and graphs to enlighten (Vol. 1)", Analytics Press Oakland, CA, 2004.
- [31] S. Few, "Eenie, meenie, minie, Moe: selecting the right graph for your message", https://www.perceptualedge.com/articles/ie/the_right_graph.pdf, Accessed October 2016, September 8, 2004.
- [32] American College of Rheumatology, Rheumatoid Arthritis, <http://www.rheumatology.org/I-Am-A/Patient-Caregiver/Diseases-Conditions/Rheumatoid-Arthritis>, Accessed September 2016, 2016.
- [33] University of Cambridge, Inclusive Design Toolkit, Retrieved April 22, 2016, from <http://www.inclusivedesigntoolkit.com/betterdesign2/gloves/gloves.html#p20>, Accessed September 2016, 2015.

Towards Development of Real-Time Handwritten Urdu Character to Speech Conversion System for Visually Impaired

Tajwar Sultana

Biomedical Engineering Department
NED University of Engineering &
Technology
Karachi,
Pakistan

Abdul Rehman Abbasi

Design Engineering & Applied Research
Laboratory
KINPOE (affiliated with PIEAS)
Karachi,
Pakistan

Bilal Ahmed Usmani, Sadeem
Khan, Wajeeha Ahmed, Naima
Qaseem, Sidra

Biomedical Engineering Department
NED University of Engineering &
Technology
Karachi, Pakistan

Abstract—Text to Speech (TTS) Conversion Systems have been an area of research for decades and have been developed for both handwritten and typed text in various languages. Existing research shows that it has been a challenging task to deal with Urdu language due to the complexity of Urdu ‘Nastaliq’ (rich variety in writing styles), therefore, to the best of our knowledge, not much work has been carried out in this area. Keeping in view the importance of Urdu language and the lack of development in this domain, our research focuses on ‘handwritten’ Urdu TTS system. The idea is to first recognize a handwritten Urdu character and then convert it into an audible human speech. Since handwriting styles of different people vary greatly from each other, a machine learning technique for the recognition part is used i.e., Artificial Neural Networks (ANN). Correctly recognized characters, then, undergo processing which converts them into human speech. Using this methodology, a working prototype has been successfully implemented in MATLAB that gives an overall accuracy of 91.4%. Our design serves as a platform for further research and future enhancements for word and sentence processing, especially for visually impaired people.

Keywords—Artificial Neural Network; Classification; OCR; Text To Speech; Urdu Handwritten Character

I. INTRODUCTION

Urdu is the national language of Pakistan and there are more than 100 million Urdu speakers worldwide¹. Urdu is predominantly the combination of two languages i.e. Arabic and Persian which contains variety of features, properties, scripts and writing styles that makes it more difficult for common algorithms to work on it [1].

A TTS System is an application used to read text aloud. TTS systems take text (handwritten or typed) as an input and produce audible speech as an output. They have a wide range of application in different areas like games and education, vocal monitoring, voice enabled email and very useful for visually impaired, etc.

A TTS system is composed of two parts: Optical Character Recognition (OCR) and Speech Synthesis.

OCR is a process of converting an image into machine code. It may be classified into two categories namely online

and offline [2]. In online character recognition, the recognition process requires real time data from user and in case of offline character recognition existing (stored) data is used. The complex task of performing accurate recognition is based on the nature of the text to be read and on its quality [3]. The process of OCR comprises of a series of steps that are essential for the preprocessing of input image. Usually, these steps include: Binarization, Segmentation, Feature Extraction and Classification.

The process of speech synthesis creates speech artificially on the basis of the input text. The aim of speech synthesis is to acquire speech that is easily understandable.

In this reported work, we have constructed a mechanism to develop an efficient TTS system. The paper advances with the review of the literature. Then, the proposed methodology is presented that highlights different phases of TTS construction. The major parts of algorithm are image acquisition, preprocessing, classification, speech synthesis and GUI development. The manuscript ends with the discussion of the important results with possible extension of the work.

II. LITERATURE REVIEW

TTS Systems have been an area of research for decades. The complete TTS system was first developed for English language by Noriko Umeda [4]. An overview of the early attempts to develop TTS systems is done by Klatt [5] that gives an extensive database of the methodologies employed to develop these systems.

In fact, the OCR systems should be efficient enough to read handwritten or typed text in different languages such as English, Sindhi, Persian and Arabic etc. M. Farhad et al. [6] proposed a novel methodology for OCR of English alphabets using ANN as the classification algorithm with curvature features of characters as input to the network. They used different seeking angles for the recognition of characters considering the predetermined features of them. This technique yields ~90% accuracy for different character seeking angles but it was computationally expensive as feature extraction proves to be time consuming.

Amit Choudhary et al. [7] presented an extensive work on offline handwritten English character recognition using multilayer feed forward neural network reporting an accuracy of 85.62%. Ganai et al. [8] focused on improving the speech quality of existing system by combining the methods of Hidden Markov Model (HMM)-based speech synthesis and waveform-based speech synthesis to develop human like speech. Despite of the different techniques used for character recognition and speech synthesis, the overall performance of TTS systems developed by both authors led to lesser accurate results and reduced overall performance. Moreover, both TTS systems were developed for English language whose alphabets are easier to detect.

Sarmad Hussain [9] presented his work on Urdu text to speech system. The work emphasized on the use of Urdu phonological processes and divided it into three stages. In the first stage, text was converted into its respective phonemes. In second stage, these phonemes were converted into numerical parameters known as text parameterization and at final stage; speech was synthesized through these parameters. However, this work was based on typed Urdu words.

Kashif Shabeeb and D.S Singh [10] developed a GUI for handwritten Urdu Text to Speech Converter. It was based on the recognition of isolated typed Urdu characters using Artificial Neural Networks (ANN). However, the accuracy of OCR was not mentioned and it did not provide facility for online handwritten Urdu character recognition.

III. PROPOSED METHODOLOGY

Unlike [9] & [10], our methodology is based on recognizing 'online handwritten' Urdu text. The framework of the proposed methodology is illustrated in Fig 1 and the details of each step are provided here:

A. Image Acquisition

Handwritten Urdu characters are input to the system in the form of images which are captured with the help of a webcam or smart phone as shown in Fig 2. The acquired images may be utilized to function in two modes i.e. offline mode and online mode.

In offline mode, the system uses images which are already stored in dataset whereas in online mode a webcam is used to capture images in real time. The images acquired are then preprocessed for further analysis.

B. Preprocessing

The steps involved in preprocessing of an input image are binarization, boundary detection, thinning, feature extraction and padding as shown in Fig 1.

1) Binarization

In the first step, the acquired colored image is converted into grayscale. In order to change any color to its gray level, it is necessary to obtain the value of its primary colors (Red, Green, and Blue). Then, by adding 30% of red, 59% of green and 11% of blue of each value together, we may get our desired grayscale value. Once the image is converted to grayscale, it is then binarized by assigning the value '0' to the

weaker intensity of gray showing black and '1' to the stronger intensity of gray showing white.

In fact, a single threshold value is determined using Otsu's method [11] above which a pixel value is considered as '1' and below it as '0'. This is a global binarization technique which is very simple and efficient for separating background and foreground pixels with high accuracy in minimum time. Sample result is shown in Fig 3.

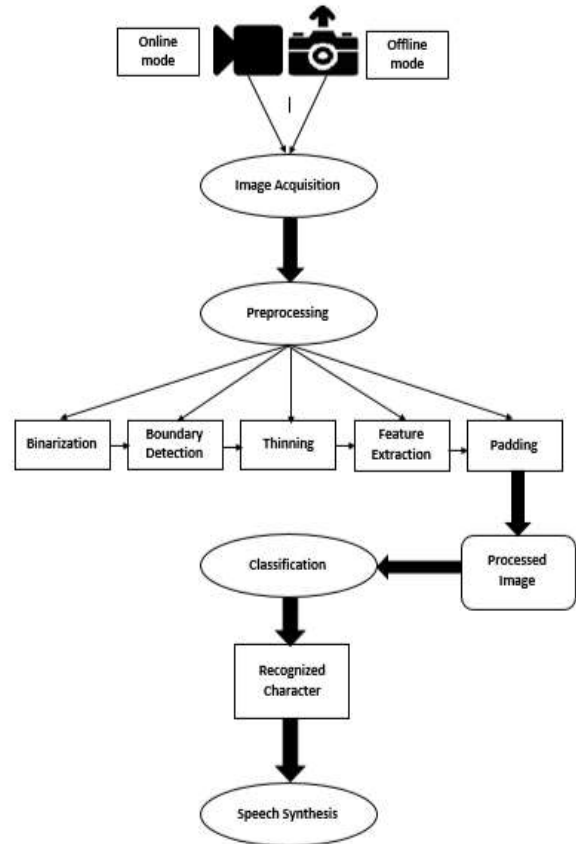


Fig. 1. Methodology of Proposed Framework



Fig. 2. Image Acquisition

2) Boundary Detection

In order to detect the character in an image, it is essential to detect its boundary. By locating regions having abrupt dark-light transfigurations and suppressing regions with homogenous intensity, the boundaries of the characters present in the image can be found. This also provides information about the number of connected elements in an image.



Fig. 3. Input image (left), Binarized image (right)

3) Thinning

When applied to binary images, image thinning is used to remove selected foreground pixels that may be presented as noise. The end result of this is another binary image that has these undesired pixels removed. The process of median filtering, which is a non-linear method is applied to perform thinning.

4) Feature Extraction

Features are distinctive characteristics present in the image of a character such as dots, strokes, edges, etc. These are extracted and cropped so that the task of classifying characters becomes less rigorous as shown in Fig 4.

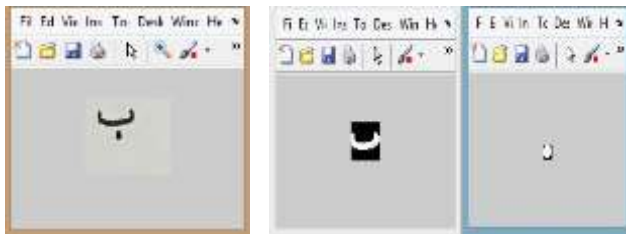


Fig. 4. The 'nuqta' of character 'baay' is extracted here

5) Padding

To reduce computational complexity, the processed images are resized and padded so that the dimensions of each image are the same before processing to the classifier as shown in Fig 5.

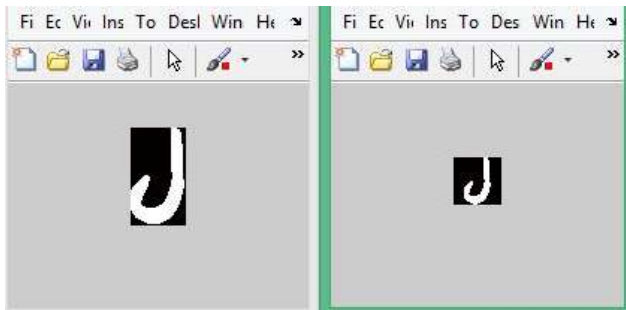


Fig. 5. Cropped image (left), Padded image (right)

C. Classification

In this work, an efficient technique of Artificial Intelligence is utilized for the purpose of classification that is Artificial Neural Network (ANN). ANN is a computational tool that replicates the structure and function of biological nervous system. This model can be changed and adapted according to the information that is passed through the network for processing. It consists of three layers: input layer, hidden layer and output layer. These layers comprise of a number of interconnected neurons and weights. All these parameters are set according to the requirement through trial and error method. ANN are very useful for finding patterns in data [12].

1) Designing the Neural Network

In this study, the neural network that is used has specific parameters as tabulated in Table 1. Here validation shows network generalization.

TABLE I. PARAMETERS OF NEURAL NETWORK

Network Specification	
Type	Feed forward neural network
Learning method	Back propagation
Number of layers	3
Number of hidden layers	1
Number of nodes in hidden layer	16
Activation function used	Gradient descent
Training set volume	70%
Validation set volume	15%
Testing set volume	15%
Input, Output nodes	1024,24

2) Sample Preparation and Training

For the purpose of training the neural network, all the characters are first divided into distinct classes. Characters that have similar primary structure like 'baay', 'paay', 'taay' are placed in a single class and 24 such classes are created on the basis of primary structural discrimination as shown in Table 2. Similarly, based on the number of connected elements, characters are further classified within a class. For example, if the character 'taay' is taken as an input, the primary structure of 'taay' is first classified into the second class as shown in Table 2 and then based on the number of connected elements, which are three in this case, it is recognized as 'taay'. In this way all the characters are recognized into their respective classes. Further classification of individual characters is based on the number of connected elements in each character. Network was trained on 60 samples where each sample represents a matrix of 1024×24 .

A target matrix of 24×24 is also set which represents '1' diagonally at the index of each class with rest of the indices being 0. Network is then trained and ready for implementation as shown in Fig 7.

TABLE II. 24 CLASSES OF URDU ALPHABETS

Class No	Characters/Groups
1	ا
2	ب پ ت ٹ
3	ج
4	چ
5	ح خ
6	د ڈ ذ
7	ر ژ ز
8	س ش
9	ص ض
10	ط
11	ظ
12	ع غ
13	ف
14	ق
15	ک
16	گ
17	ل
18	م
19	ن
20	و
21	ہ
22	ء
23	ی
24	ے

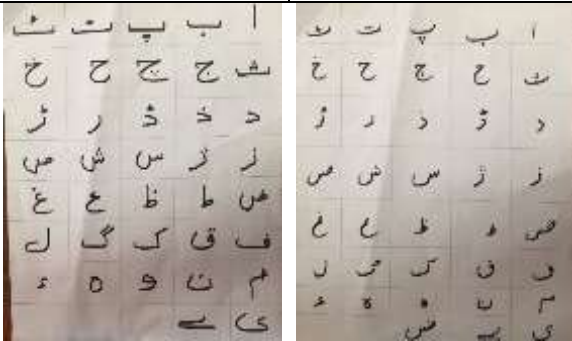


Fig. 6. Sample handwritten Urdu Text

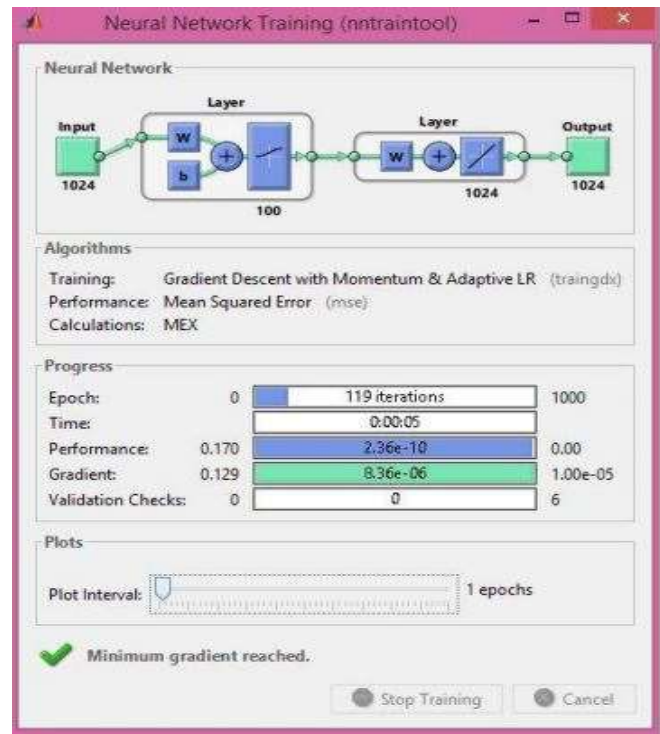


Fig. 7. Neural Network training

3) Results of OCR

To test the system, a novel input is given to the network. This novel input is an image of a character. If the character is correctly recognized, an output matrix of 24x1 is displayed which shows '1' at the place of that character's index and 0 at the rest of the indices as shown in Fig 8. After 1000 epochs (iterations), an overall accuracy was computed as 91.4%. The 37 characters are classified into 24 distinct classes and there is no major misclassification of characters as shown in Fig 9. An enlarged view of the confusion matrix showing classification of two character classes i.e. 23 and 24 is shown in Fig 10.

D. Speech Synthesis

Speech synthesis is the final step of the proposed methodology which is achieved using MATLAB to acquire human like speech. For this purpose, Digital Signal Processing (DSP) toolbox is used to manually record prosodies of each character which are then stored in a format of .wav file. A database is created which contains the recorded sounds of all characters. Once the character is recognized, stored sound is retrieved by the system through program for audible output. The speech synthesis system works effectively.

E. Graphical User Interface (GUI) Development

For the purpose of testing, a Graphical User Interface (GUI) is also developed which displays the following features:

- Input image: Shows the uploaded character image.
- Output character image: Shows the image of character recognized by the system.
- Output character text: Shows the character text, recognized by the system.
- Output speech: Shows the speech generation of recognized character.

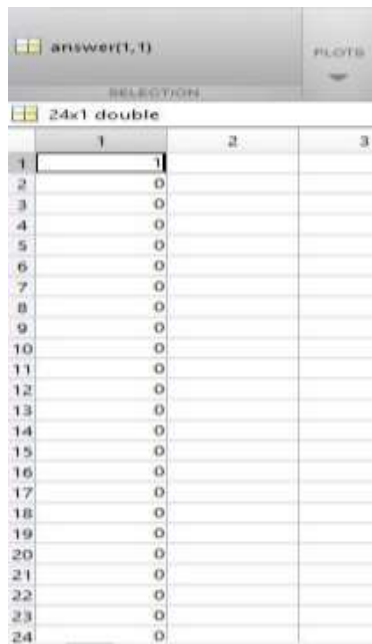


Fig. 8. Output matrix of character ‘alif’ displaying 1at first index and 0 at other indices

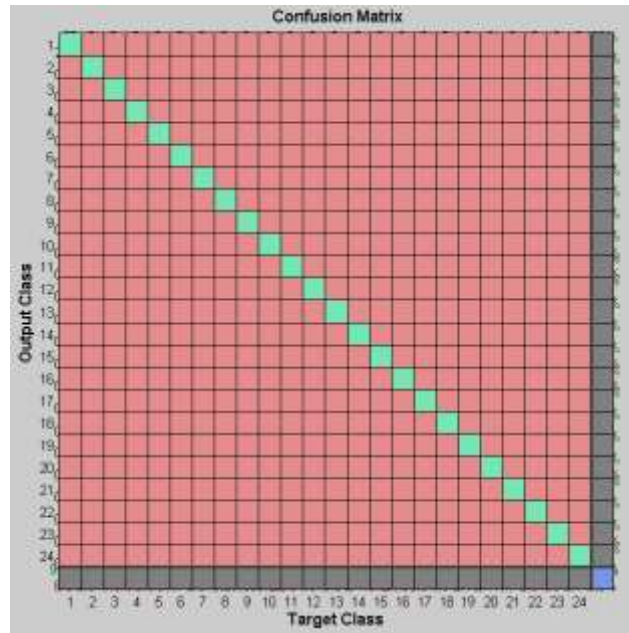


Fig. 9. Confusion Plot

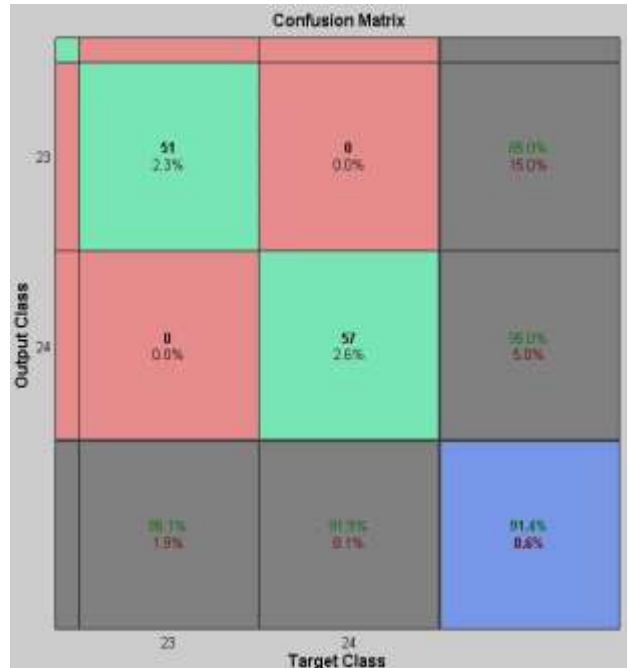


Fig. 10. Enlarged view of confusion plot

IV. CONCLUSION AND DISCUSSION

The system proposed here has two parts; handwritten Urdu character recognition and speech conversion. The Urdu alphabets were initially divided into twenty four classes grouping similar characters. After that, sixty samples of different handwritings were collected and presented to the classifier for training the network. Once the training is completed, novel samples were used for testing and validation. For every input character, a matrix of 24×1 is displayed as an output. Results show 91.4% accuracy for 60 sample data set thus ending the recognition process. The recognized character is then passed through MATLAB's digital signal processing toolbox which converts it into its corresponding human speech recorded earlier.

TABLE III. COMPARISON OF DIFFERENT OCR TECHNIQUES

Paper	Language	Online/Offline	OCR (%-accuracy)
[7]	English	Offline	85.62
[13]	Latin & Bengali	Offline	98.3
[14]	Urdu	Offline	94.97

The proposed approach accomplishes the aim of recognizing Urdu characters in real time and its conversion into human speech. This system has an advantage over other systems as it serves as a basic architecture for handwritten Urdu characters captured in real time. In Table 3, TTS systems developed for different languages are compared and their character recognition accuracies are highlighted. In comparison, the overall OCR accuracy for the proposed methodology is 91%. In addition, the TTS developed here uses simple algorithms, has online recognition feature and a dedicated GUI for easy implementation. Most of the literature available doesn't incorporate online character recognition. Moreover, although a dedicated GUI for TTS is included in many studies [1, 10], the GUI proposed here is very easy to use. On the basis on these advantages, this system can be extended to use for people with limited vision or are illiterate and unable to read important text messages and instructions.

Like other TTS systems, the reliability and efficiency of this system can be affected due to certain environment constraints (such as light intensity and direction) while taking real time data as input. It is observed that poor visibility acts as a barrier for correct OCR process. The accuracy of OCR and classification can further be enhanced by including other features like estimating the curve angles of characters [6]. We anticipate that although this approach produces better results, improved algorithms will be needed to improve the computational time.

The database used for training classifier only consists of handwriting styles of the people aged between 18 and 24 years. The above system can be improved by presenting the handwritten samples of children and senior citizens to the classifier. The network trained on the basis of the handwriting of these age groups covers a wide range of handwritten text and improves the OCR process. In addition, this modification is beneficial so that the TTS system can be used for the senior citizens having poor muscle control due to disease or illness.

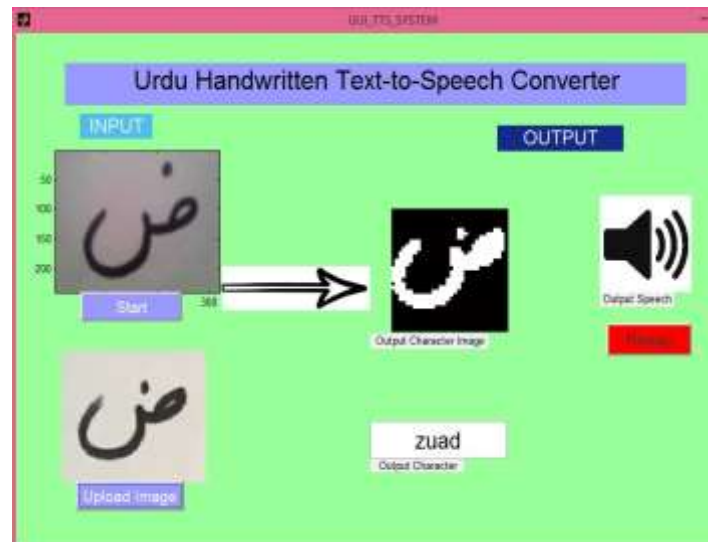


Fig. 11. Graphical User Interface showing character to speech Conversion of Urdu Character 'Zuad'

In addition to the technique proposed above, we have also attempted template matching rather than ANN but it did not produce good results. This was mainly because of the obvious differences in typed character's topology with the handwritten character's shape.

This research project can be further extended for complete Urdu words and complete sentences for a fully functional TTS system that may serve the visually impaired people. The system may also be extended as platform independent to any particular software such as MATLAB, etc.

REFERENCES

- [1] S. A. S. S.-u. Haque and M. K. Pathan, "A finite state model for urdu nastaliq optical character recognition," IJCSNS, vol. 9, p. 116, 2009.
- [2] S. Sardar and A. Wahab, "Optical character recognition system for Urdu," in Information and Emerging Technologies (ICIET), 2010 International Conference on, 2010, pp. 1-5.
- [3] S. G. Dedgaonkar, et al., "Survey of methods for character recognition," International Journal of Engineering and Innovative Technology (IJEIT) Volume, vol. 1, pp. 180-189, 2012.
- [4] N. Umeda, et al., "Synthesis of fairy tales using an analog vocal tract," in Proceedings of 6th International Congress on Acoustics, 1968, pp. B159-162.
- [5] D. H. Klatt, "Review of text-to-speech conversion for English," The Journal of the Acoustical Society of America, vol. 82, pp. 737-793, 1987.
- [6] M. Farhad, et al., "An efficient Optical Character Recognition algorithm using artificial neural network by curvature properties of characters," in Informatics, Electronics & Vision (ICIEV), 2014 International Conference on, 2014, pp. 1-5.
- [7] Choudhary, et al., "Off-line handwritten character recognition using features extracted from binarization technique," AASRI Procedia, vol. 4, pp. 306-312, 2013.
- [8] M. B. Ganai and E. J. Arora, "Text-to-Speech Conversion," 2016.
- [9] S. Hussain, "Phonological Processing for Urdu Text to Speech System," Yadava, Y, Bhattarai, G, Lohani, RR, Prasain, B and Parajuli, K (eds.) Contemporary issues in Nepalese linguistics, 2005.
- [10] D. S. S. Kashif Shabeeb, "Urdu Text to Speech Converter: Database Creation and GUI Development," International Journal of Computer Science And Technology, vol. Vol. 6, pp. 191 - 193, 2015.
- [11] N. Otsu, "A threshold selection method from gray-level histograms," Automatica, vol. 11, pp. 23-27, 1975.

- [12] S. Barve, "Artificial Neural Network Based on Optical Character Recognition," in *International Journal of Engineering Research and Technology*, 2012.
- [13] S. Pal, et al., "Line-wise text identification in comic books: A support vector machine-based approach," in *2016 International Joint Conference on Neural Networks (IJCNN)*, 2016, pp. 3995-4000.
- [14] S. Naz, et al., "Urdu Nasta'liq text recognition system based on multi-dimensional recurrent neural network and statistical features," *Neural Computing and Applications*, pp. 1-13, 2015.

Scheduling of Distributed Algorithms for Low Power Embedded Systems

Stanislaw Deniziak
Department of Information Systems
Kielce University of Technology
Kielce, Poland

Albert Dzitkowski
Department of Information Systems
Kielce University of Technology
Kielce, Poland

Abstract—Recently, the advent of embedded multicore processors has created interesting technologies for power management. Systems consisting of low-power and high-efficient cores create new possibilities for the optimization of power consumption. However, new design methods, dedicated to these technologies should be developed. In this paper we present a method of static task scheduling for low-power real-time embedded systems. We assume that the system is specified as a distributed algorithm, then it is implemented using multi-core embedded processor with low-power processing capabilities. We propose a new scheduling method to create the optimal or suboptimal schedule. The goal of optimization is to minimize the power consumption while all time constraints will be satisfied or the quality of service will be as high as possible. We present experimental results, obtained for sample systems, showing advantages of our method.

Keywords—Embedded system; distributed algorithm; task scheduling; big.LITTLE; low power system

I. INTRODUCTION

Embedded systems are dedicated computer-based systems that are highly optimized for a given application. Besides the cost and performance, power consumption is one of the most important issue considered in the optimization of embedded systems. Design of energy-efficient embedded systems is important especially for battery-operated devices. Although the minimization of power consumption is always important, because it reduces the cost of running and cooling the system. It was observed that power demands are increasing rapidly, yet battery capacity cannot keep up [1].

Embedded systems are usually real-time systems, i.e. for some tasks time constraints are defined. Therefore, power optimization should take into consideration that all time requirements should be met. In general, higher performance requires more power, hence, the optimization of embedded system should consider the trade-off between power, performance and cost. Performance of the system may be increased by applying a distributed architecture. The function of the system is specified as a set of tasks, then during the co-design process, the optimal architecture is searched [2]. Distributed architecture may consist of different processors, dedicated hardware modules, memories, buses and other components. Recently, the advent of embedded multicore processors has created an interesting alternative to dedicated architectures. First, the co-design process may be reduced to

task scheduling for multiprocessors systems. Second, advanced technologies for power management, like DVFS (Dynamic Voltage and Frequency Scaling) or ARM big.LITTLE [3], create new possibilities for designing of low-power embedded systems.

Although there are a lot of synthesis methods for low-power embedded systems [4], the problem of optimal mapping of a distributed specification onto the multicore processor is rather a variant of the resource constrained project scheduling (RCPSP) [5] one, than the co-synthesis. Since the RCPSP is NP-complete, only heuristic approach may be applied to real-life systems. According to the best of our knowledge there is no synthesis methods taking into consideration ARM big.LITTLE architecture as a target platform for real-time embedded systems. Only, some work considering run-time scheduling were done [6].

The most of RCPSP approaches are dedicated to the task graph specification of a system. But in many cases, especially in case of embedded software, more general distributed models [7] would be more convenient. It was occurred that the function of a real-time distributed system may be efficiently specified as a distributed echo algorithm [8]. Moreover, such specification may also be statically scheduled [9].

In this paper we present the novel method for synthesis of the power-aware scheduler for real-time embedded systems. We assume that the function of the system is specified as a distributed echo algorithm [10] that should be executed by the multicore processor supporting the ARM big.LITTLE technology. The goal of the static scheduling is the reduction of power consumption by moving some tasks to low-power cores (LPCs), while critical tasks are assigned to high-performance cores (HPCs), to satisfy all time constraints. The proposed method is dedicated to high performance embedded computing systems.

II. RELATED WORK

The problem of design of low-power embedded systems has attracted researchers for many years. One direction of these research is finding the low-power architecture by optimizing the allocation of resources and task assignment according to the power consumption (e.g. COSYN-LP [11], SLOPES [12], LOPOCOS [13]). The overview of some power aware codesign methods is presented in [4]. But all above methods create the dedicated hardware/software architecture and cannot

be applied to multicore processors.

Another direction of research concerning the design for low-power is to develop methodologies that takes into consideration dynamic reduction of the power consumption during runtime. AVR (Average Rate heuristic) [14] is a task scheduling method for variable speed processor. Dynamic Power Management [15] tries to assign optimal power saving states. Other methods reduces power consumption by efficiently using voltage scale processors [16]. All above methods are based on power-aware scheduling called YDS. Above methods schedules dynamically a set of tasks by selecting the proper speed for each task. ARM big.LITTLE uses only 2 predefined speeds, thus it is rather not possible to adopt above methods to this technology.

There are a lot of scheduling methods for real-time embedded systems. Earliest Deadline First (EDF) [17] or Least Laxity First (LLF) [18] is ones of the most efficient dynamic scheduling methods. But above methods are dedicated to homogeneous architectures (SMP). Discussion concerning the problems of task scheduling in real-time systems is presented in [19]. Most of them optimize schedule length.

Embedded software consists of the given set of tasks. Usually it is possible to estimate the task parameters like execution time, power consumption, memory requirements. Most static scheduling methods are based on specification represented as task graph [20]. But in many cases it is difficult to specify function as a task graph, some other models e.g. distributed algorithms [7] are more suitable. It seems that the echo algorithm [10] would be attractive for this purpose.

According to our best knowledge there is no scheduling method for real-time systems specified as distributed echo algorithm, as well as the static scheduling method optimizing energy consumption in embedded systems based on the big.LITTLE platform.

III. PRELIMINARIES

We assume that the target embedded system is based on multi-core processor with LPCs and HPCs. LPC requires less power to execute tasks but execution times are longer. HPC executes tasks faster but consumes more energy. We consider soft real-time systems, i.e. all tasks should be executed before the specified deadline. But it is acceptable to slightly exceed the deadline. In this case the quality of service (QoS) decreases with increasing delay. The goal of optimization is to find schedule for which the power consumption is minimal while time constraints are satisfied or QoS is maximal. Since we consider shared memory architecture, transmissions between tasks may be neglected

A. Echo algorithms

Echo algorithms [18] are a class of wave algorithms [7] used for describing distributed computations. The system is specified as a set of tasks communicating by message passing. One task is an initiator, which starts all computations. After finishing its execution the initiator sends explorer messages to all neighbours. After receiving the first explorer message the task stores source node as an activator and after execution sends explorer message to all neighbour nodes except the

activator. After finishing execution of all tasks, all tasks which were not activators execute again to compute echo message which is sent to their activators only. Each task, after receiving echo messages from all activated task, executes again and sends echo message to its activator. Finally, the initiator should receive all echo messages and then it computes the final result.

Fig. 1 presents sample echo algorithm consisting of 10 processes. Assume that task 0 is the initiator. Therefore this task will be executed first. Then, tasks 1, 5 and 4 should be executed. It should be noted that the order of activation of tasks depends on times of execution of the following tasks, e.g. task 6 may be activated by task 5 but also it may be activated by task 7, in case when tasks 1, 2, 3, and 7 will finish their execution before finishing task 5. Thus, the scheduling on heterogeneous processors is complex even when the execution times of all tasks are known e.g. are estimated or when the worst case execution times are assumed.

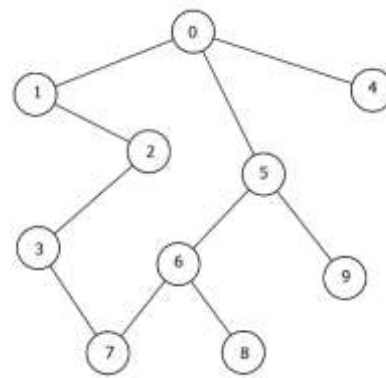


Fig. 1. Sample distributed algorithm

B. Functional Specification of Distributed Systems

We assume that the system is specified as a collection of sequential processes coordinating their activities by sending messages. Specification is represented by a graph $G = \{V, E\}$, where V is a set of nodes corresponding to the processes and E is a set of edges. Edges exist only between nodes corresponding to communicating processes. Tasks are activated when required set of events will appear. As a result, the task may generate other events. External input events will be called requests (Q), external output events are responses (O) and internal events correspond to messages (M). The function of the system is specified as finite sequences of activation of processes. There is a finite set of all possible events $\Lambda = Q \cup O \cup M = \{\lambda_i; i = 1, \dots, r\}$. System activity is defined as the following function:

$$\Phi: V \times C \rightarrow \Omega \times \Pi \times 2^A \quad (1)$$

where C is an event expression (logical expression consisting of logical operators and Boolean variables representing events), $\Omega = [\omega_L, \omega_H]$ are workloads of the activated process defined for LPC and HPC respectively, and $\Pi = [\pi_L, \pi_H]$ defines power consumption.

Using function Φ it is possible to specify various classes of distributed algorithms. The algorithm from Fig.1 may be

described using 20 actions. Assume that estimation of task workloads and energy consumption are given (Tab. I). Thus, actions will be the following:

- $A_0: \Phi(v_0, \{q_0\}) \rightarrow ([3, 2], [9, 20], \{m1_1, m2_5, m3_4\})$
 $A_1: \Phi(v_1, \{m1_1\}) \rightarrow ([13, 8], [34, 81], \{x_1, m4_2\}) /$
 $\Phi(v_1, \{m10_1\}) \rightarrow ([13, 8], [34, 81], \{x_2, m5_0\})$
 $A_2: \Phi(v_5, \{m2_5\}) \rightarrow ([6, 4], [16, 40], \{x_3, m6_6, m7_9\}) /$
 $\Phi(v_5, \{m15_5\}) \rightarrow ([6, 4], [16, 40], \{x_4, m8_0, m7_9\})$
 $A_3: \Phi(v_2, \{m4_2\}) \rightarrow ([10, 5], [26, 52], \{x_5, m9_3\}) /$
 $\Phi(v_2, \{m12_2\}) \rightarrow ([10, 5], [26, 52], \{x_6, m10_1\})$
 $A_4: \Phi(v_3, \{m9_3\}) \rightarrow ([7, 4], [18, 40], \{x_7, m11_7\}) /$
 $\Phi(v_3, \{m17_3\}) \rightarrow ([7, 4], [18, 40], \{x_8, m12_2\})$
 $A_5: \Phi(v_6, \{m6_6\}) \rightarrow ([5, 3], [13, 29], \{x_9, m13_7, m14_8\}) /$
 $\Phi(v_6, \{m16_6\}) \rightarrow ([5, 3], [13, 29], \{x_{10}, m15_5, m14_8\})$
 $A_6: \Phi(v_7, \{m11_7\}) \rightarrow ([9, 5], [23, 50], \{x_{11}, m16_6\}) /$
 $\Phi(v_7, \{m13_7\}) \rightarrow ([9, 5], [23, 50], \{x_{12}, m17_3\})$
 $A_7: \Phi(v_4, \{m3_4\}) \rightarrow ([11, 6], [28, 58], \{x_{13}\})$
 $A_8: \Phi(v_9, \{m7_9\}) \rightarrow ([12, 7], [30, 67], \{x_{14}\})$
 $A_9: \Phi(v_8, \{m14_8\}) \rightarrow ([4, 2], [11, 22], \{x_{15}\})$
 $A_{10}: \Phi(v_0, (\{m5_0/m18_0\} \& \{m8_0/m19_0\} \& \{m20_0\})) \rightarrow ([9, 5], [23, 52],$
 $\{r_1\})$
 $A_{11}: \Phi(v_1, \{x_1 \& m21_1\}) \rightarrow ([17, 9], [42, 93], \{m18_0\}) /$
 $\Phi(v_1, \{x_2 \& m1_1\}) \rightarrow ([17, 9], [42, 93], \{m22_2\})$
 $A_{12}: \Phi(v_2, \{x_5 \& m23_2\}) \rightarrow ([7, 4], [17, 40], \{m21_1\}) /$
 $\Phi(v_2, \{x_6 \& m22_2\}) \rightarrow ([7, 4], [17, 40], \{m24_3\})$
 $A_{13}: \Phi(v_3, \{x_7 \& m25_3\}) \rightarrow ([2, 1], [4, 10], \{m23_2\}) /$
 $\Phi(v_3, \{x_8 \& m24_3\}) \rightarrow ([2, 1], [4, 10], \{m26_7\})$
 $A_{14}: \Phi(v_5, \{x_3 \& m27_5 \& m28_5\}) \rightarrow ([11, 6], [27, 59], \{m19_0\}) /$
 $\Phi(v_5, \{x_4 \& m2_5 \& m28_5\}) \rightarrow ([11, 6], [27, 59], \{m32_6\})$
 $A_{15}: \Phi(v_6, \{x_9 \& m29_6 \& m30_6\}) \rightarrow ([6, 3], [15, 31], \{m27_5\}) /$
 $\Phi(v_6, \{x_{10} \& m32_6 \& m30_6\}) \rightarrow ([6, 3], [15, 31], \{m31_7\})$
 $A_{16}: \Phi(v_7, \{x_{11} \& m31_7\}) \rightarrow ([3, 2], [8, 20], \{m25_3\}) /$
 $\Phi(v_7, \{x_{12} \& m26_7\}) \rightarrow ([3, 2], [8, 20], \{m29_6\})$
 $A_{17}: \Phi(v_4, \{x_{13}\}) \rightarrow ([3, 2], [8, 21], \{m20_0\})$
 $A_{18}: \Phi(v_8, \{x_{15}\}) \rightarrow ([2, 1], [4, 9], \{m30_6\})$
 $A_{19}: \Phi(v_9, \{x_{14}\}) \rightarrow ([5, 3], [12, 30], \{m28_5\})$

Each action is activated only once, when the corresponding condition will be equal to true. Actions $A_7 \div A_6$, and $A_{11} \div A_{16}$ contain alternative sub-actions. Only the first action, for which the condition will be satisfied, will be activated. According to the echo algorithm specification, process v_0 is the initiator, messages $m1_1, \dots, m17_3$ are explorer messages, while $m18_0, \dots, m31_7$ are echo messages (indices are added only for readability, mx_i means that message mx is sent to v_i . Events x_1, \dots, x_{15} are internal events, used for storing the state of processes between successive executions.

TABLE I. TASK CHARACTERISTICS

Task no.	Task execution time [ms]				Energy consumption [mJ]			
	Exploration mode		Echo mode		Exploration mode		Echo mode	
	HPC	LPC	HPC	LPC	HPC	LPC	HPC	LPC
0	2	3	5	9	20	9	52	23
1	8	13	9	17	81	34	93	42
2	5	10	4	7	52	26	40	17
3	4	7	1	2	40	18	10	4
4	6	11	2	3	58	28	21	8
5	4	6	6	11	40	16	59	27
6	3	5	3	6	29	13	31	15
7	5	9	2	3	50	23	20	8
8	2	4	1	2	22	11	9	4
9	7	12	3	5	67	30	30	12

Since different requests may be processed by distinct algorithms, the function of a system may be specified using a set of functions Φ sharing the same processes. Each function has only one initiator (process activated by the request). Processes may be activated many times, but the algorithm should consists of the finite number of actions and infinite loops are not allowed.

C. ARM big.LITTLE technology

ARM big.LITTLE technology is an architecture where high-performance CPU cores are combined with the most efficient ones. In this way the peak-performance capacity, higher sustained performance, and increased parallel processing performance, at significantly lower average power, are achieved. It was shown that using this technology it is possible to save up to 75% CPU energy in low to moderate performance systems and it is possible to increase the performance by 40% in highly threaded workloads.

Three different methods of applying big.LITTLE technology for minimizing the power consumption were proposed [3]:

1) In the cluster switching, LPCs are grouped into "little cluster", while HPCs are arranged into "big cluster". The system uses only one cluster at a time. If at least one HPC core is required then the system switches to the "big cluster", otherwise the "little cluster" is used. Unused cluster is powered off.

2) In CPU migration approach, LPCs and HPCs are paired. At a time only one core is used while the other is switched off. At any time it is possible to switch paired cores.

3) The most powerful model is a Global Task Scheduling (GTS). In this model all cores are available at the same time i.e. tasks may be scheduled on all HPC as well as LPC cores.

Different configurations of LPC/HPC core are available.

For example Samsung Exynos 5 Octa consists of 4 LPCs (Cortex-A7) and 4 HPCs (Cortex-A15), Exynos 5 Hexa uses 2LPC/4HPC configuration, while the MediaTek MT8173 contains only 2 LPCs (Cortex-A53) and 2 HPCS (Cortex-A72). Big.LITTLE technology is applied also in Qualcomm Snapdragon, NVidia Tegra X1, Apple A10 Fusion and HiSilicon processors.

Our approach is dedicated to the global task scheduling model. GTS is the most flexible and the most efficient method of applying big.LITTLE architecture. Moving tasks between HPCs and LPCs is fast, it requires less time than a DVFS state transition or SMP load balancing action.

IV. POWER-AWARE SCHEDULING

The draft of our algorithm of power-aware scheduling is given in Fig.2. First, a list of schedulable tasks (S_{list}) consists of the initiator, only. Then time marker (T) is initialized to 0. The main loop schedules the successive tasks, ordered according to their priorities. Priority of each task is based on the laxity (L), defined as a difference between task start times, obtained using ALAP (As Late As Possible) and ASAP (As Soon As Possible) methods, assuming the deadline (TL). These methods are applied assuming non limited number of cores. The *Sort()* method orders all schedulable tasks according to increasing laxity.

Tasks with the lowest laxity are scheduled first. If the laxity is higher than the difference between task execution times for LPC and HPC, then the task is scheduled on the LPC (if any LPC is available). If the laxity is lower than above difference, then the task is scheduled on the HPC (if any HPC is available). If no HPC is available, the task is scheduled on the LPC (if any LPC is available). If the difference between the time limit (deadline) and the time maker is higher or equal the system execution time obtained from ASAP method (in version for LPC), then the task is scheduled on the LPC. If none of the above conditions is fulfilled, the task stay in S_{list} and will be attempted to schedule in the next time frame.

Finally, all scheduled tasks are removed from the S_{list} . Before starting the next iteration of the main loop, the next tasks are added to the S_{list} using *NextReadyTasks()* method. The tasks are chosen according to rules of distributed echo algorithm. When all cores are busy or S_{list} is empty, the time marker is moved to the next time frame (function *NextAvailableTimeFrame()*), i.e. the nearest time when any core will finish executing task.

The presented algorithm is a greedy approach. First, it tries to reduce the power consumption by assigning tasks to LPC whenever it is possible. Although it is heuristic, we observed that in most cases it is able to find the solution for which all time constraints are satisfied.

```
Slist = all source nodes;
T=0;
while Slist≠∅ do
{
  ASAPh scheduling of all unscheduled tasks (HPC);
  ALAPh scheduling of all unscheduled tasks (HPC);
  ASAPl scheduling of all unscheduled tasks (LPC);
  for each ti
  {
    Li = ALAPh(ti) - ASAPh(ti);
  }
  Sort(Slist);
  for each ti ∈ Slist{
    if Li > |ti - hti and available(T,LPC) then
    {
      Assign ti to LPC;
      Mark ti as scheduled;
    }
    else
    if systemExecutionTime(ASAP) ≤ TL - T
      and available(T,LPC) then
    {
      Assign ti to LPC;
      Mark ti as scheduled;
    }
    else
    if Li ≤ hti - |ti then
      if available(T,HPC) then
      {
        Assign ti to HPC;
        Mark ti as scheduled;
      }
      else if available(T,LPC) then
      {
        Assign ti to LPC;
        Mark ti as scheduled;
      }
    }
    if scheduled(ti) then
      remove ti from Slist;
  }
  add NextReadyTasks() to Slist;
  T=NextAvailableTimeFrame();
}
```

Fig. 2. Power-aware scheduling algorithm

V. EXAMPLE

Assume that the target embedded system is based on multi-core processor with 2 LPCs and 4 HPCs. The sample system specification (Fig.1) consists of 10 tasks that are executed twice, first time in the exploration phase and the second time during the echo phase. The initiator is defined as task 0. It starts the computations in the exploration mode and it returns the final result after execution in the echo mode. Assume that the soft deadline is equal 37 ms.

The algorithm starts with $S_{list}=\{0\}$ and $T=0$. During the first pass all tasks are initially scheduled using the ASAP and ALAP methods. Results are given in Tab. II.

TABLE II. INITIAL TASK SCHEDULING

Exploration phase										
Task	0	1	2	3	4	5	6	7	8	9
ASAP _b	0	2	10	14	2	2	6	9	9	6
ALAP _b	1	6	14	15	24	3	7	10	20	16
ASAP _f	0	3	16	23	3	3	9	14	14	9
L	1	4	4	1	22	1	1	1	11	10
Echo phase										
Task	0e	1e	2e	3e	4e	5e	6e	7e	8e	9e
ASAP _b	30	19	15	18	8	24	21	19	11	13
ALAP _b	32	23	19	19	30	26	23	20	22	23
ASAP _f	52	33	26	30	14	41	35	32	18	21
L	2	4	4	1	22	2	2	1	11	10

During the exploration phase tasks are identified by the task number, for the echo mode tasks are identified by adding suffix “e” to the task number. It may be observed that according to the ASAP_L method scheduling on LPCs, the minimal system execution time is equal 61 ms and it requires 5 cores. The energy consumption equals 368 mJ. Initial ASAP_L scheduling gives an information about minimal execution time using LPCs only. It gives also the solution with minimal energy consumption. The initial ASAP_H scheduling returns the following results: execution time=35 ms, energy consumption=824 mJ, and requires 5 HPCs. Above results specifies the fastest solution, which consumes the maximal power.

The algorithm proceeds as follows:

- T=0: $S_{list}=\{0\}$
Task 0: $L_0=1, lt_0-ht_0=1, (65<37-T)=false, 0 \rightarrow$ HPC1

- T=3: $S_{list}=\{5,1,4\}$
Task 5: $L_5=1, lt_5-ht_5=2, (64<37-T)=false, 5 \rightarrow$ HPC1
Task 1: $L_1=4, lt_1-ht_1=5, (64<37-T)=false, 1 \rightarrow$ HPC2
Task 4: $L_4=22, lt_4-ht_4=5, 4 \rightarrow$ LPC1
- T=6: $S_{list}=\{6,9\}$
Task 6: $L_6=1, lt_6-ht_6=2, (62<37-T)=false, 6 \rightarrow$ HPC1
Task 9: $L_9=10, lt_9-ht_9=5, 9 \rightarrow$ LPC2
- T=9: $S_{list}=\{7,8\}$
Task 7: $L_7=1, lt_7-ht_7=4, (60<37-T)=false, 7 \rightarrow$ HPC1
Task 8: $L_8=11, lt_8-ht_8=2, LPC$ not available
- T=10: $S_{list}=\{2,8\}$
Task 2: $L_2=4, lt_2-ht_2=5, (60>37-T)=false, 2 \rightarrow$ HPC2
Task 8: $L_8=10, lt_8-ht_8=2, LPC$ not available
- T=13: $S_{list}=\{8,4e\}$
Task 8: $L_8=8, lt_8-ht_8=2, 8 \rightarrow$ LPC1
Task 4e: $L_{4e}=22, lt_{4e}-ht_{4e}=1, LPC$ not available
- T=14: $S_{list}=\{3,4e\}$
Task 3: $L_3=1, lt_3-ht_3=3, (56<37-T)=false, 3 \rightarrow$ HPC1
Task 4e: $L_{4e}=21, lt_{4e}-ht_{4e}=1, LPC$ not available
- T=15: $S_{list}=\{4e\}$
Task 4e: $L_{4e}=20, lt_{4e}-ht_{4e}=1, LPC$ not available
- T=17: $S_{list}=\{8e,4e\}$
Task 8e: $L_{8e}=11, lt_{8e}-ht_{8e}=1, 8e \rightarrow$ LPC1
Task 4e: $L_{4e}=18, lt_{4e}-ht_{4e}=1, LPC$ not available
- T=18: $S_{list}=\{3e,2e,9e,4e\}$
Task 3e: $L_{3e}=1, lt_{3e}-ht_{3e}=1, (53<37-T)=false, 3e \rightarrow$ HPC1
Task 2e: $L_{2e}=1, lt_{2e}-ht_{2e}=1, (53<37-T)=false, 2e \rightarrow$ HPC2
Task 9e: $L_{9e}=10, lt_{9e}-ht_{9e}=2, 9e \rightarrow$ LPC2
Task 4e: $L_{4e}=17, lt_{4e}-ht_{4e}=1, LPC$ not available
- T=19: $S_{list}=\{7e,4e\}$
Task 7e: $L_{7e}=1, lt_{7e}-ht_{7e}=1, 7e \rightarrow$ LPC1
Task 4e: $L_{4e}=16, lt_{4e}-ht_{4e}=1, LPC$ not available
- T=22: $S_{list}=\{1e,6e,4e\}$
Task 1e: $L_{1e}=1, lt_{1e}-ht_{1e}=8, (52<37-T)=false, 1e \rightarrow$ HPC1
Task 6e: $L_{6e}=1, lt_{6e}-ht_{6e}=3, (52<37-T)=false, 6e \rightarrow$ HPC2
Task 4e: $L_{4e}=13, lt_{4e}-ht_{4e}=1, 4e \rightarrow$ LPC1
- T=25: $S_{list}=\{5e\}$
Task 5e: $L_{5e}=1, lt_{5e}-ht_{5e}=5, (49<37-T)=false, 5e \rightarrow$ HPC2
- T=31: $S_{list}=\{0e\}$
Task 0e: $L_{0e}=1, lt_{0e}-ht_{0e}=4, (6<37-T)=false, 0e \rightarrow$ HPC1

The final schedule is presented in Fig. 3. After executing ASAP and ALAP initial scheduling, task 0 has laxity equal 1 and difference between execution time for LPC and HPC equals to 1. Since the first two conditions specified in *if*



Fig. 3. Sample schedule for algorithm from Fig.1

statements evaluate to *false*, task 0 is scheduled on the HPC1. Next, tasks 1, 4 and 5 are added to the list to be scheduled in the next time frame. Tasks 1 and 5 have lower laxity than the difference between LPC and HPC, therefore they are assigned to HPC. Otherwise, the laxity of task 4 is significantly greater than the above difference, thereby the task is scheduled on the LPC. Similar cases take place for tasks 9, 8, 8e, 7e, 9e and 4e. All other tasks are scheduled on HPCs in order to fulfil given time constraint. The energy used by the processor is equal to 698 mJ. It gives 15% power saving, in comparison with the fastest solution. We observed that for lower time constraints our method can give even 55% of energy savings.

VI. EXPERIMENTAL RESULTS

The efficiency of our method was evaluated using the example from Fig.1 as well as using other examples consisting of 25 and 45 tasks. Unfortunately there is no standard benchmark sets for echo algorithms. There is also no similar approaches of scheduling that may be compared with our approach. Therefore for comparison the classical list scheduling and ASAP methods were chosen.

Tables III, IV and V present results obtained for all sample algorithms using our method (EchoLPS) and list scheduling. Two different big.LITTLE architectures were examined, the first consists of 4 LPCs and 2 HPCs, the second one consists of 2 LPCs and 4 HPCs. For each architecture 4 different deadlines were examined. The mildest constraint was chosen in such a way that all tasks may be scheduled on LPCs. Such systems are found for reference, as the most power savings systems. Experimental results show how the tightening of time constraints affects the energy consumption. It should be noted that, nevertheless that our method is heuristic, in all cases solutions satisfying the deadline were found. But of course EchoLPS does not guarantee the fulfilment of hard real-time constraints.

For comparison the results obtained using classical list scheduling was given. List scheduling, first assigns tasks to HPCs i.e. it tries to find the fastest solution. Lists of tasks are ordered according to priority that is based on ALAP-ASAP values. We may observe that for comparable results (as far as the execution time is concerned) the solution found using the List Scheduling consumes significantly more energy than solutions obtained using our method.

For reference we also performed scheduling of all sample systems using List Scheduling, ASAP and ALAP methods. Table VI presents the results. For each solution the minimal number of LPC or HPC cores was found. Using List Scheduling it was possible to find the lowest energy consuming solutions. In some cases solutions are faster than obtained our method, but more LPC cores are required. Solutions found using ASAP/ALAP methods usually found the fastest solutions, but these methods do not minimize the number of cores required to execute task.

VII. CONCLUSIONS

In this paper a power-aware static scheduling method for embedded systems was presented. The method schedules real-time tasks on multi-core processor with power management capabilities. We applied our method to processors supporting ARM big.LITTLE technology, but the method may be adopted also to DVFS. The method gives better results than classical scheduling methods adopted to low-power embedded systems.

The method assumes the specification of the system in the form of a distributed echo algorithm. Such specification is more general than task graphs used in the most of existing static scheduling methods for real-time embedded systems. According to our best knowledge this is the first static scheduling method for real-time embedded software specified as the echo algorithm.

Our future work will concentrate on extending our method to systems specified using other classes of distributed algorithms, systems using other power management technologies as well as adaptive systems [21], considering the dynamic power optimization. Other direction of our work is to perform scheduling of the set of applications on the same system. Another interesting result may be obtained by developing quasi-static or quasi-dynamic scheduling method for distributed specifications. Such methods may be applicable to systems where the time of execution for tasks is not known or it is difficult to estimate.

The presented method uses simple heuristic to find the best tradeoff between the power consumption and efficiency of the system. Although the method gives quite good results, we will consider to apply more sophisticated optimization methods like constraint logic programming, mathematical programming [22] and developmental genetic programming [23].

TABLE III. RESULTS FOR 10 TASKS

System size	10					10				
Architecture	2 HPC and 4 LPC					4 HPC and 2 LPC				
Algorithm	EchoLPS				List Scheduling	EchoLPS				List Scheduling
Time constraint	65	56	46	37	NO	79	65	51	37	NO
Execution time	65	56	45	36	37	79	65	51	36	37
Energy consumption	368	499	637	698	716	368	458	570	698	813
Power increase	100%	136%	173%	190%	195%	100%	124%	155%	190%	221%
Time decrease	100%	86%	69%	57%	57%	100%	82%	65%	47%	47%

TABLE IV. RESULTS FOR 25 TASKS

System size	25					25				
Architecture	2 HPC and 4 LPC					4 HPC and 2 LPC				
Algorithm	EchoLPS				List Scheduling	EchoLPS				List Scheduling
Time constraint	201	168	143	117	NO	357	280	204	127	NO
Execution time	194	167	142	117	125	357	279	202	127	99
Energy consumption	1672	2033	2280	2604	2864	1672	2165	2631	3177	3431
Power increase	100%	122%	136%	156%	171%	100%	129%	157%	190%	205%
Time decrease	100%	86%	73%	60%	64%	100%	78%	57%	36%	28%

TABLE V. RESULTS FOR 45 TASKS

System size	45					45				
Architecture	2 HPC and 4 LPC					4 HPC and 2 LPC				
Algorithm	EchoLPS				List Scheduling	EchoLPS				List Scheduling
Time constraint	246	215	185	154	NO	466	368	271	171	NO
Execution time	246	215	185	154	133	466	363	271	171	130
Energy consumption	2169	2559	2900	3313	3630	2169	2821	3437	4169	4537
Power increase	100%	118%	134%	153%	167%	100%	130%	158%	192%	209%
Time decrease	100%	87%	75%	63%	54%	100%	78%	58%	37%	28%

TABLE VI. RESULTS FOR LIST SCHEDULING, ASAP AND ALAP

System size	10	25	45	10	25	45	10	25	45
Architecture	6 LPC			5 HPC	9 HPC	15 HPC	4 HPC	8 HPC	13 HPC
Execution time	65	193	230	37	109	130	37	109	130
Energy consumption	368	1672	2169	824	3864	5202	824	3864	5202
Algorithm	List Scheduling			ASAP			ALAP		

REFERENCES

- [1] M. Ditzel, R.H.Otten, W.A.Serdijn, Power-Aware Architecting for data-dominated applications, Springer, 2007.
- [2] S. Deniziak, Cost-efficient synthesis of multiprocessor heterogeneous systems. Control and Cybernetics, vol.33, 2004, pp.341-355.
- [3] big.LITTLE Processing with ARMCortexTM - A15 & Cortex-A7, ARM Holdings, http://www.arm.com/files/downloads/big.LITTLE_Final.pdf, September 2013,
- [4] L.Benini, A.Bogliolo, G. De Michelli, A Survey of Design Techniques for System-Level Dynamic Power Management, IEEE Transactions on Very Large Scale Integration (VLSI) Systems, vol.8, no.3, June 2000, pp.299-316.
- [5] S. Hartmann, D. Briskorn, A survey of variants and extensions of the resource-constrained project scheduling problem, European journal of operational research : EJOR. - Amsterdam : Elsevier, Vol. 207., 1 (16.11.), 2010, pp. 1-15.
- [6] L. Costero, F. D. Igual, K. Olcoz, S. Catalán, R. Rodríguez-Sánchez and E. S. Quintana-Ortí, "Refactoring Conventional Task Schedulers to Exploit Asymmetric ARM big.LITTLE Architectures in Dense Linear Algebra," 2016 IEEE International Parallel and Distributed Processing Symposium Workshops (IPDPSW), Chicago, IL, 2016, pp. 692-701.
- [7] G. Tel, "Introduction to Distributed Algorithms" Cambridge University Press, 2nd edition, 2001.
- [8] S. Bık, R. Czarnecki, S. Deniziak "Synthesis of real-time cloud applications for Internet of things" Turkish Journal of Electrical Engineering and Computer Sciences, vol.23, no.3, 2015, pp. 913- 929.
- [9] S. Bık, S. Deniziak "Synthesis of real-time distributed applications for cloud computing", IEEE Federated Conference on Computer Science and Information Systems, IEEE, 2014.

- [10] Ernest J.H. Chang: Echo Algorithms: Depth Parallel Operations on General Graphs. IEEE Transactions on Software Engineering, Vol. 8, No. 4, July 1982.
- [11] B. P. Dave, G. Lakshminarayana and N. K. Jha, "COSYN: Hardware-software co-synthesis of heterogeneous distributed embedded systems," in IEEE Transactions on Very Large Scale Integration (VLSI) Systems, vol. 7, no. 1, March 1999, pp. 92-104.
- [12] L.Shang, R. P. Dick, N.Jha. SLOPES: Hardware/Software Cosynthesis of Low-Power Real-Time Distributed Embedded Systems With Dynamically Reconfigurable FPGAs, IEEE Trans on Computer-Aided Design of Integrated Circuits and Systems, vol.26, no.3, 2007, pp.508-526.
- [13] M. T. Schmitz, B. M. Al-Hashimi, P. Eles, System-Level Design Techniques for Energy-Efficient Embedded Systems, Kluwer Academic Publishers, 2004.
- [14] F.F. Yao, A.J. Demers and S. Shenker. A scheduling model for reduced CPU energy. Proc. 36th IEEE Symposium on Foundations of Computer Science, 1995, pp.374-382.
- [15] J.Luo, N.K. Jha, Low Power Distributed Embedded Systems: Dynamic Voltage Scaling and Synthesis, Proc. 9th Int. Conference High Performance Computing - HiPC 2002, Lecture Notes in Computer Science, vol. 2552, 2002, pp. 679-693.
- [16] C.Steger, C.Bachmann, A. Genser, R. Weiss, J. Haid, Power-aware hardware/software codesign of mobile devices, e & i Elektrotechnik und Informationstechnik, vol.127, no. 11, 2010.
- [17] J. Anderson, V. Bud, and U. C. Devi. An edf-based scheduling algorithm for multiprocessor soft real-time systems. In IEEE ECRTS, July 2005, pp. 199-208.
- [18] Han, Sangchul and Park, Minkyu, Predictability of Least Laxity First Scheduling Algorithm on Multiprocessor Real-Time Systems, Proc. of EUC Workshops, Lecture Notes in Computer Science, vol.4097, 2006, pp.755-764.
- [19] Li Jie, Guo Ruifeng and Shao Zhixiang, "The research of scheduling algorithms in real-time system," 2010 International Conference on Computer and Communication Technologies in Agriculture Engineering, Chengdu, 2010, pp. 333-336.
- [20] Abusayeed Saifullah, David Ferry, Jing Li, Kunal Agrawal, Chenyang Lu, Christopher Gill, "Parallel Real-Time Scheduling of DAGs," IEEE Transactions on Parallel and Distributed Systems, vol. 25, no. 12, Dec., 2014, pp. 3242-3252.
- [21] S.Deniziak, L.Ciopinski, "Synthesis of power aware adaptive schedulers for embedded systems using developmental genetic programming", Proc. *Federated Conference on Computer Science and Information Systems (FedCSIS)*, 2015, pp.449-459.
- [22] P. Sitek, J. Wikarek, "A Hybrid Programming Framework for Modeling and Solving Constraint Satisfaction and Optimization Problems", Scientific Programming, vol. 2016, Article ID 5102616, 2016.
- [23] S. Deniziak, L. Ciopinski, G. Pawinski, K. Wieczorek, and S. Bak, "Cost optimization of real-time cloud applications using developmental genetic programming", in IEEE/ACM 7th International Conference on Utility and Cloud Computing (UCC 2014), December 2014, pp.774-779.

RSECM: Robust Search Engine using Context-based Mining for Educational Big Data

D. Pratiba
Dept. of CSE, RVCE
Bangalore, Karnataka

Dr. G. Shobha
Dept. of CSE, RVCE
Bangalore, Karnataka

Abstract—With an accelerating growth in the educational sector along with the aid of ICT and cloud-based services, there is a consistent rise of educational big data, where storage and processing become the prime matter of challenge. Although many recent attempts have used open source framework e.g. Hadoop for storage, still there are reported issues in sufficient security management and data analyzing problems. Hence, there is less applicability of mining techniques for upcoming search engine due to unstructured educational data. The proposed system introduces a technique called as RSECM i.e. Robust Search Engine using Context-based Modeling that presents a novel archival and search engine. RSECM generates its own massive stream of educational big data and performs the efficient search of data. Outcome exhibits RSECM outperforms SQL based approaches concerning faster retrieval of the dynamic user-defined query.

Keywords—Big Data; Context; Cloud; Educational Data; Hadoop; Search Engine

I. INTRODUCTION

There is a revolutionary change in the educational system in the modern times, where ICT plays a crucial role right from primary to advance technical education [1]. At present, it is not possible for an educational institution to provide extra knowledge and skills required for getting through any competitive examination or cracking the interviews for top notch Multinational organization. In order to cater up to the educational need, various enterprises have come forward to furnish educational knowledge and skill. This system is also called as online learning or e-learning system [2]. The conventional online learning system is not interactive, and it is one way communication dominantly, where students have to listen to the instructions presented in the form of the webinar. However, with the changing requirement of education, the needs of the students are also changing that demands the Learning Management System to be highly interactive [3]. Students requires the Learning Management System to be more real-time and more interactive to feel them a virtual presence:-

- e.g. i) omnidirectional communication system among students-instructors, instructor-instructor, and student-student,
ii) availability of more offline assessments,
iii) exchange of course materials,
iv) sharing of students or instructor-centric study materials,
v) application to support a wide variety of plugins and various add-on features,

vi) access policy to be controlled by user owing to the collaborative educational network. Another trend observed in the present era is the migration of the majority of the enterprise applications over the cloud in order to give pervasiveness to the data and services. Our prior studies [4][5][6] has showcased an existing system towards digital learning along with a novel framework for providing security to big educational data. It also considers the design of interactive digital learning framework. However, the existing studies were quite analytical and need much more focus on query handling, complexities handling, and ensuring faster response rate for the stream of educational big data. Our prior framework [5][6] have discussed a system that can generate the big data efficiently. However, there is a presence of tradeoff found in our prior work introduced most recently in the research community and the actual need. When we conducted a thorough review, we found that there exists various industrial standards and tools for analyzing big data e.g. Hadoop, Hive, Pig, Cassandra, etc. We potentially felt that our existing framework have the better scope of enhancement and could bring the most additional feature that can potentially enhance the teaching and learning experience. It was also explored that till now there exist a massive archival of search engines on conventional data but never on big educational data. From any existing archival or digital repository, the outcome of the search for some specific content is either time consuming or gives irrelevant outcomes. The prime factor behind this is that existing search engines are not capable enough to identify the exact data that is valuable to the user [7]. Apart from this problem, the existing data mining algorithms are also not applicable for analyzing big educational data owing to the problem of high dimensionality and problems in the extraction of appropriate feature vector [8][9][10].

This paper reviews the existing system specifically about the mining techniques over the cloud and the techniques that are based on context mining. A significant problem statement is derived and then it proposes a novel technique that performs efficient, secure, and faster mining operation over educational big data using context-based approach. The technique introduced is quite simple and cost effective. Section II discusses the existing review of literature followed by problem identification in Section III. Discussion on proposed model is carried out in Section IV followed by research methodology discussion in Section V. Section VI illustrates the implementation techniques focusing on the algorithm and their respective operations. Outcomes being accomplished from the study are discussed on Section VII while the conclusion of the paper is made in Section VIII.

II. RELATED WORK

This section provides the glimpse of various significant studies that are being carried out by different researcher and the different mechanisms used by them to evaluate the performance of their work. Since the evolution of dataset for an educational sector is still in infancy stage; therefore different disciplines of application are considered for studying the mechanisms of approach with a common factor called Big Data. There has been remarkable work and literature available in the field of medical analytics on big data, one of such work by Belle et al. [11], where medical image analysis, physiological signal processing, and genomics data processing is discussed. The author recommended building a reconstructed network with close co-operation among clinicians, computational scientist, and experimentalists.

This can be mimicked in the case of digital learning framework to have a collaborative learning – teaching intelligent mechanism. Such collaborative platforms of learning require an efficient mechanism of context retrievals, which needs robust aggregation techniques, one of such work in the context of image data is carried out by Cao et al. [12] for web-scale image retrieval, which uses distributed learning for ranking. It supports for billions of images. Data mining is an integral part in BigData where less informative words are ignored, and only significant words are considered. One such work is carried by Chen et al. [13] by reviewing data mining in IoT (Internet-of-Things). The authors have used data mining to enhance the performance as well as to save storage. The storage of ever growing data for the analytical purpose requires a large storage which is achieved using the cloud. One such work towards using the cloud as storage of analytical data was carried out by Khan et al. [14] about the smart cities. The prototype work is developed using Hadoop and Spark. The proposed work also makes use of cloud for storage using HBase in Hadoop framework. An increase in data is also associated with tedious work of managing, analyzing and integrating the data using big data. Reviewing the challenges and future perspective in managing, analyzing and integrating big data in the field of Medical Bioinformatics is carried out by Merelli et al. [15]. The system uses data management, performs data analysis along with the integration of data from various actors like students and faculties. Usage of deep learning can contribute the effective implementation of any work. One such work is carried out by Najafabadi et al. [16] who have implemented the concept of deep learning of big data analytics. The efficiency of any system depends on the effectiveness of the algorithms or techniques used in the system. One such kind of work is carried out by Oyana [17] where disease identification and analytics of visual data was achieved using Fangled FES-k means clustering algorithm. Different algorithms are used for various functionalities like multiple logins or in the case of search operations. In any educational system, the credibility of the system depends on the quality of the information posted by the system as well as its source. Refinement of Quality Information was carried out by Ramachandramurthy et al. [18]. This is achieved by using fuzzy Bayesian process which helps in improving the truthfulness in big data.

Effectiveness and efficiency of the system are dependent on the nature of its design modeling, and performance enhancement is based on optimization. One such work is carried out by Slavakis et al. [19] in signal processing domain, wherein the authors have presented encompassing models which capture huge range of signal processing relevant data for analytics (includes Principal Component Analysis (PCA), Dictionary Learning (DL) and Compressive Sampling (CS)). In an educational system, the queries submitted by the user or clients need to be appropriately addressed. This addressing requires individual search mechanism to provide a suitable solution. One of such work is carried by Cataldi et al. [20] wherein the author's present context-based search and navigation system based on the KBC (keyword-by-concepts) graph. Santini and Dumitrescu [21] have presented a search system which provides the search result considering the context related to certain activities. Fisher and Hanrahan [22] presented a mechanism for the context-based search of the 3D scene. They also proved that context-based performs better than the keyword-based search. Lane et al. [23] presented a local search technology which in comparison to other context-based searches also uses various factors such as location, time, user activity as well as weather. It also constructs a behavioral model and provides the result of the basis of personal requirement making using of similarity among users rather than the conventional result. Adomavicius [24] has emphasized on the significance of relevant contextual data in a recommendation system. Authors have introduced different framework such as contextual pre-filtering, post filtering, as well as modeling to facilitate the incorporation of contextual data in recommendation system. Li et al. [25] have formulated context-based people search using a grouping-based mechanism in a labeled social networking. Silva et al. [26] have introduced a context-based system which allows the evaluation of related data that is associated with a concept. It performed by certain distinct contextual information considering certain facts like user domain as well task, perspective and task intended to use the data. Thangaraj and Gayathri [27] have proposed searching techniques which consider not only context but also synonyms in comparison to the conventional keyword search engines. Vasnik et al. [28] presented a semantic and context-based search engine for the Hindi language. It is developed by lexical variance, user context as well as a combination of these two mechanisms. Gupta [29] has proposed a focused searched based on contextual data where the search engine is devised to such that it can decide the relevance of the data by certain context of user query keyword.

Depending on the quality as well as desired relevance, the result set size is minimized by eliminating irrelevant documents. Rahman et al. [30] have demonstrated a context-aware meta-search engine based on Eclipse IDE. Authors have taken advantage of the API's provided by different search engines like Bing, Google, and Yahoo as well as Stack Overflow site to provide the basic solution to errors and exceptions. The search engine works by content relevance; popularity as well context relevance. In the system, a search operation is carried in two ways in a conventional way as well

as advanced way whereas the conventional way uses conventional keyword search whereas advanced search is performed by context.

Hence, it can be seen that there are various studies towards developing search engines using typical mechanism. Each mechanism has its advantages as well as pitfalls. The next section discusses the problems identified after reviewing the existing literature.

III. PROBLEM IDENTIFICATION

After going through the contribution of existing literature from prior section, it was seen that conventional relational database management system (RDBMS) is adopted for reporting as well as archiving the data. However, Hadoop is deployed to deposit a massive quantity of data over a distributed cluster nodes and at the same it processes it as well. Performing data mining or analysis over the structured data can be easily done over RDBMS as it structures the enterprise data in the patterns of rows and columns. One interesting finding is that there is a myth that conventional data mining approach cannot be applied as the data is unstructured. However, the statement is not completely true. It is because, whenever there is a need for analyzing a part of the data from the big data, RDBMS may be a perfect choice. However, there are various challenges posed by the big data to be working on conventional RDBMS system. The inherent characteristics of big data (e.g. high dimensionality, heterogeneity, data veracity, data velocity, etc.) make the RDBMS system out of the picture when it comes to deploying mining approaches. Adoption of Hadoop mitigates this problem as it has various characteristics that support processing big data. With HDFS (Hadoop Distributed File System), it supports processing big data with complete optimization of the unused space too. HDFS is the frequently used approach even for storing and processing (mining) big data. However, there are certain issues in it. The problem identifications of the proposed study are as follows:

- The SQL-based database system cannot be used to store and process educational big data owing to its incapability of handling unstructured data. Existing data mining algorithms are not applicable directly over the massive streams of big data owing to the unstructured pattern of data.
- The security features of Hadoop are highly challenging and potentially complex to be configured. It doesn't have any form of standard encryption mechanism over its storage as well as network levels giving rise to authentication-based attacks. Hadoop is designed in Java, and same Java is also used by cyber criminals to launch an attack.
- The frequently used HDFS is not good enough for handling smaller files and incapable of performing an effective data compression. The design principle of HDFS is even capable of handling random reads of smaller files.

- The biggest problem is that although Map Reduce, another frequently used software framework, supports batch-based architecture, which will eventually mean that it will never permit itself to be deployed as the use case that will require real-time access to data.

Owing to the problems as mentioned above, existing data mining algorithms cannot be integrated over Hadoop and will thereby pose a challenge to generate a precise search of specific data in the cluster node. Therefore, after briefing the problems above, the problem statement of the proposed study can be stated as – *"It is the quite computational challenging task to evolve up with a mechanism that supports highly relevant search engine over complex and unstructured educational big data."* The prime goal of the proposed system is thereby to overcome this problem.

IV. PROPOSED SYSTEM

The prime aim of the proposed system is to develop a technique that can perform both archival and search of the relevant data from the massive stream of educational big data. The technique is termed as RSECM i.e. Robust Search Engine using Context-based Mining for educational big data. The contributions of the proposed system are as follows:

- To develop an efficient archival process that can store the educational big data.
- To develop a precise search engine that can perform faster retrieval of the outcome with better accuracy.
- To show that proposed system is the better approach than conventional SQL-based approach.

In order to achieve 1st research objective of RSECM, the proposed system first develops three different actors associated with the educational domain and develops a prototype application for generating real-time educational big data. The big data is designed in the highly unstructured way as it consists of multiple forms of data with higher dimensionality. The next part of the RSECM technique is to provide enough security features to address the problems of security from Section III. Supported by a recent version of the cryptographic hash function, SHA3, the proposed system ensures higher secrecy in data transaction as well as system security. The next part of the functional operation is to perform conversion of unstructured data to structured data using Hbase. All the problems of frequently used HDFS highlighted in Section III can be addressed potentially using Hbase. The next functional operation of RSECM is to perform a search from the education data over the cloud. A novel search engine is designed using context based mining approach that initially preprocesses and then it applies post processing to generate the feature vector. The feature vector is stored in the cluster node. The proposed system will also introduce a simple query system using simple search mechanism and contextual search mechanism. The architecture of RSECM is highlighted in Fig.1

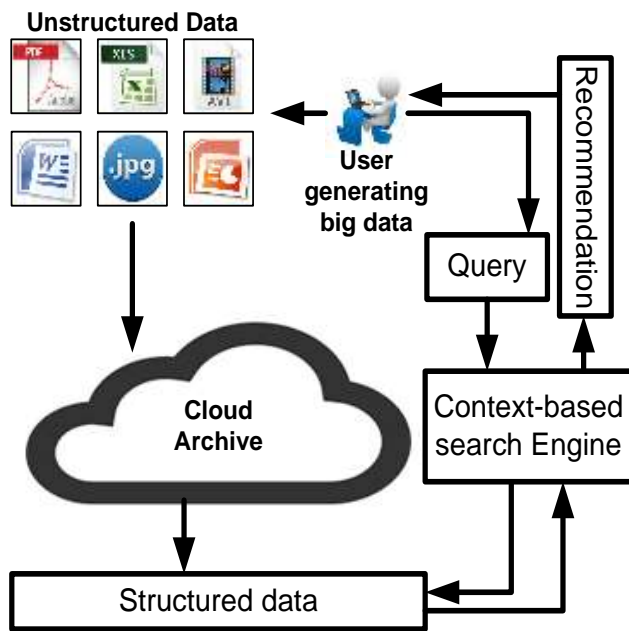


Fig. 1. RSECM Architecture of RSECM

V. RESEARCH METHODOLOGY

The proposed research work has adopted the analytical as well as experimental research methodology. Analytical modeling was developed for designing the context-based search, while experimental approach was considered to validate the outcomes on machines mapping with the cloud infrastructure. RSECM has the capability to generate real-time educational data rather than using existing available database. This section discusses the various significant task handled by the proposed RSECM for educational big data.

a) Actor Modelling

The proposed RSECM possess multiple forms of an actor of the cloud-based educational domain as well as learning management system to leverage teaching and learning experiences. RSECM has been developed over Java using a common interface protected by a novel authentication system. The interface supports accessibility to three types of actors i.e. i) students, ii) instructors and iii) policy makers. Fig.2 shows the system architecture associated with the actor modeling of RSECM. It also shows three actors associated with the interactive educational system. Initial state consists of profiling the student that records all the necessary information e.g. student's name, contact information, educational history, professional experience, etc.

A conventional database system can be used to store all profiling information. Upon successful profiling operation, the student is provided with access id and a static password originated from the cloud server. RSECM assumes that the static password is secured by the security patches practiced by the enterprise. As the existing security patches over cloud runs over the internet, we also assume that it is not safe and it requires to be protected too.

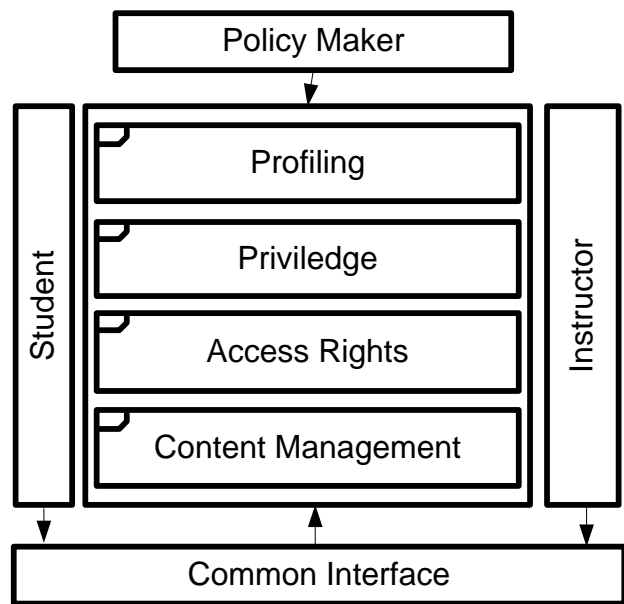


Fig. 2. System Architecture of RSECM Actor Modelling

The protection mechanism of RSECM is given by a novel authentication policy (discussed in next sub-Section B). RSECM possessed the feature of single as well as multiple authentication mechanisms, where the verification of the legitimacy of the user is done over cloud environment. The static password is only used for single authentication operation while in multiple authentication system prompts for multiple interfaces to validate the user multiple times over the internet. After successful authentication, the student actor is provided with feature to opt for an online educational system. The features about student actor are as follows:

- Can make the selection of the available list of course materials.
- Can visualize the skills and professional experience of their online instructors.
- Can download the study materials for the specific course enrolled.
- Can upload the study materials in the form of office files, PDF files, image files, audio files, video files.
- Can upload a particular file of new extension permitted by policy makers.
- Can take up the online test to assess their skill set on particular course.
- Can check their ratings provided by the instructors as an outcome of the test.
- Can communicate and share heterogeneous data with other members (students) as an open discussion forum.
- Can able to perform contextual-based search mechanism on appropriate educational data.

The second actor of RSECM modeling is an instructor, who is responsible for knowledge delivery services to the students using the remote connectivity applications in ICT. Before starting using their individual feature, the instructor will need to authenticate themselves on the same uniform interface (even used for authentication by the student actor). Similar profiling features will also be used to store the unique identity-based information of the instructor. The features pertaining to instructor actor are as follows:

- Can create a course on a particular subject and stream.
- Can upload various forms of study materials of multiple file formats permitted by policy makers.
- Can communicate with students by sharing and exchanging various forms of study contents.

The third actor of RSECM modeling is policy-maker, who is responsible for supervising the complete operations by instructors and students. RSECM emphasizes on the policy-maker as it is the only actor that monitors the activities as well as the privilege of student and instructors. The system also provides various forms of features in order to assist proper operations of the users e.g. it is policy-maker who can configure about the allowances of upload and download of the study contents. It can also configure the type of file extension (.doc, .xls, .ppt, .pdf, .avi, .jpg, WMV, .mp3 etc). As the policy-maker acts almost like the administrator of RSECM, hence it is skipped from the profiling process. However, they will be required to get themselves authenticated in order to execute their privileges.

Hence, the existing database consists of the high dimensional data which is massively growing and also is highly unstructured data. Before attempting to create a search, it is essential that such data should be stored efficiently as existing data mining approaches cannot be applied. RSECM uses Hbase data management, which is elaborated in next sub-section.

b) Security Management

The proposed system of RSECM uses the SHA3 algorithm in order to secure the authentication mechanism. Our work is the first attempt to implement the most recent cryptographic standards introduced in the year 2014. The schematic architecture of the security modeling of RSECM is discussed in Fig.3. The static input password of the user is considered as seed, where the SHA3 algorithm is applied. The system then generates two arbitrary functions for generating pseudonym A and B. The SHA3 is subjected to the pseudonym some iteration for the seed i.e. SHA3 (seed)A in order to generate 512 bits of fingerprint that is again subjected to the MD5 algorithm. This operation further generates 128 bit of print that is again split into two sub-keys of equal size in order to re-encrypt with AES. The final encrypted key is hidden in QR barcode, while one of the sub-keys generated from the 128-bit fingerprint is forwarded to user's email using email APIs in Java.

The proposed framework is now able to perform secure authentication of the user (student and instructors); however, as the proposed study relates the user to student actors mainly. The next process relates to an effective data management using

H-base.

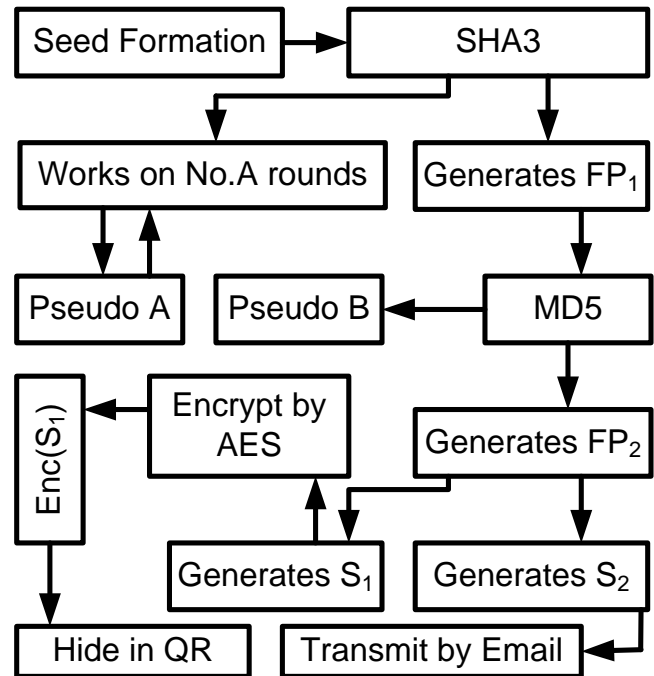


Fig. 3. RSECM Security Management

c) H-base Data Management

The proposed system of RSECM essentially generates a massive stream of random educational data which is highly unstructured and is not possible to store in the conventional database management system. However, at present, Hadoop is said to be made up of i) file system i.e. HDFS and ii) computational framework i.e. Map Reduce. Although HDFS permits repositing massive amount of extensive data in highly parallel as well as distributed manner, it doesn't support arbitrary read and write features being a file system. Although such feature is quite suitable for HDFS to access sequential data, in reality, it is not necessary that massive streams of data should be sequential in order. That's why the design principle of RSECM doesn't use HDFS but uses Hbase as it strongly supports random data with read and writes features on it. In a nutshell, Hbase has strong support to process and store unstructured data. Adoption of Hbase has another advantage of faster data access. Owing to storage characteristics of data in columnar pattern considering data as keys, Hbase can process and store the data quite faster than HDFS. Another interesting point about HBase usage is its potential for replica management with the aid of the feature termed as "region replication." According to this framework, it is possible to store and access multiple replicas over the region servers. An added advantage of replica management using HBase is its flexibility where it can manage multiple replicas in one region. The system uses a distinct replication identity to complete available replica initializing from 0. Hence, we call the primary region for any region whose replication identity corresponds to 0. Similarly, there are secondary replication regions too. All the significant writers are possessed by primary replication region along with all the updated alternations on the data. Therefore, with this feature, HBase provides a better data consistency.

Although, there is certain search engine like ElasticSearch [31] that can perform the search over cloud using graphical exploration tool, the proposed system chooses to stick on to the usage of HBase owing to its better editable properties of HDFS

architecture. The data modeling in RSECM is designed in order to facilitate the unstructured data that significantly differs in size of the field, data type, and columns.

rowkey	Column family	Column qualifier	Timestamp	Value
a	Cf1	“bar”	“1368394583”	7
			“1368394261”	“hello”
		“foo”	“1368394583”	22
			“1368394925”	136
	Cf2	“2011-07-04”	“1368396302”	“fourth of July”
		“1.0001”	“1368397684”	“almost the loneliest number”
b	Cf2	“thumb”	“1368397684”	“[3.6 kb png data]”

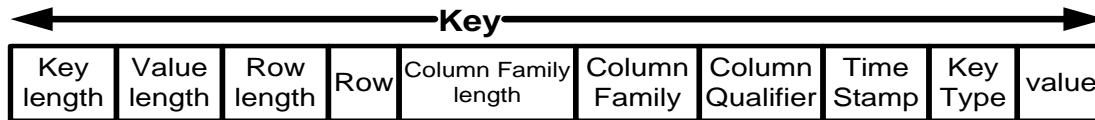


Fig. 4. Components of Hbase used in RSECM

The data modeling supported by RSECM possess multiple components are as shown in Fig.4. The functions of each component are briefly discussed below:

- **Tables:** All the unstructured data is organized in tables which are coined by string-based name and is consist of multiple collections of rows repositied in discrete partitions that are called as regions.
- **Rows:** It is a position where the data is repositied and is identified using the respective key. There is no data type for a row keys. It is also called as the byte array.
- **Column families:** It is group under which row each data resides. It is a string and is made of characters that are safe for deployment.
- **Column Qualifier:** It is a type of flag that is used for addressing the column family. It doesn't possess any form of data type and is often considered as a byte array.
- **Cell:** A cell is a combination column family, a key of a row, and column qualifier. The value of the cell is used to flag the data stored in it. It doesn't possess any form of data type and is often considered as a byte array.
- **Version:** It is a number that is used for signifying the time of generation of the cell. The default number of version of cell in HBase is 3.

Therefore, the storage framework of the RSECM will consist of the database with columnar pattern and table with rows. There is a primary key for each row also called as row keys. It is also possible to have multiple columns in each row with timestamp data stored in each cell. The method to access the data is only through the row key, table, family, timestamp, and column. The system has also used the simple APIs e.g. get, put, scan, and delete. This the way how unstructured data is converted to structured data and stored in Hbase storage. We choose to use Hbase as it supports transactional data exchanging mechanism in Hadoop that is essentially required by the user to get the updates and do personalization of their educational data.

d) Mining with Contextual Search Engine

The proposed system carries out a novel design of data analytics by carrying out mining operation as well as contextual-based search operation. The proposed system offers the generation of a query through HBase that already uses Hadoop metrics framework. The system then inherits the features as well as its classes. The mining operation of the proposed system is carried out by a simple statistical method. The presented method aggregates the statistics of a varied relationship among the words from the educational data in order to provide query specification and comparison of the objects. A contextual database is built by initially compiling the relationship between the words in order to encapsulate the statistics of similarity measures among the words. During the data retrieval, we compute a search matrix of keywords given.

The schematic diagram for this is shown in Fig.5.

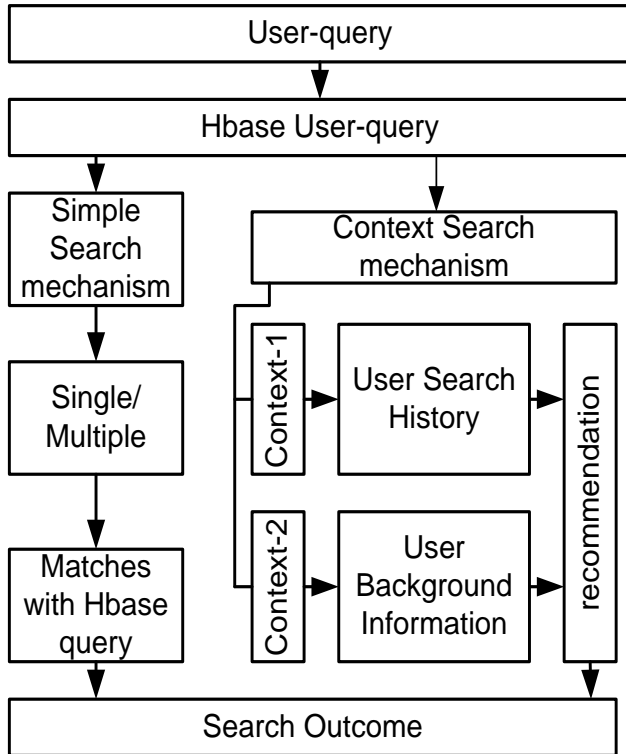


Fig. 5. Mining with Contextual Search Engine

Fig.5 shows that the transactional education big data is initially an unstructured data for which reason; it is not feasible for carrying out data mining technique. The problem is mitigated after directing the stream of unstructured data to the Hbase that performs self-indexing of the data. The unstructured data is first processed to become compatible with the Hbase index. This operation is carried out using data mining technique that performs both preprocessing as well as post processing. The preprocessing operation includes identification and removal of noise in the data, redundant data, etc., while post-processing operation involves feature extraction operation. Finally, a significant feature is extracted and stored in cluster node (or Hbase). The next process is about the search technique implementation that is initiated using user-based query keywords. The search technique can be both single as well as multiple searches. The second step is to convert the user query to the Hbase query, where depending on the number of the words, it generates multiple HBase queries. As per the number of the words in a user-based query, the loop will work for generating some Hbase query. Finally, the Hbase query returns results in sequential form for each HBase query. Finally, it matches queries from the source of files and matching sentences. The entire process is called as simple search design that is functional when the users access the common interface of RSECM. The proposed system develops context-based search in two ways,

- *Historical Context:* The proposed system considers the search history as the prime factor of developing context. If the user-centric search history, as well as user query, are found similar than the result of the

Hbase query will act as recommended result of the context-based search.

- *Background Context:* The background of the user is also included for forming the context-based search. If the information pertaining to the background of the user (from profiling data) as well as the user-centric query is found to be similar than the result generated by the Hbase query will be considered as recommended results of the context-based search.

VI. IMPLEMENTATION

As the proposed system considers the experimental approach, so it is essential to have a standard and perfect prototyping of the experimental test-bed. RSECM experiments over Oracle VirtualBox in Linux machine that provides a standard virtualization with a supportability of guest operating platform. For this purpose, a virtual machine is created and configured with the necessary parameters as well as settings for creating a cluster node (or Hbase). Cloning of this reference virtual machine is carried out multiple times for an experimental purpose. The inclusion schema used of VirtualBox integration is shown in Fig.6.

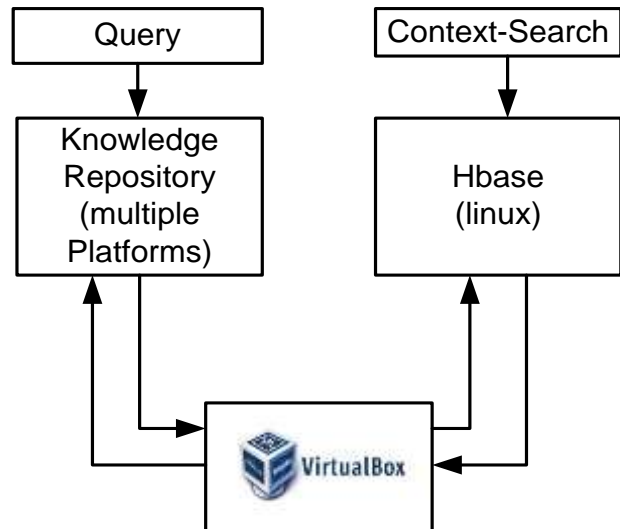


Fig. 6. Inclusion Schema of VirtualBox

The above Fig.6 shows the use of multiple forms of operating system, where the knowledge base is created. It means that user application interface lies on the 1st block where the operating system and machine configuration may quite differ from each other. It is the block that is responsible for the generation of big educational data, which is characterized by unstructured and massive streams. The user-based search is also generated from this block. The second block consists of the virtual environment where VirtualBox is configured to create Hbase in Linux machine. The contextual-based search is carried out in this block. Both the blocks are connected via cloud environment and query processing in order to accomplish better data synchronization. The implementation of the RSECM is carried out in 32/64 bit operating system consisting of 8GB RAM, and a storage capacity of 1TB. The interface designing, as well as HBase work, is carried on Java platform using JDK 1.7, using NetBeans IDE and Oracle Virtual Box. A

laboratory prototype is a setup performs this implementation using the cloud. The proposed system is supported by essentially four types of algorithms actor modeling, security management, Hbase data management, and mining with the contextual search engine.

TABLE I. ALGORITHM FOR GENERATING UNSTRUCTURED DATA

Algorithm-1: Generation of Unstructured Data

Input: n (number of actors), p (number of characteristics)

Output: unstructured data generation

Start

1. Define type of actors [$i_n | n = 3$]
2. Define characteristics of actors [$i_n=C_p$]
3. $i_n \rightarrow \text{files}(m) \forall m \in 14$
4. Stream data to Hbase

End

Table 1 highlights the algorithm that has used in the generation of the unstructured data. The algorithm takes the input of n number of actors where n is considered to be three i.e. i) student, ii) instructor, and iii) policy maker. It is also feasible for enhancing some actors depending on the type of application. Each actor is defined a particular set of characteristics p to represents their privilege. Any event of p will lead to generation of m files (.doc, .docx, .xls, .xlsx, .ppt, .pptx, .pdf, .jpg, .bmp, .tif, .png, .avi, .mpeg, .wmv). The higher limit of m is controlled by policy-maker. Line-3 of the algorithm-1 represents the generation of transactional data by the users leading to a generation of highly unstructured data that is now streamed to cluster node (or Hbase). The security features responsible for maintaining authentication for the actors are as discussed next.

TABLE II. ALGORITHM FOR SECURITY MANAGEMENT

Algorithm-2: Security Management

Input: $pswd$ (password)

Output: Key generation and authentication

Start

1. $\text{str}(pswd) \rightarrow S$
2. $g(x) = (Z_1, Z_2)$
3. Apply hash $\rightarrow \text{SHA3}(S)Z_1 \rightarrow \text{FP}_1$
4. Apply hash $\rightarrow \text{MD5}(\text{FP}_1)Z_2 \rightarrow \text{FP}_2$
5. $\text{Div}(\text{FP}_2) \rightarrow [S_1(64 \text{ bit}), S_2(64 \text{ bit})]$
6. $\text{Enc}(S_1) \rightarrow S_{e1}$
7. Embed S_{e1} in QR barcode
8. Forward S_2 to user-email
9. Extract S_{e1} and S_2
10. Authenticate using S_2
6. Allow access

End

The working of the Algorithm-2 is illustrated as follows. Initially, the unique data i.e. confidential data such as password from the user profile is retrieved. This unique data is used to generate the secured key for authentication. The unique data undergoes two kinds of the hashing function. The first hashing function is denoted by Z_1 and is performed using the SHA3 algorithm. The next hashing function is denoted by the Z_2 and is carried on the unique data using the MD5 algorithm. The SHA3 encrypted output resulting Z_1 acts on the unique data for

x iteration, whereas the MD5 encrypted data resulting Z_2 acts on unique data, and the result of SHA3 encrypted unique data represented by Z_1 for y iterations. These results in the generation of the desired secured key required for authentication of the login process.

After the generation of the secure key, the authentication process continues as follows. The secured key resulted from the multi-login Algorithm is 128 bit. The 128-bit key is then split into two parts by dividing it using a simple division. This results in a generation of two subsets of secured key denoted by S_1 and S_2 each of which is of 64-bit long. The first subset S_1 is sent to the user mail. These subset keys are further subjected to encryption using the AES algorithm, i.e. The Subset key act as data and plaintext for the encryption algorithm. Here the first subset key is used as data/plaintext and the second subset key acts as an encryption key. The first subset key is encrypted by using the second subset key using AES algorithm. The output of this operation results in a bit data which is converted into a string. This string is used to generate a QR Barcode. This QR Barcode consists of the encrypted string. In order to generate the authentication key, we require two sets of keys; the two keys are one which is present in the user mail (first subset S_1), and the other key is hidden in the QR Barcode. This QR Barcode is scanned using a user developed the application. The decryption operation is performed using the key. In simple words, the authentication needs the two key one in the user mail and the key in the barcode. This feature provides robust security since the chances of comprise of both the keys are negligible. As the secured authentication requires both keys, a user having single key will never be successful in log in to the system. This multi login algorithm is applicable for both faculty and student who have multi login option. On successful login, the user will be directed to a page containing details about courses which will facilitate various operations such as download information; syllabus and other queries like FAQ will also provide details related to faculty. The student with the privileges will be provided different options like, upload, download, search, thread, start a new thread so on.

- **Upload:** Here if the student is granted privilege from the admin staff, a student can upload his own file.
- **Search:** Allows the student to perform context based search.
- **Thread:** Provides platform for discussion for students. This can be used for knowledge sharing.
- **Start a new thread:** Allows the user to start a new discussion. It should be noted that all these threads are used in the background for context generation.

After the RSECM provides enhanced security capabilities using the most recent version of the cryptographic hash function, the next step is to perform data conversion using Hbase management. The algorithm used for big data conversion is shown in Algorithm-3.

TABLE III. EXTRACTING STRUCTURED DATA USING HBASE

Algorithm-3: HBase Data Management

Input: m (unstructured data)

Output: structured data

Start

1. Generate db (m)
2. Classify j [db (m)]
3. Configure p
4. For $p=1 \dots k$
5. $q \subseteq 1, 2, \dots, 2k$
6. $r \subseteq k$
3. Pass j to reducer
4. Reducer j forwards to Hbase (j_{hbase})
5. Represent $j_{\text{hbase}} \rightarrow \text{dis}(\text{row}, \text{col})$
6. Stream $j_{\text{hbase}(\text{row}, \text{col})}$.

End

Table 3 shows the process of conversion of the unstructured educational data $db(m)$ to the structured one. Although from the Algorithm-1, it was discussed that we choose to experiment with 14 file types; however, for further challenges, we also consider multiple forms of files or types of educational data. The variable j represents such forms of education data which are normally log files, streams of events, and various forms of educational course materials. Although there can be many more categorizations, RSECM chooses only these forms of educational file and subject it to Hadoop. The variable p basically represents *HRegion*, and q represents *MemoryStorage* and *HFile* of Hbase. The variable k represents the number of blocks of *HRegions* in Hbase, while r represents *HLog*. The data j is then finally passed on to the reducer that forwards the data to Hbase and thereby converting the entire data to structured one.

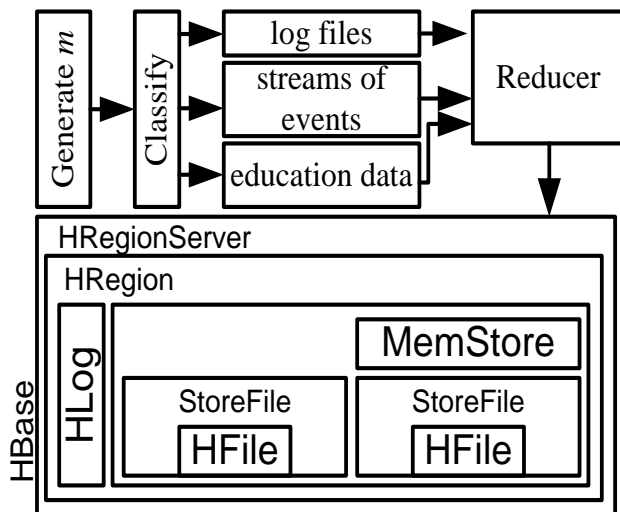


Fig. 7. HBase Architecture

HBase architecture essentially acts as the filter to eliminate the complexities associated with unstructured data (Fig.7). The context-based search in the secure educational interactive digital library provides various features to the instructor and student. The privileges are controlled by the Policy maker. The student and instructor are provided with single as well as multiple authentication schemes. The policy maker performs the action of enrolling of instructor and students. The instructor and students are entitled to different kind of privileges such as downloading, uploading or both as provided by the policy

maker who acts as administrator. The instructor and student are required to satisfy certain requirement to access the uniform interface successfully. The policymaker will provide a single or multiple authentication schemes to the instructor and student. Each time a student or instructor is enrolled into the digital library, he/she is required to provide certain information's, for instance, such as his credentials, background interests, prior knowledge and so on. All these information is used to generate context and are saved in the form of simple text in the cloud, which will contain all other information such as credentials like passwords, blog history and so on. In order to have access to the digital library, instructor and students must provide certain credentials such as username/email and password for single login. In a case of multiple authentication schemes, the procedure is illustrated in the form of the algorithm. The algorithm for performing data mining using the contextual search engine is highlighted in Table 4.

TABLE IV. DATA MINING WITH CONTEXTUAL SEARCH ENGINE

Algorithm-4: Mining with Contextual Search Engine

Input: $j_{\text{hbase}(\text{row}, \text{col})}$ (Structured data)

Output: Matched data

Start

1. $j_{\text{hbase}(\text{row}, \text{col})} \rightarrow \text{preprocess}$
2. Extract FV
3. Store FV in $j_{\text{hbase}(\text{row}, \text{col})}$
4. For Simple Search
5. $\text{query}_{\text{user}} \rightarrow \text{query}_{\text{hbase}}$
6. For $l=1:\text{size}(\text{query}_{\text{user}})$
7. Match $\text{query}_{\text{hbase}}$ with source file
8. Match $\text{query}_{\text{hbase}}$ with matching contents
9. Return r_{hbase} ;
10. For Contextual Search
11. If $(U_{\text{SH}}, \text{query}_{\text{user}}) = r_{\text{hbase}}$
12. $\text{recom}_{\text{cont}} = r_{\text{hbase}}$
13. If $(U_{\text{BI}}, \text{query}_{\text{user}}) = r_{\text{hbase}}$
14. $\text{recom}_{\text{cont}} = r_{\text{hbase}}$

End

The output of Algorithm-3 i.e. structured data from Hbase is considered as input for Algorithm-4. A simple preprocessing is applied to the structured data and feature vector FV is extracted that is ultimately stored back to the same cluster node i.e. Hbase. The entire algorithm works in two methods e.g. i) simple search and ii) contextual search. In simple search method, the size of the user-defined query is considered to be the highest limit of *for* loop in order to perform an iteration of similarity match in the search mechanism of RSECM. The user-defined query is matched with source file as well as matching contents to finally return a result from Hbase i.e. r_{hbase} .

In contextual-based search, the system checks if the search history of the user U_{SH} , as well as their query $\text{query}_{\text{user}}$, is found equivalent to outcomes of Hbase i.e. r_{hbase} than the system considers r_{hbase} as recommended outcome against the user-defined the query. Similarly, if the background information U_{BI} and user query are found equivalent to r_{hbase} , that the system considers r_{hbase} as recommended outcomes against the user search. Therefore, the search operation supports two kinds of search; one is the simple search whereas the other is contextual

search. These two search operations are illustrated using algorithms. The search operation is preceded by the streaming of data, wherein the data is received, mined, and stored in the HBase in order to perform the search operation, data mining of the unstructured data which is collected as plaintext from the various context and stored in the cloud is used. The mining operation is as follows.

- Reads the unstructured data from the cloud
- Perform operations like preprocessing which include removal of stop word, URL, HTML content, removing spaces, noisy data, special characters and less informative or less significant words.
- Feature Extraction performs the tokenization or vectorization of string; extracts featured data, and stores these featured data into HBase.

A simple keyword-based search is initiated by the user. The system performs tokenization on this basis and searches for relevant data based on a keyword is searched. Here the user authentication is not needed. Be it simple or advance search mechanism, the system keeps a consistent check of the statistical information i.e. frequencies of the word and word proximity for all the input objects. Simple inferential statistics could be used for better inference mechanism in order to extract better knowledge after every query processing. Algorithm-4 uses the advantage of statistical computation carried out by Hbase in order to perform discrete query processing. In advanced search, the algorithm differs slightly from the earlier one used for the simple search. Here also the search begins with the keyword provided by the user, and the same principle of tokenization is also followed here. The search here differs from prior step in the sense, here the search performed is based on the context basis, i.e. the search here considers different parameters like the user's search history, context related to his background, context from his profile, and various context related to the user available within the cloud. The important thing to be noted here is the user authentication is needed here; the user needs to be in active session, so it has to access the user profile. One more difference between the simple search and the advanced search is the output of the advanced search is recommended whereas the simple search provides relevant data. The recommended data is obtained by checking the user profile history and other parameters based on the context. When this context matches with the keyword for search, these are generated as recommended search and provided to the user. When the search query is not matched with the result of user background or user profile history, the result returned is simple search result without recommendation. In case of multiple keywords each of the keyword is checked within the user profile history and when matched with the result are provided as recommended output. Compared to simple search, the advanced search gives more precise and more accurate data required by the user as it involves the searching of the user profile history, it also searches the most searched content or data by the user during the process of recommending advanced search result. The complete operation of the novel contextual-based search is highlighted in Fig.8. Hence, the proposed system uses quite a novel and simple process for extracting the features in order to provide a relevant

search outcome for the users of this framework. The search engine is designed to provide both extensive search outcomes as well as narrowed and highly relevant search outcomes.

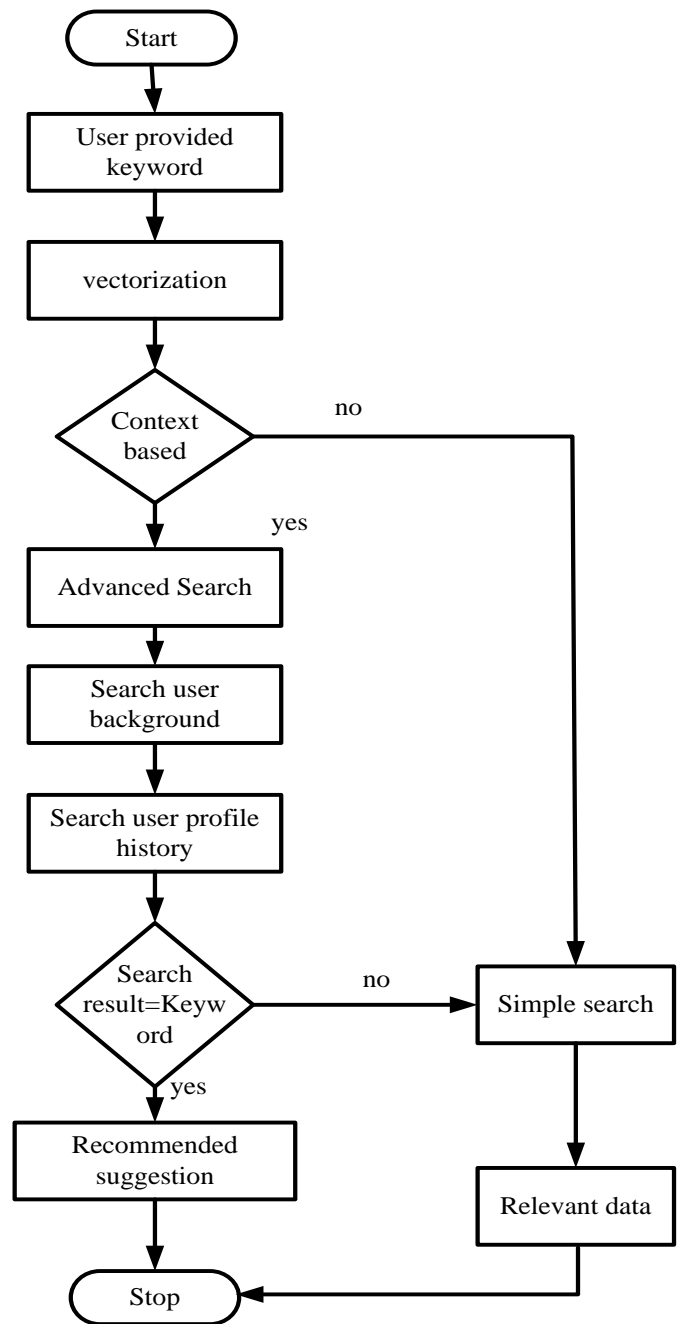


Fig. 8. Process flowchart of search operation

VII. RESULT AND DISCUSSION

This section discusses about the outcomes of the study that is compared with the conventional data mining technique using the SQL-based search engine. In order to talk about the results, it is necessary that we generate data on real-time basis. We have already developed an experimental prototype over Java to

generate educational big data [6] along with security features incorporated in it [5]. Hence, the output of unstructured or semi-structured data is fed to Hbase and proposed algorithm to design and develop contextual-based search engine. The software testing is done using black-box testing, unit-testing, integration testing, and system testing. The formulations of text-cases are done on the basis of evaluating the core objectives of proposed system i.e. accuracy of search outcomes. Owing to the nature of novelty in the proposed study, we choose to craft novel performance parameters in order to gauge the effectiveness of the study. Following are the performance parameters:

- *Processing Time (PT)*: It is the total time consumed to process the entire algorithm processing right from query origination to recommendation generation from Hbase cluster node.
- *Actually Recognized Context (ARC)*: It is a measure of actual context being correctly matched with that of user-defined query.
- *Falsely Identified Context (FIC)*: It is a measure of outcome for context that doesn't completely match with the query of the user.
- *Missing Context (MC)*: It is a measure of an outcome that doesn't have any matching context for the user query.

The technique uses manual approach for evaluating the Total Context (TC) where the Context Identification Rate (CIR) can be computed as:

$$CIR = ARC / TC$$

TC can be initialized to a number corresponding to some search history as well as background information of the user. And the error in the context identification rate (ECIR) is evaluated as,

$$ECIR = FIC / [ARC + FIC]$$

The system also has computation of Non-Context identification rate (NCIR) as

$$NCIR = MC / ARC$$

The numerical outcome of the study is shown in Table 5. In order to make the analysis easier, we consider the equal number of TC. A closer look into the outcomes will show that proposed study offers significantly lesser rate of error in contextual search as witnessed by the values of ECIR and NCIR as compared to the SQL. The prime reason behind this is SQL uses relational structuring of the database while proposed RSECM is based on wide column data storage on Hbase. This results in maximum processing time for SQL which is never recommended for analyzing big educational data. Moreover, SQL based mining approach is based on tabular data stream, JDBC, and ODBC, while the RSECM is designed based on Java API with supportability of Hbase resulting in an efficient conversion of unstructured to structured database. Another interesting part is the inclusion of MapReduce that allows processing the distributed file system.

TABLE V. COMPARATIVE ANALYSIS OUTCOME

	TC	ARC	FIC	MC	CIR	ECIR	NCIR
RSECM	500	393	17	19	0.786	4.146341	4.834606
	500	349	14	11	0.698	3.856749	3.151862
	500	251	27	22	0.502	9.71223	8.76494
	500	458	18	25	0.916	3.781513	5.458515
	500	350	17	19	0.7	4.632153	5.428571
	500	485	27	21	0.97	5.273438	4.329897
SQL	500	175	87	79	0.35	33.20611	45.14286
	500	161	50	35	0.322	23.69668	21.73913
	500	251	94	94	0.502	27.24638	37.4502
	500	188	39	55	0.376	17.18062	29.25532
	500	167	55	70	0.334	24.77477	41.91617
	500	105	38	37	0.21	26.57343	35.2381

Map Reduce is highly essential to be used for data mining process as the data is actually stored in distributed nodes and Map Reduce can process the data in highly distributed manner on the cluster nodes. This capability is quite missing in the SQL based data analyzing techniques. Every node has the capability to process the data potentially rather than simply moving the data on the network. Apart from the conventional database (SQL or any other RDBMS) system, RSECM enables to carry out the querying of the data in real-time by building the data over columnar fashion using Hbase. Originally, this columnar pattern in Hbase acts like a hash table resulting in faster query processing as compared to conventional SQL. Fig.9 is the evidence of it.

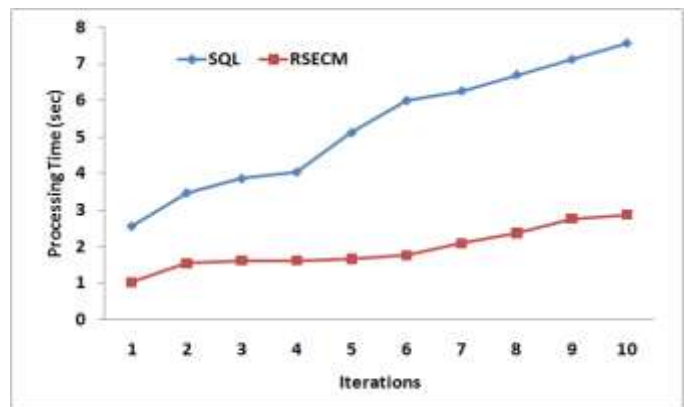


Fig. 9. Processing Time of RSECM and SQL

After reviewing the cumulative outcomes, it can be said that RSECM is highly suitable if there is a need to process massive educational data which lies in idle servers in educational institutions. The approach is also quite cost effective as RSECM doesn't require any particular modeling, however, SQL based approach of context mining is 100% dependent on data modeling. The system also offers an enormous scale of processing capabilities as well as storage facilities at a

comparatively lower cost as compared to any SQL-based search engines. Another interesting point of optimistic outcome is RSECM also supports parallel processing and can even run various set of data in parallel and yield the outcomes as faster as possible.

VIII. CONCLUSION

From the study of existing literature as well as observing the industrial trends, it is found that Hadoop has been familiarized too much. One of the most challenging facts explored is that the existing technique based on Hadoop for storing and processing the big data is just beginning. The fact of familiarization is only because of the open source nature. There are multiple sources which say advantageous features of Hadoop as well as disadvantageous features of Hadoop not only for data storage but also for mining approaches. The phenomenon of inapplicability of conventional mining technique is another reason to boost various research attempts. This paper has focused on one of the rising arenas of education system where the entire data management of educational system will give rise to big data, which is not possible for any conventional RDBMS framework or data mining technique to normalize it and make it valuable for us. Hence, this paper has developed a technique with the aid of Oracle Virtual Box where the unstructured data is converted to structured data, and then a context based mining is used to extract the knowledge of the data. The proposed system has been tested on multiple platforms as well as multiple machines in order to cross-check its performance of processing the educational big data. The outcomes are quite optimistic and highly encouraging. We gave more emphases on computational speed as it is an only problem that many researchers are encountering to achieve in developing data mining techniques over cloud.

For the future research prospective considering scope of educational big data, the proposed framework can be used to improvise the students learning skills. This work gives the hints for future researches to improve further more computational speed along with the futuristic real time educational data.

REFERENCES

- [1] H. Kanematsu, D. M. Barry, *STEM and ICT Education in Intelligent Environments*, Springer, 2015.
- [2] G. Vincenti, A. Bucciero, C. V. Carvalho, *E-Learning, E-Education, and Online Training*, Springer International Publishing, 2014.
- [3] L. Uden, J. Sinclair, Y-H Tao, D Liberona, *Learning Technology for Education in Cloud - MOOC and Big Data*, Springer, 2014.
- [4] D. Pratiba, G. Shobha, "Educational BigData Mining Approach in Cloud: Reviewing the Trend", *International Journal of Computer Applications*, Vol. 92, no.13, April 2014.
- [5] D. Pratiba, G. Shobha, "S-DILS: Framework for Secured Digital Interaction Learning System Using keccak", *Springer-Software Engineering in Intelligent System, Advances in Intelligent Systems and Computing* vol.349, pp.175-187, 2015.
- [6] D. Pratiba, G. Shobha, "IDLS: Framework for Interactive Digital Learning System with Efficient Component Modelling", *Springer-Proceedings of Third International Conference on Emerging Research in Computing, Information, Communication and Applications*, 2015.
- [7] M. Levene, "An Introduction to Search Engines and Web Navigation, John Wiley & Sons", 2011.
- [8] I. Koch, "Analysis of Multivariate and High-Dimensional Data", Cambridge University Press, 2013

- [9] J. Leskovec, A. Rajaraman, J. D. Ullman, "Mining of Massive Datasets", Cambridge University Press, 13-Nov-2014.
- [10] S. E. Ahmed, "Perspectives on Big Data Analysis: Methodologies and Applications", American Mathematical Society, 20-Aug-2014.
- [11] A.Belle, R.Thiagarajan, S. M. Reza Soroushmehr, F.Navidi, D.A. Beard, and K. Najarian, "Review Article Big Data Analytics in Healthcare", Hindawi Publishing Corporation BioMed Research International, pp. 16, 2015.
- [12] G. Cao, I. Ahmad, H. Zhang, W. Xie, and M. Gabbouj, "Balance learning to rank in big data", *Proceedings of the 22nd European in Signal Processing Conference (EUSIPCO)*, pp. 1422-1426, 2014.
- [13] F. Chen, P. Deng, J.Wan, D. Zhang, A. V. Vasilakos, and X. Rong, "Review Article Data Mining for the Internet of Things: Literature Review and Challenges", Hindawi Publishing Corporation International Journal of Distributed Sensor Networks, Article ID 431047, 2015.
- [14] Z. Khan, A. Anjum, K. Soomro, and M.A. Tahir, "Towards cloud based big data analytics for smart future cities", *Journal of Cloud Computing*, Vol. 4, No. 1, pp.1-11, 2015.
- [15] I. Merelli, H. P-Sánchez, S. Gesing, and D.D. Agostino, "Review Article Managing, Analysing, and Integrating Big Data in Medical Bioinformatics: Open Problems and Future Perspectives", Hindawi Publishing Corporation Bio-Med Research International, 2014.
- [16] M.M. Najafabadi, F. Villanustre, T. M. Khoshgoftaar, N. Seliya, R. Wald, and E. Muharemagic, "Deep learning applications and challenges in big data analytics", *Journal of Big Data*, Vol. 2, no. 1, pp.1-21, 2015.
- [17] T.J. Oyana, "Research Article A New-Fangled FES-k -Means Clustering Algorithm for Disease Discovery and Visual Analytics", Hindawi Publishing Corporation EURASIP Journal on Bioinformatics and Systems Biology, pp. 14, 2010.
- [18] S.Ramachandramurthy, S.Subramaniam, and C. Ramasamy, "Research Article Distilling Big Data: Refining Quality Information in the Era of Yottabytes", Hindawi Publishing Corporation Scientific World Journal, 2015.
- [19] K. Slavakis, G.B. Giannakis, and G. Mateos, "Modeling and Optimization for Big Data Analytics", *IEEE Signal Processing Magazine*, 2014.
- [20] M. Cataldi, C. Schifanella, K. S. Candan, M. L. Sapino, and L. D. Caro, "Cosena: a context-based search and navigation system", *Proceedings of the International Conference on Management of Emergent Digital Eco Systems*, pp. 33, 2009.
- [21] S. Santini, and A. Dumitrescu, "Context based semantic data retrieval", *Proceedings of JSWEB*, 9th Sep, 2015.
- [22] M. Fisher, and P. Hanrahan, "Context-based search for 3D models", *ACM Transactions on Graphics (TOG)*, Vol. 29, No. 6, pp. 182, 2010.
- [23] N.D. Lane, D. Lymberopoulos, F. Zhao, and A. T. Campbell, "Hapori: context-based local search for mobile phones using community behavioral modeling and similarity", *Proceedings of the 12th ACM international conference on Ubiquitous computing*, pp. 109-118, 2010.
- [24] G. Adomavicius, and A. Tuzhilin, "Context-aware recommender systems", *Recommender systems handbook*, Springer US, pp. 217-253, 2011.
- [25] C-T. Li, M-K. Shan, and S-D. Lin, "Context-based people search in labeled social networks", *Proceedings of the 20th ACM international conference on Information and knowledge management*, pp. 1607-1612, 2011.
- [26] C.F.D. Silva, P.Hoffmann and P.Ghodous, "Improve Business Interoperability through Context-based Ontology Reconciliation", *International Journal of Electronic Business Management*, Vol. 9, no. 4, pp. 281-295, 2011.
- [27] M. Thangaraj, and V. Gayatri, "A new context oriented synonym based searching technique for digital collection", *International Journal of Machine Learning and Computing*, Vol. 1, no. 1, 2011.
- [28] N. Vashnik, S. Sahu, D. Roy, "TALASH: A Semantic and Context based Optimized Hindi Search Engine", *International Journal of Computer Science, Engineering and Information Technology (IJCEIT)*, Vol.2, no.3, 2012.

- [29] P. Gupta, "A novel approach for context based focused search engine", PhD diss., JAYPEE Institute of Information Technology, 2013.
- [30] M.M. Rahman, S. Yeasmin, and C.K. Roy, "Towards a context-aware IDE-based meta search engine for recommendation about programming errors and exceptions", IEEE Conference of Software Maintenance, Reengineering and Reverse Engineering (CSMR-WCRE), Software Evolution Week-, pp. 194-203, 2014.
- [31] Gormley, Clinton, and Zachary Tong. "Elasticsearch: The Definitive Guide", O'Reilly Media, Inc.", 2015.

A Heterogeneous Framework to Detect Intruder Attacks in Wireless Sensor Networks

Mustafa Al-Fayoumi

Computer Science Department
Prince Sattam bin Abdulaziz University,
KSA
Princess Sumaya University for
Technology
(PSUT), Amman, Jordan

Yasir Ahmad

Computer Science Department
Prince Sattam bin Abdulaziz University
Riyadh,
Saudi Arabia

Usman Tariq

Information Systems Department
Prince Sattam bin Abdulaziz University
Riyadh,
Saudi Arabia

Abstract—Wireless sensor network (WSN) has been broadly implemented in real world applications, such as monitoring of forest fire, military targets detection, medical and/or science areas and above all in our daily home life as well. Nevertheless, WSNs are effortlessly compromised by adversaries due to their broadcast transmission medium as a means of communication which are lacking in tamper resistance. Consequently, an intruder can over hear all traffic, replay previous messages, inject malicious data packets, or can compromise a node. Commonly, sensor nodes are very much vulnerable of two main issues in security aspect that are node authentication and compromising a node. In this paper, a heterogeneous framework of node capture and intrusion detection for WSNs is proposed. This framework efficiently detects the captured nodes by using a novel technique, embedded with an Intrusion Detection mechanism which aggregates Signature and Anomaly based approach with Neural Network Multi-Layer Perceptron (MLP) classification in a clustering environment. Moreover, the proposed framework achieves efficiency at reasonable computation and communication costs and it can be a security shield to real WSN applications.

Keywords—Intrusion; node compromise; anomaly; signature; MLP

I. INTRODUCTION

Sensor networks are immensely distributive networks of tiny, light-weight wireless nodes, deployed in huge numbers for the monitoring of environment by the calculation of physical parameters e.g., pressure, temperature, or relative humidity. The current advances in (MEMS) Micro electro mechanical systems technology made possible to build sensors [1]. Some of the important applications of wireless sensor networks are as follows:

- Wireless sensor networks could be an essential part of military command, computing control, communications, surveillance, intelligence, and targeting systems [2].
- Sensor networks are also largely applied in agriculture research, habitat monitoring, fire detection and traffic management [3].

- Sensor networks are extensively used in home appliances, health care, classroom operations, and structural monitoring [4-8]

The topology design in the WSNs differs from an easy star network to a complex wireless multi-hop mesh network. Data propagation technique used in between the different network hops could be flooding or routing. Conventional WSNs are susceptible to various kinds of attacks. These attacks could be typically classified into following types [9-10]: (i) attack on the authentication and secrecy, (ii) attack on availability of the network, and (iii) hidden attacks on service integrity. The focus of this paper is on the first and third types of attacks on sensor networks. Currently, security mechanisms for sensor networks focus on external attacks, and these mechanisms fails to protect internal attacks where a group of sensor nodes being compromised. In hidden attacks, an intruder tries to compromise a sensor node so as to inject fake data. In this form of attack, an intruder accesses the codes and encryption keys utilized by the network. The adversary can constantly interrupt or halt the normal functions of the sensor network e.g., building routing loops. A compromised node might impact the sensor network by sending the authenticated data to the base station. By physically accessing the sensor nodes an intruder can fully control the operations of few sensor nodes. Compromising a node is normally contemplated as one of a most challenging problem in WSN security [11].

An adversary attacking a node tries straightaway to tamper the captured node physically to retrieve the cryptographic information. This attack can harm the security in the architecture of the underlying network. Furthermore, it can possibly increase many consecutive power-full insider threats [12]. Once compromised by an adversary, the node can perform variety of tasks which it is commanded to do. The node can be directed to be a launch pad for spam posting, stealing private information, or spread spyware. Considering the operation of a WSN depends on the accuracy of the secret information exchanged between the nodes, the node compromise poses detrimental impact in WSNs. Consequently, a single compromised node could be a mighty weapon for an adversary in WSNs.

Since, wireless communication is susceptible to eavesdropping, an intruder can oversee the flow of data and tries to modify, intercept, disrupt, or falsify data packets [13] and disseminates incorrect information to the sink. Typically, sensor nodes have scarce resources and short transmission range, an intruder possessing huge processing capability and farther range of communication could compromise many sensors at a time in order to modify the real data during communication.

A large number of security relevant solutions are previously proposed e.g., exchanging the key, authentication, secure routing, safety mechanisms for particular attacks. To some level these security techniques are able to ensure the security; however, they can't remove the security attacks completely [14]. To overwhelm the challenge faced by WSNs, this paper proposes a scheme which efficiently detects the captured nodes by using a novel technique, embedded with an Intrusion Detection mechanism which utilizes Anomaly and Signature based approach in the combination of Clustering, and Neural Network Multi-Layer Perceptron (MLP) classification algorithm [15].

The remaining parts of this paper are organized as follows: Section 2, gives the literature review and related works. Section 3 describes the framework with details of algorithms of the proposed solution. The experimental results are demonstrated in section 4. The paper is concluded in section 5.

II. LITERATURE REVIEW

In [9] the authors propose 'software based attestation for embedded devices' (SWATT) to discover an immediate change in the content of sensor memory which indicates the chance of an attack.

In [16], Hartung et. al., retrieve the cryptography secrets on a sensor node of MICA2 type by removing its inner memory via the JTAG interface. This attack is further explored in [17], where Becher et. al., displays how to retrieve many components of node hardware like external memory, and the boot-strap loader or the JTAG-interface. The authors suggested that the programming interfaces should be disabled so that unauthorized access to the microcontroller is prevented. They also indicated that if the node is captured it certainly remains absent for a considerable period which is enough to figure out node captivity.

[18] presents an absolute distributed-detection system which cooperates with nearest node(s) to yield a decision regarding the malicious behavior of the sensors. The authors enhance the starting security framework and develop a more promising Intrusion Detection System agent architecture which is known as LIDeA (lightweight-intrusion detection architecture) in [19]. They proposed a new encryption scheme which secures the network from external attacks and also devised few rules to detect sinkhole attack. They focused on MintRoute-routing protocol, and the approach they proposed is not applicable to the routing protocols like LEACH protocol and more.

In [20] the authors developed an Intrusion Detection system which is based upon SEP (Stable Election Protocol) for

clustered-heterogeneous WSNs. The advantage of adopting SEP protocol is its heterogeneity awareness in order to increase the life time of the first node before its death. They trained their system to identify four-types of attacks that are DOS, Probe, R2L, and U2R. Their proposed scheme used the KNN (K-nearest neighbor) classifier to detect an anomaly in the system.

In [21] the authors proposed the IP address, MAC address, and Port Number based intruder sniffing system for cluster-based WSNs. According to them, the proposed approach is truly efficient in energy consumption for initial detection & prevention of security risks and attacks. They argued that initial detection & prevention of the adversary by effective security system restricts several problems such as network slowdown, injecting of fake data, and much more. They also believed that by designing a security mechanism where a Base Station has the responsibility of the overall network security, higher security measures are expected without draining the energy levels of the cluster heads as well as individual sensor nodes.

In [22], Coppolino et.al, has shown a light weight, hybrid and distributed IDS for WSNs. They utilized both anomaly based and misuse based techniques. Their technique consists of a central agent (CA) which carries out an extremely accurate intrusion detection by devising data mining methods and they consider local agents (LA) that are lighter running on motes to detect intrusions.

In [23], Yassine et.al, proposed an IDS model which uses anomaly detection based on SVM technique and a set of attacks that are represented by fixed rule signatures. These signatures are designed to detect the malicious behavior of the intruder by anomaly detection method. This approach is implemented in a cluster based topology to increase the network lifetime.

III. THE PROPOSED FRAMEWORK

The proposed framework defends the network from various types of attacks on service integrity, authentication and secrecy etc., and at the same time it doesn't depend on a particular routing protocol. The proposed framework is assumed geographic routing with a slight modification in multi-hop topology. In the proposed routing protocol, nodes need to only be aware about the locations of nearest neighbors' in the cluster; through the network the data packets are routed by being forwarded to a cluster. The major advantages of geographic routing over other routing strategies of WSNs include; (i) stateless, and therefore highly energy efficient, nature of routing, (ii) fast adaptability to network's topological changes, and (iii) scalability [24-25] which should be the main objectives while deploying any type of WSN. These distinguished characteristics makes the protocol efficient, simple, and physically deployable, averting the use of practical routing that can originate complexity and also overhead in the mobile framework. The methodology of the proposed framework as follows:

A. Hidden attacks on Service integrity:

The sensor nodes are deployed sparsely in the network. After the deployment the sensors those are physically closer chooses a cluster head unanimously which depends upon

various parameters like battery power etc at the selection time. This selection is dynamic in the sense the node with higher battery power is selected as a CH. The sensors in a cluster dynamically create the node ID lists of the neighboring nodes and the CH. This list is maintained until the nodes changes the cluster itself or by the deployed authority or an adversary who tries to displace/compromise the node. The cluster head is responsible for the data transmission between the clusters which finally arrives to the sink. The deployed sensor reads/senses the data from the environment and disseminates it to the cluster head by applying geographic routing protocol. Then it is the responsibility of the cluster head to transmit the data to another CH or to the sink. This paper proposes an algorithm to prevent the possible node compromise by an adversary:

ALGORITHM 1:

Begin

1) If ' n_1 ' and any other neighboring node ' n_2 ' talks to each other (by transmitting messages) after a specified interval of time about their presence and non-compromising behavior in the network. Two cases arise about this scenario:

a) If a node ' n_1 ' is not sending the message to its neighboring nodes due to some other reason except node compromise in the specified period of time say ' t ', there may be many possible reasons like traffic congestion, re-configuring its hardware etc.

b) If a node ' n_1 ' is compromised, the neighboring node ' n_2 ' waits for the message for a specified period of time say ' t ', and then broadcasts the failure mode of node ' n_1 ' all the neighboring node blocks the node ID in their lists temporarily for a certain threshold time ' T '. When the compromised node doesn't acknowledge its presence after the expiration of the threshold is blocked permanently and black listed from the network.

2) If an adversary tries to shift the location of any particular node(s) from the deployed area so as to compromise its immediate neighboring node ID list, retrieve the cryptographic keys etc. Two cases arise:

a) The attacked node senses the displacement by an unauthorized authority without a certain predefined verification shuts down the system immediately and erases its memory and node ID list.

b) The displaced node before shutting the system down raises an alarm and notifies about the attack to the neighboring nodes and the CH.

End

Below is the flow chart representation of proposed node compromise algorithm, as shown in Fig. 1.

B. Attack on the authentication and the secrecy:

An Intrusion Detection System is one potential resolution for several security attacks in WSNs. IDS can only detect the attacks but are unable to prevent them. Once detected, the IDSs can raise an alarm to apprise the controller to take appropriate action. The standard classification of intrusion in networks fall into four major categories: DoS, Probe, U2R and R2L Two

main classes of IDSs exists. (1) rule based IDS and (2) anomaly based IDS [26]. Rule based or signature based IDS is used for the detection of intrusions with the assistance of built in signatures. Rule based IDS has the ability to detect known attacks with greater accuracy, however, it is not able to detect attacks that are new and for which there are no signatures present in the intrusion database. Whereas, Anomaly based IDSs are able to detect new and novel intrusions using the matching of routine traffic patterns and/or resource utilizations.

For authentication and secure data transmission in the wireless sensor network, a hybrid Intrusion Detection System, anomaly & Signature based is proposed. The proposed IDS scheme is also distributed in the following way; (i) misuse based IDS are implemented locally in the nodes. The network is trained to detect several types of known attacks before the deployment phase, and the signatures are added in the nodes profile. This misuse (signature) based IDS is a light weight scheme and is used to detect known attacks on the network.

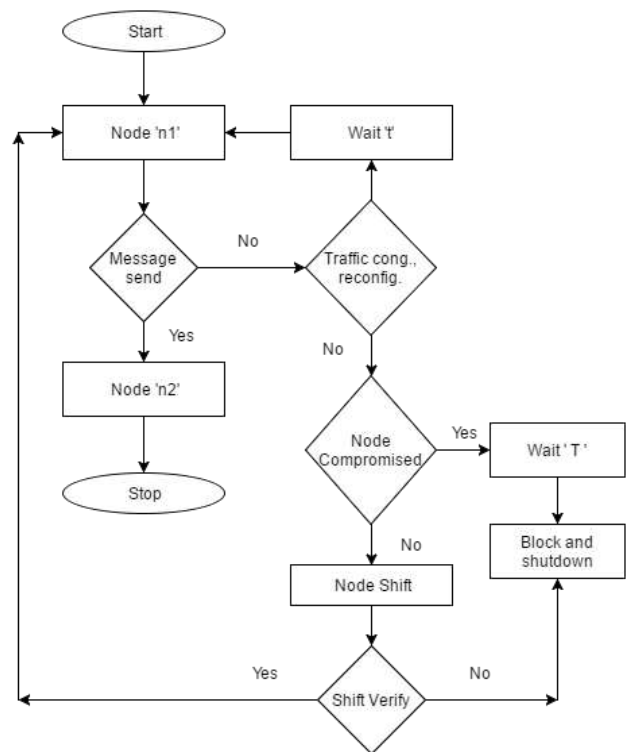


Fig. 1. Algorithm #1 Flowchart

In case of new or novel attacks which can't be detected by the signature based scheme in the sensor nodes, (ii) anomaly based IDS which is implemented in the CHs comes into action. Anomaly based IDS scheme in the CHs detects any deviation from the normal functioning of the network. If a deviation is being detected, the CH immediately stops the transmission of data and informs the neighboring CHs by raising some kind of alarm. Simultaneously, the new signature pattern which is based on this deviation is added to the misuse based IDS profile in the sensor nodes for future detection.

In this way, both the IDS techniques are utilized in a very efficient and optimal manner. This technique makes the proposed network robust and secure from several kinds of

intruder attacks. This scheme is basically a blend of stand-alone and hierarchical architecture in WSNs. The proposed IDS scheme has an advantage over the monitoring node schemes in the literature, IDS is implemented in all the sensor nodes which makes them self-dependable to resist any kind of attack to a large extent, and at the same time not to rely on any other monitoring node for the intrusion detection purpose, which if compromised disrupts all the network functionality.

C. Anomaly based detection model:

This model is proposed to implement the Multi-Layer Perceptron (MLP) (Fig. 2) and the backpropagation algorithm for the training of anomaly based detection system. It is a supervised learning algorithm [27]. The MLP is an artificial neural network which is extensively used to solve different problems like pattern recognition, digression etc. Multi-layer Perceptron is a network that is composed of several neurons, which are divided into input layer, output layer, and one or more hidden layers. The function that connects the input and the target output is what the perceptron must find. The way it accomplishes this is by this very simple rule:

$$y_i = f \left(\sum_{j=1}^m w_{ij} x_j + b_i \right) \quad (1)$$

Equation (1) calculates y_i which is the output of the node, w denotes the vector of weights, x is the vector of inputs, b is the bias and f is the activation function.

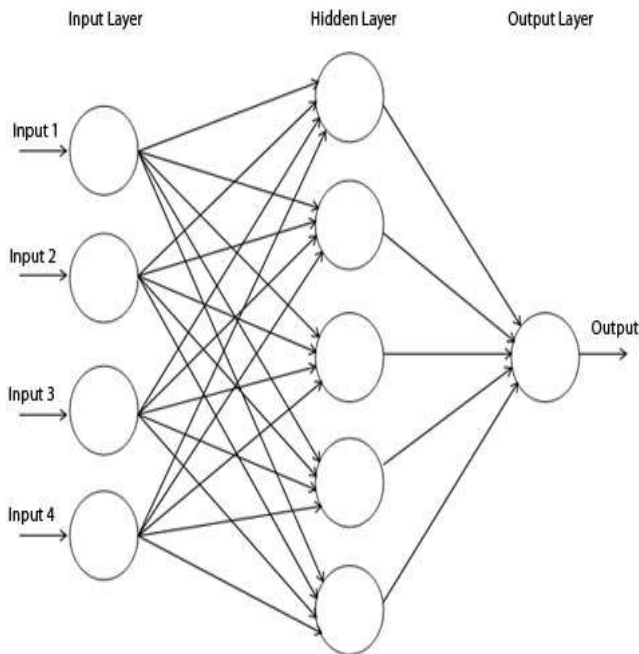


Fig. 2. MLP Diagram

Design: In this case, the proposed IDS consist of several neural networks which operate in parallel [28]. Every CH is a three-layer neural network and has its own training data sets for intrusion detection. The back-propagation algorithm is used to train the individual CH nodes. The parameters were implemented are listed below:

- Back propagation algorithm used for CH IDS learning.
- MLP structure is utilized with input, hidden, and output layers.
- Learning rate is set to η (0.1 – 1.0).
- Sigmoid function is used as activation function.

The MLP algorithm which is implemented in CHs for anomaly based IDS is defined as follows:

ALGORITHM 2:

Begin

- Initialize weights at random, choose a learning rate η
- Train the network for each training example (input pattern and target output (s)):
 - Do - Until output is produced:
 - Do - forward pass through network layer by layer:
 - Apply Inputs
 - Multiply by weights
 - Sum up the outputs
 - Apply sigmoid activation function
 - Pass the output to next layer
 - Done
 - Compute error (delta or local gradient) for each output unit δ_k
 - By backpropagation Layer-by-layer, compute error (delta or local gradient) for each hidden unit δ_j
 - Correct the output layer of weights.
 - Correct the input weights.
 - Update all the weights Δw_{ij}
- Done

End

Below is the flow chart representation of the proposed anomaly detection (MLP) algorithm, as shown in Fig. 3.

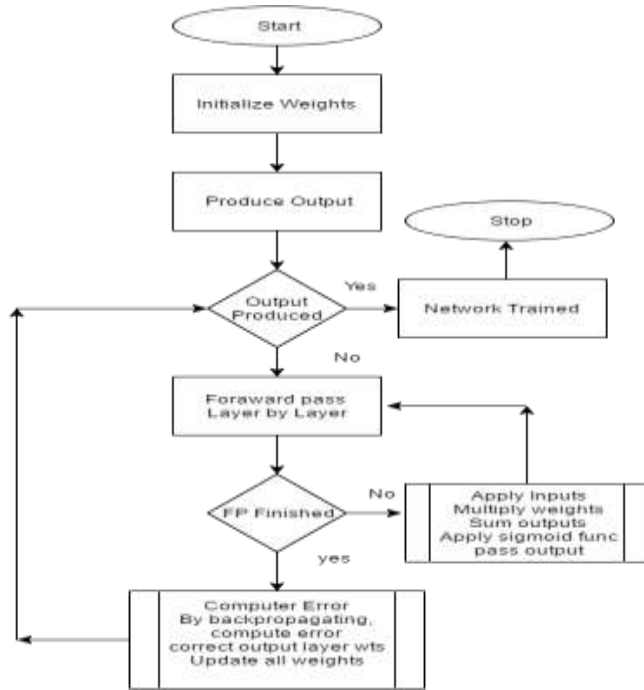


Fig. 3. Algorithm #2 Flowchart

The structure of neural networks and WSNs has similar characteristics i.e., inter-connected components. Both types of networks implement functions which maps the input values to the output values. Artificial neural networks (ANN) have general characteristics which are desirable in WSNs also. The selection of ANN MLP classification algorithm for the training of anomaly based detection in CHs has many reasons which are defined as under:

- This technique is designed to be parallelized.
- It is very fast to evaluate new attacks.
- It is also robust on noisy training data which is inherent in WSNs.

MLP classifies the data into five categories which are Normal, Probe, DoS, U2R, and R2L. This approach reduces the (FA) false alarm at the same time maintains accuracy and detection at higher range. With respect to previous researches in intrusion detection, the performance of IDS is calculated and evaluated by measure of accuracy, detection rate and false alarm which are defined in the “(2)”, “(3)” and “(4)” as follows:

$$Accuracy (A) = \frac{TP + TN}{TP + TN + FP + FN} \quad (2)$$

$$Detection Rate (DR) = \frac{TP}{TP + FP} \quad (3)$$

$$False Alarm (FA) = \frac{FP}{FP + TN} \quad (4)$$

IV. EXPERIMENTAL RESULTS

The performed experiments have been conducted to evaluate the proposed framework in terms of accuracy, attack detection rate and false alarm. The evaluation of proposed IDS detection system is conducted using KDD Cup 99 dataset [29]. The specified dataset is denounced for repetition of records. This repetition of records precludes the learning algorithms to detect unknown attacks [30]. Notwithstanding, it is the only publicly available labelled dataset which has been used extensively in the research field of intrusion detection. By experiments the proposed approach on KDD Cup 99 dataset provides a significant evaluation and makes the performance comparison with other advanced technique proportionate.

Two experiments have been carried out on MLP classifier and SVM using the KDD Cup 99 dataset. All experiments were performed on an Intel® core™ 2 Duo CPU T7500 @2.20 as computing machine with the following specifications: 4 GB main memory, and running Microsoft Windows 8. During the evaluation, the 10 percent labeled data of KDD Cup 99 dataset is utilized, where three types of legal traffic (TCP, UDP and ICMP) are available.

The evaluation of these experiments is based in terms of accuracy, attack detection rate and false alarm. Fig. 4 classifies the result for each type of data using testing dataset. Data from Table 1 is represented graphically in Fig. 5 which clearly shows that for the given attack categories, MLP performs better than K-M algorithm. Moreover, the data collected from Table 2 which is represented in Fig. 6 shows that in detecting false alarm MLP lags behind only in the probing category. MLP shows better detection performance more than 85% of attack records for probing category, more than 95% in DoS and more than 97% in R2L category.

TABLE I. DETECTION PROBABILITY OF ATTACKS

Comparison Criteria	Approaches	
	MLP	K-M
Probe	0.887	0.876
DoS	0.973	0.973
U2R	0.298	0.298
R2L	0.096	0.064

TABLE II. DETECTION PROBABILITY OF FALSE ALARMS

Comparison Criteria	Approaches	
	MLP	K-M
Probe	0.004	0.026
DoS	0.004	0.004
U2R	0.004	0.004
R2L	0.003	0.001

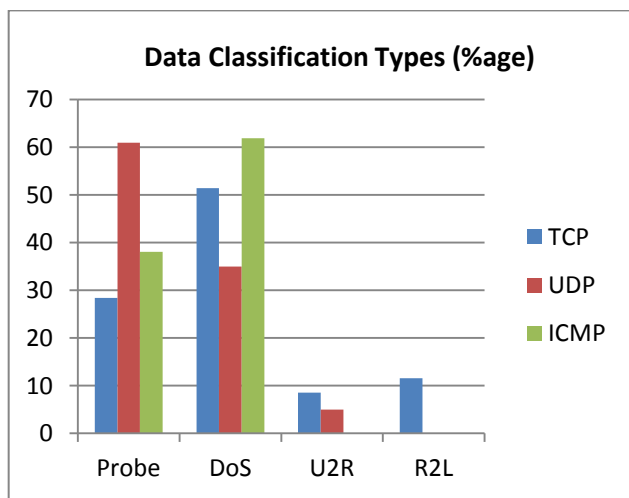


Fig. 4. Result of different classification Data types (Testing Dataset)

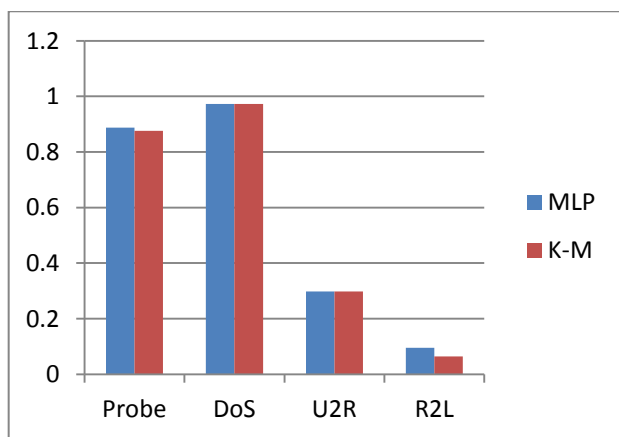


Fig. 5. Comparison of Detection probability of different Attacks

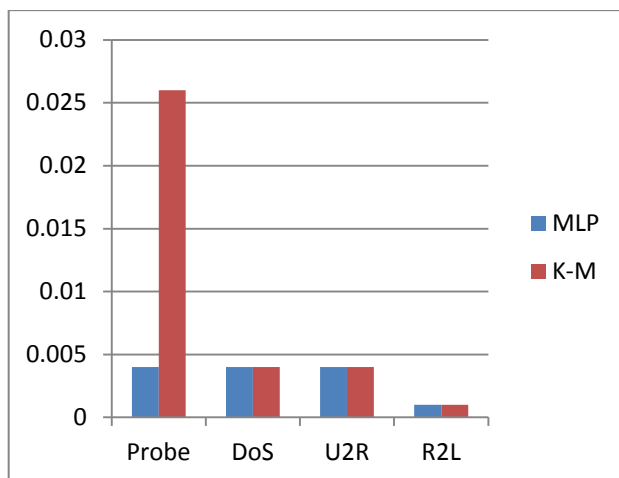


Fig. 6. Comparison of Detection probability of False Alarm

The Fig. 7 and 8 represent how different types of data (PN=Predicted Normal; PA=Predicted Attack) are classified by MLP network using the testing data set. As it can be seen clearly in Fig. 7 and 8 MLP Neural Network resulted fewer false positives and Negatives.

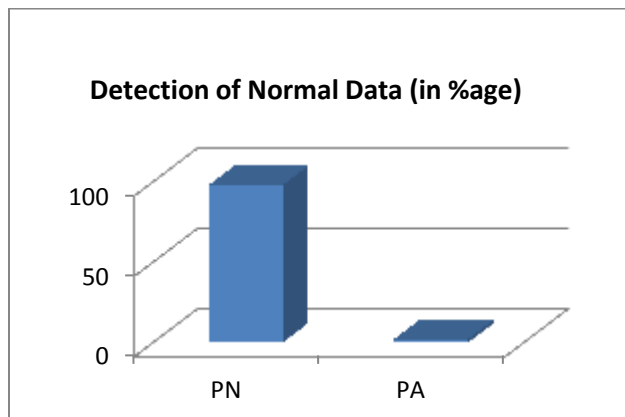


Fig. 7. Detection of Normal Data (Testing Dataset)

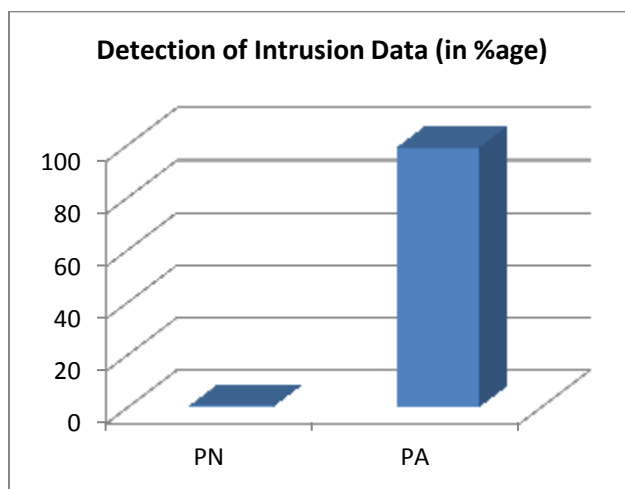


Fig. 8. Detection of Intrusion Data (Testing Dataset)

V. CONCLUSION AND FUTURE WORK

The proposed framework aims to protect the network from the attacks on service integrity, authentication and secrecy by employing a heterogeneous approach of intrusion detection. A heterogeneous IDS framework which utilizes many state-of-the-art approaches together to achieve the maximum probability of intrusion detection in WSNs. The different experiments which were carried out in comparison with K-M algorithm evaluates the performance of proposed technique of IDS on the KDD 1999 Cup dataset which showed that MLP detects more than 85% of attack records for probing category, more than 95% in DoS and also more than 97% in R2L category. It also showed promising results in detecting false alarms. In future, will be considered some more innovative techniques for intrusion detection in WSNs.

ACKNOWLEDGMENT

This project was supported by the deanship of scientific research at Prince Sattam bin Abdulaziz University under the research project # 2015/01/4646.

REFERENCES

- [1] I.F. Akyildiz, W. Su, Y. Sankarasubramaniam, and E. Cayirci, "A Survey on Sensor Networks," IEEE Communications Magazine, vol. 40, no. 8, pp. 102-116, August 2002.
- [2] Chee-Yee Chong, S.P. Kumar, "Sensor networks: evolution, opportunities, and challenges," Proceedings of the IEEE, vol.91, no.8, pp.1247,1256, Aug. 2003 doi: 10.1109/JPROC.2003.814918.
- [3] K. Martinez, J. K. Hart and R. Ong, "Environmental sensor networks," IEEE Computer, vol. 37, no. 8, pp. 50-56, Aug. 2004. doi: 10.1109/MC.2004.91.
- [4] L. Schwiebert, S.D.S. Gupta, J. Weinmann, "Research challenges in wireless networks of biomedical sensors," 7th annual international conference on Mobile computing and networking, (MobiCom2001), pp.151-165, July 2001, Rome, Italy. doi:10.1145/381677.381692.
- [5] G. Amato, S. Chessa, F. Conforti, A. Macerata, C. Marchesi, "Health Care Monitoring of Mobile Patients," ERCIM News No. 60 pp. 69-70, January 2005.
- [6] I. A. Essa, "Ubiquitous sensing for smart and aware environments," IEEE Personal Communications, vol. 7, no. 5, pp. 47-49, Oct 2000. doi: 10.1109/98.878538
- [7] M. Srivastava, R. Muntz, M. Potkonjak, 2001. "Smart Kindergarten: Sensor-based Wireless Networks for Smart Developmental Problem-solving Environments," 7th Annual Int. Conf. on Mobile Computing and Networking (MobiCom2001), pp.132-138 July 2001, Rome, Italy. doi: 10.1145/381677..381690.
- [8] N. Xu, S. Rangwala, K.K. Chintalapudi, D.Ganesan, A. Broad, R. Govindan, D. Estrin, "A Wireless Sensor Network for Structural Monitoring," SenSys '04 Proceedings of the 2nd international conference on Embedded networked sensor systems, Baltimore,MD,USA, , pp.13-24, November 20014. doi:10.1145/1031495.1031498.
- [9] P. Adrian, S. John, W. David, "Security in wireless sensor networks, "Communications of the ACM" vol. 47 no.6, June 2004. doi: 10.1145/990680.990707..
- [10] W. Wei, Q. Xu, L. Wang, X.H. Hei, P. Shen, W.Shi, L.Shan, "GI/Geom/1 queue based on communication model for mesh networks," International Journal of Communication Systems, vol. 27, no. 11, pp. 3013-3029, 2014.
- [11] C. Krauß, M. Schneider, C. Eckert, "On handling insider attacks in wireless sensor networks," Information Security Technical Report, vol. 13, no. 3, pp. 165-172, 2008.
- [12] C.P. Pfleeger, S.L. Pfleeger, Security in Computing, 3rd edition, Prentice Hall 2003.
- [13] Y. Ping, J. Xinghao, W. Yue, and L. Ning, "Distributed intrusion detection for mobile ad hoc networks," Journal of Systems Engineering and Electronics, vol. 19, no. 4, pp. 851-859, 2008.
- [14] C. Hartung, J. Balasalle, R. Han, "Node Compromise in Sensor Networks: The Need for Secure Systems," CU-CS-990-05. Computer Science Technical Report, Paper 926, January 2005. http://scholar.colorado.edu/csci_techreports/926.
- [15] W. Wei, X.L. Yang, P.Y. Shen, B. Zhou, "Holes detection in anisotropic sensor networks: Topological methods," International Journal of Distributed Sensor Networks, vol. 2012, pp. 1-9, 2012. doi:10.1155/2012/135054.
- [16] B. Alexander, B.Zinaida, D. Maximillian, "Tampering with motes: real-world physical attacks on wireless sensor networks," Third international conference on Security in Pervasive Computing, pp 104-118, York, UK, April 2006. doi: 10.1007/11734666_9.
- [17] I. Krontiris, T. Dimitriou, "Towards intrusion detection in wireless sensor networks," 13th European wireless conference, Paris, 2007.
- [18] L. Krontiris, T. Dimitriou, T. Giannetos, "LIDeA: A distributed lightweight intrusion detection architecture for sensor networks," 4th International Conference on Security and Privacy in Communication Networks, pp. 1-10, September 2008, [SecureComm '08, Istanbul, Turkey]. doi:10.1145/1460877.1460903.
- [19] A. Manal, A. Ebtessam, A. Nada, "Energy Efficient Cluster-Based Intrusion Detection System for Wireless Sensor Networks," International Journal of Advanced Computer Science and Applications (IJACSA), vol. 5, no. 9, 2014.
- [20] S.S. Patil, P. S. Khanagoudar. "Intrusion Detection Based Security Solution for Cluster Based WSN," International Journal of Advanced Research in Computer Engineering & Technology (IJARCET), vol.1 no.4, pp: 331-340, 2012.
- [21] L. Coppolino, S. D'Antonio, A. Garofalo, L. Romano, "Applying data mining techniques to intrusion detection in wireless sensor networks," Eighth International Conference on P2P, Parallel, Grid, Cloud and Internet Computing (3PGCIC), pp. 247-254, October 2103. doi: 10.1109/3PGCIC.2013.43
- [22] M. Yassine, A. Ezzati, Y. Qasmaoui, M. Mbida, "A Global Hybrid Intrusion Detection System for Wireless Sensor Networks," Procedia Computer Science, vol. 52, pp. 1047-1052, 2015.
- [23] Feng Zhao, Leonidas Guibas, Wireless Sensor Networks: An Information Processing Approach, Morgan Kaufmann Publishers Inc., San Francisco, CA, 2004.
- [24] M.R. Norouzian, S. Merati, "Classifying Attacks in a Network Intrusion Detection System Based on Artificial Neural Networks," Conference Advanced Communication Technology (ICACT), 13th International Conference on Publication, pp. 868 - 873, 2011.
- [25] S. Sahin, Y. Becerikli, and S. Yazici, "Neural Network Implementation in Hardware Using FPGAs," Neural Information Processing, Lecture notes in Computer Science, Berlin Germany: Springer, vol. 4234, 2006.
- [26] S. J. Stolfo, W. Fan, W. Lee, A. Prodromidis, and P. K. Chan, "Costbased modeling for fraud and intrusion detection: results from the JAM project," The DARPA Information Survivability Conference and Exposition 2000 (DISCEX '00), Vol.2, pp. 130-144, 2000.
- [27] W. Wang, X. Zhang, S. Gombault, and S. J. Knapkog, "Attribute Normalization in Network Intrusion Detection," The 10th International Symposium on Pervasive Systems, Algorithms, and Networks (ISpan), 2009, pp. 448-453.
- [28] W. Wei, Y. Qi, "Information potential fields navigation in wireless Ad-Hoc sensor networks," Sensors, vol. 1, no. 5, pp. 4794-4807, 2011.
- [29] H. Song, M. Brandt-Pearce, "A 2-D discrete-time model of physical impairments in wavelength-division multiplexing systems," Journal of Lightwave Technology, vol. 30, no. 5, pp. 713-726, 2012. doi: 10.1109/JLT.2011.2180360.
- [30] H. Song, M. Brandt-Pearce, "Range of influence and impact of physical impairments in long-haul DWDM systems," Journal of Lightwave Technology, vol. 31, no. 6, pp. 846-854, March 2013. doi: 10.1109/JLT.2012.2235409.
- [31] H. Song, M. Brandt-Pearce, "Model-centric nonlinear equalizer for coherent long-haul fiber-optic communication systems," 2013 IEEE Global Communications Conference (GLOBECOM), pp. 2394-2399, Atlanta, GA, 2013. doi: 10.1109/GLOCOM.2013.6831432.
- [32] H. Song, M. Brandt-Pearce, "A 2-D discrete-time model of physical impairments in wavelength-division multiplexing systems," Journal of Lightwave Technology, vol. 30, no. 5, pp. 713-726, 2012. doi: 10.1109/JLT.2011.2180360.
- [33] H. Song, M. Brandt-Pearce, "Range of influence and impact of physical impairments in long-haul DWDM systems," Journal of Lightwave Technology, vol. 31, no. 6, pp. 846-854, March 2013. doi: 10.1109/JLT.2012.2235409.
- [34] H. Song, M. Brandt-Pearce, "Model-centric nonlinear equalizer for coherent long-haul fiber-optic communication systems," 2013 IEEE Global Communications Conference (GLOBECOM), pp. 2394-2399, Atlanta, GA, 2013. doi: 10.1109/GLOCOM.2013.6831432.

Segmentation using Codebook Index Statistics for Vector Quantized Images

Hsuan T. Chang* and Jian-Tein Su
Photonics and Information Laboratory
Department of Electrical Engineering
National Yunlin University of Science and Technology
Douliu Yunlin, Taiwan

Abstract—In this paper, the segmentation using codebook index statistics (SUCIS) method is proposed for vector-quantized images. Three different codebooks are constructed according to the statistical characteristics (mean, variance, and gradient) of the codewords. Then they are employed to generate three different index images, which can be used to analyze the image contents including the homogeneous, edge, and texture blocks. An adaptive thresholding method is proposed to assign all image blocks in the compressed image to several disjoint regions with different characteristics. In order to make the segmentation result more accurate, two post-processing methods: the region merging and boundary smoothing schemes, are proposed. Finally, the pixel-wise segmentation result can be obtained by partitioning the image blocks at the single-pixel level. Experimental results demonstrate the effectiveness of the proposed SUCIS method on image segmentation, especially for the applications on object extraction.

Keywords—image segmentation; vector quantization; index image; adaptive thresholding; codebook statistics

I. INTRODUCTION

Vector quantization (VQ) has been a simple, efficient and attractive image compression scheme since the past three decades [1], [2]. The basic VQ scheme partitions an image into small blocks (vectors) and each vector is assigned by an index of the codeword in the codebook for encoding [3]. If the indices of the codewords are arranged in a specific form, they can effectively represent the image characteristics in terms of image blocks. For example, Yeh proposed a content-based image retrieval algorithm for VQ images by analyzing the indices of codewords [4]. Moreover, the correlations among these indices can be used to develop an efficient image segmentation scheme. Most of previous studies performed segmentation operations in the pixel level [5], [6]. However, block-based image segmentation schemes can provide several advantages [7], [8]. The block-based scheme is very suitable for the VQ-based image segmentation because VQ techniques usually divide an image into non-overlapping image blocks. Block-based segmentation schemes segment an image with blocks rather than pixels by considering the relative information of the neighboring image blocks. Large homogeneous regions can be detected by means of this technique. Moreover, the computational complexity can be saved by segmenting an image in the block level rather than in the pixel level.

In this paper, the segmentation using codeword index statistics (SUCIS) method is proposed for the vector quantized images. First, an image of size $N \times N$ is divided into non-overlapping image blocks of size $B \times B$. A training set of images is first used to generate an image codebook based on the well-known Linde-Buzo-Gray (LBG) algorithm [1]. The codewords in the image codebook are then sorted in an incremental order according to their mean, variance, and gradient to obtain three different codebooks. For a vector quantized image, the corresponding index from the sorting results is treated as a pixel's grayscale value to obtain the index image. Therefore, three corresponding index images can be obtained. An index image intrinsically demonstrate the correlations among image blocks, which can be used as the features to label image blocks into homogeneous, edge, or texture blocks. Several image-dependent threshold values are adaptively determined for region labeling. Then, a region number is assigned to all connected homogeneous blocks with the same label to obtain disjoint regions. Finally, the pixel-based image segmentation result can be obtained by partitioning the size of edge blocks further into the pixel level.

The rest of this paper is organized as follows: Section 2 deals with the proposed SUCIS method for VQ-coded images. Section 3 shows the experimental results for various test images. Conclusions are finally drawn in Section 4.

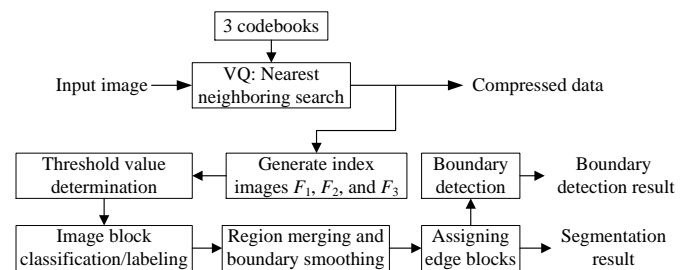


Fig. 1. The schematic diagram of the proposed SUCIS method

II. THE PROPOSED METHOD

Figure 1 shows the block diagram of the overall image segmentation system by using the proposed SUCIS method. The overall system consists of six stages: (1) codebook generation, (2) VQ encoding, (3) index image generation, (4) region labeling, merging, and boundary smoothing, (5)

boundary detection, and (6) edge block assignment for image segmentation. The first and second stages have been well studied in image compression framework based on VQ. The third stage describes how to rearrange the indices of the codewords in the codebook using three different mapping functions. Then, three different index images can be generated and are used to label all image blocks, which are classified into three types: (1) homogeneous blocks, (2) edge blocks, and (3) texture blocks. Figures 2(a) – 2(f) show six typical image blocks in the block labeling configurations. The fourth stage discusses two post-processing methods: the region-merging and boundary-smoothing schemes which can refine the boundaries of regions of special interest. In the region-merging process, many homogeneous regions are merged into certain regions and this achieves the rough image segmentation result. In the boundary-smoothing process, the boundaries of the image segmentation result can be more refined by smoothing the boundaries of regions of special interest. In the fifth stage, the result of boundary detection will be obtained by extracting the edge blocks in the image segmentation result. The final stage describes how to partition and assign the edge blocks from the block level to the pixel level. The segmentation results under the three different pixel levels will be obtained through assigning the edge blocks continuously.

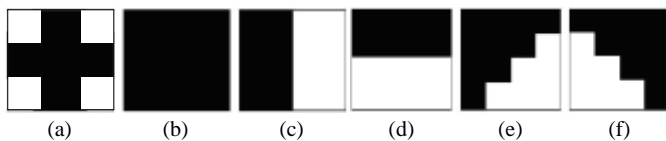


Fig. 2. Some typical image blocks in block labeling: (a) texture block; (b) monotone block; (c) vertical edge block; (d) horizontal edge block; (e) and (f) diagonal edge blocks

A. Codeword Index Assignment and Index Image Generation

VQ is a generalization of scalar quantization to quantize a vector and a mapping of q -dimensional positive Euclidean space R^q into a finite subset C of R^q . Suppose that there are L codewords in the codebook. Let c_i and C denote the codewords and codebook in VQ, respectively, where $C = \{c_i | c_i \in R^q, \text{ for } i = 0, 1, \dots, L-1\}$. The subscript i is the index of the codeword and is represented as a b -bit ($2^b = L$) binary word. It is usually written as a decimal integer for notational brevity.

Figure 3 shows the flowchart of the proposed scheme for codebook generation. If the codeword c_i is considered as a discrete random sequence $X_i = (c_{i,1}, c_{i,2}, \dots, c_{i,L})$ and every random variable $c_{i,k}, k=1, 2, \dots, L$ in X_i is uniform distributed between 0 and 255 (because of the 8-bit resolution in digital images), then the J^{th} moment of the random sequence X_i is expressed by [9]

$$E[(X_i)^J] = \frac{1}{B \times B} \sum_{k=1}^{B \times B} c_{i,k}^J \times p(c_{i,k}), \quad (1)$$

where $p(c_{i,k})$ is the probability density function of the random variable $c_{i,k}$ [7]. The codewords c_i can be sorted in an incremental order based on their J^{th} moment (where $J=1, 2$) to obtain $c_{j(J)}$ where $j(J)$ is the rank of c_i based on its J^{th} moment. From a given image codebook C , two mapping functions between indices i and $j(J)$ for mean $J=1$ and variance ($J=2$) are created. The first mapping function f_1 computes the mean value

of the codewords in the codebook, where f_1 is a linear function. The second mapping function f_2 computes the variance value of the codewords, where f_2 is a nonlinear function. Moreover, the third mapping function f_3 computes the edge density of the codewords. Here, the edge density δ_i represents the texture feature of the i^{th} 4×4 codeword. The edge density is defined as [10]:

$$\delta_i = \frac{|\{c_k | \text{Mag}_{\text{gradient}}(c_i) \geq T\}|}{B^2}, \quad (2)$$

where T denotes the average gradient magnitude of all codewords. First, the mapping function f_1 is a straight line with unit slope because the codewords in the codebook C have been already sorted in the incremental order with mean. Alternatively, the codebooks C_{F1} , C_{F2} , and C_{F3} are directly derived from image codebook C if codewords are sorted according to their mean, variance, and gradient, respectively. The codewords in the three codebooks represent the different meanings. In the first codebook C_{F1} , the indices of the codewords distribute from low mean values to high mean values. In other two codebooks C_{F2} , and C_{F3} , the high indices of the codewords represent the edge and texture blocks in the test image, respectively. We utilize the codewords in the codebook to label the total homogeneous blocks in the test image.

If the index of the codeword is treated as the grayscale value of a pixel, then an $N \times N$ image can be quantized into $N/B \times N/B$ indices and be converted into the index images F_1, F_2 and F_3 of size $N/B \times N/B$ by the use of the codebooks C_{F1}, C_{F2} , and C_{F3} , respectively, based on the three different mapping functions f_1, f_2 and f_3 . For the codebook whose size is larger than 256, to make the indices fall into the range between 1 and 256, the codewords in the codebook must be uniformly divided into 256 classes according to their incremental order. Therefore, numerous codewords can be represented by the same index.

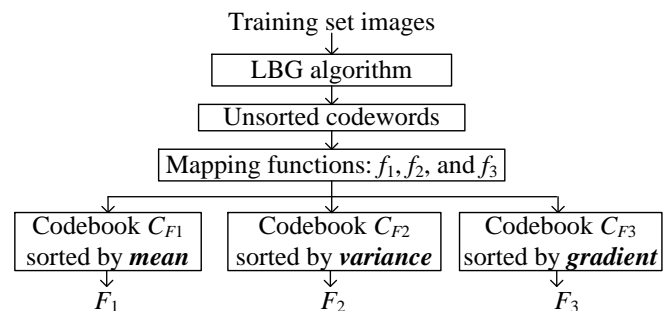


Fig. 3. Flowchart of the image codebook generation

The characteristics of all image blocks in a test image can be classified into three typical image blocks. According to the characteristics in three index images F_1, F_2 and F_3 , the regions and boundary of objects of our interest are extracted. The index image F_1 is a thumbnail version of the original image. It reveals the mean order of image blocks and is used to label all corresponding image blocks. The label of the image block is indeed the corresponding pixel value in the index image F_1 . Both the index images F_2 and F_3 strongly reveal the structural

arrangement (edge and texture information) in the image blocks and are used to determine whether the image blocks belong to the homogeneous blocks or not. The larger values in the index images F_2 and F_3 represent that the gray-level distribution of an image block is closer to the edge or texture block. If the index image F_1 is used to label all image blocks and a region number is assigned to all connected image blocks to obtain disjoint regions, the rough segmentation result can be obtained and can be used as the initial segmentation result for the following pixel-based image segmentation problem.

B. Adaptive Thresholding for Block Labeling

To classify the image blocks in a VQ-coded image, the threshold values are employed. Here, two threshold values T_M and T_F for the mean and fused index images, respectively, are determined at first. The histogram of the index image F_1 is used to determine the initial threshold value T_M . On the other hand, the histogram of fused index image (the fusion of index images F_2 and F_3) is used to determine the initial threshold value T_F . In the image fusion method, the pixel values with the same position in two index images F_2 and F_3 are compared. Then, the larger value in the two pixels is chosen as the pixel value of the fused index image. The image fusion equation is given by

$$F_f(i, j) = \begin{cases} F_2(i, j), & \text{if } F_2(i, j) > F_3(i, j) \\ F_3(i, j), & \text{otherwise} \end{cases} \quad (3)$$

Finally, the fused index image can be created by combining two index images F_2 and F_3 . The overall procedure of the parameter setting for the index image F_1 is as follows:

Step 1: Compute the histogram of index image F_1 and its average value as the initial threshold value T_M which is determined by

$$T_M = \frac{\sum_{i=0}^{255} i \times \text{Pixel number}(i)}{(N/B)^2} \quad (4)$$

Step 2: Determine the accumulated distribution of the histogram by gradually accumulating every five percent of total pixels in the index image.

Step 3: In order to obtain four regions with different grayscale distributions, two more threshold values T_{ML} and T_{MH} are calculated as follows:

$$T_{ML} = \frac{T_M}{2}; \quad T_{MH} = \frac{T_M + 255}{2} \quad (5)$$

Step 4: Calculate the difference values between the three average values T_M , T_{ML} , and T_{MH} and every grayscale level in the accumulated distribution, respectively.

Step 5: Separately update these average values by using the grayscale levels that have the minimum difference among them,

Step 6: Compute the differences between first and last three grayscale levels. Set T_L and T_H are equal to the first and last second grayscale levels, respectively, if the difference is the smallest.

If the pixel values are greater than T_{MH} , these pixel values in the index image F_1 represent the light homogeneous blocks. On the other hand, if they are smaller than T_{ML} , they represent the dark homogeneous blocks. The threshold values T_H and T_L are used to label the lightest and darkest homogeneous blocks, respectively. As mentioned above, we can employ these threshold values to label all homogeneous blocks in a VQ-coded image. After all the homogeneous blocks in a VQ-coded image are labeled, some similar image blocks can be merged into the same region. Thus, we find that many different homogeneous regions spread over a VQ-coded image. Finally, the rough image segmentation result can be obtained.

In order to make the segmentation result more accurate, it must distinguish the edge and texture blocks separately from all image blocks in a test image. The index images F_2 and F_3 are employed to determine which image blocks belong to the edge and texture blocks, respectively. Finally, the edge blocks in the index image F_2 and the texture blocks in the index image F_3 are fused and used to generate a new index image F_f by using Eq. (3). These pixel values in the index image F_f represent the bright texture blocks, if the pixel values are greater than T_F . On the other hand, they represent the dark texture blocks and are smaller than T_F . After all texture blocks in a test image are labeled, some similar image blocks can be merged into the same region. The overall procedure of the parameter setting for the fused index image is similar to that used for the mean index image except that two threshold values T_{MH} and T_{ML} are not used here.

After we remove the labels of these image blocks in the rough segmentation result and mark them as edge or texture labels, the rest of image blocks which have labels in the rough segmentation result are called the homogeneous blocks. Finally, all image blocks in a test image are classified into three classes including the homogeneous, edge, and texture image blocks. In the post-processing, the region-merging process and boundary smoothing will be used to modify the rough image segmentation result. The region-merging process can avoid the over-segmentation for a test image. More accurate contours of the objects can be obtained by means of boundary smoothing.

C. Region Merging and Boundary Smoothing

As a result of the block classification and labeling shown above, the labels for all image blocks can be obtained. A region number can be assigned to all connected blocks [11]. In numbering the connected blocks, we must check whether a candidate block and its neighboring blocks have the same label. In order to reduce the number of regions, the small-size and non-interested regions should be ignored such that the complete and large regions are left. For a given block, if the number of connected image blocks is less than a defined smallest region (SR) in a region, it will be merged into one of its neighboring regions. At the same time, the mean difference between a candidate region and one of its neighboring regions is also checked based on their corresponding codewords. A candidate region will be assigned to the neighboring region which has the smallest mean difference with the candidate region. Since only the large regions in a VQ-coded image are left, the number of regions can be reduced. Therefore, the

rough segmentation result can be obtained and the over-segmentation problem can be avoided.

After the operation of region merging has been finished, we find that the boundaries of the large and interested regions in a VQ-coded image are unsmoothed, which may lead to the erroneous segmentation. The final segmentation result might not be accurate. Thus, to obtain the higher accurate segmentation result, the operation of boundary smoothing is used to refine the boundaries of the large and interested regions. The procedure of boundary smoothing is described as follows: First, all regions in a VQ-coded image are divided into two different type regions. If a region whose label of the only neighboring region is different from that of it, it is called the independent region. On the other hand, if a region whose labels of many neighboring regions are different from that of it, it is called the dependent region. Let a mask of size 3×3 be mapped to all regions in a VQ-coded image. Then, the ratio of every image blocks in a mask is computed. If a number of image blocks of objects in a mask of size 3×3 are smaller than that of its neighboring regions, then the image blocks that lies in the center position of a mask are merged into one of its neighboring regions. Otherwise, the image blocks will not be changed. The above steps are repeatedly executed until the image blocks of all regions in a VQ-coded image are never changed again. Finally, the boundary smoothing results can be obtained.

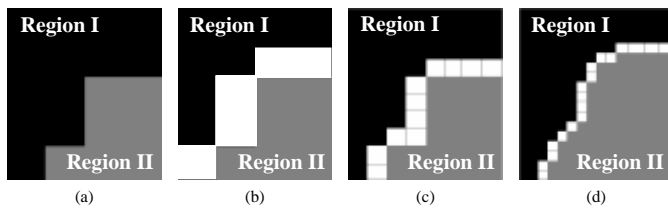


Fig. 4. Homogeneous regions and edge blocks labeling: (a) Homogeneous regions labeling. Edge blocks labeling in (b) Level 0; (c) Level 1; (d) Level 2

D. Assignments of Edge Blocks

Here we describe how to assign the edge blocks and to refine the segmentation results from the block level to pixel level. There are many homogeneous and texture regions in a test image and the image blocks in their boundaries are labeled as the edge blocks. Figure 4(a) shows two different regions, where Region I and Region II stand for the object region and the background region, respectively. Figure 4(b) shows the boundaries in the object region that is labeled as the edge blocks, where every edge block is of size 4×4 .

After all edge blocks have been labeled, they are partitioned into half size and assigned to one of its neighboring regions. The procedure of assignments of edge blocks is described as follows: First, the mean difference between a candidate edge block and each of its neighboring (4-connected neighbors [12]) regions is examined based on their corresponding codewords. Then, a candidate edge block will be assigned to the neighboring region which has the smallest mean difference with it. The size of edge blocks can be reduced to be its sub-level. As the size of edge blocks is reduced, the contour of objects can be more accurate.

Finally, the refined image segmentation result can be obtained when none of the edge block is left. The segmentation results for three different levels from the block level to the pixel level can be obtained. The basic units for assignment in the Level-0, Level-1, and Level-2 segmentation results are the blocks of size 4×4 , 2×2 , and single pixel, respectively.

TABLE I. THE PARAMETER LIST FOR TWO TEST IMAGES

Image	Parameters						
	T_M	T_{ML}	T_{MH}	T_L	T_H	T_F	SR
Lena	139	70	197	NA	NA	104	40
Tower	132	66	194	NA	NA	137	30

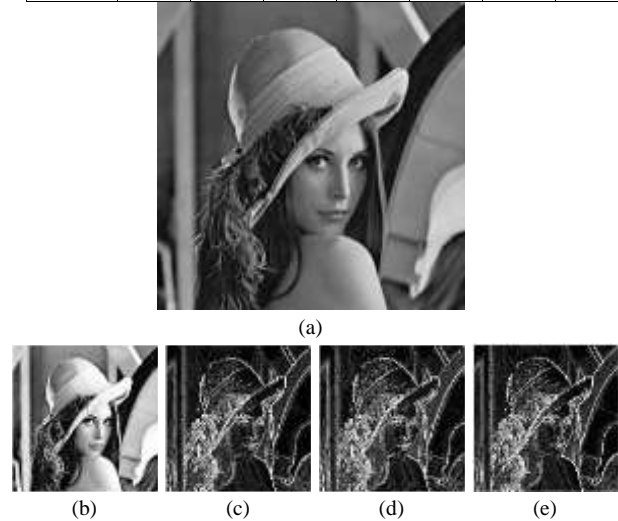


Fig. 5. (a) The original Lena image and three index images of size 128×128 : (b) F_1 , (c) F_2 , (d) F_3 , and (e) the fusion result of (c) and (d)

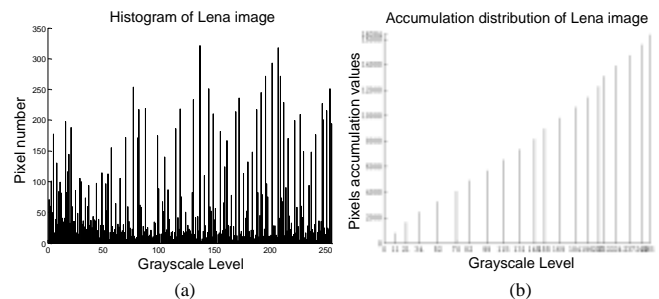


Fig. 6. (a) The histogram for the Lena index image (ordered by mean); (b) The accumulation distribution determined from (a)

III. EXPERIMENTAL RESULTS

In this paper, the Lena image of size 512×512 and the Tower image of size 360×288 are used to test the proposed SUCIS method. The unsorted codebook can be generated by using the LBG algorithm. Before the two test images are segmented, some parameters must be determined for them. Every image should have the different parameters because the complexity in each image is different. Table I shows the threshold values and the SR parameter for two test images. Both the threshold values T_L and T_H in these two images are not available because the conditions described in Section II.B

are not satisfied. Figure 5(a) shows the original Lena image. Figures 5(b)-5(d) shows the three index images F_1 , F_2 , and F_3 , which are generated by image codebooks C_{F1} , C_{F2} , and C_{F3} , respectively. The mean image shown in Fig. 5(b) looks very similar to the original image. As shown in Figs. 5(c) and 5(d), the brighter pixels represent higher variance and gradient values of the blocks in the original image. The fusion result of Figs. 5(c) and 5(d) is shown in Fig. 5(e). Figures 6(a) and 6(b) show the histogram and its accumulation distribution of the index image of the Lena image, respectively.

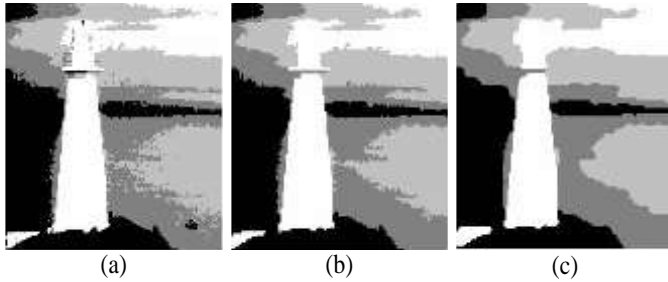


Fig. 7. Regions merging for the Tower index image F_1 (order by mean): (a) Before region merging; (b) After region merging with SR=30 and the 4-connected condition; (c) After boundary smoothing

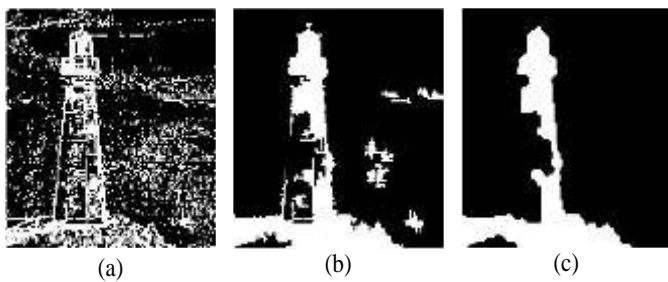


Fig. 8. Regions merging for the fused index image F_f of the Tower image: (a) Before region merging; (b) After regions merging with SR=30 and the 4-connected condition; (c) After boundary smoothing

Consider the Tower image for the proposed SUCIS method. Figures 7(a)-7(c) show some results of region merging with SR=30 and using the 4-connected condition for the mean index image. As shown in Fig. 7(c), a rough segmentation result can be observed in the smoothed regions. Figures 8(a)-8(c) show the boundary smoothing effects for the fused index image F_f . Finally, Figs. 9(a) and 9(b) show the boundary detection results for the test Lena and Tower images, respectively. According to these two figures, Figs. 10 and 11 show the segmentation results in three different levels for the Lena and Tower images which are VQ-coded. The different image segmentation results can be obtained. Obviously, the image segmentation results with better accuracy can be obtained with the edge block labeling in Level 2.

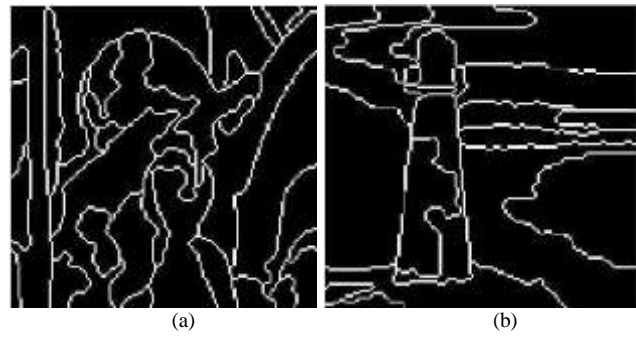


Fig. 9. Boundary detection results for the (a) Lena and (b) Tower images



Fig. 10. Segmentation results for the Lena image of size 512x512: (a) Level 0; (b) Level 1; (c) Level 2

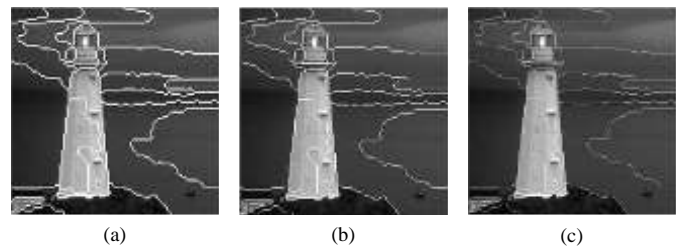


Fig. 11. Segmentation results for the Tower image of size 360x288: (a) Level 0; (b) Level 1; (c) Level 2

The proposed SUCIS method is compared with the benchmark watershed method [13] to verify the effectiveness especially for the foreground object segmentation. Four test images downloaded from the Berkeley Segmentation Dataset [14] are utilized in our experiments. Figures 12(a), 12(c), 12(e), and 12(g) show the segmentation results of the proposed SUCIS method. By using the watershed function provided in MATLAB, Figs. 12(b), 12(d), 12(f), and 12(h) show the segmentation results of the watershed method. As shown in both figures, the foreground objects can be successfully segmented. In Figs. 12(a) and 12(b), the proposed method also segments the tree branches in addition to the mother bird. The most difference results are shown in Figs. 12(e) and 12(f). The proposed method segment the foreground only in one region, while the watershed method can segment the more detail shapes for the owls.

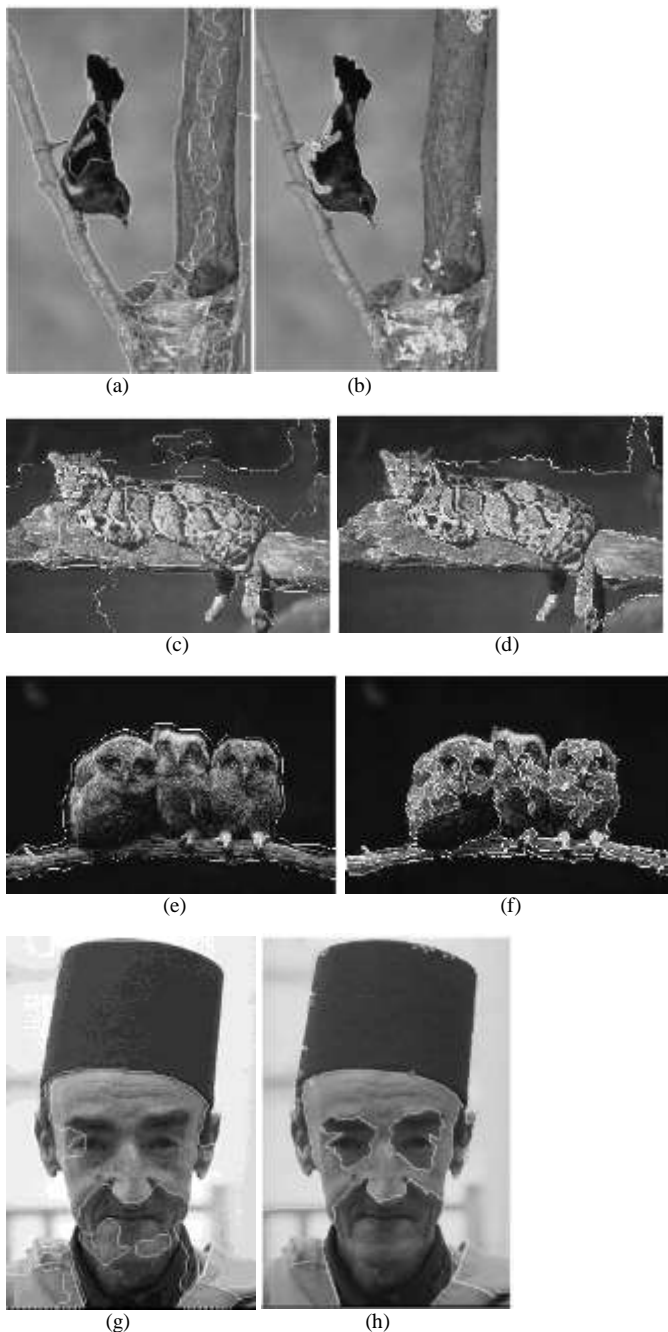


Fig. 12. Comparison of the segmentation results between the proposed SUCIS and the watershed methods: (a), (c), (e), (g) are the level-2 results of the proposed SUCIS method and (b), (d), (f), (h) are the results of the watershed method

IV. CONCLUSIONS

In this paper, the SUCIS method is proposed based on the index statistics of VQ-coded images to perform the image segmentation especially for the VQ-coded images. The SUCIS method uses three different index images to label and classify image blocks in a VQ-coded image and distinguish them into homogeneous, edge, and texture blocks to obtain disjoint regions such that the segmentation result can be obtained. Although our SUCIS method segments an image in terms of blocks rather than pixels, the pixel-based segmentation result

can be obtained by partitioning the edge blocks into the half size and assigning to one of their neighbor regions until to the pixel level. Moreover, the computational complexity can be reduced by segmenting images in the compressed domain and with blocks rather than pixels. In summary, the proposed SUCIS method is effective and efficient for image segmentation and the results can be applied on VQ-based image/video coding schemes. Our future work may focus on extracting the objects from the segmented results and/or describing the semantic meanings in the processed images. The proposed method may be extended by cooperating the local robust statistics [15] or the machine learning methods based on the artificial neural network [16] and fuzzy theory [17]. The effectiveness of applying the proposed SUCIS method onto the medical image processing [16], [18] can be investigated as well.

ACKNOWLEDGMENT

This work is partially supported by Ministry of Science and Technology (MOST), Taiwan under Contract Number MOST 105-2221-E-224-021-MY2.

REFERENCES

- [1] Y. Linde, A. Buzo, and R.M. Gray, "An algorithm for vector quantizer design," *IEEE Transactions on Communication*, vol. 28, no. 1, pp. 84-95, Jan. 1980
- [2] R. M. Gray, "Vector quantization," *IEEE ASSP Magazine*, vol. 1, no. 2, pp. 4-29, 1984
- [3] A. Gersho and R. M. Gray, *Vector Quantization and Signal Compression*, Boston, MA:Kluwer, 1992
- [4] C.-H. Yeh and C. J. Kuo, "Content-based image retrieval through compressed indices based on vector quantized images," *Optical Engineering*, vol. 45, no. 1, pp. 1-8, Jan. 2006
- [5] Y.T. Hsiao, C.L. Chuang, J.A. Jiang, and C.C. Chien, "A contour based image segmentation algorithm using morphological edge detection," *2005 IEEE International Conference on Systems, Man and Cybernetics*, vol. 3, pp. 2962-2967, Oct. 2005.
- [6] H. Gao, W.C. Siu, and C.H. Hou, "Improved techniques for automatic image segmentation," *IEEE Transactions on Circuits and Systems for Video Technology*, vol. 11, no. 12, pp. 1273-1280, Dec. 2001
- [7] C.S. Won, "A block-based MAP segmentation for image compression," *IEEE Transactions on Circuit and System for Video Technology*, vol. 8, no. 5, pp. 592-601, 1998
- [8] X. Li and S. Lei, "Block-based segmentation and adaptive coding for visually lossless compression of scanned documents," *2001 IEEE International Conference on Image Processing*, vol. 3, pp. 450-453, Oct. 2001
- [9] W.K. Pratt, *Digital Image Processing*, John Wiley and Sons, Inc, 1991
- [10] G.C. Stockman and L.G. Shapiro, *Computer Vision*, Chapter 7, pp. 216, Prentice hall, New Jersey, 2001
- [11] Y.L. Leng and X. Li, "Adaptive image region-growing," *IEEE Transactions on Image Processing*, vol. 3, no. 6, pp. 868-872, Nov. 1994
- [12] Y. Deng and B.S. Manjunath, "Unsupervised segmentation of color-texture regions in images and video," *IEEE Transactions on Pattern Analysis and Machine Intelligence*, vol. 23, no. 8, pp. 800-810, Aug. 2001
- [13] L. Vincent and P. Soille, "Watersheds in digital space: An efficient algorithm based on immersion simulations," *IEEE Transactions on Pattern Analysis and Machine Intelligence*, vol. 13, no. 6, pp. 583-597, Jun. 1991
- [14] D. Martin, C. Fowlkes, D. Tal, and J. Malik, "Database of human segmented natural images and its application to evaluating segmentation algorithms and measuring ecological statistics," *Proc. 8th International Conference on Computer Vision*, vol. 2, pp. 416-423, July 2001

- [15] C. Huang and L. Zeng, "Robust image segmentation using local robust statistics and correntropy-based K-meansclustering," *Optics and Laser in Engineering*, vol. 66, pp. 187-203, Mar. 2015
- [16] A. De and C. Guo, "An adaptive vector quantization approach for image segmentation based on SOM network," *Neurocomputing*, vol. 149, Part A, 3, pp. 48-58, Feb. 2015.
- [17] Y. Li, "Wavelet-based fuzzy multiphase image segmentation method," *Pattern Recognition Letters*, vol. 53, pp. 1-8, Feb. 2015
- [18] A. De and C. Guo, "An image segmentation method based on the fusion of vector quantization and edge detection with applications to medical image processing," *International Journal of Machine Learning and Cybernetics*, vol. 5, no. 4, pp. 543-551, Aug. 2014

An Enhanced Partial Transmit Sequence Segmentation Schemes to Reduce the PAPR in OFDM Systems

Yasir Amer Al-Jawhar and Nor
Shahida M. Shah
Dept. of Communication
Faculty of Electrical and Electronic
Engineering
Universiti Tun Hussein Onn
Malaysia
Batu Pahat, Johor, Malaysia

Montadar Abas Taher
Dept. of Communications
Engineering
College of Engineering
University of Diyala
Ba'aqubah, Diyala, Iraq

Mustafa Sami Ahmed and
Khairun N. Ramli
Dept. of Communication
Faculty of Electrical and Electronic
Engineering
Universiti Tun Hussein Onn
Malaysia
Batu Pahat, Johor, Malaysia

Abstract—Although the orthogonal frequency division multiplexing system (OFDM) is widely used in high-speed data rate wire and wireless environment, the peak-to-average-power-ratio (PAPR) is one of its major obstacles for the real applications. The high PAPR value leads some devices of the OFDM system such as power amplifiers and analog to digital converters to work out of band of these devices. Thus the system efficiency is degraded. Many techniques have been proposed to overcome the high PAPR in OFDM systems such as partial transmit sequences (PTS), selected mapping and interleaving technique. PTS is considered as one of the effective PAPR reduction methods; this scheme depends on segmentation of the input data into several subblocks and then combined again. The three well-known segmentation schemes are pseudo-random, adjacent and interleaving; each scheme has PAPR reduction performance, and computational complexity differs from one to another. In this paper, five types of segmentation schemes are proposed to improve the PAPR reduction execution including sine and cosine shape as well as hybrid interleaving and adjacent schemes in new approaches. From the simulation results, the proposed methods can achieve PAPR reduction performance greater than that of the adjacent and interleaving partition schemes, without increasing the computational complexity of the system. Moreover, the enhanced schemes can realize better PAPR performance with any number of subcarriers.

Keywords—OFDM; PAPR; PTS; adjacent PTS; interleaving PTS

I. INTRODUCTION

Orthogonal frequency division multiplexing (OFDM) is widely used in the high-speed data rate communication environment. This is because of the OFDM system provides many advantages such as its robustness to multipath fading, immunity to inter-symbol interference (ISI), the ability for high data transmission rate, and bandwidth efficiency [1] [2] [3] [4]. OFDM system has been considered as a multiplexing technique for many digital communication systems such as wireless local area network (WLAN) IEEE.802.11a/b/g/n [5], worldwide interoperability for microwave access IEEE.802.16 [6], digital video broadcasting (DVB) [7], and digital audio

broadcasting (DAB) [8]. Also, OFDM system is used in Long-Term Evaluation (LTE) which is the standard for the fourth generation (4G) technology [9] [10]. Moreover, because of its distinct features, OFDM is considered as an attractive candidate for the fifth generation (5G) of the mobile communication systems [11] [12]. However, the main disadvantage of the OFDM system is the high peak-to-average power ratio (PAPR), which leads to out-of-band radiation and in-band distortion. This is because the nonlinearity of the high power amplifier (HPA) at the transmitter. Hence, the spectral inefficiency and the bit error rate (BER) of the system are increased [13].

In order to reduce the PAPR, many methods have been proposed, such as clipping [14] [15], clipping and filtering [16], coding techniques [17], selective mapping (SLM) [18] [19], partial transmit sequence (PTS) [20] and tone injection [21]. Among these methods PTS is an effective technique, and it can improve the PAPR reduction performance. The principle idea of the PTS method is based on partitioning the input data into several subblocks, and then each subblock weights by the phase rotation factors before combining the subblocks again. The OFDM signal which has the lowest PAPR value is selected for transmission. Therefore, PTS technique depends on segmentation schemes and, phase rotation factors.

In literature, several scenarios have been proposed to modify the ordinary PTS method in terms of the segmentation schemes such as (Hong 2013) [22] and (Zeyid 2014) [12], where combining two types of the partitioning schemes is proposed. Reference [10] (Jawhar 2016) introduced a new method by combining two types of segmentation schemes. In [23] and [24], Xia analyzed the coloration between the subcarriers within the subblocks of PTS technique; he concluded that the PAPR reduction depends on the subcarriers correlation and it decided by subblocks segmentation and phase rotation factors, while it is unconcerned with the input data sequence. Furthermore, Xiao in 2007 [25] improved the PAPR interpretation by reduce the correlation among the candidate signals in the time-domain. On the other hand, the authors in the [26] combined random and interleaving

The authors would like to thank to University Tun Hussein Onn Malaysia (UTHM) for sponsoring this work under Research Supporting Grant Scheme (RSGS) Vot No. U 102.

segmentation to enhance the PAPR performance, while Singh in [27] proposed hybrid combination of PTS and SLM in order to achieve better PAPR execution.

In this paper, new partition schemes are proposed to improve the PAPR performance of the PTS technique in OFDM system. Moreover, the adjacent segmentation scheme and interleaving segmentation scheme are combined in a new approach. Furthermore, the proposed methods are compared with ordinary PTS method. The proposed PTS methods can significantly enhance the PAPR performance without increasing the computational complexity.

This paper is organized as follows: Section II illustrates the PAPR problem. Section III discusses the ordinary PTS method. The PTS segmentation schemes are analyzed in Section IV. The proposed method introduced in Section V. Simulation results and discussions are given in section VI. Finally, the conclusions have been written in section VII.

II. OFDM SYSTEM

In OFDM system, the input data block is mapped by one of the mapping techniques such as, phase shift keying (PSK) and quadrature amplitude modulation (QAM). The data symbols transmitted in parallel to generate the frequency domain signal, where N is the number of subcarriers. The discrete time domain signal can be generated by applying N -point inverse fast Fourier transform (IFFT) on X_k , which can be expressed as [28]

$$x(n) = \frac{1}{\sqrt{N}} \sum_{k=0}^{N-1} X_k e^{j2\pi k \frac{n}{N}}, \quad 0 \leq n \leq N-1 \quad (1)$$

where $j = \sqrt{-1}$.

The PAPR is the ratio of the maximum peak power signal to average power of OFDM signal, which can be written as [29]

$$PAPR = \frac{\max_{0 \leq n \leq N-1} |x(n)|^2}{P_{av, x(n)}} \quad (2)$$

$$P_{av, x(n)} = E\{|x(n)|^2\} \quad (3)$$

where $E\{\cdot\}$ represents the average power of the OFDM signal. When the subcarriers in the time domain have the same phases, the peaks of the subcarriers are added together constructively, and thus lead to increasing in the PAPR value of the OFDM signal.

The complementary cumulative distribution function (CCDF) is used to evaluate the distribution PAPR performance. The CCDF denotes the probability that the PAPR of the OFDM signal exceeding the threshold value, which can be defined as [30]

$$Pr(PAPR > PAPR_0) = 1 - (\exp(-PAPR_0))^N \quad (4)$$

where the $PAPR_0$ is the threshold value. To catch some peaks of the signal that do not appear in the PAPR calculation, oversampling is employed in the discrete baseband signal by

inserting $(L-1)N$ zeros to the OFDM signal. Therefore, the CCDF of the continuous OFDM signal is given as [31]

$$Pr(PAPR > PAPR_0) = 1 - (\exp(-PAPR_0))^{NL} \quad (5)$$

where L is the oversampling factor.

III. CONVENTIONAL PARTIAL TRANSMIT SEQUENCE (C-PTS)

C-PTS technique proposed to reduce the PAPR value of the OFDM system. Fig. 1 illustrates the block diagram of the PTS method, in which the input data sequence X_k is partitioned into V non-overlapping subblocks. In each subblock, only N/V samples are assigned, and the rest samples are set to zero. Therefore, the subblock X_v is represented

$$X = \sum_{v=1}^V X_v \quad (6)$$

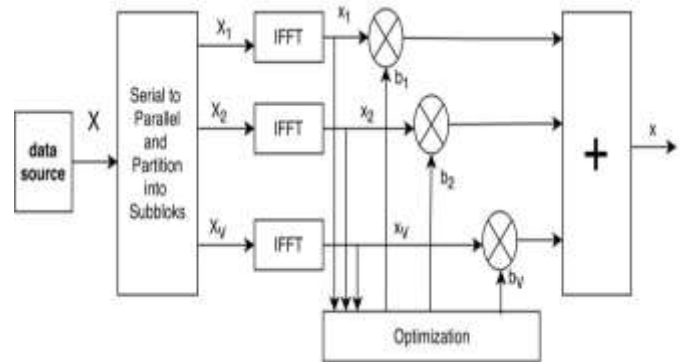


Fig. 1. PTS block diagram

The partitioned subblocks X_v is transformed from the frequency domain into the time domain by applying IFFT operation. After that, each subblock rotates by phase weighting vectors b_v , and combines with other subblocks to generate a set of candidates. The candidate sequence which achieves the minimum PAPR value is selected for transmission [32]. Therefore, the time domain signal after combining the subblocks is given by

$$x = IFFT\left\{\sum_{v=1}^V b_v X_v\right\} = \sum_{v=1}^V b_v \cdot IFFT\{X_v\} = \sum_{v=1}^V b_v x_v \quad (7)$$

where the phase factor $b = \{b_v = e^{j2\pi v W} | v = 0, 1, \dots, W-1\}$, and W is the number of the allowed phase factors. The first element of the phase factors b_1 usually set to 1, without loss of PAPR performance. Moreover, the different number of phase factors W is usually constant, so that $b_v \in \{\pm 1\}$ or $\{\pm 1, \pm j\}$ to avoid complex multiplication operations [33].

In general, there are W^{V-1} sets of the phase factors should also be searched to find the optimum phase factor and, the transmitter should send bits as side information (SI) to the receiver in order to recover the original data [18].

IV. PTS SEGMENTATION SCHEMES

In PTS method, there are three common types of the segmentation schemes, including interleaving partition,

adjacent partition and, pseudo-random partition as shown in Fig. 2. In interleaving segmentation scheme (IL-PTS), N/V subcarriers are allocated within a certain distance interval of V for each subblock. The adjacent segmentation scheme (Ad-PTS) allocates N/V successive subcarriers within subblocks sequentially. The pseudo-random segmentation scheme (PR-PTS) assigns the subcarriers randomly in the subblocks. The segmentation schemes must be under the following conditions: the subblocks should be equally in size, and the subcarrier must appear only one time within the subblock. Moreover, the subblocks must be non-overlapping with each other [34].

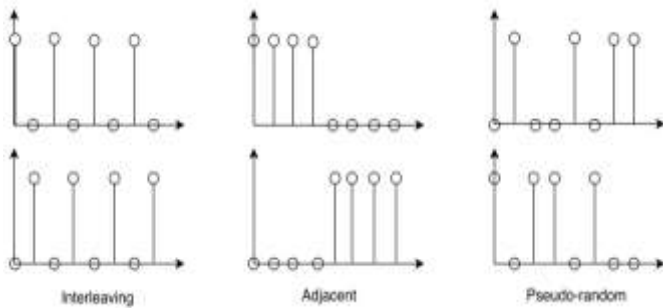


Fig. 2. Ordinary PTS segmentation schemes

The three types of partitioning influence on the PAPR reduction performance, which depend on the autocorrelation between the subcarriers. PR-PTS scheme can achieve the best PAPR performance among partitioning schemes, but the cost is an increased complexity. Ad-PTS scheme is lower PAPR reduction gain than PR-PTS scheme. In contrast, IL-PTS scheme considers the worst PAPR reduction performance, but its computational complexity is lower than other methods [30].

V. PROPOSED METHODS

A. Symmetrical Interleaving Scheme-Cosine Wave Shape

As mention, IL-PTS is one of the segmentation schemes, and its PAPR performance considered as the worse than the other schemes. However, the computational complexity of IL-PTS is lower than that of Ad-PTS and PR-PTS scheme. The symmetrical interleaving scheme cosine wave shape PTS method (S-IL-C-PTS) can improve the PAPR reduction performance better than IL-PTS and Ad-PTS without increasing the computational complexity.

Fig. 3 illustrates the proposed method, which begins with segmenting the data sequence into V subblocks similar to that of the IL-PTS scheme. After that, the IL-PTS matrix divided into S_G groups, where $G = \{1, 2, 3, \dots, N/V\}$, and each group has V rows. Then, only the even S_G groups from the IL-PTS matrix are chosen for processing. Afterward, in each even S_G groups, the first row is changed with last one and the second row with the one before the last, and so on. The IL-PTS matrix is changed into a new matrix, in which the subcarriers are allocated symmetrically as cosine wave shape. Finally, the procedure of PTS technique is applied to the proposed partitioning scheme, and the OFDM signal with the lowest PAPR value is chosen for transmission. The S-IL-C-PTS scheme can decrease the autocorrelation among the subcarriers

within the subblocks. Hence, the PAPR reduction performance will be enhanced accordingly.

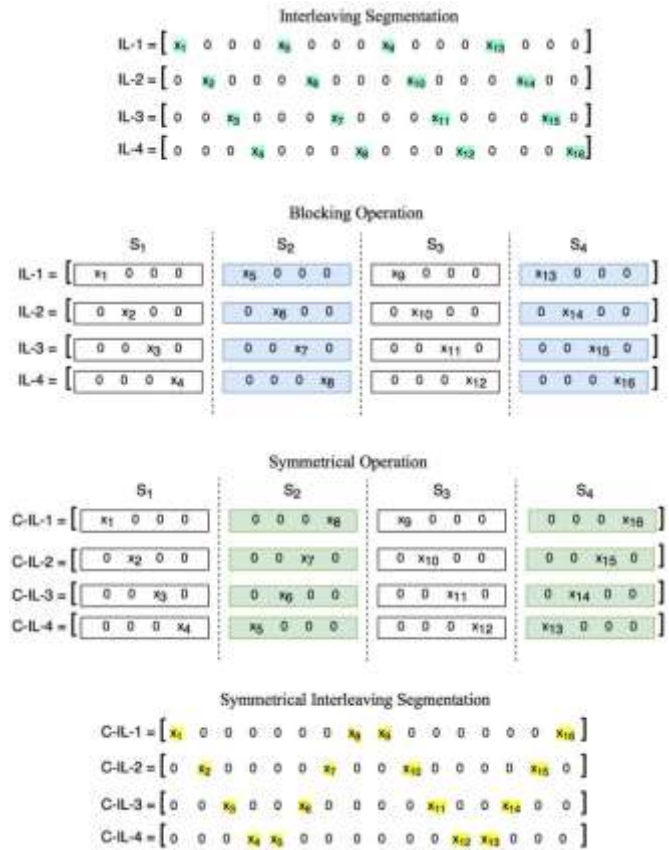


Fig. 3. S-IL-C-PTS scheme when $V=4$ and $N=16$

B. Symmetrical Interleaving Scheme-Sine Wave Shape

The symmetrical interleaving sine wave shape PTS method (S-IL-S-PTS) is the same as that of S-IL-C-PTS, but the difference is the S-IL-S-PTS scheme deals with the odd S_G groups only, while the S-IL-C-PTS method is processed with the even S_G groups from the Interleaving matrix.

Fig. 4 shows the S-IL-S-PTS segmentation operation, in which the input data X is partitioned into disjoint subsets to generate the interleaving matrix. After that, the interleaving matrix is split into S_G groups, and each S_G group contains V rows, where $G = \{1, 2, 3, \dots, N/V\}$. Afterward, only the odd S_G groups are chosen for processing, and then the first row is changed with the last one and the second row with the one before the last, etc. lastly, the S-IL-S-PTS segmentation matrix is obtained, and the subcarriers allocated symmetrically, similar to the sine wave shape.

The S-IL-S-PTS segmentation is applied to PTS algorithm, and the OFDM signal with the lowest PAPR value is selected for transmission. The S-IL-S-PTS method works to reduce the autocorrelation between the subcarriers of the subblocks. Therefore, the PAPR reduction performance is improved accordingly. Moreover, the computational complexity of the S-IL-S-PTS is the same as that of the IL-PTS method.

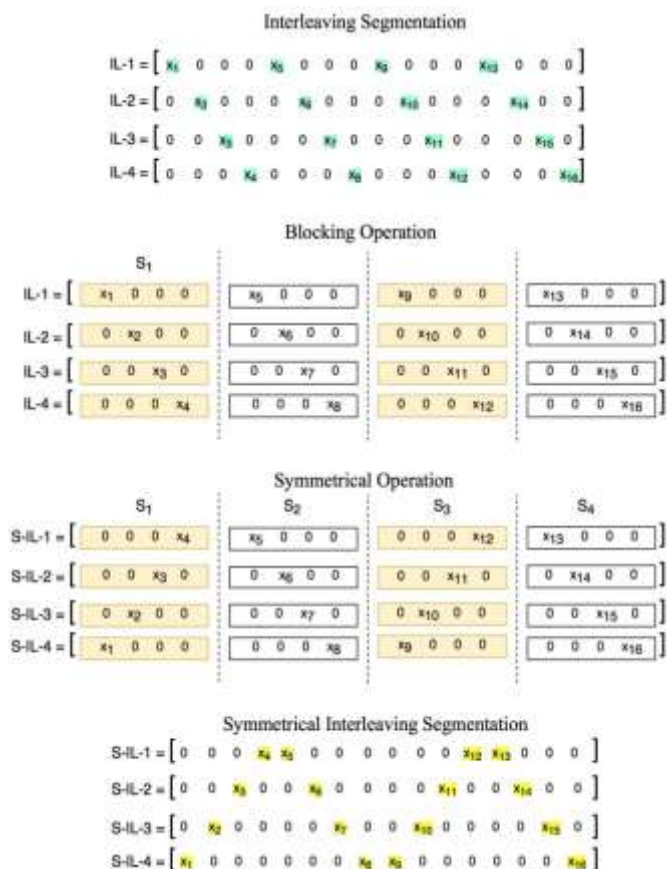


Fig. 4. S-IL-S-PTS scheme when V=4 and N=16

C. Hybrid adjacent and interleaving segmentation PTS

Ad-PTS is one of the segmentation methods for PTS algorithm, in which the successive subcarriers are assigned within subblocks sequentially. This approach can be achieved PAPR reduction performance better than that of IL-PTS, but the computational complexity is higher than that of IL-PTS.

Hybrid adjacent and interleaving segmentation PTS method (H-Ad-IL-PTS) is a new hybrid scheme that combines the features of both adjacent partitioning and interleaving partitioning schemes. H-Ad-IL-PTS can improve the PAPR reduction performance better than of both Ad-PTS and IL-PTS schemes. Moreover, its computational complexity is the same as that of IL-PTS scheme.

Fig. 5 illustrates the H-Ad-IL-PTS where the input data sequence is partitioned into V subblocks by using Ad-PTS method. Then, each row of the adjacent matrix is sub-divided into B_G blocks, and each block contains V/2 subcarriers, where G = {1, 2, ..., N/(V/2)}. Afterward, the interleaving method is applied to the modified adjacent matrix; with the consideration that; the original subcarriers of each S_G block are kept in the

same positions. Finally, the obtained H-Ad-IL-PTS scheme is fed to PTS algorithm to generate the OFDM signal. The proposed scheme exploits the capability of the Ad-PTS for reducing the PAPR performance and the tendency of the IL-PTS for decreasing the computational complexity. Therefore, H-Ad-IL-PTS method outperforms to the Ad-PTS and IL-PTS methods.

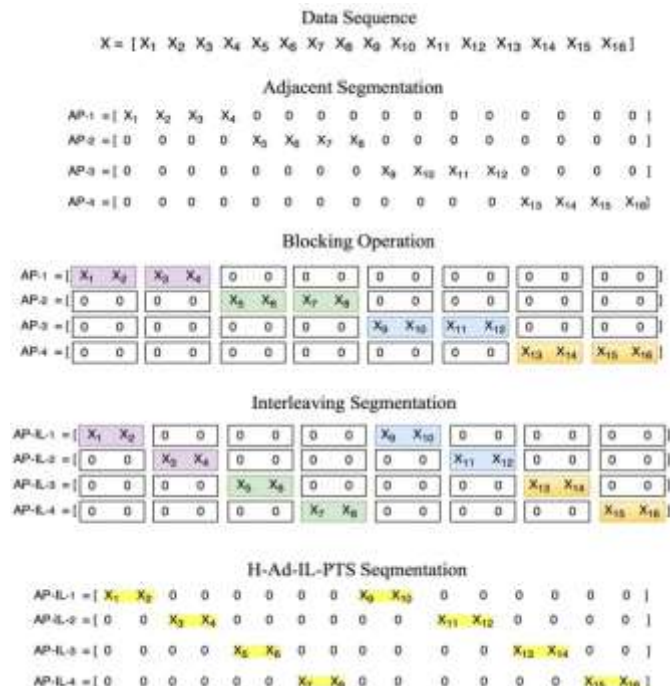


Fig. 5. H-Ad-IL-PTS scheme when V=4 and N=16

D. Symmetrical H-Ad-IL-PTS Cosine Wave Shape

The basic algorithm of the symmetrical H-Ad-IL-PTS cosine wave shape (SC-H-Ad-IL-PTS) is a combination of H-Ad-IL-PTS scheme and S-IL-C-PTS scheme. This method works to break down the autocorrelation between the subcarriers within the subblocks. Thus the PAPR reduction rendering will be improved accordingly. In addition, the computational complexity of the proposed scheme is the same as that of the IL-PTS method.

Fig. 6 clarifies the SC-H-Ad-IL-PTS scheme, in which the H-Ad-IL-PTS matrix is applied to the S-IL-C-PTS algorithm to generate the new scheme. The procedure is division the H-Ad-IL-PTS matrix into B_G groups, where G = {1, 2, ..., N/2V}. After that, only even groups are selected for processing. In every even group, the first row is changed with the last one and the second row with the one before the last, and so on. Finally, the proposed scheme is implemented on the PTS procedure, and the OFDM signal that has the lowest PAPR value is elected for transmission.

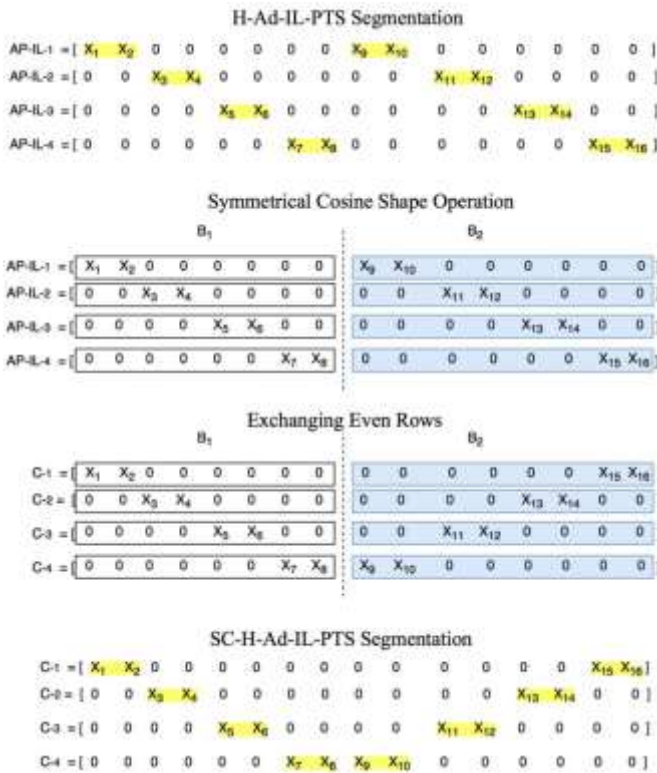


Fig. 6. SC-H-Ad-IL-PTS scheme when V=4 and N=16

E. Symmetrical H-Ad-IL-PTS Sine Wave Shape

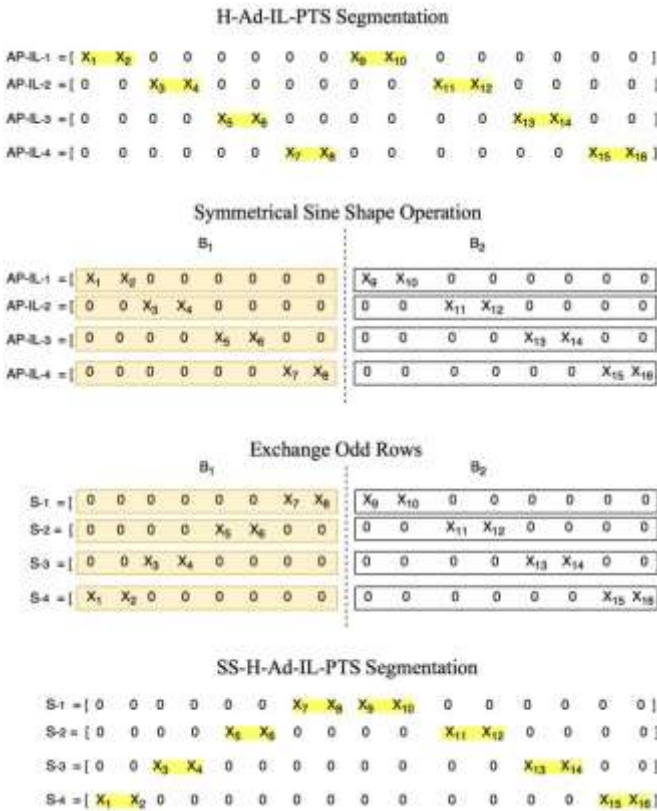


Fig. 7. SS-H-Ad-IL-PTS scheme when V=4 and N=16

This method merges the H-Ad-IL-PTS scheme with S-IL-S-PTS scheme in the frequency domain to produce a new scheme named symmetrical H-Ad-IL-PTS sine wave shape (SS-H-Ad-IL-PTS). The proposed method can diminish the PAPR value better than Ad-PTS and IL-PTS because the autocorrelation between the subcarriers is decreased. Moreover, SS-H-Ad-IL-PTS method can achieve computational complexity less than that of the Ad-PTS method and the same computational complexity of the IL-PTS method.

The proposed method is shown in Fig. 7, where the H-Ad-IL-PTS is established, and then the matrix is divided into B_G groups, where $G = \{1, 2, \dots, N/2V\}$. Afterward, only the odd B_G groups are selected from the H-IL-Ad-PTS matrix for processing, in which the first row of the odd B_G groups is changed with the last row and the second row with the one preceding the last, etc. Lastly, the PTS pattern performs on the new scheme to create a set of candidate signals. The candidate signal which can realize the lower PAPR value is selected for transmission.

VI. RESULTS AND DISCUSSION

In this section, a computer simulation has been implemented to evaluate and analysis the proposed methods and ordinary PTS method. The simulation parameters that used in this simulation are: the number of subcarriers $N=128$ and 256 , the number of subblocks $V=4$, the number of allowed phase rotation factors $W=4$ and the data samples are mapped by 16-QAM. In addition, 1000 OFDM symbols are generated randomly to evaluate the PAPR performance, and the oversampling factor is set to 8.

Firstly, the three common types of the segmentation schemes are simulated when $N=128$ and 256 , as shown in Fig. 8 and Fig. 9, respectively. As can be seen from Fig. 8, the PAPR reduction rendering of the PR-PTS scheme is superior to Ad-PTS, IL-PTS and the original OFDM signal by 0.84dB, 1.27dB, and 4dB, respectively. Moreover, Fig. 9 shows the PAPR performance of the PR-PTS, Ad-PTS, IL-PTS, and the original signal when $N=256$. The CCDF of the PR-PTS achieved better PAPR reduction performance at 7.77dB and Ad-PTS was the next best at 8.51dB. However, IL-PTS scheme realized the worst among the three segmentation schemes at 9.17dB.

In simulation result as shown in Fig. 10, the S-IL-C-PTS method is compared with Ad-PTS and IL-PTS methods when the $CCDF=10^{-5}$ and $N=128$. The PAPR value of the original signal was 11dB, IL-PTS was 8.4dB, and Ad-PTS was 8.15dB. However, the S-IL-C-PTS algorithm can achieve better PAPR reduction performance at 7.45dB. In addition, Fig. 11 simulates the same parameters that conducted in Fig. 10 except the subcarriers number increased to 256. S-IL-C-PTS was also achieved greater PAPR performance at 8.1dB compared with Ad-PTS and IL-PTS schemes. Therefore, S-IL-C-PTS scheme considers better performance than Ad-PTS and IL-PTS schemes for any number of the subcarriers.

Simulation comparison of PAPR reduction rendering is implemented by using S-IL-S-PTS scheme and Ad-PTS, IL-PTS as well as the original signal, with the consideration that; the number of subcarriers N is 128 and 256. It shown in Fig.

12, the PAPR performance of the S-IL-S-PTS scheme is 7.44dB. However, the PAPR value of the Ad-PTS, IL-PTS, and the original signal is 8.15 dB, 8.40 dB, and 11 dB, respectively. Moreover, Fig. 13 shows the PAPR performance of the S-IL-S-PTS when the number of subcarriers increased to 256. It is clearly, the proposed method can minimize the PAPR value by 3.85dB from the original OFDM signal. Therefore, the S-IL-S-PTS method is superior to Ad-PTS and IL-PTS schemes for various numbers of subcarriers.

The observation result as shown in Fig. 14, the new hybrid method is compared with Ad-PTS and IL-PTS when $N=128$. The H-Ad-IL-PTS algorithm achieved PAPR performance better than Ad-PTS and IL-PTS schemes by 0.71dB and 0.96 dB, respectively. In the same manner, the H-Ad-IL-PTS algorithm compared with adjacent and interleaving segmentation schemes when $N=256$, as shown in Fig. 15. The hybrid PTS method overcomes to the Ad-PTS and IL-PTS by 0.6dB and 1.1dB, respectively. Therefore, the H-Ad-IL-PTS scheme can be realized greater PAPR reduction performance than other ordinary schemes with the same number of subcarriers.

As can be seen from Fig. 16 and Fig. 17, The SC-H-Ad-IL-PTS method can reduce the PAPR value by 3.42dB and 4dB compared with the original OFDM signal, when the number of subcarriers is fixed at 128 and 256, respectively. Therefore, the enhanced method can improve the PAPR performance more valuable than Ad-PTS and IL-PTS schemes.

Similarly, Fig. 18 and Fig. 19 presents the simulation result for SS-H-Ad-IL-PTS algorithm compared with Ad-PTS and IL-PTS schemes when the subcarriers number is 128 and 256. The enhanced method can get better PAPR performance than Ad-PTS by 0.77dB and IL-PTS by 1.12dB when $N=128$. However, the PAPR performance of the SS-H-Ad-IL-PTS method is greater than the Ad-PTS and IL-PTS schemes by 0.7dB and 1.2dB when the number of subcarriers is 256.

TABLE I. NUMERICAL SIMULATION RESULTS OF THE VARIOUS SEGMENTATION SCHEMES

V=4, W=4		
PTS Methods	PAPR[dB]	
	N=128	N=256
Original signal	11	12.05
Ad-PTS	8.15	8.55
IL-PTS	8.4	9.05
S-IL-C-PTS	7.45	8.1
S-IL-S-PTS	7.44	8.1
H-Ad-IL-PTS	7.58	8.1
SC- H-Ad-IL-PTS	7.28	7.85
SS- H-Ad-IL-PTS	7.26	7.76

Table I summarizes all the numerical simulation results. It is clearly, the proposed methods can be achieved greater PAPR reduction rendering than the ordinary methods. In addition, Table II and Table III demonstrate the PAPR reduction ratio according to the original OFDM signal for different PTS schemes. It can be concluded that the proposed schemes can achieve better PAPR reduction percentages than the conventional schemes IL-PTS and IL-PTS in both scenarios. On the other hand, the proposed methods can improve the PAPR performance without any increasing in complexity.

TABLE II. PAPR REDUCTION RATIO OF THE VARIOUS SEGMENTATION SCHEMES WHEN N= 128

V= 4, W= 4, N= 128			
PTS Methods	PAPR of Original Signal [dB]	PAPR of PTS Method [dB]	PAPR Reduction Ratio
Ad-PTS	11	8.15	25.9%
IL-PTS		8.4	23.63%
S-IL-C-PTS		7.45	32.27%
S-IL-S-PTS		7.44	32.36%
H-Ad-IL-PTS		7.58	31.09%
SC-H-Ad-IL-PTS		7.28	33.81%
SS-H-Ad-IL-PTS		7.26	34%

TABLE III. PAPR REDUCTION RATIO OF THE VARIOUS SEGMENTATION SCHEMES WHEN N= 256

V= 4, W= 4, N= 256			
PTS Method	PAPR of Original Signal [dB]	PAPR of PTS Method [dB]	PAPR Reduction Ratio
Ad-PTS	12	8.55	28.75%
IL-PTS		9.05	24.58%
S-IL-C-PTS		8.1	32.5%
S-IL-S-PTS		8.1	32.5%
H-Ad-IL-PTS		8.1	32.5%
SC-H-Ad-IL-PTS		7.85	34.58%
SS-H-Ad-IL-PTS		7.76	35.33%

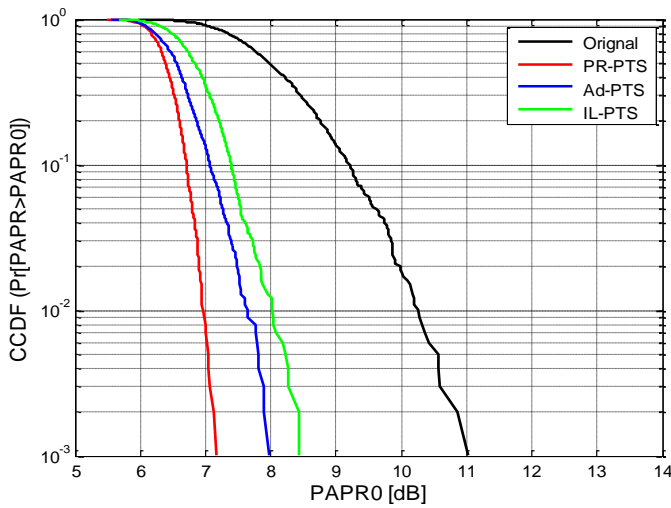


Fig. 8. PAPR comparison of the three ordinary PTS segmentation schemes for N=128

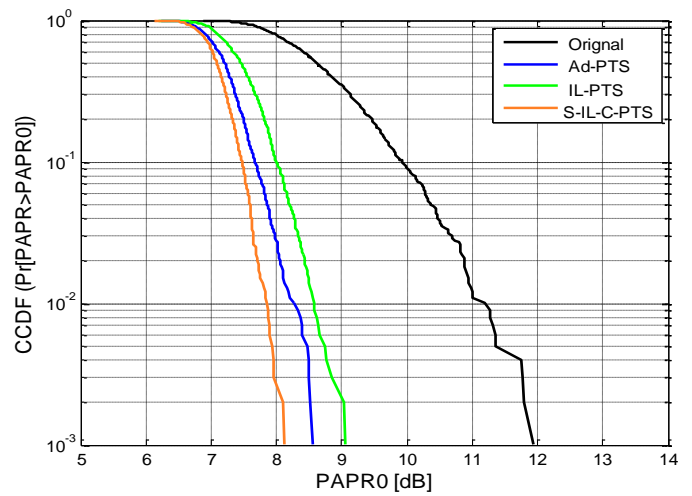


Fig. 11. PAPR comparison of the S-IL-C-PTS scheme and the ordinary PTS schemes for N=256

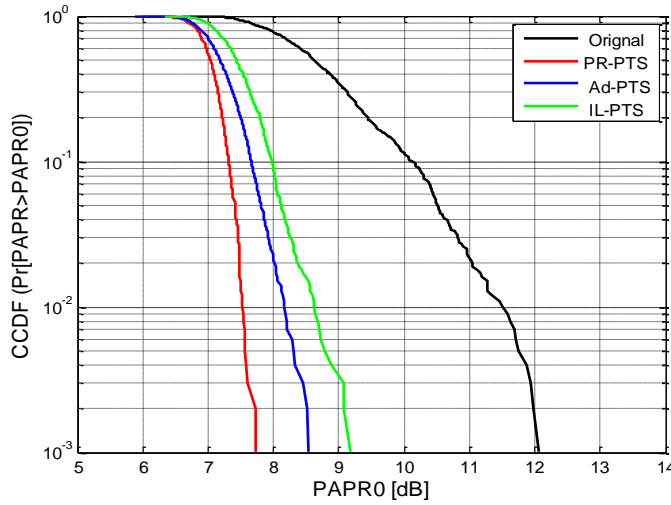


Fig. 9. PAPR comparison of the three ordinary PTS segmentation schemes for N=256

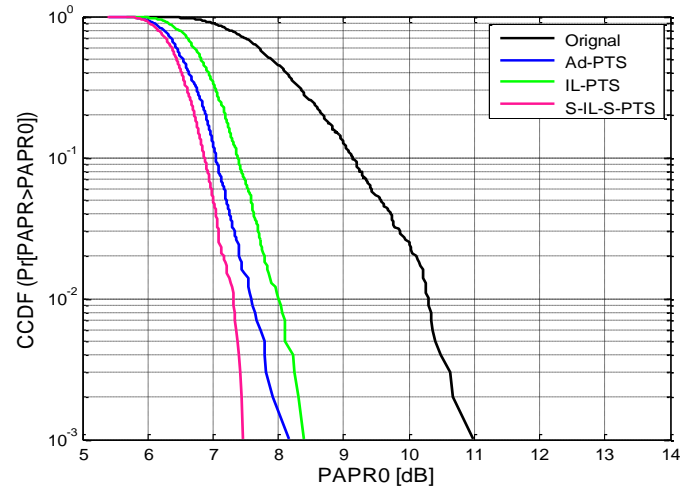


Fig. 12. PAPR comparison of the S-IL-S-PTS scheme and the ordinary PTS schemes for N=128

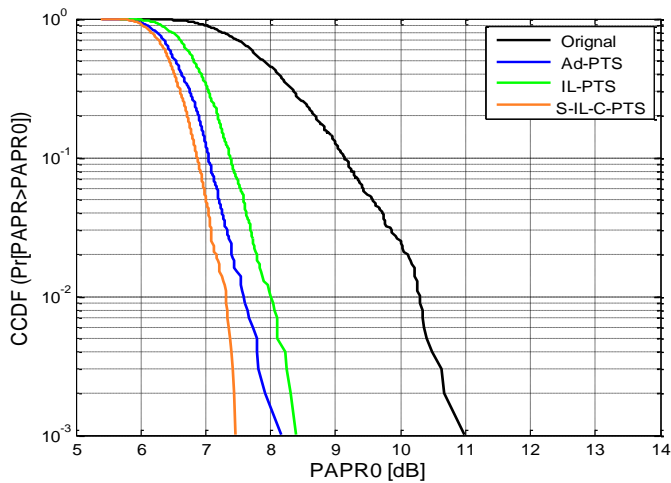


Fig. 10. PAPR comparison of the S-IL-C-PTS scheme and the ordinary PTS schemes for N=128

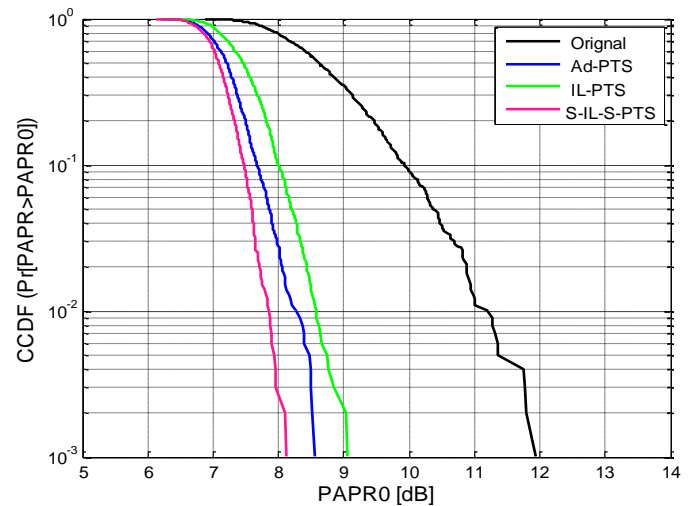


Fig. 13. PAPR comparison of the S-IL-S-PTS scheme and the ordinary PTS schemes for N=256

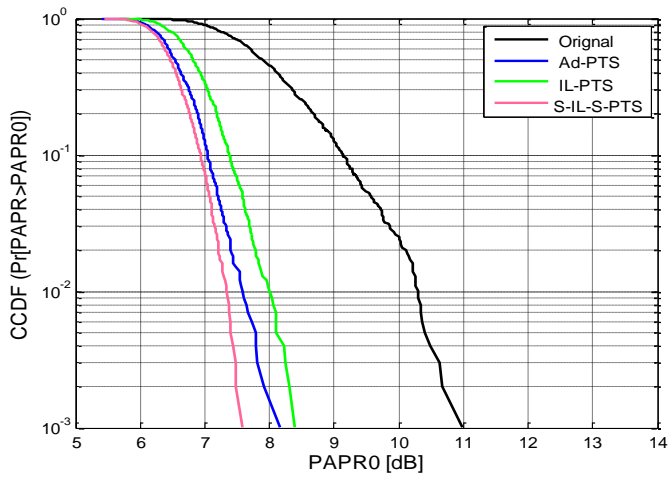


Fig. 14. PAPR comparison of the H-Ad-IL-PTS scheme and the ordinary PTS schemes for N=128

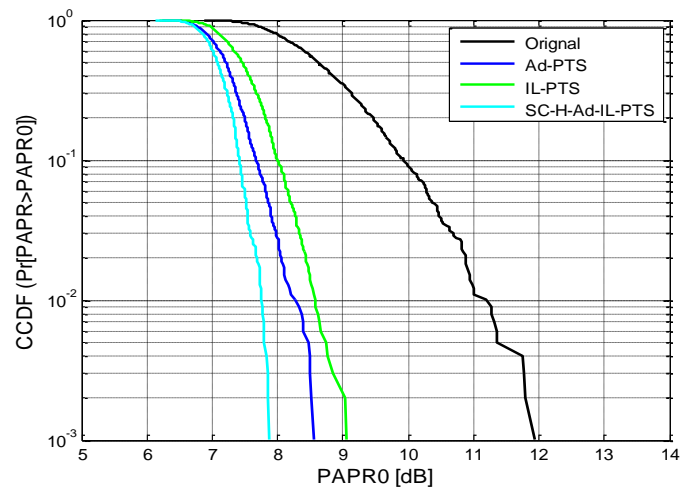


Fig. 17. PAPR comparison of the SC-H-Ad-IL-PTS scheme and the ordinary PTS schemes for N=256

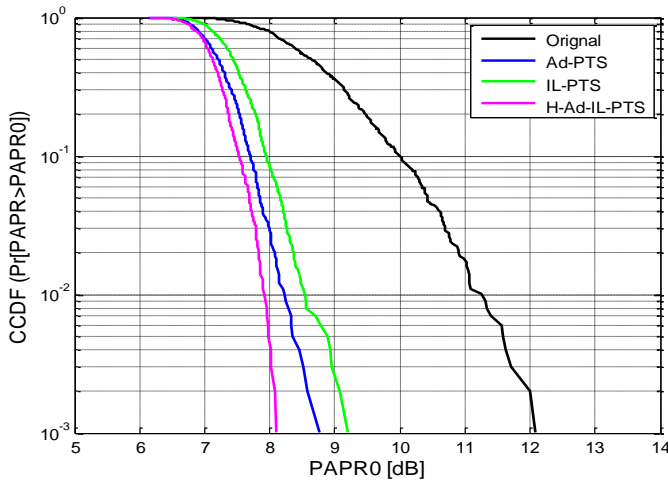


Fig. 15. PAPR comparison of the H-Ad-IL-PTS scheme and the ordinary PTS schemes for N=256

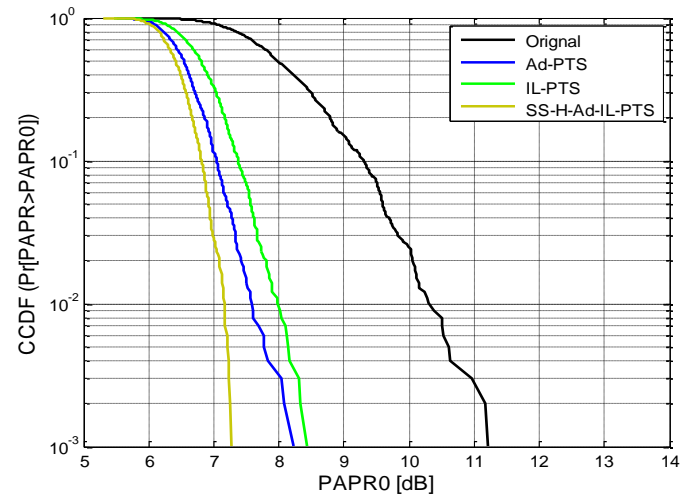


Fig. 18. PAPR comparison of the SS-H-Ad-IL-PTS scheme and the ordinary PTS schemes for N=128

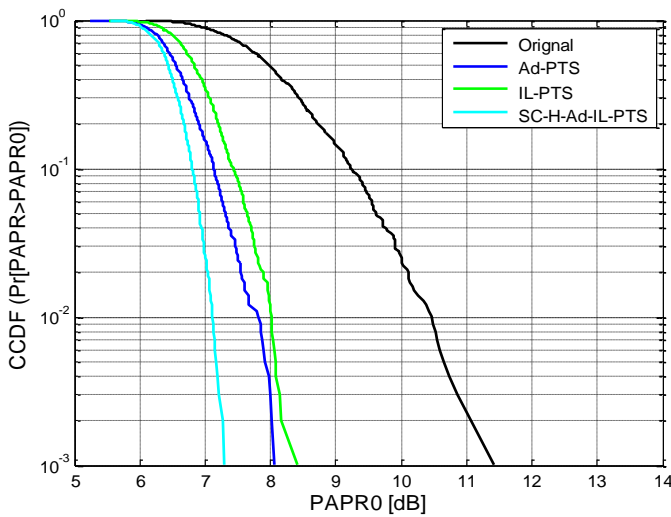


Fig. 16. PAPR comparison of the SC-H-Ad-IL-PTS scheme and three ordinary PTS schemes for N=128

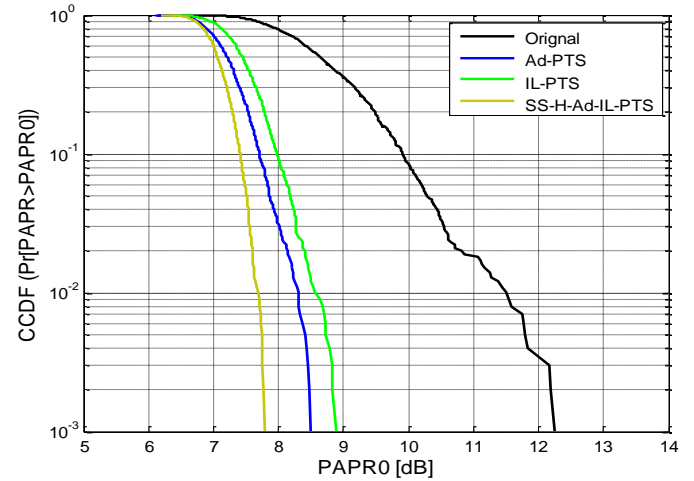


Fig. 19. PAPR comparison of the SS-H-Ad-IL-PTS scheme and the ordinary PTS schemes for N=256

VII. CONCLUSION

In this paper, the new PTS segmentation methods to reduce the PAPR in OFDM systems are proposed. The subblocks partition matrix of the PTS scheme is employed to generate the new types of the of segmentation schemes including S-IL-C-PTS, S-IL-S-PTS, H-Ad-IL-PTS, SC-H-Ad-IL-PTS, and SS-H-Ad-IL-PTS. The simulation results show the proposed methods can improve up the PAPR reduction execution compared with two well-known segmentation schemes adjacent and interleaving partition schemes. It has been seen that the proposed approaches can enhance the PAPR performance with any number of subcarriers, and the computational complexity of the new methods is kept low similar as that of the interleaving segmentation method. Therefore, the proposed schemes can be made the PTS technique more suitable for high-speed data rate wireless system, and the proposed methods could be applying in MIMO-OFDM for future work.

REFERENCES

- [1] K. Pachori and A. Mishra, "An efficient combinational approach for PAPR reduction in MIMO-OFDM system," *Wireless Networks*, vol. 22, pp. 417-425, 2016.
- [2] P. Praveenkumar, R. Amirtharajan, K. Thenmozhi, and J. B. B. Rayappan, "OFDM with low PAPR: A novel role of partial transmit sequence," *Res. J. Inform. Technol.*, vol. 5, pp. 35-44, 2013.
- [3] Z. Chen and S. G. Kang, "A three-dimensional OFDM system with PAPR reduction method for wireless sensor networks," *International Journal of Distributed Sensor Networks*, vol. 2014, pp. 1-6, 2014.
- [4] M. Vidya, M. Vijayalakshmi, and K. Ramalingareddy, "Performance enhancement of efficient partitioning technique for PAPR reduction in MIMO-OFDM system using PTS," *2015 Conference on Power, Control, Communication and Computational Technologies for Sustainable Growth (PCCCTSG)*, pp. 247-253, 2015.
- [5] Y. A. Jawhar, R. A. Abdulhasan, and K. N. Ramli, "Influencing Parameters in Peak to Average Power Ratio Performance on Orthogonal Frequency-Division Multiplexing System," *ARNP journal of engineering and applied sciences*, vol. 11(7), pp. 4322-4332, 2016.
- [6] B. H. Alhasson and M. A. Matin, "PAPR distribution analysis of OFDM signals with partial transmit sequence," *14th International Conference on in Computer and Information Technology (ICCIIT)*, pp. 652-656, 2011.
- [7] F.-S. FET-SSGI, "A Novel Approach to Reduce PAPR in OFDM Using combined DCT Precoding Technique and Clipping Method," *ARNP journal of engineering and applied sciences*, vol. 10(5), pp. 2182-2186, 2015.
- [8] L. Yang, K. K. Soo, S. Li, and Y. M. Siu, "PAPR reduction using low complexity PTS to construct of OFDM signals without side information," *IEEE Transactions on Broadcasting*, vol. 57, pp. 284-290, 2011.
- [9] M. I. Abdullah, "Comparative study of PAPR reduction techniques in OFDM," *ARNP journal of systemes and software*, vol. 1(8), pp. 263-269, 2011.
- [10] Yasir Amer Jawhar, Raed A. Abdulhasan and Khairun Nidzam Ramli, "A New Hybrid Sub-Block Partition Scheme of PTS Technique for Reduction PAPR Performance in OFDM System," *ARNP journal of engineering and applied sciences*, vol. 11(6), pp. 3904-3910, 2016.
- [11] S. P. Mohammad and K. Gopal, "Hybrid Technique for BER and Paper Analysis of OFDM Systems," *Indian Journal of Science and Technology*, vol. 9(15), pp. 1-5, 2016.
- [12] Z. T. Ibraheem, M. M. Rahman, S. Yaakob, M. S. Razalli, F. Salman, and K. K. Ahmed, "PTS Method with Combined Partitioning Schemes for Improved PAPR Reduction in OFDM System," *Indonesian Journal of Electrical Engineering and Computer Science*, vol. 12, pp. 7845-7853, 2014.
- [13] X. Wu, J. Wang, Z. Mao, and J. Zhang, "Conjugate interleaved partitioning PTS scheme for PAPR reduction of OFDM signals," *Circuits, Systems and Signal Processing*, vol. 29, pp. 499-514, 2010.
- [14] D. W. Lim, S. J. Heo, and J. S. No, "An overview of peak-to-average power ratio reduction schemes for OFDM signals," *Communications and Networks Journal*, vol. 11, pp. 229-239, 2009.
- [15] M. A. Taher, J. Mandeep, M. Ismail, S. A. Samad, and M. T. Islam, "Reducing the power envelope fluctuation of OFDM systems using side information supported amplitude clipping approach," *International Journal of Circuit Theory and Applications*, vol. 42, pp. 425-435, 2014.
- [16] L. Wang and C. Tellambura, "An overview of peak-to-average power ratio reduction techniques for OFDM systems," *2006 IEEE International Symposium on Signal Processing and Information Technology*, pp. 840-845, 2006.
- [17] T. Jiang and Y. Wu, "An overview: peak-to-average power ratio reduction techniques for OFDM signals," *IEEE transactions on Broadcasting*, vol. 54, pp. 257-268, 2008.
- [18] S. H. Müller and J. B. Huber, "A comparison of peak power reduction schemes for OFDM," *IEEE Global Telecommunications Conference, GLOBECOM'97*, pp. 1-5, 1997.
- [19] M. A. Taher, M. J. Singh, M. Ismail, S. A. Samad, M. T. Islam, and H. F. Mahdi, "Post-IFFT-Modified Selected Mapping to Reduce the PAPR of an OFDM System," *Circuits, Systems, and Signal Processing*, vol. 34, pp. 535-555, 2015.
- [20] S. H. Müller and J. B. Huber, "OFDM with reduced peak-to-average power ratio by optimum combination of partial transmit sequences," *Electronics letters*, vol. 33, pp. 368-369, 1997.
- [21] S. H. Han and J. H. Lee, "An overview of peak-to-average power ratio reduction techniques for multicarrier transmission," *IEEE Wireless Communications*, vol. 12, pp. 56-65, 2005.
- [22] C. Hong, Q. Qin, and T. Chao, "An PTS optimization algorithm for PAPR reduction of OFDM system," *2013 International Conference on Mechatronic Sciences, Electric Engineering and Computer (MEC)*, pp. 3775-3778, 2013.
- [23] L. Xia, X. Yue, L. Shaoqian, H. Kayama, and C. Yan, "Analysis of the performance of partial transmit sequences with different subblock partitions," *2006 International Conference on Communications, Circuits and Systems Proceedings*, pp. 875-878, 2006.
- [24] L. Xia, X. Yue, T. Youxi, and L. Shaoqian, "A novel method to design phase factor for PTS based on pseudo-random sub-block partition in OFDM system," *2007 IEEE 66th Vehicular Technology Conference, VTC-2007 Fall*, pp. 1269-127, 2007.
- [25] Y. Xiao, Q. Wen, X. Lei, and S. Li, "Improved PTS for PAPR reduction in OFDM systems," *The Third Advanced International Conference on Telecommunications, AICT 2007*, pp. 37-37, 2007.
- [26] L. Miao and Z. Sun, "PTS algorithm for PAPR suppression of WOFDM system," *Proceedings 2013 International Conference on Mechatronic Sciences, Electric Engineering and Computer (MEC)*, pp. 1144-1147, 2013.
- [27] A. Singh and H. Singh, "Peak to average power ratio reduction in OFDM system using hybrid technique," *Optik-International Journal for Light and Electron Optics*, vol. 127, pp. 3368-3371, 2016.
- [28] J. Zhou, E. Dutkiewicz, R. P. Liu, G. Fang, Y. Liu, and X. Huang, "A modified shuffled frog leaping algorithm for PAPR reduction in OFDM systems," *IEEE Region 10 Conference TENCON 2014*, pp. 1-6, 2014.
- [29] M. Taher, M. Singh, M. Ismail, S. A. Samad, and M. T. Islam, "Sliding the SLM-technique to reduce the non-linear distortion in OFDM systems," *Elektronika ir Elektrotechnika*, vol. 19, pp. 103-111, 2013.
- [30] L. Amhaimar, S. Ahyoud, A. Aselman, and E. Said, "Peak-to-Average Power ratio reduction based varied Phase for MIMO-OFDM Systems," *International Journal of Advanced Computer Science and Applications*, vol. 7, pp. 432-437, 2016.
- [31] S. G. Kang, J. G. Kim, and E. K. Joo, "A novel subblock partition scheme for partial transmit sequence OFDM," *IEEE Transactions on Broadcasting*, vol. 45, pp. 333-338, 1999.
- [32] L. Yang, R. S. Chen, Y. M. Siu, and K. K. Soo, "PAPR reduction of an OFDM signal by use of PTS with low computational complexity," *IEEE Transactions on Broadcasting*, vol. 52, pp. 83-86, 2006.

- [33] T. Jiang, W. Xiang, P. C. Richardson, J. Guo, and G. Zhu, "PAPR reduction of OFDM signals using partial transmit sequences with low computational complexity," *IEEE Transactions on Broadcasting*, vol. 53, pp. 719-724, 2007.
- [34] L. Miao and Z. Sun, "PTS algorithm for PAPR suppression of WOFDM system," *International Conference on Mechatronic Sciences, Electric Engineering and Computer (MEC)*, pp. 1144-1147, 2013.

Model and Criteria for the Automated Refactoring of the UML Class Diagrams

Evgeny Nikulchev
Moscow Technological Institute
Moscow, Russia

Olga Deryugina
Moscow Technological University MIREA
Moscow, Russia

Abstract—Many papers have been written on the challenges of the software refactoring. The question is which refactorings can be applied on the modelling level. Based on the UML model, for example. With the aim of evaluating this possibility the algorithm and the software tool of automated UML class diagram refactoring were introduced. The software tool proposed reduces the level of the UML class diagram complexity metric.

Keywords—UML; refactoring; class diagrams; software architecture; software design; UML transformation

I. INTRODUCTION

MDA (Model Driven Architecture) [1] approach is supported by OMG (Object Management Group). In the MDA approach design process starts with the creation of the PIM (Platform Independent Model). Then the PIM is automatically transformed into the PSM (Platform Specific Model).

MDA proposes standards of model creation, transformation and exchange. For example, UML (Unified Modelling Language) [2] is used to describe models, XMI (XML Metadata Interchange) [3] is used to exchange models between tools. One tool can be used to create a model, and another one – to analyze or transform it. Thus, model transformations play an important role in the MDA conception. One of the possible model transformation objectives can be model refactoring.

Refactoring means restructuring of the system without changing its behavior. Originally, refactoring was connected with the code-level transformations. A number of studies have investigated different means of the software refactoring [4, 5, 6].

Some refactorings apply design patterns to the existing code. First design patterns were proposed by Erich Gamma et al. in [7]. Software design patterns describe solutions of commonly occurring problems. Design patterns are aimed at the improvement of such software characteristics as modifiability, reusability, maintainability, etc.

Many papers have been written on the challenges of the software refactoring. The question is which refactorings can be applied on the PIM level described with the UML.

There are two main approaches to the problem of UML refactoring. The first one is connected with the search based software engineering [8] (SBSE), which is a topic of growing interest nowadays. In SBSE software engineering problems are formulated as optimization problems, which then are solved by search algorithms (Genetic algorithm, Simulated annealing,

Swarm intelligence algorithms, etc.) SBSE is used in order to solve UML class diagram refactoring problem in [9–14]. However, the result of applying search algorithms to class diagrams sometimes can be meaningless.

The second approach is connected with the developing frameworks of automated model refactoring [15–18], where the main role is given to the software designer. And the framework applies transformations, using some transformation rules in interaction with the designer.

This paper explores the problem of the automated UML class diagram refactoring. This problem is significant as long as the model refactoring is less time-consuming than the code refactoring. Furthermore, model refactoring is connected with the creation of PIM rather than PSM.

The rest of this paper is organized as follows: First, the problem of the automated UML class diagram refactoring is formulated in Section 2. Then an algorithm of the automated UML class diagram refactoring is proposed in Section 3. In Section 4, the software tool UML Refactoring is introduced before concluding in Section 5.

II. FORMULATION OF THE PROBLEM

The scheme of the UML class diagram analysis is shown in Fig. 1. Algorithm takes as input UML class diagram d , fitness function $f(d)$ and a set of semantically equivalent transformations T . The output is a list of transformations T^* , which reduce fitness function value and are recommended to apply.

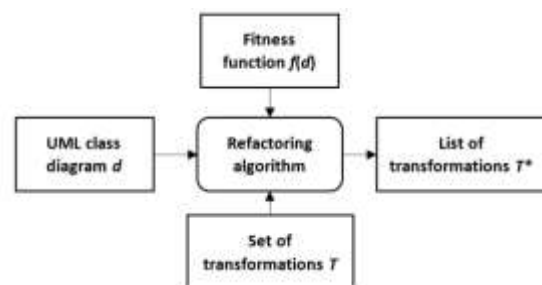


Fig. 1. Scheme of the UML class diagram analysis

Let d be a UML class diagram $d = \{C, I, R\}$, where C is a set of classes $C = \{c_0, \dots, c_k\}$, I is a set of interfaces $I = \{i_0, \dots, i_l\}$, R is a set of relations $R = \{r_0, \dots, r_g\}$.

Then c_i is a class $c_i = \{A_i, M_i, F_i\}$, where A_i is a set of attributes $A_i = \{a_0^i, a_1^i, \dots, a_n^i\}$, M_i is a set of methods $M_i = \{m_0^i, m_1^i, \dots, m_m^i\}$, F_i is a set of features $F_i = \{st_i, v_i, abs_i, \dots\}$, $st \in \{0,1\}$ is isStatic feature, v_i is visibility parameter $v_i \in \{public, private, protected\}$, abs_i is isAbstract feature $abs_i \in \{0,1\}$.

In addition, i_i is an interface which defines a set of methods $M_i = \{m_0^i, m_1^i, \dots, m_m^i\}$.

Let us assume that UML class diagram transformation t can be described as the following mapping function:

$$t(d, E) : d \rightarrow d', \quad (1)$$

where E is a set of diagram elements $e_i \in d$, $e_i \in \{C, R, I\}$.

Assume that the semantically equivalent transformation t is such a transformation $t(d, E) : d \rightarrow d'$, that:

$$S(d) \sim S(d'), \quad (2)$$

where $S(d)$ is a structural semantic value of the diagram d , which can be described as follows:

$$S_i = \{\{c_1^i = \{\dots\}, c_2^i = \{\dots\}, \dots, c_k^i = \{\dots\}\}, \{i_1^i = \{\dots\}, i_2^i = \{\dots\}, \dots, i_l^i = \{\dots\}\}, \{r_1^i, r_2^i, \dots, r_m^i\}\}, \quad (3)$$

where $c_1, \dots, c_k \in d_i$ are the classes of the diagram d ; $i_1, \dots, i_l \in d_i$ are the interfaces of the diagram d ; $r_1, \dots, r_m \in d_i$ are the relations of the diagram d .

The automated UML class diagram refactoring problem can be formulated as follows:

Assume that there is a UML class diagram d , a set of semantically equivalent transformations T , and a fitness function $f(d)$.

Then it is required to find such a set of pairs $\{t, E\}$, that:

$$d' = t(d, E), \Delta f(d') < 0.$$

III. AUTOMATIC UML CLASS DIAGRAM REFACTORING ALGORITHM

Then the CDTA (Class Diagram Transformation Analysis) Algorithm can be described as follows:

```

for each  $t \in T$ 
 $L = \text{search}(t, d, f)$  //search pairs  $\{t, E\}$  for which  $\Delta f(d') < 0$ 
 $Q.add(L)$  //add pairs  $\{t, E\}$  to the resulting list
return  $Q$ 
    
```

The search(t, d, f) function can be defined as follows:

```

 $L1 = \text{analyze}(t, d)$  //search element sets  $E \in d$  for the transformation
for each  $e \in L1$ 
    
```

```

 $d' = \text{refactor}(e, t, d)$  //apply transformation  $t$  to the diagram  $d$ 
if ( $f(d') < f(d)$ ) //check the decrease of the  $f(d)$  value
 $L2.add(t, e)$  //add  $t$  and  $e$  to the resulting list
return  $L2$ 
    
```

The analyze (t, d) method is specific for each transformation. For example, the algorithm of searching sets of diagram elements E on which the Strategy transformation can be conducted can be described as follows:

- 1) Make a list of classes having inheritors $I1$.
- 2) 2. For each class from $I1$ check whether its inheritors implement any interfaces. If yes – add them to the list $I2$.
- 3) 3. For each class from $I1$ calculate $\Delta K(d)$. If $\Delta K(d) < 0$ – add to the list $I3$: $\{\text{parent_id}, \{\text{child_classes_ids}\}, \{\text{interfaces_ids}\}\}$.
- 4) 4. Return $I3$.

Let us formulate an example of the fitness function – structural complexity metric $K(d)$:

$$K(d) = k_1 \cdot |C| + k_2 \cdot |I| + k_3 \cdot |R| + k_4 \cdot \sum_{i=0}^n |A_i| + k_5 \cdot \sum_{i=0}^n |M_i| + k_6 \cdot \sum_{i=0}^m |M_j'|, \quad (4)$$

where $K(d)$ is the structural complexity of the diagram d ; $|C|$ is the number of classes $c_i \in d$; $|I|$ is the number of interfaces $i_i \in d$; $|R|$ is the number of relations $r_i \in d$; A_i is a set of attributes $a_j \in c_i, c_i \in d$; M_i is a set of class methods (except of the methods, declared in implemented interfaces) $m_i \in c_i, c_i \in d$; M_j' is a set of interface methods $m_j \in i_i, i_i \in d$; $k_1, k_2, k_3, k_4, k_5, k_6$ are weights for each group of elements.

IV. UML CLASS DIAGRAM REFACTORING TOOL

Class diagram refactoring software should solve the following tasks:

1) UML class diagram analysis: searching the transformations which can be conducted to decrease the fitness function value;

2) UML class diagram transformation.

Main functional blocks of the UML refactoring tool are shown in Fig. 2. XMI parser translates XMI document to the abstract data structure UML Map [19], which stores UML class diagram elements in hash-maps. Then Analyzer searches pairs $\{t, E\}$, which reduce fitness function value and forms the Transformations table on the screen. OOM Calculator calculates various object-oriented metrics for the UML class diagram and forms the Metrics table on the screen. If a user has chosen some transformation from the table, the Transformer applies it to the diagram. User can export an attained diagram to XMI document.

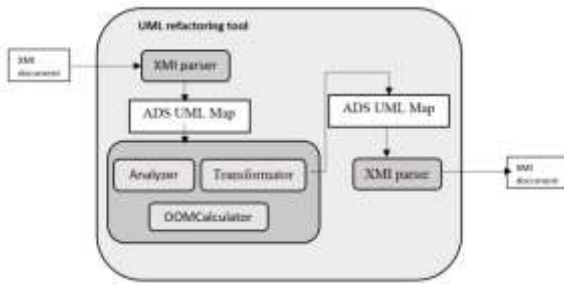


Fig. 2. Functional blocks of the UML class diagram refactoring tool

Let us introduce an example of applying the UML refactoring tool to the class diagram *d* shown in Fig. 3.

Assume that it is required to minimize relations count value. First, weight values for the fitness function should be set: $k_1 = 0.01; k_2 = 0.01; k_3 = 1; k_4 = 0.01; k_5 = 0.01; k_6 = 0.01$. Then it is attained, that:

$$K(d) = 0.06 + 0.02 + 12 + 0.03 + 0.06 + 0.02 = 12.19.$$

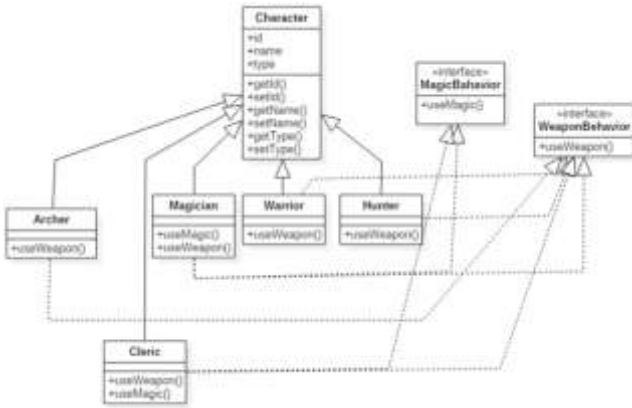


Fig. 3. Initial UML class diagram *d*

The UML Refactoring tool proposes the following transformations (see Fig. 4):

- Interface insertion for the classes Magician, Cleric and for methods useWeapon(), useMagic();
- Strategy insertion for the interfaces MagicBehaviour, WeaponBehaviour, parent class Character and child classes Archer, Magician, Warrior, Hunter, Cleric.

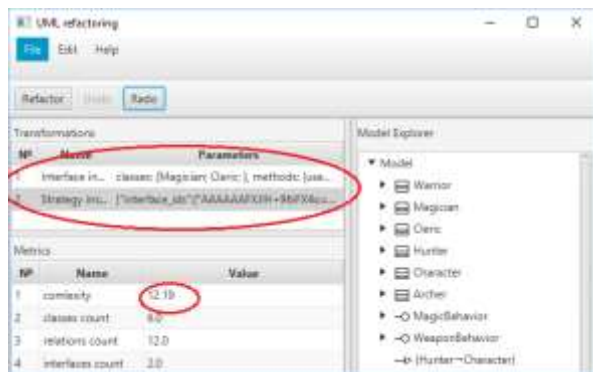


Fig. 4. Transformations proposed by the UML refactoring tool

The result of applying the Strategy transformation to the diagram *d* is shown in Fig. 5 and Fig. 6.

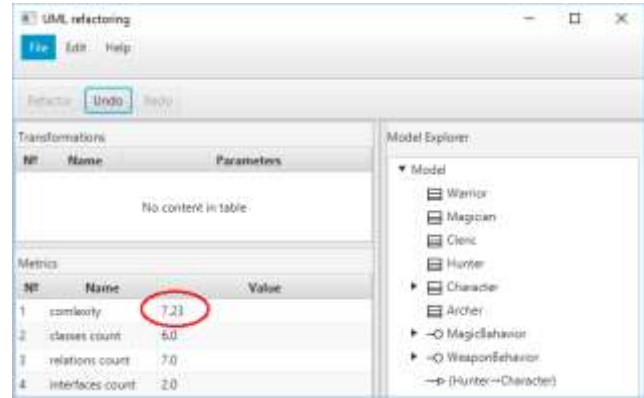


Fig. 5. The result of applying the Strategy transformation to the diagram *d*

After the transformation, the following is attained:

$$\Delta K(d') = 0.06 + 0.02 + 7 + 0.05 + 0.08 + 0.02 = 7.23,$$

$$\Delta K(d) = -4.96.$$

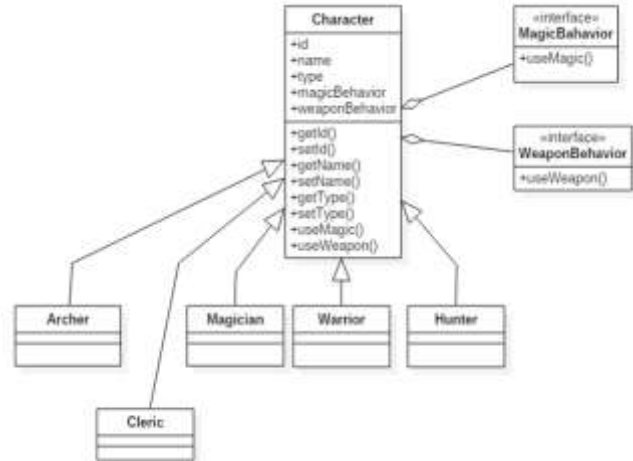


Fig. 6. Diagram *d'* attained as the result of the Strategy transformation

V. CONCLUSIONS

The presented framework gives the possibility to analyze and automatically restructure UML class diagrams in accordance with aims of the refactoring, which can be formulated based on the fitness function (4).

The main role is given to the software designer, who can import/export UML class diagrams in XMI format, refactor them and save the results.

The framework calculates metrics and proposes a list of transformations, which minimize the fitness function value. Available transformations include Strategy, Façade, Interface insertion, etc.

Future research should examine the effectiveness of the proposed framework to the large software systems. Furthermore, lists of available transformations and calculated metrics should be expanded.

REFERENCES

- [1] OMG Model Driven Architecture (<http://www.omg.org/mda>)
- [2] OMG Unified Modelling Language UML. Version 2.5 (<http://www.omg.org/spec/UML/2.5>)
- [3] XML Metadata Interchange (XMI) Specification. Version 2.4.2 (<http://www.omg.org/spec/XMI/2.4.2>)
- [4] J. Kerievsky, "Refactoring to Patterns. Boston M. A.: Addison-Wesley, 2004.
- [5] M. Fowler, Refactoring: Improving the Design of Existing Code", Boston M. A.: Addison-Wesley, 2000.
- [6] T. Mens, T. Tourwe, "A survey of software refactoring", IEEE Transactions on Software Engineering, vol. 30, no. 2, 2004, pp. 126 – 139.
- [7] E. Gamma, H. Richard, J. Ralph, and V. John, "Design patterns: Abstraction and reuse of object-oriented design", Springer Berlin Heidelberg, 1993.
- [8] M. Harman, S. Mansouri, Y. Zhang, "Search-based software engineering: Trends, techniques and applications", ACM Computing Surveys, vol. 45, no. 1, 2012.
- [9] M. Amoui, S. Mirarab, S. Ansari and C. Lucas, "A genetic algorithm approach to design evolution using design pattern transformation", International Journal of Information Technology and Intelligent Computing, vol. 1, 2006, pp. 235 – 245.
- [10] M. Bowman, L. Briand, and Y. Labiche, "Solving the class responsibility assignment problem in object-oriented analysis with multi-objective genetic algorithms", Technical report SCE-07-02, Carleton University.
- [11] S. Hadaytullah, Vathsavayi, O. Rähä, and K. Koskimies, "Tool support for software architecture design with genetic algorithms", Proceedings of ICSEA'10. IEEE CS Press, August 2010, pp. 359–366.
- [12] R. Lutz, "Evolving good hierarchical decompositions of complex systems, Journal of Systems Architecture", vol. 47, 2001, pp. 613 – 634
- [13] C. Simons C., I. Parmee, "Single and multi-objective genetic operators in object-oriented conceptual software design", Proceedings of the Genetic and Evolutionary Computation Conference (GECCO'07), 2007, pp. 1957 – 1958.
- [14] O. Deryugina, "Improving the structural quality of UML class diagrams with the genetic algorithm", 6th Seminar on Industrial Control Systems: Analysis, Modeling and Computation, vol. 6., 2016, art. 03003.
- [15] Y. Rhazali, Y. Hadi, A. Mouloudi, "A Model Transformation According Model Driven Architecture", Proceedings of 3rd International Conference on Computing Engineering & Enterprise Management (ICCEEM-2015), 2015, pp. 6 – 14.
- [16] Y. Rahmoune, A. Chaoui, E. Kerkouche, "A Framework for Modeling and Analysis UML Activity Diagram using Graph Transformation", International Workshop on the Use of Formal Methods in Future Communication Networks (UFMFCN 2015), 2015, pp. 612 – 617.
- [17] E. Kerkouche, A. Chaoui, E. Bourenane, O. Labbani, "A UML and Colored Petri Nets Integrated Modeling and Analysis Approach using Graph Transformation", Journal of Object Technology", vol. 9, no. 4, 2010. pp. 25–43.
- [18] Sergievskiy Maxim, "N-ary relations of association in class diagrams: design patterns," International Journal of Advanced Computer Science and Applications, vol. 7, no. 2, 2016, pp. 265-268.
- [19] O. A. Deryugina "Transformation of UML class diagrams using genetic algorithm", Russian Technological Journal, vol.1, no. 4 (9), 2015, pp. 36-42.

Improved Sliding Mode Nonlinear Extended State Observer based Active Disturbance Rejection Control for Uncertain Systems with Unknown Total Disturbance

Wameedh Riyadh Abdul-Adheem
Electrical Engineering Department
College of Engineering, Baghdad University
Baghdad, Iraq

Ibraheem Kasim Ibraheem
Electrical Engineering Department
College of Engineering, Baghdad University
Baghdad, Iraq

Abstract—This paper presents a new strategy for the active disturbance rejection control (ADRC) of a general uncertain system with unknown bounded disturbance based on a nonlinear sliding mode extended state observer (SMESO). Firstly, a nonlinear extended state observer is synthesized using sliding mode technique for a general uncertain system assuming asymptotic stability. Then the convergence characteristics of the estimation error are analyzed by Lyapunov strategy. It revealed that the proposed SMESO is asymptotically stable and accurately estimates the states of the system in addition to estimating the total disturbance. Then, an ADRC is implemented by using a nonlinear state error feedback (NLSEF) controller; that is suggested by J. Han and the proposed SMESO to control and actively reject the total disturbance of a permanent magnet DC (PMDC) motor. These disturbances caused by the unknown exogenous disturbances and the matched uncertainties of the controlled model. The proposed SMESO is compared with the linear extended state observer (LESO). Through digital simulations using MATLAB / SIMULINK, the chattering phenomenon has been reduced dramatically on the control input channel compared to LESO. Finally, the closed-loop system exhibits a high immunity to torque disturbance and quite robustness to matched uncertainties in the system.

Keywords—*extended state observer; sliding mode; rejection control; tracking differentiator; DC motor; nonlinear state feedback*

I. INTRODUCTION

Disturbances and uncertainties widely exist in all industrial systems and bring adverse effects on performance and even stability of control systems [1]–[3]. Not surprisingly, disturbance and uncertainty rejection is a key objective in control system design. When a disturbance is measurable, it is well known that a feed forward strategy could attenuate or eliminate the influence of disturbance. However, quite often, the external disturbance cannot be directly measured or is too expensive to measure. One intuitive idea to deal with this problem is to estimate the disturbance (or the influence of the disturbance) from measurable variables, and then, a control action can be taken, based on the disturbance estimate, to compensate for the influence of the disturbance. This basic idea can be intuitively extended to deal with uncertainties where the

influence of the uncertainties or unmodeled dynamics could be considered as a part of the disturbance. So, a new terminology of disturbance appeared, i.e. the total disturbance, which defines the aggregation of the input disturbances and system uncertainties (in this work the matched uncertainties) [4].

Many observers were designed in the last two decades like, high gain observers [5], disturbance observers [6] sliding mode observers [7]. The main advantages of sliding-mode observers (SMO) over their linear counterparts are that while in sliding, they are insensitive to the unknown inputs, and, moreover, they can be used to reconstruct unknown inputs which could be a combination of system disturbances, faults or nonlinearities [8]. Another useful property of SMO is that the analysis of the average value of the applied observer injection signal, the so-called equivalent injection signal, contains useful information about the mismatch between the model used to define the observer and the actual plant. In [9] comparison study of different advanced state, observers are carried out. Generally speaking, the ESO estimates the uncertainties, disturbances, and sensor noise efficiently. The beauty of ESO is that the lumped uncertainties and disturbances are estimated as a total disturbance by the ESO.

Firstly, the ESO proposed by Huang and Han in [10] is the key step of ADRC that is taking off as a technology after numerous successful applications in engineering. ESO has a simple structure, and it can estimate unmodeled dynamics precisely in many cases. Regarding ADRC, a class of nonlinear ESOs is designed to estimate the sum of both the states and external disturbances [11]. After that, Gao [12] proposed a class of linear ESOs (LESO) and provided guidance on how to choose the optimal parameters in the controller design. At present, ESO is mainly used in the control system to estimate disturbances and to compensate them via a feed-forward cancellation technique [13–15]. Moreover, ESO can be extended to multi-input–multi-output systems as well [15].

A class of nonlinear extended state observers (NESO) was proposed by J. Han [16] in 1995 as a unique observer design. It is rather independent of a mathematical model of the plants, thus achieving inherent robustness. It was tested and verified in key industrial control problems [17, 18].

ADRC design method was proposed to deal with both robust stability and performance specifications for a multivariable process with time delay in the input [19]. Veluvolu K.C *et al.* in [20] incorporated A sliding mode term into the nonlinear observer for a class of uncertain nonlinear systems so as to improve the estimation accuracy. While others proposed robust sliding mode control for uncertain time-delay systems against the mismatched uncertainties and matched external disturbance [21]. The researchers in [22] suggested a nonlinear disturbance observer-based robust control method for nonlinear systems in the presence of mismatched disturbances and uncertainties. People in [23] presented an adaptive fuzzy observer design for the fuzzy system with unknown output disturbance and bounded constant parameter uncertainty. The fuzzy observer was designed under the existence of uncertain parameters and output disturbance.

The application side of this work is highly related to fields where the disturbances or unwanted signals or uncertainties need to be measured or estimated. So, the main application of The technique proposed in this paper is used as an essential part of the Active Disturbance Rejection Control (ADRC) which consists of a tracking differentiator, extended state observer, and nonlinear state error feedback to solve some problems in various reference applications with promising results. The ADRC as an entire system has been applied in the medical field for the management of an artificial blood pump for terminal congestive heart failure [24]. In real manufacturing applications, the ADRC method has been used to accomplish the high-precision control of ball screw feed drives [25]. In [26], The ADRC based Load Frequency Control (LFC) has considered for both, single-area power system and multi-area power system network, where the area control error (ACE) is controlled in the existence of uncertainties in system dynamics and external disturbances, which are all estimated by the extended state observer. Also, a dual-loop ADRC algorithm that is used for an active hydraulic suspension system, which can help the six-wheel off-road vehicle to improve the performance transition [27]. In computer networks, the ADRC technique has been applied to maintain the stability of a network operating system in the presence of a delay caused by the network (sensor-controller delay and delay of the controller actuator), this delay is considered as a disturbance and is handled by the extended state observer [28]. In the field of robots, the ADRC is useful in quad helicopter control due to superiority to solve control problems and disturbance estimation of the nonlinear models with uncertainty and intense disturbances superiority [29].

The contribution of this paper is the design and robustness verification of the SMESO based ADRC in the presence of system matched uncertainties and exogenous disturbances for the PMDC motor. Firstly, we replace the ESO of the standard ADRC by a nonlinear observer designed by sliding mode technique. Then, a proper mathematical model for the PMDC motor is derived based on state-space representation by a careful choice of the states to get a model that fits the standard form of the chain integrators nonlinear form used in the design of the ADRC strategy. The mathematical model includes of an exogenous disturbance, which is called the *load torque* for the PMDC motor, the total disturbances, and the uncertainties are

all modeled and lumped in an augmented state to be estimated perfectly later by the proposed SMESO. Next, the SMESO is modeled and designed under the assumption that the closed-loop system is asymptotically stable. Otherwise, a suitable state feedback or another control design technique has to be set and applied to stabilize the unstable system. We show after that the stability of the proposed SMESO is already guaranteed if the nonlinear gain of the SMESO is above the critical gain threshold imposed by the SMESO observer stability. Finally, several numerical simulations are performed, and the results are compared with the standard ADRC proposed by J. Han ADRC [10, 11, 16, 24] based on LESO.

The rest of the paper is organized as follows: Section II presents the traditional ADRC, components of ADRC, and total disturbance estimation and rejection via ESO. The derivation of the mathematical model of the PMDC is introduced in section III. While the proposed SMESO design is presented and discussed in details, i.e. the derivation of the state-space model of the proposed observer and the stability conditions for the proposed SMESO are all discussed in section IV. Section V illustrates the numerical simulations and some comments and highlights on the work. Finally, conclusions are given in section VI.

II. ACTIVE DISTURBANCE REJECTION CONTROL (ADRC)

The ADRC can be constructed by combining the transient profile generation, the nonlinear feedback combination, and the total disturbance estimation and rejection; the ADRC takes the form as shown in Fig. 1 [30].

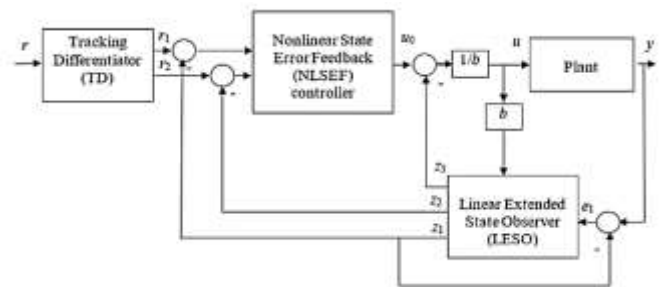


Fig. 1. ADRC topology

The desired transient profile is obtained by solving the following differential equation [30]:

$$\left. \begin{aligned} \dot{r}_1 &= r_2 \\ \dot{r}_2 &= -R \operatorname{sign}(r_1 - r(t) + \frac{r_2 |r_2|}{2r}) \end{aligned} \right\} \quad (1)$$

where r_1 is the desired trajectory and r_2 is its derivative. Note that, the parameter R is an application dependent and it is set accordingly to speed up or slow down the transient profile. It is in this sense that (1) is denoted as the “tracking differentiator” of $r(t)$.

As a control law, State Error Feedback employs a nonlinear combination of the present, accumulative, and predictive forms of the tracking error and has, for a long time, ignored other possibilities of this combination that are potentially much more effective. As an alternative, Han [11] proposed the following nonlinear function:

$$fal(e, \alpha, \delta) = \begin{cases} \frac{e}{\delta^{1-\alpha}} & |x| \leq \delta \\ |e|^\alpha sign(e) & |x| \geq \delta \end{cases} \quad (2)$$

An important concept called the total disturbance [31], its estimation, and rejection will be introduced in the following. Although such concept is, in general, applicable to most nonlinear multi-input–multi-output (MIMO) time varying systems, we will use a general second-order single-input–single-output (SISO) example for the sake of simplicity and clarity. Considering a single-input–single-output (possibly nonlinear) system with disturbance, depicted by [31]:

$$y^{(n)}(t) = f(y(t), \dot{y}(t), \dots, y^{(n-1)}(t), d(t), t) + bu(t) \quad (3)$$

where $y^{(i)}$ denotes the i^{th} derivative of the output y and u and d denote the input and the disturbance, respectively. This description represents a wide range of systems, which could be linear, or nonlinear and time invariant or time varying. To simplify the notation, the time variable will be dropped if no confusion is caused. Letting $x_1 = y, x_2 = \dot{y}, \dots, x_n = y^{(n-1)}$, one has

$$\left. \begin{aligned} \dot{x}_i &= x_{i+1}, \quad i = 1, \dots, n-1 \\ \dot{x}_n &= f(x_1, x_2, \dots, x_n, d, t) + bu \end{aligned} \right\} \quad (4)$$

Choose a new state as

$$\left. \begin{aligned} x_{n+1} &= f(x_1, x_2, \dots, x_n, d, t) \\ \dot{x}_{n+1} &= h(t) \end{aligned} \right\} \quad (5)$$

with

$$h(t) = \dot{f}(x_1, x_2, \dots, x_n, d, t) \quad (6)$$

A LESO is designed to estimate all of the states and lumped uncertainties and disturbance term f ,

$$\left. \begin{aligned} \dot{\hat{x}}_i &= \hat{x}_{i+1} + \beta_i(y - \hat{x}_1), \quad i = 1, \dots, n \\ \dot{\hat{x}}_{n+1} &= \beta_{n+1}(y - \hat{x}_1) \end{aligned} \right\} \quad (7)$$

It is obvious that both the influences of model dynamics (including unmodeled dynamics and uncertainties) and external disturbance are estimated in the LESO. Only the relative degree of the system under consideration is required in the LESO design. Therefore, the significant feature of LESO is that it requires minimum information about a dynamic system. Various extensions have been made to extend the basic LESO design to a wider range of dynamic systems [30].

III. MATHEMATICAL MODELING OF THE PERMANENT MAGNET DC (PMDC) MOTOR

Most electromechanical systems driven by DC motor such as weight belt feeder exhibits nonlinear behaviour because of motor friction, motor saturation, and quantization noise in the measurement sensors. The dynamics of the system are dominated by the motor. The PMDC motor is an example of electromechanical systems with electrical and mechanical components. Table I lists the description of the PMDC motor parameters.

The total equivalent inertia, J_{eq} and total equivalent

damping, B_{eq} at the armature of the motor are given by:

$$J_{eq} = J_m + \frac{J_L}{n^2}, \quad B_{eq} = B_m + \frac{B_L}{n^2}$$

The differential equation of the PMDC motor with exogenous disturbance is given by:

$$\ddot{\omega} = -\frac{R_a B_{eq} + K_t K_b}{L_a J_{eq}} \omega - \frac{(L_a B_{eq} + R_a J_{eq})}{L_a J_{eq}} \dot{\omega} + \frac{1}{n} \frac{K_t}{L_a J_{eq}} v_a + \frac{1}{n} \frac{1}{J_{eq}} \dot{T}_L + \frac{1}{n} \frac{R_a}{L_a J_{eq}} T_L \quad (8)$$

$$\text{Let } x_1 = \omega, \quad x_2 = \dot{x}_1 = \dot{\omega}$$

Then, the state space representation of the PMDC motor after simplifications becomes:

$$\left. \begin{aligned} \dot{x}_1 &= x_2 \\ \dot{x}_2 &= -\frac{R_a B_{eq} + K_t K_b}{L_a J_{eq}} x_1 - \frac{(L_a B_{eq} + R_a J_{eq})}{L_a J_{eq}} x_2 + \frac{1}{n} \frac{K_t}{L_a J_{eq}} (v_a + d) + \frac{L_a}{K_t} \dot{T}_L + \frac{R_a}{K_t} T_L \end{aligned} \right\} \quad (9)$$

Where d is the equivalent exogenous disturbance at the input. Finally

$$\left. \begin{aligned} \dot{x}_1 &= x_2 \\ \dot{x}_2 &= -\frac{R_a B_{eq} + K_t K_b}{L_a J_{eq}} x_1 - \frac{(L_a B_{eq} + R_a J_{eq})}{L_a J_{eq}} x_2 + \frac{1}{n} \frac{K_t}{L_a J_{eq}} (v_a + d) \\ y &= x_1 \end{aligned} \right\} \quad (10)$$

TABLE I. PMDC MOTOR PARAMETERS

Parameter (unit)	Description
Va (V)	Applied voltage
Vb (V)	Back EMF of the motor
Ra (Ω)	Armature resistance
La (H)	Armature inductance
Jm (kg/m ²)	Inertia of the motor
Bm (N.s/m)	Friction coefficient of the motor
N	gearbox ratio
JL (kg/m ²)	Inertia of the load
BL (N.s/m)	Friction coefficient of the load
ωm (rad/s)	the speed of the motor
ω (rad/s)	the speed of the shaft
Va (V)	Applied voltage

IV. PROPOSED SLIDING MODE EXTENDED STATE OBSERVER (SMESO)

In this section, the proposed SMESO is presented, and the stability analysis is considered based on Lyapunov method. Figure 2 Shows the ADRC with the proposed SMESO.

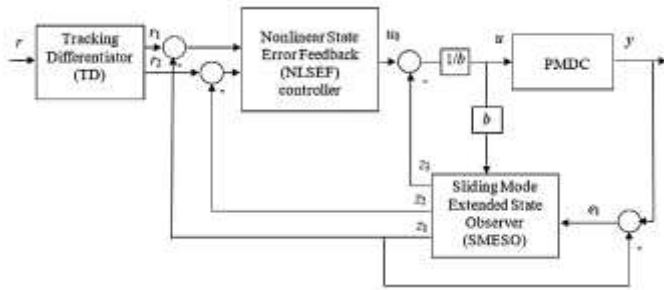


Fig. 2. ADRC topology based the SMESO

A. The Nonlinear State-Space Model representation of the Proposed SMESO

The proposed SMESO has the following state space representation:

$$\dot{\mathbf{Z}} = \mathbf{F}\mathbf{Z} + \mathbf{B}_1\mathbf{u} + \mathbf{B}_2g(y - z_1) \quad (11)$$

where $\mathbf{Z} \in \mathbf{R}^{(n+1) \times 1}$, is a vector that contains the estimated plant states and the total disturbance, $\dot{\mathbf{Z}} \in \mathbf{R}^{(n+1) \times 1}$, $\mathbf{B}_1 \in \mathbf{R}^{(n+1) \times 1}$, $\mathbf{B}_2 \in \mathbf{R}^{(n+1) \times 1}$, $\mathbf{F} \in \mathbf{R}^{(n+1) \times (n+1)}$.

$$\mathbf{Z} = [z_1 \ z_2 \ \dots \ z_{n+1}]^T, \quad \dot{\mathbf{Z}} = [\dot{z}_1 \ \dot{z}_2 \ \dots \ \dot{z}_{n+1}]^T$$

$$\mathbf{F} = \begin{bmatrix} 0 & 1 & 0 & 0 & \dots & 0 \\ 0 & 0 & 1 & 0 & \dots & 0 \\ 0 & 0 & 0 & 1 & \dots & 0 \\ 0 & \vdots & \vdots & \vdots & \ddots & \vdots \\ 0 & 0 & 0 & 0 & \dots & 1 \\ 0 & 0 & 0 & 0 & 0 & 0 \end{bmatrix}$$

$$\mathbf{B}_1 = [0 \ 0 \ \dots \ 1 \ 0]^T, \quad \mathbf{B}_2 = [\beta_1 \ \beta_2 \ \dots \ \beta_{n+1}]^T$$

Now,

$$g(y - z_1) = K_\alpha |y - z_1|^\alpha \text{sign}(y - z_1) + K_\beta |y - z_1|^\beta (y - z_1) \quad (12)$$

Assumption 1

$g(\cdot)$ is an odd nonlinear function with the following features,

- $g(0) = 0$
- $g(l) = k(l)$. l where $k_{min} \leq k(l) < \infty$.

Rewriting (12) as,

$$g(y - z_1) = \left(K_\alpha \frac{|y - z_1|^\alpha}{|y - z_1|} \text{sign}(y - z_1) + K_\beta |y - z_1|^\beta (y - z_1) \right)$$

Since

$$\text{sign}(y - z_1) = y - z_1 / |y - z_1|, \text{ for } |y - z_1| \neq 0.$$

Then,

$$k(y - z_1) = K_\alpha |y - z_1|^{\alpha-1} + K_\beta |y - z_1|^\beta$$

and,

$$g(y - z_1) = k(y - z_1)(y - z_1)$$

Or equivalently, $g(e_1) = k(e_1)e_1$

where, $e_1 = y - z_1$, and

$$k(e_1) = K_\alpha |e_1|^{\alpha-1} + K_\beta |e_1|^\beta \quad (13)$$

For $n = 2$, the nonlinear state space representation of the proposed SMESO is given as:

$$\left. \begin{aligned} \dot{z}_1 &= z_2 + \beta_1 (K_\alpha |y - z_1|^\alpha \text{sign}(y - z_1) + K_\beta |y - z_1|^\beta (y - z_1)) \\ \dot{z}_2 &= z_3 + bu + \beta_2 (K_\alpha |y - z_1|^\alpha \text{sign}(y - z_1) + K_\beta |y - z_1|^\beta (y - z_1)) \\ \dot{z}_3 &= \beta_3 (K_\alpha |y - z_1|^\alpha \text{sign}(y - z_1) + K_\beta |y - z_1|^\beta (y - z_1)) \end{aligned} \right\} \quad (14)$$

Figure 3 illustrates the proposed SMESO with order 3.

B. Stability Analysis of the SMESO

Consider an uncertain 2nd order single input-single output nonlinear plant described by:

$$\left. \begin{aligned} \dot{x}_1 &= x_2 \\ \dot{x}_2 &= f(x_1, x_2) + b(u + d) \\ y &= x_1 \end{aligned} \right\} \quad (15)$$

where $x = [x_1 \ x_2]^T \in \mathbf{R}^2$ is the state vector, $u \in \mathbf{R}$ is the control input, $y \in \mathbf{R}$ is the plant output, $d \in \mathbf{R}$ is bounded exogenous disturbance, and $f: \mathbf{R}^{2 \times 1} \rightarrow \mathbf{R}$ with $f(0,0) = 0$. The total disturbance state is represented by the augmented state

$$x_3 = f(x_1, x_2) + bd = \varphi(x_1, x_2, d)$$

Then,

$$\dot{x}_3 = \dot{f}(x_1, x_2) + b\dot{d} = \psi(x_1, x_2, \dot{d})$$

Assumption 2

1) $d(t)$ is continuously differentiable, both $d(t)$ and $\dot{d}(t)$ are bounded and $\dot{d} \rightarrow 0$ as $t \rightarrow \infty$, and $d(t) \in D$ (a compact subset of \mathbf{R}).

2) $f(x_1, x_2)$ and $\dot{f}(x_1, x_2)$ are both locally Lipschitz functions in x_1 and x_2 .

3) The closed-loop system of (15) w.r.t (1), (2), and (16) given below is uniformly asymptotically stable. i.e. \dot{x} approaches zero as t goes to infinity.

4) Both $\varphi(x_1, x_2, d)$ and $\psi(x_1, x_2, \dot{d})$ are both locally Lipschitz functions in x_1 and x_2 , bounded, and uniformly in d , over the domain of interest.

5) Only the output y is available.

6) $\left| \frac{\partial f}{\partial x_1} \right| < L_1, \left| \frac{\partial f}{\partial x_2} \right| < L_2$.

The 3rd order nonlinear SMESO that estimates the system's states and the total disturbance is given by (14) rewritten as:

$$\left. \begin{aligned} \dot{z}_1 &= z_2 + \beta_1 g(y - z_1) \\ \dot{z}_2 &= z_3 + \beta_2 g(y - z_1) + bu \\ \dot{z}_3 &= \beta_3 g(y - z_1) \end{aligned} \right\} \quad (16)$$

where $\mathbf{z} = [z_1 \ z_2 \ z_3]^T \in \mathbf{R}^{3 \times 1}$ is the state vector of the SMESO, and $B = [\beta_1 \ \beta_2 \ \beta_3]^T \in \mathbf{R}^{3 \times 1}$ is a parameter vector.

Lemma 1: Consider the plant dynamics in (15) with the augmented state x_3 to be observed by SMESO in (16). Then, the error dynamics can be described by,

$$\dot{\mathbf{e}} = \mathbf{M}\mathbf{e} + \mathbf{N}\Delta$$

Where $\mathbf{e} = [e_1 \ e_2 \ e_3]^T = [z_1 - x_1 \ z_2 - x_2 \ z_3 - x_3]^T \in \mathbf{R}^{3 \times 1}$ is the error vector,

$$\Delta(x_1, x_2, \dot{d}) = -\psi(x_1, x_2, \dot{d}) = -\dot{f}(x_1, x_2) - b\dot{d} \in \mathbf{R}^{3 \times 1},$$

$$\mathbf{M} = \begin{bmatrix} -\beta_1 k(e_1) & 1 & 0 \\ -\beta_2 k(e_1) & 0 & 1 \\ -\beta_3 k(e_1) & 0 & 0 \end{bmatrix} \in \mathbf{R}^{3 \times 3}, \quad \mathbf{N} = \begin{bmatrix} 0 \\ 0 \\ 1 \end{bmatrix} \in \mathbf{R}^{3 \times 1}$$

Proof:

To obtain the error dynamics subtract (15) from (16), then

$$\dot{z}_1 - \dot{x}_1 = z_2 - x_2 + \beta_1 g(y - z_1)$$

$$\begin{aligned} \dot{z}_2 - \dot{x}_2 &= z_3 - f(x_1, x_2) - b(u + d) + \beta_2 g(y - z_1) \\ &\quad + bu \\ &= z_3 - x_3 + \beta_2 g(y - z_1) \end{aligned}$$

$$\dot{z}_3 = -\dot{f}(x_1, x_2) - b\dot{d} + \beta_3 g(y - z_1)$$

Then

$$\dot{e}_1 = e_2 + \beta_1 g(-e_1)$$

$$\dot{e}_2 = e_3 + \beta_2 g(-e_1)$$

$$\dot{e}_3 = \Delta(x_1, x_2, \dot{d}) + \beta_3 g(-e_1)$$

Since $g(\cdot)$ is odd function and $g(e_1) = k(e_1) e_1$, then,

$$\dot{e}_1 = -\beta_1 k(e_1) e_1 + e_2$$

$$\dot{e}_2 = -\beta_2 k(e_1) e_1 + e_3$$

$$\dot{e}_3 = -\beta_3 k(e_1) e_1 + \Delta(x_1, x_2, \dot{d})$$

Hence,

$$\begin{bmatrix} \dot{e}_1 \\ \dot{e}_2 \\ \dot{e}_3 \end{bmatrix} = \begin{bmatrix} -\beta_1 k(e_1) & 1 & 0 \\ -\beta_2 k(e_1) & 0 & 1 \\ -\beta_3 k(e_1) & 0 & 0 \end{bmatrix} \begin{bmatrix} e_1 \\ e_2 \\ e_3 \end{bmatrix} + \begin{bmatrix} 0 \\ 0 \\ 1 \end{bmatrix} \Delta(x_1, x_2, \dot{d})$$

and in a compact form

$$\dot{\mathbf{e}} = \mathbf{M}\mathbf{e} + \mathbf{N}\Delta \quad \square$$

Lemma 2: Consider the plant dynamics given in (15) with assumption 2 holds. Also, consider $\left| \frac{\partial f}{\partial x_1} \right| < L_1$, $\left| \frac{\partial f}{\partial x_2} \right| < L_2$, then $\lim_{t \rightarrow \infty} \Delta(x_1, x_2, \dot{d}) = 0$.

Proof:

Writing $\dot{f}(x_1, x_2) = \frac{\partial f}{\partial x_1} \dot{x}_1 + \frac{\partial f}{\partial x_2} \dot{x}_2$. For bounded first partial derivatives and if and only if assumption 2 holds true, then

$$\lim_{t \rightarrow \infty} \Delta(x_1, x_2, \dot{d}) = \lim_{t \rightarrow \infty} -\dot{f}(x_1, x_2) - b\dot{d} = 0 \quad \square$$

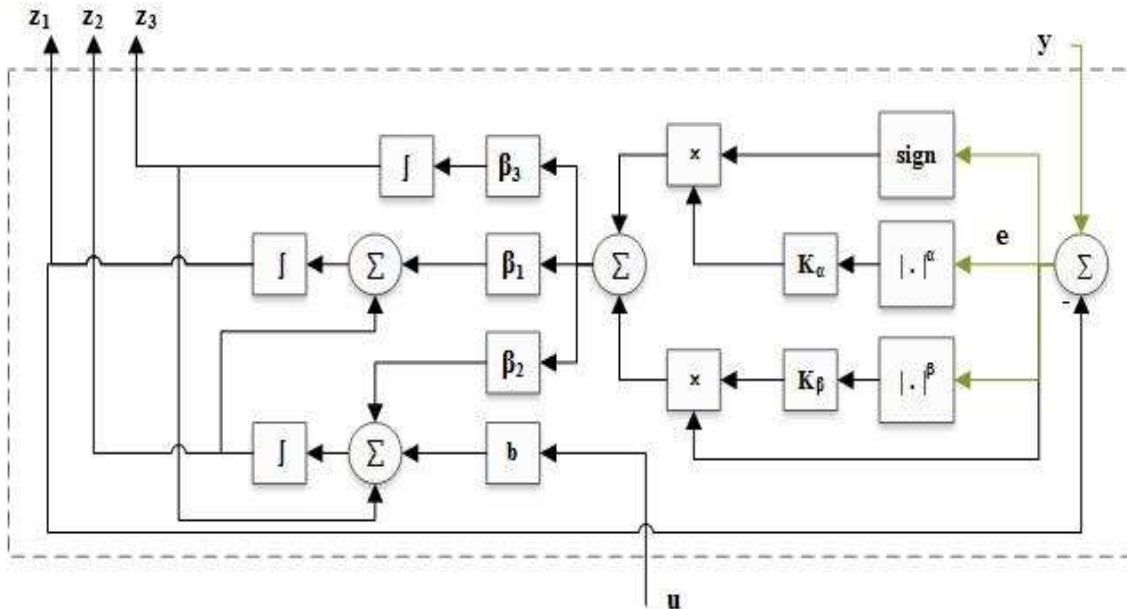


Fig. 3. Proposed SMESO for ADRC

Theorem 1: Consider the plant in (15) and the nonlinear extended state observer (16) with the error dynamics in Lemma 1 with $S = e_1$, where, $S: \mathbf{R} \rightarrow \mathbf{R}$ is the switching function for the SMESO Then,

1) The SMESO is globally asymptotically stable if $k(e_1) > k_{cr}$ (17)

where $k_{cr} = \frac{\beta_3}{\beta_2 \beta_1}$, that is for any initial conditions $\mathbf{e}(0)$, we have $\lim_{t \rightarrow \infty} \mathbf{e}(t) = 0$.

2) The SMESO has a sliding mode given that (17) is satisfied.

Proof:

Assume the candidate positive definite, radially unbounded Lyapunov function $V_{SMESO} = \frac{1}{2} \mathbf{e}^T \mathbf{e}$. Then,

$$\dot{V}_{SMESO} = \mathbf{e}^T \dot{\mathbf{e}}.$$

Moreover,

$$\dot{V}_{SMESO} = [e_1 \quad e_2 \quad e_3] \begin{bmatrix} -\beta_1 k(e_1) & 1 & 0 \\ -\beta_2 k(e_1) & 0 & 1 \\ -\beta_3 k(e_1) & 0 & 0 \end{bmatrix} \begin{bmatrix} e_1 \\ e_2 \\ e_3 \end{bmatrix} + [e_1 \quad e_2 \quad e_3] \Delta(x_1, x_2, d) e_3$$

according to lemma 2, $\lim_{t \rightarrow \infty} \Delta(x_1, x_2, d) = 0$, this leads to

$$\dot{V}_{SMESO} = [e_1 \quad e_2 \quad e_3] \begin{bmatrix} -\beta_1 k(e_1) & 1 & 0 \\ -\beta_2 k(e_1) & 0 & 1 \\ -\beta_3 k(e_1) & 0 & 0 \end{bmatrix} \begin{bmatrix} e_1 \\ e_2 \\ e_3 \end{bmatrix}$$

Or in compact form

$$\dot{V}_{SMESO} = \mathbf{e}^T \mathbf{P} \mathbf{e}$$

$$\text{where } \mathbf{e}^T = [e_1 \quad e_2 \quad e_3], \mathbf{P} = \begin{bmatrix} -\beta_1 k(e_1) & 1 & 0 \\ -\beta_2 k(e_1) & 0 & 1 \\ -\beta_3 k(e_1) & 0 & 0 \end{bmatrix}$$

If \mathbf{P} is a stable matrix then,

$$\dot{V}_{SMESO}(\mathbf{e}) < 0 \text{ for } \mathbf{e} \neq 0, \quad \dot{V}_{SMESO}(\mathbf{e}) = 0 \text{ for } \mathbf{e} = 0$$

A tabular method based on Routh-Hurwitz criterion can be used to determine the stability limits of the matrix \mathbf{P} as follows:

Firstly, compute the characteristic equation of the matrix \mathbf{P}

$$|\lambda \mathbf{I} - \mathbf{P}| = 0$$

$$\begin{vmatrix} \lambda + \beta_1 k(e) & -1 & 0 \\ \beta_2 k(e) & \lambda & -1 \\ \beta_3 k(e) & 0 & \lambda \end{vmatrix} = 0$$

Then, the characteristic equation of the matrix \mathbf{P} is given as

$$\lambda^3 + \beta_1 k(e) \lambda^2 + \beta_2 k(e) \lambda + \beta_3 k(e) = 0 \quad (18)$$

Next, fill the table that has 4 rows like the following

TABLE II. ROUTH STABILITY CRITERION

1	$\beta_2 k(e)$
$\beta_1 k(e)$	$\beta_3 k(e)$
$\frac{\beta_1 \beta_2 k(e)^2 - \beta_3 k(e)}{\beta_1 k(e)} = \beta_2 k(e) - \frac{\beta_3}{\beta_1}$	0
$\beta_3 k(e)$	0

Finally, based on above; it can be concluded that for stability, the coefficients with the nonlinear gains must satisfy

$$\beta_2 k(e) - \frac{\beta_3}{\beta_1} > 0, \quad k(e) > \frac{\beta_3}{\beta_2 \beta_1},$$

Then, the critical gain $k_{Cr} = \frac{\beta_3}{\beta_2 \beta_1}$. □

To prove 2, consider a Lyapunov function candidate:

$$V = \frac{1}{2} S^2$$

A sufficient condition for the existence of a sliding mode is that

$$\dot{V} = S\dot{S} < 0 \text{ or, } e_1 \dot{e}_1 < 0 \quad (19)$$

This can be explained as follows, from proof of point (1) and given (17) true, the SMESO is asymptotically stable, i.e., that, then means, $\dot{e}_1 < 0$. Or $\lim_{t \rightarrow \infty} e(t) = 0$ with negative $e(t)$, then $\dot{e}_1 > 0$. in both cases

$$e_1 \dot{e}_1 = (z_1 - x_1) [(z_2 - x_2) - \beta_1 k(z_1 - x_1) (z_1 - x_1)] < 0. \quad \square$$

V. NUMERICAL SIMULATIONS

The ADRC based on the proposed SMESO and the PMDC motor mathematical models are designed and numerically simulated using Matlab® /Simulink® as shown in Figure 4. These models are summarized below:

LESO:

$$\begin{aligned} \dot{z}_1 &= z_2 + \beta_1(e_1) \\ \dot{z}_2 &= z_3 + \beta_2(e_1) + bu \\ \dot{z}_3 &= \beta_3(e_1) \\ e_1 &= y - z_1 \end{aligned}$$

SMESO:

$$\begin{aligned} \dot{z}_1 &= z_2 + \beta_1 k(e_1) e_1 \\ \dot{z}_2 &= z_3 + \beta_2 k(e_1) e_1 + bu \\ \dot{z}_3 &= \beta_3 k(e_1) e_1 \\ k(e_1) &= K_\alpha |e_1|^{\alpha-1} + K_\beta |e_1|^\beta \end{aligned}$$

TD:

$$\begin{aligned} \dot{r}_1 &= r_2 \\ \dot{r}_2 &= -R \text{sign}(r_1 - r + \frac{r_2 |r_2|}{2R}) \end{aligned}$$

NLSEF controller:

$$u_0 = \text{fal}(r_1 - z_1, \alpha_1, \delta_1) + \text{fal}(r_2 - z_2, \alpha_2, \delta_2)$$

PMDC motor:

$$\begin{aligned} \dot{x}_1 &= x_2 \\ \dot{x}_2 &= f(x_1, x_2) + b(u + d) \\ f(x_1, x_2) &= -a_1 x_1 - a_2 x_2, \\ u &= u_0 - \frac{z_3}{b}, a_1 = \frac{R_a B_{eq} + K_t K_b}{L_a J_{eq}}, a_2 = \frac{(L_a B_{eq} + R_a J_{eq})}{L_a J_{eq}}, \\ b &= \frac{1}{n} \frac{K_t}{L_a J_{eq}} \end{aligned}$$

The values of the parameters for the whole system are listed in tables III-VII.

TABLE III. NLSEF PARAMETERS

Parameter	Value
δ_1	0.5656
δ_2	0.8269
α_1	0.4679
α_2	0.7440

TABLE IV. THE PARAMETERS OF THE PROPOSED SMESO

Parameter	Value
α	0.6825
β	0.9048
k_α	0.6138
k_β	0.0809

TABLE V. LESO PARAMETERS

Parameter	Value
β_1	30.4
β_2	523.4
β_3	2970.8

TABLE VI. TD PARAMETERS

Parameter	Value
R	100

TABLE VII. PMDC MOTOR PARAMETERS

Parameter	Value
R_a	0.1557
L_a	0.82
K_b	1.185
K_t	1.1882
n	3.0
J_{eq}	0.2752
b_{eq}	0.3922

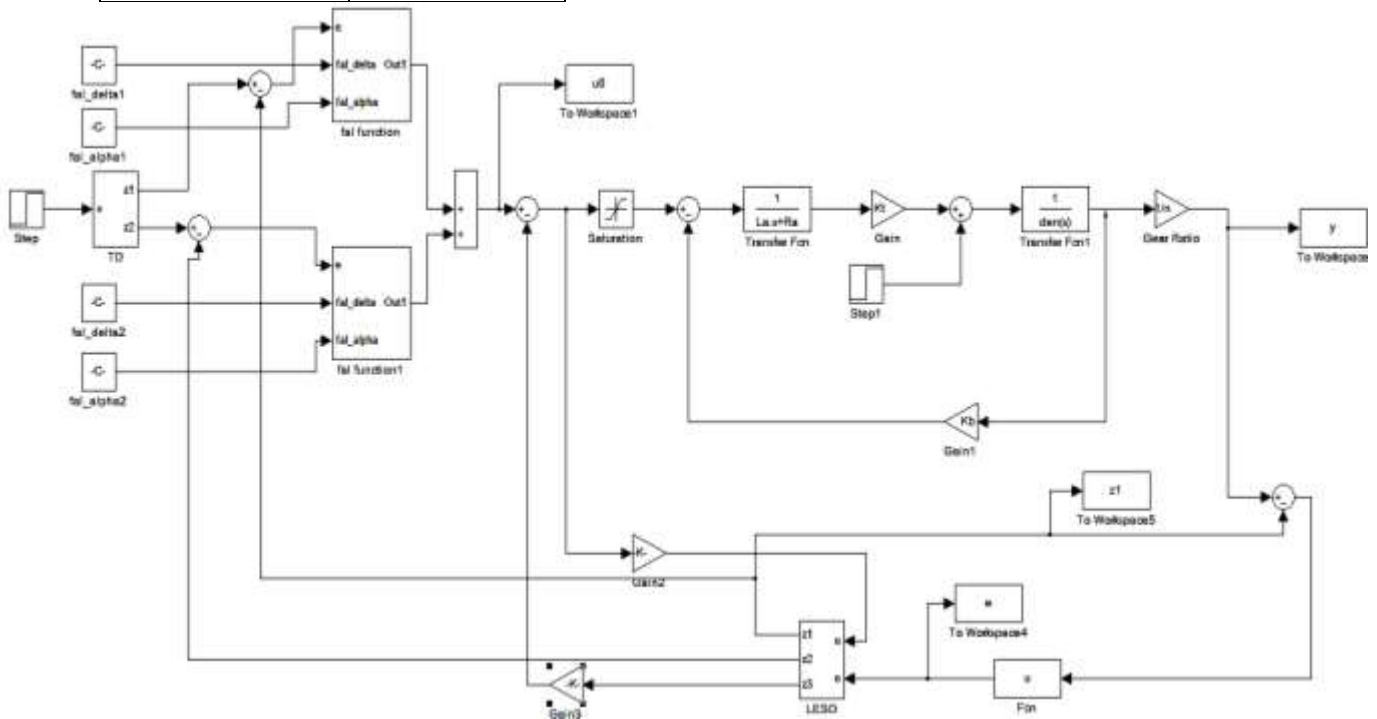


Fig. 4. The Simulink® model for the proposed ADRC based on the SMESO

The numerical simulations are done by using Matlab@ ODE45 solver for the models with continuous states. This Runge-Kutta ODE45 solver is a fifth-order method that performs a fourth-order estimate of the error. The reference input to the system is constant angular velocity equals to 1 rad/s

applied at $t = 0$ sec. The disturbance signal is applied to the motor output at $t = 10$ sec, which equals to 1 N.m.

The simulation results of ADRC based on both LESO and SMESO are shown in figures 5, and 6 respectively. The control signal u_0 , which is generated by the NLSEF controller shows a

significant reduction in chattering (compare Fig. 5(a) and Fig. 6(a)). This removal is due to the inclusion of a nonlinear function in the SMESO, and the behaviour of this observer provides a counter effect to the discontinuous function in the NLSEF. It is the main advantage of the using ADRC that relies in large extent on the total disturbance observer in cancelling the disturbances and system uncertainties than depending totally on the nonlinear controller to achieve this goal. As can be seen from the graph of the control signal for the case of the proposed SMESO that less energy will be used than the LESO to get the required tracking and disturbance cancellation. Moreover, the range of the state error e_1 reduced from $[-0.013037, 0.023414]$ for LESO to $[-0.001810, 0.010721]$ for SMESO. This reduction reflects the accuracy of the proposed SMESO to estimate the states of the system in addition to the total disturbance which comprises the exogenous disturbance and the uncertainties. An Objective Performance Index (OPI) is proposed to evaluate the performance of the proposed SMESO observer, which is represented as:

$$OPI = w_0 \times ITAE + w_1 \times IAU + w_2 \times ISU$$

Where,

$ITAE = \int_0^{20} t \times |r - y| dt$ is the integration of the time absolute error for the output signal,

$IAU = \int_0^{20} |u_0| dt$ is the integration of absolute of the NLSEF control signal, and

$ISU = \int_0^{20} u_0^2 dt$ is the integration of square of the NLSEF control signal.

The ITAE is commonly used in the performance measure of the closed-loop feedback control system to minimize the error signal. While the second term IAU minimizes the amplitude of the control signal u_0 through time. The peaking phenomenon that occurs at the starting has been reduced dramatically for both observers by including the ISU in the OPI. Table VIII shows the numerical simulation results with $w_0, w_1,$ and w_2 equal to 0.6420, 1.000, and 0.4906 respectively. The OPI in the case of LESO is 5.3502 and the OPI for the proposed SMESO are 3.3712. This means a reduction equals to 37%.

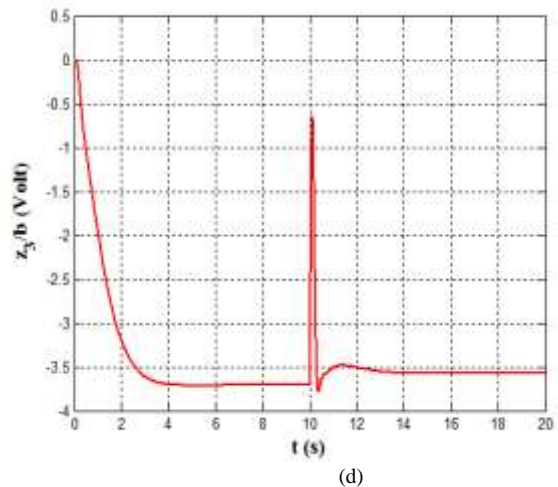
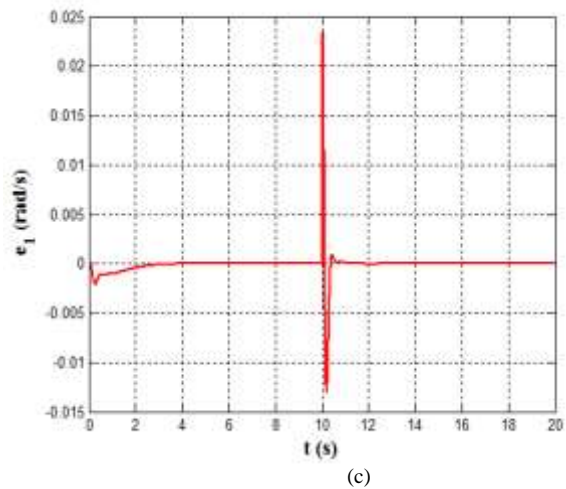
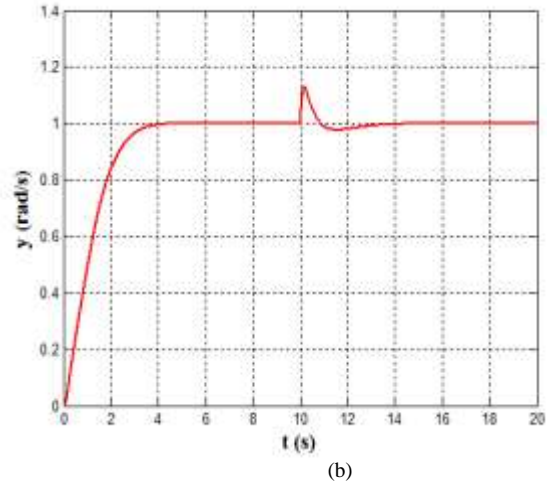
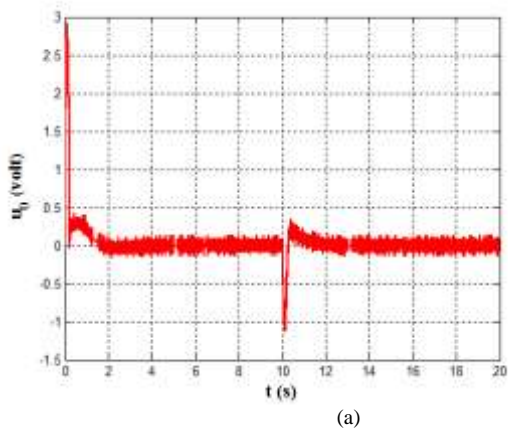
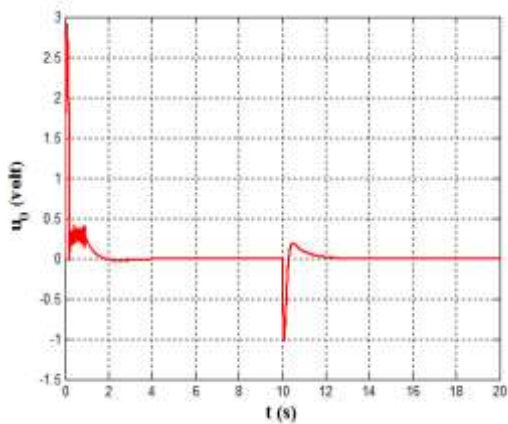
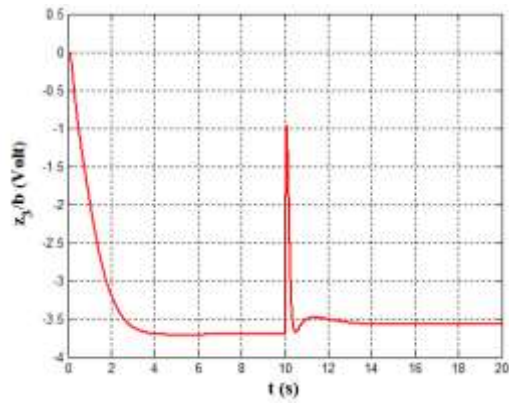


Fig. 5. The simulation results of the ADRC based on LESO, (a) The control signal u_0 (b) The plant output y (c) The LESO state error e_1 (d) The estimated input equivalent total disturbance

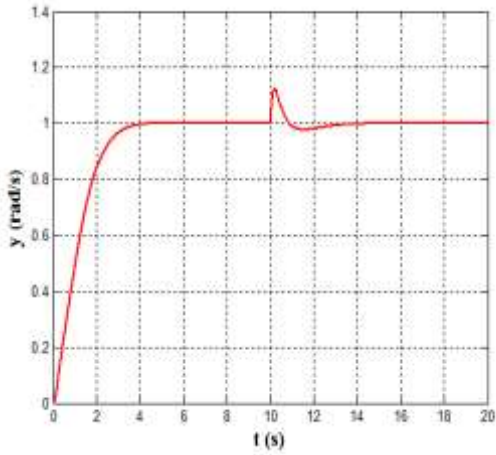


(a)

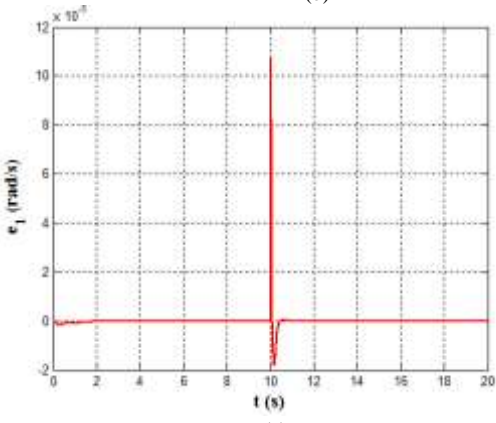


(d)

Fig. 6. The simulation results of the ADRC based on SMESO, (a) The control signal u_0 (b) The plant output y (c) The SMESO state error e_1 (d) The estimated input equivalent total disturbance



(b)



(c)

TABLE VIII. THE NUMERICAL SIMULATION RESULTS

Performance indices	LESO	SMESO
ITAE	3.5224	2.3070
IAU	2.2751	1.2701
ISU	1.6586	1.2637
OPI	5.3502	3.3712

TABLE IX. THE PARAMETERS OF THE PROPOSED SMESO

(Case 1)

Parameter	Value
α	0.6825
β	0.9048
k_α	0.1000
k_β	0.1000

TABLE X. THE PARAMETERS OF THE PROPOSED SMESO

(case 2)

Parameter	Value
α	0.7000
β	0.9000
k_α	0.0100
k_β	0.0100

TABLE XI. THE PARAMETERS OF THE PROPOSED SMESO
(case 3)

Parameter	Value
α	0.7000
β	0.9000
k_α	-0.001000
k_β	-0.001000

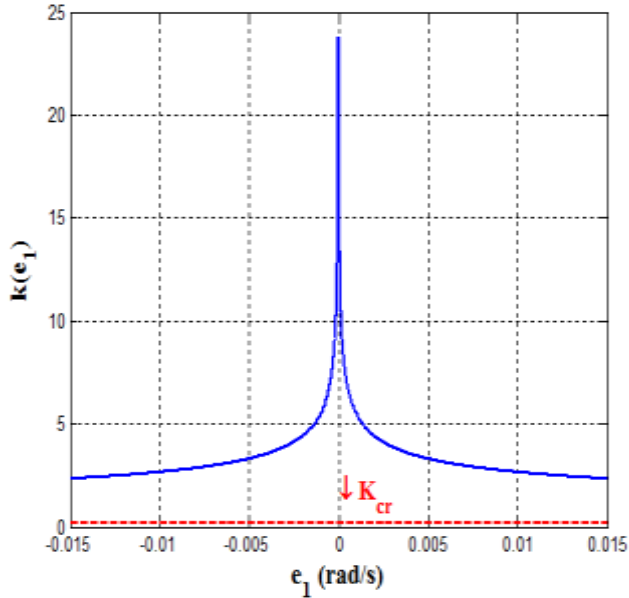
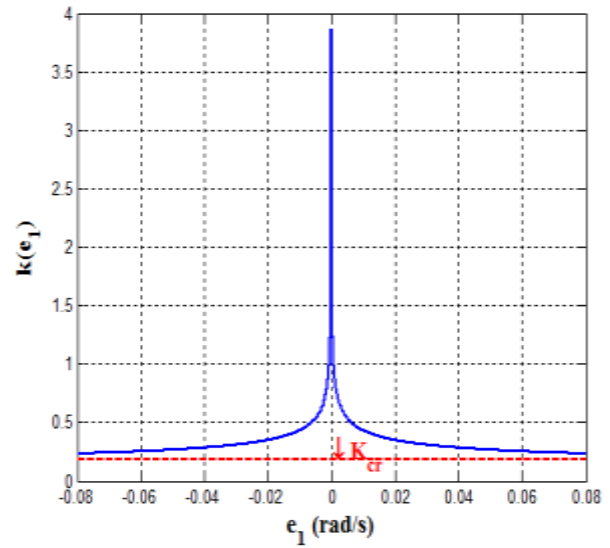
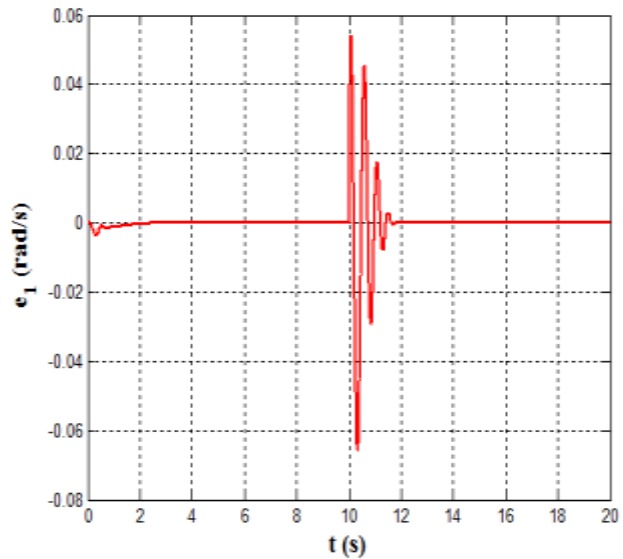


Fig. 7. The gain function of the proposed SMESO with its parameters listed in table VI

The nonlinear gain function $k(e_1)$ over the domain of the state error for the SMESO is shown in figure 7. The value of $k(e_1)$ at $e_1 = 0$ goes to infinity as can be seen from (13). But because MATLAB draws a sampled version of the signal, it does not appear graphically as supposedly to be. As the gain function $k(e_1)$ is reduced to approach the critical gain k_{cr} the ESO shows oscillation behaviour because that the roots of (18) approaches the imaginary axis, with $k(e_1)$ violates (17), the roots are in the right half plane. This phenomenon can be shown for three cases as shown in figures 8-10 by using the parameters listed in tables IX-XI for the SMESO.



(a)



(b)

Fig. 8. Reducing the gain function for case 1, (a) The gain function (b) The oscillation behaviour in e_1

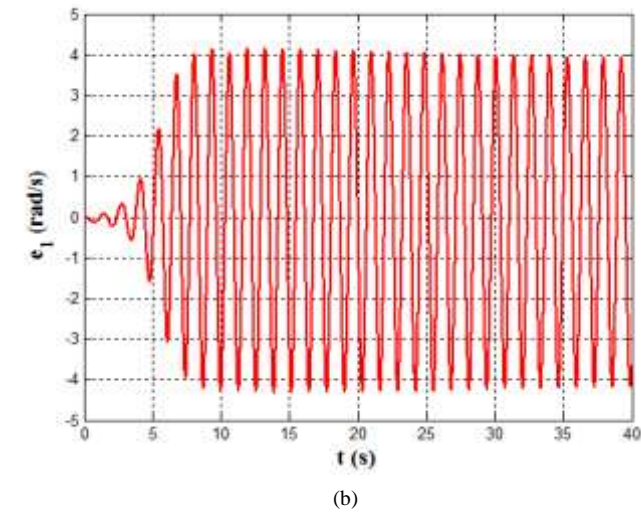
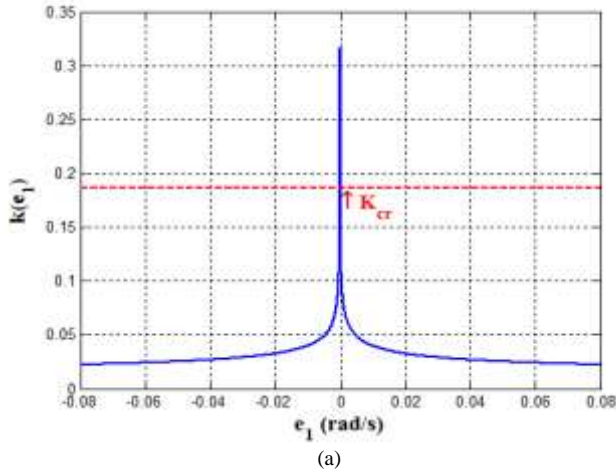


Fig. 9. Reducing the gain function for case 2, (a) The gain function (b) The oscillation behaviour in e_1

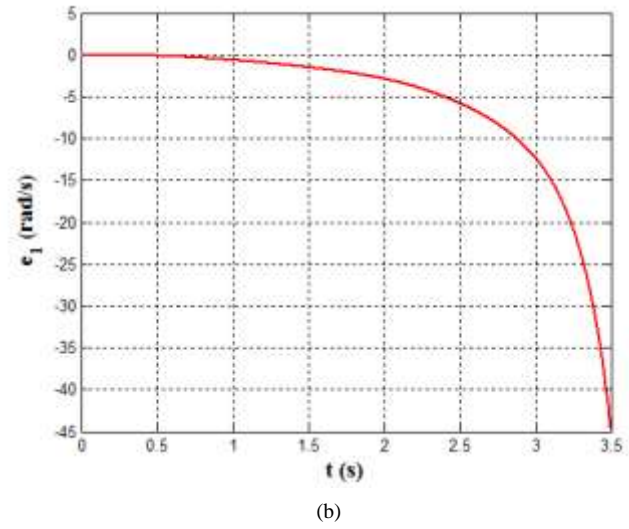
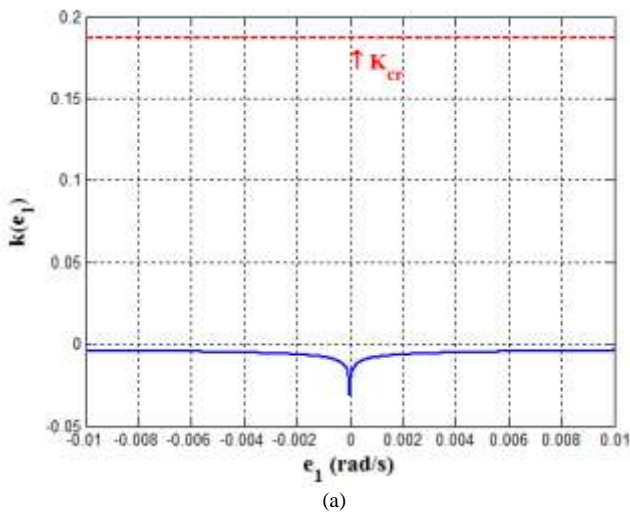
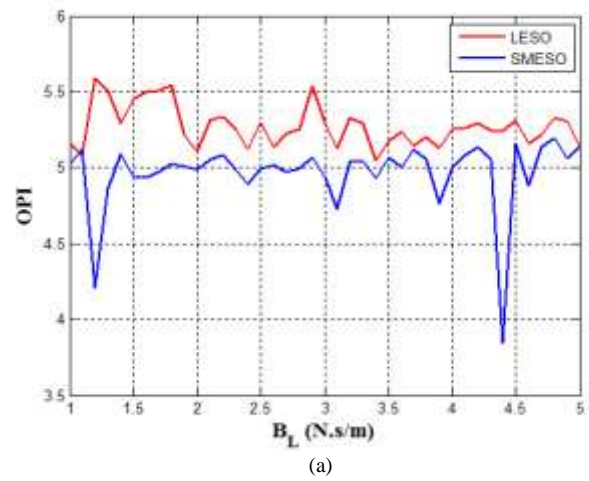


Fig. 10. Reducing the gain function for case 3, (a) The gain function (b) The oscillation behaviour in e_1

The immunity of the system to the parameter uncertainty is tested for two cases. The first case is tested by varying the factor of load viscous friction B_L in the range [1,5] N.s/m and the OPI is evaluated for that range as shown in figure 11(a). Next, the second case includes varying the value of the armature resistance R_a in the range [0.1,1] Ω . The OPI for the second case is shown in figure 11(b). It can be inferred that the OPI of the proposed SMESO is less than that for the LESO for the underlying operating range. Figures 12 and 13 show the performance of the ADRC against system uncertainties for the PMDC motor. Figure 12 is the variation in B_L , while Figure 13 is for variation in R_a . Finally, the main characteristic of the proposed design of the SMESO is asymptotic stability which can be verified by plotting $e_1 \dot{e}_1$ versus time. The negative definiteness of (18) is clear from the figure 14.



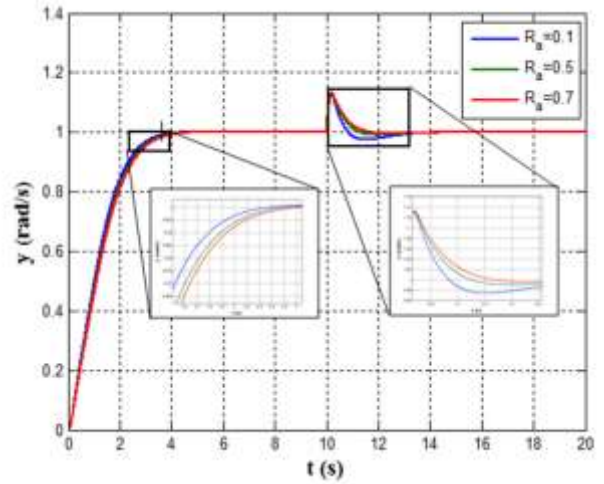
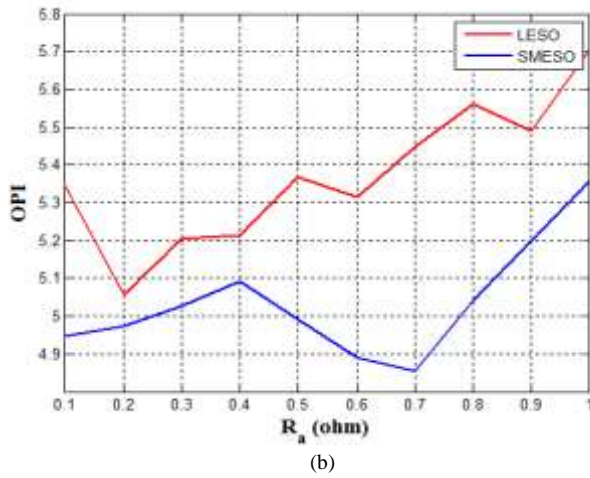
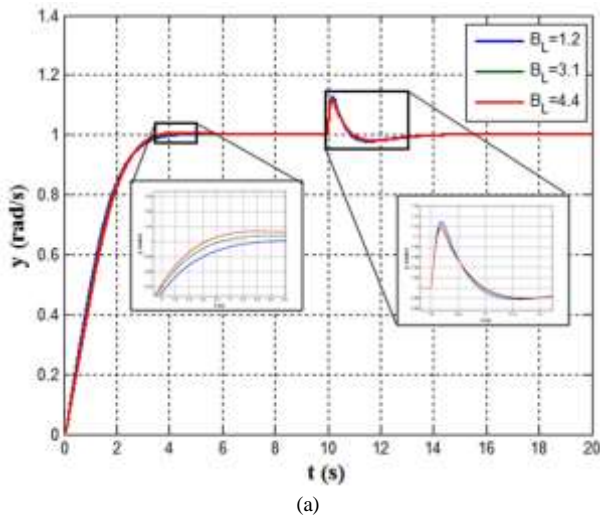
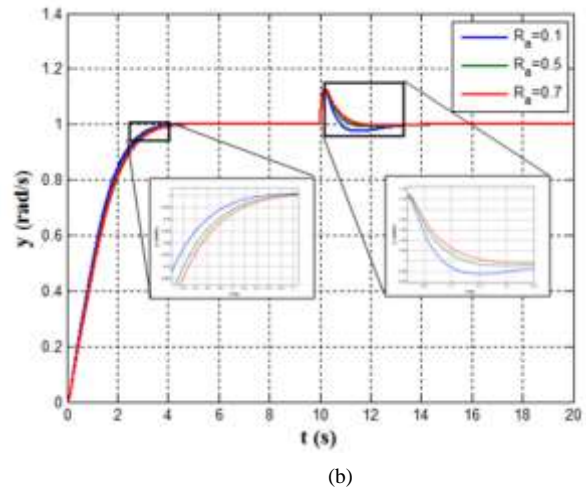


Fig. 11. The OPI against uncertainty, (a) uncertainty in BL (b) uncertainty in R_a

(a)

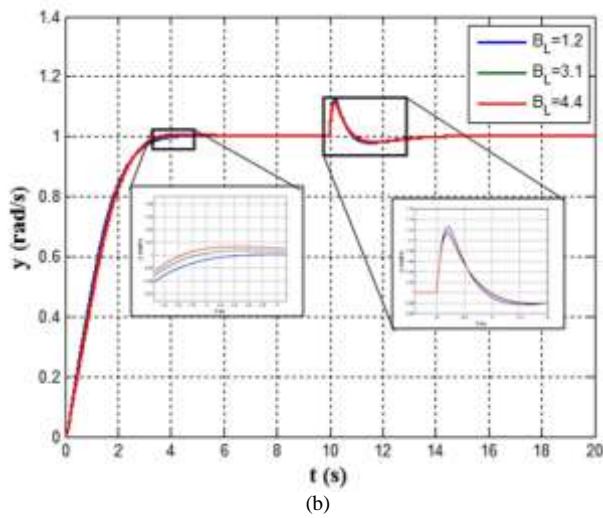


(a)



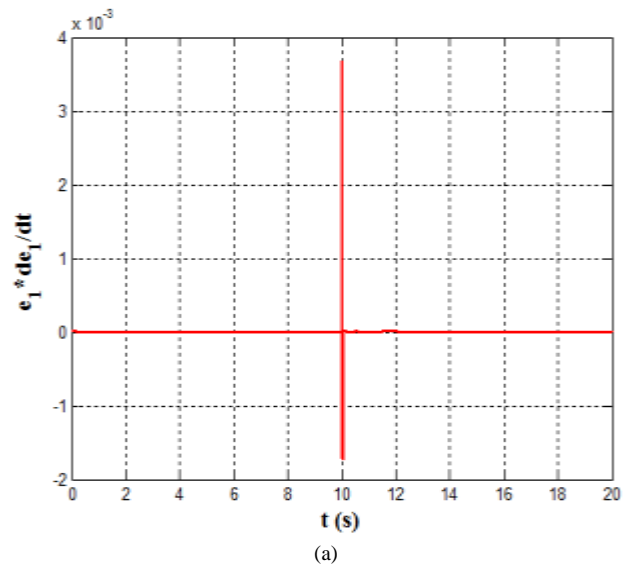
(b)

Fig. 13. The plant output y in presence of uncertainty in the parameter R_a (Ω), (a) for LESO (b) for SMESO



(b)

Fig. 12. The plant output y in presence of uncertainty in the parameter BL (N.s/m), (a) for LESO (b) for SMESO



(a)

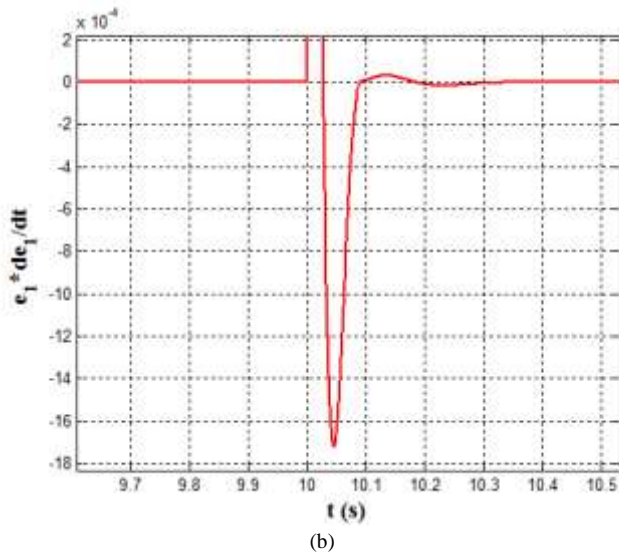


Fig. 14. The asymptotic stability characteristic of the proposed SMESO. (a) Plot of $e_1 \dot{e}_1$ against time (b) close-up for $e_1 \dot{e}_1$ around the time of disturbance trigger $t = 10$ sec

VI. CONCLUSIONS

Through this work, we designed an active disturbance rejection control based on the sliding mode extended state observer (SMESO) for the PMDC motor. The basic idea of modified ADRC is to use the SMESO to guess, in real time, both the states of the system and the lumped disturbance (or extended state) which may arise from external disturbance, unknown system dynamics, and system parameters variations, and then cancelling all these uncertainties in the closed-loop feedback system. The SMESO is an extension of the LESO method, which as a state estimator; it performs better than the LESO observer in terms of chattering reduction in the control signal. It has been proven that the estimation error is asymptotically convergent to zero under certain conditions in the nonlinear gain function. The estimation accuracy has been increased by adding the sliding term in the nonlinear extended state observer. It effectively rejects both matched uncertainties and exogenous disturbances without requiring any prior information about them and does not use an inverse model of the plant. Experimental results have shown that even the SMESO gives same performance in terms of timing and total disturbance rejection, the proposed method achieves an outstanding performance in terms of smoothness in the control signal which means less control energy is required to achieve the desired performance.

ACKNOWLEDGEMENT

The authors thank the electrical engineering department at the University of Baghdad for the direct support and encouragement.

REFERENCES

[1] Xie, L. L., Guo, L.: 'How much uncertainty can be dealt with by feedback?', IEEE Trans. Autom. Control, Dec. 2000, 45, (12), pp. 2203–2217
[2] Gao, Z.: 'On the centrality of disturbance rejection in automatic control', ISA Trans., Jul. 2014., vol. 4, no. 53, pp. 850–857

[3] Li, S. H., Yang, J., Chen, W.H., et al.: 'Disturbance Observer Based Control: Methods and Applications', Boca Raton, FL, USA: CRC Press, 2014.
[4] Chen, W., Yang, J., Guo, L., et al.: 'Disturbance-Observer-Based Control and Related Methods—An Overview', IEEE Transactions on Industrial Electronics, Feb. 2016, 63, (2).
[5] Khalil, H. K.: 'High-gain observers in nonlinear feedback control'. New Directions in Nonlinear Observer Design, 1999, 24, (4), pp. 249–268.
[6] Slotine, J. J. E., Hednck, J. K., Misawa, E. A.: 'On sliding observers for nonlinear system', Journal of Dynamic Systems, Measurement, and Control, 1987, 109, pp. 245–252
[7] Radke, A., Gao, Z.: 'A survey of state and disturbance observers for practitioners'. American Control Conference, June 2006, pp. 5183–5188.
[8] Kalsi, K., Lian, J., Hui, S., et al.: 'Sliding-Mode Observers for Uncertain Systems'. American Control Conference, June 2009, pp. 10–12.
[9] Wang, W., Gao, Z.: 'A comparison study of advanced state observer design techniques'. In Proceeding of the American Control Conference, Denver, Colorado, 2003, pp. 4754–4759.
[10] Huang, Y., Han, J.: 'Analysis and design for the second order nonlinear continuous extended states observer', Chinese Science Bulletin, 2000, 45, (21), pp. 1938–1944.
[11] Han, J.: 'From PID to active disturbance rejection control', IEEE Transactions on Industrial Electronics, 2009, 56, (3), pp. 900–906.
[12] Gao Z.: 'Scaling and Bandwidth Parametrization Based Controller tuning', IEEE, Proceedings of the ACC, Jun. 2003, 6, pp. 4989–4996.
[13] Xia, Y., Zhu, Z., Fu, M.: 'Back-stepping sliding mode control for missile systems based on an extended state observer', IET Control Theory and Applications, 2011, 5, (1), pp. 93–102
[14] Li, X., Li, S.: 'Extended state observer based adaptive control scheme for PMSM system'. Proceedings of the 33rd IEEE Chinese Control Conference, 2014.
[15] Guo, Z., Zhao, Z.L.: 'On convergence of non-linear extended state observer for multi-input-multi-output systems with uncertainty', IET Control Theory & Applications, 2012, 6, (15), pp. 2375–2386.
[16] Han, J.: 'A class of extended state observers for uncertain systems', Control and Decision, 1995, 10, (1), pp. 85–88.
[17] Hou, Y., Gao, Z., Jiang, F., et al.: 'Active disturbance rejection control for web tension regulation'. Proceedings of the 40th IEEE Conference on Decision and Control, Orlando, Florida USA, December 2001, pp. 4974–4979.
[18] Gao, Z., Hu, S., Jiang, F.: 'A novel motion control design approach based on active disturbance rejection'. Proceedings of the 40th IEEE Conference on Decision and Control, Orlando, Florida USA, December 2001, pp. 4877–4882.
[19] Xia, Y., Shi, P., Liu, G.P., et al.: 'Active disturbance rejection control for uncertain multivariable systems with time-delay', IET Control Theory Appl., 1, (1), January 2007.
[20] Veluvolu, K.C., Soh, Y.C., Cao, W.: 'Robust observer with sliding mode estimation for nonlinear systems', IET Control Theory Appl., 2007, 1, (5), pp. 1533–1540.
[21] Xia, Y., Fu, M., Shi, P., et al.: 'Robust sliding mode control for uncertain discrete-time systems with time delay', IET Control Theory Appl., 2010, 4, (4), pp. 613–624.
[22] Yang, J., Chen, W.H., Li, S.: 'Non-linear disturbance observer-based robust control for systems with mismatched disturbances/uncertainties', IET Control Theory Appl., 2011, Vol. 5, Iss. 18, pp. 2053–2062.
[23] Dang, T. V., Wang, W.J., Luoh, L., et al.: 'Adaptive observer design for the uncertain Takagi–Sugeno fuzzy system with output disturbance', IET Control Theory Appl., 2012, 6, (10), pp. 1351–1366.
[24] Wu, Y., Zheng, Q.: 'ADRC or adaptive controller – A simulation study on artificial blood pump,' Computers in Biology and Medicine, 2015, Vol. 66, pp. 135–143.
[25] Zhang, C., Chen Y.: 'Tracking Control of Ball Screw Drives Using ADRC and Equivalent-Error-Model-Based Feedforward Control,' IEEE Transactions on Industrial Electronics, 2016, Vol. 63, Iss. 12.
[26] Rahman, M. M., Chowdhury, A. H.: 'Comparative study of ADRC and PID based Load Frequency Control', International Conference

- on Electrical Engineering and Information Communication Technology (ICEEICT), 2015.
- [27] Shi. M., Liu, X., Shi, Y.: 'Research n Enhanced ADRC algorithm for hydraulic active suspension,' International Conference on Transportation, Mechanical, and Electrical Engineering (TMEE), 2011.
- [28] Ahmed, A., Ullah, H. A., Haider I., et al.: 'Analysis of Middleware and ADRC based Techniques for Networked Control,' 16th International Conference on Sciences and Techniques of Automatic control & computer engineering, At Tunisia, Vol. 16, 2015.
- [29] Chenlu, W., Zengqiang, C., Qinglin, S., et al.: ' Design of PID and ADRC based quadrotor helicopter control system,' Control and Decision Conference (CCDC), 2016.
- [30] Han. J.: 'From PID to Active Disturbance Rejection Control', IEEE Transactions on Industrial Electronics, March 2009, 56, (3).
- [31] Mahfouz, A. , Aly, A. , Salem, F. : 'Mechatronics Design of a Mobile Robot System', I.J. Intelligent Systems and Applications, 2013, 03,pp. 23-36.

Towards A Broader Adoption of Agile Software Development Methods

Abdallah Alashqur

Software Engineering Department
Faculty of Information
Applied Science Private University
Amman, JORDAN

Abstract—Traditionally, software design and development has been following the engineering approach as exemplified by the waterfall model, where specifications have to be fully detailed and agreed upon prior to starting the software construction process. Agile software development is a relatively new approach in which specifications are allowed to evolve even after the beginning of the development process, among other characteristics. Thus, agile methods provide more flexibility than the waterfall model, which is a very useful feature in many projects. To benefit from the advantages provided by agile methods, the adoption rate of these methods in software development projects can be further encouraged if certain practices and techniques in agile methods are improved. In this paper, an analysis is provided of several practices and techniques that are part of agile methods that may hinder their broader acceptance. Further, solutions are proposed to improve such practices and consequently facilitate a wider adoption rate of agile methods in software development.

Keywords—Agile Methods; Agile software development; SCRUM

I. INTRODUCTION

Software systems research and development has resulted in many applications covering various aspects of our lives [1-5]. Over the years, two major approaches for managing the software development process have evolved. These approaches are the traditional engineering approach exemplified by the *waterfall model* and its variations [6-8] and the more recent approach called *agile software development methods* [9-12]. The waterfall model as was originally introduced by Winston Royce [13] does not allow feedback from later steps to earlier steps in the process, thus adopting the engineering approach. In the engineering approach (e.g., civil engineering) requirements and specifications have to be fully completed and approved before construction starts.

Some level of flexibility has been incorporated in later versions of the waterfall model as shown in Figure 1. This flexibility is achieved by enabling feedback to previous steps of the model, which makes it possible to perform limited modifications to prior phases of the development lifecycle. Another disadvantage of the waterfall approach is that the user cannot see any running components of the software being developed until the entire system is completed, which is normally way too far down the road. Furthermore, a lot of

focus and effort is invested upfront in just documentation and planning.

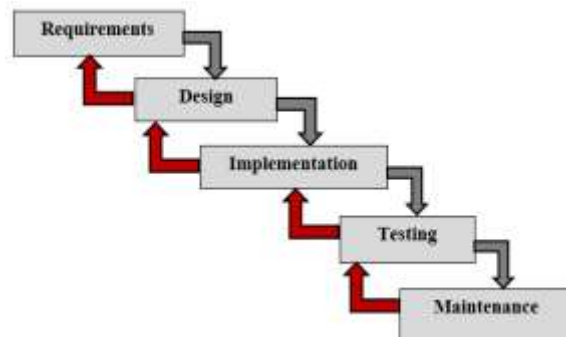


Fig. 1. Enhanced Waterfall Model

Due to the shortcomings of the waterfall-based development methods, a new approach called *agile software development*, or sometimes called Agile Methodology or just *Agile Methods (AM)*, has emerged as a viable and powerful approach to software development. In agile software development, portions of the software are designed and developed in short iterations in an incremental way. After each iteration, the user has a chance to see the outcome in the form of a running subsystem and to provide more feedback to the development team. This iterative approach allows for flexibility and takes into consideration the fact that the user may not know for sure, and in detail, what he/she wants prior to starting the development process.

Despite the advantages provided by agile methods over traditional methods, there are still several aspects in which agile methods can be further improved and several issues that need to be addressed. This paper aims at exposing several of these issues for the purpose of understanding them and being able to identify workarounds and solutions to handle them. In addition, in this paper some solutions to tackle these issues are proposed. The overall objective is to make agile methods more appealing to a wider audience in the software development community.

The rest of this paper is organized as follows. In section 2 a brief description of agile methods is provided with a focus on the values and principles of agile software development. Also a brief description of one of the agile methods is

described in some briefly. Section 3 describes several of the issues with agile methods with a description of each one of these issues and its impact. Solutions are proposed in Section 4 on how to deal with these issues. Conclusions are given in Section 5.

II. AGILE METHODOLOGY AND SCRUM

In this section a brief description of the agile values and principles is provided. Then a brief descriptions of SCRUM [14], which is an important agile methodology is given. Some terms and concepts of SCRUM will be used in subsequent sections of this paper.

A. Agile Methodology

The term *agile software development* was introduced after extensive meetings and discussions conducted by seventeen experienced individuals in the area of software development in 2001. The outcome of those meetings was summarized in a document called *The Agile Manifesto* [15], which describes the values and principles of agile software development.

The authors of *The Agile Manifesto* [15] cited four qualities that they value in agile development over four related qualities that exist in traditional software development. These four qualities are:

1) Individuals and interactions are valued more than processes and tools. Individuals are team members of the agile development teams. Agile teams are usually self-organizing and cross-functional teams.

2) Working software is valued more than comprehensive documentation. The primary objective of agile teams is to provide the client with early and working subsystems to keep the customer engaged and to obtain feedback.

3) Customer collaboration is valued more than contract negotiation. Collaboration between the customer and the agile team on a continuous basis is necessary to obtain feedback and make sure that deliverables meet customers' expectations.

4) Responding to change is valued more than following a plan. Permitting flexibility and providing a culture where requirements are allowed to evolve results in a final software that better meets the customer's needs. On the contrary, adhering to a fixed plan may result in software that is not exactly what the customer needs.

The *Agile Manifesto* [15] cited twelve principles for agile software development. These principles are summarized in Table 1.

TABLE I. PRINCIPLES OF AGILE METHODS

No	Principle
1	Satisfy the customer through early and continuous delivery of valuable software.
2	Welcome changing requirements during the development phases.
3	Produce working software on a frequent basis.
4	Business people and developers must work jointly and daily throughout the project.
5	Build projects around motivated individuals. Provide them the environment and support they need.
6	Face-to-face conversation is the best way of communication.
7	Working software is the primary measure of progress.
8	Promote sustainable development. Maintain a constant pace indefinitely.
9	Continuous attention to technical excellence and good design.
10	Simplicity (the art of minimizing the amount of work that is done) is essential.
11	The best architectures, requirements, and designs emerge from self-organizing teams.
12	At regular intervals, the team reflects on how to become more effective.

B. SCRUM

SCRUM is the most popular agile methodology [16-18]. Development in SCRUM is performed as a series of iterations called *sprints* as shown in Figure 2. A sprint is a time-box whose duration is 2 to 4 weeks. The output of a spring is an increment or subsystem of the overall system being developed. Each sprint can be viewed as a small project that has its own system development life cycle (SDLC). The final, aggregate product is the result of integrating the subsystems produced by these sprints.

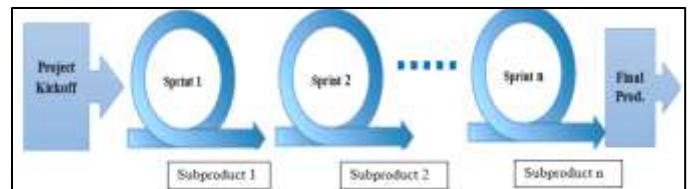


Fig. 2. SCRUM sequence of sprints

Figure 3 details a single sprint. The *Product Backlog* shown on the left side of Figure 3 is a list of requirements and features that need to be included in the end product. In addition to requirements, the Product Backlog contains

description for any changes to be made to what has been produced so far. The content of the Product Backlog evolves overtime to permit requirements to change. The *Sprint Backlog* is a subset of the items in the Product Backlog that are selected for implementation in the current sprint.

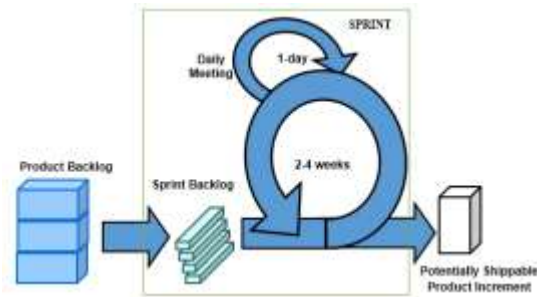


Fig. 3. Details of a single sprint

On a daily basis, the SCRUM team holds a short meeting, also called daily-standup meeting (or SCRUM meeting). This meeting is represented in Figure 3 with the arrow labeled “Daily Meeting.” In this meeting, team members present what was done in the past 24 hours and discuss the plan for the coming 24 hours. In SCRUM the product that is produced at the end of a sprint is called potentially shippable product increment, which is the release or subsystem produced by the sprint.

Scaling up the agile process. Sprints can be performed serially by the team. However in large projects, there can be several parallel sprints, where multiple teams can be working on different sub-products simultaneously. In this case we can have what is referred to as “team of teams” or “scrum of scrums” [19]. In its purist form, agile methods do not allow for team-of-teams structure in order to stay away from forming a hierarchical management structure. The scrum of scrums technique is used to scale-up SCRUM to handle large projects. However when this is done, coordination and collaboration between the teams become an overhead. Teams have their own daily meetings as usual. But then each team selects a representative to attend the scrum of scrums meeting to plan the overall project and coordinate the various development efforts. The scrum of scrums meetings may be scheduled less frequently than the scrum (or sprint) meetings.

III. AGILE PRACTICES THAT MAY DISCOURAGE WIDER ACCEPTANCE

Below are the agile practices that need improvement and can be considered obstacles preventing many organization from adopting agile methods fully. They are based on the author’s extensive experience in software research, design, and development.

1) Pushing items back to the product backlog. Whenever a team encounters or discovers a major bug, the team may push it back in the product backlog (with the approval of the product owner or user). In reality this bug can be a problem with current sprint implementation. But instead of solving it during the current sprint, the team postpones it to a future sprint by “kicking the can down the road.” Because of scheduling pressures, the team may be tempted to postpone

some genuine current-sprint work by hiding it as a bug, thus effectively taking it out of the sprint backlog and pushing it back to the product backlog. That way the team can meet strict deadlines and appear as a team of high performance.

2) Not valuing individuals. In agile methods, a team is treated and measured as a single entity. The performance of the entire team is measured without much regard to differences in the performance of individual members of a team (except may be for the purposes of discovering very low performers and taking some measures towards them). By not allowing the “stars” in a team to shine and not giving them credit for their achievements, their incentive for doing outstanding work diminishes. This negatively impacts the overall project. In a team of twenty individuals, the real stars of overachievers could be three or four individuals. These are the ones who can do magic in solving very hard problems and overcoming tough obstacles. You don’t incentivize them by telling them that no matter what they do, their work will be considered as a team achievement and that they will not be rewarded for it.

3) Treating programmers as interchangeable resources. A tendency may exist in some development environments to treat programmers just as a bunch of interchangeable “techies” or “resources”. This behavior negatively affects moral and enthusiasm towards the work environment as a whole and makes it harder to attract talented individuals to fill future open positions. This problem is aggravated if most of those “techies” are people who have language accents that are different from the main stream accent. This usually gives a false impression that “accent” is an intentional line of segregation where people with accent are given low-level implementation tasks and are treated as pluggable resources. A similar problem can happen in a distributed agile team, where some members of the team are in one country and other members are in another country. Team members in one country may perceive themselves as the “thinkers” and decision makers whereas team members in the other country are perceived as just “doers.”

4) Agile Methods focus on short term iterations. This means that the time available for developers to learn and experiment with new ideas is limited if not totally eliminated. Many of those developers are highly intellectual individuals who would dislike it if their work is transformed to cookie-cutter, non-intellectual, and repetitive task patterns. Computer science is a fast-evolving field and giving developers some room to experiment with new ideas is important. In traditional software engineering methods tasks and modules are usually large in size and not very limited and short-term as in the case of agile methods. This gives developers who use traditional methods the leeway to perform some level of research and experimentation that will not only benefit the specific task at hand but the overall project.

5) Scaling-up to handle Large Projects. Agile methods emphasize teams but avoid the adoption of a management hierarchy. In traditional methods, there is normally a

management hierarchy that can expand in size (in either depth or breadth) as much as needed to accommodate all components of a project. Because of this, traditional software engineering methods are more capable of scaling up to handle projects of large size. Agile methods are more appropriate for handling small size projects and, to some extent, medium size projects. A need exists to scale-up agile methods to handle larger projects.

6) High complexity of the system Integration process. Because agile methods emphasize short iterations that produce small subsystems, the integration of these many small subsystems into a coherent, working, and bug-free system becomes a very complex task that is difficult to accomplish.

7) Determining a project budget upfront. At the heart of agile methods is the idea of not freezing the requirements at the very beginning of a project in order to give the client the ability to introduce new requirements and modify existing requirements on an on-going basis. But this gives rise to the problem of not being able to have a clear agreement with the client regarding budget and schedule before the start of a project. This opens the door for potential disputes between the client and the developer during project execution, which is a major risk factor. How can we preserve the agility and benefit from the flexibility it provides, but at the same time avoid running into budget-related issues during project execution? This is a big question. The problem can be less severe if the client and developer are two different departments within the same company. However, if they are two different companies, the budget issue becomes a high risk area that hinders the adoption of agile methods especially in projects of large size.

IV. PROPOSED WAYS OF DEALING WITH THE ABOVE ISSUES

1) Pushing items back to the product backlog. The following three solutions can be implemented. (1) A titer approval process needs to be put in place, in order to avoid pushing items back to the product backlog unless it is absolutely necessary. (2) A record of these incidents need to be saved, in order to expose situations in which a team frequently resorts to pushing items back to the product backlog, which may indicate a potential problem. (3) The number of items placed by a team on the product backlog during a sprint implementation needs to be used as one of the metrics for measuring team performance. Less items pushed to the product backlog contribute to a higher performance measure.

2) Not valuing individuals. In addition to performing team appraisals, individual appraisals are necessary. Some sort of reporting hierarchy needs to exist in order for a manager or team leader to perform individual reviews and reward exceptional achievers. Even though the agile methodology tries to avoid having a management hierarchy, it is necessary to have some form of reporting hierarchy for the purposes of assessing and rewarding team members.

3) Treating programmers as interchangeable resources. Involving some of those programmers, especially the senior

ones, in the decision making process at the strategic level as well as at the tactical level may help alleviate this problem. Recognizing that the skills and experience of each individual are distinguished and appreciating the uniqueness of each individual is a step in the right direction.

4) Agile Methodology focuses on short term iterations. Allowing for extra time during a sprint or between sprints to reflect, learn, and experiment is one way to reduce the impact of sprints of the agile methods being very short term and tactically focused. Sending agile team members to short training courses (e.g., one week) on a quarterly or semi-annual basis may partially satisfy the need of those individuals to progress at their careers. This elevates their moral and enthusiasm towards the work environment and the projects they work on.

5) Scaling-up to handle Large Projects. Because of the nature of agile methods, it may be hard to solve this problem. Drastic modification to the agile methodology may be required to make handling large projects more natural and systematic. Formalizing the idea of “team of teams” or “scrum of scrums” may be a necessary prerequisite to enable scaling-up agile projects in a smooth way. A lot of research is needed in this area to be able scale-up to handle large projects but at the same time try to preserve the agile spirit and core concepts.

6) High complexity of the system integration process. The best solution here is to use CASE tools that aid in the integration process and track versions of components. Few CASE tools tailored to agile methods have started to appear on the market such as JIRA Software by Atlassian.

7) Determining a project budget upfront. Though in agile methods it is impossible to have an exact budget estimate, it may be possible to come up with reasonably correct estimate if we limit the variability of the requirements. One can think of demanding that 75% or more of the requirements be specified, detailed and finalized before starting the project and allowing up to 25% to be identified, modified, or added later. This gives a better guideline for estimating the budget. Again, more research is needed here.

Overall, it seems the time is ripe for blending best practices from agile methods and from traditional methods to come up with a new model of software development. The new methodology should try to avoid many of the shortcomings of agile methods as well as many of the shortcomings of traditional methods, which requires loosening some restrictions in both worlds. This approach is sometimes referred to as *hybrid* software development. Examples of pioneering research in this area can be found in [20, 21]. More research is needed in order to crystallize and identify the nature and characteristics of such a hybrid software development methodology.

V. CONCLUSION

Agile methods have proven over the years that they provide many advantages over traditional methods in the area of software development. Enabling the user to modify

requirement or add new requirements after the start of a project, providing the user with working subsystems at early phases of a project, and emphasizing a closer interaction between the development team and the user are some of these advantages. However, there are many issues pertaining to agile methods that act as barriers to its adoption by a wider community of software developers. Some of these issues are practices that can easily be improved, whereas others are deeply rooted in the methodology itself. In this paper, many of these issues are highlighted and a brief description of each one is provided. Furthermore, the paper proposed possible solutions/guidelines on how to deal with these issues in order to minimize their negative impact. This, in the end, will contribute towards improving the quality of software products developed using agile methods, which results in increased customer satisfaction. Consequently agile methods are expected to gain more momentum.

REFERENCES

- [1] Wang, Lizhe, Rajiv Ranjan, Joanna Kolodziej, Albert Y. Zomaya, and Leila Alem. "Software Tools and Techniques for Big Data Computing in Healthcare Clouds." *Future Generation Comp. Syst.* 43 (2015): 38-39.
- [2] Alashqur, Abdallah. "Mapping Data Between Probability Spaces In Probabilistic Databases." *International Journal Of Database Management Systems (IJDBMS)*, Vol. 7, No. 3, pages 1-12, June 2015.
- [3] Dvorak, Carl, Khiang Seow, and Charles Young. "Healthcare Information System with Clinical Information Exchange." U.S. Patent Application No. 15/131,738.
- [4] Zhai, Huixia. "Application of Information Construction in University Financial Management." *2015 8th International Conference on Intelligent Networks and Intelligent Systems (ICINIS)*. IEEE, 2015.
- [5] Ian Sommerville, *Software Engineering*, 10 edition, 2015. Publisher: Pearson,
- [6] Balaji, S., and M. Sundararajan Murugaiyan. "Waterfall vs. V-Model vs. Agile: A comparative study on SDLC." *International Journal of Information Technology and Business Management* 2.1 (2012): 26-30.
- [7] Elghondakly, Roaa, Sherin Moussa, and Nagwa Badr. "Waterfall and agile requirements-based model for automated test cases generation." *2015 IEEE Seventh International Conference on Intelligent Computing and Information Systems (ICICIS)*. IEEE, 2015.
- [8] Hasnine, M. N., Chayon, M. K. H., & Rahman, M. M. (2015). A Cost Effective Approach to Develop Mid-size Enterprise Software Adopted the Waterfall Model. *World Academy of Science, Engineering and Technology, International Journal of Computer, Electrical, Automation, Control and Information Engineering*, 9(5), 1140-1149.
- [9] Lassenius, Casper, Torgeir Dingsøy, and Maria Paasivaara, eds. *Agile Processes, in Software Engineering, and Extreme Programming: 16th International Conference, XP 2015, Helsinki, Finland, May 25-29, 2015, Proceedings*. Vol. 212. Springer, 2015.
- [10] Brhel, Manuel, Hendrik Meth, Alexander Maedche, and Karl Werder. "Exploring principles of user-centered agile software development: A literature review." *Information and Software Technology* 61 (2015): 163-181.
- [11] S. Ambler. Agile software development at scale. *Balancing Agility and Formalism in Software Engineering*, pages 1–12, 2008.
- [12] Brenner, Richard, and Stefan Wunder. "Scaled Agile Framework: Presentation and real world example." *Software Testing, Verification and Validation Workshops (ICSTW), 2015 IEEE Eighth International Conference on*. IEEE, 2015.
- [13] W. Royce. Managing the development of large software systems: Concepts and techniques. In *Proceedings of IEEE WESCON*, pages 328–339. IEEE CS Press, 1970
- [14] Mahnič, Viljan. "Scrum in software engineering courses: an outline of the literature." *Global Journal of Engineering Education* 17.2 (2015).
- [15] M. Fowler and J. Highsmith. The agile manifesto. *Software Development*, 9(8):28–35, 2001.
- [16] Rubin, Kenneth S. *Essential Scrum: a practical guide to the most popular agile process*. Addison-Wesley, 2013.
- [17] Akif, R., and H. Majeed. "Issues and challenges in Scrum implementation." *International Journal of Scientific & Engineering Research* 3, no. 8 (2012): 1-4.
- [18] Almseidin, M., Khaled Alrfou, Nidal Alnidami, and Ahmed Tarawneh. "A Comparative Study of Agile Methods: XP versus SCRUM'." *International Journal of Computer Science and Software Engineering (IJCSSE)* 4, no. 5 (2015): 126-129.
- [19] Scheerer, Alexander, Tobias Hildenbrand, and Thomas Kude. "Coordination in large-scale agile software development: A multiteam systems perspective." In *2014 47th Hawaii International Conference on System Sciences*, pp. 4780-4788. IEEE, 2014.
- [20] Hayata, Tomohiro, and Jianchao Han. "A hybrid model for IT project with Scrum." In *Service Operations, Logistics, and Informatics (SOLI), 2011 IEEE International Conference on*, pp. 285-290. IEEE, 2011.
- [21] Batra, Dinesh, Weidong Xia, Debra VanderMeer, and Kaushik Dutta. "Balancing agile and structured development approaches to successfully manage large distributed software projects: A case study from the cruise line industry." *Communications of the Association for Information Systems* 27, no. 1 (2010): 21.

A Bayesian Approach to Predicting Water Supply and Rehabilitation of Water Distribution Networks

Abdelaziz Lakehal

Department of Mechanical Engineering
Mohamed Chérif Messaadia University
P.O. Box 1553, Souk-Ahras, 41000, Algeria

Fares Laouacheria

Department of Hydraulic
Badji Mokhtar Annaba University
P.O. Box 12, 23000, Annaba, Algeria

Abstract—Water distribution network (WDN) consists of several elements the main ones: pipes and valves. The work developed in this article focuses on a water supply prediction in the short and long term. To this end, reliability data were conjugated in decision making tools on water distribution network rehabilitation in a forecasting context. The pipes are static elements that allow the transport of water to customers, while the valves are dynamic components which perform ensure management of water flow. This paper presents a Bayesian approach that allows management of water distribution network based on the evaluation of the reliability of network components. Modeling based on a Static Bayesian Network (SBN) is implemented to analyze qualitatively and quantitatively the availability of water in the different segments of the network. Dynamic Bayesian networks (DBN) are then used to assess the valves reliability as function of time, which allows management of water distribution based on water availability assessment in different segments. Finally an application on data of a fraction of a distribution network supplying a town is presented to show the effectiveness and the strong contribution of Bayesian networks (BN) in this research field.

Keywords—Water distribution network (WDN) management; Rehabilitation; Pipes and valves reliability; Bayesian Networks (BN); Water supply

I. INTRODUCTION

The water distribution networks (WDN) are underground infrastructure; they are intended for water supply to the consumers at working pressure in a specific range. These networks mainly include pipes, connection of water, metering systems and valves. Today, water grids are made up primarily of polyethylene pipes. At the downstream of these networks are situated individual or collective connections themselves shall be constructed of polyethylene or other equivalent material.

Through this article we will try to give a contribution to WDN management by assessing their reliability. The availability of water in the WDN depends on the availability of the pumping system, water quality, the mechanical behaviour of network components, and hydraulic parameters. All these parameters contribute to the assessment and the reliability analysis of WDN. Ostfeld [1] defined the reliability on the basis of the water quality by the fraction of the delivered quality. Kansal and Arora [2] defined the reliability on the basis of the water quality by the proportion of time in which the network was able to provide the desired water quality. The above two parameters are based on the proportion

of time during which the network provided high-quality of water. Kansal and Arora [2] proposed a widely accepted methodology for analyzing the reliability of WDN based on the water quality assessment using two parameters: the reliability of hydraulic system and the quality of water. These reliability parameters: hydraulic and water quality described as well the reliability of WDN. The major disadvantage in obtaining these parameters is highly related on the mathematical modelling methodology [3]. Quantitatively, the reliability of a water distribution system can be defined as the complement of the probability that the system fails, a failure is defined as the inability of the system to provide consumers with a drinking water (quality and continuity of service). Two types of events can cause the failure of a water distribution system: the failure of the system components (eg tubes and / or hydraulic control elements) and / or demand (transportation of the desired quantities of water to the desired pressure at desired appropriate locations and at desired appropriate times). These definitions show that the reliability of WDN can be classified into two main categories: topological and hydraulic reliability [4].

The above paragraphs show that the management of a WDN is based primarily on the quality, topological reliability and hydraulic reliability. In the following, we focus on the topological reliability and specifically the mechanical reliability of the components of the WDN, the failure of one of these elements can leave a fraction of the WDN out of service and consequently interrupting the water supply of a population.

Several authors have based their studies in the field of WDN on the reliability assessment by artificial intelligence methods either in the design phase [5] or the operation phase [6]. The methodology presented below is based on the assessment of the water availability in the WDN on the basis of the reliability modelling of pipe and valves by using Bayesian network (BN).

II. THE BAYESIAN MODELS

Each adverse event is related to one or more causes, so in the operation of WDN each failure scenario has a cause and effect structure. For example an interruption in water supply is a direct consequence of water leak, or maintenance work on the water distribution system. In this example, each cause has an individual probability of occurrence, which affects our beliefs and changes the probability of the final consequence. In addition, the causes have a probability of occurrence

defined a priori by measurement, or following investigations (expert opinion). The causes and consequences are uncertain or "stochastic" variables. They are discrete but there are belief scenarios where analysis involving continuous variables. In situations of uncertainty where expert knowledge and measurement data is incomplete, the use of posterior observations by a Bayesian approach reduces and eliminates this uncertainty.

In Bayesian methods, a priori information, the likelihood and a posteriori information are represented by probability distributions. A priori probability represents the probability distribution of knowledge on a variable before that the parameter it represents is observed. The likelihood is a function of parameters of a statistical model reflecting the possibility of observing a variable if these parameters has a value. A posteriori probability is the conditional probability of the data collected by combination of prior probability and likelihood via Bayes' theorem [7].

In a BN, dependence and causality is represented by edges. An edge between two variables implies a direct dependence between these two variables: one is called the parent, and the other named child. In a Bayesian model, the behaviour of the child variable should be given in view of the behaviour of its parent or parents (if there are several). To do this, each node in the network has a conditional probability table (CPT). A CPT associated with a node allows quantifying the effect of the parent node on that node: it describes the probabilities associated with child nodes according to the different values of the parent nodes. For root nodes (without parents), the probability table is no longer conditional and gives them a priori probabilities [8].

The BN prohibit child dependencies to parents. Thus, the set of variables and edges will form a directed (edges have a

sense) and acyclic graph (no cycle in the graph). Therefore, a BN (Figure 1) is defined by a directed acyclic graph (DAG) as [9]:

$$p(V_1, V_2, \dots, V_n) = \prod_{i=1}^n p(V_i/C(V_i)) \quad (1)$$

Where C (Vi) is the set of parents (or causes) of Vi in DAG.

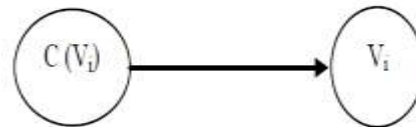


Fig. 1. Example of a simple Bayesian network

III. BAYESIAN MODEL DEVELOPMENT FOR WATER SUPPLY PREDICTION

A. Modeling with Static Bayesian Network

Modelling with BN is similar to that of the fault tree [10]. The fault tree is a systematic and comprehensive approach to determine the sequence and combinations of events that could lead to a top event taken as a reference (Figure 2.a). Whatever the nature of the basic elements identified, fault tree analysis found on the basis that the events are independent. In a BN, the connections between events will be represented by edges that reflect the dependence between these events, and cause-effect relationship. The different types of events will be represented by nodes on the basis that basic events will be the input nodes for the model (Figure 2.b).

The availability of water in a section depends on the reliability of the pipe and that of the valve. A BN models the events with the nodes, while the distinction between the various logic gates of a fault tree is made by adjusting the CPT [10].

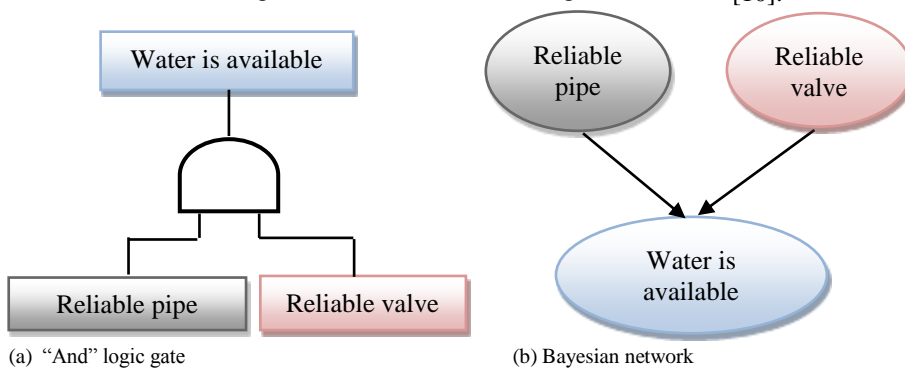


Fig. 2. Conversion of fault tree into Bayesian network

B. Modelling with Dynamic Bayesian Network

A BN is a modelling tool that treats problematic where the variable is static. In this field, each variable has a unique and fixed value. Unfortunately, this static variable hypothesis does not always take. As many domains exist where the variables are dynamic and reasoning in time is necessary such as dynamic systems. Dynamic Bayesian Networks (DBNs) are graphical models allowing to compactly representing the inherent uncertainties in dynamic systems evolving over time. The BNs and DBNs have given a strong contribution in the studies of analysis and assessment of the reliability. As two

illustrative examples, we can cite the work of [11] for modelling reliability of a complex system using BNs, and [12] for modelling reliability by DBNs.

In the framework of this study we will use the DBN for assessing the reliability of the valves and therefore predicting the different supply situations of the various sections. In order to master the water supply, it is necessary to control and monitor over time the evolution of variables (water availability) for each segment of the WDN. To achieve this objective the idea is to infer, what is the possibility for example that water is available in a WDN fraction based on

opening sequences of the valve. In this case the random hidden variable is (water availability)_t with two state (true) and (false), and the observed variable is (the status of the

valve)_t, and the satisfaction of these suppositions is modelled by the dependencies between all variables in the model that is given by the BDN in Figure 3:

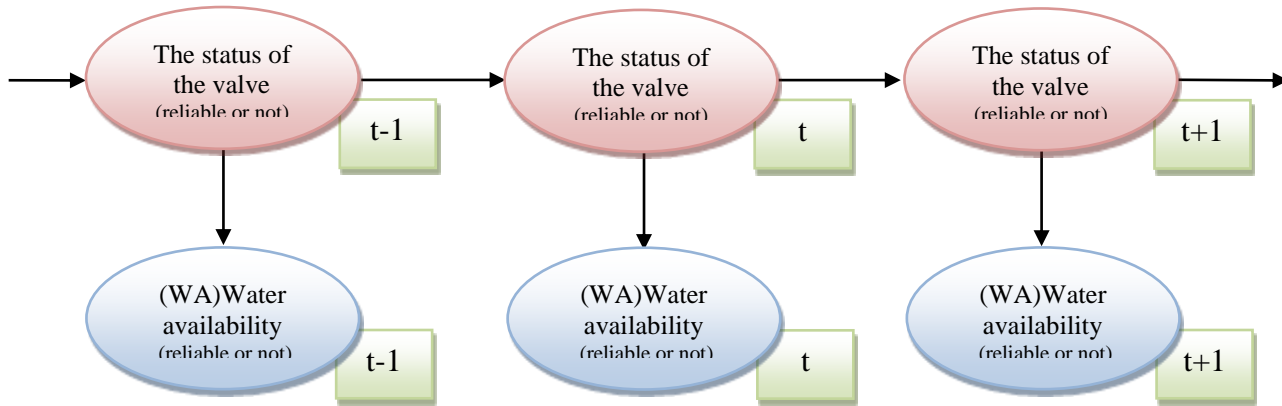


Fig. 3. Modelling of water supply of a network segment by Dynamic Bayesian Network

In Figure 3, the fact indicate an edge between the two variables (water availability)_t and (the status of the valve)_t, this means that the availability of water depends on the status and reliability of the valve at time t and similarly, the reliability of the valve at time t depends on its reliability at time t-1. From this DBN it is possible to calculate the most recent a posteriori distribution of the variable (water availability)_t by filtering, also it is possible to calculate the a posteriori probability of the variable (water availability)_{t+n} in a future time, where n the number of time steps, such as:

$$P(V_t/V_{t-1}) = \prod_{i=1}^N P(V_{i,t}/C(V_i)_{i,t}) \quad (2)$$

IV. APPLICATION AND DISCUSSION

The data used in the examples that will be presented in the rest of this paper concern a WDN supplying a city. There are two architectures for networks either meshed network (or ringed) or network in a radial arrangement. In the first case, the network segment is controlled by one valve, so the availability of water in the framework of this study is mainly dependent on the reliability of the pipe and of the valve (Figure 4.a). In the second case the water availability depends essentially on the reliability of piping and block valves (in the case study there are two valves) (Figure 4.b).

The modelling of the failure rate (breaks or leaks) by segment requires a significant history of maintenance data. Alternatively, the approach of the entire WDN is insufficient because it does not allow to plan and implement short-term actions. However, the design of reliable models must be adapted with the available data and analysis must be done on a scale segments according to several criteria: material, diameter, when it was laid, flow, pressure, and road.

Pipe failure rates in a distribution system can be determined from historical failure/repair data. In the case where historical failure data indicate a deteriorating network, a classical reliability assessment of the network can be done using Poisson process for modelling the pipe failures. In this case, the reliability measure is based on individual pipe failure probabilities. Here, the probability of failure of an individual pipe is given by:

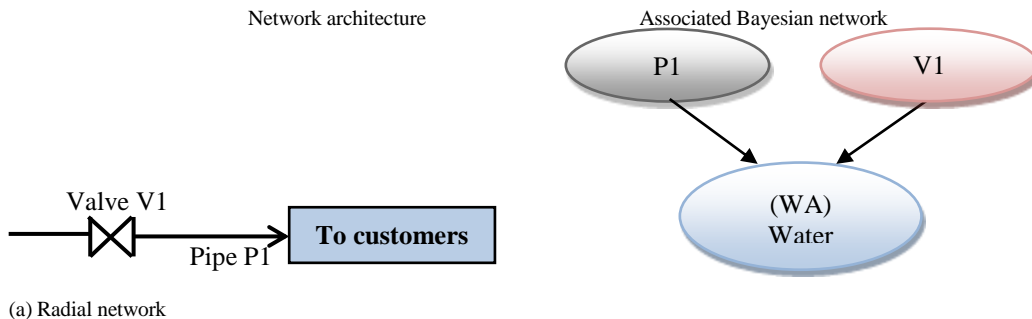
$$P = 1 - e^{-\lambda t} \quad (3)$$

Where:

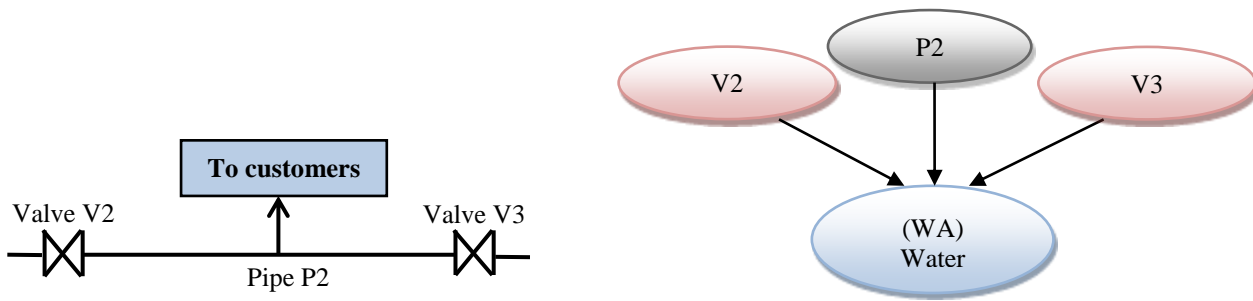
P: Probability of failure

λ : Failure rate

t: Time



(a) Radial network



(b) Mesh network

Fig. 4. Bayesian network models for the two network architectures

An estimation of $\lambda(t)$ by time slice is determined by the following calculation:

$$\lambda(t_i) = \frac{n_i}{N_i \times \Delta t_i} \quad (4)$$

Where:

n_i : the number of failed during Δt_i

N_i : the number of survivors at the beginning of the slice t_i

$\Delta t_i = t_{i+1} - t_i$: the observed time interval

By applying the formula (4) to the WDN $\lambda(t)$ is given by:

$$\lambda(t_i) = \frac{\sum_i n_i}{\sum_i (L_i \times \Delta t_i)} : \text{Number of failures/ 100m/ year} \quad (5)$$

Where:

n_i : the number of observed failures on segment i

L_i : length corresponds to each segment i (in meters)

Δt_i : the observation period for each segment i (in year)

The proposed Bayesian approach gives the probability of failure of an individual pipe from the equation (1). For a leak on the pipeline (LP), the reliability decreases (RP), provided that P (reliability of pipe) $\neq 0$:

$$P(LP/RP) = \frac{P(RP/LP)P(LP)}{P(RP)} \quad (6)$$

Bayes' theorem can reverse the probabilities. That is to say, if we know the reliability of the pipe as a consequence of leaking pipe, observing the effects allows estimating the probability of failure.

$$P(RP/LP) = \frac{P(LP/RP)P(RP)}{P(LP)} \quad (7)$$

The definition of a priori probabilities is the most difficult step in the model development; it is based on knowledge held

by experts or the feedback. It also requires special attention because the results obviously depend on the available data and on some hypothetical models.

A valve is defined as a dynamic mechanical device by which the flow of fluid may be started, stopped, or regulated by a movable part that opens or obstructs passage. Control valves are used to regulate flow or pressure at different points of the system by creating headless or pressure differential between upstream and downstream sections. The mission of isolation valves is to isolate a portion of the system whenever system repair, inspection, or maintenance is required at that segment; in the following we are interested in the isolation valves. The reliability of valves themselves has not been implicitly or explicitly incorporated in reliability assessments to date. Perhaps the main reason for this is that the human factor is the most important factor in determining their reliability. The more frequent the valve exercising programs, the greater the chance that they will operate when needed.

The water availability depends on the state of the valve. Following a closing valve, if it will not open there will be no water. From Equation (2) it's possible to define the valve reliability as a function of the valve failure (Valve won't open).

$$P(RV_t/RV_{t-1}) = \prod_{i=1}^N P(RV_{i,t}/VWO_{i,t}) \quad (8)$$

For experimentally determine the failure rate λ which corresponds to the probability of having failure in the time intervals constituting the life cycle of the studied WDN, the historical files and the formula (5) are used. Table 1 gives the failure rates (leaking pipe) for pipes P1 and P2, with two states (true) and (false) and the valves V1, V2, and V3 with regard to fault: the valve not open (Valve won't open), with two states (true) and (false).

TABLE I. A PRIORI PROBABILITIES

Element	Failure	State	Probability
P1	Leaking pipe (LP1)	True (T)	$\lambda = 0.136$
P2	Leaking pipe (LP2)	True (T)	$\lambda = 0.213$
V1	Valve won't open (VWO1)	True (T)	$\lambda = 0.057$
V2	Valve won't open (VWO2)	True (T)	$\lambda = 0.026$
V3	Valve won't open (VWO3)	True (T)	$\lambda = 0.033$

T : True, **F** : False

DBN encodes the joint probability distribution of a time-evolving set of variables $V(t) = \{V1(t), \dots, Vi(t)\}$. If we consider t time slices (time step) of variables, the DBN can be considered as a "static" BN with $T \times i$ variables. In this context the probability of supplying (water availability WA) the subscribers connected to the network of Figure 4.a is calculated as follows:

$$\begin{aligned}
 P(WA=T) &= P(WA=T / LP1=T, VWO1=T) \times P(LP1=T) \times P(VWO1=T) + \\
 &P(WA=T / LP1=T, VWO1=F) \times P(LP1=T) \times P(VWO1=F) + \\
 &P(WA=T / LP1=F, VWO1=T) \times P(LP1=F) \times P(VWO1=T) + \\
 &P(WA=T / LP1=F, VWO1=F) \times P(LP1=F) \times P(VWO1=F)
 \end{aligned}$$

Using the data collected in the table 1 we find:

$$\begin{aligned}
 P(WA=T) &= 0 \times 0.136 \times 0.057 + \\
 &0 \times 0.136 \times 0.943 + \\
 &0 \times 0.864 \times 0.057 + \\
 &1 \times 0.864 \times 0.943
 \end{aligned}$$

$$P(WA=T) = 0.814$$

As soon as the number of nodes increases the calculations become difficult. Similarly calculations are made more

complicated for modelling the dynamic behaviour of valves with DBN. To relax these constraints a program was used.

Table 2 and Table 3 give the conditional probability tables for the two network architectures.

TABLE II. CONDITIONAL PROBABILITY TABLE FOR RADIAL NETWORK

	VWO1	T		F	
	LP1	T	F	T	F
Water Availability (WA)	True (T)	0	0	0	1
	False (F)	1	1	1	0

TABLE III. CONDITIONAL PROBABILITY TABLE FOR MESH NETWORK

	VWO2	T				F			
	VWO3	T		F		T		F	
	LP2	T	F	T	F	T	F	T	F
Water Availability (WA)	True (T)	0	0	0	1	0	1	0	1
	False (F)	1	1	1	0	1	0	1	0

The interpretation of CPTs is as follows: for the first architecture, if the valve does not open, water is not available, and also if the pipe is faulty, water is unavailable. One of these two conditions implies that water is not available (OR gat in Fault tree analysis). For the second architecture, water is available, if at least one of the valves opens and pipe is not leaking (reliable pipe).

The valves have a dynamic behaviour; however, and from equation (8) the temporal probability distributions of the three valves V1, V2, and V3 are shown in Figure 5.

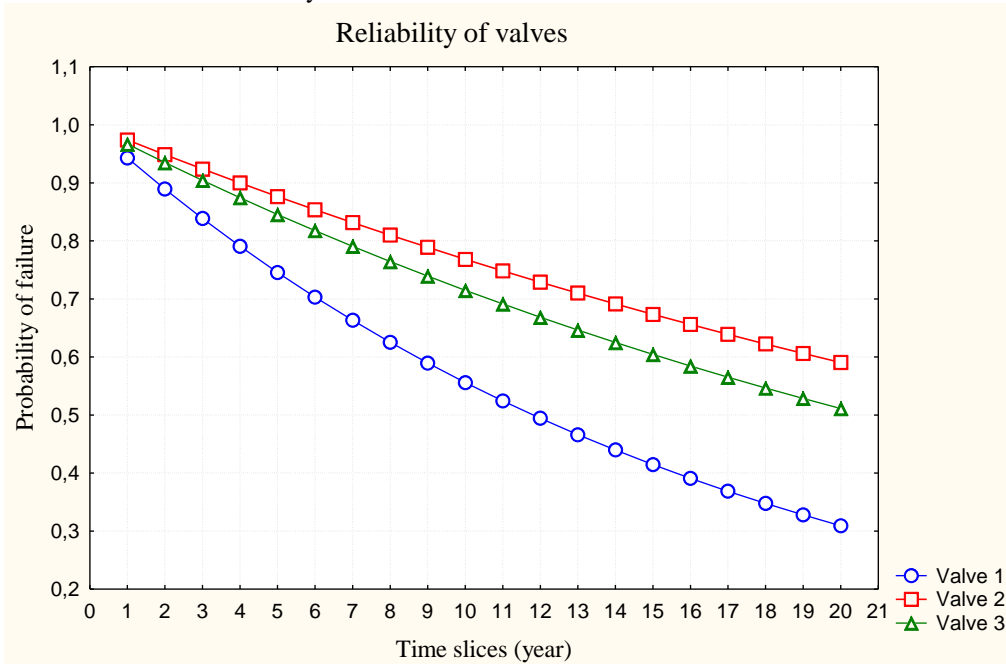


Fig. 5. Temporal probability distributions of the three valves V1, V2, and V3

Applying formula (2) and on the basis of CPTs shown in Tables 2 and Table 3, the water availability probabilities as a function of time are obtained. The results are shown in

Figure.6 and Figure 7, they depend on the reliability data of the valves V1, V2, V3, the two segments of network P1, and P2 and also the two architectures (defined by CPTs):

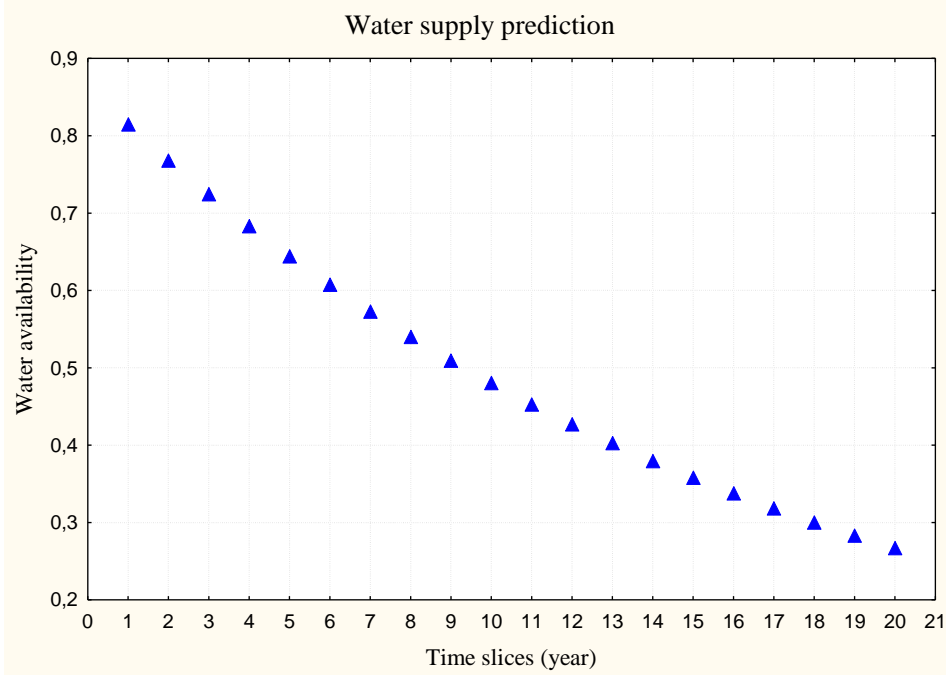


Fig. 6. Water supply for radial network

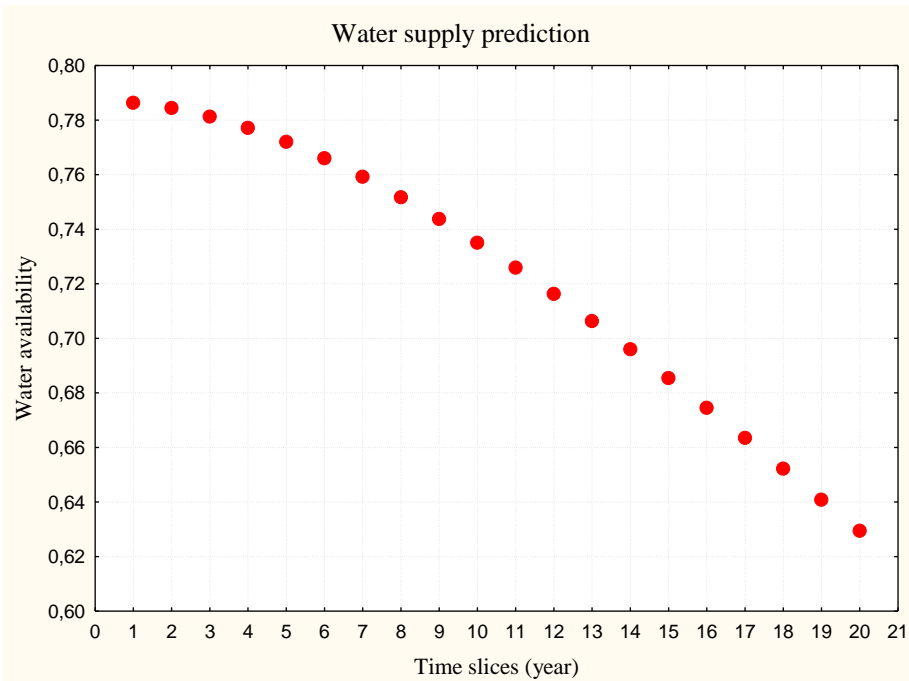


Fig. 7. Water supply for meshed network

This section presents predictive results on water supply; results were based on the reliability of the pipes and valves (Figure 6 and Figure 7). From the results of the developed model it's possible to easily extract information and transform them into quantitative and qualitative data. This approach allows predicting the behaviour of WDN gives the possibility

of a predictive management of water supply and anticipates failures of network elements. On the other hand, it is possible from the developed Bayesian approach to simulate the maintenance actions and investment reflections.

From the results shown in Figures 6 and Figure 7, it is remarkable that despite that there are two water intakes for

meshed architecture, but the probability that the mesh network is supplied is 78.63% for the first year. Lower value than that of the radial network (81,74%). This is due mainly to the failure rate $\lambda(P2)$ which is higher than $\lambda(P1)$. After 10 years of service, the supply from the radial network is found with a probability of 48.04%, low value. After the same period the subscribers connected to the mesh network will have a water supply probability equal to 73.50%, higher value compared with that of the network in a radial arrangement. Now, after 20 years the radial network is at the end of service life, on the other hand, the mesh network is still profitable (a water supply probability greater than 62%).

From these results it is also possible to define a plan of action for the rehabilitation of WDN. For example, if the probability of 60% is fixed as the threshold value on the probability of water supply for the rehabilitation of the WDN, it is necessary to provide the rehabilitation for the radial network from the seventh year, whereas for the mesh network rehabilitation is not needed for the 20 years.

The proposed Bayesian model has a great interest compared to the Poisson model. It classifies sections with low failure rates, or who have not experienced failures (failure rate equal to 0) with similar sections. When new information is available on the individual failure rate, the results will be updated by inference without increasing the calculation time.

In order to expand the study by taking into account hydraulic reliability and reliability-based quality (the level of chlorine in the water) it is possible to develop the model by adding the quality and hydraulic parameters as input variables in the model. The same goes with adding new information; add a new variable in Bayesian models is not difficult and the inference process will not take a significant time for calculating the new a posteriori probabilities.

A WDN operates as a system of dependent components (valve, pipe, individual and collective water connection). The hydraulics of each component is relatively straightforward; however, these components depend directly upon each other and as a result affect each other's performance. The purpose of the Bayesian analysis is to determine how the systems perform hydraulically under various demands and operating conditions. In this paper, a segment of network has been studied. If the study is generalized over the entire network with its multitude of valves; pipe and connections, the results found in the examples are used for the following situations:

- Evaluation of WDN reliability
- WDN performance and operation optimization: prioritize actions and supporting any strategic decisions.
- Determination of rehabilitation priorities
- Design of a new WDN: best choice of the network design (radial or mesh network) by considering the reliability as a central element in this design in parallel with the hydraulic elements
- Modification and expansion of an existing WDN: the implantation and the management of the boundary

valve in the network is essential in maintaining the integrity of the hydraulic structure

- Preparation for maintenance: optimizing the systematic and predictive maintenance

Analysis of WDN malfunction: such as water connection breaks, leakage, valve failure

V. CONCLUSION

In this paper, the Bayesian approach presented will be a useful tool in the decision-making process. The model developed in this work helps operators of WDN to assess the water availability as function of time which allows a predictive management of water supply. The use of DBN is due to the dynamic character of flow control components which are valves. The Bayesian approach used for modelling the reliability of pipe which has experienced failures, pipes without failures, and valves, represents a new and unique tool for the three cases compared to existing models in the literature. The found results have contributed greatly to estimating in a realistic and practical estimation of foreseeable demand to improve management of the quantities of water and to improve the operational capability of operation and maintenance services. Also in the operation of WDN and in general, maintenance and investment actions must be included in the time. To do this, the DBNs are powerful simulation tools of the impact of these actions on the future management of WDN.

In the future work, we will look forward to developing the model by taking into account the hydraulic reliability and the reliability based quality on the one hand and on the other hand by considering the human factor that also represents an influence factor in determining the reliability of the valves.

REFERENCES

- [1] A. Ostfeld, "Reliability analysis of water distribution systems," *J. Hydroinform.* vol. 6, 4, 281–294, 2004.
- [2] M.L. Kansal, and G. Arora, : Water quality reliability analysis in an urban distribution network, " *J. Indian Water Works Assoc.* vol. 36, 3, 185–198, 2004.
- [3] R. Gupta, S. Dhapade , S. Ganguly and P.R. Bhawe, : Water quality based reliability analysis for water distribution networks," *ISH Journal of Hydraulic Engineering.* vol. 18, 2, 80–89, 2012.
- [4] A. Ostfeld, : Reliability analysis of regional water distribution systems," *Urban Water.* vol. 3, 4, 253–260, 2001.
- [5] T. D. Prasad, S.H Hong, and N. Park, : Reliability based design of water distribution networks using multi-objective genetic algorithms," *KSCE Journal of Civil Engineering.* vol. 7, 3, 351–361, 2003.
- [6] V. Kanakoudis, S. Tsitsifli, : Water pipe network reliability assessment using the DAC method," *Desalination and Water Treatment.* vol. 33, 97–106, 2011.
- [7] A. Darwiche, *Modeling and Reasoning with Bayesian Networks.* Cambridge University Press, 2009.
- [8] Jensen, F, V. An Introduction to Bayesian Networks. UCL Press; 1996.
- [9] P. Naim, P.H. Wuillemin, P. Leray, O. Pourret, and A. Becker, : *Réseaux bayésiens.* 2 ed. France: Eyrolles; 2004.
- [10] A. Bobbio, L. Portinale, M. Minichino, and E. Ciancamerla, : Improving the analysis of dependable systems by mapping fault trees into Bayesian networks," *Reliability Engineering System Safety.* vol. 71, 3, 249–60, 2001.

- [11] H. Boudali, and J.B. Dugan, : A discrete-time Bayesian network reliability modeling and analysis framework,” Reliability Engineering and System Safety. vol. 87, 3, 337-349, 2005.
- [12] P. Weber, and L. Jouffé, “Complex system reliability modelling with Dynamic Object Oriented Bayesian Networks (DOOBN).” Reliability Engineering and System Safety. Vol. 91, 149-162, 2006.

Reducing Energy Consumption in Wireless Sensor Networks using Ant Colony Algorithm and Autonomy Mechanisms

Javad Mozaffari

Department of Computer, Ardabil Science and Research Branch, Islamic Azad University, Ardabil, Iran
Department of Computer, Ardabil Branch, Islamic Azad University, Ardabil, Iran

Mehdi EffatParvar*

Department of Computer, Ardabil Branch, Islamic Azad University, Ardabil, Iran

Abstract—Wireless sensor network includes hundreds or thousands of nodes with limited energy. Since the lifetime of each sensor is as the battery life of the sensor, the energy issue is discussed as a fundamental challenge. In this article, parallel ant algorithm and exclusive territoriality algorithm have been used by providing the ability of nodes self-determination, in order to improve the parameters of energy consumption, extend the life and network coverage. For routing nodes also is used direct send method, sending by hierarchical clustering, along with carrier head cluster. This article is evaluated by focusing on network stability, based on two main factors: reduce energy consumption and extend the network life and increase network coverage. The simulated output in this paper represents an increase of energy consumption balance and network lifetime approach (the first death time) and network imperative life (the last death time), which represents network high-performance than latch, direct transmission and other methods. Therefore, also in this article the purpose is to provide a better way than previous methods based on developed ant algorithm to reduce energy consumption against hardware limitations.

Keywords—wireless sensor networks; ant algorithm; network stability; energy consumption reduction; network coverage; network lifetime

I. INTRODUCTION

Nowadays, wireless sensor networks are attractive for academic and industrial circles as a new and efficient technology in information collecting and mobile communication, as that is the one area that has seen the most development and this rapid development reveals some major problems that it has which include the hardware limitations and energy consumption. These two issues caused a lot of researches in the field of hardware, i.e. reducing the size and increasing energy efficiency and in the field of software, i.e. energy efficiency. Sensor node includes a processing unit, transmission unit, the receiving unit and the unit positioning unit. Wireless sensor network includes relay typical nodes, head cluster and base station, which the requirement to all this equipment and facilities has caused that downsizing technology, fails to reach its ultimate goals, and, in fact, reduce energy consumption needs energy consumption management to increase these networks lifetimes by this way. Routing is the most important approach in energy consumption, because

wireless networks generally varies inversely with distance, so, efforts to reduce energy consumption is often in terms of routing and reduce the mean distance, in which always the goal of algorithms, was routing parameters improvement, including routing algorithms we can refer to routing algorithms based on clustering. However, the clustering will be useful in situations that the distance from the sink in the total of network be greater than base distance, if the distance average from sink be lower than or close to base distance, clustering will not be useful. But with increasing distance from the sink and distribution network area development, single step and multi steps clustering will have the highest efficiency in reducing energy consumption respectively.

Nodes in each cluster receive information from environment and send it to head cluster. Head cluster aggregate them after receiving. After integration, information is transmitted to the base station through the single step path or multi step path. Cluster size, number of node (head cluster) per cluster and selecting the head cluster are considered as important factors in clustering (7). On the other hand the head cluster position is considered as a major issue in clustering. As the energy model, energy consumption has a direct relationship with the square of the distance (8, 13). We used of ant colony optimization techniques in sizing Meso-Structures for in Non Pneumatic Tires (9), thus the head cluster inappropriate choice will increase gap and more energy consumption. Therefore, an approach that would take into account all aspects and give to network flexibility is often of interest.

In other words, an algorithm that can show flexibility in various conditions and by relying on the conditions (such as changing the size of the network, change the shape and dimensions of the network, etc.) uses a particular method in sending and receiving information, this algorithm would be appropriate. We also used of ant colony optimization Analysis of the graph complexity connectivity method for Procedia (15) Based on the above principles, the designed network in this paper is used the ant algorithm and exclusive territoriality and to choose the optimal head clusters and autonomy and to increase the flexibility it used of the autonomy ability and change the clustering type (directly and hierarchy transmission).

Corresponding author: Mehdi Effatparvar

A. Ant colony optimization algorithm

Ant colony optimization algorithm is also one of the methods based on the behaviour of ants to find food. Ants create a route with the shortest length between their nest and the food source to prepare food. This algorithm is presented as the standard mode for discrete optimization problems. In fact, the ants' way in reality is that they initially look for food randomly. Once they find a source of food, they return some food with themselves to the colony. Along the way, ants leave a chemical substance called pheromones. This chemical substance does somehow related to the information exchange of bees dancing act. Pheromone is a volatile substance that evaporates over time. Consequently, if the ants in their various searches find many sources, most favourable (closest) food sources have been accessed by more ants and in turn, the path that supreme from colony to that resource containing greater amounts of pheromones it should be noted that the process of evaporation would be to avoid getting stuck in local optimum. Pheromones values in this algorithm update as follows in each iteration:

$$P_{ij}^k = \begin{cases} \frac{(\tau_{ij})^\alpha (\eta_{ij})^\beta}{\sum_{m \in N_i^k} (\tau_{im})^\alpha (\eta_{im})^\beta} & j \in N_i^k \\ 0 & \text{otherwise} \end{cases} \quad (1)$$

According to equation (1) p_{ij}^k is the probability that ant k chooses to go from node i to node j , N_i^k is a set of all the probable neighbours that have still not met by ant k . η_{ij} is heuristic function, τ_{ij} is the pheromone on edge i to j , α and β are parameters that determine heuristic information importance or relative weight and pheromone scale.

Pheromone update is done through the following formula:

$$\tau_{ij} = \tau_{ij} + \Delta \tau_{ij}^k$$

$$\Delta \tau_{ij}^k = \begin{cases} \frac{Q}{f(\psi^k)} & l_{ij} \in \psi^k \\ 0 & \text{otherwise} \end{cases} \quad (2)$$

Evaporation is updated through the following formula:

$$\tau_{ij} = (1 - \rho)\tau_{ij} \quad (3)$$

Where ρ is pheromones reduction constant coefficient, $f(\psi^k)$ is cost solution made by ant k , and Q is a constant value. This process is repeated until to get a certain number (7), (10, 18). Presented Second Edition Leach algorithm and selecting the number of head clusters is central station responsibility. In the preparation phase, each node sends

location information and its residual energy to the central station. Base station computes the average value of the energy network. It do not let to those nodes that their energy levels are lower than the mean value to be head cluster, Its function $T(n)$ is calculated in the form below.

$$T(x) = \begin{cases} \frac{p*\lambda}{1-p[\lceil r \bmod (\frac{1}{p}) \rceil]^*} & \text{if } n \in G \\ 0, & \text{otherwise} \end{cases} \quad (4)$$

$$\lambda = \frac{\text{residual energy}}{\text{primal energy}}$$

The disadvantage of this version is wasting energy when it occurs in notice of the location situation and its residual energy (7). (11,14).present an performed model of leach using the **PSO** algorithm, the assumptions used in this algorithm are higher energy of head cluster and head cluster closer distance to the main station, to achieve this assumption the following equations is used.

$$f_i = \alpha 1. f1 + \alpha 2. f2 \quad (5)$$

$$f1 = \sum_{i=1}^n qi / \sum_{i=1}^k qk \quad (6)$$

$$f2 = \sum_{i=1}^n li / \sum_{i=1}^k lk \quad (7)$$

According to the above equations $f1$ is to achieve higher energy and $f2$ is for closer head cluster to the main station and the sum of the coefficients equal to 1, the effectiveness of any of the above functions is done by setting the alpha 1 and alpha 2 parameters, in the first run of leach, due to the amount of energy equality we just consider parameter P , so P value is calculated as follows. (12, 16)

$$p = \frac{\sqrt{n}}{\sqrt{2\pi}} \frac{D\sqrt{\epsilon fs}}{\sqrt{Elect(N+1) + \epsilon mpl4}} \quad (8)$$

By doing this, it reached to the longer life and more equitable use of energy, due to the use of energy level and distance, but despite this, optimization has been done to clustering step. (17)

Now, a lot of research have been done about reduce energy consumption, routing optimization and increase reliability of wireless networks, and each of them used the specific methods and procedures to improve the situation,

But in general, data processing for routing and network stability increasing stability is significantly high in them, and in a few of them is emphasized about appropriate and essential use of nodes, that in this study this goal is noticed by the use of a particular type of ant algorithm and disable unnecessary nodes.

B. Suggested method

For a better visual understanding of an issue that is considered to be established, with a few examples, challenging initial deployment of sensors in a wireless sensor network is explained. The goal here is to test the clustering effect in different situations. It is assumed that to select the 9 point on the coordinates screen, and this 9 point be placed in a

symmetrical situation, so that all states, including the points with greatest distance from the sink, points with the shortest distance from the sink and the points with medium distance from the sink could be selected as a head cluster.

And each time the remaining energy to be considered for a round, i.e. each time a node is selected as head cluster and once send and receive act is done and then the network residual energy is done and then the remaining energy to be reviewed. As shown in Figure 1, all nodes are distributed symmetrically around a point and in symmetrical form and also a sink is located in zero point with red color and solid in the figure below, the node in points 40 and 25, or start node, is selected as head cluster for the first time and then in counter-clockwise in the other nodes is selected as head cluster and finally central node is selected as a head cluster and each time entire network consumed energy is tested, according to Table 1, nodes distances from the sink nodes is calculated respectively as shown below.

TABLE I. NODES DISTANCES FROM THE SINK

47.1699	42.4264	47.1699	58.3095	68.0074	70.7107	68.0074	58.3095	56.5685
---------	---------	---------	---------	---------	---------	---------	---------	---------

That their average from base distance about (87), is less

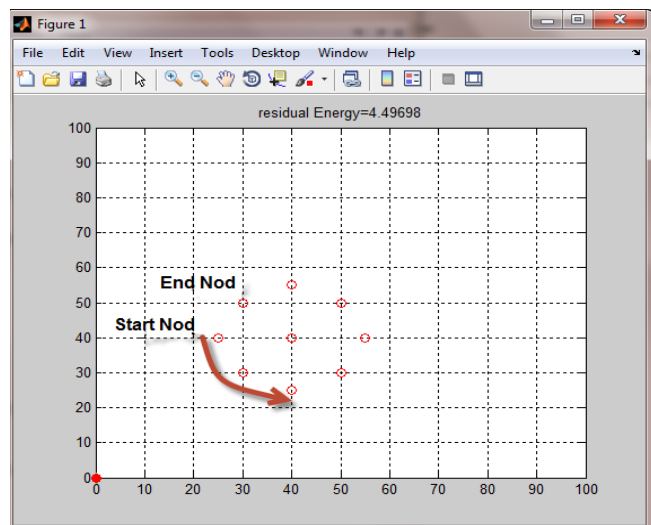


Fig. 1. The positioning graph of the nodes in a page

II. HOW TO CHOOSE THE HEAD CLUSTER

Most of the residual energy occurs when nodes send information directly; it means that, when an average distance of nodes is less than the base distance, clustering is not considered as a good strategy for reducing energy consumption. So we should withdraw from that, i.e., when the sizes of the area is close to the base distance, direct transmission is considered as the best method of sending information and any other method, including single-step head clustering such as latch and multi-step head clustering such as hierarchical clustering is rejected, also, if the optimal mode of clustering be done, for example, in an area with dimensions of 100 * 100 or 87 * 87, direct transmission even is better than

single step clustering and also from multi steps clustering. But it seems that when the average distance from the sink, is greater than base distance, send data directly is costly and clustering is needed in such circumstances very much. Then the network is going to set that, the nodes average distance from the sink be greater the distance of the base.

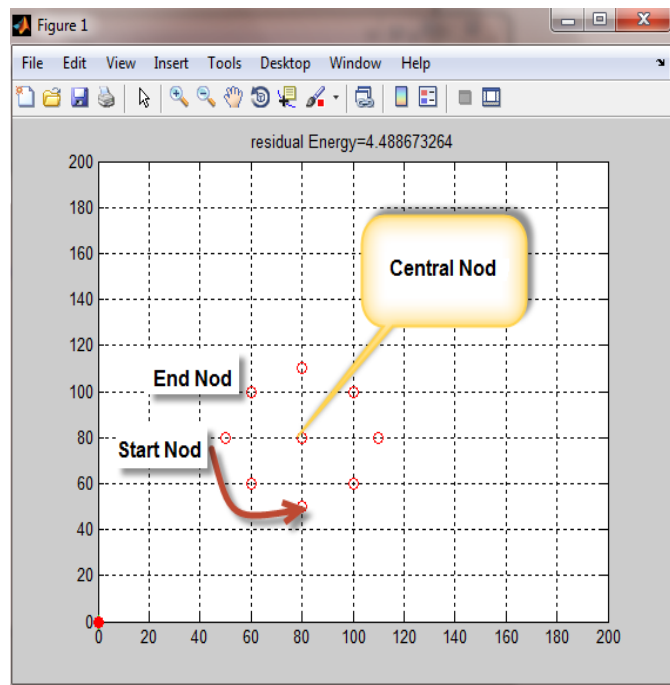


Fig. 2. Nodes placement graph in a page, with the distance more than base distance

In the network nodes head clustering does not occur any difference and sinusoidal modes is repeated between beside nodes and when the central node is selected as the head cluster, the highest efficiency in energy consumption occurs too, but when none of the nodes in accordance with the 10th stage isn't selected as head cluster, the residual energy unlike the previous case decreases than clustering and if this conditions is maintained for the case that 50 percent of nodes are in less distance and 50 percent of node are in greater distance, then energy consumption in direct transmission also will be greater because of more efficacy of large numbers power (large distances). That is, if the node average distance from the sink be more than base distance, is greater than first, latch single-stage method and then multi-stage method can be useful, in other words, each of the routing algorithms, in a certain range, has an advantage. Now, to improve the conditions so that the network can be balanced in terms of energy consumption it is necessary to: First, clustering is specific for areas that are at a greater distance from the base distance. Second, the nodes around head cluster must be placed on its base distances; otherwise it should be prevented receiving data from beyond nodes or be created a new head cluster for nodes on the outskirts. Thirdly, in areas less than from the base distance, there should be connecting rings to connect beyond head clusters to sink, that this nodes in this article introduced as carrier nodes.

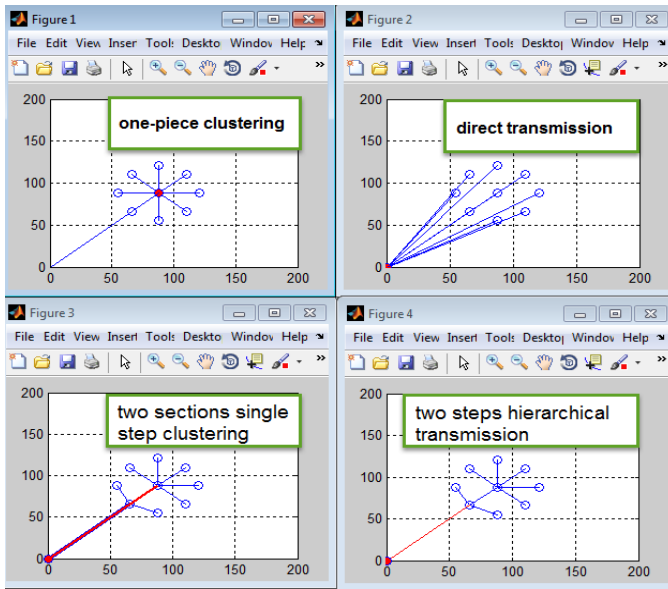


Fig. 3. Different routing algorithms

In the distance between the base distance near the 100 meters, two sections single step clustering algorithms (Figure 3) has the best performance. But then, this average distance is increased gradually and when the distance is going to be more than 130 meters, two steps hierarchical transmission is presented as the best performance and transmission with single step clustering (leach) is presented as the second useful transmission method in energy consumption and direct transmission is the worst way at such distances and this rating is always maintained. Therefore, we can say that direct transmission, at least from the base, single step and multi-step hierarchical transmission at distances greater than 130 meters and two-pieces single step and one-piece single step transmission in the middle distance have the best usage.

III. ROUTING MODEL INFLUENCED BY TERRITORY

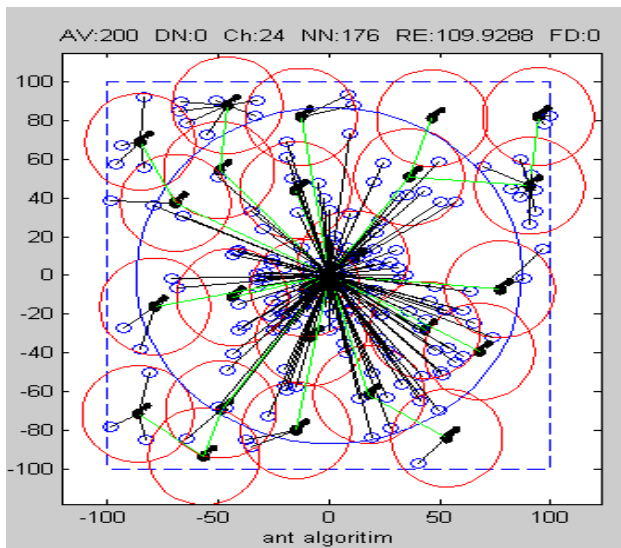


Fig. 4. Routing model affected by territory

IV. RESULTS SIMULATION AND EVALUATION

The idea Experimental evaluation proved that when the size of network area is larger than the base area, hierarchical clustering is the best mode for routing head clusters, but with increasing the number of nodes or the size of the network, this performance is better for single step transmission, for example, at a time when network is 200*200 and the number of nodes increased from 100 to 200 or more, the results of latch will be better therefore, it is necessary to increase network capabilities, appropriate control parameters to be created in accordance with changing network conditions and always maintain network functionality. Experimental evaluation showed that the single step routing length between the head clusters should be decreased by increasing the number of nodes and by increasing the size of the simulation it should be increased, in the other words, with increasing the number of nodes, the layers radius between head clusters must be reduced and by increasing the size of the simulation area, the radius should be increased.

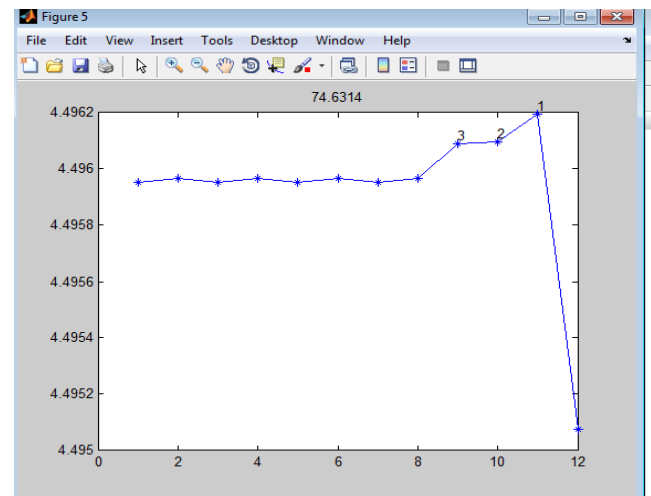


Fig. 5. The energy consumption graph based on head cluster point

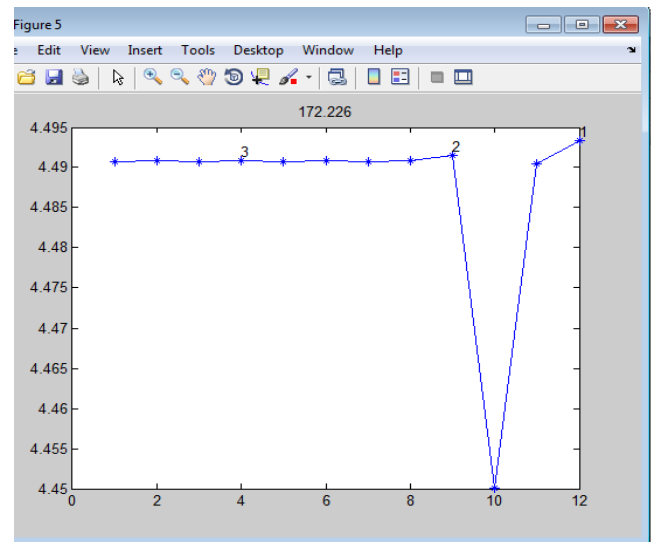


Fig. 6. Energy consumption diagram according to the head cluster point

TABLE II. SIMULATION PARAMETERS

parameter	parameters	
area	area	1000, 500, 200, 100, 70
Number of nodes	N	400, 100, 70
Sink location	BS location	0 and 0
Base distance	d0	87 m
Primary energy	E0	0.5 J
Near distance supportive energy	EFS	10 pj/bit
Near distance supportive energy	EMP	0.0013 pj/bit
Collecting energy	EDA	5 nj/bit
Pocket size	Packet size	4000 bit

V. SIMULATION SCENARIOS AND ANALYSIS OF RESULTS

To show the proposed algorithm ability, various scenarios were considered with two important variables, area size and number of nodes. The results in Table 3 indicate the increasing network longevity in proposed algorithm than other algorithms in large areas and by decreasing the simulation area, the longevity distance of proposed method will decrease than other methods that this agent is because of the nature of energy consumption in the base and limited areas and also observed that the lifetime of the network in networks with several nodes often is more than networks with fewer nodes.

TABLE III. SIX ALGORITHM LONGEVITY RESULTS COMPARING

		area space		area space		area space		area space		Death of the last node	
		1000*1000		500*500		200*200		100*100			
		Number of nodes		Number of nodes		Number of nodes		Number of nodes		Number of nodes	
		100	400	100	400	100	400	100	400	100	400
Longevity	LEACH_D	2	2	28	63	835	900	10101	1065	2500	2500
	LEACH_A	-	-	-	-	-	-	567	713	1857	2184
	LEACH_C	-	-	-	-	-	-	626	867	987	1087
	EBCS	-	-	-	-	-	-	785	879	992	1104
	Dls	2	2	10	10	337	274	1405	1505	2500	2500
	E_ANT	89	150	668	923	878	980	1714	1585	2500	2500

The lifetime of the network in 1000*1000, with the proposed algorithm, is much more compared to networks with typical latch algorithms and direct transmission diversely, but the network coverage is very limited than its life.

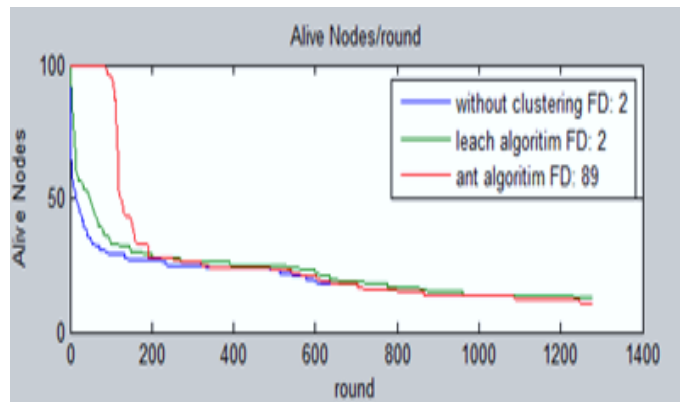


Fig. 7. Output charts in 1000*1000 areas with 100 nodes

As figure 7, the head cluster selecting chart patterns, the number of ordinary nodes, the number of live nodes, the number of dead nodes and energy consumption scale has been shown, that the proposed algorithm is shown in red.

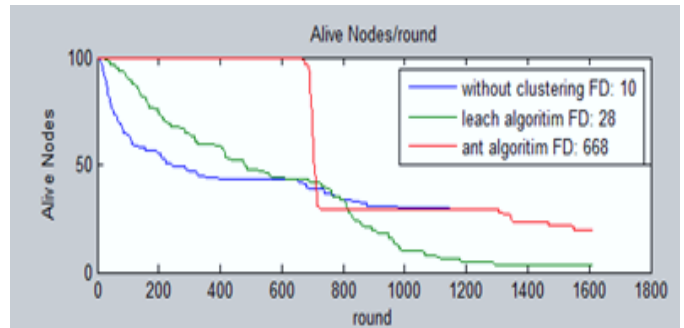


Fig. 8. Output charts in the 500*500 with 100 nodes

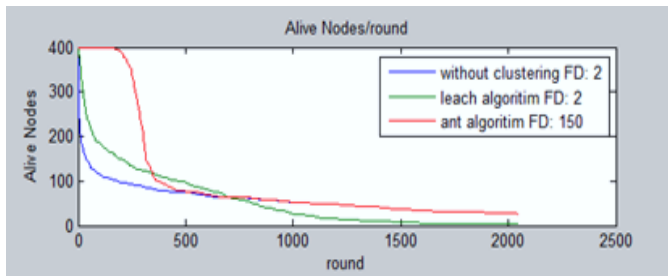


Fig. 9. Output charts in 1000*1000 area with 400 nodes

VI. CONCLUSION AND FUTURE WORK

The goal of this article is modifying the conditions for extensive use of wireless networks. This means that the network aims a kind of broad intelligence so it can manage network in terms of longevity, energy consumption and network coverage under different conditions. The output of the simulation and results graphs shows that network can work under different conditions and shows high flexibility in different areas and develops this intelligence by reducing or increasing the size of the territory of each node, reducing or increasing the single step and multi steps length of routes and the number of head cluster nodes and finally the use of self-determination property outside of the realm confine. Also in this article we try to present comparable useful features with innovative methods of proposed algorithm as an important factor in maintaining the superiority of the proposed algorithm by identifying useful work area for various algorithms and compared in this article and using the method of them in the form combination. The proposed algorithm, working in all areas except the work area that only features in its self-determination was important, and we could improve the situation by changing some parameters. Therefore it is recommended that routing methods be balanced at the base areas that include have about 1×87 m with an average sink position. In other words, if there is a significant method of routing or clustering in base area that can perform better than direct transmission, an critical event will occur in the field of wireless networks energy consumption.

REFERENCES

[1] Anaami, n. (2010). Reduce energy consumption in wireless sensor network using SOM neural network, Tehran, central Tehran branch of Payame Noor University technical and Engineering College.

[2] Rezaei-Nejad, M., Rahimi Nasab, m., Mousavi, s. (2013, Spring 1). Aware energy routing in wireless sensor Networks by using of Harmony Search Algorithm. (1), p. 2-15.

[3] Kazem Beshkani, m., Vejdani Mahmoudi, M. (2015). Reduce energy consumption in wireless sensor networks and reliability improvement by using clustering algorithm based on the latch. First Langerud Branch Islamic Azad University Electrical Engineering National Conference.

[4] Mortazavi, S., Malek Zadeh, M., Asgari Moghaddam, R. (2013, December 28). Eighth Development Conference in Sciences and technology, reducing energy consumption in wireless sensor networks by head cluster optimal locating with colonial competitive algorithm. Khavaran Higher Education Institute.

[5] Nasirian, S., Faghani, f. (2015, June 18). a hierarchical routing algorithm presentation for wireless sensor networks to reduce energy and increase the longevity of the network using the tree-radial structure. Second National Conference of Information Technology Engineering and Management.

[6] Al-karaki, J., & Kamal, A. (2004). Routing Techniques in Wireless Sensor Networks: A Survey. IEEE Wireless Communication x, 6-28.

[7] Gautam, N., & Jae-Young, P. (2010, Apr). Distance Aware Intelligent Clustering Protocol for Wireless Sensor Networks. Journal of Communication and Networks, 2(2), 122-129.

[8] Hall, A. (2009). Wireless Sensor Network Designs, vol. 1: Wiley (2009. Journal of Engineering Research & Technology (1), 50-62.

[9] Shankar, Prabhu, Mohammad Fazelpour, and Joshua D. Summers. "Comparative Study of Optimization Techniques in Sizing Mesosstructures for Use in NonPneumatic Tires." Journal of Computing and Information Science in Engineering 15.4 (2015): 041009

[10] Han, Z., Wu, J., Zhang, J., Liu, L., & Tian, K. (2014). A General Self-Organized Tree-Based Energy-Balance Routing Protocol for Wireless Sensor Network. IEEE Transactions on Nuclear Sciences, 61(2), 732-740.

[11] Heinzelman, W., Chandrakasan, A., & Balakrishnan, H. (2002). Energy-Efficient Communication Protocol for Wireless Micro sensor Networks. 33rd Hawaii Int'l. Conf.

[12] Intanagon Wiwat, C., & Govindan, E. (2000). a Scalable and Robust Communication Paradigm for Sensor Networks. ACM Mobi-Com , 56-67.

[13] Kang, Y., Lee, H., Kim, H., & Lee, B. (2007). A Clustering Method for Energy Efficient Routing in Wireless Sensor Networks. in 6th WSEAS International conf. on Electronics (Hardware (Wireless and Optical Communication), 133-138.

[14] Lee, S., JuneJae, Y., & TaeChoong, C. (567 - 568). Distance-Based Energy Efficient Clustering for Wireless Sensor Networks . in 29th Annual IEEE International Conference on Local Computer Networks, 2004.

[15] Sridhar, S., Fazelpour, M., Gill, A. S., & summers, J. D. (2016). Accuracy and Precision Analysis of the Graph Complexity Connectivity Method.Procedia CIRP, 44, 163-168

[16] Lindsey, S., & Raghavendra, C. (2002). Power-Efficient Gathering in Sensor Information Systems. IEEE Aerospace Conf, 3, 9-1.

[17] Murata, T., & Ishibuchi, H. (2008). Performance evaluation of genetic algorithms for flowshop scheduling problems. 1st IEEE Conf. Evolutionary Computation, 2, 812-817.

[18] Shiung Chang, R. (2008). An Energy Efficient Routing Mechanism for Wireless Sensor Networks. 20th International Conference on Advanced Information Networking and Applications, 1-5.

Measuring the Data Openness for the Open Data in Saudi Arabia e-Government – A Case Study

Marwah W. AlRushaid and Abdul Khader Jilani Saudagar
Information Systems Department, College of Computer and Information Sciences
Al Imam Mohammad Ibn Saud Islamic University (IMSIU)
Riyadh, Saudi Arabia

Abstract—Conceptually, data can be found at the lowest level of abstraction from where information and knowledge are being extracted. Furthermore, data itself has no meaning, unless it's being interpreted and transferred into information and knowledge. Thus, all governments have come to appreciate the relevance between releasing data and obtaining information and knowledge in return. However, the abstract nature of data with the undefined benefits to everyday life has slowed down the awareness of public to open data and its relevance. Thus, the increasing efforts by governments in embracing open data agendas may not be clear and shared among people. Most of the open government data initiatives focus on the technology needed to support the usability and accessibility of data. However, this focus has not been proven to increase citizens' awareness. Citizens' awareness of open data practices must be carefully measured as without citizen engagement, open government data is useless.

The purpose of this research is to measure data openness level of Saudi Arabia e-Government Data Portal. Moreover, a proposed model by the researcher, which is based on a scoring model by Global Open data index, is used to measure data openness level of Saudi Arabia e-Government Data Portal.

Keywords—*abstraction; accessibility; awareness; benchmarking; e-Government; knowledge; information; openness*

I. INTRODUCTION

Governments across the world are now releasing vast amounts of data in an accelerated fashion. Yet while some of the released data is easily reachable, some are still trapped in paper. Thus, there is a degree to how "open" data is, and then, how much value data can create as a result. Through all levels of government, millions of data records are collected and stored ranging from unemployment rate to energy use. Much of this data can be readily shared to the public, enabling third parties to create innovative services and products¹. Thus, by making government data available, public services can be better analyzed by organizations and citizens. Therefore, it can help to identify the subsequent improvement and even inefficiencies. This innovative use of open government data by entrepreneurs and volunteers can greatly stimulate economic growth. In specific, the value that the data can create depends on how open is the data. This imposes a need for an evaluation assessment of Open Government data in

term of data openness². The evaluation of data openness level attracts academic's attention to be one of the extensively covered topics over the past several years. Some of the approaches include evaluating a set of chosen open data characteristics to determine specific aspect such as (data quality), whereas others are oriented toward evaluating data openness in general. For example, a five-stage model [1] is proposed to evaluate the availability feature of open data. If data are not available, the availability is considered stage 0. If data are obtainable, availability reaches stage 1. When data are available in a non- machine- readable format, the availability is in stage 2. If data are in a machine-readable format, the availability reaches stage 3. Finally, when all requirements are fulfilled and data become visualizable, the availability reaches stage 4.

Sir- Berners- Lee proposed a star rating system model for evaluating the extent of public data availability³. According to the model, data receive one star if they are available on the web and license- free. If data are published in a machine-readable format, two stars will be appointed. Three stars are given if data are published in a nonproprietary format. When data comply with all previous conditions and additionally use semantic web standards related to identifying things, data receives four stars. If all mentioned rules are met and data are provided with context, data receives five stars.

The first three stages of the star-rating model match the three stages from Osimo's models, whereas the latter two of the star- rating models focus on the linked feature of data. Thus, a higher value is given to data, which can be reused and whose context is defined through linked information. The star-rating model promotes a need to focus on data structuring and formatting rather than publishing it on a simple format such as PDF Files. Both Osimo's model and star- rating model focus only in one feature of open data: data availability. Although data availability is one of the major features that defines open data; it's not the only one. Thus, none of the mentioned models can be used solely to measure the level of data openness.

The European commission⁴ has performed a study on open data portals through a web-survey and in-depth interviews

¹ <http://beyondtransparency.org/chapters/part-3/generating-economic-value-through-open-data/>

² <http://www.opendataimpacts.net/2011/11/evaluating-open-government-data-initiatives-can-a-5-star-framework-work/>

³ <https://www.w3.org/DesignIssues/LinkedData.html>

⁴ <https://ec.europa.eu/digital-single-market/en/news/pricing-public-sector-information-study-popsis-open-data-portals-e-final-report>

with government representatives. The survey was made on selected data portals worldwide. The European commission has used a star rating system model by Sir- Berners- Lee to measure data availability. However, more detailed sub-indicators were defined to clearly measure the result. Unfortunately, the study didn't go any further rather than listing the obtained results. They didn't create a path nor provided a calculation for measuring data portals openness [2]. Therefore, this study can be considered as a great resource for benchmarking methodology, but it lacks processing methods, which are crucial in measuring, classifying and comparing different open government data portals.

Socrata Company⁵ has also shown an interest in assessing open government data. The company performed a study of open government data through three surveys targeting: government, citizens, and developers. The survey was published in a form of questionnaires with the goal of assessing open government data from the perspective of government, data consumers and data contributors. Later, the results of the survey were categorized into five groups: attitudes and motivation, current states of open data, current states of data availability, high value data, engagement and participation.

The open knowledge foundation group has defined a scoring model, which contains a set of nine principles of open government data. These are: Data Exist, Data in Digital Format, Publicly Available, Free of charge, Available Online, Openly Licensed, Machine- Readable, Available in Bulk, Updated. Those principles are based on the eight principles of open government data established by the open data working group⁶. Thus, unlike other models, the scoring model contains well-defined Open Government data principles; it provides a practical determination of the extent of fulfillment of open government's primary goals. Other initiative focus on one feature of open government data and can't be used solely to measure the level of data openness. The model now is globally accepted as guidelines for open governmental data. Moreover, the recognized indicators in other benchmarks models can be mapped onto these nine principles/indicators of scoring model. For example, The European commission model provides many indicators, which are similar to the scoring model by open knowledge foundation such as: timeliness, machine- readable, license-free). However, the European commission went beyond the scope of open government data by defining additional indicators such as pricing.

A. Open Government Data in Saudi Arabia (2012- 2016)

As the concept of open government data gained momentum all over the world, Saudi Arabia was not left behind. Although the tech-based modernization in Saudi Arabia has started decades ago, its official e-government program started only a few years ago with the launch of "Yesser" in 2005 [3]. The primary aim of YESSER, an e-government initiative was to create and encourage the use of digital programs by the government. The implementation of the program was in two stages. The first phase was from the year 2006 to 2010, and the second phase is from 2012 to 2016

("The National Strategy and The e-Government Action Plan, 2016"). As a start, the aim of the program was to assist the government in offering better services to the citizens. Later, a new era of e-government has started in Saudi Arabia by launching Open Government Data Initiatives⁷ in 2011. Delivering data through the national portal as well as through the website of the ministry of the economy was the approach that Saudi Arabia followed in term of launching its Open Government Data [4]. The government aim was to enable transparency, promote citizens participation and inspire innovation. Therefore, open government data was implemented in all the ministries. However, the implementation and adoption of open government data in Saudi Arabia had faced many challenges and criticism, and it explains why the data dissemination scored low in the international threshold⁸. An overview of the different models for measuring open government data is as shown in Table 1.

TABLE I. OVERVIEW OF THE DIFFERENT MODELS FOR MEASURING OPEN GOVERNMENT DATA

Model's Name	Indicators / Aspects to be measured
Four- Stage Model of data availability (David Osimo, 2008).	✓ Availability
Five- Star Model of data availability (Sir- Berners- Lee (2010)	✓ Availability
(European Commission Model, 2011)	✓ Number of open datasets available ✓ Timeliness ✓ Data format ✓ Reuse Conditions ✓ Pricing ✓ Accessibility ✓ Take-up by citizens ✓ Take-up by app developers ✓ Number of application developed based on open data
Open data benchmark (Socrata, 2011)	✓ Accessibility ✓ Availability
Scoring model by open knowledge foundation.	✓ Data Exist ✓ Data in Digital Format ✓ Publicly Available ✓ Free of charge ✓ Available Online ✓ Openly Licensed ✓ Machine- Readable ✓ Available in Bulk ✓ Updated.

II. METHODOLOGY

A. Measuring Data Openness Level

The purpose of the research presented in this section is to suggest and apply a model for measuring data openness, which relies on global data index' scoring model established by Open Knowledge Foundation. The literature review has entailed that unlike other models, the scoring model contains

⁵ <https://socrata.com/>

⁶ <http://www.opengovpartnership.org/groups/opendata>

⁷ <https://dohanews.co/opinions-sought-new-policy-open-govt-data-public/>

⁸ <https://www.capgemini.com/resources/the-open-data-economy-unlocking-economic-value-by-opening-government-and-public-data>

well-defined Open Government data principles. Moreover, it provides a practical determination of the extent of fulfillment of open government's primary goals plus neither of the other existing models can be used alone to measure data openness level. In specific, the exclusivity and non-overlapping nature of the model's factors enable the model to be used for evaluation purposes. In fact, the scoring model was used by the organization to measure the openness level of 122 governments' data portals around the world (including Saudi Arabia). The evaluation was accomplished with the assistance of volunteers and organization members based on the information made available via governments' datasets on its online data portals. This enables government progress by giving them a baseline and measurement tool for enhancement of the open government data ecosystem in their country. Like any other evaluation tool, the scoring model by Global Data Index tries to answer a question: "What's the status of open data around the world?" and then other questions emerge: "Which is the most/least open country?," "Which is the most/least open datasets within each evaluated country?"

Since each country has a different governance structure as well as different policies in regard to open data, key assumptions were developed by the organization to be taken into consideration when assessing and collecting the data.

Assumption 1: Unified definition of Open Government Data Global Open Data Index has defined open data in accordance with 'Open Definition'⁹. The Open definition is a simple and easy to operationalize a set of principles which define data openness in relation to content and data.

Assumption 2: The role of government is to publish data there have been questions about the role of the government when some of the government data are privatized (produced and owned by a third- party).

Assumption 3: National government is accountable to publish data for all its sub- governments each country has a different governance structure and varies in the centralization of its services. Some have a major government with municipalities; others have sub-governments with much more complicated structures. Open data index assumptions is that national government must be the aggregator of all sub-governments data.

B. Datasets Assessment

Since the evaluation is based on the information made available via governments' datasets on its online data portals, it's crucial to set guidelines for each dataset to ensure it's comparable across countries and to enable accurate assessment. This year, open data index have refined the guidelines for the datasets¹⁰.

1) Each dataset must have at least 3 key data criteria: open data index has set at least 3 key data characteristic for each dataset.

2) Datasets need to be updated but how often each dataset need to be updated varies: a timeframe was assigned for each dataset since they have different times in which they need to be updated. Thus, the question "is data updated?" can be easily answered.

3) There must be a list of unified datasets for evaluation: Table 2 below shows the full list of the selected datasets for evaluation.

TABLE II. LIST OF THE SELECTED DATASETS FOR EVALUATION

Dataset's name	Description
National Statistic	Major national statistic and economic indicators (population, GDP, employment rate, etc.) Criteria: <ul style="list-style-type: none">- GDP must be updated at least quarterly.- Population must be updated at least once a year.- Unemployment rate should be updated monthly.
Government Budget	This category includes budgets and planned government expenditure for the upcoming year (not the actual expenditure). Criteria: <ul style="list-style-type: none">- Planned budget should be divided by all government department as well as sub-department.- Descriptions about different budget sections must be included.- Must be updated once a year.
Government Spending	Record of past and actual government spending in a detailed and transactional level. Criteria: <ul style="list-style-type: none">- Access to individual transaction.- Date of transactions- Amount of transactions- Vender's name- Updated on a monthly basis.
Legislation	Record of all national laws and statutes. Criteria: <ul style="list-style-type: none">- Content of the statutes/ law.- All relevant amendments to law/statutes.- Date of the amendments.- Updated quarterly.
Election results	This category must cover all results by district/ constituency for all electoral contests. Criteria: <ul style="list-style-type: none">- Result for all electoral contests.- Number of valid votes.- Number of invalid votes- Number of spoiled ballots.- Report of all data must be at the level of the polling station.
National Map	A high level national map. Criteria: <ul style="list-style-type: none">- National roads markings.- National borders.- Marking of Streams, lakes, rivers and mountains- Updated on a yearly basis.

⁹ <http://opendefinition.org/>

¹⁰ <http://index.okfn.org/>

Pollutant Emissions	Record of data in regard to emission of air pollutants (especially those which are harmful to human health). Criteria: <ul style="list-style-type: none"> - Published data must be on a national level or at least for three major cities. - Updated once a week. - Particulate matter (PM) Levels. - Carbon monoxide (CO) - Nitrogen oxides (NOx) - Sulphur oxides (SOx) - Volatile organic compounds (VOCs)
Company Register	List of all registered companies. Criteria: <ul style="list-style-type: none"> - Company's Name. - Company's unique identifier. - Company's address. - Updated once a month.
Location Datasets.	Databases of zipcodes/postcodes and its corresponding spatial locations in a latitude/ longitude. If the country does not use a postcode/zipcode system, data of administrative borders must be provided. Criteria: <ul style="list-style-type: none"> - Zipcodes includes: <ul style="list-style-type: none"> o Address o Coordinate (latitude & Longitude) o National level o Updated once a year. - Administrative boundaries: <ul style="list-style-type: none"> o Poligone's Name (neighborhood) o Borders poligone. o National level o Updated once a year.
Tenders of Government Procurement (past and current).	Record of all tenders/ awards of the national government, which help in increasing government compliance. Criteria: <ul style="list-style-type: none"> - Tenders: <ul style="list-style-type: none"> o Name o Description o Status - Awards: <ul style="list-style-type: none"> o Title o Description o Value of the award o Suppliers name.
Water quality	Records on the quality of water for the prevention of disease and delivery of services. Criteria: <ul style="list-style-type: none"> o Total dissolved solids o Fecal coliform o Arsenic o Fluoride levels o Nitrates.
Weather forecast	Records of 5 days forecast of precipitation, temperature and wind as well as recorded data for the past year. Criteria: <ul style="list-style-type: none"> o Daily update of 5 days forecast for temperature. o Daily update of 5 days forecast for wind. o Daily update of 5 days forecast for precipitation. o Historical data about temperature for the past year.
Land ownership	Maps that shows the ownership of all lands with metadata on each land. Criteria: <ul style="list-style-type: none"> - Land Size - Land Borders - Owners Name - National Level. - Updated Yearly.

C. Measuring Each Datasets by using Open Data Index Scoring Model

Each dataset is evaluated by using open data index's scoring model. The model uses nine questions/indicators based on the open definition to examine the openness of each dataset. After reviewing each dataset, final percentages are calculated by adding the scores of all datasets as shown in Table 3 and divide them by 1300 (a maximum score which a country can get, assuming that all 13th datasets have scored 100). Later, numbers are rounded to the nearest whole number.

$$\text{Index percentage} = \frac{\text{Sum of (13 datasets)}}{13 \times 100} \quad (1)$$

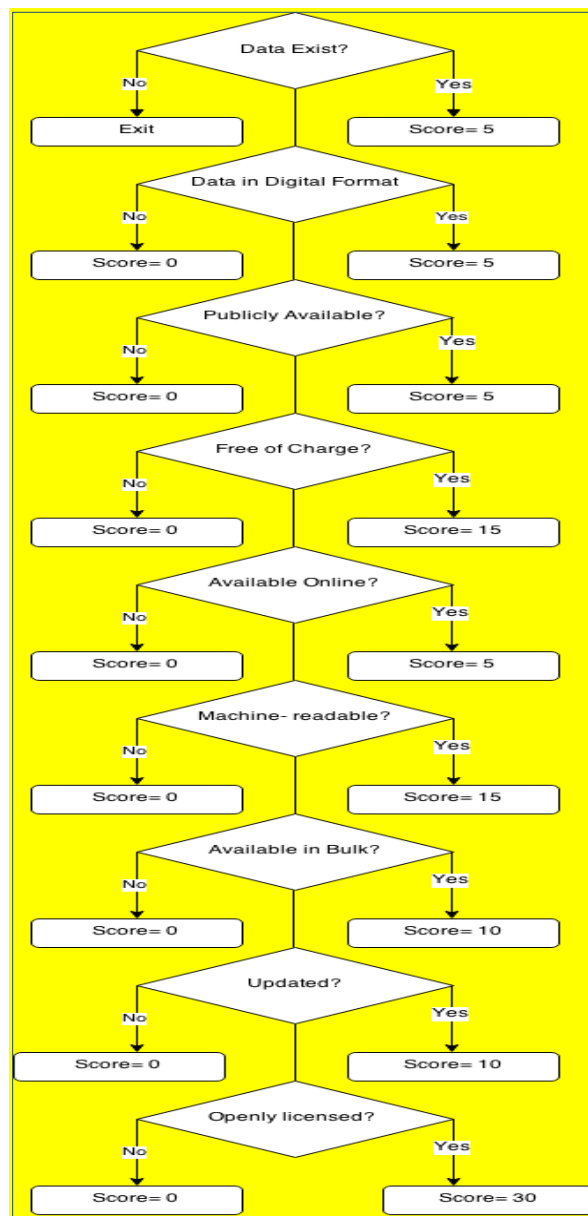


Fig. 1. Flow Chart of the Scoring Model

Fig. 1 and Table 3 describe the models' questions and their scoring weights:

TABLE III. LIST OF THE SELECTED DATASETS FOR EVALUATION

Question	Details	Weighting
Data Exist?	The question asks about data in general in any form (paper, digital, online or offline). If data doesn't exist, then all other questions in the model will not be answered.	5
Data in digital format?	The question addresses if data is in digital format (stored in a computer or in any digital format).	5
Publicly available?	The questions addressed if data is public (public data refer to data which can be accessed from outside of the government, this doesn't require data to be free). Example: data available for purchase.	5
Free of charge?	The question addresses if data is available without charges.	15
Available Online?	The question addresses if data is available online from an official source.	5
Machine-Readable?	Machine-Readable refer to data in a format which can be easily structured by a computer. The appropriate machine- readable format varies depending on data type. For example, machine- readable formats for tabular data may be different than geographic data.	15
Available in Bulk?	Data is available in bulk if the whole datasets (not partly) can be downloaded/ accessed easily.	10
Updated?	The question addresses if data is timely- updated or if it's long delayed.	10
Openly Licensed?	Data is openly licensed if the terms of use/ license are clearly mentioned to allow the use, reuse, and redistribute of data.	30

D. Benchmarking Model for Measuring Government Data Openness

Research regarding open government data assessment has led to a benchmark model for measuring government data openness in accordance with well-defined openness principles. The purpose of this section is to suggest and apply an enhanced model for measuring government data openness, which relies on global data index' scoring model. The model represents a new tactic to evaluate the openness of government data and is fully described in this section. A debate will also be provided about the reason behind the researcher's choice to develop an enhanced data openness assessment model rather than using the existing ones. To proof the model's capabilities, the model will be applied to measure the openness level of Saudi Open e-Government Data portal along with other five data portals with comparisons, analysis of results followed by conclusion.

Open government revolved around data openness and citizen engagement. According to [5], the open government is defined as "transparent, accessible and responsive governance system, where information moves freely both to and from the government, through a multitude of channels". It is obligatory

to define the term of Open Government Data as two elements: a) open data are "data that can be freely used, re-used and distributed by anyone only subject to (at the most) the requirement that users attribute the data and that they make their work available to be shared as well": b) Government data is "any data and information produced or commissioned by government". In the era of open government data, citizens become partners and take an active role where information and services are co-producing by both government and citizens. To further foster openness, on January 21, 2009, president Obama issued the Open Government Directive to which government institutions should take actions to implement the three cornerstones of Open Government data principles: Transparency, Participation, and Collaboration. Later, on May 2010, The Digital Agenda for Europe was launched to support the open government approach in fostering citizen participation and engagement. According to the digital agenda, government transformation should be triggered by web 2.0, ubiquitous mobile connectivity and social media to allow mass dissemination of data and promotes the collaboration between government and citizens. In the literature, models that have been developed to measure open government data openness were presented in details along with their perspectives and properties. Although it was concluded that the scoring model as shown in Fig. 3, is the most comprehensive model in term of measuring data openness level, there is still room for improvement. Lee and Kwak [6] argued that existing models are not 100% designed to fulfill the main principles of open government data (participation, collaboration, and transparency), which are empowered by emerging technologies such as social media, and ubiquitous mobile technology. According to Open Government Maturity Model as shown in Fig. 2, there are five levels of maturity in regard to Open Government Data 1. Initial conditions, 2. Data transparency, 3. Open Participation, 4. Open Collaboration, 5. Ubiquitous Engagement. Thus, higher maturity levels suggest increased public engagement and public value.

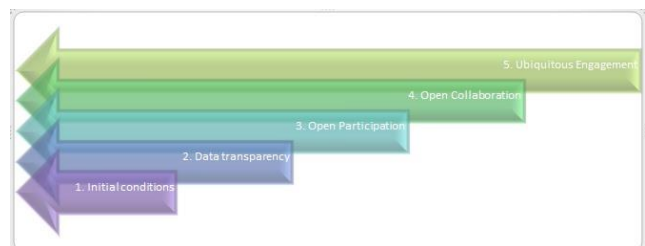


Fig. 2. Lee & Kwak Five Level of Maturity Model

Stage 1- Initial condition: this stage implies that government agencies are aggregating, gathering and publishing data in one- way communication where citizens can access in a wide range. However, the published data may be difficult to reuse (outdated, duplicated, and inaccurate).

Stage 2 – Data Transparency: at this stage, the government provides unified data, which are derived from different government sources. The focus at this stage is on the quality of data and consequently data here is complete, precise, and timely without contradictions and duplicates. Therefore, citizens have access to high – value government data that are

accessible and easily reusable which increases the transparency and public awareness of government work.

Stage 3- Open Participation: the focus at this stage is on the open participation; the government here is open to public knowledge and ideas. Thus, government data are enriched with none- government and informal data such as public’ feedback, comments, ideas, knowledge and experiences that are collected from expressive social media.

Stage 4- Open Collaboration: this stage implies that government is engaging citizens in complex government tasks and projects by providing relative solutions for increasing citizens’ value- added products and services.

Stage 5- Ubiquitous Engagement: at this stage, the benefits of open government data are totally realized and a high level of maturity is achieved. Public engagement becomes ubiquitous with mobile Government (M- Government). Furthermore, governments’ are promoting their data and services via mobile applications where citizens can easily access through their mobile devices.



Fig. 3. Scoring Model and Five Level of Maturity Model

It’s been evident after reviewing Open Government Maturity Model that Open Government Data has shifted the focus of government from traditional practices into citizens’ empowerment, information sharing, and collaboration. However, the new principles of government may not be fully attained unless governments’ progress is being measured accordingly. In specific, governments will not achieve a highest level of Open Government Maturity Model unless they are aware of being measured with relative parameters. For example, every year, governments around the world are waiting impatiently for the results of open data index report to know exactly where they are standing, and what improvements they can make on their government’s data portal. However, the scoring model used by open data index to measure each government’s data portal only satisfies the first two stages of Open Government Maturity Model. Thus,

government efforts to enhance their portals will be limited to the model’s parameters, which only satisfy the first two stages of Open Government Maturity Model (initial conditions and data transparency).

Initial conditions Stage: the first 5 questions of the scoring models only satisfy the first stage of Open Government Maturity Model where Government agencies are aggregating, gathering and publishing data for citizens to access in a one-way communication.

Data Transparency: the last three questions of the scoring models satisfy the second stage of Open Government Maturity Model where governments’ agencies are focusing on the quality of data (updated, Machine- readable, available in bulk).

E. Proposed Enhanced Model

Since the scoring model only satisfies the first two stages of Open Government Data maturity model, more questions/ indicators must be added to satisfy each stage until reaching an optimal level of maturity (stage 5). To do so, the researcher proposes enhancing the model as shown in Fig. 4 by adding three questions/indicators derived from each unsatisfied stage of Open Government Data.



Fig. 4. Proposed Enhanced Model

1) Do Governments' portals use Social Media tools? This question is proposed to satisfy stage Three of Open Government Data Maturity Level (Open Participation) since open participation is mainly concerned about social media.

2) Is API- Enabled in Governments' Data? This question is proposed to satisfy stage four of Open Government Data Maturity Level (Open Collaboration) where governments are providing relative solutions for increasing citizens' value-added products and services. In specific, an Application Programming Interface (API) increase the effective collaboration between government organizations and citizens by making data more usable which leads to more value- added apps, product, and services ("Apis Should Be The Default For Publishing Open Data - Socrata, Inc.").

Do Governments' portals have mobile applications? This question is proposed to satisfy stage five of Open Government Data Maturity Level (Ubiquitous Engagement) since this stage is mainly concerned about citizen accessibility to governments' data through mobile applications.

The enhanced/proposed scoring model perceives the openness of governments' data portals through the following indicators: Data Exist, Data in Digital Format, Publicly Available, Free of charge, Available Online, Openly Licensed, Machine- Readable, Available in Bulk, Updated, Use Social Media tools, API- Enabled and Have Mobile Applications. These indicators match both open government data principles and Open Government Data Maturity model.

F. Measurement of the Proposed Model's Indicators

Since a special weight/ score was assigned to each indicator in the original model by open data index to allow measuring the openness of governments' data portals. Enhancing the model by adding more indicators demanded the recalculation of each indicator plus assigning a score/weight to each new proposed indicator. The challenge here was to know the main methodology followed by Open Data Index to score each indicator in the original model. Unfortunately, secondary data was not helpful in this regard. To overcome this difficulty, email 'interview' was conducted with high-end team at Global Open Data Index (responsible for methodology and crowdsourcing data).

The obtained information from the interview has contributed building a methodology for scoring the new model. To do so, the researcher's conducted an online survey to seek the opinions of experts in 14 different open data institutions as shown in Table 4. The institutions were carefully selected because of their value- added projects and research in promoting open data. For this study, the researcher's sought to identify at least one open data expert in each institution by examining the institution's website looking for contact details. Some institutions were contacted directly to request the email of the relevant person. In the initial contact, the researcher ensured that the interlocutor indeed has a relevant experience/knowledge. Then, a general explanation of the survey's purpose was clarified followed by guidance on

how to fill the survey and a corresponding link. A total of 9 experts from 9 institutions responded to the survey (64.28%) from the list as shown in Table 4. The study was carried out by means of a questionnaire and the focus of the study was to get feedback on the proposed model and to assign a weight for each indicator.

TABLE IV. LIST OF SURVEYED INSTITUTIONS

Institution Name	Brief Description
1. Open Data Institute	Established by Sirs Tim Berners-Lee and Nigel Shadbolt. Open Data Institute is an independent, non-profit organization that nurture, train and collaborate with individuals around the world to promote the innovation through open data.
2. Open Data Working Group	Open Data Working group act as a central point of reference for individuals around the world who are interested in Open Government Data. The organization develop documents, principles and catalogues to make official information open in different countries
3. The Open Data Foundation	Non- profit organization dedicated to the development of open-source solutions to promote the use of statistical data in Open Government. The focus of the organization is to improve data and overall quality in support of research and policy making.
4. Open Data Nation	The Open Data Nation host events to spark the engagement and increase the visibility of open data to stakeholders Such as entrepreneurs, advocates, and investors. In particular, the organization helps stakeholders to make data-driven decisions, and operate more efficiently.
5. Global Open Data Initiative	The Global Open Data Initiative (GODI) is an enterprise led by civil society organizations for the purpose of sharing principles, resources for governments and societies on how to best employ the opportunities created by opening government data.
6. Open State Foundation	Open State Foundation is an organization based in Amsterdam, which promotes revealing/unlocking open government data and stimulates its re-use.
7. Engage Data	Engage data is a project funded by European Commission Program. The main goal of Engage is to empower the deployment of open governmental data towards citizens. By using Engage platform, researchers/ citizens can submit, search and visualize data from all the countries of the European Union.
8. Open Data Soft	Open Data Soft is an organization based on Paris-France, which provides a platform for easy publishing, reuse and sharing of all types of data. The main goal of the organization is to promote the transformation of data into innovative services and products.
9. Socrata	Socrata is a privately held software company headquartered in Seattle, Washington, D.C. and London. Socrata's team consists of open government advocates, software engineers and business professionals who are working together to unleash the power of data to transform the world.

10. Open Data Charter	Open data charter main goal is to sets open data principles. The organization was build by the efforts of open data champions from governments, civil society, multilateral organizations, and private sectors.
11. SPARC	SPARC is a global organization committed to make Open data the default for research and education. It empowers people to solve big problems and make new discoveries through the use of policies/ practices that advance Open Access and Open Data.
12. Sunlight Foundation	Sunlight Foundation is a non- profit organization that advocates for open government. The focus of Sunlight Foundation is to Make government and politics more open, accountable and transparent.
13. GovEx	GovEx refer to the center of government excellence at Johns Hopkins University. The center helps government to make decisions based on open data evidence and community engagement.
14. Factual	Factual is an organization founded by Gil Elbaz. The main goal of the organization is to gather raw data from millions different sources then clean, structure, package and distribute it in multiple ways to make the data ready- for- use.

As stated above, respondents were asked to score each indicator of the enhanced model based on its priority/importance and relevance in measuring data Openness level with the condition that the sum of all indicators must be one hundred. After calculating the total average of the responses, a weight was assigned to each indicator as shown in Fig. 5. Thus, the enhanced model became ready to be used as a measurement tool.

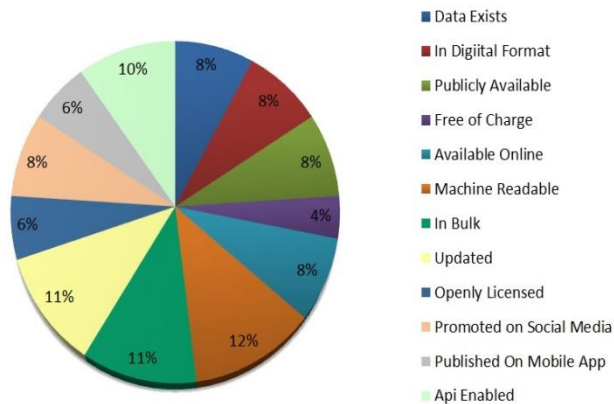


Fig. 5. Score of each indicator in the Enhanced Model

III. RESULTS

To proof the model’s capabilities, the model will be applied to measure the openness level of Saudi Open Government Data portal along with other five data portals with comparisons, analyses, and conclusion about the results.

For the results to be comparable, the datasets selected for evaluation for each data portals are the same datasets

selected/evaluated by Open Data Index. The goal here is to compare the results of using the original model versus the enhanced model.

The researcher has performed an evaluation of data openness for the following data portals: Saudi Arabia, Taiwan, United Kingdom, Denmark Colombia, and Finland. The researcher has chosen Saudi Arabia data portal because it’s the main focus of this research. Further, the other five data portals were chosen because of their top and sequence ranking among others. For example, Taiwan has achieved the highest ranking of data openness (87%) among 122 countries and areas in the 2015 Global Open Data Index followed by United Kingdom (76%), Denmark (70%), Colombia (68%) and Finland (67%). Since the chosen data portals have a sequence ranking, it was interesting to see how applying the enhanced model has affected their ranking.

The UK represents the oldest portals, launched in 2009 respectively¹¹, and the first initiator of “Open Data” movement along with United States. By contrast, Colombia is the youngest, officially published in 2013 [7]. Taiwan and Saudi Arabia in the middle¹², having been published in 2011, followed by Denmark and Finland 2012 [8]. It was interested to compare between these portals and see whether their attained maturity and age has any influence on their final score.

For each portal, the evaluation was accomplished by applying the enhanced model on a 13th dataset. The model uses eleventh questions/indicators where each question has a determined score as explained earlier in the previous chapter to examine the openness of each dataset. After reviewing each dataset, final percentages of each data portal are calculated by adding the scores of all datasets and divide them by 1300 (a maximum score which a country can get).

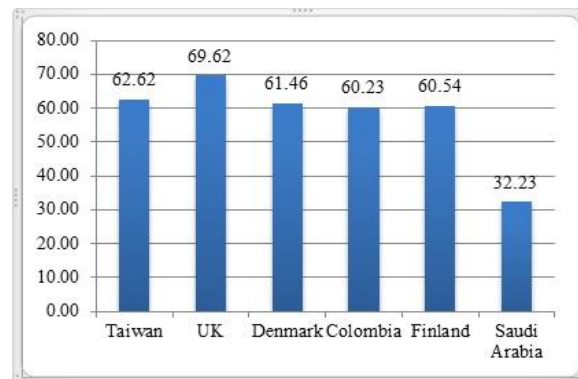


Fig. 6. Data openness percentage for analyzed portal

The Fig. 6 shows the result of applying the enhanced model on each data portals. As illustrated, the highest score was achieved by the UK data portals 69.62%, which indicated 69.62% openness, followed by Taiwan 62.62%, Denmark 61.46%, Finland 60.54%, Colombia 60.23 % and Saudi Arabia 32.23%. A closer look at the results provides insights

¹¹ <http://ckan.org/>

¹² <https://knowledgedialogues.com/>

about the successful, less successful and areas of improvement for each analyzed data portal.

Saudi Arabia's final score (32.23%) points to the necessity for further improvements. From Saudi Arabia's detailed information per datasets Fig. 7, it was found that four out of 13th mandatory datasets are empty. Other datasets are ranging from 8% openness to 75%. Therefore, to improve the final score, Saudi Arabia should focus on launching data to the missing datasets as well as improving the existing ones. As the chart indicates, the overall highest scoring dataset was achieved by location datasets (75%) whereas the worst graded datasets, if the researchers exclude those with a score of zero, were Pollutant Emissions (8%), and Land Ownership (8%). For example, by analyzing in details the results of the highest scoring dataset "location datasets", researchers can conclude that the critical indicators were Data in Bulk, Openly Licensed and open data promoted through social media. Achieving zero in those indicators indicates a complete lack of openly licensed and bulk data as well as a complete absence of this dataset in social media. Consequently, improving those indicators would inevitably lead to an improved overall score for the location dataset in Saudi Open Government Data Portal.

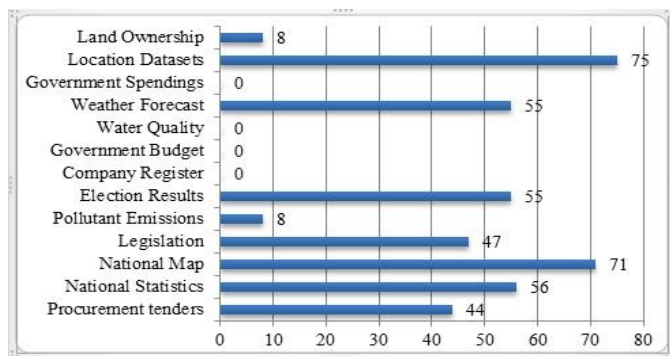


Fig. 7. Saudi Arabia score per dataset

Saudi Open Government data portal has achieved a score of 15% in the 2015 Global Open Data Index. However, when the portal was evaluated by using the enhanced model where three more measurement indicators were added (API enabled, Data promote through social media and Data promoted through mobile applications), a score of 32.23% was obtained. The gap between the results of the two assessments relies on two things.

First, Saudi Arabia has enabled API data and launched mobile applications for two of its datasets (National map, location datasets) as shown in Fig. 8. This has contributed slightly to increase its final score. Moreover, the score was further enhanced after finding that Saudi Arabia is using Social Media platforms (Twitter, Facebook, LinkedIn, YouTube) to promote the open data of five datasets (Procurement tenders, National Statistics, National Map, Election Results, and Weather Forecast).

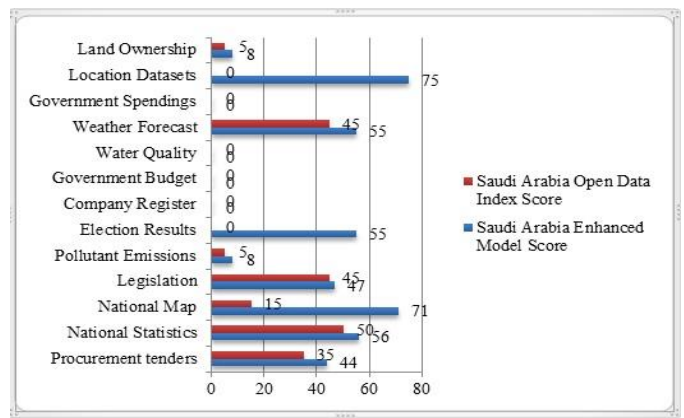


Fig. 8. Saudi Arabia: enhanced model results versus open data index results

Second, by double-checking the results of Open Data Index 2015 in regard to Saudi Arabia, the researcher has found that three out of six datasets, which were scored mistakenly zero by the organization actually exists. Those datasets are: Location datasets¹³, election results¹⁴ and National Map¹⁵. The existence of the three datasets had contributed rapidly to increase Saudi Arabia's final score. In this regard, the researcher had contacted Open Data Index to inform them about the existence of the three datasets and the necessity for modifying Saudi Arabia's final score. However, since the assigned time for reviewing the results of 2015 had been closed by the organization, Open Data Index replied with a confirmation that the researcher's feedback will be considered in 2016 report.

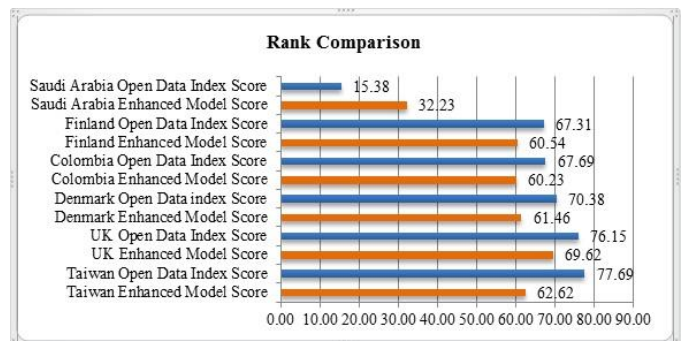


Fig. 9. Comparison of the analyzed data portals among countries by using open data index model versus the enhanced model

Fig. 9 above provides a comparison of the analyzed data portals among countries by using Open Data Index model versus the enhanced model. It is observed that after applying the enhanced model, the overall score and global ranking of data portals have been changed as shown in Table 5.

After applying the enhanced model, two phenomena were noticed. First, all data portals' scores have been decreased respectively except Saudi Arabia for the reasons explained earlier. Second, UK Data Portal has taken Taiwan place by achieving the highest ranking of data openness while Finland

¹³ <https://address.gov.sa/en/default.aspx>

¹⁴ <http://www.intekhab.gov.sa/>

¹⁵ <https://address.gov.sa/en/default.aspx>

has taken Colombia's place by achieving a global ranking of number 4. Since the enhanced model uses three additional indicators: API-enabled data, the use of social media and mobile applications in each dataset, The gap between the results of the two assessments rely basically on each data portal's efforts in achieving those additional indicators.

TABLE V. OVERALL SCORE AND GLOBAL RANKING OF DATA PORTALS

Data Portal	Year Launched	Score by Open Data Index.	Global Ranking	Score by Enhanced Model.	Global Ranking
Taiwan	2011	78%	1	62.62 %	2
United Kingdom	2009	76%	2	69.62 %	1
Denmark	2012	70%	3	61.46%	3
Colombia	2013	68%	4	60.23%	5
Finland	2012	67%	5	60.54%	4
Saudi Arabia	2011	15%	103	32.23 %	58

IV. CONCLUSION

Saudi Arabia is making major milestones in implementing Open Government Data in all levels. However, it is important to point out that the nation has long way to go for improvements. From the evidence collected throughout this research, the researcher can conclude:

- The lack of introduction of Open Government Data by Saudi Government affected the publics' knowledge about the benefits and advantages of utilizing such program. This indicates that the Saudi government is yet to persuade citizens to participate in the initiative.
- The fruits of Open Government data are still not harvested in Saudi Arabia where there are no much product/services created by using the data released by the government.
- The fact that citizens are using other online programs offered by Saudi e-government mean that citizens have the potential to participate in Open Government Data "if it's marketed right".
- The score given to Saudi Open Government Data Portal by Global Data Index was not correct. Saudi Arabia has achieved a global ranking score of 103 out of 122 among other countries in term of Open Government Data. By double- checking the results, the

researcher has found that three out of six datasets, which were scored mistakenly zero by the organization actually exists. Those datasets are: Location datasets, National Map and election results.

- Obtained result gained from the enhanced model applied in this research, shows that Saudi Arabia' final openness score (32.23%) points to the necessity for further improvements. The criteria/ indicators used by the model to evaluate the portal, provides an insight about the areas of improvements and the way it should be done.

Recommendation for future research

Open Government data in Saudi Arabia is a relatively new topic and there are many areas that need to be studied in depth. Although the researcher suggests going beyond the scope of the present research, there are some areas that relate to this research, which are working of future investigation. These include:

- Developing strategies to spread the awareness of Open Government Data among citizens in Saudi Arabia.
- Automating the model suggested throughout this research by converting it into a web- tool. Automating the assessment of data openness offer a significant advantage as the process can be performed at any time, quickly and without human intervention.

REFERENCES

- [1] O. David, "Benchmarking e-government in the web 2.0 era: what to measure and how," European Journal of e-Practice, pp. 33-43, August 2008.
- [2] B. Sanja, V. Natasa, and S. Leonid, "How open are public government data? an assessment of seven open data portals," Measuring E-Government Efficiency, vol. 5, pp. 25-44, February 2014.
- [3] M. Alshehri, and S. Drew, "Challenges of eGovernment service adoption in Saudi Arabia from e-ready citizen perspective," World Academy of Science, pp. 1053-1059, June 2010.
- [4] I. A. Elbadawi, "The state of open government data in GCC countries," In Proceedings of the 12 th European Conference on e-Government, Barcelona, 2012, pp. 193-200.
- [5] B. Ubaldi, "Open government data: Towards empirical analysis of open government data initiatives," OECD Publishing, France, May 2013.
- [6] G. Lee, and Y. H. Kwak, "Open government implementation model: a stage model for achieving increased public engagement", In Proceedings of the 12 th Annual International Digital Government Research Conference: Digital Government Innovation in Challenging Times, Maryland, USA, 12-15 June, 2011, pp. 254-261.
- [7] T. Obi, and N. Iwasaki, "A Decade of World E-Government Rankings," IOS Press, 2015.
- [8] I. Carlos, "A year of open data in the EMEA region", ePSIplatform Topic Report No. 2013/12, 2013.

Automatic Fall Detection using Smartphone Acceleration Sensor

Tran Tri Dang

Faculty of Computer Science and Engineering
Ho Chi Minh City University of Technology, VNU-HCM
Ho Chi Minh city, Vietnam

Hai Truong

Faculty of Computer Science and Engineering
Ho Chi Minh City University of Technology, VNU-HCM
Ho Chi Minh city, Vietnam

Tran Khanh Dang

Faculty of Computer Science and Engineering
Ho Chi Minh City University of Technology, VNU-HCM
Ho Chi Minh city, Vietnam

Abstract—In this paper, we describe our work on developing an automatic fall detection technique using smart phone. Fall is detected based on analyzing acceleration patterns generated during various activities. An additional long lie detection algorithm is used to improve fall detection rate while keeping false positive rate at an acceptable value. An application prototype is implemented on Android operating system and is used to evaluate the proposed technique performance. Experiment results show the potential of using this app for fall detection. However, more realistic experiment setting is needed to make this technique suitable for use in real life situations.

Keywords—fall detection; long lie detection; acceleration sensor; smartphone; personal healthcare

I. INTRODUCTION

The proportion of old people in the world population is increasing. According to a report prepared by the Population Division of the United Nations, this number is projected to reach 21 percent in 2050, although it was only 10 percent in 2000 [1]. Translating these ratios into absolute values, there are approximately 600 million elderly people at the start of the twenty-first century, and 50 years later the number of people whose ages are 60 or more will be around 2 billion. The high number of older people brings challenges for the healthcare system, especially at developing countries, where public healthcare service is of limited and expensive.

One of the most popular problems elderly people face is falling. According to the Centers for Disease Control and Prevention, one out of three older people falls each year [2]. The consequences of falls are serious and include: broken bones, head injury [3][4], traumatic brain injuries [5]. If prevention solutions are not invested in the immediate future, the number of injuries caused by falls will be double in 2030 due to the increasing portion of old people [6].

The definition of fall is very common, however, it is difficult to precisely describe a fallen behavior, and thus, to specify the means of detection. In 1987, Gibson [7] defines a fall as "unintentionally coming to ground, or some lower level not as a consequence of sustaining a violent blow, loss of consciousness, sudden onset of paralysis as in stroke or an epileptic seizure", or in an informal explanation, a fall could be fast changes of upstanding/sitting posture to the lolling position without being controlled or without intentional behavior such as lying down. The Gibson's definition is widely applied in

many research aspects because it is broad enough to even cover specific falls caused by syncope or dizziness which could be a consequence of an epileptic fit or cardiovascular collapses. A fall detection system must be able to classify, or distinguish between a fall event with normal behavior to decrease the false positive alarm bothering the elderly people. Concurrently, this system possesses the ability of covering all fall for safety requirement. As a result, how to design a detection system which can balance these two requirements is a challenging mission.

A fall detection system is first designed not to reduce the occurrence of fallen but aims to alert when a fall event happens. However, fall detectors have been demonstrated to direct impact on the reduction of fall fear. In fact, falls and fear of falling is not independent. An individual who is frequently falls appears to be fear of falling and this fear afterwards may increase the risk of suffering from a fall [8]. Fear of fall majorly negative impacts on the life quality of elderly which can cause depression, activities limitation, social interaction decreasing, falling, lower life quality. The relationship between automatic fall detection system and fall fear has been proved by Brownsel [9] et al. They conducted a study on elderly who experienced at least one fall in the previous six months. At the end of the experiment, people who wore the fall detector feel more confident and diminish the fear of fallen, as well as consider the detector had improved their safety.

The other important objective of a fall detector is to limit the time the elderly remains on the floor after falling. The period of laying on the floor after falling determines the severity of a fall because long lie may lead to hypothermia, dehydration and pressure sores [10,11]. This is extremely critical in case the person lives alone without any assistances from their families and neighbors. Lord et al. [12] indicates that about 20% of fallen patients admitted in the hospital after laying on the ground for more than one hour. Although there is no direct injury at the fallen time, the morbidity rates are very high compared with the patients who entered the hospital in less than 30 minutes. The ultimate goal of the detector system is to realize a fall event and manage to notify an assistant immediately. A robust fall detector should be able to classify the falls as falls and the non-falls as non-falls in real life condition because people sometimes intentionally up stand or sit rapidly, which could confuse the system. Certainly, if an elderly falls and the system is unable to detect, the outcome

could be dramatic. In addition, people is losing confidence in the detector system, which leads to increase the fear of falling and fallen probability consequently. On the other hand, an overestimated detector system may alert excessive number of false activations, thus, caregivers may assume it as ineffective or useless. Balancing these two objectives is a challenging objective and although several commercial products are available on the market, they are not truly impact on the elders' lives yet [13,14].

II. RELATED WORKS

Based on whether the system is attaching on the customer's body or not, the detector could be classified as context-aware systems and wearable devices.

The context-aware systems deploy sensors in the environment to recognize a fall event. One of the drawback of this approach is that fallen could be only alerted limited in places attached with sensors. By contrast, person does not need to wear any special devices which emit many electromagnetic radiations. The most common sensors are cameras, microphones, floor sensors, infrared sensors and pressure sensors. Based on the specific sensor type, detection techniques vary a lot. Most of them utilize the common approach of extracting the personal features and comparing with the model to determine a fallen event. Features which could be collected are the ratio of weight and height [15], changes in light and illumination [16], direction of main axis of the body [17], skin color to detect the body region [18]. These features are then analyzed to distinguish between normal behaviors and fall events by different techniques. For example, Hazelhoff [19] et al. first performs the object segmentation based on the background subtraction and then tracks the object by its motion and head region. Finally, a multi-frame Gaussian classifier is utilized to determine a fall event. Liu et al. [20] use the frame differencing approach to identify the human body. Then, image processing techniques are applied to smooth the input. The authors use k-nearest neighbor classifier to categorize the body posture and a fall is decided based on the time difference of event transitions. Several other approaches are also employed such as Rule-based techniques [21], Bayesian filtering [22], Hidden Markov Models [23], Threshold techniques [24] and Fuzzy Logic [25]. Among these decision and extraction techniques, none of them shows outstanding performance to the others and no appropriate comparison has been done yet. As a result, there is no standardized context-aware technique which is widely accepted by the research community.

Wearable device is defined as electronic sensors which must be worn by the user under, with or on top of clothing. About 90% of these systems are in the form of accelerometer devices. Some of them also integrate with gyroscopes to extract information about the position of the patient. This trend is rapidly developing due to the cheap embedded sensors. The wearable devices could further be divided into two groups which are accelerometers attached to the body and smartphone built-in accelerometer.

For the accelerometer attached to the body, data is continuously collected during normal activities and falls using independent tri-axial accelerometers attached to different parts of the body. Doukas et al. [26] applied the sensor to the

patient's foot in order to transmit patient movement data wirelessly to the monitoring center. The center generalizes data in the three axis and uses machine learning method to classify an event a fall or not. The experiment of this research achieved high sensitivity (SE) and specificity (SP) at SE equals 98.2% and SP equals 96.7%. The system is also enhanced by transmitting video images for remote decision for any suspected, indecisive falls. However, the authors just perform the experiment on 1 subject, thus, the result is not truly supportive. In another research, Cheng et al. [27] tried to monitor daily activity and fall detection by using sensors attached in the chest and thigh. For the decision, the authors used a decision tree which was constructed on the body posture angels to recognize posture transition and the impact magnitude is thresholded to detect falls. The system is able to detect four different fallen types: from standing to face-up lying, face-down lying, left-side lying and right-side lying. The experiments are performed on 6 males and 4 females from age 22-26 and achieve SE equals 95.33% and SP equals 97.66%. Most of the existing researches apply thresholding techniques for automatic fall detection. However, since 2010, machine learning approach has increasingly influenced in this area. These methods include Support Vector Machine, Gaussian Distribution of Cluster Knowledge [28] and Decision tree. Among them, multilayer perceptron seems to prevail although standardized technique still has not widely accepted [29]. In term of sensor placement, waist seems to be optimal because it is close to the center of body gravity, supporting reliable information on patient body movements.

Another direction of the wearable devices is smartphone built-in accelerometer. The advantage of this approach is today's smartphones embeds multiple sensors such as camera, microphone, GPS, accelerometer, digital compass and gyroscope. Sposaro et al. [30] proposed an alert system using smartphone which is assume to hold at the thigh (pocket). This system uses thresholding to consider the impact, the difference in position before and after the fall. This approach is also applied in other studies [31,32]. Similar to the attached accelerometer mentioned in previous part, machine learning methods such as support vector machines, Sparse Multinomial Logistic Regression are used to classify a fallen event on the mobilephone. Regarding the position and direction of the phone, waist is still the preferred part of the body. Some of these studies published their result into application which are available for downloading in Google Play. However, when searching with the keyword "fall detector" or "fall detection", 10 results are returned. The number of download is quite low and an average of about 10 people give comments about their opinion which can infer that these application does not attract people much. Therefore, studies in this approach of using smartphone should be invested more because it is anticipated to be an emerging field in the near future.

III. OUR FALL DETECTION APPROACH

In this work, our main objective is to determine whether a person is doing her daily activities (e.g. walking, sitting, standing, etc.) or just falls to the ground. We observe that the body of the target person moves significantly differently between these 2 situations. As a result, if we attach a smart phone to a fixed position of the person body, and make that

smart phone record the body movements, recorded data could be analyzed to spot the differences between 2 situations. By recognizing the movement differences, we can deduce when a fall happens.

When a body is moving, many types of data are generated. Among them, acceleration is considered as one of the most suitable data type for the purpose of fall detection. The reason behind this consideration is that a body acceleration maintains a strong relationship with the force exerting on that body, according to physical laws, and when there is a fall, the exerting force will be changed accordingly. This transitive relationship between a body fall and its acceleration explains for the reason to apply acceleration data for fall detection. Furthermore, accelerometer is a popular sensor type. It is equipped on most smart phones nowadays. Therefore, using acceleration as the data source to detect fall can make our solution reach a large number of users.

To propose an appropriate algorithm for fall detection, at first, the patterns of acceleration data generated in a fall as well as in other normal activities must be discovered. This helps us in designing an effective classification algorithm and in determining the classification parameters for example the number of parameters and relationships among them. To achieve this objective, data acquisition and analysis phase are executed, which will be described in detailed later. Data is acquired by volunteers who perform intentional activities. Then, acquired data values are visualized to learn the attributes and patterns.

A. Data acquisition

To acquire acceleration data, a simple Android app is created to read the values provided by a smart phone's accelerometer. A person is invited to use this smart phone to generate data. Because at this stage, we only want to understand the generic different patterns generated during various activities, so one individual is enough to collect the desired data. The smart phone is assumed to be kept at a fixed position on the individual's body. In this research, the individual's front pant pocket is chosen as the position of the smart phone because people frequently keep their phones at that place. In addition, putting a smart phone in pant pocket helps them to keep the phone longer without tiredness.

We ask a volunteer to do the following actions: sitting on a chair, walking, standing up, sitting down, and falling onto a soft mattress, all with a monitoring smart phone in his front pant pocket. The generated acceleration data is processed as follow:

- When there is a change in acceleration value, Android raises an event and also supplies current value in 3 coordinate axes (A_x , A_y , A_z).
- The amplitude of the current acceleration is calculated as:

$$A = \sqrt{A_x^2 + A_y^2 + A_z^2}$$

B. Data analysis

For each activity, the acceleration amplitudes are stored as time series. Microsoft Excel is utilized to plot these series to see the pattern of various activities. Figure 2. shows the results of the plotting.

Based on the illustration images of acceleration data in various cases, some important features are indicated:

- In sitting state, acceleration value is quite stable. It is easy to understand because the experiment smart phone is almost static in sitting state.
- In walking state, acceleration value falls down, rises up, then repeats this cycle again. The difference between minimum and maximum value in a cycle is about $2m/s^2$.
- The acceleration value rises up then falls down in standing up state, and it goes in opposite direction (i.e. falls down then rises up) in sitting down stage. In both states, the difference between the maximum and minimum value is less than $3m/s^2$.

The pattern generated in falling state is somewhat similar to the pattern generated in sitting down state. But the difference between minimum and maximum value is much higher in the former state, around $8m/s^2$ compared to less than $2m/s^2$.

IV. PROPOSED ALGORITHM

A. Algorithm description

Based on the above observation, an algorithm for fall detection based on thresholds is developed. Specifically, the following terms is used in the algorithm:

- Detection period: the duration in which acceleration values are extracted and analyzed to determine a fall event. Based on the previous step, detection period is about 1 to 2 seconds.
- Low threshold acceleration: this is the acceleration value that is lower than the acceleration values generated by most activities. In other words, only a fall event can generate acceleration values which are lower than this threshold.
- High threshold acceleration: this value has an opposite meaning with the low threshold acceleration value defined above. It is the acceleration value that is higher than the acceleration values generated by most activities, except the acceleration value generated in a fall.

In a detection period, a fall event is alerted if the following conditions are met:

- There is at least one acceleration value v_1 which is lower than the low threshold acceleration.
- There is at least one acceleration value v_2 which is higher than the high threshold acceleration.

- The time point t_1 when v_1 happens must be preceded the time point t_2 when v_2 happens.

The pseudocode for the above fall detection algorithm is given below:

```
/* Fall detection based on thresholds */
/* Assume lowThreshold and highThreshold
are decided already */
/* Input: an array of acceleration values
extracted in detection period */
/* Output: fall (true) or not (false) */

bool fallDetection(float[] a) {
    n = a.length;
    for (i = 0; i < n; i++) {
        if (a[i] < lowThreshold) {
            for (j = i + 1; j < n; j++) {
                if (a[j] > highThreshold)
                    return true;
            }
        }
    }
    return false;
}
```

B. Algorithm refinement

In the above algorithm, the actual values of low threshold acceleration and high threshold acceleration are the main factors affecting the performance of our proposed fall detection technique. Specifically, the performance of the fall detection technique is evaluated by the 2 following criteria:

- True positive rate: the number of detected falls over the total number of falls. A good system must possess high true positive rate.
- False positive rate: the number of wrongly detected falls over the total number of normal events. We want this number as low as possible.

According to our experiments, achieving a good balancing of the trade-off between true positive rate and false positive rate is challenging. In the fall detection algorithm, if the range between low and high threshold acceleration is set to be broad enough, the false positive rate may achieve at zero percent. However, at that point, the true positive rate is concurrently very low. On the other hand, if the range between low and high threshold is so tight, the true positive rate may reach a perfect score at 100%, but the false positive rate may be too high. This situation is quite dangerous because an individual could have fallen without being detected by the system.

To improve concurrently both true positive rate and false positive rate, an additional checking layer is added after a fall is detected. This check verifies if a person can return to normal activities after a fall is detected. In case the individual does not perform any actions after the suspected fall in about 3 seconds, there is a high possibility that a real fall event has just occurred and caused “long lie” [33]. In the long lie state, the generated acceleration values are stable due to inactivity of the fallen

person. As a result, we define several new terms to apply in the long lie detection algorithm:

- long lie period: the duration in which no activities are detected after of a suspected fallen event.
- low long lie threshold acceleration: the acceleration value that is lower than all acceleration values generated during long lie period.
- high long lie threshold acceleration: the acceleration value that is higher than all acceleration values generated during long lie period.

With these terms, the pseudocode for proposed long lie detection algorithm is given below:

```
/* Long lie detection after a detected
fall */
/* Assume lowLongLieThres and
highLongLieThres are already determined
*/
/* Input: an array of acceleration values
extracted in long lie period */
/* Output: long lie (true) or not (false)
*/

bool longlieDetection(float[] a) {
    float min = Math.min(a);
    float max = Math.max(a);
    if (min >= lowLongLieThres && max
        <= highLongLieThres) {
        return true;
    }
    return false;
}
```

V. EXPERIMENTS

A. Application prototype

To evaluate the performance of the proposed fall detection technique, we develop a working prototype on Android platform and perform the experiment with volunteers. Android is chosen solely because of its popularity. In fact, the detection algorithm is independent of the underlying operating system, therefore could be deployed in any OS.

The components of the prototype are illustrated in Figure 1.

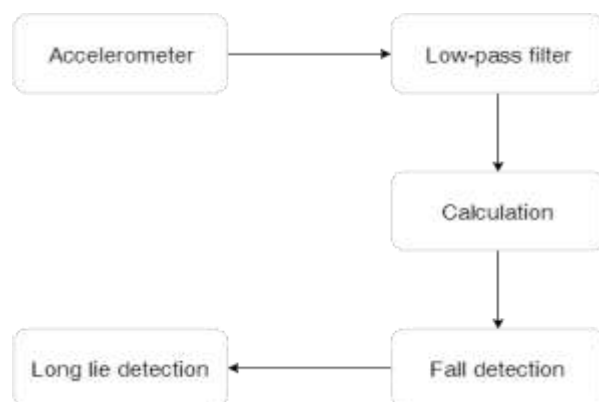


Fig. 1. Components of the working prototype

As illustrated in Figure 2., the working prototype contains 5 main components. At first, acceleration values are retrieved from mobile accelerometer; these acceleration values then go through a low-pass filter to remove noises. After that, the smoothed output data is utilized to calculate acceleration amplitudes; Finally, fall detection and long lie detection algorithms will determine if a fall event occurs or not based on the calculated amplitudes.

B. Experiment setting

Five volunteers participate in the experiment to evaluate the performance of the proposed fall detection technique. The group consists 3 men and 2 women from 25 to 35, weights from 50 kg to 70 kg, and heights from 155 cm to 170 cm. Although the target users of fall detection system are elderly, it is difficult to invite them into the experiments because of safety requirements. Therefore, our experiment is evaluated on 5 young and healthy individuals.

Each volunteer is requested to put an Android-powered ASUS Zenfone 2 into his/her front pant pocket. This device contains a 5.5-inches screen, an Intel Atom CPU (quad core 2.3GHz) and 4GB RAM memory. The device's weight is 170g and has built-in Android 5.0. Our application prototype has been installed into the devices before the experiments.

The volunteers are required to perform these following activities twice:

- Stand up from the sitting posture,
- Sit down from the standing posture,
- Walk normally in 5 seconds,
- Fall down onto a soft mattress,
- Lie down in 5 seconds.

The purpose of the first 4 activities is to achieve data to decide the detection period, low detection threshold acceleration, and high detection threshold acceleration. The purpose of the last activity is to determine the long lie period, low long lie threshold acceleration and high long lie acceleration. In the first 4 activities, the volunteers are requested to fall hard enough to be able to classify of other normal activities. In other words, for any individual, if the acceleration generated in a fall cannot be differentiated from the acceleration generated in other activities, we discard all the related data and ask that person to perform these 4 activities again.

C. Experiment result and discussion

Beside the fall detection algorithm, long lie detection approach is an enhancement algorithm to confirm the suspicious fall event. For that reason, we can tolerate a little bit high false positive rate to compensate for a higher true positive rate. Therefore, for each volunteer, the higher value between 2 low detection threshold accelerations attained in 2 falls is chosen. The lower value between 2 high detection threshold acceleration values attained in 2 falls is chosen also. Similarly, the detection period for each individual is chosen as the longer one between the 2 periods attained in experiments.

The long lie period is set to 3 seconds. The low long lie threshold acceleration and high long lie threshold acceleration for each person are set to the minimum and maximum acceleration values attained during 10 seconds (we combine 2 lying down experiments together) lying down respectively.

Table 1 displays the fall and long lie detection algorithms' parameters after the experiments:

TABLE I. FALL AND LONG LIE DETECTION PARAMETERS

ID	Low detection threshold acceleration (m/s ²)	High detection threshold acceleration (m/s ²)	Detection period (s)	Low long lie threshold acceleration (m/s ²)	High long lie threshold acceleration (m/s ²)
1	8.4	17.3	1.6	9.6	9.9
2	8.0	16.5	2.2	9.7	9.9
3	8.3	16.8	2.0	9.7	10.0
4	7.5	15.6	1.8	9.7	10.1
5	8.2	16.2	1.6	9.6	10.0

After collecting all the fall detection and long lie detection parameters, the 2 proposed detection algorithms are modified to utilize these parameters for decision making. Then, each volunteer is asked to use the application for an extended period of time, i.e. about 2 minutes. During that time, each volunteer is requested to either walking, running, or falling. Each person needs to fall at least 5 times, and stays lying down for at least 5 seconds after each fall. The result of these experiments is given in Table 2.

TABLE II. RESULT WHEN USING THE APP FOR AN EXTENDED PERIOD

Person	Number of falls	Number of detected falls	Number of false positives without long lie check	Number of false positives with long lie check
1	5	5	5	1
2	5	4	3	0
3	6	6	0	0
4	5	5	0	0
5	6	4	3	0

The data in Table 2 shows that our proposed technique achieves the true detection rate of 93%. Without long lie check, total of 11 false alarms occurs, whereas this measurement reduces to 1 if the long lie check is integrated. In our experiments, all false positives are created during quick running and they come together, not as separated ones. When long lie detection is added, most of the fall positive cases are eliminated. That exceptional case is caused by one person' standing still after running due to his tiredness.

VI. CONCLUSIONS AND FUTURE WORKS

In this paper, we have proposed a technique for automatic fall detection using smartphones. The approach utilizes the phone accelerometer's captured data to make decision. The proposed technique consists of 2 algorithms: fall detection and long lie detection. The former is used to check the occurrence of a fall, while the latter is used to find out if there is a lying down state after that fall. By combining these 2 algorithms, we can partly solve the trade-off issue between achieving a high true positive rate and keeping a low false positive rate.

The proposed technique is then implemented as an Android application for experiment. Due to safety constraints, only young and healthy people are invited to participate. They are asked to perform intentional falls as well as other normal activities. The data generated during these actions are used to get detection parameters. These parameters are then applied in detection algorithms to evaluate the application performance for an extended period. Experiment results show the potential of using this application for fall detection when achieving a true positive rate of 93% and only generates 1 false positive during 10 minutes experiment of 5 volunteer people.

There are still some drawbacks that cannot be completely solved by the algorithm. The first one is not able to organize a realistic environment for experiments. Because falls may cause serious injuries, the experiment's volunteers just consist of young and healthy individuals, who are particularly not the main target of the fall detection technique. This may make the parameters learnt in experiments not match with the practical conditions. Furthermore, volunteers only fall onto a soft surface during evaluation which makes the result may be very different when comparing with real falls onto hard surfaces.

Another problem is the limitation in the extensive experiments with large number of volunteers. Due to time and cost constraints, we do not have many people to join our experiments which may cause the achieved results not representative enough. In addition, the activities performed are insufficient which do not produce all possible acceleration patterns in reality. For example, we do not examine strong activities such as jumping, which may create similar acceleration patterns falling. By experimenting more with such activities, we can fine-tune the proposed algorithms and make our application more suitable in real-world utilization.

ACKNOWLEDGMENT

This research is funded by Vietnam National University HoChiMinh City (VNU-HCM) under grant number C2015-20-06

REFERENCES

- [1] Department of Economic and Social Affairs United Nations, 2002. *World population ageing: 1950-2050*. UN.
- [2] Centers for Disease Control and Prevention. Important Facts about Falls. Available at <http://www.cdc.gov/homeandrecreationsafety/falls/adultfalls.html> (accessed 3/2016)
- [3] Alexander, B.H., Rivara, F.P. and Wolf, M.E., 1992. The cost and frequency of hospitalization for fall-related injuries in older adults. *American journal of public health*, 82(7), pp.1020-1023.
- [4] Sterling, D.A., O'Connor, J.A. and Bonadies, J., 2001. Geriatric falls: injury severity is high and disproportionate to mechanism. *Journal of Trauma and Acute Care Surgery*, 50(1), pp.116-119.
- [5] Stevens, J.A., Corso, P.S., Finkelstein, E.A. and Miller, T.R., 2006. The costs of fatal and non-fatal falls among older adults. *Injury prevention*, 12(5), pp.290-295.
- [6] Igual, R., Medrano, C. and Plaza, I., 2013. Challenges, issues and trends in fall detection systems. *Biomedical engineering online*, 12(1), p.1.
- [7] Gibson, M.J., Andres, R.O., Isaacs, B., Radebaugh, T. and Wormpetersen, J., 1987. The Prevention of Falls in Later Life-A Report of the Kellogg-International-Work-Group on the Prevention of Falls by the Elderly. *Danish Medical Bulletin*, 34, pp.1-24.
- [8] Friedman, S.M., Munoz, B., West, S.K., BandeenRoche, K. and Fried, L.P., 1997, September. Falls and fear of falling: Which comes first?. In

JOURNAL OF THE AMERICAN GERIATRICS SOCIETY (Vol. 45, No. 9, pp. P186-P186). 351 WEST CAMDEN ST, BALTIMORE, MD 21201-2436: WILLIAMS & WILKINS.

- [9] Brownsell, S. and Hawley, M.S., 2004. Automatic fall detectors and the fear of falling. *Journal of telemedicine and telecare*, 10(5), pp.262-266.
- [10] Rubenstein, L.Z. and Josephson, K.R., 2002. The epidemiology of falls and syncope. *Clinics in geriatric medicine*, 18(2), pp.141-158.
- [11] Tinetti, M.E., Liu, W.L. and Claus, E.B., 1993. Predictors and prognosis of inability to get up after falls among elderly persons. *Jama*, 269(1), pp.65-70.
- [12] Lord, S.R., Sherrington, C., Menz, H.B. and Close, J.C., 2007. *Falls in older people: risk factors and strategies for prevention*. Cambridge University Press.
- [13] Noury, N., Fleury, A., Rumeau, P., Bourke, A.K., Laighin, G.O., Rialle, V. and Lundy, J.E., 2007, August. Fall detection-principles and methods. In *2007 29th Annual International Conference of the IEEE Engineering in Medicine and Biology Society* (pp. 1663-1666). IEEE.
- [14] Bagalà, F., Becker, C., Cappello, A., Chiari, L., Aminian, K., Hausdorff, J.M., Zijlstra, W. and Klenk, J., 2012. Evaluation of accelerometer-based fall detection algorithms on real-world falls. *PLoS one*, 7(5), p.e37062.
- [15] Miaou, S.G., Sung, P.H. and Huang, C.Y., 2006, April. A customized human fall detection system using omni-camera images and personal information. In *1st Transdisciplinary Conference on Distributed Diagnosis and Home Healthcare, 2006. D2H2*. (pp. 39-42). IEEE.
- [16] Fu, Z., Delbruck, T., Lichtsteiner, P. and Culurciello, E., 2008. An address-event fall detector for assisted living applications. *IEEE transactions on biomedical circuits and systems*, 2(2), pp.88-96.
- [17] Hazelhoff, L. and Han, J., 2008, October. Video-based fall detection in the home using principal component analysis. In *International Conference on Advanced Concepts for Intelligent Vision Systems* (pp. 298-309). Springer Berlin Heidelberg.
- [18] Cucchiara, R., Prati, A. and Vezzani, R., 2007. A multi-camera vision system for fall detection and alarm generation. *Expert Systems*, 24(5), pp.334-345.
- [19] Hazelhoff, L. and Han, J., 2008, October. Video-based fall detection in the home using principal component analysis. In *International Conference on Advanced Concepts for Intelligent Vision Systems* (pp. 298-309). Springer Berlin Heidelberg.
- [20] Liu, C.L., Lee, C.H. and Lin, P.M., 2010. A fall detection system using k-nearest neighbor classifier. *Expert systems with applications*, 37(10), pp.7174-7181.
- [21] Vishwakarma, V., Mandal, C. and Sural, S., 2007, December. Automatic detection of human fall in video. In *International conference on pattern recognition and machine intelligence* (pp. 616-623). Springer Berlin Heidelberg.
- [22] Rimminen, H., Lindström, J., Linnavuo, M. and Sepponen, R., 2010. Detection of falls among the elderly by a floor sensor using the electric near field. *IEEE transactions on information technology in biomedicine: a publication of the IEEE Engineering in Medicine and Biology Society*, 14(6), pp.1475-1476.
- [23] Cucchiara, R., Prati, A. and Vezzani, R., 2007. A multi-camera vision system for fall detection and alarm generation. *Expert Systems*, 24(5), pp.334-345.
- [24] Miaou, S.G., Sung, P.H. and Huang, C.Y., 2006, April. A customized human fall detection system using omni-camera images and personal information. In *1st Transdisciplinary Conference on Distributed Diagnosis and Home Healthcare, 2006. D2H2*. (pp. 39-42). IEEE.
- [25] Anderson, D., Luke, R.H., Keller, J.M., Skubic, M., Rantz, M. and Aud, M., 2009. Linguistic summarization of video for fall detection using voxel person and fuzzy logic. *Computer vision and image understanding*, 113(1), pp.80-89.
- [26] Doukas, C., Maglogiannis, I., Tragas, P., Liapis, D. and Yovanof, G., 2007, September. Patient fall detection using support vector machines. In *IFIP International Conference on Artificial Intelligence Applications and Innovations* (pp. 147-156). Springer US.
- [27] Cheng, J., Chen, X. and Shen, M., 2013. A framework for daily activity monitoring and fall detection based on surface electromyography and

accelerometer signals. *IEEE journal of biomedical and health informatics*, 17(1), pp.38-45.

[28] Yuwono, M., Moulton, B.D., Su, S.W., Celler, B.G. and Nguyen, H.T., 2012. Unsupervised machine-learning method for improving the performance of ambulatory fall-detection systems. *Biomedical engineering online*, 11(1), p.1.

[29] Kerdegari, H., Samsudin, K., Ramli, A.R. and Mokaram, S., 2012, June. Evaluation of fall detection classification approaches. In *Intelligent and Advanced Systems (ICIAS), 2012 4th International Conference on* (Vol. 1, pp. 131-136). IEEE.

[30] Sposaro, F. and Tyson, G., 2009, September. iFall: an Android application for fall monitoring and response. In *2009 Annual International Conference of the IEEE Engineering in Medicine and Biology Society* (pp. 6119-6122). IEEE.

[31] Lee, R.Y. and Carlisle, A.J., 2011. Detection of falls using accelerometers and mobile phone technology. *Age and ageing*, p.afr050.

[32] Fang, S.H., Liang, Y.C. and Chiu, K.M., 2012, January. Developing a mobile phone-based fall detection system on android platform. In *Computing, Communications and Applications Conference (ComComAp), 2012* (pp. 143-146). IEEE.

[33] Nevitt, M.C., Cummings, S.R. and Hudes, E.S., 1991. Risk factors for injurious falls: a prospective study. *Journal of gerontology*, 46(5), pp.M164-M170.

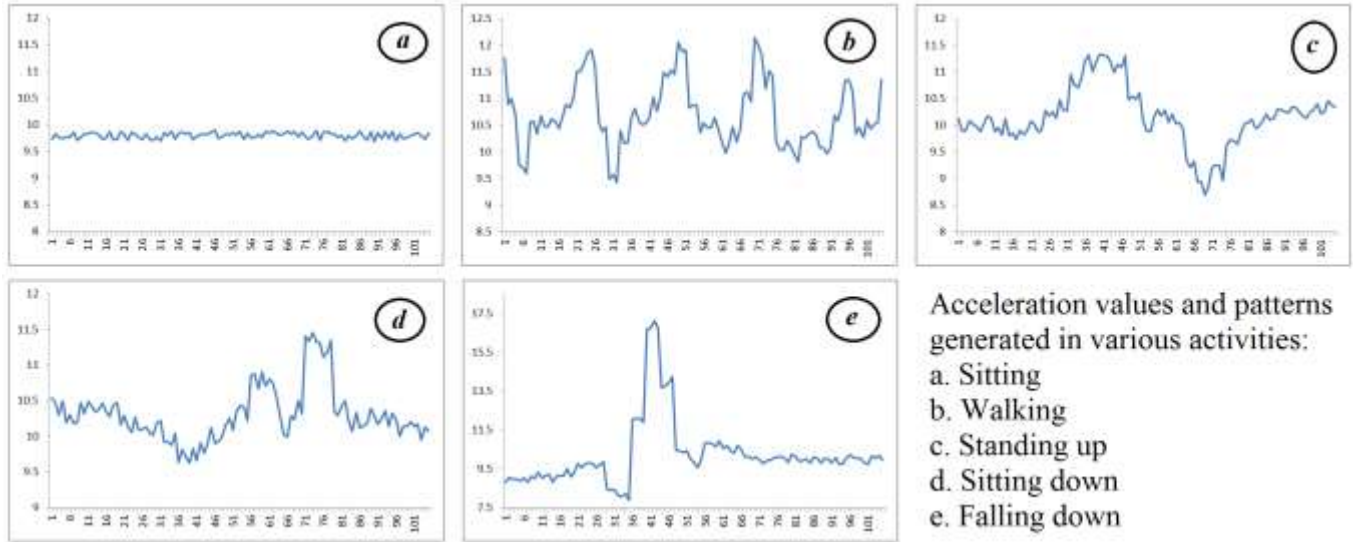


Fig. 2. Plotting of acceleration values and patterns in various activities

All in Focus Image Generation based on New Focusing Measure Operators

Hossam Eldeen M. Shamardan ¹

¹ Department of Information Technology
Faculty of Computers and information
University of Helwan
Egypt

Abstract—To generate an all in focus image, the Shape-From-Focus (SFF) is used. The SFF key is finding the optimal focus depth at each pixel or area in an image within sequence of images. In this paper two new focusing measure operators are suggested to be used for SFF. The suggested operators are based on modification for the state of art tool for time-frequency analysis, the Stockwell Transform (ST). The first operator depends on Discrete Orthogonal Stockwell Transform (DOST) which represents a pared version of ST, while the other depends on Pixelwise DOST (P-DOST) which provides a local spatial frequency description. Both of the operators provides the computational complexity and memory demand efficiency compared to the operator depending on ST. A comparison between the suggested operators to operators based on ST are performed and showed that the suggested operators' performances are as analogous to that of ST.

Keywords—Focus Measure; All In Focus; Stockwell Transform; DOST

I. INTRODUCTION

SFF is an essential process to overcome a specific limitation of imaging systems which is the different depth of field (DOF) for each part in an image [1, 2, 3]. The SFF solves this problem by providing fully sharp focused image. The SFF depends on measuring the optimal focus by using the focus measure (FM) operator, the main key, for shape estimating. The usual SFF methods compute optimal focus and its depth by applying FM operator on every area in a frame within a sequence of images and seek the optimal focused part along the sequence. The fully focused image can be constructed from merging the focuses optimal parts [4, 5].

The sharp focused area is characterized by its energy for high frequency components, and The FM operator is used to measure the amount of energy in every part. Many FM operators have been proposed in the literature for both autofocus (AF) and SFF applications [5]. In [6], the performance of multiple FM operators were examined. FM operators can be classified into two broad types: space domain and, frequency domain [7] [8], and others such as compression operators [5] [9].

The ST has been used as a base for FM operator in [10] and compared to other FM operators. The suggested idea is to measure the high frequency components energy located in a region of interest in the ST domain. The ST gives good results but it suffers from high computational cost. To overcome the

problem of high cost for ST, a pared version of ST, DOST was provided in [11]. The DOST provides efficiency in both computational cost and memory usage. Another version of DOST, pixel-wise local spatial frequency description (P-DOST) was given in [12]. The P-DOST provides a tool for studying a specific frequency at specific pixel or area. Both of DOST and P-DOST have low computational cost and robustness to Gaussian noise.

In this paper two new FM operators are presented based on DOST and P-DOST for their low computational cost and memory usage.

This paper is organized as follows. In section 2, the background for ST, DOST and P-DOST are presented. The proposed algorithm and FM operators are described in section 3. Finally, experimental results and conclusion are presented in sections 4 and 5 respectively.

II. BACKGROUND

ST has been shown as a generalization of the short-time Fourier transform (STFT), and the wavelet transforms [13]. From [10] the 2D-ST, H_{st} for an image $h(x, y)$ of size $N * M$ for pixel (x, y) is given by

$$H_{st}[x, y, k_x, k_y] = \sum_{n=0}^{N-1} \sum_{m=0}^{M-1} H[n + k_x, m + k_y]^* \exp(-2\pi^2 (\frac{n^2}{k_x^2} + \frac{m^2}{k_y^2})) \exp(2\pi i(nx + my)) \quad (1)$$

Where H is the 2D Fourier transform of h , x , and y are x-coordinates and y-coordinates in space respectively and k_x , and k_y are indices in the frequency along x-axis and y-axis.

From [14], it has been demonstrated that the ST redundancy comes from the equal sampling rate for both low and high frequency bands despite the fact of Nyquist criterion which states that the sampling rate depends on the frequency of the sampled data. A detailed study for the 2D-ST computational complexity for an image of size $N * N$ is given in [12]. It has been shown that ST has a computational cost of $O(N^4 + N^4 \log N)$ and a storage requirement of $O(N^4)$.

The DOST suggested in [11] gives lower sampling rates for lower frequencies, and higher sample rates for higher

frequencies to solve the ST redundancy. It does so by building a set of N orthogonal unit-length basis vectors, each of which targets a particular region in the time-frequency domain. The regions defined by DOST are described by a set of parameters: ν specifies the center of each frequency band (voice) p , β is the width of that band, and τ specifies the location in time.

DOST basis vectors for a particular band p and the parameters describing these basis vectors are defined in the following cases according to p where $p = 0, 1, \dots, \log_2(N) - 1$

$$\text{for } p = 0, \nu = 0, \beta = 1,$$

$$D(kT)_{[\nu, \beta, \tau]} = 1$$

$$\text{for } p = 1, \nu = 1, \beta = 1,$$

$$D(kT)_{[\nu, \beta, \tau]} = e^{(-2ik\pi/N)} \quad (2)$$

$$\text{for } p > 1, \nu = 2^{(p-1)} + 2^{(p-2)},$$

$$\beta = 2^{(p-1)}, \tau = 0, \dots, \beta - 1$$

$$D(kT)_{[\nu, \beta, \tau]} = ie^{(-i\pi k)} * \frac{e^{-2i\alpha(\nu - \beta/2 - 1/2)} - e^{-2i\alpha(\nu + \beta/2 - 1/2)}}{2\sqrt{\beta} \sin(\alpha)}$$

where $\alpha = \pi(k/N - \tau/\beta)$ is the center of the temporal window, and $k = 0, 1, \dots, N-1$ is the index of time interval. The time-frequency distribution for a family of vectors for a signal of length 16 is shown in Fig. 1 [15].

Calculating DOST is determined by taking the inner product between the basis vectors mentioned above and the input signal. By taking linear combinations of the Fourier complex sinusoids in band-limited subspaces and applying appropriate phase and frequency shifts, the 2D-DOST of $M * N$ image $h[x, y]$ is defined in [12] as follows:

$$S[x', y', \nu_x, \nu_y] = \frac{1}{\sqrt{\beta}} \sum_{m=-2^{p_x-2}}^{2^{p_x-2}-1} \sum_{n=-2^{p_y-2}}^{2^{p_y-2}-1} H(m + \nu_x, n + \nu_y) * \exp(2i\pi(\frac{mx'}{2^{p_x-1}} + \frac{ny'}{2^{p_y-1}})) \quad (3)$$

Where $\nu_x = 2^{p_x-1} + 2^{p_x-2}$ and $\nu_y = 2^{p_y-1} + 2^{p_y-2}$ are representing the horizontal and vertical voice frequencies, and $\beta = 2^{p_x p_y - 2}$ is representing the number of points in the partition, and $H(m, n)$ is the 2D Fourier transform for image $h[x, y]$.

The 2D-DOST due to using orthonormal set of basic functions as described above, has computational complexity of $O(N^2 + N^2 \log N)$ and storage requirements of $O(N^2)$ which was proved in [16]. It is obvious DOST has less computational complexity required than for the 2D-ST.

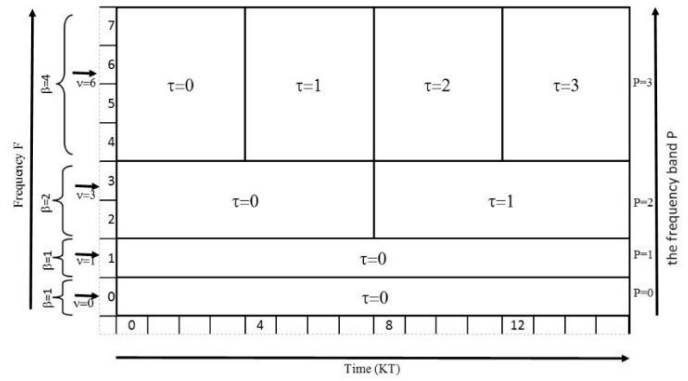


Fig. 1. Time-Frequency distribution for DOST components in positive direction

The P-DOST suggested in [12] aims to find the voice frequency distribution for a pixel or region within the image. By choosing a set of (x, y) coordinates representing a single pixel or area, all the values of $s[x, y, \nu_x, \nu_y]$ for all horizontal and vertical voices (ν_x, ν_y) can be determined for position (x, y) . Due to the variable size and limits of every DOST components at each band, the P-DOST is constructed by obtaining all components of DOST at each band (p_x, p_y) by:

$$S[x/N * 2^{p_x-1}, y/N * 2^{p_y-1}, \nu_x, \nu_y] \quad (4)$$

From (4), the P-DOST corresponding response is occupying part of the DOST response space. Hence. It only requires size of, considering the negative side, $2\log_2(N) * 2\log_2(N) (2\beta * 2\beta)$. The P-DOST response is referred to as the local domain (or spectrum). Since P-DOST selects only some components from the whole components set for DOST, a reduction will consequently go further for the computational complexity and memory demands. Consequently, the computational complexity for calculating P-DOST for single pixel is of order $O((2 * \log_2(N))^2)$. Considering the DOST calculations, it is obvious that P-DOST is less demanding for computational complexity than for DOST.

III. PROPOSED ALGORITHM

The algorithm suggests a stack of L frames $I_1 \dots I_L$ with the same size, and same scene pictures an object at different focusing depths. The frames are divided into windows $W(x, y, z)$ each of size $M * N$ located at position (x, y) in every frame z . The Suggested algorithm is described as follows:

- 1) Divide every frame $I_1 \dots I_L$ into windows. Each window $W(x, y, z)$ is located at position (x, y) in frame I_z
- 2) Apply the FM_D or FM_p for window $W_{x,y,z}$ using formulas in (5) or (6) along all the L frames.
- 3) Find $Z_{optimal}$ by using (7).
- 4) Repeat steps from 1 to 3 and merge all windows to get the generated fully focused image.

The formulas for calculating FM_D is given as follows:

$$FM_D(Z) = \sum_{v_y=v(p=-M-1)}^{v_y=v(p=M)} \sum_{v_x=v(p=-N-1)}^{v_x=v(p=N)} \xi(x, y, v_x, v_y) \quad (5)$$

where

$$\xi(x, y, v_x, v_y) = \sum_{y=0}^{M-1} \sum_{x=0}^{N-1} abs(S[x, y, v_x, v_y]) \quad (v_x, v_y) \neq (0,0)$$

And for FM_p

$$FM_P(x_0, y_0) = \sum_{v_y=v(p=-M-1)}^{v_y=v(p=M)} \sum_{v_x=v(p=-N-1)}^{v_x=v(p=N)} \xi(x_0, y_0, v_x, v_y), \quad (6)$$

where

$$\xi(x_0, y_0, v_x, v_y) = abs(S[x_0, y_0, v_x, v_y]) \quad (v_x, v_y) \neq (0,0)$$

For determining $Z_{optimal}$

$$Z_{Optimal} = \arg \max_z (FM(Z)), \quad z = 1 \dots L \quad (7)$$

The suggested FM_D and FM_p in the algorithm are based on DOST and P-DOST respectively and both of them measure the energy in high frequencies components (frequency > 0 (DC)). A formula used for the suggested operators are given in (5) and (6). The operators are used to find the optimal focused window by measuring the highest response resulted by the operator. By merging the optimal focused window a fully focused image of the scene can be reconstructed. The idea for measuring the energy is the of the energy for the components within an area reflects the sharpness and hence the focusing. For FM_p , the pixel (x_0, y_0) is selected at the center of the targeted window and used to represent the window.

IV. EXPERIMENTAL RESULTS

To evaluate the performance of the proposed algorithm and its robustness, three experiments for three sequences of images were conducted each of 256 gray levels. The first experiment contains sequence of 60 images of cone. The size for this sequence is 360*360. A simulation software was used to generate the images focused at different parts of the image Fig. 2a through 2d, the proposed algorithm has been used to construct all in focus image through FM_D and FM_p operators on this sequence. The resulting images are shown in Fig. 2e, 2f. The second experiment contains a sequence of 30 natural images, each of size 299*215. The sequence and the generated all in focus image are shown in Fig. 3. The third experiment contains also 30 natural images of size 215 * 215. Results are shown in Fig. 4.

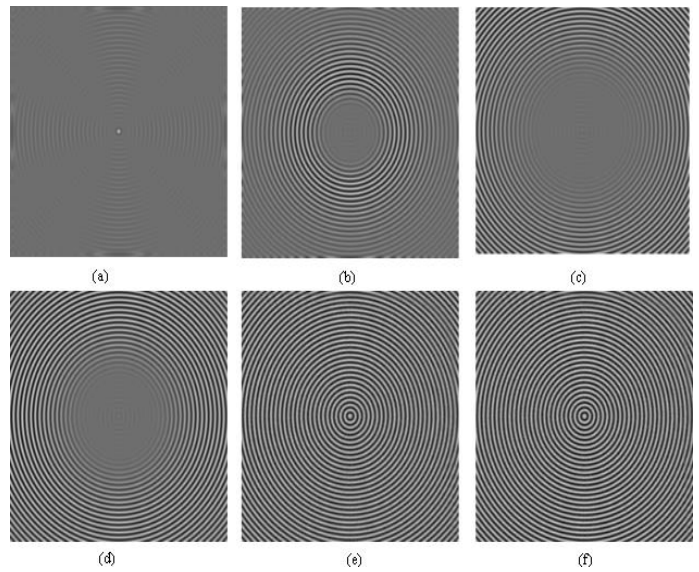


Fig. 2. Pictures from (a) to (d) are defocus cone images at different focusing level, e) SFF by using FM_D , f) SFF by using FM_p

The first sequence of images was adopted and used for next evaluating tests. To evaluate the robustness of the algorithm against noise, three different measures were adopted to measure the all in focus image quantitatively. The first measure is the rmse (root mean square error) which is defined as follows

$$rmse = \sqrt{\frac{1}{MN} \sum_{x=1}^M \sum_{y=1}^N (I(x, y) - I'(x, y))^2} \quad (8)$$

Where $I(x, y)$ the original is image, and $I'(x, y)$ is the all in focus image from the sequence of images

To test the performance of the algorithm, the algorithm was applied to the sequence with added Gaussian noise of variance ranging from 0 to 10 and the window size is ranging from 4 to 64 Fig. 5 shows the results of this test.

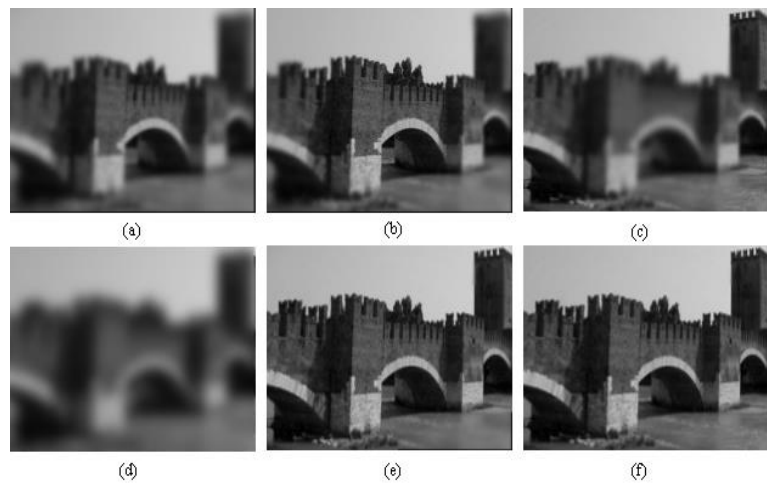


Fig. 3. Pictures from (a) to (d) are defocus cone images at different focusing level, (e) SFF by using FM_D , (f) SFF by using FM_p

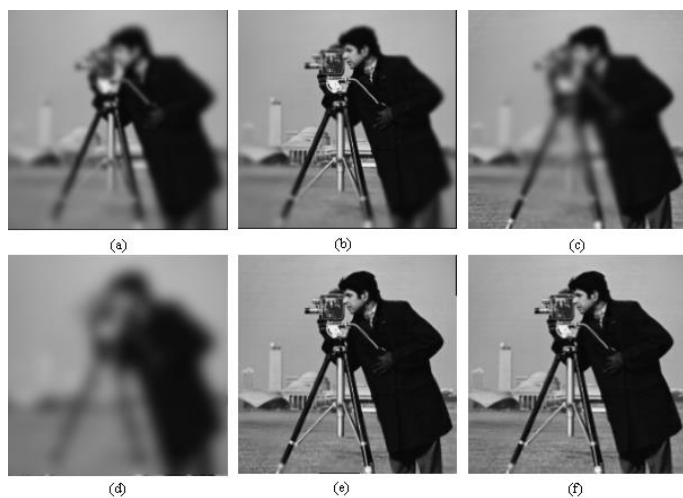


Fig. 4. Pictures from (a) to (d) are defocus cone images at different focusing level, e) SFF by using FM_D , f) SFF by using FM_P

To compare between FM_D and FM_P performance, a test was applied showing the rmse performance of the two operators against the window size and for different noise variances. The results are shown in Fig. 6. It is obvious that the FM_D is advantageous than the FM_P since it considers all the pixels rather than a single central one.

The next measures are the UIQI (universal image quality index) and SSIM (structural similarity index measure) [10] and are defined as following:

$$UIQI = \frac{4\sigma_u \bar{I}'}{(\sigma_i^2 + \sigma_i'^2)(\bar{I}^2 + \bar{I}'^2)} \quad (9)$$

$$SSIM = \frac{(2\bar{I} + c_1)(2\sigma_i \sigma_i' + c_2)}{((\bar{I}^2 + \bar{I}'^2) + c_1)(\sigma_i^2 + \sigma_i'^2 + c_2)} \quad (10)$$

Where \bar{I} and \bar{I}' represent mean of the original and all in focus image constructed from the sequence of images respectively. The results are shown in Fig. 7,8. It is clear that both UIQI and SSIM gives similar performance for both FM_D and FM_P .

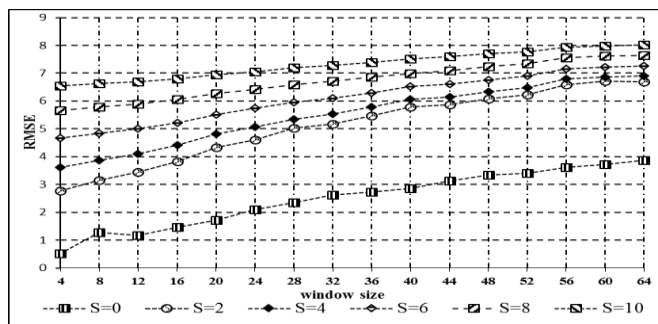


Fig. 5. rmse against window size for different variance levels of gaussian noise

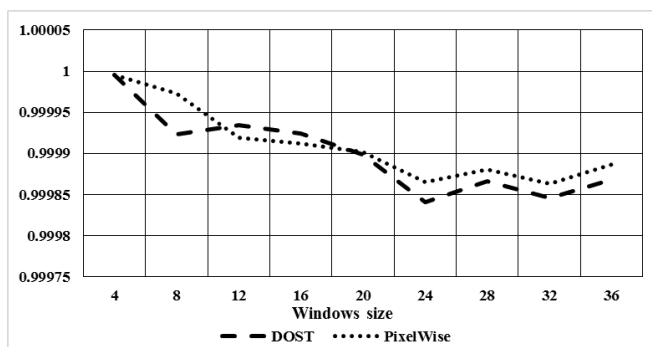


Fig. 6. Comparison between FM_D and FM_P operators performance (UIQI) versus window size

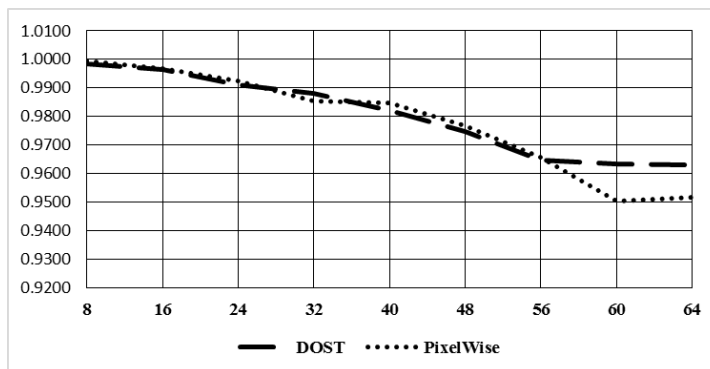


Fig. 7. Comparison between FM_D and FM_P operators performance (SSIM) versus window size

Another experiment was conducted to compare between FM_{ST} and FM_D performances for generating the cone image give in Fig. 2, assuming window is of size 4. The results showed that FM_{ST} provides performance little bit better than FM_D . The achievable rmse for the ST is 0.52 while the DOST achieved 0.72. Of course the FM_{ST} provides better performance (38%) however, the resultant performance is very minor (less than 1) out of 256 gray level. Compared to the computational complexity, the FM_{ST} is of order $O(N^4 + N^4 \log N)$ while the FM_D is of order $O(N^2 + N^2 \log N)$.

V. CONCLUSION AND FUTURE WORK

In this paper, two new FM operators are suggested to reconstruct all-in-focus image. The two operators are built on extensions of Stockwell Transform, a space-frequency transformation tool. Stockwell Transform has been proved to suffer from excessive abundant computations and high memory requirements and to reduce the computational complexity that is the reason the FM_D and FM_P are adopted as bases for the suggested FM operators. Results have shown to

be as good as for FM_{ST} . The two suggested methods are of almost similar performance and with less computational complexity and memory demands. The future research can extend the usage of those tools to get automatic focusing and to enhance the robustness

REFERENCES

- [1] Z. Li, A. Fischer and G. Li, "Volumetric retinal fluorescence microscopic imaging with extended depth of field," in SPIE 9713, Three-Dimensional and Multidimensional Microscopy: Image Acquisition and Processing XXIII, San Francisco, 2016.
- [2] E. Anderes, B. Yu, V. Jovanovic, C. Moroney, M. Garay, A. Braverman and E. Clothiaux, "Maximum likelihood estimation of cloud height from multi-angle satellite imagery," The Annals of Applied Statistics, pp. 902-921, 5 October 2009.
- [3] Y. Song, Y. Xie, V. Malyarchuk, J. Xiao, I. Jung, K. Choi, Z. Liu, H. Park, C. Lu, R. Kim, R. Li, K. Crozier, Y. Huang and J. Rogers, "Digital cameras with designs inspired by the arthropod eye," Nature, vol. 497, no. 7447, p. 95-99, 2 May 2013.
- [4] A. Anish and T. J. Jebaseeli, "A survey on multi-focus image fusion methods," International Journal of Advanced Research in Computer Engineering & Technolog, vol. 1, no. 8, p. 319-324, October 2012.
- [5] S. Pertuz, D. Puig and M. A. Garcia, "Analysis of focus measure operators for shape-from-focus," Pattern Recognition, vol. 46, no. 5, p. 1415-1432, May 2013.
- [6] A. S. Malik and T. S. Choi, "Consideration of illumination effects and optimization of window size for accurate calculation of depth map for 3D shape recovery," Pattern Recognition, vol. 40, no. 1, pp. 154-170, 2007.
- [7] T. M. Mahmood, S. O. Shim and T. S. Choi, "Shape from focus using principal component analysis in discrete wavelet transform," Optical Engineering, vol. 48, no. 5, p. 057203, 28 May 2009.
- [8] J. Baina and J. Dublet, "Automatic focus and iris control for video cameras," in Image Processing and its Applications, 1995., Fifth International Conference on, Edinburgh, 1995.
- [9] H. Mir, P. Xu and P. V. Beek, "An extensive empirical evaluation of focus measures for digital photography," in SPIE 9023, Digital Photography X, 90230I, 2014.
- [10] T. M. Mahmood and T. S. Choi, "Focus measure based on the energy of high-frequency components in the S transform.," in Depth Map and 3D Imaging Applications: Algorithms and Technologies., vol. 35, IGI Global, 2012, pp. 189-208.
- [11] R. G. Stockwell, "A basis for efficient representation of the S-transform," Digital Signal Processing, p. 371-393, January 2007.
- [12] S. Drabycz, R. G. Stockwell and J. R. Mitchell, "Image Texture Characterization Using the Discrete Orthonormal S-Transform," Journal of Digital Imaging, vol. 22, no. 6, pp. 696-708, December 2009.
- [13] Y. Wang and J. Orchard, "On the use of the Stockwell transform for image compression," in Image Processing: Algorithms and Systems VII, 724504, 2009.
- [14] Y. Wang, Efficient stockwell transform with applications to image processing (Ph.D. thesis), Waterloo, Ontario: The University of Waterloo, 2011.
- [15] Y. Wang and J. Orchard, "Fast Discrete Orthonormal Stockwell Transform," SIAM Journal on Scientific Computing, vol. 31, no. 5, p. 4000-4012, 11 November 2009.
- [16] M. K. N. B. and P. K., "Palmprint Authentication System Based on Local and Global Feature Fusion Using DOST," Journal of Applied Mathematics, vol. 2014, p. 11, 16 December 2014.

Stemmer Impact on Quranic Mobile Information Retrieval Performance

Huda Omar Aljaloud

Computer Science Department
King Abdulaziz University
Jeddah, Saudi Arabia

Mohammed Dahab

Computer Science Department
King Abdulaziz University
Jeddah, Saudi Arabia

Mahmoud Kamal

Information Systems Department
King Abdulaziz University
Jeddah, Saudi Arabia

Abstract—Stemming algorithms are employed in information retrieval (IR) to reduce verity variants of the same word with several endings to a standard stem. Stemmers can also help IR systems by unifying vocabulary, reducing term variants, reducing storage space, and increasing the likelihood of matching documents, all of which make stemming very attractive for use in IR. This paper aims to study the impact of using stemming techniques in mobile effectiveness. Two-word extraction stemming techniques will be used: a light stemmer and a dictionary-lookup stemmer. Also, three sets of experiments were conducted in this research in order to raise the efficiency of mobile applications. Implementing the two stemming approaches and assessing their accuracy by calculating the precision, recall, MAP, and f-measure, produced results which show that the light10 stemmer outperforms the dictionary-lookup stemmer in precision and MAP. Furthermore, the mobile performance of the light10 stemmer exceeds that of the dictionary-based stemmer.

Keywords—stemming; information retrieval; light10; Quran lexicon; mobile performance; natural language processing

I. INTRODUCTION

The Holy Quran is a global source of knowledge for humanity in general and Muslims in particular. Studying and learning the Holy Quran plays a central role in the lives of all Muslims. Since the Holy Quran is the divine revelation and the word of God, it needs careful handling when processed by automated methods of natural language processing (NLP). The Holy Quran is written in the Arabic language, which is known to be one of the more challenging natural languages in the field [1]. Most researchers have been interested in the development of search techniques for the Quranic text. The techniques employed to retrieve information from the Quran can be classified into two types: semantic-based and lexical-based. The lexical-based search yields results according to the morphological analysis for a query.

Compared to any other kind of communication device, the mobile phone has proved its superiority in communicating and in gaining information. Recognizing this, many companies have focused unprecedented attention on technologies and mobile applications [2]. As a result, the development and evaluation of new technologies for mobile phones occurs very quickly. According to a recent study, smartphone devices will surpass computers as the primary tool by 2020 [3]. This development has inspired researchers to exploit smartphones

in various areas, especially in the field of mobile information retrieval (IR) and necessary preprocess phases like stemming. Mobile IR is considered a subset of traditional IR [3].

Stemming has been shown to be more efficient for Arabic retrieval than for English [4]. After several decades of intensive research activity on English stemmers, the techniques of Arabic morphological analysis have become a popular area of research. Early research in this field was performed using small collections until the TREC 2001 Arabic track became available [5]. Root-based stemming, light stemming, and dictionary-lookup stemming are three different types of stemming [6].

To motivate researchers and develop more advanced techniques, Al-sughaiyer et al. in [5] introduced, classified, and surveyed Arabic morphological analysis techniques in an attempt to summarize and organize the information available in the literature of this research area. However, stemmers achieve a noticeable improvement in related NLP tasks [7]. Also, in [8], a comparative study was conducted on most of the existing stemmers (almost twenty) that used different approaches for stemming. The results showed that from 2000 to 2014, the stemmers were used mostly in information retrieval, followed by text classification, with light stemmers being the most commonly used.

A review of semantic search methods was done to retrieve information from the Qur'an corpus in [9]. A proposal for further research in Quranic Knowledge Map was presented in [10]. Moreover, although the Holy Quran is written in Arabic, many efforts to improve word-stemming algorithms are done in other languages [11]. For example, Atwell et al., in [12], investigated the effectiveness of information retrieval in the verse retrieval problem for translated Quranic text in Malay, English, and stemmed English language. A thorough research of the relevant literature found that no research study was done that examined and compared automatic stemming versus manual stemming techniques on Quranic mobile application performance the way it is done in this paper.

In this paper, three questions were investigated: 1) Are automated stemmers more effective than manual-based dictionary-lookup stemmers? 2) Do light stemmers enhance mobile application performance compared to other stemmers? 3) Does using stemmers offline and storing processed tokens with the dataset in the mobile application increase the performance?

Dictionary-lookup stemming is based on the manual construction of dictionaries. The root of each processed word is found in the lexicon [14]. Dictionary-lookup stemming is fast since it does not require word analysis, but it does require space and precision in preparing the dictionary [4]. In contrast, light stems use morphological rules to strip off suffixes; light stemming is therefore considered to be a less complicated type of stemming analysis.

Accordingly, to study the impact of different stemming approaches on the accuracy of Quranic IR, dictionary-lookup and light10 stemmers were used in the mobile application. The dictionary-lookup stemmer was based on the Lexicon of the Raw Stems of the Words of the Holy Quran, a manual dictionary by Mohamed Aldabbagh [15]. The electronic database version of the afore-mentioned dictionary was obtained by direct contact with the author. Table 3 shows the effect of stemming on the Quranic word. As can be seen from the first verse word in the table, (بسم), the Light10 stemmer returned the same word (بسم), while the dictionary stemmer resulted in the root word (سمو).

TABLE III. THE EFFECT OF STEMMING ON THE QURANIC WORD

Verse Word	Light10 Stem	Dictionary Root
بسم	بسم	سمو
الله	له	الله
الرحمن	رحمن	رحم
الرحيم	رحيم	رحم

III. EXPERIMENTS

For this research, the Holy Quran was used as a dataset. The dataset contained a total of 6,236 verses, obtained from <http://tanzil.net/>, and a collection of fifty queries. The queries with corresponding relevance judgments were generated by the authors of this paper. To study the impact of stemming in mobile performance, three experiments were conducted. First, the impact of two stemmer algorithms on IR performance results was evaluated. Second, the mobile performance results of the selected stemmer techniques were compared. The last experiment investigated the ability of offline and online stemmers to raise mobile efficiency.

A. Impact of Stemmer Technique on IR Performance

To examine the impact of text preprocessing on Quranic IR performance, two stemmer techniques were applied. In this experiment, a stem-based technique was employed using light10 and dictionary-lookup stemmers based on the Lexicon of the Raw Stems of the Words of the Holy Quran [15]. In order to determine the effectiveness of verse retrieval in the Holy Quran, the recall, precision, F-measure, and MAP were calculated [16].

B. Impact of Stemmer Technique on Mobile Performance

The effectiveness of a mobile application is usually

measured in terms of processing time and memory requirements. SystemPanel 1.4 Task Manager Application was used to examine the CPU and memory usage. Also, the overall Android application package (APK) size was calculated. APK is the package file format used by the Android operating system for distribution and installation of mobile applications.

To gauge the tradeoff between the storage capacity and CPU efficiency, the next two experimental studies were applied. The experiments in this study set were calculated in seconds to figure out the CPU time consumed. The experiments studied the influence of two stemmer techniques used to manipulate smartphone performance. The light10 and dictionary-based stemmers were applied and then demonstrated which allowed more efficient use of the resources.

In the last experiment, two different preprocessing stage periods were applied. Preprocessing involved extracting words from documents, normalization, removing stopwords, and stemming. First, the preprocessing stage was completed before uploading the data collection to a smartphone. Therefore, the verse text preprocessing was completed before the mobile application launched (an offline preprocess). Second, the preprocessing of the verse text was completed after the mobile application launched (an online preprocess).

IV. RESULTS AND DISCUSSION

In this paper, experiments were performed on the Holy Quran (the dataset) with fifty queries between two and three words. Additionally, three sets of experiments were conducted to raise the performance of the mobile application.

Most of the research related to Arabic stemmers is either based on a dictionary of Arabic roots or uses a set of rules to identify the stem of Arabic words [17]. The results of the first experiment, displayed in Table 4, showed that using the light10 system and MAP would give the highest precision rather than using the dictionary-based system. MAP provided a brief summary of ranking effectiveness used by the IR system. In this case, a higher MAP score indicated that the relevant verses were distributed at the top ranks. Similarly, the light10 stemmer outperformed various stemmers in IR. It is widely utilized, as some studies have proven [14][18][7][19]. On the other hand, dictionary stemming for Quranic words achieved better recall than did the light10 system, as shown in Fig. 2.

TABLE IV. STEMMER ALGORITHMS PERFORMANCE MEASURE RESULTS

Stemmer	Recall	Precision	F-measure	MAP
Light10	0.7401	0.9046	0.7700	0.9359
Dictionary Based	0.9891	0.7447	0.8087	0.8318

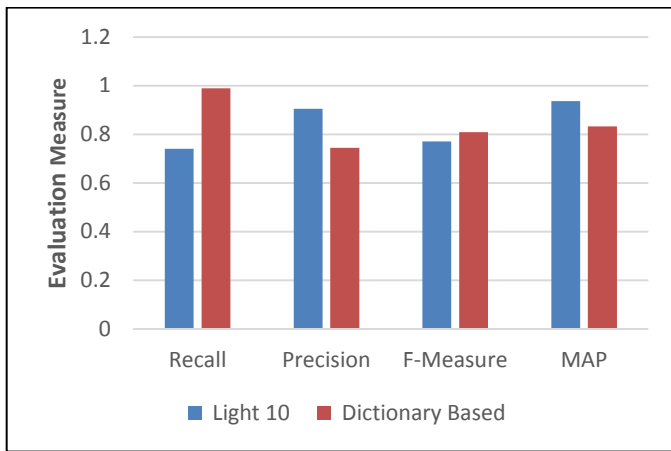


Fig. 2. IR Performance results for stemmers

Table 5 and Fig. 3 present the performance results of the second experiment. The performance of the light10 stemmer, exceeded that of the dictionary-based stemmer in terms of the speed of the CPU. Even the light10 APK file was smaller than the other; 1.918 MB compared to 2.252 MB for the dictionary based stemmer’s APK size. The dictionary-based stemmer consumed the CPU without credit in memory usage.

TABLE V. SECOND EXPERIMENT RESULTS

Stemmer	APK Size	CPU Time	Memory Usage
Light 10	1.918 MB	2.75 s	3.44 MB
Dictionary Based	2.252 MB	4.8 s	3.38 MB

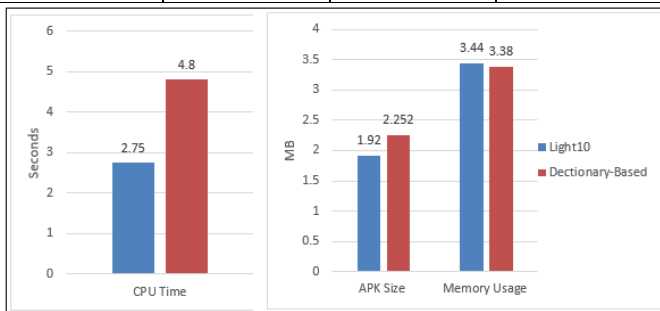


Fig. 3. Second experiment performance

For the third experiment, Table 6 illustrates that the offline preprocessing surpassed the online preprocessing in smartphone performance, despite the fact that the APK size file was slightly larger in offline preprocessing. Offline preprocessing contributed to increasing the performance, as shown in Fig. 4.

TABLE VI. THIRD EXPERIMENT RESULTS

Experiment	APK Size	CPU Time	Memory Usage
Offline Preprocess	1.918 MB	2.75 s	3.44 MB
Online Preprocess	1.789 MB	3.65 s	5.26 MB

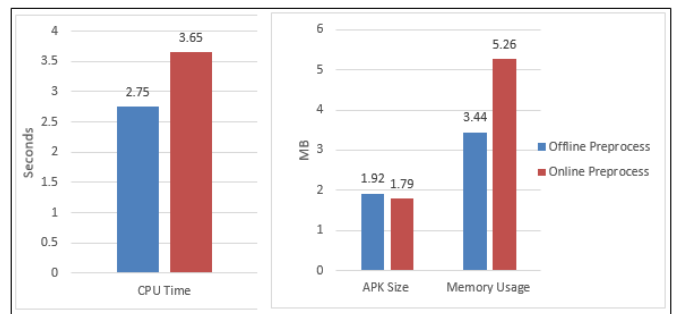


Fig. 4. Third experiment performance

V. CONCLUSION

In this paper, the efficacy of stemmer techniques was examined by studying the impact of different stemming approaches on the accuracy of Quranic IR and mobile performance. Dictionary-lookup and light10 stemmers were used in the mobile application.

In addition, three sets of experiments were conducted in this research to raise the efficiency of the mobile application. First, an experiment was conducted to evaluate the impact of two stemmer algorithms on IR performance results. In the second experiment, the mobile performance results of the selected stemmer techniques were compared. In the final experiment, the impact of offline and online stemmers on mobile efficiency was investigated.

Based on the results of the first experiment, the light10 stemmer demonstrates the highest precision and MAP. Most modern studies indicate that using stems outperforms roots [20]; which these results confirm.

Moreover, to improve the mobile application performance, the results suggested using an offline preprocessing stemmer stage which allows the light10 stem-based system to use mobile resources more efficiently.

Future work based on this study would be to compare automatic root extraction with the manual one used. As for the manual dictionary-based stemmer root approach, the main limitation was in extracting all words to tri-roots only. This can be improved by using an automatic root extractor and including more root patterns.

ACKNOWLEDGMENT

The authors thank Mohamed Aldabbagh for obtaining the electronic database version from the root Quranic lexicon.

Also, the authors thank tanzil.net for providing the data for this research. They also appreciate the efforts of the Zekr Quran Project and Quran Code Desktop Software, which was used to obtain the relevant judgments for the query terms.

REFERENCES

- [1] A. Mohammad, H. Mohamed, and H. Anwer, "Processing the Text of the Holy Quran: a Text Mining Study," International Journal of Advanced Computer Science and Applications (IJACSA), vol. 6, no. 2, pp. 262–267, 2015.
- [2] P. Racherla and J. Hills, "What We Know and Do Not Know About Mobile App Usage and Stickiness.," International Journal of E-Services and Mobile Applications, vol. 7, no. 3, pp. 48–69, 2015.

- [3] F. S. Tsai, M. Etoh, X. Xie, W. Lee, and Q. Yang, "Introduction to Mobile Information Retrieval," *IEEE Intelligent Systems*, vol. 25, pp. 11–15, 2010.
- [4] A. Nwesri, "Effective Retrieval Techniques for Arabic Text," RMIT University, 2008.
- [5] I. a. Al-sughaiyer and I. a. Al-kharashi, "Arabic morphological analysis techniques: A comprehensive survey," *Journal of the American Society for Information Science and Technology*, vol. 55, no. 3, pp. 189–213, 2004.
- [6] F. Harrag, E. El-Qawasmah, A. M. S. Al-Salman, E. El-Qawasmah, and F. Harrag, "Stemming as a Feature Reduction Technique for Arabic Text Categorization," in *Programming and Systems (ISPS)*, 2011 10th International Symposium on. IEEE, pp. 128–133, 2011.
- [7] M. El-defrawy, "Enhancing Root Extractors Using Light Stemmers," in *29th Pacific Asia Conference on Language, Information and Computation*, pp. 157–166, 2015.
- [8] M. Y. Dahab, A. Al Ibrahim, and R. Al-Mutawa, "A Comparative Study on Arabic Stemmers," *International Journal of Computer Applications*, vol. 125, no. 8, 2015.
- [9] E. Atwell and M. Algahtani, "A Review of Semantic Search Methods to Retrieve Information from the Qur ' an Corpus," in *corpus Linguistics 2015*, pp. 7–9, 2015.
- [10] E. Atwell, C. Brierley, K. Dukes, M. Sawalha, and A. Sharaf, "An Artificial Intelligence approach to Arabic and Islamic content on the internet," *Proceedings of NITS 3rd National Information Technology Symposium*. Leeds, pp. 1–13, 2011.
- [11] K. Mohamad Nizam, A. W. Amirudin, M. Mohd Aizaini, and Z. Anazida, "Word stemming challenges in Malay texts: A literature review," in *Information and Communication Technology (ICoICT)*, 4th International Conference, 2016.
- [12] A. M. Sultan, A. Azman, R. A. Kadir, and M. T. Abdullah, "Evaluation of Quranic text retrieval system based on manually indexed topics," *2011 International Conference on Semantic Technology and Information Retrieval*. IEEE, pp. 156–161, 2011.
- [13] M. Y. Ai-nashashibi, D. Neagu, and A. A. Yaghi, "an Improved Root Extraction Technique for Arabic Words," *Computer Technology and Development (ICCTD)*, 2010 second International Conference on. IEEE, pp. 264–269, 2010.
- [14] L. S. Larkey, L. Ballesteros, and M. E. Connell, "Light Stemming for Arabic Information Retrieval," *Arabic computational morphology*. Springer Netherlands, pp. 221–243, 2007.
- [15] M. Aldabbagh, *Lexicon of the Raw Stems of the Words of the Holy Quran*, First edit. Baghdad: available on line by archive.org, 2015.
- [16] H. Aljaloud, M. Dahab, and M. Kamal, "Intelligent Information Retrieval Approach Using Discrete Wavelet Transform for the Holy Quran in a Smartphone Application," in *4th International Conference on Islamic Applications in Computer Science and Technology*, 2016, in press.
- [17] M. N. Al-Kabi, S. A. Kazakzeh, B. M. Abu Ata, S. A. Al-Rababah, and I. M. Alsmadi, "A novel root based Arabic stemmer," *Journal of King Saud University-Computer and Information Sciences*, vol. 27, no. 2, pp. 94–103, 2015.
- [18] M. A. Otair, "Comparative analysis of arabic stemming algorithms," *International Journal of Managing Information Technology*, vol. 5, no. 2, pp. 1–12, 2013.
- [19] M. Ahmed and R. Mamoun, "Arabic text stemming: Comparative analysis," in *Basic Sciences and Engineering Studies (SGCAC)*, 2016.
- [20] M. I. Eldesouki and W. M. Arafa, "Stemming techniques of Arabic Language: Comparative Study from the Information Retrieval Perspective," *The Egyptian Computer Journal*, vol. 36, no. 1, pp. 30–50, 2009.

Internal Model Control of A Class of Continuous Linear Underactuated Systems

Asma Mezzi

Tunis El Manar University,
Automatic Control Research Laboratory, L.A.R.A.,
National Engineering School of Tunis (ENIT),
BP 37, Le Belvédère, 1002 Tunis, Tunisia

Dhaou Soudani

Tunis El Manar University,
Automatic Control Research Laboratory, L.A.R.A.,
National Engineering School of Tunis (ENIT),
BP 37, Le Belvédère, 1002 Tunis, Tunisia

Abstract—This paper presents an Internal Model Control (IMC) structure designed for a class of continuous linear underactuated systems. The study treats the case of Minimum Phase (MP) systems and those whose zero dynamics are not necessarily stable. The proposed IMC structure is based on a specific controller which is obtained by the realization of an approximate inverse of the model plant. It is shown that, using such IMC structure, it is possible to remedy the problem of system underactuation and Non-Minimum Phase (NMP) behavior. The case of non-zero initial conditions and imperfect modeling are also presented and model parameters effects on the system evolution are discussed. Simulated examples are presented to prove the effectiveness of the proposed control method to ensure set-point tracking, stability and disturbance rejection.

Keywords—Internal Model Control; continuous linear underactuated systems; specific controller; minimum phase systems; non-minimum phase behavior; non-zero initial conditions; model parameters effects; set-point tracking; stability; disturbance rejection

I. INTRODUCTION

Multivariable underactuated systems, i.e., systems having fewer control inputs than degrees of freedom, are widely used in industry. Aircraft, helicopters, underwater vehicles, surface vessels, mobile systems and many of today's walking and underwater robots are some examples of underactuated systems. They are used for reducing cost, weight or energy consumption. Some other advantages of underactuated systems include tolerance for actuators failure and less damage while hitting an object. The dynamics of some underactuated systems may contain NMP behavior which causes much more challenging control problems.

Over the last years, research in the field of underactuated control systems have led to significant advance and several control methodologies have been proposed. In order to contribute to this research area, we propose to extend an interesting control approach (called IMC) to a class of continuous linear underactuated systems.

The IMC is considered as one of the most powerful control approaches thanks to its robustness and simplicity. In 1982, it was defined for Single-Input Single-Output systems (SISO) by Morari and Garcia and extended to Multi-Input Multi-Output (MIMO) ones in 1985 [3, 8]. Since then, several structures of continuous-time, discrete-time, linear and non-linear IMC have

been proposed [1, 2, 4, 5, 6, 7]. These studies have covered many classes of SISO systems and MIMO fully-actuated ones where the number of control inputs is equal to that of the outputs. Among the proposed IMC approaches, we are mostly interested in the IMC structure proposed in [7]. The specificity of this IMC structure resides in the use of a special controller which is an approximate inverse of the model plant. The use of this controller ensures a high level of robustness and system performance reservation even in the case of NMP systems and those with a time-delay [1, 5]. A number of studies of this IMC structure have been applied to both linear and non-linear SISO systems [1, 6, 7] as well as multivariable fully-actuated ones [2, 4]. The obtained results are very satisfactory which led us to extend the approach to a class of continuous linear multivariable underactuated systems.

An internal model controller of a class of continuous linear multivariable underactuated systems is presented in this paper. Cases of linear MP and NMP underactuated systems are studied. Simulation results confirm the effectiveness of the approach to ensure stability, accuracy and system performance reservation in spite of the presence of external disturbances, unstable zeros and non-zero initial conditions. The influence of the model parameters on the system behavior is also discussed.

The rest of this paper is divided into three sections. Firstly, the proposed approach is described beginning with a review of the IMC basic structure which was designed for linear multivariable fully-actuated systems, followed by the explanation of the encountered basic problems and the proposed solutions. Secondly, two illustrative examples, in which our proposed IMC structure is applied to cases of MP and NMP linear underactuated systems, are presented. Thirdly, the influence of non-zero initial conditions on the system evolution is treated and finally, effects of the model parameters are discussed.

II. THE PROPOSED APPROACH

A. The basic IMC structure

As presented in Fig. 1, the basic IMC structure consists of three principal parts: an internal model M chosen very close to the process allowing to predict the effect of the manipulated variables on the outputs, a controller C used to compute values of the manipulated variables that are based on present and past errors as well as set-point trajectories, and a filter which can be inserted to achieve a desired degree of robustness [1, 3, 7, 8].

The IMC structure has several advantages. For example, it guarantees the closed loop system stability, anticipates constraint violations and allows for corrective actions. Also, a perfect set-point satisfaction can be achieved despite the presence of external disturbances.

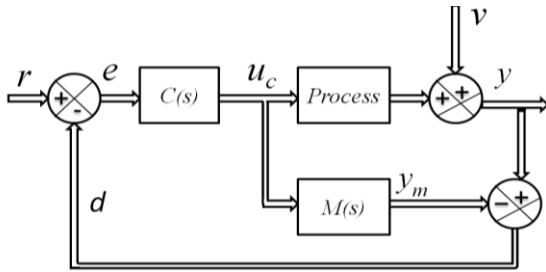


Fig. 1. IMC basic structure (MIMO fully-actuated systems)

The controller C is the inverse of the chosen model if it is realizable. Its structure and parameters are known a priori which simplifies the process of finding a suitable approximation for a practical implementation.

In the case of multivariable fully-actuated systems, n is the number of the system inputs and outputs, r is a reference signal of a dimension $(n \times 1)$, y is the process output vector of a dimension $(n \times 1)$, y_m is the model output vector of a dimension $(n \times 1)$, v is a disturbance signal affecting the system and u_c is the control input signal of a dimension $(n \times 1)$ [2, 4]. As shown in Fig. 1, the signal u_c , which is generated by the controller C , is applied to the plant and the model M alike. The signal d represents the calculated difference between the process output signal y and the model output signal y_m . It also represents the disturbance effect and the modeling errors, as shown in (1).

$$e = r - d = r - ((G(s) - M(s))u(s) + v(s)) \quad (1)$$

The signal d is then compared to the reference signal r to generate the controller input signal e .

In the case of linear multivariable fully-actuated systems, the process and its model can be presented by their square transfer matrices of dimension $(n \times n)$ or their space state representations [2, 4].

The internal model control structure is stable if and only if during the process, the model M and the controller C are stable in the open loop. In other words, the characteristic polynomials of the plant, the model and the controller state matrices should verify the Routh-Hurwitz stability criterion. The controller synthesis and stability conditions will be discussed in more details in the following section.

B. Main problems

The synthesis of an IMC controller that is equal to the inverse of the model expression is essential in order to ensure perfect set-point tracking. This inversion represents the basic problem of the IMC approach. In fact, the realization of the direct model inverse is difficult or not possible for most physical systems. This difficulty is due to the denominator order on the model expression, which is usually greater than the numerator one, or the presence of unstable zeros or/and

time delay. The direct model inversion is also impossible in the case of underactuated plants. In fact, the model must provide an accurate description of the process dynamics and characteristics. Therefore, the model expression must be very close to that of the plant. For underactuated systems, the number of control inputs is equal to m , the number of outputs is equal to n , and the transfer matrix of the plant is of a dimension $(n \times m)$ making it a non-square matrix. In this case, the model cannot be invertible. This represents the major problem encountered.

In addition to the system underactuation, the presence of NMP dynamics complicates the system control and makes it much more challenging. In fact, an NMP system, i.e., a system with zeros in the Right Half of the Plane (RHP), is presented by an NMP model. As explained previously, the controller which must be stable is an inverse of the model expression. This inversion may generate an unstable controller. To remedy these problems, we propose firstly to modify the IMC basic structure so that it becomes applicable to underactuated systems. Secondly, we design an approximate inverse of the model plant which is inspired of studies of [1, 7] in the case of SISO systems, and those of [2, 4] in the case of multivariable fully-actuated systems. This proposed controller represents a remedy for NMP systems.

These proposed solutions will be detailed in the following section. The system and model transfer matrix representations will be considered in order to simplify the study and the proposed approach explanation.

C. Proposed IMC structure for linear underactuated systems

1) The proposed IMC design

Underactuated systems are systems with more outputs than control inputs. Therefore, the transfer matrix of a linear underactuated system cannot be square. As mentioned in the previous section, on the one hand, the model M must be chosen as very close to the process G ; and on the other hand, the controller C is an approximate inverse of the model which requires a square transfer matrix M . The suggested solution consists of utilising a square model then eliminating the excess control inputs which are applied to the system. This procedure has led to the proposed IMC structure as presented in Fig. 2 [9, 10].

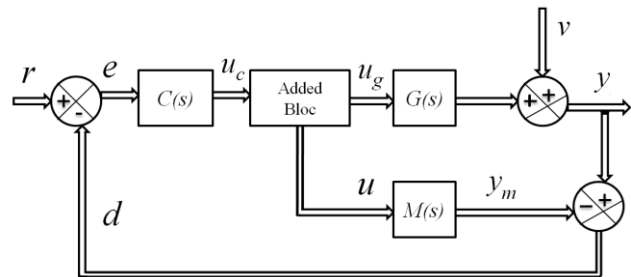


Fig. 2. IMC structure for linear multivariable underactuated systems

In fact, the transfer matrix $G(s)$ of a linear underactuated system (such that m is the number of system inputs, n is the system outputs one, and m is less than n) is of dimension $(n \times m)$. $G(s)$ is expressed by the following matrix.

$$G(s) = \begin{bmatrix} G_{11}(s) & \cdots & G_{1m}(s) \\ \vdots & & \vdots \\ G_{n1}(s) & \cdots & G_{nm}(s) \end{bmatrix} \quad (2)$$

The matrix $M(s)$ must be chosen close to $G(s)$, but as explained previously, the inversion problem requires that the matrix $M(s)$ must be square [2]. To solve this problem, a number of $(n \times (n-m))$ transfer functions are added to the matrix $M(s)$ in order to make it a square matrix having a dimension of $(n \times n)$ [9, 10]. Therefore, the IMC structure designed for multivariable fully-actuated systems (where $(m = n)$) can be applied. The $(n \times (n-m))$ added functions can be chosen as first-order transfer functions which verify the Routh- Hurwitz stability criterion in order to simplify the study and avoid inversion problems [9, 10]. The obtained matrix M is expressed by (3).

$$M(s) = \underbrace{\begin{bmatrix} M_{11}(s) & \cdots & M_{1m}(s) \\ \vdots & & \vdots \\ M_{n1}(s) & \cdots & M_{nm}(s) \end{bmatrix}}_{\substack{\text{Initial transfer} \\ \text{functions} \\ (n \times m)}} \underbrace{\begin{bmatrix} M_{1m+1}(s) & \cdots & M_{1n}(s) \\ \vdots & & \vdots \\ M_{mm+1}(s) & \cdots & M_{mn}(s) \end{bmatrix}}_{\substack{\text{added transfer} \\ \text{functions} \\ (n \times (n-m))}} \quad (3)$$

Secondly, the IMC structure designed for multivariable fully-actuated systems (proposed in [2]) is modified in order to eliminate the $(n-m)$ excess control inputs. To do so, a bloc is added to the basic IMC structure as shown in Fig. 2 [9, 10]. It is used to eliminate the $(n-m)$ excess control inputs acting on the process G by the use of usual arithmetic operators, as shown in Fig. 3.

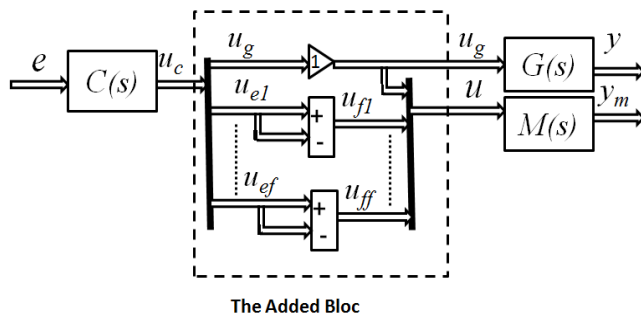


Fig. 3. The added bloc

Where u_g is the vector of the m control inputs acting on the process G ;

$u_e = [u_{e1} \dots u_{ef}]^T$ is the vector of the $(n-m)$ excess control inputs ;

$u_f = [u_{f1} \dots u_{ff}]^T$ is the vector of the $(n-m)$ eliminated excess control inputs.

u_f is the control input vector acting on the $(n \times (n-m))$ added transfer functions of the model M and u is the control input vector acting on the model M .

The control inputs vectors u and u_g , the signals d and e , and the system output vector y are given respectively by these following expressions and equations.

$$u = \underbrace{\begin{bmatrix} u_1 & \dots & u_m \end{bmatrix}}_{\substack{\text{Control inputs acting} \\ \text{on the plant} \\ (m \times 1)}} \underbrace{\begin{bmatrix} u_{m+1} = 0 & \dots & u_n = 0 \end{bmatrix}}_{\substack{\text{Eliminated excess control inputs} \\ ((n-m) \times 1)}}^T$$

$$u_g = [u_1 \dots u_m]^T \quad (4)$$

$$d(s) = G(s)u_g - M(s)u + v(s) \quad (5)$$

$$e(s) = r(s) - \underbrace{(G(s)u_g - M(s)u + v(s))}_{d(s)} \quad (6)$$

$$u_g(s) = u_{g1}(s) + u_{g2}(s) \quad (7)$$

where

$$\begin{cases} u_{g1}(s) = (C(s)G(s))^{-1}C(s)[r(s) - v(s)] \\ u_{g2}(s) = (C(s)G(s))^{-1}[C(s)M(s) - I_n]u(s) \end{cases} \quad (8)$$

$$y(s) = y_r(s)r(s) + y_v(s)v(s) + y_u(s)u(s) \quad (9)$$

where

$$\begin{cases} y_r(s) = G(s)(C(s)G(s))^{-1}C(s) \\ y_v(s) = I_n - G(s)(C(s)G(s))^{-1}C(s) \\ y_u(s) = G(s)(C(s)G(s))^{-1}[C(s)M(s) - I_n] \end{cases} \quad (10)$$

2) The controller design

The controller structure of multivariable linear systems that can be NMP is presented in Fig. 4 [1, 2, 7].

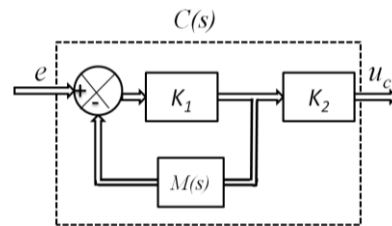


Fig. 4. The controller structure

Where $M(s)$ is the transfer matrix of the proposed model. It is of a $(n \times n)$ dimension. K_1 is a chosen square matrix of a $(n \times n)$ dimension and K_2 is a gain matrix of a $(n \times n)$ dimension. e is the controller input vector of a dimension $(n \times 1)$ and u_c is the control input vector of a dimension $(n \times 1)$.

The gain matrix K_2 is used to compensate the static errors, and the gain matrix K_1 is used to ensure the controller stability. In fact, the first part of this proposed controller which represents the approximate inversion approach is shown in Fig. 5. In this case, the controller can be expressed by (11).

$$C(s) = (I_n + K_1M(s))^{-1}K_1 = (K_1^{-1} + M(s))^{-1} \quad (11)$$

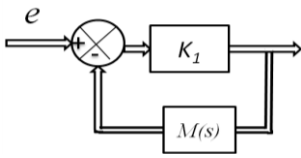


Fig. 5. The approximate inversion (multivariable systems)

Where I_n is the identity matrix of a dimension n and K_1 is an invertible square matrix ensuring the stability of the controller. In order to simplify our study, K_1 can be expressed by (12) where $a \in \mathbb{R}^+$.

$$K_1 = a I_n \quad (12)$$

If we choose a high value of a in (12), we obtain a small value of $\frac{1}{a}$ which allows to approximate $(K_1^{-1} + M(s))^{-1}$ with $M(s)^{-1}$. In this case, $C(s)$ is approximately equal to the model expression inverse as follows.

$$C(s) \approx M(s)^{-1} \quad (13)$$

Therefore, the system output vector expression given in (9) can be expressed by (14).

$$y(s) \approx y_r(s)r(s) + y_v(s)v(s) \quad (14)$$

The coefficients of the characteristic polynomial of the controller state matrix whose values depend on the value of a in (12) must satisfy the Routh-Hurwitz criterion in order to ensure the controller stability. Since $M(s)$ is stable, a suitable choice of the matrix K_1 ensures the controller stability. However, in the case of NMP systems, the adequate coefficient value of a cannot be chosen to be very high which can lead to the system accuracy degradation. In fact, in order to ensure the system accuracy, i.e., a zero static error, the controller static gain matrix $C(0)$ must be very close to the inverse of the model static gain matrix $M(0)$ as shown in (15), which is not possible in the case of a small value of a [2].

$$C(0) \approx M(0)^{-1} \quad (15)$$

In order to remedy this problem, the gain matrix K_2 presented in Fig. 4 is added. It allows to compensate the system static errors thanks to its expression given by (16) and ensures that $C(s)M(s) = I_n$.

$$K_2 = K_1^{-1}(I_n + K_1 M(0))M(0)^{-1} \quad (16)$$

The general controller expression for NMP multivariable systems is therefore presented by (17) as follows [2].

$$C(s) = K_2(I_n + K_1 M(s))^{-1} K_1 \quad (17)$$

III. ILLUSTRATIVE EXAMPLES

Two set-point signals r_1 and r_2 of type steps having an amplitude equal to 1 are applied to the following two examples, such that $r = [r_1 \ r_2]^T$. Nominal cases are considered, i.e., systems with no external disturbances.

A. The case of a linear MP underactuated system

Considering the following linear MP underactuated system with one control input u_1 and two outputs y_1 and y_2 . The system transfer matrix $G(s)$ is given by (18).

$$G(s) = \begin{pmatrix} \frac{s+2}{s^2+3s+2} \\ \frac{s+1}{4s^2+3s+1} \end{pmatrix} = \begin{pmatrix} G_1 \\ G_2 \end{pmatrix} \quad (18)$$

The model transfer matrix $M(s)$ is of a dimension (2×2) as explained previously. The system and the model outputs are expressed respectively by (19) and (20).

$$\begin{bmatrix} y_1 & y_2 \end{bmatrix}^T = G u_g = G u_1 \quad (19)$$

$$\begin{bmatrix} y_{m1} \\ y_{m2} \end{bmatrix} = \underbrace{\begin{pmatrix} M_{11} & M_{12} \\ M_{21} & M_{22} \end{pmatrix}}_{\text{The Model M}} \underbrace{\begin{bmatrix} u_1 \\ u_2 = 0 \end{bmatrix}}_{\substack{\text{The control} \\ \text{input vector} \\ u}} = M u \quad (20)$$

The model transfer functions M_{11} and M_{21} are successively chosen to be close to G_1 and G_2 . We consider the case of a perfect modeling, such that M_{11} is equal to G_1 and M_{21} is equal to G_2 . M_{12} and M_{22} are chosen as first order transfer functions so that they ensure the invertibility conditions of the matrix M . The chosen model is expressed by the following transfer matrix $M(s)$.

$$M(s) = \begin{pmatrix} \frac{s+2}{s^2+3s+2} & \frac{1}{s+2} \\ \frac{s+1}{4s^2+3s+2} & \frac{3}{s+4} \end{pmatrix} \quad (21)$$

The application of the Routh-Hurwitz stability criterion allows to assess the necessary and sufficient condition of the controller stability. In the case of this system, we must choose $a > -0.72$ such that $K_1 = a \times I_2$. The proposed IMC design presented in Fig. 2 is applied and the controller of Fig. 4 is used in order to ensure a greater accuracy.

In this study, two cases are considered. In the first case, the gain matrix K_1 is chosen to be equal to $1 \times I_2$ ($a = 1$), and in the second case, K_1 is equal to $40 \times I_2$ ($a = 40$).

The gain matrix K_2 which is relative to $K_1 = 1 \times I_2$ is given by (22).

$$K_2 = \begin{pmatrix} 2.5 & -1 \\ -1 & 3 \end{pmatrix} \quad (22)$$

The gain matrix K_2 which is relative to $K_1 = 40 \times I_2$ is given by (23).

$$K_2 = \begin{pmatrix} 1.0375 & -0.0250 \\ -0.0250 & 1.0500 \end{pmatrix} \quad (23)$$

Fig. 6 and Fig. 7 show the system control inputs evolution in the cases where $a = 1$ and $a = 40$, respectively.

Fig. 8 and Fig. 9 show the system outputs signals in the cases where $a = 1$ and $a = 40$, respectively.

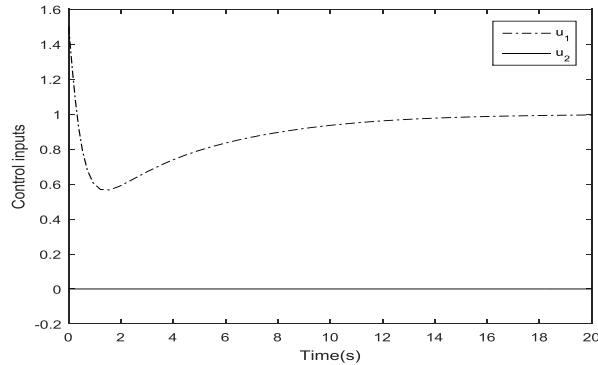


Fig. 6. Control inputs (linear MP underactuated system, case of $a = 1$)

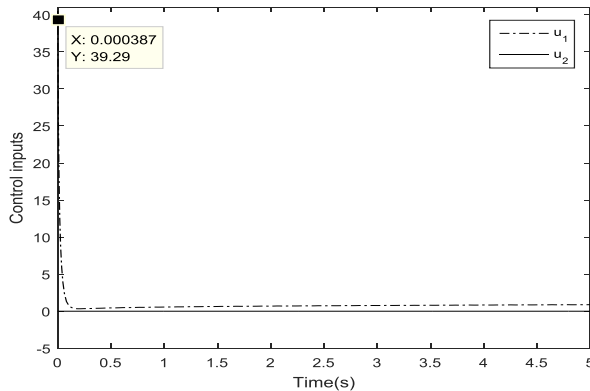


Fig. 7. Control inputs (linear MP underactuated system, case of $a = 40$)

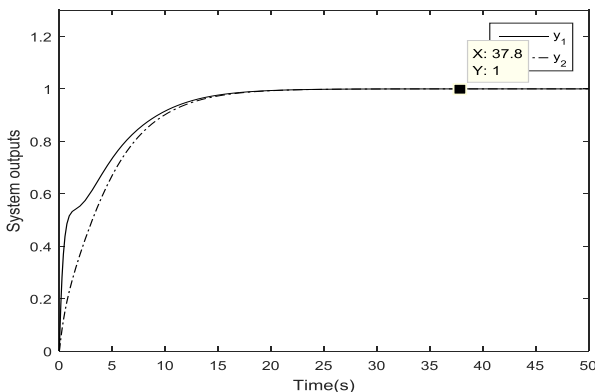


Fig. 8. System outputs (linear MP underactuated system, case of $a = 1$)

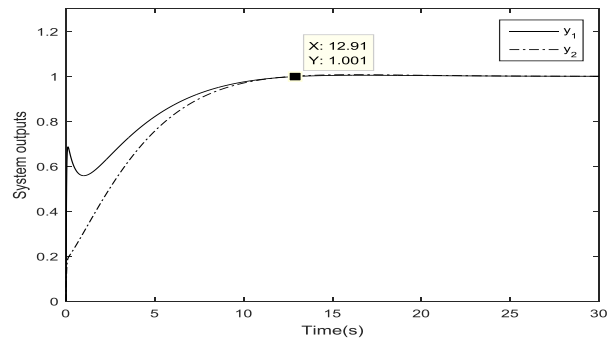


Fig. 9. System outputs (linear MP underactuated system, case of $a = 40$)

It can be shown in Fig. 6 and Fig. 7 that the excess control input u_2 is successfully eliminated. Simulation results also show the effects of the choice of the coefficient a on the system behavior. The more the value of a increases, the more the system responses are fast and accurate. This is explained by the fact that the approximated inverse is closer to the real inverse of the model. However, we note a significant peak of the control input u_1 which appears at the initial instants in Fig. 7 which is due to the high value of a . The more the value of a increases, the more the peak is high. This is due to the fact that the system at boot acts as an open-loop system controlled by a control signal vector $C(s)$ which is equal to $a \times r(s)$. The peak is then eliminated by the feedback effect.

The problem of the control input peak can be solved by the use of a saturation bloc that is added to the controller configuration as shown in Fig. 10 [1].

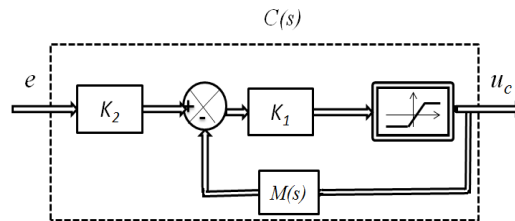


Fig. 10. Controller structure with a saturation bloc

The same linear MP underactuated system presented in (18) and the case where $K_1 = 40$ are considered. The gain matrix K_2 is presented in (23).

Fig. 11 shows the control input evolution after having applied the controller structure in Fig. 10. Maximum eligible values of the control input u_1 must be equal to -10 and 10. It is shown that u_1 has not exceeded the landmarks. It is also noted that the addition of the saturation block does not affect the system accuracy and stability.

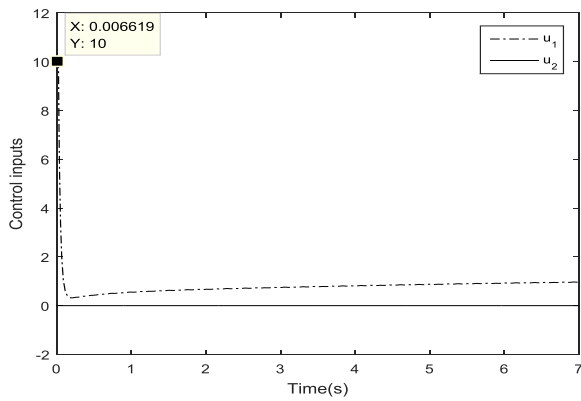


Fig. 11. Control inputs

The next example presents the case of a linear NMP underactuated system.

B. The case of linear NMP underactuated system

We present in this example one control input/two outputs NMP system. It is represented by the following transfer matrix

$$G(s) = \begin{pmatrix} \frac{1-s}{s^2+s+1} \\ \frac{s+1}{s^2+2s+1} \end{pmatrix} = \begin{pmatrix} G_1 \\ G_2 \end{pmatrix} \quad (24)$$

where the unstable zero of $G(s)$ is equal to 1.

The case of a perfect modeling is considered. So, the transfer function M_{11} is chosen to be equal to G_1 and M_{21} is chosen to be equal to G_2 . M_{12} and M_{22} are chosen as first order transfer functions with stable poles and zeros in order to simplify the calculations and avoid model inversion and controller stability problems.

The model M is presented by the transfer matrix given in as follows.

$$M(s) = \begin{pmatrix} M_{11} & M_{12} \\ M_{21} & M_{22} \end{pmatrix} = \begin{pmatrix} \frac{1-s}{s^2+s+1} & \frac{1}{s+2} \\ \frac{s+1}{s^2+2s+1} & \frac{1}{s+1} \end{pmatrix} \quad (25)$$

The model has one unstable zero (equal to 1) which may cause instability of the controller if we apply a direct inversion of the model. The controller structure described in Fig. 4 allows us to overcome this blocking problem. In fact, the application of the Routh–Hurwitz stability criterion on the controller characteristic polynomial whose coefficients depend on the value of a allows us to determine the necessary and sufficient condition of the controller stability which is found to be $a < 0.87$. In this case, the stabilizing value of a is small. So, the approximated inverse model is different from the real one which requires the addition of the gain matrix K_2 expressed in (16). In our case, the gain matrices K_1 and K_2 are respectively equal to (26) and (27).

$$K_1 = 0.1 I_2 \quad (26)$$

$$K_2 = \begin{pmatrix} 21 & -10 \\ -20 & 21 \end{pmatrix} \quad (27)$$

The control inputs and the system outputs are respectively presented in Fig. 12 and Fig. 13.

Simulation results prove the effectiveness of the approach to ensure a fast set-point tracking and to preserve the system performances in spite of the presence of underactuation and non-minimum phase behavior.

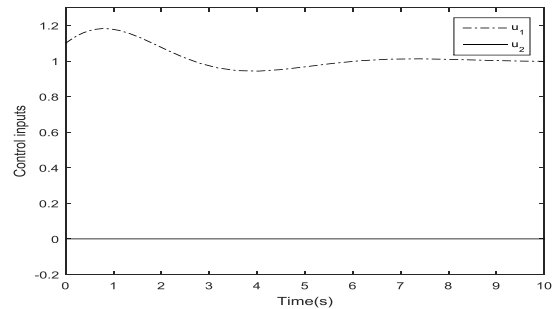


Fig. 12. Control inputs

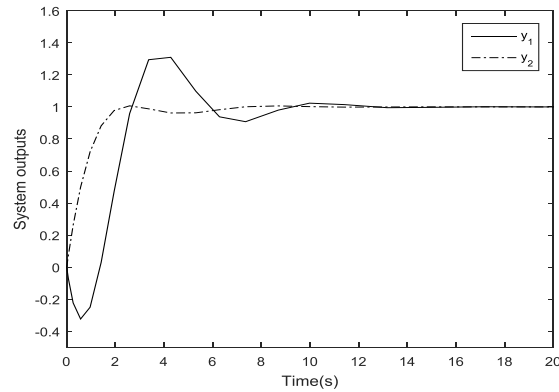


Fig. 13. System outputs

In what follows, the implementation problems of the proposed IMC structure are discussed. Indeed, the influences of external disturbances, initial conditions and model parameters on the system behavior are studied.

IV. IMPLEMENTATION OF THE PROPOSED IMC STRUCTURE

The linear underactuated system which is presented in (18) is considered in all the following examples and the controller structure of Fig. 4 is used. The chosen gain matrix K_1 is equal to $40 \times I$ and the reference signals are chosen to be steps of amplitude equal to 1.

A. The case of disturbed system

In order to show a significant improvement of the accuracy and the disturbance rejection capability of the proposed IMC structure, we consider the case of a disturbed system where the disturbance signals v_1 and v_2 are chosen to be steps of amplitude 1 that occurs at $t = 20s$ as in (28).

$$v(s) = [v_1 \quad v_2]^T = \begin{bmatrix} \frac{e^{-20s}}{s} & \frac{e^{-20s}}{s} \end{bmatrix}^T \quad (28)$$

The case of a perfect modeling is considered. The model is expressed by its transfer matrix given by (21). The gain matrix K_2 is presented in (23).

Control inputs and system outputs are respectively presented in Fig. 14 and Fig. 15. Simulation results show that the IMC designed for linear underactuated systems guarantee an accurate set-point tracking and a fast disturbance rejection proving the robustness of the proposed approach.

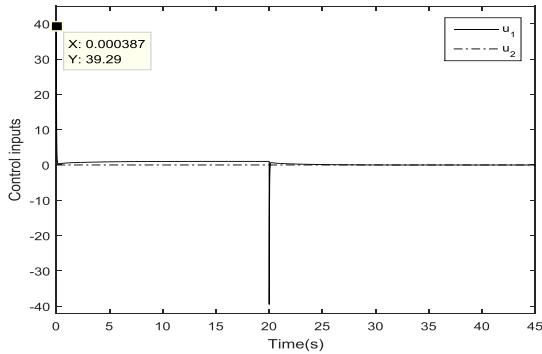


Fig. 14. Control inputs

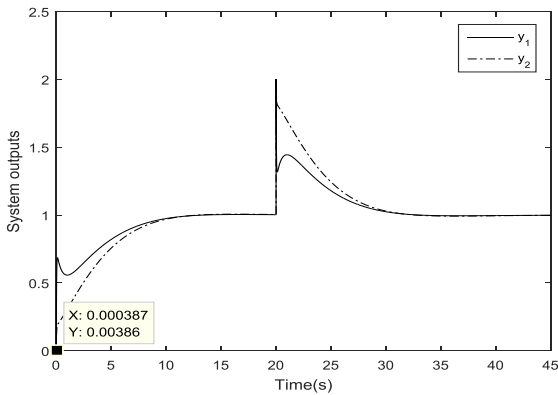


Fig. 15. System outputs

As we mentioned in the previous section, the control inputs peaks values can be reduced by the use of the controller structure with saturation bloc which was presented in Fig. 10.

B. The case of non-zero initial conditions

We consider the model presented in (21) and the gain matrix K_2 given by (23).

The transfer matrix representation does not reveal the system evolution if it is not initially relaxed. So, we convert it into an equivalent state-space representation. This model and process representations are given respectively by (29) and (30) in a canonical form.

$$A_G = \begin{pmatrix} -3 & -2 & 0 & 0 \\ 1 & 0 & 0 & 0 \\ 0 & 0 & -0.75 & -0.5 \\ 0 & 0 & 0.5 & 0 \end{pmatrix} \quad B_G = \begin{bmatrix} 2 \\ 0 \\ 1 \\ 0 \end{bmatrix} \quad (29)$$

$$C_G = \begin{pmatrix} 0.5 & 1 & 0 & 0 \\ 0 & 0 & 0.25 & 0.5 \end{pmatrix}$$

$$A_M = \begin{pmatrix} -3 & -2 & 0 & 0 & 0 & 0 \\ 1 & 0 & 0 & 0 & 0 & 0 \\ 0 & 0 & -0.75 & -0.5 & 0 & 0 \\ 0 & 0 & 1 & 0 & 0 & 0 \\ 0 & 0 & 0 & 0 & -2 & 0 \\ 0 & 0 & 0 & 0 & 0 & -4 \end{pmatrix} \quad B_M = \begin{bmatrix} 2 & 0 \\ 0 & 0 \\ 0.5 & 0 \\ 0 & 0 \\ 0 & 1 \\ 0 & 2 \end{bmatrix} \quad (30)$$

$$C_M = \begin{pmatrix} 0.5 & 1 & 0 & 0 & 1 & 0 \\ 0 & 0 & 0.5 & 0.5 & 0 & 1.5 \end{pmatrix}$$

The disturbance vector presented in (28) is considered. We study these two examples of non-zero initial conditions of the system outputs:

$$y(t = 0s) = [y_{01} \ y_{02}]^T = [0.75 \ 0.375]^T ;$$

$$y(t = 0s) = [y_{01} \ y_{02}]^T = [1.53 \ 0.675]^T .$$

The resulting simulations are illustrated in Fig. 16 and Fig. 17 respectively. It can be shown that even for model and system initial conditions that may be non-zero and different, only the transient region of the output signals is affected which proves the robustness of the proposed control structure.

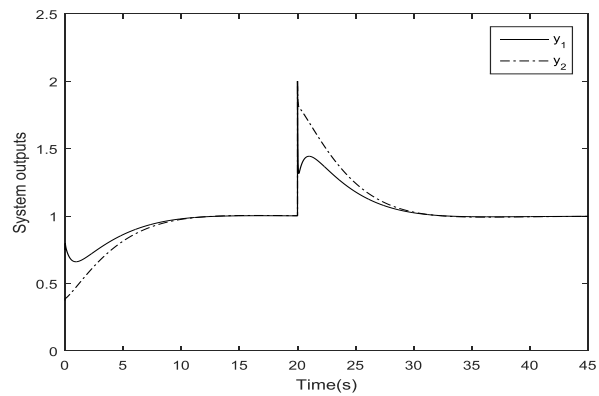


Fig. 16. System outputs

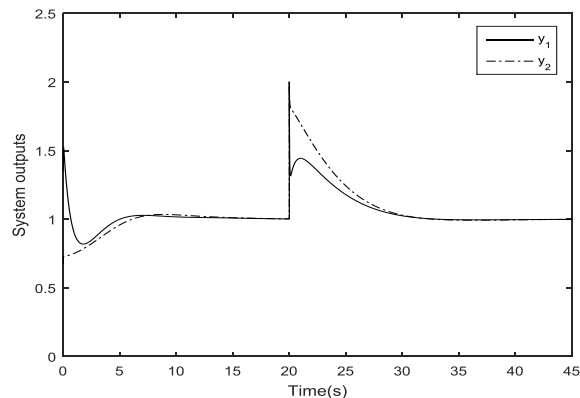


Fig. 17. System outputs

C. The case of imperfect modeling: model parameters effects

The IMC approach is based on an accurate linear model, but in many cases such as changes in process settings, sensors measuring imprecision, the system linearization, system parametric uncertainties, etc, modelling cannot be highly

precise. Such model cannot provide a perfect description of the process behavior. Therefore, it can affect the process stability and/or precision which has led us to study the case of an imperfect model and test its parameter effects on the system evolution. These tests can help us to choose the model that best describes the controlled system and does not affect its stability.

The studied system is the linear underactuated system presented in (18). The gain matrix K_2 is given by (23). We present in the following the case of an imperfect modeling caused by the difference between the value of the process Damping Ratio (DR) and that of the model. We consider the model presented by the transfer matrix given by (31). The nominal case is studied.

The model and system DR values are denoted respectively as DRM and DRS.

$$M(s) = \begin{pmatrix} M_{11}(s) & \frac{1}{s+2} \\ \frac{s+1}{4s^2+3s+2} & \frac{3}{s+4} \end{pmatrix} \quad (31)$$

In the following tests, the DR value of the model transfer function (M_{11}) is chosen to be very different from that of the process (G_1).

1) Test 1: $DRM \gg DRS$

In this case, the transfer matrix $M_{11}(s)$ is given by (32).

$$M_{11}(s) = \frac{s+2}{s^2+30s+2} \quad (32)$$

The system outputs are illustrated by Fig. 18. It can be shown that even for a high value of DRM, the system stability is maintained while the reference signal tracking becomes much slower.

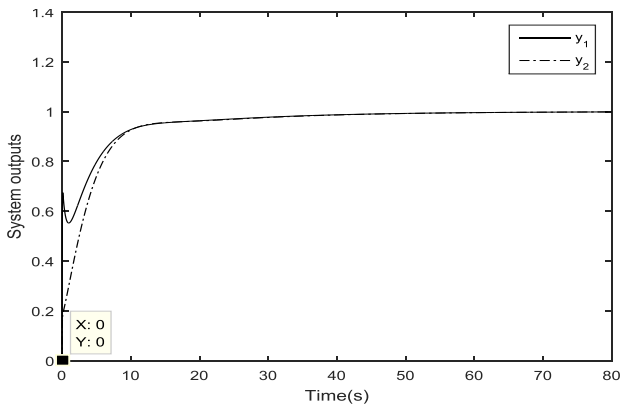


Fig. 18. System outputs

2) Test 2: $DRM \ll DRS$

The chosen transfer matrix $M_{11}(s)$ is given by (33).

$$M_{11}(s) = \frac{s+2}{s^2+0.01s+2} \quad (33)$$

The system outputs are presented in Fig. 19.

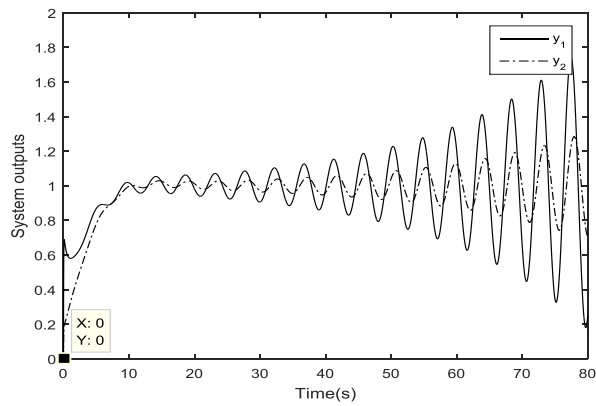


Fig. 19. System outputs

The obtained simulation results show that, in the case of a much smaller value of the DRM as compared to the DRS, the system becomes unstable.

In fact, the model response becomes much faster than that of the system. As a result, their outputs are added instead of being compared and the process behavior becomes equivalent to that of an open-loop system.

V. CONCLUSION

In this paper, a new approach to the IMC of continuous linear multivariable underactuated systems is presented. The realized research treats the case of underactuated MP and NMP systems.

Effects of non-zero initial conditions and model parameters on the system evolution are discussed.

Simulation results show the accuracy and the rapid disturbance rejection capability of the proposed IMC structure proving its robustness and its ability to remedy the problems caused by the system underactuation, the system NMP behavior, and non-zero initial conditions.

REFERENCES

- [1] M. Naceur, "Sur la commande par modèle interne des systèmes dynamiques continus et échantillonnés," PhD dissertation, ENIT, Tunis, 2008.
- [2] N. Touati, D. Soudani, M. Naceur and M. Benrejeb, "On the internal model control of multivariable linear system," International Conference on Sciences and Techniques of Automatic control and computer engineering, STA, Sousse, 2011.
- [3] M. Morari and E. Zafiriou, "Robust Process Control," Ed. Prentice Hall, Englewood cliffs, N.J., 1989.
- [4] N. Touati, D. Soudani, M. Naceur and M. Benrejeb, "On an internal multimodel control for nonlinear multivariable system – A comparative study," International Journal of Advanced Computer Science and Applications, IJACSA, Vol. 4, No.7, 2013.
- [5] M. Touzri, M. Naceur and D. Soudani, "A new design method of an Internal Multi-Model controller for a linear process with a variable time delay," International Conference on Control, Engineering & Information, CEIT, Sousse, 2013.
- [6] C. Othman, I. Ben Cheikh, and D. Soudani, "On the Internal Multi-Model Control of Uncertain Discrete-Time Systems," International Journal of Advanced Computer Science and Applications, IJACSA, Vol. 7, No.9, 2016.

- [7] M. Benrejeb, M. Naceur, D. Soudani, "On an internal model controller based on the use of a specific inverse model," International Conference on Machine Intelligence, ACIDCA, Tozeur, 2005.
- [8] C.E. Garcia and M. Morari, "Internal model control. I. A unifying review and some results," *Ind Eng.Chem. Process. Des.*, Vol.21, 1982.
- [9] A. Mezzi, D. Soudani and M. Benrejeb, "On the Internal Model Control of Multivariable Linear Underactuated Systems," Multi-Conference on Computational Engineering in Systems Applications, CESA, Marrakech, 2015.
- [10] A. Mezzi, and D. Soudani, "On the Internal Model Control of Multivariable Linear Underactuated Systems : Effects Of Initial Conditions," International Conference on Automation, Control, Engineering and Computer Science, ACECS, Sousse, 2015.

Comparison Study of Different Lossy Compression Techniques Applied on Digital Mammogram Images

Ayman AbuBaker*

Electrical and Computer Eng. Dept.
Applied Science Private University
Amman, Jordan

Mohammed Eshtay

Faculty of Information Technology
Applied Science Private University
Amman, Jordan

Maryam AkhoZahia

Electrical and Computer Eng. Dept.
Applied Science Private University
Amman, Jordan

Abstract—The huge growth of the usage of internet increases the need to transfer and save multimedia files. Mammogram images are part of these files that have large image size with high resolution. The compression of these images is used to reduce the size of the files without degrading the quality especially the suspicious regions in the mammogram images. Reduction of the size of these images gives more chance to store more images and minimize the cost of transmission in the case of exchanging information between radiologists. Many techniques exist in the literature to solve the loss of information in images. In this paper, two types of compression transformations are used which are Singular Value Decomposition (SVD) that transforms the image into series of Eigen vectors that depends on the dimensions of the image and Discrete Cosine Transform (DCT) that convert the image from spatial domain into frequency domain. In this paper, the Computer Aided Diagnosis (CAD) system is implemented to evaluate the microcalcification appearance in mammogram images after using the two transformation compressions. The performance of both transformations SVD and DCT is subjectively compared by a radiologist. As a result, the DCT algorithm can effectively reduce the size of the mammogram images by 65% with high quality microcalcification appearance regions.

Keywords—Mammogram Images; DCT Compression; SVD compression; Microcalcifications

I. INTRODUCTION

The emergence of internet and the vast development of web technologies in addition to the popularity of social networks, image sharing and video application triggered the inevitable need for minimizing the amount of digital information stored and transmitted. The size of images is increasing with the advancement in digital cameras and the more availability of storage devices. Hence as the size increases, more storage we need for storing these files and the higher bandwidth we need for transmission [1]. Suppose we have a color image of 3200 pixel width and 2500 pixel height, the color image usually has three components for each picture, red, green and blue (RGB). The size of such an image will be 22.9 MB.

The solution for these challenges is to apply compression to minimize the size needed for storage and transmission of such images taking into account keeping the image with good quality [2,3]. The aim of the compression techniques is to reduce the redundancy and the irrelevant data. Many techniques used to compress images, predictive coding uses the decorrelation between the pixels of the image to eliminate or reduce redundancy. Huffman coding is an example of such a

technique where we give variable length coding for redundant data depending on statistical information. Wavelet transform is another type of compression techniques that deals with the image as a series of wavelets. Wavelet transforms separate signals into wavelets and then it uses the coefficients for compression by discarding some of these coefficients that will not cause big effect on the quality of the image. Wavelet transforms are very useful for compression because it reveals the fine details of the signal [1,4]. JPEG uses the discrete cosine transform (DCT) which is one of the most popular techniques used for image compression. Another technique uses the linear approximation of matrices for compression is singular value decomposition (SVD) [4].

Moreover, using the image compression techniques in medical image is crucial since it relates directly to the human life. The digital mammogram image is one of the medical images that varies in the size between 8 MB and 55 MB. Also, many studies indicated that the detection accuracy may decrease of microcalcifications tumors by radiologists if the images are digitized less than at 0.1 mm x 0.1 mm. Therefore, the mammogram images need to be reduced using compression techniques that minimize the required storage as well as maintain the microcalcification clear for the radiologist.

This paper will evaluate the performance of two compression techniques: full frame discrete cosine transform (DCT) with entropy coding and singular value decomposition (SVD) on digital mammogram images. The dependence of their efficiency on the compression parameters was investigated. The techniques are compared in terms of the trade-off between the bit rate and the detection accuracy of subtle microcalcifications by a specialist radiologist.

The remainder of this paper is organized as follows. Section II reviews some basic preliminaries like Singular Value Decomposition (SVD) and Discrete Cosine Transform (DCT). In Section III, literature review is visited. The implementation of SVD and DCT on mammogram images is presented in section IV. Experiments and evaluation of the results have been presented in Section V. Section VI concludes the work with some future directions.

II. THEORETICAL BACKGROUND

Compression is a term that describes the process of reducing the number of bytes required to store or transmit the image without degrading the quality of the image to an unacceptable level.

The objective of image compression is reducing or eliminating irrelevant and redundant data to efficiently store and transmit images. The sources of redundancy can be divided into the following three categories [2].

1) Coding redundancy: Huffman coding is a famous example of coding redundancy. The idea is to assign variable length codes to combinations depending on the frequency of appearances of these combinations in the original data. Statistical approach is used to bind the appropriate combination with the appropriate code [1].

2) Spatial redundancy: Spatial redundancy is term that describes the elements that are duplicated in the structure. In digital images the neighboring pixels are usually similar, one of the techniques that uses this type is constant area encoding [1].

3) Irrelevant data: Many of the information existed in 2D arrays that represent images are ignored by the human vision systems. The idea is to discard the data that is less important and hardly noticed by the human. Human eye is less sensitive to higher level frequencies. Many of the compression techniques use this property to eliminate or reduce redundancies of such type of information. Discrete cosine transform is a well-known technique of this type [1].

The compression techniques are usually classified into two major categories: lossless and lossy techniques. Lossless algorithms preserve the same information so we can get the original data anytime and they are actually exploits the data redundancy in the original data. Examples of lossless techniques are Huffman, run length encoding and Lempel-Ziv-Welch (LZW) Coding. Lossy algorithms do not retain the original so they are called irreversible. Lossy algorithms exploit both data redundancy and human perception properties. As a result of eliminating part of information we can get higher compression rates using lossy techniques [5].

A. Singular Value Decomposition (SVD)

SVD can be viewed through three different points of view: the first one is that SVD is a method to transform set of correlated variable into set of uncorrelated variables that describes the relationships between the data items. The second point of view sees SVD as a method to specify the dimensions in which the data items represent high variations. The third one is that as we recognize the biggest variation of data we can reach the best approximation using fewer dimensions Fig. 1[8].

The main idea of SVD is taking high data set dimensions and reduces it to fewer dimensions with retaining the original substructure of the data. The main reason behind using SVD in compression is that we can work with it as a method for data reduction.

In linear algebra SVD is a way to compose matrix into series of linear approximations. SVD factorize the matrix into product of matrices [9]. So, SVD of matrix M is a factorization of the form as in (1):

$$M_{mn} = U_{mm} \Sigma_{mn} V_{nn}^T \quad (1)$$

Where Σ is a diagonal matrix that only contains the diagonal entries σ_i . σ_i of Σ are called the singular values of M . The columns of U are called the left-singular vectors of M and

the columns of V are called the right-singular vectors of M [8] as in (2).

$$UTU=I, VTV=I \quad (2)$$

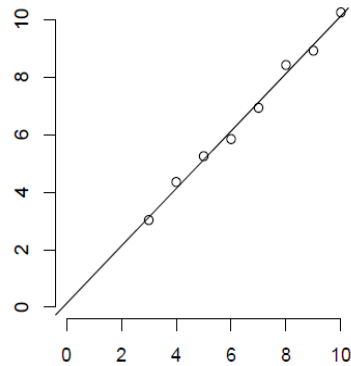


Fig. 1. SVD reduce data from two dimensions to one dimension

Each column in U is one of the orthonormal eigenvectors of MM^T , and each column of V is one of the orthonormal eigenvectors of $M^T M$. The singular values of M are the square roots of eigenvalues of U or V in descending order.

Applying SVD decompose the image into three matrices but doing this only does not compress the image actually. To perform the compression we need only to retain few number of singular values of the diagonal matrix [9].

Since the singular values $\sigma_1 \geq \dots \geq \sigma_n$ then the first value of the diagonal matrix has the biggest impact on the total sum, followed by the second value and so on. Thus the singular values in the bottom of the list contain negligible value and can be discarded for the sake of compression.

The approximation is performed by taking only the first few terms of the diagonal matrix as shown in (3).

$$M_{approx} = \sum_{i=1}^k \sigma_i u_i v_i \quad (3)$$

As k increases the image quality increase but also the needed memory of storage is also increased.

B. Discrete Cosine Transform (DCT)

The DCT works by transforming image from spatial representation into frequency domain. The image is separated into parts of differing frequencies. Image is represented as a sum of sinusoids of varying magnitude and frequencies. DCT is high energy compact so the most significant image information is concentrated in few coefficient of DCT [5].

The less important frequencies are discarded hence the lossy compression. The only important frequencies are used to retrieve the image in the decompression process.

The steps of DCT compression that shown in Fig.2 are summarized as follows:

- 4) Input image (MxN).
- 5) Initiate subimages blocks (8x8).
- 6) Apply DCT on each block.
- 7) Quantization process.
- 8) Use symbol encoder such as Huffman coding.

The step of quantization will normalize the resultant matrix taking into account the psycho visual properties. Selecting of the quantization matrix has effect on the compression ratio.

One of the most attractive properties of DCT is that it preserves the most information of the image in fewest coefficients [7].

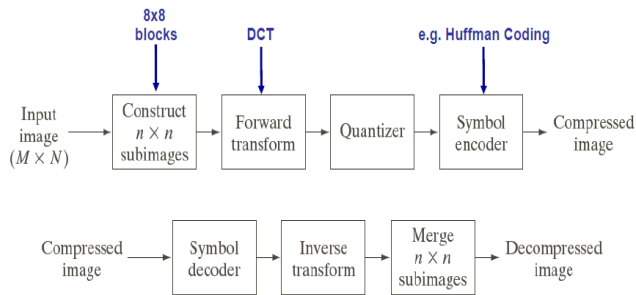


Fig. 2. DCT compression steps

III. LITERATURE REVIEW

Image size reduction is a critical stage in many image processing systems for applications such as mammography, multimedia and electronic publishing [14, 27]. Many techniques are available to magnify or reduce images ranging from linear interpolation to cubic spline interpolation [10, 19, 20, 26].

Image interpolation has a central role in many applications [27, 24]. One was changing the size of a digital image according to the nature of the display device. According to Chuah and Leou [12], three categories exist for image interpolation: static image interpolation [13, 23], multi-frame image interpolation [11, 26], and image sequence (video) interpolation [11].

One of the simplest techniques for image interpolation is the nearest neighbor pixel. In this approach, the intensity of every pixel in the resultant image is set equal to the intensity of its nearest corresponding pixel in the original image. This method is extremely simple to implement but tends to produce images with a clustered or blocky appearance due to the low interpolation order. Bi-linear interpolation is another interpolation technique that uses the weighted average value of the four pixels nearest the exact position of a pixel in the source image corresponding to a pixel in the final image [21, 24]. However, small points in high resolution images, such as mammogram images, will be eliminated by this bi-linear interpolation since interpolation using 4 neighbor pixels was not enough for small or so hazy points. Another interesting interpolation method is the bi-cubic interpolation technique. Bi-cubic interpolation is a sophisticated technique that produces smoother edges than bi-linear interpolation [16]. This method combines better effectiveness and lower complexity compared to other interpolation techniques [21]. In mammogram images there are no abrupt changes between the neighboring pixels. Therefore, using bi-cubic interpolation will generate a representative pixel from 16 neighboring pixels that will facilitate scaling down mammogram images. Herasa et al. [17] compared the visual appearance of three interpolation methods linear, bi-cubic and the parametric spline method,

which was a compromise between the previous two methods. They build a robust algorithm OPED for the reconstruction of images from Radon data using these interpolation methods. The bi-cubic interpolation showed a good performance with a significantly lower Normalized Mean Square Error (NMSE) than the other methods.

Other algorithms have been developed with modified interpolation processes. Kim et al. [16] proposed a new image scaling algorithm called the Winscale algorithm. The scaling (up/down) in this algorithm was based on the use of an area pixel model rather than a point pixel model. As a result, the Winscale algorithm produced effective results for image processing systems that required high visual quality and low computational complexity. However, its performance was similar to the bi-linear interpolation technique [15]. An adaptive algorithm was proposed by Chuah and Leou [12] to interpolate low resolution (decimated) image frames. In this algorithm, two nonlinear filters were used to generate high-frequency components iteratively that were lost during the implementation of the resolution reduction procedure, then a blocking artefacts-reduction scheme was adopted to improve the image quality. Abe and Iiguni [25] investigated the discrete cosine transform (DCT) in down-sampled images and proposed high-resolution (HR) image restoration from a down-sampled low-resolution (LR) image using the discrete cosine transform (DCT). Their algorithm showed a superior performance compared to cubic spline interpolation in the HR image restoration as long as the amount of the additive noise was small.

Many reduction techniques were based on image interpolation that was followed by a re-sampling process. These techniques were simple to implement but produce sub-optimal results [20]. Another technique used in image reduction utilizes the mean of each non-overlapping 8x8 pixel neighbourhood [18]. This blurred the breast boundary since the boundary was averaged with the background. As a result, an important breast regions such as microcalcification are lost which means that there are a significant loss of the information in the original mammogram images.

IV. THE ALGORITHM IMPLEMENTATION

Mammogram images show abnormal structures inside a breast, and one of the important breast tumors is microcalcification (MC). Since microcalcifications are small (less than 1mm across [26]), there is a necessity for high resolution images in order to show MCs clearly in the mammogram images. Therefore, mammogram images are high-resolution and large size images that require specialized computing capabilities to process. Moreover, transmitting these images over computer networks can be difficult and may require image compression. Therefore, a size-reduction pre-processing stage is needed for most mammography-based systems. During this size-reduction stage, two aspects have to be carefully considered and preserved; the image quality and the MC appearance in the mammogram images.

As preprocessing stage, the images segmentation algorithm is implemented on the digital mammogram images as in [28]. The breast region covers up to 75% of the mammogram image.

This involves partitioning a given image into breast and background regions. This segmentation method is robust enough to handle the wide range of mammographic images that are obtained from different acquisition systems and from different types of breast glandular tissues. Breasts can be classified to three categories based on their glandular tissues density as fatty, normal, and dense. In the segmentation process, fatty breasts present the most difficulty because the intensities of some regions of the breast are very close to the background region intensity. Another challenge was in removing artefacts, such as the image name and labels from the mammogram images.

In this work, 40 microcalcification mammogram images are selected from the University of South Florida (USF). These images are collected from different medical schools and hospitals across the USA. These images all have the same specification (3000 pixel \times 4500 pixel and 16-bit pixel depth). These MC images are processed using two types of compression techniques (SVD and DCT). The MATLAB platform was used to formulate these techniques also, the code of these techniques is presented in Appendix A. Fig. 3 shows the result of image compression of both SVD and DCT techniques.

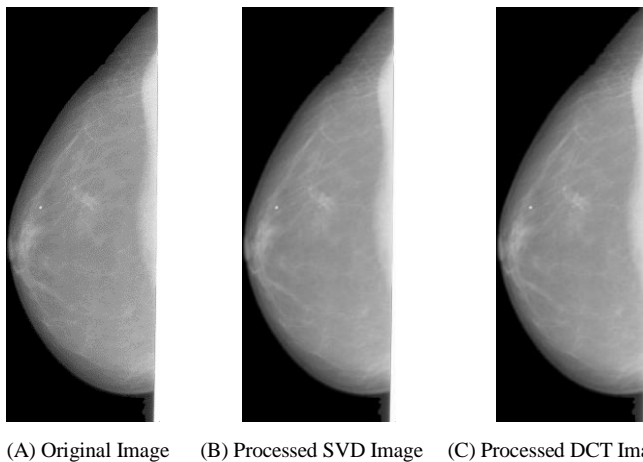


Fig. 3. Implementation SVD and DCT compressions on Mammogram Images

V. IMAGE COMPRESSION EVALUATION

Forty mammogram images from USF databases are used in this evaluation process. The processed images are later subjectively compared with the original images and specially focused on the microcalcifications regions. The compression ratio and image quality for both SVD and DCT techniques are reported. The image quality for the microcalcification is reported based on the radiologist diagnoses for each resulted image. The following subsection presented the evaluation process for both compression techniques.

A. SVD Evaluation Results

In the first step, the microcalcification mammogram images are processed using the SVD compression technique as shown in Fig. 4. The algorithm performance is reported as shown in Table I.

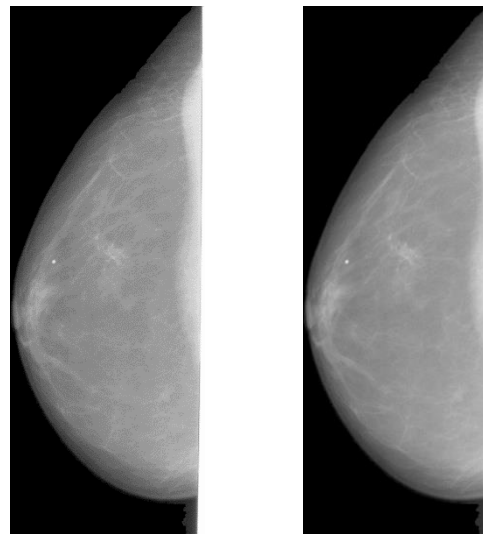


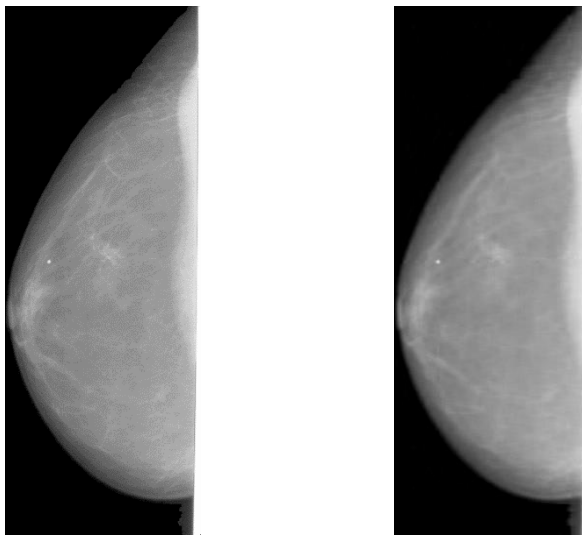
Fig. 4. Processed Mammogram images using SVD Compression

TABLE I. EVALUATION THE PERFORMANCE OF SVD COMPRESSION TECHNIQUE

Singular Values	Compression Ratio	Image Quality(%)
5	2.14	0
30	1.95	0
55	1.79	25
80	1.67	50
105	1.59	75
130	1.54	80
155	1.49	100
180	1.43	100
205	1.42	100
230	1.41	100

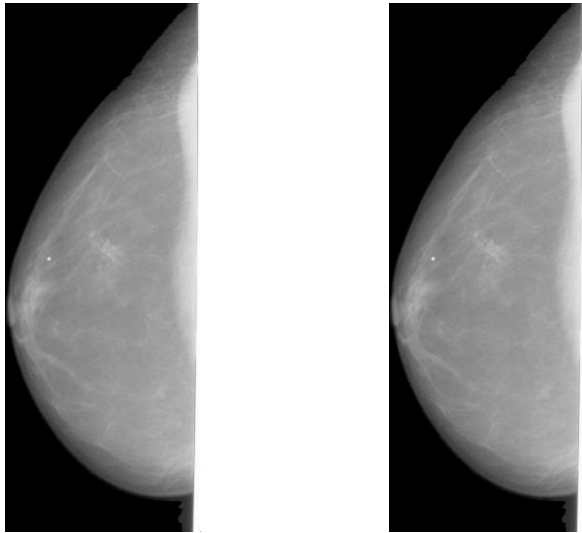
As shown in the Table I, the performance of SVD is very bad for low number of singular values and becomes better when this number is increased. So, the optimum value that can has a high compression ratio with high quality is 155 singular value. Whereas, the 230 singular value has also high quality image but the compression ratio is decreased. Figure 5, show the results of SVD compression image with different singular values.

The criteria of reduction storage in SVD is calculated using the formula $k \times (m + n + 1)$ bytes instead of $m \times n$ bytes of the original image, where the k is number of top singular values. The k values should be smaller than $\frac{m \times n}{(m+n+1)}$.



(A) Original image

(B) SVD 30



(C) SVD 80

(D) SVD 155 Singular Value

Fig. 5. Processed Mammogram images using different SVD levels

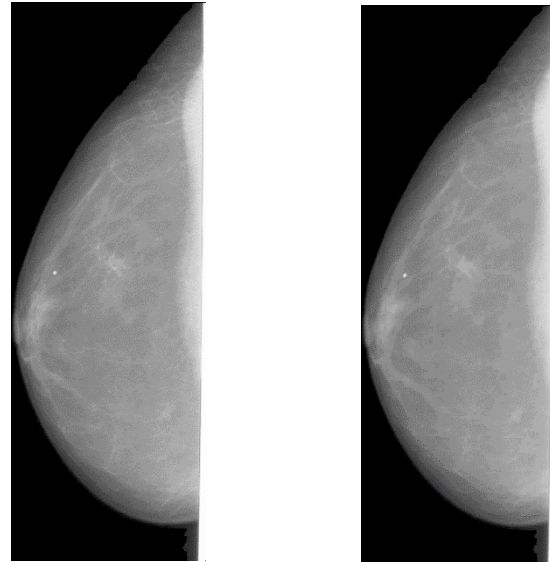
B. DCT Evaluation results:

The same microcalcification mammogram images are also processed using the DCT compression technique. The compression ratio and image quality is also considered in this evaluation as shown in Table II.

The experiment is tested using seven different threshold from 5 to 60. As shown in Table II, the most significant value for the threshold for DCT compression is 10 with image quality 95% as measured from the radiologist. Some of the processed mammogram image using DCT with different threshold value are shown in Fig. 6.

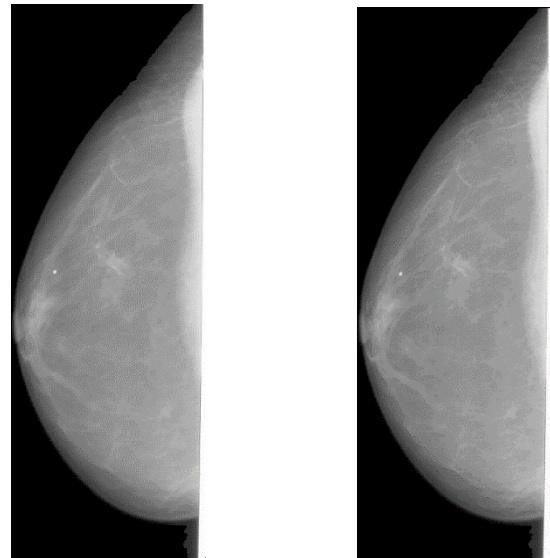
TABLE II. EVALUATION THE PERFORMANCE OF DCT COMPRESSION TECHNIQUE

Threshold	Compression Ratio	Image Quality (%)
60	5.88	5
50	5.74	10
40	5.62	30
30	5.33	50
20	4.676	75
10	3.005	95
5	2.02	100



(A) Original Image

(B) DCT with Threshold 60



(C) DCT with Threshold 40

(D) Threshold with Threshold 10

Fig. 6. Processed Mammogram images using DCT with different Threshold Values

A comparison is carried out between two compression techniques on mammogram images. As a result, the DCT compression technique shows good results in both image compression ratio and image quality comparing with SVD compression technique. For example, a mammogram image of size 5.17 MB will be compressed to 1.72MB using DCT technique and 3.496 MB using SVD Technique with good image quality at this ratio. The use of SVD in the process of compressing mammograms images does not benefit us as hoped in reaching the main goal which is compressing mammograms images as much as possible and keeping the quality needed by radiologist at the same time.

VI. CONCLUSION

The mammogram images are one of the large medical images that need to be processed and transmitted through the media. This paper presents an ongoing effort to reduce the image size in order to be easily processed and transmitted through the media. Two of lossy compression algorithms are presented in this paper which are singular value decomposition and discrete cosine transformation. Those compression algorithms are implemented on 40 microcalcification images and an intensive comparisons are carried out to evaluate the performance of those techniques based on compression ratio and image quality. The SVD compression is applied to the mammogram images with different singular values that is from 5 to 230. The optimum value, that have a largest compression value with high quality result, was 155. The DCT compression is also applied of the same mammogram images using different threshold value that is from 5 to 60. The optimum threshold value, that have a largest compression value with high quality image, was at 10.

As a result, the DCT compression technique can effectively reduce the mammogram image size by 65% from the original size without affecting the suspicious regions such as microcalcifications. Whereas, the SVD compression technique can reduce the image by 33% from the original image size.

An interesting extension will be in using the Principal component analysis (PCA) to compress the mammogram images and compare it with the techniques listed in this paper. Another future work, CAD system will be implemented using the compressed database resulted from this paper. The true positive and false positive ratio in detection the microcalcification in mammogram images will highlighted for both compression techniques.

ACKNOWLEDGMENT

The authors are grateful to the Applied Science Private University, Amman, Jordan, for the full financial

REFERENCES

- [1] V. J. Rehna & A. Dasgupt. "JPEG Image Compression using Singular Value Decomposition". International Journal of Advances in Electronics Engineering, Vol. 1, No(1), 2001, pp.81-86.
- [2] S. Kahu, & R. Rahate. "Image compression using singular value decomposition". Int. J. Adv. Res. Technol, Vol. 2, No(8), 2013, pp.244-248.
- [3] K. C. Sekaran, & K. Kuppusamy. "Performance Analysis of Compression Techniques Using SVD, BTC, DCT and GP". IOSR Journal of Computer Engineering , Vol. 17, No.(1), 2015, pp.06-11.
- [4] D. Gupta, P. Singh, & S. S. Nivedita."A comparative study of image compression between Singular value decomposition, Block truncating coding, Discrete cosine transform and Wavelet". International Journal of Computer Science and Network Security Vol. 12, No. (2), 2012, pp.100-108.
- [5] K. Cabeen, & P. Gent. Image compression and the discrete cosine transform. College of the Redwoods.
- [6] M. Dobrovolný, "The Quality Comparison Of Svd And Dct Based Image Compression Methods For Embedded Devices". J. of computer engineering, Vol. 5, No. (6), 2011, pp. 201-2012.
- [7] A. Kaur, & J. Kaur. "comparison of DCT and DWT of Image Compression Techniques". International Journal of Engineering Research and Development, 2012, pp. 49-52.
- [8] K. Baker. "Singular value decomposition tutorial". The Ohio State University, Vol. 24, 2005, .
- [9] A. B. Watson. "Image compression using the discrete cosine transform". Mathematica journal, Vol. 4, No.(1), 1994., pp. 81-95.
- [10] A. Aldroubi, M. Unser and M. Eden, "Cardinal spline filters: Stability and convergence to the ideal sinc interpolation," IEEE Signal Process, Vol. 28, 1992, pp. 127-138.
- [11] A.J. Patti, M.I. Sezan and A.M. Tekalp, "High-resolution image reconstruction from a low-resolution image sequence in the presence of time-varying blur," Proc. IEEE Intl. Conf. Image Processing, Austin, TX, 1994, pp. 343-347.
- [12] C.S. Chuah, and J.J. Leou, "An adaptive image interpolation algorithm for image/video processing," Pattern Recognition, Elsevier, Vol. 34, 2001, pp. 2383-2393.
- [13] H.S. Hou, and H.C. Andrews, "Cubic splines for image interpolation and digital altering," IEEE Trans. Acoust. Speech Signal Process, ASSP, Vol. 26, 1978, pp. 508-517.
- [14] K. Wakabayashi, "Evaluation of the effective information preservation method for binary image reduction," System and Computers in Japan, Vol. 32, 2001, pp. 1-11.
- [15] E. Aho, J. Vanne, K. Kuusilinna and T.D. Hämäläinen, "Comments on Winscale: An image-scaling algorithm using an area pixel model," IEEE Trans. Circuits and Systems for Video Technology, Vol. 15, No.3, 2005, pp. 345-355.
- [16] C.H. Kim, S.M. Seong, J.A. Lee and L.S. Kim, "Winscale: An image-scaling algorithm using an area pixel model," IEEE Trans. Circuits and Systems for Video Technology, Vol. 13, No. 6, 2003, pp. 1-4.
- [17] Hugo de las Herasa, Oleg Tischenkoa, Yuan Xub, Christoph Hoeschena, "Comparison of interpolation functions to improve a rebinning-free CT-reconstruction algorithm," IEEE of Medical Physics, Vol. 4, 2007, pp. 430-445..
- [18] M. Masek, "Hierarchical segmentation of mammograms based on pixel intensity," Ph.D. Thesis, The University of Western Australia, Australia, 2004
- [19] M. Unser, A. Aldroubi and E. Eden, "Fast B-spline transforms for continuous image representation and interpolation," IEEE Trans. Pattern Anal. Machine Intell., Vol. 13, 1991, pp. 277-285.
- [20] M. Unser, A. Aldroubi and M. Eden, "Enlargement or reduction of digital images with minimum loss of information," IEEE Trans. Image Processing, Vol. 4, 1995, pp. 247-258.
- [21] R.G. Keys, "Cubic convolution interpolation for digital image processing," IEEE Trans. Acoustics Speech and Signal Processing, Vol. 29, 1981, pp. 1153-1160.
- [22] R.Y. Tsai, and T.S. Huang, "Multiframe Image Restoration and Registration," Advance in Computer Vision and Image Processing, JAI Press, Greenwich, CT, Vol. 1, 1984, pp. 317-339.
- [23] R.R. Schultz, and R.L. Stevenson, "A Bayesian approach to image expansion for improved definition," IEEE Trans. Image Process., Vol. 3, 1994, pp. 233-242..
- [24] W.K. Pratt, "Digital Image Processing," 3rd edition, John Wiley & Sons Inc, 1991.
- [25] Yoshinori Abe, Youji Iiguni, "Image restoration from a down-sampled image by using the DCT," IEEE of Signal Processing Vol. 87, 2007, pp. 2370-2380.

- [26] Ravi kumar Mulemajalu , Shivaprakash Koliwad, "Lossless compression of digital mammography using base switching method", J. Biomedical Science and Engineering, 2009, 2, 336-344
- [27] Zhigang Liang, Xiangying Du, Jiabin Liu, Yanhui Yang, Dongdong Rong, Xinyu Yao & Kuncheng Li, "Effects Of Different Compression Techniques On Diagnostic Accuracies Of Breast Masses On Digitized Mammograms", Acta Radiologica, Vol. 49, No.(7), 2009, 747-751.
- [28] A. AbuBaker. "Automatic Detection of Breast Cancer Microcalcifications in Digitized X-ray Mammograms". Ph.D., thesis, School of Informatics, University of Bradford-UK. (2008).

APPENDIX

Matlab Code for SVD

```
inImage=imread('Image');
inImage=rgb2gray(inImage);
inImageD=double(inImage);
% decomposing the image using singular value decomposition
[U,S,V]=svd(inImageD);
dispEr = [];
numSVals = [];
for N=5:25:300
    C = S;
    % discard the diagonal values not required for compression
    C(N+1:end,:)=0;
    C(:,N+1:end)=0;
    % Construct an Image using the selected singular values
    D=U*C*V';
display and compute error
figure;
buffer = sprintf('Image %d singular values', N)
imshow(uint8(D));
title(buffer);
```

```
error = sqrt(sum(sum(S(N+1:end,N+1:end))));
    imwrite(uint8(D),strcat(buffer,'.jpg') );
dispEr = [dispEr; error];
    numSVals = [numSVals; N];
End
figure;
title('Error in compression');
plot(numSVals, dispEr);
grid on
xlabel('Number of Singular Values used');
ylabel('Error between compress and original image');
```

Matlab Code for DCT

```
f1 = @(block_struct) dct2(block_struct.data);
f2 = @(block_struct) idct2(block_struct.data);
Im = imread('Image');
Im1 = rgb2gray(Im);
%imwrite(Im1,'tigergray.jpg');
figure,imshow(Im);
J=blockproc(Im1,[8,8],f1);
depth=find(abs(J)<40);
J(depth) = zeros(size(depth));
K = blockproc(J,[8,8],f2)/255;
figure,imshow(K);
title('threshold:40');
imwrite(K,'Image');
```

Evaluating Confidentiality Impact in Security Risk Scoring Models

Eli Weintraub

Department of Industrial Engineering and Management
Afeka Tel Aviv Academic College of Engineering
Tel Aviv, Israel

Abstract—Risk scoring models assume that confidentiality evaluation is based on user estimations. Confidentiality evaluation incorporates the impacts of various factors including systems' technical configuration, on the processes relating to users' confidentiality. The assumption underlying this research is that system users are not capable of estimating systems' confidentiality since they lack the knowledge on the technical structure. According to the proposed model, systems' confidentiality is calculated using technical information of systems' components. The proposed model evaluates confidentiality based on quantitative metrics rather than qualitative estimates which are currently being used. Frameworks' presentation includes system design, an algorithm calculating confidentiality measures and an illustration of risk scoring computations.

Keywords—information security; risk management; continuous monitoring; vulnerability; confidentiality; risk assessment; access control; authorization system

I. INTRODUCTION

Cyber-attackers cause damage to organizations and personal computers by stealing their business or private data and by making changes in their software and hardware [1]. The damages are usually categorized by security experts to three kinds: loss of confidentiality, integrity or availability. Vulnerabilities are software weaknesses or exposures. An attack is performed by exploiting software vulnerabilities in the target system. Attackers make use of vulnerabilities stemming from bugs that are potential causes to security failures. Exploits are planned to attack certain components having specific vulnerabilities. Users' computers might be damaged by exploited vulnerabilities. Defending computers depends on the amount of knowledge an organization has of their computing systems' vulnerabilities. This work focuses on gaining accurate knowledge of computers' configuration, thus enabling improved risk mitigation to defend computers from threats caused by attackers. Accurate knowledge of computers' risks assist security managers to adopt security measures effectively. Reference [2] states that Stuxnet worm included a process of checking hardware models and configuration details before launching an attack. Risk managers make decisions on activities actions they have to perform in order to limit their exposure to risks according to the amount of potential damage and vulnerability characteristics [3].

Risk has many definitions in research publications. This research uses the definition of [4]: "An event where the

outcome is uncertain". Accordingly, this work is aimed at lessening risk uncertainty. The proposed model focuses on an improved confidentiality impact assessment algorithm which is based on the real-time information on systems configuration, as proposed by [5].

Several software products are used to defend computers from cyber-attackers. Antivirus software, antispayware and firewalls are examples to some of these tools based on periodic assessment of the target computer by comparing computers' software to the known published vulnerabilities. Continuous Monitoring Systems (CMS) monitor systems in a near real time process aimed at detecting vulnerabilities and notifying security managers. Contemporary systems use vulnerabilities databases which are continually updated as new vulnerabilities are detected and a scoring algorithm which predicts potential business damages. This work focuses on measuring the confidentiality impacts on the overall risk score. Confidentiality refers to limiting information access and disclosure to only authorized users, as well as preventing access by, or disclosure to unauthorized ones. Evaluating confidentiality impacts on business risk will be based on an algorithm which compares the actual access users are gaining, to the rules defined by the authorization system. The proposed CMS evaluates business risk scores relating to the actual technical configuration. This model focuses on measuring confidentiality potential losses related to known vulnerabilities. According to the proposed model each time a system is breached, systems' risk score is re-evaluated to reflect the impacts of the new breach.

Computers are at risk to known threats until the time a patch is prepared for defending the vulnerable software, an activity that may last weeks or months. In today's environment of zero-day exploits, conventional systems updating for security mitigation activities has become a cumbersome process. There is an urgent need for a solution that can rapidly evaluate system vulnerabilities' potential damages for immediate risk mitigation [6].

Security Continuous Monitoring (SCM) is a specific subgroup of CMSs that use techniques for monitoring, detecting and notifying of security threats. After identifying these risks, the tools evaluate the potential impacts on the organization. Reference [7] states that SCM systems are aimed at closing the gap between the zero-day of identifying the vulnerability, until the moment the computer is loaded by a patch.

This paper describes the mechanisms of a new SCM framework that will produce better risk scores than current known systems. The proposed framework defines processes on two grounds: 1) knowledge concerning real computers' configuration of the target system, and 2) an algorithm which runs continuously and computes confidentiality impact assessments.

The rest of the paper is organized as follows: In section II a description of current known security scoring solutions. In section III a description of access control systems. In section IV a presentation of the proposed framework including systems architecture. In section V a description of the confidentiality algorithm and risk scoring model. In section VI presentation of the results. In section VII conclusions and future research directions.

II. EXISTING SOLUTIONS

SCM systems are using external vulnerabilities databases for evaluation of the target computers' risk. There are several owners of vulnerability databases [6], for example the Sans Internet Storm Center services and The National Vulnerability Database (NVD). Vulnerability Identification Systems (VIS) aimed to identify vulnerabilities. Examples for VIS systems are The Common Vulnerabilities and Exposures (CVE), and The Common Weakness Enumeration (CWE).

This work uses NVD vulnerabilities database as an illustration of the proposed model.

Risk evaluation uses scoring systems which makes use of systems' characteristic parameters for estimating vulnerabilities' impacts on the organization. The Common Vulnerability Scoring System (CVSS) is a framework that enables user organizations benefit by receiving IT vulnerabilities characteristics [1].

CVSS uses three groups of parameters to score potential risks: basic parameters, temporal parameters and environmental parameters. Each group is represented a vector of parameters which are used to compute the score. Basic parameters represent the intrinsic specifications of the vulnerability. Temporal parameters represent the specifications of a vulnerability that might change over time due to technical changes. Environmental parameters represent the specifications of vulnerabilities derived from the local IT specific environment used by users' organization. CVSS enables omitting the environmental metrics from score calculations in cases the users do not specify the detailed description of environment and components.

CVSS is a common framework for characterizing vulnerabilities and predicting risks, used by IT risk managers, researchers and IT vendors. It uses an open framework which enables managers to deal with organizations' risks based on systems' characteristics. Organizations adopting CVSS framework may gain the following benefits:

- A standard scale for characterizing vulnerabilities and scoring risks.
- Normalizing vulnerabilities according to specific IT platforms.

- An open framework. Organizations can see the characteristics of vulnerabilities and the logical process of scoring evaluation.
- Environmental scores. Considering changes in its IT environment according to predicted risk scores.

There are few other vulnerability scoring systems besides CVSS differing by the parameters' specifications and scoring scales. CERT/CC emphasizes internet infrastructure risks. SANS vulnerability system considers users' IT configuration. Microsoft emphasizes attack vectors and vulnerabilities' impacts.

Using CVSS scoring system, basic and temporal parameters are specified and published by products' vendors who have the best knowledge of their product. Environmental parameters are specified by the users who have the best knowledge of their environments and business impacts.

This paper focuses on environmental metrics.

Business damages caused by a vulnerability are influenced by the IT exploited component. CVSS environmental parameters specify the characteristics of a vulnerability that is associated with user's IT configurations' components. Environmental parameters are of three groups:

1) Collateral Damage Potential (CDP).

Measures specifying the economic potential damage caused by a vulnerability.

2) Target Distribution (TD).

The percentage of vulnerable components in users' environment.

3) Security Requirements (CR, IR, AR).

Security importance measures in users' organization. Those parameters are subdivided to parameters indicating the Confidentiality Requirement (CR), integrity (IR), and availability (AR). Higher security requirements may cause higher security damages on the organization.

Confidentiality impacts measure the impact on confidentiality of a successfully exploited vulnerability. Confidentiality refers to limiting information access and disclosure to only authorized users, as well as preventing access by, or disclosure to unauthorized ones. Confidentiality is evaluated using two parameters: Confidentiality Impact (CI) which is a basic parameter, and Confidentiality Requirement (CR) which is an environmental parameter. CI may be assigned three values: N, P, and C. Increased CI increases the vulnerability score. None (N) is defined whenever there is no impact to the confidentiality of the system. Partial (P) is whenever there is considerable informational disclosure, access to some system files is possible, but the attacker does not have control over what is obtained, or the scope of the loss is constrained. Complete (C) is defined when there is total information disclosure, resulting in all system files being revealed. CR is an environmental parameter used for different environments which may have varying impacts on the final evaluation of business risk. CR is one out of three Security Requirement parameters belonging to the environmental group.

The environmental group of metrics enables the analyst to customize the CVSS score depending on the importance of the affected IT asset to a user's organization, measured in terms of confidentiality, integrity, and availability, that is, if an IT asset supports a business function for which availability is most important, the analyst can assign a greater value to availability, relative to confidentiality and integrity. Each security requirement has three possible values: "low," "medium," or "high". The full effect on the environmental score is determined by the corresponding base impact metrics. That is, these metrics modify the environmental score by reweighting the base confidentiality, integrity, and availability impact metrics. The CI metric has increased weight if the CR is "high". The greater the security requirement, the higher the score.

CR may get four values. Low (L) for cases of loss of confidentiality which have only a limited adverse effect on the organization or individuals associated with the organization (e.g., employees, customers). Medium (M) for loss of confidentiality for cases having serious adverse effects on the organization or individuals associated with the organization. High (H) for cases of confidentiality losses which have a catastrophic adverse effect on the organization. Not Defined (ND) for situations having no environmental impact on confidentiality score.

Categorization of IT components according to security requirement measures should encompass all assets to raise the possibility of predicting organizational risks. Federal Information Processing Standards (FIPS) requirements demands implementation of a categorization [7], but does not require using any particular scale, thus risk comparison of users' systems is difficult.

III. ACCESS CONTROL

Access Control refers to control how Information Technology resources are accessed so that they are protected from unauthorized modifications or disclosure [8]. Access controls are security features that control how users and systems interact with other systems and resources and protect the resources from unauthorized access. Access controls give organizations the ability to control, restrict, monitor and protect resource availability, integrity and confidentiality. This paper focuses on confidentiality. Several kinds of information are more sensitive than other and require a higher level of confidentiality. Information such as health records, financial information and military plans are high confidential and need more control mechanisms and monitoring to provide confidentiality. Organizations should identify the data that must be classified to ensure that the top priority of security protects this information. On the other end organizations should allocate less budgets to protect information which is less sensitive. Organizations should define varying access controls techniques to limit access to the sensitive information in accordance to the sensitivity level of the information. Organizations should define rules that outline the sensitivity levels of the varying kinds of information, and define the identity of users which will gain legal access to each information.

A decision whether a user may access specific resource is a process comprising two steps: authentication and authorization. Authentication is a process of decision if the user is who he claims to be, and authorization is a process of decision whether he is authorized to access a particular source and what actions he is permitted to perform on the resource. Authorization is a core component of every operating system, but application and the resources themselves sometimes perform this functionality. Authorization processes use access criteria matrixes to provide their decisions. Access matrixes manage the information whether a user has the permissions to perform varied operations on particular resources. Granting access rights to users should be based on the level of trust an organization has on a user and the users' need-to-know. The different access criteria can be enforced by roles, groups, location, time, and transaction type. Roles are based on organizational functions the user may perform during his work. Group is a couple of users who require the same types of access to information and resources. Using groups is easier to manage then assigning permissions to each user. The need-to-know principle is similar to the least-privilege principle. It is based on the concept that users should be given access only to the information they require in order to perform their job duties. Giving any more rights to a user rises the possibility of that user to abuse the permissions assigned to him, thus raising the risks of illegal usage. An Access Control Model is a framework that dictates how users access resources. It uses mechanisms to enforce the rules of the model.

There are three main access control models. Discretionary Access Control (DAC), Mandatory Access Control, and Role-Based Access Control (RBAC). In DAC data owners decide who has access to resources. Access Control Lists (ACL) are used to enforce access decisions. In MAC, operating systems enforce the systems' policy through security labels. In RBAC access decisions are based on each subjects' role and his hierarchical functional level. According to [9] RBAC has become the predominant model for advanced access control because it reduces development and management costs. A variety of IT vendors, including IBM, Sybase, Secure Computing, and Siemens developed products based on this model.

Once an organization determines what type of access control model it will use, it needs to decide what technique to use to support the access control model. There are several techniques: Rule-Based, Constrained User Interfaces, Matrix. Content-Dependent and Context-Dependent. Rule-Based Access Control techniques are based on specific rules that indicate what can and cannot do a user on a resource. Constrained User Interfaces restrict users' access abilities to resources. Access Control Matrix is a table of subjects and objects indicating what actions each subject can perform on a specific object. Subject may represent users or roles or groups of users, object may represent technological resources. Content-Dependent Access Control is determined by the content within the object. The content dictates which user is authorized to access the object. Context-Dependent Access Control uses collection of information residing in the environment of the subject and object.

The model presented in this paper will use a RBAC model, using an Access Control Matrix technique.

IV. THE PROPOSED FRAMEWORK

Federal organizations are moving from periodic to continuous monitoring implementing SCM's which will improve national cyber security posture [10]. The proposed framework includes two capabilities not found in current practices. First, the environmental parameters are based on the components of the system as updated in the systems' Configuration Management Data Base (CMDB) [11]. This capability enables basing the scoring models to predict organizational damages to organizations' confidentiality scores relating to actual IT configuration rather than on user's estimates as proposed by [12]. According to [13] it is impossible for organizations to make precise estimates of the

economic damages caused by an attack without having full knowledge of users' IT environment. Ref. [14] [5] state that network configuration should be monitored continually and available vulnerabilities must be analyzed in order to provide the necessary security level.

The proposed Security Continuous Monitoring System (SCMS) examines a database of published asset vulnerabilities, compares in real time computers' assets for existing exposures and calculates confidentiality impact measures for business risk score computations. The SCMS proposed architecture presented in Fig. I. Following, a description of systems' structure and modules, followed by modules functionality.

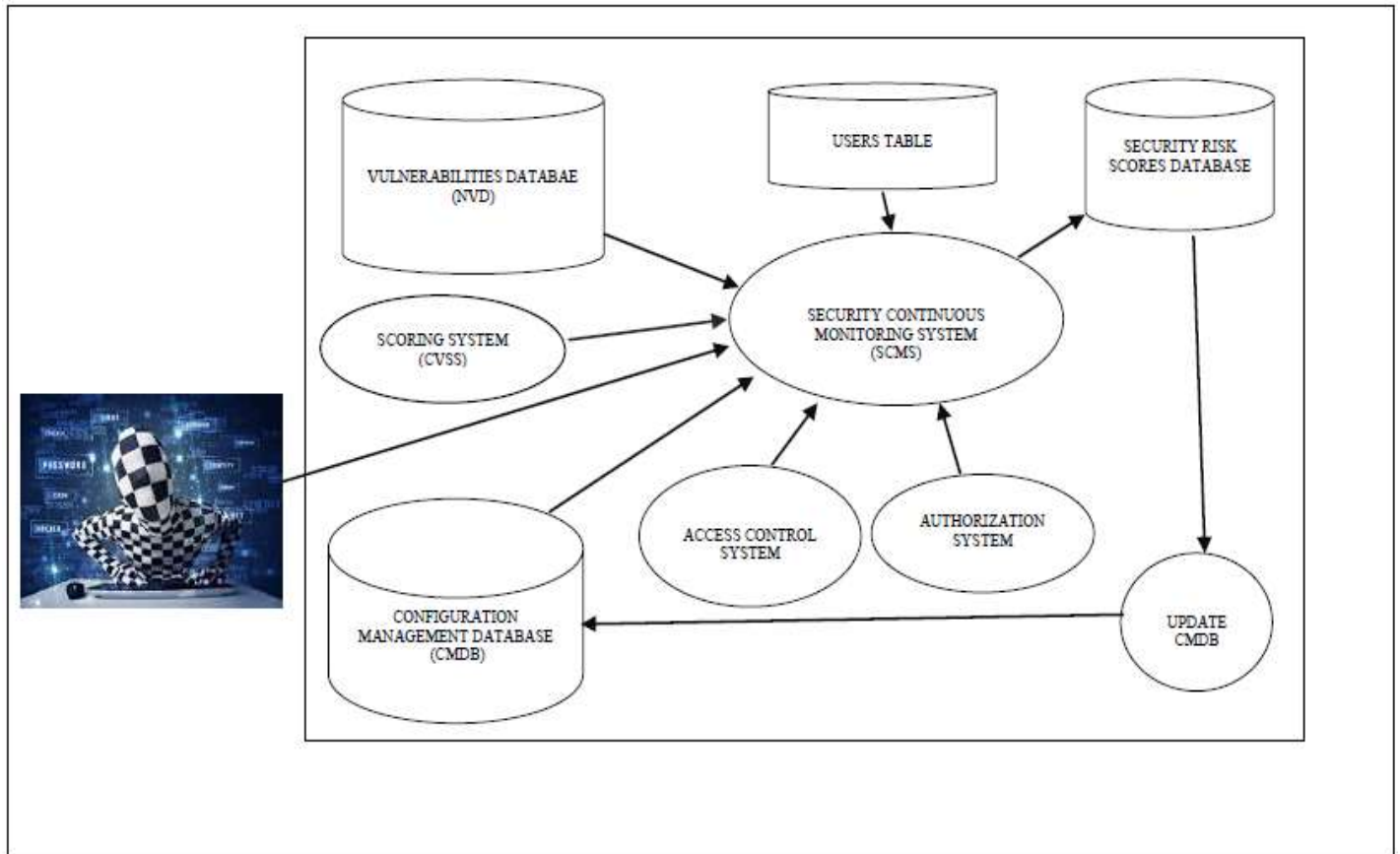


Fig. 1. Security Continuous Monitoring System architecture

- Security Continuous Monitoring System (SCMS)

The system runs continuously computing risk scores. Computations of confidentiality scores are performed in three cases:

- When a new vulnerability is published and indicated in NVD.
- When a change is made in a systems' component and indicated in CMDB.
- When the Access Control System signals that a certain component was illegally accessed or breached.

SCMS makes use of the Confidentiality Impact scoring algorithm defined in this paper.

- Vulnerabilities database (NVD).

Vulnerabilities database includes all known vulnerabilities and their specification as published by database owners. Examples of vulnerability specifications used by NVD are: vulnerability category, vendor name, product name, published vulnerability start and end dates, vulnerability update dates, vulnerability severity, access vector, and access complexity [7].

- The Common Vulnerability Scoring System (CVSS)

CVSS is the algorithm this research uses for illustration of the proposed model. CVSS computes security risk scores according to parameter groups: basic, temporal and environmental. There are also other known scoring algorithms, some of them for public use other commercial.

- Configuration Management Database (CMDB).

CMDB is a database which manages all the information of hardware and software components of the target system. The target system might be one computer or a group of organizations' network computers. According to the proposed model the CMDB includes detailed information of components' risk scores as well as detailed information of all software components. CMDB includes the information on software programs and services, and of data managed by the target system. Data is specified in the resolution of databases, tables and data items. Input/output interfaces are handled using screen-names, reports and messages. The CMDB includes information relating to risks: Security requirements (CR, IR, AR) of each component in the system. CMDB manages also the calculated CI's of systems' components. CI's are calculated using the algorithm described in this paper. CI scores are re-weighted according the environmental CR computed scores. In every activation of the SCMS system, the CI is calculated, written to the Security Risk Scores database. While calculating the CIs the CVSS module calculates the updated risk score.

- Security Risk Scores Database.

The database includes all computed risk scores and confidentiality impact scores calculated computed by SCMS. The computed scores are then updated in the CMDB by the Update CMDB module.

- Update CMDB

In cases of updates to systems' risk scores as calculated by the SCMS, CI scores and risk scores are passed to the Update CMDB module for CMDB updating. CMDB risk scores represent the updated risk scores and confidentiality impact scores for all systems' components. This update process is needed to prevent unnecessary risk scoring heavy computations which were already evaluated and has been written in the CMDB.

- Users Table

This Table includes all systems' users, whether manual or machine. Each user is identified by a User-ID. A user may include several user-roles for interfacing with the authorization system. Each user-role resembles a set of access rights to specified systems' components. For example a bank teller may have two roles which define two processes performed by him. Those processes access system components. For example, giving a loan to a customer uses a role which needs access to the loans table and customers table. Second role may be depositing cash to customers' account, which needs access to deposits table, customers table and current accounts module. In order to find out what the user is authorized to do interacting the system, one has to read all his roles in users' table, then get each user-roles' authorizations from the authorization system.

- Authorization system.

This system is responsible for management of all system applications' accesses to systems' components related to a role. Whenever an application wants to perform a users' task, it calls the authorization system by supplying the user-ID, user-role and the operation needed. The Authorization systems' reply includes an answer whether the user is authorized to perform the requested operation on the component or he is not. Operations may be read, write, update or view the component. Usually, Authorization Systems are planned as rule-base systems which uses the parameters: user-role and requested operation and other parameters such as time and place of the needed operation. Regularly, Authorization Systems manage access to database items, not to other system components such as processes, operating systems utilities, and hardware devices. Such other components are regularly managed by an Access Control System.

- Access Control System

This system controls and monitors all computers' components: hardware, software, databases, communication, system software and utilities. When the system recognizes an illegal access to a certain component it alerts operators and according to rules, interrupts or terminates processes. Illegal access to systems' components may be caused by hackers or software bugs. Hackers look for vulnerabilities or backdoors which let them bypass the authorization system rules, thus reaching illegally data or software components. In such cases it will notice the SCMS about illegal users for dropping down their authorizations and computing the new components' risk score.

V. THE RISK SCORING ALGORITHM

CVSS's framework is based on three kinds of parameters: basic, temporal and environmental parameters. According to [7], in many organizations IT resources are labeled with criticality ratings based on network location, business function, and potential losses. For example, the U.S. government assigns every unclassified IT asset to a grouping of assets called a system. Every system must be assigned three "potential impact" ratings to show the potential impact on the organization if the system is compromised according to three security objectives: Confidentiality, Integrity, and Availability. Thus, every unclassified IT asset in the U.S. government has a potential impact rating of low, moderate, or high with respect to the security objectives of confidentiality, integrity, and availability. This rating system is described within Federal Information Processing Standards (FIPS) 199.5 [15]. CVSS follows this general model of FIPS 199, but does not require organizations to use any particular system for assigning the low, medium, and high security impact ratings. References [15] [16] state that organizations should define security risk specifications of their environment, but does not define the ways organizations have to specify that information. The Department of State has implemented an application called iPost and a risk scoring program that is intended to provide continuous monitoring capabilities of information security risk to elements of its information technology infrastructure. According to [17] the iPOST scoring model does not refine the base scores of CVSS to reflect the unique characteristics of its environment. Instead, it applied a mathematical formula to the base scores to provide greater separation between the scores for higher-risk vulnerabilities and the scores for lower-risk vulnerabilities. This technique provides ordinal qualitative scores but not real quantitative measures. This work is targeted to fill-in this vacuum.

The CMDB defined in this work presented in Table I, handles configurations' information of the target system including the following entities: database tables, software components, system components such as operating system, database management systems, utility programs, development components, UI screens, etc. Each component is describes including knowledge relating to security requirements needed for operation of the risk scoring algorithm. The CMDB manages five kinds of environmental information for every system component. Table I includes information concerning the characteristics assigned to systems' components. Characteristic values are based on [15] definitions. The information is categorized according to its security type which is defined as a specific category of information (e.g., privacy, medical, proprietary, financial, investigative, contractor sensitive, security management). Reference [15] states that the potential impact is low if the loss of confidentiality, integrity, or availability could be expected to have a limited adverse effect on organizational operations, organizational assets, or individuals. The potential impact is moderate if the loss of confidentiality, integrity, or availability could be expected to have a serious adverse effect on organizational operations, organizational assets, or individuals. The potential impact is high if the loss of confidentiality, integrity, or availability could be expected to have a severe or catastrophic adverse

effect on organizational operations, organizational assets, or individuals.

TABLE I. CMDB – COMPONENTS TABLE

Column ID	Column Name	Column Description	Values (*)
COMPONENT ID	Software or Hardware, Vendor, Serial No', Version...	Value is equal to component ID in NVD	unique
COMPONENT TYPE	Hardware Type (cpu, printer, disk...), Software type, etc'	For example: Database, Table, Column....	H, S, UI, COMM ...
CONFIDENTIALITY IMPACT (CI)	Basic parameter	None, Partial, Complete	N, P, C
CR	Confidentiality Requirement	The importance of the affected IT asset to a user's organization, measured in terms of confidentiality.	L,M,H
IR	Integrity Requirement	Guarding against improper information modification or destruction.	L,M,H
AR	Availability Requirement	"Ensuring timely and reliable access to and use of information...".	L,M,H
FINAL EVALUATED RISK SCORE	CVSS final Risk Score based on all basic, temporal and env' parameters.	Based on all parameters including CI and CR.	0-10

(*) N=none, L=low, LM=low medium, M=medium, MH=medium high, H=high

• Confidentiality Scoring

Confidentiality of a component refers to limiting information access and disclosure to only authorized users, as well as preventing access by, or disclosure to, unauthorized ones. CVSS model uses the CR environmental parameter which is assigned three values: Low, Medium and High. According to the proposed model, suggested by [18] CR will get quantitative values on the scale [0, 1] assigning real values instead of three qualitative ordinal values H, M, and L. A new algorithm will compute the CR values according to the following formula (1):

$$(1) \quad CR(c) = \frac{\text{LegalLost}(c)}{2 * \text{LegalNorm}(c)} + \frac{\text{ILegalPermitted}(c)}{2 * \text{ILegalNorm}(c)}$$

LegalLost = Legal users who lost their permissions.

LegalNorm = Number of users authorized according to the Authorization system to perform operations on component c.

IlegalPermitted = Ilegal users who actually got permissions.

IlegalNorm = Users who normally have no legal access.

CR is computed by summing the quotient of users who lost their permissions out of all legal authorized users, added to the quotient of illegal users who got permissions out of all illegal users, according to the authorizations' norm.

$$0 \leq CR \leq 1$$

Following the pseudo code for parameter calculations:

LegalNorm (c) = Count number of users authorized to access component c, over all their roles for each role having at least one legal authorization to c.

IlegalNorm (c) = Count number of users authorized to access component c, over all their roles for each role having no legal authorization to c.

LegalLost (c) = Count number of users authorized to access component c who have NO ACTUAL access to c and have at least one DEFINED legal authorization to c.

IlegalPermitted (c) = Count number of users who have ACTUAL access to c and are not defined as legal authorizations for c.

To illustrate the rational of the formula we assume an application planned for 10 workers, among them 3 legal authorized users and 7 illegal users, which use other applications. The illustration includes five cases of CR computations.

Implementation of the formula involves performing an algorithm which simulates accesses to the target components for all users in all possible roles counting the number of legal and illegal authorizations. The algorithm is performed twice, first on the before-attack system, second on the post-attack system.

- Case study illustration

The case study assumes users are assigned 4 roles: System administrator (Admin), Deposit services (Depos) and Loans services (Loan). The Database consists of three tables: Customers, Deposits and Loans. The Admin role is authorized to access all tables, The Depos role authorized to access to deposits tables, The Loan role is authorized access to loans table. Following the contents of Roles table (Table II) and Users table (Table III).

TABLE II. ROLES TABLE

ROLE	AUTHORIZATION
Depos	Deposits
Loan	Deposits, Loans
Admin	Customers, Deposits, Loans

TABLE III. USERS TABLE

User ID	Role
User1	Admin
User2	Depos
User3	Depos, Loans
User4	No
User5	No
User6	No
User7	No
User8	No
User9	No
User10	No

Following in Table IV the values of Confidentiality impact scores for all system components according to the normal authorizations, and also values of actual access permissions after a cyber-attack has occurred. Norm authorizations are according to legal authorizations' definitions. Actual permissions assumed number of illegal and lost permissions given after illustrating three kinds of cyber-attacks. At the rightmost column the evaluated CR according to Formula (1).

TABLE IV. CONFIDENTIALITY IMPACT EVALUATION

Attack Number	Components Table	Legal Norm	Legal Lost	Ilegal Norm	Ilegal Permitted	CR
1	Deposits	3	0	7	0	$(0/3 + 0/7)/2 = 0$
1	Loans	2	1	8	5	$(1/2 + 5/8)/2 = 0.56$
1	Customers	1	1	9	9	$(1/1 + 9/9)/2 = 1$
2	Deposits	3	1	7	5	$(1/3 + 5/7)/2 = 0.52$
3	Deposits	3	3	7	5	$(3/3 + 5/7)/2 = 0.86$

VI. RESULTS

As illustrated, during attack number 1 Deposits table was not impacted by the attack, thus CR is zero. Customers table lost all user legal authorizations and in addition all illegal

users got permissions, thus CR is scored maximal hence 1. Loans table lost 1 users' permissions and 5 illegal users got permissions, hence the calculated CR is 0.56.

Comparing impacts of attack 2 on Deposits table to attack 1 on Loans table shows that although both attacks caused loss of access to one user and an addition of 5 illegal users, the calculated CR of attack 2 is less harmful ($0.52 < 0.56$). This is due to the fact that there are still 2 users having access to the table, while only 1 user has access to loans table.

Comparing impacts of attacks 2 and 3 on Deposits table shows that although the impacts on illegal users are similar, the impacts on legal number user is more harmful ($0.86 > 0.52$) in attack 3, since all legal users lost their access rights.

VII. CONCLUSIONS

This work presents a new framework of a Security Continuous Monitoring System, structure and mechanisms. The SCMS uses the CVSS scoring model for risk scoring operating in real time. According to the proposed model CVSS uses CR environmental parameters which are evaluated by the new algorithm, based on the technological configuration of the system, instead of CR figures which according to current practices, is based on users' personal intuitive knowledge. The structure of the system, modules and the scoring algorithm is presented and illustrated using a use case.

The model helps risk managers in estimating the organizational risks, basing their risk management decisions on the specific technological structure by using the algorithm. Using the proposed model will bring more accurate estimates to vulnerability risks, thus enabling efficient risk mitigation plans and improved defense strategies to organizations.

Confidentiality metric is used by risk scoring algorithm CVSS to measure the impact on confidentiality of a successfully exploited vulnerability.

The value of confidentiality score is calculated by using the basic parameter CI and the environmental parameter CR. Increased confidentiality impact raise the vulnerability score. CR metric enables customizing the CVSS algorithm to the importance of the affected IT asset to a user's organization. That is, if an IT asset supports a business function for which availability is most important, the metric will be assigned a higher value. CR has three possible values: "low," "medium," or "high". The proposed model presents an algorithm which enables assigning quantitative values to confidentiality impact based on the real planned and actual impact of an attack on the specific component. The calculated values are based on the actual impacts of cyber-attacks on that component, compared to the organizational needs as specified in the authorizations system. The formula and metrics are presented and illustrated in a use case example. The evaluated score is assigned real values instead of current qualitative estimates, thus enabling higher resolutions of confidentiality scores. The proposed model outlines the structure of a SCMS which uses the real organizational configuration, components, and processes. The model will enable getting more accurate measure, which are based dynamically on users' configuration thus enabling the organization making better risk management decisions,

allocating risk management budgets to the relevant threats Incorporating the CR computed values in CVSS scoring model needs a minor modification to CVSS algorithm: using the calculated CR instead of the estimated values for all systems' components.

Future improvements to confidentiality impacts formulas and algorithm needs more research. Confidentiality impacts may be considerably elaborated in the following directions:

- Assigning different weights by the confidentiality formula to differentiate users who lost their access from un-authorized users who got illegal access.
- Assigning different weights to components according to business losses caused by attacks on the components.
- Assigning different weights to kinds of components such as software or hardware, operating system component or application components.
- Computing components' confidentiality score in relation to the amount of roles to a component a user is authorized, compared to the number of actual lost roles.
- Computing score according to the types of access a user is authorized in certain roles, for example differentiating between write and read access rights.
- Calculating scores according to the amount of interrelationships of the evaluated component with other components, measuring indirect impacts on other components, and including interrelationships' kinds such as reads or writes operations between components.
- Measuring impacts on types of users. Higher level organizational users and key personnel might be hurt more by loss of access then operational low-level workers.

More research is needed in supplying quantitative measures to the CVSS model. In our view CVSS model uses additional qualitative measures which could be improved adding quantifiable measures. Parameters such as target distribution may use the technological aspects of the configuration instead of users' intuitive estimates. Other environmental parameters such as integrity and availability scores should be based on figures representing the actual technological environment.

REFERENCES

- [1] P. Mell, K. Scarfone, and S. Romanosky, "CVSS – A complete guide to the common vulnerability scoring system, version 2.0", 2007.
- [2] L. Langer, "Stuxnet: dissecting a cyber warfare weapon, security and privacy", IEEE, Volume 9 Issue 3, pages 49-51, NJ, USA, 2011.
- [3] S. Tom and D. Berrett, "Recommended practice for patch management of control systems", DHS National Cyber Security Division Control Systems Security Program, 2008.
- [4] A. Terje and R. Ortwin, "On risk defined as an event where the outcome is uncertain", Journal of Risk Research Vol. 12, 2009.
- [5] E. Weintraub, "Security Risk Scoring Incorporating Computers' Environment", (IJACSA) International Journal of Advanced Computer Science and Applications, Vol. 7, No. 4, April 2016.
- [6] Y. F. Nñez, "Maximizing an organizations' security posture by distributedly assessing and remedying system vulnerabilities", IEEE –

- International Conference on Networking, Sensing and Control, China, April 6-8, 2008.
- [7] K. Dempsey, N. S. Chawia, A. Johnson, R. Johnson, A. C. Jones, A. Orebaugh, M. Scholl and K. Stine, "Information security continuous monitoring (ISCM) for federal information systems and organizations", NIST, 2011.
- [8] S. Harris, All in one CISSP Exam Guide. 6Th Ed. McGraw Hill Education, 2013.
- [9] R. Sandhu, D. Ferraiolo and R. Kuhn", "The NIST Model for Role-Based Access Control: Towards A Unified Standard", George Mason Univ., 1999.
- [10] M. G. Hardy, "Beyond continuous monitoring: threat modeling for real-time response", SANS Institute, 2012.
- [11] A. Keller and S. Subramanianm, "Best practices for deploying a CMDB in large-scale environments", Proceedings of the IFIP/IEEE International conference and Symposium on Integrated Network Management, pages 732-745, NJ, IEEE Press Piscataway, 2009.
- [12] E. Weintraub, "Evaluating Damage Potential in Security Risk Scoring Models" *International Journal of Advanced Computer Science and Applications(IJACSA)*, 7(5), 2016.
- [13] M. R. Grimalia, L. W. Fortson and J. L. Sutton, "Design considerations for a cyber incident mission impact assessment process", Proceedings of the International Conference on Security and Management (SAM09), Las Vegas, 2009.
- [14] I. Kotenko and A. Chechulin, "Fast network attack modeling and security evaluation based on attack graphs", *Journal of Cyber Security and Mobility* Vol. 3 No. 1 pp 27-46, 2014.
- [15] FIPS Publication 199 - Federal Information processing standards publication, "Standards for security categorization of federal information and information systems", Department of Commerce, USA, February, 2004.
- [16] E. Weintraub and Y. Cohen, "Continuous monitoring system based on systems' environment", ADFSL - Conference on Digital Forensics, Security and Law, Florida, USA, May 19, 2015.
- [17] GAO – United States Government Accountability Office Report to Congressional Request, "Information security – state has taken steps to implement a continuous monitoring application but key challenges remain", July, 2011.
- [18] E. Weintraub, "Quantitative measurement for estimation Confidentiality impacts after Cyber Attacks", ICSCCT - International Conference on Secure Computing and Technology, Washington, USA, 11/2016.

Formal Modeling and Verification of Smart Traffic Environment with Design Aided by UML

Umber Noureen Abbas

Department of Computer Science
COMSATS Institute of Information
Technology Sahiwal
Sahiwal, Pakistan

Nazir Ahmad Zafar

Department of Computer Science
COMSATS Institute of Information
Technology Sahiwal
Sahiwal, Pakistan

Farhan Ullah

Department of Computer Science
COMSATS Institute of Information
Technology Sahiwal
Sahiwal, Pakistan

Abstract—Issue challan in response to rules violation, LED (Light Emitting Diode) and Bridge components of this proposed Smart Traffic Monitoring and Guidance System are presented in this paper to monitor violation of rules, update users about traffic congestion through LED and to provide central hub to communicate with sensors to update server about the traffic situation. It involves the Wireless Sensors and actors to communicate with the system. The proposed components require fewer resources in terms of sensors and actors. Further sensors identify violation of rules through issue challan. Secondly, LED component provides information to users about the traffic situations. Thirdly, Bridge component is used to provide central hub to communicate with different components in the proposed model and to update the server. The proposed components of this model are implemented by developing formal specification using VDM-SL. VDM-SL is a formal specification language used for analysis of complex systems. The developed specification is validated, verified and analyzed using VDM-SL Toolbox.

Keywords—Formal specification; Formal analysis; VDM; Sequence Diagram; Issue Challan; LED

I. INTRODUCTION

Traffic congestion is a big problem in developed countries. In advanced countries better transportation management system has the ability to handle complex situations. It is quite important to suppress traffic problems because it can contribute a lot in the development of a country. Traffic congestion can cause, accidents, wasting of time, minimize trade opportunity, increases energy consumption and inversely affect the education system and the impact of all these can be dangerous for living societies [2].

The main objectives of traffic management system should be the ability to reduce congestion, overcome traffic pollution and smooth traffic flow. Researchers have proposed different models to make traffic system robust, smarter and reliable. In order to maintain the change in demand of speed and efficiency, a reliable traffic system is required that can manage and monitor traffic in a dynamic environment. With the growth of population traffic becomes a critical issue, irregular traffic is a big problem in populated cities of Pakistan. To sort out these issues we have to develop a smart traffic management system in which data can be collected from sensors in real time, processed at the same time and update the system to remove

congestion. This paper has proposed a model and formalized few components in VDM-SL, which are discussed in [1]. Researchers have proposed different models with the involvement of different tools and technologies. These models have the capability of collecting road traffic information through wireless sensors and other employed devices. They collect information about vehicles, pedestrians and other moving objects in real time that can affect road network. This collected information can also be presented to pedestrians and vehicles so they can decide their route. We need all these things to minimize any distraction on roads that can cause to accident or disaster. Real-time systems can recognize the road traffic make certain decisions and predict the flow of traffic. This paper has also proposed certain functions in the model that works in real-time like to change the signal timings and to identify the occlusion. Developing intelligent traffic management system with the integration of IoT has more advantages than employing other related technologies. IoT save more cost, reliability, and safety than other mechanisms [21]. This proposed model and different other models employed IoT devices which have a number of RFIDs and wireless sensors that communicate with each other and sends data to the administrator. This is a challenge for future researchers to ensure the security of smart objects and their transmitted data so no intruders can attack on data [3]. The proposed traffic monitoring and guidance system provides an efficient way of monitoring traffic flow and it helps to avoid congestion, provide smooth traffic flow better utilization of resources and decrease the management cost.

Currently, this study is focused on the bridge, Issue Challan, and LED Information components in this system model. Bridge is the central location where all the wireless sensors from any location connect and communicate. Issue Challan is the procedure of issuing Challan to vehicles who violate the traffic rules. The last module is related to the procedure of changing information on the LED that is employed on roads to help drivers. The formalization of this system is done in Vienna development method specification language, some of the modules are already presented in a previous article and remaining is presented in this paper. This paper consists of different sections which are Introduction, Literature Review, Problem statement, Formalization of modules, Sequence diagrams of these modules and conclusion.

II. LITERATURE REVIEW

The problem of traffic management is quite critical so different researchers have dealt with the problem and gave their solutions, indeed different intelligent traffic monitoring and controlling systems have been described and proposed as a result of their efforts. Pang et al. [19] proposed a system of traffic flow prediction based on a fuzzy neural network. Bhadra et al. [7] presented a technique based on applied agent-based

fuzzy logic for traffic, involving multiple approaches and vehicle movements. In [15] authors have proposed a technique that can integrate dynamic data into intelligent Transportation Systems. Patrik et al. [23] proposed a service-oriented architecture (SOA) for an effective integration of IoT in enterprise services.

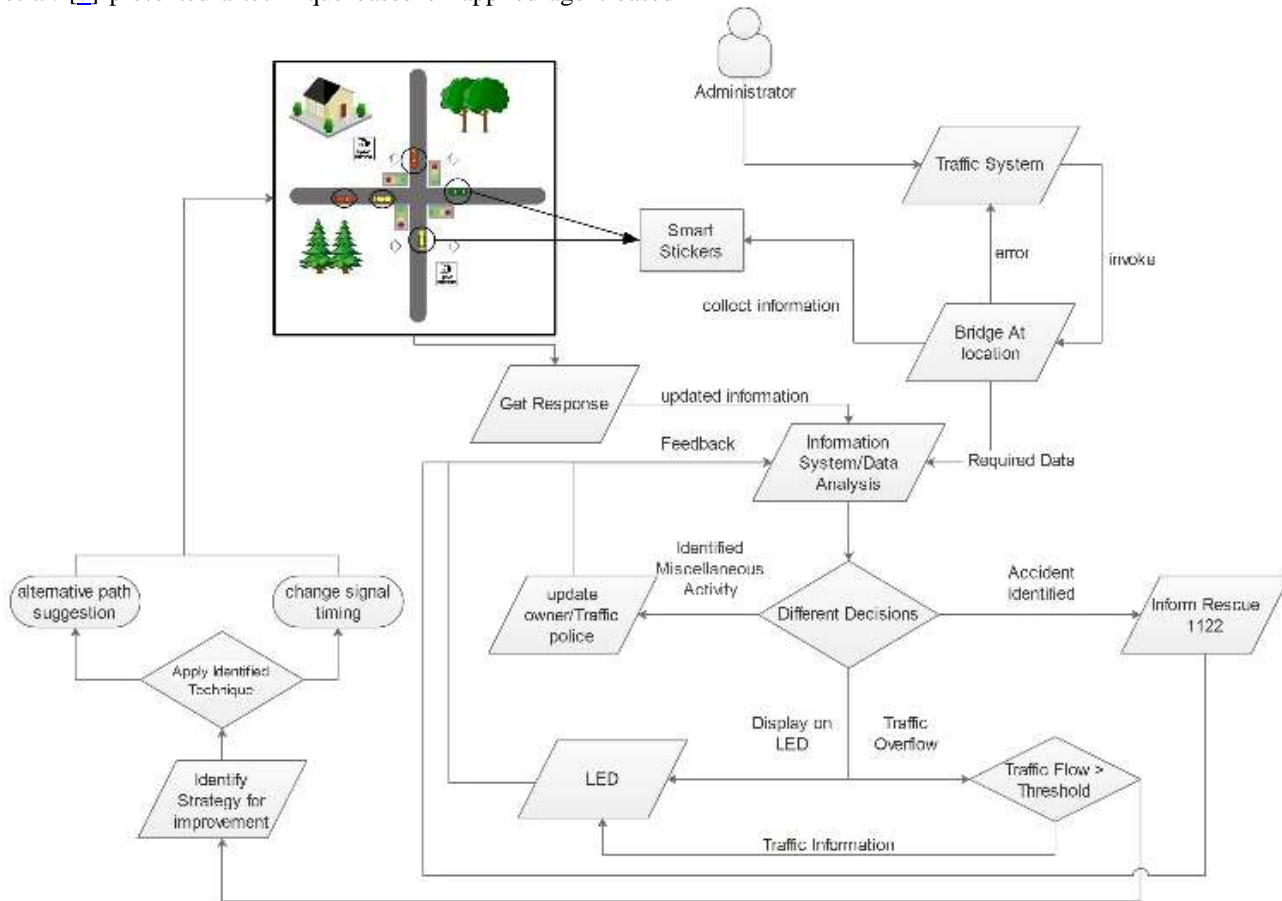


Fig. 1. Smart Traffic model with Design Aided by UML

Different researchers developed different paradigm for IoT composed of different intelligent systems. The domain of such intelligent systems in [4, 10, 17, 22] are health care, business inventories, smart environment, smart home, retail smart agriculture, supply chain logistics, monitoring electrical equipment. In this case of the intelligent transportation system is the earlier stage with respect to their needs [8, 20, 24, 25]. Various IoT smart systems such as FeDNet [16, 18], UbiComp [12] are using the simple message passing communication techniques. Such techniques using a large amount of energy and bandwidth.

Fortino et. al [11] have proposed cloud computing and architecture integrating agents techniques for developed reorganized smart objects within IoT. Godfrey et al. [9] have proposed the mobile based agent technique. This technique is not just handling the communication among the different devices, it also conduct searching for needed resources [9, 14, 18].

III. MODEL OF TRAFFIC MONITORING AND GUIDANCE SYSTEM

In this proposed model Authors have explored main and important problems of traffic system. The major problems are traffic congestion, road accidents, identification of illegal and rules violating vehicles and emergency incidents. Another aspect is, large number of drivers are illiterate. They cannot read or effectively understand the traffic rules, signs and guidance provided on road. In this proposed model it provides guidance on road through Light Emitted diode (LED) at different points and intersections. In this study the focus is on display information on LEDs, issue challan on rules violation. LED display information related to current traffic state, future congestion prediction, path information, signal timings and other related information. Sensors installed at different point will scan the traffic situation on different intervals and then system will be updated with that information. Further, Bridge is another component to provide central hub for

communication among different components of the system. The Light Emitted Diodes will provide the display information to every user.

Issue challan will active in response to violation of rules, challan will be issued by the administrator and sent to owners mobile also system will inform nearby traffic wardens about violation. During processing system will also detect any miscellaneous activity and inform to related department if detected. In a previous study, Authors have described the traffic signals and smart stickers, traffic signals are controlled by the system automatically and it will also update the signal timing according to the situation.

IV. UML SEQUENCE DIAGRAMS

A. Traffic System Sequence Diagram

In a typical traffic system, all the equipment's are required to be online. The reason is system can request anytime. A mature information system has strong behavior. Therefore the work is done in a sequence. So that this diagram is called as sequence diagram. The first sequence of operation is related to maintenance of traffic system and at initial point any of the sequence can be initiated that belongs to system. First, the admin make a request for system. After this, the system makes a request for information system that collects all the information that is necessary from sensors. Now at this point the sensors receive the raw fact and send it to information system. Information system is required to process that coming information in real time and send back to LED or system admin. So the loop represents the working of information system.

This all due to sensors because information sending and receiving at the same time is much difficult task. In this way it identifies the flow of traffic. The processed information then used for changing the signal timings or other necessary actions.

The analyzer is checking or comparing the updated traffic information with the previous signal timings either there is any need to change the signals or not. After analysis the data it again sends to system and all this happens in fraction of second. The information is collected by sensors and stored in a system. If it is successful then make a normal feedback to the admin. Improvement centre also maintain history of situations and signals timings that perform well at certain time, this historical data is necessary while making a system automate. Now after completing all the stages admin have information that is completely correct.

To show the interaction between objects or sequential functionality of a system objects generally developers use sequence diagram. Sequence diagrams helps developers to develop that particular task easily, so developers think sequence diagrams are meant for them [5]. However traffic system sequence diagram can find the sequence between admin and system. First of all, admin give command to get information from sensors. System communicate and gather information from activate sensors because the system is using different types of sensors to get different information so system gather information from different type of sensors.

Unified modeling language have another technique to model the system, it is called class diagram. A class diagram represents the static behaviour of any system, in previous diagrams author was looking into dynamic behaviour of the system. Class diagram is a modeling technique in which anyone can represent the structure of system with its attributes and functionalities associated with it. All the previous functionalities are represented in this diagram and it also show the relationship between them [6] how a complete system is linked from inside and what information sharing is going on can be seen with this diagram. Class is also one way to represent a system as object oriented system.

B. LED Information Update Sequence Diagram

Sequence diagram is a timely or sequence based system interaction diagram that shows, how many process will be in the current system module and either they are communicating with each other or not. Which operation comes first and which comes later, how and why a process is dependent on other process [13]. It provides the sequence between processes, in sequence diagram interaction between operations arranged in time sequence. As discussed earlier in this scenario the pattern of reading a sequence diagram is standard way of reading from left to right and top to bottom. The figure shows the admin start the processing by sending the command to traffic system.

The bridge collects all information from the desired location and sends it to system for processing and then system put back that processed information on the LEDs. In this way the information is updated and displayed on LED. Here there are two cases which are:

Case I: If there is a request for update information then the admin give a request to system to call a bridge and ensure that all the information that are collected by the bridge is correct and make a request to display updated information on LEDs.

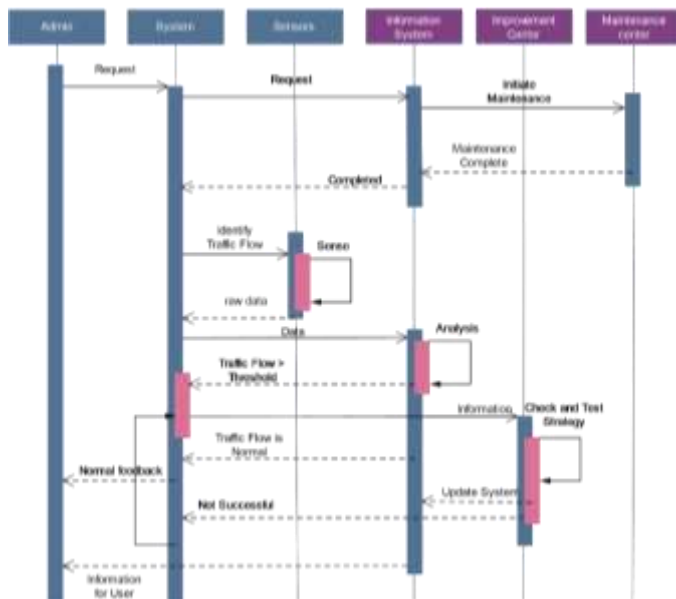


Fig. 2. Traffic System Sequence Diagram

Case II: If there is no request for update information then the old information is displayed on LEDs.

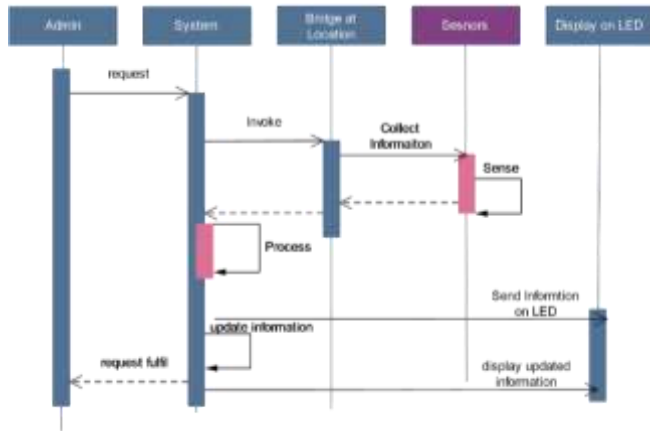


Fig. 3. LED Information Update Sequence Diagram

C. Issue Challan Sequence Diagram

Interactive diagrams model define the behaviour of system in a way that when different group of users interacts with the same system, it can give different output behaviour according to users group. There are two diagrams in common for modeling interactivity of system those are collaborative and sequence. UML sequence diagram shown below, different lines represent different functions applied to system. Sequence diagram read from left to right (fig) shows that the object of system activate the behaviour by sending the request at bridge location. Then the object bridge at central location collect the information from sensors, then these sensor can detect the vehicle its speed, geo-location, direction and other metadata required to make decisions. The collected data will be processed by information system, if the information relates with miscellaneous activity or rule violation then, the system updates its database and send the situation and all other necessary information to nearest traffic police representative. Related information may also be sent to vehicle owner.

The word violation means to break the law for some reason or no reason. The violation might be high speed, don't fasten the seat belt and wrong overtaking etc. How to reduce the traffic violations? If the violation occurs then where it is occurring? Identify it and how to engage it? These are basic questions to be answered in a well-suited manner first of all the system makes a request for the nearby bridge at a central location. Sensor device has short range as compared to bridge. If we say the range is enough for sensor then the problem will, all the sensors cannot make direct connection with the server. Bridge is basically collector that is why the system use bridge is to group sensors that receive all the information from sensors and directly connect to the server. Working of bridge is like a Wi-Fi device to receive and collect the signal from host devices or server then send it to all main and major devices that are attached or connected with Wi-Fi. So, in the same way, the bridge collects all the information from the sensors and then convey this to server. The bridge collects the information in the form of raw data. Then the data is forwarded to information system. At this stage, the information system identifies either the activity is miscellaneous or not. Miscellaneous activities

involve all types of rules violation if it identifies then that activity will be reported to police representative and system admin.

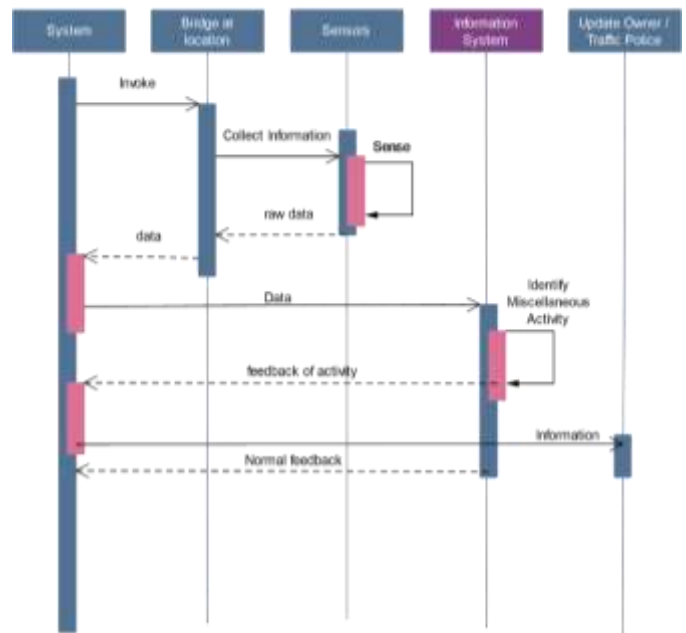


Fig. 4. Traffic Rules Violation Sequence Diagram

V. FORMALIZATION OF MODULES

A. Bridge

Bridge is a device that is used to connect all the sensors with the server. All the sensors cannot connect directly with the server, because it will make a mess. So the system needs a central point (bridge) where all the sensors of a certain location connected and then bridge will be connected to server.

In the formal specification of bridge, the first part this system has is types in which all the variables are declared. The system used different variables like bridge status that is quote type, Bridge, sensor information that is the token type, location, and sensor that is a string. Other variable is traffic situation and the last one is restricted area. The system used these variables for storage of different values as name suggests traffic situation will store the current state either it is jammed congestion, smooth or accident. Restricted area store different areas that are restricted. Same as location will store the locations.

```

types
String = seq of char;
bridgestatus =
<AVAILABLE>|<BUSY>|<IDLE>|<ERROR>;
Bridge::name : String
      Status : bridgestatus;
Sensorinformation = token;
Location = String;
Sensors = String;
trafficSituations =
<JAMMED>|<CONGESTION>|<SMOOTH>|<ACCIDENT
>;
restrictedAreas = set of token;
    
```

The system is not assigned with any predefined value so the values portion is empty. The most important part of any specification is its state. State defined the starting behaviour of any program and it gave values to different variables that remained in the memory. Different variables defined in the state with their data types, the state also has invariant and initialization, invariant is a condition that must be satisfied before the declaration of object, and initialization define the values of all the variables in the state on declaration. So the system is checking Bridge and restricted area must not be empty.

```
state theBridge of
loc : map Sensors to Location
bridge : set of Bridge
getinformation : map Sensors to Sensorinformation
restrictedArea : set of restrictedAreas
currentTraffic : set of trafficSituations
inv mk_theBridge(-,b,-,r,-) == (b << {}[2]) and (r << {})
init i == i = mk_theBridge({|->}, {}, {|->}, {}, {})
end
```

The system can perform different operations on Bridge; these are add sensor, get information and status update. First Operation is ADD SENSOR that has two inputs, first is a sensor that is to be added in network and the other is location where the sensor is to be deployed. The precondition is checking, is this sensor is new or already used, so if the sensor is not already used map that sensor to the location.

```
operations
Addsensor(sensorin:Sensors,locationIn:Location)
ext wr loc:map Sensors to Location
pre sensorin not in set dom loc
post loc = loc munion{sensorin|->locationIn};
```

Another important operation is GET INFORMATION FROM SENSORS. It has also two inputs and it will give the information from the sensors after sensing. The precondition is checking the information that is not already stored in the system and the sensor is in the domain of location. It will get the information and store in the get information variable.

```
Getinformtionformsensors(getinformationin:Sensorinformatio
n, sensorin:Sensors)
ext wr getinformation: map Sensors to Sensorinformation
wr loc:map Sensors to Location
pre (getinformationin not in set rng getinformation) and
(sensorin in set dom loc)
post getinformation = getinformation munion{getinformationin
|-> sensorin};
```

SENSE INFORMATION operation defining the context of information from where it is coming, giving the location, the bridge and the type of information is to be sense. The precondition is used to check either the bridge exist, post condition is used to check either the bridge status is available or the traffic situation is also known. If all these conditions are true, then take information from the sensors and store it to get information variable.

```
SenseInformation(nameIn:String,statusIn:bridgestatus,locatio
nIn:restrictedAreas,sensorIn:Sensorinformation,anyTrafficSitu
tion: trafficSituations)
ext wr restrictedArea : set of restrictedAreas
wr getinformation: map Sensors to Sensorinformation
wr bridge : set of Bridge
```

```
wr currentTraffic: set of trafficSituations
pre (mk_Bridge(nameIn,statusIn).Status << <ERROR>)
post (mk_Bridge(nameIn,statusIn).Status = <AVAILABLE>
and (locationIn in set restrictedArea) or (anyTrafficSituation in
set currentTraffic ) or getinformation = getinformation
munion{getinformation|->sensorIn});
```

The last operation is STATUS UPDATE that is used to update the status of bridge. It is necessary to maintain all the devices so during maintenance, bridge status might be changed to busy or error and update status might be converted back to active.

```
StatusUpdate(statusIn:bridgestatus,bridgeIn:Bridge)
ext wr bridge : set of Bridge
pre true
post bridgeIn.Status=statusIn;
```

B. Issue Challan

Issue challan is common when somebody breaks the rule. This specification defined different situations when somebody got challan with different processes involved in it. The system has used different variables, vehicle owner that is a composite type, reasons that stored the reason of a challan. Sensors information that is either information about the vehicle or information about the reasons for challan. The system also store location.

```
types
String = seq of char;
Vehicleowner :: id:String
License:String;
Resons=<OVERSPEED>|<CROSSREDSIGNAL>|<TAXESO
VERDUE>;
Challan=String;
Sensorinformation=<VEHICLEOWER>|<RESONS>;
Location = String;
Sensors = String;
```

In the values the system has used speed limit, its type is integer and value is sixty, it may be used inside the city for checking over speed.

```
values
SPEEDLIMIT:int=60
```

The state is an important part of any specification, in the invariant of this state, the system is checking for reasons, because if the system is issuing a challan then there must be a reason for it. So the cardinality of reasons must be equal to the cardinality of challan. The detail of challan will come later and for the initialization, yet all the variables are empty.

```
state issuechallan of
loc: map Sensors to Location
sensors : set of Sensors
getinformation: map Sensors to Sensorinformation
cardriver : set of Vehicleowner
resons: set of Resons
challan:set of Challan
inv mk_issuechallan(-,-,-,r,c) == (card(c)=card(r)) and
(r={<OVERSPEED>} or r={<CROSSREDSIGNAL>} or r =
{<TAXESOVERDUE>}) and (SPEEDLIMIT > 60 )
init i == i = mk_issuechallan({|->}, {}, {|->}, {}, {})
end
```

Next part is operations that define the behaviour for any system. In this module the first operation is add sensor same as

in other modules management can add sensor to any location. The ADD SENSORS is used to add sensor and where to deploy it. For adding a sensor, management uses mapping function that Maps a Sensor to the given location.

```
operations
AddSensors(sensorin:Sensors,locationIn:Location)
ext wr loc: map Sensors to Location
wr sensors : set of Sensors
pre sensorin not in set dom loc
post loc= loc munion{sensorin/->locationIn};
```

The GET INFORMATION FROM SENSOR operation can be invoked manually or automatically. This method senses the information from the sensors and give it to the calling authority, for the input parameters.

```
Getinformationfromsensors(getinformationin:Sensorinformation, sensorin:Sensors)
ext wr getinformation: map Sensors to Sensorinformation
pre (getinformationin not in set rng getinformation) and (sensorin in set dom loc)
post getinformation= getinformation
munion{getinformationin /-> sensorin};
```

ISSUING CHALLAN is necessary to control the traffic on roads. To issue challan the system must have some reason, id and license of the person.

```
Issuchallan(resonIn:Resons,idIn:String,licencIn:String)
ext wr cardriver :set of Vehicleowner
wr resons: set of Resons
wr challan: set of Challan
pre true
post (resonIn=<OVERSPEED>and (SPEEDLIMIT>60)or resonIn=<CROSSREDSIGNAL>or resonIn=<TAXESOVERDUE>) and challan = challan union {mk_Vehicleowner(idIn,licencIn)};
```

The system must have an option in it to check whether the person has paid his or her previous challan or not. So IS PAID CHALLAN method takes challan and check whether it is paid or not paid.

```
Ispaidchallan(challanIn: Challan)query:bool
ext wr cardriver :set of Vehicleowner
wr challan: set of Challan
pre true
post query <=> challanIn in set challan ;
```

NUMBER OF ISSUE CHALLAN method used the total count of challans issued in a system to any user.

```
numberofissuechallan(number:int)
ext wr challan:set of Challan
pre true
post number = card challan ;
```

C. LED Information

The Authors have deployed LEDs on roads for displaying information to users. The Authors have developed this module to set and edit the LED information. The first part of the specification is types that have variables declared in it then these variables are used in operations and state of LED. LED information variable store information that is currently displayed on the LED and if management wants to change the information they have to modify the information that is currently stored in it. Second variable the system use is

information about the traffic either the traffic is jammed, is there any accident and is there any construction going on or congestion. Next variable is related to information given to a user about the path.

```
types
String = seq of char;
ledInformation = set of String;
information
=<CONGESTION>|<JAMMED>|<CONSTRUCTION>|<ACCIDENT>;
Signalforvehicleowner
=<CONTINUE>|<SUGGESTIONPATH>;
SensorinformationonLED=<INFORMATION>|<SIGNAL>;
Location = String;
Sensors=String;
```

Next part of the specification states that defined the initialization of a class. The System has used invariant that triggers before the initialization and validates some conditions, and then initializes the variables according to values if given. In this situation, the system doesn't have any values given in the initialization.

```
state LED of
loc: map Sensors to Location
sensors : set of Sensors
getinformationofLED: map Sensors to SensorinformationonLED
ledInfo:set of String
newinfo : map String to String
inv mk_LED(-,-,l,n) == (card(l) > 0 and card(l) <= 30)and (l subset dom n)
init mk_LED(-,-,l,n)== l = {} and n={/->}
end
```

The first operation is ADD SENSORS, a method is defined to take a sensor and a location and it maps the sensor to the location.

```
operations
AddSensors(sensorin:Sensors ,locationIn: Location)
ext wr loc: map Sensors to Location
wr sensors : set of Sensors
pre sensorin not in set dom loc
post loc= loc munion{sensorin/-> locationIn };
```

GET INFORMATION FOR LED method takes input to display on LEDs from sensors. It gets information from sensor after system processed that information and then display on the LED, before the pre-conditions validates that this information is not already displayed on LED.

```
GetinformationforLED(getinformationin:SensorinformationonLED, sensorin:Sensors)
ext wr getinformationofLED: map Sensors to SensorinformationonLED
wr loc:map Sensors to Location
pre (getinformationin not in set rng getinformationofLED) and (sensorin in set dom loc)
post getinformationofLED= getinformationofLED
munion{getinformationin /-> sensorin};
```

ADD INFORMATION method takes information and displays it on the LEDs. This method is manual, when admin wants to display desired information on the LEDs then admin will use this method to send the string to LEDs.

```
AddInformation(newInfo:set of String)
ext wr ledInfo:set of String
pre newInfo <> {}
post ledInfo = newInfo union ledInfo;
```

REMOVE INFORMATION works same as the previous method. It is possible that LEDs are displaying some information one after another. Therefore, any information management wants to remove from the LEDs they have to pass it to this method.

```
RemoveInformation(removeInfo:set of String)
ext wr ledInfo:set of String
pre removeInfo <> {}
post ledInfo = removeInfo \ ledInfo;
```

As the name suggests CHANGE INFORMATION method change the text from LEDs, it replaces old information with the new information. Admin needs to change information occasionally so this method is very important.

```
changeinformation(oldinfo:String,lednewinfo:String)
ext wr newinfo : map String to String
pre lednewinfo not in set dom newinfo
post newinfo =newinfo ++{lednewinfo |-> oldinfo};
```

VI. FORMAL ANALYSIS OF MODULES

A. Formal Analysis of Bridge

Formal analysis of bridge is shown in Figure 5 and Table 1.

TABLE I. FORMAL ANALYSIS OF BRIDGE

Operation	Syntax Check	Type Check	Integrity Check
Addsensors	Y	Y	Y
Getinformationfromsensor	Y	Y	Y
Senseinformation	Y	Y	Y
StatusUpdate	Y	Y	Y

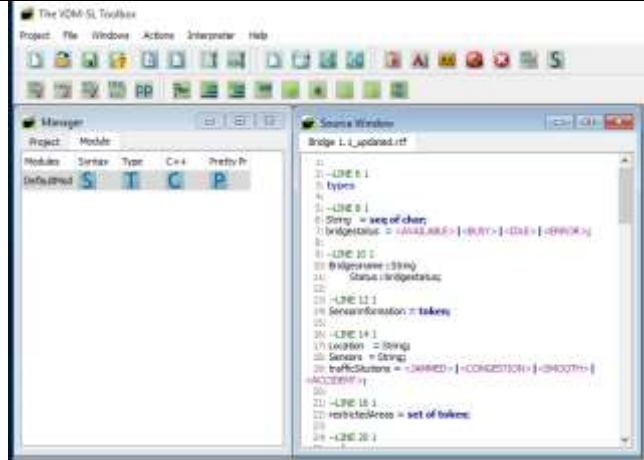


Fig. 5. Formal Analysis of Bridge

B. Formal Analysis of Issue Challan

TABLE II. FORMAL ANALYSIS OF ISSUE CHALLAN

Operation	Syntax Check	Type Check	Integrity Check
Addsensors	Y	Y	Y
Getinformationfromsensor	Y	Y	Y
Issuechallan	Y	Y	Y
IsPaidchallan	Y	Y	Y

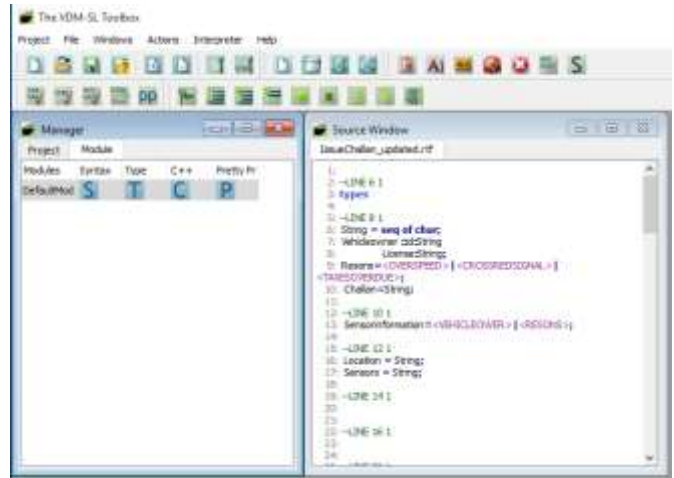


Fig. 6. Formal Analysis of Issue Challan

C. Formal Analysis of LED Information Update

The analysis is performed as shown in Table 3 and Figure 7.

TABLE III. FORMAL ANALYSIS OF LED INFORMATION UPDATE

Operation	Syntax Check	Type Check	Integrity Check
Addsensors	Y	Y	Y
Getinformationfromsensor	Y	Y	Y
Addinformation	Y	Y	Y
Changeinformation	Y	Y	Y
removeInformation	Y	Y	Y

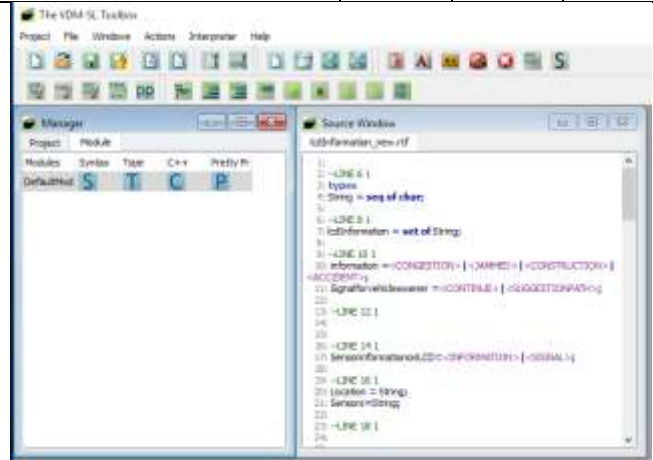


Fig. 7. Formal Analysis of LED Information Update

VII. CONCLUSION AND FUTURE DIRECTIONS

This paper presented modules of Smart Traffic Monitoring and Guidance System like issue challan, display information of traffic situation on LEDs, bridge and system maintenance. The goals of these modules are to provide information related to traffic, its rules and display information on LEDs at different locations on roads to guide users. Traffic rules violation monitored remotely through sensors, further these sensors collect information of vehicle owners and about those persons who violate the rules. First, LEDs are used to show rules and status of different roads, sensors are used to detect rules

violation, also sensors are used to detect traffic load and finally bridges are used to combine sensors from a certain location. The system needs to be maintained in its life cycle, so Authors have also proposed maintenance module in which system errors and bugs will be fixed and system values will be adjusted. Smart traffic system provides the information related to traffic situation to overcome the incidents. Formal methods based technique, i.e. VDM-SL is used to develop a formal representation of the proposed model. The proposed model components are validated, verified and analyzed using VDM-SL Toolbox. In a previous paper, the authors have already discussed the traffic signal, rescue services, and smart sticker services to provide the security and trouble-free environment.

In future, there is a need to design smart algorithms for this proposed Smart Traffic Management and Guidance System to enhance the functionality of sensors. This model can be connected to web domain in order to inform users on their desktop about traffic situations. Sensors can be connected with GSM (Global System for Mobile communications) that can be able to broadcast information through SMS (Short Message Service) to users which are in range. In future, this model can be enhanced to provide smart services in traffic management system in the country.

REFERENCES

- [1] Abbas, U.N., F. Ullah, and N.A. Zafar, Formal Model of Smart Traffic Monitoring and Guidance System. *International Journal of Computer Science and Information Security*, 2016. 14(6): p. 241.
- [2] Al-Heeti, K. and M.S. Al-Ani, Intelligent Traffic Light Control System Based Image Intensity Measurement. 2011.
- [3] Al-Sakran, H.O., Intelligent traffic information system based on integration of Internet of Things and Agent technology. *International Journal of Advanced Computer Science and Applications (IJACSA)*, 2015. 6(2): p. 37-43.
- [4] Asin, A. and D. Gascon, 50 sensor applications for a smarter world. *Libelium Comunicaciones Distribuidas*, Tech. Rep, 2012.
- [5] Bell, D., UML basics: The sequence diagram. IBM Corporation, Feb, 2004. 16: p. 15.
- [6] Bertini, R.L., M. Leal, and D.J. Lovell, Generating Performance Measures from Portland's Archived Advanced Traffic Management System Data. *Transportation Research Board*, 2002.
- [7] Bhadra, S., A. Kundu, and S.K. Guha. An agent based efficient traffic framework using fuzzy. in *2014 Fourth International Conference on Advanced Computing & Communication Technologies*. 2014. IEEE.
- [8] Cao, Y., W. Li, and J. Zhang. Real-time traffic information collecting and monitoring system based on the internet of things. in *Pervasive Computing and Applications (ICPCA)*, 2011 6th International Conference on. 2011. IEEE.
- [9] Chen, B., H.H. Cheng, and J. Palen, Integrating mobile agent technology with multi-agent systems for distributed traffic detection and management systems. *Transportation Research Part C: Emerging Technologies*, 2009. 17(1): p. 1-10.
- [10] Domingo, M.C., An overview of the Internet of Things for people with disabilities. *Journal of Network and Computer Applications*, 2012. 35(2): p. 584-596.
- [11] Fortino, G., et al. Integration of agent-based and cloud computing for the smart objects-oriented iot. in *Computer Supported Cooperative Work in Design (CSCWD)*, Proceedings of the 2014 IEEE 18th International Conference on. 2014. IEEE.
- [12] Goumopoulos, C., A. Kameas, and P. Hellas, Smart objects as components of ubicomp applications. 2009.
- [13] Johnson, W.W., et al., Development and demonstration of a prototype free flight cockpit display of traffic information. 1997.
- [14] Karthikeyan, T. and S. Sujatha, Optimization of traffic System using TCL Algorithm through FMSA and IMAC Agents. *International Journal of Advanced Research in Computer Engineering & Technology (IJARCET)*, Voulme, 2012. 1.
- [15] Katiyar, V., P. Kumar, and N. Chand, An intelligent transportation systems architecture using wireless sensor networks. *International Journal of Computer Applications*, 2011. 14(2): p. 22-26.
- [16] Kawsar, F., A document-based framework for user centric smart object systems. PhD in Computer Science, Waseda University, Japan, 2009.
- [17] Miorandi, D., et al., Internet of things: Vision, applications and research challenges. *Ad Hoc Networks*, 2012. 10(7): p. 1497-1516.
- [18] Nakamiti, G., et al. An agent-based simulation system for traffic control in the Brazilian Intelligent Cities Project context. in *Proceedings of the 2012 Symposium on Agent Directed Simulation*. 2012. Society for Computer Simulation International.
- [19] Pang, M.-b. and X.-p. Zhao. Traffic flow prediction of chaos time series by using subtractive clustering for fuzzy neural network modeling. in *Intelligent Information Technology Application*, 2008. IITA'08. Second International Symposium on. 2008. IEEE.
- [20] Pyykönen, P., et al. Iot for intelligent traffic system. in *Intelligent Computer Communication and Processing (ICCP)*, 2013 IEEE International Conference on. 2013. IEEE.
- [21] Rodríguez-Molina, J., et al., Combining wireless sensor networks and semantic middleware for an internet of things-based sportsman/woman monitoring application. *Sensors*, 2013. 13(2): p. 1787-1835.
- [22] Sanchez, T., et al., Adding sense to the internet of things—an architecture framework for smart object systems. *Pers Ubiquitous Comput*, 2012. 16(3): p. 291-308.
- [23] Spiess, P., et al. SOA-based integration of the internet of things in enterprise services. in *Web Services*, 2009. ICWS 2009. IEEE International Conference on. 2009. IEEE.
- [24] Yin, Y. and D. Jiang. Research and application on intelligent parking solution based on internet of things. in *Intelligent Human-Machine Systems and Cybernetics (IHMSC)*, 2013 5th International Conference on. 2013. IEEE.
- [25] Yu, X., F. Sun, and X. Cheng. Intelligent urban traffic management system based on cloud computing and Internet of Things. in *Computer Science & Service System (CSSS)*, 2012 International Conference on. 2012. IEEE.

Response Prediction for Chronic HCV Genotype 4 Patients to DAAs

Mohammed A.Farahat

Faculty of Computers and Information
Helwan University
Cairo, Egypt

A. Abdo

Faculty of Computers and Information
Helwan University
Cairo, Egypt

Samar K. Kassim

Faculty of Medicine
Ain Shams University
Cairo, Egypt

Khaled A.Bahnasy

Faculty of Computers and Information
Ain Shams University
Cairo, Egypt

Sanaa M.Kamal

Faculty of Medicine
Ain Shams University
Cairo, Egypt

Ahmed Sharaf Eldin

Faculty of Computers and Information
Helwan University
Cairo, Egypt

Abstract—Hepatitis C virus (HCV) is a major cause of chronic liver disease, end stage liver disease and liver cancer in Egypt. Genotype 4 is the prevalent genotype in Egypt and has recently spread to Southern Europe particularly France, Italy, Greece and Spain. Recently, new direct acting antivirals (DAAs) have caused a revolution in HCV therapy with response rates approaching 100%. Despite the diversity of DAAs, treatment of chronic hepatitis C genotype 4 has not yet been optimized. The aim of this study is to build a framework to predict the response of chronic HCV genotype 4 patients to various DAAs by applying Data Mining Techniques (DMT) on clinical information. The framework consists of three phases which are data preprocessing phase to prepare the data before applying the DMT; DM phase to apply DMT, evaluation phase to evaluate the performance and accuracy of the built prediction model using a data mining evaluation technique. The experimental results showed that the model obtained acceptable results.

Keywords—HCV; DMT; Decision Tree; DAAs; Prediction Model

I. INTRODUCTION

Hepatitis C virus (HCV) is a major cause of liver disease worldwide. The WHO estimated that more than 170 million persons are infected by this virus [1]. The HCV infection is transmitted parentally through injections which are unsafe; inadequate sterilization of medical equipment in some health-care places; transfusion of unscreened blood or blood products, sexual transmission or vertical transmission from mother to infant¹. HCV causes an acute infection which evolves to chronic hepatitis in 80% of cases [3]. Some patients with chronic hepatitis C infection develop liver cirrhosis, end stage liver disease or liver cancer [4, 5]. There are six genotypes of hepatitis C which may respond differently to the treatment. Approximately, 350000 to 500000 people die each year because of hepatitis C-related liver diseases [6].

Egypt has the highest incidence and prevalence of HCV infection worldwide [7]. HCV represents a huge public health and socio-economic problem in Egypt. The prevalence of

HCV in Egypt is 12% of the population (about 11 million Egyptians) [8]. The prevalent genotype in Egypt is genotype 4. Recently, HCV genotype 4 started to spread to Europe particularly France, Italy, Greece and Spain now. Thus, HCV genotype 4 became a growing problem in other areas of the world.

The treatment of HCV has progressed from interferon monotherapy to interferon and ribavirin (RBV) combination therapy then pegylated interferon (PEG-INF) and ribavirin therapy. However, interferon based therapies were associated with multiple adverse events in addition to limited response rates especially in genotypes 1 and 4. Recently, new direct acting antivirals (DAAs) resulted in very high success rates exceeding 90% with minimal adverse events. DAAs are either given as interferon free regimen or administered with pegylated interferon. DAAs represent a breakthrough in HCV treatments since the response rate exceeds 90% Thus, DAAs represent a breakthrough in eradication of HCV. However, DAAs have not been adequately evaluated in chronic HCV genotype 4.

Data mining is not all about the used tools or database software. Data mining itself depends on building a suitable data model and structure which can be used to process, identify, and build the needed medical and clinical information. In spite of the source data form and structure, structuring and organizing the clinical information in a format which allows the data mining techniques to run in as efficient a model as possible.

Therefore, this study is designed to build an application to predict the response of chronic HCV genotype 4 patients to DAAs by applying Data Mining Techniques (DMT) on clinical information.

The remainder of this paper is structured as follows. First, we discussed the related work in Section II. This is followed by a description of the clinical data and the phases of our framework in Section III. The experimental results are discussed in Section IV. We conclude our paper in Section V and give an outlook to the future work.

¹ <http://www.who.int/mediacentre/factsheets/fs164/en/>

II. RELATED WORK

Many researches have been developed to predict patients' response to treatment of HCV from clinical information using different data mining techniques.

In [2], Mohammed M.Eissa et al. used Rough Granular Neural Network model and Artificial Neural Network (ANN) for Making Treatment Decisions of Hepatitis C. This data was collected from clinical trials of a newly developed medication for HCV. It consists of 119 cases; each of which is described by 28 attributes: 23 numerical and 5 categorical attributes, the intention of the dataset is to forecast the presence or absence of the hepatitis virus related to the proposed medication. The rough set technique had been used to discover the dependency among the attributes, and to reduce the attributes and their values before the original information, remove redundant information, reduce the dimension of the information space, provide a simpler neural network training sets, and then construct and train the neural network. The experimental results show that the proposed hybrid model can acquire the advantages from the two data-mining methods (Rune Space (RS) and ANN). In addition, the integration of the Rough Sets and ANN together can produce a positive effect, enhancing model performance.

In [6] E. M. F. El Houby, et. al. applied knowledge discovery technique to predict HCV patients' response to treatment, which is a combined therapy Peg-IFN and RBV, according to a set of features. The proposed framework consists of two phases which are pre-processing and data mining. A database of 200 Egyptian cases was constructed from patients with hepatitis C virus genotype 4, who treated with combined therapy Peg-IFN and RBV for two years. This data was collected at Cairo University hospital. For each patient a record composed 12 features was registered, in addition to response feature. Associative Classification (AC) has been used to predict response to treatment in patients. AC technique has been used to generate a set of Class Association Rules (CARs). The most suitable CARs are selected to build a classifier which predicts patient's response to treatment from the selected features. The accuracy of the algorithm is high reach up to 90%.

In [7] M. ElHefnawi, et. al. made a prediction of response to Interferon-based therapy in Egyptian patients with Chronic Hepatitis C using machine-learning approaches. They used ANN and DT techniques. The study included 200 Hepatitis C patients with genotype 4 at Cairo University Hospital who were treated with combined therapy PEG-IFN- α and RBV for 48 weeks. The data was divided into 150 cases for training and 50 for validation; the maximum accuracy for ANN and DT were 0.76 and 0.80 respectively.

In [8] M. M. Eissa, et. al. introduced a Hybrid Rough Genetic Model to classify the effects of a new medication for HCV treatment through Hybrid Rough Genetic Model which has been used to predict response to new medications for HCV treatment in patients with hepatitis C virus (HCV). This data was collected from clinical trials of a newly developed medication for HCV [32, 33]. It consists of 119 cases; each of which is described by 28 attributes: 23 numerical and 5 categorical attributes. During the experiment HCV Dataset

was divided into training set and test set with splitting factor 0.25. The proposed model included 4 phases (data preprocessing, data reduction, rule generation and classifications of HCV data). the proposed hybrid model can acquire the advantages from the two data-mining methods (Rough Sets and Genetic Algorithms) and therefore, produce superlative results .The Integrating Rough Sets and Genetic Algorithms together can produce a positive effect, enhancing model performance.

In [9] a framework has been developed to compare different data mining techniques' performance in predicting patients' response to treatment of HCV from clinical information. Three data mining techniques which are: (ANN, AC and DT). Data from 200 Egyptian patients with hepatitis C virus genotype 4, who were treated with combined therapy IFN plus RBV for 2 years, was collected at Cairo University Hospital. In evaluation phase, all the models built using different DM techniques for various candidate features subsets have been evaluated using test dataset of 50 cases which have been selected randomly in each iteration. This dataset is independent of the model building dataset (i.e., training dataset). According to evaluation results, the highest performance model can be selected. The best accuracy for the AC is 92% while for ANN it is 78% and it is 80% for DT.

In [10], Lin E, et. al. have used two families of classification algorithms, including Multilayer Feed Forward Neural Network (MFNN) and logistic regression as a basis for comparisons. An MFNN is one type of ANN models where connections between the units do not form a directed cycle. These classifiers were performed using the Waikato Environment for Knowledge Analysis (WEKA) software. There were 523 participants, including 350 Sustained virological response (SVRs) and 173 Non-viral response (NRs). They further converted the clinical diagnostic data into numerical forms, that is, 1 for "SVR" and 0 for "NR", respectively. To measure the performance of prediction models, they defined the accuracy as the proportion of true predicted participants of all tested participants. In addition, they used the receiver operating characteristic (ROC) methodology and calculated the area under the ROC curve (AUC).

In [11], Masayuki Kurosaki, et. al. used classification and regression tree (CART) and Statistical analysis to build a predictive model of response to the treatment in HCV. The software automatically explore the data to search for optimal split variables, builds a decision tree structure and finally classifies all subjects into particular subgroups that are homogeneous with respect to the outcome of interest. The CART analysis was carried out on the model building set of 269 patients using the same variables as logistic regression analysis.

In [12], Kazuaki Chayama et al. made a statistical analysis using the R software package (<http://www.r-project.org>). CART analysis was used to generate a decision tree by classifying patients by SVR, based on a recursive partitioning algorithm with minimal cost-complexity pruning to identify optimal classification factors. The association between SVR and individual clinical factors was assessed using logistic

regression. Data was collected from 840 genotype 1b chronic hepatitis C patients. In this study 465 patients achieved an SVR, whereas 375 patients were either non-responders or relapsers, yielding an overall SVR rate of 55.4%. The rate of SVR did not differ significantly between the 48- and 72-week treatment groups (55.3 vs. 56.4%, respectively; $P = 0.81$), but the NR rate was significantly lower in patients who were treated for 72 weeks.

In [13], Naglaa Zayed et al. made a study on retrospective data belonging to 3719 adult patients with chronic HCV infection of both sexes who were diagnosed by anti-HCV antibodies. Data cleansing was applied for detecting, correcting or removing corrupt or inaccurate record from database in addition to the removing of typographical errors or validating and correcting values against a known list of entities. High quality data was characterized by accuracy, integrity, completeness, validity, consistency, uniformity and unique-ness. Weka implementation of C4.5 (WEKA J48) decision-tree learning algorithm was applied using 19 clinical, bio-chemical, virologic and histologic pre-treatment attributes form the data of 3719 Egyptian patients with chronic HCV. The universality of the decision-tree model was validated using both internal and external validation to confirm the reproducibility of the results. They applied Statistical and Multivariable logistic regression analysis on the data. They concluded that the Prediction of treatment outcome in chronic HCV patients genotype-4 (HCV-G4) has been an important debate since even with the application of combination therapy for 48 weeks only around 50% of patients will respond.

In this research we are going to build an application to predict the response of chronic HCV genotype 4 patients to DAAs as it has not been adequately evaluated in chronic HCV genotype 4.

III. MATERIAL AND METHODS

A. Clinical Data

Data from 420 patients infected with hepatitis C virus genotype 4 from different centers in Europe and Egypt are analyzed. Patients were treated with four different regimens of DAAs with or without pegylated interferon. For each patient there is a record that contains 13 main features which are age, treatment regimen group, gender, body mass index (BMI), white blood cells (WBC), hemoglobin, platelets, baseline PCR, baseline core antigen, aspartate aminotransferase (AST), alanine aminotransferase (ALT), histologic grading and histologic staging. All patients were evaluated at baseline and at different time points during treatment and follow up. The treatment endpoint was sustained virologic response defines as undetectable HCV RNA 12 weeks following termination of therapy.

B. Prediction Model

In this research, a framework has been built to predict the response of Chronic HCV genotype four patients to DAAs by applying Data Mining Techniques (DMT) on clinical information, and then extract the result of DMT to be a Knowledge Base for our application to perform the prediction process. Fig. 1 shows the proposed framework which consists of (1) Data preprocessing phase to prepare the data before

applying the DMT; (2) DM phase to apply DMT, (3) evaluation phase to evaluate the performance and accuracy of the built model using a data mining evaluation technique.

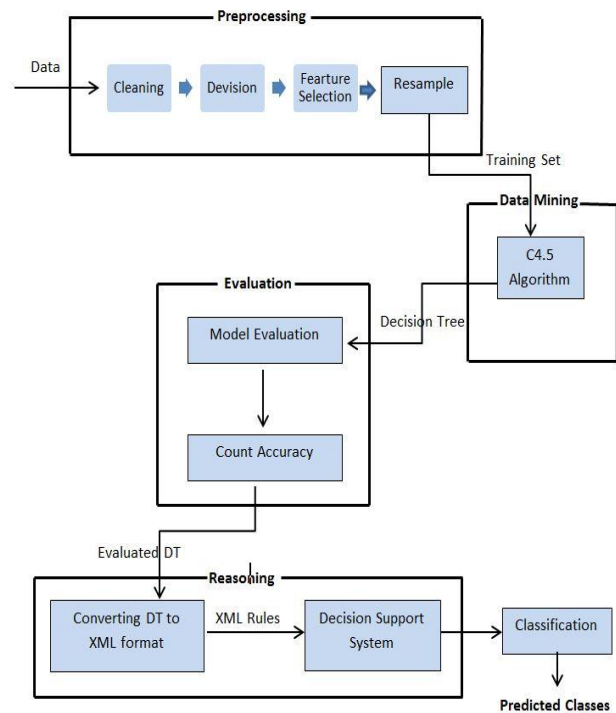


Fig. 1. The Framework of predicting the response of HCV genotype 4 to DAAs

1) Data Preprocessing Phase

In this phase, a series of steps were applied to clean, divide, select the most suitable features for the model from the patient data for applying DMT and resample the data sets into training and test sets.

Data cleaning phase is to clean the data and remove the records that contains empty values. Then the clinical data has been divided into four groups according to the regimen of DAAs treatments which are labeled as (TR1, TR2, TR3 and TR4).

Feature Selection phase is to select a subset of features relevant to the target DMT from all the features of the data set. In the filtering approach; the feature selection algorithm is independent of the DMT which applied to the selected features.

In this research eight features of 13 were selected for TR1, seven for TR2, five for TR3 and nine for TR4. The class label (Result) is considered as the PCR of the 48th week (24 weeks following termination of therapy)

For Resampling; each treatment group has been divided into: 90% of the data as a training set and 10% as a testing set using unsupervised resample filter in Weka.

2) Data Mining Phase

Weka implementation of C4.5 (Weka J48) decision-tree learning algorithm was applied the four training data sets.

C4.5; is based on the ID3 algorithm and tries to find simple (or small) decision trees (DT's). Some premises on which this algorithm is based will be presented in the following sections.

a) Construction

Some premises guide this algorithm, such as:

- If all cases are of the same class, the tree is a leaf and the leaf is returned labeled with this class;
- For each attribute, calculate the potential information provided by a test on the attribute (based on the probabilities of each case having a particular value for the attribute). Also calculate the gain in information that would result from a test on the attribute (based on the probabilities of each case with a particular value for the attribute being of a particular class);
- Depending on the current selection criterion, find the best attribute to branch on.

b) Counting gain

This process uses the "Entropy", i.e. a measure of the disorder of the data. The Entropy of \vec{y} is calculated by

$$\text{Entropy}(\vec{y}) = -\sum_{j=1}^n \frac{|y_j|}{|\vec{y}|} \log \frac{|y_j|}{|\vec{y}|} \quad (1)$$

Iterating over all possible values of \vec{y} . The conditional Entropy is

$$\text{Entropy}(j|\vec{y}) = \frac{|y_j|}{|\vec{y}|} \log \frac{|y_j|}{|\vec{y}|} \quad (2)$$

and finally, we define Gain by

$$\text{Gain}(\vec{y}, j) = \text{Entropy}(\vec{y}) - \text{Entropy}(j|\vec{y}) \quad (3)$$

The aim is to maximize the Gain, dividing by overall entropy due to split argument \vec{y} by value j [15].

c) Pruning

Pruning is a significant step to the result because of the outliers. All data sets include a little subset of instances which are not well-defined, and vary from the other ones in its neighborhood. After the whole creation processes of the tree, which classify all the training set instances, it is pruned. This is to minimize classification errors which can be occurred because of specialization in the training set; we do this to make the tree more general.

d) Results

To show concrete examples of the C4.5 algorithm application, WEKA software tool has been used on training sets. The resulting classes are about the effect of the four treatments on the PCR result, e.g. TR1_Yes or TR1_No. Fig. 2 shows the resulting DT, using C4.5 implementation from WEKA on TR3 data set (as the smallest tree).

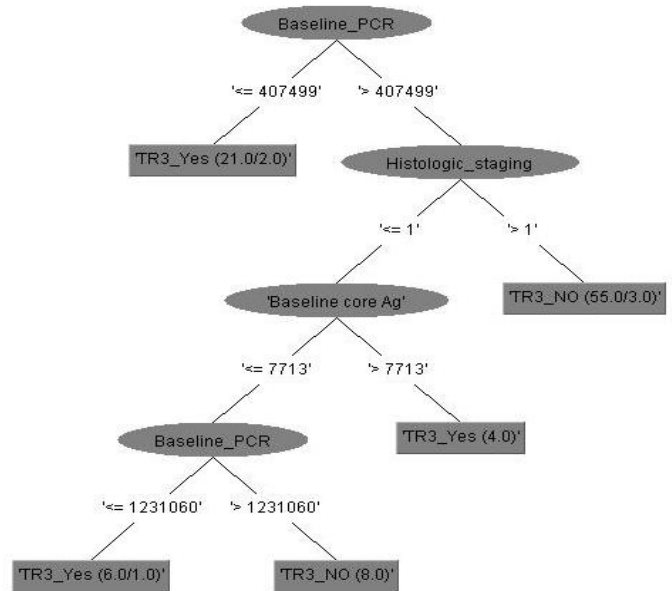


Fig. 2. DT of TR3, Created by the C4.5 algorithm

3) Evaluation Phase

The universality of the four DT models was validated using the test data sets by the hold-out validation method.

The holdout method is considered as the simplest type of cross validation. The data set is divided into two different sets, which are known as the training set and the testing set [14]. The function approximator uses the training set only to fit a function which is used to predict the output values for the testing set data which has never seen these output values before. Then the errors it makes are gathered as before to give the mean absolute test set error, which will be used to evaluate the model. This method is usually preferable to the other methods and takes less time to compute.

C. Reasoning

In the reasoning phase an application has been developed with C# programming language to perform the prediction operation. It can be considered as an expert system.

The knowledge base of this application is the model of decision tree algorithm. It is applied on Weka which delivers rules which has been converted into XML rules format to be used as an input to our DSS application.

IV. EXPERIMENTAL RESULTS

This section shows an empirical performance evaluation of the proposed framework using the applied DM techniques. Data from 420 patients infected with hepatitis C virus genotype 4 from different centers in Europe and Egypt were

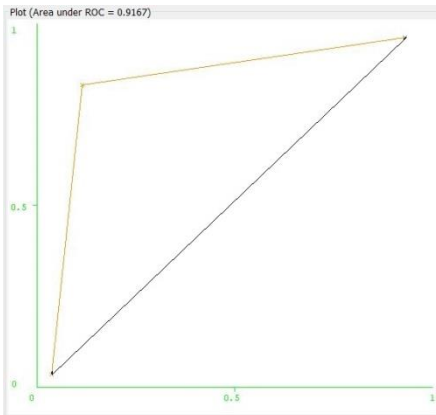
used. Extensive experimental studies had been conducted in order to evaluate the model performance. The clinical data has been divided into four groups according to the regimen of DAAs treatments. Feature selection algorithm has been applied on each group. Eight features of 13 were selected for TR1, seven for TR2, five for TR3 and nine for TR4. A subset of 10% of the data had been selected to test the model and the 90% used to build the classifier.

After applying the model; a large scale of statistical information were obtained. These performance measures had been used to evaluate the model as shown in Table 1. This

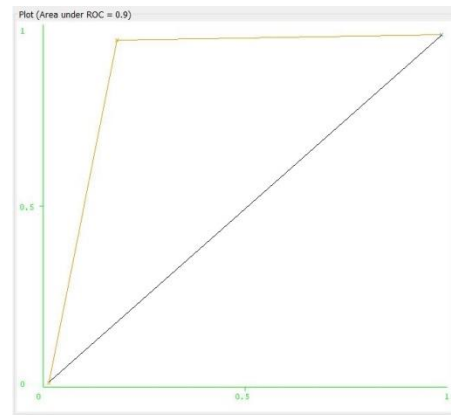
table shows the performance for each treatment group. The DT of the 1st treatment had 83.3% sensitivity, 100% specificity and 90.9% accuracy. The DT of the 2nd treatment had 80% sensitivity, 100% specificity and 90% accuracy. The DT of the 3rd treatment had 100% sensitivity, 71.4% specificity and 81.8% accuracy. Finally the DT of the 4th treatment had 57.1% sensitivity, 100% specificity and 75% accuracy. The averages of the four decision trees are 80% of sensitivity, 93% of specificity and 84% of accuracy.

TABLE I. Performance of the Decision Trees of the 4 DAAs Combination After Testing

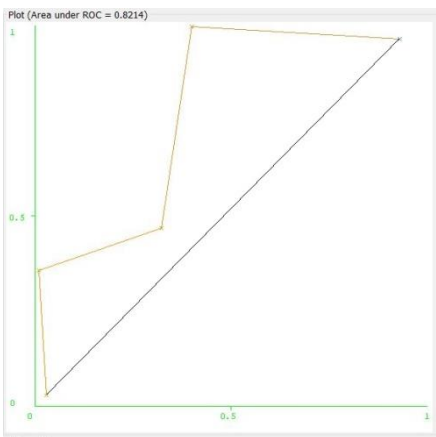
DT number	Size of the tree	Number of leaves	TP	TN	Positive Predictive value %	Negative Predictive value %	Sensitivity	Specificity	AUC%	Accuracy%
TR1_DT	25	13	5	5	100%	83.3%	83.3%	100%	91.67%	90.9%
TR2_DT	31	16	4	5	100%	83.3%	80%	100%	90%	90%
TR3_DT	9	5	4	5	66.7%	100%	100%	71.4%	82.1%	81.8%
TR4_DT	25	13	4	5	100%	62.5%	57.1%	100%	80%	75%
Average			4	5	92%	82%	80%	93%	86%	84%



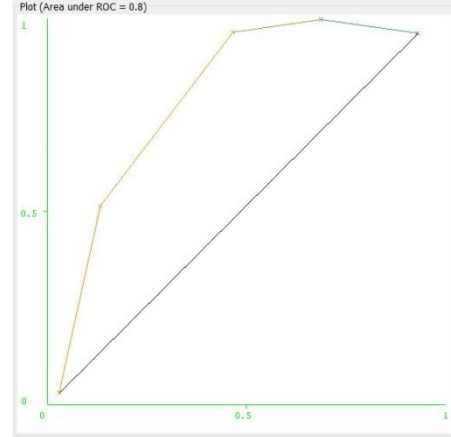
TR1_DT



TR2_DT



TR3_DT



TR4_DT

Fig. 3. The ROC curves for the 4 models with their sensitivity and specificity

Fig. 3 shows a Comparison between the Receiver Operating Characteristic (ROC) curves for the four models and their sensitivity and specificity values at the optimal cutoff points.

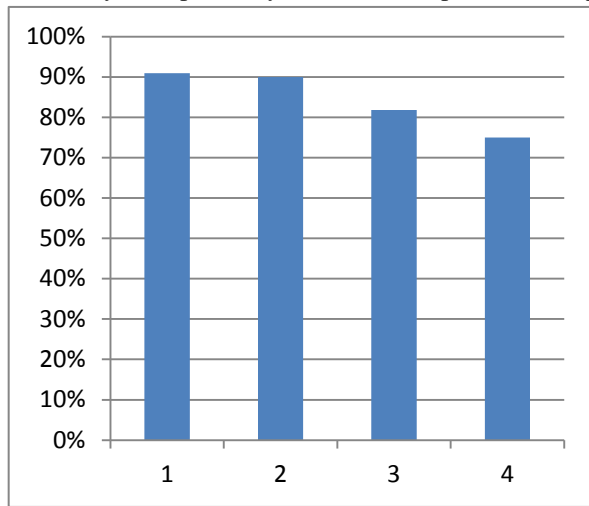


Fig. 4. Comparison of accuracy for the 4 models

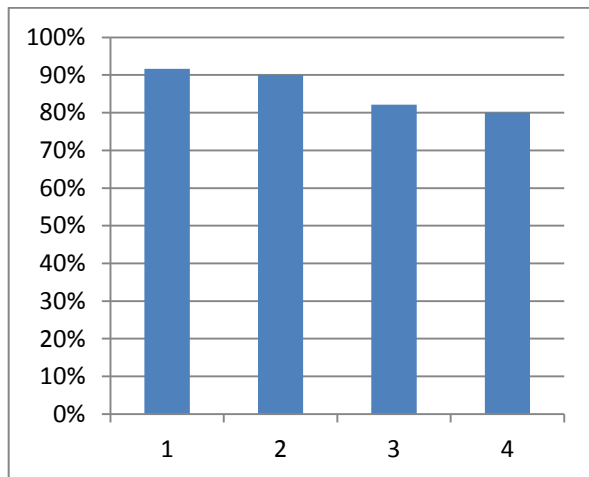


Fig. 5. Comparison of AUC for the 4 models

Fig. 4 shows a comparison between the four models regarding their accuracy. While Fig. 5 shows the comparison of Area Under Curve (AUC) for the model.

V. CONCLUSION AND FUTURE WORK

In this research, a framework has been built to predict the response of Chronic HCV genotype 4 patients to DAAs by applying Data Mining Techniques (DMT) on clinical information. Data from 420 patients infected with hepatitis C virus genotype 4 from different centers in Europe and Egypt has been analyzed. Patients were treated with four different regimens of DAAs with or without pegylated interferon. The clinical data has been divided into four groups according to the regimen of DAAs treatments. Feature selection algorithm has been applied on each group. Decision Tree has been

applied for the prediction, after that extraction of the result of DTs was performed. This constructed a Knowledge Base for our application to perform the prediction operation. The experimental results showed that the four groups give acceptable results. The best accuracy was 90.9% for the 1st group.

In the future, more data sets will be used to train other classifiers and to try more experiments. Also other techniques will be applied and more than one technique will be combined to reach as high accuracy as possible.

REFERENCES

- [1] S.M. Kamal, I.A. Nasser, "Hepatitis C genotype 4: What we know and what we don't yet know," *Hepatology*, vol. 47, no. 4, pp. 1371-83, Apr 2008.
- [2] Mohammed M.Eissa et al., "Rough - Granular Neural Network Model for Making Treatment Decisions of Hepatitis C," the 9th International Conference on INFormatics and Systems (INFOS2014), December, 2014.
- [3] Jiawei Han and Micheline Kamber, *Data Mining Concepts and Techniques* 3rd edition, 2011.
- [4] A. A. Freitas, "A survey of evolutionary algorithms for data mining and knowledge discovery," in *Advances in Evolutionary Computation*, pp. 819-845, Springer, Berlin, Germany, 2001.
- [5] M. F. Enas, "Analysis of associative classification for prediction of HCV response to treatment," *International Journal of Computer Applications*, vol. 63, no. 15, pp. 38-44, 2013.
- [6] E. M. F. El Houby and M. S. Hassan, "Using associative classification for treatment response prediction," *Journal of Applied Sciences Research*, vol. 8, no. 10, pp. 5089-5095, 2012.
- [7] M. ElHefnawi, M. Abdalla, S. Ahmed et al., "Accurate prediction of response to Interferon-based therapy in Egyptian patients with Chronic Hepatitis C using machine-learning approaches," in *Proceedings of the IEEE/ACM International Conference on Advances in Social Networks Analysis and Mining*, pp. 803-810, August, 2012.
- [8] M. M. Eissa, M. Elmogy, M. Hashem, and F. A. Badria, "Hybrid rough genetic algorithm model for making treatment decisions of hepatitis C," in *Proceedings of the 2nd Conference of Engineering and Technology and International (ICET '14)*, German University in Egypt, Cairo, Egypt, 2014.
- [9] Enas M. F. El Houby, "A Framework for Prediction of Response to HCV Therapy Using Different Data Mining Techniques," *Hindawi Publishing Corporation*, 2014.
- [10] Lin E, Hwang Y, Wang SC, "Pharmacogenomics of drug efficacy in the interferon treatment of chronic hepatitis C using classification algorithms," *Advances and Applications in Bioinformatics and Chemistry journal*, 2010.
- [11] Masayuki Kurosaki, et al, "A predictive model of response to peginterferon ribavirin in chronic hepatitis C using classification and regression tree analysis," *Hepatology Research*, 2010.
- [12] Kazuaki Chayama et al., "Factors predictive of sustained virological response following 72 weeks of combination therapy for genotype 1b hepatitis C," *J Gastroenterol* (2011) 46:545-555, 2011.
- [13] Naglaa Zayed et al., "The assessment of data mining for the prediction of therapeutic outcome in 3719 Egyptian patients with chronic hepatitis C," *clinics and Research in Hepatology and Gastroenterology*, 2012.
- [14] Vijay Kumar Mago and Nitin Bhatia, *Cross-Disciplinary Applications of Artificial Intelligence and Pattern Recognition: Advancing Technologies*, 2011
- [15] A. Sivasankari, S. Sudarvizhi and S. Radhika Amirtha Bai, "Comparative study of different clustering and decision tree for data mining algorithm," *International Journal of Computer Science and Information Technology Research*, Vol. 2, Issue 3, pp. 221-232, 2014.S

RAX System to Rank Arabic XML Documents

Hesham Elzentani
Faculty of Informatics and
Computing
Singidunum University
Belgrade, Serbia

Mladen Veinović
Faculty of Informatics and
Computing
Singidunum University
Belgrade, Serbia

Goran Šimić
Military Academy of the Ministry of
Defense
Belgrade, Serbia

Abstract—This paper describes an RAX System designed for ranking Arabic documents in information retrieval processes. The proposed solution basically depends on the similarity of textual content. The model we have designed can be used for documents stored in the different formats and written in Arabic language. Due the complex lingual semantics of this language the proposed solution uses a pure statistical approach. The design and implementation are based on existing text processing frameworks and referent Arabic grammar. The main focus of our research has been the evaluation of different similarity measures used for classifying Arabic documents from different domains and different document categories based on query criteria provided by the user.

Keywords—Text similarity measures; Text classification; Processing Arabic documents

I. INTRODUCTION

Arabic is a widely spoken Semitic language. It has morphology, vocabulary and vowels. Like other Semitic languages an Arabic statement consists of a (Subject-Verb-Object) or (Verb-Subject-Object) chain. The Arabic word is structured by adding infixes, prefixes and/or suffixes as well as

diacritics to the root. The Arabic language has 28 letters which are written from right to left, unlike Latin based languages which are written from left to right. The shape of letters changes according to their positions in the words. Arabic words are divided into nouns and verbs. Nouns include adjectives and adverbs while verbs include prepositions, pronouns and conjunctions. Nouns are masculine or feminine and singular, dual or plural. Verbs are derived from roots [1]. This will be described in further detail in the Related Works section.

In recent years the growth of Arabic content and numbers of users on the Internet has greatly increased as can be seen from the table of top ten languages in the Internet (Table I). Arabic is a widely spoken language with more than 375 million speakers and over 155 million, or over forty percent of these Arabic speaking people use the Internet. This represents nearly five percent of all the Internet users in the world. The number of Arabian speaking Internet users has grown by a factor of sixty in the last fifteen years (2000-2015). This growth in usage has outpaced the growth in information retrieval systems, summarization of Arabic text (such as documents and web pages), query processes and natural language processors [2].

TABLE I. NUMBER OF INTERNET USERS BY LANGUAGE

Top Ten Languages In The Internet	Internet Users by Language	Internet Penetration (% Population)	Users Growth in Internet (2000 - 2015)	Internet Users % of World Total (Participation)	World Population for this Language (2015 Estimate)
English	851,623,892	60.9 %	505.0 %	26.0 %	1,398,277,986
Chinese	704,484,396	50.4 %	2,080.9 %	21.5 %	1,398,335,970
Spanish	245,150,733	55.5 %	1,248.4 %	7.5 %	441,778,696
Arabic	155,595,439	41.5 %	6,091.9 %	4.8 %	375,241,253
Portuguese	131,615,190	50.0 %	1,637.3 %	4.0 %	263,260,385
Japanese	114,963,827	90.6 %	144.2 %	3.5 %	126,919,659
Russian	103,147,691	70.5 %	3,227.3 %	3.2 %	146,267,288
Malay	93,915,747	32.7 %	1,539.0 %	2.9 %	286,937,168
French	92,265,199	23.9 %	669.0 %	2.8 %	385,389,434
German	83,738,911	87.8 %	204.3 %	2.6 %	95,324,471
TOP 10 LANGUAGES	2,576,501,025	52.4 %	768.2 %	78.8 %	4,917,732,310
Rest of the Languages	693,989,559	29.6 %	980.6 %	21.2 %	2,342,888,808
WORLD TOTAL	3,270,490,584	45.0 %	806.0 %	100.0 %	7,260,621,118

An Arabic word has different forms of syntax and morphologies with different meanings. Grammatically, documents contain different forms of words including derivations. This causes problems in text processing, document summarization and information retrieval systems. Furthermore, there is a high level of information loss during the processes of querying, document summarizing and information retrieval, especially with large documents, as information loss is directly proportional to the size of documents during these processes.

This paper describes an RAX System which is designed for ranking Arabic documents stored in the different formats in information retrieval processes. It consists of the following sections: (1) Introduction, which introduces the Arabic language and current internet statistics; (2) Related works that have informed the research; (3) Arabic document management, which introduces the XQuery and Sedna XML database management systems; (4) Proposed solution, which describes

the processing and ranking of Arabic documents; (5) Conclusions.

II. RELATED WORKS

There is currently a high level of interest within the research community for text processing of Arabic documents as well as queries, stemmers, ranking, keyword extraction. The retrieval of formal Arabic language, as used in media such as news domains, as well as the retrieval of Arabic dialects is among the problems that face information retrieval systems. Natural language processing of Arabic information to enable retrieval is considered in [1].

XML documents and querying XML data and databases using XQuery and XML indexing (which summarize large XML data structure into a tree) are discussed in [3] and [4].

Different Arabic text stemmers, as well as constructed Arabic stopwords lists used in information retrieval systems, are described in [5] and [6].

Stemming methodologies and query terms affect the information retrieval systems according to the word and stem. In contrast, term importance can be computed according to term frequency and inverse document frequency as described in [7].

The use of similarity measures in a vector space model, according to term frequency (TF) and inverse document frequency (IDF) of documents and structural of terms, is described in [8].

Automatic keyword extraction according to candidate keywords (that are extracted from a document and selected based on term frequency of words within these documents), word degree and ratio of degree to frequency are covered in [9].

Arabic natural language processing techniques have used linguistic resources such as Corpora and Lexicon to develop parser and POS-tagger. This has enabled the creation and evaluation of a framework for use in Islamic sciences written in the Arabic language. This framework could adapt the theories, resources, tools and applications of other NLPs such as English and French as described in [10].

Three vector space models (Cosine, Dice and Jaccard coefficients) for classifying Arabic text using the K-Nearest algorithm and the IDF term are compared in [11].

Finally, there is currently a high level of activity in the production of tools that provide automatic annotation and translation of Arabic texts. The linguistic difference of the Arabic language to western culture languages results in complexity of implementation. In [NP Subject Detection in Verb-Initial Arabic Clauses] the focus is on the words-in-sentence ordering problem and the different way Arabic phrases are formed. For example the sentence in Fig. 1, which in English is ordered from left-to-right compared to the Arabic phrase which is ordered right-to-left, illustrates the ordering problem [12].

A. Standard Arabic reference background

The following is a brief introduction to standard Arabic based on [5] and [13].

The Arabic language is sematic language. It consists of masculine and feminine and includes grammatical cases (nominative, genitive and accusative) as well as morphology. Arabic nouns in the nominative case have a root (*stem*) which is the standard word in a list or the *base form* in a dictionary. For instance خريطة means *a map*. The definitive noun of *a map* is created by adding the prefix article ال to the beginning of the noun to create the feminine Arabic word الخريطة which means *the map*. One can also attach a preposition such as ل (to) or ب (by) to the front of the definitive article of the noun. Thus the masculine plural of the Arabic word بالخرائط means by *the maps*.

A possessive pronoun can take prefixes and suffixes. For example the Arabic word بسيارتي, meaning *by my car*, could be resolved into ب + سيارة + ي (remembering that writing in Arabic is in the opposite direction to western culture languages). This contains a prefix ب, meaning *by*, and a pronoun suffix ي, meaning *my*.

In the Arabic language plural has a regular (sound) plural form and irregular (broken) plural form. To create the sound plural for feminine nouns one adds suffix ات while for masculine nouns one adds ون in the nominative and ين in the genitive and accusative. For example the Arabic word مدرسة means *teacher* (feminine). The plural is مدرّسات and means *teachers* (feminine) in nominative, genitive and accusative. The Arabic word مدرّس means *teacher* (masculine). The plural in the nominative is مدرّسون, which means *teachers* (masculine), while the plural in the genitive is مدرّسين, which also means *teachers* (masculine).

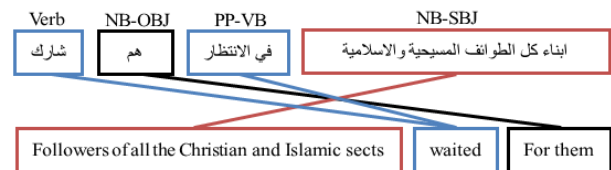


Fig. 1. Phrase reordering [12]

Moreover, the Arabic word رجل means *man*. The broken plural is رجال meaning *men*, which is created by adding infix ل. The plural form of the noun غرفة, meaning *room* is غرف, meaning *rooms*, which is created by stripping out the suffix ة. Another familiar example of broken plural is the Arabic word امرأة, meaning *woman*, while the plural is a completely different word نساء, meaning *women*.

Root is the main characteristic of Arabic language. Every root has many derivative forms. So regarding the problems discussed above, Arabic text in documents must be stemmed to get the root for every word in the text, and then rank these documents (stemmed text) using similarity measures.

B. Preliminaries to XML trees and paths

Arabic documents are written within Arabic character encoding formats such as ISO 8859-6, Windows-1256 and UTF-8. Listing 1 shows the XML tree of an Arabic document and its translation. Hierarchically structured XML documents are the result of these transformations. A document tree consists of a set of nodes which form the root of a tree [14,15,16] and a set of edges including attributes, tags and strings (#PCDATA).

XML is a tree $T = (r_T, N_T, E_T, F_T)$, where $N_T \subseteq \mathbb{N}$. This means that every element of N_T is also an element of a natural numbers nodes set. $r_T \in N_T$ is root of T , which is an element of N_T , $E_T \subseteq N_T \times N_T$. This means that all element of E_T are elements of the set of edges. $F_T : N_T \mapsto \alpha$ means that the function F_T maps the element N_T to α , where α is *attributes* \cup *tags* \cup *strings*.

An XML path p is a sequence from the tree root element to a specific node, which is $p = s_1.s_2....s_m$ symbols of nodes in α , where s_i is the tag name of root element and s_m is a tag name of the specific node including attributes and strings. An XML path has two types, the incomplete path which is *tag path* and the *complete path* including α . This paper will focus on the complete path #PCDATA (string) content.

C. Text similarity measures

There are many methods for measuring text similarity according to query and document terms such as Dice's Listing 1. XML tree of Arabic document and its translation.

coefficient and Cosine similarity. The following is a brief introduction to these methods.

Dice's coefficient, defined in [17], is a statistical method used to measure the similarity between two sets or two strings, or to measure the similarity between queries and documents in terms of common n-grams. An n-gram is an adjacent section of letters in the string. Dice's coefficient is given in "(1)". The similarity values vary between 0 and 1.

$$\text{Dice}(Q, D) = \frac{2 \times n\text{-grams}(Q) \cap n\text{-grams}(D)}{n\text{-grams}(Q) + n\text{-grams}(D)} \quad (1)$$

where $n\text{-grams}(Q)$ are a multi-set of letter n-grams in Query and $n\text{-grams}(D)$ is a multi-set of letter n-grams in Document.

Furthermore, the main idea is breaking a string to n-grams. For example, the string "right", the set of bigrams would be {"ri", "ig", "gh", "ht"}. Likewise, the string "write" would break down into {"wr", "ri", "it", "te"}.

However, after bigrams have been created, the "(1)" can be applied. So, the set $Q = \{\text{"ri"}, \text{"ig"}, \text{"gh"}, \text{"ht"}\}$, then $|Q| = 4$ and $D = \{\text{"wr"}, \text{"ri"}, \text{"it"}, \text{"te"}\}$, then $|D| = 4$. The intersection of the bigram sets $(Q \cap D)$ is {"ri"}, only one element exists in the set. The union of the bigram sets $(Q \cup D)$ is {"ri", "ig", "gh", "ht", "wr", "it", "te"}, only seven elements exit in the set. So, according to "(1)", the similarity measurement between "right" and "write" is $\frac{2}{7}$.

```
<?xml version="1.0" encoding="UTF-8"?>
<articles>
  <article id="25">
    <title>التكاليف الاقتصادية للمشكلات البيئية وأهم طرق التقييم البيئي المستخدمة</title>
    <author>سلمى عائشة كهللي, سليمة غدير أحمد, يوسف قريشي</author>
    <subject>بيئة</subject>
    <keywords>بيئة, المشكلات البيئية, التلوث</keywords>
    <contents>
      ... الملخص: ينطوي التطور الاقتصادي والاجتماعي على تكما ينعكس على البيئة
    </contents>
  </article>
</articles>
```

```
<?xml version="1.0" encoding="utf-8"?>
<articles>
  <article id="25">
    <title>The economic costs of environmental ... </title>
    <author>Salma Aisha Kehli, Salema Ghadeer Ahmad, Yousef Qureshi </author>
    <subject>environment </subject>
    <keywords>environment, environmental problems, pollution </keywords>
    <contents>Abstract: Involves economic and social ... </contents>
  </article>
</articles>
```

A collection of XML documents can be represented by a vector space model in which each document is represented by a vector of terms and their weights. A query (an expression that requests information from database) is represented as terms with weights to represent the importance of query terms. Term frequency (TF) and Inverse document frequency (IDF) are used for the weighting of terms [7,8,18,19]. This commonly used statistical measure uses:

- The frequency of a term j in a document i (tf_{ij})
- The frequency of the term j in the whole collection (df_j)
- The inverse document frequency of term j in document i (idf_j)

Equation (2) gives the inverse document frequency of term j in the collection and “(3)” gives the weight of the term j in the document i .

$$idf_j = \log_e \left(1 + \frac{N}{df_j} \right) \quad (2)$$

$$w_{i,j} = tf_{i,j} \times idf_j \quad (3)$$

where N denotes the number of documents in the collection.

Term weights using TF IDF for measuring the similarity between Query and Document.

Cosine similarity is used to calculate the angle between Query and Document. If a vector is considered in a V -dimensional Euclidean space, the angle between Query and Document represents their mutual similarity. A smaller angle means greater similarity. Equation (4) defined the similarity between a document D_i and a query Q .

$$sim(Q, D_i) = \frac{\sum_{j=1}^V w_{Q,j} \times w_{i,j}}{\sqrt{\sum_{j=1}^V w_{Q,j}^2 \times \sum_{j=1}^V w_{i,j}^2}} \quad (4)$$

where $w_{Q,j}$ is weight of query term j , and $w_{i,j}$ is weight of term j in document i as mentioned in “(3)”, (Example of cosine similarity is illustrated in section 4.1 and 4.2).

III. ARABIC DOCUMENT MANAGEMENT

Arabic documents represented in different formats are used as information resources. They are structured in different ways and for information retrieval purposes their content should be preserved regardless of the processing necessary for information retrieval. Therefore they must be stored and manipulated in a non-relational content management system. XML data management systems, as well as filtering technologies as XPath and XQuery, were recognized as being suitable for this purpose.

A. XQuery

The RAX System developed during the course of this research ranks documents based on criteria given by the end user (or client application). XQuery is utilized for this purpose as the documents are represented in XML format. XQuery is a query language for querying collections of XML documents as introduced by the World Wide Web Consortium (W3C). XQuery uses XPath expression to address specific nodes on XML document including FLWOR expression (FOR, LET, WHERE, ORDER BY and RETURN) [20]. The example in listing 2 illustrates XQuery expression for getting terms that appear in the text by using iteration (FOR clause) and criteria (term frequency > 0 in WHERE clause).

XQuery runs many operations to access XML documents including selecting information based on identified standards, filtering, seeking, joining data from multiple documents or collections, sorting, clustering, restructuring XML data into another XML structure and performing arithmetic calculations [21].

B. Sedna XML database management system

Many database management system producers offer support for the management of data stored in XML formats (IBM DB2, MS SQL Server, Oracle DB, PostgreSQL, etc.). For example Sedna XML DBMS can be used for managing XML documents [22]. Sedna is an XML DBMS with full database functionality. Sedna gives flexible XML processing capability including W3C XQuery implementation and integration of XQuery with full-text searching. The Sedna client application programming interfaces (APIs) can access databases of the Sedna DBMS and treat data using XML database query languages (e.g. XPath and XQuery). API enables access to Sedna from other client systems programmed in high-level languages such as Java APIs.

IV. PROPOSED SOLUTION

The aim of this paper is to find a suitable solution to the problems mentioned in the introduction section i.e. the rapid growth in demand for Arabic language content; the complexity of the language and its differences to existing tools based on western culture/Latin based languages causing problems in text processing, document summarization and information retrieval systems; and the high information loss rates especially for larger documents. To achieve this following steps were followed:

- Collect data from Arabic PDF documents from different domains and categories (agriculture, sciences, geography, ecology, engineering, development, energy, industry, administration, accounting, education, information technology and computers).
- Use an Arabic normalizer to normalize the Arabic text extracted from Arabic PDF documents.
- Remove Arabic stopwords from normalized text.

Listing 2. Example of XQuery with FLWOR expressions.

```
for $article_text in // contents /text()
let $tokenized_text := tokenize($article_text, ' environmental ')
let $term_freq:= count($tokenized_text) where $term_freq>0
return $term_freq
```

- Use an Arabic stemmer to stem every normalized word in the text and get the base form (dictionary word).
- Create XML documents according to the stemmed text because XML is used to exchange and represent semi-structured data on the Internet.
- Load the XML documents to the XML database management system.
- Apply queries and weight and rank XML documents to define an appropriate concept of similarity between the XML documents and queries.

To carry out the above steps the *RAX system* was developed and used to rank Arabic documents via an XML database

management system. Basically, processing of Arabic documents is performed in two stages; document preparation stage and implementation stage. Fig. 2 illustrates the overall system architecture and dataflow through its steps. Portable document format is used as the input format due to fact that there are many tools and functional libraries designed for conversion of different document formats to PDF. These include Apache OpenOffice [23] and documents4j library [24]. Text extraction from PDF is also well supported e.g. via Apache PDFBox [25] and iText library [26].

Document preparation is represented with a dataflow from PDF input to XML DBMS while the document implementation stage is represented with a dataflow from XML DBMS to the user. More details about these two stages are given in the next two sub-sections.

A. Document preparation stage

The first stage begins with the loading of PDF documents into a PDF Box library. This process is described in the following seven steps:

1) Apache PDFBox is used to extract of pure text and metadata from PDF files. PDFBox represents a class library

written in Java and used in many advanced content management tools (e.g. Alfresco, Lucene, Apache Tika and REWOO Scope). It is an open source tool for dealing with PDF documents. The RAX system used the Apache PDFBox library to test a set of 100 Arabic PDF documents from different domains and categories [27].

2) An Arabic normalizer performs the normalization process in which Arabic diacritics, punctuation, non-letters and stretching letters are removed and different versions of a letter are converted into the standard letter. For instance the letters أ , إ , آ , أ are all forms of the letter أ (letter A in the English language). These various forms would each be converted into letter أ . Other examples are the normalization of the letters ى and ه which are transformed into ي and ة . A diacritic word مَدْرَسَةٌ meaning *school* will normalize to مدرسة without diacritics. The stretched word كِتَاب meaning *book* will normalize to كتاب without stretching. The word أَحَدٌ contains diacritics and one form of letter أ . This normalizes to احمد with the standard form of letter أ and without diacritics.

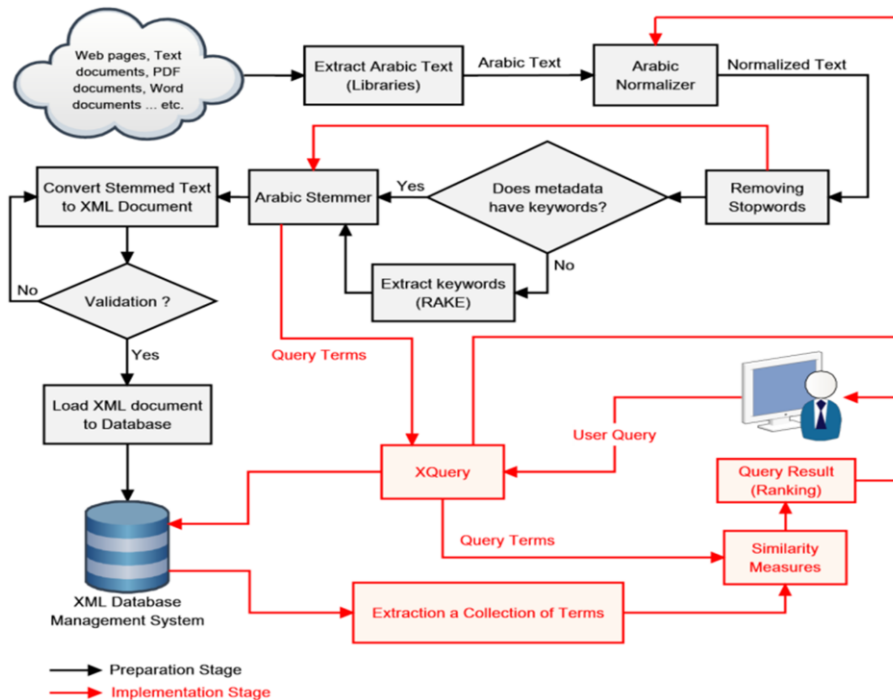


Fig. 2. RAX system model

3) The RAX system then removes Arabic stopwords, such as و , ان and في . A list of Arabic stopwords has been created consisting of 168 stopwords including pronouns and prepositions [13].

4) Following normalization and removal of stopwords. If there are no keywords in the document's metadata the RAX system uses rapid automatic keyword extraction (RAKE) technology to extract keywords from text. RAKE

contains a list of stopwords, phrase and word delimiters that is used to identify candidate keywords – a series of words by priority of occurrence in the text. Each candidate keyword is scored according to the ratio of word degree to word frequency. The top scoring candidates are selected as keywords, which calculated as $\frac{1}{3}$ number of words [9].

5) Since it is difficult to process Arabic language in summarization and information retrieval due to its complex

morphology, an Arabic stemmer is used to reduce derivational forms of a word to a stem or a root word (base form). Each root gives rise to many different words, such as nouns, adjectives, and verb stems. For example the words مَكْتَبٌ (maktab) office, كُتُبٌ (kutub) books, كِتَابٌ (kitAb) book, كَتَبَ (kataba) he wrote, and نَكْتُبُ (naktubu) we write all come from the root كَتَبَ (ktb). The RAX system uses its own stemmer to strip off prefixes such as ل ل ل ا و س ب ي ن م ت and suffixes such as ف ها تما كما ان ها واتم كم تن كن نا ة ت ا ي ات. To illustrate the processes mentioned above, fragments of three documents are used:

- **D₁**: "الأنظمة الحكومية هي الأنظمة الموثوق بها والتي تحتفظ "Government systems are the trusted systems that hold information about citizens...."
- **D₂**: "قواعد البيانات هي الجوهر لنظم المعلومات" "Data bases are the core of information systems."
- **D₃**: "قواعد البيانات في أنظمة الحكومة التي تحتفظ بمعلومات عن "Data bases in government systems hold information about citizens and they are the core of these information systems."

In the first step the system eliminates stop words and the sentences are modified as follows:

- **D₁**: الأنظمة الحكومية الأنظمة الموثوق تحتفظ بمعلومات المواطنين - Government systems trusted systems hold information citizens.
- **D₂**: قواعد البيانات الجوهر لنظم المعلومات - Data bases core information systems.
- **D₃**: قواعد البيانات أنظمة الحكومة تحتفظ بمعلومات المواطنين - Data bases government systems hold information citizens core information systems.

In the next step (stemming) all of the words are transformed into normal form. In this way the sentences are put into their final form as follows:

- **D₁**: Government system - نظم حكم نظم وثق حفظ علم وطن trust system hold information citizen.
- **D₂**: Data base core information system - قعد بين جوهر نظم علم: علم.
- **D₃**: Data base government system hold information citizen core information system - قعد بين نظم حكم حفظ علم وطن جوهر نظم علم: علم.

6) Document Creation; XML is a simple textual data, which supports different Unicode standards for different languages and well as benefiting from simplicity and usability over the Internet. XML syntax is widely used as a default format to represent data structure and create documents e.g. in Microsoft Office, OpenOffice.org, and web services. By this stage RAX has initialized the XML document and converted normalized stemmed Arabic text originating from PDFs to well-formed Arabic XML

documents using Java API for XML Processing [28] and Simple API for XML [29]. Listing 3 shows the fragment of the first document (D₁) in this step represented in XML form.

Listing 3. XML form of fragment D₁.

```
<?xml version="1.0" encoding="UTF-8"?>
<articles>
  <article id="1">
    <title>الانظمة الحكومية</title>
    <author>محمد نصر</author>
    <subject>سياسة</subject>
    <keywords>نظام الحكم</keywords>
    <statistics>
      <percentstemmed>100.0</percentstemmed>
      <stemmingtime>0.30</stemmingtime>
      <stemmedwords>7</stemmedwords>
      <nonstemmedwords>0</nonstemmedwords>
      <stopwords>4</stopwords>
      <punctuationwords>0</punctuationwords>
      <nonletterwords>0</nonletterwords>
      <totalwords>11</totalwords>
      <totalstemmedwords>7</totalstemmedwords>
    </statistics>
    <stemmedtext>وطن حفظ علم نظم وثق</stemmedtext>
    <notstemmedwords/>
  </article>
</articles>
```

The XML database management systems enable storage of XML documents and transfer of data between relational databases. These documents can be queried, transformed, transported and returned to a calling system. So after the documents are preprocessed and XML formed they are ready to be stored in an XML DBMS The Sedna DBMS, which has full ability of database services and gives flexible XML processing facilities including W3C XQuery accomplishment with full-text search, is used. This is the end of preparation stage and RAX system is ready for implementation.

B. Implementation stage

One of the obvious facts about information retrieval systems, as opposed to sorting and searching algorithms, is that the more documents are stored into the database the better it performs. Next is a description how the system works during implementation:

1) When the end user enters a query the RAX system performs its processing in the same way as with documents (normalization, the removing of stopwords and stemming). As a result the query expression is transformed into vector of terms.

2) Next the RAX system executes XQuery on the document base in the XML DBMS (Sedna DBMS) expression which includes the vector of query terms. XQuery uses XPath syntax for accessing different nodes of

XML documents. A set of XML documents is returned as a result of the query. Listing 4 shows an XQuery expression; this query returns a collection of documents including the term frequency for each document that contains the query term.

Listing 4. XQuery expression used by RAX system.

```
let $query_term := 'نظم'
for $document_terms in //article, $id in $ document_terms/@id
let $output_terms := tokenize($document_terms/stemmedtext/text(), $query_term)
let $freq := count($output_terms)where $freq>0
return <document id="{ $id }"><frequency>{ $freq }</frequency></ document>
```

3) To rank documents the RAX system calculates weights for each particular term in the document. Term frequency and inverse document frequency are used for this purpose (“(2)” and “(3)”). This means that the vector space model in which the documents are transformed is enriched with additional information: each document’s vector is represented by an array of term-weight pairs. The user query is processed in the same way. Final comparison between these two is performed using cosine similarity as a

measure of the documents’ ranking (“(4)”). The following example shows how the documents’ samples fragments (described in section 4.1) are used in this process. Transformation in the improved vector model is the most crucial and processor intensive phase. After this each fragment of document being considered for ranking is represented with two vectors. The original XML document consists of a vector of terms. The terms are collections of words and each word is represented by its weight (TF*IDF) value. In this way the documents are represented with two vectors. Original words are filtered and transformed into normal form and for convenience are labeled terms. For clarity, TF and IDF are represented separately i.e. (term₁, tf₁, idf₁), ... , (term_n, tf_n, idf_n), where n is the full number of terms in the document set. Thus there are 9 different terms for our example and the vector space model (VSM) for each document should contain these. TF is represented by row frequency, which represents the number of occurrences of a specific term in the document, and IDF is calculated according to “(2)”. See table II.

TABLE II. TF AND IDF CALCULATIONS FOR SAMPLES USED IN EXAMPLE

Document: D ₁									
Term	نظم System	حکم Government	وثق Trust	حفظ Hold	علم Information	وطن Citizen	بین Data	قعد Base	جوهر Core
TF	2	1	1	1	1	1	0	0	0
IDF	0.30102	0.39794	0.60206	0.39794	0.30102	0.39794	0	0	0
W _{D1}	0.60204	0.39794	0.60206	0.39794	0.30102	0.39794	0	0	0
Document: D ₂									
Term	نظم System	حکم Government	وثق Trust	حفظ Hold	علم Information	وطن Citizen	بین Data	قعد Base	جوهر Core
TF	1	0	0	0	1	0	1	1	1
IDF	0.30102	0	0	0	0.30102	0	0.39794	0.39794	0.39794
W _{D2}	0.30102	0	0	0	0.30102	0	0.39794	0.39794	0.39794
Document: D ₃									
Term	نظم System	حکم Government	وثق Trust	حفظ Hold	علم Information	وطن Citizen	بین Data	قعد Base	جوهر Core
TF	2	1	0	1	2	1	1	1	1
IDF	0.30102	0.39794	0	0.39794	0.30102	0.39794	0.39794	0.39794	0.39794
W _{D3}	0.60204	0.39794	0	0.39794	0.60204	0.39794	0.39794	0.39794	0.39794

The next step is to determine the cosine similarity between the query and the previous collection which is represented in

table II. Let us consider a query which contains two words: علم نظم - information system (in stemming form). Table III shows that the query has transformed into VSM.

TABLE III. TF AND IDF CALCULATIONS FOR QUERY

Query: Q ₁ نظم علم - Information System									
Term	نظم System	حکم Government	وثق Trust	حفظ Hold	علم Information	وطن Citizen	بین Data	قعد Base	جوهر Core
TF	1	0	0	0	1	0	0	0	0
IDF	0.30102	0	0	0	0.30102	0	0	0	0
W _{Q1}	0.30102	0	0	0	0.30102	0	0	0	0

Finally, table IV shows the calculated cosine similarity according to “(4)”. The document D₃ is the best fit to the query and the ranking is D₃, D₁, D₂.

TABLE IV. COSINE CALCULATIONS

Cosine Similarity	
Cosine(Q ₁ ,D ₁)	0.52230
Cosine(Q ₁ ,D ₂)	0.45894
Cosine(Q ₁ ,D ₃)	0.64904

4) Practical Evaluation and Comparison

Regarding the system complexity and hardware limitations the collection of 100 of random documents was found to be optimal for the different scenarios used in the research. The random documents are obtained from different categories [27]. The next table (table V) illustrates these categories:

TABLE V. CATEGORIES OF INTEREST

Category	No. of documents
General reference	1
Culture and the arts	2
Geography and places	1
Health and fitness	3
Mathematics and logic	5
Natural and physical sciences	9
People and self	11
Philosophy and thinking	3
Society and social sciences	21
Technology and applied sciences	44
Total	100

First of all, the RAX stemmer is compared with others. Fig. 3 represents the comparison of summarization process over the collection between RAX stemmer and other stemmers, such as Khoja and Light10. It's clear from Fig. 3 that RAX system is much powerful than the others, because RAX System has used wider list of stopwords.

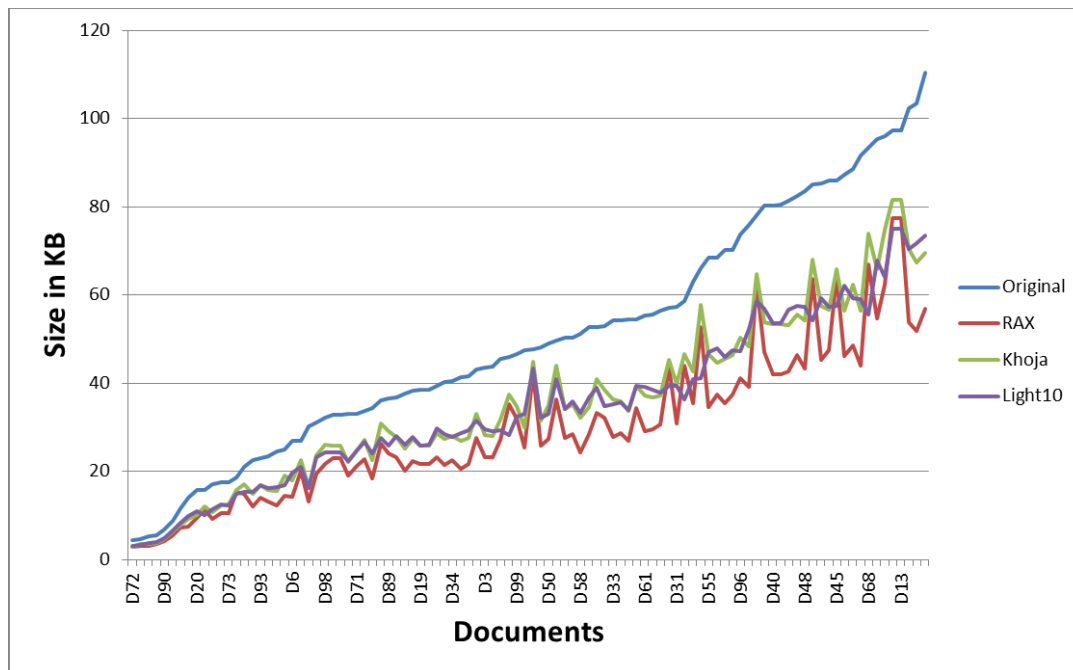


Fig. 3. Summarization comparison between RAX stemmer and other stemmers in ascending order according to original XML documents size

Following we mentioned just two queries from Computer Science and Ecology domains. These queries are used in the experiment in order to cover all of the documents. The RAX system is used for measuring similarity by using TF, IDF and cosine similarity as previously described as well as compares results with Dice coefficient measurements:

- Query₁ = { نظم المعلومات - Information Systems }, after stemming process has taken place, Query₁ = { نظم علم - Information System }. Query₁ has two terms; the (Information) term which occurred once (TF=1) and the (System) term which occurred also once (TF=1). So the inverse document frequency and the weight of query₁ were determined from “(2)” and “(3)”. As a result of query₁ we have found 77 documents contain the term (Information), and 92 documents

contain the term (System). The cosine similarity measures are calculated between query₁ terms and document terms according to “(4)”. The top ranked documents which contain both terms are D₇₈, D₈₄, D₄₆, D₂₃, D₅₉, D₁₈ and D₆₁ (see Fig. 4).

RAX system has used N-grams=3 to calculate Dice Coefficients similarity measures according to “(1)” because the whole roots in the Arabic language have three letters. Fig. 5 represents the percentage of similarity measurements. The most ranked documents are D₅₁, D₈₇, D₂₀, D₄₆, D₁, D₅ and D₉ respectively.

- Query₂ = { التنمية البيئية المستدامة - Sustainable Environmental Development }, after stemming

process has taken place, $Query_2 = \{ \text{نمى دوم بيئية} - \text{Sustain Environment Develop} \}$. $Query_2$ has three terms; the (*Sustain*) term which occurred once (TF=1), the (*Environment*) term which occurred once (TF=1) and the (*Develop*) term which also occurred once (TF=1). So the inverse document frequency and the weight of $query_2$ were determined from “(2)” and “(3)”. We have found 46 documents contain the term (*Sustain*); no document contains the term (*Environment*), and 82 documents contain the term (*Develop*). As none of the collection match the

term (*Environment*) it is impossible to calculate IDF due to the denominator df_j being zero, so the RAX system has excluded the term (*Environment*) from further consideration. The cosine similarity measures are calculated between $query_2$ terms and document terms according to “(4)”. We conclude that the RAX system will exclude terms which are not matched. The top ranked documents which contain both terms are D_{71} , D_{44} , D_6 , D_{36} , D_1 , D_9 and D_{17} (see Fig. 6).

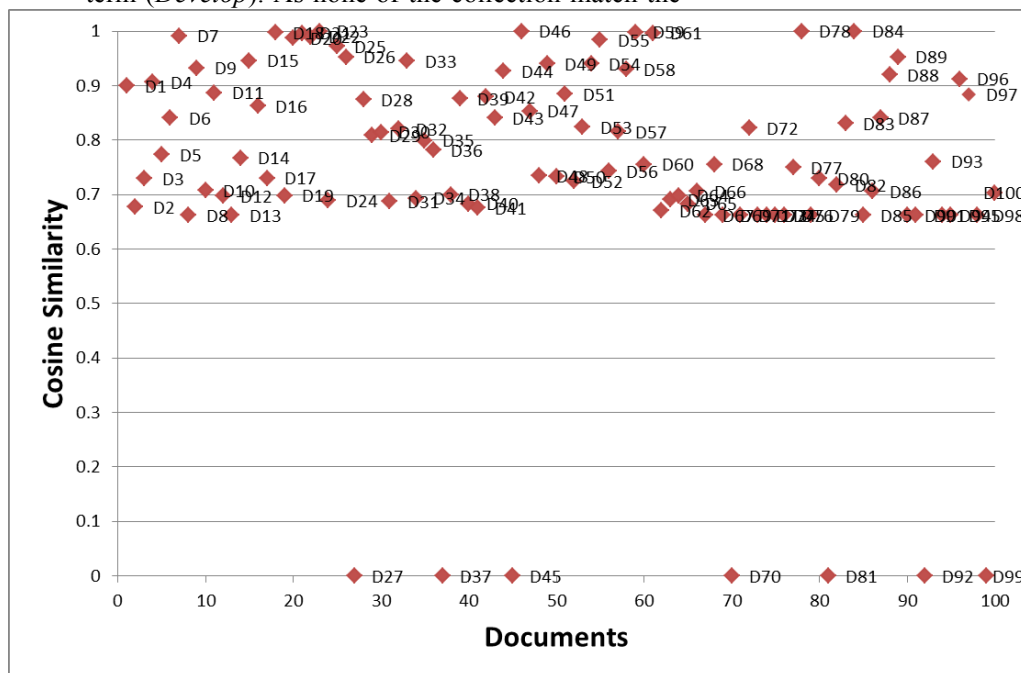


Fig. 4. Similarity measures of query

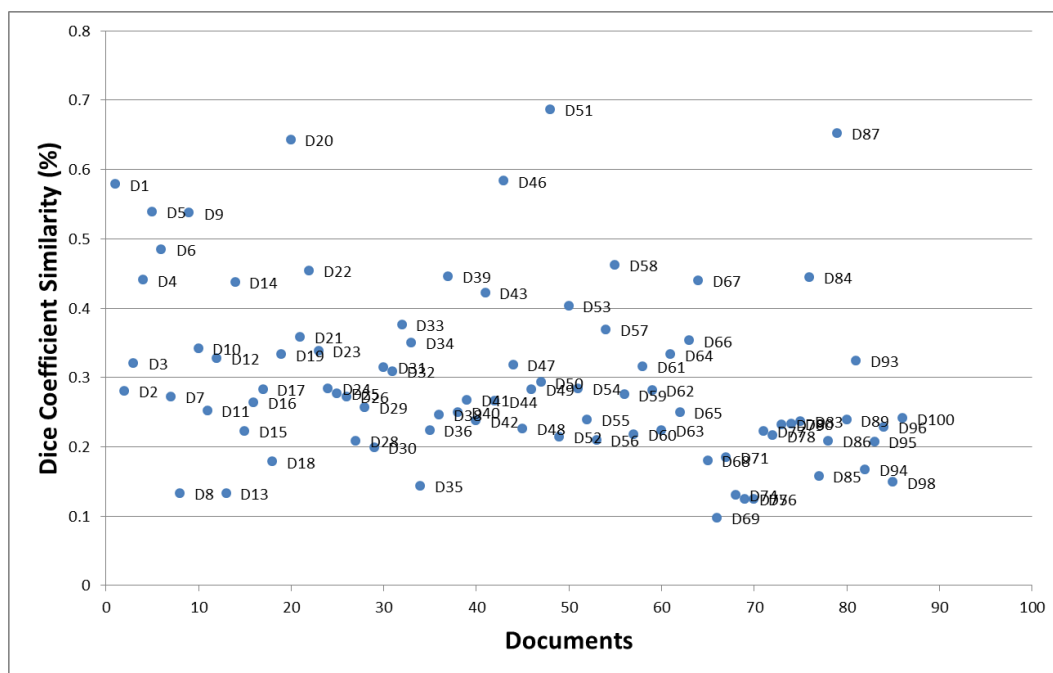


Fig. 5. Dice coefficient measures of documents that match Q_1 terms

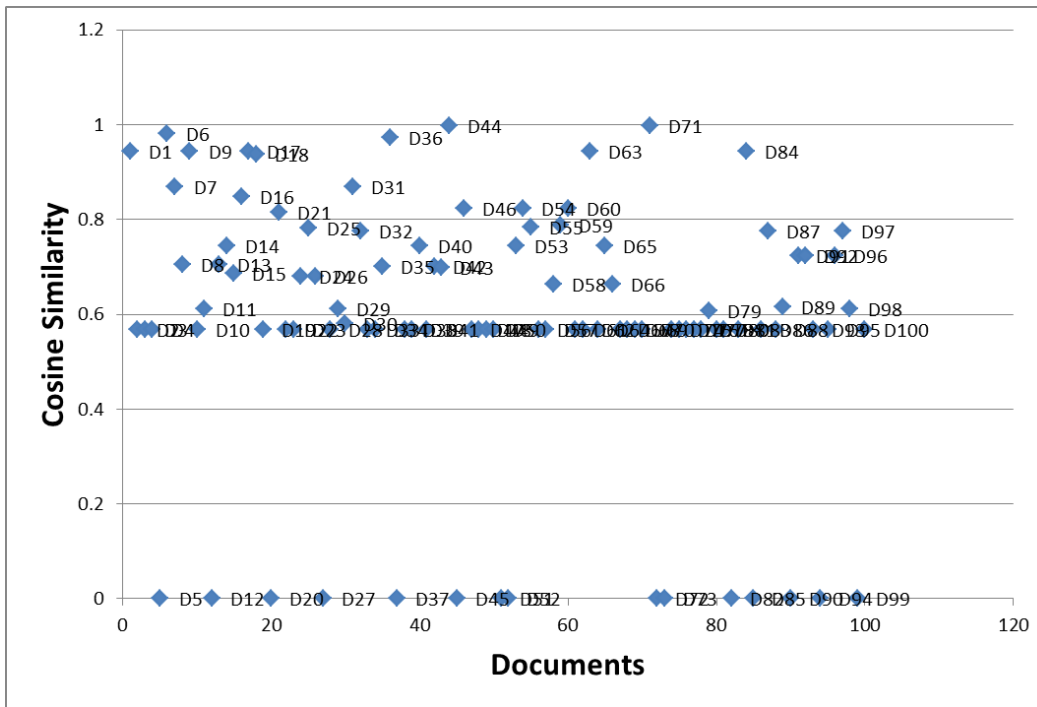


Fig. 6. Similarity measures of query₂

RAX system also has used N-grams=3 to calculate Dice Coefficients similarity measures according to “(1)”. Fig. 7 represents the percentage of similarity measurements.

The most ranked documents are D₈₇, D₁, D₆₇, D₈₄, D₆, D₅₈, and D₉ respectively.

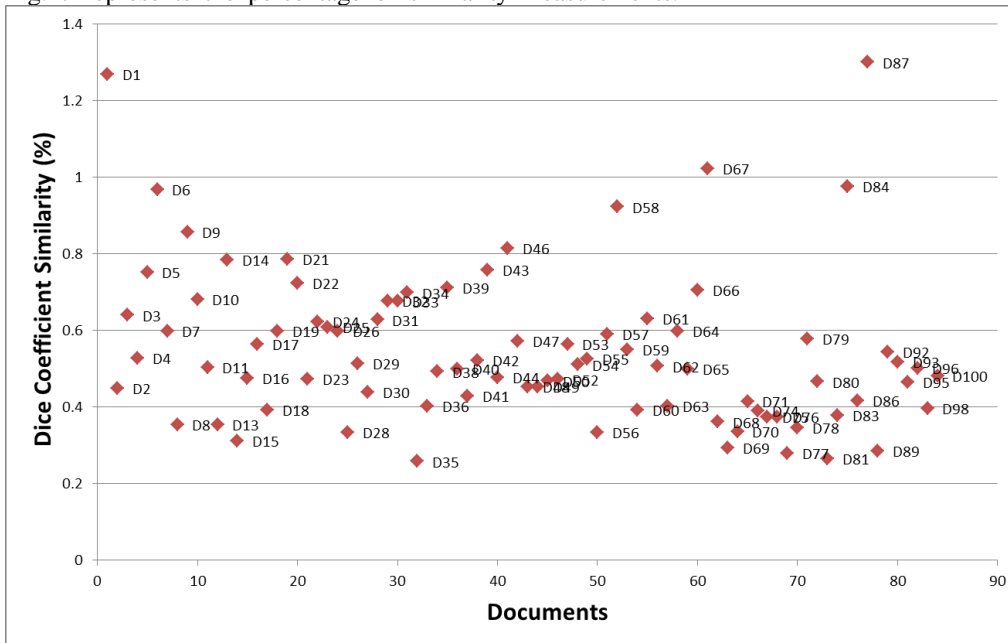


Fig. 7. Dice coefficient of the resulted documents and the Q₂ as three terms

From above results, we noticed that there was difference in the documents ranking between Cosine and Dice because cosine similarity depends on term frequency and inverse document frequency. In contrast, Dice coefficient similarity depends on n-grams, every time the n-grams is changed the ranked document will change too. So, Cosine similarity is much accurate than Dice similarity.

V. CONCLUSION

This paper described the RAX System which has been designed for ranking Arabic documents based on content similarity. Our model was applicable to documents stored in different formats and written in Arabic language. The design and implementation were based on existing text processing

frameworks and referent Arabic grammar. The main focus of the research was on evaluating different similarity measures used for classifying Arabic documents from different domains and different categories.

In the preparation stage the *RAX* system was used to process Arabic text taking in account the character encoding for the Arabic language (UTF-8, Windows-1256 etc). In the implementation stage the *RAX* system managed XML documents via an XML database management system using Xpath and XQuery languages. The *RAX* system uses cosine similarity to measure the similarity metric in n-dimensional space. This is based on the finding that when two vectors are similar in rate and direction from the origin to their end points, they will be close to each other in the vector space, with a small angular separation, and vice versa. The cosine value lies between 1 and -1. Therefore the cosines of small angles are close to 1, which means high similarity, while the cosines of large angles are close to -1, which means low similarity.

The preparation stage of the processing of Arabic text was established in 4 steps: extraction of full text from documents; normalization (remove diacritics, remove non-letters and remove punctuation marks); removal of stopwords from the normalized text and stemming (remove prefixes, remove suffixes and finally extract roots or stems words). The well-formed Arabic XML document was created from the stemmed text and loaded into XDBMS which manages end user queries over a collection of XML documents. The Arabic text in queries was processed in 3 steps: normalization, removal of stopwords and stemming (Implementation stage).

When were no documents in the collection which match one of the terms i.e. *Environment*. In this case it was impossible to calculate IDF due to the denominator df_j being equal to zero. In this case the *RAX* system excluded the term *Environment* from further consideration.

We conclude that the Arabic text was fully represented in the processing of Arabic documents.

There was a proportional relationship between the number of terms of a query and its result. The *RAX* system excludes terms which are not matched. Some factors such as the position of nodes in the XML tree and the query expressions (structure of expressions) could affect the operation of the *RAX* system. System performance could be improved by changing the type of stemmer.

There are two main advantages of the *RAX* system. Firstly, the query results are more comprehensive and wider when using the roots of words or stems. Secondly, the similarity measures are calculated after the completion of the query process.

As regards future work the *RAX* system could be improved in various ways. We plan to work on making it more efficient. This will mean that the stemmer will need to be improved and enhanced in capabilities and effectiveness to deal with the huge volume of Arabic roots in large data sets (stopword list, compatibility between prefixes and suffixes in stemming process, etc). We also aim to use DTD and XML schema to create XML documents as well as to enhance their summarization. Finally, we plan to upgrade the *RAX* system to

find and replace any query term which has a zero term frequency.

REFERENCES

- [1] K. Darwish and W. Magdy, "Arabic information retrieval," Foundations and Trends in Information Retrieval, vol. 7(4), pp. 239-342, 2013.
- [2] Internet world stats, retrieved on June 30, 2015, <http://www.internetworldstats.com/stats7.htm>.
- [3] L. Zhang, X. Shen and W. Xiong, "The query and application of XML data based on XQuery," 4th International Conference on Computational and Information Sciences, 2012.
- [4] Q. Zou, S. Liu and W. Chu, "Using a compact tree to index and query XML data," Proceedings of the 13th ACM International Conference on Information and Knowledge Management, pp. 234-235, 2004.
- [5] A. Chen and F. Gey, "Building an Arabic stemmer for information retrieval," 11th Text Retrieval Conference (TREC 2002), 2003.
- [6] L. Larkey, L. Ballesteros and M. Connell, "Light stemming for Arabic information retrieval," in Arabic Computational Morphology: Text, Speech and Language Technology, vol. 38, pp. 221-243, Springer, 2007.
- [7] H. Abu-Salem, M. Al-Omari and M. Evens, "Stemming methodologies over individual query words for an Arabic information retrieval system," Journal of the American Society for Information Science, vol. 50(6), pp. 524-529, 1999.
- [8] T. Shlieder and H. Meuss, "Querying and ranking XML documents," Journal of the American Society for Information Science and Technology, vol. 53(6), pp. 489-503, 2002.
- [9] S. Rose, D. Engel, N. Cramer and W. Cowley, "Automatic keyword extraction from individual documents," in Text Mining: Applications and Theory, edited by Michael W. Berry and Jacob Kogan, 2010.
- [10] M. Najeeb, A. Abdelkader and M. Al-Zghoul, "Arabic natural language processing laboratory serving Islamic sciences," International Journal of Advanced Computer Science and Applications, vol. 5(3), pp. 114-117, 2014.
- [11] J. Ababneh, O. Almomani, W. Hadi, N. El-Omari and A. Al-Ibrahim, "Vector space models to classify Arabic text," International Journal of Computer Trends and Technology, vol. 7(4), pp. 219-223, 2014.
- [12] S. Green, C. Sathi and C. Manning, "NP subject detection in verb-initial Arabic clauses," Proceedings of the Third Workshop on Computational Approaches to Arabic Script-based Languages, 2009.
- [13] K. Ryding, A reference grammar of modern standard Arabic. Cambridge University Press, 2005.
- [14] A. Tagarelli and S. Greco, "Toward semantic XML clustering," Siam Conference on Data Mining, 2006.
- [15] M. Hachicha and J. Darmont, "A survey of XML tree patterns," IEEE Transactions on Knowledge and Data Engineering, vol. 25(1), pp. 29-46, 2013.
- [16] S. Flesca, F. Furfaro, S. Greco and E. Zumpano, "Repairs and consistent answers for XML data with functional dependencies," In Z. Bellahsene, A. Chaudhri, E. Rahm, M. Rys, R. Unland (Eds), Database and XML Technologies, First International XML Database Symposium, XSym 2003, Berlin, Germany, September 8, 2003, Proceedings. Lecture Notes in Computer Science 2824, pp. 238-253, Springer 2003.
- [17] G. Kondrak, "N-gram similarity and distance," String Processing and Information Retrieval, Lecture Notes in Computer Science, vol. 3772, pp. 115-126, 2005.
- [18] G. Šimić, Z. Jeremić, E. Kajan, D. Randjelović and A. Presnall, "A framework for delivering e-government support," Acta Polytechnica Hungarica, vol. 11(1), pp. 79-96, 2014.
- [19] D. Lee, H. Chuang and K. Seamons, "Document ranking and the vector-space model," IEEE Software, vol. 14(2), pp. 67-75, 1997.
- [20] W3C Recommendation, "XQuery 3.0: An XML Query Language," 2014, <http://www.w3.org/TR/xquery-30/>.
- [21] P. Walmsley, XQuery, O'Reilly Media Inc, 2007.

- [22] Sedna, "Native XML database system," 2015, <http://www.sedna.org/>.
- [23] Apache OpenOffice, retrieved on December 24, 2016, <https://www.openoffice.org/>.
- [24] Documents4j library, retrieved on December 24, 2016, <http://documents4j.com/#/>.
- [25] Apache PDFBox® - A Java PDF library, retrieved on December 24, 2016, <http://pdfbox.apache.org/>.
- [26] iText library, retrieved on December 24, 2016, <http://itextpdf.com/>.
- [27] Wikipedia, portal:contents/categories, retrieved on December 24, 2016, <https://en.wikipedia.org/wiki/Portal:Contents/Categories>.
- [28] Java API for XML processing (JAXP), retrieved on December 24, 2016, <https://docs.oracle.com/javase/tutorial/jaxp/>.
- [29] Simple API for XML (SAX), retrieved on December 24, 2016, <http://www.saxproject.org>.

A Novel Method for Measuring the Performance of Software Project Managers

Jasem M. Alostad

The Public Authority for Applied Education and Training (PAAET), College of Basic Education
P.O. Box.23167, Safat 13092, Kuwait

Abstract—This paper is focused on providing a novel method for measuring the performance of software project managers. It clarifies the fundamental concepts of software project management, knowledge areas, life cycle phases of software project, and performance metrics. It presents some examples of processes and common performance metrics related to knowledge areas of software project management. The researcher extracts an enhanced list of performance metrics using a questionnaire that is passed to 60 experts and specialists in the field of software projects. Their responses are collected and filtered for reaching to effective performance metrics and the importance degree of each one. The researcher adapts Goal Question Metrics method to include an additional step that dedicated to calculate a performance indicator for each knowledge area of software project management. Finally, the new method has been applied on 3 real software projects to measure the performance of their managers. Measuring the performance of software project managers can be helpful in controlling and improving the performance.

Keywords—software project manager; performance; measurement; metrics; indicators; Goal Question Metrics method; schedule management

I. INTRODUCTION AND PROBLEM DEFINITION

The knowledge and skills required for effective project managers in an Information Technology (IT) environment fall into four domains [1]: project management competencies, industry and/or business competencies, IT management practices, and general management competencies. In this paper, the researcher focuses on the project management competencies which include the IT practices. The researcher doesn't focus on the industry and/or business competencies because they differ from one project to another. Also, the researcher doesn't focus on the general management competencies because they are basic knowledge and skills required for any project manager. Each project management competency and its IT ramifications will be explained as a specific knowledge area of Software Project Management (SPM).

Software development is a mentally complicated process. Therefore, SPM is the art and science of planning and leading software projects [2]. SPM is the on-going activities for planning, organizing, directing, and controlling progress to develop an acceptable system, i.e. conform to the quality standards within the allocated time and budget [3]. Software Project (SP) manager is a person who undertakes the responsibility of executing the SP. Software project manager is thoroughly aware of all the phases of software development

process that the software would go through. A project manager closely monitors the development process, prepares and executes various plans, arranges necessary and adequate resources, maintains communication among all team members in order to address issues of cost, budget, resources, time, quality, and customer satisfaction [4].

The mismanaged projects may lead to: unfulfilled or unidentified requirements, uncontrolled change of the project scope, uncontrolled change of technology, uncontrolled risk of the project, uncontrolled subcontracting and integration, cost overruns, and/or late delivery [5]. However the number of successful SPs is few compared to the total number of software projects [6]. Figure 1 illustrates a part of a research performed by Standish Group that includes the percentage of successful, failed, and challenged software projects from year 2004 to year 2012 resulted from CHAOS manifesto [7].

	2004	2006	2008	2010	2012
Successful	29%	35%	32%	37%	39%
Failed	18%	19%	24%	21%	18%
Challenged	53%	46%	44%	42%	43%

Fig. 1. Project resolution results from CHAOS research [7]

This research finds that around 60% of software projects were challenged or failed through the years 2004 to 2012. Because of the high percentage of failure, some research efforts are initiated to improve the performance of SP managers.

This paper contributes in these efforts by providing a quantitative method for measuring the performance of SP managers at any point of time in the project life or at the end of a specific phase. The proposed method depends on an enhanced list of performance metrics and simple mathematical and statistical techniques. In addition, the proposed method depends on an adapted version of GQM method that can provide an organized method of thinking in this field. GQMI delivers an enhanced list of metrics and indicators that can be used for evaluating the performance of SP manager in order to improve and develop it. Performance indicators give a significant image about the pitfalls in the performance and then assist the management to direct the SP managers to improve their performance.

The rest of the paper is organized as follows: Section II provides a background overview about the main concepts related to the research topic. Section III presents some

significant related work focusing on measuring the performance of SP managers. Section IV presents how to reach to the enhanced list of performance metrics and GQMI. Section V presents how to apply GQMI on real projects. Section VI concludes the paper with final remarks. The last section includes the ideas that are expected to be focused on the future.

II. BACKGROUND OVERVIEW

This section consists of three parts. The first part presents the main concepts related to SPM. The second part provides an overview of performance metrics of SPM. The final part gives an explanation of GQM.

A. SPM Areas and Project Phases

SPM is the process of planning, organizing, staffing, monitoring, controlling and leading a software project. SPM activities can be organized in nine knowledge areas [1]: integration management, scope management, schedule/time management, costs management, quality management, human resources management, communications management, risk management, and procurement management. A new knowledge area was added in PMBOK 5th edition [8, 9], which is “stakeholder management”.

- Project integration management includes the processes required to ensure that the various elements of the project are properly coordinated [1]. It involves bringing people and things together to perform effectively. It includes the integration of functionality, data, and/or interfaces.
- Project scope management involves activities to define and control what is included in the project and what is out of its scope.
- Project schedule/time management is the administration and control of the finite resource of time to prevent or correct any slippages [8].
- Project cost management is the planning and control required to ensure that a project is completed within the approved budget.
- Project quality management involves those activities that ensure the project delivers the systems that satisfy the project objectives. The project manager must ensure that the quality activities are implemented and applied throughout the project life cycle.
- Project human resources management involves those processes required to make the most effective use of the people involved in a project [1]. The project manager must identify and implement strategies to re-skill the existing IT workforce and acquire external expertise through vendors and consultants when needed [10]. Also, the project manager should establish procedures for involving the system users [11].
- Project communications management involves the timely and appropriate generation, collection, dissemination, storage, and ultimate disposition of project information. Effective communication is one of the critical success factors for IS projects [12].

- Project risk management includes the processes concerned with identifying, analyzing and responding to the project risks, maximizing the results of positive events and minimizing the consequences of adverse events [1].
- Project procurement management includes managing subcontractors because if one of the subcontractors late, this may lead to project slippage. So, the project manager must make everything is clear to subcontractors [11]. Also, the project manager must know the legal and financial issues of subcontracting.
- Project stakeholder management includes the processes required to identify the people, groups, or organizations that could impact or be impacted by the project, to analyze stakeholder expectations and their impact on the project, and to develop appropriate management strategies for effectively engaging stakeholders in project decisions and execution [8].

Each knowledge area includes a set of processes related to a specific field in SPM practices. Table I illustrates the processes required to achieve project schedule/time management, project cost management, project scope management, and project stakeholder management.

TABLE I. EXAMPLE OF THE PROCESSES REQUIRED FOR ACHIEVING SPM KNOWLEDGE AREAS [8]

Knowledge Area	Processes
Project Schedule/Time Management	<ol style="list-style-type: none"> 1. Plan Schedule Management 2. Define Activities 3. Sequence Activities 4. Estimate Activity Resources 5. Estimate Activity Durations 6. Develop Schedule 7. Control Schedule
Project Cost Management	<ol style="list-style-type: none"> 1. Plan Cost Management 2. Estimate Costs 3. Determine Budget 4. Control Costs
Project Scope Management	<ol style="list-style-type: none"> 1. Plan Scope Management 2. Collect Requirements 3. Define Scope 4. Create WBS 5. Validate Scope 6. Control Scope
Project Stakeholder Management	<ol style="list-style-type: none"> 1. Identify Stakeholders 2. Plan Stakeholder Management 3. Management Stakeholder Engagement 4. Control Stakeholder Engagement

For achieving the purpose of this paper, the researcher will focus on schedule/time management as an example of knowledge areas to explain the novel measuring method. According to PMBOK 5th edition [8] and [9, 13], the inputs, possible tools and techniques, and outputs for each process required for project schedule/time management is illustrated in table II.

TABLE II. THE INPUTS, TOOLS AND TECHNIQUES, AND OUTPUTS FOR PROJECT SCHEDULE/TIME MANAGEMENT [8, 9, 13]

Process	Inputs	Possible tools and techniques	Outputs
Plan Schedule Management	- Project management plan - Project charter - Enterprise Environmental Factors (EEF) - Organizational Process Assets (OPA)	- Expert judgment - Meetings - Analytical techniques	- Schedule management plan
Define Activities	- Schedule Management Plan - Scope baseline - EEF - OPA	- Decomposition - Rolling wave planning - Expert judgment	- Activity List - Activity Attributes - Milestone list
Sequence Activities	- Schedule management plan - Activity List - Activity Attributes - Milestone list - Project scope management - EEF - OPA	- Precedence Diagramming Method (PDM) - Dependencies - Leads and lags	- Project Schedule Network Diagrams - Project document updates
Estimate Activity Resources	- Schedule management plan - Activity list - Activity attributes - Resource calendar - Risk register - EEF - OPA	- Expert judgment - Alternative analysis - Published estimating data - Bottom-up estimating - PM software	- Activity resource requirements - Resource breakdown structure (RBS) - Project document updates
Estimate Activity Durations	- Schedule management plan - Activity list - Activity attributes - Activity resource requirements - Resource calendars - Project scope statement - Risk register - RBS - EEF - OPA	- Expert judgment - Analogous estimating - Parametric estimating - Three-point estimating - Group decision making - Reserve analysis	- Activity duration estimates - Project documents updates
Develop Schedule	- Schedule management plan - Activity list - Activity attributes - Project schedule network diagrams - Activity resource requirements - Resource calendars - Activity duration estimates - Project scope statement - Risk register - Project staff assignments - RBS - EEF - OPA	- Schedule network analysis - Critical path method - Critical chain method - Resource optimization techniques - Modeling techniques - Leads and lags - Schedule compression - Scheduling tool	- Schedule baseline - Project schedule - Schedule date - Project calendars - PM plan updates - Project documents updates
Control Schedule	- Project management plan - Project schedule - Work performance data - Project calendars - Schedule data - OPA	- Performance reviews - PM software - Resource optimization - Modeling techniques - Leads and lags - Schedule compression - Scheduling tool	- Work performance information - Schedule forecasts - Change requests - PM plan updates - Project documents updates - OPA updates

Project life cycle consists of four phases [14, 15]: project initiation, project planning, project execution, and project closure. Figure 2 illustrates the project life cycle [16]. There is

a feedback between each two phases. For example, through the planning phase, the SP manager may discover that the documented project background ignores some facts in the reality. Therefore, there is a feedback between initiating the project and planning the project to redefine the project background. Each phase includes a set of processes to achieve it, but it is out of this paper scope. The performance of project managers can be effectively measured for a specific SPM knowledge area because each area includes a set of processes and skills related to a specific SPM competency. The knowledge areas are a handy way to group together theory and practical techniques [13]. It can help in discovering the weaknesses in a specific area that can be led to more attention to this area. Therefore, this is the main focus of the novel measuring method proposed in the paper.

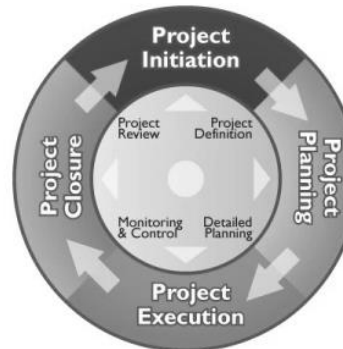


Fig. 2. Project life cycle [16]

B. SPM Performace Metrics and Indicators

Performance measurement is the ongoing monitoring and reporting of project accomplishments, particularly progress towards pre-established goals [17]. This process is used in project management and quality processes to determine and communicate status and accomplishments measured against specific objectives, schedules, and milestones. These measurements extend to include delivery of desired products and services to customers, whether external or internal. Performance measurement can be useful to improve future work estimates [18]. Performance measures may address: the type or level of project process conducted, the direct products and services delivered by a program, and/or the results of those products and services [17].

A metric is a quantitative measure of the degree to which a system, component, or process possesses a given attribute [19]. Metrics can be used for measuring the performance of SP manager. Performance metrics should be objective, timely, simple, accurate, useful, and cost-effective. Performance metrics can be divided into three basic categories [17]: measures of efforts, measures of accomplishments, and measures that relate efforts to accomplishments.

- Measures of efforts: Efforts are the amount of resources, in terms of money, people, etc., applied to a project. Examples: The amount of money spent and the number of person-hours burned on a project.
- Measures of accomplishments: Accomplishments are milestones achieved with the resources used. Examples

include: number of modules coded and number of deliverables.

- Measures that relate efforts to accomplishments: These measures are associated with resources or cost relative to accomplishments achieved. Examples may include: amount of money expended for the portion of project completed versus the amount of money planned to be expended for this portion of work.

Mike Denley proposes a list of metrics related to project cost and schedule management [20] that shown in table III.

TABLE III. METRICS OF PROJECT COST AND SCHEDULE MANAGEMENT [20]

Knowledge Area	Metric
Project Cost Management	% Deviation Planned Vs. Actual Margin
	% Hours billed vs. project hours completed
	% of actual project hours completed /estimated Project hours
	% unplanned hours / total hours
	Cost Deviation From Planned Budget
	Estimate to Complete (ETC) (cost)
	Value at Completion (VAC) Budget at Completion (BAC)
Project Schedule Management	% or Number of Milestones Missed
	Deviation From Project / Program Time Schedule
	Planned Vs. Actual Project End Date
	Schedule Variance

Performance metrics can be useful in calculating performance indicators for SP manager. An indicator can be defined as a function of metrics. Figure 3 illustrates the relationships between SPM knowledge areas, metrics, measures, and indicators.

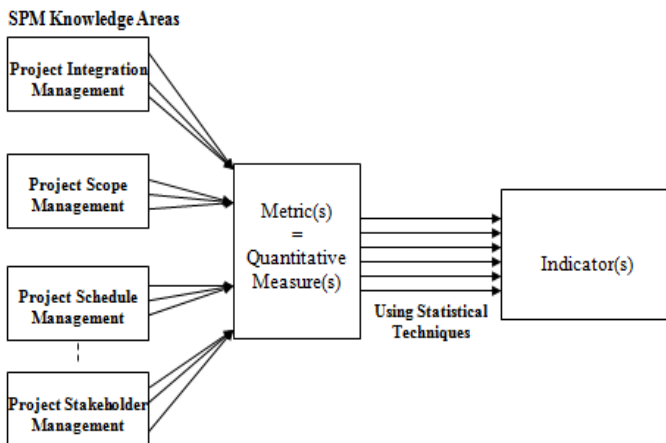


Fig. 3. SPM knowledge areas, metrics, measures, and indicators

Calculating metrics is a simple process because it depends on simple or known mathematical formulas such as percentage, ratio, present value, and time deviation (in hours, days, weeks, or months). On the other hand, calculating indicators from metrics is not an easy process because the indicator value may depend on a combination of metrics and each of them doesn't have the same level of importance and they may not have the same nature [17].

C. Goal Question Metrics (GQM) Method

Victor Basili and et al at Maryland University developed a goal oriented approach for measurement [21]. GQM method was developed for multi-purpose evaluation of software [22]. This method depends on three steps:

- 1) Set goals specific to needs in terms of purpose, perspective, and environment.
- 2) Refine the goals into quantifiable questions that are tractable.
- 3) Deduce the metrics and data to be collected (and the means for collecting them) to answer the questions.

In GQM method, each goal generates a set of quantifiable questions that attempt to define and quantify this goal. The question can only be answered relative to, and as completely as, the available metrics allow. In GQM, the same question can be used to define multiple goals. Also, metrics can be used to answer more than one question. Figure 4 illustrates the hierarchy of goals, questions, and metrics of GQM method [23]. In this paper, the researcher provides a new adapted version of GQM method to measure the performance of SP managers.

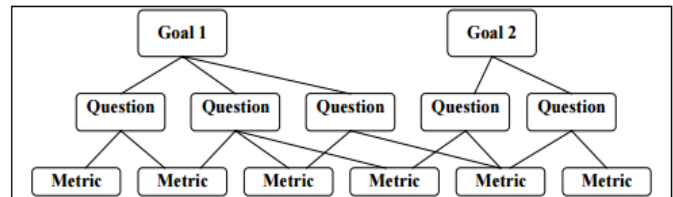


Fig. 4. GQM method [23]

III. RELATED WORK

There are many studies conducted to describe the performance of SP managers and provide some guidance on the factors affecting their success. Some other studies provide simple and little ideas about performance measurement. In the following, some examples of these studies are presented:

- Andrew Stellman and Jennifer Greene [2] provide a practical guide for managing a software project effectively. They present the common pitfalls that plague all software projects and rookie mistakes that are made repeatedly. They present the tools, techniques, best practices, and practical advices that can be used on software projects for building better software. They cover many performance issues, but they don't cover performance metrics issues.
- Basharat et al. [24] describes different factors that cause the success or failure of projects. Their results present general guidance for project managers to make sure that their projects be successful. This study shows the importance of project management tools and techniques in the industry. It also shows how project management is important for a successful and quality software product.
- J. Procaccino and J. Verner [25] examine the mindset of software development project managers with regard to how they define a successful project in order to arrive at

a richer perspective of success. They investigated components of the developed system in order to place traditional measures of success in context with other organizational and managerial measures that have been suggested in the literature. They conclude that involvement of users and stakeholders during project development is an important success factor.

- Mirza and et al. [26] discuss that scope should be properly defined and controlled and what can be the major factors behind mismanagement of scope and how it can be overcome. It is concluded that a better appreciation of the distinction between project and product scope can bring a higher possibility of project success within the planned cost and schedule.
- J. Verner and W. Evanco [27] surveyed 42 software projects in Australia in order to understand what project management practices are used in these projects. The relationship between practices and software project outcomes enables the authors to investigate why some projects succeed and others fail. They found that nearly 20% of projects had no lifecycle methodology and 10% of the respondents did not understand what was meant by a software development lifecycle methodology. Many recognized software practices are not being applied consistently in the projects investigated. Fifty percent of projects began with unclear requirements. Risk assessment is not normally a part of the development process and the organizations are not learning from their mistakes as post mortem reviews are much more likely to be held for successful projects than they are for failed projects.
- Paul Pocatilu [28] stated that in order to have successful projects, lessons learned have to be used, historical data to be collected and metrics and indicators have to be computed and used to compare them with past projects and avoid failure to happen. He presents some metrics that can be used for IT project management. He concluded that the quality of calculating metrics depends on the quality of data used in the model.
- Kanhaiya Jethani [29] discusses the benefits of choosing appropriate metrics and analysis method based on observations in several organizations. It also discusses the pitfalls of choosing wrong metrics. Organizations can define useful metrics for the software development process by using the GQM method, which ensures that the metrics are aligned with the goals of the organization. Examples of metrics for software development process and some of the pitfalls of inappropriate metrics definition based on observations in various organizations have been provided for guidance. Simple metrics analysis methods for various metrics have also been provided for reference.
- Julio Menezes and et al. [30] present the application of a systematic mapping study that aims to raise related work to the usage of metrics and indicators for risk assessment in multiple projects' environments. They conclude that the study of risk measurement in software development environments should be seen more carefully, taking into account the aspects of software processes, especially with the increasing of agile methods, which requires a more sophisticated development culture, impacting directly on software processes.
- Terence L. Woodings and Gary A. Bundell [31] define a taxonomy of software metrics which is derived from the needs of users, developers, and management. The properties of the classifications are discussed. A number of approaches (e.g. the Software Factory, CMM, Bootstrap, SPICE, GQM, Balanced Scorecard), have been advocated for the systematic design and introduction of software metrics for the purposes of process improvement and capability assessment in an organization. Rules are then derived which generate a new set of metrics from an existing class. The rules complement standard approaches by focusing attention on user driven aspects of an organization's measurement program. They do this by directly linking product characteristics with organizational improvements. The method also has promise as an approach for validating process models and metrics. Examples of the theoretical and pragmatic use of the taxonomy are provided. The paper concludes with a discussion of useful applications.
- Maarit Tihinen [32] discusses challenges in current measurement practices have been summarized and described in detail from a GSD viewpoint. Further, requirements for dynamic measurements derived from GSD-related challenges in current measurement practices have been introduced. This thesis defines dynamic measurements as actions where metrics are defined or updated based on the needs of each project and demands of each project's collaboration setting. The actual metrics data are collected and analyzed continuously from various tools and databases, even from stakeholders' databases, and results of measurements are analyzed with visualized indicators that are easy to read. This thesis introduced a technical implementation that was utilized as a proof of concept for the measurement-based management of GSD projects.
- Ž. Antolić [33] presents an overview of possible Key Performance Indicators (KPI) that can be used for software process efficiency evaluation. The overview is based on currently used KPIs in software development projects on Cello Packet Platform (CPP) platform. The most important KPIs are analyzed, and their usage in the process efficiency evaluation is discussed. The outcome of the measurement is used to initiate further process adjustments and improvements.

IV. GOAL QUESTION METRIC INDICATOR (GQMI) METHOD

The researcher proposes an adapted version of GQM method which is illustrated in figure 5. The adapted version of GQM method exceeds one step rather than the original one. The additional step is calculating the performance indicator for

each SPM knowledge area, therefore the adapted version of GQM will be entitled Goal Question Metric Indicator (GQMI) Method. However, the four steps of GQMI are:

- 1) Define goals for each SPM knowledge area.
- 2) Refine the goals into quantifiable questions that must be answered for each goal.
- 3) Deduce performance metrics that can be used to answer the questions. Then, calculate the value of performance metrics.
- 4) Calculate performance indicators that can be calculated for each SPM knowledge area.

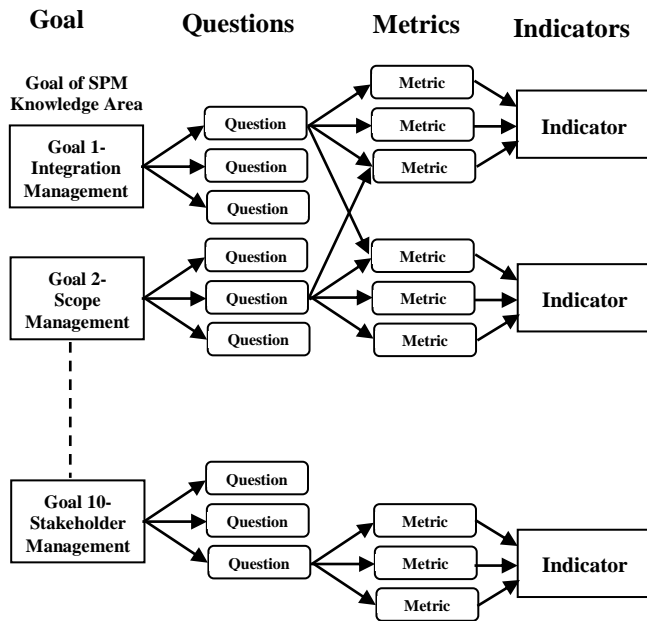


Fig. 5. GQMI Method

A. Define Goals for each SPM Knowledge Area

Each SPM knowledge area has a goal that represents the conceptual level of GQM method. A goal is defined for an object, for a variety of reasons, with respect to various models of quality, from various points of view, relative to a particular environment [23]. In this paper, the performance of SP managers is the main focus; therefore a goal is expressed as the performance of the project manager in a specific SPM knowledge area. For example, the goal related to the knowledge area “project integration management” is “improving the performance of the project manager in project integration management”. Similarly, the goals of the rest nine SPM knowledge areas can be defined.

B. Refine the Goals into Quantifiable Questions

A set of questions is used to characterize the way the assessment/achievement of a specific goal is going to be performed [23]. The questions that are typically used for

characterizing the performance of the SP manager are collected from various references and then purified and classified into groups, where each group relates to a specific SPM knowledge area. The result is a list of questions that represents each knowledge area and can be used for deducing performance metrics that will be explained in the next sub-section. The following is an example of questions related to project schedule/time management:

- Q1: How is the schedule management plan developed?
- Q2: How are the activities defined?
- Q3: How are the activities sequenced?
- Q4: How is the activity resources estimated?
- Q5: How is the activity durations estimated?
- Q6: How is the schedule developed?
- Q7: How is the schedule controlled?

C. Deduce Performance Metrics

There are many performance metrics of SPM that can be used for answering the questions of each SPM knowledge area. These metrics can be used for evaluating the performance of SP manager. But, not all metrics have the same degree of importance or efficiency in measuring the performance, therefore each metric must have a weight to express its importance. The typical method of weighting is assigning the weights 1, 2, or 3 for each metric. A weight 3 is used to show the performance metric of the most importance. A weight 1 is used to show the performance metric of the lowest importance. A weight 2 is used to show the performance metric of the average importance. The researcher tries to prepare an enhanced list of performance metrics and their weights.

For the purpose of this paper, an initial list of performance metrics is prepared from published SPM literatures and opinions of experts. Then, the initial list of metrics is subjected to validation process to produce the enhanced list of performance metrics. The researcher validates the performance metrics using a questionnaire that is prepared and delivered to 60 experts and specialists in SPM. The questionnaire includes the nine SPM knowledge areas as goals, each goal decomposes into a set of questions that is used to characterize the way of achieving it, and each question can be answered through a set of metrics. The respondents were originally classified into three equal groups:

- The first group includes 20 SP managers in different domains.
- The second group includes 20 professionals who work as team members in SPs.
- The third group includes 20 academic staff members who are interested in SPs.

The actual number of respondents who completed the questionnaire was 48. The respondents were required to select the effective metrics from the available list in the questionnaire. In addition, they were required to determine the weight of each metric. After collecting the responses, the researcher filtered the questions and metrics to reach an enhanced list of metrics. The definition of each metric should include the mathematical or statistical techniques for calculating this metric. The enhanced list will include the most effective questions and metrics that may make it more practical and efficient. Table IV presents the enhanced list of questions and performance metrics for schedule/time project management as an example of SPM knowledge areas. The majority of metrics in table IV have the importance degree 3; that is because the researcher attempts to extract the most effective metrics. In addition, the metric “M5” in question “Q1” is same as the metric “M4” in question “Q7”. Similarly, the metric “M3” in question “Q2” and the metric “M3” in question “Q7”. The complete definition of the performance metrics should also include:

- The mathematical or statistical techniques for calculating each metric.
- The planning and/or actual data required for calculating each metric.
- The required implementation range for each performance metric. The required implementation range is the acceptable range of the performance metric.

At the end of this step, a complete definition of performance metrics is reached in the form of an enhanced list. Then, the performance metrics can be calculated either for one or more SPM knowledge areas.

D. Calculate Performance Indicators

The enhanced list of performance metrics resulted from the previous sub-section is used for calculating performance indicators for SP manager in each SPM knowledge area. This process can help in improving capability level, productivity, and performance. Calculating indicators from metrics is not an easy process because the indicator value may depend on a combination of metrics and each of them doesn’t have the same level of importance and they may not have the same nature [17]. The source of complexity is due to the different nature of the data types of the performance metrics. They may include ROI, PV, percentage, ratio, number of days, or/and numeric amounts.

Therefore, it is important to use a method to unify these values to be entered into indicators calculation process. Therefore, the researcher uses a rating scale for measuring the implementation of the performance metrics. The proposed scale is based on that each performance metric value is compared with the required implementation range, and typically the following rules are applied:

- If the metric value is in the required range, the implementation value will be “Accepted” or equal the numeric value “2”.

TABLE IV. THE ENHANCED LIST OF QUESTIONS AND PERFORMANCE METRICS FOR SCHEDULE/TIME MANAGEMENT

Questions	Metrics	W
Q1: How is the schedule management plan developed?	M1. Percentage of schedule management procedures included in the plan vs the standard or predefined procedures.	3
	M2. Percentage of actual inputs included in the process vs planned inputs.	3
	M3. Percentage of techniques and tool used vs possible or effective techniques and tool for this activity.	2
	M4. Percentage of the attributes of schedule management plan implemented vs required.	3
	M5. Ratio of number of modifications applied to schedule management plan vs required.	3
Q2: How are the activities defined?	M1. Percentage of actual inputs included in the process vs planned inputs.	3
	M2. Percentage of techniques and tool used vs possible or effective techniques and tool for this activity.	3
	M3. Percentage of schedule management procedures applied vs planned.	3
	M4. Percentage of activities included in the activity list resulted from this process vs all defined.	3
	M5. Percentage of activities that have completed attributes vs all activities in the activity list.	3
	M6. Percentage of external milestones included in the external milestone list vs identified in the contract.	3
	M7. Percentage of internal milestones included in the internal milestone list vs identified by the custom.	2
	M8. Ratio of internal milestones to external milestones included in the milestone list.	1
Q3: How are the activities sequenced?	M1. Percentage of actual inputs included in the process vs planned inputs.	3
	M2. Percentage of techniques and tool used vs possible or effective techniques and tool for this activity.	3
	M3. Percentage of activities that were subjected to dependency analysis vs all activities in the activity list.	3
	M4. Percentage of project activities sequenced in project schedule network diagrams vs all activities in the activity list.	3
Q4: How is the activity resources estimated?	M1. Percentage of actual inputs included in the process vs planned inputs.	3
	M2. Percentage of techniques and tool used vs possible or effective techniques and tool for this activity.	3
	M3. Percentage of alternatives were analyzed vs all alternatives.	3
	M4. Percentage of activities that were subjected to resources estimation vs all activities in the activity list.	3
Q5: How is the activity durations estimated?	M1. Percentage of actual inputs included in the process vs planned inputs.	3
	M2. Percentage of techniques and tool used vs possible or effective techniques and tool for this activity.	3
	M3. Percentage of activities that were subjected to duration estimation vs all activities in the activity list.	3
	M4. Percentage of estimates that were subjected to reviews vs all estimates.	2
Q6: How is the schedule developed?	M1. Percentage of actual inputs included in the process vs planned inputs.	3
	M2. Percentage of techniques and tool used vs possible or effective techniques and tool for this activity.	3
	M3. Percentage of activities used in developing schedule vs all activities in the activity list.	3
	M4. Percentage of schedule reviews that were performed before finalizing the schedule vs identified by the custom.	2
Q7: How is the schedule controlled?	M1. Percentage of actual inputs included in the process vs planned inputs.	3
	M2. Percentage of techniques and tool used vs possible or effective techniques and tool for this activity.	3
	M3. Percentage of schedule management procedures applied vs planned.	3
	M4. Ratio of number of modifications applied to schedule management plan vs required.	3
	M5. Percentage of tasks completed vs. planned at a point of time.	3
	M6. Percentage of external milestones met vs. planned.	3
	M7. Percentage of internal milestones met vs. planned.	2
	M8. Percentage of project deliverables achieved vs. planned.	3
	M9. Slippage time of the project schedule (in days).	3

- If the metric value is greater than the required range, the implementation value will be “Highly Accepted” or equal the numeric value “3”. Some metrics can’t exceed the required range; therefore this rule isn’t applied in this case.
- If the metric value is less than the required range, the implementation value will be “Not Accepted” or equal the numeric value “1”.

The previous rules can’t be applied to some metrics such as the metrics “M9” in question “Q7”. If the slippage time is greater than the required range, the implementation value will be “Not Accepted” or equal the numeric value “1”. If the slippage time is less than the required range, the implementation value will be “Highly Accepted” or equal the numeric value “3”. In addition, some performance metrics may be Not Applicable (NA) in some cases [34]. During computing the performance indicators, the not applicable quality metrics will be eliminated.

For achieving the purpose of the proposed model, the performance metrics are organized in a table as in table V. The performance indicator can be calculated using the weighted mean method. The weighted mean method is appropriate because it takes the weights into account during calculations [34]. The basic formula of the weighted mean is [35]:

$$\text{Weighted Mean} = \frac{\sum X_i \cdot W_i}{\sum W_i}$$

Where:

- X_i is the implementation value of the performance metric i
 X_i may take the value 1, 2, or 3 according to the rating the lowest importance, average importance, or the most importance respectively.
- W_i is the metric weight of each performance metric i . It may take the value 1, 2, or 3.

Based on to the rating scale that is used, the performance indicator value will range from 1 to 3. According to the proposed measuring method and the data listed in table V, the performance indicator for schedule/time can be calculated using the weighted mean equation for each question or for all the knowledge area.

Performance indicator for “Q1” = $(3 \times 2 + 3 \times 3 + 2 \times 2 + 3 \times 1 + 3 \times 1) / (2 + 3 + 2 + 1 + 1) = 2.78$ out of 3 = 92.67 %

Similarly, the performance indicator for “project schedule/time management” can be calculated = 1.8 out of 3 = 60 %

After calculating the value of the performance indicator for a specific SPM knowledge area, this value must be compared with the acceptable value of performance indicator. Then, the result of comparison should be analyzed to discover the weakness and strength points of SPM performance. The analysis may return to the performance indicators of questions to reveal which of them contribute in increasing or decreasing the value of the performance indicator. Based on the analysis of results, top management may take supportive or corrective actions. The acceptable value of the performance indicator is

used for judging the calculated value. If the acceptable value of performance indicator is 2.4 out of 3. Therefore, performance indicator of “project schedule/time management” isn’t acceptable and the value of the performance indicator for each question should be analyzed because each one represents a process required for achieving the knowledge area.

TABLE V. THE ACTUAL VALUES OF PERFORMANCE METRICS FOR SCHEDULE/TIME MANAGEMENT

Question	Metric	Metric Weight W_i	Required Range	Actual Value of the Metrics	NA	Implementation Value X_i
Q1	M1	3	80-90 %	90 %		2
	M2	3	80-90 %	95 %		3
	M3	2	70-80 %	75 %		2
	M4	3	85-95 %	60 %		1
	M5	3	1:1	4:6 i.e. <1:1		1
Q2	M1	3	80-90 %	80 %		2
	M2	3	70-80 %	80 %		2
	M3	3	85-95 %	80 %		1
	M4	3	90-95 %	100 %		3
	M5	3	90-95 %	100 %		3
	M6	3	100 %	80 %		1
	M7	2	85-95 %	95 %		2
	M8	1	1:1	1:1		2
Q3	M1	3	80-90 %	80 %		2
	M2	3	70-80 %	80 %		2
	M3	3	100 %	100 %		2
	M4	3	100 %	100 %		2
Q4	M1	3	80-90 %	95 %		3
	M2	3	70-80 %	70 %		2
	M3	3	80-90 %		✓	
	M4	3	80-90 %	80 %		2
Q5	M1	3	80-90 %	80 %		2
	M2	3	70-80 %	80 %		2
	M3	3	80-90 %	80 %		2
	M4	2	80-90 %	70 %		1
Q6	M1	3	80-90 %	90 %		2
	M2	3	70-80 %	60 %		1
	M3	3	100 %	100 %		2
	M4	2	85-95 %	70 %		1
Q7	M1	3	80-90 %	80 %		2
	M2	3	70-80 %	80 %		2
	M3	3	85-95 %	80 %		1
	M4	3	1:1	4:6 i.e. <1:1		1
	M5	3	85-95 %	70 %		1
	M6	3	80-90 %	80 %		2
	M7	2	80-90 %	70 %		1
	M8	3	85-95 %	95 %		2
	M9	*	3	14 days	25 days	

V. APPLYING GQMI METHOD ON REAL SOFTWARE PROJECTS

To achieve the purpose of this paper, GQMI has been applied on 3 real SPs to evaluate the performance of SP managers.

- The first project aimed to develop a software application for inventory control in an agriculture company.
- The second project aimed to develop a software application for managing training department in a pharmaceutical company.

- The third project aimed to develop a software application for managing procurement department in a beverage company.

The performance metrics were calculated for schedule/time management. Table VI illustrates the actual data of the three projects.

TABLE VI. THE APPLICATION OF GQMI ON THREE SOFTWARE PROJECTS

Question	Metric	Metric Weight W_i	Implementation Value X_i		
			Project (1)	Project (2)	Project (3)
Q1	M1	3	2	3	2
	M2	3	3	3	2
	M3	2	2	3	2
	M4	3	1	3	2
	M5	3	1	1	2
Q2	M1	3	2	2	1
	M2	3	2	3	2
	M3	3	1	3	1
	M4	3	3	2	2
	M5	3	3	2	3
	M6	3	1	2	2
	M7	2	2	3	3
	M8	1	1	2	1
Q3	M1	3	2	2	2
	M2	3	2	2	2
	M3	3	2	2	1
	M4	3	2	2	2
Q4	M1	3	3	2	1
	M2	3	2	2	2
	M3	3	1	2	3
	M4	3	2	3	3
Q5	M1	3	2	2	1
	M2	3	2	3	2
	M3	3	2	2	1
	M4	2	1	2	2
Q6	M5	3	2	3	2
	M6	3	1	3	3
	M7	3	2	2	2
	M8	2	1	2	3
Q7	M1	3	2	3	3
	M2	3	2	3	1
	M3	3	1	3	2
	M4	3	2	2	2
	M5	3	1	3	3
	M6	3	2	3	2
	M7	2	1	2	3
	M8	3	2	3	2
	M9	3	1	2	1
Σ		$\Sigma W_i=107$	$\Sigma X_i.W_i=192$	$\Sigma X_i.W_i=260$	$\Sigma X_i.W_i=213$
The Indicator Value= Weighted Mean= $(\Sigma X_i.W_i) / \Sigma W_i$			1.79	2.43	1.99

According to table VI, the performance of the project manager for schedule/time management of project (2) is the best because he has more experience and applies some agile practices. The performance of the project manager for schedule/time management of project (1) is the worst because he hasn't the sufficient experience and there are problems in the project team. Figure 6 illustrates the comparison between the performances of the three project managers for schedule/time management of the three projects. Figure 7 illustrates the value of the performance indicator for each

question related to project (1).

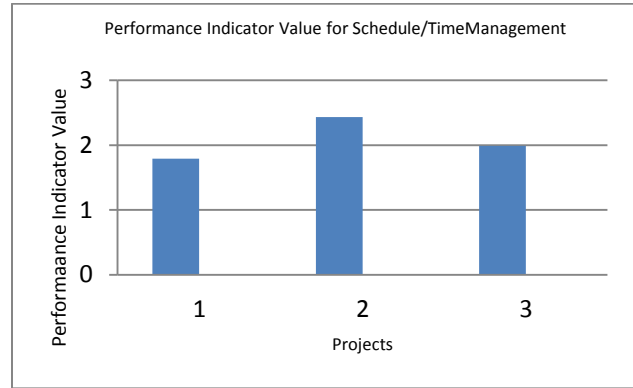


Fig. 6. The comparison between the performances of the three project managers

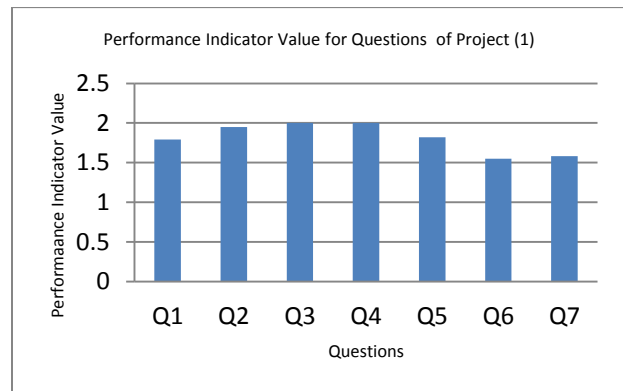


Fig. 7. The value of the performance indicator for each question related to project (1)

VI. CONCLUSION

The performance of project managers can be effectively measured for a specific SPM knowledge area because each area includes a set of processes and skills related to a specific SPM competency. This paper aimed to measure the performance of SP managers through a novel method that is based on GQM method, an enhanced list of performance metrics for SPM knowledge areas, and a combination of simple mathematical and statistical techniques to calculate performance indicators for SP managers. The novel method depends on defining goals for each SPM knowledge area, refining the goals into quantifiable questions that must be answered for each goal, deducing performance metrics that can be used to answer the questions, and calculating performance indicators for each SPM knowledge area. In addition, the performance indicator can be calculated for each question that represents a process related to the knowledge area. The researcher focused on schedule/time management as an example of knowledge areas to explain the novel measuring method. In addition, he applied the novel method on three real SPs. Finally, the researcher concludes that measuring the performance of SP managers can provide an attention to pitfalls in their performance and may be helpful in controlling and improving the performance.

VII. FUTURE WORK

There are many issues related to the performance of SP managers can be tackled in the future:

- Expanding the work to build an automated software tool for evaluating the performance indicators of SPM knowledge areas.
- Adapting GQMI method to be used for agile SPs.
- Adapting GQMI method to be used in cloud computing applications.
- Measuring the performance of the project managers of e-government projects.

REFERENCES

- [1] Information Systems Audit and Control Foundation (ISACF), "Project Management: Skill and Knowledge Requirements in an Information Technology Environment", 2002.
- [2] Andrew Stellman and Jennifer Greene, "Applied Software Project Management", O'Reilly Media, ISBN 978-0-596-00948-9, 2005.
- [3] Jeffrey A. Hoffer, Joey F. George, and Joseph S. Valacich, "Modern System Analysis and Design", Addison Wesley Longman, Inc, 1999.
- [4] https://www.tutorialspoint.com/software_engineering/software_project_management.htm Last visit: 4/10/2016
- [5] Jeffrey L. Whitten, Lonnie D. Bentley and Kevin C. Dittman, "System Analysis and Design Methods", Fifth edition, Mc Graw Hill Companies, Inc, 2001.
- [6] Nagy Ramadan Darwish and Nancy M. Rizk, "Multi-Dimensional Success Factors of Agile Software Development Projects", International Journal of Computer Applications (IJCA), Vol. 118 No. 15, Page: 23-30, Foundation of Computer Science, New York, USA, May 2015.
- [7] CHAOS manifesto 2013, Standish Group International.
- [8] Project Management Institute (PMI), "A Guide to the Project Management Body of Knowledge – PMBOK Guide", 5th edition, 2013.
- [9] Project Management Institute (PMI) and IEEE Computer Society, "Software Extension to the PMBOK Guide (5th Edition)", 2013.
- [10] Mary Sumner, "Risk Factors in Enterprise Wide Information Management Systems Projects", ACM press, New York, NY, USA, Proceedings of the 2000 ACM SIGCPR Conference on Computer Personnel Research, 180-187.
- [11] Hallows, Jolyon E., CMC, "Information Systems Project Management: How to Deliver Function and Value in Information Technology Projects", AMACOM, a division of American Management Association, 1998.
- [12] Mary Sumner, "Critical Success Factors in Enterprise Wide Information Management Systems Projects", ACM press, New York, NY, USA, Proceedings of the 1999 ACM SIGCPR Conference on Computer Personnel Research, 297-303, 1999.
- [13] <https://www.project-management-prepcast.com/pmbok-knowledge-areas-and-pmi-process-groups> last visit: 22/10/2016.
- [14] Daniele Di Filippo, Russell D. Archibald, and Ivano Di Filippo, "Six-Phase Comprehensive Project Life Cycle Model", Vol. I, Issue V, December 2012.
- [15] Jason Westland, "Project management guidebook", Method123, 2003.
- [16] <http://www.method123.com/project-lifecycle.php> last visit: 4/10/2016.
- [17] Department of Energy (DOE), "Basic Performance Measures for Information Technology Projects", 2002, <http://energy.gov/sites/prod/files/cioprod/documents/PerMeasTech-V3-011502.pdf> Last visit: 29/9/2016.
- [18] Karl E. Wiegers, "A Software Metrics Primer", Process Impact, 1999, http://www.processimpact.com/articles/metrics_primer.html
- [19] IEEE Standard 610, "Glossary of Software Engineering", 1990.
- [20] Mike Denley, "Metric-Driven Project Management Driving Success by Design", Siemens PLM Software, http://www.elysiuminc.com/gpdis/2015/Siemens-Denley_DrivingtoSuccessbyDesign_PDST_Open.pdf Last visit: 4/10/2016.
- [21] Fenton, Norman, Robin Whitty and Yoshinori Iizuka, "Software Quality Assurance and Measurement", International Thomson Computer Press, 1995.
- [22] Zdena Dobešová¹ and Dagmar Kusendová², "Goal-Question-Metric method for evaluation of cartographic functionality in GIS software", proceedings GIS Ostrava, 2009, www.geoinformatics.upol.cz/app/visegrad/images/GISOstrava.pdf
- [23] Victor R. Basili, Gianluigi Caldiera, and H. Dieter Rombach, "THE GOAL QUESTION METRIC APPROACH", 1994.
- [24] Basharat Jehan, Kamran Ghani, and Muhammad Shafiq, "Assessment of Project Management Practices in Pakistan Software Industry", IEEE SCONEST 2014, At Hyderabad Pakistan, 2014.
- [25] J. Procaccino and J. Verner, "Software project managers and project success: An exploratory study", Journal of Systems and Software, Vol. 79, No. 11, pp. 1541-1551, 2006.
- [26] Muhammad Nabeel Mirza, Zohreh Pourzolfaghar, and Mojde Shahnazari, "Significance of Scope in Project Success", Procedia Technology, Volume 9, Pages 722-729, 2013.
- [27] J. Verner and N. Cerpa, "Australian Software Development: What Software Project Management Practices Lead to Success?", Proceedings of the 2005 Australian Software Engineering Conference (ASWEC'05), IEEE, 2005.
- [28] Paul Pocatilu, "IT Project Management Metrics", Revista Informatica, 4 (44), 2007.
- [29] Kanhaiya Jethani, "Software Metrics for Effective Project Management", International Journal of System Assurance Engineering and Management, pages 335-340, Vol. 4 No. 4, December 2013.
- [30] Júlio Menezes Jr., Cristine Gusmão, and Hermano Moura, "Indicators and Metrics for Risk Assessment in Software Projects: A Mapping Study", Laboratório de Banco de Dados, Universidade Federal de Minas Gerais, 2012.
- [31] Terence L. Woodings and Gary A. Bundell, "A framework for software project metrics", Proceedings of the 12th European Conference on Software Control and Metrics, 2001.
- [32] Maarit Tihinen, "Measurement-based management of global software development projects", Ph.D. Thesis, VTT SCIENCE 70, University of Oulu, Finland, October 2014.
- [33] Ž. Antolić, "An Example of Using Key Performance Indicators for Software Development Process Efficiency Evaluation", Internal Ericsson Documentation, Croatia, January 2008.
- [34] William E Perry, "Quality Assurance for Information Systems: Methods, Tools, and Techniques", QED technical publishing Group, 1991.
- [35] Abdul Quader Miah, "Applied Statistics for Social and Management Sciences", Springer 2016.

A Topic based Approach for Sentiment Analysis on Twitter Data

Pierre FICAMOS*, Yan LIU[†]
School of Software Engineering
TONGJI University
Shanghai, China

Abstract—Twitter has grown in popularity during the past decades. It is now used by millions of users who share information about their daily life and their feelings. In order to automatically process and analyze these data, applications can rely on analysis methods such as sentiment analysis and topic modeling. This paper contributes to the sentiment analysis research field. First, the preprocessing steps required to extract features from Twitter data are described. Then, a topic based method is proposed so as to estimate the sentiment of a tweet. This method requires to extract topics from the training dataset, and train models for each of these topics. The method allows to increase the accuracy of the sentiment estimation compared to using a single model for every topic.

Keywords—sentiment analysis; opinion mining; natural language processing; feature extraction; topic modeling

I. INTRODUCTION

Twitter is a social network which allows its users to post and share short messages (up to 140 characters) called tweets¹. Over the past decades, Twitter has spread worldwide and has become one of the major social networks. Overall, social media are growing more and more popular, they are now one of the main way of communication for both people and companies. Twitter's slogan is: "Twitter it's what's happening". Indeed, many users are sharing about events of their daily life. Hence, following Twitter's flow of data may allow to monitor events which are occurring and understand people's feelings.

In order to automatically process Twitter data, several data analysis methods, such as sentiment analysis and topic modeling, can be applied. The outcomes of these analyses may be used by several applications, such as event monitoring, and opinion mining about products or brands. Indeed, companies always need fast and accurate information in order to be able to react the market trends.

This paper proposes a sentiment analysis method: First, topics are extracted from the training dataset. Then an algorithm is trained for each topic. Finally, the method estimates the sentiment of a sentence according the best topic related algorithm results.

This paper's contributions contain: 1) Detail the possible steps for data preprocessing in order to extract bags of words from Twitter data. 2) Propose a sentiment analysis method which relies on tweets topics for improving the estimation

accuracy.

This paper is organized as follows. Section II describes related works on the sentiment analysis research field. Then, the section III introduces the preprocessing steps which are applied in order to extract bags of words from the samples. The method applied so as to estimate the sentiment of a tweet is explained in section IV, and section V presents the evaluation of this method. Finally, the section VI concludes and introduces future works.

II. RELATED WORK

A. General Research Field

Sentiment analysis research field is anterior to the social network era. Most of the first studies led on sentiment analysis were focusing on review, such as movie review, since reviews are often associated to a score. Hence, it was simple to get the sentiment score of a review. The researchers did not have to manually label their datasets.

The first approaches for extracting sentiments from texts were relying on human generated baseline. These methods were not able to handle the complexity of the language, and were providing low accuracy results. Indeed, a random approach for classifying a text between positive and negative would already be 50% accurate. The human generated baselines seems to have difficulty to provide better accuracy than 70% for the sentiment prediction [1], [2].

One of the most popular approach for sentiment analysis is to rely on supervised machine learning techniques. The three main machine learning algorithms which are applied for sentiment analysis are: Naive Bayes [3], Maximum Entropy [4], and Support Vector Machine (SVM) [5]. The accuracy of these three algorithm depends on the feature extraction method which is applied and the analyzed datasets. For example, SVM shows better performance when it only use unigrams, and adding bigrams features will reduce its accuracy [1], [2].

According to anterior research, the feature extraction methods have to take the following specificity into account:

- **Presence is better than Frequency:** Two possible methods for extracting features from a text are either to generate a bag of words which contains each words present in the text, or to count the frequency at which each word appears in the text. Previous researches have shown that analyses are more accurate when focusing on the word presence [1].

¹<https://twitter.com/>

- **Negation Handling:** Negation allows to alter the meaning of a word to its opposite meaning. Therefore, during the feature extraction, it is important to indicate process whether or not a word is negated [3]. If the negation is not handling the algorithm will understand the opposite meaning of the sentence, and will have less accurate predictions.
- **Bigrams:** Several feature extraction methods will use bigrams in order to extract a more accurate representation of the sample [2], [3]. Indeed, n-grams allow to capture the context of a word, thus it allows the algorithms to be more accurate.
- **Part of Speech (POS) tags:** POS (Part Of Speech) tags are representation of the lexical category of a word [6]. Part of speech may allow to disambiguate words meaning [1], and it may also be used so as to generate pattern for extracting features from the samples [7].
- **Lemmatizing / stemming word:** Both lemmatization and stemming allow to ignore the possible variation of a word. These methods are often applied for extracting features from a text. They allow to reduce the amount of features generated, and regroup similar features [8].

B. Sentiment Analysis on Twitter

Since social network has become more and more popular, several researchers have been focusing on applying sentiment analysis on short text message. The majority of these researches are dealing with Twitter samples. Indeed, it is convenient to retrieve data from Twitter with its available APIs. Then, in order to train the algorithms, sentiment analysis requires to have annotated samples. Contrary to review, twitter data does not have associated scores, the data have to be manually annotated. An alternative method for annotating these data relies on the emoticons which are contained in the samples. Emoticons are used to convey the sentiment of the writer, thus it is possible to label every text which contains positive emoticons to positive and negative ones to negative [2], [9]. This method is convenient since it allows to automatically generate important set of data, but the dataset generation will be less accurate than a manually annotated dataset.

Performing feature extraction on Twitter messages rises new challenges:

- **Short messages:** Sentiment analysis is usually performed on longer text. Because of the text limitations, Twitter messages are short, and the algorithm has less features available for analysis.
- **Internet language:** Twitter users adopt the “internet language” when writing their messages. This language differs from the traditional English: new words, repeated letters [2], emoticons.
- **Twitter characteristics:** Twitter allows users to add three specific entities to their messages: hashtags, user references, and URLs. These entities require to be processed differently than common words.

III. DATA PREPROCESSING

The preprocessing steps aim to begin the feature extraction process and start extracting bags of words from the samples. One of the main focus is to reduce the final amount of features extracted. Indeed, features reduction is important in order to improve the accuracy of the prediction for both topic modeling and sentiment analysis. Features are used to represent the samples, and the more the algorithm will be trained for a specific feature the more accurate the results will be. Hence, if two features are similar it is convenient to combine them as one unique feature. Moreover, if a feature is not relevant for the analysis, it can be removed from the bag of words.

- **Lower uppercase letters:** The first step in the preprocessing is to go through all the data and change every uppercase letter to their corresponding lowercase letter. When processing a word, the analysis will be case sensitive and the program will consider “data” and “Data” as two totally different words. It is important that, these two words are considered as the same features. Otherwise, the algorithms will affect sentiments which may differ to these two words. For example, on these three sentences: “data are good”, “Awesome data”, and “Bad Data”. The first and second sentences both contain “data” and are positive, the third sentence contains “Data” and is negative. The algorithm will guess that sentences containing “data” are more likely to be positive and those containing “Data” negative. If the uppercases had been removed the algorithm would have been able to guess that the fact that the sentence contains “data” is not very relevant to detect whether or the sentence is positive. This preprocessing step is even more important since the data are retrieved from Twitter. Social media users are often writing in uppercase even if it is not required, thus this preprocessing step will have a better impact on social media data than other “classical” data.
- **Remove URLs and user references:** Twitter allows user to include hashtags, user references and URLs in their messages. In most cases, user references and URLs are not relevant for analyzing the content of a text. Therefore, this preprocessing step relies on regular expression to find and replace every URLs by “URL” and user reference by “AT_USER”, this allows to reduce the total amount of features extracted from the corpus [2]. The hashtags are not removed since they often contain a word which is relevant for the analysis, and the “#” characters will be removed during the tokenization process.
- **Remove digits:** Digits are not relevant for analyzing the data, so they can be removed from the sentences. Furthermore, in some cases digits will be mixed with words, removing them may allow to associate two features which may have been considered different by the algorithm otherwise. For example, some data may contain “iphone”, when other will contain “iphone7”. The tokenization process, which will be introduced later,

will not separate “iphone” from “7”, so these two features will be considered as different. Removing the “7” will allow the features representing these two words to be the same.

- **Remove stop words:** In natural language processing, stop words are often removed from the sample. These stop words are words which are commonly used in a language, and are not relevant for several natural language processing methods such as topic modeling and sentiment analysis [10]. Removing these words allows to reduce the amount of features extracted from the samples.
- **Remove repeated letters:** This preprocessing step refers to the fact that Twitter users will often repeat some letters several times when they want to highlight a word [2]. For example, the following tweets contain the word “love” with several repeated letters: “I loooovvveee that!”. Repeated letter will be reduced to their first two occurrences. Hence, for the previous example “loooovvveee” will become “loovvee”.
- **Tokenize:** Tokenization is almost implicit since the English language is already segmented. Each word is separated by space, thus the token can be created by splitting the sentence on each space. The tokenization applied for this project also include other functionalities such as separated punctuation tokens from the word. The experiments will use the NLTK word_tokenize method for tokenizing its samples [11].
- **Detect POS tags:** Part of speech may have two uses for data analysis. First, it may be used so as to disambiguate the meaning of a word. Even if it makes sense for a reader that in the sentences: “I like that” and “I am not like you”, “like” have two different meaning, when computing the bag of words, the algorithm will consider them as the same [1]. The second use for POS tags is to allow to categorize words and process them differently according to which type they correspond to [7]. The detection of the samples POS tags will rely on the NLTK method pos_tag [11].
- **Lemmatize:** When processing samples, “word” and “words” would be considered as two different features. Hence, in order to improve the features reduction process, the unigrams can be lemmatized. This preprocessing step mainly allows to remove plurals and conjugations. The lemmatization will be based on the WordNet implementation which is including in the NLTK distribution [11].

IV. METHODOLOGY

This paper proposes an approach which can be extended to several sentiment analysis problems. The concept of this approach is that sentiment analysis algorithms can perform better when the data, which are processed, deal with a less wide category of topic. Hence, topic modeling techniques may help to divide data into several datasets. The vocabulary diversity of these dataset will be inferior to the original data, thus training the sentiment analysis is more simple.

After the data preprocessing, the tweets are represented by bags of words. These bags of words contain words which has been lemmatized and their associated POS tags. The proposed method uses this bag of words in order to extract topics from the text and train its algorithms.

A. Topics extraction

The first requirement of this method is to extract topics from the samples. Topic extraction can either be supervised or unsupervised. Supervised topic extraction require to have manually analyzed the training dataset, and to associate a topic to each tweet. Therefore, unsupervised topic modeling technique is more simple to implement and will be applied for this paper.

First, features have to be extracted from the training data set. The testing dataset is ignored for the topics extraction process since, in real application cases, these testing data would not be available. In order to represent the samples: nouns, verbs, adjectives, adverbs and interjections are extracted from the bags of words according to their POS tags. By empirical study, this feature extraction method has provided better topic distribution for applying sentiment analysis. Then, these features are used to train the model and extract topics from the samples.

The topic modeling model which is applied is a Latent Dirichlet Allocation (LDA), the core estimation is based on the algorithm of Hoffman *et al.* [12]. This model has been chosen since it allows inference of topic distribution. Other equivalent model could also be applied.

B. Train the Algorithms

After having extracted the topics from the samples, the training dataset can be split in several subsets. The topics extraction process provides a probability distribution of the topics for each sample. Hence, a sample may be associated to several topics. The training process takes into account this probability distribution: each topic subset contains all the samples which probability distribution is superior to a threshold. Thus, some samples may be contained in several subsets, when others may be contained by only one.

```
FOR each topic related to the tweet
  FOR each sample
    estimate the topic probability distribution
    IF probability > threshold THEN
      ADD sample to the training subset
    END IF
  END FOR
  extract features from the subset
  train algorithm
END FOR
```

Fig. 1. Algorithms training process (pseudocode)

Once all the subsets have been generated, sentiment analysis algorithms can be trained for each of these subsets. The training of these algorithms requires to extract features from the subsets. After the preprocessing, the samples are already represented by bags of words, thus features can be directly extracted from these bags of words. The feature extraction method which have been applied allows to extract unigrams from the bag of words, and handle negation words.

Other alternative feature extraction could also be applied. The pseudocode of the training process is detailed in Fig 1.

C. Sentiment estimation

Since a tweet may be associated to several topics and a sentiment analysis algorithm has been trained for each of these topics, a method for exploiting the results of all of these algorithms needs to be defined.

In order to estimate the sentiment of a tweet, the sentence is first preprocessed, and then features are extracted from the bag of words. Finally, the topic probability distribution of the tweet is estimated. For each topic whose probability is superior to a threshold, the algorithm trained for this specific topic is applied in order to estimate the sentiment of the tweet. The estimation which has the highest probability is kept as the final estimation. This estimation process is described as a pseudocode in Fig 2.

```
FOR each topic related to the tweet
  IF topic probability distribution > threshold THEN
    estimate the sentiment of the tweet
  END IF
END FOR
sentiment = maximum probability of the estimation
```

Fig. 2. Sentiment estimation process (pseudocode)

V. EVALUATION

The experiments of this paper mainly rely on the NLTK libraries [11]. As it has been introduced in the third section, several preprocessing steps rely on these libraries. Furthermore, the algorithm which will be applied for this experiments, Naive Bayes (NB), is also implemented by NLTK. Other sentiment analysis algorithm such as maximum entropy or SVM could also have been selected.

So as to train the algorithm and estimate its accuracy, the experiments will process the same dataset which was introduced by Go *et al.* [2]. The data have been retrieved from Twitter: the training set of 1.6 million tweets, was annotated according their emoticons, and the testing set composed of 177 negative tweets and 182 positive ones were manually annotated. Because of the processing time required for training the algorithms, the training dataset has been reduced to 5 000 positive tweets, and 5 000 negative ones. Three dataset have been generated by randomly extracting samples from the complete dataset. Then the experiments have been conducted on these three dataset. The results obtained are the average results of these three experiments.

The experiment focuses on two parameters: N the total amount which will be extracted from the samples, and ξ the threshold for the topic probability distribution. The aim is to demonstrate that these two parameters are linked, and the correct combination of these parameters allows to increase the global estimation accuracy.

First, the method has been applied with one unique topic (N = 1). The results of this first experiment will be used as a reference for the other experiments. Indeed, with only one topic, this method corresponds to the basic sentiment analysis method. This method has provided 74.09% accurate results.

When the size of training dataset is increased to its maximum, this method can provide 81.34% accuracy which is consistent with the results obtained by Go *et al.* [2].

TABLE I. AVERAGE ACCURACY OF THE ESTIMATION FOR N AND ξ GIVEN

$\xi \backslash N$	2%	4%	6%	8%	10%
1	74.09	74.09	74.09	74.09	74.09
2	74.09	74.06	74.22	74.16	74.25
3	74.05	74.08	74.12	74.22	74.59
4	74.50	74.24	74.61	74.35	73.64
5	74.22	74.31	74.95	73.48	73.51
6	73.59	74.20	73.28	73.20	73.44
7	74.58	74.86	73.53	73.52	73.57
8	74.39	75.17	73.45	73.40	73.24
9	73.44	74.07	73.31	73.23	73.29
10	73.54	73.17	73.14	73.16	73.13

Then different combinations have been tried for N and ξ , the results are shown in Table I. Since LDA model uses randomness in the topic extraction process, the estimations have been repeated ten times, and the final results correspond to the average of these results.

According to these results, it can be estimated that as N increases, the threshold ξ needs to be reduced. This observation can be explained: the more the amount of topics increase, the more spread are the distributions of topics, thus the threshold needs to be decreased.

VI. CONCLUSION AND FUTURE WORK

This paper's first contribution to the sentiment analysis research field is to detail the preprocessing steps which have to be applied to extract bags of words from Twitter data. The second contribution is to propose a topic based sentiment analysis approach. This approach relies on the fact that the complexity of an analysis can be reduced when the algorithm focus on a smaller range of topic. The algorithms have to deal with less vocabulary and its estimation can be more accurate. Hence, the experiments have shown that, applying this method performs better than the classical sentiment analysis model. The proposed approach can be extended to other sentiment analysis problems.

The method can be improved. The paper has focused on exploiting the results of the default parameter for the topic modeling method. More research on the topic extraction may allow to have more distinct topics, hence the estimation should be more accurate.

Moreover, the method proposed here cannot handle neutral data. In order to apply sentiment analysis on real application cases, neutral data need to be handled. Therefore, future works should focus on these neutral data. Two methods may allow to detect neutrality:

- Use supervised topic modeling techniques to differentiate opinionated data from the neutral data.
- Adapt the sentiment analysis method for detecting either opinionated data or neutral data.

REFERENCES

- [1] B. Pang, L. Lee, and S. Vaithyanathan, "Thumbs up?: sentiment classification using machine learning techniques," in Proceedings of the ACL-02 conference on Empirical methods in natural language processing, vol. 10, pp.79-86, Association for Computational Linguistics, July 2002.
- [2] A. Go, R. Bhayani, and L. Huang, "Twitter sentiment classification using distant supervision," CS224N Project Report, Stanford, 1, 12, 2009
- [3] V. Narayanan, I. Arora, and A. Bhatia "Fast and accurate sentiment classification using an enhanced Naive Bayes model," in International Conference on Intelligent Data Engineering and Automated Learning, pp. 194-201. Springer Berlin Heidelberg, October 2013.
- [4] A. L. Berger, V. J. D. Pietra, and S. A. D. Pietra, "A maximum entropy approach to natural language processing" Computational linguistics, 22(1), 39-71, 1996.
- [5] C. J. Burges, "A tutorial on support vector machines for pattern recognition," Data mining and knowledge discovery, 2(2), 121-167, 1998.
- [6] E. Brill, "A simple rule-based part of speech tagger," in Proceedings of the workshop on Speech and Natural Language, pp. 112-116, Association for Computational Linguistics, February 1992.
- [7] P. D. Turney, "Thumbs up or thumbs down?: semantic orientation applied to unsupervised classification of reviews," in Proceedings of the 40th annual meeting on association for computational linguistics, pp. 417-424, Association for Computational Linguistics, July 2002.
- [8] M. Hu and B. Liu, "Mining Opinion Features in Customer Reviews," in AAAI, vol 4, no. 4, pp. 755-760, July 2004.
- [9] A. Pak, and P. Paroubek, "Twitter as a Corpus for Sentiment Analysis and Opinion Mining," in LREc, vol. 10, pp.1320-1326, May 2010.
- [10] C. Fox, "A stop list for general text," *ACM SIGIR Forum*, vol. 24, no 1-2, pp. 19-21, September 1989.
- [11] S. Bird, E. Loper and E. Klein "Natural language processing with python," O'Reilly Media Inc. 2009.
- [12] M. Hoffman, D.M. Blei, and F.R. Bach, "Online learning for latent dirichlet allocation," in advances in neural information processing systems, pp. 856-864, 2010.

An Improved Malicious Behaviour Detection Via k -Means and Decision Tree

Warusia Yassin, Siti Rahayu, Faizal Abdollah and Hazlin Zin
Faculty of Information and Communication Technology
Universiti Teknikal Malaysia Melaka
Malaysia

Abstract—Data Mining algorithm which is applied as an anomaly detection system has been considered as one of the essential techniques in malicious behaviour detection. Unfortunately, such detection system is known for its inclination in detecting a cyber-malicious activity more accurately (i.e. maximizing malicious and non-malicious behaviours detection) and has become a persistent limitation in the deployment of intrusion detection systems. Consequently, these constraints will affect a number of important performance factors such as the accuracy, detection rate and false alarms. In this research, KMDT proposed as an anomaly detection model that utilized k -means clustering and decision tree classifier to maximize the detection of malicious behaviours by scrutinizing packet headers. The k -means clustering employed for labelling and plots the whole behaviours into identical cluster, which characterized the behaviours into suspicious or non-suspicious composition. Subsequently, these dissimilar clustered behaviours are reordered within two classes of types such as malicious and non-malicious via decision tree classifier. KMDT is a profitable finding which improved the anomaly detection performance in identifying suspicious and non-suspicious behaviours as well as characterizes it into malicious and non-malicious behaviours more accurately. These criteria have been validated by the result from the experiments throughout banking system environment dataset 2016. KMDT have detected more malicious behaviours accurately as contrast to discrete and diversely combined methods.

Keywords—Intrusion Detection; Malicious Behaviours; Clustering; Decision Tree Classifier; Packet Headers

I. INTRODUCTION

Safekeeping confidential information and computing assets from cyber threats, has turned into a foremost dispute as a consequence from sudden increases on network based malicious activities. As such, various Intrusion Detection Systems (IDSs) used to recognize, gather and analyse security infractions from diverse systems or networks [1]. In addition, the research societies have been classified these IDSs into misuse and anomaly based detection systems [2]–[6].

Misuse based detection recognizing acknowledge malicious traffic throughout the signatures which are defined and gathered earlier in the database. This facilitates the security personnel to easily create those signatures based on the seen behaviours of a malicious behaviours and determine which specific behaviours they want to detect [7]. Despite, the incapability to identifying the novel malicious behaviours

remain as challenging task as these detection systems required frequent signature updates for each time novel behaviours are discovered [5].

Conversely, the research communities have claimed that the finest solution to observe unforeseen malicious behaviours without concerning signatures are with anomaly based detection systems [8]. This detection system is dependent on forming of ordinary behavioural models and conclude any attempt that is not covered within this model as malicious behaviours [9]. Nonetheless, higher false alarm or false positives are the main imperfection of this detection systems [10].

Seeing facts, for last two decades, an anomaly detection system that utilizes data mining approaches has attracted researcher interest, particularly within the concept of intrusion detection [10]–[12]. Nevertheless, maximizing the true positive (malicious behaviours which detected as malicious) and true negative (non-malicious behaviours which detected as non-malicious) as well as minimizing the false positive (non-malicious behaviours which detected as malicious) and false negative (malicious behaviours which detected as non-malicious) are not much enhanced as a whole. Consequently, this situation drags into poor performance in term of detection rate, accuracy and false alarm [13], [14] and as a result, research in data mining as anomaly detection system particularly for malicious behaviours is still in a process of improvement [15], [16].

In this research, k -means and Decision Tree, namely KMDT proposed in order to prevail over the aforementioned inadequacy. Even if so, much more focuses has been given to identify malicious activity than the non-malicious activities because failure in detecting malicious behaviours could lead to the losses of confidential information and computing assets. KMDT uniquely designed with clustering and classification scheme in scrutinizing malicious and non-malicious behaviours more accurately.

Figuratively, the foremost contributions of this paper include: (i) k -means clustering as an initial stage able to accumulate the similar and dissimilar malicious behaviours into unlike clusters. (ii) The dissimilar clustered behaviours are reorganized with decision tree classifier to increase the malicious prediction rate. By utilizing this two detection approach, the performance of the detection metric such as accuracy, detection rate and false alarm has improved.

The rest of the paper is organized as follows: In Section 2, the former similar fundamental works are briefly represented. The proposed detection model methodology has detailed out in Section 2. The experimental analysis discussed in Section 4 while conclusion and future work are covered in Section 5.

II. RELATED WORK

Data mining approach extensively discovered and applied as detection methods in these few years in a field of an anomaly detection system. The major concentration of these whole detection methods is direct to observe, differentiate and identify i.e malicious or non-malicious behaviours [6]. Procedure of discovering fundamental patterns and concealed relationships systematically from valuable information within the data to visualize and model interrelationship of the data itself are known as data mining process [17]. Clustering and classification are common data mining algorithms and widely discovered and employed within the field of intrusion detection [6], [18], [19].

Clustering is ordinarily applied in anomaly detection to explore assemblage without prior knowledge on relationship within the data. Thus, clustering groups objects based on characterization of data points, where every single data point in a cluster is alike to those within its cluster, but different from those in different or other clusters [20], [21]. Clustering has capabilities to group similar malicious data points collectively into one or more cluster including previously unseen malicious data points [22]. In addition, *k*-means clustering is much more efficient as a contrast to other existing clustering methods as the fact that this algorithm able to process huge volumes of instances quickly and have non-linear complexity. In contrary, the challenges of such method are to define the *k* centroids for every single cluster, in which different location of a centroids possible to produce different outcome that is not much favourable [23]–[25] has tested and proven that the *k*-means algorithm is capable to detect malicious behaviours with high detection rates. They applied the algorithm to categorize normal and abnormal data points into different clusters to detect malicious behaviours more correctly, identifying unknown malicious behaviours without having prior knowledge. However, this algorithm also usually contributes in increasing false positive rates [26] even though it shows a high success rate in identifying suspicious behaviours. Such a high rate of false positives could downgrade the detection performance of IDSs as too many alerts are generated for non-suspicious behaviours wrongly detected as malicious data. Therefore, classification is introduced to reclassify the entire behaviours processed through *k*-means during the pre-processing stage [27].

Classification is a supervised learning method intended to build a detection model which could explain a data class, sort out data points or elements into classes that correspond to their features based on a sequence of pre-determined class label [13], [22]. Consequently, the structured label elements will be further used to predict the class label of new elements. For example, using training data with a pre-determined label to predict each class label in testing data [28]. Among various classification techniques, Decision Tree is faster and able to construct rules that are easy to interpret and understand [29].

However, a single classifier's impact or contributions is improved when it is integrated with other data mining algorithms even though each of these methods individually has been proven to achieve well in intrusion detection [6].

Integrated forms basically are made up of multiple clustering and classification algorithms, where clustering is executed at the beginning as a pre-processing method to reduce the noise within the dataset or to label the data for the subsequent classification stage [30], [31]. In another word, clustering is used in earlier phases to separate or label data into different clusters with a reasonable clustered data rate, so that the classifier can perform better to classify those data more correctly in the next phase. *K*-means clustering and Naive Bayes classifier has proposed as a an anomaly detection method. As an initial stage, the clustering method has applied to isolate a group of malicious and non-malicious activities which act analogously and un-analogously while Naive Bayes applied in the further stage to re-organize the clustered data more precisely into rightful class categories. The aim of above mentioned clustering algorithm is to minimize squared error-function, so that the optimal distance between two different data points and cluster centroids could be calculated more effectively. On the other hand, the naive bayes algorithm used to scrutinize the relationship between dependent and independent variables in deriving a conditional probability of every single relationship. This method has been evaluated and its slightly enhanced the detection performance in term of accuracy, the detection rate and false alarm [32]. A variety of combinations have been efficiently applied as intrusion detection recently. For instance, [31] integrated both *k*-means and *k*-nearest neighbour (KNN) algorithms to identify a specific form of attacks in an anomaly detection method named Triangle Area based Nearest Neighbour (TANN). *K*-means clustering is employed to categorize data into specific sets and type of attacks, and further reassembled through the *K*-NN classifier based on a feature of the triangle area. TANN is capable to identify certain types of attacks, but performs moderately in reducing the false alarm rate. Furthermore, *k*-means clustering has been combined with a decision tree algorithm as a network anomaly detection method [33]. In the initial phase, *k*-means clustering has applied to split the training data into *k* disjoint clusters, in which every single cluster correspond to a boundary of comparable data. Next, the above data is input into a decision tree algorithm to be classified either as normal or anomaly. The method contributes notable true positive and false positive rates with a reasonable accuracy rate which can be further improved. In contrast to these methods, an innovative anomaly detection method that distinctively combined *k*-means clustering, Naive Bayes as feature selection and the Kruskal-Wallis statistical test is used to discover important features prior to classification. Then, this subset is classified with the Decision Tree algorithm to identify intrusion with the maximum amount of accuracy [6]. Furthermore, in [34] performance analysis on Decision Tree and Naive Bayes for data classification has been conducted. The aim of this comparison is to find the most accurate classifier with high true positive and lower false positive rates. The author has concluded that the efficiency and accuracy of Decision Tree classifier are much better than Naive Bayes. In addition, in [35] conducted a

similar analysis for intrusion detection using well-known data mining classifiers such as Decision Tree, Bayesnet, OneR and Naïve Bayes. In their study, they discovered that the best classification algorithm which could be applied for intrusion detection particularly novel intrusions is Decision Tree. Most researchers have claimed that the Decision Tree classifier is much more effective than others in maximizing novel malicious behaviour detection Such as from [29], [34]–[37]. Therefore Decision Tree classifier considered in this work.

In summary, even though the data mining approach, particularly clustering and classification mechanism has been applied widely in detecting malicious and non-malicious behaviours, the shortcomings such as maintaining the highest detection, accuracy and false alarm rates prohibit in assembling a proficient detection method [38], [39]. Moreover, these constraints still exist as a result of that, the whole focuses is not being given to maximizing the unseen and seen malicious as well as non-malicious behaviours identification rate. Therefore, there is also a critical requirement in designing efficient anomaly detection to identify malicious and non-malicious behaviours more accurately.

III. K-MEANS AND DECISION TREE ANOMALY DETECTION METHOD

The proposed detection method *k*-means clustering and Decision Tree classifier called (KMDT) uses packet header information for anomaly detection which relies on a series of methods, i.e. employing *k*-means clustering in labelling data based on a clustered arrangement as a pre-processing stage and decision tree for classifying data which is affected with suspected outliers or miss-classified data during the pre-processing stage. The KMDT aim to identify the malicious behaviours more accurately and overcome the drawbacks currently faced in research in anomaly detection method. The process involves in each stage is as follows:

A. *K*-means Clustering

An unsupervised algorithm such as clustering method directly to discover separate data boundaries into an amount of sections called *clusters* without concerning labelled information for the learning process, in which every single data point can be apportioned or allocated a degree of relationship to each of the clusters [40], [41]. In another expression, given a sort of data that does not have any label associated with it $\{x^1, x^2, x^3 \dots x^n\}$, whereas unsupervised algorithm (i.e. *k*-means) applied to find the structure or pattern of these data and gather it into coherent subset. Moreover, the procedure of casting clusters includes merging numerous alterable (variable) into a dissimilar or a distance dimension whose measure are thenceforth expended to construct clusters. An iterative clustering method such as *k*-means is an admired algorithm worthy for its easiness, immediate convergence and short period intricacy (complexity). These methods intended to the clusters sort of *i* input data points $\{x^1, x^2, x^3 \dots x^n\}$ into *K* coherent (disjoint) subsets of $S_{(i)}$ to minimize mean-square-error, JMSE as in Equation (3):

$$JMSE = \sum_{i=1}^K \sum_{x_{(i)} \in S_{(i)}} dist(x_{(i)} - \mu_{r(i)})^2 \quad (1)$$

TABLE I. BANKING SYSTEM DATASET 2016 TRAINING AND TESTING BEHAVIOUR DISTRIBUTION

Variant	Non-Malicious Behaviours	Malicious Behaviours	Volume
Training	16,797	60,729	77526
Testing	33,579	22,842	56421

where $x_{(i)}$ is a vector representing the *i*-th input data point and $\mu_{r(i)}$ is the geometric centroid of the data points $x_{(i)}$ in $S_{(i)}$, and $(x_{(i)} - \mu_{r(i)})^2$ is selected as matrix of distances to be minimized between input data points $x_{(i)}$ and $\mu_{r(i)}$ cluster centroid [40]. In addition, Euclidean Distance (Dist) function applied to calculate the distance in a basis of similarity or dissimilarity between $x_{(i)}$ and $\mu_{r(i)}$.

K-means has been chosen and utilized in the proposed model among various conceivable clustering algorithms on the grounds that it have the capabilities to collectively cluster the suspicious and non-suspicious data points without prior knowledge. Secondly, the clustered collection can then be beneficial to label the data points into malicious and non-malicious for the classification stage as presented in the later sections. Based on preliminary studies, MacQueen *et al.* [42], is the researcher whom developed and introduce *k*-means algorithm in 1967. *K*-means algorithm can be described as in Algorithm 1.

K-means is one of the many clustering algorithms extensively used for the reason of its in complexity, proficiency and easy to implement. Once the clustered set has been identified and data points have been labelled, it is feasible to carry on the classification procedure as in the next section.

B. Decision Tree Classifier

The Decision Tree (DT) classifier is the well-known data mining method enforced these days and was firstly introduced

Algorithm 1: *K*-Means Clustering Steps

- 1 Define the total number of *K* clusters centroids. Evaluation phase involving a total number of *K* clusters in a variant of $2 < K < 7$.
- 2 Initialize the *K* clusters centroids, $\mu^1, \mu^2, \mu^3 \dots \mu^K \in \mathbb{R}^n$. For instance, μ^1 and μ^2 for two different clusters (i.e. suspicious and non-suspicious).
- 3 Compute Euclidean Distance $dist(x_{(i)} - \mu_{r(i)})^2$. It is usually applied to calculate the distance between data points and cluster centroids.
- 4 Assigning data points to the nearest centroid, such that every single cluster will be occupied by possible similar data points.
- 5 Re-compute the mean of each cluster centroid. The location of the cluster centroids changes hereon.
- 6 Repeat steps (3)-(5) until the convergence conditions are fulfilled and the data point is label appropriately according to its clusters.

by Quinlan (1986) [43]. Using similar methodology in [44], a tree classifier known as decision tree has been created. This developed classifier consisting three major elements i.e. decision node which signifies the conditions on an instances, a split that matches close to one of the possibility attribute values and a leaf that chooses the class whereabouts the instances fits in. In order to classify the instances, the initial

point defined from top of the leaf which referred as the root and subsequently the branches is established based on the outcome of every single test down along a leaf node is reached. The last part of the leaf node is considered as the classification criteria. The information gain methodology has been applied to select the optimum attribute splitting for each subset on each stage, in which the attributes that has maximum information value choose to form a decision. The formulated algorithm of above-mentioned decision tree illustrated in Algorithm 2.

In the proposed detection approach, the k -means clustering helps in labelling and arranging the suspicious and non-suspicious data in some form that could be usable for a classification method such as early notification on possible malicious and non-malicious data to obtain better accuracies and detection outcomes on the subsequent phase using the decision tree classifier. The next section presents the assessment to validate that the proposed method is considerably better in anomaly detection.

IV. EVALUATION AND DISCUSSION

In this section, the proposed KMDT evaluated with latest

Algorithm 2: Decision Tree Steps

- 1 While every single leaf node comprises more than one instances category, remaining attributes and noteworthy information gain do the below steps,
 - 2 Let choose the root node and single attributes,
 - 3 Let Segregate the node population and compute an information gain values,
 - 4 Let discover the split which have highest information gain values for an attribute,
 - 5 Let re-compute these process for entire attributes,
 - 6 Let discover the finest splitting attribute and split rule,
 - 7 Utilize these attributes to split the node,
 - 8 Repeat step 2 to 7 until no child node is remains.
-

datasets. In the following section, the dataset used as well as measurement of detection applied for evaluation purpose have been described and then the assessment result presented.

A. Banking System Dataset 2016

Recently, there are huge recommendations among the research community to evaluate the detection method using an appropriate and latest dataset. As such, an analysed and validated packet header which has captured and correlated from the real-time banking system environment applied to perform intrusion detection using proposed KMDT. The detection procedure is supervised on an offline mode and the original class label i.e. malicious or non-malicious ignored for use during the prediction phase. However, those labels have been used to calculate and validate the value of false positive, false negative, true positive and true negative. Table I illustrate the distribution of training and testing behaviours. A variant of experiments were run separately to validate KMDT using aforesaid dataset.

B. Detection Measurement

The detection performance was evaluated using benchmark measurement as recommended by research

communities [22], [45], in which the measurement or indicator includes detection rate, accuracy and false alarms. The formulas used to calculate those values are as follows:

$$Accuracy = (tp + tn)/(tp + tn + fp + fn) \quad (2)$$

$$Detection\ Rate = (tp)/(tp + fp) \quad (3)$$

$$False\ Alarm = (fp)/(fp + tn) \quad (4)$$

Non-malicious behaviours which is incorrectly identified as malicious is called *false positive (fp)*, while *false negative (fn)* refers to the incorrect identification of malicious behaviours as non-malicious. Conversely, malicious behaviours which is correctly identified as malicious is called *true positive (tp)*, while *true negative (tn)* is the correct identification of non-malicious behaviours as non-malicious. For better understanding, the entire above-mentioned performance metric described in percentage form in this article.

Under the circumstances of failure to achieve the best degrees in previous metrics, the current detection methods cannot contribute in high accurate detection for accuracy, detection rate and false alarm indicators. Moreover, the major significant task that necessary to be met is to come with applicable scheme that can increase the detection percentage of non-malicious behaviours (NMB) and detection percentage of malicious behaviours (MB) with the development of anomaly based detection. In addition, once the detection percentage of non-malicious and malicious behaviours is maximized, the conventional limitation in having high accuracy and detection rate as well as lowest false alarm is now achievable. The formulas used to calculate those values are as follows:

$$NMB = \left(\frac{tn}{tn+fp}\right) * 100 \quad (5)$$

$$MB = \left(\frac{tp}{tp+fn}\right) * 100 \quad (6)$$

The proposed model is promising to maximize the above-mentioned indicators rate as justified in the next section.

C. Detection Result

In order to appraise the proposed method more meticulously, various experiments have been performed using banking system dataset 2016. The banking system dataset is used to validate the effectiveness of the proposed method in terms of prediction of the malicious and non-malicious behaviours. Different stages of analysis have been conducted using clustering to choose the best optimized cluster sets while decision tree for classification purpose that can contribute to higher accuracy, detection rate and lowest false alarm as well as with the maximum non-malicious and malicious behaviours percentage. In other words, the entire behaviours have been clustered into different variants of (k -th) clusters and the most accurate cluster (i.e. highest true positive and true negative) arrangement is chosen for the clustering stage. Once the clustered arrangement has been identified and behaviours have labelled (i.e. suspicious or non-suspicious), the value of the behaviours was entered into the Decision Tree (DT) classification task. The DT classifier classified these

behaviours into non-malicious or malicious classes more accurately.

High detection accuracy and lowest false alarm rate represent the best model of anomaly detection. However, high NMB and MB detection percentage also need to be considered in selecting such detection model. The experimental result confirmed that the proposed KMDT (*k*-means and decision tree) is substantially effective and improve the anomaly-based detection capabilities based on the above-mentioned performance factors as compared to other combinational and individual method. The result of a variant of K-Means (*k-th*), Decision Tree (DT) as an individual method and a variant of K-Means and Decision Tree (*k-th*-DT) as a combinational method from each experiment conducted have been presented from Table 2 through Table 5.

TABLE II. DETECTION PERCENTAGE OF NON-MALICIOUS AND MALICIOUS DATA OF *K*-TH K-MEANS USING BANKING SYSTEM TRAINING DATASET

Cluster <i>k</i> -th	<i>k</i> -2	<i>k</i> -3	<i>k</i> -4	<i>k</i> -5	<i>k</i> -6	<i>k</i> -7	<i>k</i> -8	<i>k</i> -9	<i>k</i> -10
DP-NMD	75.4	75.4	80.5	75.4	65.1	79.8	75.4	75.2	81.3
DP-MD	100	100	100	100	100	100	100	100	100

TABLE III. DETECTION PERCENTAGE OF *K*-TH K-MEANS USING BANKING SYSTEM TRAINING DATASET

Cluster <i>k</i> -th	<i>k</i> -2	<i>k</i> -3	<i>k</i> -4	<i>k</i> -5	<i>k</i> -6	<i>k</i> -7	<i>k</i> -8	<i>k</i> -9	<i>k</i> -10
Accuracy	42.3	42.3	52.5	42.3	30.6	50.9	42.3	42	54.6
Detection Rate	4.6	4.6	5.5	4.5	3.85	5.35	4.6	4.6	5.8
False Alarm	59.4	59.4	48.9	59.3	71.4	50.5	59.3	59.6	46.7

TABLE IV. DETECTION PERCENTAGE OF *K*-8 K-MEANS & DECISION TREE USING BANKING SYSTEM TRAINING DATASET

Method	DP-NMD	DP-MD	Accuracy	Detection Rate	False Alarm
<i>k</i> -8	75.4	100	42.3	4.6	59.3
DT	9.38	99.31	79.83	79.84	90.61
<i>k</i> -8-DT	99.98	99.44	99.97	99.53	0.01

TABLE V. DETECTION PERCENTAGE OF *K*-8 K-MEANS + DECISION TREE USING BANKING SYSTEM TESTING DATASET

Method	DP-NMD	DP-MD	Accuracy	Detection Rate	False Alarm
<i>k</i> -8	50.98	99.98	83.25	79.73	49.01
DT	88.39	67.27	79.84	79.77	11.60
<i>k</i> -8-DT	99.81	99.88	99.86	99.90	0.18

TABLE VI. DETECTION PERCENTAGE OF KNOWN & UNKNOWN MALICIOUS BEHAVIOURS OF *K*-8 K-MEANS + DECISION TREE USING BANKING SYSTEM TESTING DATASET

Method	Unknown Malicious Behaviours		Known Malicious Behaviours	
	M-UMB	D-UMB	M-KMB	D-KMB
<i>k</i> -8+DT	281	27894	58	3805
	0.01%	99.9%	0.15%	99.85%

In Table II, in a series of *k*-th cluster trials, from $2 < k < 10$, the entire clusters able to clusters the malicious behaviours accurately with 100% detection (MB). In contrast, for the NMB, clustering outcome are not much satisfactory. For example, *k*-10 and *k*-4 recorded approximately less than 82% as NMB while the remaining *k*-th is below than 80%. Failure in achieving high NMB and NB has caused the computed false alarm, accuracy and detection rate for overall *k*-th clusters recorded the poorest result as in Table III. Based on the analysis, the entire clusters are less effective in grouping the behaviours which are similar to each other.

In Table IV, the result of the KMDT that only has performed better during the assessment period is presented. It is noticeable that the KM-DT which employs *k*-8 clusters and Decision Tree (i.e. *k*-8+DT) perform better with higher accuracy, higher detection rate and much lower false alarm rate compared to *k*-8 and Decision Tree (DT). Taking *k*-8, DT and *k*-8-DT as an example, the accuracy and detection rate have increased from 42.3%, 79.83% to 99.97%, and 4.6%, 79.84 to 99.53, respectively, and false alarm has decreased from 59.3%, 90.61% to 0.01%. This table also demonstrates the percentages of detection for the NMB and MB which vary between 75.4%, 9.38% to 99.98% and 100%, 99.31% to 99.44%, respectively. Unlike DT and *k*-8-DT which has only 2 final classes for grouping, *k*-8 has a set of clusters which facilitates to group malicious data effectively. Thus, the result of *k*-8 in MB is much better as compare to others. However, single detection method is not capable to improve the entire performance metrics using banking dataset.

In contrast to the above experiments that only use training data in assessing the proposed method, a different experiment have been further conducted using testing data. The reason is to identify the optimized clusters during the training phase (i.e. *k*-8) and apply these clusters during the testing phase evaluation. In addition, it could be helpful in practical solution and real deployment in selecting the number of cluster set (*k*) by only assessing the available data.

Table V represents the dimensions in terms of accuracy, the detection rate and false alarm of the KMDT method of *k*-8-DT that exercised on testing data. Combinational methods *k*-8+DT have outperformed with higher accuracy and detection rate and lowest false alarm at 99.86%, 99.90% and 0.18%, while *k*-8 at 83.25%, 79.73% and 49.01% as well as the DT classifier at 79.84%, 79.77% and 11.60%, respectively. In addition, these combinations are more accurate as compared to *k*-8 clusters set and decision tree classifier for grouping and classifying malicious and non-malicious behaviours. For example, the detection percentages of both NMB and MB for the *k*-8+DT combination have achieved 99.81% and 99.88% which are much better than others, i.e. *k*-8 and DT with 50.98, 99.98% and 88.39%, 67.27%, respectively. The MB of *k*-8 is slightly higher than *k*-8+DT because the clustering (*k*-8) has the advantage to manipulate continuous data as compared to a Decision Tree. Thus, the value of true positive of *k*-8 at 37153 is much higher than *k*-8 +DT at 37117. The entire result signifies that a better performance can be attained using the *k*-th value of 8 combined with DT (*k*-8+DT).

D. Discussion and Further Analysis

This finding proves that the combination of k -means and Decision Tree (KMDT) classifier with appropriate clusters set i.e. k -8+DT observed earlier during the training phase could give a much better result during the testing phase or in real environment. In addition, k -8+DT also contribute in increasing both non-malicious and malicious behaviours detection percentage. The main reason is because the clustering is utilized as the initial element for grouping and labelling of similar data into analogous sorts (i.e. suspicious and non-suspicious), and the capability in handling continuous-value contributes in maximizing detection percentage particularly for malicious classes. For example, as in Table V, the MB of k -8 at 99.98% is higher than DT at 67.27% and k -8+DT at 99.88%. Based on the investigation, k -8 detected 37153 malicious behaviours (true positive), thus yields in higher MB while DT and k -8+DT merely achieves 15368 and 37117. However, referring to Table V, the most significant performance is shown through k -8+DT, found to greatly improve the detection rate and accuracy above 99% and false alarm below 1% as compared to others. The entire results signify that a better performance could be attained using k -8+DT. To support this fact, practically, various experiments conducted and each experiment has shown a remarkable performance for k -8+DT. In contrast, the individual k -8 clustering and DT classifier which are incapable to identify non-malicious and malicious data more precisely also shown.

The detection of malicious behaviours is most concern in developing a detection system. Failures in identifying more malicious behaviours can cause data and confidential assets compromised by another party. These facts include the identification of known and unknown malicious behaviours. Taking these facts into account, four different performance variants have been considered such as missing known malicious behaviours (M-KMB), missed unknown malicious behaviours (M-UMB), detected known malicious behaviours (D-KMB) and detected unknown malicious behaviours (D-UMB). The M-KMB refers to the percentage where the known malicious behaviours during the training phase are failed to be identified during the testing phase while M-UMB are the percentage where the unknown malicious behaviours which not been covered during the training phase also failed to be detectable during the testing phase. On the other hand, D-KMB refers to refers to the percentage where the known malicious behaviours during the training phase are correctly identified during the testing phase while D-UMB is the percentage where the unknown malicious behaviours which not been covered during the training phase also correctly detectable during the testing phase.

Further experiments and analysis has been conducted to evaluate the proposed k -8+DT using aforesaid variants against banking dataset. Total number of unique malicious behaviours used is 32,038 in which 28,175 are known malicious behaviours while remaining 3836 are unknown malicious behaviours. Table VI exhibits the distribution of known and unknown malicious behaviours, and the outcome of k -8+DT. Surprisingly, based on the result, the rate of D-UMB and D-KMB for k -8+DT is 99.9% and 99.85%, which means k -8+DT able to detect more unforeseen malicious behaviours as a

contrast to seen behaviours accurately. Moreover, k -8+DT also recorded the lowest rate of M-UMB and M-KMB at 0.01% and 0.15%. Therefore, k -8+DT are more suitable to be utilized as anomaly detection systems particularly for detecting unknown malicious behaviours.

V. CONCLUSION AND FUTURE WORKS

Packet header for intrusion detection has attracted researchers' attention in the field of data mining based anomaly detection. Although a number of anomaly detection methods have been proposed, the common drawback is to achieve a high rate of accuracy, detection rate as well as a lower false alarm with high non-malicious and malicious behaviours detection remain as an unsolved problem, and directly affects the integrity of the said detection method to be widely adopted. In this work, a combined anomaly detection model named KMDT based on data mining methods that focuses on examining the entire features of a packet header to detect malicious behaviours is proposed. The k -means clustering is utilized to label the entire behaviour based on the behaviour characteristic such as suspicious or non-suspicious. In subsequent stages, the clustered behaviours input into Decision Tree classifier for classification purpose. The evaluation phase using banking dataset 2016 validates that the combinational method between k -means and Decision Tree shows an effective performance, such as higher accuracy and detection rate with lower false alarm as contrast to others. Thus, the KMDT approach could be a better anomaly detection method in identifying abnormal behaviour and determining it to be malicious or non-malicious behaviour more correctly. Besides, the ability of the KMDT focuses on identifying cyber-attack without emphasis on processing time or prompt detection can be considered for future research. For example, efforts to reduce the number of features that need to be examined are necessary and could be performing through feature reduction approach. This directly improves the processing time and the malicious data can be observed quickly.

ACKNOWLEDGMENT

The authors would like to thank the anonymous reviewers for their significant comments. Furthermore, the research project has been conducted in Universiti Teknikal Malaysia Melaka using Grant Scheme FRGS/1/2014/ICT4/FTMK?02/F00212.

REFERENCES

- [1] M. A. Faysel and S. S. Haque, "Towards Cyber Defense : Research in Intrusion Detection and Intrusion Prevention Systems," vol. 10, no. 7, pp. 316–325, 2010.
- [2] A. Patcha and J.-M. Park, "An overview of anomaly detection techniques: Existing solutions and latest technological trends," *Comput. Networks*, vol. 51, no. 12, pp. 3448–3470, Aug. 2007.
- [3] C.-M. Chen, Y.-L. Chen, and H.-C. Lin, "An efficient network intrusion detection," *Comput. Commun.*, vol. 33, no. 4, pp. 477–484, 2010.
- [4] Y. Waizumi, Y. Sato, and Y. Nemoto, "A Network-Based Anomaly Detection System Based on Three Different Network Traffic Characteristics," *J. Commun. Comput.*, vol. 9, no. 7, p. 805, 2012.
- [5] H.-J. Liao, C.-H. Richard Lin, Y.-C. Lin, and K.-Y. Tung, "Intrusion detection system: A comprehensive review," *J. Netw. Comput. Appl.*, vol. 36, no. 1, pp. 16–24, Jan. 2013.

- [6] P. Louvieris, N. Clewley, and X. Liu, "Effects-based feature identification for network intrusion detection," *Neurocomputing*, vol. 121, no. 0, pp. 265–273, 2013.
- [7] S. Juma, Z. Muda, and W. Yassin, "Machine Learning Techniques For Intrusion Detection System: A Review.," *J. Theor. Appl. Inf. Technol.*, vol. 72, no. 3, 2015.
- [8] M. Woźniak, M. Graña, and E. Corchado, "A survey of multiple classifier systems as hybrid systems," *Inf. Fusion*, vol. 16, no. 0, pp. 3–17, 2014.
- [9] Y. Cho, K. Kang, I. Kim, and K. Jeong, "Baseline Traffic Modeling for Anomalous Traffic Detection on Network Transit Points," in *Proceeding APNOMS'09 Proceedings of the 12th Asia-Pacific network operations and management conference on Management enabling the future internet for changing business and new computing services, 2009*, pp. 385–394.
- [10] Y. Xie, S. Tang, X. Huang, C. Tang, and X. Liu, "Detecting Latent Attack Behavior from Aggregated Web Traffic," *Comput. Commun.*, vol. 36, no. 8, pp. 895–907, 2013.
- [11] K.-C. Lee, J. Chang, and M.-S. Chen, "PAID: Packet Analysis for Anomaly Intrusion Detection," in *Advances in Knowledge Discovery and Data Mining SE - 58*, vol. 5012, T. Washio, E. Suzuki, K. Ting, and A. Inokuchi, Eds. Springer Berlin Heidelberg, 2008, pp. 626–633.
- [12] M. Z. Mas`ud, S. Sahib, M. F. Abdollah, S. R. Selamat, and R. Yusof, "Analysis of Features Selection and Machine Learning Classifier in Android Malware Detection," in *2014 International Conference on Information Science & Applications (ICISA), 2014*, pp. 1–5.
- [13] L. Koc, T. A. Mazzuchi, and S. Sarkani, "A network intrusion detection system based on a Hidden Naïve Bayes multiclass classifier," *Expert Syst. Appl.*, vol. 39, no. 18, pp. 13492–13500, 2012.
- [14] S. Juma, Z. Muda, and W. Yassin, "Reducing False Alarm Using Hybrid Intrusion Detection Based On X-Means Clustering and Random Forest Classification," *J. Theor. Appl. Inf. Technol.*, vol. 68, no. 2, pp. 249–254, 2014.
- [15] W. Yassin, N. Udzir, A. Abdullah, M. Abdullah, Z. Muda, and H. Zulzalil, "Packet Header Anomaly Detection Using Statistical Analysis," in *International Joint Conference SOCO'14-CISIS'14-ICEUTE'14 SE - 47*, vol. 299, J. G. de la Puerta, I. G. Ferreira, P. G. Bringas, F. Klett, A. Abraham, A. C. P. L. F. de Carvalho, Á. Herrero, B. Baruque, H. Quintián, and E. Corchado, Eds. Springer International Publishing, 2014, pp. 473–482.
- [16] M. Z. Mas`ud, S. Sahib, ..., M. F. Abdollah, S. R. Selamat, and R. Yusof, "Android Malware Detection System Classification," *Res. J. Inf. Technol.*, vol. 6, no. 4, pp. 325–341, Apr. 2014.
- [17] A. Urtubia, J. R. Pérez-Correa, A. Soto, and P. Pszczółkowski, "Using data mining techniques to predict industrial wine problem fermentations," *Food Control*, vol. 18, no. 12, pp. 1512–1517, 2007.
- [18] K. Abhaya, R. Jha, and S. Afroz, "Data Mining Techniques for Intrusion Detection: A Review," *Int. J. Adv. Res. Comput. Commun. Eng.*, vol. 3, no. 6, pp. 6938–6942, 2014.
- [19] S. Agrawal and J. Agrawal, "Survey on Anomaly Detection using Data Mining Techniques," *Procedia Comput. Sci.*, vol. 60, pp. 708–713, 2015.
- [20] J. F. Hair, R. Tatham, R. E. Anderson, C. T. Reviews, and B. Black, *Multivariate Data Analysis*, 6th ed. Academic Internet Publ., 2006.
- [21] A. B. S. Serapião, G. S. Corrêa, F. B. Gonçalves, and V. O. Carvalho, "Combining K-Means and K-Harmonic with Fish School Search Algorithm for data clustering task on graphics processing units," *Appl. Soft Comput.*, vol. 41, pp. 290–304, Apr. 2016.
- [22] D. M. Farid, L. Zhang, C. M. Rahman, M. A. Hossain, and R. Strachan, "Hybrid decision tree and naïve Bayes classifiers for multi-class classification tasks," *Expert Syst. Appl.*, vol. 41, no. 4, Part 2, pp. 1937–1946, 2014.
- [23] Y. Guan, A. A. Ghorbani, and N. Belacel, "Y-means: a clustering method for intrusion detection," in *Electrical and Computer Engineering, 2003. IEEE CCECE 2003. Canadian Conference on, 2003*, vol. 2, pp. 1083–1086 vol.2.
- [24] M. Kaushik and B. Mathur, "Comparative Study of Various Clustering Techniques," *Int. J. Softw. Hardw. Res. Eng.*, vol. 3, no. 10, pp. 497–504, 2014.
- [25] M. Ahmed, A. Naser Mahmood, and J. Hu, "A survey of network anomaly detection techniques," *J. Netw. Comput. Appl.*, vol. 60, pp. 19–31, Jan. 2016.
- [26] Y. Zhang, W. Lee, and Y.-A. Huang, "Intrusion Detection Techniques for Mobile Wireless Networks," *Wirel. Netw.*, vol. 9, no. 5, pp. 545–556, Sep. 2003.
- [27] S. Duque and M. N. bin Omar, "Using Data Mining Algorithms for Developing a Model for Intrusion Detection System (IDS)," *Procedia Comput. Sci.*, vol. 61, pp. 46–51, 2015.
- [28] P. García-Teodoro, J. Díaz-Verdejo, G. Maciá-Fernández, and E. Vázquez, "Anomaly-based network intrusion detection: Techniques, systems and challenges," *Comput. Secur.*, vol. 28, no. 1–2, pp. 18–28, 2009.
- [29] P. Kapoor and R. Rani, "Efficient Decision Tree Algorithm Using J48 and Reduced Error Pruning," *Int. J. Eng. Res. Gen. Sci.*, vol. 3, no. 3, pp. 1613–1621, 2015.
- [30] S. Zhong, T. M. Khoshgoftaar, and N. Seliya, "Clustering-Based Network Intrusion Detection," *Int. J. Reliab. Qual. Saf. Eng.*, vol. 14, no. 02, pp. 169–187, Apr. 2007.
- [31] C.-F. Tsai and C.-Y. Lin, "A triangle area based nearest neighbors approach to intrusion detection," *Pattern Recognit.*, vol. 43, no. 1, pp. 222–229, 2010.
- [32] M. Mohammadi, Z. Muda, W. Yassin, and N. Izura Udzi, "KM-NEU: An Efficient Hybrid Approach for Intrusion Detection System," *Res. J. Inf. Technol.*, vol. 6, no. 1, pp. 46–57, Jan. 2014.
- [33] A. P. Muniyandi, R. Rajeswari, and R. Rajaram, "Network Anomaly Detection by Cascading K-Means Clustering and C4.5 Decision Tree algorithm," *Procedia Eng.*, vol. 30, no. 0, pp. 174–182, 2012.
- [34] T. R. Patil, "Performance Analysis of Naive Bayes and J48 Classification Algorithm for Data Classification," *Int. J. Comput. Sci. Appl. ISSN 0974-1011*, vol. 6, no. 2, pp. 256–261, 2013.
- [35] Y. K. Jain, "An Efficient Intrusion Detection Based on Decision Tree Classifier Using Feature Reduction," *Int. J. Sci. Res. Publ.*, vol. 2, no. 1, pp. 1–6, 2012.
- [36] D. P. Gaikwad and R. C. Thool, "Intrusion Detection System Using Bagging with Partial Decision TreeBase Classifier," *Procedia Comput. Sci.*, vol. 49, pp. 92–98, 2015.
- [37] A. Rai, K. Devi, M.S. and Guleria, "Decision Tree Based Algorithm for Intrusion Detection," *Int. J. Adv. Netw. Appl.*, vol. 2834, pp. 2828–2834, 2016.
- [38] C. A. Catania and C. G. Garino, "Automatic network intrusion detection: Current techniques and open issues," *Comput. Electr. Eng.*, vol. 38, no. 5, pp. 1062–1072, 2012.
- [39] M. Panda, A. Abraham, and M. R. Patra, "A Hybrid Intelligent Approach for Network Intrusion Detection," *Procedia Eng.*, vol. 30, pp. 1–9, Jan. 2012.
- [40] A. K. Jain, "Data Clustering: 50 Years Beyond K-means," *Pattern Recogn. Lett.*, vol. 31, no. 8, pp. 651–666, 2010.
- [41] N. Jain and V. Srivastava, "Data Mining Techniques: A Survey Paper," *IJRET Int. J. Res. ...*, vol. 2, no. 11, pp. 116–119, 2013.
- [42] J. MacQueen, "Some methods for classification and analysis of multivariate observations," in *Proceedings of the Fifth Berkeley Symposium on Mathematical Statistics and Probability, 1967*, pp. 281–297.
- [43] J. R. Quinlan, "Induction of decision trees," *Mach. Learn.*, vol. 1, no. 1, pp. 81–106, 1986.
- [44] D. AL-Nabi and S. Ahmed, "Survey on Classification Algorithms for Data Mining:(Comparison and Evaluation)," *Comput. Eng. Intell. Syst.*, vol. 4, no. 8, pp. 18–25, 2013.
- [45] W. Xiong, N. Xiong, L. T. Yang, J. H. Park, H. Hu, and Q. Wang, "An Anomaly-based Detection in Ubiquitous Network Using the Equilibrium State of the Catastrophe Theory," *J. Supercomput.*, vol. 64, no. 2, pp. 274–294, 2013.

Integrated Approach to Conceptual Modeling

Lindita Nebiu Hyseni

Faculty of Contemporary Sciences and Technologies
South East European University
Tetovo, Macedonia

Zamir Dika

Faculty of Contemporary Sciences and Technologies
South East European University
Tetovo, Macedonia

Abstract—Conceptual modeling is supporting understanding and communication of the requirements in developing the information system (IS). The nature of requirements is usually divided into the functional (FRs) and non-functional requirements (NFRs). Thus, the scholars who are representing the conceptual modeling separate FRs and NFRs. Attempting to create an integrated framework for conceptual modeling of FRs and NFRs a new approach is being represented. In order to justify the approach, the research work and relevant literature in the field by using integrated perspective has been analyzed in this paper. As an outcome of this review, the need for an integrated approach to the requirement determination and proposed an integrated framework for conceptual modeling, which shall include the functional and non-functional requirements in one conceptual model has been identified. There is also identified that a small number of researchers have worked in this field, whilst the failure rate of the IS implementation which continues to be high has been the motivation, therefore the concept of proposing an integrated framework which will contribute to the increase of the efficacy of the requirements from the analysis phase in order to secure the sustainability of the IS has been approached.

Keywords—*Integrated Framework; Conceptual Model; Functional Requirements; Non-Functional Requirements; Research Gaps; Joint Approval Requirements (JAR)*

I. INTRODUCTION

The information system (IS) is an integrated set of the Information and Communication Technology (ICT) components, human resources and processes which supports individuals, groups, organizations and society in achieving their business and societal goals. Therefore, it is very important to support communication and understanding of the requirements in the development of the information system by using the conceptual model. The conceptual model is the model of the information system represented in a simple way in order to be understood by all participants in the project team and to be developed faster in fulfilling the requirements during the knowledge acquisition [1]. Conceptual model plays crucial role in the success of the information system [2], [3], [4]. After proven that the success of conceptual model affects the success of the information system, is asked the research question, what is needed to improve the conceptual modeling? Based on this research questions, the focus turns to the nature of the functional and non-functional requirements and their integration in one conceptual model, source used for the conceptual modeling, quality applied in the conceptual modeling, instrument used to design the conceptual model and method which is used by the client for approval of the requirements and conceptual model.

System requirements importance in developing the successful information system is also treated by scholars in 2016, who showed that participants involved in the project of the information system, start to clarify incompleteness and inconsistencies only during the phase of the system implementation but not at the phase of the system requirements, thus having an impact on the failure rate of the information system [5], [6]. Accordingly, is needed to conduct research by identifying if the scholars have started to initiate the integration of the functional and non-functional requirements in one conceptual model. Based on this, the objective in this paper is to present the rationale behind the proposal for integration of functional and non-functional requirements in one conceptual model, through a state of the art review for the identification of the research gap. This paper is organized as follows: in the section 2 is state of the art; in the section 3 are presented identified research gaps in the conceptual modeling; in the section 4 is presented the proposed integrated framework for conceptual modeling; in the section 5 is conclusion and future work; at the end, in the section 6 are presented the references used in this paper.

II. STATE OF THE ART

Based on the literature reviewed, development of the conceptual model is treated from different research outcomes, but in this section, are presented researches relevant to the functional and non-functional requirements.

A. Conceptual model

During the research conducted it is identified that the researchers nowadays have initiated to consider the non-functional requirements during the information system development. The authors Zubcoff, Garrigos, Casteleyn, Mazon, and Aguilar (2016), presented the Pareto method in which they considered the non-functional requirements during analysis and modeling of the requirements, in order to increase the quality of the web application, improve the design decision accuracy during the requirements analysis phase and they also stated the possibility for reducing the time needed by the designers [7]. Even though the issue of the non-functional requirements is initiated by above mentioned authors; Afreen, Khatoon and Sadiq (2016) in their article highlighted that most of the work is related to the functional requirements, while the non-functional requirements have received less consideration by the goal-oriented requirements engineering community [8]. In the article proposed by Neto, Vargas-Solar, da Costa, and Musicante (2016) it is also concluded that the non-functional requirements are not considered sufficiently in all software engineering phases [9]. The above articles treated the issue of

consideration of the non-functional requirements during information system modeling, but they did not introduce the method how to integrate the non-functional requirements. A hint about the possibility of the integration of the functional and non-functional requirements is presented by the authors Eckhardt, Vogelsang, and Fernández (2016), who presented the differences between FRs & NFRs whilst their results suggested that many non-functional requirements can be handled similarly to functional requirements [10]. This opens the possibility to propose a solution for consideration of the non-functional requirements and functional requirements during the conceptual modeling in order to closely resemble the conceptual model of the information system with the real world.

Most of the research articles about the conceptual modeling are not making any distinction, nor putting the argumentation about the effects of the conceptual model versus functional or non-functional requirements. Therefore, the following articles define what type of the requirements belong to conceptual model; two of the articles presented by authors Fatwanto and Boughton (2008) treated the functional and non-functional requirements in separate conceptual models. They have proposed a method to analyze, specify and develop the conceptual models of functional requirements, especially in the context of the translative model-driven development. Whereas, the other article proposes a method to analyze, specify and develop conceptual models of non-functional requirements. They validated these methods by using a case study of the Voter Tracking System [11], [12]. Also, the article presented by Cysneiros and Leite (2004) tackled the issue of the non-functional requirements not being treated as first class requirements. In the article, they presented a process to elicit, analyze and trace the non-functional requirements to the functional conceptual model. They also proposed a UML extension in order to allow non-functional requirements to be expressed. Their proposal is tested by three case studies but the results suggested that their proposal can improve quality of the conceptual model. The strategy used by them has some problems in the functional model and its impact. It is not significant in the overall development process [13]. The development process of the information system was also treated in early 1986 by the author Borgida (1986), when he introduced the paper about conceptual modeling of the information system. In this paper the author stated that the information system development can easily be done and used in the natural way by concentrating on the semantic of the application domain [14]. Unlike the author Borgida (1986), Bogumila, Zbigniew, Lech and Iwona (2016) have presented a method for development of domain models based on knowledge represented by domain ontology [15]. As seen in the last two articles, during the period 1986-2016 is dealt with semantic of application domain and development of domain models.

B. Designing the conceptual model

In designing the conceptual model, it is very important the source used for modeling. Based on the researches it is noticed that small number of articles related to the guides for documentation of the functional and non-functional requirements are published. This documentation is used as a

source for conceptual modeling. Despite the small number of the articles published, contribution to the requirements engineering is high. One of the relevant article is presented by Sommerville, I., & Sawyer, P. (1997), in which they presented a practical guide to the functional requirements documentation which contains what system should do and is applicable to any type of the information system [16]. Another guide for the functional requirements documentation was presented by authors Gorschek, T., & Wohlin, C. (2006), who presented the Requirements Abstraction Model (RAM) which enables prioritizing and packaging the requirements in the document before the development of the information system. This document contains what system should do but not how the system should do [17]. That the functional requirements document should contain what system should do, was also agreed by the authors Sommerville, I., & Sawyer, P. (2015). The authors in their article presented a guide for functional and non-functional requirements, where they divided these two types of requirements in two separated documents, one document for the functional requirements which contains what the system should do and the other document for the non-functional requirements [18].

The other important element in designing the conceptual model is the quality in the conceptual modeling, which based on this research is treated by different scholars. The authors Siau and Tan (2005) used the cognitive mapping techniques regarding the quality in the conceptual modeling [19]. While the authors Nelson, Poels, Genero, and Piattini (2012) regarding the quality in the conceptual modeling presented the Conceptual Modeling Quality Framework, when they brought together the framework of Lindland, Sindre, and Sølvsberg (LSS) and the one of the Wand and Weber based on Bunge's ontology (BWW) [20]. Unlike the above authors that presented techniques and frameworks, the following authors presented guides which should be considered in order to apply quality during the conceptual modeling. The authors Alencar, Marín, Giachetti, Pastor, Castro, and Pimentel (2009) proposed a guide to solve the gap between specifications of the requirements and the final software products by integrating the Goal-Oriented Requirements Engineering (GORE) and the Model Driven Development (MDD). This guide was proposed for the transformation of the initial requirements into automatically generated software [21]. Another helpful guide presented by authors Silva, Pinheiro, Albuquerque, and Barroso (2016), aims to help the analyst in identifying the functional and non-functional requirements in the contexts of the customer software. In their article, they emphasized that the elicitation of the functional and non-functional requirements is a hard task and time consuming [22]. Unlike the above authors, Andreas, J., & Frank, T. (2016) treated quality in conceptual modeling by presenting the highlights which are provided by conceptual models [23]. Based on his article the conceptual models provide blueprints for a reasonable, good design of the information system and underlying organizational settings. He also highlighted the IS` researchers assume that the application of conceptual model allows time and cost savings and increases the quality.

Moreover, the instrument for designing the conceptual model is very important in the conceptual modeling. Based on

the research conducted, a small number of articles which treated the instruments for designing the conceptual model is published. The author Wohed (2000) presented his article by introducing an instrument for the complex modern information system jointly with the requirements for shorter development time [24]. Also, the authors Lu and Parsons (2013) presented the instrument called a UML CASE tool for constructing of the UML diagrams which reflect the real world by using the well-defined ontological rules proposed by Evermann and Wand [25]. Another relevant article is presented by authors Ribeiro, Pereira, Rettberg, and Soares (2016), who treated the combination of the UML with the other instruments as SysML and MARTE in order to do modeling of the hardware and software requirements of real-time-systems. The UML and SysML are used for modeling of the functional requirements, while the MARTE is used for modeling of the non-functional requirements. This article also defines which type of requirements can be modeled by which instrument [26]. An instrument which differs from the above instruments due to the cloud computing technology used, is a novel, web-and-based, collaborative, and scalable (meta) modeling tool which supports designing of the domain specific modeling languages and creation of the corresponding domain models. This instrument was presented by authors Maróti, Kecskés, Kereskényi, Broll, Völgyesi, Jurác, and Lédeczi (2014) [27].

During the conducted literature review it is identified that most of the authors have treated more the impact of cloud computing at system analysis and design giving less importance to the instruments which are used to design conceptual model. The authors Soon and David (2010) presented their article about the impact of the cloud computing on system analysis and design, where they found no differences in the phase of analysis for creating a Cloud based solution, but in the design stage they highlighted the challenges to the database schema, queues, access control, workflow, service bus and query efficiency [28]. The impact of the cloud computing technology is also treated by authors Agarwal and Dhar (2014), who presented the critical issues in predictive modeling for big data and data science [29].

C. Requirements approval

The conceptual model is the representation of the information system. Therefore, it is necessary to be reviewed

and approved by all participants in the project team from the client side in order for the information system to be completed within time, scope, budget and quality. Based on literature review, is identified that most of the scholars' work was focused on the requirements determination during the session with participants from the client side, even though they have started to initiate the requirements validation but not requirements approval. One of the techniques presented by Bentley, L. D., & Jeffrey, L. (2007) mentioned requirements validation as optional during the session with participants from the client side. This technique is called Joint Requirements Planning (JRP) and it is for identification, analysis and definition of the requirements during the JRP session. It also includes JRP session planning and JRP session conducting. Benefits of using this technique are that actively involves users and management in the project development, decreases time for finding facts in planning and analysis phase, confirms requirements and approves prototypes if available, produces a formal written document which is published immediately following the JRP session in order to maintain the momentum of the JRP session [30].

The other technique for the requirements definition, but not for the requirements validation or approval, is presented by Dennis, A., Wixom, B. H., & Roth, R. M. (2012). This technique is called Joint Application Development (JAD) and allows project team, users and management to identify requirements for the information system. It specifies the way of selecting participants in JAD session, the location for the JAD session, the way how to design, prepare and conduct the JAD session and what will JAD post-session report consist of. This JAD technique is used in the analysis and design phase [31].

If is compared the layout of the session room of JRP and JAD technique, the room of the JRP session presents how the room is arranged and the way of the organization of the session by showing in which place is each participant positioned, while the room of the JAD meeting presents only how the room is arranged. Both techniques use "U" shape meeting room.

D. The summary table

In the following Table 1 is presented the summary of the state of the art section, where research for conceptual modeling and its concepts is conducted in the period of 1986 to 2016.

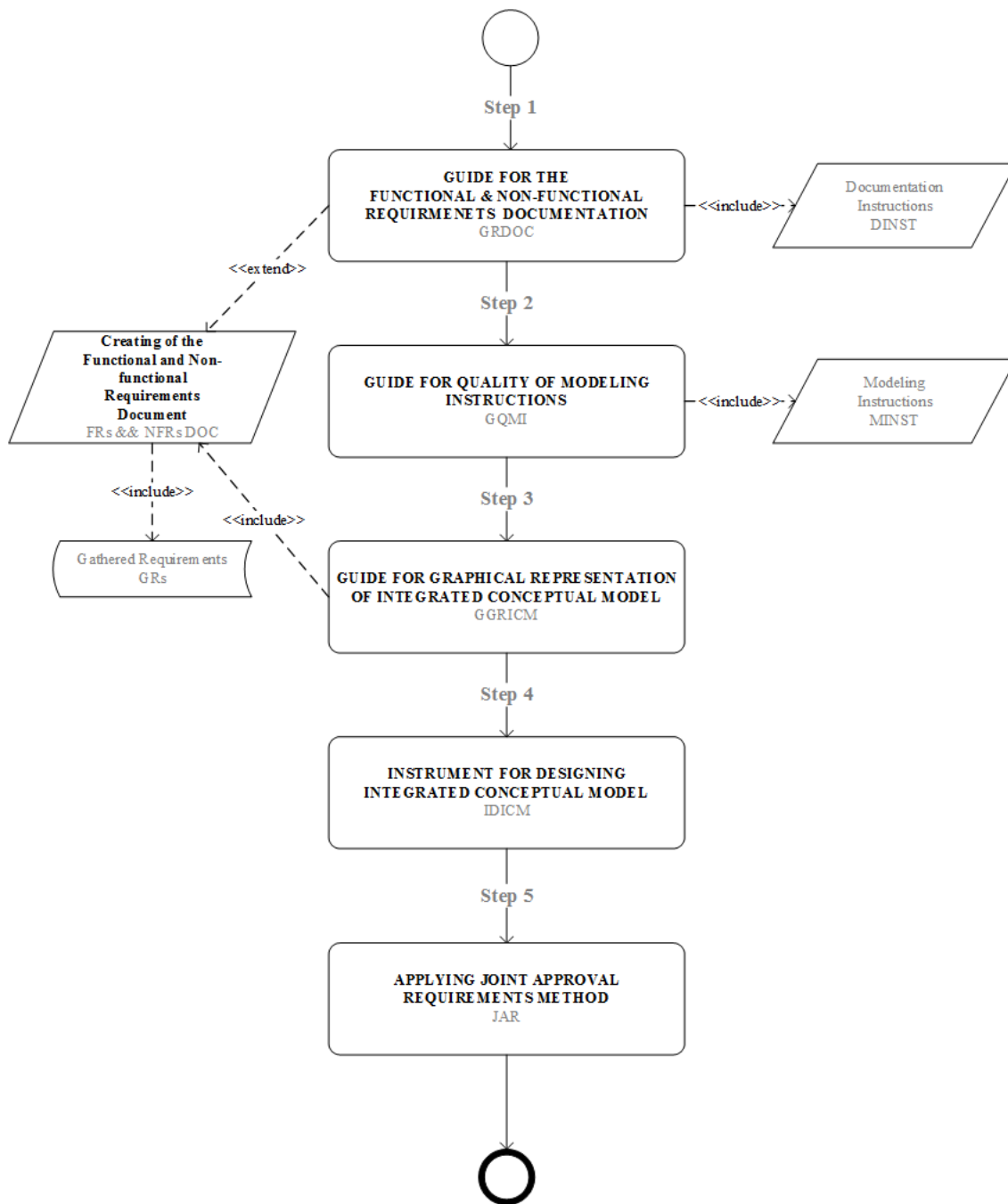


Fig. 1. The algorithm of the Integrated Framework for Conceptual Modeling (IFCMod)

In the Fig. 1, is presented the algorithm of the proposed integrated framework for conceptual modeling (IFCMod) which consists five steps, in the first step is proposed the guide for the functional and non-functional requirements documentation (GRDOC) which should be considered during creation of the requirements document (FRs & NFRs DOC) based on the documentation instructions (DINST) proposed in this guide and on the gathered requirements (GRs) from documents and texts, the analyst's impressions and reactions, observations, interviews and questionnaires, in the second step is proposed the guide for quality of modeling instructions

(GQMI) which shall be used to apply the quality in the integrated conceptual modeling by using the modeling instruction (MINST), in the third step is proposed the guide for graphical representation of integrated conceptual model (GGRICM) which shows the way of modeling based on proposed guide for quality of modeling instruction (GQMI) and the requirements document (FRs & NFRs DOC), in the fourth step is the proposed instrument for designing integrated conceptual model (IDICM), and in the fifth step is the method called Joint Approval Requirements (JAR) which is for review and approve the requirements by client in the JAR meetings.

Based on the Fig. 1, is proposed also the model of the integrated framework for conceptual modeling (IFCMod), which is shown in the Fig. 2.

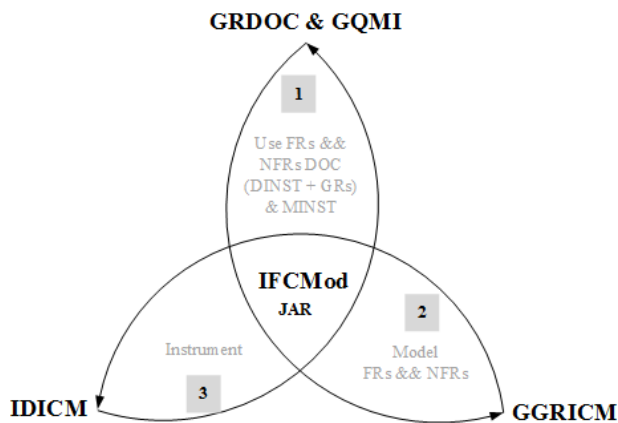


Fig. 2. Conceptual model of IFCMod

The research questions derived from the study about conceptual modeling are presented in the following. Is it possible to create the proposed integrated framework for conceptual modeling (IFCMod)? What will be the documentation instruction (DINST) in the proposed guide for the functional and non-functional requirements documentation (GRDOC) and what will be the impact of this guide in document creation for the functional and non-functional requirements (FRs & NFRs DOC)? Does have impacted the gathered requirements (GRs) in creating of the functional and non-functional requirements documentation (FRs & NFRs DOC)? What will be the modeling instruction (MINST) in the proposed guide for quality of modeling instructions (GQMI) and what will be the impact of this guide in the modeling of the integrated conceptual model? Does have impact those two type of guides (GRDOC & GQMI) in the guide for graphical representation of integrated conceptual model (GGRICM)? What will be the proposed instrument for designing integrated conceptual model (IDICM), will it be flexible to work on-premises and cloud computing technology? Is it possible to create the Joint Approval Requirements (JAR) method? Does have impact the proposed integrated framework for conceptual modeling (IFCMod) in the quality of the system requirements and information system?

V. THE CONCLUSIONS AND FUTURE WORK

Based on the identified research gaps through the literature review and work experience, the integrated framework for conceptual modeling (IFCMod) is proposed in this paper. This integrated framework consists of guide for the functional and non-functional requirements documentation (GRDOC), the guide for quality of modeling instructions (GQMI), the guide for graphical representation of integrated conceptual model (GGRICM), the proposed instrument for designing integrated conceptual model (IDICM) and the method called Joint Approval Requirements (JAR). Thus, in the near future, the intention is to continue working on this integrated framework for conceptual modeling (IFCMod) by answering the research questions related to.

REFERENCES

- [1] Robinson, S. (2012, December). Tutorial: Choosing what to model—Conceptual modeling for simulation. In Simulation Conference (WSC), Proceedings of the 2012 Winter (pp. 1-12). IEEE.
- [2] Bera, P., Krasnoperova, A., & Wand, Y. (2011). Using ontology languages for conceptual modeling. *Cross-Disciplinary Models and Applications of Database Management: Advancing Approaches: Advancing Approaches*, 1.
- [3] Braga, B. F., Almeida, J. P. A., Guizzardi, G., & Benevides, A. B. (2010). Transforming OntoUML into Alloy: towards conceptual model validation using a lightweight formal method. *Innovations in Systems and Software Engineering*, 6(1-2), 55-63.
- [4] Mehmood, K., Cherfi, S. S. S., & Comyn-Wattiau, I. (2010, September). CM-Quality: a pattern-based method and tool for conceptual modeling evaluation and improvement. In *Advances in Databases and Information Systems* (pp. 406-420). Springer Berlin Heidelberg.
- [5] Brinkkemper, S. (2016, March). Gamified Requirements Engineering: Model and Experimentation. In *Requirements Engineering: Foundation for Software Quality: 22nd International Working Conference, REFSQ 2016, Gothenburg, Sweden, March 14-17, 2016, Proceedings* (Vol. 9619, p. 171). Springer.
- [6] Wagner, D. N. (2016). Breakin'the Project Wave: Understanding and avoiding failure in project management.
- [7] Zubcoff, J. J., Garrigos, I., Casteleyn, S., Mazon, J. N., & Aguilar, J. A. (2016). Evaluating the use of Pareto Efficiency to Optimize Non-Functional Requirements Satisfaction in i* Modeling. *IEEE Latin America Transactions*, 14(1), 331-338.
- [8] Afreen, N., Khatoon, A., & Sadiq, M. (2016). A Taxonomy of Software's Non-functional Requirements. In *Proceedings of the Second International Conference on Computer and Communication Technologies* (pp. 47-53). Springer India.
- [9] Neto, P. A. S., Vargas-Solar, G., da Costa, U. S., & Musicante, M. A. (2016). Designing service-based applications in the presence of non-functional properties: A mapping study. *Information and Software Technology*, 69, 84-105.
- [10] Eckhardt, J., Vogelsang, A., & Fernández, D. M. (2016, May). Are non-functional requirements really non-functional: an investigation of non-functional requirements in practice. In *Proceedings of the 38th International Conference on Software Engineering* (pp. 832-842). ACM.
- [11] Fatwanto, A., & Boughton, C. (2008, December). Analysis, Specification and Modeling of Functional Requirements for Translative Model-Driven Development. In *Knowledge Acquisition and Modeling, 2008. KAM'08. International Symposium on* (pp. 859-863). IEEE.
- [12] Fatwanto, A., & Boughton, C. (2008, December). Analysis, Specification and Modeling of Non-Functional Requirements for Translative Model-Driven Development. In *Computational Intelligence and Security, 2008. CIS'08. International Conference on* (Vol. 2, pp. 405-410). IEEE.
- [13] Cysneiros, L. M., & Leite, J. C. S. D. P. (2004). Nonfunctional requirements: From elicitation to conceptual model. *Software Engineering, IEEE Transactions on*, 30(5), 328-350.
- [14] Borgida, A. (1986). Conceptual modeling of information systems. In *on Knowledge Base Management Systems* (pp. 461-469). Springer New York.
- [15] Bogumila, H., Zbigniew, H., Lech, T., & Iwona, D. (2016). Conceptual Modeling Using Knowledge of Domain Ontology. In *Intelligent Information and Database Systems* (pp. 554-564). Springer Berlin Heidelberg.
- [16] Sommerville, I., & Sawyer, P. (1997). *Requirements engineering: a good practice guide*. John Wiley & Sons, Inc.
- [17] Gorschek, T., & Wohlin, C. (2006). Requirements abstraction model. *Requirements Engineering*, 11(1), 79-101.
- [18] Sommerville, I., & Sawyer, P. (2015). *Requirements engineering* (10th Edition). Pearson.
- [19] Siau, K., & Tan, X. (2005). Improving the quality of conceptual modeling using cognitive mapping techniques. *Data & Knowledge Engineering*, 55(3), 343-365.

- [20] Nelson, H. J., Poels, G., Genero, M., & Piattini, M. (2012). A conceptual modeling quality framework. *Software Quality Journal*, 20(1), 201-228.
- [21] Alencar, F., Marín, B., Giachetti, G., Pastor, O., Castro, J., & Pimentel, J. H. (2009). From i* requirements models to conceptual model of a model driven development process. In *The Practice of Enterprise Modeling* (pp. 99-114). Springer Berlin Heidelberg.
- [22] Silva, A., Pinheiro, P., Albuquerque, A., & Barroso, J. (2016). A Process for Creating the Elicitation Guide of Non-functional Requirements. In *Software Engineering Perspectives and Application in Intelligent Systems* (pp. 293-302). Springer International Publishing.
- [23] Andreas, J., & Frank, T. (2016). Towards a document-driven approach for designing reference models: From a conceptual process model to its application. *Journal of Systems and Software*, 111, 254-269.
- [24] Wohed, P. (2000). Tool support for reuse of analysis patterns—a case study. In *Conceptual Modeling—ER 2000* (pp. 196-209). Springer Berlin Heidelberg.
- [25] Lu, S., & Parsons, J. (2013). Ontological Rules for UML-Based Conceptual Modeling: Design Considerations and Frameworks for Developing Efficient Information Systems: Models, Theory, and Practice: Models, Theory, and Practice, 177.
- [26] Ribeiro, F. G. C., Pereira, C. E., Rettberg, A., & Soares, M. S. (2016). Model-based requirements specification of real-time systems with UML, SysML and MARTE. *Software & Systems Modeling*, 1-19.
- [27] Maróti, M., Kecskés, T., Kereskényi, R., Broll, B., Völgyesi, P., Jurác, L., ... & Lédeczi, Á. (2014). Next Generation (Meta) Modeling: Web- and Cloud-based Collaborative Tool Infrastructure. In *MPM@ MoDELS* (pp. 41-60).
- [28] Chin Boo Soon; David C. W. (2010, May) "How Cloud Computing Changes Systems Analysis and Design" International Conference on Cloud Computing & Virtualization; (pp. 148)
- [29] Agarwal, R., & Dhar, V. (2014). Editorial—Big data, data science, and analytics: The opportunity and challenge for IS research. *Information Systems Research*, 25(3), 443-448.
- [30] Bentley, L. D., & Jeffrey, L. (2007). *System Analysis & Design Methods* (pp. 229-235).
- [31] Dennis, A., Wixom, B. H., & Roth, R. M. (2012). *Systems analysis and design*. John Wiley & Sons (pp. 119-143).

Low Complexity for Scalable Video Coding Extension of H.264 based on the Complexity of Video

Mayada Khairy

Dept. of Computers and Systems,
Electronics Research ERI
Giza, Egypt

Amr Elsayed

Dept. Telecomm. and Electronics
Faculty of Engineering, Helwan, Univ.
Cairo, Egypt

Alaa Hamdy

Dept. Telecomm. and Electronics
Faculty of Engineering, Helwan, Univ.
Cairo, Egypt

Hesham Farouk Ali

Dept. of Computers and Systems,
Electronics Research ERI
Giza, Egypt

Abstract—Scalable Video Coding (SVC) / H.264 is one type of video compression techniques. Which provided more reality in dealing with video compression to provide an efficient video coding based on H.264/AVC. This ensures higher performance through high compression ratio. SVC/H.264 is a complexity technique whereas the takes considerable time for computation the best mode of macroblock and motion estimation through using the exhaustive search techniques. This work reducing the processing time through matching between the complexity of the video and the method of selection macroblock and motion estimation. The goal of this approach is reducing the encoding time and improving the quality of video stream the efficiency of the proposed approach makes it suitable for are many applications as video conference application and security application.

Keywords—Scalable video coding; motion estimation; SVC layers; quality scalability

I. INTRODUCTION

Scalable video coding (SVC) has been standardised to extend the capabilities of the H.264 advanced video coding (AVC) [1]. Whereas the objective of SVC is to enable the generation of the one-bit stream. In other words, it allows decoding partial streams depending on the specific rate, quality and resolution required by certain applications [2-3].

The SVC consists of a base layer (BL) and one or more enhancement layer (EL). The BL represents the main information of the video and should be transmitted with very high reliability [4]. On the other hand, the EL sent part of a bit stream according to the destination required [5]. SVC supports spatial, temporal and quality [6]. To encoded video using the SVC, divide frames to macroblocks (MBs). To encode this macroblock using two modes; first: intra-mode, which coded MB referring to the data in the same frame. The intra mode is utilised two types of MB there are (4×4 and 16×16) modes [7].

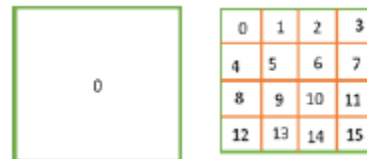


Fig. 1. Macroblock modes for intra prediction

Another one: Inter - mode; the MB coded referring data in the previously coded frames there are nine candidate mode of inter-modes (skip, 16×16, 16×8, 8×16, 8×8, 8×4, 4×8, and 4×4), Figure. 2 illustrates all the candidate inter-modes of H.264/SVC [8-9]. The process of the select best motion vector is called motion estimation as will be described in the next subsection.

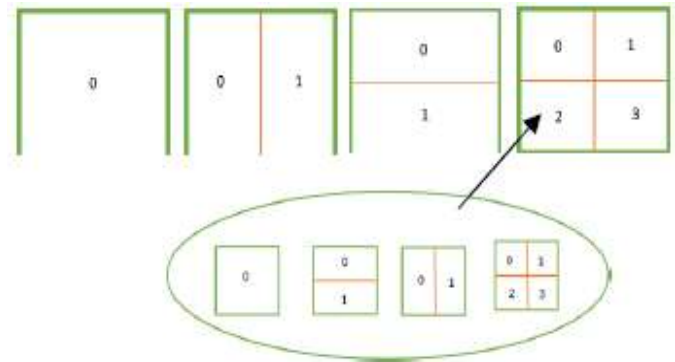


Fig. 2. Macroblock and sub-macroblock modes for inter prediction

A. Motion estimation in SVC

Motion estimation is one of the key elements of SVC technique. It is used to get benefit from the redundancy between frames in a video sequence, to investigate the high video compress rate of data.

The motion between frames estimates the prediction for the next frame. Once a motion estimate has been made, the algorithm only transmits the difference between two frames, which is contained in the motion information and the estimation error. The efficiency of the compression depends on the quality of motion estimation [10].

In this technique the picture is divided into two parts; the motion vectors which estimate the motion in the image, and the residual, which is the error between the current frame and its estimate [11]. There are two broad categories of motion compensation is block-based motion compensation and pixel-recursive motion compensation [12].

The Block Matching Algorithms (BMA) is a preferable method with SVC more computationally realistic than other methods [13-14]. The BMA frames are divided into non-overlapping blocks as discussed in the previous section, and each block is compared with its counterpart in the previous frame[15-16]. To find an area that is similar. The same area in the reference frame is known as the best match.

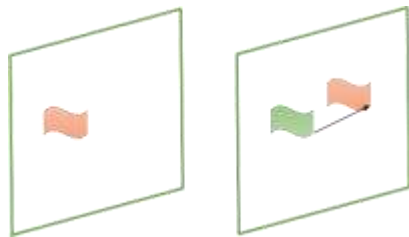


Fig. 3. Block matching algorithm

The relative difference in locations is the MV [17-19]. As illustrates in fig.3 the most common approach for block matching in ME is three steps search algorithm. It executes at three cascaded steps: first, is full-pixel ME here the ME start find the best match by the integer-pixel motion which performed for each square block of the frame to be encoded to the fine displacement vector(s) within a search range. To decide The best match, the Lagrangian cost function is used as follows [20]:

$$J = D + \lambda R \quad (1)$$

Where λ is a Lagrangian multiplier, D is an error measure between the candidate MB taken from the reference frame(s) and the current MB, R stands for the number of bits required to encode the difference between the motion vector(s) and its prediction from the neighboring MBs (differential coding). The second step is half-pixel ME after the integer-pixel motion search finds the best match, the values at half-pixel positions around the best match are interpolate. At the last, the values of the quarter-pixel positions are generated by averaging pixels at integer and half-pixel positions. Figure 4 illustrates the interpolated fractional pixel positions. Upper-case letters indicate pixels on the full pixel grid, while numeric pixels indicate pixels at half-pixel positions and lowercase letters indicate pixels in between at quarter-pixel positions [21-22].

The SVC has many different MB modes, although the significantly improve the RD performance.

Several fast algorithms proceed to reduce the implementation complexity [23-25] most of them share the

same concept of using the correlation between macroblocks and it's neighbouring in different layers and also that MB in the bland its corresponding position in the EL. But these algorithms have a limitation when applied to the fast video sequence or with complexity background [26].

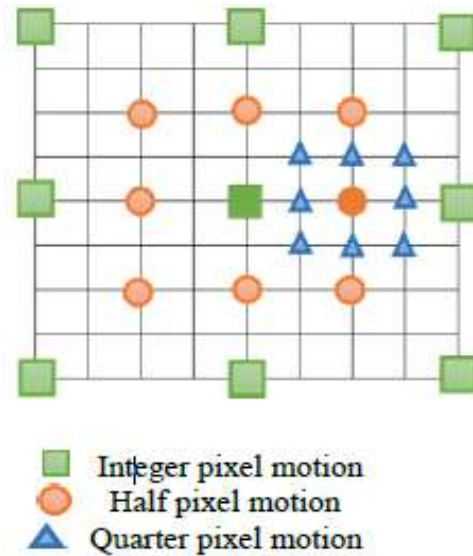


Fig. 4. Fractional pixel search positions

This paper focuses on decreasing the complexity of SVC encoding processing through reducing the time spent on the selection of both the mode of MB and motion estimation.

The proposed approach differs from the previous method in aspects: it linking the value of the difference between video sequences with the concept of correlation between MB in frames. To decide if we can utilise this concept or not and who it can be used to select the macroblocks mode and motion estimation. To solve the shortage of the previously proposed algorithms as will be discussed in the next section.

II. THE PROPOSED APPROACH

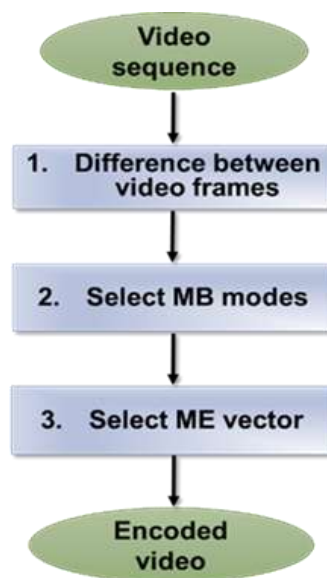


Fig. 5. The stages of proposed approach

This paper proposed a new approach to reducing encoding time for SVC. Through the minimizing time of; motion estimation (ME) and selection of macroblocks mode.

The proposed approach constants of three stages; first: Measuring the difference between video sequence test frames, second: select macroblocks modes and last stage: choose the method of motion estimation to calculate the motion vector. As outlined in fig. 5. Each of them will be discussed in details in the next subsections.

A. The first stage

The first stage in the proposed method as mention before is determination the difference between in the video sequence. This difference refers to the complexity and the motions of the video sequence.

There are many methods can detect the difference between frames. This work utilised sum of absolute differences (SAD) is used to determine the difference between frames. Seeing that the SAD has a higher quality precision and involves lower computational cost as. The SAD represent by the following equation:

$$SAD_n(P, Q) = \sum_{ij} |P_{ij} - Q_{ij}| \quad (2)$$

Where P_{ij} is a pixel of the current frame, and Q_{ij} is the corresponding pixel next frame. After calculating SAD between every cascaded frame in a video sequence, determine the average (η) of SAD at the percentage of the difference between the frames according to the certain threshold as follow:

$$\eta = \frac{1}{n} * \sum_{i=1}^n SAD_i \quad (3)$$

if $\eta > th1$ then the difference is high.
else if $th1 > \eta > th2$ then the difference is medium.
else $\eta < th2$ then the difference is low

B. The second stage

Select the MB mode –outlined in figure 6- depends on the value of η which calculated in the first stage as following:

For $\eta > th1$: meaning there is significant change between frames hence the selected MB mode should achieve high efficient. Hence, we cannot depend on the concept of correlation between macroblocks in different frames. In this case, the proposed approach reduce the complexity depends on two factors; out some of the modes from the competition from the start, and using the correlation equation to detriment the best MB instead of Lagrangian cost function.

The two concept applied as follows: According the smaller MB modes give highest Coding efficient, so the inter 16*16 and intra 16*16 modes should be out from the competition.

- If the frame should be encoded is I frame selected intra 4*4 mode to encode it.
- Else if the frame is p frame test all candidate modes accept 16*16 inter mode.

The proposed approach select The MB modes, which give the best correlation between the current MB and candidate modes of MB using the following equation of correlation:

$$\text{Correlation} = \frac{\sum_{mn} (W_{mn} - W') (F_{mn} - F')}{\sqrt{(\sum_m \sum_n (W_{mn} - W')^2)} \sqrt{(\sum_m \sum_n (F_{mn} - F')^2)}} \quad (4)$$

Where W, F are two MB, W' , F' are the average (μ) value of W, F

$$W' = \mu(w) = \frac{1}{K} \sum_{i=1}^n W_i \quad (5)$$

$$F' = \mu(F) = \frac{1}{K} \sum_{i=1}^n F_i \quad (6)$$

Where K is the total number of elements in the matrix and W_i are a number of elements in column.

For $th2 > \eta < th1$: Here there are medium changes between frames. The processes of select MB for frames in EL can be built on the tradeoff between the finer mode of corresponding MB in the BL and the mode of the previous encoded MB at the same frame.

For $\eta < th2$: Which meaning there is small change between frames. So, the MB mode depends on the tradeoff between the finer mode of the corresponding MB in the BL and the same mode of the previously encoded frame.

C. The third stage:

As discussed in Sec 1.1 the search of best motion vector execute at cascade three levels; full-pixel, half-pixel fraction and quarter pixel fraction

Which meaning the meager of encoding time consume in the motion estimation.

Our proposed approach reducing the time of motion estimation depends on the two previous stage discussed in sec.2.1 and sec.2.3, as following:

For $\eta > th1$: applied the smaller pixel fraction of the corresponding MB in the BL

For $h2 > \eta < th1$: The ME depends on which mode of the macroblock selected -as discussed in Sec. 2.2 as follows:

If the mode of macroblock selected depends on the corresponding MB in EL. Hence, select of motion estimation method depends on the same method of Pixel and half-pixel for ME in selected mode of MB in EL layer

For $h2 > \eta < th1$: The ME depends on which mode of the macroblock selected -as discussed 2.2 as follows:

If the mode of macroblock selected depends on the corresponding MB in EL. Hence, select of motion estimation method depends on

The tradeoff between the current pixel fraction and the smaller one meaning:

- If the ME method is full-pixel; then using tradeoff between full- Pixel and half-pixel for ME in selected mode of MB in EL layer

else If the ME in selected MB is half -pixel than using tradeoff between the half-pixel and quarter-pixel for ME in selected mode of MB in the enhancement layer

- Else selected using the using quarter pixel.

For $\eta < th2$: meaning there is no significant change from frames to cascade so using the same

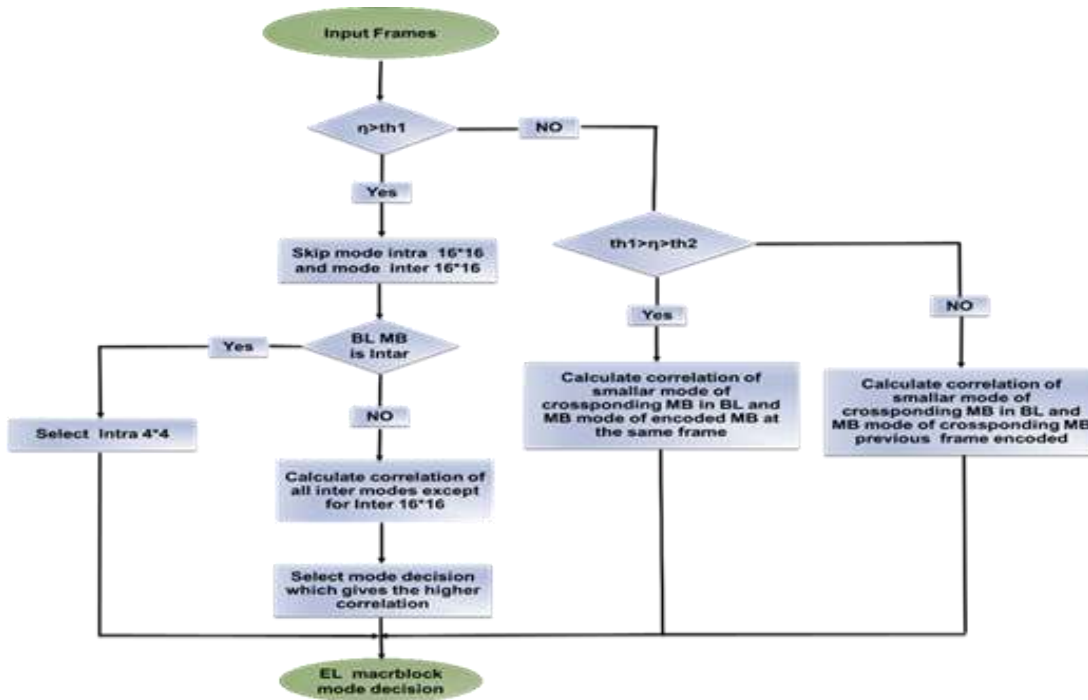


Fig. 6. Select MB mode

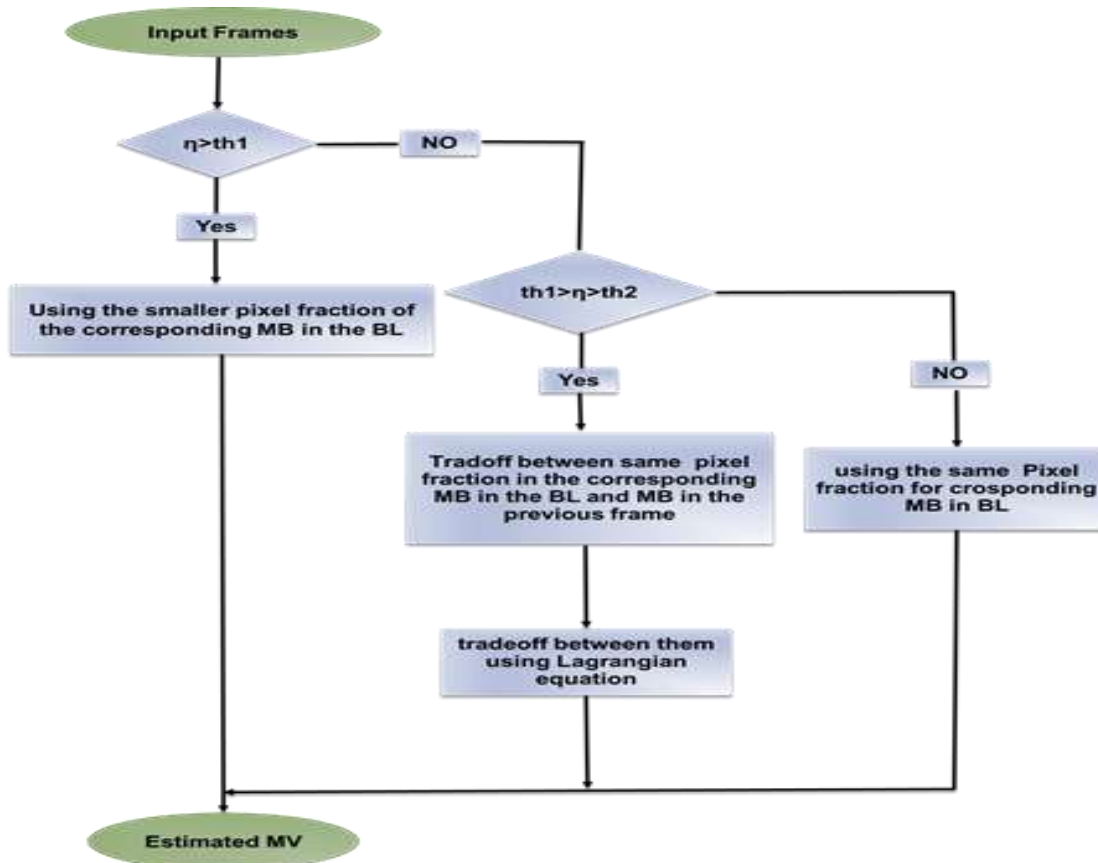


Fig. 7. Select MV

III. RESULTS AND EXPERIMENT

The proposed algorithm was implemented and evaluated using the “JSVM 9.18” software and Lu and Martin’s method [27]. Six standard video test sequences Bus, City, Crew, Football, Foreman, Harbour.

Table 1 shows the experiment conditions. Were selected based on the commonly used values in similar research work

TABLE I. EXPERIMENTAL CONDITIONS

	BL	EL
Quantization parameters	30	25
Resolution	QCI	QCIF
	F	
GOP		16
MV Search range		32
Number of frames		150
Frame per second		30

The metrics used for evaluation The video test are time saving (TS), (ΔT), the number of sending bits (ΔN), and degradation of peak signal-to-noise ratio (Y-PSNR) representing as following equation:

$$\Delta TS = \frac{TS(\text{proposed}) - TS(\text{reference})}{TS(\text{reference})} * 100 \quad (7)$$

$$R = \frac{BR(\text{proposed}) - BR(\text{reference})}{BR(\text{reference})} * 100 \quad (8)$$

$$Y - PSNR = PSNR(\text{proposed}) - PSNR(\text{reference}) \quad (9)$$

All the results were expressed as percentages about reference software. The experimental results of the proposed approach were variously compared with those of the JSVM reference software, and with Lu and Martin’s method.

The results demonstrate that the proposed approach achieved significant saving in time and improvement video quality with neglecting increasing in BR comparing with JSVM reference software, and with Lu and Martin’s method. From the results in table 2 posted the following:

First for the time-saving parameter: Overall the proposed approach achieve good enhancement in decreasing the encoding time for all video sequence test especially with video represent the low complexity video as Foreman.

Second for the quality parameter: improvement the quality comparing with the Lu and Martin’s method, however, there is small degradation in the quality relative to the original software JSVC 9.81.

The last for the Bit Rate: there are negligible increasing in BR comparing with JSVM reference software, and with Lu and Martin’s method.

IV. CONCLUSION

This paper proposes an effective and efficient video compression approach that is suitable for multi user required the video with different quality. This approach is summarised as follows. Firstly, this measure difference between video sequence frames, second depends on the output from the first step to select macroblocks modes, last minimising the search method to choose the motion vector depending on the complexity and motion for video.

The efficiency of our approach compares it with reference software JSVC and another similar approach. It is shown that our approach has a high saving time up to (85.9 %) with improving quality and smaller decreasing in bit rate

TABLE II. RESULTS OF THE PROPOSED APPROACH

Video Sequence Test	Proposed algorithm Vs. JSVM 9.18			Proposed algorithm Vs. Lu and Martin’s		
	ΔTS	$\Delta PSNR$	ΔBR	ΔTS	$\Delta PSNR$	ΔBR
Bus	70.45%	-0.05	1.81	8.20%	0.07	0.3
City	85.93%	-0.02	2.00	18.09%	0.02	0.24
Crew	72.18%	-0.01	2.01	11.6%	0.02	0.05
Football	61.07%	-0.03	1.41	3.28%	0.02	0.49
Foreman	81.47%	-0.08	1.94	18.47%	0.66	0.08
Harbour	75.77%	-0.04	1.01	7.58%	0.12	0.29

ACKNOWLEDGMENT

The authors greatly appreciate the support of Engr. Gamel Saleh, Chairman of Systems Design Company.

REFERENCE

- [1] T. Wiegand, L. Noblet, and F. Rovati, "Scalable video coding for IPTV services," *IEEE Transactions on Broadcasting*, vol. 55, no. 2, pp. 527–538, 2009.
- [2] C. Bouras, S. Charalambides, K. Stamos, S. Stroumpis, and G. Zaoudis, "Power management for SVC video over wireless networks," in *Broadband and Wireless Computing, Communication and Applications (BWCCA)*, 2011 International Conference on, 2011, pp. 270–276.
- [3] W.-H. Peng et al., "Rate-distortion optimised SVC bitstream extraction for heterogeneous devices: A preliminary investigation," in *Multimedia Workshops, 2007. ISMW'07. Ninth IEEE International Symposium on*, 2007, pp. 407–412.
- [4] M. M. Hassan and U. Farooq, "Adaptive and ubiquitous video streaming over Wireless Mesh Networks," *Journal of King Saud University-Computer and Information Sciences*, 2016.
- [5] T. Schierl, C. Hellge, S. Mirta, K. Gruneberg, and T. Wiegand, "Using H. 264/AVC-based scalable video coding (SVC) for real time streaming in wireless IP networks," *IEEE International Symposium on Circuits and Systems*, pp. 3455–3458, 2007.
- [6] T. Varisetty and P. Edara, "Systematic Overview of Savings versus Quality for H. 264/SVC," 2012.
- [7] R. Ruolin, H. Ruimin, and C. Hao, "An adaptive selection algorithm of macroblock coding candidate modes," in *Computer Science and Education (ICCSE)*, 2010 5th International Conference on, 2010, pp. 1499–1502.
- [8] A. Kessentini, A. Samet, M. A. B. Ayed, and N. Masmoudi, "Performance analysis of inter-layer prediction module for H. 264/SVC," *AEU-International Journal of Electronics and Communications*, vol. 69, no. 1, pp. 344–350, 2015.
- [9] X. Li, P. Amon, A. Hutter, and A. Kaup, "Performance analysis of inter-layer prediction in scalable video coding extension of H. 264/AVC," *IEEE Transactions on broadcasting*, vol. 57, no. 1, pp. 66–74, 2011.
- [10] M. Usha, "Motion detection in compressed video using macroblock classification," *Advanced Computing*, vol. 5, no. 2/3, p. 1, 2014.
- [11] J. Ratnottar, R. Joshi, and M. Shrivastav, "Comparative study of motion estimation & motion compensation for video compression," *International Journal of Emerging Trends & Technology in Computer Science (IJETTCS)* Vol. 1, 2012.
- [12] S. Mattoccia, F. Tombari, L. Di Stefano, and M. Pignoloni, "Efficient and optimal block matching for motion estimation," in *Image Analysis and Processing, 2007. ICIAP 2007. 14th International Conference on*, 2007, pp. 705–710.
- [13] C. Kas and H. Nicolas, "H. 264/SVC scene motion analysis," in *2009 IEEE International Conference on Acoustics, Speech and Signal Processing*, 2009, pp. 957–960.
- [14] S. Kamp, D. Heyden, and J.-R. Ohm, "Inter-temporal vector prediction for motion estimation in scalable video coding," in *Intelligent Signal Processing and Communication Systems, 2007. ISPACS 2007. International Symposium on*, 2007, pp. 586–589.
- [15] S. Mattoccia, F. Tombari, L. Di Stefano, and M. Pignoloni, "Efficient and optimal block matching for motion estimation," in *Image Analysis and Processing, 2007. ICIAP 2007. 14th International Conference on*, 2007, pp. 705–710.
- [16] X. Lu and G. R. Martin, "Fast H. 264/SVC inter-frame and inter-layer mode decisions based on motion activity," *Electronics letters*, vol. 48, no. 2, pp. 84–86, 2012.
- [17] L. Kulkarni, T. M. Manu, and B. S. Anami, "A Two-Step Methodology for Minimization of Computational Overhead on Full Search Block Motion Estimation," *International Journal of u-and e-Service, Science and Technology*, vol. 7, no. 4, pp. 339–348, 2014.
- [18] X. Yi and N. Ling, "Scalable complexity-distortion model for fast motion estimation," in *Visual Communications and Image Processing*, p. 59603Y–59603Y, 2005.
- [19] E. Cuevas, D. Zaldívar, M. Pérez-Cisneros, and D. Oliva, "Block-matching algorithm based on differential evolution for motion estimation," *Engineering Applications of Artificial Intelligence*, vol. 26, no. 1, pp. 488–498, 2013.
- [20] K. R. Rao, D. N. Kim, and J. J. Hwang, "Video coding standards," *The Netherlands: Springer*, 2014.
- [21] A. Luthra and P. N. Topiwala, "Overview of the H. 264/AVC video coding standard," in *Optical Science and Technology, SPIE's 48th Annual Meeting*, pp. 417–431, 2003.
- [22] T. Wedi and H. G. Musmann, "Motion-and aliasing-compensated prediction for hybrid video coding," *IEEE transactions on circuits and systems for video technology*, vol. 13, no. 7, pp. 577–586, 2003.
- [23] H. Li, Z. G. Li, and C. Wen, "Fast mode decision algorithm for inter-frame coding in fully scalable video coding," *IEEE Transactions on Circuits and Systems for Video Technology*, vol. 16, no. 7, pp. 889–895, 2006.
- [24] J. Ren and N. Kehtarnavaz, "Fast adaptive early termination for mode selection in H.264 scalable video coding," in *2008 15th IEEE International Conference on Image Processing*, pp. 2464–2467, 2008.
- [25] G. Goh, J. Kang, M. Cho, and K. Chung, "Fast mode decision for scalable video coding based on neighboring macroblock analysis," in *Proceedings of the 2009 ACM symposium on Applied Computing*, pp. 1845–1846, 2009.
- [26] A. Abdelazim, S. Mein, M. Varley, and D. Ait-Boudaoud, "Low complexity hierarchical prediction algorithm for H. 264/SVC," in *Image and Video Technology (PSIVT)*, 2010 Fourth Pacific-Rim Symposium on, pp. 252–257, 2010.
- [27] X. Lu and G. R. Martin, "Fast mode decision algorithm for the H. 264/AVC scalable video coding extension," *IEEE Transactions on Circuits and Systems for Video Technology*, vol. 23, no. 5, pp. 846–855, 2013.

An M-Learning Framework in the Podcast Form (MPF) using Context-Aware Technology

*Mohamed A. Amasha

Department of Computer Preparing Teacher
Dumyat University
Dumyat, Egypt

Elsaeed E. Abdelrazek

Department of Computer Preparing Teacher
Dumyat University
Dumyat, Egypt

Abstract—Mobile computing is rapidly transforming the world in which we live, with the advent of iPhones, iPads, tablet computers, and Android smartphones. M-learning in the podcast form (MPF) is a recent development for conveying course content to students in higher education. Context-aware technologies use temporal and environmental information to determine context. This study presents a theoretical framework for using context awareness, M-learning in the podcast form to investigate the effectiveness of using MPF engagement with context-aware technology in Teaching and Learning a multimedia course. The framework is based on two principal dimensions (MPF and context-aware technology), and it contributes to support researchers in e-learning and ubiquitous learning. The study was conducted on students (n = 42) enrolled in a multimedia course (IS 450) at Qassim University. After finishing the course, they completed an online survey to give their feedback on the effectiveness of using MPF with context-aware technology. The results indicate that learners had a positive attitude towards using MPF with context aware technology, and that they considered it a great way to develop their knowledge and receive course information. This study demonstrates the ability of context-aware technology to enhance the behaviour of learners by using m-learning in the podcast form.

Keywords—M-Learning; Context Aware; E-Learning; RSS; Podcast

I. INTRODUCTION

Mobile learning (m-learning) is defined as the use of smart phones in education and training, and it allows students to access educational content through mobile devices [9]. It also permits students to follow training activities, helps in publishing the communication content, and makes communication tools like discussion boards, forums, and social media available to the learner. M-learning has become the new version of E-learning [12].

U-learning is a combination of both M-learning and E-learning. It is a new model based on context-aware technology, and it allows autonomous learning at any time and any place using mobile devices, radio frequency identification (RFID), and sensor technologies. M-learning depends on podcasting to disseminate educational content from the instructor to the students, who receive it through podcatchers on their computing devices (PADs, iPhone, android, laptop, and pc). In order for the learner to complete the learning process properly, the environment surrounding them (place, time, location, and status) should be defined. The following questions should be answered using this strategy: “Who is the

learner? Where is the learner? When is he/she now? What is he/she doing? Why is he/she doing so? What are the surrounding environmental characteristics? Where is the learner’s location? Context-aware technology can answer these questions.

MPF describes any information that characterizes a situation that involves the interaction between learners, content of the course, and the real world. Previous studies mainly focused on using podcasting as a teaching tool and its impact on the learning process, without any consideration of the status and surroundings of learners. This study will focus on these aspects, especially since there is insufficient research on using MPF with context-aware technology in the field of e-learning. Therefore, the current study presents a framework of using context-aware technology in M-learning in the podcast form (MPF) and scope to investigate the effectiveness of using MPF engagement with context-aware technology in teaching and learning multimedia courses. We hope this study can achieve an improvement in pedagogical effectiveness, and reveal the educational value in e-learning courses that depend on a podcast form.

II. LITERATURE REVIEW

M-learning is the second revolution of e-learning, arriving with the great spate of mobile devices and wireless technologies. To support and develop the learning experience, it uses mobile computing technologies that can be mixed together to involve and motivate learners anywhere, at any time [21]. The employment of mobile devices such as cell phones, smartphones, netbooks, and tablet PCs enables learners to deliver e-content to their own locations, in any environment suitable for learning [14]. Context awareness techniques help students have their academic content regardless of the time or place of the learner, and to relate their learning activities to the real world. [5][6]. “Context awareness technology” in M-learning is a situation in which the student is involved in a reality, while using mobile devices to support his or her learning [7]. Radio-frequency identification (RFID) can also be used to facilitate the context-aware mechanism and enhance ubiquitous and mobile learning [12][15].

Mobile computing is rapidly transforming the world in which we live, with the advent of iPhones, iPads, tablet computers, and Android smartphones [19] [16][13]. Nowadays, M-learning uses podcast technology, which appeared in 2004 with the emergence of the second generation of web (web 2.0), to transform content for the learners. A

podcast is defined as an MP3 or MP4 media file that has been uploaded onto a website, and can thus be transmitted directly to the audience via their smart devices, or through social media, using RSS.

The appearance of podcasts has revolutionized the way of dealing with multimedia, and also introduced an innovative method for learning and teaching. Additionally, research has proven the efficiency of using iPod devices in transmitting content. Lately, the use of podcasts has widely increased, coinciding with the revolution and reevaluation of smart devices. Transmitting educational content started with smartphones (instead of iPhones) using podcasters, in a process known as m-learning or u-learning. Whatever the name used for this kind of learning, it is clear that communication between teacher and learner can now be facilitated through smart devices, with the content rendered into a podcast format.[1]

Using this method in the learning process has many advantages, such as:

- The flexibility in being able to listen to the content anywhere.
- The ability to listen to the content many times.
- Clarifying ambiguous points.
- It could be a substitution for going to campus.
- It can be used for exam revision.

However, as with anything else, this technology may have some shortcomings, such as the inability to identify the learner or make a link between the real world and the virtual world. Additionally, the teacher cannot identify the special content for the individual learner (place – time – status). In this research, we strive to develop a framework for using devices for MPF, and to link it with the individual context for the learner. Moreover, in order to link the real and virtual environments, we will clarify how this kind of learning enables communication between learners and teachers in a virtual environment and recognizes the individual context for each learner.

III. THEORETICAL FRAMEWORK

This study suggests a model to develop context-aware programs in M-Learning applications, which are provided in podcast form (MPF). We provide a framework that supports the application developer in the following key ways:

- It provides a communication method between the teacher and the learner, as well as dispensing the educational content through mobile devices.
- It provides a methodological framework for using context technology in MPF.
- It provides an interaction mechanism between the sensors devices, the objects, the learner, and the content provider.
- It provides an easy mechanism to use programming and programming tools in MPF design.

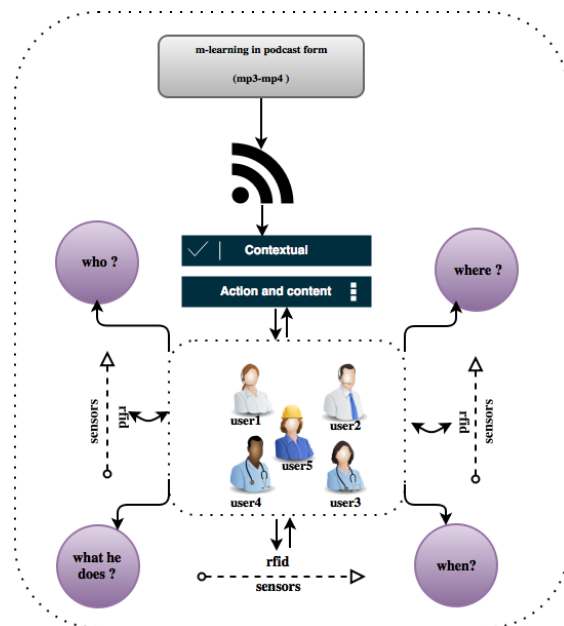


Fig. 1. Using context awareness in podcast form

In this section, we present an m-learning framework based on context-aware technology. It consists of two sections: m-learning in the podcast form and context-aware categories.

A. M-learning in the podcast form (MPF)

A podcast is an MP3 or MP4 (audio or video) file that is uploaded to a webhosting server and then automatically broadcast to the users' devices, enabling the user to listen to file directly or download it to listen later [10][3]. The applications of educational m-learning are based on broadcasting lessons to students' devices as a podcast. The following steps show how a podcast is created and delivered to the learners. [20]

a) Record sound (MP3) and video (MP4)

An MP3 output file can be created using all types of sound-recording software. For the purposes of this study, a free, open-source program called Audacity was used for recording the educational content. Audacity is widely available for download from the internet, and it is compatible with most operating systems (OS). It needs to be installed and configured to capture the input at the right settings, since the wrong settings can produce a variety of negative results such as poor sound quality.

Using Audacity as an example, we will provide a walk-through of software settings. First of all, we set Sample rate to 44,100 Hz and Sample format to a 32-bit float. Next, we need to adjust the settings for the format to which the file will be exported, which should be the MP3 format. We should also pay attention to the bit rate for the exported file, which should be the same as the bit rate used for recording the original audio file. [17]

Similarly, to create an MP4 file we can use any video capture software, such as SnagIt, which enables the user to create AVI (Audio Video Interleave) files. We first record the lesson, using print screen key, save it as AVI, and then upload

the file on www.archive.org(hosting). The AVI file will be automatically converted to MP4 as it uploads to the archive. We use the upload link on the archive homepage use the upload link to upload the file, copy the URL of the MP4 page that is created, and paste it on the desired web page or blog.

b) Hosting podcast

There are three methods to hosting the episodes on server. A private server can be set up using server software. A number of websites produce web server software, but one of the most popular is Apache, which can be found at www.apache.org. To connect the server to a network, an unchanging static Internet Protocol (IP) address is needed, to allow users to find the server online. The Second method is to share the server, and this can be done through creating an account on blogsites like Blogger or WordPress. These blog sites use a database, which can be used for uploading the podcast episode. The third and final method is by using host services, which are specialized services configured to host the episode. With these services, we only need to upload the file and update the podcast blog. The podcast will have a name that includes the service domain, like this one for our podcast on LibSyn: “fir.libsyn.com.” If having a unique URL is important to podcasters, they can get a dedicated domain and redirect it to the actual location of the file. Host services like LibSyn (Liberated Syndication) at <http://www.libsyn.com> and Switchpod at www.switchpod.com host podcasts and provide RSS feed for each episodes. Since the second method is the easiest, we chose to use it in this study.

The next step is creating a web page or a blog to upload episodes from the hosting site, with a dedicated page named “podcast” that is linked to the MP3 or MP4 files, and containing information on how to subscribe. A weblog or blog is a website created using template with html code linked to a database. In weblog setting, changing “Enable Title Links and Enclosure Links” from “No” to “Yes” allows the blog to provide subscriptions to the hosted files. For each episode, a new post is created, the file URL is inputted into the “Enclosure Links,” and an RSS is obtained from FeedBurner or the blog setting. From blog overview, “add a gadget” is selected and the RSS feed is inputted. The RSS feed is then shared with learners, who use it with dedicated RSS readers like iTunes.

c) Really simple syndication (RSS)

To distribute and publish podcast episodes, an RSS feed is needed. It can be obtained using special software or any web RSS generator like FeedBurner, or by using their XML code. Feed readers should be able to identify the generated feed as an RSS feed. These include:

- Feed for all: Runs on Windows operating systems. Available at www.feedforall.net.
- Feed editor: Runs on MAC operating systems. Available at www.extralabs.net.
- RSS editor: Runs on Windows operating systems. Available at www.rss-info.com.
- Feedy: An online tool. Available at <http://feedity.com/>.

- Feedburner: An online tool from Google provides RSS feeds for blogs like WordPress, Bloggers and Tumblr. Available at <http://www.feedburner.com/>.

The widely used hosting site www.archive.org was used for this study. It enables users to upload MP3 files, MP4 files, and document files. It helps convert AVI files to MP4, it saves files to a database for as long as possible, and it enables users export URLs of uploaded files to any webpage or blog.

d) Publishing podcasts

Publishing a podcast means delivering it to listeners as it is uploaded on the website or hosting site. The episode can be delivered in three ways: smartphones, personal computers, or SNSs (social network services). An RSS reader such as Coolsteache feed reader, iTunes, and RSS graffiti (for SNS) must be used. RSS reader applications can be uploaded from the Google Play Store or the Apple Store, and RSS graffiti can also be used through SNS as Facebook or twitter. Figure 2 shows how the episode is delivered to the learners.



Fig. 2. How the episode is delivered to the learners

IV. CONTEXT-AWARE CATEGORIES

“Context” can be defined as the information used to describe the situation of an entity. An entity is any relevant person, place, or object that can be related to the interaction between a user and an application. It can also include the user and the applications themselves [8]. Generally, context-aware technology provides information (location, social, time, physical context) about the learners to allow the teacher to continuously communicate with them. It enables the student to describe educational situations, communicate with the teacher, and to respond to class questions and discussions. Although there are many definitions of “context-awareness,” its relationship to education is less defined. It can be described as a technique to help communication between the teacher and the learner in the learning environment, in order to create e-learning-specific instruction to connect real world learning and reality environment. When content is sent to learners, the context-awareness detects their location and enables the instructor to be aware of the large amount of information surrounding them. It guides us through the information surrounding the students and adapts to their environment. [11][22]

A. User Context

a) User Profile

User profiles are important for determining the context of the learner for MPF. The instructor must identify the personality and identity of the learners, as MPF sends content to the learner but cannot identify him or her. MPF cannot answer the following questions: “who is the learner?”, “What is his or her identity?”, and “How can I communicate with him or her?” An ontology-based user profile model allows the user to have situation-aware MPF by controlling how many

learners there are for specific categories of people in a given situation. Learner profiles must contain general information about learners, as they help determine the basic features of the learner and some details about the educational situation.

User profiles contain three details that help in recognizing the learner's identity. They first identify unchangeable features like the name, the date of birth, and the address. Next, they contain a service profile, which is related to the volume of the sound, its style, and the manner of the performance. The third identifier is called a situation-dependent profile, which contains the information related to the context such as the learner's locations. This information helps to identify individual learners, and makes it easier to communicate with them. Jellybean 4.3 is an application that helps the instructor identify the profile of the learner. It is a multi-user Google application, that can be used to add and manage user profiles and allows instructors to identify learners through their pictures.

b) Location

In MPF, the teacher will be aware of primary location but not of other locations, since the content is delivered electronically. "Location" involves information about the learner's surrounding environment. Glympse is an application that helps learners share their location using GPS. It does not require signing up for the service, but instead works anywhere the learners have GPS and a data connection. The instructor asks the learners to share their locations since it is very important for the learning situation.

c) Location-based social network

Some applications can be used to determine users' preferences. Friend's Latitude is an application from Google store that helps learners share their location directly during the learning process. It allows learners to share their location using GPS, and sends it through mobile and social media. Students can add some details about their places, which permit the instructors to know their precise location, or simply if anyone will be nearby.

d) Computing context

With the use of smart devices in the transferring of the educational content to the learner through podcast technology, the teachers can facilitate the transfer process using a variety of programs and applications. It now becomes necessary to understand the context of computing, as it is considered an essential part in the design of e-learning processes. The user interfaces for m-learning applications, which are based on podcast form, can be simple or complex according to the educational situation and the context of learner environment. Choosing colours, background, font size, button, and links is determined according to the context and the environment surrounding the learner. For example,

using the application in sunny places is different from using it in the dark, since the purpose is providing an interface suitable for the user. [2][3]

Context computing is a process of transferring a computing application from desktop to mobile computing devices, which are adaptable to the environment. This is considered the third wave of computing, and it depends on a new paradigm of applications: sensor-based applications. In fact, using context computing creates applications that are able to adapt automatically with changes in their physical surroundings, and helps strengthen the interaction between the learner and the mobile device. During the design of podcast applications on mobile phones, the location of the students during the learning process should be taken into account, and the application should be allowed to identify specific situations. [18]

Making a link between the MPF applications and learning programs should identify the location and other student details by means of a learning style, which uses multimedia (sound, animation, and video file). RFID (Radio-Frequency Identification) is a technology capable of providing students with some information about educational places they expect to visit [4]. RFID can be used to identify the learner using a RFID reader and a smart card that sends stored reader data wirelessly. The reader receives data from an identification card, which contains antenna that sends wireless waves that urge the card to send the storage data to the reader. These data are received and processed by the database. The context data cloud helps in learning more about learners, their profile, locations, and semantic locations. Friend's Latitude also provides the instructor with more information about learners and their location.

e) Physical context

The student's physical context is the setting where your place is and where the learner is co-located. It is the state of the place where the learner exists. A number of questions can be posed about this, such as where the location is, what the weather conditions are like, what the temperature is, and what are the noise levels. The learner's surrounding environment deeply affects the learning process, because learning is not only comprised of content and learner but also the environment. The temperature of the room and the equipped place generally affect the learning process. The surrounding environment, emotional status, and school performance are all very influential.

Identifying the surrounding environment of the learner, while communicating and conveying the content, is very essential. The designer of the content should therefore provide application tools to help identify the learner's surrounding environment, and aid in receiving responses from

the student during the learning process, especially for practical subjects where the learner is sent to special places such as the Internal Medicine department of a hospital. In these situations, the teacher also needs to make sure that the learner is in the right place, and can accomplish this through Google's Beacons platform, which can find nearby beacons with real-time distance estimates. Beacons enable the user to locate any beacon, even without prior knowledge of its identifiers. Additionally, users can detect and decode beacons as well as calibrate their own.

f) Sensors

U-learning uses a large number of cooperative nodes with communication abilities, such as smart phones, sensors, network nodes, RFID, handheld terminals, and mobile IPs. Using RFID tags, these sensors can detect the spatiotemporal conditions for the students. Wireless sensors networks (WSN) are the tool to collect important information everywhere, as they contain spatially autonomous sensors that detect physical conditions such as sound, temperature, motion vibration, or pressure, and convey these data to the main location. These wireless networks, which need little power, are able to acquire data quickly and communicate with other networks through a radio link. Data stored in the sensor nodes is compressed and sent to a base station "gateway," either directly or through other wireless sensor nodes.

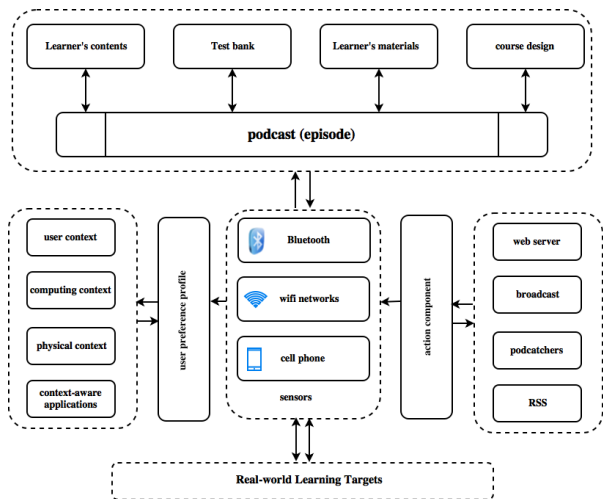


Fig. 3. The theoretical framework of context-aware technology in the podcast form (MPF)

V. RESEARCH OBJECTIVES

This study aims to:

- Present a framework for using context-aware technology in M-learning in the podcast form (MPF)

- Examine the effectiveness of using MPF engagement with context-aware technology in teaching and learning a multimedia course (IS 450).

VI. METHOD

a) Participants

This study sought to investigate the effectiveness of using MPF with context-aware technology to learn multimedia IS 450 course. The perspective of learners were identified by collecting data from students (n= 42) enrolled in the IS 450 course. Participants completed an online survey (available at <https://goo.gl/forms/U8vQBUj5pXo3ERzb2>) after course completion.

b) Instrument

The survey instrument was developed through the following steps. First, the aim of the scale was described as obtaining feedback on the effectiveness of using MPF with context-aware technology. A literature review to address the topic followed, and the areas of research were determined according to aforementioned aims. The instrument was then designed to have six components: *Attitude towards Podcast (AP)*, *Intention to podcast (IP)*, *Availability of applications (AA)*, *Ease of podcast use (EP)*, *Motivation to learn (ML)* and *Monitoring and Evaluation (ME)*. It consisted of (23) items distributed over six constructs, all of which used a five point Likert scale that ranged from 1 "strongly disagree," to 5 "strongly agree." Cronbach's α for the instrument was 0.928 and the revised consistency reliability was 0.82, therefore the instrument exceeded generally accepted validity and reliability standards for basic research. The correlation matrix between constructs were collected as shown in table:

TABLE I. A CORRELATION MATRIX BETWEEN CONSTRUCTS

Constructs	UA	CC	EL	CL	AU	IP
AP	-					
IP	.514*	-				
AA	.760*	.558*	-			
EP	.819*	.444*	.574*	-		
ML	.784*	.558*	.862*	.691*	-	
ME	.954*	.491*	.823*	.809*	.852*	1.00*

2-tailed p values; *p < 0.05, **p < 0.01

Attitude towards Podcast (AP), *Intention to podcast (IP)*, *Availability of applications (AA)*, *Ease of podcast use (EP)*, *Motivation to learn (ML)*, *Monitoring and Evaluation (ME)*.

c) Procedures

The study was conducted as a part of a college course, namely IS 450 multimedia course, and all study participants were enrolled in it. This course aimed to teach the students how to use multimedia in e-learning, and twelve lectures were created in PowerPoint format and then converted to video

podcasts. A weblog (<http://is450.blogspot.com/>) was set up to upload lecturers, and GoogleFeedBurner (<https://feedburner.google.com/>) was used to obtain RSS for the blog. The podcasts were made available online by uploading them on archive-web site (<https://feedburner.google.com/>) and linking them with the weblog. The RSS feed was sent to students via mail, and they were asked to download CoolersTeach Feed Reader to their mobile phones, then input the RSS into the feed URL icon. They also received a video tutorial that explains how to do this. Context data cloud was used to follow students and connect with them. Lensoo Create application was used to respond to student inquiries. Figure 3 illustrates this process.

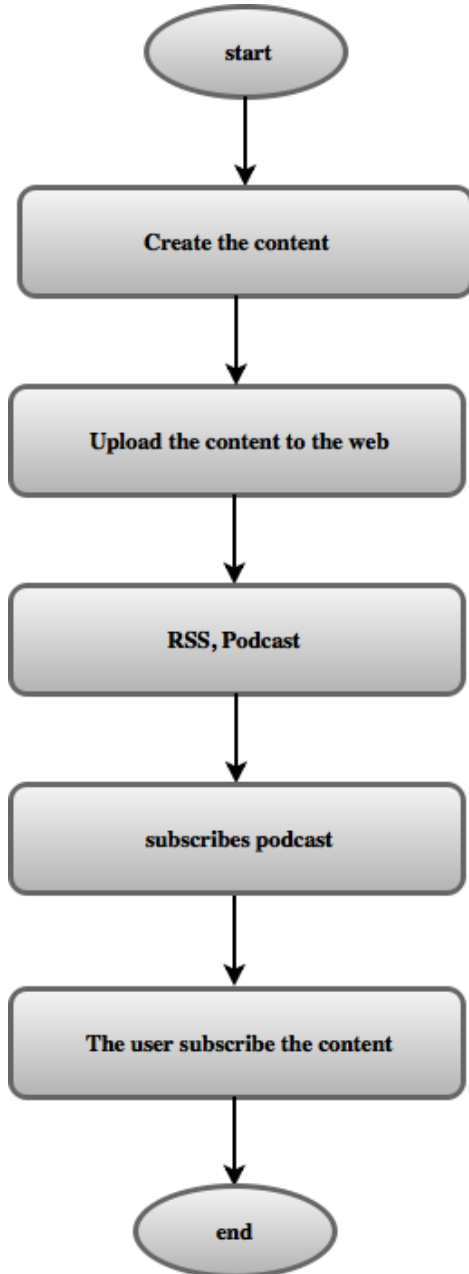


Fig. 4. Content delivered to users as podcast stack

VII. RESULTS

a) Attitude towards Podcast (AP)

As Table 2 shows, students were asked to estimate their *Attitude towards Podcast* using context-aware applications in their studying for the IS450 course. Nearly 71.4% stated that they understood the ambiguity and subtle details when listening to the episodes ($M=3.81$, $SD= (1.087)$, and a chi-square analysis revealed that there is a significant difference between the actual and the expected opinion of the student ($X^2 (4, 42) = 13.95$, $p < 0.002$) two-tails. 71.4% of the students also reported revising the lectures many times ($M=3.29$, $SD = 1.330$), ($X^2 (4, 42) = 10.85$, $p < 0.028$). In general, students gave a positive impression towards podcast use. A comparison of students' *Attitude towards Podcast* is present in Figure 5, however, the percentage of student responses about this construct is quite high.

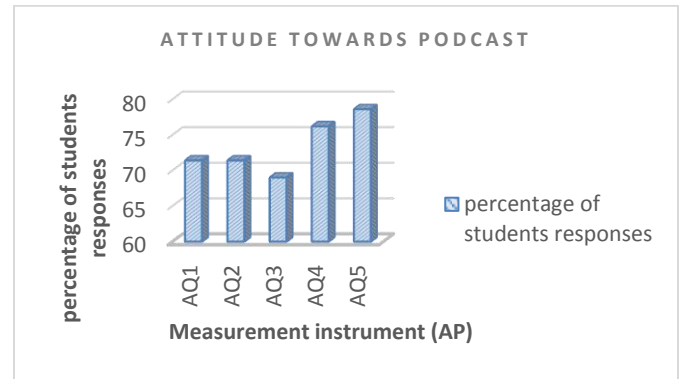


Fig. 5. Student's responses about Attitude toward Podcast

b) Intention to podcast (IP)

Students' responses about their *Intention to podcast* indicate that podcasts are an attractive format for them, as depicted in table 2. Nearly half of the students (47%) reported that it provided good feedback. The results also indicate that there are significant differences between the students' actual and expected opinion ($M=4.29$, $SD = 0.805$), ($X^2 (4, 42) = 36.81$, $p < 0.000$) two-tails. A comparison of students' *Intention to podcast* is presented in Figure 6.

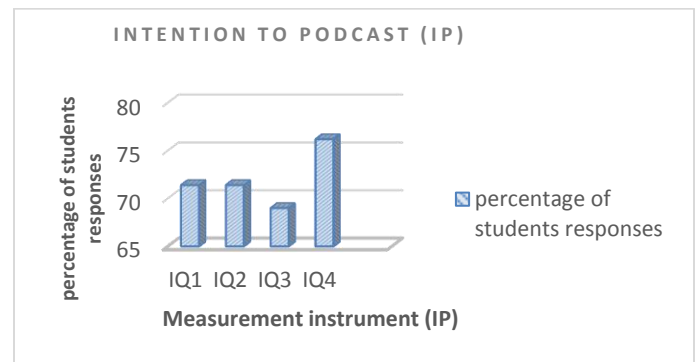


Fig. 6. Student's responses about Intention to podcast

c) Availability of Applications (AA)

All applications used to publish the episodes were available to students, as table 1 demonstrates. 64.3% of the students reported that all podcast applications were available and easy to use ($M=3.48$, $SD =1.31$), ($X^2(4, 42) =13.47$, $p<0.000$). They also reported that all context-aware applications were available and easy to use ($M=3.24$, $SD =1.52$), ($X^2(4, 42) =5.61$, $p<0.003$). Students' responses about the *Availability of Applications* are shown in figure 7.

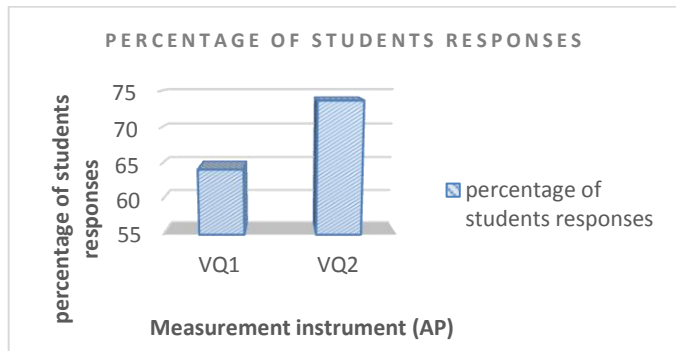


Fig. 7. Student's responses about Availability of Applications

d) Motivation to Learn (ML)

Students were asked if the use of podcasts in the learning process of the IS450 course motivated them to learn. More than half the students (57.6%) reported that the use of podcasts increased their motivation toward learning ($M=4.29$, $SD =0.805$), ($X^2(4, 42) =18.23$, $p<0.000$). Students also reported that the use of podcasting supported cooperation between them ($M=3.57$, $SD =1.72$), ($X^2(4, 42) =21.57$, $p<0.007$). These results show that MPF motivates both individual and collective learning. Students' responses about *Motivation to Learn* are shown in figure 8.

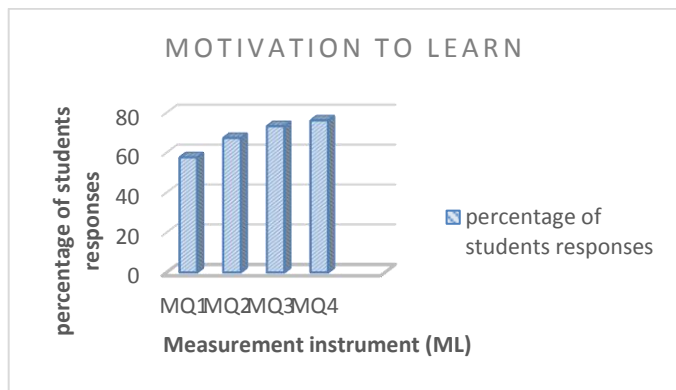


Fig. 8. Student's responses about Motivation to Learn

e) Ease of Podcast use (EP)

Students reported that the episodes were clear, simple, and appropriate to their levels ($M=3.57$, $SD =1.15$), ($X^2(4, 42)=12.28$, $p<0.000$). 42.6% of respondents indicated that the episodes were flexible and integrated. Students also had the opinion that the use of podcasts through their devices was an easy and well-paced way to learn. Students' responses about *Ease of Podcast use* are shown in figure 9.

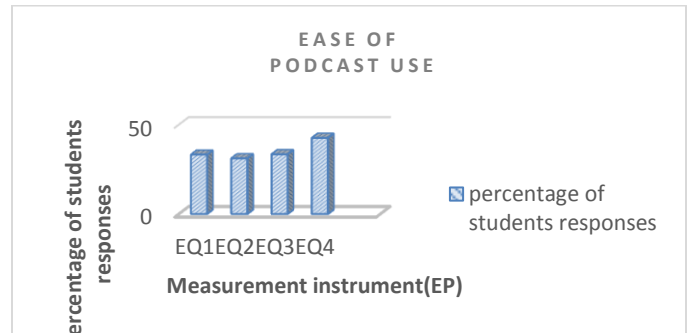


Fig. 9. Student's responses about Ease of Podcast use

f) Monitoring and Evaluation (ME)

The main purpose of using context-aware applications is following up with students and communicating with them. Students were asked about *Monitoring and Evaluation*, and 65.1% of them responded that the teacher's follow up made them more careful ($M=3.67$, $SD =1.20$), ($X^2(4, 42) =18.23$, $p<0.002$). Additionally, a sizable group (71.3%) reported that the fact that the teacher care to know about their surroundings made them more considerate ($M=3.36$, $SD =1.34$), ($X^2(4, 42) =10.61$, $p<0.034$). In general, student had a positive attitude toward the teacher's follow up. Students' responses about *Monitoring and Evaluation* are shown in figure 9.

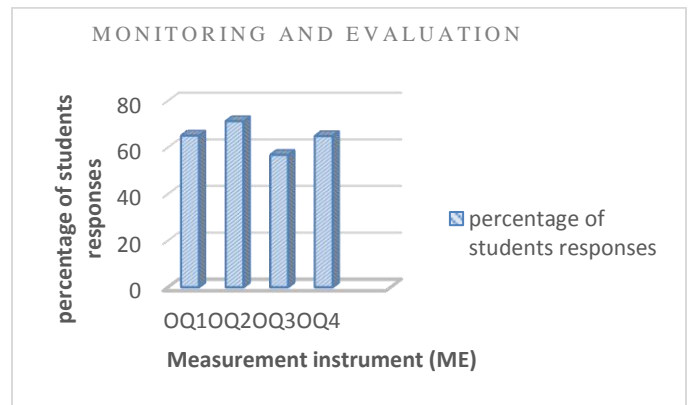


Fig. 10. Student's responses about Monitoring and Evaluation

TABLE II. MEANS, STANDARD DEVIATION, CHI SQUARED AND CONSTRUCT RELIABILITY

Constructs	Measurement instrument	Mean (SD)	%	Construct reliability	Chi Squared ^a	p-value
Attitude towards Podcast	AQ1: It helps me download missed lectures.	3.60(1.14)	71.4	.863	13.95	0.007
	AQ2: It helps me revise the lectures multiple times.	3.29(1.33)	71.4		10.85	0.028
	AQ3: It helps me understand ambiguous and subtle points.	3.81(1.08)	69		16.81	0.002
	AQ4 It helps me follow course-related news	3.74(1.037)	76.2		19.19	0.001
	AQ5: It presents a better learning source	3.19(1.23)	78.6		12.76	0.012
Intention to podcast	IQ1: It is a very useful for exam revisions.	4.36(.79)	45.8	.909	43.00	0.000
	IQ2: It is a way for attracting students.	4.33(.68)	45.2		42.52	0.000
	IQ3: It provides good feedback.	4.29(.80)	47.6		36.81	0.000
	IQ4: It covered the concepts of the course.	4.07(.86)	40.5		27.28	0.000
Availability of applications	VQ1 All podcast applications are available and easy to use	3.48(1.33)	64.3	.910	13.47	0.000
	VQ2: All context-aware applications are available and easy to use.	3.24(1.52)	73.8		5.61	0.003
	EQ1: The episodes are clear and simple.	3.07(1.17)	33.2		10.61	0.019
Ease of podcast use	EQ2The episodes are appropriate to the students' levels.	3.57(1.15)	31.1	.649	12.28	0.006
	EQ3: The episodes are present in an easy and well-paced format.	3.24(1.10)	33.4		11.33	0.033
	EQ4: Motivate individual and collective learning.	3.10(1.20)	42.6		15.61	0.001
	MQ1: It increases my motivation toward learning.	4.24(0.85)	57.6		18.23	0.000
Motivation to learn	MQ2 I feel safe when I listen to the episodes.	4.29(.77)	67.3	.889	10.61	0.000
	MQ3: It supports cooperation between students.	3.57(1.17)	73.2		21.57	0.007
	MQ4 Motivate individual and collective learning.	3.19(1.13)	76.1		19.19	0.017
Monitoring and Evaluation	OQ1: Teacher's follow up makes me more careful.	3.67(1.20)	65.1	.891	18.23	0.002
	OQ2:Teacher's caring to know about my surrounding makes me more considerate.	3.36(1.34)	71.3		10.61	0.034
	OQ3: Teacher's constant demand for feedback makes me always ready.	3.93(1.15)	56.8		21.57	0.012
	OQ4 The constant communication with the teacher gives me a positive attitude towards learning.	3.74(1.03)	64.9		19.19	0.000

^a chi-squared used to test time trends; *df*= 4

VIII. CONCLUSION

MPF is m-learning that depends on the podcast form to send educational content uploaded by the instructor to the students, who receive it through podcatchers on PADS, iPhones, Android devices, laptops, and PCs. Using podcast technology by itself doesn't enable instructors to be aware of the learners' identity, current status, or their surrounding environment during the learning process, which reflects poorly on the completeness of the educational process.

Due to the importance of completing the learning process properly, the environment surrounding the learners (the place, the time, the location, and the status) should be defined. This study presents a theoretical framework of using "context-

awareness" in M-learning in the podcast form (MPF). It takes into account the clarity and the simplicity in the presentation of the framework, in order to help MPF research and design. Additionally, it presents a context-aware calendar application built according to an out-of-context framework.

This research presents a case study of a computer department multimedia course (IS 450) at Qassim University. Course lectures were presented through podcast episodes, and students were followed up via context-aware applications. We asked the students to complete a questionnaire, after completing the course, to measure the effectiveness of this learning method. The results indicate that students have a positive attitude toward using (MPF) for coursework, and confirmed that podcasting and context-aware technology had a

significant impact on learning in the multimedia IS 450 course.

REFERENCES

- [1] Aparici, M., Bacao, F., & Oliveira, T. (2016). An e-Learning Theoretical Framework. *Educational Technology & Society*, 19 (1), 292–307.
- [2] Baran, E. (2014). A Review of Research on Mobile Learning in Teacher Education. A Review of Research on Mobile Learning in Teacher Education. A Review of Research on Mobile Learning in Teacher Education. A Review of R. *Educational Technology & Society*, 17(4), 17–32.
- [3] Bogdanovic, Z., Barac, D., Jovanic, B., Popovic, S., & Radenkovic, B. (2015). Evaluation of mobile assessment in a learning management system. *British Journal of Educational Technology*, 45(2), 231–244.
- [4] Chen, C. C., & Uang, T. C. (2012). Learning in a u-Museum: Developing a context-aware ubiquitous learning environment. *Computers & Education*, Elsevier, 59, 873–883.
- [5] Chia-Chen, C., & Tien-Chi., H. (2012., Nov). Learning in a u-Museum: Developing a Context-Aware Ubiquitous Learning Environment. *Computers & Education*, v59 n3, 873-883.
- [6] Chih Lai, H., Yen Chang, C., Shiane Li, W., Lin Fan, Y., & Tien Wu, Y. (2013). The implementation of mobile learning in outdoor education: Application of QR codes. *British Journal of Educational Technology*, 44(2), E57–E62.
- [7] Crompton, H. (2015). Understanding Angle and Angle Measure: A Design-Based Research Study Using Context Aware Ubiquitous Learning. *International Journal for Technology in Mathematics Education*, v22 n1 (1744-2710.), p19-30.
- [8] Dey, A. K. & Abowd, G. D. (2000). Towards a Better Understanding of Context and Context-Awareness, CHI 2000 Workshop on the What, Who, Where, When, and How of Context-Awareness.
- [9] Evans, C. (2008). The effectiveness of m-learning in the form of podcast revision lectures in higher education. *Computers & Education*, Elsevier, 50, 491–498.
- [10] H. Kay, R. (2012). Exploring the use of video podcasts in education: A comprehensive review of the literature. *Computers in Human Behavior*, 820–831.
- [11] Huang, Y. M., & Chiu, P.-S. (2015). The effectiveness of a meaningful learning-based evaluation model for context-aware mobile learning. *British Journal of Educational Technology*, 46(2), 437–447.
- [12] Ju-Ling, S., Hui-Chun, C., Gwo-Jen, H., & Kinshuk. (2011, May). An Investigation of Attitudes of Students and Teachers about Participating in a Context-Aware Ubiquitous Learning Activity. *British Journal of Educational Technology*, v42 n3(0007-1013.), 373-394.
- [13] Li, M., Ogata, H., Hou, B., Uosaki, N., & Mouri, K. (2013). Context-aware and Personalization Method in Ubiquitous Learning Log System. *Educational Technology & Society*, 16(3), 362–373.
- [14] Mandula, K., Rao Meda, S., Kumar Jain, D., & Kambham, R. (July 2011). Implementation of Ubiquitous Learning System Using Sensor Technologies. *Technology for Education (T4E), 2011 IEEE International Conference* (pp. 142 - 148). Chennai, Tamil Nadu: IEEE.
- [15] Mohammad A. Amasha and Salem Alkhalaf (2016) Using RSS 2.00 as a Model for u-Learning to Develop e-Training in Saudi Arabia/Using RSS 2.00 as a Model for u-Learning to Develop e-Training in Saudi Arabia, *IJIT 2016 Vol.6(7): 516-521 ISSN: 2010-3689*.
- [16] Nguyen, L., Barton, S. M., & Nguyen, L. T. (2015). iPads in higher education—Hype and hope. *British Journal of Educational Technology*, 46(1), 190–203.
- [17] Ouwehand, K., Gog, T. v., & Paas, F. (2015). Designing Effective Video-Based Modeling Examples Using Gaze and Gesture Cues. *Educational Technology & Society*, 18 (4), 78–88.
- [18] P.-S, T., C.-C, T., & G.-J, H. (2012, Jun). Developing a Survey for Assessing Preferences in Constructivist Context-Aware Ubiquitous Learning Environments. *Journal of Computer Assisted Learning*, v28 n3(0266-4909.), 250-264.
- [19] S. Fallahkhair, L. Pemberton, & R. Griffiths. (2007). Development of a cross-platform ubiquitous language learning service via mobile phone and interactive television. *Journal of Computer Assisted Learning*, 23, 312–325.
- [20] S, S. N., & Göktas, Ö. (2014). Preservice teachers' perceptions about using mobile phones and laptops in education as mobile learning tools. *British Journal of Educational Technology*, 45(4), 606–618.
- [21] T.-Y., L. (2009, Dec). A Context-Aware Ubiquitous Learning Environment for Language Listening and Speaking. *Journal of Computer Assisted Learning*, v25 n6(0266-4909), 515-527.
- [22] You, J. W. (2015). Examining the Effect of Academic Procrastination on Achievement Using LMS Data in e-Learning. *Educational Technology & Society*, 18 (3), 64–74.

An Inclusive Comparison in LAN Environment between Conventional and Hybrid Methods for Spectral Amplitude Coding Optical CDMA Systems

Hassan Yousif Ahmed

Electrical Engineering Department
College of Engineering at Wadi Aldawaser, PSAU
Wadi Aldawaser, KSA

Z. M Gharsseldien

Mathematics Department
College of Art and Science, PSAU
Wadi Aldawaser, KSA

Nisar K.S

Mathematics Department
College of Art and Science, PSAU
Wadi Aldawaser, KSA

S. A. Aljunid

School of Computer and Communication Engineering
Universiti Malaysia Perlis
Kangar, Malaysia

Abstract—In this paper, performance analysis of conventional spectral amplitude coding (CSAC) with hybrid (HSAC) for OCDMA system is investigated in local area network (LAN) environment. The CSAC is built based on arithmetic sequence with simple algebraic ways. The HSAC technique is used in which spectral amplitude coding (SAC) combined with wavelength division multiplexing (WDM) to effectively reduce multiple access interference (MAI) and mitigate the influence of phase induced intensity noise (PIIN) arising in photodetecting process. The main idea is to construct the code sequences in SAC domain then repeat it diagonally in the wavelength domain as groups which maintains the same cardinality of a given code weight. Results show that HSAC outperforms CSAC when the number of active users is high due to its better correlation properties. It has been shown that the HSAC can suppress intensity noise effectively and improve the bandwidth utilization significantly up to 4.2 nm.

Keywords—Conventional SAC (CSAC); Hybrid SAC (HSAC); WDM; OCDMA; MAI

I. INTRODUCTION

The demand for networks with higher capabilities at lower cost is increasing daily. This demand is fueled by many different factors. The tremendous growth of the internet has brought huge amount of users consuming large amount of bandwidth since data transfers involving video and image. To fulfill the demands for bandwidth and to deploy new services, new technology must be deployed and fiber optic is such one key technology. There is not much difference between multiple access and multiplexing techniques, in simple word, multiple access is a technique that allows communication media to be shared between different users while multiplexing is a combination of signals into single transmission signal [1]. Wavelength division multiplexing (WDM) has been considered as an ideal solution to extend the capacity of optical networks without drastically changing the fiber infrastructure. Various architectures that incorporate WDM into access networks have been proposed by both academia and industry [1-2]. Optical

code division multiple access (OCDMA) has been considered lately as an efficient scheme for optical communication networks [3]. Among all OCDMA techniques, spectral amplitude coding (SAC) systems have been considered since multiple access interference (MAI) can be completely eliminated by spectral coding [4-6]. However, as long as the number of users increases, phase induced intensity noise (PIIN) arises during balance photodetecting process which results in higher bit error probability. This eventually limits the network capacity. Several schemes have been introduced to be combined with OCDMA technique to improve the MAI cancellation and support more users in fiber optical networks [7-13]. Among all of them temporal/spatial OCDMA networks to improve autocorrelation sidelobes and cross-correlation have been proposed in [7]. Applying an optical pulse to represent one chip in the wavelength and time domain is one way of the MAI improvement schemes [8-10]. Some proposals [11-13] have employed differential detection to reduce the MAI. However, these systems are suffered from different problems one way or another to remove all the MAI at the receiver, resulting in severe interference, which limits the number of active users in the network. In SAC system, fiber Bragg grating (FBG) can be used as main part of encoder-decoder structure of each user. When the number of active users becomes large the sizes of FBG will become impractical. One way to relax impracticality of FBGs is to use two dimensional coding schemes but at the cost of additional fiber ribbons and star couplers are required [14]. In this paper, firstly a conventional SAC (CSAC) code family is built by using simple algebraic ways. Secondly a hybrid SAC scheme is modeled by combining WDM and SAC which maintains MAI cancellation property and PIIN alleviation in OCDMA network. The CSAC code sequences is characterized by the parameters L , N , W , λ_c , where L is the code length, N is the number of users, W is the code weight (number of marks) and λ_c is the cross correlation ($\lambda_c=1$). The CSAC scheme is built with fixed in-phase cross correlation aiming to completely remove the MAI by differential detection at the receiver side.

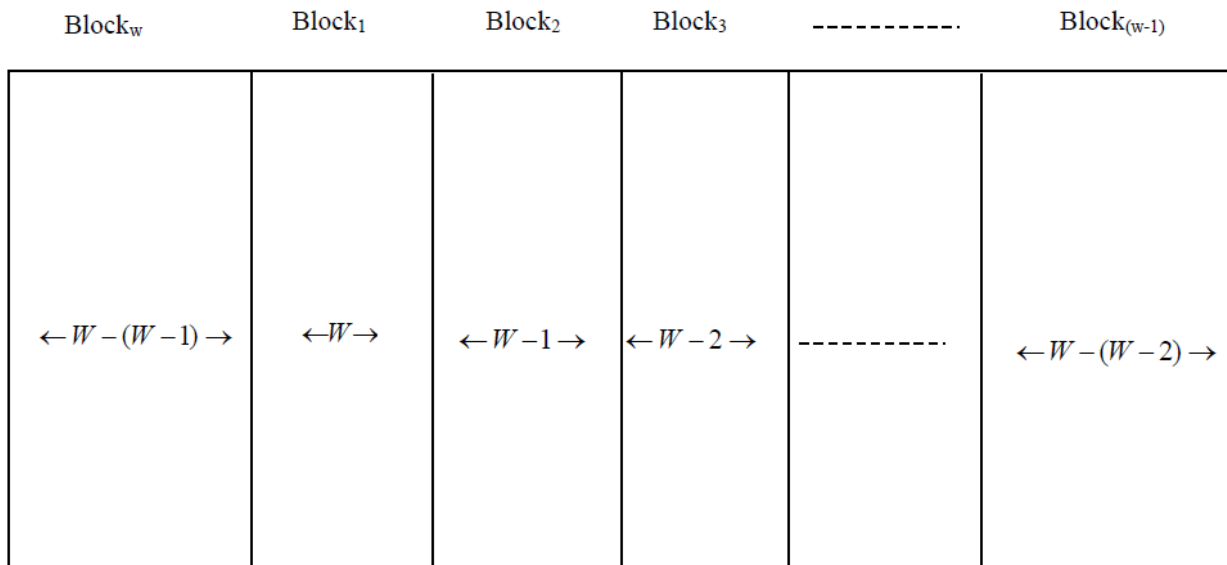


Fig. 1. Mapping elements in AS to blocks in CSAC matrix

The PIIN with the power square at photodiodes (PDs) is noticeably suppressed due to the space for spreading the received power which makes the PDs get less power for the PIIN, while maintaining the same signal power in the receiver [4], [15]. The rest of the paper is organized as follows. Section 2 shows steps of construction of CSAC code family. The HSAC model is described in Section 3. The HSAC encoder/decoder structure is explained in Section 4. In Section 5, the performance analysis of the CSAC and HSAC in the OCDMA network is elaborated. Theoretical analysis and numerical results are presented in Section 6. Finally, the conclusions are drawn in Section 7.

II. CODE CONSTRUCTION AND PROPERTIES

A. Definitions

Let $AS = (W, W-1, W-2, W-3, W-4, \dots, 1)$ denotes an arithmetic sequence. The sum of W terms of the arithmetic sequence (AS) can be calculated by.

$$S_w = \frac{W}{2} (W + 1) \quad (1)$$

The value of S_w represents the number of columns of conventional SAC (CSAC). Fig. 1 illustrates the mapping process of AS to CS, where each element in AS will be mapped to corresponding block in CSAC. The length of each block can be calculated by the formula.

$$L_g = W - g + 1 \quad (2)$$

where W is the code weight and $g = 1, 2, 3, \dots, N$

B. Construction steps of CSAC code family

Step1: Form the arithmetic sequence (AS) as follows.

$$AS = (W, W-1, W-2, W-3, W-4, \dots, 1) \quad (3)$$

Step 2: Calculate value(s) of m , such that:

$$M_1 \leq m \leq M_2 \quad (4)$$

where,

$$M_1 = 2 + (r-1) \left(W - \frac{r-2}{2} \right) \quad (5)$$

$$M_2 = 1 + r \left(W - \frac{r-1}{2} \right) \quad (6)$$

Notice that, if the value of M_1 exceeds the value of L then m carries the value 1 (i.e., if $M_1 > L$ then m, M_1, M_2 assign the value 1).

Step 3: Calculate the code length

$$L = \frac{(W \times N)}{2} \quad (7)$$

Step 4: Calculate the position of “1s” in the first row of each block using

$$p = (r, m) \quad (8)$$

Step 5: Calculate the positions of cross-correlated “1s” in each block using

$$q = (r + m - M_1 + 1, m) \quad (9)$$

Step 6: Fill each row with $\frac{W(N-2)}{W-1}$ “0s” , where N is

the number of users.

C. Code Examples

To clarify the steps mentioned in Section 2.2, we consider the following two cases.

Case 1: for $W = 3, N = 4$

Step1: Form the arithmetic sequence, so the block of CSAC is $r = 1, 2, 3$.

Step 2: Calculate M_1 and M_2 using Eq. (4) and Eq. (5).

For $r=1$,

$$M_1 = 2 + (1-1)\left(3 - \frac{1-2}{2}\right) = 2$$

$$M_2 = 1 + 1\left(3 - \frac{1-1}{2}\right) = 4$$

hence $m = 2, 3, 4$ using (2).
For $r=2$,

$$M_1 = 2 + (2-1)\left(3 - \frac{2-2}{2}\right) = 5$$

$$M_2 = 1 + 2\left(3 - \frac{2-1}{2}\right) = 6$$

hence $m = 5, 6$ using (2).
For $r=3$,

$$M_1 = 2 + (3-1)\left(3 - \frac{3-2}{2}\right) = 7$$

$$M_2 = 1 + 3\left(3 - \frac{3-1}{2}\right) = 7$$

hence $m, M_1, M_2 = 1$ as $M_1 > L$.

Step 3: Calculate the code length using (6).

$$L = \frac{(3 \times 4)}{2} = 6$$

Step 4: Calculate p using (7)

For $r=1$ and $m = 2, p = (1, 2)$

For $r=1$ and $m = 3, p = (1, 3)$

For $r=1$ and $m = 4, p = (1, 4)$

For $r=2$ and $m = 5, p = (2, 5)$

For $r=2$ and $m = 6, p = (2, 6)$

For $r=3$ and $m = 1, p = (3, 1)$

Step 5: Calculate q using (8)

For $r = 1, M_1 = 2$ and $m = 2, 3, 4$

$q = (1 + 2 - 2 + 1, 2) = (2, 2)$

$q = (1 + 3 - 2 + 1, 3) = (3, 3)$

$q = (1 + 4 - 2 + 1, 4) = (4, 4)$

For $r = 2, M_1 = 5$ and $m = 5, 6$.

$q = (2 + 5 - 5 + 1, 5) = (3, 5)$

$q = (2 + 6 - 5 + 1, 6) = (4, 6)$

For $r = 3, M_1 = 1$ and $m = 1$ (as $M_1 > L$)

$q = (3 + 1 - 1 + 1, 1) = (4, 1)$

Step 6: Pad each row with a $\frac{W(N-2)}{2}$ "0s"

$$= \frac{3(4-2)}{2} = \frac{3(2)}{2} = 3 \text{ "0s"}$$

Using the above steps of construction in Section 2.2, we have listed some code sequences in Eq. (10). In this equation, the coordinates of p obtained in step 3 are (1,2), (1,3), (1,4), (2,5), (2,6), and (3,1) while the coordinates of q obtained in step 4 are (2,2), (3,3), (4,4), (3,5), (4,6), and (4,1). It should be pointed out that, all these coordinates represent the positions of "1s" whereas the positions of "0s" calculated by using step 6. Therefore, using step 4, step 5 and step 6, the code patterns can be generated

$$CSAC = \begin{bmatrix} 0 & 1 & 1 & 1 & 0 & 0 \\ 0 & 1 & 0 & 0 & 1 & 1 \\ 1 & 0 & 1 & 0 & 1 & 0 \\ 1 & 0 & 0 & 1 & 0 & 1 \end{bmatrix} \quad (10)$$

Case 2: for $W = 4, N = 5$

Step 1: Form the arithmetic sequence

$$AS = (4, 4 - 1, 4 - 2, 4 - 3) = (4, 3, 2, 1)$$

, so the block of CSAC is $r = 1, 2, 3, 4$.

Step 2: Calculate M_1 and M_2 using Eq. (4) and Eq. (5).

For $r=1$,

$$M_1 = 2 + (1-1)\left(4 - \frac{1-2}{2}\right) = 2$$

$$M_2 = 1 + 1\left(4 - \frac{1-1}{2}\right) = 5$$

hence $m = 2, 3, 4, 5$ using (2).

For $r=2$,

$$M_1 = 2 + (2-1)\left(4 - \frac{2-2}{2}\right) = 6$$

$$M_2 = 1 + 2\left(4 - \frac{2-1}{2}\right) = 8$$

hence $m = 6, 7, 8$ using (2).

For $r=3$,

$$M_1 = 2 + (3-1)\left(4 - \frac{3-2}{2}\right) = 9$$

$$M_2 = 1 + 3\left(4 - \frac{3-1}{2}\right) = 10$$

hence $m = 9, 10$ using (2).

For $r=4$,

$$M_1 = 2 + (4-1)\left(4 - \frac{4-2}{2}\right) = 11$$

$$M_2 = 1 + 4\left(4 - \frac{4-1}{2}\right) = 11$$

Step 3: Calculate the code length using (6).

$$L = \frac{(4 \times 5)}{2} = 10$$

hence $m = M_1 = M_2 = 1$ as $M_1 > L$.

Step4: Calculate p using (7)

For $r=1$ and $m = 2, p = (1, 2)$

For $r=1$ and $m = 3, p = (1, 3)$

For $r=1$ and $m = 4, p = (1, 4)$

For $r=1$ and $m = 5, p = (1, 5)$

For $r=2$ and $m = 6, p = (2, 6)$

For $r=2$ and $m = 7, p = (2, 7)$

For $r=2$ and $m = 8, p = (2, 8)$

For $r=3$ and $m = 1, p = (3, 9)$

For $r=3$ and $m = 1, p = (3, 10)$

For $r=4$ and $m = 1, p = (4, 1)$

Step 5: Calculate q using (8)

For $r = 1, M_1 = 2$ and $m = 2, 3, 4, 5$.

$$q = (1+2-2+1,2) = (2,2)$$

$$q = (1+3-2+1,3) = (3,3)$$

$$q = (1+4-2+1,4) = (4,4)$$

$$q = (1+5-2+1,5) = (5,5)$$

For $r = 2, M_1 = 6$ and $m = 6, 7, 8$.

$$q = (2+6-6+1,6) = (3,6)$$

$$q = (2+7-6+1,7) = (4,7)$$

$$q = (2+8-6+1,8) = (5,8)$$

For $r = 3, M_1=9$ and $m = 9, 10$.

$$q = (3+9-9+1,9) = (4,9)$$

$$q = (3+10-9+1,10) = (5,10)$$

For $r = 4, M_1 = 1$ and $m = 1$ (as $M_1 > L$)

$$q = (4+1-1+1,1) = (5,1)$$

Step6: Pad each row with a

$$\frac{W(N-2)}{2} \text{ "0s"} = \frac{4(5-2)}{2} = \frac{4(3)}{2} = 6 \text{ "0s"}$$

Using the above steps of construction in Section 2.2, we have listed some code sequences in Eq. (11). In this equation, the coordinates of p obtained in *step 3* are (1,2), (1,3), (1, 4) (1, 5) (2, 6) (2, 7) (2, 8) (3, 9) (3, 10) and (4, 1) while the coordinates of q obtained in *step 4* are (2,2), (3,3), (4,4), (5,5), (3,6), (4,7), (5,8), (4,9), (5,10), and (5,1) . It should be pointed out that, all these coordinates represent the positions of "1s" whereas the positions of "0s" calculated by using *step 6*.

Therefore, using step 4, step 5 and step 6, the code patterns can be generated as follows.

$$CSAC = \begin{bmatrix} 0 & 1 & 1 & 1 & 1 & 0 & 0 & 0 & 0 & 0 \\ 0 & 1 & 0 & 0 & 0 & 1 & 1 & 1 & 0 & 0 \\ 0 & 0 & 1 & 0 & 0 & 1 & 0 & 0 & 1 & 1 \\ 1 & 0 & 0 & 1 & 0 & 0 & 1 & 0 & 1 & 0 \\ 1 & 0 & 0 & 0 & 1 & 0 & 0 & 1 & 0 & 1 \end{bmatrix} \quad (11)$$

III. MODEL DESCRIPTION OF HSAC SYSTEM

$$\begin{bmatrix} (CSAC)_1 & 0 & 0 & \dots & 0 \\ 0 & (CSAC)_2 & 0 & \dots & 0 \\ 0 & 0 & \ddots & \ddots & \vdots \\ \vdots & \vdots & \ddots & \ddots & 0 \\ 0 & 0 & \dots & 0 & (CSAC)_N \end{bmatrix}$$

Fig. 2. Matrix representation of HSAC code

An HSAC is a system where the whole code constructed in SAC domain (CSAC) then repeated in a diagonal fashion in the wavelength domain as groups. Each group maintains the same cardinality of a given code's weight of SAC code as shown in Fig. 2. In this HSAC system, the code words are divided in to g groups, where $g = 1, 2, 3, \dots$. Each user indexed as user $\#(z,t)$ and assigned a code sequence $C_{z,t}$, $z = 1,2,3,\dots,g$ and $t = 1,2,3,\dots,N$. The code length L can be calculated using the formula (11).

$$L = g \frac{(W \times N)}{2} \quad (12)$$

In Eq. (12) and Eq. (13) p and q represent the positions of "1s" in the first row of each block and the positions of cross-correlated "1s" in each block respectively.

$$p = (r+(g-1)N, m+(g-1)L) \quad (13)$$

$$q = (r + m - M_1 + (g - 1)N + 1, m + (g - 1)L) \tag{14}$$

To clarify HSAC system let us consider the following two cases.

Case 1: for $W=3, N=8$ and $g=2$

Using the steps 1, 2, 5 in Section II-B and equations (13) and (14) in Section III to calculate the position of “1s” in the first row of each block and the positions of cross-correlated “1s” in each block respectively (see Fig.1), where Table.I can be easily generated. Therefore, the points coordinates obtained for p are (1,2), (1,3), (1,4), (2,5), (2,6), (3,1) using Eq. (7) and (5,8), (5,9), (5,10), (6,11), (6,12), (7,7) using Eq. (13). While for q are (2,2), (3,3), (4,4), (3,5), (4,6), (4,1) using (8) and (6,8), (7,9), (8,10), (7,11), (8,12), (8,7) using Eq. (14).

TABLE I. HSAC CODE WORDS FOR $G = 2$ AND $N = 8$

z	t	HSAC code sequences $C_{z,t}$											
1	1	0	1	1	1	0	0	0	0	0	0	0	0
1	2	0	1	0	0	1	1	0	0	0	0	0	0
1	3	1	0	1	0	1	0	0	0	0	0	0	0
1	4	1	0	0	1	0	1	0	0	0	0	0	0
2	5	0	0	0	0	0	0	0	1	1	1	0	0
2	6	0	0	0	0	0	0	0	1	0	0	1	1
2	7	0	0	0	0	0	0	1	0	1	0	1	0
2	8	0	0	0	0	0	0	1	0	0	1	0	1

Case 2: for $W=4, N=10$ and $g=2$

Using the steps 1, 3, 6 in Section 2.1 and equations (12), (13) in section 3 to calculate the position of “1s” in the first row of each block and the positions of cross-correlated “1s” in each block respectively (see Fig.1), where Table. II can be easily generated. Therefore, the points coordinates obtained for p are (1,2), (1,3), (1, 4) (1, 5) (2, 6) (2, 7) (2, 8) (3, 9) (3, 10) (4, 1) using Eq. (7) and (5,8), (5,9), (5,10), (6,11), (6,12), (7,7) using Eq. (12). While for q are (2,2), (3,3), (4,4), (5,5), (3,6), (4,7), (5,8), (4,9), (5,10), (5,1) using (8) and (6,8), (7,9), (8,10), (7,11), (8,12), and (8,7) using Eq. (14).

IV. CONFIGURATION OF TRANSMITTER AND RECEIVER SECTIONS

Table II shows an example of the HSAC code words of two groups (8 users) are obtained by applying the steps of code construction mentioned in Section II-B.

TABLE II. CODE WORDS FOR $G = 2$ AND $N = 10$

z	t	HSAC code sequences $C_{z,t}$																			
1	1	0	1	1	1	1	0	0	0	0	0	0	0	0	0	0	0	0	0	0	
1	2	0	1	0	0	0	1	1	1	0	0	0	0	0	0	0	0	0	0	0	
1	3	0	0	1	0	0	1	0	0	1	1	0	0	0	0	0	0	0	0	0	
1	4	1	0	0	1	0	0	1	0	1	0	0	0	0	0	0	0	0	0	0	
1	5	1	0	0	0	1	0	0	1	0	1	0	0	0	0	0	0	0	0	0	
2	6	0	0	0	0	0	0	0	0	0	0	0	1	1	1	1	0	0	0	0	
2	7	0	0	0	0	0	0	0	0	0	0	0	1	0	0	0	1	1	1	0	
2	8	0	0	0	0	0	0	0	0	0	0	0	1	0	0	1	0	0	1	1	
2	9	0	0	0	0	0	0	0	0	0	0	1	0	0	1	0	0	1	0	1	
2	10	0	0	0	0	0	0	0	0	0	0	1	0	0	0	1	0	0	1	1	

Table III represents the corresponding amplitude spectra of the code sequences shown in Table I, where the violet bell-shaped curves represent “1s” chips and the blank spaces represent “0s” chips. The in phase cross correlation between codes words within the same group (from Table III, $C_{(1,1)}$, $C_{(1,2)}$, $C_{(1,3)}$, $C_{(1,4)}$) is one ($\lambda = 1$), while the codes from different groups (from Table III, $C_{(2,5)}$, $C_{(2,6)}$, $C_{(2,7)}$, $C_{(2,8)}$) is zero ($\lambda = 0$).

From Table III we can observe that the CSAC code has six spectral bins while HSAC code has twelve spectral bins. The bin bandwidth for CSAC code is set to 0.4 nm, which results in a 2.4 nm total bandwidth (1547.2 nm to 1549.2 nm). In the meantime, the bin bandwidth of HSAC codes were set to 0.4 nm resulting in 4.8 nm total bandwidth (1549.6 nm to 1551.6 nm).

The transmitter/receiver structure based on the HSAC code sequence for $W=3$ is shown Fig. 3. The principle idea behind the HSAC detection technique is that only intended signal spectrum and overlapping spectrum interferences in the same group are detected and cancelled detected (from Table I users #1, #2, #3, #4). Code sequences that belong to different groups pass through the decoder without being detected (from Table I users #5, #6, #7, #8). As listed in Table I, the information of user#1, which was coded as 011100, has been modulated using ON-OFF Keying (OOK) technique as shown in Fig. 3. The optical pulses are then reflected to an FBG set, where specific wavelengths ($\lambda_2 \lambda_3 \lambda_4$) are assigned to the chips of specific code given to the desired user. In the code sequences, the positions of the “1s” determine the center wavelengths of FBGs. The

corresponding decoder decodes the received optical pulses. For the data to be recovered the decoder should have the same spectral response to the intended encoder [3]. The detected sequences comprise the HSAC code spectrum of the desired user in company with overlapping spectra from other interference of HSAC code sequences. The complementary decoder detects the complementary wavelengths, $\lambda_1 \lambda_5 \lambda_6$ of the

intended user where the received wavelengths are processed via FBG sets. Subsequently the results are circulated to balanced photo-detectors [3]. A subtraction process is needed where a subtractor is used to strike the unwanted from the wanted signal. Finally, the original data is recovered after photo detections, low pass filter (LPF) and thresholding processes.

TABLE III. SPECTRAL BINS OF HSAC CODE WORDS FOR 8 USERS

Spectral bin (nm)	λ_1	λ_2	λ_3	λ_4	λ_5	λ_6	λ_7	λ_8	λ_9	λ_{10}	λ_{11}	λ_{12}
Users												
User# 1 $C_{(1,1)}$		█	█	█								
User# 2 $C_{(1,2)}$		█			█	█						
User# 3 $C_{(1,3)}$	█		█		█							
User# 4 $C_{(1,4)}$	█			█		█						
User# 5 $C_{(2,5)}$							█	█	█			
User# 6 $C_{(2,6)}$								█		█	█	
User# 7 $C_{(2,7)}$							█		█		█	
User# 8 $C_{(2,8)}$							█			█		█

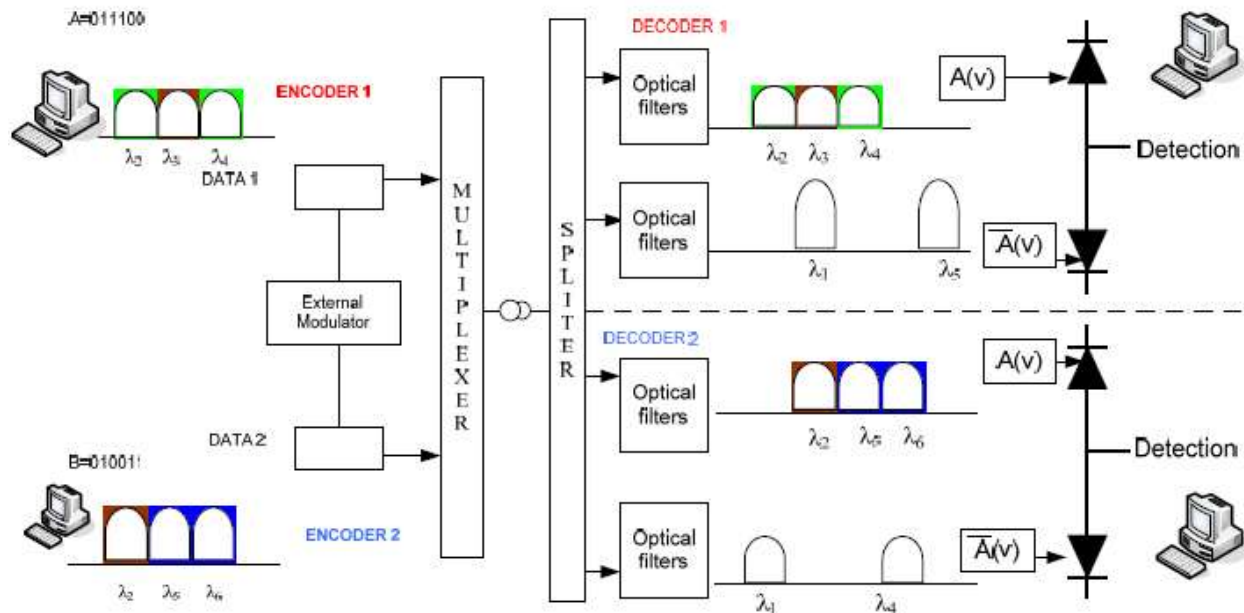


Fig. 3. Transmitter-receiver structure in LAN environment based on HSAC system

V. SYSTEM PERFORMANCE

To analyze the system with transmitter and receiver as shown in Fig. 3 for HSAC, let $C_x(i)$ denotes the i th element of the x th HSAC code sequences, the code properties based on XOR subtraction technique can be written as [17,18]:

$$\sum_{i=1}^L C_x(i)C_y(i) = \begin{cases} W, x = y \\ 1, x \neq y \end{cases} \quad \text{In the same group (g=1)} \quad (15)$$

$$\begin{cases} 0, x \neq y \end{cases} \quad \text{Not in the same group (g \ge 2)}$$

$$\sum_{i=1}^L (C_x(i) \oplus C_y(i))C_x(i) = \begin{cases} 0, & x = y \\ W - 1, & x \neq y \end{cases} \quad \text{In the same group (g=1)} \quad (16)$$

$$\begin{cases} 0, & x \neq y \end{cases} \quad \text{Not in the same group (g \ge 2)}$$

The condition of x and y in the same group ($g = 1$) meaning that both code sequences are in $CSAC_{(1)}$ or $CSAC_{(2)}$ or $CSAC_{(m)}$ as shown Fig. 2. The condition of x and y not in the same group ($g \geq 2$) meaning that one of the code sequence might be located in $CSAC_{(1)}$ and the other code sequence is located in $CSAC_{(2)}$ or $CSAC_{(m)}$. Therefore, the XOR operation of $(C_x(i) \oplus C_y(i)) C_x(i)$ is valid for $x \neq y$ only. However, the cross correlation of $(C_x(i) \oplus C_y(i)) C_x(i)$ is valid for $x \neq y$ only in Eq. (15) while from Eq. (14), the cross correlation of $C_x(i) C_y(i)$ is W when $x = y$.

Therefore, the MAI can be eliminated as the cross correlation $\sum_{i=1}^L (C_x(i) \oplus C_y(i))C_x(i)$ can be subtracted from $\sum_{i=1}^L C_x(i)C_y(i)$ when $x \neq y$. Therefore, the decoder that computes Eq. (17) rejects the MAI coming from interfering users and obtains the desired information bits.

Thus

$$\sum_{i=1}^L C_x(i)C_y(i) - \frac{\sum_{i=1}^L (C_x(i) \oplus C_y(i))C_x(i)}{W - 1} = \begin{cases} W, & x = y \\ 0, & x \neq y \end{cases} \quad (17)$$

From Eq. (17) the weight is zero when $x \neq y$, means that an MAI impact can be completely removed by using XOR subtraction detection technique. Referring to the methods described in [4, 17] the SNRs of CSAC and HSAC can be calculated as follows.

$$SNR_{CSAC} = \frac{\frac{\eta^2 P_{sr}^2 (W-1)^2}{L^2}}{\frac{P_{sr} e B \eta}{L} [(2(N-1) + W + 1)] + \frac{P_{sr}^2 B \eta^2 N}{2 \Delta V L^2} [W + 1 + 2(N-1)] + \frac{4K_B T_n B}{R_L}} \quad (18)$$

$$SNR_{HSAC} = \frac{\frac{\eta^2 P_{sr}^2 (W-1)^2}{L^2}}{\frac{P_{sr} e B \eta}{L} [(2(N-1) + W + 1)] + \frac{P_{sr}^2 B \eta^2 N}{2 \Delta V L^2} \left[W + 1 + \frac{2(N-1)}{g} \right] + \frac{4K_B T_n B}{R_L}} \quad (19)$$

where η is the photodiode responsivity, P_{sr} is the effective power of a broad-band source at the receiver, e is the electron charge, B is the electrical equivalent noise bandwidth of the receiver, K_B is Boltzmann's constant, T_n the absolute receiver noise temperature, R_L is the receiver load resistor, ΔV is the optical source bandwidth, W, N, L are the code weight, the number of users and the code length respectively, as being the parameters of the HSAC code itself. The bit error rate (BER) is computed from the SNR using Gaussian approximation as [4-5].

The bit error rate (BER) can be calculated using

$$P_e = \frac{1}{2} \operatorname{erfc} \left(\sqrt{SNR / 8} \right) \quad (20)$$

VI. RESULTS AND DISCUSSION FOR THEORETICAL PERFORMANCE ANALYSIS

A sufficient amount of signal-to-noise ratio (SNR) is important because it states the quality of the signal in the system. BER and SNR are interconnected; a better SNR yields a better BER. In this section, the numerical results analyses are based on the SNR, BER, received output power for different type of noises, and noise power.

A. Relationship between the number of active users (N) and BER

In Fig. 4, the BER is plotted against the number of active users when $P_{sr} = -10$ dBm at 622Mbit/s. From the figure, it is observed that the BER of HSAC code is lower compared to the CSAC, MQC and MFH codes even though the weight is far less, which is 4 in this case. For acceptable BER of 10^{-12} was achieved by the HSAC code with ≈ 140 active users than for ≈ 65 by CSAC code. This is evident from the fact that HSAC code has an in-phase cross correlation property that would eliminate the MAI effects by g value. However, MQC and MFH codes used with a fixed in-phase cross-correlation exactly equal to one since the in-phase cross-correlation of these codes is always one, the PIIN induced in the system utilizing these codes is still significant, thus limiting the system performance for further improvement.

B. The Effect of on system Performance by considering different Noises

Fig. 5 shows the BER plotted against for HSAC code ($W=4, g = 4$) when the number of active users is 30 and the data rate is 622Mbit/s. The red dashed line with circles represents the BER of HSAC code performance when intensity noise, shot noise and thermal noise are considered. The blue line with squares represents the BER of CSAC code performance taking into account the effects of the intensity and thermal noises. The green solid line with stars represents the BER of CSAC code performance when intensity noise and shot noise are considered. It is shown that, when g is large, both the shot and thermal noises are negligibly small compared to intensity noise, which becomes the main drawback factor of the system performance.

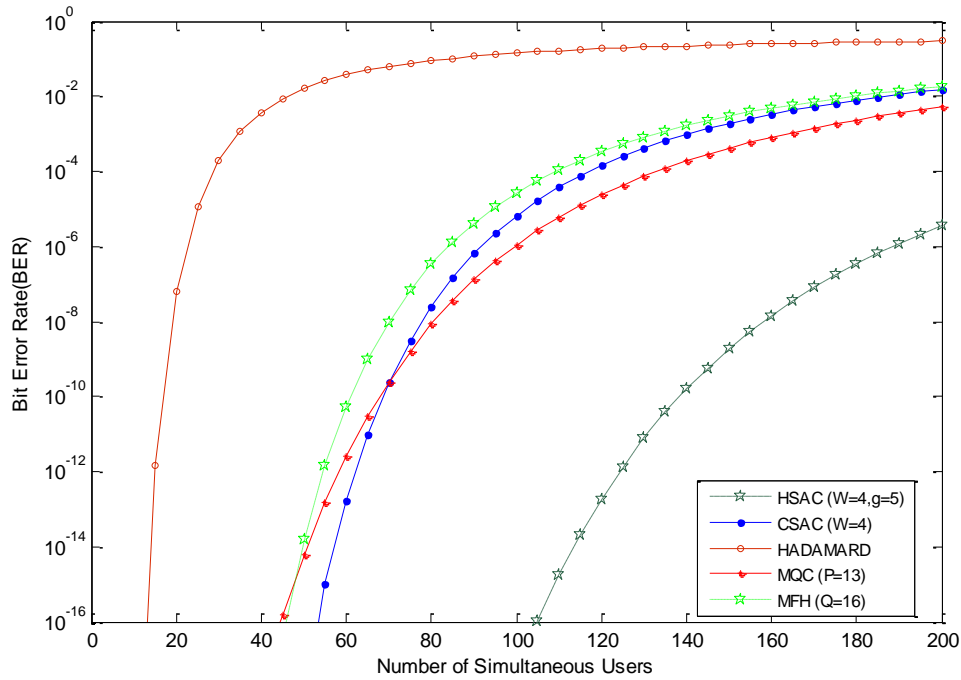


Fig. 4. BER versus number of active users when $P_{sr} = -10\text{dBm}$ at 622Mb/s

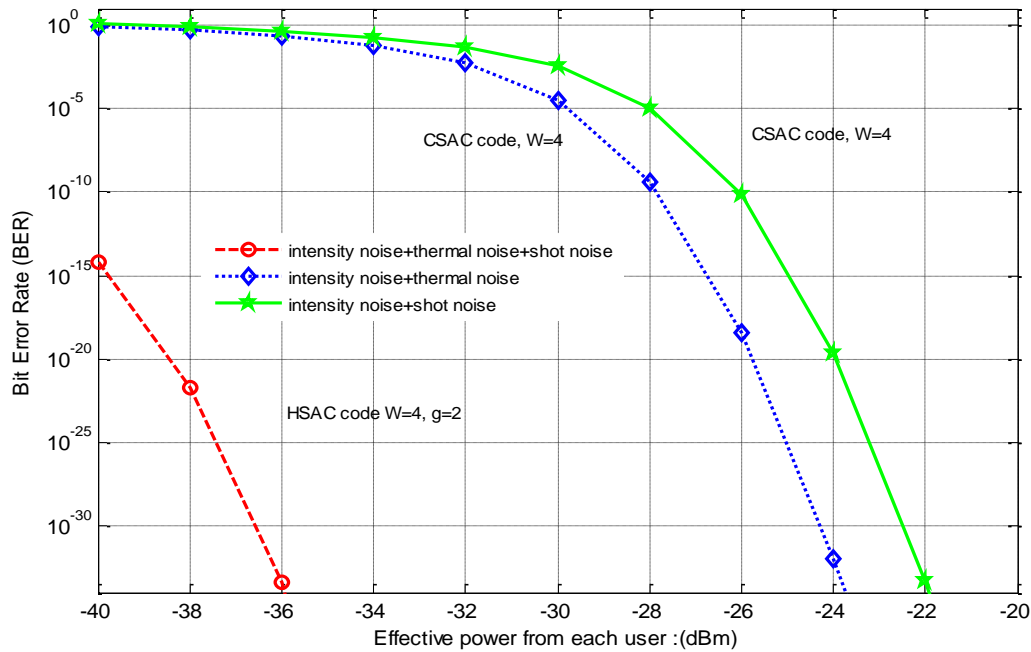


Fig. 5. BER versus effective source power P_{sr} when the number of active users is 30, taking into account the intensity noise, shot noise, and thermal noise at the data rate 622Mb/s

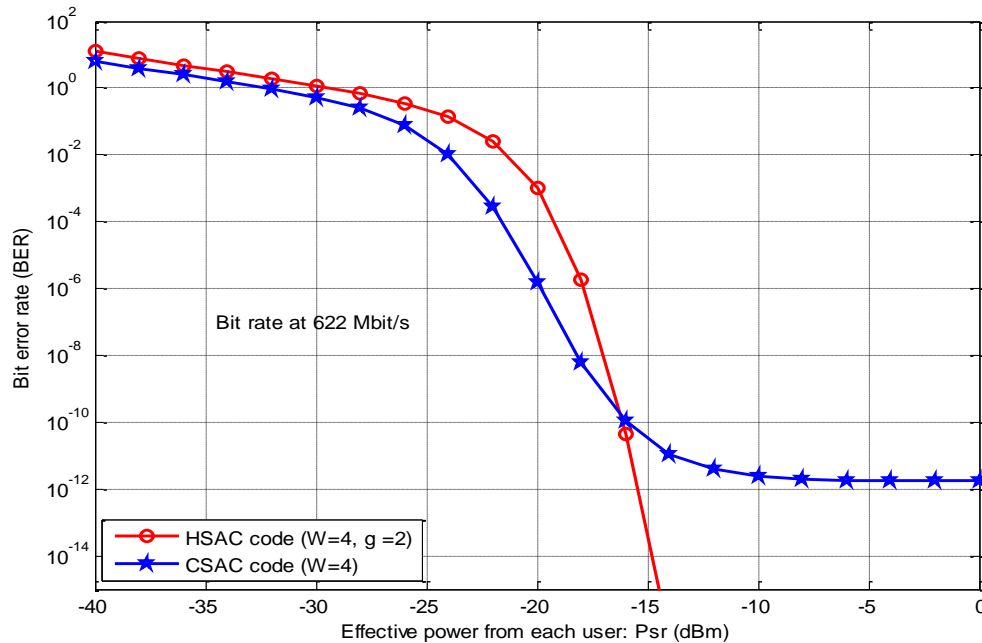


Fig. 6. BER versus effective source power P_{sr} when the number of active users is 15, taking into account the intensity noise, shot noise, and thermal noise at the data rate 622Mb/s

On the other hand, when P_{sr} is low, the effect of intensity noise becomes minimal, and thus, the thermal source becomes the main factor that impairs the system performance.

Fig. 6 shows the BER variations with the effective power P_{sr} when the number of active users is 15 at data rate of 622Mb/s for each user, taking into account the effects of the intensity noise, thermal noise and shot noise for HSAC and CSAC codes.

CSAC is adopted with the parameters $W=4$ and $g=2$ (two groups); CSAC code is adopted with the parameter $W=4$. The figure shows that the effective power P_{sr} of acceptable BER of 10^{-10} for the CSAC code is lower ($\approx P_{sr} > -15$ dBm) than that for the CSAC code ($\approx P_{sr} > 0$ dBm) when the number of active users is the same. This is because the interference from other users is reduced by the value of g which is 2 in this case for HSAC while for CSAC is fixed as the number of simultaneous users increases. This figure reveals that HSAC code outperforms CSAC code by the magnitude of almost fifteen times.

For comparison purpose, the properties of the HSAC and MQC codes are listed in Table IV. Table IV shows that HSAC codes exist for any number of weight W , free code size, and maximum in-phase cross correlation between any two code sequences is one. MQC code exists for prime number of users which limits the addressing flexibility of the system utilizing these codes to P2. HSAC has better performance and can

support almost double number of users compared to MQC code.

VII. CONCLUSION

In this paper, a new code family for SAC-OCDMA systems is presented. The properties of this code family have been proved and discussed. The results of system performance are compared with the reported codes. The HSAC code is a SAC code repeated in a diagonal fashion in wavelength domain. The in-phase cross correlation has maximum value of one ($\lambda = 1$) in the same group and zero ($\lambda = 0$) with codes in different groups.

It has been shown that the new code family can suppress intensity noise effectively and improve the system performance considerably. It shows that when a larger number of users are involved, the HSAC outperforms almost fifteen times the conventional ones and the bit-error rate is decreased as the number of groups g is increased. An improvement in bandwidth utilization is reported where HSAC surpassed CSAC by double amount which promising burst environment like LAN to be its favorable candidate in high-speed applications. In addition to its improved performance, the HSAC codes are requiring less complexity in the encoder and decoder structure design.

ACKNOWLEDGEMENT

This project was supported by the Deanship of Scientific Research at Prince Sattam bin Abdulaziz University under the research project # 2014/1/877.

TABLE IV. COMPARISON BETWEEN HSAC AND MQC CODES

Property	MQC-technique	HSAC-technique	Remarks
λ	1	≤ 1	1- the maximum cross correlation is one between all code sets for MQC 2- the maximum cross correlation is zero when $g \geq 2$ for HSAC codes
Existence	Prime number	Any integer number	More flexibility in code weight selection for HSAC and limited selection for MQC codes
Size	P^2	Free	Free cardinality for HSAC and limited codes
Code length	P^2+P	$L = g \frac{(W \times N)}{2}$	
Number of variables and parameters	$(\alpha, \beta, b, d, \text{ and } k)$	W, g	HSAC has two parameters in construction while MQC has five parameters
Matrix Form	Yes	Yes	less steps in HSAC compared to MQC

REFERENCES

- [1] Frigo N, Iannone P, Reichmann K. Spectral slicing in WDM passive optical networks for local access, in IEEE Proc. Europ. Conf. Optical Commun. Tech. Dig, vol. 1, pp. 119–120, 1998.
- [2] Froberg ., Henion, Rao H, Hazzard B, Parikh S, Romkey, Kuznetsov M, “The NGI ONRAMP test bed: Reconfigurable WDMtechnology for next generation regional access networks,” J. LightwaveTechnol, vol.18, pp. 1697–1708, 2000.
- [3] Salehi J. A, Brackett C. A, “Code division multiple access techniques in optical fiber network—Part II: System performance analysis,” IEEE Transaction on Communications, vol. 37, pp. 834–842, 1989.
- [4] Zou Wei, Shalaby H. M. H, Ghafouri-Shiraz H, “Modified Quadratic Congruence codes for Fiber Bragg-Grating-Based SAC-OCDMA,” Journal of Lightwave Technology, vol. 19, pp. 1274-1281, 2001.
- [5] Wei Z, Ghafouri-Shiraz H, “Code for spectral amplitude-coding optical CDMA systems,” J. Lightwave Technol, vol. 20, pp. 1284-1291, 2002.
- [6] Abd T. H, Aljunid S. A, Fadhil H. A, Ahmad R. B, Junita M. N, “Enhancement of performance of a hybrid SAC-OCDMA system using dynamic cyclic shift code,” Ukr. J. Phys. Opt, vol. 13, pp. 12-27, 2012.
- [7] Park E, Mendez A.J, Garmire E. M, “Temporal/spatial optical CDMA networks-design, demonstration, and comparison with temporal networks,” IEEE Photonics Technol Lett, vol. 4, pp. 1160-1162, 1992.
- [8] Yim R.M.H, Chen L.R, Bajcsy J, “Design and performance of 2-D codes for wavelength-time optical CDMA,” IEEE Photonics Technol. Lett, vol. 14, pp. 714-716, 2002.
- [9] Mendez Antonio, J, Gagliardi Robert M, Vincent J. Hernandez, Bennett Corey V, Lennon William J, “Design and performance analysis of wavelength/time (W/T) matrix codes for optical CDMA,” IEEE J. Lightwave Technol, vol. 21, pp. 2524-2533, 2003.
- [10] Song-Ming Lin, Jen-Fa Huang, Chao-Chin Yang, “Optical CDMA network codecs with merged-M-coded wavelength-hopping and prime-coded time-spreading,” Opt. Fiber Technol, vol. 13, pp. 117-128, 2007.
- [11] Sheng Peng Wan, Hu Yu, “Two-dimensional optical CDMA differential system with prime/OOC codes,” IEEE Photonics Technol. Lett, vol. 13, pp.1373-1375, 2001.
- [12] Yim R.M.H, Bajcsy J, Chen L.R, “A new family of 2-D wavelength-time codes for optical CDMA with differential detection,” IEEE Photonics Technol. Lett, vol. 15, pp.165-167, 2003.
- [13] Heo H, Seong-sik Min, Won Yong Hyub, Yeon Y, Bong Kyu Kim, Byoung Whi Kim, “A new family of 2-D wavelength-time spreading code for optical code-division multiple-access system with balanced detection,” IEEE Photonics Technol. Lett, vol. 16, pp. 2189-2191, 2004.
- [14] Yang C. C, Huang J. F, “Two-Dimensional M-matrices coding in spatial/frequency optical CDMA networks,” IEEE Photon. Technol. Lett, vol.15, pp. 168–170, 2003.
- [15] Smith E. D. J, Blaikie R. J, Taylor D. P, “Performance enhancement of spectral-amplitude-coding optical CDMA using pulse-position modulation,” IEEE Trans. Commun, vol. 46, pp. 1176–1185, 1998.
- [16] Chao-Chin Yang, “Hybrid wavelength-division multiplexing/spectral-amplitude-coding optical CDMA system,” IEEE Photon. Technol. Lett, vol. 17, pp. 1343–1345, 2005.
- [17] Hassan Yousif Ahmed, Nisar K.S, “Diagonal Eigenvalue Unity (DEU) code for spectral amplitude coding-optical code division multiple access,” Optical Fiber Technology, vol. 19, pp. 335–347, 2013.
- [18] Hassan Yousif Ahmed, Nisar K.S, “Reduction of the fiber dispersion effects on MAI for long span high-speed OCDMA networks using Diagonal Eigenvalue Unity (DEU) code,” Optik, vol. 124, pp. 5765–5773, 2013.
- [19] Goodman J.W, Statistical optics. Wiley: New York, 1985.

An Approach for Analyzing ISO / IEC 25010 Product Quality Requirements based on Fuzzy Logic and Likert Scale for Decision Support Systems

Hasnain Iqbal
Computing and Technology
Iqra University
Islamabad, Pakistan

Muhammad Babar
Computing and Technology
Iqra University
Islamabad, Pakistan

Abstract—Decision Support Systems (DSS) are collaborative software systems that are built to support controlling of an organization in decision making process when faced with non-routine problems in a specific application domain. It's important to measure portability, maintainability, security, reliability, functional suitability, performance efficiency, compatibility, and usability quality requirements of DSS properly. ISO / IEC 25010 which replaced ISO 9126, used for three different quality models for software products, such as: a) Quality in use model, b) Product quality model, and c) Data quality model. There is a lack of methodologies to measure and quantify these quality requirements. Fuzzy logic used to specify quality requirements of DSS, because it's an approach to computing based on degrees of truth, rather than true or false logics. Likert scale is a method in which it converts qualitative values into quantitative values to make a best statistical analysis. The measurement and quantification of quality requirements of DSS is a challenging task, because these quality requirements are in qualitative form and can't be represented in quantitative way. Although, several quality requirements methods for DSS have been proposed so far, but the research on analyzing quality requirements of DSS are still limited. In this paper, quantitative approach proposed for analyzing ISO / IEC 25010 product quality requirements based on fuzzy logic and likert scale for DSS which aims to quantify quality requirements. Moreover implemented proposed framework on a case study 'Internet Banking' and got data from 25 respondents i.e. System Analysts and Domain Experts of banking sector.

Keywords—ISO / IEC 25010; Product Quality Requirements; Fuzzy Logic; Likert Scale; Functional Requirements; Non-Functional Requirements; Internet Banking; Decision Support Systems

I. INTRODUCTION

In this paper, mainly focused for analyzing ISO / IEC 25010 product quality requirements based on the fuzzy logic and likert scale for DSS which aims to quantify the quality requirements.

ISO / IEC 25010 "Systems and Software Engineering – Systems and Software Quality Requirements and Evaluation (SQuARE) – Systems and Software Quality Models"; which replaced ISO 9126 "Software Engineering – Product Quality", used for three different quality models for software products: 1) Quality in use model, 2) Product quality model, and 3) Data

quality model [8].

DSS are collaborative software systems that are built to support the controlling of an organization in decision making process when faced with non-routine problems in a specific application domain. It's important to measure portability, maintainability, security, reliability, functional suitability, performance efficiency, compatibility, and usability quality requirements of DSS properly.

Non-Functional Requirements (NFRs) are requirements that specifies criteria that can be used to judge the operation of a system, rather than specific behaviors of the system. These requirements must be distinguished with the major Functional Requirements (FRs) that define specific behavior or functions of the systems. There are some major quality attributes of NFRs framework that must be measurable before start working on the system like; risk analysis, configurability, modifiability, performance, efficiency, traceability, recoverability, reliability, reusability, security, availability, interfaces, design constraints, and failure management.

There is a lack of methodologies to measure and quantify these quality requirements. Fuzzy logic used to specify quality requirements of DSS, because it's an approach to computing based on the degrees of the truth, rather than the true or false logics.

As a scaling method, likert scale is a method in which it converts qualitative values into quantitative values to make a best statistical analysis. It is commonly used to measure defendant's attitudes or behaviors by asking the extent to which they agree or disagree with a particular statement.

The measurement and quantification of the quality requirements of DSS is a challenging task, because these quality requirements are in the qualitative form and can't be represented in a specific quantitative way. Although, several quality requirements methods for DSS have been proposed so far, but the research on analyzing quality requirements of DSS is limited.

In this study, our objectives to provide a quantitative approach for analyzing ISO / IEC 25010 product quality requirements based on the fuzzy logic and likert scale for DSS which quantify the quality requirements.

The rest of the paper is organized as follows. The literature review of product quality requirements of DSS discussed in Section II. Section III contained proposed framework that consists upon five steps. Section IV validated the results of respective 280 rules. Section V consists of a case study and finally Section VI concluded the paper.

II. LITERATURE REVIEW

In [10], discussed about DSS Life Cycle and highlighted its importance for interactive software systems while decision making process for an organization when facing non-repetitive difficulties in a specific application domain. For this, author mentioned a list of NFRs that were divided into three categories i.e. DSS development and pre-development, DSS operation, and DSS maintenance and evaluation.

In [1], highlighted NFRs importance, implementation, and its overall effects on software architecture. Author proposed an approach that provides decision support in a software development process for designing decision model in the field of NFRs. By using this, developer's productivity will be increase by reusing design decisions.

In [2], proposed a quantitative approach that based on fuzzy logic and Alpha cut approach which objectives to achieve process of prioritizing NFRs. Proposed approach divided into four different steps; first step identify FRs and NFRs, second step generates decision matrix ($n \times m$), third step stimulate importance degree of each NFR with admiration to each FR, whereas fourth step calculates all NFRs with respect to all FRs by using fuzzy logic and Alpha cut approach.

In [13], presented a fuzzy model for software reliability prediction. Authors proposed three parameters i.e. availability, failure probability, and recoverability for combined measure of the software reliability. Proposed approach also helped to progressed intermediary stages among reliable and unreliable state of a system.

In [17], showed an approach that participates FRs, measurable NFRs, and scalable NFRs. Authors originated use of fuzzy logic and likert scale for treatment of separately quantifiable as well as scalable NFRs.

In [11], discussed capability of fuzzy logic in control fuzziness and ambiguity to come up with an efficient maintainability prediction model. Authors proposed a model that was constructed using by object-oriented metrics data as there are at-least two major important sources of information for building the prediction model, such as: historical data, and human experts.

In [15], survey paper reviewed an improvement of performance of DSS to meet the challenges and development of integrated DSS. It determines that by measuring integration, well support will be provided to decision makers, with anticipation of both better decisions and enhanced decision making processes.

In [8], discussed about measuring performance of cloud computing based applications by using ISO / IEC 25010 quality characteristics. Authors used Bautista's proposed performance measurement framework for measuring overall

performance of cloud computing based applications. There were three key challenges become deceptive as a result of this case study analysis, such as: collecting, processing, and representing data.

In [3], highlighted importance of measuring software quality in use, also described that why software quality in use measurement is so much difficult especially in the e-government applications, embedded systems, and mobile based applications. Authors divided paper into two contributions: a) classification and definition of key issues and challenges while measuring software quality in use in context of ISO SQuaRE series, and b) prediction of software quality in use.

In [4], discussed about NFRs, as it's difficult to identify them for specific domains. Authors introduced model based approach that based on fuzzy logic and DSS, which helped to classify different design alternatives. Proposed approach were accomplished by building a model of the NFRs and then performing analysis on the model.

In [19], discussed about major difference between business intelligence and decision support systems or applications. Authors also highlighted software decision making difficulties while taking any decisions and focused on two basic types of software solutions that used to support software decision making, such as: DSS, and business intelligence.

In [6], highlighted that most of time project fails due to NFRs. Authors mentioned that NFRs are very vital in any software project that supports in finalizing major functionality of system. Authors declared that NFRs is very difficult to identify, so in most of cases developers ignored NFRS regardless of significant their importance in functionality of system.

In [14], discussed about importance of NFRs for an effective development and deployment of software product. Authors projected a four layered analysis approach for identification of NFRs, and some rules also proposed for each layer. Proposed approach successfully applied on two case studies i.e. online library management system, and ATM system. They identified NFRS and then validated by using a check list.

In [7], discussed regarding importance of service oriented architecture in organizations and underlined that quality should be preserved as a key issue. Authors mentioned that there is a need for development of a specific quality model for service oriented architecture based on the latest ISO / IEC 25010.

In [18], addressed about clashes among NFRs that identified individually, whereas existing approaches were fail to detention nature of clashes among those NFRs. Proposed framework categorizes and examines the clashes that based on relationships among quality attributes, functionalities and constraints.

In [16], highlighted about importance of NFRs in software architecture and its contribution to success of a software project. Authors identify different types of NFRs that based on different types of systems and application domains, and originate that there are some other NFRs which have no explained yet. Only 20.18% NFRs have definition and

attributes, 26.32% NFRs have definition, whereas 53.51% NFRs were without definition and attributes.

In [12], discussed about NFRs that how much these are difficult to software engineers for many years, although since long time different methods and techniques have been proposed to improve the elicitation, documentation, and validation. Authors mentioned that by knowing more about these issues will be beneficial for both parties i.e. practitioners and researchers in their daily routine work. Authors presented an empirical study which based on thirteen interviews with software architects.

In [9], highlighted regarding quality attributes, eliciting quality attributes requirements, quality attribute workshop and quality attribute workshop eight steps, and quality attribute scenarios. Paper were consists on these questions: a) what is the best time to specify quality attribute requirements, b) what is an approach that an organization uses to identify quality attributes requirements.

In [5], showed importance of online banking for development and improvement over the world and manipulating organizations, society and individuals. NFRs are as important as NFs, and NFRs should be specify in initial phase. Many of software projects fails due to not considering NFRs. NFRs such as accuracy, usability, security and performance are regularly critical to online banking system. For conducting survey, authors set a questionnaire and send to 122 online banking customers and measured results.

However in above mentioned studies, no particular method or approach has been proposed for analyzing ISO / IEC 25010 product quality requirements for DSS based on fuzzy logic and likert scale. In this study, proposed an enhanced approach for analyzing ISO / IEC 25010 product quality requirements for DSS based on fuzzy logic and likert scale. By this approach, we can classify different quality requirements of DSS from multiple views of stakeholders, that how much quality requirements are High Important, Important, Low Important, or Not Important.

III. PROPOSED FRAMEWORK

In order for analyzing, maintaining, and determining the quality requirements of DSS; proposed a framework as showed in TABLE I.

TABLE I. STEPS OF PROPOSED FRAMEWORK FOR ANALYZING QUALITY REQUIREMENTS FOR DSS

Step No.	Description
1	Compare quality requirements of DSS with ISO / IEC 25010:2012 with respect to the product quality
2	Set the values of importance of quality requirements by using likert scale
3	Use of Fuzzy Model four modules i.e. Rule Base, Fuzzification, Inference Engine, and Defuzzification for determining the quality requirements
4	Calculating quality requirements of DSS and plot values by using Mamdani Style Inference Mechanism
5	Defuzzify the fuzzified outputs by using Joint Membership Function plotting on Two-Dimensional Surface View

Fig. 1. shows overall steps of proposed framework for analyzing quality requirements of DSS.

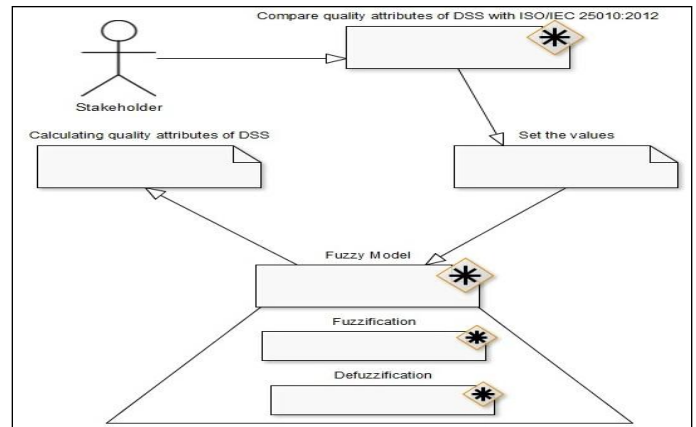


Fig. 1. Steps of Proposed Framework for Analyzing Quality Requirements of DSS

Step 1

Comparison between quality requirements of DSS with ISO / IEC 25010:2012 with respect to the product quality:

TABLE II. COMPARISON BETWEEN ISO / IEC 25010 PRODUCT QUALITY REQUIREMENTS OF DSS

Sr.	ISO / IEC 25010: 2012 General Characteristics (Product Quality)	ISO / IEC 25010: 2012 Sub – Characteristics (Product Quality)	Quality Requirements of DSS [1]
1	Portability	Adaptability	YES
		Installability	YES
		Replaceability	YES
2	Maintainability	Modularity	YES
		Reusability	YES
		Analyzability	YES
		Modifiability	YES
3	Security	Testability	YES
		Confidentiality	YES
		Integrity	YES
		Non-repudiation	YES
		Accountability	YES
4	Reliability	Authenticity	YES
		Maturity	YES
		Availability	YES
		Fault Tolerance	YES
5	Functional Suitability	Recoverability	YES
		Functional Completeness	YES
		Functional Correctness	YES
6	Performance Efficiency	Functional Appropriateness	YES
		Time Behavior	YES
		Resource Utilization	YES
7	Compatibility	Capacity	YES
		Co-existence	YES
8	Usability	Interoperability	YES
		Appropriateness Recognisibility	YES
		Learnability	YES
		Operability	YES
		User Error Protection	YES
		User Interface Aesthetics	YES
		Accessibility	YES

Step 2

Set the values of importance of quality requirements by using the Likert Scale. Here Likert Scale will give a value to each quality requirement of DSS as shown in TABLE III. The inputs of quality requirements of DSS are Portability (PORT), Maintainability (MAIN), Security (SEC), Reliability (REL), Functional Suitability (SUIT), Performance Efficiency (PER), Compatibility (COMP), and Usability (USA). Levels of all eight inputs nominal values are: Portability, Maintainability, Security, Reliability, Functional Suitability, Performance Efficiency, Compatibility, Usability = {High Important (I_H), Important (I), Low Important (I_L), Not Important (I_N)}.

TABLE III. LIKERT SCALE FOR NOMINAL VARIABLES WITH ACTUAL VALUES OF PORTABILITY, MAINTAINABILITY, SECURITY, RELIABILITY, FUNCTIONAL SUITABILITY, PERFORMANCE EFFICIENCY, COMPATIBILITY, AND USABILITY

Portability, Maintainability, Security, Reliability, Functional Suitability, Performance Efficiency, Compatibility, Usability	
Nominal Variables	Actual Values
High Important (I _H)	4
Important (I)	3
Low Important (I _L)	2
Not Important (I _N)	1

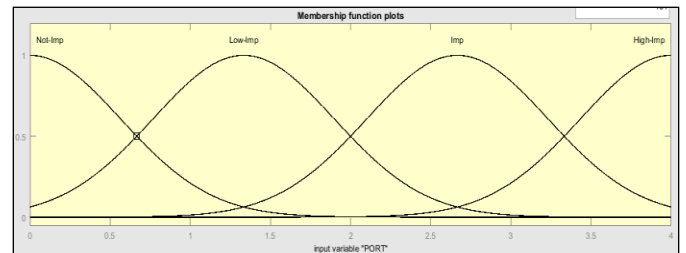


Fig. 2. Fuzzification of Input Variable: PORT (Portability)

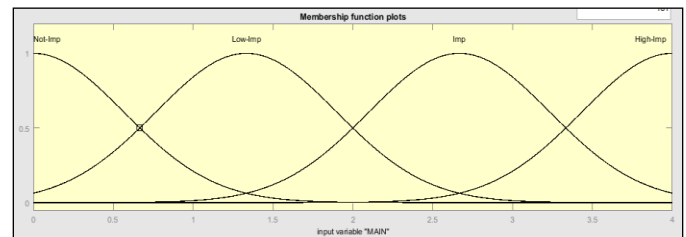


Fig. 3. Fuzzification of Input Variable: MAIN (Maintainability)

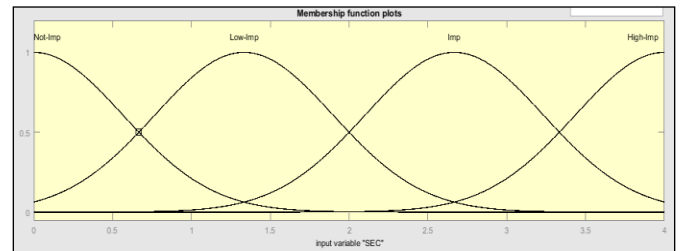


Fig. 4. Fuzzification of Input Variable: SEC (Security)

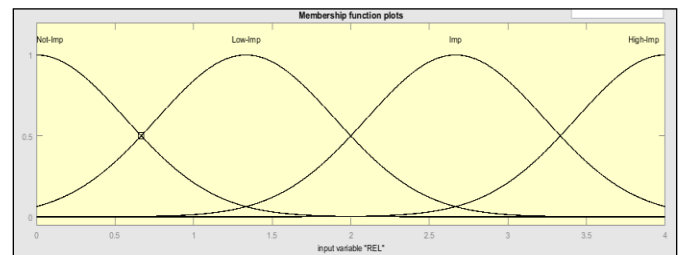


Fig. 5. Fuzzification of Input Variable: REL (Reliability)

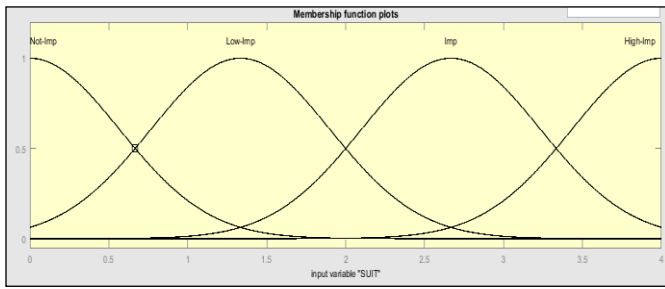


Fig. 6. Fuzzification of Input Variable: SUIT (Functional Suitability)

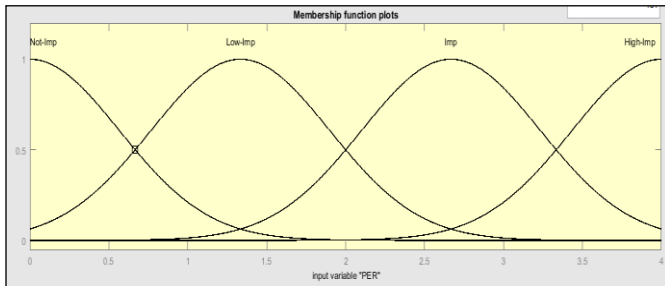


Fig. 7. Fuzzification of Input Variable: PER (Performance Efficiency)

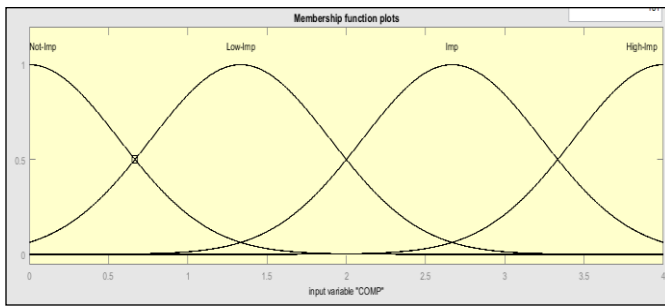


Fig. 8. Fuzzification of Input Variable: COMP (Compatibility)

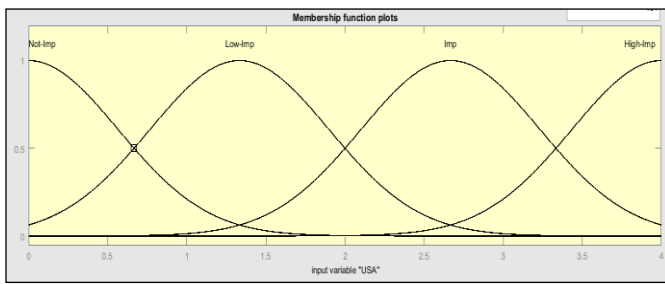


Fig. 9. Fuzzification of Input Variable: USA (Usability)

Step 3

Fuzzy Model is a greatest choice for analyzing, maintaining, and determining the quality requirements of DSS in the form of quantitative way. Here we used Fuzzy Model four modules i.e. Rule Base, Fuzzification, Inference Engine, and Defuzzification for this as shown in Fig. 10.

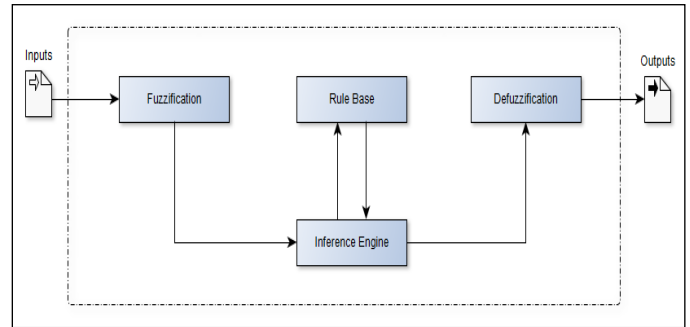


Fig. 10. Fuzzy Logic Controller Block Diagram (Fuzzy Model)

Fig. 10. describes the Fuzzy Logic Controller Fuzzy Model that converts the crisp inputs into the fuzzy values, after that these values are handled by the Inference Engine in Fuzzy Domain via Rule Base. Finally the handled output is converted from fuzzy domain to the crisp domain by the defuzzification module [11].

Here we fuzzified the inputs of quality requirements of DSS by using rule base Fuzzification and assign them Product Quality Range Values as shown in TABLE IV.

TABLE IV. LIKERT SCALE FOR NOMINAL VARIABLES WITH ACTUAL RANGE VALUES OF PRODUCT QUALITY

Nominal Variables	Actual Range Values
High	24 – 32
Average	17 – 23
Low	0 – 16

TABLE IV. shows likert scale for nominal variables with actual range values of product quality. Here we used Product Quality High (PQ_{High}), Product Quality Average ($PQ_{Average}$), and Product Quality Low (PQ_{Low}) as a nominal values having (24 - 32), (17 - 23), and (0 - 16) actual range values respectively.

After completing the Fuzzification, we defuzzify the fuzzified output and then plot them by using MATLAB Fuzzy Tool Box through Mamdani Style Inference Mechanism and displayed the results.

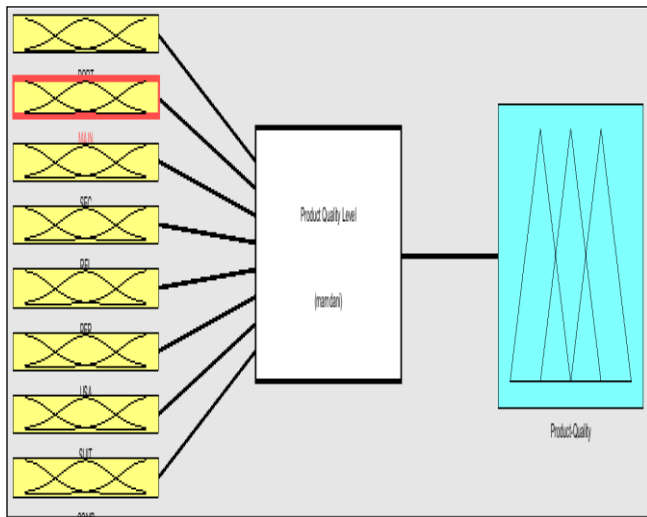


Fig. 11. Product-Quality Model Diagram by Mamdani Style Inference Mechanism

Fig. 11. describes the product-quality model diagram by using Mamdani Style Inference Mechanism. Here inputs parameters for Mamdani Style Inference Mechanism are PORT, MAIN, SEC, REL, SUIT, PER, COMP, and USA. Whereas Product-Quality is the output of Product-Quality Model.

The proposed framework integrates the quality requirements of DSS that analyzes PORT, MAIN, SEC, REL, SUIT, PER, COMP, and USA for determining Product-Quality level based on the following rule base Fuzzification. Here all 280 possible sets of inputs (rules) are consider, as per given Mathematical Combination Formula:

$$C(n, r) = n! / (r! (n - r)!) \\ C(8, 4) = 8! / (4! (8 - 4)!) \\ C(n, r) = 70$$

In the given formula, ‘C’ used for Total Combinations, ‘n’ used for ‘Total Number of Objects / Parameters’, whereas ‘r’ used for ‘Total Number of Elements’ without any repetition. In this study, total eight objects / parameters used i.e. PORT, MAIN, SEC, REL, SUIT, PER, COMP, and USA. Whereas 4 total numbers of elements i.e. I_N , I_L , I, and I_H have been used.

As in this study, we used four elements for each parameter (total 8 parameters), so that for calculating total inputs multiply possible combinations (70 Combinations) with 4, such as:

$$70 \times 4 = 280 \text{ Total Inputs}$$

These rules are classified as Product Quality High (PQ_{High}), Product Quality Average ($PQ_{Average}$), and Product Quality Low (PQ_{Low}) as given below in TABLE V (all 280 rules given in Annexure A):

TABLE V. ANALYZING PORTABILITY, MAINTAINABILITY, SECURITY, RELIABILITY, FUNCTIONAL SUITABILITY, PERFORMANCE EFFICIENCY, COMPATIBILITY, AND USABILITY QUALITY REQUIREMENTS OF DSS FOR DETERMINING PRODUCT QUALITY LEVEL

Sr.	(Quality Requirements Inputs)								Product Quality Level
	PORT	MAIN	SEC	REL	SUIT	PER	COMP	USA	
1	I_N	I_N	I_N	I_N	I_N	I_N	I_N	I_N	PQ_{Low}
28	I_L	I_N	I_H	I_N	I_N	I_N	I_N	I_N	PQ_{Low}
56	I	I_N	I_N	I_N	I_H	I_N	I_N	I_N	PQ_{Low}
84	I_H	I_N	I_N	I_N	I_N	I_N	I_H	I_N	PQ_{Low}
112	I	I	I_N	I_N	I_L	I_N	I_N	I_N	PQ_{Low}
140	I_H	I_H	I_N	I_N	I_N	I_N	I_N	I	PQ_{Low}
168	I	I	I	I_N	I_N	I_N	I_H	I_N	$PQ_{Average}$
196	I_L	I_L	I_L	I_L	I_N	I_N	I_N	I_L	PQ_{Low}
224	I_L	I_L	I_L	I_L	I_L	I_L	I_N	I_N	PQ_{Low}
252	I_L	I_L	I_L	I_L	I_L	I_L	I	I_N	PQ_{Low}
256	I_L	I_L	I_L	I_L	I_L	I_L	I_N	I_H	$PQ_{Average}$
260	I	I	I	I	I	I	I_N	I_L	$PQ_{Average}$
276	I	I	I	I	I	I	I	I_H	PQ_{High}
280	I_H	I_H	I_H	I_H	I_H	I_H	I_H	I_H	PQ_{High}

TABLE V. shows respective rules (all 280 rules given in Annexure A) for analyzing PORT, MAIN, SEC, REL, SUIT, PER, COMP, and USA quality requirements of DSS for determining Product-Quality Level, that were classified as Product Quality High (PQ_{High}), Product Quality Average ($PQ_{Average}$), and Product Quality Low (PQ_{Low}).

Step 4

All 280 possible rules were implanted and then created a rule base. In this model, Mamdani Style Inference Mechanism has been castoff. Output variable Product-Quality is observed by using the MATLAB Fuzzy Tool Box for a particular 280 sets of inputs. For respective given set of input parameters i.e. [PORT, MAIN, SEC, REL, SUIT, PER, COMP, USA] as [3.25, 3, 3.75, 3.25, 3, 3.50, 3, 3.25] and then Rule Viewer help to realize the output Product-Quality level generated i.e 24.6 corresponding to this assumed set of input variables which is shown at Fig. 12.

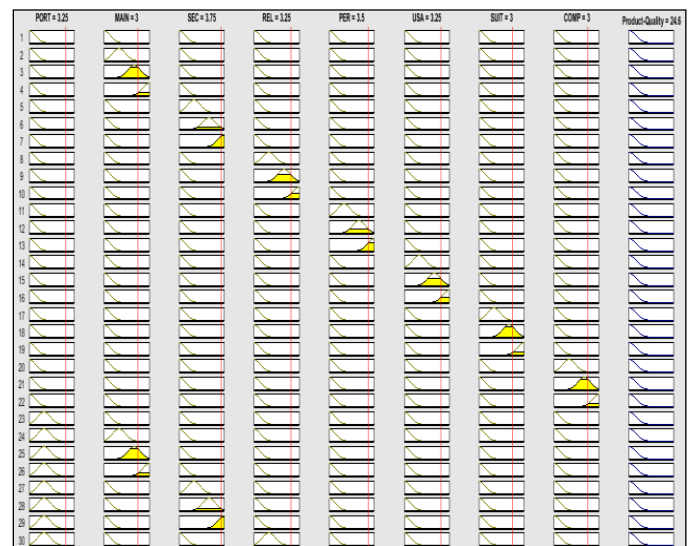


Fig. 12. Rule Viewer for Product-Quality Model

Step 5

After creating all possible 280 rules by using MATLAB Fuzzy Tool Box through Mamdani Style Inference Mechanism, we defuzzify the fuzzified outputs by using the Joint Membership Function by plotting on Two-Dimensional Surface View, as shown in Fig. 13. to 26 accordingly:

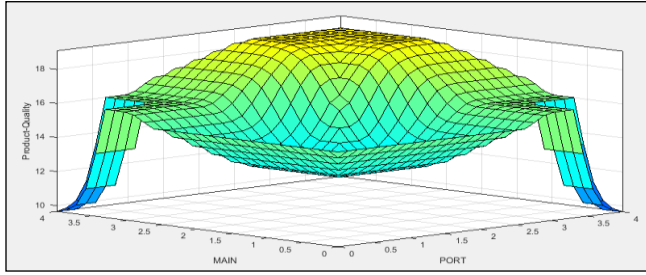


Fig. 13. Two-Dimensional Surface View with PORT (input) on X-axis, MAIN (input) on Y-axis, Product-Quality (output) on Z-axis

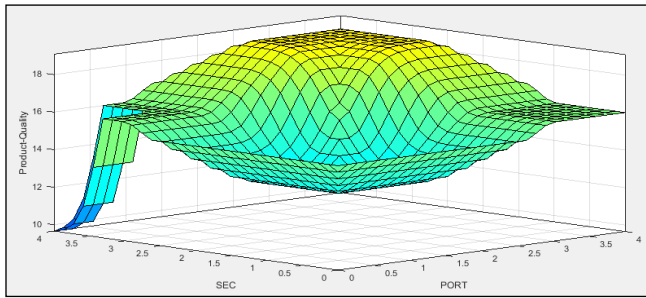


Fig. 14. Two-Dimensional Surface View with PORT (input) on X-axis, SEC (input) on Y-axis, Product-Quality (output) on Z-axis

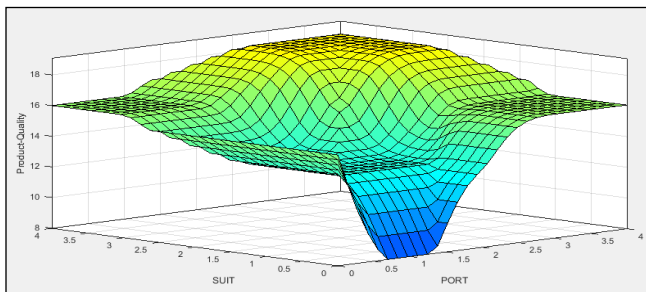


Fig. 15. Two-Dimensional Surface View with PORT (input) on X-axis, SUIT (input) on Y-axis, and Product-Quality (output) on Z-axis

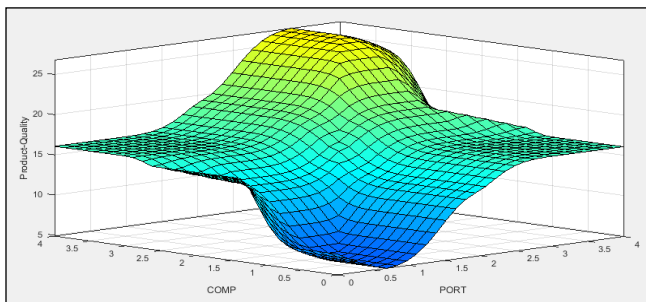


Fig. 16. Two-Dimensional Surface View with PORT (input) on X-axis, COMP (input) on Y-axis, and Product-Quality (output) on Z-axis

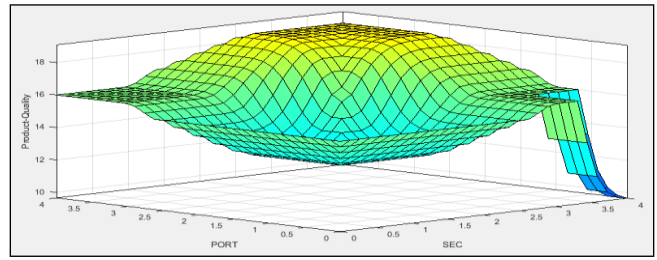


Fig. 17. Two-Dimensional Surface View with SEC (input) on X-axis, PORT (input) on Y-axis, and Product-Quality (output) on Z-axis

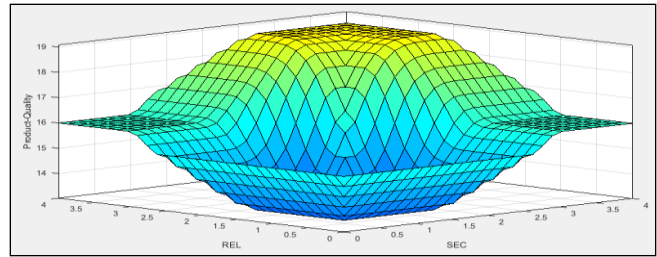


Fig. 18. Two-Dimensional Surface View with SEC (input) on X-axis, REL (input) on Y-axis, and Product-Quality (output) on Z-axis

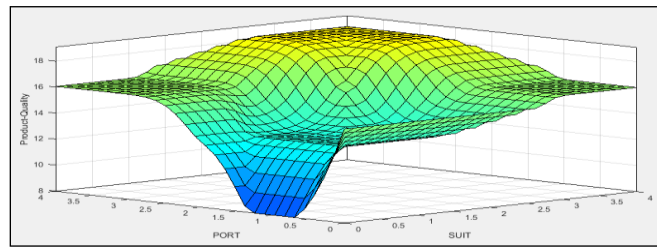


Fig. 19. Two-Dimensional Surface View with SUIT (input) on X-axis, PORT (input) on Y-axis, and Product-Quality (output) on Z-axis

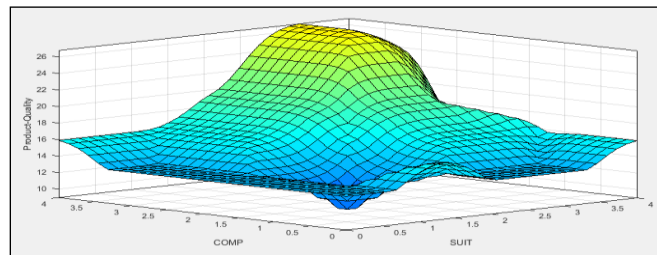


Fig. 20. Two-Dimensional Surface View with SUIT (input) on X-axis, COMP (input) on Y-axis, and Product-Quality (output) on Z-axis

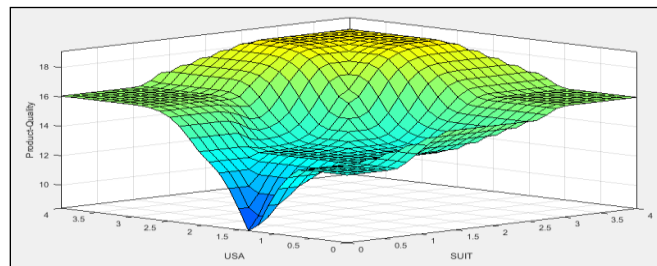


Fig. 21. Two-Dimensional Surface View with SUIT (input) on X-axis, USA (input) on Y-axis, and Product-Quality (output) on Z-axis

IV. RESULTS

After doing experiments on respective rules (as given in Annexure A), got following results as given on TABLE VI. regarding eight parameters i.e. PORT, MAIN, SEC, REL, SUIT, PER, COMP, and USA with respect to Product-Quality Level and Membership Grade of Product-Quality:

TABLE VI. PRODUCT QUALITY LEVEL AND MEMBERSHIP GRADE OF PRODUCT QUALITY FOR GIVEN RULES

Rule No.	PORT	MAIN	SEC	REL	SUIT	PER	COMP	USA	PQ Level	Membership Grade of Product-Quality
1	I _N	Low (8)	Min 1, Max 16							
28	I _L	I _N	I _H	I _N	Low (12)	Min 1, Max 16				
56	I	I _N	I _N	I _N	I _H	I _N	I _N	I _N	Low (13)	Min 1, Max 16
84	I _H	I _N	I _H	I _N	Avg (14)	Min 17, Max 23				
112	I	I	I _N	I _N	I _L	I _N	I _N	I _N	Avg (13)	Min 17, Max 23
140	I _H	I _H	I _N	I	Avg (16)	Min 17, Max 23				
168	I	I	I	I _N	I _N	I _N	I _H	I _N	Avg (17)	Min 17, Max 23
196	I _L	I _L	I _L	I _L	I _N	I _N	I _N	I _L	Low (12)	Min 1, Max 16
224	I _L	I _N	I _N	Low (14)	Min 1, Max 16					
252	I _L	I	I _N	Low (16)	Min 1, Max 16					
256	I _L	I _N	I _H	Avg (17)	Min 17, Max 23					
260	I	I	I	I	I	I	I _N	I _L	Avg (21)	Min 17, Max 23
276	I	I	I	I	I	I	I	I _H	High (25)	Min 24, Max 32
280	I _H	High (32)	Min 24, Max 32							

V. CASE STUDY

Internet banking is a major innovation in the field of banking. Earlier banking was in a very traditional manner, and there were no such innovations. Internet Banking is actually a facility under which the customers can perform the basic banking transactions electronically, round the clock throughout the world.

A system of banking in which customers can view their account details, pay bills, and transfer money through personal computers or from other devices by means of the internet. Normally internet banking provides account information, bill payments, online shopping payments, ticket booking, recharging prepaid phone, fund transfer, insurances services, investments services, credit cards facilities, and general customer services.

Data Collection Procedure

Useful data was collected from system analysts and domain experts of banking sector. For this, a set of questionnaire was given to respondents. This questionnaire was divided into two parts. First part of the questionnaire covers overall importance of product quality requirements for internet banking, whereas second part of questionnaire comprises how much each product quality requirement is important for internet banking by using scale from 1 to 4, such as: Not Important = 1, Low Important = 2, Important = 3, and High Important = 4.

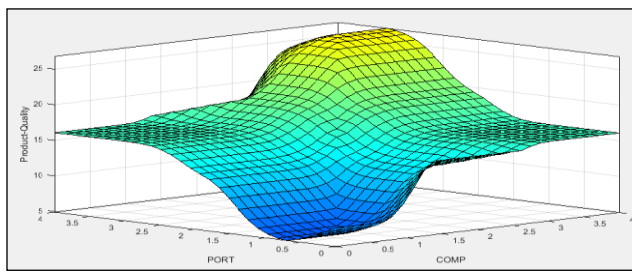


Fig. 22. Two-Dimensional Surface View with COMP (input) on X-axis, PORT (input) on Y-axis, and Product-Quality (output) on Z-axis

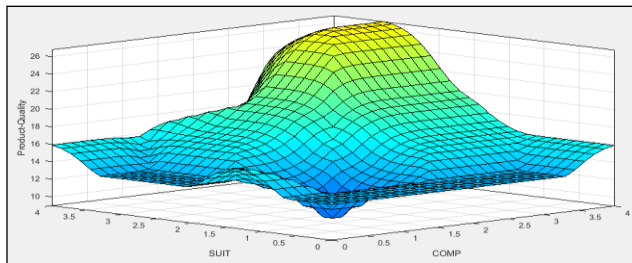


Fig. 23. Two-Dimensional Surface View with COMP (input) on X-axis, SUIT (input) on Y-axis, and Product-Quality (output) on Z-axis

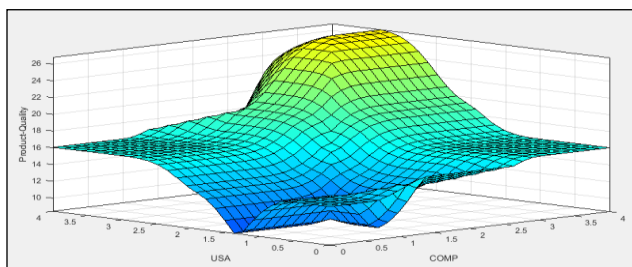


Fig. 24. Two-Dimensional Surface View with COMP (input) on X-axis, USA (input) on Y-axis, and Product-Quality (output) on Z-axis

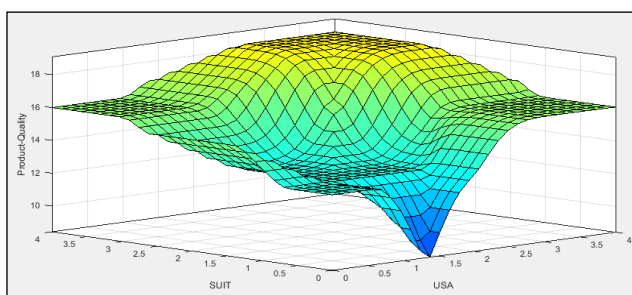


Fig. 25. Two-Dimensional Surface View with USA (input) on X-axis, SUIT (input) on Y-axis, and Product-Quality (output) on Z-axis

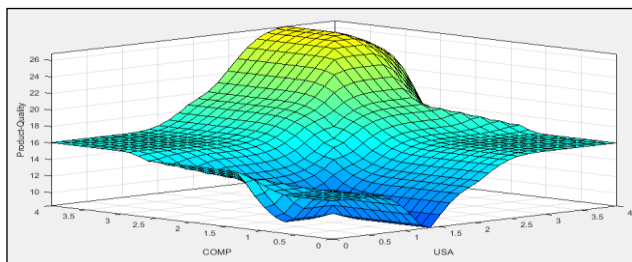


Fig. 26. Two-Dimensional Surface View with USA (input) on X-axis, COMP (input) on Y-axis, and Product-Quality (output) on Z-axis

25 respondents provided essential information regarding product quality requirements of internet banking, and further mentioned that which product quality requirement is high important for internet banking.

Data Analysis

While gathering the information, it was perceived that 72% of males and 28% of females were respondents. In which 44% of respondents were belongs to the age of above 45 years, 28% of respondents were belongs to the age of 35 - 44 years, 20% respondents were belongs to the age of 26 - 34 years, and 08% of respondents were belongs to the age of 18 - 25 years.

Information gathered analyzed and total weightage score were computed from observation of analysis. It was discovered that in the online banking, respondents were more worried about the security followed by performance efficiency, usability, reliability, portability, compatibility, maintainability, and functional suitability of internet banking services as per graph indicated in Fig. 27.



Fig. 27. Total Weightage of Product Quality Requirements

During that survey it was observed that security is the most important product quality requirement having 96 total weightage for internet banking from all other product quality requirements, so that is the reason Security is at first place. Here security consists of confidentiality, integrity, non-repudiation, accountability, and authenticity. Performance efficiency is also very important product quality requirement having 94 total weightage for internet banking, so that's why performance efficiency is at second place. Performance efficiency comprises of time behaviour, resource utilisation, and capacity. To have the disturbance free operations, respondents were concerned about usability having 89 total weightage of the internet banking that is at third place. Usability comprises on appropriateness recognisability, learnability, operability, user error protection, user interface aesthetics, and accessibility. Reliability is at fourth place having 87 total weightage that consists of maturity, availability, fault tolerance, and recoverability. Portability is at fifth place having 84 total weightage that comprises of adaptability, installability and replaceability. Compatibility is at sixth place having 81 total weightage that consists of co-existence, and interoperability. Maintainability is at seventh place having 78 total weightage, as it comprises of modularity, reusability, analysability, modifiability, and testability. Functional suitability is at eighth place having 76 total weightage that

consists of functional completeness, functional correctness, and functional appropriateness.

After completing survey, got data from respondents that were based on following inputs as shown in TABLE VII. regarding eight parameters i.e. PORT, MAIN, SEC, REL, SUIT, PER, COMP, and USA with respect to Product-Quality Level and Membership Grade of Product-Quality:

TABLE VII. PRODUCT QUALITY REQUIREMENTS INPUTS FROM SYSTEM ANALYSTS AND DOMAIN EXPERTS OF INTERNET BANKING WITH RESPECT TO THE PRODUCT QUALITY LEVEL AND MEMBERSHIP GRADE OF PRODUCT QUALITY

PORT	MAIN	SEC	REL	SUIT	PER	COMP	USA	PO Level	Membership Grade of Product-Quality
I ₂₄	High (32)	Min 24, Max 32							
I ₂₄	High (32)	Min 24, Max 32							
I	I ₂₄	I ₂₄	I	I ₂₄	I	I ₂₄	I	Avg (22)	Min 17, Max 23
I ₂₄	High (32)	Min 24, Max 32							
I ₂₄	High (32)	Min 24, Max 32							
I	I	I	I	I ₂₄	I ₂₄	I	I	High (24)	Min 24, Max 32
I	I ₂₄	I ₂₄	I	I ₂₄	I	I ₂₄	I	Avg (22)	Min 17, Max 23
I ₂₄	High (32)	Min 24, Max 32							
I	I	I ₂₄	I	I ₂₄	I ₂₄	I	I	High (25)	Min 24, Max 32
I	I ₂₄	I ₂₄	I	I ₂₄	I	I ₂₄	I	Avg (22)	Min 17, Max 23
I ₂₄	High (32)	Min 24, Max 32							
I	I	I ₂₄	I ₂₄	I	I ₂₄	I ₂₄	I ₂₄	High (29)	Min 24, Max 32
I	I ₂₄	I	I	I ₂₄	I ₂₄	I	I	Avg (23)	Min 17, Max 23
I	I ₂₄	I ₂₄	I	I ₂₄	I	I ₂₄	I	Avg (22)	Min 17, Max 23
I	I	I ₂₄	I	I	I ₂₄	I	I ₂₄	High (27)	Min 24, Max 32
I ₂₄	High (32)	Min 24, Max 32							
I	I	I ₂₄	I	I	I ₂₄	I	I ₂₄	High (27)	Min 24, Max 32
I	I ₂₄	I ₂₄	I	I ₂₄	I	I ₂₄	I	Avg (22)	Min 17, Max 23
I	I	I	I	I	I ₂₄	I	I	High (25)	Min 24, Max 32
I	I	I ₂₄	I ₂₄	I	I ₂₄	I ₂₄	I ₂₄	High (29)	Min 24, Max 32
I ₂₄	High (32)	Min 24, Max 32							
I	I ₂₄	I ₂₄	I	I ₂₄	I	I ₂₄	I	Avg (22)	Min 17, Max 23
I	I ₂₄	High (31)	Min 24, Max 32						
I	I	I	I	I	I ₂₄	I	I	High (25)	Min 24, Max 32
I ₂₄	High (32)	Min 24, Max 32							

For this model, Mamdani Style Inference Mechanism has been castoff. Output variable Product-Quality is observed by using the MATLAB Fuzzy Tool Box for a particular 25 sets of inputs received from respondents. For respective given set of input parameters i.e. [PORT, MAIN, SEC, REL, SUIT, PER, COMP, USA] as [3.36, 3.12, 3.84, 3.48, 3.04, 3.76, 3.24, 3.56] and then Rule Viewer helps to realize the output Product-Quality level generated i.e 26.2 corresponding to this assumed set of input variables which is shown below at Fig. 28.

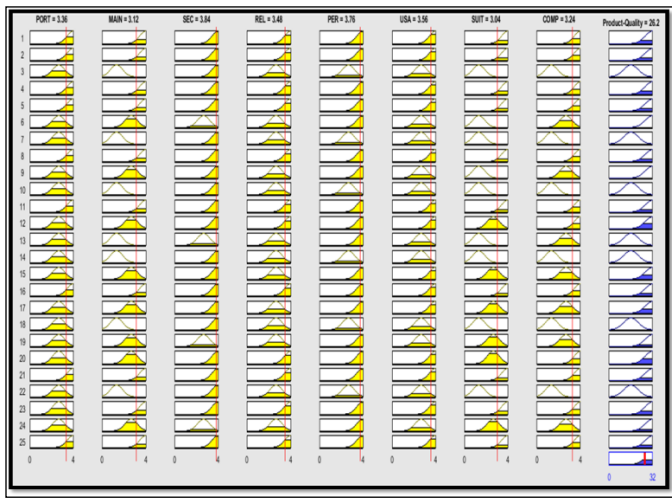


Fig. 28. Rule Viewer for Product-Quality Model with respect to the Respondents Inputs

After creating all 25 rules by using MATLAB Fuzzy Tool Box through Mamdani Style Inference Mechanism, defuzzifying the fuzzified outputs by using the Joint Membership Function by plotting on Two-Dimensional Surface View, as shown in Fig. 29 to 38 accordingly:

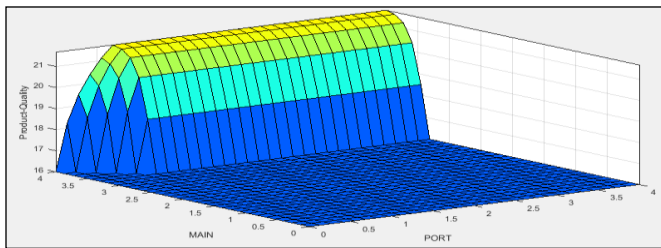


Fig. 29. Two-Dimensional Surface View with PORT (input) on X-axis, MAIN (input) on Y-axis, and Product-Quality (output) on Z-axis with respect to the Respondents Inputs

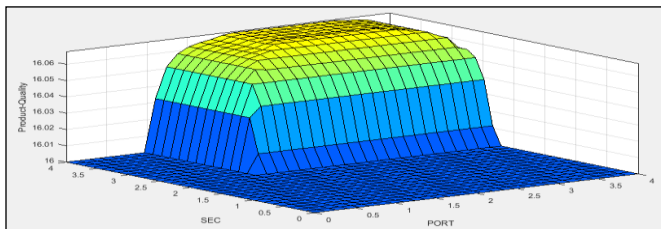


Fig. 30. Two-Dimensional Surface View with PORT (input) on X-axis, SEC (input) on Y-axis, and Product-Quality (output) on Z-axis with respect to the Respondents Inputs

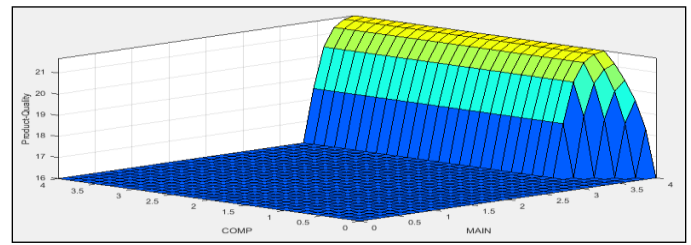


Fig. 31. Two-Dimensional Surface View with MAIN (input) on X-axis, COMP (input) on Y-axis, and Product-Quality (output) on Z-axis with respect to the Respondents Inputs

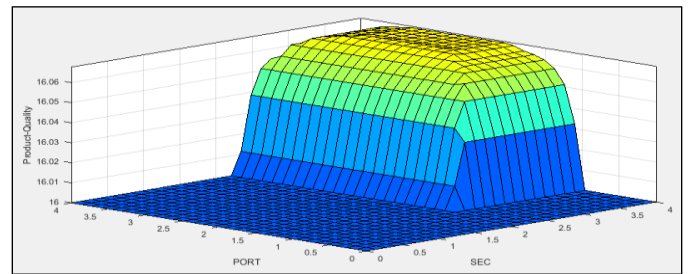


Fig. 32. Two-Dimensional Surface View with SEC (input) on X-axis, PORT (input) on Y-axis, and Product-Quality (output) on Z-axis with respect to the Respondents Inputs

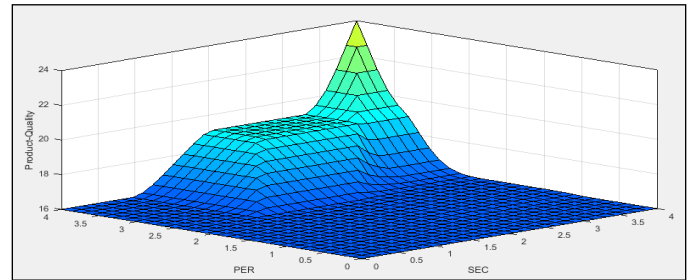


Fig. 33. Two-Dimensional Surface View with SEC (input) on X-axis, PER (input) on Y-axis, and Product-Quality (output) on Z-axis with respect to the Respondents Inputs

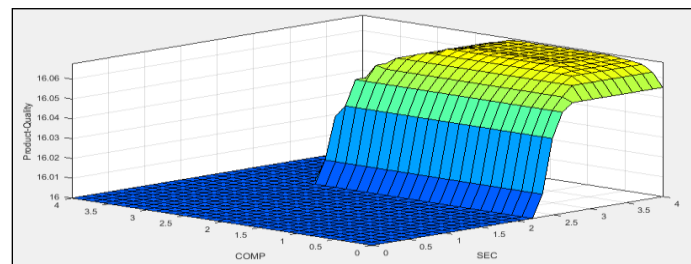


Fig. 34. Two-Dimensional Surface View with SEC (input) on X-axis, COMP (input) on Y-axis, and Product-Quality (output) on Z-axis with respect to the Respondents Inputs

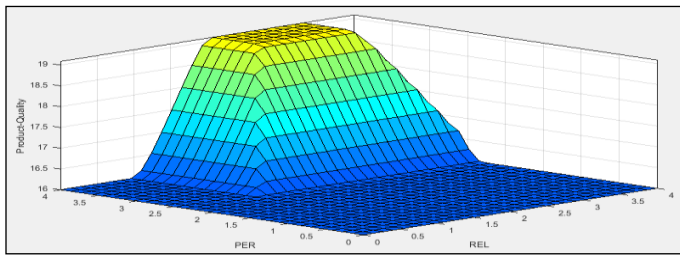


Fig. 35. Two-Dimensional Surface View with REL (input) on X-axis, PER (input) on Y-axis, and Product-Quality (output) on Z-axis with respect to the Respondents Inputs

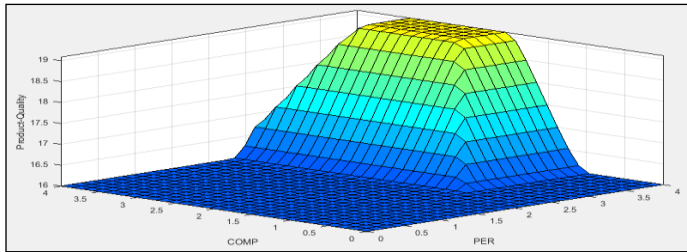


Fig. 36. Two-Dimensional Surface View with PER (input) on X-axis, COMP (input) on Y-axis, and Product-Quality (output) on Z-axis with respect to the Respondents Inputs

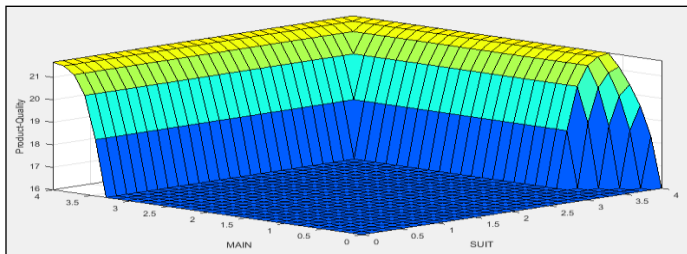


Fig. 37. Two-Dimensional Surface View with SUIT (input) on X-axis, MAIN (input) on Y-axis, and Product-Quality (output) on Z-axis with respect to the Respondents Inputs

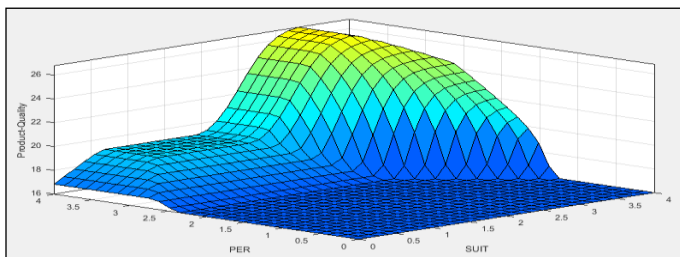


Fig. 38. Two-Dimensional Surface View with SUIT (input) on X-axis, PER (input) on Y-axis, and Product-Quality (output) on Z-axis with respect to the Respondents Inputs

VI. CONCLUSION

The measurement and quantification of quality requirements of DSS is a challenging task, because these quality requirements are in the qualitative form and can't be represented in a specific quantitative way. Although, several quality requirements methods for DSS have been proposed so far, but the research on analyzing quality requirements of DSS were limited.

Since last decades, researchers are focusing on quality requirements, because most of DSS only unsuccessful due to the inattention of quality requirements. As stakeholders requires a best quality DSS software, so we can't neglect quality requirements because of its primary importance into systems.

In this paper, a quantitative approach proposed for analyzing ISO / IEC 25010 product quality requirements based on fuzzy logic and likert scale for DSS which aims to quantify the quality requirements.

Proposed model has validated combined measure of Product-Quality based on PORT, MAIN, SEC, REL, SUIT, PER, COMP, and USA. After that, implemented proposed framework on a case study 'Internet Banking'. Got data from 25 system analysts and domain experts of banking sector and during that survey, we learned that respondents were more worried about the security followed by performance efficiency, usability, reliability, portability, compatibility, maintainability, and functional suitability.

In future, we are planning to develop a specific tool that will internment and manuscript these requirements.

REFERENCES

- [1] Busch, Axel. "Automated Decision Support for Recurring Design Decisions Considering Non-Functional Requirements." *Software Engineering & Management*. 2015.
- [2] Dabbagh, Mohammad, and Sai Peck Lee. "An Approach for Prioritizing NFRs According to Their Relationship with FRs." *Lecture Notes on Software Engineering 3.1* (2015): 1.
- [3] Atoum, Issa, and Chih How Bong. "Measuring Software Quality in Use: State-of-the-Art and Research Challenges." *arXiv preprint arXiv: 1503 - 06934* (2015).
- [4] Saadatmand, Mehrdad, and Sahar Tahvili. "A Fuzzy Decision Support Approach for Model-Based Tradeoff Analysis of Non-Functional Requirements." *Information Technology-New Generations (ITNG)*, 2015 12th International Conference on. IEEE, 2015.
- [5] Kaur, Harmeet, and Gurbinder N. Verma. "A Case Study upon Non-functional Requirements of Online Banking System". *International Journal of Computer Applications Technology and Research* Volume 4 – Issue 4, 220 - 225, (2015): 2319 –8656.
- [6] Zaib, Amna, Maha Chauhan, and Mehreen Sirshar. "A Review Analysis on Non-Functional Requirements and Causes of Failure of Projects." *International Journal of Computer and Communication System Engineering (IJCCSE)*, Vol. 2 (3), (2015): 490 -497.
- [7] Franca, Joyce MS, and Michel S. Soares. "SOAQM: Quality Model for SOA Applications based on ISO 25010." *Proceedings of the 17th International Conference on Enterprise Information Systems (ICEIS-2015)*, 60-70: 978 – 989 – 758 – 097 – 0.
- [8] Ravanello, Anderson, et al. "Performance measurement for cloud computing applications using ISO 25010 standard characteristics." *Software Measurement and the International Conference on Software Process and Product Measurement (IWSM-MENSURA)*, 2014 Joint Conference of the International Workshop on. IEEE, 2014.
- [9] Wojcik, Rob. "Eliciting and Specifying Quality Attribute Requirements." *Carnegie - Mellon Univ Pittsburgh PA Software Engineering Institute (SEI)*, 2013.
- [10] Saleh, Kassem. "Development of Non-functional Requirements for Decision Support Systems." *Proceedings of World Academy of Science, Engineering and Technology*. No. 65. World Academy of Science, Engineering and Technology, 2012.
- [11] Al-Jamimi, Hamdi A., and Moataz Ahmed. "Prediction of software maintainability using fuzzy logic." *Software Engineering and Service*

Science (ICSESS), 2012 IEEE 3rd International Conference on. IEEE, 2012.

[12] Ameller, David, et al. "How do software architects consider non-functional requirements: An exploratory study." 2012 20th IEEE International Requirements Engineering Conference (RE). IEEE, 2012.

[13] Kumar, Ravinder, Kiran Khatter, and Arvind Kalia. "Measuring software reliability: a fuzzy model." ACM SIGSOFT Software Engineering Notes 36.6 (2011): 1 - 6.

[14] Rao, A. Ananda, and Merugu Gopichand. "Four layered approach to non-functional requirements analysis." International Journal of Computer Science Issues 8.6 (2011).

[15] Liu, Shaofeng, et al. "Integration of decision support systems to improve decision support performance." Knowledge and Information Systems 22.3 (2010): 261 - 286.

[16] Mairiza, Dewi, Didar Zowghi, and Nurie Nurmuliani. "An investigation into the notion of non-functional requirements." Proceedings of the 2010 ACM Symposium on Applied Computing. ACM, 2010.

[17] Malik, Nasir Mahmood, et al. "Measurable & scalable NFRs using fuzzy logic and Likert scale." arXiv preprint arXiv: 0906 - 5393 (2009).

[18] Sadana, Vishal, and Xiaoqing Frank Liu. "Analysis of conflicts among non-functional requirements using integrated analysis of functional and non-functional requirements." Computer Software and Applications Conference, 2007. COMPSAC 2007. 31st Annual International. Vol. 1. IEEE, 2007.

[19] Skrobaková, Marketa, and Hana Kopacková. "Decision support systems or business intelligence: what can help in decision making?." Scientific papers of the University of Pardubice. Series D, Faculty of Economics and Administration. 10 (2006) (2006).

ANNEXURE

Analyzing PORT, MAIN, SEC, REL, SUIT, PER, COMP, USA Quality Requirements of DSS for Determining Product-Quality Level (Annexure A)

TABLE VIII. ANALYZING PORTABILITY, MAINTAINABILITY, SECURITY, RELIABILITY, FUNCTIONAL SUITABILITY, PERFORMANCE EFFICIENCY, COMPATIBILITY, AND USABILITY QUALITY REQUIREMENTS OF DSS FOR DETERMINING PRODUCT QUALITY LEVEL (ANNEXURE A)

Sr.	(Quality Requirements Inputs)								PQ Level
	PORT	MAIN	SEC	REL	SUIT	PER	COMP	USA	
1	I _N	I _N	I _N	I _N	I _N	I _N	I _N	I _N	PQ _{Low}
2	I _N	I _L	I _N	PQ _{Low}					
3	I _N	I	I _N	PQ _{Low}					
4	I _N	I _H	I _N	PQ _{Low}					
5	I _N	I _N	I _L	I _N	PQ _{Low}				
6	I _N	I _N	I	I _N	PQ _{Low}				
7	I _N	I _N	I _H	I _N	PQ _{Low}				
8	I _N	I _N	I _N	I _L	I _N	I _N	I _N	I _N	PQ _{Low}
9	I _N	I _N	I _N	I	I _N	I _N	I _N	I _N	PQ _{Low}
10	I _N	I _N	I _N	I _H	I _N	I _N	I _N	I _N	PQ _{Low}
11	I _N	I _N	I _N	I _N	I _L	I _N	I _N	I _N	PQ _{Low}
12	I _N	I _N	I _N	I _N	I	I _N	I _N	I _N	PQ _{Low}
13	I _N	I _N	I _N	I _N	I _H	I _N	I _N	I _N	PQ _{Low}
14	I _N	I _N	I _N	I _N	I _N	I _L	I _N	I _N	PQ _{Low}
15	I _N	I _N	I _N	I _N	I _N	I	I _N	I _N	PQ _{Low}
16	I _N	I _N	I _N	I _N	I _N	I _H	I _N	I _N	PQ _{Low}
17	I _N	I _N	I _N	I _N	I _N	I _N	I _L	I _N	PQ _{Low}
18	I _N	I _N	I _N	I _N	I _N	I _N	I	I _N	PQ _{Low}
19	I _N	I _N	I _N	I _N	I _N	I _N	I _H	I _N	PQ _{Low}
20	I _N	I _N	I _N	I _N	I _N	I _N	I _N	I _L	PQ _{Low}
21	I _N	I _N	I _N	I _N	I _N	I _N	I _N	I	PQ _{Low}
22	I _N	I _N	I _N	I _N	I _N	I _N	I _N	I _H	PQ _{Low}
23	I _L	I _L	I _N	PQ _{Low}					
24	I _L	I	I _N	PQ _{Low}					
25	I _L	I _H	I _N	PQ _{Low}					
26	I _L	I _N	I _L	I _N	PQ _{Low}				
27	I _L	I _N	I	I _N	PQ _{Low}				
28	I _L	I _N	I _H	I _N	PQ _{Low}				
29	I _L	I _N	I _N	I _L	I _N	I _N	I _N	I _N	PQ _{Low}
30	I _L	I _N	I _N	I	I _N	I _N	I _N	I _N	PQ _{Low}
31	I _L	I _N	I _N	I _H	I _N	I _N	I _N	I _N	PQ _{Low}
32	I _L	I _N	I _N	I _N	I _L	I _N	I _N	I _N	PQ _{Low}
33	I _L	I _N	I _N	I _N	I	I _N	I _N	I _N	PQ _{Low}
34	I _L	I _N	I _N	I _N	I _H	I _N	I _N	I _N	PQ _{Low}
35	I _L	I _N	I _N	I _N	I _N	I _L	I _N	I _N	PQ _{Low}
36	I _L	I _N	I _N	I _N	I _N	I	I _N	I _N	PQ _{Low}
37	I _L	I _N	I _N	I _N	I _N	I _H	I _N	I _N	PQ _{Low}
38	I _L	I _N	I _L	I _N	PQ _{Low}				
39	I _L	I _N	I	I _N	PQ _{Low}				
40	I _L	I _N	I _H	I _N	PQ _{Low}				
41	I _L	I _N	I _L	PQ _{Low}					
42	I _L	I _N	I	PQ _{Low}					
43	I _L	I _N	I _H	PQ _{Low}					
44	I	I _N	PQ _{Low}						
45	I	I _L	I _N	PQ _{Low}					
46	I	I	I _N	PQ _{Low}					

47	I	I _H	I _N	PQ _{Low}					
48	I	I _N	I _L	I _N	PQ _{Low}				
49	I	I _N	I	I _N	PQ _{Low}				
50	I	I _N	I _H	I _N	PQ _{Low}				
51	I	I _N	I _N	I _L	I _N	I _N	I _N	I _N	PQ _{Low}
52	I	I _N	I _N	I	I _N	I _N	I _N	I _N	PQ _{Low}
53	I	I _N	I _N	I _H	I _N	I _N	I _N	I _N	PQ _{Low}
54	I	I _N	I _N	I _N	I _L	I _N	I _N	I _N	PQ _{Low}
55	I	I _N	I _N	I _N	I	I _N	I _N	I _N	PQ _{Low}
56	I	I _N	I _N	I _N	I _H	I _N	I _N	I _N	PQ _{Low}
57	I	I _N	I _N	I _N	I _N	I _L	I _N	I _N	PQ _{Low}
58	I	I _N	I _N	I _N	I _N	I	I _N	I _N	PQ _{Low}
59	I	I _N	I _N	I _N	I _N	I _H	I _N	I _N	PQ _{Low}
60	I	I _N	I _L	I _N	PQ _{Low}				
61	I	I _N	I	I _N	PQ _{Low}				
62	I	I _N	I _H	I _N	PQ _{Low}				
63	I	I _N	I _L	PQ _{Low}					
64	I	I _N	I	PQ _{Low}					
65	I	I _N	I _H	PQ _{Low}					
66	I _H	I _N	PQ _{Low}						
67	I _H	I _L	I _N	PQ _{Low}					
68	I _H	I	I _N	PQ _{Low}					
69	I _H	I _H	I _N	PQ _{Low}					
70	I _H	I _N	I _L	I _N	PQ _{Low}				
71	I _H	I _N	I	I _N	PQ _{Low}				
72	I _H	I _N	I _H	I _N	PQ _{Low}				
73	I _H	I _N	I _N	I _L	I _N	I _N	I _N	I _N	PQ _{Low}
74	I _H	I _N	I _N	I	I _N	I _N	I _N	I _N	PQ _{Low}
75	I _H	I _N	I _N	I _H	I _N	I _N	I _N	I _N	PQ _{Low}
76	I _H	I _N	I _N	I _N	I _L	I _N	I _N	I _N	PQ _{Low}
77	I _H	I _N	I _N	I _N	I	I _N	I _N	I _N	PQ _{Low}
78	I _H	I _N	I _N	I _N	I _H	I _N	I _N	I _N	PQ _{Low}
79	I _H	I _N	I _N	I _N	I _N	I _L	I _N	I _N	PQ _{Low}
80	I _H	I _N	I _N	I _N	I _N	I	I _N	I _N	PQ _{Low}
81	I _H	I _N	I _N	I _N	I _N	I _H	I _N	I _N	PQ _{Low}
82	I _H	I _N	I _L	I _N	PQ _{Low}				
83	I _H	I _N	I	I _N	PQ _{Low}				
84	I _H	I _N	I _H	I _N	PQ _{Low}				
85	I _H	I _N	I _L	PQ _{Low}					
86	I _H	I _N	I	PQ _{Low}					
87	I _H	I _N	I _H	PQ _{Low}					
88	I _L	I _L	I _L	I _N	PQ _{Low}				
89	I _L	I _L	I	I _N	PQ _{Low}				
90	I _L	I _L	I _H	I _N	PQ _{Low}				
91	I _L	I _L	I _N	I _L	I _N	I _N	I _N	I _N	PQ _{Low}
92	I _L	I _L	I _N	I	I _N	I _N	I _N	I _N	PQ _{Low}
93	I _L	I _L	I _N	I _H	I _N	I _N	I _N	I _N	PQ _{Low}
94	I _L	I _L	I _N	I _N	I _L	I _N	I _N	I _N	PQ _{Low}
95	I _L	I _L	I _N	I _N	I	I _N	I _N	I _N	PQ _{Low}
96	I _L	I _L	I _N	I _N	I _H	I _N	I _N	I _N	PQ _{Low}
97	I _L	I _L	I _N	I _N	I _N	I _L	I _N	I _N	PQ _{Low}
98	I _L	I _L	I _N	I _N	I _N	I	I _N	I _N	PQ _{Low}
99	I _L	I _L	I _N	I _N	I _N	I _H	I _N	I _N	PQ _{Low}
100	I _L	I _L	I _N	I _N	I _N	I _N	I _L	I _N	PQ _{Low}
101	I _L	I _L	I _N	I _N	I _N	I _N	I	I _N	PQ _{Low}
102	I _L	I _L	I _N	I _N	I _N	I _N	I _H	I _N	PQ _{Low}
103	I _L	I _L	I _N	I _L	PQ _{Low}				
104	I _L	I _L	I _N	I	PQ _{Low}				
105	I _L	I _L	I _N	I _H	PQ _{Low}				
106	I	I	I _L	I _N	PQ _{Low}				
107	I	I	I	I _N	PQ _{Low}				
108	I	I	I _H	I _N	PQ _{Low}				
109	I	I	I _N	I _L	I _N	I _N	I _N	I _N	PQ _{Low}
110	I	I	I _N	I	I _N	I _N	I _N	I _N	PQ _{Low}
111	I	I	I _N	I _H	I _N	I _N	I _N	I _N	PQ _{Low}
112	I	I	I _N	I _N	I _L	I _N	I _N	I _N	PQ _{Low}
113	I	I	I _N	I _N	I	I _N	I _N	I _N	PQ _{Low}
114	I	I	I _N	I _N	I _H	I _N	I _N	I _N	PQ _{Low}

115	I	I	I _N	I _N	I _N	I _L	I _N	I _N	PQ _{Low}
116	I	I	I _N	I _N	I _N	I	I _N	I _N	PQ _{Low}
117	I	I	I _N	I _N	I _N	I _H	I _N	I _N	PQ _{Low}
118	I	I	I _N	I _N	I _N	I _N	I _L	I _N	PQ _{Low}
119	I	I	I _N	I _N	I _N	I _N	I	I _N	PQ _{Low}
120	I	I	I _N	I _N	I _N	I _N	I _H	I _N	PQ _{Low}
121	I	I	I _N	I _L	PQ _{Low}				
122	I	I	I _N	I	PQ _{Low}				
123	I	I	I _N	I _H	PQ _{Low}				
124	I _H	I _H	I _L	I _N	PQ _{Low}				
125	I _H	I _H	I	I _N	PQ _{Low}				
126	I _H	I _H	I _H	I _N	PQ _{Average}				
127	I _H	I _H	I _N	I _L	I _N	I _N	I _N	I _N	PQ _{Low}
128	I _H	I _H	I _N	I	I _N	I _N	I _N	I _N	PQ _{Low}
129	I _H	I _H	I _N	I _H	I _N	I _N	I _N	I _N	PQ _{Average}
130	I _H	I _H	I _N	I _N	I _L	I _N	I _N	I _N	PQ _{Low}
131	I _H	I _H	I _N	I _N	I	I _N	I _N	I _N	PQ _{Low}
132	I _H	I _H	I _N	I _N	I _H	I _N	I _N	I _N	PQ _{Low}
133	I _H	I _H	I _N	I _N	I _N	I _L	I _N	I _N	PQ _{Low}
134	I _H	I _H	I _N	I _N	I _N	I	I _N	I _N	PQ _{Low}
135	I _H	I _H	I _N	I _N	I _N	I _H	I _N	I _N	PQ _{Average}
136	I _H	I _H	I _N	I _N	I _N	I _N	I _L	I _N	PQ _{Low}
137	I _H	I _H	I _N	I _N	I _N	I _N	I	I _N	PQ _{Low}
138	I _H	I _H	I _N	I _N	I _N	I _N	I _H	I _N	PQ _{Average}
139	I _H	I _H	I _N	I _L	PQ _{Low}				
140	I _H	I _H	I _N	I	PQ _{Low}				
141	I _H	I _H	I _N	I _H	PQ _{Average}				
142	I _L	I _L	I _L	I _L	I _N	I _N	I _N	I _N	PQ _{Low}
143	I _N	I _N	I _N	I	I _N	I _N	I _N	I _N	PQ _{Low}
144	I _N	I _N	I _N	I _H	I _N	I _N	I _N	I _N	PQ _{Low}
145	I _N	I _N	I _N	I _N	I _L	I _N	I _N	I _N	PQ _{Low}
146	I _N	I _N	I _N	I _N	I	I _N	I _N	I _N	PQ _{Low}
147	I _N	I _N	I _N	I _N	I _H	I _N	I _N	I _N	PQ _{Low}
148	I _N	I _L	I _N	I _N	PQ _{Low}				
149	I _N	I	I _N	I _N	PQ _{Low}				
150	I _N	I _H	I _N	I _N	PQ _{Low}				
151	I _N	I _L	I _N	PQ _{Low}					
152	I _N	I	I _N	PQ _{Low}					
153	I _N	I _H	I _N	PQ _{Low}					
154	I _N	I _L	PQ _{Low}						
155	I _N	I	PQ _{Low}						
156	I _N	I _H	PQ _{Low}						
157	I	I	I	I _L	I _N	I _N	I _N	I _N	PQ _{Low}
158	I	I	I	I	I _N	I _N	I _N	I _N	PQ _{Low}
159	I	I	I	I _H	I _N	I _N	I _N	I _N	PQ _{Average}
160	I	I	I	I _N	I _L	I _N	I _N	I _N	PQ _{Low}
161	I	I	I	I _N	I	I _N	I _N	I _N	PQ _{Low}
162	I	I	I	I _N	I _H	I _N	I _N	I _N	PQ _{Average}
163	I	I	I	I _N	I _N	I _L	I _N	I _N	PQ _{Low}
164	I	I	I	I _N	I _N	I	I _N	I _N	PQ _{Low}
165	I	I	I	I _N	I _N	I _H	I _N	I _N	PQ _{Average}
166	I	I	I	I _N	I _N	I _N	I _L	I _N	PQ _{Low}
167	I	I	I	I _N	I _N	I _N	I	I _N	PQ _{Low}
168	I	I	I	I _N	I _N	I _N	I _H	I _N	PQ _{Average}
169	I	I	I	I _N	I _N	I _N	I _N	I _L	PQ _{Low}
170	I	I	I	I _N	I _N	I _N	I _N	I	PQ _{Low}
171	I	I	I	I _N	I _N	I _N	I _N	I _H	PQ _{Average}
172	I _H	I _H	I _H	I _L	I _N	I _N	I _N	I _N	PQ _{Average}
173	I _H	I _H	I _H	I	I _N	I _N	I _N	I _N	PQ _{Average}
174	I _H	I _H	I _H	I _H	I _N	I _N	I _N	I _N	PQ _{Average}
175	I _H	I _H	I _H	I _N	I _L	I _N	I _N	I _N	PQ _{Average}
176	I _H	I _H	I _H	I _N	I	I _N	I _N	I _N	PQ _{Average}
177	I _H	I _H	I _H	I _N	I _H	I _N	I _N	I _N	PQ _{Average}
178	I _H	I _H	I _H	I _N	I _N	I _L	I _N	I _N	PQ _{Average}
179	I _H	I _H	I _H	I _N	I _N	I	I _N	I _N	PQ _{Average}
180	I _H	I _H	I _H	I _N	I _N	I _H	I _N	I _N	PQ _{Average}
181	I _H	I _H	I _H	I _N	I _N	I _N	I _L	I _N	PQ _{Average}
182	I _H	I _H	I _H	I _N	I _N	I _N	I	I _N	PQ _{Average}

183	I _H	I _H	I _H	I _N	I _N	I _N	I _H	I _N	PQ _{Average}
184	I _H	I _H	I _H	I _N	I _N	I _N	I _N	I _L	PQ _{Average}
185	I _H	I _H	I _H	I _N	I _N	I _N	I _N	I	PQ _{Average}
186	I _H	I _H	I _H	I _N	I _N	I _N	I _N	I _H	PQ _{Average}
187	I _L	I _N	I _N	I _N	PQ _{Low}				
188	I _L	I _L	I _L	I _L	I	I _N	I _N	I _N	PQ _{Low}
189	I _L	I _L	I _L	I _L	I _H	I _N	I _N	I _N	PQ _{Low}
190	I _L	I _L	I _L	I _L	I _N	I _L	I _N	I _N	PQ _{Low}
191	I _L	I _L	I _L	I _L	I _N	I	I _N	I _N	PQ _{Low}
192	I _L	I _L	I _L	I _L	I _N	I _H	I _N	I _N	PQ _{Low}
193	I _L	I _L	I _L	I _L	I _N	I _N	I _L	I _N	PQ _{Low}
194	I _L	I _L	I _L	I _L	I _N	I _N	I	I _N	PQ _{Low}
195	I _L	I _L	I _L	I _L	I _N	I _N	I _H	I _N	PQ _{Low}
196	I _L	I _L	I _L	I _L	I _N	I _N	I _N	I _L	PQ _{Low}
197	I _L	I _L	I _L	I _L	I _N	I _N	I _N	I	PQ _{Low}
198	I _L	I _L	I _L	I _L	I _N	I _N	I _N	I _H	PQ _{Low}
199	I	I	I	I	I	I _L	I _N	I _N	PQ _{Average}
200	I	I	I	I	I	I _N	I _N	I _N	PQ _{Average}
201	I	I	I	I	I _H	I _N	I _N	I _N	PQ _{Average}
202	I	I	I	I	I _N	I _L	I _N	I _N	PQ _{Average}
203	I	I	I	I	I	I _N	I	I _N	PQ _{Average}
204	I	I	I	I	I	I _N	I _H	I _N	PQ _{Average}
205	I	I	I	I	I _N	I _N	I _L	I _N	PQ _{Average}
206	I	I	I	I	I _N	I _N	I	I _N	PQ _{Average}
207	I	I	I	I	I _N	I _N	I _H	I _N	PQ _{Average}
208	I	I	I	I	I	I _N	I _N	I _L	PQ _{Average}
209	I	I	I	I	I	I _N	I _N	I	PQ _{Average}
210	I	I	I	I	I _N	I _N	I _N	I _H	PQ _{Average}
211	I _H	I _H	I _H	I _H	I _L	I _N	I _N	I _N	PQ _{Average}
212	I _H	I _H	I _H	I _H	I	I _N	I _N	I _N	PQ _{Average}
213	I _H	I _N	I _N	I _N	PQ _{Average}				
214	I _H	I _N	I _L	I _N	PQ _{Average}				
215	I _H	I _H	I _H	I _H	I _N	I	I _N	I _N	PQ _{Average}
216	I _H	I _H	I _H	I _H	I _N	I _H	I _N	I _N	PQ _{Average}
217	I _H	I _H	I _H	I _H	I _N	I _N	I _L	I _N	PQ _{Average}
218	I _H	I _H	I _H	I _H	I _N	I _N	I	I _N	PQ _{Average}
219	I _H	I _H	I _H	I _H	I _N	I _N	I _H	I _N	PQ _{Average}
220	I _H	I _H	I _H	I _H	I _N	I _N	I _N	I _L	PQ _{Average}
221	I _H	I _H	I _H	I _H	I _N	I _N	I _N	I	PQ _{Average}
222	I _H	I _H	I _H	I _H	I _N	I _N	I _N	I _H	PQ _{Average}
223	I _H	I _H	I _H	I _H	I _N	I _N	I _N	I _N	PQ _{Average}
224	I _L	I _N	I _N	PQ _{Low}					
225	I _L	I	I _N	PQ _{Low}					
226	I _L	I _H	I _N	PQ _{Low}					
227	I _L	I _N	I _L	PQ _{Low}					
228	I _L	I _N	I	I _N	PQ _{Low}				
229	I _L	I _N	I _H	I _N	PQ _{Low}				
230	I _L	I _N	I _N	I _L	PQ _{Low}				
231	I _L	I _N	I _N	I	PQ _{Low}				
232	I _L	I _N	I _N	I _H	PQ _{Average}				
233	I	I	I	I	I	I _L	I _N	I _N	PQ _{Average}
234	I	I	I	I	I	I	I _N	I _N	PQ _{Average}
235	I	I	I	I	I	I	I _H	I _N	PQ _{Average}
236	I	I	I	I	I	I	I _N	I _L	PQ _{Average}
237	I	I	I	I	I	I	I _N	I	PQ _{Average}
238	I	I	I	I	I	I	I _N	I _H	PQ _{Average}
239	I	I	I	I	I	I	I _N	I _N	PQ _{Average}
240	I	I	I	I	I	I	I _N	I _N	PQ _{Average}
241	I	I	I	I	I	I	I _N	I _N	PQ _{Average}
242	I _H	I _L	I _N	PQ _{High}					
243	I _H	I	I _N	PQ _{High}					
244	I _H	I _N	I _N	PQ _{High}					
245	I _H	I _N	I _L	PQ _{High}					
246	I _H	I _N	I	PQ _{High}					
247	I _H	I _N	I _H	PQ _{High}					
248	I _H	I _N	I _L	PQ _{High}					
249	I _H	I _N	I _N	PQ _{High}					
250	I _H	I _N	I _N	PQ _{High}					

251	I _L	I _N	PQ _{Low}						
252	I _L	I	I _N	PQ _{Low}					
253	I _L	I _H	I _N	PQ _{Average}					
254	I _L	I _N	I _L	PQ _{Low}					
255	I _L	I _N	I	PQ _{Low}					
256	I _L	I _N	I _H	PQ _{Average}					
257	I	I	I	I	I	I	I _L	I _N	PQ _{Average}
258	I	I	I	I	I	I	I	I _N	PQ _{Average}
259	I	I	I	I	I	I	I _H	I _N	PQ _{Average}
260	I	I	I	I	I	I	I _N	I _L	PQ _{Average}
261	I	I	I	I	I	I	I _N	I	PQ _{Average}
262	I	I	I	I	I	I	I _N	I _H	PQ _{Average}
263	I _H	I _L	I _N	PQ _{High}					
264	I _H	I	I _N	PQ _{High}					
265	I _H	I _N	PQ _{High}						
266	I _H	I _N	I _L	PQ _{High}					
267	I _H	I _N	I	PQ _{High}					
268	I _H	I _N	I _H	PQ _{High}					
269	I _L	I _N	PQ _{Low}						
270	I _L	PQ _{Low}							
271	I _L	I	PQ _{Average}						
272	I _L	I _H	PQ _{Average}						
273	I	I	I	I	I	I	I	I _N	PQ _{Average}
274	I	I	I	I	I	I	I	I _L	PQ _{Average}
275	I	I	I	I	I	I	I	I	PQ _{High}
276	I	I	I	I	I	I	I	I _H	PQ _{High}
277	I _H	I _N	PQ _{High}						
278	I _H	I _L	PQ _{High}						
279	I _H	I	PQ _{High}						
280	I _H	PQ _{High}							

Analysis of IPv4 vs IPv6 Traffic in US

Mahmood-ul-Hassan^{1,4}, Muhammad Amir Khan^{2,3,4}, Khalid Mahmood^{2,4}, Ansar Munir Shah^{2,4}

¹Al-Jouf University, College of Science and Arts, Tabarjal Saudi Arabia

²College of Science and Arts, Department of Information Systems, Mahayel Aseer

King Khalid University, Abha Saudi Arabia

³Department of Electrical Engineering,

COMSATS Institute of Information Technology, University Road, Tobe Camp, 22060, Abbottabad, Pakistan

⁴Department of Computer Science

IIC University of Technology Cambodia

Abstract—It is still an accepted assumption that internet traffic is dominated by IPv4. However, due to introduction of modern technologies and concepts like Internet of Things (IoT) IPv6 has become the essential element. So keeping in mind the advancements in new technologies and introduced concepts to update the adoption of IPv6 on the internet. We want to find out what percentage of the IPv6 traffic is present in the Internet from last 6 years (2008-14) and to obtain the adoption curve of IPv6 native traffic by years to analyze if it is slow or fast. Also what are factors, constraints and limitations involve in the adoption of IPv6. Therefore, we have taken two data sets from the Caida website. The dataset belongs to OC-48 and OC-192 links from two data center of Equinix located at Chicago and Sanjose in the US. Finally compare the final curve with infographic of World IPv6 Launch to know how realistic it is and applied Linear Prediction techniques to see the future trend of the dataset obtained from the US population.

Keywords—IPv4; IPv6; Mobile node; IP Traffic; IID Testing

I. INTRODUCTION

Everything on Internet is identified with the IP and IoT has made the new paradigm of the Internet by recognising the devices with IP even if it is your camera or TV. And old IPv4 is not at all capable to provide IP addresses to such increasing number of connected devices which is more in number than the users themselves. According to cisco there will be 25 billion devices by 2015 and 50 billion by 2020 which is more than the population. Also from World IPv6 Launch there will be 20 billion devices online by the end of 2016. So we want to know how far the dreams have become the realities.

Internet was designed as an experiment in 1973 and launched in 1983. However, since 1981 IPv4 has been the de facto standard in the world of Internet routing. In the early 1980s, the benefits of IPv4 were unambiguous and that is why its adoption rates increased enormously. Later on in early 1990s, due to accrued demand for Internet end users, the adoption was grown exponentially, which has lifted concerns within the Internet Engineering Task Force (IETF) and other ISPs. At this point, we realized that a point will come when all of the IPv4 address space will be out of capacity. The questionable, 2^{32} i.e. 4.3 billion largest address space, now seemed to be finite. This caused the necessity for superior technology that would be able to cater the need for a larger address space and also allow for improved services. [1]

Prediction done by Cisco in September 2005, that the unadvertised address space of IPv4 will be exhausted in more or less 10 years [2]. US IPv4 policies revision began in 2008 to see what arrangements can be done to utilize the used pool of IPv4 [3]. But, still the last block was sold in 2011, there is some address space with major Internet service providers that have not yet been used, for instance according to an article publicized by MIT; US still has 1.5 billion IPv4 addresses out of 3.7 billion IPv4 addresses. This is the main reason, the US has a lot of these unused IPv4 address space and this caused a slow transformation to IPv6. [4]

Researchers are of the view, according to statistical analysis that by the end of 2012, there will be a need for IP addresses to connect approximately 3.6 billion devices throughout the world [5]. Several of these devices due to technology advancements would need multiple IP addresses to perform functions accordingly. Hence, 4.3 billion IPv4 address space is even less than sufficient for the whole networking world to work efficiently. Moreover, scalability of Network Address Translation (NAT), to translate multiple private addresses is limited. It provides with a disadvantage of limiting a peer to peer communication session with VOIP (Voice Over Internet Protocol) and IPsec (IP security) [6]. Also, some researchers have found that NAT transversal cost for the vendor of the application is so high to reach 500 million dollars per year [7,10]. However, using the IPv6 which allows peer to peer communication without the need of the intermediate server involving no cost.

Route aggregation is another benefit provided by IPv6 in an organised manner to analyze the network with geographically significance features. Summuration of routes can be done in a sequential manner. Such ease, reduces the total size of the routing information or table and hence cause the reduction in the load throughout the network. Memory usage is minimized to reduced rates if such an efficient IP protocol is to be utilized. In this way, less network resources are consumed in an efficient way with minimized associated cost.

Day by day, the availableness of the IPv4 address space is detractive so internet is in need for an enhanced technology for its survival. IPv6 has thousand trillions of a address space that would be sufficient enough to cater the exponentially increasing advancements of multiple IP usage technology

[8,9]. However, it is not the case that IPv6 only provides the advantage of enormous address space. Mobility is one of the important features of the IPv6 that helps in providing more than one IP addresses to multiple network interface[11]. By network interface we mean to say if let say we have a smart phone, then it has to network interface one is the WiFi and the other is the GSM internet interface. Seamless roaming can be achieved through the use of IPv6 as compared to IPv4. Moreover, both vendor and operator of telecom companies has the big benefit of utilizing the IPv6. Wireless Sensors devices used in BCI is significantly a decent example of IPv6 mobility.

Our contribution in this paper starts from the description of the some important features of IPv6 protocol. Then we analyse the dataset taken from the Caida website to know the percentage of the IPv6 and IPv4 traffic in the data networks of Chicago and Sanjose. In the final section of the article we have analysed and applied the Linear Prediction tools on the same dataset for further analysis.

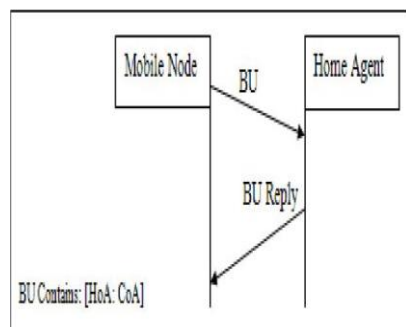


Fig. 1. Mobility Handshake between MN and HA using BU Messages

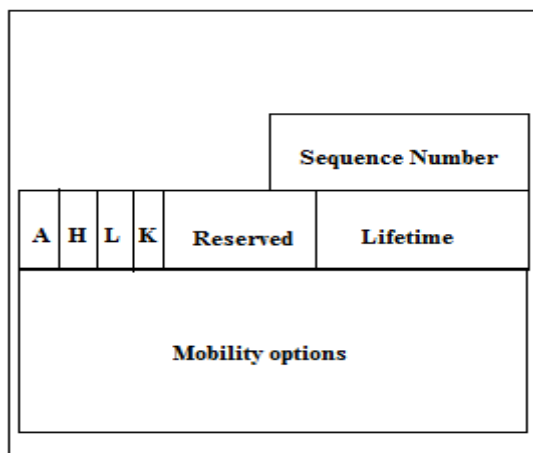


Fig. 2. BU Message send by a MN to HA or Correspondence Node

II. MOBILITY IN IPV6

In this section, we have assumed that a mobile device is IPv6 enabled and has moved to some other network. Now, we will describe that what steps are involved in its mobility procedure.

Registration in Home Agent (HA) Signaling messages:

Information included and why it is needed.

Home Agent Registration: Once a Mobile Node (MN) has completed agent discovery, it knows whether it is on its home network or a foreign network. If on its home network it communicates as a regular IP device, but if on a foreign network it must activate Mobile IP. This requires that it communicate with its home agent so information and instructions can be exchanged between the two. This process is called Home Agent Registration, or more simply, just registration. Describe through Figure 1.

Included Information: The BU (Binding Update) message is used and send by MN to notify the HA or the correspondent node of the binding information of CoA and HoA of the MN. A MN sends the BU message with its CoA and its HoA whenever it changes the point of attachment to internet and changes its CoA. The receiving node after receiving the BU message will create an entry to keep the binding information that also includes CoA and HoA. More information included in the single BU message is described below as seen in the Figure 2.

Sequence Number: It contains a sequence number (16 bit variable) for BU message to avoid replay attack. Also if present sequence number in the database is smaller then it will be removed with new greater sequence number having the recent update information.

Lifetime: This field specifies the proposed lifetime of the binding information included. When BU message is used for HA registration, the value must not be greater than the remaining lifetime of either HoA or the CoA of the MN. The value is in units of 4 s.

Mobility Options: BU message may have following mobility options:

- The Binding Authorization Data Option
- The Nonce Indices Option
- The Alternate CoA Option

Why this Information is Included:

This information is needed in order to tell the HA about the current location or more correctly current point of attachment of the MN with the respective network. This current point of MN refers to the temporary network in which MN is assigned a CoA to act as Locator. Whereas the permanent address of MN is HoA that will continue to act as Identifier. In this way, HA knows that MN is in other network and HA has to send the packets to MN using the CoA.

Security of the procedure: Security in this procedure is to have a unique key which is only known to MN and HA. This key is to be encrypted by using some cryptographic algorithms. The BU message must be secured by IPSec. IPSec stands for Internet Protocol security.

This protocol (IPSec) makes the virtual tunnel of each packet by encryption.

It ensures the confidentiality and integrity of each packet by ensuring a Virtual Private Network between nodes.

In the network given above in Figure 3, if Node1 wants to send data to MN which has been moved to a new point of attachment with the Router Rb, then it has two routes to use. Keeping in mind the cost of each link is 1.

Route1: Node1-Ra-HA-Rb-MN with Cost:4 and

Route2: Node1-Ra-Rb-MN with Cost:3.

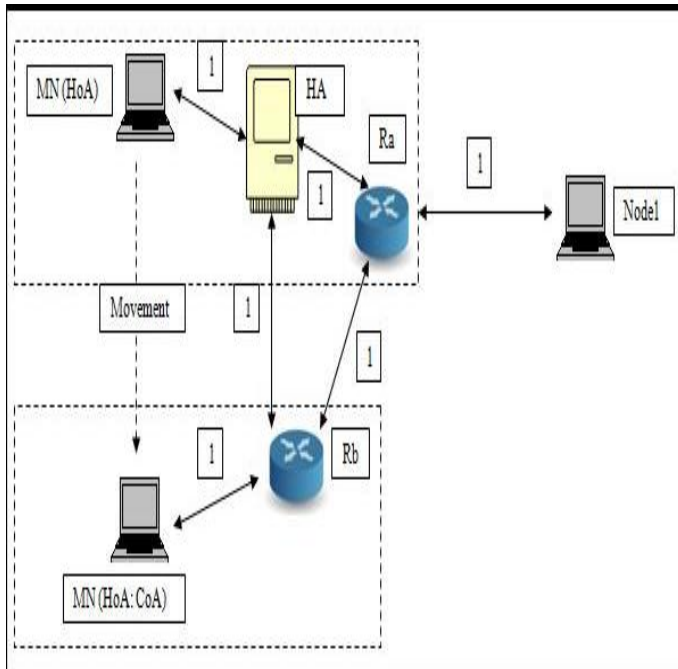


Fig. 3. Mobility in IPv6

Due to the mobility procedure adopted in IPv6, Route2 can not be utilized because it is not suitable due to security concerns and other limitations. However, Route2 has minimum cost then Route1. Therefore, traffic should only go through the HA to the MN which is actually the traffic exchange without route optimization. (A tunnel is established between the Home Agent and a reachable point for the Mobile Node in the foreign network.)

How the HA gets the packets sent to the HoA:

Consider the Figure 3 again, If Node1 wants to send data to MN which is in the temporary Network and having HoA and CoA respectively. Then it will send the data through HA using the IPv6 addresses.

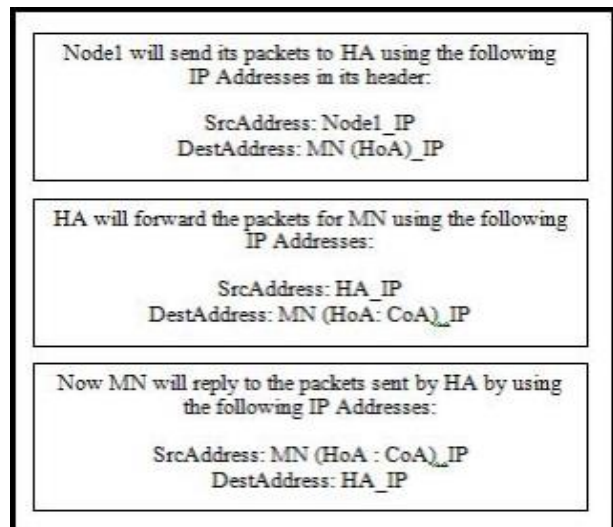


Fig. 4. Packets sent to HoA

III. ANALYSIS OF IP TRAFFIC

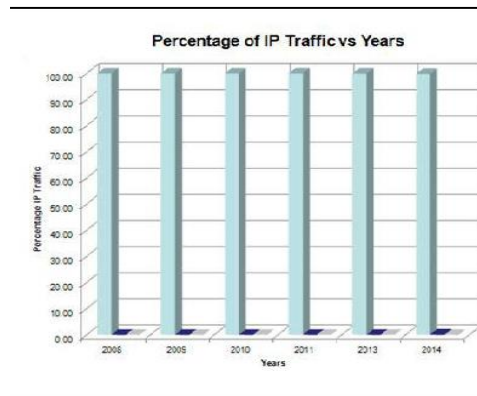
Before we start the analysis of the dataset taken from the Caida website, it is important to know and understand the terms we are going to use in our analysis which are as follows:

Allocation: The Entire IPv4 address space is maintained by IANA (Internet Assigned Number Authority)

IANA allocates blocks of addresses to 5 Regional Internets Registries (RIRs); US-Europe-Asia-LatinAmerica-Africa.

Assignment: The RIRs assigns IPv4 addresses to several ISPs or Network operators.

Advertisement: It denotes the part of assigned IPv4 addresses that are in real use in traffic.



(a)

TABLE I. PERCENTAGE IP TRAFFIC BY YEARS FROM CAIDA DATASET [1]

Chicago	Sanjose
IPv4:99.84 IPv6:0.15	IPv4:99.49 IPv6:0.51
IPv4:99.94 IPv6:0.03	IPv4:99.69 IPv6:0.31
IPv4:99.97 IPv6:0.02	IPv4:99.94 IPv6:0.64
IPv4:99.98 IPv6:0.01	IPv4:99.99 IPv6:0.01
IPv4:99.96 IPv6:0.04	IPv4:99.98 IPv6:0.02
IPv4:99.98 IPv6:0.01	IPv4:99.99 IPv6:0.01

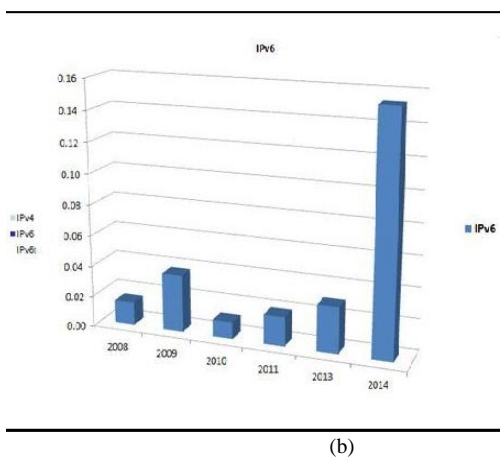


Fig. 5. (a). Percentage of IP Traffic vs Years in Chicago monitor (b).IPv4 vs IPv6

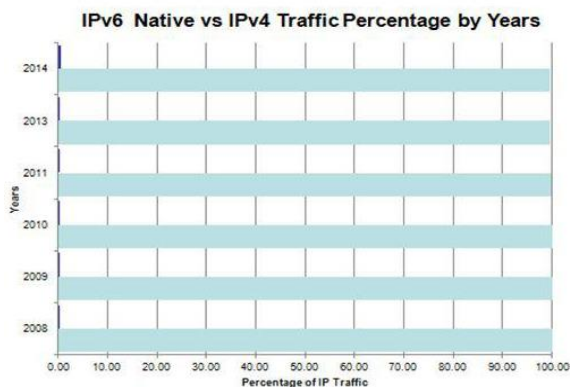


Fig. 7. (a) Percentage of IP Traffic vs Years in Sanjose monitor (b) Percentage of IPv4 and IPv6 Traffic

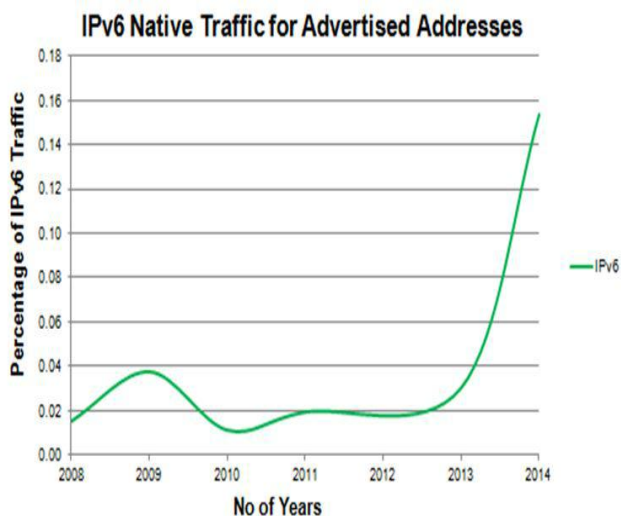
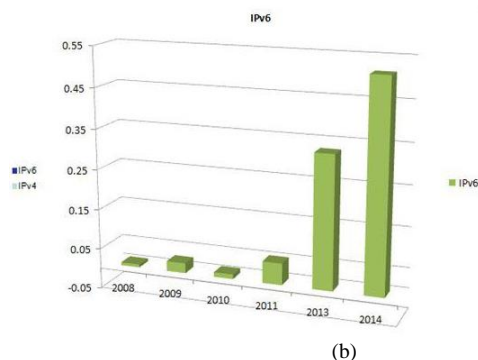


Fig. 6. Percentage Growth of IPv6 Native Traffic by Years in Chicago



In Figure 5, the data set belongs to the Chicago monitor and as I have mentioned in the first presentation that Chicago is the third largest city in the US after NY and LA with 9.5 million people. So analysis of this data is very important as it belongs to the huge population. IPv4, IPv6 and IPv6t (tunnel) traffic shown in the bar graph. As you have seen that over the last 6 years IPv4 is maintain the IP traffic percentage of more than 98-99 percent on average. However, if you analyse the Figure 6 as shown below you will come to know that overall progress of IPv6 traffic over six years is in increasing manner. Although increasing manner is shown but still the percentage is not more than 0.16 at the end of the Month of April 2014. IPv6 traffic tends to increase since the July 2012 as shown in the graph. And the affective reason for this is the event WorldIPv6Launch that has happened in the same time span. And in this launch was conducted by Internet Society in which major ISPs, AT and T, Google, Akamai and many more united to redefine the global internet by enabling all of their devices and equipment to use IPv6 permanently. More and more big companies are still joining this launch up till now and that is the reason that IPv6 traffic is continuously increasing.

Fig. 7. (a) Percentage of IP Traffic vs Years in Sanjose monitor (b) Percentage of IPv4 and IPv6 Traffic

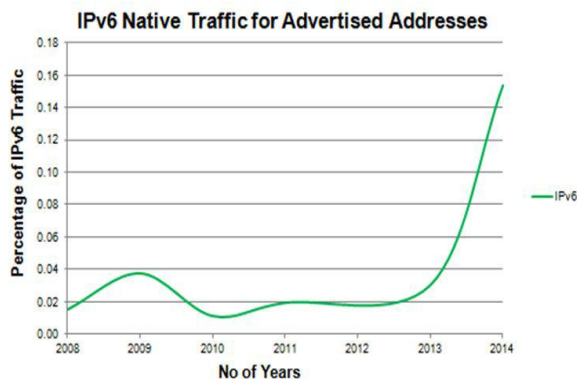


Fig. 8. Percentage Growth of IPv6 Native Traffic by Years in Sanjose

IV. RESULTS AND DISCUSSION

Reasons for Minimal IPv6 Traffic in the Backbone

As our data set belongs to the data centre in US so I am

only going to explain the specific reasons belongs to the region and some over all general issues in the IPv6 slow growth.

A. IPv4 Unadvertised Block

Referring again to my second presentation in which I have shown some statistics from the ARIN website also shown in Figure 7. If you see the bar from the ARIN which is responsible for allocation of IP blocks in US, there are more than 30 percent of the IPv4 addresses that are still unadvertised at the end of 2012 onwards. According to Colorado State University this percentage of unadvertised block was 42 percent i.e. 1.5 billion of addresses. So the first reason of very little IPv6 traffic is that in US IPv4 addresses are still unadvertised.

B. Transition Cost

It is one of the important issue raised and discussed by many analysts while talking about the migration to IPv6. There is a report issued by Arbor Networks in 2012 in which US Department of Commerce says that to implement an end to end IPv6 network the estimated cost is 25billion dollars for all the ISPs in the US.

C. Governmental Initiative

There are no official initiatives reported until 2012 from US government for the adoption of IPv6. Might be because of availability of IPv4 blocks or may be some other reasons as well. US government is not very active as of European, Japan and China. Japan has taken his lead in the adoption since 1999 and very next year IPv6 RFC 2460 been published. There government has taken a solid initiative by the name e-Japan initiative for the adoption of IPv6 since 2001 and declared as national mission. In the same manner China government has taken the initiative in the same year with the name China Next Generation Internet. So the point to make here is that US government should take some initiatives to announce some funds and technical support for ISPs to provide end to end IPv6 networks if they want to be in race of IPv6 adoption.

After the text edit has been completed, the paper is ready for the template. Duplicate the template file by using the Save As command, and use the naming convention prescribed by your conference for the name of your paper. In this newly created file, highlight all of the contents and import your prepared text file. You are now ready to style your paper; use the scroll down window on the left of the MS Word Formatting toolbar.

D. Linear Prediction Analysis

The first step that was taken in applying linear analysis and prediction to our dataset was to remove any trends, seasonal components, etc. associated with the dataset. In particular, the data used for this study does, in fact, have a trend associated with it. To estimate the trend, a polyfit function of order 1 was used. The trend was then removed from the data. After doing so, it needed to be determined whether or not the data was independently and identically distributed (IID). There are five hypotheses that can be tested to determine whether a process is IID. If the majority of the hypotheses are rejected, the data cannot be considered to be IID. Section 4.a, below, describes

the process in which the dataset is tested to determine whether or not it is IID.

E. IID Testing

The first of hypothesis is the Sample ACF. An autocorrelation function is performed on the data. Then, if three or more stems in the autocorrelation have a value greater than $1.96/\sqrt{n}$ (approximately 0.27), the process is said to not be IID. The second hypothesis that is tested is the Portmanteau test which takes a single statistic Q which is defined in the equation below.

$$Q = n \sum_{h=1}^H \epsilon_h p^2 \dots \dots \dots (1)$$

If the value Q is greater than the inverse of the chi-square distribution with h degrees of freedom, the hypothesis is rejected. This is because a higher Q signifies a higher correlation. The third hypothesis that is employed is the Turning Point Test. Where C is the number of turning points in the data, the following two equations show the average value for C and its variance for any IID sequence with length n .

$$\mu_c = \frac{2}{3}(n - 2) \dots \dots \dots (2)$$

$$\theta_c^2 = \frac{16n-29}{90} \dots \dots \dots (3)$$

The hypothesis is rejected if $\frac{|C-\mu_c|}{\theta_c} > 1.96$. The fourth hypothesis, the Difference-Sign Test, is similar to the third hypothesis except that instead of counting a value C , a new value S is counted. S corresponds to the number of instances where there is an increase in the value of the data at time index i , compared to the value of the data at time index $i-1$. (i.e. $y_i > y_{(i-1)}$) For a sequence to be considered IID, the following two equations must hold. $\mu_s = \frac{1}{2}(n - 1)$ and $\theta_s^2 = \frac{n+1}{12} \text{If } \frac{|S-\mu_s|}{\theta_s} > 1.96$, the hypothesis is rejected. The fifth and final hypothesis to be tested is called the Rank Test. This hypothesis is very similar to the Difference-Sign Test. The difference is that instead of finding a value S (the number of times when there is an increase from one time instance to the next time, $i-1$, instance, i), the test finds a value P , where P is the number of times that there is an increase from the value at one time index to another value at some future time index. (i.e. $y_i > y_{(i-1)}$) For an IID process, the following two equations give the statistical mean and variance for P . $\mu_p = \frac{1}{4n(n-1)}$

$\theta_p^2 = \frac{n(n-1)(2n+5)}{8}$ the hypothesis is rejected. The following is a section from the output of the MATLAB program, displaying the results of each IID hypothesis test.

IID hypothesis not rejected: Sample ACF
IID hypothesis not rejected: Portmanteau
IID hypothesis rejected: Turning Point

IID hypothesis rejected: Difference-Sign
IID hypothesis not rejected: Rank

F. Autocorrelation and Partial Autocorrelation Functions

With the trend removed from the dataset, the autocorrelation and partial autocorrelation functions are used to determine which type of process the data can be modelled after. The options available are as follows: autoregressive

(AR), moving-average (MA), and autoregressive-moving-average (ARMA). Although, it is possible to use more than one of these models for making predictions, it is better to search for and identify the one that is suited best to the dataset of interest. Once, we have settled on a choice, we can then employ that model to make a prediction about the adoption of IPv6 based on the traffic of IPv4. Also of note, it can be observed that the readings do appear to represent an IID process, despite the fact that one would expect a dependency on a number of factors such as time, transition cost, equipment cost, government policies, etc. The figure 9 is the result of the autocorrelation being performed on the data. As seen in the figure, the autocorrelation slowly decays to zero. After performing the partial autocorrelation function to the dataset, the following figure 10 was produced.

As demonstrated by Figure 10, it is suggested there exists a high correlation in the dataset between distant entries. However, this is not the case since the dataset is relatively small (53 entries) and, therefore, the most reliable statistics come from the first 12 lags. For this reason, the partial autocorrelation statistics after lag 20 have been removed, resulting in Figure 11 below. From both Figures 10 and 11, it can be determined that the appropriate model to use for making predictions based on this dataset is the AR (autoregressive) model of order AR Processes: We are given two procedures for predicting AR processes: the Yule-Walker method and the Burg method. For the analysis performed, both methods were employed and compared. Discussion of the comparison can be found in the following section.

Error Measurement and Comparison: To compare the Yule-Walker and the Burg method, the Mean Squared Error (MSE) and Mean Absolute Percentage Error (MAPE) of each method were taken. To accomplish this, the predicted values of each technique were compared against the test values (the last three values) of the

- MSE in Yule-Walker = 0.0022998
- MSE in Burg = 0.0022978
- MAPE in Yule-Walker = 0.024427 percent

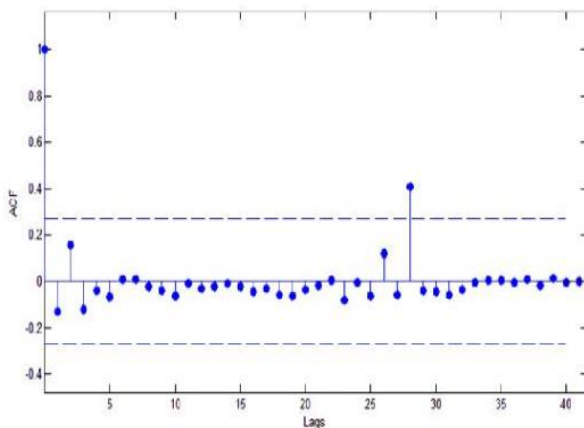


Fig. 9. Autocorrelation function

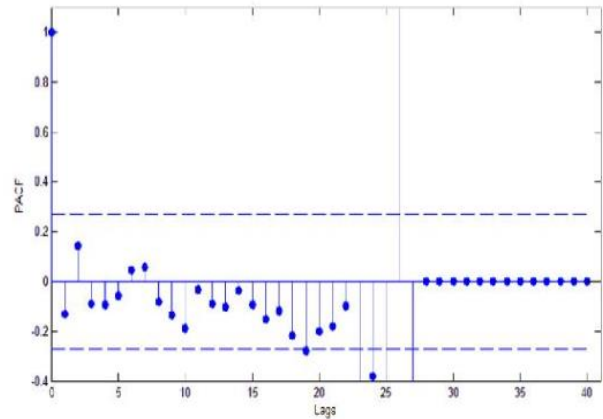


Fig. 10. Partial Autocorrelation function

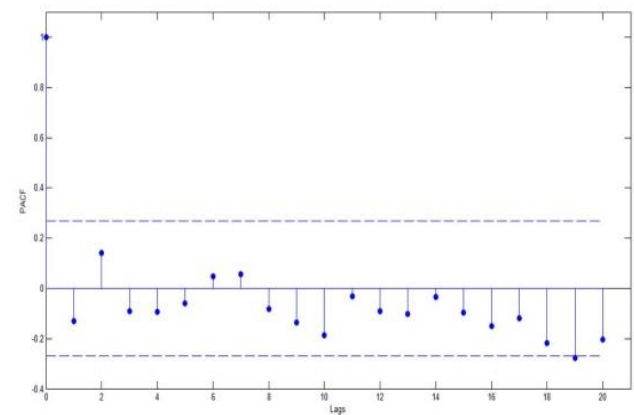


Fig. 11. Partial Autocorrelation function

V. CONCLUSION

As seen from these results, the Burg method yields a slightly lower error for both statistics. However, the difference is almost negligible, indicating that either method would be suitable from linear prediction. Additionally, both statistics (MAPE and MSE) are equally useful since the data is being compared does not come from different datasets and, therefore, the scale is not an issue in this case. Also from the analysis of the IP traffic, it is very clear that IPv6 traffic growth rate is increasing year by year. There is a constant increasing manner shown in the traffic, however it is the fact that IPv4 still the dominant protocol of the internet traffic today.

REFERENCES

- [1] M. Gomez et al., IPv6: A New Business Opportunity, 2008
- [2] T. Hain, A Pragmatic Report on IPv4 Address Space Consumption, The Internet Protocol Journal, vol. 8, pp.2-19, Sep.2005
- [3] <http://www.icann.org/en/news/announcements/announcement-2-05feb09-en.htm>
- [4] M. Orcutt, End of the Internet as we know it, June 24, 2011. http://www.technologyreview.com/printer_friendly_article.aspx?id=37859
- [5] C. Marsan, IPv6 vs. Carrier-grade NAT, June 7, 2010. <http://www.networkworld.com/news/2010/060710-tech-argument-ipv6-nat.html>

- [6] S. Shih-Pyng, H. Fu-Shen, H. Yu-Lun, L. Jia-Ning, "Network address translators: effects on security protocols and applications in the TCP/IP stack," *Internet Computing, IEEE*, vol.4, no.6, pp.42-49, Nov/Dec 2000; doi: 10.1109/4236.895015
- [7] M. P. Gallaher and B. Rowe, IPv6 Economic Impact Assessment, NIST, October, 2005.
- [8] N. Jauhari, Advantages of IPv6 - The next generation Internet, <http://linuxpoison.blogspot.com/2009/01/advantages-of-ipv6-next-generation.html>
- [9] M. Nikkhah, R. Guerin, Y. Lee, and R. Woundy, Assessing IPv6 Through Web Access: A Measurement Study and Its Findings, in *Proceedings of the Seventh Conference on emerging Networking EXperiments and Technologies*, 2011.
- [10] N. Sarrar, G. Maier, B. Ager, R. Sommer, and S. Uhlig, Investigating IPv6 Traffic - What Happened at the World IPv6 Day? in *Proceedings of the 13th International Conference on Passive and Active Network Measurement*, 2012.
- [11] E. Karpilovsky, A. Gerber, D. Pei, J. Rexford, and A. Shaikh, Quantifying the Extent of IPv6 Deployment, in *Proceedings of the 10th International Conference on Passive and Active Network Measurement*, 2009.

Clustering-based Spam Image Filtering Considering Fuzziness of the Spam Image

Master Prince

Department of Computer Science
Qasim University, College of Computer
Al Qasim, Kingdom of Saudi Arabia

Abstract—If there are pros, cons are always there. As email becomes a part of individual's need in our busy life with its benefits, it has negative aspect too by means of email spamming. Nowadays basic images with embedded text called image spamming have been used by the spammers as effective text spam filtering methods already been introduced. Tracking and stopping spam become challenge in the internet world because of versatility in the spam images. In this paper a novel model AFSIF (Autonomous Fuzzy Spam Image Filter) has been introduced. The basic idea behind AFSIF is, an spam image can combine several basic features of different spam images, so feature fusion weight of the image has been generated, which keeps combined feature of spam images and user preference as well. Here user preference has not been applied separately; it is used to calculate the fusion weight in terms of predefined topics (rule table).

Keywords—*versatility of spam image; feature fusion weight; cluster; rule table*

I. INTRODUCTION

As internet comes under the reach of majority of the people the email becomes the cheapest and effective way of advertisement. Spammers are using this medium by sending unwanted email message through junk email, earlier text-based spam emails have been used but now to by-pass the conventional email filtering technique they are using image-based spam. Image spam is actually a technique of embedding text (commercial content) into image by means of penetrating the text spam filter. Most email readers spend a non-trivial amount of time regularly deleting junk email messages, even as an expanding volume of such email occupies sever storage space and consume network bandwidth [1].

To protect the inbox from image spam emails, the filter should be able to distinguish between spam and ham images. The use of computer vision and pattern recognition techniques has been investigated in recent years and several text-based spam image filtering methods have been developed. Consequently some researchers proposed techniques based on detecting the presence of embedded text, and on characterizing text areas with low level feature like their size [2, 3] or their color distribution [2, 4].

However, some realistic problems that are not dealt well by the prevalent models. Like a spam image may belongs to several categories of spam images and similarity measurement is not able to discriminate because of small difference from

each of the class. And user preference we usually place at the end, an intelligent spammer can send every time new image to defeat the spam filter as the result end user spam it after seeing it.

In this paper a novel approach called AFSIF has been presented. The AFSIF comprises two steps filtration tasks. First stage is cluster based filter. The training data set is divided into clusters based on their similar features. The image is mapped with each of the cluster and declares as spam or ham depending on degree of similarity and dissimilarity respectively. If image is labeled as ham second stage comes into action, the feature fusion weight of the image has been calculated, which will be describe in subsequent sections. Finally, if image has been declared as spam by the user from inbox at the same time according to the similarity measure the spam image is associated with the closest cluster training data set. In this method user will experience negligible number of spam email because in second stage the fusion weight of the image contains user predefined topics.

The proposed AFSIF model has two advantages: 1) Incremental Learning System, 2) Features of spam image is fused with user pre-defined topics through feature fusion weight.

The rest of the paper is structured as follows. Section II gives the brief overview of literature reviewed, Section III presents the proposed AFSIF model, Section IV presents experiment and results, and finally in Section V some conclusions are drawn.

II. RELATED WORK

The wide use of image spam fetches the attention of researchers. Several attempts have been made to address filtering spam images by utilizing specific feature of image [3, 5]. For feature extraction there are various algorithms, such as principle component analysis (PCA), Independent component analysis (ICA), Partial Least squares (PLS) to transform graphical image into feature vector. In this paper, PCA has been used because of its suitability for data set in multiple dimensions.

Yih et al.[6] first address the grey mail problem and train two spam filters - the gray and b&w (ham/spam)filter on two disjoint subsets. Ming-wei Chang et al. [7] propose using the portioned logistic regression (PLR) to learn content and user model separately.

Here, Dataset accompanies combined set of gray and b&w and spam archive data provided by Giorgio Fumera's group has been considered.

III. AFSIF MODEL IMPLEMENTATION

Fig. 1 as shown is the proposed AFSIF model with two level filtering.

A. Feature Extraction & Clustering

First and very important task is to extract the feature of all the training set images; it plays a very vital role to improve the classification system. The spam archive images were taken from the spam archive data provided by Giorgio Fumera's group. In total, the images consider to this proposed work is 1204 JPG images with 964 spam images and 240 ham images and some personal data set.

Principle component analysis (PCA) is applied to convert the high dimension images into reduced set of feature vector without much loss of information. After feature extraction an image x_i will be represented as a feature vector with d dimension, where d is the number of image x_i features. Once all the images are represented with feature vector they clustered into group based on similarity measurement between the feature vectors [8] and user predefined topics. The weight of each image within each cluster is calculated by multiplying the difference form mean image of that cluster and feature vector of the image. The representative weight of each cluster is that whose average dissimilarity to all the images in the cluster is minimal.

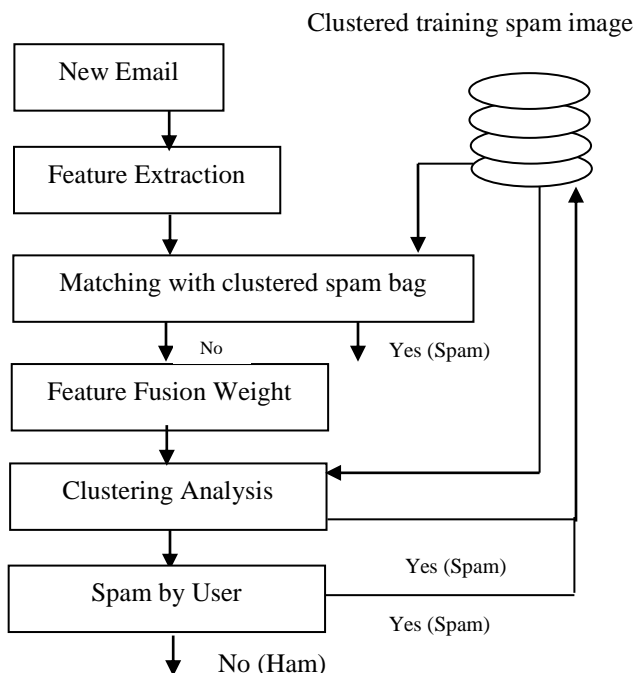


Fig. 1. AFSIF Model for spam image filtering

B. Similarity Measurement

For discrimination between spam and ham image the degree of similarity is measured. Let $p = \{p_1, p_2, \dots, p_{25}\}$ and $q = \{q_1, q_2, \dots, q_{25}\}$ are the feature vectors of two images p and

q . When calculating the degree of similarity of p and q , we use Euclidean distance defined by

The smaller the distance value is, the more similar the two images. In the matching process, the similarity evaluation leads to the mapping $R_{25} \rightarrow \{-1, +1\}$, where R_{25} represents the normalized 25 edge features of a new coming image, -1 and $+1$ denote ham, spam image respectively. So, Euclidean distance between new coming image and representative image of each cluster is compared. The new image is categorized as spam if smallest distance value is not more than a dissimilarity threshold otherwise treated as normal image.

If the image is labeled as ham the next level of filter comes into action.

C. Feature Fusion Weight Generation

The objective of FFW (Feature Fusion Weight) generation of the image is to obtain the feature vector of the given image whose feature slightly matches with more than one cluster. And smallest distance value from representative weight may be more than a dissimilarity threshold as the result spam image may bypass the filter. At the same time the user preference is also considered by means of rule table and fused with the feature vector to obtained FFW.

Fuzzy kohonen clustering network (FKCN) is employed to determine the fusion weight of the coming image corresponding to each cluster.

In Fig. 2 the input layer of the network, the feature vector of the coming image is given, the distance between the input image and cluster's representative image is calculated such that

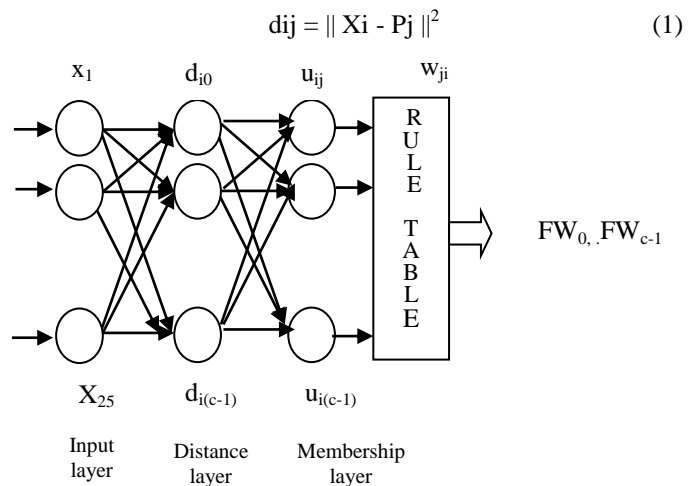


Fig. 2. Feature Fusion Weight Generation

where X_i denotes the input image and P_j denotes the j th representative image. In this layer degree of dissimilarity between coming image and the representative images is calculated. The membership layer calculates the similarity degree between coming image and representative images. If smallest distance value of the coming image from each of the representative is more than a dissimilarity threshold, then the similarity between the coming image and individual

representative image is represented by membership value from 0 to 1.

$$FW_i = \sum_{j=0}^{c-1} w_{ji} u_{ij} \quad (2)$$

where w_{ji} represents the representative image weight of the i th cluster. The representative image weights are designed in a rule table according to the user preference.

Table 1 describes the weight of the i th cluster representative image according to user preference. The size of the table may increase as much as clusters and user preferences increases

TABLE I. USER PREFERENCE RULE TABLE

If Similarity degree from RI						SPAM	HAM
C ₁	C ₂	C ₃			C _n		
1	>.65	<0.34				1	
	⋮	⋮			⋮	⋮	
	1						1
		>0.68				1	

D. Clustering Analysis

After calculating the FFW of the incoming image feature fusion weight is calculated such as,

$$FFW_i = \sum_{j=0}^{c-1} RI_j FW_j \quad (3)$$

Then compare with the clustered training image set by similarity evaluation as described in section B and label accordingly. If labeled as spam, the image is added to the closest cluster and trained, so the model justify the incremental learning system.

E. Filter by User

At the end there are possibility of leaking of filter, so when marked as spam by the user from inbox, the image added to the training set and rule table may also be updated with the new user preference.

IV. EXPERIMENTAL RESULTS

A. Training dataset

In order to evaluate the performance, the experiments are carried out by using the Personal dataset in [5] for two reasons. First, the Personal dataset is one of few public corpuses containing both spam images and normal images appeared in real email exchange. Furthermore, the spam images in this dataset can reflect the property of similarity among spam images. And 1204 JPG images with 964 spam images and 240 ham images (Giorgio Fumera’s group). After preprocessing through similarity measure and user preference these images are divided in to 25 clusters.

B. Performance measure

Two measurements are applied to evaluate the

performance of the proposed method; True Positive Rate (TPR) and False Positive Rate (FPR) which are computed as follows:

$$\text{True Positive Rate} = \frac{\text{Correctly detected}}{\text{Total number of images}}$$

$$\text{False Positive Rate} = \frac{\text{Incorrectly detected}}{\text{Total number of images}}$$

C. Results

Table II describes the results on personal and full dataset.

TABLE II. RESULTS ON PERSONAL & FULL DATASET

	Classified	TPR	FPR
Personal (350)	341	0.9742	0.02
Full (1554)	1456	0.9399	0.063

On personal dataset the results are more efficient than the general dataset.

V. CONCLUSION AND FUTURE WORK

As user preferences are added with the weight of the incoming image through rule table very less number of spam images bounces to the inbox. So, eliminating the need of extra filter for gray/spam for user preference.

For future work, further enhancement is needed in the rule table. Machine learning can be employed to prepare standard rule table and user can set their preference. Big Five Model of Personality can also be used to automate the system.

REFERENCES

- [1] Ian Stuart, sung-Hyuk cha and Charles tappert, “A Neural Network Classifiers for Junk Mail”, springerLink2004, pp-442-450.
- [2] H. B Aradhye, G. K. Myers, and J. A Herson. Image Analysis for Efficient Categorization of image-based Spam E-mail, Eighth International Conference on Document Analysis and Recognition (ICDAR’05), August 2005, pp. 914-918.
- [3] B. Biggio, G. Fumera, I. Pillai, and F. Roli. Image Spam Filtering Using Visual Information, 14th international Conference on Image Analysis and Processing (ICIAP 2007), September 2007, pp. 105-110.
- [4] Y. Gao, M. Yang, X. Zhao, B. Pardo, Y. Wu, T. N. Pappas, A. Choudhary. Image Spam Hunter, IEEE International Conference on Acoustics, Speech, and Signal Processing, pp. 1765-1768, 2008.
- [5] M. dredze, R. Gevanyahu, and A.E Bechrach, “ Learning Fast Classifiers for Image Spam”, in proc. CEAS ‘2007-2007.
- [6] W. Yih, R. McCann, and A. Kolcz. “Improving Spam Filtering by Detecting Gray Mail”, in proc CEAS’2007, 2007.
- [7] Ming-wei Chang , wen Tau Yih, and Robert McCnn. “Personalized Spam Filtering for Gray Mail”, in proc.’2008, 2008.
- [8] Ying He, Wengang Man, and Haibo He “Incremental Clustering-based Spam Image Filtering using Representative Images”, proc ICSEDMI 2011, 2011.

Overview of Technical Elements of Liver Segmentation

Nazish Khan*

Institute of Management Sciences,
Peshawar, Pakistan

Imran Ahmed

Institute of Management Sciences,
Peshawar, Pakistan

Mehreen Kiran

Institute of Management Sciences,
Peshawar, Pakistan

Awais Adnan

Institute of Management Sciences,
Peshawar, Pakistan

Abstract—Liver diseases are life-threatening, it's important to detect it tumor in early stages. So, for tumor detection Segmentation of the liver is a first and significant stride. Segmentation of the liver is a yet difficult undertaking in view of its intra patient variability in intensity, shape and size of the liver. The aim of this paper is to assemble a wide assortment of techniques and used CT scan dataset information for liver segmentation that will provide a decent beginning to the new researcher. There are different strategies from basic to advance like thresholding, active contour, region growing to graph cut is briefly abridge to give an outline of existing segmentation strategies. We review the concept of particular strategies and review their original ideas. Our idea is to provide information under which condition a chosen strategy will work or utilize.

Keywords—component; CT Scan; Liver; Dataset; Segmentation technique

I. INTRODUCTION

The liver is key and biggest organ among different organs of the body and provide exceptionally crucial task to our body to keep it free from toxins and harmful substances such as alcohol and medications. Its primary vital functions are: to filter the blood coming from digestive track, it supports all other organs of the body in some way, regulate the supply of body fuel by managing glucose level in our body, cleanse the blood by metabolizing alcohol and obliterating and neutralizing destructive substances, produce bile, which helps in digestion, manufacture many primary and essential proteins which provide resistance to infection and help in blood clotting and thickening. Its direct the supply of vitamins and mineral in our body.

According to Global Cancer Statistics [26] liver cancer fifth the most commonly diagnosed and the second driving reason for death among men and seventh in women. Distinct methods for liver cancer is a blood test, screening and biopsy. A biopsy is intrusive procedure and is exceptionally painful diagnostic technique for patients. That is why researchers are attempting to develop noninvasive techniques. In this way, before the detection of the liver pathology, liver must be segmented accurately.

Liver segmentation is challenging task to develop robust strategies for liver segmentation. Researchers are coping with this challenge to automatically segment the liver; exceedingly unique shapes and volume of liver, similar intensity value among adjacent organs (stomach, spleen, Aorta and abdominal wall), complicated liver structure and contrast media injection cause liver tissue to have different grey level value. Liver segmentation is still an open problem as a result of these challenges. At the time being, researchers are dealing with challenging tasks to increase accuracy in diagnosis and maintain the strategic distance from the need for biopsy (a small tissue of tumor is removed and analyzed) and surgery. These systems do not replace the radiologist, but only provide the second opinion in diagnosis and support radiologist to settle on their choice. Segmentation methods are categorized into 2 main categories; automatic and interactive method. An automatic method has no user intervention and are fully automated and free from user error. It potentially saves the time of operators. The semi-automatic required user intervention like refinement of binary mask and in the selection of seed points. General approach to deal with follow in automated and semi-automatic CAD (Computer Aided System) system is: Pre-processing, Liver segmentation, Lesion Detection, Feature extraction, Classification, Evaluation. Some paper applies the post processing also as indicated by their prerequisite. In pre-processing phase filters are utilized to enhance the image quality and features, furthermore to remove noise and contortion from images. liver segmentation, the liver is sectioned from other encompassing organs. Lesion are detected from segmented liver. Then features are extracted from the lesion area to categorize them either benign or malignant, primary or secondary tumors.

Different modalities are utilized for the diagnosis of liver pathology (liver cancer, cirrhosis, hepatitis) such as CT (Computed Tomography), MRI (Magnetic Resonance Imaging), (US)ultrasounds. According to research CT is the most preferred modality because CT is less costly than MRI. The CT data is collected in the form of DICOM (Digital Imaging and Communication in Medicine) image. DICOM images can be converted to many types, however, for medical

imaging it is ideal to utilize .PNG or .BMP. Many researchers work on Liver segmentation and propose different techniques. Each technique has its own merits and shortcomings.

The rest of the Paper is organized as follows section II Literature Review, section III we organize liver segmentation techniques overview, section IV we include conclusion to summarize our views. we place the dataset comparison table and techniques overview table at the end of paper.

II. LITERATURE REVIEW

Lim et al [2] Develop automatic liver segmentation using previous knowledge of liver position and use a deformable contour method based on morphological filtering operation. On the gradient label map Algorithm [2] perform deformable contouring. To reduce computational complexity and to decide suitable threshold histogram analysis is performed in the ELP (Estimated liver position). Proposed method uses multi scale morphological filter recursively with region labeling and clustering to detect search rang for deformable contouring. They use private dataset of 10 patients. Results are compared with manual segmentation by a radiologist. Graphical representation is shown below in Fig. 1

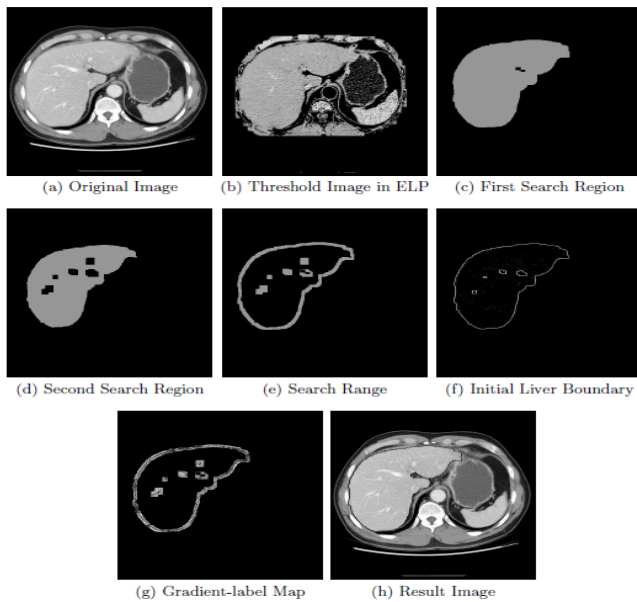


Fig. 1. Final Segmentation result

Suzuki et al [4] developed automatic liver extraction technique for contrast enhance CT images. The anisotropic diffusion filter uses for image denoising and preserving the shape of the liver. Scale specific gradient magnitude use to enhance liver boundary. These preprocessing results are passed to fast marching level set algorithm that initially refines the liver boundary and use as a rough estimate of liver shape and geodesic active contour combine with level set to extract liver shape. And estimate liver volume. Liver manually trace by the expert radiologist is use as a gold standard to compare the evaluation results of liver volume. Their local dataset consists of 15 patients. Overall accuracy is 98.4 %. Sensitivity, specificity and percent volume error is 91.1%, 99.1%, and 7.2 respectively. Limitation of the paper is small dataset. Graphical representation is shown in Fig. 2

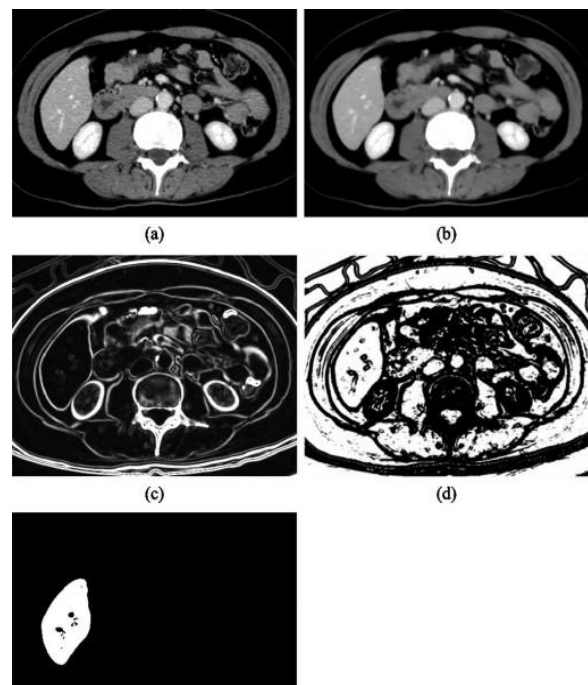


Fig. 2. (a) Original CT image (b) Anisotropic diffusion noise reduction (c) Scale specific gradient magnitude calculation (d) Non-linear grey scale conversion (e) Geodesic active contour segmentation

Massoptier et al [7] Develop innovative statistical model based approach. Active contour and gradient vector flow (GVF) are also used for hepatic segmentation. They analyzed nonlinear anisotropic diffusion and mean shift filter based on the processing time. To save processing time they follow mean shift filter. Clustering technique was used with their powerful initialization method for hepatic lesion segmentation. For lesion detection 82.6% Sensitivity and 87.6% specificity were achieved. Liver volume overlapping was evaluated by DSC (Dice Similarity Coefficient), FNR (false negative ratio), FPR (false positive ratio). They use their own private data set of 21 patient CT data set. From 46 lesions, they diagnosed different type of tumor 6 were HCC (Hepatocellular carcinoma), 2HDG (Hemangioma), 8HM (Hepatic metastases) and 5 have healthy patients.

Yusuf et al [10] proposed automatic 3D liver segmentation algorithm using a hybrid technique that combines morphological operations with graph cut method. Anisotropic diffusion filter for noise removal. In liver region estimation histogram analysis was performed and give their assumption that liver, grey value always lies between 75 to 200. For liver segmentation 2D and 3D Connected Component Labeling was performed. The graph cut technique was used for the refinement of CCL segmented liver and for reconstruction of liver surface. Accuracy check is performed in 10 cases of silver07 dataset. Computation time is less than 6 min. For evaluation of segmentation results, use 5 different evaluation metrics. Volumetric overlap error (VOE), Relative volume difference (RVD), Average symmetric surface difference (SD), Maximum symmetric surface difference (MSD) and Root mean square symmetric surface difference (RMSD). On average results VOE is less than 10%, RVD is 2.99% and RMSD is close to 2mm. Limitation of their

paper is, they face under segmentation problem when lesions are close to liver boundary. The dataset is very small.

Militzer et al [12] Proposed a novel system for automatically detecting and segmenting focal liver region from CT images. For classification, it utilizes a probabilistic boosting and thus provide fully automated detection and segmentation of the liver lesion simultaneously. They use hierarchical mesh-based shape representation for liver segmentation. Features selected in this paper are gray level statistical feature and Haar like features. Detection rate 77% could be achieved with the specificity of 0.93% and a sensitivity of 0.95% at the same time for lesion segmentation at the same setting.

S.S Kumar [15] presented an automatic segmentation of the liver lesion from CT radiographs. This paper utilizes medium filter, erosion, dilation, largest connected component as a pre-processing step. In post-processing, morphological operators are utilized to additionally refine the image and utilize basic region growing techniques for live segmentation and an alternate Fuzzy C-Means Clustering for tumor segmentation. He used 10 cases in his research work. The Technique result was contrasted and evaluated with the manual segmentation based on false positive rate, false negative rate, volume measurement error, spatial overlap and visual overlap. Pictorial results are shown in Figure .1 below.

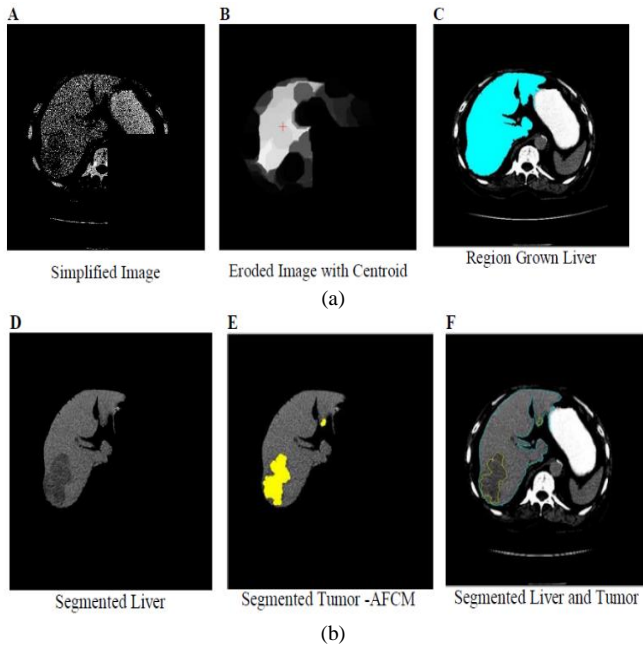


Fig. 3. (a) results of final liver segmentation using AFCM (b) results of final liver segmentation using AFCM

Belgherbi et al [17] A semi-automatic method developed for liver lesion extraction using mathematical morphology from CT images. In pre-processing for refinement of the liver they use dilation, erosion and anisotropic diffusion filter. For liver lesion, they use mathematical morphology, especially on the water shed technique. They use private data set. The proposed scheme achieves 92% Sensitivity & 99% Specificity. Brief graphical representation is shown in Fig.4. Here we

focus only on the graphical representation of the liver. Pictorial representation of liver lesion is not represented here.

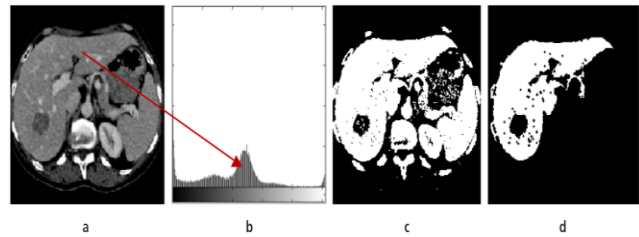


Fig. 4. Original image Histogram Thresholding Liver extraction

Marcin Ciecholewski [18] present novel method which automatically segments the liver shape. In CT scan images lumber section of the spine is utilized as seed point. After seed point selection, joint polylines are drawn to approximate the liver contour. These component polylines frames the components of two polygons eliminated from the image, which leaves only the segmented liver shape inside the image. Results are accessed on 13,30 images using Dice's similarity. Fig. 5 shows the results graphically.

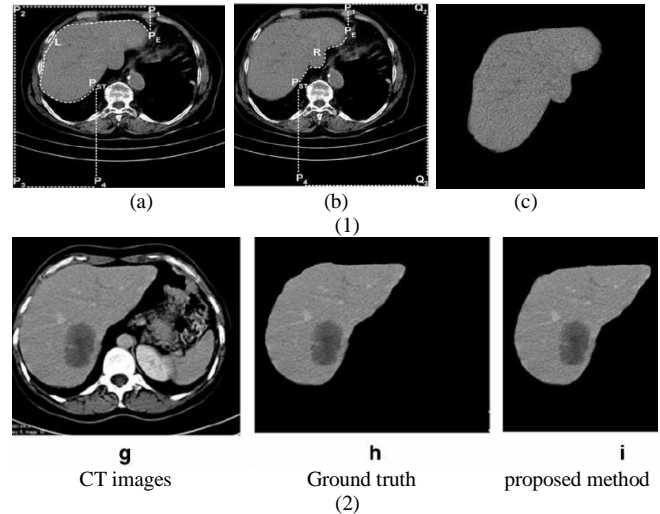


Fig. 5. (1) (a) Polygon with polyline L (b) Polygon with polyline R (c) segmented liver (2) Segmentation of liver shape using connected polylines

Anter et al [20] proposed hybrid approach using adaptive threshold and CCL for liver segmentation. For liver lesion segmentation, their method based on watershed [14] and region growing. RG algorithm has their limitation such as initial point position and its selection highly affects the segmentation result if they are not properly handling well. So, to overcome these limitations the integrate RG with watershed algorithm. Their 2 dataset consist of 112 Patients, one of radiopaedia website and aother is a local dataset collected from a local hospital. The computational time is 0.15s/slice. Overall, liver extraction accuracy is 93%. (CY) cyst (hepatocellular carcinoma), (HG)hemangioma, (HA) hepatic adenoma, (FNH) Focal nodular hyper plasma, (CC) cholangiocarcinoma, (MS)metastases achieve the accuracy 0.91, 0.90, 0.93, 0.95, 0.91, 0.94, 0.94 % respectively.

Aldeek et al [21] develop semiautomatic method using a Bayesian classifier for liver segmentation. In post processing, median filter and some filling operation are performed to further refine the classifier results. Dataset consists of 44 cases. Average area overlaps accuracy is over 87% They evaluate their results with the manual segmentation done by the expert radiologist. Graphical representation is shown in Fig.6.



Fig. 6. Bayesian classifier segmentation results

Altarawneh et al. [30] in this paper researcher modify DLSR (Distance regularization level set) [1] method because it does not work well in case of weak or without edges of liver images. [30] overcome this issue by introducing new Balloon force that control weak and without the edges region by slowing down and controlling the evaluation process. Balloon force was created by utilizing probability density energy function to control the speed and energy of the evaluation process. Experiments were performed on 10 cases of 512*512 pixels Slices. Graphical representation of comparison are shown in Fig. 7 below.

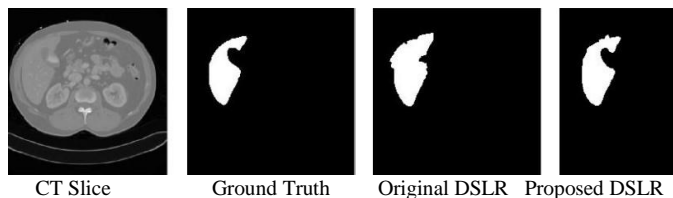


Fig. 7. Comparison of DLSR with proposed DSLR with balloon force

III. LIVER SEGMENTATION TECHNIQUES

A. Active contour

Active Contour is the energy minimizing, deformable curves that moves due to the effects of internal and external object forces to detect object boundary. Internal forces prevent deformation. "The contours are classified broadly into two categories as: parametric active contours and geometric active

contours. Parametric active contours are again classified into three types: Traditional snake, GVF snake and Ballon forces. Geometric active contours are Level set".

Basically, snakes use energy minimization to match a deformable model of an image.

General snake or active contour faces two problems:

- Initial model must be close to the boundary, otherwise it will show wrong result
- This model confronting issue to progress into boundary concavities.

AC [9][6][7] [13] model generally need manual initialization which is close to the image contour, otherwise it will give under or over segmentation problem. In case of liver segmentation, it causes over segmentation problem because liver share same intensity with the adjacent organs. It easily streams to the neighboring organ and cause over segmentation problem. Its performance is degraded if there should be an occurrence of irregular and higher intensities. Some of online available matlab codes are: [34] [35][36].

B. Gradient vector flow

Gradient Vector Flow [5] deal with two issues of the active contour model. It can converge into boundary concavities by calculating both concave and convex features. The traditional snake model must start close to the boundary while GVF [6][7] have the ability to start far from the boundary and till can converge to the image boundary. By and large, GVF demonstrate insensitivity to the initialization. GVF contour can handle broken object edges and subjective contour. Some of available code for GVF are in [37]

C. Level set

LS [13][16][30] semi-automatic techniques since it oblige user to select seed point. LS performance is very rely on the initial position, its performance increase when initial contour is placed close to the hepatic boundary. Its performance is degraded when the object is without edges or have weak edges[1]. The liver has the same intensity as the neighboring organs, hence cause over segmentation issues. Level set is time consuming for large computation. Level set strategy is additionally utilized for refinement of the liver segmentation. Some Matlab code accessible online is [38].

D. Graph cut

Graph Cuts, or max-flow/min-cut, is a generic technique for minimizing a specific form of energy called Markov random field (MRF) energy. In GC, image is represented using undirected weight graph. Each pixel represents every node of the graph. Each edge associated a couple of adjoining pixels. Similarity of grey level demonstrates the weight of edges between every match. Segmentation is the cut of graph. Every region speaks to a subgraph. The best cut is to make the subgraph similitude in a subgraph maximum and the closeness between the subgraph minimum. It is semi-automatic method since it requires user intervention for seed point selection which label the foreground and background. GC is not iterative method Graph cut is functioning admirably in homogenous area. Graph cut [3] can be made fully automatic

using different algorithms. In case of liver tumor segmentation general active contour come up short when tumor is near liver surface, graph cut handle this kind of active contour issues extremely well.

E. Adaptive thresholding

Adaptive Thresholding [3] is additionally called local or dynamic thresholding. The principal idea of adaptive threshold is to apply different threshold on the different region of the image. Adaptive threshold divide the image into small areas and apply different threshold in different areas. On adaptive threshold value at each pixel location is depends on the neighboring pixel intensity. This type of thresholding is functioning admirably in irregular intensities and can handle the lightening condition extremely well. Adaptive threshold work on a pixel level, it sets all the pixel as foreground whose intensity value is greater than a certain threshold and all other pixels as background. Adaptive threshold work on color and grey scale image by converting it into a binary image. Adaptive threshold follow two approaches to find the threshold for every pixel: (i) the *Chow and Kaneko* approach and (ii) *local* thresholding. General online link for adaptive matlab code in [39].

F. Region growing

Region Growing [15][20][23][19] technique is semi-automatic strategy, since user interaction is required as the seed point is chosen by the user. RG method divides the image into regions according to predefine basis. This technique is initiates utilizing seed point, and examine the neighboring pixel either utilizing 4 connectivity or 8 connectivity, it iteratively adds the pixel to different region as indicated by predefined criteria. The criteria could be pixel intensity, gray level texture or color. In case of liver segmentation this technique gives great outcomes in contrast enhance images. Its effectiveness is relying on the determination of the seed point. Some of the RG code available online are [31][32][33].

G. Fuzzy clustering mean(fcm)

FCM is developed by dunn [40] is widely utilized in medical image processing. Its originate from the k mean algorithm. In k mean algorithm, each pixel is belonging to only one k cluster which is not feasible in case the of liver segmentation. FCM overcomes this issue by utilizing membership function which shows the belongings of the pixel to the cluster. FCM is fuzzy clustering technique which allows a pixel to belong to one or more clusters. FCM is a semi-automatic method. Some parameters like the selection of centroid, the degree of fuzziness and stopping criteria highly effects the performance of the FCM. In case of liver segmentation. FCM is mostly used for tumor segmentation [15] from the CT data.

H. Statistical shape model(ssm)

SSM [28][29][11] are find extremely effective in liver segmentation. The liver has an exceptionally varying shape. In this approach, probabilistic model is made to adapt to the varying shape of the liver. SSM can deal with the limitation of gray level techniques extremely well. During segmentation of liver, grey level techniques frequently appear under or over segmentation issues when the tumor is close to liver boundary.

This constraint of grey level techniques can handle utilizing SSM. Utilizing the prior knowledge SSM can deal unclear boundary of the liver extremely well. SSM focus on the shape of the liver. Limitation of shape based method and classifier based method [8][23] is they require great number of training dataset.

IV. CONCLUSION

The different segmentation techniques review has been done in this paper. Here the review of preprocessing, main segmentation technique, and their dataset information is provided in the form of a table. Comparative evaluation of different method is not possible in light of the fact that every author utilizes small private dataset set and different performance measure criteria are utilized. For objective comparison, for the most part acknowledge performance measures are required. From review of the techniques, it is concluded that there is still need to discover robust and efficient method for liver segmentation. As the liver is exceptionally difficult organ to handle and segment. Each existing method has its own advantage and disadvantages they are not full robust. Future work is to cover the classification techniques for liver tumor.

REFERENCES

- [1] Li, Chunming, et al. "Distance regularized level set evolution and its application to image segmentation." *IEEE transactions on image processing* 19.12 (2010): 3243-3254.
- [2] Lim, Seong-Jae, Yong-Yeon Jeong, and Yo-Sung Ho. "Automatic liver segmentation for volume measurement in CT Images." *Journal of Visual Communication and Image Representation* 17.4 (2006): 860-875.
- [3] Massotier, Laurent, and Sergio Casciaro. "Fully automatic liver segmentation through graph-cut technique." *2007 29th Annual International Conference of the IEEE Engineering in Medicine and Biology Society*. IEEE, 2007.
- [4] Rusko, Laszlo, et al. "Fully automatic liver segmentation for contrast-enhanced CT images." *MICCAI Wshp. 3D Segmentation in the Clinic: A Grand Challenge 2.7* (2007).
- [5] Gui, Tianyi, Lin-Lin Huang, and Akinobu Shimizu. "Liver segmentation for CT images using an improved GGVF-snake." *SICE, 2007 Annual Conference*. IEEE, 2007.
- [6] Alomari, Raja S., Suryaprakash Kompalli, and Vipin Chaudhary. "Segmentation of the liver from abdominal CT using Markov random field model and GVF snakes." *Complex, Intelligent and Software Intensive Systems, 2008. CISIS 2008. International Conference on*. IEEE, 2008.
- [7] Massotier, L., & Casciaro, S. (2008). A new fully automatic and robust algorithm for fast segmentation of liver tissue and tumors from CT scans. *European radiology*, 18(8), 1658-1665.
- [8] Mala, K., V. Sadasivam, and S. Alagappan. "Neural network based texture analysis of liver tumor from computed tomography images." *International Journal of Biological and Life Sciences* 2.1 (2006): 33-40.
- [9] Jiang, Huiyan, and Qingshui Cheng. "Automatic 3D segmentation of CT images based on active contour models." *Computer-Aided Design and Computer Graphics, 2009. CAD/Graphics' 09. 11th IEEE International Conference on*. IEEE, 2009.
- [10] Yussuf, Wan Nural Jawahir Hj Wan, and Hans Burkhardt. "Integration of Morphology and Graph-based Techniques for Fully Automatic Liver Segmentation." *Majlesi Journal of Electrical Engineering* 4.3 (2010): 59-66.
- [11] Lamecker, Hans, Thomas Lange, and Martin Seebass. *Segmentation of the liver using a 3D statistical shape model*. Konrad-Zuse-Zentrum für Informationstechnik, 2004.

- [12] Militzer, Arne, et al. "Automatic detection and segmentation of focal liver lesions in contrast enhanced CT images." *Pattern Recognition (ICPR), 2010 20th International Conference on*. IEEE, 2010.
- [13] Suzuki, Kenji, et al. "Computer-aided measurement of liver volumes in CT by means of geodesic active contour segmentation coupled with level-set algorithms." *Medical physics* 37.5 (2010): 2159-2166.
- [14] Wang, Ning, Lin-Lin Huang, and Baochang Zhang. "A fast hybrid method for interactive liver segmentation." *Pattern Recognition (CCPR), 2010 Chinese Conference on*. IEEE, 2010.
- [15] Kumar, S. S., R. S. Moni, and J. Rajeesh. "Automatic segmentation of liver and tumor for CAD of liver." *Journal of advances in information technology* 2.1 (2011): 63-70.
- [16] Li, Bing Nan, et al. "Integrating FCM and level sets for liver tumor segmentation." *13th International Conference on Biomedical Engineering*. Springer Berlin Heidelberg, 2009.
- [17] Belgherbi, A., I. Hadjidj, and A. Bessaid. "A Semi-automated Method for the Liver Lesion Extraction From a CT Images Based on Mathematical Morphology." *Journal of Biomedical Sciences* 2.2 (2013).
- [18] Ciecholewski, Marcin. "Automatic liver segmentation from 2D CT images using an approximate contour model." *Journal of Signal Processing Systems* 74.2 (2014): 151-174.
- [19] López-Mir, Fernando, et al. "Liver Segmentation on CT Images. A Fast Computational Method Based on 3D Morphology and a Statistical Filter." *IWBIO*. 2013.
- [20] Anter, Ahmed M., et al. "Automatic computer aided segmentation for liver and hepatic lesions using hybrid segmentations techniques." *Computer Science and Information Systems (FedCSIS), 2013 Federated Conference on*. IEEE, 2013.
- [21] ALDEEK, NIDAA, et al. "LIVER SEGMENTATION FROM ABDOMEN CT IMAGES WITH BAYESIAN MODEL." *Journal of Theoretical & Applied Information Technology* 60.3 (2014).
- [22] Mostafa, Abdalla, et al. "CT liver segmentation using artificial bee colony optimisation." *Procedia Computer Science* 60 (2015): 1622-1630.
- [23] Cheng, Ching-Hsue, and Liang-Ying Wei. "Rough Classifier Based on Region Growth Algorithm for Identifying Liver CT Image." *淡江理工學刊* 19.1 (2016): 65-74.
- [24] Sayed, Gehad Ismail, Aboul Ella Hassanien, and Gerald Schaefer. "An Automated Computer-aided Diagnosis System for Abdominal CT Liver Images." *Procedia Computer Science* 90 (2016): 68-73.
- [25] Sayed, Gehad Ismail, and Aboul Ella Hassanien. "Abdominal CT Liver Parenchyma Segmentation Based on Particle Swarm Optimization." *The 1st International Conference on Advanced Intelligent System and Informatics (AISI2015), November 28-30, 2015, Beni Suef, Egypt*. Springer International Publishing, 2016.
- [26] Jemal, Ahmedin, et al. "Global cancer statistics." *CA: a cancer journal for clinicians* 61.2 (2011): 69-90.
- [27] Wu, Kesheng, Ekow Otoo, and Arie Shoshani. "Optimizing connected component labeling algorithms." *Medical Imaging. International Society for Optics and Photonics*, 2005.
- [28] Heimann, Tobias, H. Meinzer, and Ivo Wolf. "A Statistical Deformable Model for the Segmentation of Liver CT Volumes Using Extended Training Data." *Proc. MICCAI Work (2007)*: 161-166.
- [29] Li, Guodong, et al. "Automatic liver segmentation based on shape constraints and deformable graph cut in CT images." *IEEE Transactions on Image Processing* 24.12 (2015): 5315-5329.
- [30] Altarawneh, Nuseiba, et al. "Liver Segmentation from CT Images Using a Modified Distance Regularized Level Set Model Based on a Novel Balloon Force| NOVA. The University of Newcastle's Digital Repository." (2014).
- [31] <https://www.mathworks.com/matlabcentral/fileexchange/50782-region-growing-segmentation>
- [32] <https://www.mathworks.com/matlabcentral/fileexchange/32532-region-growing--2d-3d-grayscale->
- [33] <https://www.mathworks.com/matlabcentral/fileexchange/19084-region-growing>
- [34] <https://www.mathworks.com/matlabcentral/fileexchange/19567-active-contour-segmentation>
- [35] <https://www.mathworks.com/matlabcentral/fileexchange/23445-chan-ve-se-active-contours-without-edges>
- [36] <http://www.shawnlankton.com/2008/04/active-contour-matlab-code-demo/>
- [37] <https://www.mathworks.com/matlabcentral/fileexchange/45896-fast-gradient-vector-flow--gvf->
- [38] <https://www.mathworks.com/matlabcentral/fileexchange/12711-level-set-for-image-segmentation>
- [39] <https://www.mathworks.com/matlabcentral/fileexchange/8647-local-adaptive-thresholding>
- [40] Dunn, Joseph C. "A fuzzy relative of the ISODATA process and its use in detecting compact well-separated clusters." (1973): 32-57.

TABLE I. COMPARISON OF DATASET

Ref	Author	Year	Images used	Datatypes	Image size
[2]	Lim et al	2005	10cases	Private dataset	512*512
[3]	Massoptier et al	2007	10cases	Private dataset	-
[4]	Rusko et al	2007	10cases	-	-
[5]	Gui et al	2007	4cases ,200images	Private dataset	170*170
[6]	Alomari et al	2008	13cases	Private dataset	512*512
[7]	Massoptier et al	2008	21cases	Private dataset	512*512
[8]	Mala et al	2008	105 images	Private dataset	256*256
[9]	Jiang et al	2009	5 cases	-	-
[10]	Yussof et al	2010	10cases	-	512*512
[11]	Akram et al	2010	100images	Private dataset	512*512
[12]	Militzer et al	2010	15cases	Private dataset	-
[13]	Suzuki et al	2010	15cases	Private dataset	-
[14]	Wang et al	2010	100images	Private dataset	512*512
[15]	S.S Kumar	2011	10cases	-	512*512
[16]	Li et al	2009	15cases	LTSCdataset NUHdataset	512*512
[17]	Belgerbi et al	2013	-	Private dataset	-
[18]	Ciecholewski	2014	1330 images 120 cases	Private dataset	-
[19]	Lopez-mir et al	2013	30 cases	Private dataset	512*512
[20]	M.Anther et al	2013	112cases 860 images	2 Private datasets	630*630
[21]	ALDEEK et al	2014	44cases	Private dataset	512*512
[22]	Mostafa, et al	2015	38CT images	Private dataset	-
[23]	Cheng et al	2016	800images	Open NBIA Private dataset	512*512
[24]	Sayed et al	2016	62 Images	-	256*256
[25]	Sayed et al	2016	43 images	-	256*256

TABLE II. LIVER SEGMENTATION TECHNIQUES OVERVIEW

REF NO	PRE-PROCESSING	LIVER SEGMENTATION	EVALUATION
[3]	Mean shift filter Adaptive threshold	Graph cut	Accuracy 96%
[4]	Hough transform Erosion/dilation Largest CCL	Region growing	Accuracy 76%
[5]	Canny edge detector Hermit spline curve Anisotropic diffusion filter	GGVF	-
[2]	Multilevel thresholding Morphological filter	Gradient label map K mean clustering Label based search algorithm	Accuracy 96%
[6]	Histogram analysis Markov random field	Gradient vector flow Active contour	Similarity matrix
[7]	Adaptive threshold Mean shift filter	Gradient vector flow Active contour	A volume overlap of liver 94.2% Sensitivity & specificity for tumor 82.6% & 87.5% respectively
[9]	Sobel operator Erosion/dilation	Active contour	Accuracy 94%
[10]	Opening Multiscale filtering Anisotropic diffusion filter	CCL Graph Cut	-
[11]	Median filter Adaptive Histogram Power law transformation	Closing Largest area Global threshold	Accuracy 96%
[13]	Anisotropic diffusion filter Median filter Scale specific gradient magnitude filter	Fast marching Level set Geodesic active contour	Manual tracing method
[14]	Gradient magnitude Anisotropic diffusion filter	Random walk algorithm Watershed	TP, TN, FP, FN Manual tracing method
[15]	Median filter/ Erosion Largest CCL	Region growing Alternate FCM	Manual tracing method
[16]	Morphological operations	Fuzzy Clustering Mean/ Level set Balloon force	-
[17]	LIVER: H max transform Dilation/erosion Lesion: Anisotropic diffusion filter Hmaxima transform filter	Watershed algorithm	Sensitivity & specificity 92% & 99 % respectively
[18]	-	Connected poly lines	DICE similarity co efficient 81.3%
[19]	Adaptive filter Dilation/erosion	Region Growing	-
[20]	Erosion/dilation Adaptive threshold	CCL Region Growing Watershed	Accuracy 96%
[21]	Convert intensity value into Hounsfield units Median filter	Bayesian Model	Accuracy 87%
[22]	Median filter Contrast Stretching Thresholding to separate Ribs	Artificial bee colony Optimization algorithm	Accuracy 93.73%
[24]	Median filter	FCM Grey Wolf Optimization SVM	Accuracy 96%

Automatic Cloud Resource Scaling Algorithm based on Long Short-Term Memory Recurrent Neural Network

Ashraf A. Shahin^{1,2}

¹College of Computer and Information Sciences,
Al Imam Mohammad Ibn Saud Islamic University (IMSIU)
Riyadh, Kingdom of Saudi Arabia

²Department of Computer and Information Sciences, Institute of Statistical Studies & Research,
Cairo University,
Cairo, Egypt

Abstract—Scalability is an important characteristic of cloud computing. With scalability, cost is minimized by provisioning and releasing resources according to demand. Most of current Infrastructure as a Service (IaaS) providers deliver threshold-based auto-scaling techniques. However, setting up thresholds with right values that minimize cost and achieve Service Level Agreement is not an easy task, especially with variant and sudden workload changes. This paper has proposed dynamic threshold based auto-scaling algorithms that predict required resources using Long Short-Term Memory Recurrent Neural Network and auto-scale virtual resources based on predicted values. The proposed algorithms have been evaluated and compared with some of existing algorithms. Experimental results show that the proposed algorithms outperform other algorithms.

Keywords—auto-scaling; cloud computing; cloud resource scaling; recurrent neural networks; resource provisioning; virtualized resources

I. INTRODUCTION

One of the important features provided by cloud computing is Scalability, which is the ability to scale allocated computational resources on-demand [1]. Scalability feature allows users to run their applications in an elastic manner, use only computational resources they need, and pay only for what they use. However, the process of instantiating new virtual machines takes 5-15 minutes [2]. Therefore, predicting future demand might be required to deal with variable demands and being able to scale in advance. In the current literature, many diverse auto-scaling techniques have been proposed to scale computational resources according to predicted workload [3, 4, 5, 6].

However, one of the most famous problems that face current auto-scaling techniques is Slashdot problem; where auto-scaling technique might not be able to scale in case of sudden influx of valid traffic. Slashdot is unpredictable flash-crowd workload. Flash-crowd workload reduces cloud service providers' revenue by violating Service Level Agreement.

Slashdot effects can be reduced by detecting Slashdot situations at earlier stages and performing appropriate scaling actions. However, detecting Slashdot situations at earlier

stages is not an easy task. Even if Slashdot is detected, finding suitable scaling action is a very hard task. Recently, several machine-learning techniques (e.g. Support Vector Machine, Neural Networks, and Linear Regression) have been used to predict cloud workload [7, 8, 9]. However, most of currently used techniques cannot remember events if there are very long and variant time lags between events, as in Slashdot.

To improve memorization of standard feed forward neural network, Jeff Elman has proposed recurrent neural network (RNN), which extends standard feed forward neural network by adding internal memory [10]. RNNs can learn when the gap between relevant events is small (less than 10-step time lags). Unfortunately, conventional RNNs still unable to learn when gap between relevant events grows [1]. In 1997, Hochreiter & Schmidhuber have proposed a special type of RNN, called Long Short-Term Memory network (LSTM), with ability to recognize and learn long-term dependencies (up to 1000-step time lags between relevant events)[1].

This paper tries to answer the question: can we reduce Slashdot effects by using LSTM-RNN? To answer this question, this paper has proposed two auto-scaling algorithms. The first algorithm avoids long and variant time lags between Slashdot situations by using two different LSTM-RNNs. The first LSTM-RNN is employed to deal with normal workload while the second LSTM-RNN is exploited to deal with Slashdot workload. The second algorithm investigates applicability of using one LSTM-RNN to deal with both normal and Slashdot workloads. Performance of the proposed algorithms have been evaluated and compared with some of existing algorithms using CloudSim with real traces. Experimental results show that the first auto-scaling algorithm, which uses two LSTM-RNNs, outperforms other algorithms.

The rest of this paper is structured as follows. Section 2 gives a brief background on Long Short-Term Memory recurrent neural network (LSTM-RNN). Section 3 overviews related work in the area of automatic cloud resources scaling. Section 4 briefly describes the proposed algorithms. Following this, Section 5 evaluates performance of the proposed algorithms using CloudSim simulator with real workloads and

compares their performance with some of existing algorithms. Finally, Section 6 concludes.

II. LSTM-RNN

Feed forward neural network is a set of connected neurons that try to capture and represent underlying relationships in a set of data [10]. One of the major limitations of feed forward neural network is that it does not consider order in time and only remember few moments of training from their recent past. Therefore, feed forward neural network cannot recognize or learn sequential or time-varying patterns [10].

Alternatively, recurrent neural networks (RNN) determine new response by using feedback loops, which combine current inputs with outputs of the previous moment. Feedback loops allow sequential information to persist and allow recurrent networks to perform tasks that cannot be performed by feed forward neural networks [1].

Figure 1 shows simple recurrent neural network design, which was proposed by Elman. New layer (called *context layer*) has been added to standard feed forward neural network. Context units receive inputs from, and return their results to hidden units. Context units allow RNN to memorize its previous state [10].

Unfortunately, regular RNN still loses its memory very fast. In 1997, Hochreiter & Schmidhuber have proposed a special type of RNN, called Long Short-Term Memory network (LSTM), with ability to recognize and learn long-term dependencies. Long Short-Term Memory blocks have been added to the hidden layers of RNN [11]. As shown in Fig. 2, each memory block contains memory cell to store internal state and contains three different types of gates (input, output and forget gates) to manage cell state and output using activation function (usually sigmoid). The input gate decides what information to store in the memory cell. The output gate decides when to read information from the memory cell. The forget gate decides how long to store information in the memory cell. In 2002, Schmidhuber et al. have enhanced memory block by adding peephole connections from its internal cell to its gates. Peephole connections allow LSTM to learn precise timing between relevant events [1].

III. RELATED WORK

Recently, several auto-scaling techniques have been proposed. In [12], Gandhi et al. have proposed auto-scaling approach, called Dependable Compute Cloud, to scale infrastructure automatically without accessing application-level and without offline application profiling. The proposed approach proactively scales application deployment based on monitoring information from resource-level and based on performance requirements that are specified by users. Multi-tier cloud application is approximated using product-form queueing-network model. Kalman filtering technique is employed to predict required parameters without accessing user's application. However, the proposed approach has not considered Slashdot and has assumed that incoming requests have Poisson arrivals.

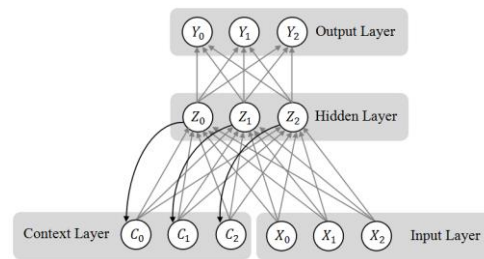


Fig. 1. Simple Recurrent Neural Network Design

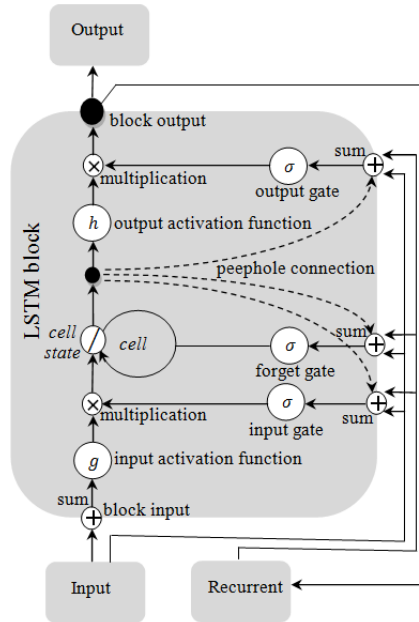


Fig. 2. Long Short-Term Memory block [11]

In [13], Moore et al. proposed a hybrid elasticity controller that coordinates between reactive and predictive scalability controllers to enhance cloud applications scalability. Both controllers act concurrently. Cloud applications' administrators configure scaling rules, which are monitored by reactive controller. After some condition has already been met, reactive controller submits scaling requests to centralized decision manager. If the predictive controller is certain of what action to take then it submits scaling requests to centralized decision manager. Otherwise, the predictive controller continues to learn. Decision manager receives, validates, and executes all triggered scaling requests. Although, performance of the proposed elasticity controller has been evaluated using two real traces (ClarkNet web server trace logs and FIFA 1998 World Cup Access logs), none of these traces has Slashdot. Therefore, performance of the proposed elasticity controller has not been evaluated with Slashdot.

Lin et al. [3, 6] proposed auto-scaling system, which monitors incoming requests and HTTP response time to recognize cloud applications' performance. Auto-scaling algorithm was proposed based on recognized performance.

Furthermore, Lin et al. proposed an algorithm to analyze the workload trend to reduce the number of peaks in response time caused by the variability of workload. Although, the authors have mentioned that the proposed scaling strategy can respond to variant and sudden workload changes in short time, the proposed strategy has not been evaluated using sudden workload changes and only evaluated using short workload (200 minutes) with predictable seasonality.

Kanagala and Sekaran [14] have proposed Threshold-based auto-scaling approach, which minimizes violation of service level agreement by considering virtual machine turnaround time and virtual machine stabilization time during adapting thresholds. Thresholds are dynamically specified by using double exponential smoothing. To set upper threshold, double exponential smoothing is used to predict at which time the system will reach max load and specify point before this time to be used as upper threshold. To scale down, double exponential smoothing is used to predict point before reaching the minimum system load and use it as lower threshold. However, weights that are assigned to observations by double exponential smoothing method are decreased exponentially while observations get older. Therefore, double exponential smoothing method does not able to remember Slashdot when there are long time lags.

Mao et al. [4, 5, 15] proposed auto-scaling mechanism, which considers both user performance requirements and cost concerns. Performance requirements are specified by assigning soft deadline for each job. The proposed auto-scaling mechanism allocates/deallocates virtual machines and schedules tasks on virtual machines to finish each job within its deadline with minimum cost. However, instantiating new VMs requires at least 10 minutes. Thus, probability of violating Service Level Agreement is increased.

Nikraves et al. [16] proposed a proactive auto-scaling system based on Hidden Markov Model. Their experiments shown that scaling decisions that are generated using Hidden Markov Model are more accurate than scaling decisions that are generated using support vector machine, neural networks, and linear regression. In [7, 8, 9], Bankole and Ajila have applied three machine-learning techniques: Support Vector Machine, Neural Networks, and Linear Regression to proactively scale provisioned cloud resources for multitier web applications. Their results show that Support Vector Machine outperforms other techniques in predicting future resource demands. Although, several auto-scaling techniques have been proposed during the last few years, most of them do not consider Slashdot.

IV. PROPOSED ALGORITHMS

As shown in Algorithm 1, inputs are as following. The first input, CPU_H , is the history of total required CPU. Total required CPU at time t , $CPU_H(t)$, is calculated as sum of all

required CPU for coming requests at time t .

To enhance prediction accuracy of the proposed algorithms, sliding window technique is utilized. Sliding window has been used in many areas to improve prediction accuracy [2]. The input W_{length} specifies size of sliding window that will be used during prediction.

The input VM_{delay} represents delay of starting up new VM. CPU_{PH1} and CPU_{PH2} are history of previously predicted CPU by using first and second LSTM-RNN respectively. $MAPE_{Normal}$ and $MAPE_{Slashdot}$ represent prediction accuracy of first and second LSTM-RNN respectively. Prediction accuracy is calculated as Mean Absolute Percentage Error (MAPE).

The first auto-scaling algorithm uses two different LSTM-RNNs for forecasting future demand. The first LSTM-RNN is trained by normal workload without Slashdot and the second LSTM-RNN is trained with Slashdot workload only. $MAPE_{Normal}$ and $MAPE_{Slashdot}$ are continuously updated using predicted and observed CPU. Required CPU after VM_{delay} step-ahead is forecasted by using LSTM-RNN with lowest MAPE. Predicted CPU is sent to Scaling Decision Maker algorithm to decide appropriate scaling action. Number of VMs to scale up or down is specified according to the difference between predicted and provisioned resources after VM_{delay} step-ahead.

Algorithm 2 shows steps of the second auto-scaling algorithm, which uses only one LSTM-RNN to predict required CPU with normal and Slashdot workloads.

ALGORITHM 1: Auto-scaling with two LSTM-RNN

INPUTS:

CPU_H : history of total required CPU
 W_{length} : sliding window length
 VM_{delay} : VM startup delay
 CPU_{PH1} : history of predicted CPU using $LSTM_RNN_{Normal}$
 CPU_{PH2} : history of predicted CPU using $LSTM_RNN_{Slashdot}$
 $MAPE_{Normal}$: prediction accuracy of $LSTM_RNN_{Normal}$
 $MAPE_{Slashdot}$: prediction accuracy of $LSTM_RNN_{Slashdot}$

OUTPUTS:

Scaling decision

Begin

- 1: $w_t =$ Get sliding window from CPU_H with length W_{length}
- 2: $CPU_{PH1}(t) =$ Predict required CPU after VM_{delay} step-ahead using $LSTM_RNN_{Normal}(w_t)$
- 3: $CPU_{PH2}(t) =$ Predict required CPU after VM_{delay} step-ahead using $LSTM_RNN_{Slashdot}(w_t)$
- 4: Update $MAPE_{Normal}$ and $MAPE_{Slashdot}$
- 5: **if** $MAPE_{Normal} < MAPE_{Slashdot}$
- 6: Call Scaling Decision Maker using $CPU_{PH1}(t)$
- 7: **else**
- 8: Call Scaling Decision Maker using $CPU_{PH2}(t)$
- 9: **endif**
- 10: **return** scaling decision

End

ALGORITHM 2: Auto-scaling with one LSTM-RNN

INPUTS:

CPU_H : history of total required CPU
 W_{length} : sliding window length
 VM_{delay} : VM startup delay
 CPU_{pH} : history of predicted CPU

OUTPUTS:

Scaling decision

Begin

- 1: $w_t =$ Get sliding window from CPU_H with length W_{length}
- 2: $CPU_{pH}(t) =$ Predict required CPU after VM_{delay} step-ahead
- 3: Call Scaling Decision Maker using $CPU_{pH}(t)$
- 4: **return** scaling decision

End

Scaling decision maker algorithm is shown in Algorithm 3. Scaling decision maker algorithm uses three thresholds: upper threshold $ThrU$, lower threshold $ThrL$, and $ThrbU$, which is slightly below the upper threshold $ThrU$. If required CPU crosses above $ThrU$, virtual resources are considered over utilized and have to be scaled up. If required CPU crosses above $ThrbU$ and does not cross above $ThrU$ for a pre-specified number of times, virtual resources are considered over utilized and virtual resources have to be scaled up. In another hand, if required CPU crosses below $ThrL$ for a pre-specified number of times, virtual resources are considered underutilized and some virtual resources have to be released.

Thresholds are initialized by the same values for all applications. However, due to variation nature of workloads, setting the same values for all applications increases the probability of violating service level agreements. Therefore, all thresholds are periodically and automatically adapted using Median Absolute Deviation of required CPU history for each application.

$$ThrU = 1 - c_1 \cdot MAD,$$

$$ThrbU = 1 - c_2 \cdot MAD,$$

$$ThrL = 1 - c_3 \cdot MAD,$$

where $c_1, c_2,$ and $c_3 \in \mathbb{R}^+$, such that $c_1 < c_2 < c_3$, and MAD is median of absolute deviations from median of required CPU. Using $c_1, c_2,$ and c_3 , we can adapt the safety of the proposed algorithm. For example, lower values for $c_1,$ and c_2 decrease the cost, but increase the probability of violating service level agreements.

V. PERFORMANCE EVALUATION

Proposed algorithms have been implemented using Cloudsim simulator with deep-learning library called Deeplearning4j [20]. Performances of the proposed algorithms have been compared with two auto-scaling approaches, which are proposed by Kanagala et al. [14], and Hasan et al. [17]. The following subsections describe evaluation environment settings and discuss simulations' results.

A. Evaluation environment settings

The proposed algorithms have been evaluated using CloudSim simulator with real trace called NASA Log [18].

NASA Log contains two month's *HTTP* requests to the NASA Kennedy Space Center WWW server, which is located in Florida. This log was collected from 00:00:00 July 1, 1995 to 23:59:59 July 31, 1995 and from 00:00:00 August 1, 1995 to 23:59:59 August 31, 1995. Fig. 3 shows number of requests that are generated according to NASA Log from August 1 to August 31.

Slashdot has been added to NASA Log from [19], which contains number of hits for July 26 2000; the day the AUUG/LinuxSA InstallFest story hit Slashdot (Fig. 4 shows number of requests versus time). Fig. 5 shows NASA Log after adding Slashdot.

ALGORITHM 3: Scaling Decision Maker

INPUTS:

CPU_H : history of total required CPU
 $CPU_p(t)$: predicted CPU at time t
 $Scaling_{delay}$: duration before scaling

OUTPUTS:

Scaling Action

Begin

- 1: $MAD =$ Get Median Absolute Deviation of CPU_H
- 2: $ThrU = 1 - c_1 \cdot MAD$
- 3: $ThrbU = 1 - c_2 \cdot MAD$
- 4: $ThrL = 1 - c_3 \cdot MAD$
- 5: $Tick_Up_Timer = 0$
- 6: $Tick_Down_Timer = 0$
- 7: **if** ($CPU_p(t) > ThrU$)
- 8: $Scaling_Action = scale_Up$
- 9: $Tick_Down_Timer = 0$
- 10: $Tick_Up_Timer = 0$
- 11: **else**
- 12: **if** ($CPU_p(t) > ThrbU$)
- 13: $Tick_Down_Timer = 0$
- 14: $Tick_Up_Timer ++$
- 15: **if** ($Tick_Up_Timer > Scaling_{delay}$)
- 16: $Scaling_Action = scale_Up$
- 17: **endif**
- 18: **else**
- 19: **if** ($CPU_p(t) < ThrL$)
- 20: $Tick_Up_Timer = 0$
- 21: $Tick_Down_Timer ++$
- 22: **if** ($Tick_Down_Timer > Scaling_{delay}$)
- 23: $Scaling_Action = scale_Down$
- 24: **endif**
- 25: **else**
- 26: $Tick_Down_Timer = 0$
- 27: $Tick_Up_Timer = 0$
- 28: **endif**
- 29: **endif**
- 30: **endif**
- 31: **return** $Scaling_Action$

End

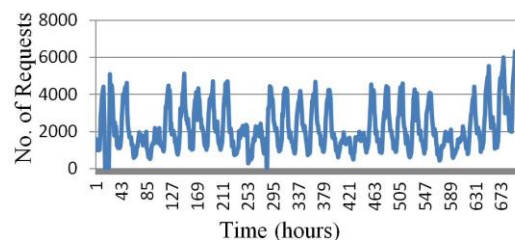


Fig. 3. Generated requests according NASA Log from August 1 to August 31

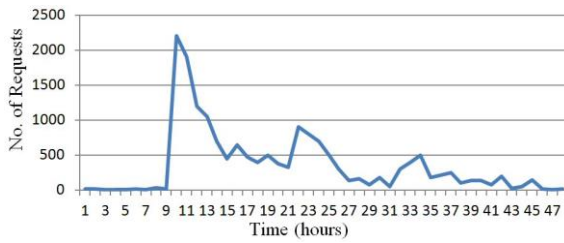


Fig. 4. Number of requests versus time for Slashdot

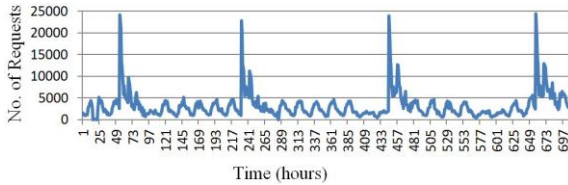


Fig. 5. NASA Log with Slashdot

To implement LSTM-RNN, *Deeplearning4j* library has been used. *Deeplearning4j* is an open-source deep-learning library in Java. *Deeplearning4j* is developed by San Francisco-based business intelligence and enterprise software firm [20].

B. Evaluation results

Fig. 6 and Table 1 show number of running VMs during period from hour 221 to hour 248, which contains the second Slashdot (as shown in Fig. 5). The proposed algorithms increase number of running VMs (between 221 and 230) among other approaches to deal with Slashdot and rapidly decrease number of running VMs (between 230 and 250) to minimize cost.

Fig. 6 and Table 1 show that number of provisioned VMs by the proposed algorithms is higher than provisioned VMs by the related approaches. These VMs are incorporated to achieve large number of requests in short response time as shown in Fig. 7, Table 2, Fig. 8, and Table 3.

In [17], fixed number of VMs is defined to be allocated or de-allocated during scaling up or down. This fixed number limits scaling speed through Slashdot. In the proposed algorithms, number of VMs is variant and depends on growth or decrease of the workload.

In [14] and [17], if workload goes across the upper threshold for a pre-specified duration, they start to scale up. During this period, Service Level Agreement (SLA) will be violated and some penalty has to be incurred by providers. Moreover, duration of SLA violation will be extended to include startup delay of new VMs, which sometimes takes around 10 minutes. In the proposed algorithms, VMs will be scaled up directly if predicted workload goes across the upper threshold. Therefore, the proposed algorithms act faster to provide enough resources to achieve coming requests.

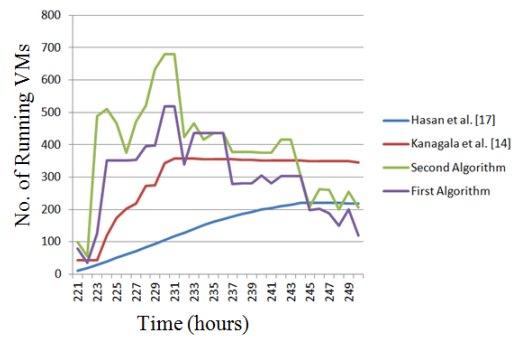


Fig. 6. Number of running VMs versus time

TABLE I. NUMBER OF RUNNING VMS VERSUS TIME

Time (hour)	First Algorithm	Second Algorithm	Kanagala et al. [14]	Hasan et al. [17]
221	79	100	43	11
222	36	55	43	19
223	125	488	44	28
224	352	510	119	40
225	352	466	173	51
226	352	376	203	62
227	353	472	219	72
228	396	520	272	83
229	397	633	274	94
230	519	680	344	106
231	519	680	357	117
232	339	424	357	128
233	435	466	357	139
234	435	416	356	151
235	435	435	356	161
236	435	435	356	169
237	279	378	355	178
238	280	378	353	187
239	281	378	353	193
240	305	376	352	201
241	281	376	352	205
242	303	416	352	211
243	303	415	352	215
244	303	305	351	220
245	199	209	350	220
246	202	262	349	220
247	188	261	349	220
248	150	200	349	220
249	200	254	349	219
250	120	207	346	218

In [17], they scale down if the trend is down even if the load does not cross the lower threshold, which means that VMs will be shrunken even if we do not need that. Moreover, in [17], it terminates VM after marking it to be terminated after 5 minutes even if it is already finished, which sometimes increases the cost if these few minutes add more hour cost. In addition, it can increase SLA violation if there are running requests need more time.

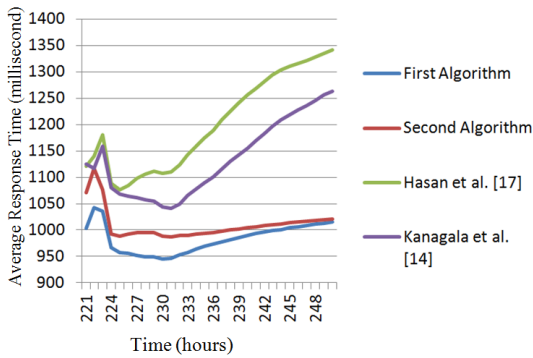


Fig. 7. Average response time

TABLE II. AVERAGE RESPONSE TIME (MILLISECOND)

Time (hour)	First Algorithm	Second Algorithm	Kanagala et al. [14]	Hasan et al. [17]
221	1003	1071	1125	1121
222	1042	1117	1116	1139
223	1036	1076	1159	1181
224	967	993	1080	1089
225	958	988	1068	1077
226	956	993	1064	1084
227	952	995	1061	1098
228	949	996	1057	1106
229	950	996	1055	1111
230	946	988	1044	1108
231	947	988	1042	1110
232	953	990	1050	1123
233	958	990	1065	1143
234	964	992	1078	1159
235	969	993	1090	1175
236	974	996	1100	1189
237	978	998	1116	1209
238	982	1000	1130	1226
239	986	1003	1143	1241
240	990	1005	1155	1256
241	994	1007	1169	1269
242	996	1008	1184	1282
243	999	1010	1197	1293
244	1001	1012	1208	1304
245	1004	1014	1218	1310
246	1006	1016	1228	1316
247	1009	1017	1236	1321
248	1011	1018	1245	1327
249	1013	1019	1256	1335
250	1015	1021	1263	1341

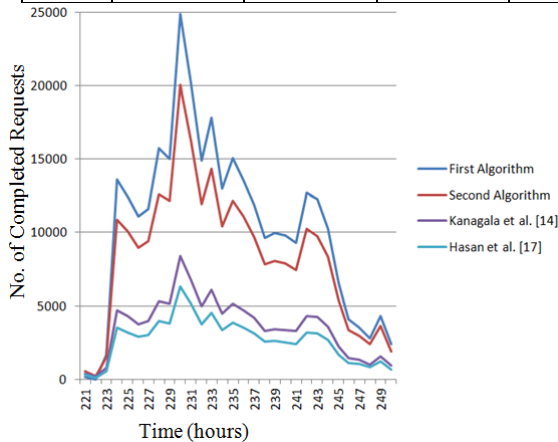


Fig. 8. Number of completed requests

VI. CONCLUSION

Although, elasticity is one of cloud computing cornerstones that attract many companies to host their applications in the cloud, most of current dynamic resource scaling systems do not have ability to deal with Slashdot. Slashdot prevents companies from gaining benefits of cloud computing elasticity and increases the probability of losing customers. Motivated by this problem, this paper has proposed two auto-scaling algorithms based on Long Short-Term Memory Recurrent Neural Network to minimize Slashdot effects.

TABLE III. NUMBER OF COMPLETED REQUESTS

Time (hour)	First Algorithm	Second Algorithm	Kanagala et al. [14]	Hasan et al. [17]
221	30	530	412	323
222	155	92	91	153
223	1908	1646	649	585
224	13456	10992	4658	3513
225	12597	10142	4305	3266
226	11049	8884	3776	2881
227	11543	9471	3995	3008
228	15729	12508	5393	4039
229	15151	12154	5159	3891
230	25011	20060	8517	6335
231	20104	16158	6759	5145
232	14872	12034	5060	3754
233	17741	14364	6115	4503
234	12797	10316	4369	3377
235	15011	12175	5119	3838
236	13742	11056	4759	3521
237	11873	9612	4159	3108
238	9758	7937	3290	2500
239	9832	8067	3406	2570
240	9833	7887	3386	2566
241	9187	7582	3147	2355
242	12763	10144	4353	3281
243	12247	9877	4097	3174
244	10265	8252	3607	2649
245	6397	5350	2278	1742
246	4072	3374	1452	1115
247	3535	2948	1347	1047
248	2903	2356	1040	766
249	4429	3634	1591	1224
250	2340	2052	874	735

The proposed algorithms have been empirically evaluated against some of existing approaches. Experiment results have showed that the proposed algorithms outperform others on both cost and service level agreement. Based on these results, this paper concludes that using Long Short-Term Memory Recurrent Neural Network to recognize and deal with Slashdot can minimize its effects.

In the future, deep Long Short-Term Memory Recurrent Neural Network will be exploited to recognize Slashdot behavior. Deep LSTM-RNN has been effectively applied in many areas and has proved its efficiency throughout the years. Deep LSTM-RNN offers more benefits over standard LSTM RNNs by having several hidden layers. Each layer processes some part of the task before sending it to the next layer.

REFERENCES

[1] J. S. Felix A. Gers, Nicol N. Schraudolph, "Learning precise timing with lstm recurrent networks," *Journal of Machine Learning Research*,

- vol. 3, pp. 115–143, 2002. [Online]. Available: <http://www.jmlr.org/papers/volume3/gers02a/gers02a.pdf>
- [2] S. Islam, J. Keung, K. Lee, and A. Liu, “Empirical prediction models for adaptive resource provisioning in the cloud,” *Future Gener. Comput. Syst.*, vol. 28, no. 1, pp. 155–162, Jan. 2012. [Online]. Available: <http://dx.doi.org/10.1016/j.future.2011.05.027>
- [3] C.-C. Lin, J.-J. Wu, P. Liu, J.-A. Lin, and L.-C. Song, “EnglishAutomatic resource scaling for web applications in the cloud,” in *EnglishGrid and Pervasive Computing*, ser. Lecture Notes in Computer Science, J. Park, H. Arabnia, C. Kim, W. Shi, and J.-M. Gil, Eds. Springer Berlin Heidelberg, vol. 7861, pp. 81–90, 2013. [Online]. Available: http://dx.doi.org/10.1007/978-3-642-38027-3_9
- [4] M. Mao and M. Humphrey, “Auto-scaling to minimize cost and meet application deadlines in cloud workflows,” in *2011 International Conference for High Performance Computing, Networking, Storage and Analysis (SC)*, pp. 1–12, Nov 2011.
- [5] M. Mao, J. Li, and M. Humphrey, “Cloud auto-scaling with deadline and budget constraints,” in *2010 11th IEEE/ACM International Conference on Grid Computing (GRID)*, pp. 41–48, Oct 2010.
- [6] C.-C. Lin, J.-J. Wu, J.-A. Lin, L.-C. Song, and P. Liu, “Automatic resource scaling based on application service requirements,” in *2012 IEEE 5th International Conference on Cloud Computing (CLOUD)*, pp. 941–942, June 2012.
- [7] A. Bankole and S. Ajila, “Cloud client prediction models for cloud resource provisioning in a multitier web application environment,” in *2013 IEEE 7th International Symposium on Service Oriented System Engineering (SOSE)*, pp. 156–161, March 2013.
- [8] S. Ajila and A. Bankole, “Cloud client prediction models using machine learning techniques,” in *2013 IEEE 37th Annual Computer Software and Applications Conference (COMPSAC)*, pp. 134–142, July 2013.
- [9] A. Bankole and S. Ajila, “Predicting cloud resource provisioning using machine learning techniques,” in *2013 26th Annual IEEE Canadian Conference on Electrical and Computer Engineering (CCECE)*, pp. 1–4, May 2013.
- [10] J. S. Sepp Hochreiter, “Long short-term memory,” *Neural Computation*, vol. 9(8), pp. 1735–1780, 1997. [Online]. Available: http://deeplearning.cs.cmu.edu/pdfs/Hochreiter97_lstm.pdf
- [11] F. B. Hasim Sak, Andrew Senior, “Long short-term memory recurrent neural network architectures for large scale acoustic modeling,” in *INTERSPEECH 2014, 15th Annual Conference of the International Speech Communication Association, Singapore, September 14-18*, pp. 338–342, 2014. [Online]. Available: <http://static.googleusercontent.com/media/research.google.com/en/pubs/archive/43905.pdf>
- [12] A. Gandhi, P. Dube, A. Karve, A. Kochut, and L. Zhang, “Adaptive, model-driven autoscaling for cloud applications,” in *11th International Conference on Autonomic Computing (ICAC 14)*. Philadelphia, PA: USENIX Association, pp. 57–64, Jun. 2014. [Online]. Available: <https://www.usenix.org/conference/icac14/technical-sessions/-presentation/gandhi>
- [13] K. B. Laura R. Moore and T. Ellahi, “A coordinated reactive and predictive approach to cloud elasticity,” in *CLOUD COMPUTING 2013 : The Fourth International Conference on Cloud Computing, GRIDs, and Virtualization*, 2013.
- [14] K. Kanagala and K. Sekaran, “An approach for dynamic scaling of resources in enterprise cloud,” in *2013 IEEE 5th International Conference on Cloud Computing Technology and Science (CloudCom)*, vol. 2, pp. 345–348, Dec 2013.
- [15] Y. Wadia, R. Gaonkar, and J. Namjoshi, “Portable autoscaler for managing multi-cloud elasticity,” in *2013 International Conference on Cloud Ubiquitous Computing Emerging Technologies (CUBE)*, pp. 48–51, Nov 2013.
- [16] A. Nikraves, S. Ajila, and C.-H. Lung, “Cloud resource auto-scaling system based on hidden markov model (hmm),” in *2014 IEEE International Conference on Semantic Computing (ICSC)*, pp. 124–127, June 2014.
- [17] M. Z. Hasan, E. Magana, A. Clemm, L. Tucker, and S. L. D. Gudreddi, “Integrated and autonomic cloud resource scaling,” in *2012 IEEE Network Operations and Management Symposium*, pp. 1327–1334, April 2012. DOI:10.1109/NOMS.2012.6212070
- [18] Nasa-http, two months of http logs from NASA Kennedy Space Center WWW server in Florida, USA. [online] <http://ita.ee.lbl.gov/html/contrib/NASA-HTTP.html> (Accessed on October 1, 2016)
- [19] The Slashdot Effect, hits-vs-time for the AUUG/LinuxSA InstallFest Slashdot, July 26 2000. [online] <http://slash.dotat.org/~newton/installpics/slashdot-effect.html> (Accessed on October 1, 2016)
- [20] Deeplearning4j, open-source deep-learning library in Java, San Francisco-based business intelligence and enterprise software firm. [online] <https://deeplearning4j.org> (Accessed on October 1, 2016)

U Patch Antenna using Variable Substrates for Wireless Communication Systems

Saad Hassan Kiani¹, Khalid Mahmood², Umar Farooq Khattak³, Burhan-Ud-Din⁴, Mehre Munir⁵

Electrical Engineering Department^{1,4,5}

Computer Science Department³

City University of Science and Information Technology^{1,3,4,5}, Member IEEE²
Peshawar, Pakistan

Abstract—Due to their smaller size and light weighted structures patch antennas are frequently now used in GPS transmitters and receivers and throughout modern communication technology. In this paper a miniaturized patch antenna is presented using stack configuration. Various parameters such as gain, directivity, return loss, efficiency of antenna is demonstrated. Using Air, Teflon, Foam and FR4 (Lossy) as substrates FR4 (lossy) is kept fixed and other substrates are combined one by one to observe response of proposed antenna. The antenna showed dual and tri band response with different combination of mentioned substrates. The proposed antenna has been found useful for W-LAN, GSM, Radio Satellite, Fixed Satellite Services (RSS) & (FSS) and satellite communication systems.

Keywords—miniaturization; directivity; gain; substrates; efficiency; VSWR; Wireless communication; Multiband response

I. INTRODUCTION

With rapid advancement in communication technology, patch antenna miniaturization and multiband response has attracted researchers and designers to involve. Applications of such patch structures embrace but not bounded to personal, military applications, vehicular communication and much more. As traditional antenna offers complex and low gain structures with difficult and long process fabrication, patch antennas have been known due to their ability of easy fabrication and light weighted structures. As Multiband response is necessity of today's communication era, different methodologies and process have been introduced. Some of them are mentioned below.

Only low amount of size reduction was achieved with use of split ring resonators [1-2]. Using H-Shape on ring antenna showed multivariable response but bandwidth and gain reduced to significantly low levels [3]. With reverse outcome of declination of radiation pattern and poor antenna bandwidth, by aggregating electric permittivity of a substrate antenna size is reduced [4]. With high increase of cost and fabrication, metamaterials have been found useful in reducing size of patch [5-6]. Expenditure of synthetic magnetic conductors resulted with lowered gain at desired resonant frequencies [7]. With fluctuating return loss plot and poor radiation pattern in [8] defected ground structure resulted in reducing 30% size and dual band response. Hence in simple words patch size reduction and multi band response has been a very common interesting topic among researchers [9-11].

Upper substrate play a vital role in resulting various antenna parameters [12]. Therefore in this paper we have proposed a multiband patch antenna using stack configuration. By use of Air, Teflon PTFEE and Foam with fix FR4 (lossy) as substrate, different parameters response has been observed. Computer Simulation technology 2014 has been used for designing and modeling of proposed design.

This paper is organized as follows:

Section I deals with introduction, Section II shows antenna Structure, Section III includes detailed result analysis and Section IV includes Conclusion.

II. ANTENNA DESIGN

The elementary patch antenna comprises of patch, substrate and ground plane as shown in fig 1.

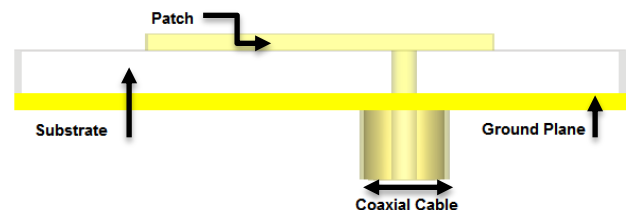


Fig. 1. Elementary patch antenna

A. Substrate

The first significant charge while scheming an antenna is selection of a proper substrate with proper dielectric constant as various parameters are linked up to substrate. In projected antenna design, due its cost success, dampness enduring competences, FR4 (lossy) is chosen as first and basic substrate with dielectric constant of 4.3. Air, Teflon and Foam are chosen as second substrates to observe antenna behavior.

B. Width

For calculating and deriving patch width following equation is used. (1).

$$W = \frac{c}{2 f_0 \sqrt{\frac{\epsilon r + 1}{2}}} \quad (1)$$

Whereas c is the speed of light in free space and f_0 is the resonating frequency and ϵr is the relative permittivity.

C. Length

In order to derive Patch length, following equation is used.

(2).

$$L = L(eff) - 2\Delta L \tag{2}$$

Where

$$L(eff) = \frac{c}{2f_0\sqrt{\epsilon_{(reff)}}} \tag{3}$$

And

$$\epsilon_{(reff)} = \frac{\epsilon_r + 1}{2} + \frac{\epsilon_r - 1}{4} \left(1 + \frac{12h}{W}\right)^{-1/2} \tag{4}$$

Where h is the height and W as mention above is the patch width. Antenna with resonating frequency of 4.5GHz is designed by calculating patch dimensions.

Various dimensions of the proposed antenna technique are provided in table 1.

TABLE I. DIMENSIONS OF PROPOSED ANTENNA

Parameters	Values in MM
Patch Length, PL	16.11
Patch Width, PW	21.43
Ground Length, GL	28.11
Ground Width, GW	33.43
Vertical Fractal Slot Length, VFSL	10.0
Vertical Fractal Slot Width, VFSL	4.0
Horizontal Fractal Slot Length, HFSL	8.0
Horizontal Fractal Slot Width, HFSL	4.0
U Slot Length, UL	6.0
U Slot Width, UW	1.0
Patch Height, PH	0.0035
Height of Ground, HG	0.08
Height of First Substrate, HS	2.0
Height of Second Substrate, H2S	1.0
Horizontal U and H Slot Width, HUU&HHW	1.0
Horizontal U Slot Length, HUL	8.0
Horizontal H Slot Length, HHL	7.0
Vertical U and H Slot Length, VUL&VHL	6.0
Vertical U and H Slot Width, VUU &VHW	1.0

After designing patch antenna for 4.5 GHz, fractal shape is implemented as following.

Patch is slotted by 8mm length and 10mm width horizontally and 10mm length and 4mm width vertically. U shape slot on fractal patch is designed with the following dimensions as shown in Fig 2. Length of slot is 6mm and width of the slot is 1mm. Now to further reduce size and for efficient frequency response defected ground structure

technique is used by adding U and H slot on a ground plane as shown in fig 2.

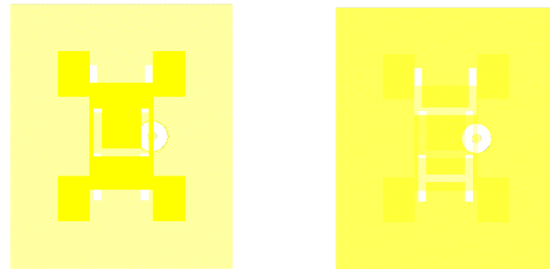


Fig. 2. (a) Frontal View of Patch with single Substrate (b) Frontal View of Ground

The antenna is fed by Co-axial cable a contacting scheme in which inner conductor is mounded to patch through hole from ground through substrate while outer conductor connected with ground plane.

Figure 2 shows the frontal view of single patch antenna. The second layer of antenna with different combinations is shown in Figure 3 and 4.

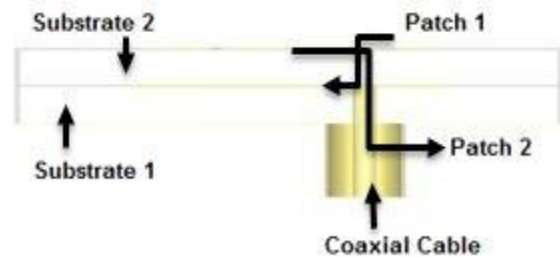


Fig. 3. Overall view of Stacked antenna

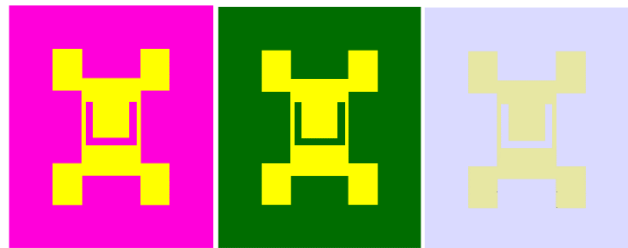


Fig. 4. (a) Front View of Patch antenna with Roggers (b) Front view of Patch antenna with Foam (c) Front view of Patch antenna with Air

The proposed antenna showed unlike response interms of gain, directivity, radiation patterns and bandwidth. Results are discussed one by one.

III. RESULTS AND DISCUSSIONS

After simulation, we got the following results in Return loss graph showing tri band response but this return loss is only of single substrate that's is FR4 (lossy) as first base results are of vital importance [12-13].

From taking a look at return loss graph we have got tri band response. For 3.349 we have got -12.05dB return loss. For frequency 4.7GHz we have got good return loss of -34.47dB and in the end we have got resonating frequency having return loss exceeding -24dB.

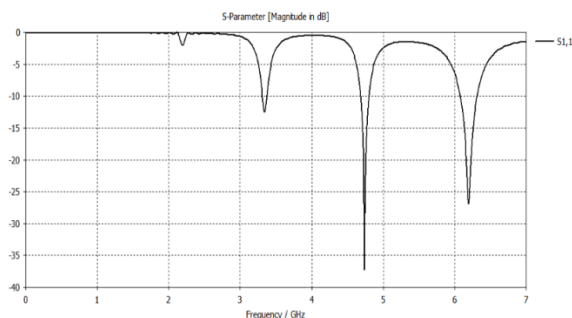


Fig. 5. Return loss graph of antenna

The impedance smith chart of proposed patch is shown below.

Our proposed antenna is operating at fixed impedance of 50 ohm hence showing antenna is fed accurately by Coaxial cable.

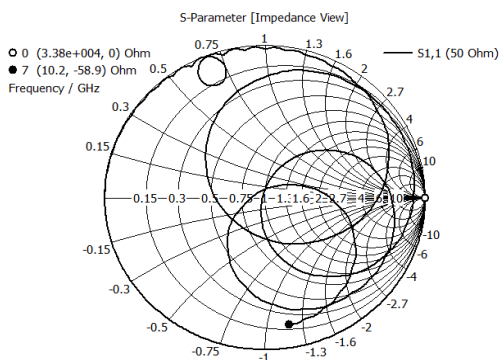


Fig. 6. Smith chart view of proposed antenna

In single patch results, all the radiation pattern showed great patterns for all the resonating frequencies.

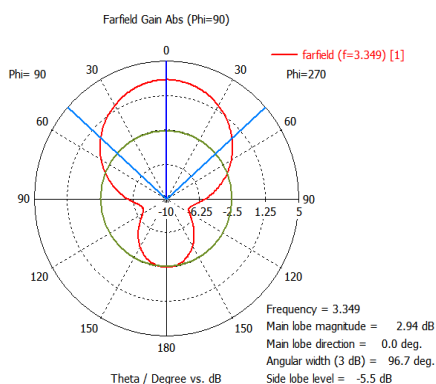


Fig. 7. 1D radiation pattern of Gain at 3.349GHz

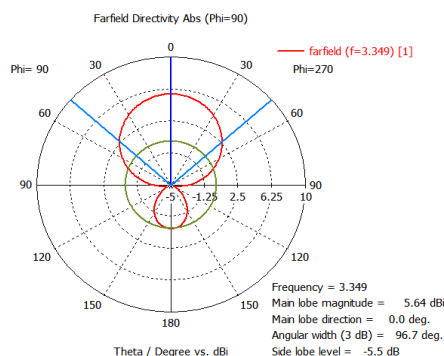


Fig. 8. 1D radiation pattern of Directivity at 3.349GHz

For 3.349 GHz single patch, the magnitude of main lobe scale is 2.91dB, main front lobe direction is 0 degrees and angular width is 96.8 degrees while back lobe scale is -5.5dB.

For directivity plot, the main front lobe scale is 5.64dBi, main lobe direction is 0.0 degrees and angular width is 96.8 degrees while back lobe scale is -5.5dB. The Radiation patterns are shown in Fig 7 and 8.

As our main concern is stack configuration patch analysis, hence we will mainly focus on stacked patches result. These cases are discussed one by one.

A. Air

Air can be seen as substrate in various patch designs, the first combination with FR4 (lossy) was chosen to be air. Following values were obtained.

TABLE II. PARAMETER RESULTS WITH OF AIR

Frequency	Return Loss	Gain	Directivity	Bandwidth
3.32GHz	-12.49dB	3.02dB	5.7dBi	60MHz
6.32GHz	-24.10dB	2.87dB	5.74dBi	200MHz

Return loss Values obtained were -12 and -24 respectively at 3.3 and 6.32GHz. Radiation pattern of fundamental (first) resonant frequency is shown in figure 9 and figure 10.

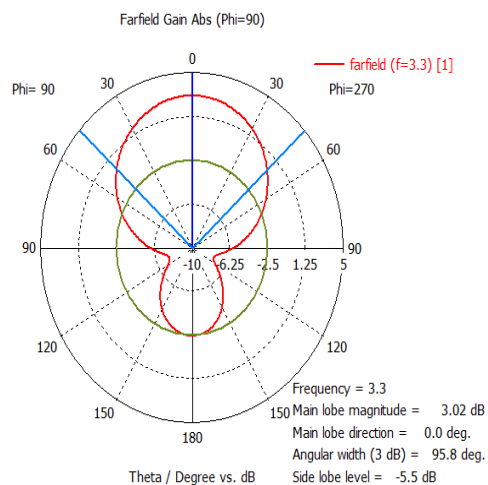


Fig. 9. 1D radiation pattern of Gin at 3.3GHz

For 3.349GHz, the magnitude of main lobe scale is 3.02dB, main front lobe direction is 0 degrees and angular width is 95.8 degrees while back lobe scale is -5.5dB.

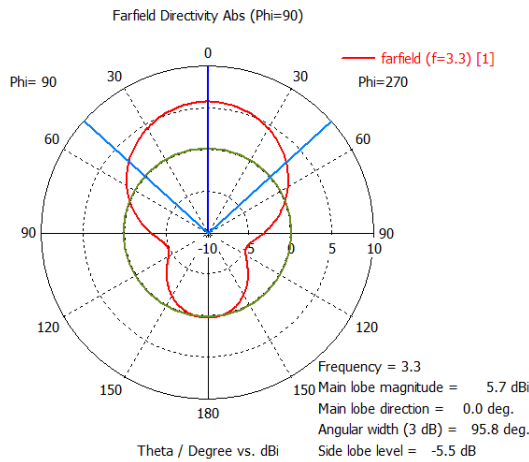


Fig. 10. 1D radiation pattern of Directivity at 3.3GHz

For directivity plot, the main front lobe scale is 5.7dBi, main lobe direction is 0.0 degrees and angular width is 95.8 degrees while back lobe scale is -5.5dB.

So overall of gain increase from 2.9 to 3.02 was seen to be increase with Air as compared to single patch.

The VSWR of proposed antenna showed good results for all resonating frequencies as all values were less than 2 with near to approximately null Mismatch loss.

Formula used for calculating VSWR is shown in eq 5.

$$VSWR = \frac{1+|r|}{1-|r|} \quad (5)$$

Where $|r|$ is the reflection coefficient also called return loss.

By inverting the formula in eq (5), reflection coefficient $|r|$ can also be determined.

$$|r| = \frac{1-VSWR}{1+VSWR} \quad (6)$$

Now the reflection coefficient obtained in eq (6) is in voltage to actually know the amount of reflected power following equation is used.

$$RP(\%) = 100 * |r|^2 \quad (7)$$

And

$$RP(dB) = 20 * \log |r| \quad (8)$$

Where in eq (7) reflected power is obtain in percentage and through eq (8) is obtained in dB

In last power is conveyed or reflected from antenna. Amount of power being lost from antenna is due to mismatch of impedance.

$$MMLoss(dB) = 10 * \log_{10} (1 - |r|^2) \quad (9)$$

All the above mention parameters were calculated for proposed antenna. The approximate values are shown in the following table.

TABLE III. VSWR VALUES OF RESONANT FREQUENCIES

Resonant Frequency	VSWR	Reflection Coefficient	Reflected Power (%)	Reflected Power (dB)	Mismatch Loss (dB)
3.3GHz	1.63	0.24	5.7	-12.41	0.26
6.1GHz	1.10	0.05	0.2	-26.44	0.01

From results shown in table III all the resonant frequencies prove that antenna impedance is matched. For 3.3GHz antenna power delivered is up to 80% and for 6.1GHz power radiated is nearly 99.99%.

B. Foam

Second substrate to be combined was chosen to be foam as due to its low permittivity values, ease of availability and ease of fabrication. Following results were observed.

TABLE IV. PARAMETER RESULTS WITH FOAM

Frequency	Return Loss	Gain	Directivity	Bandwidth
3.33GHz	-12.71dB	2.99dB	5.64dBi	60MHz
4.88GHz	-10.17dB	0.78dB	5.99dBi	30MHz
6.32GHz	-29.41dB	3.42dB	5.98dBi	200MHz

Return loss obtained were -12, -10 and -25dB at respective resonant frequencies of 3.3, 4.8 and 6.3GHz. Radiation pattern were good with minor back lobe radiation. The first resonant frequency of 3.3GHz radiation patterns of gain and frequency are shown in fig 11 and fig 12.

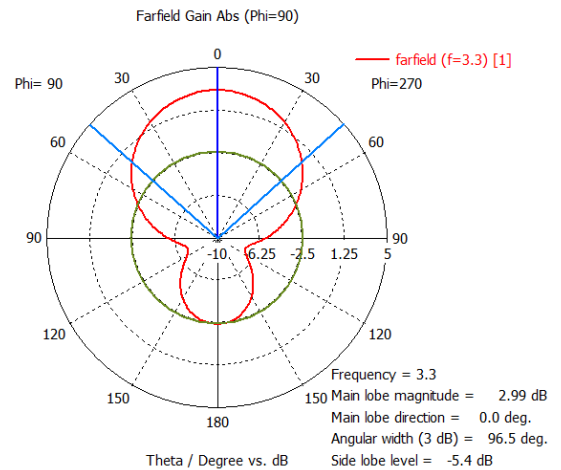


Fig. 11. 1D radiation pattern of gain at 3.3GHz

For 3.3GHz, the magnitude of main lobe scale is 2.99dB, main front lobe direction is 0 degrees and angular width is 96.5 degrees while back lobe scale is -5.4dB.

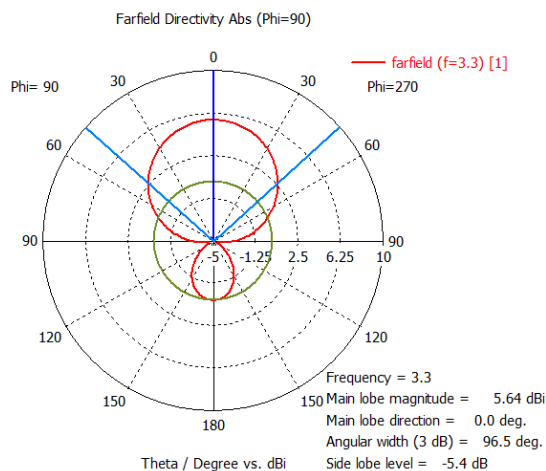


Fig. 12. 1D radiation pattern of Directivity at 3.3GHz

For directivity plot, the magnitude of main lobe scale is 5.64dBi, main front lobe direction is 0 degrees and angular width is 96.5 degrees while back lobe scale is -5.4dB.

So overall of parameters results of foam were observed to be very similar to that of air substrate results with minor changes.

The VSWR of proposed antenna showed good results for all resonating frequencies as all values were less than 2 with near to roughly null Mismatch loss.

TABLE V. VSWR VALUES OF RESONANT FREQUENCIES

Resonant Frequency	VSWR	Reflection Coefficient	Reflected Power (%)	Reflected Power (dB)	Mismatch Loss (dB)
3.3GHz	1.63	0.23	5.3	-12.41	0.26
4.8GHz	1.8	0.29	8.2	-10.08	0.37
6.1GHz	1.07	0.03	0.1	-29.42	0.01

From results shown in table V all the resonant frequencies prove that antenna impedance is matched. For 3.3GHz antenna power delivered is up to 85%. For 4.8GHz, power is delivered round about 70%. And at last for 6.1GHz power radiated is nearly 99.98%.

C. Teflon

With relative permittivity of 2.1, Teflon was chosen as third substrate with FR4 for stack configuration. Following parameter results were observed.

TABLE VI. PARAMETER RESULTS WITH TEFLON

Frequency	Return Loss	Gain	Directivity	Bandwidth
3.2GHz	-11.74dB	2.68dB	5.45dBi	50MHz
4.7GHz	-15.56dB	1.34dB	5.32dBi	90MHz
6.1GHz	-17.95dB	3.67dB	6.34dBi	200MHz

Return loss obtained were -11, -15 and -17dB at respective resonant frequencies of 3.2, 4.7 and 6.1GHz. Radiation pattern were good with minor back lobe radiation. The first resonant frequency of 3.2GHz radiation patterns of gain and frequency are shown in fig 13 and fig 14.

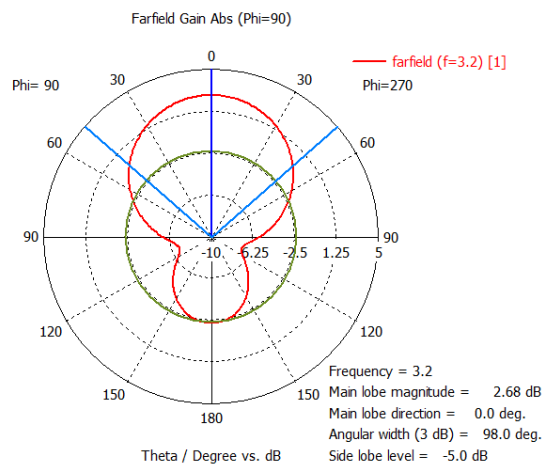


Fig. 13. 1D radiation pattern of gain at 3.2GHz

For 3.3GHz, the magnitude of main lobe scale is 2.68dB, main front lobe direction is 0 degrees and angular width is 98.0 degrees while back lobe scale is -5.0dB.

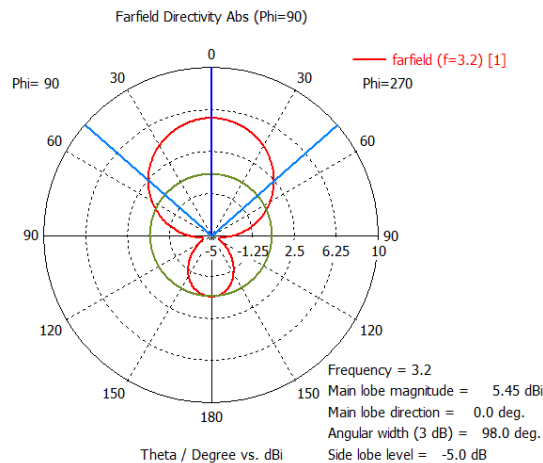


Fig. 14. 1D radiation pattern of Directivity at 3.2GHz

For directivity plot, the magnitude of main lobe scale is 5.45dBi, main front lobe direction is 0 degrees and angular width is 98.0 degrees while back lobe scale is -5.0dB.

With Teflon substrate, for fundamental resonant frequency of 3.2GHz, gain was observed to be less than that of air and foam but overall radiation pattern, directivity and other VSWR parameters were as food as air and foam. The VSWR values are shown in table VII.

TABLE VII. VSWR VALUES OF RESONANT FREQUENCIES

Resonant Frequency	VSWR	Reflection Coefficient	Reflected Power (%)	Reflected Power (dB)	Mismatch Loss (dB)
3.32GHz	1.7	0.26	6.7	-11.71	0.3
4.7GHz	1.02	0.17	2.8	-15.56	0.12
6.1GHz	1.10	0.13	1.6	-17.95	0.07

From results shown in table VII all the resonant frequencies prove that antenna impedance is nearly matched.

For 3.2GHz antenna power delivered is up to 94.3%. For 4.7GHz nearly all the power is delivered from transmitter side. And at last for 6.1GHz power radiated is nearly 99.3%.

The antenna after size reduction resonated with fundamental frequency of 3.3GHz. The fundamental antenna with resonant frequency of 3.3GHz would require dimensions of $27.94 \times 21.30 = 594.6$ where it was obtained with only dimensions of $16 \times 21 = 361 \text{mm}^2$ hence reducing the size up to 60%. It was also observed that with use of stack configuration different substrates exhibit different behavior of resonant frequencies. Higher the permittivity lower the resonant frequency as in case of Teflon fundamental frequency was down to 3.2 hence resulting in size reduction up to 57% but with expense of lower performance of antenna parameters.

IV. CONCLUSION

In this paper, U shaped patch antenna with stack configuration was presented. With use of multiple substrates antenna exhibited different result. It was concluded that through stack configuration using higher permittivity substrates results in more size reduction with expense of degradation if antenna performance parameters but with mentioned three combinational substrates proposed antenna is very useful and can be used for W-LAN, GSM, Radio Satellite, Fixed Satellite Services (RSS) & (FSS), W-LAN and Satellite communication system applications.

V. FUTURE WORK

This design can be implemented on multiple input multiple output (MIMO) technique to observe more enhance radiation response. Meanwhile by insertion of Electromagnetic band gap (EBG) structures more focused radiation pattern can be concluded with reduction in electromagnetic interaction in MIMO implementation.

ACKNOWLEDGMENT

The author would acknowledge the environment and support provided by City University of Science and Information Technology Peshawar, Pakistan.

REFERENCES

- [1] Shaw, Tarakeswar, Deepanjan Bhattacharjee, and Debasis Mitra. "Miniaturization of slot antenna using split ring resonators." Applied Electromagnetics Conference (AEMC), 2015 IEEE. IEEE, 2015.

- [2] Liu, Yanxia, et al. "A miniaturized artificial magneto-dielectric resonator antenna with split ring resonators." Antenna Technology and Applied Electromagnetics (ANTEM), 2016 17th International Symposium on. IEEE, 2016.
- [3] Liu, Y., Shafai, L. and Shafai, C., 2016, July. Gain and bandwidth enhancement of stacked H-shaped patch-open ring antenna. In Antenna Technology and Applied Electromagnetics (ANTEM), 2016 17th International Symposium on (pp. 1-2). IEEE.
- [4] Yuan, Bo, et al. "An axial-ratio beamwidth enhancement of patch antenna with digonal slot and square ring." Microwave and Optical Technology Letters 58.3 (2016): 672-675.
- [5] Dai, Yuanlong, et al. "Ultra-wideband patch antenna with metamaterial structures." 2015 IEEE 16th International Conference on Communication Technology (ICCT). IEEE, 2015.
- [6] Yuan, Hang-Ying, et al. "A metamaterial-inspired wideband high-gain FABRY-Perot resonator microstrip patch antenna." Microwave and Optical Technology Letters 58.7 (2016): 1675-1678.
- [7] Rahmadani and A. Munir, "Microstrip patch antenna miniaturization using artificial magnetic conductor," in Telecommunication Systems, Services, and Applications (TSSA), 2011 6th International Conference on, 2011, pp. 219-223.
- [8] Saad Hassan Kiani, Sharyar Shafique Qureshi, Khalid Mahmood, Mehr-e- Munir and Sajid Nawaz Khan, "Tri-Band Fractal Patch Antenna for GSM and Satellite Communication Systems" International Journal of Advanced Computer Science and Applications(IJACSA), 7(10), 2016.
- [9] Ren, Wang, and Chen Jiang. "A novel design of multiband printed anchor-shaped slot antenna." Microwave and Optical Technology Letters 58.3 (2016): 521-526.
- [10] Munir, Mehre-E., Ahsan Altaf, and Muhammad Hasnain. "Miniaturization of microstrip fractal H-Shape patch antenna using stack configuration for wireless applications." Recent Trends in Information Systems (ReTIS), 2015 IEEE 2nd International Conference on. IEEE, 2015.
- [11] Caporal Del Barrio, Samantha, Art Morris, and Gert F. Pedersen. "Antenna miniaturization with MEMS tunable capacitors: techniques and trade-offs." International Journal of Antennas and Propagation 2014 (2014).
- [12] Kiani, Saad Hassan, Khalid Mahmood, Sharyar Shafiq, Mehre Munir, and Khalil Muhammad Khan. "A Novel Design of Miniaturized Patch Antenna Using Different Substrates for S-Band and C-Band Applications." INTERNATIONAL JOURNAL OF ADVANCED COMPUTER SCIENCE AND APPLICATIONS 7, no. 7 (2016): 273-278.
- [13] Fakharian, Mohammad M., et al. "A capacitive fed microstrip patch antenna with air gap for wideband applications." International Journal of Engineering, Transactions B: Applications 27.5 (2014): 715-722.
- [14] Altaf, Ahsan, and Syed Imran Hussain Shah. "Miniaturization of multiband patch antenna using stack configuration." Multi-Topic Conference (INMIC), 2014 IEEE 17th International. IEEE, 2014.

Novel Causality in Consumer's Online Behavior: Ecommerce Success Model

Amna Khatoon

Department of Software Engineering
Bahria University Islamabad, Pakistan

Shahid Nazir Bhatti

Senior Assistant Professor
Department of Software Engineering
Bahria University Islamabad, Pakistan

Atika Tabassum, Aneesa Rida

Dept. of Software Engineering
Bahria University Islamabad, Pakistan

Sehrish Alam

Dept. of Software Engineering
Bahria University Islamabad, Pakistan

Abstract—Online shopping (e-Shopping) has grown at a rapid pace with the advancement in modern web technologies, there are then socio and technical aspects (factors) in the mentioned e-shopping. The following research paper highlights some mandatory socio-technical factors affecting consumer's behavior in online shopping environment. In this work a comprehensive conceptual model is put forward based on proposed reform DeLone and McLean Success Model for Information Systems. This model is used for the assessment of the success of eCommerce web portals. Approximately thirteen different hypotheses are proposed on the bases of this methodology which represent the cause and effect relationship among the various variables affecting consumer's online buying behavior. Further this work is simulated in iThink technology to show prominently that consumer's satisfaction and trust directly affects productivity of the organization. For development organizations the proposed methodology is valuable because it will facilitate in building the eCommerce websites, web portals whereas retailers can improve the productivity of their organization by accomplishing this.

Keywords—Online shopping; Consumer behavior; E-marketer; Usability; DeLone & McLean; eCommerce success model; Causal loop diagram; iThink; Simulation; Evaluation; Retailer

I. INTRODUCTION

In recent times eCommerce has gained recognition with the advent of internet. Retailers can sell their products online and customers can search products suitable for them. Online shopping differs from brick-and-mortar shopping businesses in many ways; be it the physical presence needed for traditional shopping, convenience, reasonable price, product variety, and promotions in online shopping, it has taken incredible acclaim amongst everyone. Retailers, suppliers, marketers can expand their business because of low distribution cost and consumers can find and get the best product available on the internet. Retailers should be aware how to gain consumer's trust and satisfy them.

Consumers can buy products and services faster, anywhere and anytime at reasonable price from an online shopping website [1]. Retailers have to understand consumer's needs and wants beforehand to give them the best online experience possible. In order to do that they have to understand the

psychological state of the consumer who shop online [2] and their behavior and what can affect it.

The online shopping behavior process consists of five steps [3]. First, the customer identifies the need or wants for a purchase and defines requirements for it. Secondly, they search for the product from the options available to them. Once they find the right product for them, they'll buy it after the process of elimination and comparison of prices. Lastly, consumers will have to decide the shipping costs, and delivery mechanism.

Several factors can affect the end user's online purchase behavior such as subjective norms (culture, trust), system quality (website quality, interactivity, ease of use, promotions) and service quality (responsiveness, security, price, reliability, alternatives).

There are eight sections in this research paper. Section I is Introduction, Section II is for Materials and methods, Related work is in Section III, Conceptual model is in Section IV, Hypotheses regarding factors affecting consumer online shopping behavior are in Section V, Causal loop diagram is in Section VI, Simulation and results are in Section VII, and finally Section VII is the conclusion.

II. MATERIALS AND METHODS

A. eCommerce

eCommerce is a business platform, where anyone can buy, sell and transfer goods, information and services through electronic means usually over the internet. Anything can be offered to the end users via ecommerce, from concert tickets to books to commercial services. eCommerce includes Business-to-Consumer model(B2C), where consumers can buy goods or services directly from the source (business). Online shopping or e-tailing is an example of B2C.

B. Online Shopping

In 1979, Michael Aldrich invented online shopping. It can also be called e-tail from 'electronic retail' or e-shopping. Online shopping is where users can use web browser to buy goods or services over internet.

Consumers can enjoy the convenience of online shopping from anywhere and businesses can thrive on low overhead. Online shopping is ideal for small business as they don't need huge amount of merchandise stocked or a retail store.

Internet has created an exceedingly cutthroat market where retailers are vying for customer's attention. Since there are so many potential consumers, it is paramount that retailer are able to understand what the consumer wants and needs and identify the influencing factors affecting consumer behavior.

C. Consumer Behavior

Sabine Kuester, [4] defines consumer behavior as the processes and ideas, the individuals and groups exercise to satisfy their needs. Every human being has a different personality so their buying behavior is also different from one another. Consumer behavior is influenced by cultural trends, social drivers (family, social status), personal factors (age, lifestyle, and revenue), psychological factors (motivation, perception and attitude) and risks perceived by the user.

III. RELATED WORK

There are multiple studies available regarding what factors influence consumer's online shopping behavior. The most important and common factors were found to be consumer's trust, e-loyalty and consumer's satisfaction.

Shankar et al. [23] discussed online trust in relation to different types of stakeholders: customers, dealers, stockholders, distributors and partners. They presented a conceptual framework for factors which are relevant to online trust including website and user attributes (such as security, brand, etc.). Trust then influences customer satisfaction, customer loyalty and performance of the ecommerce website.

Aghdaie et al. [9] suggested that consumer's trust is the main influence in eCommerce transactions. The authors made hypotheses from a survey study, discussing the factors in terms of trustee, trustor and environment to build trust, purchase and recurring purchase. Some of the factors affecting consumer's attitude of trust are promotions, government policies, payment methods and delivery mechanism, information quality and design, and usability of the website.

Uzun and Porturak [27] examined Bosnian online ecommerce customers and discussed the relationship between e-satisfaction and e-loyalty. E-loyalty was referred in terms of repurchases, demographics, age, gender, education and revenues. They proposed seven hypotheses concerning trust, satisfaction and online shopping behavior. Consumer's trust, price, convenience, web design, quality of product, delivery time, and previous experience positively affects consumer behavior and their satisfaction. Zhu et al. [22] also support that trust and customer satisfaction are the primary factors that have an impact on customer's loyalty to the eCommerce website.

Chandra and Sinha, [24] studied the factors affecting the consumers of online shopping in an Indian city, Bhilai-Durg. They presented several hypotheses that the consumer intention to buy thing online depends upon demographics, attitude of

the consumer, convenience, price and trust. These hypotheses were tested through the result from 100 questionnaires.

Park and Kim, [6] conducted a survey of 602 Koreans who bought books online. They found that UI quality, content quality, and secure payments were some of the factors influencing consumer's purchase behavior and their commitment to the website.

Akbar and James, [7] identified the nine variables (Price, Auction websites, Refund policy, Convenience, Security, Search engines, Product Brand, Promotions and malls) as the independent factors that influence consumer behavior. They gathered data from employees of "crazy domains" from Nonthaburi, Thailand. Using t-test analysis for gender they showed that females tend to shop online more than men.

Javadi et al. [25] presented a conceptual model for online consumers of Iran, which represent social and technical factors that affect consumer online shopping behavior. They surveyed 200 users and found that unsecure transactions and non-delivery of the items purchased by the user have negative impact on consumer behavior.

Li and Zhang, [8] analyzed 35 empirical articles to investigate online shopping attitudes and behaviors. Ten factors were identified as demographics, environment, user and item's attributes, attitude, buyer's intention to purchase goods and their buying behavior, and consumer satisfaction.

Hung and McQueen, [10] proposed an evaluation mechanism for the evaluation from first-time consumer's perspective of an online shopping website. Three failure points were identified to measure the satisfaction and dissatisfaction of consumer.

Khanh and Gim, [26] performed an empirical study on 238 Vietnam consumers who shop online. They proposed a conceptual model having several factors that affect consumer's online shopping behavior such as: price, ease of use, payment method, security, and content privacy of the website.

DeLone and McLean [11] presented an eCommerce success model which included six dimensions: System quality, Service quality, Information quality, Use, Customer satisfaction and Net benefits. They also reviewed old and new eCommerce success metrics from different authors, which they applied to two case studies to justify their model.

Laurae'us et al. [12] discussed that searching process and searching mechanisms for finding the perfect product, while shopping online are essential to customer's satisfaction.

Sinha and Kim [28] proposed a conceptual model for factors affecting Indian online shopping customers. This model examined there are financial, product and convenience risks associated with consumers attitude to shop online. Delivery concerns and return policies also influence consumer's behavior and attitude towards online shopping.

In Table I. multiple studies are shown in a tabular form, regarding the several factors which influence consumer's online shopping behavior.

TABLE I. DIFFERENT STUDIES ON FACTORS AFFECTING CONSUMER'S ONLINE SHOPPING BEHAVIOR

Factors	Authors
Trust	Shanker et al. [23], Chandra and Sinha [24], Aghdaie et al. [9], Khanh and Gim [26], DeLone and McLean [11], Zhu et al. [22], Cheung & Lee 2006, Crye et al. 2005, Jarvenpaa & Tractinsky 1999, Bhatnagar et al. 2000, Doolin et al., 2005, Gupta et al. 2003, Lee & Turban 2001, Gommans et al. 2001, Pavlou 2003, Uzun and Porturak [27]
Demographics	Li & Zhang [8], Chandra and Sinha [24], Uzun and Porturak [27], Bellman et al., 1999, Bhatnagar et al., 2000, Kunz 1997, Sultan & Henrichs 2000, Weiss 2001, Swinwyrd & Smith 2003
Availability of information	Aghdaie et al. [9], DeLone and McLean [11], Elliot & Speck 2005, Quinn 1999, Bart et al. 2005, Brown et al. 2001
Price	Chandra and Sinha [24], Akbar and James, [7], Khanh and Gim [26], Sinha and Kim [28], Spann & Tellis 2006, Chung & Shun 2008, Cuneit & Gautam 2004, Heim & Sinha 2001
Responsiveness	Cheung & Lee 2005
Ease of use	Shanker et al. [23], Aghdaie et al. [9], Khanh and Gim [26], Dabholkar 1996, Santos 2003, Pavlou 2003
Security	Shanker et al. [23], Park and Kim [6], Akbar and James [7], Javadi et al. [25], Aghdaie et al. [9], Khanh and Gim [26], Kesh et al., 2002, Rao 2000
Decision aids	Geiss lee & Zinkhan 1998, Haubl & Murray 2003, Xio & Benbast 2007, Huang & Sycara 2002, Huang & Lin 2007
UI quality	Li & Zhang [8], Shanker et al. [23], Park and Kim [6], Aghdaie et al. [9], Khanh and Gim [26], DeLone and McLean [11], Uzun and Porturak [27] Nali & Phing Zhang 2002, Zhang, Von Dran, Small & Barcellos (1999,2000), Zhang & Von Dran 2000
Interactivity	Shanker et al. [23], Aghdaie et al. [9], Haeckel 1998, Hoffman & Novak 1996
Reliability	Parasuraman et al., 1988, Janda et al., 2002, Kim & Lee 2002
Brand	Shanker et al. [23], Akbar and James [7]
Convenience	Chandra and Sinha [24], Akbar and James, [7], Javadi et al. [25], Sinha and Kim [28]
Customer satisfaction	Li & Zhang [8], Shanker et al. [23], Aghdaie et al. [9], Khanh and Gim [26], DeLone and McLean [11], Zhu et al. [22], Uzun and Porturak [27]
Customer loyalty	Li & Zhang [8], Shanker et al. [23], Aghdaie et al. [9], DeLone and McLean [11], Zhu et al. [22], Uzun and Porturak [27]

IV. CONCEPTUAL MODEL

The conceptual model proposed here is the modified form of DeLone and McLean model for eCommerce success. Incorporated in this conceptual model, are some social and

technical factors which influence customer shopping behavior. This model can be used to assess eCommerce website success and help retailers to keep their customers and increase their organization's productivity. Seven segments of this model are as follows:

A. Information Quality

The quality of information of an eCommerce website depends upon the completeness, correctness and relevance of the content of the website. Comprehensive information about the product has a huge impact upon buyer's intention to use the website and buyer's satisfaction.

B. System Quality

The quality of the system can be referred to as ease of use, user interface quality and interactivity, search engine optimization and decision aids. It indirectly impacts the productivity of the organization through usage intentions and consumer's satisfaction.

C. Service Quality

The service quality can be defined in terms of responsiveness of the system, secure transactions, Promotions, lower cost and reliability (refund policies, on time product delivery). It impacts consumer's usage and satisfactions which in turn impacts the productivity.

D. Intention to use

Consumer's intention to use is influenced by information, system and service quality. Culture and demographics also influence the user's usage of the system. It in turn effects user's satisfaction.

E. User satisfaction

End user's satisfaction is the extent to which a consumer is contended with the system and is influenced by consumer's usage of the system. If a consumer is pleased with the system there is a chance of repeat purchase.

F. User loyalty

User satisfaction directly impacts user's loyalty. If a consumer is satisfied with the website's quality and service, it is most likely that the consumer visits the website again to make purchase. Trust is the critical factor in consumer's loyalty which in turn also impacts user satisfaction.

G. Productivity

Customer's intent to use the system and their loyalty to the system affects the productivity of the system. It refers to how much an organization has profited from consumer's responsiveness. Productivity then impacts user's usage and user loyalty.

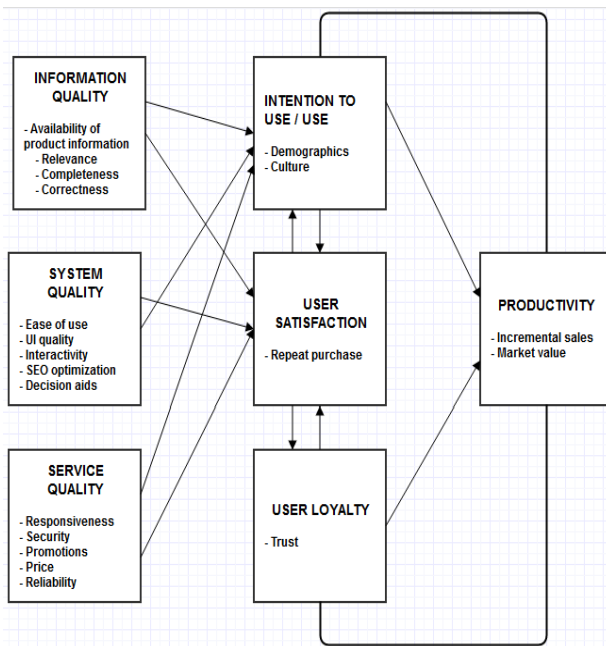


Fig. 1. Conceptual model for eCommerce website success

V. HYPOTHESIS ON FACTORS AFFECTING CUSTOMER BEHAVIOR IN AN ONLINE SHOPPING ENVIRONMENT

From the conceptual model discussed in Section IV, thirteen hypotheses can be made regarding the factors influencing customer's online shopping behavior.

A. Social Aspects

1) *Culture*: Culture can be defined as the joint characteristics of the minds that differentiate individuals from one another [13]. The values and beliefs that affect how we perform a task and make decisions are ingrained, in us from our childhood [14]. Therefore, these traits are important to e-marketers. Marketers have to understand the user's cultural background in order to predict their buying behavior. The consumer's background knowledge, their core value and norms help the marketers to produce potential goods that satisfy consumer's needs.

Internet has the capability to reach people of every culture around the globe. Marketers will have to instigate consumers in accepting the custom of online shopping in the fabric of society.

H1: Culture positively affects consumer's intention to shop online.

2) *Cost*: Price is a critical factor for consumers who shop online [15]. Several consumers don't bother to explore further if the price is not reasonable. Shopping online allow users to gather and compare product information such as price. Furthermore, extra charges such as shipping cost, customs or extended delivery times can affect consumer's decision to buy a product even if its price is reasonable.

Nevertheless, Li et al. argues that often online shoppers don't care about price as the price difference is very small and comparison of products cost is time consuming.

H2: Price of the product positively affects customer satisfaction.

3) *Demographics*: Demographics incorporate age, gender, revenue, academic qualification and time spent online of an end user. It essentially, tells whether the end users surf the internet or not, but once the end user is online, demographics doesn't affect their purchasing activities.

Consumer belonging to higher social class and higher education, shop more online, then consumers of lower social class and less education because of the availability of financial resources and awareness [5]. Some studies show that females tend to shop more online than men, while other studies show opposite.

H3: Demographics positively affect the consumer's intention to shop online.

4) *Convenience*: Something that saves time and effort is convenient. It is undeniable that a person's life has become hectic in this age, so modern technology can be reckoned as the solution to the consumer's worries of in store peak hour crowds. Shopping online is very convenient to consumers as they can access the website from anywhere anytime if they do not mind waiting for extra shipping time and delivery costs.

In the business context, the presence of internet has liberated retailers from traditional marketing practices. Online shopping has provided retailers a platform to grow their profits by developing better marketing communication strategies [16].

H4: Convenience positively affects consumer's satisfaction.

5) *Availability of product information*: Availability of product information affect consumer's trust [17], as consumer cannot physically examine the product while shopping online. Marketers have difficulty in establishing consumer's trust in online shopping environment [18].

Therefore, it is important to provide detailed information of the product to help build user confidence, that they made the right decision in buying the product. Constant updates in product information helps consumer to keep track of the product [19].

H5: Availability of product information positively affects consumer's trust.

6) *Trust*: Trust, is essentially the most significant cause that influence consumer's behavior while shopping online. The definition of online trust varies with the stakeholders. From a consumer's point of view, an eCommerce website must be secure and reliable. Whereas, from a seller's viewpoint the website key constituents may be integrity, competence and confidentiality [11].

H6: Trust positively affects consumer's satisfaction.

B. Technical Aspects

1) *User Interface Quality and interactivity*: Consumers are attracted to the websites because of their design features, quality and interactive interfaces. The higher the website

quality, the higher is a chance of consumer shopping there. The quality of the shopping website leads to consumer's satisfaction and dissatisfaction and in consumer's revisiting it. However, bad website features and quality can hinder consumer's online shopping behavior as they directly impact on users [3]. The user interface of the website should be attractive and appealing to grab consumer's attention while showing the essence of website.

Appropriate font and color schemes, clear navigation, responsive website design, cross browser functionality should be present to appeal the customer. Appropriate help and search engine optimization of the website should be provided [22]. Feedbacks from consumers can help in understanding their problems and improving website design quality.

H7: User interface quality and interactivity positively affects consumer's satisfaction.

2) *Ease of use*: Online shopping website must have ease of use, i.e. every kind of user can easily understand and use the website. The usability factor is critical in maintaining customer trust in online shopping environment.

Clear and visible navigations, consistent styles and color, concise content, appropriate help and searching means easily accessible are various usability factors to affect end user's satisfaction.

H8: Ease of use positively affects consumer's satisfaction.

3) *Decision aids*: Decision making in an online shopping environment includes searching for product information, comparison of prices, and choosing alternatives.

Typically, consumers will rather view the price of a product first, than any other information about the product. There are same products available of different brands with different prices. The consumers can choose the products through comparing prices using decision aids. Interactive decision aids are used to facilitate consumers to form intelligent decisions [13]. These decisions directly influence consumer's satisfaction and their purchasing behavior.

Recommendation agent and comparison matrix are the two main interactive decision making tools available to help consumers to make the right decision. Alternatives should be available to consumers in term of searching and payment methods. The user may choose from related products and pay through different mechanisms such as PayPal, credit card, Bit coin, cash on delivery etc.

H9: Decision aids positively affect consumer's satisfaction.

4) *Responsiveness*: In this era online shopping is preferred compared to traditional shopping because of its convenience. This means that online shopping is time effective. The consumers will prefer the system whose order processing and transaction takes less time. If the system is not responsive, the consumer will not buy from that website.

H10: Responsiveness positively affects consumer's satisfaction.

5) *Security*: There are many benefits of online shopping but there are security risks involved. Security is one of the main attributes which can limit consumer's buying over the internet, as they fear for the security of their sensitive information [21]. The consumers fear disclosure of their personal information (address, contact information) as well as their account information.

E-marketers must maintain the best possible security mechanisms to provide protection to the consumer's data and secure transactions to help consumers feel secure. If the security methods of the website are not state-of-the-art then consumer will not bother to shop there.

H11: Secure transactions positively affect consumer's trust.

6) *Promotions*: E-retailers might use deals/ offers and promotions on a product to encourage consumers to shop online [22]. Websites should advertise deals regarding a product on social media, and alert users on email address and mobile phones.

Promotions are another way to grab consumer's attention toward online shopping. If the consumer finds the deals interesting and feasible enough then the consumer will certainly buy the product and inform others about it.

H12: Promotions positively affects consumer's satisfaction.

7) *Reliability*: Reliability means the effectiveness of online order process i.e. getting the products delivered on time, refunds and reliable customer service. E- Retailers ought to provide refund policy for the customers who wish to return the product or replace it for another, if they are not satisfied with it.

H13: Reliability positively affects consumer's trust.

VI. CAUSAL LOOP DIAGRAM (CLD)

Causal loop diagram is a system dynamics tool, used to visualize relationship between different variables in term of cause and effect. It is a great way to portray how the factors affecting consumer's behavior are interrelated and how they associate with customer's satisfaction.

The thirteen hypothesis formed about the consumer's behavior in an online shopping environment are visualized here in a causal loop diagram. There are several factors that positively affect consumer's satisfaction including: Interactivity and UI Quality of the website, Convenience, Responsiveness, Promotions, Ease of use, decision aids and price. Security, Reliability, Brand, Demographics and Availability of product information positively affect customer's trust.

Trust increases the end user's satisfaction with the website and their loyalty to the website as they visit the website for repurchase of items. Customer loyalty increases the productivity of the website.

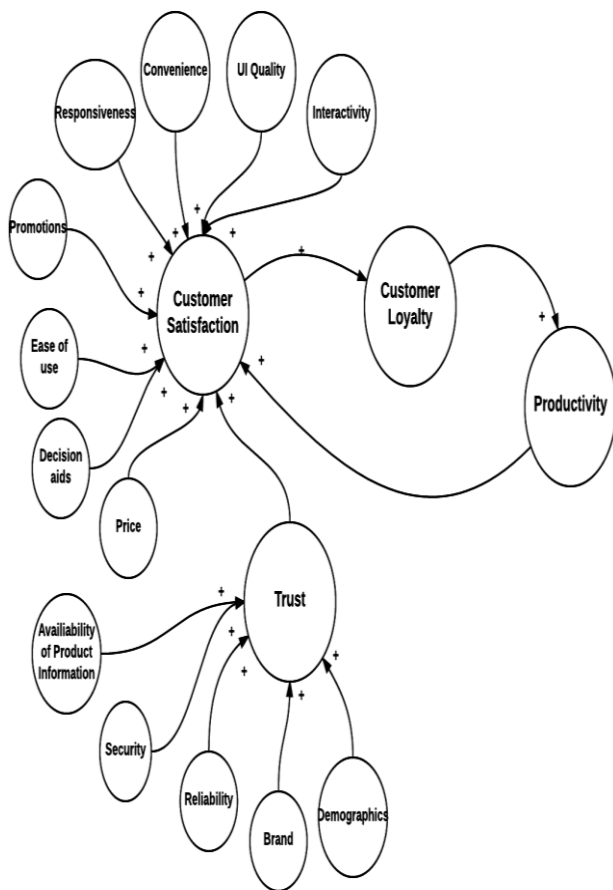


Fig. 2. Causal loop diagram for this scenario

VII. SIMULATION AND RESULTS

This section contains the simulation of the causal loop diagram in iThink tool and the results found which are also generated through the features (Table Pad and Graph Pad) of the same tool.

A questionnaire was developed from thirteen hypothesis discussed in Section-V to collect data. 20 questions having Likert scale were asked in the online survey from 100 participants. The Likert scale range started from strongly disagree having value of 1, to strongly agree having the highest value of 7. The data was analyzed to find the mean values of the factors and added to a simulation via iThink (i.e. by isee systems).

There are some negative factors which contribute to the loss of consumer’s trust such as: no delivery risk, unsecure transactions, loss of privacy, bad UI quality, poor website content and poor customer support service. For this simulation RANDOM function is used to calculate trust lost, because these negative factors may vary in websites. iThink is a system dynamics tool having an intuitive icon-based graphical interface. There have been many studies regarding factors affecting consumer’s online behavior and for evaluation of eCommerce websites.

This simulation showed how the user’s trust and satisfaction directly impact productivity of the eCommerce website.

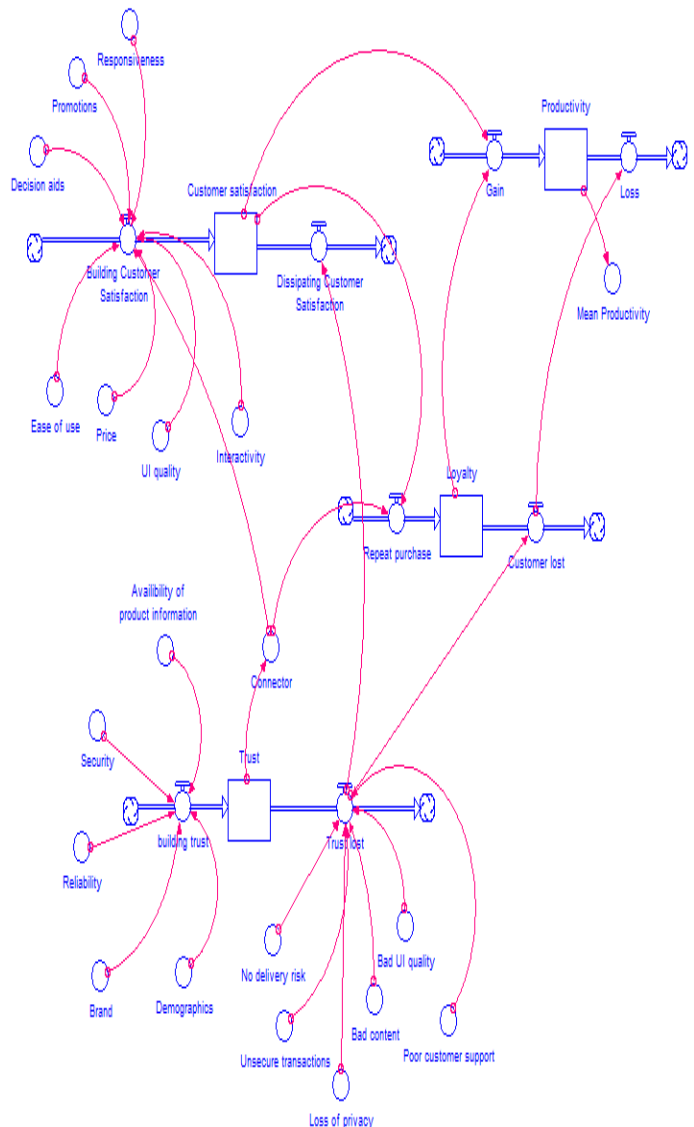


Fig. 3. Model of the causal loop diagram in iThink

TABLE II. TABULAR DATA OF 20 YEARS SHOWING INCREASE IN TRUST LEADS PRODUCTIVITY

Years	Customer sat	Trust	Loyalty	Productivity	Mean Product
Initial	0.00	0.00	0.00	0.00	0.00
1	32.84	22.29	3.55	0.00	0.00
2	89.15	45.84	65.83	51.93	0.52
3	173.24	73.38	220.97	268.70	2.67
4	275.50	93.70	488.06	781.82	7.82
5	404.89	118.19	891.05	1,689.77	16.90
6	554.22	140.82	1,451.93	3,212.37	32.12
7	730.83	166.28	2,199.81	5,528.79	55.27
8	927.73	187.85	3,152.64	8,845.52	88.46
9	1,151.20	213.47	4,338.13	13,411.72	134.12
10	1,390.98	232.04	5,770.41	19,478.99	194.79
11	1,653.00	253.19	7,473.00	27,328.67	273.29
12	1,941.09	277.90	9,473.13	37,285.21	372.85

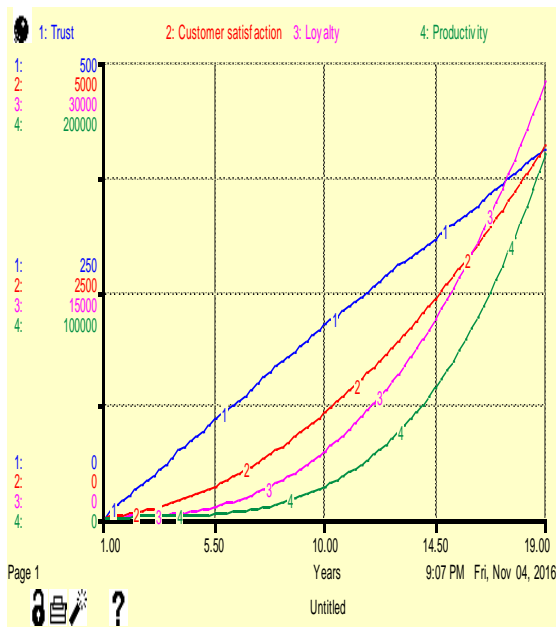


Fig. 4. Simulations Graph showing increase in productivity through trust

In Table II and figure 4 data of 20 years of an ecommerce website is shown. It shows that trust increases consumer's satisfaction which in turn increases customer loyalty. Customer loyalty refers to when the consumers come back on the website for repeat purchase. Consumer's satisfaction and e-loyalty increases productivity of the website. Retailers and marketers can benefit from using this model.

VIII. CONCLUSION

As opposed to other studies regarding factors affecting consumer's online behavior, this work provides a comprehensive amount of factors and a novel approach to represent the conceptual model.

In aforementioned work, different socio-technical factors (attributes) are highlighted, integrated and delineated comprehensively in graphical representation (simulations) those affects the way the consumer shop online. A conceptual methodology is proposed in this work to estimate and validate the success of the eCommerce website (web portal). The simulations and validations of the proposed model is then validated latter via iThink which further depicts (data & results) productivity increases if consumer is satisfied and trust the system.

This proposed methodology is beneficial to developers as well as for retailers. Developers can keep in mind the technical aspects (attributes) while developing the system to provide user the best experience possible and latter retailers can increase the productivity of their organization.

REFERENCES

[1] Koyuncu and G. Bhattacharya, "The impacts of quickness, price, payment risk, and delivery issues on on-line shopping", *The Journal of Socio-Economics*, vol. 33, no. 2, pp. 241-251, 2004.

[2] N. Li and P. Zhang, "Consumer online shopping attitudes and behavior: An assessment of research", *AMCIS 2002 Proceedings*, p. 74, 2002.

[3] T. Liang and H. Lai, "Electronic store design and consumer choice: an empirical study", *System Sciences*, 2000. Proceedings of the 33rd Annual Hawaii International Conference, 2000.

[4] S. Kuester, *MKT 301: Strategic Marketing & Marketing in Specific Industry Contexts*, University of Mannheim, p. 110, 2012.

[5] A. Smith and W. Rupp, "Strategic online customer decision making: leveraging the transformational power of the Internet", *Online Information Review*, vol. 27, no. 6, pp. 418-432, 2003.

[6] C. Park and Y. Kim, "Identifying key factors affecting consumer purchase behavior in an online shopping context", *Intl J of Retail & DistribMgt*, vol. 31, no. 1, pp. 16-29, 2003.

[7] S. Akbar and P. James, "Consumers' attitude towards online shopping: Factors influencing employees of crazy domains to shop online", *Journal of Management and Marketing Research*, vol. 14, no. 3, 2013.

[8] N. Li and P. Zhang, "Consumer online shopping attitudes and behavior: An assessment of research", *AMCIS 2002 Proceedings*, p. 74, 2002.

[9] S. F. A. Aghdaie, A. Piraman and S. Fathi, "An analysis of factors affecting the consumer's attitude of trust and their impact on internet purchasing behavior", *International Journal of Business and Social Science*, vol. 2, no. 23, pp. 147-158, 2011.

[10] W. Hung and R. McQueen, "Developing an evaluation instrument for e-commerce web sites from the first-time buyer's viewpoint", *Electronic Journal of Information Systems Evaluation*, vol. 7, no. 1, pp. 31-42, 2004.

[11] W. DeLone and E. McLean, "Measuring e-commerce success: Applying the DeLone & McLean information systems success model", *International Journal of Electronic Commerce*, vol. 9, no. 1, pp. 31-47, 2004.

[12] T. Lauraćus, T. Saarinen and A. Öörni, "Factors Affecting Consumer Satisfaction of Online Purchase," *System Sciences (HICSS)*, 2015 48th Hawaii International Conference on, Kauai, HI, 2015, pp. 3364-3373. doi: 10.1109/HICSS.2015.406

[13] G. Hofstede, "The business of international business is culture", *International Business Review*, vol. 3, no. 1, pp. 1-14, 1994.

[14] P. Kotler and G. Armstrong, *Principles of marketing*. Upper Saddle River, N.J.: Pearson Prentice Hall, 2006.

[15] G. Heim and K. Sinha, "Operational Drivers of Customer Loyalty in Electronic Retailing: An Empirical Analysis of Electronic Food Retailers", *Manufacturing & Service Operations Management*, vol. 3, no. 3, pp. 264-271, 2001.

[16] J. Joergensen and J. Blythe, "A guide to a more effective World Wide Web presence", *Journal of Marketing Communications*, vol. 9, no. 1, pp. 45-58, 2003.

[17] Y. Bart, V. Shankar, F. Sultan and G. Urban, "Are the Drivers and Role of Online Trust the Same for All Web Sites and Consumers? A Large-Scale Exploratory Empirical Study", *Journal of Marketing*, vol. 69, no. 4, pp. 133-152, 2005.

[18] A. Schlosser, T. White and S. Lloyd, "Converting Web Site Visitors into Buyers: How Web Site Investment Increases Consumer Trusting Beliefs and Online Purchase Intentions", *Journal of Marketing*, vol. 70, no. 2, pp. 133-148, 2006.

[19] C. Quinn, "How leading-edge companies are marketing, selling, and fulfilling over the Internet", *Journal of Interactive Marketing*, vol. 13, no. 4, pp. 39-50, 1999.

[20] G. Häubl and V. Trifts, "Consumer Decision Making in Online Shopping Environments: The Effects of Interactive Decision Aids", *Marketing Science*, vol. 19, no. 1, pp. 4-21, 2000.

[21] A. Bhatnagar and S. Ghose, "A latent class segmentation analysis of e-shoppers", *Journal of Business Research*, vol. 57, no. 7, pp. 758-767, 2004.

[22] D. S. Zhu, M. J. Kuo and E. Munkhbold, "Effects of E-Customer Satisfaction and E-Trust on E-Loyalty: Mongolian Online Shopping Behavior," 2016 5th IIAI International Congress on Advanced Applied Informatics (IIAI-AAI), Kumamoto, 2016, pp. 847-852.

[23] V. Shankar, G. Urban and F. Sultan, "Online trust: a stakeholder perspective, concepts, implications, and future directions", *The Journal of Strategic Information Systems*, vol. 11, no. 3-4, pp. 325-344, 2002.

- [24] A. Chandra and D. Sinha, "Factors Affecting the Online Shopping Behaviour: A Study With Reference to Bhilai Durg", *International Journal of Advanced Research in Management and Social Sciences*, vol. 2, no. 5, 2013.
- [25] M. Moshrefjavadi, H. Rezaie Dolatabadi, M. Nourbakhsh, A. Poursaeedi and A. Asadollahi, "An Analysis of Factors Affecting on Online Shopping Behavior of Consumers", *International Journal of Marketing Studies*, vol. 4, no. 5, 2012.
- [26] N. Khanh and G. Gim, "Factors Affecting the Online Shopping Behavior: An Empirical Investigation in Vietnam", *International Journal of Engineering Research and Applications*, vol. 4, no. 2, pp. 388-392, 2014.
- [27] H. Uzun and M. Poturak, "Factors Affecting Online Shopping Behavior of Consumers", *European Journal of Social and Human Sciences*, vol. 3, no. 3, pp. 163-170, 2014.
- [28] Sinha and J. Kim, "Factors affecting Indian consumers' online buying behavior", *Innovative Marketing*, vol. 8, no. 2, pp. 46-57, 2012.

Role of Requirements Elicitation & Prioritization to Optimize Quality in Scrum Agile Development

Aneesa Rida Asghar
Dept. of software engineering
Bahria University Islamabad, Pakistan

Shahid Nazir Bhatti
Senior Assistant Professor,
Department of Software Engineering,
Bahria University Islamabad, Pakistan

Atika Tabassum
Dept. of software engineering
Bahria University Islamabad, Pakistan

Zainab Sultan, Rabiya Abbas
Department of Software Engineering,
Bahria University Islamabad, Pakistan

Abstract—One of most common aspect with traditional software development is managing requirements. As requirements emerge throughout the software development process and thus are needed to be addressed through proper communication and integration between stakeholders, developers and documentation. Agile methodology is an innovative and iterative process that supports changing requirements and helps in addressing changes throughout the development process.

Requirements are elicited at the beginning of every software development process and project (product) and latter are prioritized according to their importance to the market and to the product itself. One of the most important and influencing steps while making a software product is requirements prioritization. Prioritizing requirements helps the software team to understand the existence and importance of a particular requirement, its importance of use and its urgency to time to market. There are many requirements prioritization techniques with their relative strength and weaknesses. Otherwise many of them fail to take account all the factors that must be considered while prioritizing requirements such as cost, value, risk, time to market, number of requirements and effect of non-functional requirements on functional requirements.

There are several requirements prioritization methodologies that aid in decision making but importantly many lacks to account the important factors that have significant influence in prioritizing requirements. A requirement prioritization methodology based on several factors such as time to market, cost, risk etc has been proposed. The proposed model is expected to overcome this lack. In sprints, requirements will be prioritized both on the basis of influencing factors such as cost, value, risk, time to market etc. and through the effect of non-functional requirements over functional requirements. This will improve the overall quality of software product when it is included in the development process of scrum. Requirements will not only be prioritized based on sprints, human decision but by critically analyzing the factors (sub characteristics) that can cause the product to success/ fail repeatedly thus ensuring the consistency in right requirements and hence the right prioritized requirements will be selected for a particular sprint at a time.

Keywords—Agile Software Engineering (ASE); Agile Software Development (ASD); Scrum Software Development Process; SCRUM; Product Owner (PO)

I. INTRODUCTION

Traditional requirement engineering does not support changing requirements and continuous communication with stakeholders therefore problems arise when new requirements are evolved due to change in business needs and time to market [4] [3] [1]. Thus software market is moving towards agile software development as it supports changing requirements and speedy process development. Agile practices are being acknowledged and are becoming popular day by day in the field of requirement engineering. One of the most popular methods among agile family where software is delivered in increments called sprints is known as SCRUM [8] [6]. A sprint consists of 2-4 week iteration. Scrum methodology comprises of a planning meeting and daily scrum meeting, the planning meeting is conducted at the beginning of every sprint. In this meeting team members determine the number of requirements they can oblige to manage that is they create a sprint backlog out of that. Sprint backlog contains the list of all the tasks that should be perform during a particular sprint. Daily scrum meetings are not more than 15 minutes, where product owner (PO) gets continuous updates about the development process and can provide feedback about the features being included. This way if a PO decides to add new feature to a sprint, he/she can discuss it with the development team and save time rather than reviewing it at the end and demanding change at the end. The team conducts a sprint review at the end of each sprint where they demonstrate new features and functionality to the PO or to other stakeholders that can provide any kind of feedback which could be beneficial or helpful in any way for the next sprint. This loop of feedbacks results in modifications to the recently delivered functionality, then again it is more likely reviewing or adding new requirements to the product backlog. Another activity in Scrum project management is Sprint retrospective. The Scrum Master, PO and the development team participates in this meeting. It is the chance to reproduce or review the sprint that has ended, and identify new ways to improve. Scrum consists of three artifacts, sprint backlogs, product backlogs and burn down charts. The Product backlog, prioritized by the PO is a complete list of the functionality (written as user stories) that is to be added to the product eventually. It is prioritized so that the team can always

work on the most important, urgent and valuable features first. On the other hand, sprint backlog is the list of all those tasks that the team obliged to and needs to perform during the sprint in order to deliver the required functionality. The remaining amount of work either in a sprint or a release is shown by 'Burn down' charts. It is an effective tool to conclude whether a sprint or release is on schedule to have all planned work finished in time. The traditional requirements engineering is very time consuming and requires speedy process to timely meet the needs of market so modern software industry demands rapid and iterative process like agile development to cope with the changing requirements and time.

There are many factors involved in the success or failure of a product, one of them is collecting and prioritizing requirements [2]. Requirements elicitation and prioritization is one the most challenging task during product development and it is very unlikely to be able to write down all the requirements at early stage, they evolve continuously throughout the development process and are needed to be addressed properly to meet the changing needs of market and time. As scrum is an agile methodology, therefore it allows engineers to handle changing requirements as they evolve; however, it is still a challenging task to comprehend which prerequisites are sufficiently vital to have high need and to be incorporated into early sprints. Organizing requirements into Priorities requirements helps the project team to comprehend which requirements are most essential and most urgent to implement and execute. Prioritization is likewise a helpful activity for decision making in other phases of software engineering. Therefore there should be a well-managed requirement prioritization technique included in scrum processes that improves its quality.

A requirement prioritization technique based on several factors such as time to market, cost, risk etc. has been proposed that will improve the quality of software product when it is included in the development process of scrum. The proposed model is expected to overcome the lack of quality of the prior models. Requirements will be prioritized both on the basis of influencing factors such as cost, value, risk, time to market etc. and through the effect of non-functional requirements over functional requirements. Requirements will not only be prioritized based on human decision but by critically analysing the factors that can cause the product to fail/success repeatedly thus ensuring the consistency in right requirements for a particular sprint at a time.

II. MATERIALS AND METHODS

A. Agile Requirement Engineering

In this work [1], author presented the 10 years progress of agile research and proposed some future research areas for agile researchers to hold on to an approach that is theoretical or hypothetical. A survey based methodology was used to get reliable information about the progress of agile methodologies. It is significant to remember that one can produce and enhance fields as a scientific discipline only if energies are able to convey a solid theoretic system to conduct research on agile development. Therefore, it is a need that in future when investigating into agile development proficient research areas, agile researchers hold on to a more theoretical based approach.

Ming Huo et al [3] proposed that agile methods can assure quality even agile methods are faster and have to manage changing requirements. Author basically presented a comparison between waterfall model and agile model and presented the results. Agile methods contain some practices that have QA abilities, so with the help of this quality can be achieved more appropriately through agile methods. However one thing that must be considered when documenting agile RE is that in complex software development processes, less documentation can bring some issues/ problems.

Lan Cao et al [4], presented an empirical study on agile RE practices. This study shows the difference between agile RE and traditional RE is an iterative finding approach. Developing clear and complete requirements specification is impossible in agile development. Because of such important differences a new set of agile RE practices had come into practices that are reported in this paper. The study participants recognized that the most important practice in RE is thorough communication between the developers and customers.

Numerous participants highlighted that the efficiency of this practice depends deeply & effectively on exhaustive communication and interaction between customers and developers. Risks such as incomplete requirements, ineffectively developed requirements or wrong requirements are possessed if high quality interaction lacks in any project.

In this work Pekka et al [6], proposed that there are different methods of agile process that needs the empirical evidences. Authors emphasized on the quality of methodology not the quantity. This approach was chosen for comparative analysis of these processes. Five perspectives are included in the analytical lenses. SDLC include the process aspect abstract principles vs. concrete guidance, empirical evidence, project management and universally predefined vs. situation appropriate. New directions are offered based on these 5 perspectives that focus on quality not on quantity of methods.

Amin et al [7], proposed that some lessons of RE must be considered by the agile methods if the most emphasized thing is quality. Some major aspects of RE that are not a much emphasized in agile are analysis (verification and validation), non-functional requirements and managing change. Author suggested that these practices of RE can be adopted in agile and high quality can be achieved. RE practices such as simplicity, continuing validation, short releases and frequent refactoring, can be implemented in the perspective of agile main ideas.

Deepti Mishra et al [8], proposed that agile process can be helpful for the development of complex software projects. Author supported his argument with the help of a case study. A medium enterprise (SME) that practiced agile methods, achieved many successful results. Starting a project with agile methods and then achieving optimum methods by tailoring agile methods according to vision and benefits is the main reason of the success of supply chain management. The architectural design of this large scale complex project was supported with formal documentation. In the successful completion of the project an important role was played by this design documentation.

Franek et al [11], proposed different ways of RE methods from which agile software development can get advantages. Some common and different features and attributes of traditional approaches and agile approaches are also discussed. Agile approaches such as XP involves feedback from development teams and customers, communication and simplicity. Similarly RE process also includes dictation, analysis and validation. But in agile process phases are not as clearly distinguished as in RE process and techniques can also vary. Overall both are pursuing same objectives. The major difference is of documentation that is really important to communicate with the stakeholders.

V. N. Vithana [12], conducted a research using qualitative methods to find out which requirement engineering practices are mostly being used in SCRUM methodology when developing a software product offshore. In order to collect data different job holders from nine organizations were questioned. It was found that RE practices such as Customer Involvement, prototyping, test driven development and Interaction are the least practiced activities of Requirement Engineering, although most of the team members were successfully practicing iterative requirements engineering, face to face communication, managing requirements change and requirements prioritization of SCRUM RE practice.

B. Requirements Prioritization Techniques

In this Anna Perini et al [14], proposed a strategy called Case-Based Ranking (CBRank). This method joins the preferences of the stakeholders of the project with the approximation of requirements ordering that is computed over machine learning methods. On simulated data the properties of CBRank are performed and then matched with a method called state-of-the-art prioritization, thus provided empirical results. However there are some assumptions in the CBRank prioritization process such as arbitrary selection as pair sampling policy and the monotonicity of the elicitation process. To improve the efficiency of real complex sitting methods the authors intend to work in future on non-monotonic formal logic case and pair sampling strategies that are more refined.

DAN HAO et al, [10] in this article, have presented a strategy that comprises the total and additional strategies for unified test case prioritization. These tactics prioritize test cases in light of components secured per test case, the aggregate number of program segments (or code-related) and the number of others (not yet covered) program segments (or code-related) components covered per test case, respectively. The proposed approach includes basic and extended models, which define a spectrum of test case prioritization from a purely total to a purely additional technique by specifying the value of a parameter referred to as the fp value [10].

Rahul Thakurta [15], proposed a quantitative structure that determines the priority of a list of non-functional requirements. This framework involves members from business organization and the project to provide a measurable ground for assessing the level of value addition that is considered while choosing a new non-functional requirement to the project's requirement set. However, the inputs provided to the framework by members were subjective which may result in non-optimal results. Additionally, as the requirements assessment process

involves stakeholders from both business organizations and the project, there are odds of irreconcilable interests and priorities of requirements. The author has also set the directions for future work which is to build a heuristic to bound the number of stakeholders to be preferred for assessment process.

Naila Sharif et al [16], devised a new requirements prioritization technique called FuzzyHCV which is a hybrid of two domains (SE and Computational Intelligence). It is a fusion of two methodologies which are Hierarchical Cumulative Voting (HCV) and Fuzzy Expert System. In FuzzyHCV, rather than a single crisp value a triangular fuzzy number is used. The proposed technique has been applied on 3 case studies and the results obtained are very close to the results of actual prioritization used in all of the three case studies. It is found that FuzzyHCV produces more precise results than HCV by comparing them with actual results for the chosen datasets. Authors intend to carry on work in this area by using fuzzyHCV for other domains problem such as decision making problems in employee selection and by incorporating fuzzyHCV to already existing decision making or requirements prioritization techniques so that less risky choices are made in future.

Nupul Kukreja et al [17], in this have proposed a prioritization methodology to prioritize requirements of system and software. This methodology is a two-step approach and is based on decision theoretic model using a prioritization algorithm called TOPSIS viz. In the proposed approach [13], initially, the system is fragmented into high-level Marketable Features (MMFs). The proposed methodology allows measuring the effect of fluctuating business priorities on individual requirements without much overhead. This methodology also authorizes stakeholders to perform numerous analyses which also help in accurately judging the impact of fluctuating business priorities on individual requirements.

Here authors have also presented a validation report of this methodology by implemented this with 24 project teams of students at the Software Engineering project course in the University of Southern California. Although this approach has some drawbacks that need to be tackled in future; such as, one of the drawbacks of TOPSIS is reversal of ranks i.e. the original order of requirements prioritization may change if irrelevant requirements are entered into the prioritization. This limitation was not considered while implementing the approach as the teams were result oriented therefore they resisted in adding irrelevant requirements for prioritization. Another drawback is that the ordered prioritization of requirements may not accurately reflect the anticipated rank ordering of requirements

To overcome the drawbacks of TOPSIS, several other prioritization algorithms could be used instead of TOPSIS viz such as Cost of Delay, Simple Additive Weighting or Weigers' Prioritization. Also one can simply record items to eliminate the overhead of winbook's incapability to record the items.

III. FRAMEWORK FOR REQUIREMENTS PRIORITIZATION

Missing or poorly specified quality requirements can lead to project failure or huge loss. Eliciting quality requirements effectively is a difficult task altogether especially in SCRUM

where one person i.e. the product owner [PO] has to make the list of all the requirements to be included in the project. It can be a hectic and difficult task. As 'Quality' requirements drive the architecture of software-intensive systems, they are more important than the functional requirements. Thus the success or failure of mission critical systems depends on how well the quality requirements are engineered and implemented. Prioritizing requirements is also another challenging task while developing a software product. Product Owner's commonly use following backlog prioritization techniques: Kano analysis, Moscow and Relative weighting (Karl wieger) [3] [8].

IV. METHODOLOGY

The proposed model is based on several techniques that are being used to prioritize requirements. However when combined, they are expected to give better results. The First step in this model is cumulative voting, in cumulative voting each stakeholder distributes a total of 100 points (\$, euro or coins) on the requirements, the Product Owner then will sum up the points and present the derived ordering of the requirements. Although the desired features will be selected at this point but there could be the chance that the selected feature will not provide benefit in terms of cost, time or easiness as much as it could have provided with other features selected at this time. The second step is Numerical assignment of requirements; it's the most common technique for prioritizing requirements and is based on grouping requirements into different priority groups. For example group the requirements gathered from first steps into different groups based on their nature such as risk requirements, value requirements, and complex requirements etc. After this, requirements will be grouped based on influencing factors that could be effecting these requirements in any way. For example R1 and Rn are risk requirements [11] (see fig 2 below) and they are in any way contradicting with other requirements at the moment that have also been selected to implement in the sprint. Fig.1 depicts the steps of the proposed methodology.

This will cause trouble in implementing all of these requirements, therefore it should be taken care of while selecting and prioritizing requirements for a sprint. Next the groups will be prioritized based on highest points (see fig 2). Groups with requirements R1, R3, R4 have greater number of points as a whole then the other group therefore it has higher priority than other. After this the next step is AHP, in AHP the priorities of requirements is calculated to estimate their relative importance by comparing all unique pairs of requirements. In other words, the individual performing the comparison will decide manually which requirement has more significant, and to what extent using a scale 1-9.[14] AHP provides better results than any other tested methods as it is a ratio scale methodology, and also includes a consistency check.

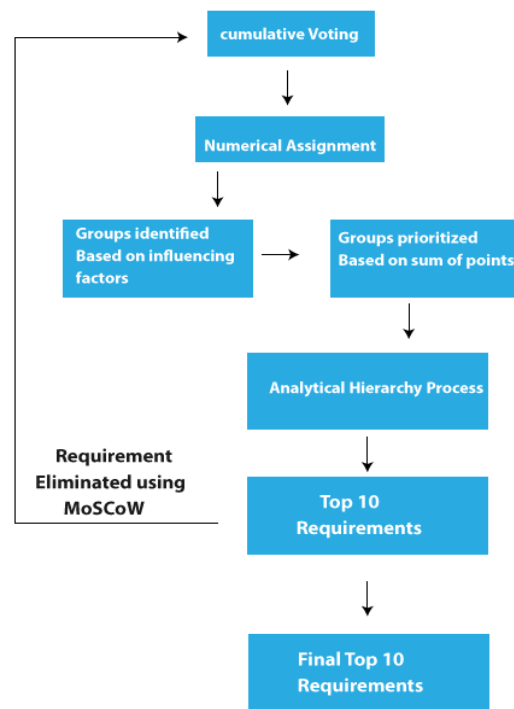


Fig. 1. Hybrid model for Requirements Prioritization

Steps involved in AHP are:

- 1) Make an $v \times v$ matrix (v represents the number of requirements) requirements are latter inserted in rows and columns of the matrix.
- 2) For each pair of requirements, insert their relative intensity of importance (where the row of X meets the column Y). At the same point, insert the reciprocal values to the transposed positions (e.g. if cell $XY=4$ then cell $YX=1/4$)
- 3) Now, calculate the eigenvalues of this matrix to get the relative priority of each requirement. The final result will be the relative priorities of the requirements.

Total no. of comparisons that AHP requires is $v \times (v-1)/2$. Redundancy is produced in pair-wise comparisons in AHP, therefore AHP also calculates the consistency ratio to check the accuracy of the comparisons [14].

At this point when small number of requirements have been selected and grouped, it is best to apply AHP at this point as grouping the requirements based on their nature and influencing factors will make it easy to check requirements with other groups and find out their relative importance, or contradiction between them. As Agile development team and

PO have best idea because of their experience in the field about the implementation of such requirements that are conflicting each other to some extent and/or the risk or cost while implementing them it is suggested to apply MoSCoW at this point. MoSCoW is based on human opinion based on their experience, desire and influencing factors at that time such as market demand, cost, risk, time and resources, the resultant selected requirements are then again filtered using MoSCoW, this is expected to filter out those requirements that may have gotten higher points during the 100 dollar test (cumulative voting) but are causing contradiction to other requirements or may be less beneficial to get them implemented in this sprint. New requirements from the backlog are added after such requirements have been filtered out. If the number of newly added requirements is greater than 3 or 4 then all the steps are repeated on those newly added requirements. If small number of requirements is being added then only MoSCoW should be applied.

Detailed diagram of the Proposed Model is presented below.

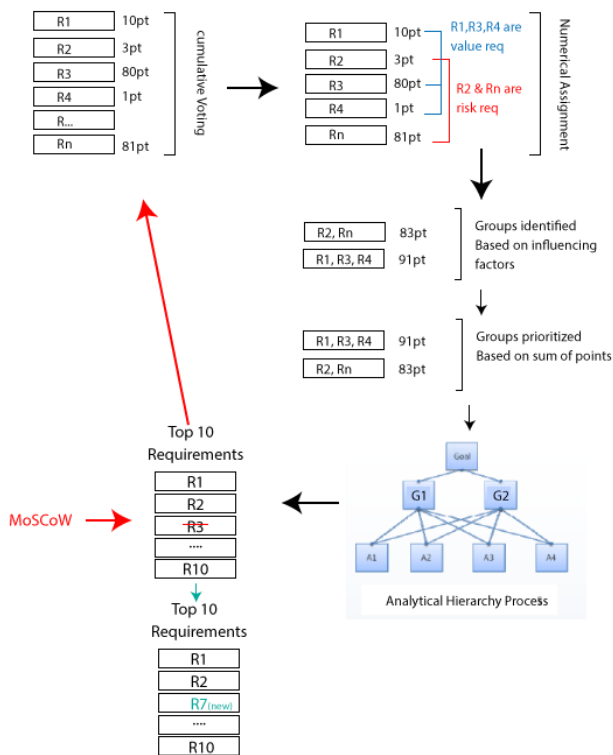


Fig. 2. Detailed presentation of the proposed model

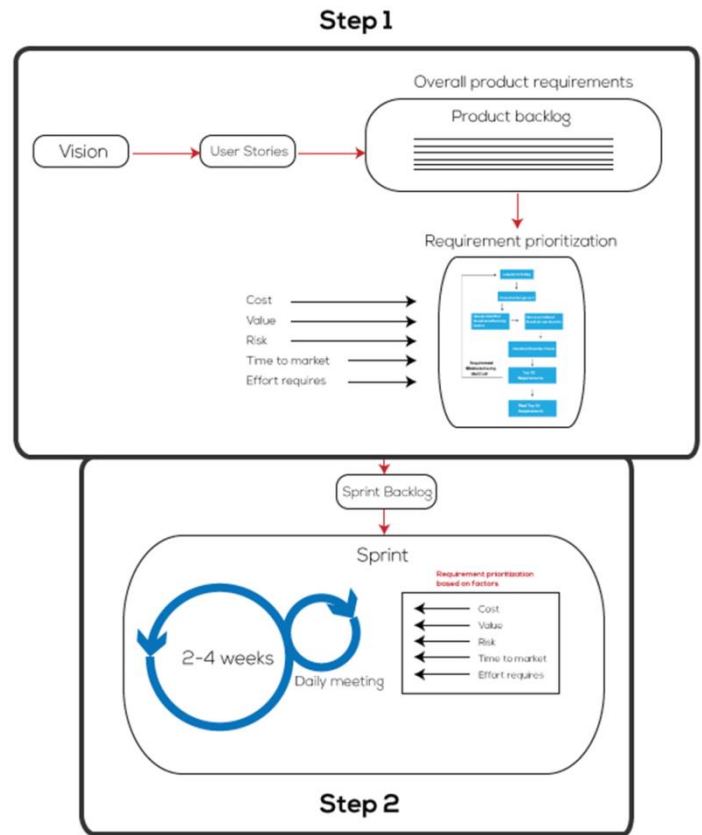


Fig. 3. Detail implementation (staging) in scrum

The validation of the proposed model is made via detail simulations using iThink software (see fig 4 below). The model is expected to increase the quality of the requirements being selected and prioritized during the sprints in SCRUM agile development. The simulation shows that as the number of requirements increases during the development process (see chart 1) and new requirements are added after filtering out requirements that were contradicting others, the priority of the requirements changes as new requirements were added after applying the selected techniques.(see chart 2) The results of these changes in requirements and prioritization shows that the quality of the selected requirements and prioritization increases (see chart 3) and is expected to give better results while implementing in SCRUM agile development.

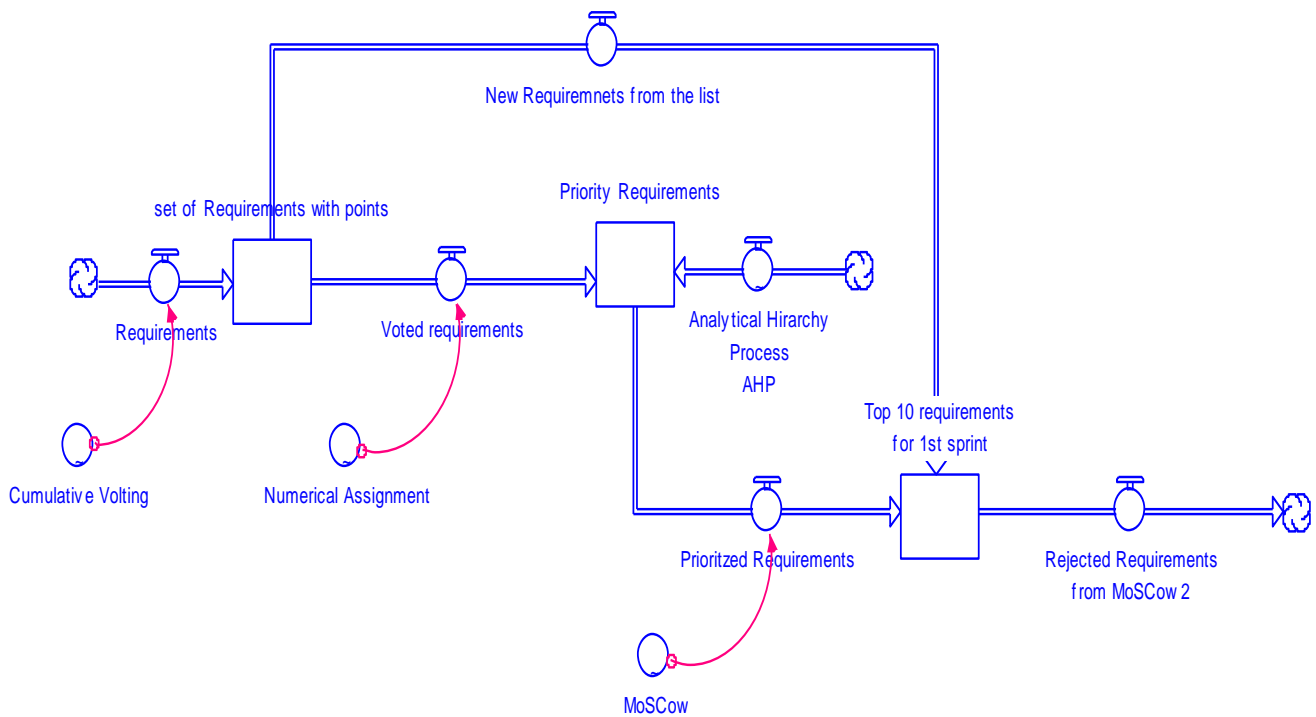


Fig. 4. Simulations of the proposed model in iThink

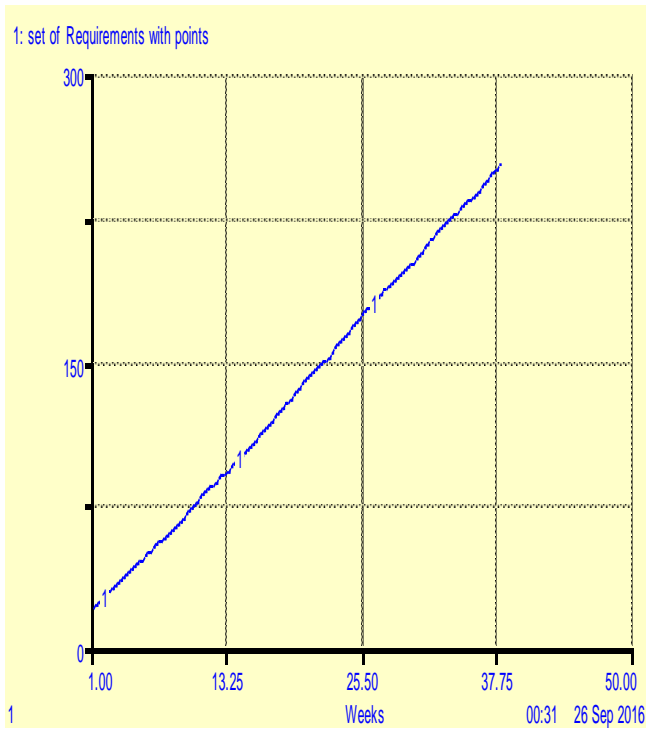


Fig. 5. Chart showing requirements upsurge during SDLC

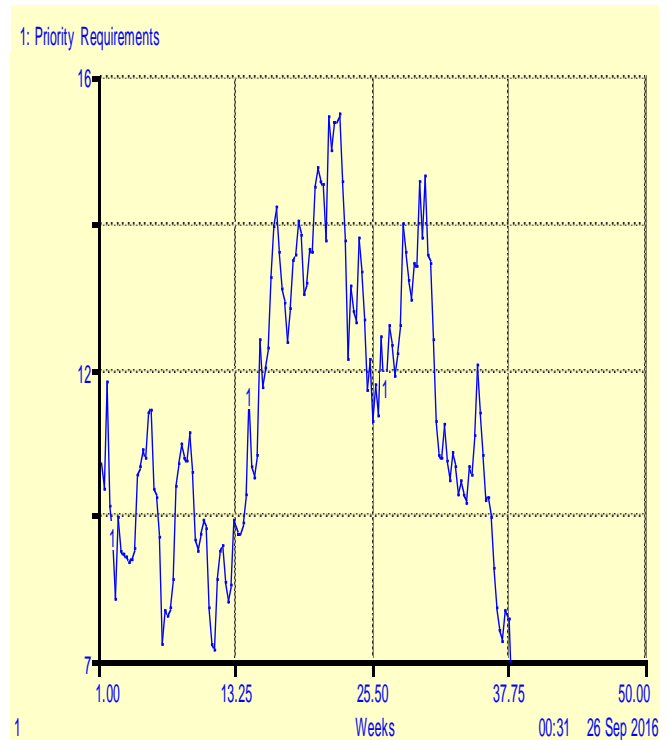


Fig. 6. Chart showing the priority of requirements change's as new requirements arrive



Fig. 7. Chart shows that the quality of requirements increases when applied to proposed model for a peculiar set of requirements

V. CONCLUSION

As requirements emerge throughout the software development process and requirements are needed to be prioritized and hence managed with highest priority, especially when the scenario is that of Agile Software Development process. As discussed and highlighted in this research work, there are many requirements prioritization techniques, methodologies proposed and been followed but most of them fail to account those classical factors (metrics) that influence the overall quality of software product being developed for example ISO (9126, 25000) external metrics. In the following research work a methodology has been proposed in which we have taken account of the mentioned ISO/ IEC external metrics (i.e. 25000, 9126) which affect the quality of process as well as product. Further as it can be seen clearly that these mentioned metrics (attributes) increase the quality of requirements being selected for the development of the product by considering all those aspects that has influence in prioritizing requirements, especially in case of ISO 25000. The proposed model here is a hybrid of other requirements prioritization techniques, it has the advantages of all the positive features already available of those ascribed techniques as mentioned and also have a consistency check that ensure that right requirements are being selected at the right time for the sprint under process in case of ASE (scrum).

REFERENCES

[1] Elsevier (2012) A decade of agile methodologies: Towards explaining agile software development, The Journal of Systems and Software

[2] Mohd. Mugeem, Dr.Mohd.Rizwan, Validation of Requirement Elicitation Framework using Finite State Machine”, IEEE International Conference on Control, Instrumentation, Communication and Computational Technologies (ICCICCT), pp 1210 – 1216, 2014.

[3] Ming Huo, June Verner, Liming Zhu, Muhammad Ali Babar (2004) Software Quality and Agile Methods, IEEE

[4] Lan Cao, Balasubramaniam Ramesh (2008) Agile Requirements Engineering Practices: An Empirical Study, IEEE.

[5] Shahid Nazir, SEN-2005, Why Quality? ISO 9126 Software Quality Metrics (Functionality) Support by UML Suite, NY, USA. DOI=<http://dl.acm.org/citation.cfm?doi=1050849.1050860>

[6] Pekka Abrahamson, Juhani Warstam, Mikko T. Siponen and Jussi Ronkainen (2003) New Directions on Agile Methods: A Comparative Analysis, IEEE.

[7] Armin Eberlein, Julio Cesar Sampaio do Prado Leite (2002) Agile Requirements Definition: A View from Requirements Engineering, Proceedings of the International Workshop on Requirement engineering.

[8] S. N. Bhatti, Deducing the complexity to quality of a system using UML. ACM SIGSOFT Software Engineering Notes 34(3): 1-7 (2009). DOI= <http://dl.acm.org/citation.cfm?doi=1527202.1527207>

[9] DAN HAO, LINGMING ZHANG, LU ZHANG, GREGG ROTHERMEL, HONG MEI, (2014) A Unified Test Case Prioritization Approach, ACM Transactions on Software Engineering and Methodology, Vol. 24, No. 2, Article 10, Pub. date: December 2014.

[10] Frauke Paetsch, Frauke Paetsch, Dr. Frank Maurer (2003) Requirements Engineering and Agile Software Development, IEEE

[11] V. N. Vithana (2015) Scrum Requirements Engineering Practices and Challenges in Offshore Software Development, International Journal of Computer Applications (0975 – 8887), Volume 116 – No. 22, April 2015.

[12] Azar, J.,Smith, R.K., “Value-Oriented Requirements Prioritization in a Small Development Organization”, IEEE Computer society, 2007, pp 32 – 37, 2007.

[13] Anna Perini , Angelo Susi , Paolo Avesani (2013) A Machine Learning Approach to Software Requirements Prioritization, IEEE TRANSACTIONS ON SOFTWARE ENGINEERING, VOL. 39, NO. 4, APRIL 2013

[14] Rahul Thakurta (2013) A framework for prioritization of quality requirements for inclusion in a software project, Software Quality Journal (2013) 21:573–597

[15] Naila Sharif, Kashif Zafar, Waqas Ziad (2014) Optimization of Requirement Prioritization using Computational Intelligence Technique, 2014 International Conference on Robotics and Emerging Allied Technologies in Engineering (iCREATE) Islamabad, Pakistan, April 22–24, 2014

[16] Nupul Kukreja, Barry Boehm (2013) Integrating Collaborative Requirements Negotiation and Prioritization Processes: A Match Made in Heaven, Proceedings of the 2013 International Conference on Software and System Process

[17] Rubaida Easmin, Alim Ul Gias, Shah Mostafa Khaled (2014) A Partial Order Assimilation Approach for Software Requirements Prioritization 3rd INTERNATIONAL CONFERENCE ON INFORMATICS, ELECTRONICS & VISION 2014

[18] Shahid N. Bhatti, Maria Usman, Amr A. Jada, 2015, Validation to the Requirement Elicitation Framework via Metrics. ACM SIGSOFT Software Engineering Notes 40(5): 17, USA. DOI=<http://dl.acm.org/citation.cfm?doi=2815021.2815031>

[19] J. Karlsson and K. Ryan. 1997, “Prioritizing requirements using a cost-value approach,” IEEE Software 14 (5), pp. 67–74.

[20] John A Mcdermid, Software Engineer’s Reference Book, Butterworth-Heinemann, 1991.

Optimizing the Locations of Intermediate Rechlorination Stations in a Drinking Water Distribution Network

Amali Said

OMEGA Research Team, LERES Laboratory
Faculty FSJES, Moulay Ismail University
Meknes, Morocco

Mourchid Mohammed

MIC Research Team, Laboratoire MISC
Faculty of Sciences, Ibn Tofail University
Kenitra, Morocco

EL Faddouli Nour-eddine

RIME Research Team, LRIE Laboratory
Mohammadia School of Engineers, Mohammed V
University
Rabat, Morocco

Zouhri Mohammed

OMEGA Research Team, LERES Laboratory
Faculty FSJES, Moulay Ismail University
Meknes, Morocco

Abstract—The preservation of the water quality in the distribution network requires maintaining permanently minimum residual chlorine at any point of the network. This is possible only if we plan chlorine's injections in various points of the network for intermediate rechlorination, or when increasing the initial level of chlorine in the tank outlet. In the latter case, there is a risk of disruption of the taste and smell of water for consumers near the tanks.

Therefore, to avoid an excessive increase in the chlorine concentration in the tanks and to avoid affecting the taste of the distributed water, intermediate rechlorination stations should be implemented. These stations will proceed with the chlorine regulation.

Given the high cost of the implementation of such stations, the optimization of the number and the choice of location of these stations are needed. This paper is focused on the implementation of an algorithm for such optimization. We used dynamic programming in this algorithm. Performance tests of our decision support system were done on real sites of the Wilaya Rabat-Sale (network of Morocco's capital).

Keywords—Simulation of chlorine distribution; drinking water distribution network; deficit nodes; optimizing the locations of rechlorination stations; Dynamic programming

I. INTRODUCTION

Water is essential for life. However, in nature, water is rarely directly consumable. Indeed, its contact with the ground, the water pollutes and its charges by suspended matter, clay particles, vegetation waste, living organisms (plankton, bacteria, viruses), salts various (nitrates, chlorides, sulfates, sodium carbonate, etc...), gas (1). The presence of these impurities requires processing before use, to make it potable. Traditionally considered as a symbol of purity, water has gradually become the nutrition product most monitored and subject to the strictest quality standards imposed by the World Health Organization (WHO).

The urban distribution is the potential seat of numerous causes of degradation of the quality of water that lead to sanitary risks as well as to organoleptic degradations directly perceived by consumers (2) (3). The evaluation of this quality requires a follow-up of control and prevention, through sampling in the network. Indeed, chlorine is an agent of effective disinfection (4) (5) which has helped solve the problem of the major epidemics of the last centuries (Typhoid, cholera, etc...) (6). This efficiency is only possible if we permanently maintain a residual of free chlorine in the distribution network (7) (8). In order to achieve this, it is necessary to plan the implantation of intermediate chlorination stations.

The objective of this work is, thus, to propose the rechlorination station locations in a distribution network. To minimize the number of deficit nodes in chlorine and the stations to be implanted, it is necessary that the choice of these locations has to be optimal.

The modeling of the distribution of chlorine is an important step in the search of optimal locations of rechlorination stations. In this regard, the second section of this paper describes the method used to simulate the chlorine distribution in every point of the network.

In the third section, we present the method retained for the optimization of the locations of intermediate rechlorination stations, particularly with regard to the approach of the dynamic programming.

The results of this study with regard to the optimization of the locations of intermediate rechlorination stations in some stages of the drinking water distribution network of Wilaya Rabat-Sale, Morocco's capital, will be the object of the fourth section.

The last section will be devoted to the description of the tool to aid decision. This tool facilitates, among others, simulating the distribution of chlorine content in every point of

the network and furthermore, it proposes the best locations of intermediate rechlorination stations.

II. SIMULATION OF CHLORINE DISTRIBUTION IN A DISTRIBUTION NETWORK

In order to control the water quality in the network, it is imperative first to model the degradation of chlorine in a pipe as a function of residence time. Other parameters needed for the concentration of chlorine, will implicitly be introduced into the reaction rate constant of chlorine. This will allow us to monitor the changes in chlorine level as a function of time in function of time throughout the distribution network.

The degradation of the chlorine concentration at each network point requires the establishment of a mathematical model describing the degradation of chlorine in the network.

The database for the chlorine distribution simulation in a network contain, firstly, information related to the geometric structure and the hydraulic regime (flow distribution and residence time) of the nodes and pipes, and secondly, the initial conditions i.e. the level of chlorine injected into the supply sources and the locations of the already implanted chlorination stations in the network.

By using these data, we simulated the distribution of chlorine in a distribution network.

We present in Fig. 1, a node j, in which the chlorine level will be determined using the known chlorine rate values in three other nodes.

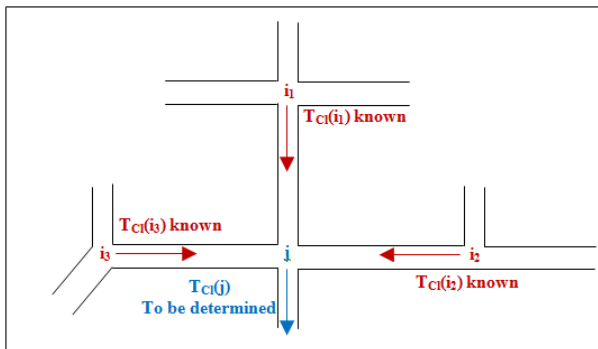


Fig. 1. Illustration schema of the chlorine concentrations in a distribution network

To calculate the chlorine level in the node j, we must first know the level of chlorine in each of the pipes (TCl (i) where $i = i_1, i_2$ and i_3) that supply the node j.

We have two cases (9) :

- First case: if the pipe(i,j) has a chlorination station, then the following is applied:

$TCl(i,j)$ = setpoint of the station (initial rate that is assumed to be known)

- Second case: if absence of chlorination station on the pipe (i, j), then the following is applied:

$$T_{Cl}(j) = \frac{\sum_1^3 T_{Cl}(i, j) \cdot Q(i, j)}{\sum_1^3 Q(i, j)} \quad (1)$$

Where : $T_{Cl}(i, j) = T_{Cl}(i) \times \exp(-k_{i,j} \times t_{i,j})$

Where:

$t_{i,j}$: the residence time of water in the pipe(i,j)

$k_{i,j}$: coefficient of chlorine degradation in the pipe(i,j)

and $Q(i,j)$: the debit of the pipe (i,j)

Equation (1) is a weighted average of the partial chlorine rate of pipes serving the node j, with weighting coefficient the debit rate $Q(i,j)$ transiting in each conduit.

Proceeding out from the source of supply (reservoir, wells, etc...) where the chlorine level is known, we can calculate step by step the rate of chlorine in every point of the network.

This simulation (10), allows us to identify the deficit nodes in chlorine, i.e. the nodes where the chlorine concentration levels are below a preset minimum value. It is necessary thereafter, remedied by implantation of rechlorination stations. Our simulation was enriched by a technique of optimization of intermediate rechlorination station locations.

III. METHOD OF OPTIMIZING THE LOCATIONS OF RECHLORINATION STATIONS

The optimization of these chlorination stations' locations in a distribution network aims mainly to reduce the number of deficit nodes in chlorine with the minimum of stations to implant.

Before the description of this algorithm, we recall the various basic principles of dynamic programming.

A. Definition

Dynamic programming can be applied to optimization by formulating them as a sequence of decisions. It was identified by mathematician Richard Bellman in 1954 (11).

A problem can be solved by the dynamic programming if it is decomposable into n phases, any phase i being defined by two vectors (state vector and decision vector) and two functions (transfer function and return function) (12) (13).

- The input state vector E_{i-1} characterizes the state of the system studied
- The decision vector X_i expresses the intervening decisions to phase i.
- The transfer function $E_i = E_i(E_{i-1}, X_i)$ giving the output vector.
- The return function $r_i = r_i(E_{i-1}, X_i)$ expressing the result of decisions taken at the phase i.

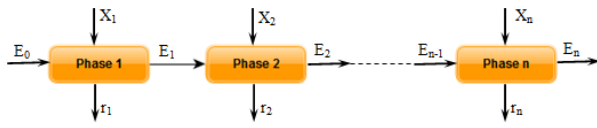


Fig. 2. Phases of a problem solved by dynamic programming

The problem amounts in the search for decisions X_1, X_2, \dots, X_n leading to the optimum of a global function "R" whose these elements are the return functions of each phase ($r_1(E_0, X_1), r_2(E_1, X_2), \dots, r_n(E_{n-1}, X_n)$) as arguments :

$$Opt_{X_1, X_2, \dots, X_n} R[r_1(E_0, X_1), r_2(E_1, X_2), \dots, r_n(E_{n-1}, X_n)] \quad (2)$$

B. Calculation method

From the calculation of the distribution of chlorine in the network, we identify deficit nodes and their number. The location of a rechlorination station that reduces this number is obtained by calculating the number of nodes deficit associated with each pipe (the number of deficit nodes associated with a pipe corresponds to the number of deficit nodes by placing a station of rechlorination on this pipe).

When all the pipes are tested, we hold positions (pipes) which give the minimum of deficit nodes.

Since a chlorination station modifies totally or partially the chlorine distribution on the network, we proceed by phase(cf Fig.2). It is therefore, in our case a dynamic programming (9).

- The states (E_i) represents the information on the network hydraulic status (pipes, nodes, setpoint at reservoirs and the threshold below which a node is declared deficit).
- The decisions (X_i) are the possible locations of a rechlorination station in the network.
- The function return (r_i) proposes the optimal locations.
- The transfer functions (E_i) calculate the distribution of chlorine in the network.

The algorithm based on dynamic programming is the following (14) (9):

```

Begin
Tclini ; Tclmin
Repeat
X : possible locations for a station;
Total_Pipes ← number of pipes of X ;
K ← 0 ;
Simulation(0) ; /* Initial distribution of chlorine */
Cout ← Cout(0) ; /* Cout(0) : initial number of deficit nodes*/
Repeat
K ← K + 1 ;
Initialize "nodes" and "pipes";
Simulation(K) ; /* Chlorination station on pipe K */
Cout(K) ← number of remaining deficit nodes ;
Until (K >= Total Pipes) ;
Cout ← min(Cout(K)) ;
Display the optimal locations ; /* pipes K whose cout(K) = cout* /
If (Cout > 0) Then
Fix a optimal station /* Chosen from the list of the optimal locations displayed */
Until (Cout = 0) ;
End.

```

Fig. 3. The algorithm based on dynamic programming

Where:

Tclini :represents the level of chlorine at the outlet of the feed points (reservoirs, wells and the existing stations).

Tclmin : rate of minimal chlorine below which a node is declared deficit

Simulation(K) :is a function that calculates the distribution of chlorine in the light of a rechlorination station on the pipe K.

Cout(K) :is a function that gives the number of deficit nodes after implantation of a station on the pipe K.

IV. OPTIMIZATION RESULTS

The performance tests of our decision support system decision we developed (See section V) were performed on real sites of the distribution networks of the Wilaya Rabat-Sale (Network of Morocco's capital). The models established within the framework of the study of the functioning of the networks of REDAL (autonomous governance of water and electricity of the Wilaya Rabat-Sale) have taken into account that the pipes ensure a transfer of water from one zone to the other of each floor. So, the pipes whose function was reduced to distribution in a street were excluded from the analysis. This is the conducts of weak diameters ($d < 150\text{mm}$), or conducts antenna.

For this study, we took as chlorine minimum threshold the value 0.25 mg / l below which a node is counted among the

deficits (15). Indeed, this value, which is defined by the World Health Organization (WHO) (16) (7) ensures effective disinfection and maintain water quality in the network.

We wish to look for the best intermediate station locations that minimize the number of nodes deficit chlorine for different stages of the distribution network of the Wilaya Rabat-Salé.

The distribution network of the Wilaya of Rabat-Salé is divided into several pressure stages (17) (18). We present in this paper the optimization results on the following:

Stages: Stage of "Temara bas", Stage "61 of Agdal", Stage of "86-réduit" and Stage of "Skhirat".

- Case of "Temara Bas"

This stage (19) is supplied by a tank with a volume of 3500 m³. The number of nodes that fall within the scheme of this stage is 26 and the number of pipes is 29 (Cf. Fig. 4).

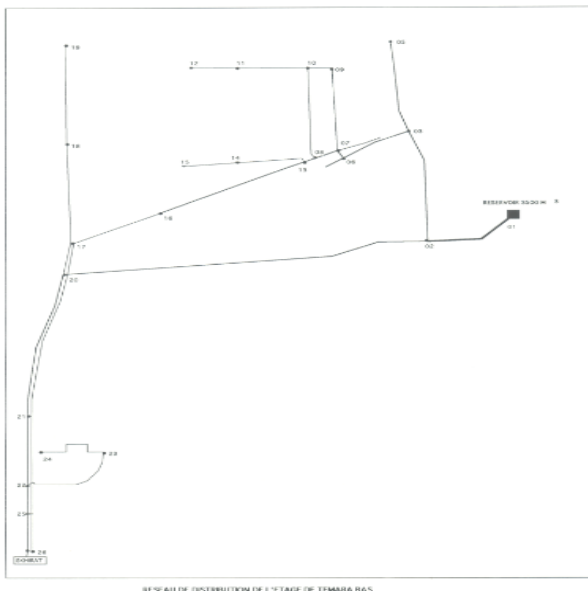


Fig. 4. Map of the stage "Temara bas"

Fig. 5 illustrates the variation in the number of deficit nodes according to the setpoint.

An iteration corresponds to implantation of the station. The study of this figure shows that to have no deficit node in this stage, it is necessary to implant two rechlorination stations.

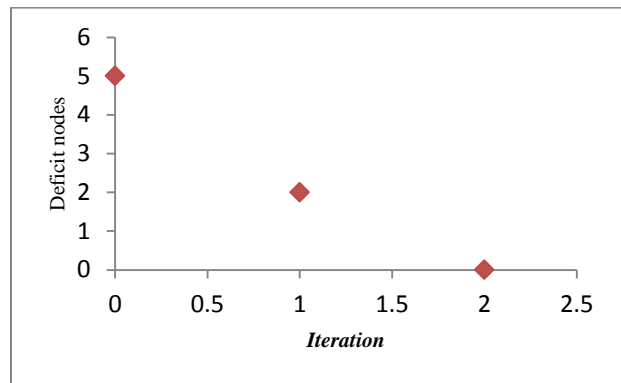


Fig. 5. Variation in the number of deficit nodes according to the iterations (the case of Temara bas)

- Case of "Stage 61 of Agdal"

The stage 61 of Agdal (17) is a distribution network that includes neighborhoods "Médina, l'Océan and Orangers". The two reservoirs of that stage have an overall storage capacity of 6000m³. It is so called because the altimetry side of the reservoirs of "stage 61" is about 61.28m. The number of nodes contained in the scheme of this stage is 52, while the number of pipes is 73 (cf Fig. 6).

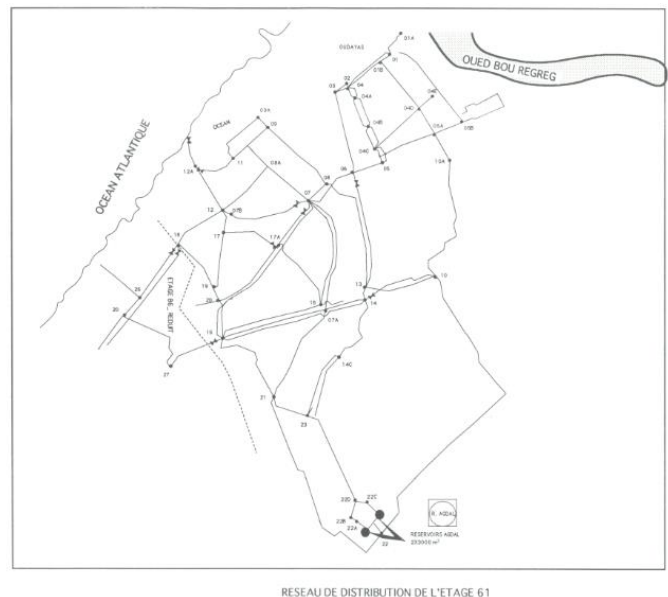


Fig. 6. Map of the stage "61 of Agdal"

We learn from Fig. 7 that the number of deficit nodes decreases with the implantation of rechlorination stations. We also note that the installation of two rechlorination stations is enough for having a null number of deficit nodes.

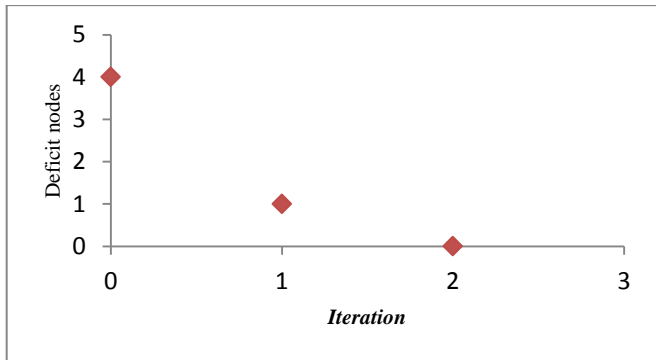


Fig. 7. Variation in the number of deficit nodes according to the iterations (the case of stage 61)

- Case of Stage "Skhirat"

This stage (20) is powered by a 2500m³ storage tank, the coast of the raft is 68.5. The number of nodes that enter into the constitution of this stage is 24, by against the pipes are 28 (see Fig. 8).

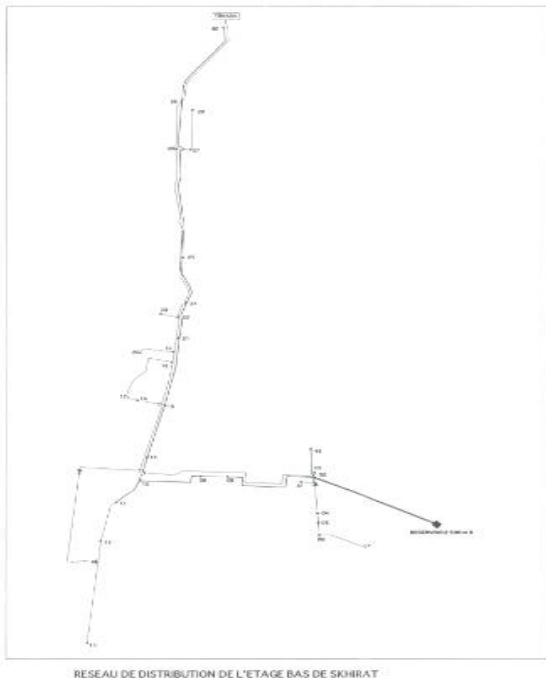


Fig. 8. Map of the stage "Skhirat"

Fig. 9 shows the evolution of number of deficits nodes according on the iterations. By this figure, we can see that the

implementation of a rechlorination station inside this stage eliminates the deficit nodes.

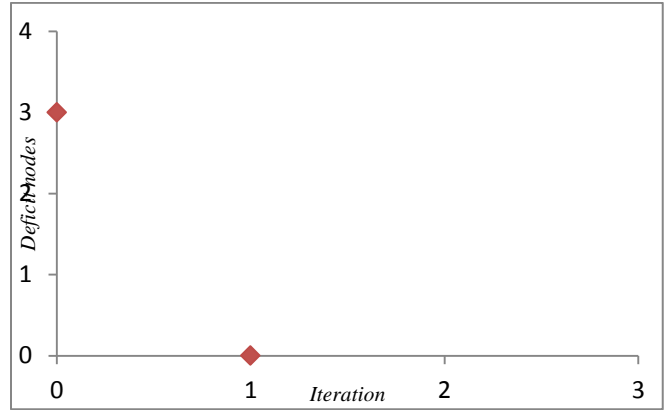


Fig. 9. Variation in the number of deficit nodes according to the iterations (the case of stage "bas de Skhirat")

- Case of stage "86-réduit"

The pressure stage "68-réduit" is a distribution network created following the separation of the stage 61 into two parts (17). The scheme of this stage consists of 105 nodes and 141 pipes (see Fig. 10).

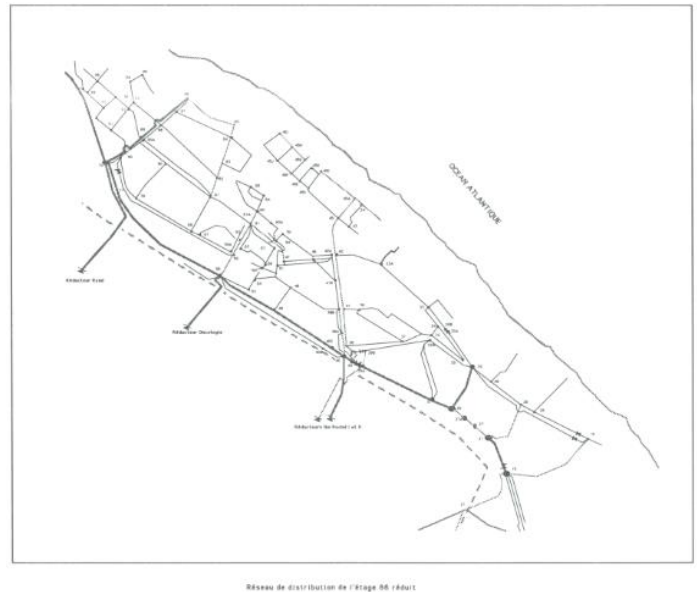


Fig. 10. Map of the stage "68-réduit"

Fig.11 shows the number of deficit nodes according to the iterations.

This figure shows that to have no deficit node in this stage, it is enough to implant two rechlorination stations.

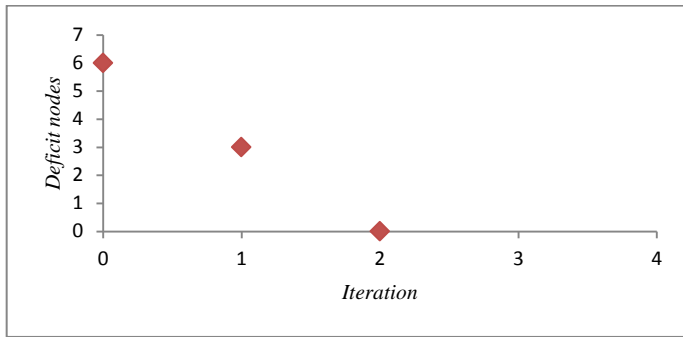


Fig. 11. Variation in the number of deficit nodes according to the iterations (the case of stage "86-réduit")

Fig. 5, 7, 9 and 11 illustrate the variation in the number of deficit nodes according to the iterations. An iteration references the execution of the algorithm of optimization following a chlorine distribution in the network that is determined based on the instruction, the minimum threshold of chlorine, and the number of stations in the network. Each iteration will consider the results of the previous (station implanted in the network). For this study, we gave priority to install a station on the pipe whose service area is the most extensive.

The interpretation of these figures shows that the number of deficit nodes decreases with the number of iterations of the optimization algorithm. Indeed, at each iteration, a chlorination station is implanted in the network, which increases the chlorine content, and therefore results in a reduction of the deficit nodes.

V. PRESENTATION OF THE TOOL TO AID DECISION

The objective of the decision aid tool is to obtain an overview of the variations of the concentrations of chlorine inside a drinking water distribution system, and determining optimal locations of rechlorination stations that minimize the number of deficit nodes in chlorine.

To accomplish its tasks, the tool uses as data input the information on nodes (name, code) and pipes (code, start node, destination node, length, diameter, velocity of water conveyed in the pipe, coefficient of chlorine degradation in driving) representing the hydraulic state (flow distribution and residence time) and the geometric network studied, the chlorine setpoint of entry points (tanks, wells and pipes having a rechlorination station) and the minimum chlorine level below which a node is declared deficit. From these data, the tool determines the distribution of chlorine in every point on the network and proposes optimal locations of rechlorination stations.



Fig. 12. Data flow of the decision aid tool

General architecture

Any real system can be decomposed into several components, each of which performs a specific processing. These components which we call modules, cooperate together to describe the operation of the complete system.

This decomposition into modules can facilitate the development, maintenance and extensibility of our system. Figure 6 shows the overall organization of the tool realized.

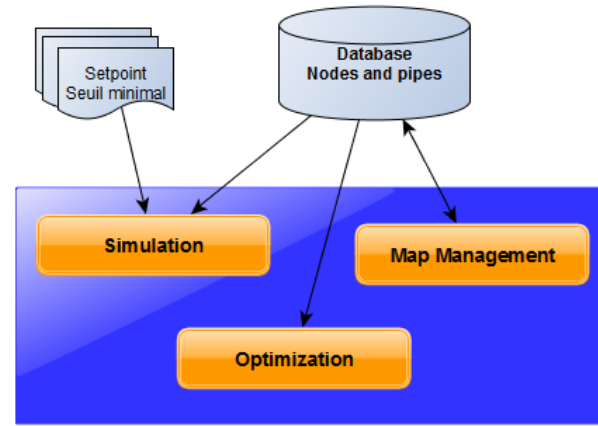


Fig. 13. Architecture of the decision aid tool

The decision support tool is an integration of the algorithms described in our rechlorination simulation work (20) and the algorithm of Fig. 3. It in fact includes two modules, simulation and optimization, using these algorithms. To enable map management, an additional module is developed.

- Module "Simulation"

This module simulates the distribution of chlorine in the network studied, compared with a definite hydraulic regime (flow distribution, and residence times). By giving the chlorine concentration at entry points, this module allows the calculation of the concentrations of chlorine in all network nodes.

It also offers the flexibility to generate the chlorine distribution in the network studied for different concentrations of chlorine in the tanks. The result of the simulation can be presented to the operator in two forms:

Graphic form: the result is displayed on screen. This mode of graphical representation is more significant. It indicates deficit nodes in a color different from those of the other nodes.

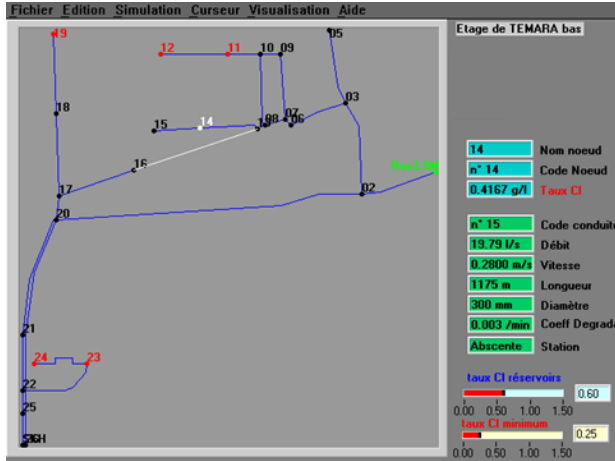


Fig. 14. Example of graphical representation (case of stage " TEMARA bas")

Textual form: the result, in this case, is a textual description of the graphic form. It contains all information related to the nodes and pipes, and can be edited or printed. Fig. 15 is an example of this mode of presentation.

Etage de TEMARA bas									
Liste des nœuds			Liste des conduites						
Nom	Code	Taux de chlore (g/l)	Code	Nœud de départ	Nœud d'arrivée	Longueur (m)	Vitesse (m/s)	Diamètre (mm)	Coefficient de dégradation (1/min)
Res3.5M	1	0.600	1	1	2	655	0.26	300	0.003
02	2	0.529	2	2	20	2865	0.66	400	0.003
03	3	0.456	3	3	6	560	0.69	300	0.003
05	5	0.434	4	2	3	1150	0.39	400	0.003
06	6	0.438	5	3	5	985	1.01	300	0.003
07	7	0.437	6	6	7	80	1.54	200	0.003
08	8	0.430	7	7	8	170	0.57	300	0.003
09	9	0.3491	8	7	9	855	0.19	200	0.003
10	10	0.300	9	8	10	925	0.06	150	0.003
11	11	0.245	10	8	13	90	0.52	300	0.003
12	12	0.156	11	9	10	170	0.13	200	0.003
13	13	0.427	12	10	11	450	0.11	200	0.003
14	14	0.416	13	11	12	450	0.05	200	0.003
15	15	0.395	14	13	14	405	0.83	150	0.003
16	16	0.346	15	13	16	1175	0.28	300	0.003
17	17	0.350	16	14	15	450	0.42	150	0.003
18	18	0.295	17	16	17	720	0.40	200	0.003
19	19	0.210	18	17	18	1290	0.38	200	0.003
20	20	0.432	19	20	17	305	0.50	125	0.003
21	21	0.386	20	18	19	1290	0.19	200	0.003
22	22	0.358	21	20	21	1355	0.34	125	0.003
23	23	0.259	22	20	21	1355	0.64	350	0.003
24	24	0.103	24	21	25	1160	0.30	125	0.003
25	25	0.348	25	22	23	710	0.08	150	0.003
26	26	0.326	26	22	25	235	0.53	350	0.003
SKH	27	0.310	27	23	24	655	0.04	150	0.003
			28	25	26	970	0.75	125	0.003
			29	25	27	970	0.42	350	0.003
			23	21	22	925	0.60	350	0.003

Fig. 15. Example of textual presentation (case of stage " TEMARA bas")

- Module « Optimization »:

We solicit this module to optimize the location of rechlorination stations inside the network studied.

The optimization function integrates the algorithm based on dynamic programming described in Section 3.

The locations of the proposed rechlorination stations are ranked in descending order of degree of influence (fig. 16). Indeed, in practice the priority when installing a station is given to the pipe which supplies a wider service area.

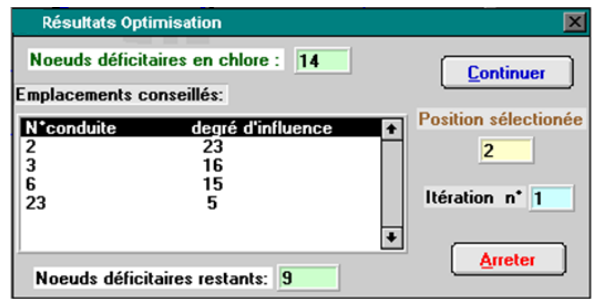


Fig. 16. Optimization interface

When a location of a station is selected among those proposed by the optimizer, the system recalculates the distribution of chlorine and the number of deficit nodes before starting the next iteration.

This process of calculating the number of remaining deficit nodes for each iteration can be continued until there are no more deficit nodes or stopped at any time by the operator.

- Module « Map Management »

This module offers the functionality of a database manager, it is composed of a set of utilities allowing the presentation, handling of graphics cards (zoom, selection, etc...), and management of the database. Management operations (adding, updating, deleting and consulting) are performed on two tables, one on the other nodes and the pipes (Fig. 17).

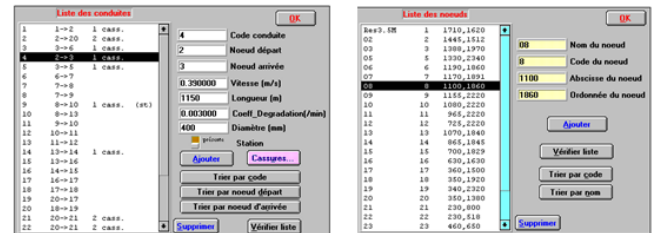


Fig. 17. The different interfaces of the database manager

VI. CONCLUSION

To assure permanently a rate of minimal chlorine in any point of a drinking water distribution system, we developed a decision aid tool. The tool proceeds, on one hand, to the IT control of the chlorine content in a network, which allows to obtain a fast knowledge on the distribution of chlorine in the network compared to a definite hydraulic regime, and to reduce the cost of measures (sampling, displacement, etc...). On the other hand, it allows to optimize the locations of intermediate rechlorination stations.

In the term of this work, the managers of REDAL (autonomous governance of water and electricity of the Wilaya Rabat-Sale (network of Morocco's capital.)) will have at their disposal an operational software adapted to their needs. However, the operation of the system within the administration concerned, requires a preliminary preparation by integrating the actual data with the current structure of the distribution network of the Wilaya Rabat-Sale. This will allow a new evaluation of our system of which the obtained results will be confronted with the data collected in the field.

REFERENCES

- [1] LOKISTAGNEPAS (eau potable AEP), La CHLORATION de l'EAU. <http://lokistagnepas.canalblog.com/archives/2007/12/04/7123046.html>. Décembre 2007.
- [2] Catherine Juery. Définitions des caractéristiques techniques de fonctionnement et domaines d'emploi des appareils de désinfection, document technique du Fonds National pour le Développement des Adductions d'Eau N° 2 (FNDAE 02), Ministère de l'Agriculture, de l'Alimentation, de la Pêche et des Affaires Rurales, 2012.
- [3] Guergazi S. et Achour S. Effet de la désinfection par le chlore sur la pollution des eaux de surface de la région de Biskra. Larhyss Journal, ISSN 1112-3680, n° 09, Décembre 2011, pp. 131-138
- [4] Organisation Mondiale de la Santé (OMS). Directives de qualité pour l'eau de boisson troisième édition, Volume 1 Recommandations, Genève 2004.
- [5] Fondation de l'Eau Potable Sûre (FEPS). La chloration. www.safewater.org. 2007.
- [6] REJSEK F. Analyse des eaux. Aspects réglementaires et techniques, Série Sciences et techniques de l'environnement, Centre régional de documentation pédagogique d'Aquitaine, Bordeaux, France. 2002.
- [7] Organisation Mondiale de la Santé (OMS), WEDC, fiches techniques eau, hygiène, et assainissement en situation d'urgence, Mesurer les niveaux de chlore dans les systèmes d'approvisionnement, en eau. http://www.pseau.org/outils/ouvrages/oms_wedc_les_niveaux_de_chlore_dans_les_systemes_d_approvisionnement_en_eau_2013.pdf. 2013.
- [8] Qualité de l'eau potable - ARS de Franche-Comté. Traitement de désinfection et taux de chlore. http://www.ars.bourgogne-franche-comte.sante.fr/fileadmin/FRANCHE-COMTE/ARS_Internet/Votre_sante/Eaux_et_aliments/Synthese_FC/7-D_Chlore.pdf. 2015.
- [9] M.ELBELKACEMI, S.AMALI, M.LIMOURI, A.ESSAID, Elaboration d'un outil d'aide à la décision. Optimisation d'emplacement de stations de rechloration dans un réseau de distribution d'eau potable. Conférence Internationale en Recherche Opérationnelle CIRO'99, Marrakech, 1999.
- [10] S. Amali, N.EL. Faddouli, M.Mourchid,A.Marhraoui Hsaini. Simulation of Chlorine Distribution in a drinking water distribution network: Case of the Wilaya Rabat-Sale Network. International Journal of Engineering Trends and Technology (IJETT) – Volume-40 Number-1 - October 2016
- [11] A.Kaufman. Méthodes et modèles de la recherche opérationnelle, Tome II, DUNOD Paris, 1972.
- [12] Sophie Jacquin. Hybridation des métaheuristiques et de la programmation dynamique pour les problèmes d'optimisation mono et multi-objectif : Application à la production d'énergie. Thèse, Laboratoire CRISTAL Lille France, 2015.
- [13] Stephane Bonnet. Approches numériques pour la commande des systèmes dynamiques, Université de Technologie Compiègne France, 2008
- [14] S.Amali. Outil d'aide à la décision. Optimisation d'emplacement de stations de rechloration intermédiaires dans un réseau de distribution d'eau potable, Thèse de 3ième cycle, LCS, Faculté des Sciences, Rabat, 1999.
- [15] Marche à suivre pour désinfecter l'eau potable en ONTARIO. <https://dr6j45jk9xcmk.cloudfront.net/documents/1183/99-disinfection-of-drinking-water-fr.pdf>. 2006.
- [16] O.Wable, J.P.Duguet, G.Elas, J.F.Depierre, P.Jarrige. Modélisation de la concentration en chlore dans les réseaux de distribution, T.S.M L'eau, Juin 1992.
- [17] Saureca, Adi, Gersar, Gibb. Plan directeur de distribution d'eau potable de la Wilaya de Rabat-Salé, « Définitions des données de base, vérification du réseau existant », Mission I, Ville de Rabat, Juin 1992.
- [18] Saureca, Adi, Gersar, Gibb. Plan directeur de distribution d'eau potable de la Wilaya de Rabat-Salé, « Définitions des données de base, vérification du réseau existant », Mission I, Ville de Salé, Juin 1992.
- [19] Saureca, Adi, Gersar, Gibb. Plan directeur de distribution d'eau potable de la Wilaya de Rabat-Salé, « Définitions des données de base, vérification du réseau existant », Mission I, Ville de Témara, Juin 1992.
- [20] Saureca, Adi, Gersar, Gibb. Plan directeur de distribution d'eau potable de la Wilaya de Rabat-Salé, « Définitions des données de base, vérification du réseau existant », Mission I, Ville de Skhirat, Juin 1992.

A Semantic Learning Object (SLO) Web-Editor based on Web Ontology Language (OWL) using a New OWL2XSLO Approach

Zouhair Rimale

Dept. of Mathematics and computer science

Faculty of Sciences Ben M'sik
Hassan II University
Casablanca, Morocco

EL Habib Benlahmar

Dept. of Mathematics and computer science

Faculty of Sciences Ben M'sik
Hassan II University
Casablanca, Morocco

Abderrahim Tragha

Dept. of Mathematics and computer science

Faculty of Sciences Ben M'sik
Hassan II University
Casablanca, Morocco

Abstract—Today, we see a strong demand for real-time information, with a rapid growth of m-learning. We also see that there are many educational resources on the Internet. Learning objects (LOs) are designed as a means of reusing these resources. Most of these LOs are built for e-learning systems based on desktop computers, which prevents their use on mobile devices. A LO is an area that is open to research and has a lot of potential in the creation, adaptation and production of learning content. There are standards that describe LOs in general as IEEE LOM, SCORM. Semantic web and its associated technologies are increasingly used in electronic document editing while separating the content from the presentation. Creating a LO with the semantic web is complex and raises difficulties because of the editing tools that require general knowledge of XML syntax and related technologies. In this paper, the authors propose a new OWL2XSLO approach based on ontologies (OWL) allowing the generation of XML-Schemas LOs. They then derive a semantic LO web editor based on OWL2XSLO approach for the generation of a content type enabling the editing of interactive LOs with XML technology and which can then be integrated into LMS and adapted to the mobile display.

Keywords—m-learning; learning objects; web semantic; XML-schema; xsd; owl; Ontology; rdf

I. INTRODUCTION

In recent years, m-learning has been boosted by the continued development of new information and communication technologies, which have become essential elements in education [1].

The design and development of teaching materials adapted to mobile devices may present difficulties for researchers and educators [2]. There is a wide variety of mobile devices and platforms; therefore, the pedagogical design of mobile content requires specific adjustments [3].

Educational content is numerous and consists of various types of media such as video, audio and presentations. Some of these LOs [4] are designed for fixed computers, which prevents their use on mobile devices. Among the problems that can occur are screen size and resolution, supported file type.

Teachers are looking for the best method to represent their courses. Since the LO becomes a smallest basic unit that can be

designed to be reused, customized and adapted, teachers prefer to find creative tools to easily create interactive and adaptive LOs.

In order to implement an effective adaptive learning system, a new LO concept is needed. It is the separation of content from the presentation that could create and update a LO for different presentations [5] [6]. XML (Extended Markup Language) [7] is appropriate for implementing this separation. XML is the most promising technology to use specific parts of LOs to adapt them while using XSLT [8] style sheets.

In addition, the research studies related to the development of LOs, found that the ontology can be used to represent the knowledge in the development of LOs and able to support the semantic web development. Thus, the ontology plays an important role in creating standards for accessing to the contents and helpful for the learning management [9]. Moreover, the ontology is applied for constructing the personalized learning contents. The ontology approach can present the LOs, content structures and learning path that are corresponding to the learning environment of each individual [10]. It can also dynamically generate personalized hypertext relations powered by reasoning mechanisms over distributed RDF annotations [11].

In a digital learning environment a number of essential services are supported such as content creation that requires an educational content editor. The use of certain tools is not an easy task for anyone who wants to create specific educational content. In general, LMS / LCMS (Moodle [12], Dokeos [13], Atutor or Calorine [14]) have traditional editing tools. These tools are hypertext based with multimedia features for content creation in HTML format that is not suitable for direct display on small screens of mobile browsers. Importing content from external formats, even standardized (Microsoft Office, Open Office), pose several problems of compatibility, filtering and structuration.

At the present time, there are not really any editing tools that allow the creation of the basic LO adapted to the specific needs of the course designers by using the semantic web and from this the generation of the adaptive presentation to the display of mobile devices. The creation of the new LO with the

semantic web raises difficulties because of the available tools that require a general knowledge of semantic web language and its related technologies such as XML technology.

In this paper, the authors propose a semantic LO web editor based on approach [15] called OWL2XSLO allowing the generation of the XML schema using two ontologies in order to create and share LOs with XML technology. The strength of the semantic LO web editor lies in its automatic generation of LO content types, which will allow organizations to organize, manage and process content in a coherent way. Beyond this synthesis, the semantic LO web editor wants to answer two fundamental questions about the creation of the new LO. The what? (What LO) and the how? (How the LO content will be represented).

II. RELATED WORK

Mobile devices offer new learning opportunities but their level of use in e-learning is still low [16]. E-learning systems and LMS have already been widely adopted to allow teachers to create learning materials [17]. For m-learning to be effective, it must be integrated with an existing e-learning platform in order to achieve better results regardless of the device used, including mobile devices [18] [16].

The important part of the interaction between the learner and a LO is the visual design of the LO. Mobile devices have several limitations, which also require specific adjustments. In earlier research, it was noted that learning content for mobile devices cannot be presented in the same way as e-learning used on computers because of the small size of the screen [16][19][20]. For the LMS to offer learning content suitable for all devices including mobile devices there should be a way for the teacher to define what to display on desktops and what to do Display on mobile devices.

In their research, Houser and Thornton [19] found that most educational web services can be modified to work on small screens. In the example of Houser and Thornton, a new course management system (CMS) called Poodle was developed as a step towards adopting the use of mobile phones in education. The Poodle system is a light version of the popular LMS Moodle, providing quizzes, a voting system, a wiki server and a flash card server to promote m-learning.

Bogdanović et al. [16] extended the Moodle platform with a mobile quiz application to study how students react to m-learning in a real context. The presented application works as a plug-and-play component that recognizes the device used and adapts the content using different CSS themes.

To support new pedagogies and technologies related to technology-enhanced learning, LOs have been developed as a new conceptual model for the creation and distribution of content [21]. Hodgins and Duval [22] defined LO as any numerical or non-numerical entity that can be used for learning, education and training. LOs are building blocks that can be combined in a virtually infinite way to build collections that can be called lessons, modules, and courses [23].

The most widely used standards for packaging and composition of LOs are IMS-LD and Moodle. It also allows for the exchange and re-use of learning design across platforms

and supports a wide range of modern educational approaches such as active learning, collaborative learning, adaptive learning And skills-based learning [24].

The problem is that the creation tools based on IMS-LD require non-mobile platforms. As well as the IMS-LD does not have adequate mobility support and there is no widely accepted theory of m-learning. Some limitations are related to the physical aspects of mobile technologies.

Sotsenko et al. [25] discuss the use of LO in m-learning environments by adding contextual information as metadata to provide the learner with the right content at the right time to solve problems related to mobile devices such as small size screen. The idea is to obtain contextual information from the learner, using the detection mechanisms in the mobile device and the contextual information provided by the learning platform, and to provide the most appropriate content that corresponds to the personal context of the learner, the environmental context, as well as the properties of the device and the connection to the network.

Metadata is essential for processing implementations of the LO. This concept allows the discovery, retrieval and reuse of LOs [26]. In recent years, the number of LO repository has been developed, such as Merlot [27], Ariadne [28], Careo [29]. Most of these repositories focus on the e-learning perspective and there is no interoperability fully achieved with mobile devices.

According to Hodgins [21], the way LOs are to be used and sequenced is also very important. It also recalls that in order for LOs to be widely adopted, there must be tools that make the process of conceptualization, design, construction and selection quick and easy. It would be important to consider how the authors could create adaptive LOs that can be both used by existing LMS and integrated with LORs to support m-learning.

III. THE PROPOSED OWL2XSLO APPROACH

A. Objective

The purpose of the OWL2XSLO approach is to generate automatically from two ontologies, an XML-schema (XSD) to create LOs with XML technology using the web ontology language (OWL). Ontology is used to provide domain knowledge such as terminology, restrictions and data types. The OWL2XSLO approach can be used in all areas including notably education m-learning, provided that ontology is available for this area. This will have a big impact on applications such as communication systems where XML is widely used. Manual labor will be reduced in professional organizations including universities and schools on the creation of LOs in XML. Once the ontology is created for a university to the description of domain knowledge of the course for example, it is possible to refer the terms used in this ontology in the XML instance documents to automatically generate the XML-schema.



Fig. 1. The conceptual model approach «OWL2XSLO»

B. Methodology

Most existing tools that allow the generation of the specific XML schema based on data in the XML document. Though the XML schema that can be generated, it will not be the most accurate diagram. The reason for this is mainly due to the lack of knowledge of the area in which the XML documents are created.

The authors use OWL2XSLO approach to overcome the above problems while providing successively two ontologies as mounted in Figure 2 below, ontology "Content Ontology" which represents the knowledge, skills, items and vocabularies an essential way to establish and develop a structure of the LO and the other ontology "Ontology of Use" which represents the know-how and allows to define how to use knowledge, skills that it necessary to include any LO (make definitions, make examples, do exercises and corrected).

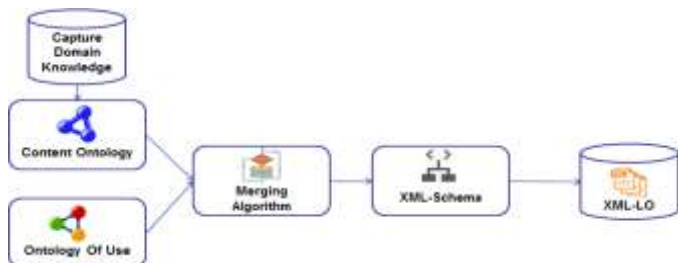


Fig. 2. The conceptual model OWL2XSLO approach

- **The Content Ontology (What):** This ontology is a structure of concepts that describe the knowledge domain. It consists of knowledge in the forms of the hierarchical data structure to describe the interested knowledge domain (Figure 3). The use of this ontology is adapted to the sharing of knowledge in the same knowledge. Thus, using this ontology for the design of LOs would be useful for providing knowledge and building a standardization of knowledge content that is also passed on to learners.

To automatically create an XML schema for each LO in XML, it is necessary to store this ontology in a form readable by the machine by using the OWL. The Ontology Web Language (OWL) is based on the RDF (Resource Description Framework) [30]. Then the SPARQL (SPARQL protocol and RDF Query Language) is applied to query the information in a RDF format [31].

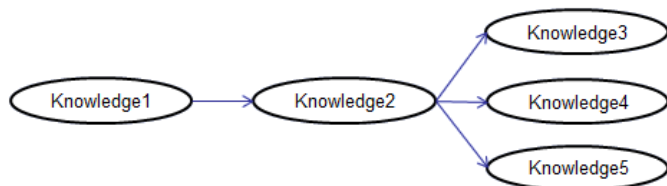


Fig. 3. Content Ontology

- **Ontology of Use (How):** The lesson plan is for the teacher a communication tool of his intentions, his expectations and the requirements of the course. Its quality rests on the consistency with the course itself, the accuracy and relevance of its content. The syllabus allows the professor

to have a faithful portrait of his course, to confirm the structure of the course and to communicate the essential elements to the persons concerned, namely the students. For the professor, writing and revising his lesson plans are opportunities to check the division into modules or lessons, to re-evaluate the time allocated to the most important objectives, to adapt or modify his course. But the course plan is also a course management tool. It makes it possible to better control its progress and to avoid deviations or delays that are detrimental to students.

As shown in Figure 4, ontology of use aims to describe how each concept (knowledge) of the content ontology will be presented in order to create a coherent LO plan.

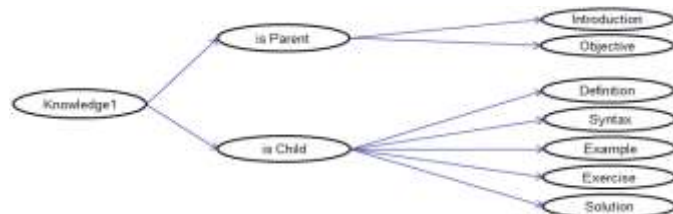


Fig. 4. Ontology of Use

- **Ontology Merging Algorithm:** After setting the Framework of ontology, the next step was the development of the algorithm as shown in Figure 6. The objective of the algorithm was to automatically merging two ontologies to create a single coherent ontology, or (2) aligning the ontologies by establishing links between them and allowing them to reuse information from one another. The process of the algorithm takes as input two (or more) source ontologies and returns a merged ontology based on the given source ontologies as shown in figure 5.

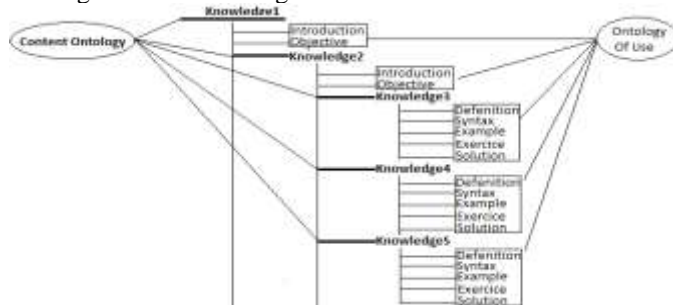


Fig. 5. Process of Ontology Algorithm Merging [15]

```

Extract root element from the owlContent « Ontology Content »
Extract root element from the owlUsing « Ontology Using »
Create an array List
Create xsSchema ()
Check the Element if has child
For each elementC in owlContent
{
  Create xsElement ()
  If elementC has child {
    Create xscomplexType
    Create sequence
    For each Element in owlUsing is parent {
      Create xsElement ()
      //Introduction//Image//Objective
    }
    For each child in elementC {
      For each Element in owlUsing is child {
        Create xsElement ()
        //Definition//Syntax//Example//Exercise//corrigé
      }
    }
  } Else {
    Create xscomplexType
    Create sequence
    For each Element in owlUsing is child {
      Create xsElement ()
    }
  }
  Add the new nodes to the Array List
}
Return xml schema
    
```

Fig. 6. Algorithm of the OWL2XSLO approach [15]

The algorithm of the OWL2XSLO approach allows the automatic generation of the XML schema (Figure 9) from two ontologies fused above (using the OWL) while successively using two conversions, basic and advanced as shown the two figures below 7 and 8. The algorithm takes each knowledge of 'Content Ontology' by checking whether it is parent or child element. If the selected knowledge is a parent element then a complex element should be created with the elements of the parent type of "ontology of use". If not a simple element should be created with the elements of child type of "ontology of use".

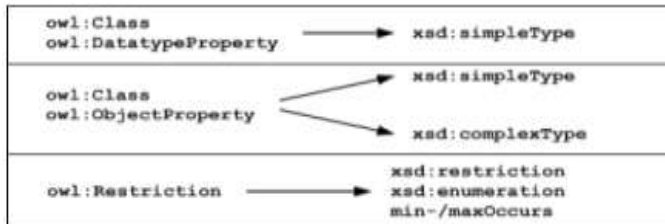


Fig. 7. Basic Conversion [15]

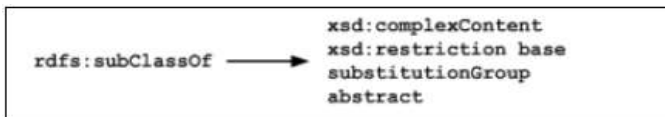


Fig. 8. Advanced Conversion [15]

IV. PROPOSAL: NEW SEMANTIC LO WEB EDITOR

A. Overview of the semantic LO web editor

The semantic LO web editor is a creative environment based on the semantic web using the ontology web language (OWL) and XML technology. It is designed to help teachers and academics in the design, development and publication of interactive LOs without the need to become proficient in XML.

The Semantic Web is a revolutionary educational tool because it presents to teachers and learners a technology that simultaneously provides content with the means of adaptation. Unfortunately, the power of the semantic web is restricted in educational settings because the vast majority of teachers and academics do not have the technical skills to build their own LOs. The semantic LO web editor is under development to overcome a number of identified limitations:

- Traditionally, existing creative tools require general semantic web knowledge, they have not been intuitive and they were not designed for publishing learning content. As a result, teachers and academics have not adopted these technologies for the publication of LO content. The semantic LO web editor aims to provide an intuitive and easy-to-use tool that will allow teachers to publish interactive LOs and can adapt for m-learning.
- Currently, LMSs do not offer sophisticated creation tools to create LO content with XML technology. The publisher is a tool that offers professional LO publishing features that will be easily referenced or imported by LMS standards;
- Many LMS do not provide an intuitive WYSIWYG environment allowing the creation of LOs with XML

technology. The semantic LO web editor mimics the WYSIWYG feature that allows authors to see what content will look like when they are published online.

With the semantic LO web editor, authors will have a content type suited to their needs enabling the construction of the flexible and easily updated LO.

B. Architecture of the Semantic Learning Object Web-Editor

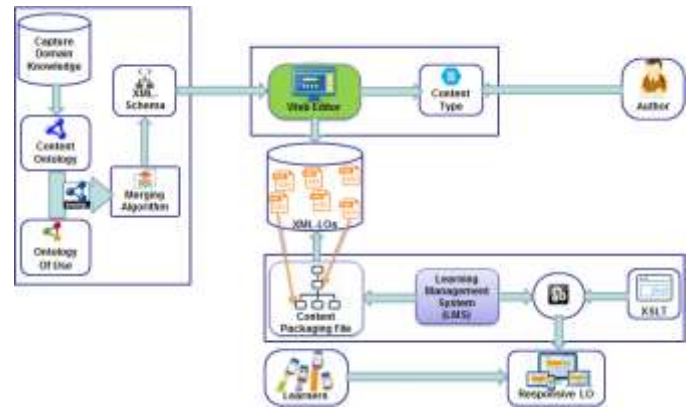


Fig. 9. Architecture of the semantic LO web editor

The architecture of the semantic LO web editor is based on 4 essential elements:

- An environment based on the OWL2XSLO approach allowing the automatic generation of the XML-schema using OWL and SPARQL.
- A semantic XML environment based on a content type allowing the creation, storage, modification and dissemination of LOs in XML.
- A storage environment for LOs in a single repository, to separate the contents from its presentation.
- An LCMS / LMS environment enabling authors to create, store, reuse, manage and distribute LOs to associate them, order them to build a coherent course. This solution is based on the choice of free software that complies with the postulates of the LCMS.
- An environment for adapting semantic XML content in a format suitable for displaying mobile devices using XSLT.

The design can be presented in the following scenario:

The course author can modify and create his LOs using a web content type (web form) that is generated automatically by respecting an XML-schema. The XML-Schema (figure 11) based on OWL2XSLO approach is also automatically generated by successively using two ontologies, the "SELECT" knowledge of the "content ontology" that allows the representation of the SQL language knowledge [9] as shown on figure 10 and "ontology of use" as shown on figure 4. The storage of these LOs is possible in their original format (XML) conforming to the metadata structure defined in an XML schema format [32] (FIG. 9). Using an LMS, the author can associate and order these LOs in order to build a coherent course. Using the XSLT transformations and the CSS3, an LO with its XML content can have several presentations generated on demand in formats suitable for displaying mobile devices.

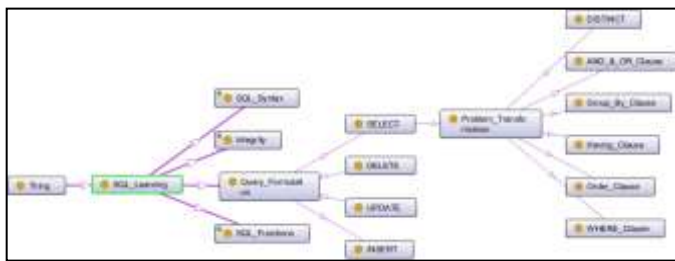


Fig. 10. Content Ontology: SQL Knowledge Domain[9]

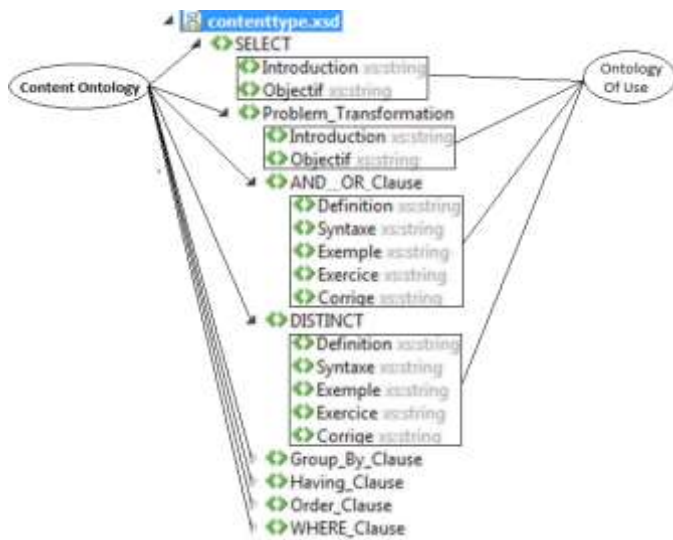


Fig. 11. Result of the OWL2XSLO approach: XML-Schema of Knowledge "SELECT"

C. Implementation of the Semantic LO Web Editor

For the validation of the proposal, the web editor is developed around ontologies and the Microsoft .Net on a Windows 7 platform. We used Protege [33] for the construction of ontologies with the ontology web language (OWL), The SPARQL query language to query and query the OWL, Microsoft Visual Studio 2015 [34] to create the platform using Microsoft ASP.NET (Active Server Page) web technology. The learning module chosen for validation is the SQL [9] language. To use of the semantic LO web editor we need an Internet Browser only without installation or update.

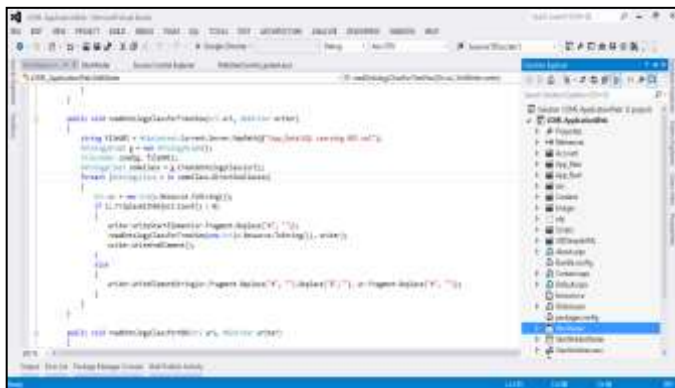


Fig. 12. Technical Architecture under microsoft visual studio 2015[34]

The user interface comprises different parts, each having a special role:

- 1) Search box: Allows the author to search, modify or create a new content type of LO.
- 2) The Tree View to the left: represents the plan, the main elements and the tree of the LO
- 3) The editing area: area where the author can create the content of the LO using the text areas.
- 4) Navigation buttons: allows the author to save and display the next or previous element of the LO.



Fig. 13. User Interface of the Semantic LO Web Editor



Fig. 14. User interface of the LO content type "SELECT"

V. CONCLUSION AND FUTURE WORK

This article presents on the one hand the conception of the original approach titled OWL2XSLO allowing the generation of the XML-schema of learning object from two ontologies and on the other hand the construction of the semantic LO web editor allows the generation of the LO content type (web form) from this XML-schema.

For the future work, the authors describe another approach based on the web services for the integration of an environment of adaptation of a pedagogical content for a mobile use. As a result, they can set up a multimodal content adaptation system for a mobile learning environment. They can adopt web services technology to provide a flexible integration model in which all components of learning and applications will be well defined. The future work has the advantage of using a mobile web browser as a universal communication environment.

REFERENCES

- [1] Zouhair Rimale, El Habib Ben Lahmar, Abderrahim Tragha, A Brief Survey and Comparison of m-Learning and e-Learning, International Journal of Computer Networks and Communications. Vol.4, Issue 4, April 2016
- [2] Alvarez, C., Alarcon, R., Nussbaum, M.. Implementing collaborative learning activities in the classroom supported by one-to-one mobile computing: A design-based process, Journal of Systems and Software, Vol. 84, 2011. p. 1961–1976. doi:10.1016/j.jss.2011.07.011.
- [3] Güler, Ç., Kılıç, E., Çavuş, H. A comparison of difficulties in instructional design processes: Mobile vs. desktop, Computer Human Behavior, Vol. 39, 2014. p. 128–135. doi:10.1016/j.chb.2014.07.008.
- [4] Moreno JER (2012) Adaptation of learning strategies in learning objects for using learning styles. IERI Procedia 2:808–814. doi:10.1016/j.ieri.2012.06.175
- [5] Parupalli R, Nelaturu SCB, Jain DK (2011) The role of content adaptation in ubiquitous learning. In: 2011 IEEE international conference on technology for education, pp 177–182. doi:10.1109/T4E.2011.35
- [6] Mohan, P., & Greer, J. (2003, June). Reusable learning objects: Current status and future directions. Paper presented at ED-MEDIA 2003 World Conference on Educational Multimedia, Hypermedia & Telecommunications, Honolulu, Hawaii. Retrieved January 3, 2006, from <http://www.campussaskatchewan.ca/pdf.asp?pdf=PMohanEdMedia03.pdf>
- [7] Extensible Markup Language (XML). <http://www.w3.org/XML>.
- [8] Extended Style Sheet Transformations <http://www.w3.org/TR/xslt>
- [9] Wilairat Yathongchai, Thara Angskun, and Jitimon Angskun “SQL Learning Object Ontology for an Intelligent Tutoring System” International Journal of e-Education, e-Business, e-Management and e-Learning, Vol. 3, No. 2, April 2013
- [10] J. Jovanovic, D. Gašević, and V. Devedžić, “TANGRAM for Personalized Learning Using the Semantic Web Technologies,” Journal of Emerging Technologies in Web Intelligence, vol. 1, no 1, 2009, pp. 6-21.
- [11] N. Henze, P. Dolog, and W. Nejdl, “Reasoning and Ontologies for Personalized E-Learning in the Semantic Web,” Educational Technology & Society, vol. 7 no 4, 2004, pp. 82-97.
- [12] Moodle open-source community-based tools for learning <http://moodle.org>
- [13] Dokeos: e-learning open source, <http://www.dokeos.com>
- [14] Atutor learning Management System, <http://www.atutor.ca>
- [15] Zouhair Rimale, El Habib Ben Lahmar, Abderrahim Tragha, (2016) An Approach for the Automatic Generation of a Content Type of a Semantic Learning Object from Ontology. In: 2016 IEEE 11th International Conference On Intelligent Systems : theories and Applications.
- [16] [Bogdanović et al., 2014] Bogdanović, Z., Barać, D., Jovanić, B., Popović, S., and Radenković, B., Evaluation of mobile assessment in a learning management system. British Journal of Educational Technology, 45 (2014), 231–244.
- [17] [Ako-Nai and Tan, 2013] Ako-Nai, F. and Tan, Q. Location-Based Learning Management System for Adaptive Mobile Learning. International Journal of Information and Education Technology 3, 5 (2013), 529-535.
- [18] [Fayed et al., 2013] Fayed, I., Yacoub, A., and Hussein, A. Exploring the impact of using tablet devices in enhancing students listening and speaking skills in tertiary 93 education. QScience Proceedings: Vol. 2013, 12th World Conference on Mobile and Contextual Learning (mLearn 2013), 1.
- [19] [Houser and Thornton, 2005] Houser, C. and Thornton, P., "Poodle: a course management system for mobile phones," Wireless and Mobile Technologies in Education, 2005. WMTE 2005. IEEE International Workshop on Wireless and Mobile Technologies in Education (Nov. 2005), 28-30.
- [20] [Shih et al., 2011] Shih, J.-L., Chu, H.-C., Hwang, G.-J., and Kinshuk. An investigation of attitudes of students and teachers about participating in a context-aware ubiquitous learning activity. British Journal of Educational Technology, 42, 3 (2011), 373–394.
- [21] [Hodgins, 2002] Hodgins, H.W. The Future of Learning Objects. In: 2002 ECI Conference on e-Technologies in Engineering Education: Learning Outcomes Providing Future Possibilities. Lohmann, J.R., Georgia Institute of Technology, USA, Corradini, M.L., University of Wisconsin-Madison, USA (Eds.). ECI Symposium Series, P01 (2002).
- [22] Hodgins W., Duval E. 1484.12.1-2002 - IEEE Standard for Learning Object Metadata, 2002. Retrieved 20.10.2014, URL:<http://ieeexplore.ieee.org/stamp/stamp.jsp?tp=&arnumber=1032843&isnumber=22180>.
- [23] Chikh, A. A general model of learning design objects, Journal of King Saud University – Computer and Information Sciences, Vol. 26, 2014. p. 29–40. doi:10.1016/j.jksuci.2013.03.001.
- [24] Koper, R., Olivier, B. Representing the Learning Design of Units of Learning, Educational Technology & Society, Vol. 7; 2004. p. 97–111
- [25] [Sotsenko et al., 2013] Sotsenko, J., Jansen, M., and Milrad, M. About the Contextualization of Learning Objects in Mobile Learning Settings. QScience Proceedings: Vol. 2013, 12th World Conference on Mobile and Contextual Learning (mLearn 2013), article 11 (Oct. 2013), 67-70.
- [26] Roy, D., Sarkar, S., Ghose, S. A Comparative Study of Learning Object Metadata, Learning Material Repositories, Metadata Annotation & an Automatic Metadata Annotation Tool, Vol. 2, 2010. p. 103–126.
- [27] Merlot, Multimedia Educational Resource for Learning and Online Teaching, 2009. Retrieved 12.10.2014, URL: <http://www.merlot.org>.
- [28] Aradne Foundation, ARIADNE, 2014. Retrieved 12.10.2014, URL: <http://ariadne-eu.org/>.
- [29] Careo project, Campus Alberta Repository of Educational Objects, 2014. Retrieved 12.10.2014, URL: <http://careo.org/>
- [30] W3C. (2004). RDF Vocabulary Description Language 1.0: RDF Schema. W3C Recommendation. [Online]. Available: <http://www.w3.org/TR/rdf-schema/>.
- [31] W3C. SPARQL Query Language for RDF. [Online]. Available: <http://www.w3.org/TR/rdf-sparql-query>
- [32] XML Schema, <http://www.w3.org/xml/schema>
- [33] webprotege [<http://webprotege.stanford.edu/>]
- [34] Microsoft Visual Studio 2015. <https://www.visualstudio.com/>

Detection and Classification of Mu Rhythm using Phase Synchronization for a Brain Computer Interface

Oana Diana Eva

Faculty of Electronics, Telecommunications and Information Technology
“Gheorghe Asachi” Technical University
Institute of Computer Science
Romanian Academy
Iasi, Romania

Abstract—Phase synchronization in a brain computer interface based on Mu rhythm is evaluated by means of phase lag index and weighted phase lag index. In order to detect and classify the important features reflected in brain signals during execution of mental tasks (imagination of left and right hand movement), the proposed methods are implemented on two datasets. The classification is performed using linear discriminant classifier, quadratic discriminant classifier, Mahalanobis distance classifier, k nearest neighbor and support vector machine. Classification accuracies up to 74% and 61% for phase lag index and weighted phase lag index were achieved. The results indicate that phase synchronization measures are relevant for classifying mental tasks recorded in the active state and the relaxation state from additional motor area and from the sensorimotor area. Phase lag index and weighted phase lag index methods are easy to implement, efficient, provide relevant features for the classification and can be used as an offline methods for motor imagery paradigms.

Keywords—brain computer interface; electroencephalogram; phase synchronization; phase lag index; weighted phase lag index; classifiers

I. INTRODUCTION

Brain computer interface (BCI) systems translate brain activities into commands for external devices. Their main goal to provide a communication channel for people with severe motor disabilities.

One of the most popular and used method in recording neurological signals is the electroencephalogram (EEG). It is simple to use, implies low costs and has a very high time resolution allowing EEG based BCIs to respond very quickly to user commands [1].

EEG based BCIs identify changes that occur while the person performs different mental tasks and make use of important features in classification. The linear classifiers, neural networks and nearest neighbor classifiers are most used in BCI applications.

The EEG signals contain amplitude and phase information. Common spatial pattern (CSP) [2], power spectral density (PSD) [1], adaptive auto regressive (AAR) parameters [3] and Hurst exponent [4] have been used to extract from EEG

amplitude distinctive features in different mental states. Phase synchrony is a mechanism for dynamic integration of distributed neural networks in the brain. Phase relationships identified between the recordings of electrophysiological activity generated within different cortical regions may provide information about functional connections between those cortical regions [5]. Such relationships are reported between cortical regions that are used in the control of a BCI where spectral coherence quantifies phase synchronization for electrophysiological data [6].

Phase synchronization can be difficult due to the presence of the common reference, the volume-conduction of source activity and the presence of noise sources [7]. To overcome these problems, methods that are focusing on phase instead of the amplitude have been proposed: the phase locking value (PLV) [8], that uses only the relative phase between signals to measure the phase-synchronization, the imaginary component of the coherency (ImC) [9] as a conservative index of phase-synchronization, phase lag index (PLI) [10] as a potential improvement of the ImC and the weighted phase lag index (WPLI) [4] in order to increase the capacity to detect true changes in phase synchronization.

Sensorimotor rhythms (SMR) refer to a brain oscillation in the specific frequency band generated from the sensorimotor area. SMRs are modulated by motor execution, motor observation and motor imagery [11].

While performing a mental activity as left/right hand movement or imagination changes appear in the sensorimotor area in the corresponding signal power of Mu (8-12 Hz) and Beta (12-30 Hz) rhythms.

An off-line analysis is performed in order to extract and classify significant features contained in the EEG signals using indexes that characterize the phase synchronization (PLI and WPLI) in a BCI paradigm based on sensorimotor rhythms. Five classifiers are used for distinguishing mental tasks.

In the section II databases and methods used are described, how the features are extracted and how the classification methods are applied. The results are depicted in section III. The paper ends with discussions based on our results (section IV) and conclusions (section V).

II. METHODOLOGY

A. Datasets

The EEG signals are recorded with a portable acquisition system from the lab of the Faculty of Medical Bioengineering. It is provided by g.tec medical engineering GmbH and is based on a g.GAMMAcap unit, a g.GAMMAbox unit and a g.MOBilab+ one. The sampling frequency of 256 Hz and BCI2000 platform [12] are used. 8 electrodes (CP3, CP4, P3, P4, C3, C4, PZ and CZ) are placed on the subject scalp according to International 10-20 System. The reference electrode is linked on the right earlobe.

Subjects (33 healthy volunteers, men and women, age range 19-59 years) are asked to perform motor imagery tasks. The subjects are sitting relaxed in front of a computer screen. At the beginning of a trial, the screen is white. After 2 s, an arrow pointing to the left or to the right appears on the screen. The subject has to imagine the hand movement indicated by the arrow and to relax when the screen is white. During the recordings, subjects are advised to try to avoid the eye blinking, eye movements, feet movements or swallowing. Each arrow appears up for 30 times. The trials are conducted in different days. All subjects provide written informed consent prior to the experiment.

The second dataset used is provided by Dr. Allen Osman in BCI Competition 2002 [13]. The EEGs are recorded by 59 electrodes. The signals are sampled at the frequency 100 Hz. The reference electrode is placed on the left mastoid. The dataset consists of EEG data recorded from 9 well trained subjects. Each session lasts 6 s and each run consists of 90 trials (45 trials for imagery of left hand movement and 45 for imagery of right hand movement). In each trial a cue is shown on the screen instructing the subject to perform one of the following motor imagery tasks: left hand, right hand, relaxation. The signals acquired from 9 electrodes (FC3, FCZ, FC4, CP3, CPZ, CP4, C3, CZ and C4) over the sensorimotor area are considered for further processing.

B. Methods

The phase lag index and the weighted phase lag index are used for measuring the synchronization between two signals $x(t)$ and $y(t)$.

The phase lag index measures the statistical interdependencies between time series. The aim of PLI is to obtain reliable estimates of phase synchronization that are invariant against the presence of common sources as active reference electrodes.

The asymmetry of the phase difference distribution means that the likelihood that the phase difference $\Delta\theta$ will be in the interval $-\pi < \Delta\theta < 0$ is different from the likelihood that it will be in the interval $0 < \Delta\theta < \pi$. This asymmetry implies the presence of a nonzero phase difference ('lag') between the two time series [10].

An index of the asymmetry of the phase difference distribution can be obtained from a time series of phase differences $\Delta\theta(t_k), k = 1 \dots N$ in the following way:

$$PLI = |\langle \text{sign}[\Delta\theta(t_k)] \rangle|, \quad (1)$$

where sign is the signum function and $-\pi \leq \Delta\theta \leq +\pi$.

The PLI ranges between 0 (no interaction) and 1 (maximum interaction), $0 \leq PLI \leq 1$. The $\langle \rangle$ denotes the average over the time t . A PLI of zero indicates either no coupling or coupling with a phase difference $\Delta\theta$ centered around $[0, \pi]$ [10].

The WPLI increases the capacity to detect real changes that occur in phase synchronization, reduces the influence of common noise sources and reduces the influence of changes in the coherence phase [7]. The weighted phase lag index is calculated using the formula:

$$WPLI = |\langle I(X) \rangle| / \langle |I(X)| \rangle = |\langle I(X) \text{sign} I(X) \rangle| / \langle |I(X)| \rangle \quad (2)$$

where $I(X)$ is the imaginary component of the cross spectrum between two signals $x(t)$ and $y(t)$.

The complex cross-spectrum $C(f)$ for two real-valued signals $x(t)$ and $y(t)$ is computed by Fourier transform.

$$C(f) = \langle X(f)Y^*(f) \rangle, \quad (3)$$

where $X(f)$ is the Fourier transform of signal $x(t)$ and $Y(f)$ is the Fourier transform of signal $y(t)$. The symbol $*$ indicates the complex conjugation and $\langle \rangle$ denotes the expectation value.

The values of the WPLI are ranged between 0 and 1, where 1 means total synchronization. Synchronization is defined by $P\{\text{sign}(I(X)) = 1\} = 1$ or $P\{\text{sign}(I(X)) = -1\} = 1$, where $P\{\cdot\}$ denotes probability. The WPLI is based on the imaginary component of the cross spectrum [7].

C. Preprocessing of the EEG signals

All EEG signals from the first dataset are loaded, and then they are band-pass filtered in the 8-12 Hz frequency band by means of 100th order Finite Impulse Response (FIR) filter in order to avoid phase distortions. Data segments corresponding to the left hand motor imagery and to the right hand motor imagery are extracted.

New obtained EEG signals are analyzed using the PLI and the WPLI. To compute the phase synchronization, it is necessary to know the instantaneous phase of the two signals involved. This can be realized using the Hilbert transform. The Hilbert transform is performed for all the channels (CP3, CP4, P3, P4, C3, C4, PZ and CZ) and the PLI and the WPLI are computed for all the possible pairs of EEG channels (both for left hand motor imagery and for right hand motor imagery).

Two electrodes from the additional motor area CZ and PZ and six electrodes from the sensorimotor areas P3, C3, CP3 (from left hemisphere) and P4, C4, CP4 (from right hemisphere) are used. Six combinations for CZ (CZ-CP3, CZ-CP4, CZ-P3, CZ-P4, CZ-C3, CZ-C4), six combinations for PZ (PZ-CP3, PZ-CP4, PZ-P3, PZ-P4, PZ-C3, PZ-C4) and three combinations left-right (CP3-CP4, P3-P4 and C3-C4) are extracted.

The approach is firstly evaluated using the PLI and then the WPLI.

The same steps are followed for the second dataset but other channels are handled. Nine combinations for left

hemisphere: FCZ-FC3, FCZ-C3, FCZ-CP3, CZ-FC3, CZ-C3, CZ-CP3, CPZ-FC3, CPZ-C3, CPZ-CP3, nine combinations for right hemisphere: FCZ-FC4, FCZ-C4, FCZ-CP4, CZ-FC4, CZ-C4, CZ-CP4, CPZ-FC4, CPZ-C4, CPZ-CP4 and three combinations left-right: CP3-CP4, FC3-FC4 and C3-C4 are formed.

D. Classifiers

In order to observe the discrimination between left or right motor activity we used 5 classifiers: linear discriminant analysis (LDA) [6], quadratic discriminant analysis (QDA) [14], Mahalanobis distance (MD) [15], k nearest neighbor (KNN) [16] and support vector machine (SVM) [17]. A 10x10 fold cross validation estimated the classification rate for each subject.

The feature vector is formed by PLI indexes for left motor imagery and right motor imagery. Data are divided into 10 parts with an equal number of features, 5 parts are used for training and the other parts for testing.

III. RESULTS

Fig. 1 displays the classification rates obtained with classifiers LDA, QDA and MD for PLI for the dataset developed with EEGs recorded in our lab. The classification rates are above 60%. 68% from the subjects obtained better results with QDA classifier and the others 32% with MD classifier.

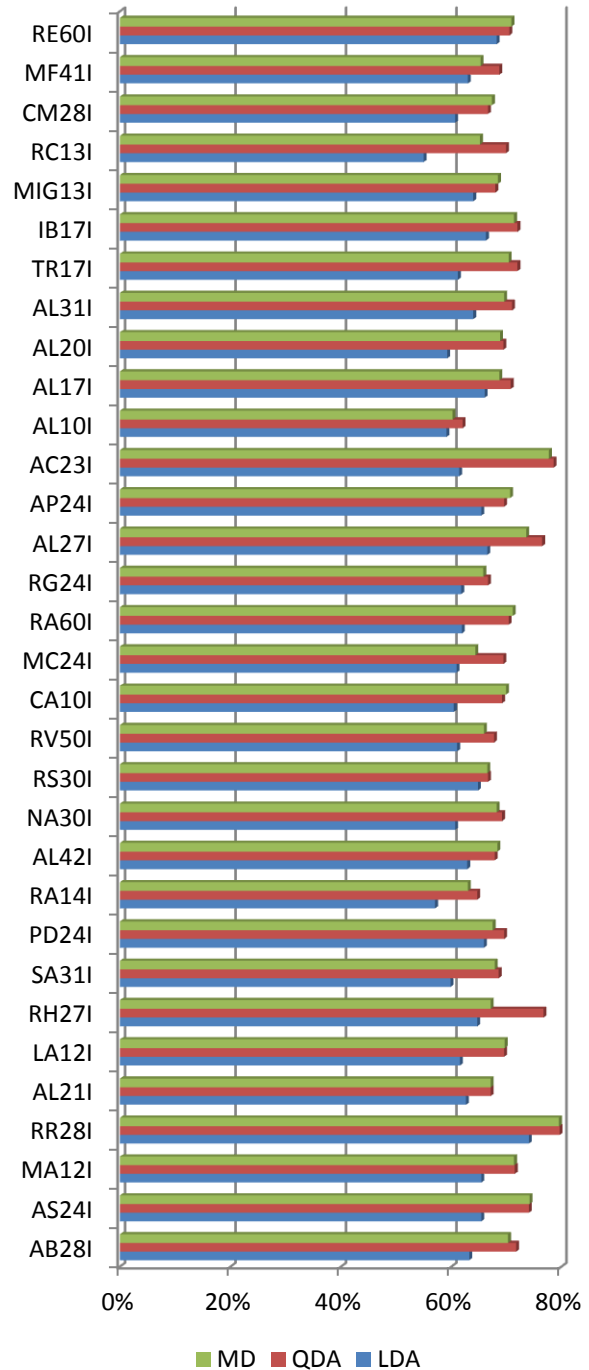


Fig. 1. The classification rates of PLI using classifiers LDA, QDA and MD

TABLE I. shows the classification rates using KNN classifier for 1, 2, 3, 4 or 5 neighbors. The higher classification rates of about 83% are obtained by subject RH27I and the smaller rates of about 68% by subject AL10I.

TABLE I. THE CLASSIFICATION RATES OBTAINED WITH KNN FOR PLI

Subjects	Number of neighbors				
	1	2	3	4	5
AB28I	79,37%	79,49%	79,59%	79,71%	79,79%
AS24I	75,93%	76,12%	76,15%	76,25%	76,24%
MA12I	75,46%	75,54%	75,71%	75,88%	75,95%
RR28I	84,67%	84,70%	84,69%	84,72%	84,63%
AL21I	69,70%	69,76%	69,88%	69,96%	69,99%
LA12I	75,56%	75,52%	75,38%	75,34%	75,24%
RH27I	83,62%	83,74%	83,83%	83,98%	84,04%
SA31I	70,94%	70,98%	70,95%	70,97%	70,99%
PD24I	73,74%	73,73%	73,70%	73,65%	73,58%
RA14I	72,89%	72,88%	73,03%	73,13%	73,28%
AL42I	73,72%	73,75%	73,74%	73,71%	73,60%
NA30I	75,07%	75,14%	75,18%	75,23%	75,26%
RS30I	73,50%	73,47%	73,43%	73,38%	73,28%
RV50I	73,89%	73,95%	74,07%	74,16%	74,29%
CA10I	75,50%	75,50%	75,50%	75,53%	75,57%
MC24I	73,57%	73,69%	73,78%	73,90%	73,97%
RA60I	78,04%	78,06%	78,13%	78,21%	78,18%
RG24I	75,26%	75,29%	75,25%	75,20%	75,08%
AL27I	81,34%	81,33%	81,31%	81,38%	81,41%
AP24I	76,85%	76,76%	76,76%	76,72%	76,58%
AC23I	83,54%	83,61%	83,68%	83,77%	83,84%
AL10I	67,90%	67,84%	67,76%	67,67%	67,70%
AL17I	73,76%	73,75%	73,70%	73,67%	73,56%
AL20I	74,07%	74,20%	74,27%	74,37%	74,41%
AL31I	75,37%	75,50%	75,59%	75,65%	75,67%
TR17I	76,98%	76,85%	76,80%	76,74%	76,62%
IB17I	77,54%	77,44%	77,39%	77,34%	77,27%
MIG13I	80,43%	80,45%	80,41%	80,33%	80,15%
RC13I	75,28%	75,33%	75,52%	75,63%	75,79%
CM28I	73,46%	73,52%	73,43%	73,44%	73,36%
MF41I	71,74%	71,77%	71,94%	72,04%	72,24%
RE60I	76,43%	76,46%	76,41%	76,35%	76,28%

Using WPLI, the classification rates for all the subjects are smaller with 20% in comparison with PLI using classifiers LDA, QDA, MD (Fig.2). The accuracy rates are below 66%.

Unlike PLI, where none of the subjects obtained higher classification rates with LDA classifier, for WPLI, 6 subjects obtained the best classification rates with LDA, 18 subjects with QDA classifier and 9 subjects with MD classifier.



Fig. 2. The classification rates (%) for WPLI using classifiers LDA, QDA and MD

Subjects MIG13I and CA10I achieved the highest classification rates by means of KNN classifier when WPLI is used as feature vector. In comparison with PLI the classification rates obtained with WPLI are also lower (TABLE II).

TABLE II. THE CLASSIFICATION RATES OBTAINED WITH KNN FOR WPLI

Subjects	Number of neighbors				
	1	2	3	4	5
AB28I	53,72%	53,79%	54,05%	54,22%	54,30%
AS24I	53,56%	53,33%	53,31%	53,18%	53,12%
MA12I	56,36%	56,51%	56,67%	56,80%	56,77%
RR28I	53,30%	53,27%	53,31%	53,38%	53,43%
AL21I	54,95%	54,95%	54,93%	54,93%	54,85%
LA12I	57,58%	57,55%	57,53%	57,53%	57,50%
RH27I	54,96%	54,96%	54,95%	54,98%	54,99%
SA31I	58,36%	58,51%	58,54%	58,60%	58,58%
PD24I	59,27%	59,26%	59,25%	59,28%	59,27%
RA14I	54,34%	54,42%	54,51%	54,66%	54,66%
AL42I	51,89%	51,71%	51,61%	51,46%	51,34%
NA30I	55,15%	55,34%	55,45%	55,55%	55,70%
RS30I	57,73%	57,75%	57,70%	57,75%	57,83%
RV50I	55,13%	55,08%	55,05%	55,01%	55,01%
CA10I	61,58%	61,63%	61,60%	61,63%	61,56%
MC24I	57,38%	57,43%	57,28%	57,26%	57,18%
RA60I	56,21%	55,95%	55,83%	55,69%	55,49%
RG24I	52,39%	52,43%	52,41%	52,39%	52,37%
AL27I	57,35%	57,46%	57,68%	57,97%	58,21%
AP24I	55,07%	55,18%	55,37%	55,54%	55,62%
AC23I	54,47%	54,50%	54,55%	54,60%	54,70%
AL10I	56,15%	56,12%	56,02%	56,00%	55,92%
AL17I	57,52%	57,47%	57,42%	57,34%	57,22%
AL20I	57,84%	57,87%	57,95%	58,02%	57,99%
AL31I	55,21%	55,34%	55,41%	55,48%	55,45%
TR17I	52,11%	52,16%	52,08%	52,00%	51,91%
IB17I	54,52%	54,57%	54,53%	54,49%	54,44%
MIG13I	62,81%	62,70%	62,71%	62,70%	62,75%
RC13I	54,13%	54,14%	54,11%	54,10%	54,03%
CM28I	57,80%	57,79%	57,76%	57,77%	57,73%
MF41I	58,60%	58,56%	58,52%	58,37%	58,23%
RE60I	54,74%	54,60%	54,45%	54,28%	54,08%

Fig. 3 presents the results for PLI compared with the results for WPLI using SVM classifier. For PLI, the highest classification rate is 86.25% – subject RR28I and for WPLI 61.56% – subject AL27I.

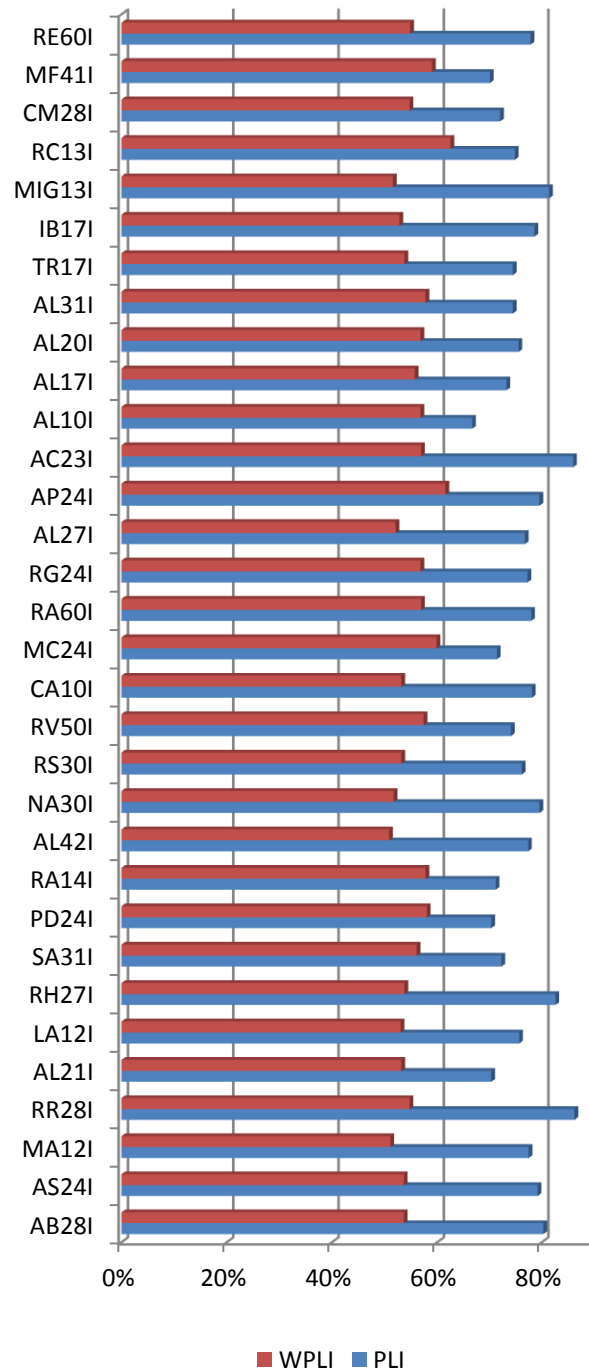


Fig. 3. The classification rates for PLI and WPLI using SVM classifier

In the next section are shown the classification results obtained on the second dataset used. Subject 1 achieved the following discrimination rates: 85.80% - LDA, 83.33% - QDA and 87.08% - MD for PLI (Fig. 4).

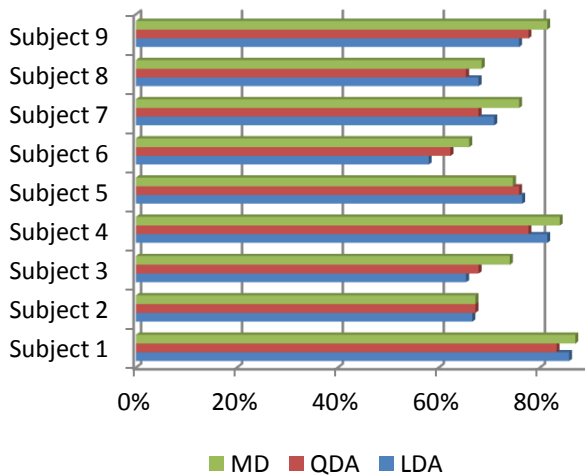


Fig. 4. The classification rates for PLI applying LDA, QDA and MD

KNN classification with 1, 2, 3, 4, 5 neighbors is depicted in TABLE III. The results are in the range of 63.99% (subject 8) and 87.34% (subject 1).

TABLE III. THE CLASSIFICATION RATES (%) OBTAINED WITH KNN FOR PLI

Subjects	Number of neighbors				
	1	2	3	4	5
Subject 1	87,22%	87,34%	87,34%	87,34%	87,24%
Subject 2	68,94%	68,72%	68,51%	68,31%	68,11%
Subject 3	72,36%	72,29%	72,13%	71,97%	71,91%
Subject 4	85,68%	85,82%	85,85%	85,98%	85,91%
Subject 5	77,75%	77,49%	77,34%	77,20%	77,26%
Subject 6	70,26%	70,02%	69,68%	69,46%	69,24%
Subject 7	72,47%	72,40%	72,23%	72,18%	72,02%
Subject 8	65,20%	65,04%	64,79%	64,44%	63,99%
Subject 9	84,47%	84,31%	84,36%	84,31%	84,26%

The discrimination rates achieved with WPLI and LDA, QDA and MD are presented in Fig. 5. For each of the three classifiers, the results are smaller compared to those when the feature vector used the PLIs.

In TABLE IV. are presented the results obtained with KNN. The higher classification is achieved by Subject 9 and the smaller one by Subject 3.

Concerning the comparison between performances achieved with SVM classifier, for PLI and WPLI the higher difference between rates is 29.01% for subject 1 and the

smaller one is 1.85% (Fig. 6). Subject 7 attained a better classification for WPLI.

The findings are consistent with other works [18], [19] in which the second dataset is exploited. So, in [18] where a time-frequency approach is investigated using six subjects (1, 2, 5, 6, 7, 9), for subject 1 and subject 9 are reported the classification rates 81.11% and 83.61%, respectively. With PLI for subject 1 the classification rates achieved are in the range 77.78% - 87.34%, while for subject 9 the classification rates were in the range 67.28% - 84.47%. For WPLI, for subject 1 the classification rates are between 48.76% - 62.34% and for subject 9: 59.25% - 62.86%.

In [20], where Itakura distance based method is used and 20 subjects from the first database, the classification rates are approximately the same with the actual results. For example, subject RR28I achieved 81.67%, 86.67%, 85.00% classification rates using LDA, QDA and MD classifiers, compared to 74.09%, 79.68%, 79.56% for PLI and 56.20%, 55.60% and 55.84% for WPLI.

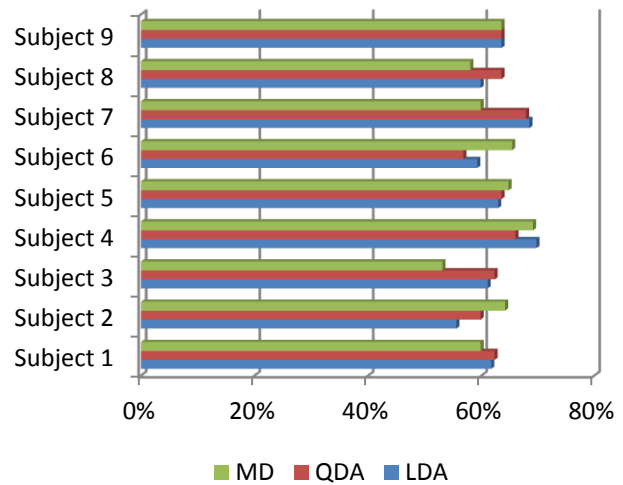


Fig. 5. LDA, QDA and MD classification corresponding to the WPLI method

TABLE IV. THE CLASSIFICATION RATES OBTAINED WITH KNN FOR WPLI

Subjects	Number of neighbors				
	1	2	3	4	5
Subject 1	61,78%	61,69%	61,70%	61,51%	61,63%
Subject 2	56,50%	56,39%	56,49%	56,49%	56,17%
Subject 3	55,18%	55,19%	55,11%	55,13%	55,35%
Subject 4	62,00%	61,90%	61,70%	61,30%	61,32%
Subject 5	62,56%	62,45%	62,45%	62,45%	62,55%
Subject 6	59,47%	59,63%	59,68%	59,62%	59,67%
Subject 7	59,03%	58,77%	58,72%	58,68%	58,54%
Subject 8	57,05%	57,03%	57,02%	57,01%	57,00%
Subject 9	62,11%	62,34%	62,55%	62,87%	62,86%

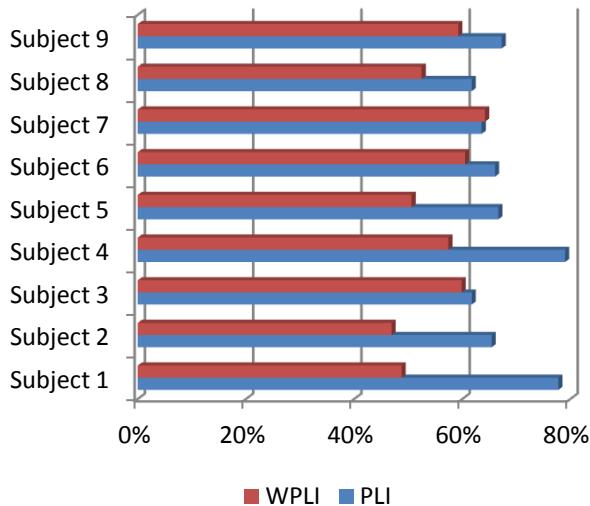


Fig. 6. The classification rates for PLI and WPLI using SVM classifier

Fig. 7 displays the highest classification rates obtained for phase lag index and weighted phase lag index with all five classifiers and for datasets used.

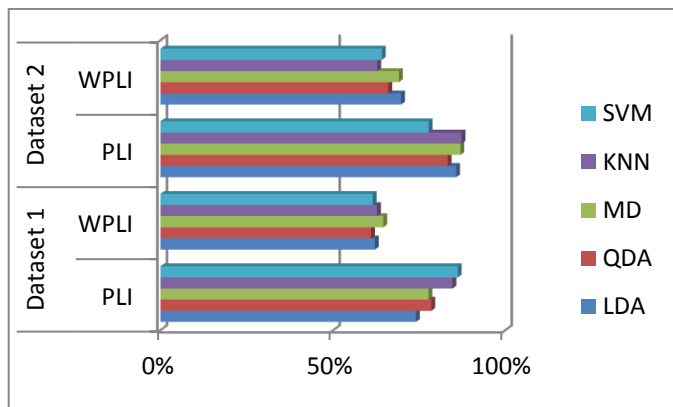


Fig. 7. The classification accuracies using all classifiers for PLI and WPLI

IV. DISCUSSIONS

The research evaluated two phase synchronization based methods with two indexes: phase lag index and weighted phase lag index, on two different datasets. Phase synchronization contains important features connected to the brain activity and in this way the discrimination can be made between left and right hand movement. The first dataset is formed by EEG recordings collected by the authors. So, in this case, the research is more efficient because all the details and conditions on which the recordings were made are known. The opinion of the voluntaries and their information regarding the experiments are also well-known. The volunteers are trained first by performing effectively the movement of the left/right hand and after that performing left/right hand imagination. For the second dataset used there are not available so many information: the acquisition system it is not described or mentioned, isn't specified if the recordings took placed in the same day or in different days and the age of the volunteers is

not known. It is mentioned that the subjects were well trained. The technical and social details are very important in developing a brain computer interface.

For the first dataset, the classification rates obtained with PLI are different from the results attained with WPLI. Using LDA classification method 5 subjects obtained differences higher with 10% for PLI in comparison with WPLI. Two subjects achieved better results with WPLI. Differences below 5% between PLI and WPLI were noticed at 8 subjects. With QDA classifier classification rates obtained are higher than LDA but also the higher differences between classification rates for PLI and WPLI. For 70% of the subjects the differences between classification rates are in the range of 10.22%-19.71%. No subject has achieved higher classification rates for WPLI. MD classification provided better results for PLI for 87% of the subjects. The smaller difference between the classification rates is obtained by one subject – 2.07%.

If we are comparing the results obtained with LDA, QDA and MD the higher classifications rates are achieved with QDA.

Regarding the KNN classification the number of neighbors is very important. We have chosen to represent all five neighbors in order to see which neighbor is the best. The average for 1 neighbor was 75.78%, 2 neighbors – 75.82, 3 neighbors – 75.84%, 4 neighbors – 75.88%, 5 neighbors 75.87% in the case of PLI. In the case of WPLI the average obtained were 56.01%, 56.01%, 56.02%, 56.03%, 56.01%. SVM classifier outperforms all classifiers used. In this cases aren't highlighted major differences between neighbors. Two subjects achieved classification rates above 86% when the feature vector is formed with and other two subjects when the feature vector is formed with WPLI.

For the second dataset used we can conclude the following: the higher difference between PLI and WPLI is 24.07% and the smaller difference is 2.47% for LDA classification.

QDA method revealed approximately the same results as LDA classification. The highest classification rate is about 83.33% and the smallest one is about 62.35%.

If we compare LDA, QDA and MD the higher classification rates are obtained with MD. For PLI the results are also better.

In KNN classification the difference between neighbors were not significant. The average was 76% for PLI and 56% for WPLI.

With SVM classification the highest classification rates are also obtained.

Overall, the classification rates are better for the second dataset.

The discrimination rates are higher with 8-10% for the second dataset compared to the first dataset.

Although WPLI is a more complex method by introducing weighted normalized phase difference, the classification rate is not higher than 60%.

The type of classifier utilized, the way how a subject could imagine the hand movement are some aspects that should be explored more deeply.

V. CONCLUSIONS AND FUTURE WORK

Offline analysis based on phase synchronization are proposed and tested.

The results suggest that methods could be exploited for BCI paradigms. It was found a large variability between subjects and between datasets.

PLI and WPLI avoid artifacts caused by the volume conductor. Volume conductor is very important for the EEG recordings because the analysis of connectivity is limited due to the low spatial resolution.

The results revealed satisfactory even although no methods for elimination of artifacts and few EEG channels were used.

Future work implies developing an ensemble classifier (a combination of classification methods) for improving the classification rates.

ACKNOWLEDGMENT

This work was supported by a grant of the Romanian National Authority for Scientific Research and Innovation, CNCS – UEFISCDI, project number PN-II-RU-TE-2014-4-0832 “Medical signal processing methods based on compressed sensing; applications and their implementation”.

REFERENCES

- [1] J.R. Wolpaw, N. Birbaumer, D.J. McFarland, G. Pfurtscheller, T.M. Vaughan, “Brain-computer interfaces for communication and control”, *Clinical Neuro-physiology*, vol. 113(6), pp. 767–791, 2002.
- [2] Y.Wang, S. Gao, X. Gao, “Common spatial pattern method for channel selection in motor imagery based brain-computer interface”, *IEEE Engineering in Medicine and Biology 27th Annual Conference*, pp. 5392-5395, 2005.
- [3] A. Schlögl et al., “Characterization of four-class motor imagery EEG data for the BCI-competition 2005”, *Journal of neural engineering*, 2.4: L14, 2005.
- [4] R. Aldea, D. Tarniceriu, “Estimating the Hurst exponent in motor imagery-based brain computer interface”, *Speech Technology and Human-Computer Dialogue (SpeD)*, IEEE, pp. 1-6, 2013.
- [5] I. Daly, S.J. Nasuto, K. Warwick, “Brain computer interface control via functional connectivity dynamics”, *Pattern recognition*, vol. 45(6), pp. 2123-2136, 2012.
- [6] F. Lotte, M. Congedo, A. Le Cuyer, F. Lamarche, B. Arnaldi, “A review of classification algorithms for EEG-based brain-computer interfaces”, *Journal of NeuralEngineering*, 4(2), 2007.
- [7] M. Vinck, R. Oostenveld et al., “An improved index of phase-synchronization for electrophysiological data in the presence of volume-conduction, noise and sample-size bias”, *Neuroimage*, vol. 55(4), pp. 1548–1565, 2011.
- [8] JP Lachaux, E. Rodriguez et al., “Measuring phase synchrony in brain signals”, *Hum Brain Mapp.*, vol. 8(4), pp. 194–208, 1999.
- [9] G. Nolte, O. Bai, L. Wheaton, Z. Mari, S. Vorbach, M. Hallett, “Identifying true brain interaction from EEG data using the imaginary part of coherency”, *Clin. Neurophysiol.*, vol. 115, pp. 2292–2307, 2004.
- [10] C.J. Stam, G. Nolte, A. Daffertshofer, “Phase lag index: assessment of functional connectivity from multi channel EEG and MEG with diminished bias from common sources”, *Hum. Brain Mapp.*, vol. 28, pp. 1178–1193, 2007.
- [11] C. Neuper, R. Scherer, S. Wriessneger, G. Pfurtscheller, “Motor imagery and action observation: modulation of sensorimotor brain rhythms during mental control of a brain-computer interface”, *Clinical Neurophysiology*, vol. 120, pp. 239–247, 2009.
- [12] J. Mellinger, G. Schalk: BCI2000: A General-Purpose Software Platform for BCI Research, In: G. Dornhege, J. del R. Millán, T. Hinterberger, D.J. McFarland, K.-R. Müller (eds.), *Toward Brain-Computer Interfacing*, MIT Press, 2007.
- [13] A. Osman, A. Robert., “Time-course of cortical activation during overt and imagined movements”, *Proc. Cognitive Neuroscience Annu. Meet.*, New York vol. 1, pp. 1842-1852, 2001.
- [14] T. Hastie, R. Tibshirani, J. Friedman, “The Elements of Statistical Learning - Data Mining, Inference and Prediction”, *Springer Series in Statistics*, pp.110-111, 2009.
- [15] F. Babiloni, L. Bianchi, F. Semeraro, J. del R Millan, J. Mouriño, A. Cattini, F. Cincotti, “Mahalanobis distance-based classifiers are able to recognize EEG patterns by using few EEG electrodes”, *Engineering in Medicine and Biology Society*, 1, pp. 651-654, 2001.
- [16] W.A. Chaovalitwongse, Y.J. Fan, R.C. Sachdeo, "On the time series k-nearest neighbor classification of abnormal brain activity", *Systems, Man and Cybernetics, Part A: Systems and Humans*, IEEE Transactions, vol. 6, pp. 1005-1016, 2007
- [17] K.P. Bennett, C. Campbell, “Support vector machines: hype or hallelujah?”, *ACM SIGKDD Explorations Newsletter*, vol. 2(2), pp.1-13, 2000.
- [18] N. F. Ince, A.H. Tewfik, S. Arica, “Extraction subject-specific motor imagery time-frequency patterns for single trial EEG classification”, *Computers in Biology and Medicine*, vol. 37(4), pp. 499-508, 2007.
- [19] B. Kamousi, Z. Liu, B. He, “An EEG inverse solution based brain-computer interface”, *The International Journal of Bioelectromagnetism*, vol. 7(2), pp. 292-294, 2005.
- [20] O.D. Eva, A.M. Lazar, “Channels selection for motor imagery paradigm - An Itakura distance based method”, *E-Health and Bioengineering Conference (EHB)*, IEEE, pp. 1-4, 2015.

Reducing the Electrical Consumption in the Humidity Control Process for Electric Cells using an Intelligent Fuzzy Logic Controller

Rafik Lasri

Dept of Computer Science,
Poly-disciplinary Faculty of Larache,
University of Abdelmalek Essaâdi,
Morocco

Larbi Choukri, Mohammed
Bouhorma

Dept of Computer Engineering, FST-
Tangier,
University of Abdelmalek Essaâdi,
Morocco

Ignacio Rojas, Héctor Pomares

Dept of Architecture & Computer
Technologies
University of Granada, Spain

Abstract—The electrical energy distribution uses a huge network to cover the urbanized areas. The network distribution incorporates an important number of electrical cells that ensure the energy transformation. These cells play a fundamental role to ensure a permanent feeding. Thus, the performance of these cells must be optimized. The main problem that affects these cells is the inside humidity that should be controlled permanently to prevent serious damage and power failure. The presented work proposes the use of a powerful intelligent Fuzzy Logic Controller that can online adapt their internal parameters according to the actually state of the controlled plant and auto-learn from the behavior of the plant how the current humidity level can be decreased. The used controller can stabilize the humidity inside the cells within the recommended range by controlling a set of heating resistances installed inside these cells and in the same time ensuring valuable advantages for the electrical energy distribution company. Unlike the rest of the controllers that are used to stabilize moisture. The intelligent controller used in these papers ensures a very precise control with very low power consumption which trains a very significant energy savings in each electrical cell. Knowing that the distribution network incorporates a very large number of electrical cells, the final savings balance would be a very high amount of energy that can be presented economically with significant savings on the electricity bills.

Keywords—humidity in electric cells; humidity control; optimization of electrical consumption; intelligent fuzzy logic controller; saving power

I. INTRODUCTION

The phenomenon of condensation of atmospheric moisture remains at the center of scientific research for aspects, the positive and the harmful effects. On the positive side, there is the production of water from atmospheric air [1], [2] in order for example to fight against drought, promote agriculture, industrial development and accompany follow demand household water in large cities. On the positive side, there is the production of water from atmospheric air in order for example to fight against drought, promote agriculture, industrial development and accompany follow demand household water in large cities. For adverse effects include the case of bad hygrothermic of buildings [3] which exacerbates the problem of indoor humidity and damage caused by the

formation of mold and corrosion. Also moisture condensation poses problems of reliability of electronic components [4], the smooth operation of metal constructions [5], and particularly arcing of electrical installations [6] that cause the interruption of power homes and stopping industrial processes and causing huge financial losses.

So some researchers are interested in determining the dew point [7], [8], temperature at which water vapor in the air condenses and turns into water droplets, and to determine the anti-condensation prevention system best suited. Other researchers have focused on the development of these anti-condensation systems and the design of their regulators to optimize their operations; particularly in [9] a Fuzzy-PID controller is developed to control a dehumidifier in high voltage electrical equipment.

In this paper, we will propose the use of an Intelligent Fuzzy Logic Controller (FLC) to optimize the operation of heating resistances installed inside a medium voltage cell to avoid the probable damage due to the formation of the mold and the corrosion. Contrary to the actually used controller and the conventional FLC, the Intelligent FLC will be able to control the environment inside the cells consuming little energy than the remaining controllers.

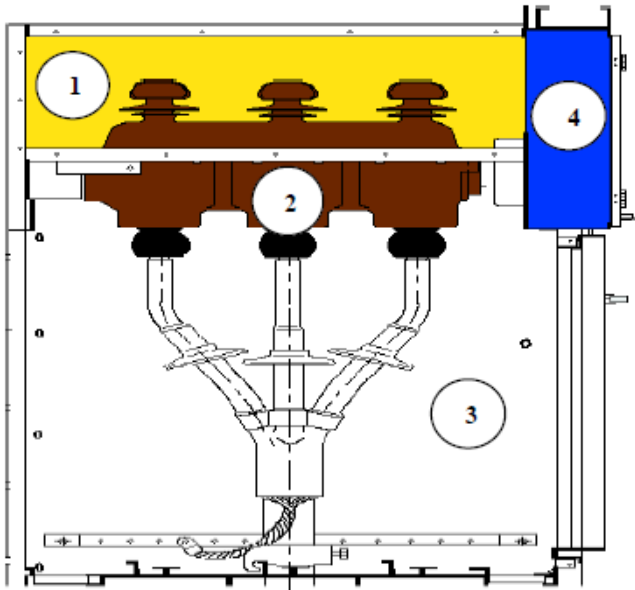
II. ELECTRIC CELLS AND CONDENSATION OF ATMOSPHERIC MOISTURE PROBLEM

Ensure a permanent power supply presents a major concern for the electrical energy distributors, for this, the studies do not cease to lute against different causes of alimentation disruptions. Priming insulators in electric cells low voltage is a common cause of power failure that disrupts the continuity of services provided by electricity distributors.

It's to note here that the role of these cells is to ensure the electricity transmission from the source to consumers by adapting the distributed power via different transformers, which justifies the significant number of these cells along the alimentation network. Therefore, the risk of power cut due to priming of the equipment of these cells is very considerable. The Fig.1 shows the internal diagram of a cell with its different blocks. A cell consists of three basic systems:

- The appliances compartment that contain: Medium Voltage (MV) breakers and switch...
- The Medium Voltage bus bar compartment for the electrical connections between several MV cells grouped into tables.
- The connections compartment to MV cables, often used for receiving the measuring sensors.

A fourth compartment used usually to complete this set, it is the control compartment (or Low Voltage, LV box) that contains the protection, monitoring and control units. Priming a switch or circuit breaker causes the power cut out for the all the Medium Voltage cables.



1: Bus bar compartment 2: Vacuum switch 3: Cable compartment
4: Compartment mechanism also serving as low voltage compartment
Fig. 1. The internal diagram of a cell with its different blocks

A. Priming due to the dew point and their risk on the electrical equipment

Inside the cells (switch or circuit breaker), when the ambient air becomes saturated with water and the metal surfaces are colder, the dew appear on these surfaces (fig.2) which encourages the ionization of the air around the conductors and the appearance of effluvia. This phenomenon liberates molecules such as ozone which recombines with other elements of the ambient air generates nitric acid which oxidizes metals that degrade the insulation and creates leakage paths to ground until priming.

In order to avoid this phenomenon, a heater is installed in the cable compartment of each Medium Volt (MV) cell to warm the sheet metal and the air. This heater (resistance) runs continuously throughout the year causing an important waste of energy and a new risk for the insulation when exceeding the maximum permissible temperature. To avoid all these inconvenient, an intelligent controller will be implemented to ensure a supportive work environment inside the MV cells by calculating dew point from the temperature and the relative

humidity measured by a sensor placed in the cable compartment of the MV cells, the intelligent controller will adjust the supply voltage (0 to 240 V) of all the heating resistors to heat in an optimal manner inside the cells beyond the critical threshold. Fig. 3 present the proposed control process of the internal Medium Volts cell temperature and humidity. The value of the dew point temperature is given by the formula Henrich Gustav Magnus - Tetens:

$$T_{DP} = b * \frac{\alpha(T,RH)}{a - \alpha(T,RH)} \tag{1}$$

while:

$$\alpha(T, RH) = a * \frac{T}{b + T} + Ln(RH) \tag{2}$$

- | | |
|--|----------------------------|
| T: Measured temperature (°C) | a = 17.27 |
| R _H : Relative humidity (%) | b = 237.7 °C |
| T _{DP} : Dew Point of Moist Air | 0 ≤ T ≤ 60°C |
| | 1% ≤ R _H ≤ 100% |



Fig. 2. Apparition of the dew inside the electric cells

III. IMPLEMENTATION OF THE FUZZY LOGIC CONTROLLER

The control process presented in these papers is considered as a regular process that not requires sophisticated implementation. Hence, the important parameters to supervise are; the internal temperature of the cell and their variations over the time. The FLC used in this case has two inputs, the temperature difference and their variations; each one of these latter has a set of triangular membership functions imposed by an expert that describes the real state of the plant at this moment. The output of the FLC is the power supply (EV, Electrical Volts) that feeds the heating resistance to establish the required temperature inside the cell. The output space is represented with a set of triangular membership functions imposed too by the expert describing the real state of the plant output. Hence, in this work a Mamdani FLC was used to perform the control process. The used fuzzy rules can be presented as:

$$\text{IF } T_{dif} \text{ is } \mu_{critical} \text{ AND } \frac{dT_{dif}}{dt} \text{ is } \mu_{regular} \quad (3)$$

$$\text{THEN } V = \mu_{high}$$

Once the output fuzzy rule is precised, the defuzzyfication stage starts by applying the method of the center of gravity as follow:

$$\hat{\Omega}(\bar{z}^l) = \frac{\sum_{j_1=1}^{n_1} \sum_{j_2=1}^{n_2} \dots \sum_{j_N=1}^{n_N} (S_{j_1 j_2 \dots j_N} \cdot \prod_{w=1}^N v_{z_w^{j_w}}(z_w^l))}{\sum_{j_1=1}^{n_1} \sum_{j_2=1}^{n_2} \dots \sum_{j_N=1}^{n_N} (\prod_{w=1}^N v_{z_w^{j_w}}(z_w^l))} \quad (4)$$

where \bar{z}^l is the input vector at the k instant with l dimension, $S_{j_1 j_2 \dots j_N}$ are the activated rules and $v_{z_w^{j_w}}$ the membership degree.

Fig. 3 present the proposed control process of the internal Medium Volts cell temperature and humidity.

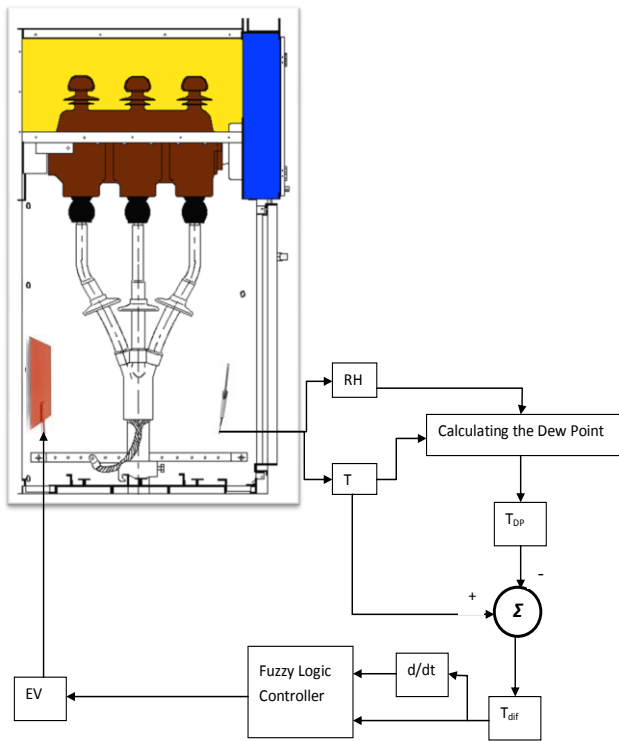


Fig. 3. The proposed control process of the internal Medium Volts cell temperature and humidity

A. Fuzzy Membership Function

In this control process each input and output variables has a set of membership function that defined as follows:

• Input Variables

Input 1: Temperature difference (T_{dif})

The difference between the measured temperature (T) and the dew point temperature (T_{DP}), is represented by four membership functions; very critical, critical, optimal, secured and very secured (table I).

TABLE I. THE SET OF MEMBERSHIP FUNCTIONS

Input 1	Range (°C)	Fuzzy Set Label
Temperature difference (T_{dif})	0-5	Very critical
	0-10	critical
	5-15	optimal
	10-20	Secured
	15-20	Very secured

$$\mu_{Very\ Critical}(x) = \begin{cases} 1, & x < 0 \\ 1 - (\frac{x}{5}), & 0 \leq x \leq 5 \end{cases}$$

$$\mu_{Critical}(x) = \begin{cases} x/5, & 0 \leq x \leq 5 \\ 2 - (\frac{x}{5}), & 5 \leq x \leq 10 \end{cases}$$

$$\mu_{Optimal}(x) = \begin{cases} (x/5) - 1, & 5 \leq x \leq 10 \\ 3 - (\frac{x}{5}), & 10 \leq x \leq 15 \end{cases} \quad (5)$$

$$\mu_{Secured}(x) = \begin{cases} (x/5) - 2, & 10 \leq x \leq 15 \\ 4 - (\frac{x}{5}), & 15 \leq x \leq 20 \end{cases}$$

$$\mu_{Very\ Secured}(x) = \begin{cases} (x/5) - 4, & 15 \leq x \leq 20 \\ 1, & x > 20 \end{cases}$$

Fig. 4 presents the input space of the first Input that represent the Temperature difference.

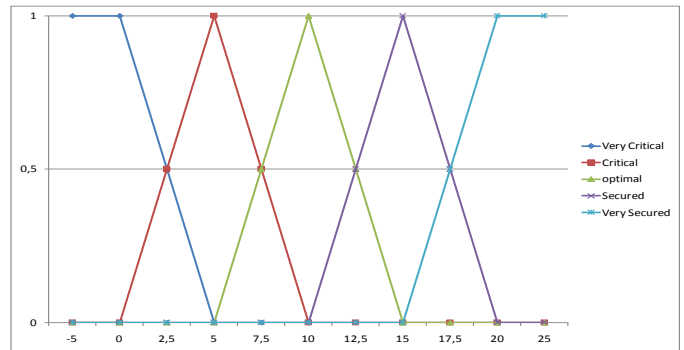


Fig. 4. The input space of temperature difference

Input 2: The temperature difference variation ($\frac{dT_{dif}}{dt}$)

The variation in the temperature difference is represented by four membership functions: very slow, slow, normal, fast and very fast (table II) and Fig. 5 presents the input space of the second Input that represent the variation in the temperature difference.

TABLE II. THE SET OF MEMBERSHIP FUNCTIONS

Input 2	Range (°C/s)	Fuzzy set
Variation in the temperature difference ($\frac{dT_{dif}}{dt}$)	0-0.5	Very slow
	0-1	slow
	0.5-1.5	normal
	1-2	fast
	1.5-2	Very fast

$$\mu_{\text{Very Slow}}(x) = \begin{cases} 1, & x < 0 \\ 1 - \left(\frac{x}{0.5}\right), & 0 \leq x \leq 0.5 \end{cases}$$

$$\mu_{\text{Slow}}(x) = \begin{cases} x/0.5, & 0 \leq x \leq 0.5 \\ 2 - 2x, & 0.5 \leq x \leq 1 \end{cases}$$

$$\mu_{\text{Normal}}(x) = \begin{cases} 2x - 1, & 0.5 \leq x \leq 1 \\ 3 - 2x, & 1 \leq x \leq 1.5 \end{cases}$$

$$\mu_{\text{Fast}}(x) = \begin{cases} 2x - 2, & 1 \leq x \leq 1.5 \\ 4 - 2x, & 1.5 \leq x \leq 2 \end{cases}$$

$$\mu_{\text{Very Fast}}(x) = \begin{cases} 2x - 3, & 1.5 \leq x \leq 2 \\ 1, & x > 2 \end{cases}$$

(6)

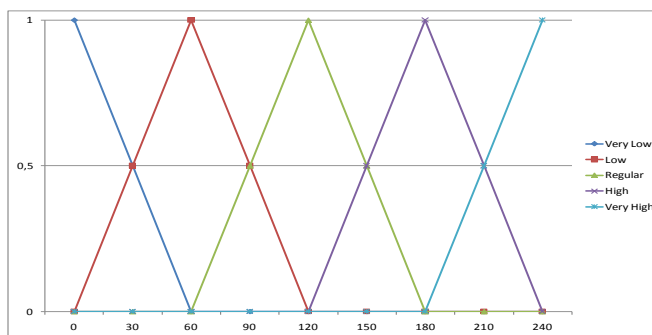


Fig. 6. The output space that represents the supply power

B. Fuzzy Rules Base

The implemented controller has two inputs, each one of them has five membership functions that cover the variation range of inputs. Therefore, the fuzzy rules base is 5x5 matrix that represent the output state of each fuzzy rule (table IV).

TABLE IV. THE FUZZY RULES OF THE FLC

	Inputs		Output
	ΔT_{dif}	$\frac{dT_{dif}}{dt}$	Supply signal
1	very critical	very slow	Very high
2	very critical	slow	Very high
3	very critical	normal	Very high
4	very critical	fast	high
5	very critical	very fast	regular
6	critical	very slow	Very high
7	critical	slow	Very high
8	critical	normal	high
9	critical	fast	regular
10	critical	very fast	low
11	optimal	very slow	Very high
12	optimal	slow	high
13	optimal	normal	regular
14	optimal	fast	low
15	optimal	very fast	Very low
16	secured	very slow	High
17	secured	slow	Regular
18	secured	normal	Low
19	secured	fast	Very low
20	secured	very fast	Very low
21	very secured	very slow	Regular
22	very secured	slow	Low
23	very secured	normal	Very low
24	very secured	fast	Very low
25	very secured	very fast	Very low

IV. THE IMPLEMENTATION OF THE INTELLIGENT FUZZY LOGIC CONTROLLER

The main objective of this work is to preserve the continuous operation of the electrical cells by consuming very less power. According to the experts, the humidity is the principal factor that can shut down the electrical cells

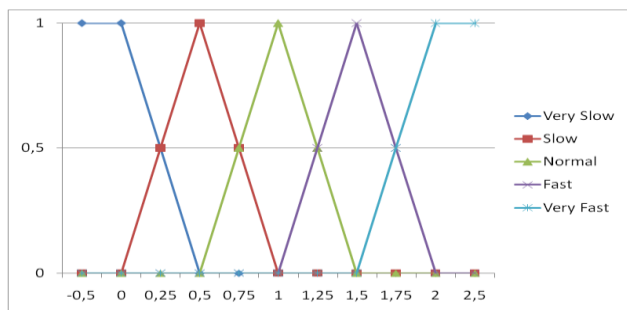


Fig. 5. The input space of the variation in the temperature difference

• Output Variable: Supply signal

The supply signal is an AC voltage applied to the heating resistor to provide adequate power to prevent condensation of moisture. The output membership function space is represented by using five membership functions: very low, low, regular, high, and very high (table III). Fig. 6 presents the output space that represents the supply power.

TABLE III. THE SET OF MEMBERSHIP FUNCTIONS

Output	Range (Volt)	Fuzzy set
Supply signal (V)	0-60	very low
	60-120	low
	120-180	regular
	180-240	high
	180-240	Very high

$$\mu_{\text{Very Low}}(x) = \begin{cases} 1 - \left(\frac{x}{60}\right), & 0 \leq x \leq 60 \end{cases}$$

$$\mu_{\text{Low}}(x) = \begin{cases} x/60, & 0 \leq x \leq 60 \\ 2 - x/60, & 60 \leq x \leq 120 \end{cases}$$

$$\mu_{\text{Regular}}(x) = \begin{cases} \left(\frac{x}{60}\right) - 1, & 60 \leq x \leq 120 \\ 3 - \left(\frac{x}{60}\right), & 120 \leq x \leq 180 \end{cases}$$

$$\mu_{\text{High}}(x) = \begin{cases} \left(\frac{x}{60}\right) - 2, & 120 \leq x \leq 180 \\ 4 - \left(\frac{x}{60}\right), & 180 \leq x \leq 240 \end{cases}$$

$$\mu_{\text{Very High}}(x) = \left\{ \left(\frac{x}{60}\right) - 3, 180 \leq x \leq 240 \right.$$

(7)

operation. For this reason a permanent control of the inside humidity is highly needed. In real case, the humidity is reduced by a heating resistances installed in the electrical cells. The feeding signal of these resistances is controlled by an On/Off controller to keep the indoor temperature within the safe range, the used controller can adjust the indoor temperature and avoid probable moisture risks but in the same time consuming an important amount of energy who represents a supplementary charge for the company expenses. For that reason, the On/Off controller should be substitute with another controller who can follow the state of the controlled plant and predicts suitable output without wasting the electrical energy. The intelligent FLC used in this piece of work was proposed by Hector et.al [10] as new methodology of self-organizing FLC able to adapt online its own parameters using only some qualitative information. The following sections describe the methodology of this intelligent FLC.

Before starting the description of the methodology of the intelligent controller, the immense tools that bring this controller must be mentioned:

- The mathematical model of the controlled plant is not required at all; also, the differential equations are not necessary.
- The intelligent FLC initiates the control of the plant with no rule base or by allocating arbitrary values.
- The intelligent FLC is very robust against disturbances, i.e., its able to adjudicate the new state imposed by the disturbance and compensate their negative effects on the control process.

Thus, to initiate a control process, the controlled plant should be described mathematically by an equivalent model. Generally, a common model of controlled plant can be presented like:

$$g(l + \tau) = f(g(l), \dots, g(l - \alpha), v(l), \dots, v(l - \beta)) \quad (8)$$

where τ is the delay of the controller system and f is an unknown continuous and derivable function. The time delay is considered as a determinist factor to achieve the maximum performance in the majority of the engineering process, for example: electrical distribution applications, signals processing, etc. The dilemma of the crucial role of the time delay was very well documented over the last decade [10], [11], [12], and [13]. In order to use the intelligent FLC, the controlled process should have an adequate delay time and the plant should be continuous and presents a constant monotonicity, i.e. the relation between the controlled process and the controller output has the same sign. The Intelligent FLC is based essentially on adapting the fuzzy rules. Throughout two stages of self-adaptation the controller can adjust en reel time their own parameters to follow the reel need of the plant and to predict the convenient output. The only information used from the system is its monotonicity sign and its delay to perform a coarse adaptation of the fuzzy rules (consequents adaptation and antecedents adaptation).

For the consequents adaptation, the evaluation of the current state of the plant leads to impose a correction of the rules responsible for the actual state of the plant. The sense of the imposed correction is deduced from the monotonicity of the plant as reward or penalty. Equation (9) presents the expression of the proposed correction:

$$\Delta S_{j_1 j_2 \dots j_N}(l) = Q \cdot \gamma_{j_1 j_2 \dots j_N}(l - \lambda) \cdot e_g(l) \quad (9)$$

$$Q \cdot \gamma_{j_1 j_2 \dots j_N}(l - \lambda) \cdot (s(l - \lambda) - g(l))$$

where $\gamma_{j_1 j_2 \dots j_N}$ is the strength or α -level of rule $S_{j_1 j_2 \dots j_N}$
 $e_g(l)$ is the error at instant l .

The Q coefficient is an absolute value that should be computed offline, where: $|Q| = \Delta u / \Delta g$.

Δg represents the output space of the controlled plant and Δu is the operation interval of the actuator.

In [13], the evaluation of the proposed modification is done at the instant l using proportionally the activation degree of the rule responsible of the plant output $u(l-\lambda)$ at the instant $(l-\lambda)$. It's very important to highlight here that if $s(l-\lambda)$ was used instead $s(l)$ it would be wrong because at the instant $l-\lambda$ a set of rules was activated to achieve the set point $s(l-\lambda)$ not $s(l)$.

As it is mentioned above, the intelligent FLC starts the adjustment of their internal parameters through adapting the consequents of the rules by applying rewards or penalties. After that, its tackles the second step through the re-organization of the membership functions in the inputs spaces to equilibrate the accumulated error that results from the adaptation process. Hence, the new rules antecedents will represent more faithfully the actual state of the controlled system.

In order to establish a balanced input space regarding the accumulated error during the first stage of learning process, the intelligent FLC incorporates an autonomous tools that can ensure the equilibrium on the registered error over different areas of the input spaces by redistributing the membership functions to make the areas with an important error accumulation covered by more membership functions so as to compensate it. Since, the area with an important accumulation of error is the most activated area during the control process. Hence, it should be well expressed by enough membership functions. The criterion that represents the accumulated error is the Integral of squared error and it's calculated by as follow:

$$ISE_i^j = \frac{1}{\sigma_y^2} \left(\int e^2(t) dt \Big|_{z_i(t) \in [p_i^{j-1}, p_i^j]} - \int e^2(t) dt \Big|_{z_i(t) \in [p_i^j, p_i^{j+1}]} \right) \quad (10)$$

In the aforementioned expression, $z_i(t)$ represents the input while p_i represents the j -th membership function center and σ_y^2 is a normalization factor that represents the variance of the

plant output. The two integrals calculate the error in two cases, the first one in the case when the input is between $(j-1)$ and j centers and the second one in the case when the input is between j and $(j+1)$ centers. It's to note here that the system is discrete that's mean the integral can be expressed as a sum, so the equation can be simplified. The result of this sum can precise in which side the center of the membership function should be moved, hence, when the sum is positive, that means the error in the right was smaller than in the left. Therefore, the center has to be moved to the left to minimize the accumulated error in this area. Otherwise, when the sum is negative the center should be moved to the right. This displacement of membership functions centers should not affect their original order. The displacement of the membership function centers is ensured by the following expression:

$$\Delta p^j = \begin{cases} \frac{p^{j-1} - p^j}{2} \frac{ISE^j}{ISE^j + \frac{1}{S^j}}, & \text{if } ISE^j \geq 0 \\ \frac{p^{j+1} - p^j}{2} \frac{|ISE^j|}{|ISE^j| + \frac{1}{S^j}}, & \text{if } ISE^j < 0 \end{cases} \quad (11)$$

where, the distance that can a center of a membership function be moved on without over passing the permitted limits is expressed by S^j . Therefore, big value of S^j implies an important displacement of the membership function center and small value of S^j implies a short displacement of this centre. The sum of the accumulated error will be computed during an enough predefined time T and the intelligent controller starts the operation with a big value of S^j to ensure an important displacement of the centers over the inputs spaces, the initial value of S^j will be exponentially decreased by time. The learning process of the intelligent controller starts until the second run. Hence, at the first run the controller proceed to tune their rules consequents and the ISE is not calculated yet. The end of the second run brings the modification of the emplacements of the membership functions centers. So, at the upcoming time T the controller will not compute the ISE and will proceed to re-tune their rules consequents according to the new centers emplacement. For every time the controller needs to compute a new ISE it will use a S^j value smaller than the value used previously.

V. THE RESULTS OF THE HUMIDITY CONTROL PROCESS

The goal of these papers is not only the presentation of a control algorithm able to replace the On/Off method used actual inside the electric cells to avoid high levels of moisture that provokes serious damage on the electrical devices and power failures. But, the main goal was the limitation of wastage of energy during the humidity control process. Since, the dew point inside the cells is avoided by implementing a set of heating resistances that need an important amount of electrical energy to heat the internal surroundings. These latter don't need a high control precision to ensure the desired conditions.

Therefore, there are a lot of used controllers that can guaranty these criterions but not the limitation of wastage of energy. For this reason the use of the Intelligent FLC

previously presented is proposed. The Intelligent FLC is a powerful control algorithm that presents several interesting control quality like: High precision, robustness against perturbation and low power consumption during the control process [14].

To present the valuable contribution that brings the intelligent controller on the energy consumption while controlling the humidity inside the electric cells we proceed to present the obtained results of different control process using firstly the On/Off controller actually used by the electricity distribution company. Secondly, a conventional Fuzzy Logic Controller (FLC) will be used in the same control process to make out the control performances regarding the energy consumption and finally the intelligent FLC will be implemented under the same conditions as the beforehand mentioned control processes. So that, we can easily highlight the effects of each one of the used controllers on the energy consumption to precise the most effective one. Table V presents the real consumption of the heating resistances installed inside the electric cells using the On/Off controller. It's to note here that the electric cells situated to close to the sea need more powerful resistances than other cells.

TABLE V. THE DETAILS OF REAL CONSUMPTION OF THE HEATING RESISTANCES USING THE ON/OFF CONTROLLER

	Power of the heating resistance in Watt	Number of resistances	Daily consumption in KWh	Annual consumption in KWh
Close to the sea	50	3	3,6	1.314
Far from the sea	100	3	7,2	2.628

Fig. 7 presents the evolution of the supply signal regarding the temperature inside the electric cell using the On/Off controller. This kind of controller starts the control process using the maximum of power feeding and keeps the supply signal constant until reaching the desired point. Therefore, the sum of the power consumed during this period will be very important.

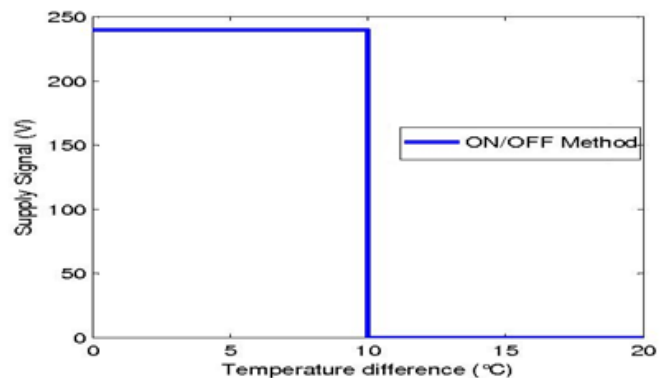


Fig. 7. The evolution of the supply signal regarding the temperature inside the electric cell using the On/Off controller

Trying to improve the control process performances vis-a-vis the power consumption, a conventional FLC was used and

the obtained results show that the energy balance of the control process can be improved with a significant gain in electrical energy. Fig. 8 presents the evolution of the supply signal regarding the temperature inside the electric cell using the conventional FLC versus the On/Off controller.

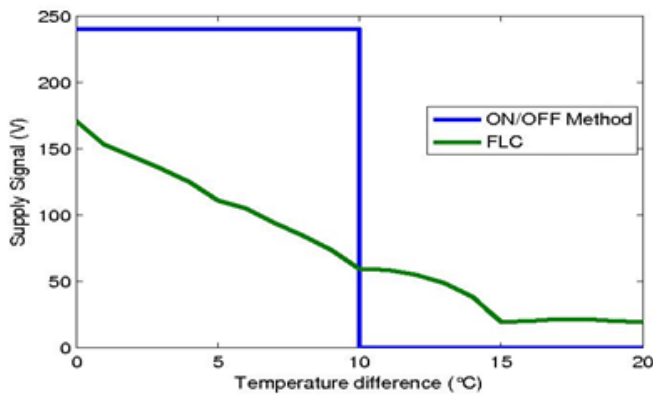


Fig. 8. The evolution of the supply signal regarding the temperature inside the electric cell using the conventional FLC versus the On/Off controller

The above figure can explain clearly that unlike the On/Off controller, the conventional FLC starts the control with a relatively small voltage and decreases this value proportionally with the registered temperature until achieving the desired temperature then the power supply will be stabilized even if the inside temperature is upper that the dew point. This operating mode generates relatively low power consumption over the time. Since, the FLC doesn't use the maximum voltage and decrease the used power by time. Hence, the sum of the power consumed during the control process will be reasonable compared to the On/Off controller.

As it's mentioned above, the control of the humidity inside the electric cells doesn't need high control precision. Nevertheless, another criterion plays a fundamental role in this control process. The challenge faced on during this process is the power consumed. Starting from the fact that the energy production has an important and direct impact on the environment - the majority of the electrical energy consumed comes from polluting sources - we are strongly concerned about how can we reduce and the optimize of our electrical energy needs. In this control process, the Intelligent FLC used has been able to carry out a very precise control process with an amazing energy balance. Fig. 8 describes the evolution of the supply signal regarding the temperature inside the electric cell using the intelligent FLC versus the remaining used controllers.

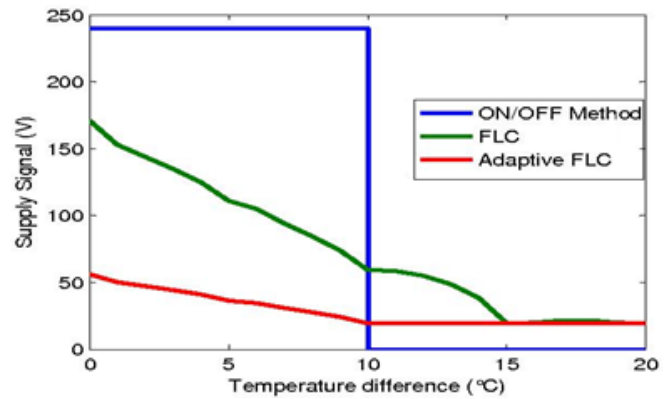


Fig. 9. The evolution of the supply signal regarding the temperature inside the electric cell using the Intelligent FLC versus the remaining used controllers

The Intelligent FLC starts the control by generating a moderated supply signal to ensure the temperature increase until reaching the safe value then the supply signal will be stabilized. Generally, the needed power to ensure this control process is very lower than the power needed using the remaining controllers. Since, the intelligent FLC begin with a smaller voltage and decreases it by the time until the stabilization at a small voltage keeping the heating resistances powered permanently. This advantage serve to optimize the energy needed to restart the heating process without requiring too much energy as in the On/Off controller and better than the conventional FLC. Table VI presents the real consumption of the heating resistances installed inside the electric cells using the On/Off controller, the conventional FLC and the Intelligent FLC.

TABLE VI. THE REAL CONSUMPTION OF THE HEATING RESISTANCES USING DIFFERENT CONTROLLER

	On/Off		FLC		Intelligent FLC	
	Close to the sea	Far from the sea	Close to the sea	Far from the sea	Close to the sea	Far from the sea
Daily consumption in KWh	3,6	7,2	3,2	6,9	2,7	6,7
Annual consumption in KWh	1.314	2.628	1.168	2.518	985	2.445

The daily and annual energy consumption of the three used controllers illustrates the efficiency of the Intelligent FLC in

terms of energy saving. The use of this latter can guarantee the saving of an important amount of the energy consumed by the resistances using the On/Off controller. Knowing that in the electrical distribution network, thousands of electric cells are installed. The sum of the energy saved in each one will be a huge gain in terms of energy and money.

VI. CONCLUSION

Nowadays, the energy and the climate changes represent an extremely important issue for the whole world. Since, the energy production usually comes from processes that affect the environment. For that, the energy saving has become the centre of interest in several research areas. This work pretend to present a new idea to reduce the energy consumption over the huge electrical power distribution networks by reducing the important energy consumed while protecting thousands of electric cells from the damage caused by the moisture. Actually the controller used to control the heating resistances installed inside the electric cells is an On/Off controller that can ensure the ideal temperature to protect the cells from moisture, but with an important waste of energy. The Intelligent Fuzzy Logic Controller that we propose to use has demonstrated that can be a very suitable alternative to protect the cells and in the same time ensure an important reduction in the power consumption that can be reflected in the electric bills. Thus, the environmental cost of energy production will be on the wane. The presented results illustrate the effectiveness of this controller compared with the On/Off controller and even the conventional FLC.

REFERENCES

- [1] B. Khalil, J. Adamowski, A. Shabbir, C. Jang, M. Rojas, K. Reilly Bogdan, Ozga-Zielinski, "A review: dew water collection from adiative passive collectors to recent developments of active collectors: Sustain". *Water Resour. Manag*, Vol.2, pp. 71–86, 2016.
- [2] O. O. Adeoye, L. E. Shephard, M. Wright, Moses West, Stacy Peters, "Atmospheric Water Generation: A Path to Net-Zero", 2016 IEEE Green Technologies Conference, pp. 45-50, April 2016.
- [3] Maisarah Ali et al., "Hygrothermal Performance of Building Envelopes in the Tropics Under Operative Conditions: Condensation and Mould Growth Risk Appraisal", *Jurnal Teknologi (Sciences & Engineering)* 87:5, pp.271-279, 2016.
- [4] Milton Ohring, Lucian Kasprzak, "Reliability and Failure of Electronic Materials and Devices", / Chapter 7, 2nd Edition Elsevier, ISBN-9780120885749.
- [5] Kallias, AN, Imam, B and Chryssanthopoulos, MK, "Performance profiles of metallic bridges subject to coating degradation and atmospheric corrosion", *Structure and Infrastructure Engineering: maintenance, management, lifecycle design and performance*, 2016.
- [6] Tony Byrne, "Humidity effects in substations", 2014 Petroleum and Chemical Industry Conference Europe, p. 1-10, June 2014.
- [7] Baghban, A, Bahadori, M, Rozyn, J, Lee, M, Abbas, A, Bahadori, A and Rahimali, A, "Estimation of air dew point temperature using computational intelligence schemes", *Applied Thermal Engineering*, vol. 93, pp. 1043-1052, 2015.
- [8] Kasra Mohammadi et.al. "Using ANFIS for selection of more relevant parameters to predict dew point temperature", *Applied Thermal Engineering*, Vol. 96, pp. 311–319, 2016.
- [9] Jinbo Zhang, Tongguang Shao, Yu Wang, Jing Wang, "A New Type of Dehumidifier for Enclosed High-voltage Switchgear Cabinet", *TELKOMNIKA*, Vol. 10, No. 7, November 2012.
- [10] H. Pomares, I. Rojas, J. González, F. Rojas, M. Damas and F. J. Fernández "A two-stage approach to selflearning direct fuzzy controllers," *International Journal of Approximate Reasoning*, Vol. 29, Issue 3, pp. 267-289, 2002.
- [11] I. Rojas, H. Pomares, F.J. Pelayo, M. Anguita, E. Ros, A. Prieto, "New methodology for the development of adaptive and self-learning fuzzy controllers in real time," *International Journal of Approximate Reasoning*, vol. 21, pp. 109-136, 1999.
- [12] Chen Peng, Li-Yan Wen, and Ji-Quan Yang, "On Delaydependent Robust Stability Criteria for Uncertain T-S Fuzzy Systems with Interval Time-varying Delay," *International Journal of Fuzzy Systems*, Vol. 13, No. 1, Mar 2011.
- [13] A. Boulkroune, M. M'Saad, M. Farza, "Adaptive fuzzy controller for multivariable nonlinear state time-varying delay systems subject to input nonlinearities," *Fuzzy sets and systems*, Vol. 164, No. 1, pp. 45- 65, Feb 2011.
- [14] R. Lasri, I. Rojas, H. Pomares and O. Valenzuela, "Innovative Strategy to Improve Precision and to Save Power of a Real-Time Control Process Using an Online Adaptive Fuzzy Logic Controller," *Advances in Fuzzy Systems*, Vol. 2013, pp. 16, Article ID 658145.

Representing Job Scheduling for Volunteer Grid Environment using Online Container Stowage

Saddaf Rubab¹, Mohd Fadzil Hassan², Ahmad Kamil Mahmood³, and Syed Nasir Mehmood Shah⁴

^{1,2,3,4}Department of Computer and Information Sciences, University Teknologi PETRONAS, Bandar Seri Iskandar, 32610, Tronoh, Perak, Malaysia

Abstract—Volunteer grid computing comprises of volunteer resources which are unpredictable in nature and as such the scheduling of jobs among these resources could be very uncertain. It is also difficult to ensure the successful completion of submitted jobs on volunteer resources as these resources may opt to withdraw from the grid system anytime or there might be a resource failure, which requires job reassignments. However, a careful consideration of future jobs can make scheduling of jobs more reliable on volunteer resources. There are two possibilities; either to forecast the future jobs or to forecast the resource availability by studying the history events. In this paper an attempt has been made to utilize the future job forecasting in improving the job scheduling experience with volunteer grid resources. A scheduling approach is proposed that uses container stowage to allocate the volunteer grid resources based on the jobs submitted. The proposed scheduling approach optimizes the number of resources actively used. The approach presents online container stowage adaptability for scheduling jobs using volunteer grid resources. The performance has been evaluated by making comparison to other scheduling algorithms adopted in volunteer grid. The simulation results have shown that the proposed approach performs better in terms of average turnaround and waiting time in comparison with existing scheduling algorithms. The job load forecast also reduced the number of job reassignments.

Keywords—Volunteer grid computing; volunteer resources; container stowage; job scheduling

I. INTRODUCTION

Volunteer grid computing environment is a type of grid consisting of volunteered resources which are distributed and heterogeneous in nature [1]. The volunteer grid is growing day by day as more number of resources is volunteered for high computational research projects. The ‘World Community Grid’ is a large-scale volunteer computing project supported by IBM [2]. The statistics for number of resources and research projects running under it is shown in Fig. 1.

The resources and jobs submitted to a volunteer grid are unpredictable which affects the performance of volunteer grid and makes resource management more challenging. It is therefore difficult to schedule the jobs as the future job rate and resource availability cannot be anticipated.

The jobs submitted to Volunteer Grid (VG) may vary in terms of requirements and load. The job requirements change due to the nature of tasks to be performed and sometimes based on the time of the day job has been submitted. There might be a few jobs submitted to volunteer grid repeatedly. These repeated jobs may have random load and resource requirements on each job submission. It is hard to forecast the resource demands. There have been studies [3-5] which suggest to allocate a few extra resources to complete a job in VG.

However, it is not an efficient way to over-provision the resources because it will leave the allocated resources as under-utilized. This underutilization of resources is negating the objective of VG to maximize the utilization of allocated resources.



Fig. 1. World Community Grid Volunteer Statistics [2]

Job migration allows a job to be transferred from one resource to another without causing any interruption in job execution. Job migration can help to balance the load and to transfer a job from underutilized resource to another one for achieving VG maximum resource utilization objective where the job can also complete within the specified deadline.

For example, when most of the jobs running on one resource and there is a possibility that a few jobs can miss their deadlines, those jobs can be transferred to other available resources which can complete the jobs within their specified deadlines.

In contrast, when jobs are being executed on a resource which is underutilized, the overall performance of resource is getting low, the jobs can be transferred to other resources which can complete the jobs within deadline and free the underutilized resources. This will not only help to maximize the resource utilization of new resource but also help to free the previous resource for other large job executions. There are practices of migrating jobs to improve the turnaround time of jobs [6-8]. The work presented in [6], proposed a job scheduling strategy which includes history events to make possible a job scheduling scheme which results in fewer job migrations and improve the turnaround time as well. Various job migration strategies are presented in [7], for migrating the unfinished jobs that are delayed or halted on any node.

The job scheduling and resource allocation problem can be demonstrated as container stowage problem where each job is considered as a container and resource as a ship or terminal to pack the containers. Container stowage itself is NP-Hard problem, which requires stowing the containers in vessels or ships in order to reduce the operating costs and deliver the containers at their destination within the budgetary values and time [9, 10]. Container stowage is illustrated in Fig. 2.

The containers are to be stowed to a ship which can deliver the containers to destination within the time and operational cost. A container can only be stowed to one ship at a time whereas many containers can be stowed to one ship. This can depict the job scheduling, as illustrated in Fig. 3. A job can be assigned to one resource at a time and a resource can be allocated to more than one job considering the time and cost constraints associated with the jobs and resources.

In this paper, a job scheduling approach has been presented that uses online container stowage to allocate the volunteer grid resources dynamically based on the job requirements. The proposed approach will also optimize the number of resources used in terms of using the allocated resources to their maximum instead of using excessive resources. The main contributions of this work are:

- To develop an online container stowage job scheduling algorithm that is able to avoid the overloading of resources while ensuring the maximum utilization
- A theoretical proof for optimal value of number of resources in use
- Simulation results to compare with existing job scheduling approaches

The outline of this paper is as follows. Section II describes a literature studied on job scheduling in volunteer grid computing and job reassignments. Section III gives a broad overview of job scheduling approach whereas Section IV focusing mainly on the proposed job scheduling algorithm. The results and simulations are discussed in Section V. Section VI concludes the paper giving the future research direction.

II. RELATED LITERATURE

This section will give a brief literature review on the job scheduling in volunteer grid which not only will outlines the practices of job scheduling but also the issues, challenges and methods on job reassignment.

Due to the growing use of distributed computing resources, the jobs scheduling becomes an important issue to be studied. Therefore, the job scheduling in volunteer grid has been studied vastly in the literature. A survey [11] has been presented on grid resource management systems, mainly discussing the grid schedulers such as Condor, AppLes, Globus and Nimrod which use batch scheduling heuristics. Few of the scheduling algorithms for volunteer grid are discussed and compared under different input conditions applied using simulation [12].

A 39-days trace of computer availability of 32 machines located in two classrooms has been collected in [13]. These traces were used for scheduling techniques analysis to improve average turnaround time in volunteer grid environment. A tool, named DGSchedSim [14] has also been presented later on to evaluate different other volunteer grid scheduling algorithms using the collected traces by [13].

A stochastic modeling based job scheduler was presented in [15]. A job scheduling architecture using performance prediction was proposed in [11], using the neural network that focuses on local job scheduling on volunteer grid resources. Cost based online job scheduling algorithm is presented by Weng et al. [18]. They have compared the performance of proposed online algorithm with the optimal offline algorithm.

The job scheduling performance in volunteer grid environment can be affected because of resource failure or resource withdrawn. These can be avoided by migrating or reassigning jobs to other available resources [6-8].

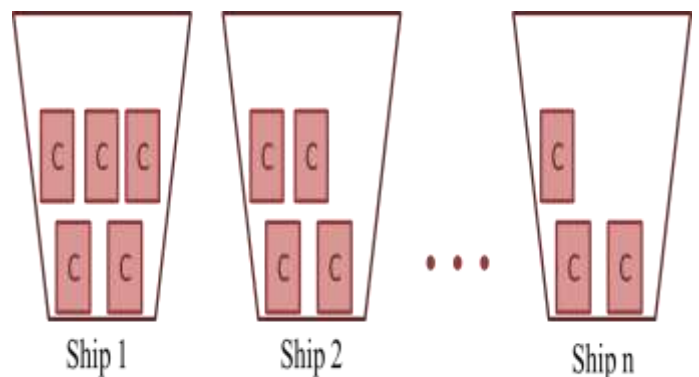


Fig. 2. Illustration of Container Stowage Problem

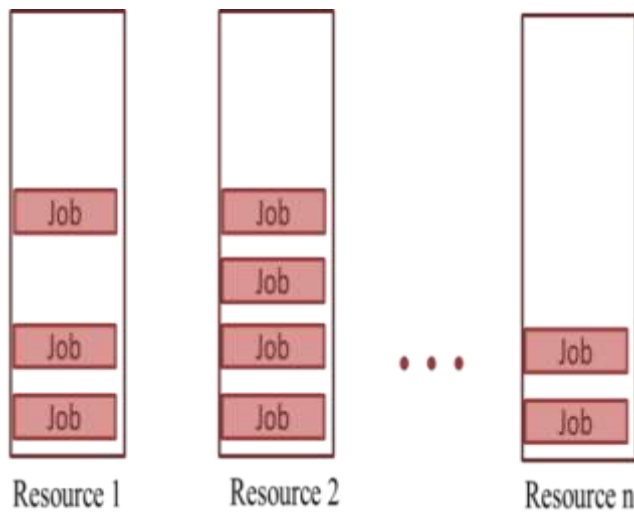


Fig. 3. Illustration of Job Scheduling

A job scheduling strategy based on neural network load predictions was proposed in [6] that reassigns the jobs from current resource to another available volunteer resource. Different job scheduling strategies including migration adaptive, wave migration and immediate migration were presented to get better turnaround time for job scheduling using volunteer grid resources [7]. The adaptive scheduling was used by Zhou et al. [7] to reassign the delayed jobs from current nodes to less load classified as night nodes. Most of the job scheduling algorithms and strategies reviewed in this section are greedy and offline algorithms.

The change in volunteer grid environment is mainly due to the resource availability and failure, which is the prime reason for reassignment of jobs. Job scheduling in volunteer grid computing environment can mimic the container stowage problem where the containers need to be stowed in ships and vessels while meeting their time and budgetary constraints. Container stowage problem has been tried to solve by using genetic algorithms, combinatorial optimization and heuristics etc. [9, 10].

Considering this fact, a job scheduling scheme is proposed in this paper which is adaptive in nature and based on container stowage problem concepts. The proposed job scheduling will also use the load prediction/forecast to improve the average turnaround time for scheduling using volunteer resources.

III. OVERVIEW OF PROPOSED JOB SCHEDULING APPROACH

The proposed scheduling approach consists of a job scheduler which can schedule the jobs optimally to complete the submitted jobs within the deadline. The job scheduler is the one responsible for running proposed scheduling algorithm. The volunteer resources will run the submitted and assigned jobs to them individually.

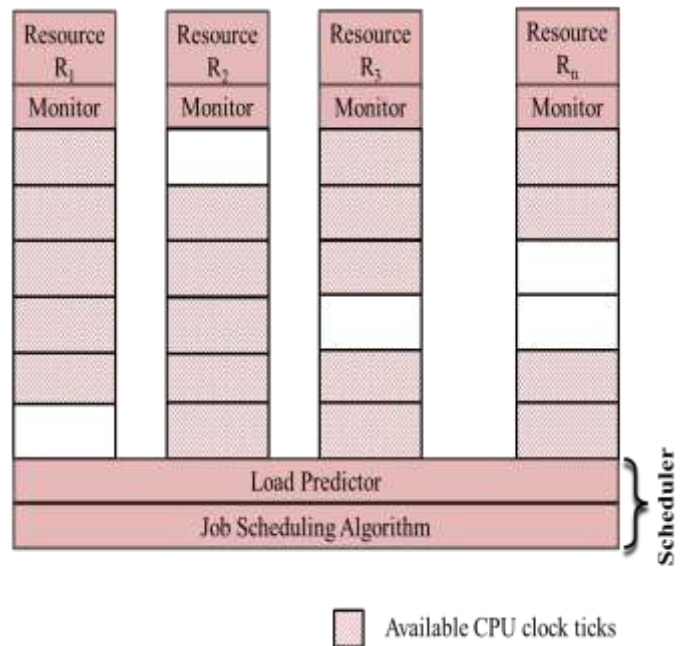


Fig. 4. Scheduling Approach

Each of the resource can have different availability times, which illustrates that there can be availability time intervals which can be further sub-divided to fit in more jobs. In such a case multiple jobs can share one resource. The resource monitor attached with each resource will collect the usage information in terms of availability time which means that for how many CPU clock ticks a resource can serve a job and how many available CPU clock ticks are still unassigned with the resource for more jobs. This usage information will be used by scheduler, which is responsible for overall job scheduling. The scheduler required the following three (03) inputs:

- resource demand history of jobs
- capacity and load history of resource
- current allocation of resources to jobs

The scheduler has two main components as well. The load predictor (LP), that is responsible for predicting the resource demands in near future. The second component of scheduler is the proposed scheduling algorithm itself, which can optimally schedule the jobs such that the jobs are completed within the deadline specified and the currently assigned resources are utilized maximum. The overview of job scheduling approach is presented in Fig. 4. The scheduler will be periodically called after a fixed number of CPU clock ticks to see if there is any new job arrived or relocation of job is required. In each of scheduler call, the load predictor will predict the resource demands of new submitted jobs and resource load based on usage information. The prediction results will be represented as CPU clock ticks i.e., the required number of CPU cycles for job and unassigned available CPU cycles.

After the load predictor, the predictions results will be passed to scheduling algorithm to find that there are enough resources available to assign more jobs and to execute the already assigned jobs. If the resources can complete the already assigned jobs and new jobs, the resource allocation will be done locally. In other case, the overload mechanism will be performed.

The scheduling algorithm also reschedules the running jobs from underutilized resources to the nearly optimal maximum utilized resource in order to free the underutilized resource for future jobs which may require more CPU clock ticks and help to use the maximum of resource. The scheduling algorithm will then generate an allocation/re-allocation list (AR list) and pass it to resource monitor to start the job execution on allocated resources. The scheduling approach makes use of live reallocation of jobs, which is itself incurring an overhead but the overall scheduling performance can be improved because the overhead is very negligible.

To analyze the load prediction, in each set of jobs e.g., 250 jobs, the first set of jobs is restricted to 10 jobs and next set is considered as predicted jobs. This scheme can be followed for all the job sets as these are multiples of 10. The load prediction can be done using any time series forecasting method like ARMA, ARCH, GARCH, and Holt-Winters [12-14] etc. The effect of load prediction will be discussed in Section 0

IV. JOB SCHEDULING AS CONTAINER STOWAGE PROBLEM

The container stowage planning for is a core activity of shipping and difficult to solve because of combinatorial nature of alternative mappings of containers to the stowage location in a ship or vessel [10]. Container stowage can be used to demonstrate the job scheduling where each of the resource is a ship and each job is a container to be stowed.

Extensive literature is available on the container stowage problem however those presented solutions are not feasible to apply in grid and volunteer grid environment specifically. The traditional container stowage solutions can show performance ratio approximately one which suggests having an approach to call upon the stowage planning solution after a fixed interval of time to assign and reassign the jobs. Due to the reassignment, there is a possibility of having many job migrations from one resource to another when the resource is underutilized or overloaded because the traditional scheduling algorithms does not take new jobs arriving to the system in consideration that can affect the overall system performance. These all algorithms are usually termed as offline algorithms.

The online container stowage algorithms can be a solution to reduce the number of job migrations. Although there are online container stowage algorithms, which does not take the following container details to avoid container/job migrations. A few online container stowage algorithms do not allow migration of already stowed container to a new ship/vessel location. If such an online container stowage algorithm is applied, this will be a limitation to our job scheduling approach although the volunteer grid environment allows migration of the jobs. Using the authors' experimental setup, it will be proved that job migration using online container stowage algorithm using volunteer grid resources will help to achieve nearly op-

timal results.

It must be considered that at time of job migration from one resource to another, the required CPU burst time of job might have been reduced as the job has an opportunity to utilize the current resource for its execution. This presents that a job requirement can be changed after its first assignment to the current resource. The changed job requirements compel to have an online algorithm which can accommodate not only the future jobs but also ensures the maximum utilization of resources in use and free the nearly idle resources. The scheduling algorithm proposed in this study is named as Online Container Stowage Job Scheduling (onCSJS). onCSJS illustrates the container stowage planning by ensuring the behavior of containers and ships/vessels. The ships/vessels are not allowed to stow the containers to the maximum limit as it unfavorable for the ship stability. The resources in onCSJS will mimic the same behavior by not allowing the jobs to fully utilize the volunteer resource as it will not only provides a possibility of overloading but also the migration of large number of jobs in case of resource failure.

A. Job Scheduling Algorithm

The main objective of onCSJS is to improve the job scheduling for volunteer grid environment to complete the jobs within deadline and to use maximum of the resources in use by freeing the nearly idle resources. The onCSJS is online relaxed job scheduling algorithm utilizing the concept of container stowage by not considering the new jobs when reassigning the old jobs and only a few reassignments are acceptable. The proposed algorithm onCSJS not only assign the new jobs but also perform the reassignment of old jobs currently running on volunteer resources. The job assignment to the available volunteer resources will be performed by calling assign(job) function. reassign(oldjobs, job) will be called to reassign the old jobs from current volunteer resource to new resource. During the reassignment operation the old jobs which have been executed partially on current resources will be considered as new jobs because the remaining CPU burst time are changed and will require less CPU clock ticks to complete the job. The description of algorithm will be clearer by understanding the following representations firstly in container stowage:

- Let c as a container to be stowed and $size(c)$ as the size of container, where $size(c) \in (0, 1]$
- Let sv as the ship/vessel. The $total_space(sv)$ is the total space available in a ship for container stowage and $space(sv)$ as the space available in sv ship for more containers, where $total_space(sv) \in (0, 1]$

The container stowage problem must satisfy the equation (1) such that the total space of ship/vessel sv must be greater than or equal to the total of already stowed containers and space left after stowing a new container c_i .

$$space_i(sv) + c_i \leq total_space_i(sv) \quad (1)$$

The representation of container stowage has been translated for job scheduling algorithm in volunteer grid environment.

- Let c as a job to be assigned and $size(c)$ as the size

of job, where $size(c) \in (0, 1]$

- Let sv as the resource. The $total_space(sv)$ is the total space available in a resource for scheduling job and $space(sv)$ as the space available in sv resource for more jobs to be assigned, where $total_space_{(sv) \in (0, 1]}$

The job scheduling must satisfy the equation (1) such that the total space of resource sv must be greater than or equal to the total of already assigned jobs and space left after assigning a new job c_i .

The $total_space$ of resource is translated in the range of 0 to 1, which requires classifying the jobs. Following are the four (04) classes of jobs:

- S-con: Small jobs $size(c) \in (0, 1/3]$
- M-con: Medium jobs $size(c) \in (1/3, 1/2]$
- L-con: Large jobs $size(c) \in (1/2, 2/3]$
- VL-con: Very Large jobs $size(c) \in (2/3, 1]$

The system performance can be increased if a threshold is set for the maximum resource to be utilized. In simulation test run of onCSJS, the 0.75 or 75% of the total resource available will be set as CPU clock ticks that a resource can contribute.

The volunteer resources are arranged considering the classification of jobs each of it will have the $total_space_{(sv) \in (0, 1]}$

- S-ship: Small resource
- M-ship: Medium resource
- L-ship: Large resource
- VL-ship: Very Large resource

Since the resources are heterogeneous in volunteer grid environment, a few combinations of these resource classes are also considered including SL-ship, MM-ship and ML-ship. There are some constraints to be considered while assigning or reassigning jobs to the resources. The S-ship resource can only have a few S-con jobs only. M-ship resource can be allocated to only two M-con jobs, whereas L-ship is for only two L-con job. The VL-ship can have two VL-con jobs only. SL-ship will be allocated to one L-con job and few S-con jobs. MM-ship will only have two M-con jobs. ML-ship can have one M-con job and one L-con job.

Further, there are groups formed from the S-con submitted jobs such that the group size of each is 1/3 of the total of S-con jobs submitted to be scheduled. This will help to assign the S-con jobs (small jobs) in a few steps and waiting time for these jobs will be less. It will also reduce the overhead in case of reassignment of jobs as overhead will be more for L-con or VL-con jobs in comparison with S-con jobs if require reassignment.

V. RESULTS AND SIMULATION

A. Experimental Setup

SETI@home [15] has been selected for resources and LCG1 [16, 17] dataset has been used for jobs submitted to be scheduled on volunteer resources. SETI@home project has recorded activities of 60883 nodes for a period of 10 months [15]. In SETI@home there are missing values such as zero or negative values in RAM size, null values are saved in location, null values in time zone and other components. These all null, zero and negative values were removed before starting the simulation using a pre-processing method. After pre-processing, only 38,166 nodes are having complete data. Table 1 shows population of nodes after pre-processing the missed values.

TABLE I. NUMBER OF NODES AFTER PRE-PROCESSING

Type of Nodes	Number of Nodes
Initial	60883
After pre-processing Location	38180
After pre-processing location RAM size, Time zone	38166

The LCG1 dataset contains 11 days of recorded node activities with 188,041 jobs of 53y 179d 7h 26m 46s CPU time. The details can be studied in an online published report [17]. For benchmarking only top 15 nodes activities for 5 days from processed resource dataset has been selected and total of 1000 jobs from LCG1 has been selected randomly.

B. Benchmarking of onCSJS

The performance of proposed algorithm onCSJS has been compared with EDF (Earliest Deadline First), LLF (Least Laxity First), RM (Rate Monotonic), FCFS (First Come First Serve) and RR (Round Robin) [18-20] using trace datasets available online.

C. Active Resources

In the simulation run, a resource with less than two jobs is considered as non-active. Fig. 5 shows the number of active resources during 5 days with 5 hours difference. It has been assumed in onCSJS that the active resources are those which are allocated to two or more jobs. The reason of a resource being non-active could be the reassignment of jobs or resources are idle from the start. If a resource has been assigned only one job, it will be reassigned to another active resource if can execute, and current resource will become non-active. It has been observed that if the number of jobs is less there will be less number of active resources.

On the contrary, if the number of jobs is increased preserving the same amount of resources, the number of active resources will be more.

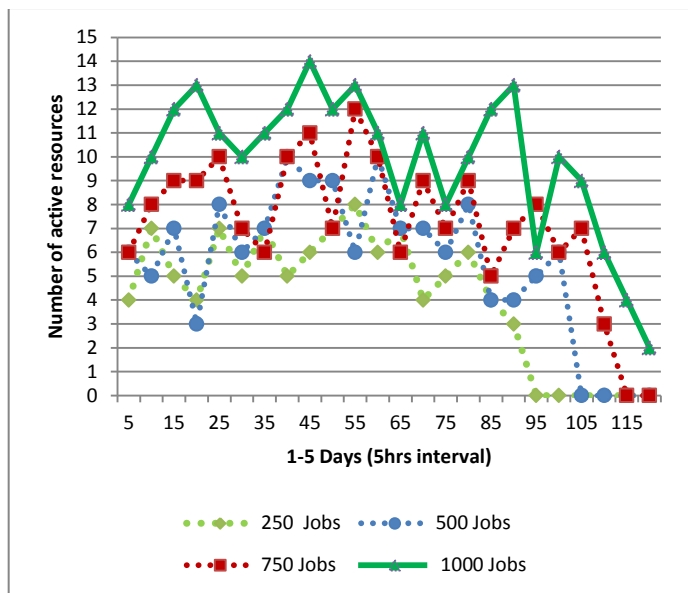


Fig. 5. Active Resources 1-5 Days

It proves our claim that active resources must be ensured that they are being used to the maximum and rest of the resources are saved for any future jobs. The scheduling algorithms chosen for benchmarking do not consider the factor of active and non-active resources; therefore, it is not a valid justification to make a comparison with the proposed algorithm.

D. Load on Active Resources

From Fig. 6, the behavior of active resources is easy to study. Fig. 3 gives more detail analysis of active resources with respect to the jobs scheduled using different algorithms. The proposed algorithm onCSJS used less number of active resources and tried to use the maximum of the active resources.

The difference will be clearer if more number of resources is used. In the simulation, only 15 volunteer resources are selected, however of the number of resources are more, the difference in number of active resources using onCSJS as compared with other scheduling algorithms will be more evident.

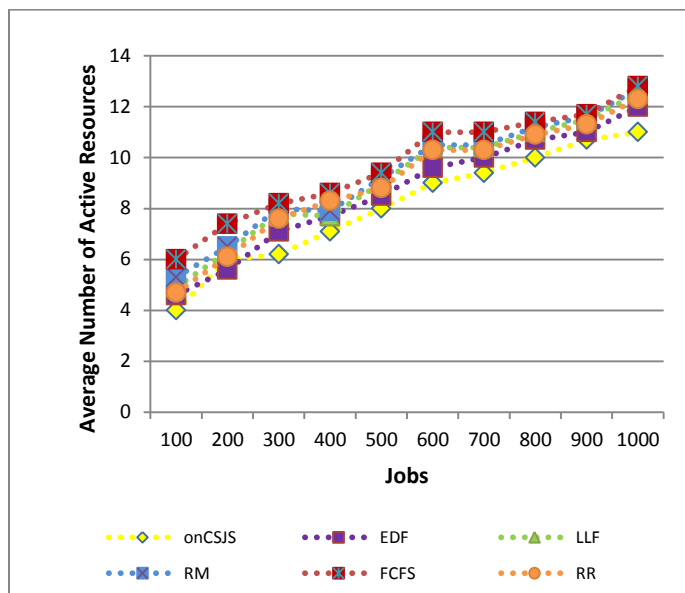


Fig. 6. Load on Active Resources

E. eassignment of Jobs

Fig. 7 presents the number of reassignments in case the job has to be migrated from one resource to another depending on the scheduling algorithm being used to test the performance. The number of reassignments is increasing as the number of jobs submitted increased. The number of job migrations is more in onCSJS as compared to the RR and RM because the proposed algorithm focuses more on the overall performance rather than on individual job runs.

F. Performance Comparisons

The performance of job scheduling algorithm can be explained briefly with the help of average waiting time and average turnaround time. The onCSJS scheduling algorithm performs better than the baseline scheduling algorithms for both the average waiting time and average turnaround time.

The average waiting time of onCSJS and baseline scheduling algorithms is presented in Fig. 8. The average waiting time of onCSJS and EDF is very close and there is a significant difference with other scheduling algorithms.

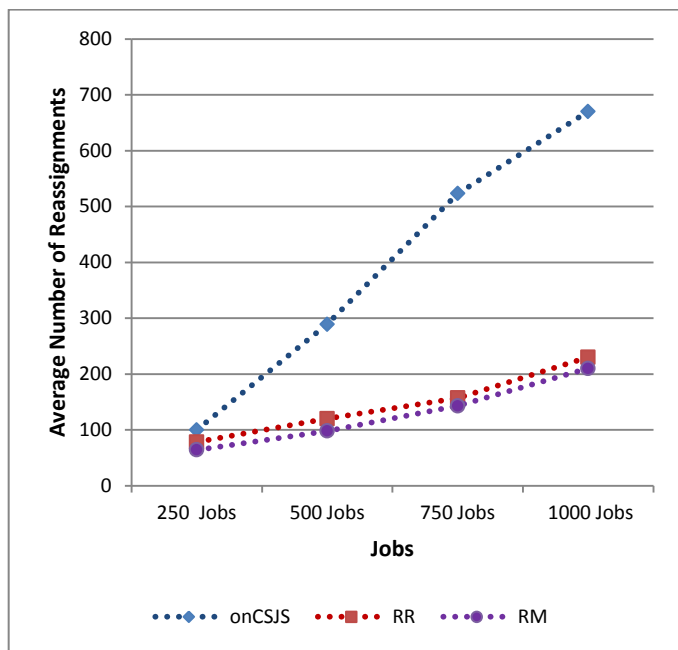


Fig. 7. Reassignments on Jobs

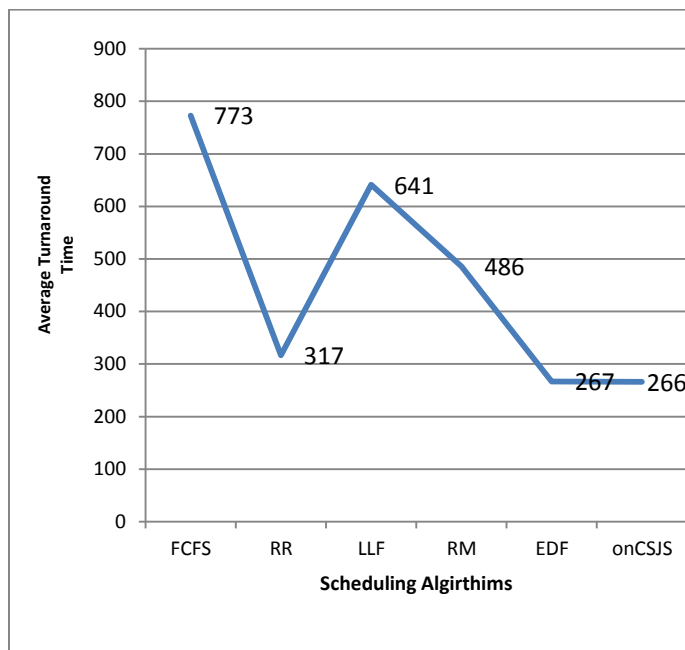


Fig. 9. Average Turnaround Time

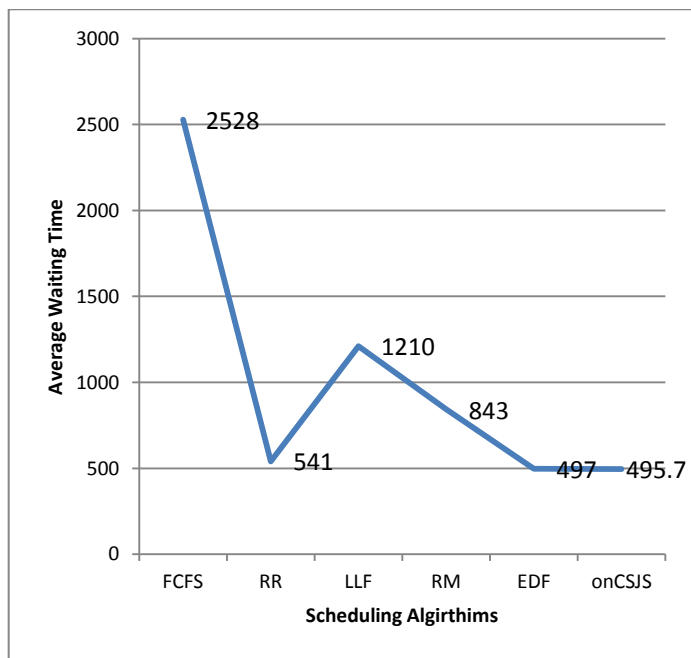


Fig. 8. Average Waiting Time

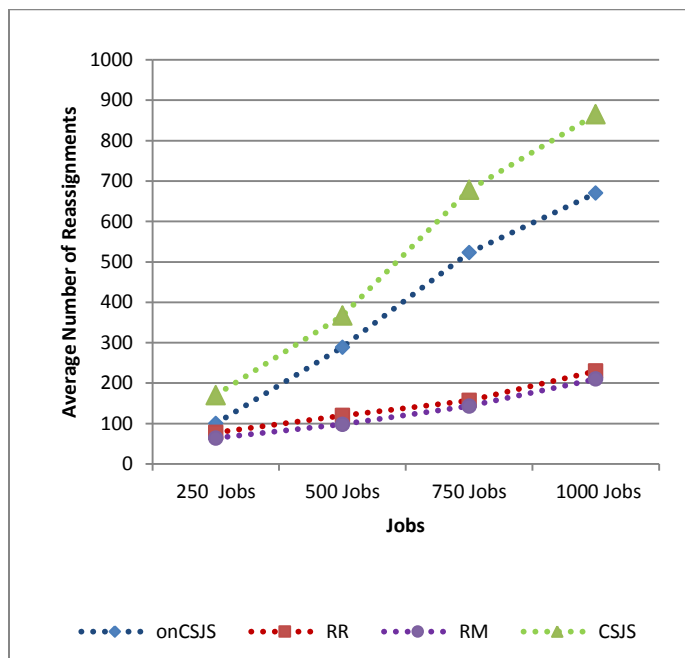


Fig. 10. Reassignment of Jobs with onCSJS

The turnaround time of onCSJS is presented in Fig. 9. It has been observed that average turnaround time calculated using onCSJS is very less than the baseline scheduling algorithms. The less turnaround time can be a similar effect for less waiting time. The less waiting time and less turnaround time are due to the reason of scheduling the jobs to a resource with available CPU clock ticks that can be allocated to submitted jobs.

G. Load Predictor Analysis

If the load prediction is not included in the proposed job scheduling algorithm onCSJS, let's call that CSJS. In CSJS the number of job reassignments will be more because there is no consideration for the future job load on volunteer re-sources and the job scheduling will be different. The number of job reassignments is very less in onCSJS (Fig. 7) as compared to CSJS (Fig. 10). This proves that if job prediction is made using any forecasting method, it can help to reduce the job reassignments overhead. The results are tabulated in Table II.

TABLE II. NUMBER OF REASSIGNMENTS

Scheduling Algorithms	Jobs			
	250	500	750	1000
onCSJS	100	289	523	670
RR	78	120	157	230
RM	64	98	143	210
CSJS	170	367	678	865

VI. CONCLUSION

There are job scheduling policies which can make use of history events. The job scheduling in volunteer grid computing environment can be aided with container stowage considering the jobs as containers and resources as ships or vessels. A job scheduling algorithm using the container stowage has been proposed for volunteer grid computing environment. The design and evaluation has been discussed in details by making comparisons with the other job scheduling algorithms including EDF, RM, RR, LLF and FCFS. The proposed algorithm considers job reassignments dynamically that's why it is named as onCSJS. The effect of not including reassignments has also been discussed. The onCSJS takes history events into account at time of assigning jobs to volunteer resources. If the history events are not taken in considerations, it will increase the number of reassignments and we call it as CSJS.

In future, the onCSJS can be incorporated in the middleware of volunteer grid to study its impact in real environment. A more accurate forecasting method can be engaged rather than taking the next batch of jobs as forecasted jobs.

ACKNOWLEDGMENT

Authors appreciatively acknowledge the High Performance Computing Center (HPCC) at Universiti Teknologi PETRONAS (UTP), Malaysia for providing the volunteer grid computing environment.

REFERENCES

- [1] M. Nouman Durrani and J. A. Shamsi, "Volunteer computing: requirements, challenges, and solutions," *Journal of Network and Computer Applications*, vol. 39, pp. 369-380, 2014.
- [2] J. W. Taylor and R. D. Snyder, "Forecasting intraday time series with multiple seasonal cycles using parsimonious seasonal exponential smoothing," *Omega*, vol. 40, pp. 748-757, 2012.
- [3] N. P. Preve, *Grid Computing: Towards a Global Interconnected Infrastructure*: Springer-Verlag London, 2011.
- [4] K. Chard, K. Bubendorfer, and P. Komisarczuk, "High occupancy resource allocation for grid and cloud systems, a study with DRIVE," in *Proceedings of the 19th ACM International Symposium on High Performance Distributed Computing*, 2010, pp. 73-84.
- [5] S. Krawczyk and K. Bubendorfer, "Grid resource allocation: allocation mechanisms and utilisation patterns," in *Proceedings of the sixth Australasian workshop on Grid computing and e-research-Volume 82*, 2008, pp. 73-81.
- [6] S. Naseera and K. M. Murthy, "Prediction Based Job Scheduling Strategy for a Volunteer Desktop Grid," in *Advances in Computing, Communication, and Control*, ed: Springer, 2013, pp. 25-38.
- [7] D. Zhou and V. Lo, "Wave scheduler: Scheduling for faster turnaround time in peer-based desktop grid systems," in *Job Scheduling Strategies for Parallel Processing*, 2005, pp. 194-218.
- [8] J. Zhang, "Flexible distributed computing with volunteered resources," 2010.
- [9] P. Giemisch and A. Jellinghaus, "Optimization models for the container-ship stowage problem," in *Operations Research Proceedings 2003*, ed: Springer, 2004, pp. 347-354.
- [10] M. Zeng, M. Y. H. Low, W. J. Hsu, S. Y. Huang, F. Liu, and C. A. Win, "Automated stowage planning for large containerhips with improved safety and stability," in *Proceedings of the Winter Simulation Conference*, 2010, pp. 1976-1989.
- [11] N. Ding, C. Benoit, G. Foggia, Y. Besanger, and F. Wurtz, "Neural Network-Based Model Design for Short-Term Load Forecast in Distribution Systems," 2015.
- [12] D. C. Montgomery, C. L. Jennings, and M. Kulahci, *Introduction to time series analysis and forecasting vol. 526*: John Wiley & Sons, 2011.
- [13] P. J. Brockwell, *Introduction to time series and forecasting vol. 1*: Taylor & Francis, 2002.
- [14] C. Chatfield, "The holt-winters forecasting procedure," *Applied Statistics*, pp. 264-279, 1978.
- [15] D. P. Anderson, J. Cobb, E. Korpela, M. Lebofsky, and D. Werthimer, "SETI@ home: an experiment in public-resource computing," *Communications of the ACM*, vol. 45, pp. 56-61, 2002.
- [16] Z. Balaton, Z. Farkas, G. Gombas, P. Kacsuk, R. Lovas, A. C. Marosi, et al., "EDGeS: the common boundary between service and desktop grids," *Parallel Processing Letters*, vol. 18, pp. 433-445, 2008.
- [17] J. Basney, M. Livny, and T. Tannenbaum, "Deploying a high throughput computing cluster," *High performance cluster computing*, vol. 1, pp. 356-361, 1999.
- [18] S. Teng, W. Zhang, H. Zhu, X. Fu, J. Su, and B. Cui, "A Least-Laxity-First Scheduling Algorithm of Variable Time Slice for Periodic Tasks," *Breakthroughs in Software Science and Computational Intelligence*, p. 316, 2012.

- [19] Y. Xu, H. Su, Y.-J. Pan, Z.-G. Wu, and W. Xu, "Stability analysis of networked control systems with round-robin scheduling and packet dropouts," *Journal of the Franklin Institute*, vol. 350, 2013.
- [20] A. Sirohi, A. Pratap, and M. Aggarwal, "Improvised Round Robin (CPU) Scheduling Algorithm," *International Journal of Computer Applications*, vol. 99, pp. 40-43, 2014.

An Incident Management System for Debt Collection in Virtual Banking

Sareh Saberi*

Department of Computer Engineering, Science and
Research Branch,
Islamic Azad University,
Tehran, Iran

Seyyed Mohsen Hashemi

Department of Computer Engineering, Science and
Research Branch,
Islamic Azad University,
Tehran, Iran

Abstract—An astonishing peak volume of bad loans in most countries, including Iran, is one of the latest manifestations of deep disorders which inhibited banking system from performing its main duty to promote development plans over a long period. Main mission of banking system is to link savers and those economic actors who need financial facilities. Banks, as intermediaries, receive interest from the second group and pay interest to the first group. During the last 10 years, millions of people have been controlling their financial lives online in the developed markets. Counters of access to electronic money and electronic wallet have increased currently. Bad loans increase as more facilities are provided for customers. Therefore, a mechanism is required for debt collection without any need for physical bank and improvement of this process using incident management system.

Keywords—virtual banking; debt collection; incident management

I. INTRODUCTION

Currently, information technology is known as an integral part of all industries and areas of activity. Few areas of industrial, commercial and service activities can be found which do not require IT to achieve their goals. Banking industry is one of the main economic activities in which IT is widely used as a key element. In current banks, IT is blood in vessels of the bank; all banking activities are through this context. Part of financial resources of banks and financial and credit institutions, which are granted to recipients of facilities, is in the form of bad loans. This group of customers discourages re-granting of financing facilities and ideal banking services to customers. Credit risk has been always a threat to banking activity. The risk of non-repayment of loans taken from banks is always considered as bad loans in financial headlines. Thus, banks have been always concerned with observation of bad loans to granted facilities. According to the studies conducted, if this ratio reaches 20%, it will be a risk for the bank. Using data analysis, this study develops a system which can improve debt collection and return these financial resources to the banking industry [1, 2, 3].

Information Technology Infrastructure Library (ITIL) is a systematic approach to quality of IT services. Details of the most important processes of an IT organization such as task list, instructions and responsibilities provides a basis to accommodate needs of various organizations. Development and dissemination of this approach provided useful guidelines

in many fields which resulted in growth and development of IT organizations. In simple terms, ITIL can be considered as a standard in the field of IT, while the reality is that ITIL is not a standard [4, 5].

II. DEFINITION OF INCIDENTS

Modified ITIL terminology defines incident as any event that is not part of a standard operation and cause service interruptions or reduced quality of the service. The purpose of ITIL is to achieve normal operation in the shortest possible time with minimal effect on trade or user by spending an affordable cost. Incidents may occur due to certain or uncertain reasons and they are recorded eventually to control problem management in Known Error Database. Incidents result from underlying IT problems and errors. The cause of incidents may be known and clear and may not need any investment in terms of time of cost for identifying. These incidents may lead to an application for maintenance, a physical presence at the site, or a change request to remove error. Where an incident is raised to be seriously and vigorously pursued or several events similar to an incident are observed, a problem could be recorded as a solution to all cases in the system. A problem may not be recorded until several similar problems are reported. Management of a problem is different from management process of an incident and it is done by different employees; for this reason, it is controlled by problem management process. When a problem is identified, the problem is recognized as a problem. Once the cause of an incident is detected, it becomes a detected error. Finally, a change request may be created for changing the system or eliminating the detected error. This process is covered by a change management process. Note that, request for an additional service is not recognized as an incident; instead, it is called a change request [4, 6].

III. INCIDENT MANAGEMENT BASED ON ITIL

Purpose of incident management is to restore normal servicing operations at minimum time possible and to minimize effect of hazards and inconsistencies in commercial operations. Normal service operation here is defined as a service operation within limits of the service level agreements. In other words, incident management is a part of the IT service management. Its primary goal is to restore normal servicing operations at minimum time possible and to minimize its negative effects such as lack of servicing in commercial operations. Incident refers to any event which is not routine

component of a service and may stop the service or reduce quality of the service. Process management monitors processing, allocates resources to different layers of this process, insures the updated database, and uses these tools efficiently; other responsibilities of management include planning and reporting [7].

IV. COMPARISON OF SERVICE DESK APPLICATIONS

To evaluate features of different service desks in order to identify characteristics of incident management, these applications are compared in terms of three following companies which annually report experiences of customers with available applications.

A. IDC MarketScape

- Leader: ServiceNow, BMC Software.
- Major Player: CherWell Software, CA Technologies, IBM, HP.
- Contenders: LANDESK, ZOHO
- Participants

B. Gartner

- Leader: ServiceNow, BMC Software
- Challengers: CherWell Software, CA Technologies
- Visionares: Landesk, Axios Systems
- Niche Players: FronRange, IBM, EasyVista, HP, ManageEngin, SysAid Technologies, TOPdesk, Hernbill

C. Forrester

- Leader: SysAid Technologies, CherWell Software, ServiceNow.
- Strong Perfomers: EasyVista, FronRange, Zendesk, TOPdesk, Vivantlo.
- Contenders: Landesk, Axios Systems
- Risky Bets

By comparing features, it is concluded that a full service desk should have following characteristics: Mobile, Web-Based, Alert/Escalation, Asset Management, Asset life Cycle Management, Automated, Assignment/Routing, Contract Management, Work Flow, Customer DataBase, Customer Self Service Ticket Management, Knowledge Base, Reporting, Incident Management, Problem Management, Change Management, Configuration Management, CRM, SMS, Social Media Integration Surveys & Feedback, Live Chat, Email Integration, Community Forums, Telephony [8, 9, 10].

V. VIRTUAL BANKING

In a virtual bank, customers and users are the same and both use banking services vie internet. Important efforts have been made for virtual banking worldwide. Statistics released by the International Monetary Fund indicate that virtual banking is mostly used in Austria, Finland, Korea, Singapore, Spain, Sweden and Switzerland where more than 75% of banks

deliver internet services. In America, those banks providing internet services possess more than 90% of assets of banking system. Although most customers have accounts in banks providing e-banking services, only 4% of them are customers of these banks. There are few virtual banks in the world; by 2001, there were only nine virtual banks with independent charter and almost 20 virtual banks with special trademark in America and two virtual banks in Asia and several virtual banks in European Union [11, 12, 13].

VI. DEBT COLLECTION

According to the latest information and formal and informal interviews, there is 800 thousand billion tomans cash operating in Iran, of which 150 thousand billion tomans as bad loans has not been returned to the banks. Portfolio of bad loans shows that about 60% of these loans are doubtful headings. Statistical analysis suggests that more than half of the portfolio of bad loans is in disposal of few people (not more than 100 people). Therefore, the crisis in bank liquidity cycle is an uncommon problem which needs to be addressed. By definition, bad loans are divided into two groups of current and non-current loans. Current loans refer to those loans that two months have passed their due date. These loans are traced in banks as current heading. Non-current loans include past due, overdue and doubtful headings. Time is involved in definition of these headings. By definition, those loans that more than two months and less than six months have passed their due date are past due loans. Overdue loans are those loans that more than six months and less than eighteen months have passed their due date. Doubtful loans are those loans that more than eighteen months have passed their due date [1, 3].

VII. METHODS

Using UML concepts, Activity Diagrams are depicted for traditional debt collection, electronic debt collection and the suggested system by using features of incident management system and results of comparison of the best service desks as well as features of virtual banking to suggest the virtual debt collection process.

VIII. TRADITIONAL DEBT COLLECTION

Three categories of information are required for filing:

- Information of loans including the type of contract signed by the customer at the time of receiving loans
- Type of collaterals and guarantees received from the customer at the time of receiving loans
- Full information of the debtor including ID, addresses, work, email address and contact information

Once this information is imported to the debt collection system, it is analyzed and separated. Then, the file is referred to a debt collection expert who sends a text message to cellphone of the debtor recorded in the file. The text message is determined by consulting with legal department. In a stepwise fashion, the text message gradually becomes a warning. As an important principle in debt collection, leverages are intensified gradually on the debtor to repay debt (Figure 1) [14,15].

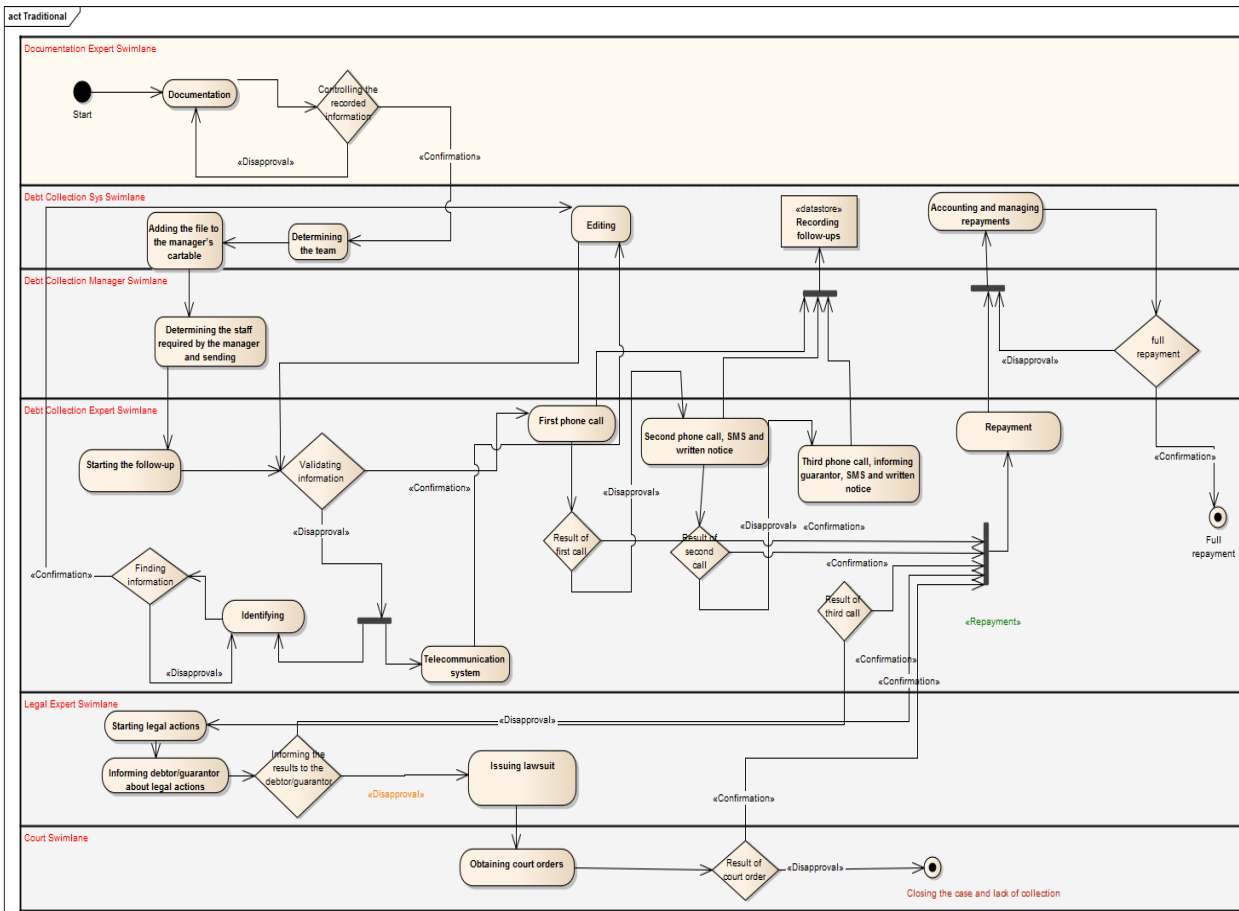


Fig. 1. Traditional Debt Collection Activity Diagram

IX. FIRST IMPROVEMENT USING VIRTUAL BANKING FEATURES, ELECTRONIC DEBT COLLECTION SYSTEM

The process starts with visiting the website and filling the application forms to obtain loans. The qualified applicant is asked to upload the scanned documents. Then, the uploaded documents are evaluated in terms of accuracy and adequacy. Validation starts by reviewing the documents and available information. Validation eventually leads to credit rating, based on which bank credit committee decides whether to grant the

loan. All records of BadPay saved in this database are considered as input for validation. By analyzing validation information, the customer will be informed if the loan is not to be granted. Otherwise, the customer is informed after the loan is deposited in customer account. The customer is informed of amount and due date of the first installment. Once the loan is deposited, the system starts accounting and payment management. If the installments are not paid in the determined due date, debt collection experts make the first follow-up contact (Figure 2).

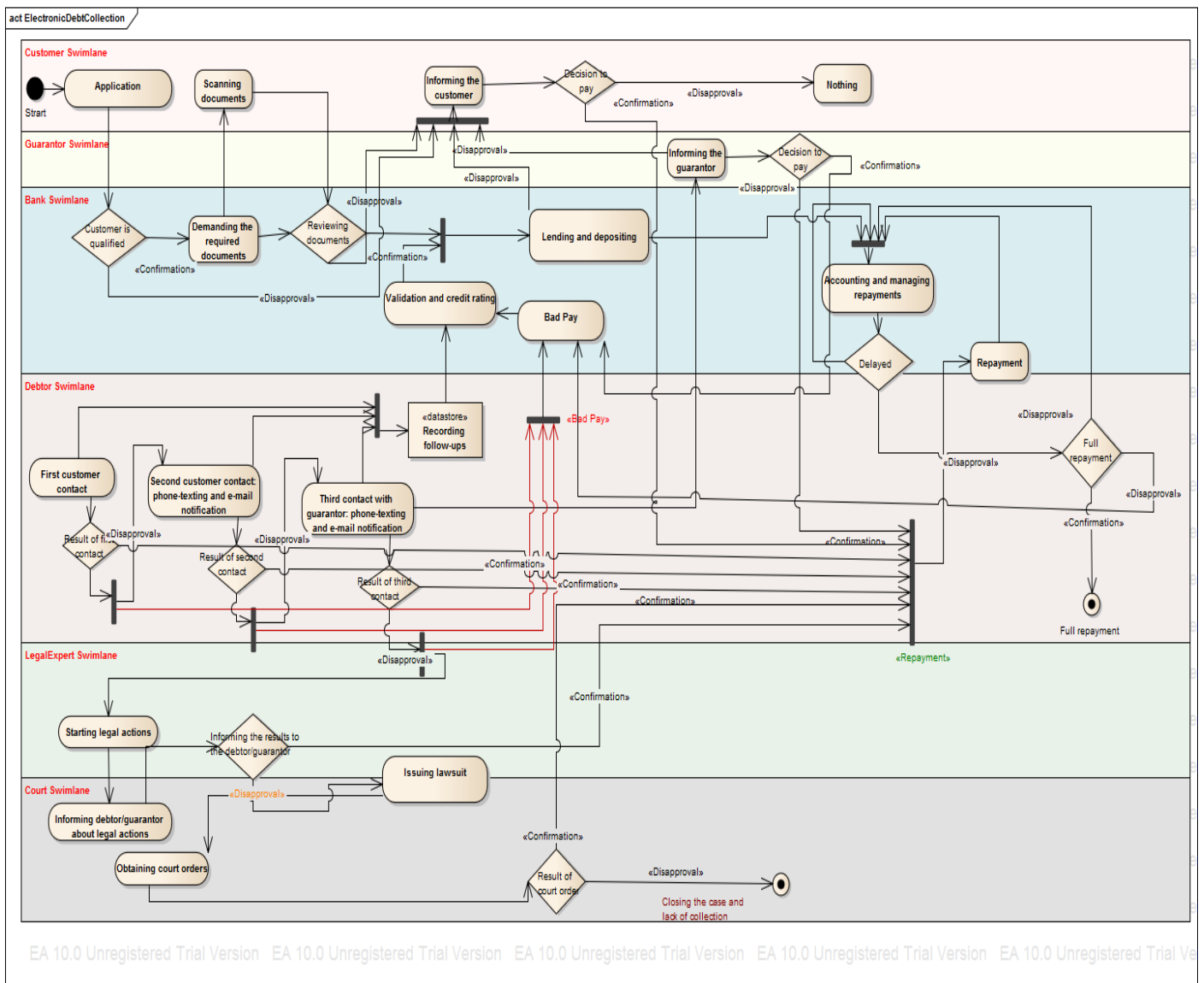


Fig. 2. Electronic Debt Collection Activity Diagram

X. THE SUGGESTED METHODOLOGY

A. Incident Management System for Debt Collection in Virtual Banking

The operation starts with visiting the website and filling the application form. The application form contains information on type of loan, rate of interest, ID and claimed collaterals. The system makes decisions automatically and online by considering customer choices, information and documents by connecting to central databases such as Document Registration Organization to investigate property collaterals announced, Civil Registration Organization to investigate claimed information and Telecommunication Organization to investigate contact numbers and addresses as well as BadPay output which is explained below. The customer is rated through BadPay outputs and payment behavior of previous loans using Knowledge Base feature of Service Desk. The output is compiled in a Black List of people who are not qualified and do not have collaterals. Once the information is

received, the system makes decision on the granting the loan. If the loan is allowed, the requested amount will be directly deposited in account of the applicant. The customer is informed of deposition, repayment period, due date of the first installments, and amount of installment. Moreover, the system informs the customer upon depositing the loan. If the applicant is not qualified, the system will inform the applicant via email and SMS. Systemic operation of accounting and repayment management starts once the loan is deposited. In fact, on time repayment is monitored in the system. At each stage of due date, lack of repayment is recorded as Badpay in this system. All Badpay records are analyzed in a database called as customer payment behaviors, containing a history of customer actions and reactions in repayment; for example, the database shows repayments after stages of follow-up. Based on these records, decisions are made on granting loans and follow-up operations of debt collection. One requirement of loan is guarantor(s). Informing system is applicable for the guarantor in the next stages. If the customer does not repay upon the first

due date, accounting system and repayment management and the follow-up debt collection systematically start to work using repayment behavior of customer. The first follow-up is through phone call using IVR which informs legal consequences of non-compliance with repayment obligations. The system extends the deadline for repayment and studies customer behavior in the extended period. If the customer does not repay at the deadline, it will be recorded as a Badpay and the system starts the next stage to continue follow-up. Next follow-ups involve phone calls, SMS and email. In case of repayment at any follow-up stages, it is recorded in the accounting system and repayment management; otherwise, the second Badpay is recorded for the customer. At the third stage of follow-up, the system informs both customer and guarantor about legal consequences of the guarantee. If the guarantor does not respond, the system records Badpay for the guarantor. If the third follow-up does not lead to repayment, the system will refer the file to the legal follow-up department. From the beginning, the customer and the guarantor are informed of

legal actions. The deadline is extended to one week; in case of non-repayment, the file is referred to the judicial authorities for follow-up by calculating interest, fines and debt to the date. This stage involves issuing of a lawsuit by sending information to online system of judicial authorities and court's decision and ultimately issuing the definitive execution to force the customer or the guarantor to repay the debt. All repayment procedures ultimately lead to complete repayment of the debt. In each stage of follow-up, the debtor may attempt to pay off debts, which is done in repayment process. In addition, payment management and accounting system constantly monitors the customer's account. According to central bank laws, lending becomes difficult and even impossible to individuals and guarantors in the banking network. By linking to judicial systems, this can lead to automatic issuing of travel bans. Some of banking services may be discontinued later. For example, Shetab network services may be disrupted or money transfer may not be available (Figure 3).

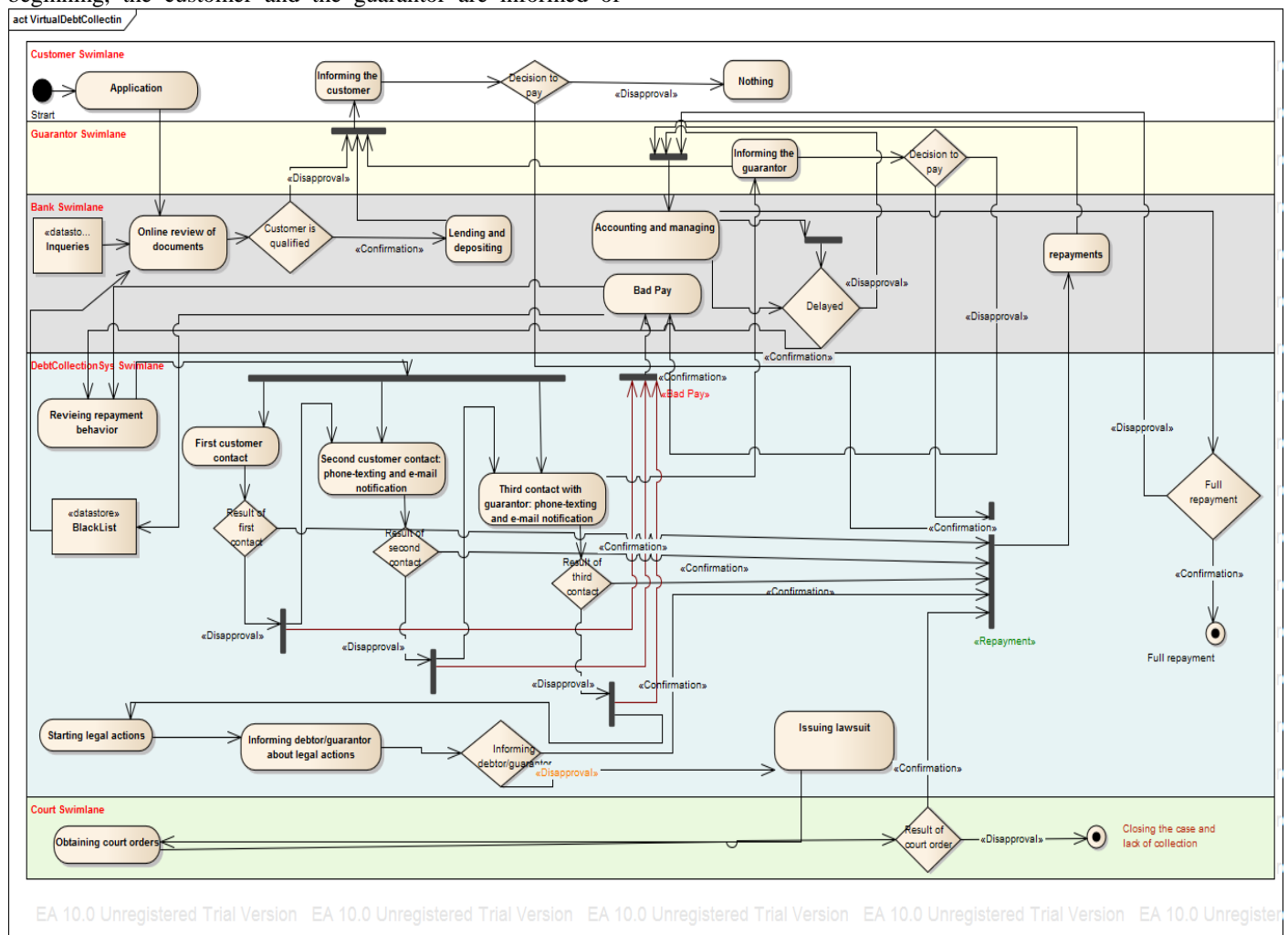


Fig. 3. Incident Management System for Debt Collection in Virtual Banking Activity Diagram

XI. SYSTEM EVALUATION

A. Measurement of Effectiveness

An inclusive study is required to evaluate systemic improvements done. The figure below determines logical chain of this study:

- 1) *Information*
 - Easily received and processed information
 - Easily validated information
- 2) *Customer satisfaction*
 - Customer self-validation
 - Easy lending
 - Transparent informing
 - Access to sufficient information at any time
- 3) *Debt collection process*
 - Reduced costs of ineffective follow-ups

- Improved repayment behavior for satisfaction
- Completed database of non-creditworthy customers and prevention of next bad loans

XII. MEASUREMENT OF CUSTOMER SATISFACTION BY KANO MODEL

Results of the survey of 100 customers analyzed by Kano model show that customers are most concerned with attractive factors followed by must-be and basic factors considered in virtual banking. The lowest score given by respondents to the questions F16 and F23 results from their lack of understanding of the menus; this can be attributed to the fact that respondents had no experience with the real website and only considered the simulated scenario. In conclusion, the results show that customer satisfaction with attractive, must-be and basic factors increases overall satisfaction of users; positive responses are expected from repayment behavior of customers (Table 1 and 2 and Figure 4) [16, 17].

TABLE I. CUSTOMER SURVEY

	Question	Class	Dislike	Live with	Neutral	Must be	Like	Total
F1	Meeting customer information needs in relation to types of lending contracts	Attractive	1	0	2	12	35	230
F2	Satisfaction with informing process	Attractive	1	2	11	25	11	193
F3	Providing sufficient information through alarms in the customer profile	Attractive	3	2	15	22	8	180
F4	Usage of promotions and forgiveness of crimes and satisfaction	Attractive	0	0	23	10	17	194
F5	Customer opinion about reduced cost of commuting due to the new method	Attractive	1	0	16	19	14	195
F6	Supporting views and reforms	Attractive	1	3	12	22	12	191
F7	New information	Attractive	1	5	19	16	9	177
F8	How lack of validation impairs customer intention	Attractive	1	1	3	32	13	205
F9	Lack of information about debt collection process has an effect on customer satisfaction	Attractive	2	2	1	29	16	205
F10	Lack of promotions and motivations (informing, forgiveness, commuting cost)	Attractive	0	1	1	38	10	207
F11	Easy communication and access to customer service	Basic	2	2	5	26	15	200
F12	Easily met customer expectations from menus	Basic	1	1	9	28	11	197
F13	Ability to search information	Basic	1	3	4	36	6	193
F14	Accurate presentation	Basic	1	2	3	38	6	196
F15	Help tables and content menus	Basic	0	2	18	24	6	184
F16	What do you think if the menus are removed?	Basic	3	1	3	11	11	113
F17	Do you agree with removal of the search feature?	Basic	0	1	3	21	25	220
F18	How would lack of help tables be effective on easy access?	Basic	4	4	3	22	17	194
F19	How do customers with bad loan evaluate the new debt collection system?	Indifferent	0	1	3	34	12	207
F20	Suitable and sufficient resolution of webpages	Indifferent	2	1	6	40	1	187
F21	Ability to monitor the status of any pending case online	Questionable	0	0	8	38	4	196
F22	Overall satisfaction with virtual debt collection services	Questionable	0	2	23	15	10	183
F23	Ability to show user's position on the website	Questionable	10	14	16	8	2	128
F24	Logical structure of information provided	Questionable	0	2	10	32	6	192
F25	Information is available on the site until needed	Questionable	3	5	9	28	5	177
F26	Statement of information along with their details	Questionable	2	3	7	23	15	196
F27	Satisfaction with responsiveness and support	Reverse	0	0	12	37	1	189
F28	Satisfaction with continuous collection and follow-up services	Reverse	0	0	11	16	23	212
F29	Ability to monitor credit rating and systemic self-evaluation and customer satisfaction	Must-be	2	1	7	20	20	205
F30	Online monitoring of bad loans and installments and customer satisfaction	Must-be	1	1	14	18	16	197
F31	Ensuring that the data imported by the user is stored and maintained	Must-be	0	0	5	42	3	198

F32	To display load time and system response	Must-be	0	1	11	22	16	203
F33	User help	Must-be	0	8	16	20	6	174
F34	Updated information	Must-be	3	5	10	21	11	182
F35	How important is the outdated information?	Must-be	1	3	10	35	1	182
F36	How effective is the lack of load display and system response on satisfaction?	Must-be	3	2	4	36	5	188
F37	What do you think if data security is not guaranteed?	Must-be	0	1	3	39	7	202

TABLE II. CLASSIFICATION OF QUESTIONS BASED ON KANO

	Dislike	Live with	Neutral	Must be	Like
Attractive	0.02	0.03	0.21	0.45	0.29
Basic	0.03	0.04	0.12	0.52	0.24
Indifferent	0.02	0.02	0.09	0.74	0.13
Questionable	0.05	0.09	0.24	0.48	0.14
Reverse	0	0	0.23	0.53	0.24
Must-be	0.02	0.05	0.18	0.56	0.19

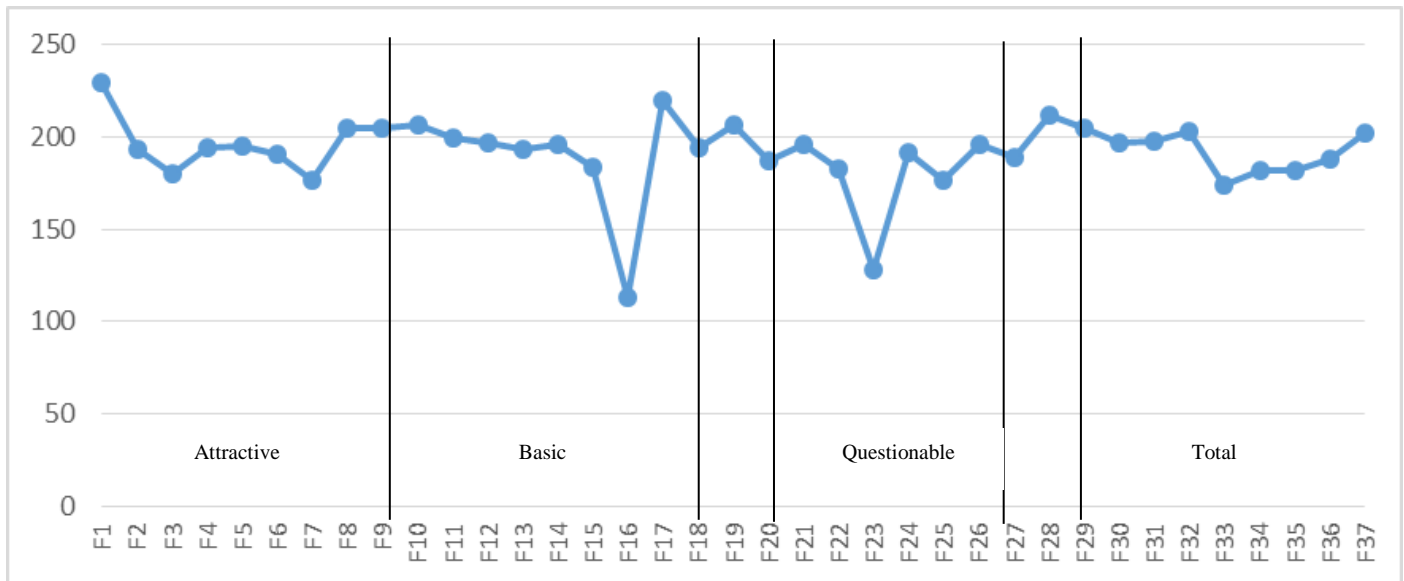


Fig. 4. Frequency of questions based on Kano

XIII. INDICATORS OF EFFECTIVENESS

By determining chain strategies used to create value added, an indicator is defined for each goal; then, methods are developed for calculating these indicators. Thus, summarized steps of this evaluation are determined for effectiveness, path control and tactics to achieve organizational goals. For this purpose, it is essential to recognize scientific and practical concepts for determining the indicators. Using balanced scorecard (BSC), performance evaluation indicators are divided into three categories [18]:

- Key result indicators (KRIs)
- Performance indicators (PIs)
- Key performance indicators (KPIs)

Indicators of debt collection are extracted from activities of a debt collection company as shown in Table 3.

XIV. CONCLUSION

Given that debt collection is based on customer data, precision and accuracy of information is important for this mission. In traditional debt collection, information is recorded

manually as input to the debt collection system; due to the size of information, human error is probable and may disrupt the debt collection process. Moreover, traditional debt collection lacks a database which can convert raw customer data using BadPay records to analytical information based on knowledge management. Moreover, the traditional system cannot monitor customer behaviors in debt collection, on time repayment or follow-up contacts. Consequently, this information gap causes latent costs. Repeated follow-ups extend the debt collection. Losses of delays and follow-ups cannot be estimated easily. Some of the costs such as written notice can be calculated; moreover, costs of each type of follow-ups can be estimated. However, latent cost is the tip of the iceberg. In addition to primary validation, repayment behavior of the customer is evaluated at the time of debt collection. The traditional system lacks this feature. In fact, customer validation prevents bad loans. Written notice requires a large amount of paper, human resources and time; moreover, the customer may not receive the notice. There may be conflicts in contracts and the relevant staff may not notice the conflicts. Traditional system suffers a considerable amount of human error. There are advantages and disadvantages in the electronic system. However, the electronic system has improvements compared to the traditional system.

Advantages of the electronic system include online application for the loan and informing process at different stages. Although the electronic system has been improved, it suffers shortcomings such as time-ineffectiveness and additional process. This system does not allow online validation simultaneously with application. It is time consuming to validate the information claimed by the applicant, because it requires inquiries from the relevant organizations. One advantage of the electronic system is that validation starts with access to the information. However, disadvantage of the system is that the applicant is required to upload the scanned documents and the bank needs to send these documents to the relevant organizations for validation; this prolongs the process. Compared to traditional and electronic systems, an inclusive database and integrated information is an advantage of virtual system. Based on incident management model, virtual banking enables a relatively smart system. In the virtual system, the customer fills the application form containing primary information, type of loans and rate of interest; by connecting to a systematic database, the system extracts and analyzes records of the applicant. To save the costs, the applicant can login to the validation system to know his credit rate and predict agreement or disagreement with his application. The database containing BadPay, BlackList records and the systems linked to DataSharing departments accelerate lending process. This system analyzes raw data and customer reactions to loans and repayments and determines a history of previous loans. For

debt collection, the system finds a suitable method based on behaviors, actions and reactions and makes decisions intelligently. The system suffers no human error in recording the information and the steps are taken rapidly. In virtual debt collection, the system receives personal information, addresses and guarantors and validates them through databases of relevant organizations such as Document Registration Organization, Civil Registration Organization, and Telecommunication Organization. Using central bank database, the customers with BadPay records are alarmed when applying for the loan and validating online. There is no need for prolonged legal process. The files are referred to the court online. In this study, virtual debt collection system was implemented by using features of incident management and service desk. A central database was developed by using mobile base and web base to integrate and validate information using features of virtual banking. Alert and email used to inform debtors save time and cost. Customer database and customer self-service enables customers to validate themselves before applying. Using a history of all banking activities, customers can validate themselves and improve their conditions if they are not qualified. Using knowledge management, previous activities and repayments of the customers can be monitored and used for validation and determination of the warning suitable for the customers. Table 4 and Table 5 summarize advantages and disadvantages of traditional, electronic and virtual banking systems.

TABLE III. EFFECTIVENESS INDICATORS OF DEBT COLLECTION IN VIRTUAL BANKING SYSTEM

Type of Indicator	Formula	Effectiveness	Indicator
KPI	Number of complaints (questions with average to weak rating) / total surveys (all questions responded) × 100	Customer satisfaction	Customer satisfaction
Correct information flow and improved quality of customer service increases customer satisfaction in surveys and indirectly influences repayment behavior of customers.			
PI	Total number of follow ups / total number of debtors × 100	Debt collection	Follow-up rate
Through a direct relationship between transparency and facilitated flow of information and increased customer satisfaction, total number of follow-ups directly decreases. Given that the number of files or debtors is constant, the follow-up rate decreases. In other words, lower follow-up is required for collection of bad loans compared to the traditional debt collection system.			
KPI	Number of depositing files / total number of bad loans × 100	Debt collection	Depositing file ratio
Given that a number of bad loans remain unpaid until they are referred to a legal entity, an important indicator must always monitor success rate of pre-legal and post-legal measures. This shows a logical relationship with customer behavior. Even decision on immediate referral to the legal department can avoid excessive time and energy spent on some files by controlling costs. Therefore, regular monitoring of the number of depositing files is important for the bank. Many debtors tend to extend or repay through re-installment. Thus, depositing files involve those who have not yet repay completely and had multiple repayments.			
KRI	Collection rate (RLS) / Total amount of bad loans × 100	Debt collection	Collection to portfolio ratio
Debt collection management calculates the ratio of collected debts to total amount of bad loans. This indicator is very important in financial management, financial statements and generally auditing of the bank. Effect of customer satisfaction which results from facilitated flow of information and quality of the services provided manifests itself in this indicator.			
PI	Number of paid loans / total number of bad loans × 100	Debt collection	Paid loan ratio
Debt collection management requires customers to accept the terms of contracts including rate of interest and penalty and pay their debts completely. Thus, debt collection system requires an indicator for determining completely paid loans. This indicator is successful when numerator and denominator approach to 1. Apart from the amount of debt, this indicator directly refers to the paid loans.			
KRI	Administrative fee of debt collection (phone, SMS, IVR, etc.) / total amount of collected debts × 100	Debt collection/information	Cost to collection ratio
One of the indicators which are directly related to facilitated flow of information and customer satisfaction is the reduced number of follow-ups and consequently reduced costs of these follow-ups. The lower the numerator, the higher the collected debts and profitability will be.			
PI	(Cost of paper + phone calls + SMS + IVR) + cost of staff salary / total organizational expenses	Debt collection/information	Cost ratio
This ratio shows the share of costs to total administrative expenses. It is in fact the bottleneck of organizational expenses and involves those costs which are directly involved in debt collection process.			
PI	The number of referrals to legal department / total number of bad loans × 100	Customer satisfaction	Number of referrals to legal department
PI	Amount of files referred to legal department / total number of bad loans × 100	Customer satisfaction	Amount of files referred to legal department
These two indicators show those customer behaviors referred to legal department for banking contracts or amount of debts. It also indicates decision of the organization to save the time and reduce costs by referring the files to the legal department immediately. On the other hand, this indicator shows effectiveness of pre-legal processes and customer satisfaction indirectly. From a win-win perspective, this indicator reduces costs of legal actions for both customers and the bank. The bank tends to refer less files to the legal department; for this, the bank needs to inform the customer and explain costs of legal actions to the customer.			

TABLE IV. COMPARISON OF DEBT COLLECTION SYSTEMS

	Information recording	Access to previous records	Customer self-validation	Validation	SMS	IVR	Written notice	e-mail	Customer behavior analysis	Integrated information	Online mobile base	Security	Easy access
Traditional system	√	×	×	×	√	√	√	×	×	×	×	×	×
Electronic system	×	√	×	√	√	√	×	√	×	√	√	√	√
Virtual system	×	√	√	√	√	√	×	√	√	√	√	√	√

unfavorable efficiency
■ Performance nearly as Good
■ Accuracy action / optimal favorable
■

TABLE V. ADVANTAGES OF VIRTUAL DEBT COLLECTION

Advantages of virtual debt collection	
Higher profitability	Reduced time of collection
Reduced bad loans	Inexpensive services
No physical money	Continuous smart validation and follow-up
Reduced possibility of misuse	Easy to use
Fast transactions	Higher quality
Record of activities	Accuracy of information
Increased customer satisfaction	Inclusiveness
Full-time services	

REFERENCES

- [1] Central Bank of the Islamic Republic of Iran. debt collection guideline for credit institutions. tehran: central bank, central bank publication, Iran, vol. 1, 2008.
- [2] M. SABETI, H. FARSIJANI, M. KASAEI, M. HAMIDIZADEH, Cumhuriyet University Faculty of Science, Science Journal (CSJ), vol. 36, No. 6, 2015.
- [3] Central Bank of the Islamic Republic of Iran, non-current debt collection guideline for credit institutions. tehran: central bank, 2015.
- [4] P. Bernard. *Foundations of ITIL® 2011 Edition*. 2012
- [5] <https://en.wikipedia.org/wiki/ITIL>
- [6] The Office of the Government Chief Information Officer, "INFORMATION SECURITY INCIDENT HANDLING GUIDELINES", The Government of the Hong Kong Special Administrative Region, vol. 1, 2012.
- [7] CityBank, "Debt Collections Standards in India Citibank Code for collection of dues & Repossession of Security" 'Version Eleven' vol. 1, April 2014.
- [8] C. Gliedman, The Forrester Wave™: Service Desk Management Tools, vol. 4, 2006.
- [9] J. M. Brooks, and G. Jarod. "Magic quadrant for IT service support management tools." vol. 7, 2012.
- [10] IDC MarketScape: Worldwide Service Desk Management Software Vendor Analysis. vol. 1, 2014.
- [11] H. Moeinzade, difference in advantages and effects of virtual banking development. virtual banking, vol. 1, 2012.
- [12] K. Naboure, comparison of virtual banking services of top 10 virtual banks . virtual banking, vol. 1, 2012.
- [13] M. Hatami, M. electronic service development in smart city. virtual banking, vol. 1, 2012.
- [14] B. Kercher, Debt Collection Harassment in Australia (Part 2). Monash UL Rev., vol. 5, pp. 204, 1978.
- [15] V. Fedaseyeu, & R. M. Hunt, The economics of debt collection: enforcement of consumer credit contracts, vol. 1, 2015.
- [16] E. Sauerwein , F. Bailom, K. Matzler, Hans H. Hinterhuber, International Working Seminar on Production Economics, Innsbruck/Igls/Austria, vol. 1, pp. 313 -327, 1996.
- [17] <http://www.parsmodir.com/thesis/kano.php>.
- [18] R. S. Kaplan, D. P. Norton, "The Balanced Scorecard: Translating Strategy into Action. Boston" 'Harvard Business School Press , vol. 1, 2004.

Credibility Evaluation of Online Distance Education Websites

Khalid Al-Omar

Department of Information Systems
King Abdulaziz University
Jeddah, Kingdom of Saudi Arabia

Abstract—Web credibility is becoming a significant factor in increasing user satisfaction, trust, and loyalty. Web credibility is particularly important for people who cannot visit an institution for one reason or other and mostly depend on the website, such as online distance education students. Accordingly, universities and educational websites need to determine the types of credibility problems they have on their websites. However, far too little attention has been paid to providing detailed information regarding the types of specific credibility problems that could be found on university websites in general, and specifically, in the Kingdom of Saudi Arabia (KSA). The aim of this paper is to study and analyze the credibility of university websites that offer distance education courses in the KSA. A total of 12 universities in Saudi Arabia were considered, which include 11 affiliated and one private university. The analysis of the data represents the level of credibility of distance education websites. Results reveal that in Saudi Arabia, distance education websites are reliable, but violate basic credibility guidelines.

Keywords—*university websites; credibility; trustworthiness; online trust; website design; Saudi Arabia; distance education*

I. INTRODUCTION

The World Wide Web (WWW) helps academic institutions distribute their messages and increase their services across the globe. Unfortunately, until now, the available technologies do not guarantee whether the web content on the Internet is reliable, up to date, and standardized, since web publishing does not involve the different stages of reviewing and filtering, as print sources do [1]. Consequently, trusting the information on websites is vital, especially for people who cannot visit an institution and depend mainly on the website—for example, online distance education students. To ensure that students join their online distance education programs and not go elsewhere, universities should be certain that their websites are aesthetic, usable, and credible. Therefore, deanships of e-learning and distance education websites at universities require reliable web-based information.

II. WHAT IS WEB CREDIBILITY?

Credibility is one of the most important characteristics of any user interface. Credibility is defined as believability [2, 3] or trustworthiness of information found on the web, which means the level to which users trust the content in a website [1]. In other words, it explains why people believe the information provided by some websites but not others. Credibility offers the ability to change user attitudes and behaviors. It can make

users comfortable interacting with the website, registering their personal information, and then returning again [2].

The vast majority of researchers identify two key components of credibility: “trustworthiness” and “expertise” [4]. Trustworthiness is defined by the terms truthful and unbiased, whereas “expertise” is defined by terms such as knowledgeable and competent. The trustworthiness dimension of credibility captures the perceived goodness or morality of the source, while the expertise dimension of credibility captures the perceived knowledge and skill of the source. Highly credible websites will be perceived to have high levels of both trustworthiness and expertise.

The remainder of the paper is organized as follows: First, there is an overview of web credibility, presented in Section 2; then, a brief description of distance education in the KSA is given in Section 3. In Section 4, e-learning website selection is discussed, and then in Section 5, there is a brief description of relevant previous studies and a literature review. In Section 6, objectives of this work are presented, and in Section 7, there is a hypothesis. Section 8 presents the methodology used, Section 9 presents and discusses the results of this research, and website evaluation using automated tools is presented in Section 10. In Section 11, tool-based results are provided; in Section 12, there is a discussion of these results; and in Section 13, suggestions are offered. Finally, conclusions and future work are discussed in Section 14.

III. A BRIEF NOTE ABOUT DISTANCE EDUCATION IN THE KSA

In the present day, the Kingdom of Saudi Arabia (KSA) has witnessed growth in the number of universities in the country. Consequently, universities are facing huge competition as far as bringing in more students, with the competition being even higher for distance education programs, since the structure of online learning gives students full control over the time and place for their study. Therefore, more than ever before, the credibility of websites in higher education is becoming an increasingly important area to consider. The aim of this paper is to study and analyze several aspects related to the credibility of distance learning websites in the Kingdom of Saudi Arabia. According to the Ministry of Higher Education in the KSA, there are 35 universities in Saudi Arabia. There are 25 government universities, 10 private universities, and one university focusing exclusively on graduate education and research—King Abdullah University of Science and

Technology (KAUST). A total of 293,665 (140,415 male and 153,250 female) students were enrolled in higher education for the 35 universities in 2014. In addition, 740 students were enrolled in KAUST (488 male and 252 female).

TABLE I. NUMBER OF ESTABLISHED UNIVERSITIES IN THE KSA

Year of Establishment	No. of Government Universities	No. of Private Universities	Percentage
Before 1960	1	0	1
Between 1960 and 1970	4	0	4
Between 1970 and 1980	3	1	4
Between 1980 and 1990	0	0	0
Between 1990 and 2000	1	1	2
Between 2000 and 2010	16	6	22
After 2010	1	2	3
Total	26	10	36

IV. E-LEARNING WEBSITE SELECTION

Among the 36 universities, only 11 government universities have been authorized by the Ministry of Higher Education to offer distance education courses ranging from bachelor's to master's degree. On the other hand, only one private university (the Arab Open University) has been accredited by the Ministry of Higher Education (see Table 2). However, the number of e-learning students enrolled is not an indication of credibility, since the location of the university affects the number of enrollees.

TABLE II. NUMBER OF ONLINE DISTANCE EDUCATION STUDENTS IN THE KSA 2014

No	University	Male	Female	Total
1	King Abdulaziz University (KAU)	1,959	1,909	3,868
2	Islamic University in Madinah	700	0	700
3	IMAUM	5,156	3,733	8,889
4	King Faisal University (KFU)	5,911	6,901	1,2812
5	TAIBUAHU	1,530	1,713	3,243
6	Taif University (TU)	2,014	1,041	3,055
7	Jazan University (JAZANU)	876	810	1,686
8	Aljouf University (JU)	199	66	265
9	Najran University (NU)	1,005	977	1,982
10	University of Dammam (UD)	957	1,241	2,198
11	Saudi Electronic University (SEU)	4,490	2,771	7,261
12	Arab Open University	1,914	2,340	4,254

Currently, there is a huge demand for online distance learning in the KSA. Mainly, there are two main factors that influence online learning. First, the KSA is a large country with very few universities open compared to its size. Second, the KSA government encourages its employees to get an advanced degree to become eligible for promotion to a higher position. However, the main reason that causes more demand for distance education programs is the acceptance of online

distance learning by the Ministry of Civil Service. Therefore, the demand for a place to study online learning at the university is still much more than is available. Thus, every academic year, thousands of students are left out of universities [5]. As a result, many universities have recently been offering distance education learning programs. As such, sooner or later, deanships of distance learning programs will face increasing pressure to enhance the credibility of their websites.

V. LITERATURE REVIEW

In recent years, factors affecting the credibility of websites have been the subject of many research projects, such as social networking sites [6], mobile website interfaces [7], e-learning, e-government [8, 9], and e-commerce (e.g. [2, 6, 10-12]). BJ Fogg's team at the Stanford Web Credibility Project conducted a remarkable study to investigate which design elements positively or negatively influence credibility. Fogg et al. conducted a large-scale online survey of more than 1,400 participants, both from the U.S. and Europe, evaluating 51 different website elements. In this study, they identified five elements that have a positive effect on the credibility of a website: real-world feel, ease of use and usefulness, expertise, trustworthiness, and tailoring [2]. Two of these credibility elements, ease of use and tailoring, closely relate to usability [13]. Also, the researchers found that the two factors hurting credibility were "commercial implications" and "amateurism." Based on these findings, Fogg et al. [2] proposed seven guidelines to create highly credible websites, which they expanded on further by setting up the Stanford Guidelines for Web Credibility [14].

Furthermore, Fogg et al. conducted a study with more than 2,500 participants to shed light on what leads people to believe, or not believe, what they find online [15]. Participants evaluated the credibility of two live websites on a similar topic (health). They concluded that the design of the site was mentioned most frequently, followed by comments about information structure and information focus. Also, in this study authors shared participants' feedback in the top 18 areas that people noticed when evaluating website credibility.

VI. OBJECTIVES

The main objective of this study is to examine the web credibility of e-learning and distance education deanships websites at universities in the KSA, compare the online distance education websites of universities in the KSA, and then offer suggestions for the design of an ideal online distance education website for a university to increase the site's credibility.

VII. HYPOTHESES

Hypotheses applied for the study were:

- A majority of the universities in Saudi Arabia have hosted websites on the Internet.
- The university websites are heterogeneous in their structure and content.
- Most of the websites do not follow established guidelines.

- The majority of the universities in Saudi Arabia have serious issues with web credibility.

VIII. METHODOLOGY

The first part of our evaluation methodology was intended to evaluate the credibility of the e-learning websites of Saudi universities by using the self-evaluation method. The data for this study was collected through this method [15], which included the following:

- Designing a checklist from previous research [1, 2].
- Evaluation of the websites.¹
- Data collection.
- Analysis and interpretation of data.

The credibility evaluation methods conducted by human involvement can assess only the external attributes of the website rather than its internal attributes. External attributes depend on the website and its usage, while the internal attributes of the website depend on how the website has been designed and developed [16]. The internal attributes of the website can be assessed and evaluated using automated tools. Both internal and external attributes are required. In this study, the total size of the website, total size of images, percentage of images in the total size, and the download times were collected. Slow websites gave an indication that the website was uncertain. However, the external attributes of the website were assessed and evaluated by self-evaluation.

IX. DATA ANALYSIS AND DISCUSSION

Among the 36 universities, only 12 have been authorized by the Ministry of Higher Education to offer distance education courses ranging from bachelors' to masters' degrees. In this study, all 12 universities were considered, evaluated, and analyzed. However, there has been a phenomenal growth of e-learning and distance education in Saudi Arabia universities since 2009 (Table 3).

TABLE III. YEAR OF ESTABLISHMENT OF E-LEARNING AND DISTANCE EDUCATION DEANSHIPS AT UNIVERSITIES IN THE KSA

No	University	Year of Establishment	
		Gregorian	Hijri
1	King Abdulaziz University (KAU)	2002	1423
2	Islamic University in Madinah	1961	1381
3	IMAUM	2007	1428
4	King Faisal University (KFU)	2009	1430
5	TAIBUAHU	2005	1426
6	Taif University (TU)	2011	1432
7	Jazan University (JAZANU)	2009	1430
8	Aljouf University (JU)	2007	1428
9	Najran University (NU)	2011	1432
10	University of Dammam (UD)	2010	1430
11	Saudi Electronic University (SEU)	2011	1432
12	Arab Open University	2002	1423

¹ www.websiteoptimization.com

In 2011 Saudi Electronic University (SEU) became the first government educational institution specializing in distance education in the KSA. SEU is offering both graduate and undergraduate degree programs.

All the universities agreed that students should attend campuses for the final test. However, not all authorized universities provide complete full-distance education programs (see Table 4). There are two universities that have adopted the Blended System in e-teaching: Saudi Electronic University (SEU) and Arab Open University in the KSA. Students at SEU have to attend 25% of classes in the form of direct lectures, and another 25% as virtual classes. The rest (50%) are distributed among educational forums and following up on the digital learning content. Students at the Arab Open University in the KSA have to attend 25% in the form of direct lectures, and the rest (75%) are distributed among educational forums and following up on the digital learning content.

TABLE IV. WAY TO STUDY DISTANCE EDUCATION AT UNIVERSITIES IN THE KSA

No	University	Learning Style
1	King Abdulaziz University (KAU)	Distance Education
2	Islamic University in Madinah	Distance Education
3	IMAUM	Distance Education
4	King Faisal University (KFU)	Distance Education
5	TAIBUAHU	Distance Education
6	Taif University (TU)	Distance Education
7	Jazan University (JAZANU)	Distance Education
8	Aljouf University (JU)	Distance Education
9	Najran University (NU)	Distance Education
10	University of Dammam (UD)	Distance Education
11	Saudi Electronic University (SEU)	Blended Learning: 25% as direct (face-to-face) lectures 25% as virtual (online) classes 50% participating in the course
12	Arab Open University in the KSA	Blended Learning: 25% as direct (face-to-face) lectures

Table 5 shows that all government universities have their URL with "edu.sa," and just a single private university used ".org" for their university URL.

TABLE V. CLASSIFICATION OF WEBSITES BY URL EXTENSION

URL	.edu.sa	.org
Number of Universities	11 Government Universities	1 Private University

X. WEBSITE EVALUATION USING AUTOMATED TOOLS

Credibility assessment methods that are conducted by human involvement (users and experts) can assess only the external attributes of the website (such as the usability of the website) rather than its internal attributes (such as webpage speed analysis). Testing website download speed and the size of the webpage is definitely essential, since it influences the usability and credibility of any website. The data obtained might not be accurate, but is used only to represent the extent and the level of website download speed and size of the

webpage possessed by the university websites in Saudi Arabia. The webpage analyzer 0.98 is a free tool from Website Optimization utilized to measure the website performance tool and webpage speed analysis to improve a website's performance. In this study, the total size of the website, total size of images, percentage of images in the total size, and the download times have been collected.

Table 6 shows that the expertise factors for websites help users gain more credibility. The majority (83 percent) of the e-learning university websites offer information in the English language. Unfortunately, 95 percent of the English content provided is not exactly the same as the Arabic content. Using a language other than English in the e-learning university websites is rarely found. Besides, one can rarely find information about research activities or research articles on the site. On the other hand, 67 percent of the e-learning university websites appear on the first page of Search Engines such as Google, Yahoo, and Bing. While the majority of the universities have information about "research activities," some of them provide the "project titles" as well.

TABLE VI. CLASSIFICATION OF WEBSITES BY EXPERTISE FACTORS

Expertise factors	Total (Percentage) n=12
The site offers information in more than one language (e.g. English and Arabic).	10 (83)
Information about research activities is given.	3 (25)
Research articles available in the site authored by students and faculty (IR).	3 (25)
The site appeared on the first page of Google search engine results	8 (67)
Yahoo search engine results	8 (67)
Bing search engine results	8 (67)
URL matches the name or acronym of the institute.	12 (100)
The site is large (e.g., not less than five pages).	12 (100)

TABLE VII. CLASSIFICATION OF WEBSITES BY EASY-TO-USE/NAVIGATION FACTOR

Website classification by easy-to-use/navigation factor	Total (Percentage) n=12
The site lets users search for past content (i.e., archives).	9 (75)
The site looks professionally designed.	10 (83)
The site is arranged in a way that makes sense to users.	6 (50)
The site takes a long time to download.	4 (33)
The site is difficult to navigate.	5 (42)
Navigation path.	9 (75)
Site map is given.	1 (8)
Search facility available.	8 (67)
Active and inactive links are clearly visible.	0 (0)
It is easy to navigate logically according to the broader category.	6 (50)
The site has a picture gallery.	8 (67)
It has thumbnail-size or full-size pictures.	4 (33)
Homepage link is available on all subpages.	7 (58)

Table 7 shows that the majority of the websites look like they have been professionally designed (83 percent), and allow

users to search past content (75 percent). However, half of the e-learning university websites in Saudi Arabia have proper structure and logically arranged content (50 percent). Unfortunately, it comes as a surprise that even large websites fail to make active and inactive links clearly visible. The structure of the website and its navigation plays a major role in website credibility, so it is odd to note that only one university website provides navigation tools such as a site map.

The "validity" factor helps to evaluate the importance and role of a website. Table 8 shows that all the websites (100 percent) are maintained without any internal or external advertisements and can "distinguish between link and line of statement" clearly. Also, half of the universities associate with other renowned institutions or organizations. Unfortunately, more than half of the websites (58 percent) maintain a dead link. Further, the top credibility criterion, "when the site was updated," is found among the universities in Saudi Arabia on the main page, whereas it is rarely found for other pages in the website. Also, even large universities do not provide information about the students' achievements, or provide students' records.

TABLE VIII. CLASSIFICATION OF WEBSITES BY VALIDITY FACTOR

Validity factor	Total (Percentage) n=12
Association with other renowned institutions/organizations is mentioned.	6 (50)
Information about students' achievements or records is given.	4 (33)
The site is maintained without any dead links.	7 (58)
Able to distinguish between link and line of statement.	12 (100)
There is information about when the site was updated.	5 (42)
Calendar of events is given.	7 (58)
The site is maintained without any internal/external advertisement	12 (100)

TABLE IX. CLASSIFICATION OF WEBSITES BY RELIABILITY FACTORS

Reliability factors	Total (Percentage) n=12
History of the university is mentioned.	10 (83)
Information about affiliation or accreditation is mentioned.	7 (58)
There is a link to send the complaint.	12 (100)
There is a link to send feedback.	12 (100)
Head of Departments and other faculty information is provided with their qualifications.	6 (50)
The site displays photos of offices or staff members	5 (42)
Information about ISO Certification is provided.	3 (25)
The site has copyright registration, and the information about same is given.	12 (100)
Postal address is given.	12 (100)
Telephone number with STD code is given.	12 (100)
Contact e-mail ID is given.	12 (100)

Table 9 explains that almost all the universities provide the contact details, history, copyright information, “feedback” feature, and give users the ability to make a complaint through their website. Only 50 percent of the universities provide information about ISO Certification.

Table 10 shows that all the websites have graphics or pictures (100 percent), and in the majority (92 percent) of the websites, the background and text color match. Unfortunately, 42 percent of the websites do not have a responsive web design. The responsive design of the websites is important since many websites do not fit into a one-page display. In addition, not all websites provide information about the screen resolution and browser compatibility. Furthermore, in half of the websites, the site’s page format is followed in all the subpages.

TABLE X. CLASSIFICATION OF WEBSITES BY DESIGN FACTOR

Classification of websites by design factor	Total (Percentage) n=12
There are graphics on the site.	12 (100)
There is animation on the site.	7 (58)
The background and font color matches.	11 (92)
Number of visitors is given.	2 (17)
View resolution is suggested.	0 (0)
Browser compatibility is suggested.	1 (8)
Responsive web design.	5 (42)
The site’s page format is followed in all the subpages.	6 (50)

XI. TOOL-BASED RESULTS

In this part of the evaluation, automated assessment tools were used to assess website credibility. The results obtained from the WebPage Analyzer are presented in Table 11.

TABLE XI. CLASSIFICATION OF WEBSITES BY WEBPAGE SIZE AND DOWNLOAD SPEED

Name of the university	Total size of the website	Total size of the images	Percentage of images in total size	Download time at 56K connections
KAU	1885781	930851	55	393.63
IU	301313	451273	98	949.76
IMAUM	284501	61956	6	61.10
KFU	1017485	734151	19	212.18
TAIBUAHU	974124	789597	74	212.74
TU	2155286	1250190	44	441.35
JAZANU	3126833	458363	99	969.56
JU	2461388	2273857	72	514.35
NU	457998	448225	11	93.88
UD	2528954	2039003	84	525.42
SEU	629	0	0	0.53

The web optimization’s WebPage Speed Report has the connection rate starting from 1.44 Mbps to 14.4K. According to the usability guidelines [17], the optimal download time for a homepage is 10 seconds. So, for better download speed, it is suggested to design 45 kb to 55 kb–sized homepages. Table 14 shows that only Arab Open University falls in the <10 seconds category, and only two universities fall under the >100 seconds category. Other homepages of universities in Saudi Arabia fall under the > 200 seconds category. Saudi Arabia has pictures, which occupies nearly 70 to 98 percent of the overall website size.

XII. RESULTS AND DISCUSSION

Table 12 presents a summary of the score for each of the 12 university websites. For the “design” factor, only the SU and KAU website scored more than half of the total, where the rest scored half or less. The SEU, NU, KAU, and IU university websites achieved the highest score (61 percent) for the “easy to use” factor, where the rest of the websites scored less than half. This indicates that half of the university websites have usability problems in their websites. On the other hand, most university websites achieved a high score on “reliability factors.” The JU university website scored the lowest for both the “validity” and “expertise” factors, followed by the NU university website. Three university (KAU, KFU, and SEU) websites achieved full marks in the expertise area.

TABLE XII. CREDIBILITY SCORE

University	Design factor (8)	Easy to use (13)	Reliability factors (11)	Validity factors (7)	Expertise (9)
KAU	6	7	10	7	9
IU	3	7	9	4	7
IMAUM	3	4	8	6	6
KFU	4	3	8	4	9
TAIBUAHU	3	2	7	5	7
TU	3	6	10	4	4
JAZANU	3	4	7	4	3
JU	3	2	6	1	0
NU	3	8	8	3	3
UD	4	5	7	2	6
SEU	6	8	10	7	9

Figure 1 shows the overall scores for each of the 12 university websites. A maximum score of 564 could be achieved, as 47 criteria for each website. The SUE website received the highest score (40), followed by KAU (39). The least credible was the JU website (12). The rest of the university websites achieved half of the score or above.

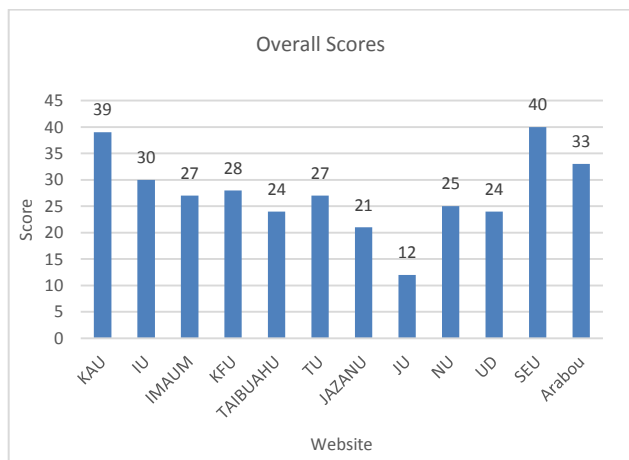


Fig. 1. Overall scores

Figure 2 reveals that, in general, the “easy to use” factor is the most violated web credibility factor among Saudi Arabia universities, followed by the “design factor.” The reliability factor achieved the highest score (75%) among Saudi Arabia universities.

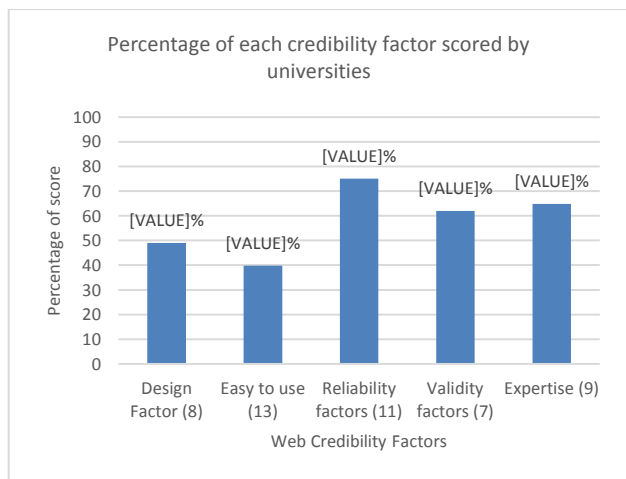


Fig. 2. Percentage of each credibility factor scored by the universities

XIII. SUGGESTIONS

1) A majority of the university websites in Saudi Arabia do not provide any information about students’ achievements or records. Hence, it is mandatory in the future to show student records.

2) A majority of the university websites in Saudi Arabia are not updated regularly and do not indicate the date of the last update. Doing so will add more credibility to the site.

3) E-learning university websites should associate their websites with other renowned institutions and organizations such as The National Center for e-Learning and Distance Learning. This association will be a value added to the website, which will increase its credibility.

4) Many websites do not fit into a one-page display, which is necessary given the large number of different devices used to access websites. Therefore, universities’ website

designs should have a responsive layout. This design will be a value added to the website, which will increase its credibility.

5) The structure of the website and its navigation plays a major role in website credibility. Therefore, universities should provide a site map, navigation path, and internal search engine, which will be a value added to the website, thereby increasing credibility.

6) The page format for the university websites should follow the same style in all the subpages, since this will help prevent user confusion and add credibility to the website.

7) The university websites should focus on maintaining their websites without any dead links, since such links will strongly undermine the websites’ credibility.

8) Normally a website will have many links; therefore, it is critical to help users distinguish between active and inactive links. This approach will be a value added to the website, which will increase its usability as well as its credibility.

9) University websites should make navigation easier by providing a site map, and the internal search engine will be a value added to the website, which will also increase its credibility.

10) Providing more than one language can help enhance the credibility of the websites. However, users sometimes switch from one language to another, so it is critical to make the websites look the same in all languages.

XIV. CONCLUSION AND FUTURE WORK

The purpose of the current study was to examine the web credibility of distance education websites in Saudi Arabia universities. The results of this investigation show that university websites are reliable and are designed well, but violate basic usability, accessibility, and credibility guidelines. Therefore, university websites in Saudi Arabia should be required to be evaluated periodically using established criteria such as usability, accessibility, and credibility. Consequently, this will help the universities improve their websites to meet users’ needs. The current study should be repeated using the user evaluation method. This approach will contribute to understanding how Saudis perceive website credibility. Another possible area of future research would be to investigate which usability and accessibility factors impact negatively on web credibility.

REFERENCES

- [1] R. Babu, A. N. Kumar, and S. Gopalakrishnan, "Credibility of university websites in Tamil Nadu," *DESIDOC Journal of Library & Information Technology*, vol. 29, pp. 16-28, 2009.
- [2] Fogg, J. Marshall, O. Laraki, A. Osipovich, C. Varma, N. Fang, et al., "What makes Web sites credible?: a report on a large quantitative study," in *Proceedings of the SIGCHI conference on Human factors in computing systems*, 2001, pp. 61-68.
- [3] S. Tseng and B. Fogg, "Credibility and computing technology," *Communications of the ACM*, vol. 42, pp. 39-44, 1999.
- [4] B. Fogg, T. Kameda, J. Boyd, J. Marshall, R. Sethi, M. Sockol, et al., "Stanford-Makovsky web credibility study 2002: investigating what makes web sites credible today," Report from the Persuasive Technology Lab, available online at <http://captology.stanford.edu/pdf/Stanford-MakovskyWebCredStudy2002-pre%20lim.pdf>, 2002.

- [5] Al-Shehri, "E-learning in Saudi Arabia: To E or not to E, that is the question," *Journal of family & community medicine*, vol. 17, pp. 147-150, 2010.
- [6] L. Song, J. Lai, and J. Li, "Identifying Factors Affecting Individual Perceived Credibility on SNS," in *Proceedings of the The 3rd Multidisciplinary International Social Networks Conference on Social Informatics 2016, Data Science 2016, 2016*, p. 2.
- [7] K. Oyibo, Y. S. Ali, and J. Vassileva, "An Empirical Analysis of the Perception of Mobile Website Interfaces and the Influence of Culture," in *Proceedings of the International Workshop on Personalization in Persuasive Technology (PPT'16)*, Salzburg, Italy, 2016.
- [8] M. A. A. Rashid, M. N. A. Othman, and M. Z. Othman, "Website Quality as a Determinant of E-government User Satisfaction Level," in *Regional Conference on Science, Technology and Social Sciences (RCSTSS 2014)*, 2016, pp. 157-168.
- [9] Z. Huang and M. Benyoucef, "Usability and credibility of e-government websites," *Government Information Quarterly*, vol. 31, pp. 584-595, 2014.
- [10] N. Wathen and J. Burkell, "Believe It or Not: Factors Influencing Credibility on the Web," *JOURNAL OF THE AMERICAN SOCIETY FOR INFORMATION SCIENCE AND TECHNOLOGY*, vol. 53, pp. 134-144, 2002.
- [11] Alsudani and M. Casey, "The effect of aesthetics on web credibility," in *Proceedings of the 23rd British HCI Group Annual Conference on People and Computers: Celebrating People and Technology*, 2009, pp. 512-519.
- [12] J. F. George, G. Giordano, and P. A. Tilley, "Website credibility and deceiver credibility: Expanding Prominence-Interpretation Theory," *Computers in Human Behavior*, vol. 54, pp. 83-93, 2016.
- [13] J. Nielsen, "Usability 101: Introduction to usability," ed, 2003.
- [14] B. Fogg, "Stanford guidelines for web credibility: A research summary from the Stanford Persuasive Technology Lab," Stanford University. Retrieved August, vol. 10, p. 2011, 2002.
- [15] B. Fogg, C. Soohoo, D. R. Danielson, L. Marable, J. Stanford, and E. R. Tauber, "How do users evaluate the credibility of Web sites?: a study with over 2,500 participants," in *Proceedings of the 2003 conference on Designing for user experiences*, 2003, pp. 1-15.
- [16] Brajnik, "Automatic web usability evaluation: what needs to be done," in *Proc. Human Factors and the Web, 6th Conference*, 2000.
- [17] J. Nielsen, "Designing web usability: the practice of simplicity New Riders Publishing," Indianapolis, Indiana, 2000.

AUTHOR PROFILE

Dr. Khalid Hamad Alomar: Assistant Professor of Information Systems, Faculty of Computing & Information Technology, King Abdul-Aziz University, major in software engineering and Human Computer Interaction. Currently, Dr. Khalid is a vice dean of the Technical Affairs of E-learning and Distance Education at King Abdul-Aziz University.

Implementation of Cooperative Spectrum Sensing Algorithm using Raspberry Pi

Engr. Ammar Ahmed Khan,
Trainee Engineer,
K electric Company, Karachi. Pakistan

Dr. Aamir Zeb Shaikh
Assistant Professor,
Dept. of Electronic Engineering,
NED University of Engg. And Technology, Karachi,
Pakistan

Dr. Shabbar Naqvi
Associate Professor,
Dept. of Computer Systems Engineering,
Baluchistan University of Engineering & Technology
Khuzdar, Pakistan

Dr. Talat Altaf
Professor,
Dept. of Electrical Engineering,
Sir Syed University of Engineering & Technology,
Karachi, Pakistan

Abstract—A novel cooperative spectrum sensing algorithm is implemented and analyzed using Raspberry Pi. In the proposed setup, Nokia cell phone is used as a spectrum sensing device while Raspberry Pi functions as a FC device to collect sensing results from local sensing devices. The investigation results of the proposed setup show significant improvement in detection performance as compared to local spectrum sensing techniques. Furthermore, results show a successful communication between sensing nodes and FC.

Keywords—Cooperative Spectrum Sensing; Cognitive Radio; Fusion Center; Raspberry Pi

I. INTRODUCTION

With the success of 4G technologies in the cellular market, more and more broadband services emerge[1]. Such fast communication has ushered in a new trend, in innovation of services offered by the service provider that brings bandwidth-hungry services in the form of ubiquitous communication resources [2]. The asynchronous nature of these services is present but they cannot be considered as real time if it weren't for the constant availability of the communication spectrum and bandwidth which is getting more complex and tedious to manage as service providers introduce more and more services that have to be accommodated on the same channel. The constantly increasing demand for bandwidth and its effective utilization is what drove the robust de-centralized 2G network to evolve into a powerful centralized 4G network. The race for more bandwidth and higher data rates continues as different research efforts concentrated towards finding more ways to increase available bandwidth per user are being done all over the world. One technology, which promises to solve these issues through opportunistic spectrum access, is cognitive radio technology [3]. Thus, more users can be accommodated on the same RF channels subject to absence of primary users. This idea results in thinking beyond the limits of a designated bandwidth and channel. The implementation of the evolutionary idea (of exploiting the spectrum in secondary manner) requires a significant amount of research and

consideration towards devising control protocols (for secondary users) that are solely designed for the purpose of coordination and update of the participating network nodes in an opportunistic network[4].

Detection techniques are employed in an opportunistic network (5G of cellular networks) to monitor a channel's usage by primary users and classify the usage in three classes; Black area i.e. channel that is exhausted in data rate and bandwidth due to traffic, a Gray area i.e. channel carrying medium traffic and finally, white area indicating a channel carrying little or no traffic at all [5]. Experimental and statistical studies show that standard spectrum usage and idle state is enough to justify cognitive radio communications over primary licensed channels[6].

Cooperative schemes involve cooperation among sensing nodes to improve performance especially under fading and shadowing [7-9]. Additionally, multiple antenna based sensing nodes can also produce improvement in detection performance [10-12]. Cooperative algorithms can be distributed into three categories i.e. centralized [7, 13-15], decentralized [7, 16, 17] and relay assisted [7, 18-21].

In centralized detection algorithms, a central node, also known as fusion center (FC), supervises and manages the detection. FC instructs the sensing nodes to sense a particular spectrum band and submits the sensing results. The results can be in form of complete sensing energies or one bit decisions showing activity of PU or its absence. The sensing results in form of likelihood ratios can be combined using soft combination strategies i.e. equal gain combining (EGC), maximal ratio combining (MRC), square law combining (SLC) and selection combining (SC) approaches[22]. On the other hand, one bit decisions can be fused through hard decision combining strategies. These include OR, AND, n-ary [13]. After computing the final outcome of the presence or absence of PU, FC broadcasts the decision regarding to SU. The transmission of sensing data from sensing nodes to FC

and the broadcast information from FC to nodes is accomplished through control channels.

Decentralized detection scheme refers to the set of algorithms where cognitive sensors group themselves based on distribution algorithm and combine their results and communicate among themselves regarding presence or absence of white spaces. This set of algorithms does not use any FC to manage the RF sensing and management task [17].

Due to dynamic wireless channel conditions, the sensing channel (between sensing node and primary user) or control channel (channel between sensing node and FC) may not be an ideal and may produce deteriorated. In such situations, relay assisted sensing can provide improved sensing performance [18, 19].

We implement a co-operative spectrum sensing strategy on Raspberry pi board. The board functions as a FC where all the users will submit the sensing results and this center will combine the results to compute the final decisions regarding presence or absence of a PU. The rest of the paper is organized as follows: Section II presents a summary of the Raspberry pi Linux ARM board, Section III presents the setup of proposed test scenario, Section IV presents local spectrum sensing model, section V presents the simulation results and discussion, Section VI concludes the paper.

II. EMBEDDED ARM LINUX BOARD

The Raspberry Pi is an embedded ARM Linux board that accompanies the peripherals on miniaturized model [23]. The board is used to simulate multiple logic blocks that are otherwise termed as software processes throughout the rest of the paper. Each software process runs in the main memory of the Linux kernel of the board alongside the other processes, which makes it a preferable choice for prototyping advanced applications with ranging requirements. The interfaces of board makes it easier to expand its functionality towards wireless sensor applications, industry process automation testing, data logging and recording through various device ports, ADC functionality and much more[23, 24]. In this paper, it's UART; USB and Ethernet interfaces are used to accompany several wired and wireless communication media. The ability to make changes in the software both remotely and on-site makes the project's architecture, quite flexible for future enhancements in the form of upgrades and software patches. Since the Raspberry Pi gives provision for expansion of hardware, each section in the implementation also demonstrates how the functionality accompanied by the software processes can be enhanced into an actual physical experiment through hardware rather than being emulated by software to give real-world results. However, the software processes are designed to be as close in proximity to the real-world hardware processes as much as possible[23, 24].

III. SETUP OF TEST SCENARIO

This section presents the proposed implementation of cooperative spectrum sensing strategy using Raspberry Pi board.

A centralized cooperative spectrum sensing based algorithm is implemented using Raspberry Pi as FC. The employed framework consists of primary user PU and several Cognitive Radio (CR) users, the primary licensed channel of interest and a control channel for reporting the results. This is to be simulated in a soft environment in either completely software defined processes or semi software defined processes.

The proposed scenario is a semi software defined process where the outcome of cooperative sensors will be simulated by the output of a software process that computes the receiver operating curves. The result will be a flag for wireless channel i.e. idle or busy. The FC will be the central router that will carry out routing functions as it is designated as the gateway. The CR users will be TCP/IPv4 network nodes connected to a LAN IP network and will carry out communication to simulate a local Base Transceiver Station and surrounding mobile station. The diagram illustrated in Fig. 1 depicts the proposed setup.

Another way to employ this setting is to replace the different devices on the LAN IP network by creating logical users communicating with the FC through local ports on the machine that is running the FC as shown in Fig. 2.

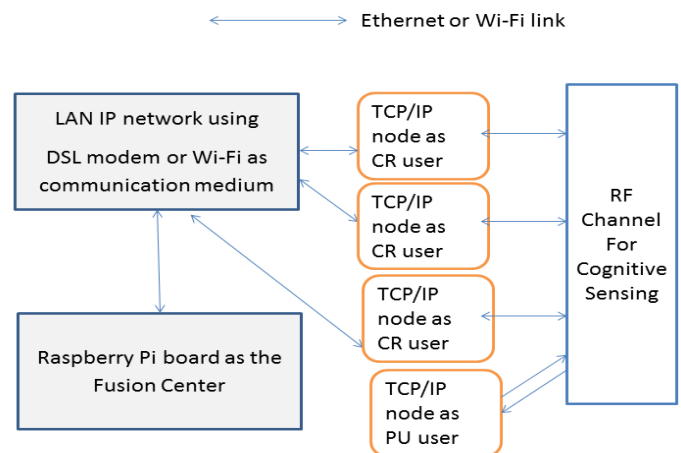


Fig. 1. Depicts the implementation setup for proposed sensing algorithm

One other change that can be made in the proposed setup without compromising the infrastructure and layout of the testing scenario is to do away with the separate TCP/IP nodes and designate the CR users as separate software processes running on the Raspberry Pi. The CR users will be software logic emulated modules that will run simultaneously on the Raspberry Pi Linux board that use TCP/IPv4 to communicate with the FC by using an IP address and port combination called a "socket". In that way, each of the CR users will have same IP as the fusion center or the Linux board but with unique port number. This setup resembles a standard cellular Base Transceiver Station (BTS) [25]. To further explain this model, the layout of the testing process components is presented in the Fig. 2.

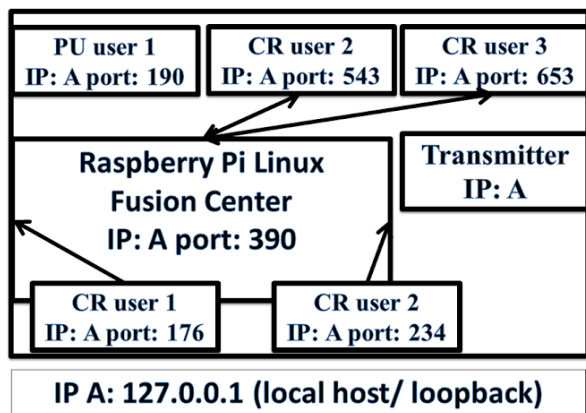


Fig. 2. Proposed setup by using Logical Users

The software processes that emulate the CR users will collect RF signal samples, compute hypothesis testing rule and transmit one bit of information to the FC. The FC will combine the results using hard combination rule ‘OR’ to come up with a final decision for a specific frequency band. The hard decision combining process will help in efficiently utilizing control bandwidth[26].

The communication between all the processes is achieved through sockets. Hence, communication can be carried out between the nodes and the FC in form of IP packets or more specifically, TCP packets as IP packets can’t carry out unique communication streams between the nodes on their own, the port number to be accommodated will be encapsulated in the TCP or UDP packet. In the proposed setup, an application layer protocol such as HTTP can also be used to carry out communication between the nodes but we wish to restrict the packet processing at the transport layer. The TCP packets received by a node will be processed by their respective software modules accordingly.

However, since the RF channel to be sensed also has to be emulated, hence we will list it as a node and assign software process to it so that it can emulate an RF channel behavior. Since the channel is being sensed by all CR users except the fusion center, this broadcast behavior of the channel can be emulated by broadcasting TCP packets of the channel’s state values to every software process or node except the FC. The software process or nodes that receive the TCP packets by the channel will read the channel values, perform digital signal processing on it which is optional and send it to the fusion center as TCP packets.

IV. PROPOSED SPECTRUM SENSING MODEL

In this section, we present the simulation setup for local spectrum sensing devices. Cellular phones and other wireless devices are assumed to work as cognitive sensors while Raspberry Pi is assumed to work as FC. A decision regarding presence or absence of PU is computed by CR. Furthermore, one bit decisions are also transmitted to FC for the computation of global results. The detection performance of

local sensors is also compared with cooperative decisions. After computation of global probability values of detection and false alarm, the results are broadcast via common control channel to all the CRs so that unused spectral bands could be utilized and occupied bands could be avoided to prevent PU from harmful interference of secondary activity. The objective of the proposed setup is to implement the sensing logic in software and communicate that to the FC node on real-time basis to the Raspberry Pi which is serving as a FC.

The binary hypothesis for local CR sensor can be formulated as:

$$r(n) = \begin{cases} n(n) & ;H_0 \\ x(n) & ;H_1 \end{cases} \quad (1)$$

In above equation, r shows the observation of received signal. Under H_0 , cognitive user detects the absence of primary user. This condition is represented by collection of Laplace distribution. Whereas under H_1 , the cognitive user collects signal samples that are drawn from Gaussian distribution, representing the presence of PU activity in the sensing band. The proposed setup of binary hypothesis is taken from [27].

Thus, CR senses the presence of non-Gaussian noise i.e. impulsive noise that follows the following PDF.

$$p(r | H_0) = \frac{1}{2} \exp(-|r|) \quad (2)$$

This probability distribution is also known as Laplace. The location parameter for this distribution is assumed as, $\mu = 0$ while scale parameter, $b = 1$. This PDF is also called double exponential distribution. Under alternative hypothesis, the CR results in following PDF.

$$p(r | H_1) = \frac{1}{\sqrt{2\pi}} \exp\left(-\frac{r^2}{2}\right) \quad (3)$$

Using Neyman-Pearson Lemma, decision statistic can be computed using following equation:

$$\Lambda_r(r) = \frac{f_r(r | H_1)}{f_r(r | H_0)} \quad (4)$$

Thus, detection probability can be derived using Neyman-Pearson Lemma:

$$P_D = 1 - 2Q(-\ln(1 - P_{FA})) \quad (5)$$

The above equation relates detection probability with false alarm rate of spectrum sensor. It is used by local sensors to produce probability values for local spectrum sensor. After computing the decision statistics, one bit information will be sent to FC to come up with global values of detection and false alarm. Authors in [14] use OR based combination strategies to compute cumulative decisions.

$$P_c = \sum_{i=a}^b \binom{b}{i} (P_l)^i (1-P_l)^{b-i} \quad (6)$$

$$Q_c = \sum_{i=a}^b \binom{b}{i} (P_F)^i (1-P_F)^{b-i} \quad (7)$$

In above equations, P_c represents cumulative probability of detection while Q_c shows the cumulative decision of false alarm based on Hard decision combining strategy at the FC.

V. PERFORMANCE EVALUATION AND RESULTS

In this section, we present the detection performance of proposed cooperative spectrum algorithm in the form of receiver operating curves (ROC). In the proposed setup CR enabled devices sense the RF spectrum for searching the unused spectral bands. After computing the decisions locally, all the sensing devices will transmit a hard decision to the FC in the form of '1' for the presence of PU and '0' for the absence of PU.

Fig. 3 shows the implementation of the proposed setup. Fig. 4 compares the local detector performance with global on FC. For 0.2 false alarm probability, local detector results in detection probability of less than 0.2 while cooperative detector installed on Raspberry pi computes almost 0.4. Thus, the FC decision maker improves the detection performance more than 100%. Similarly for other values of false alarm, detection performance of FC is better than the local detector. Additionally, FC exploits hard decision combiner that consumes lesser resources in comparison to soft decision combination strategies. After computing the decisions in terms of detection and false alarm probabilities, the results will be broadcast to secondary devices so that they may be able to use specific bands that are unused by PU.



Fig. 3. Proposed Setup

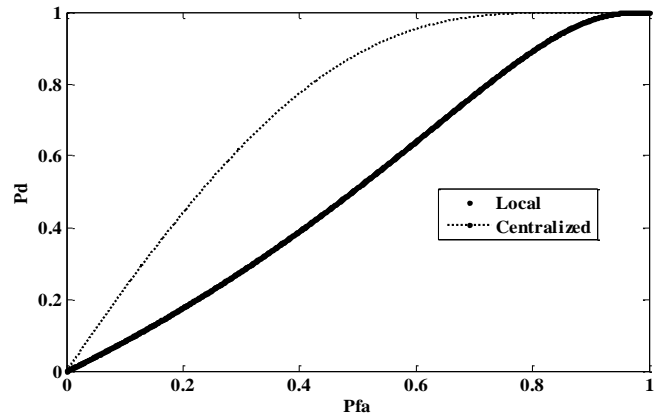


Fig. 4. Comparison of Local and Cooperative Detector

Fig. 5 depicts the successful detection of devices connected with Raspberry Pi, acting as a FC for the proposed spectrum sensing setup.

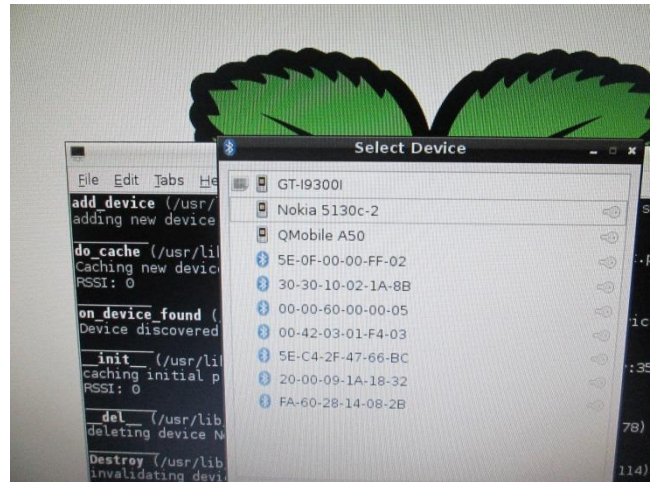


Fig. 5. Shows the number of devices detected by Raspberry Pi

Fig. 5 selects the wireless device, that is Nokia 5130c-2 for the transfer of data from FC. Furthermore, many devices can be selected that can be connected with the FC for the transmission of decision. This feature enables the FC to confirm the device before starting transmission for the purpose of gathering RF sensing data or broadcasting the final probability values of detection and false alarm.

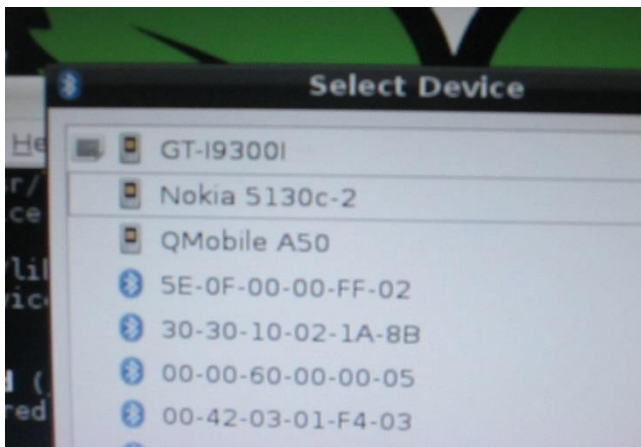


Fig. 6. Shows the selection of Nokia 5130c-2 device

Fig. 6 shows data collected by several cognitive devices to the FC and also the result outcome of FC. Based on the hard decision combining technique, FC decides the RF channel as idle by deciding the presence of noise only while the channel is tagged as Busy on computing the presence of PU activity.

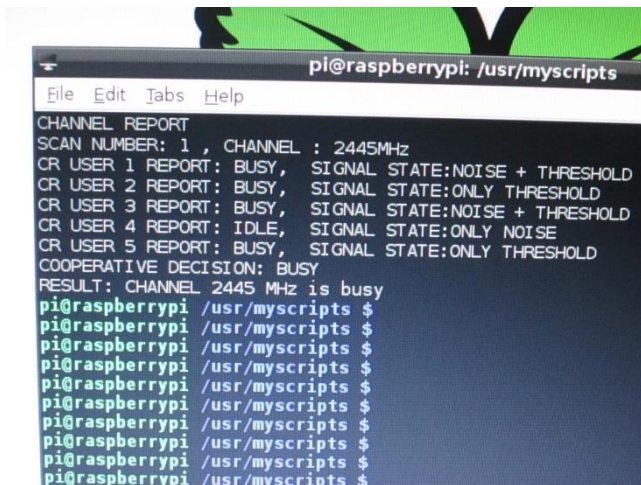


Fig. 7. Shows the report sent by FC to the sensing node regarding the channel report of 2445 MHz

VI. CONCLUSION

A cooperative spectrum sensing algorithm is implemented on Raspberry Pi board. The proposed cooperative architecture has many benefits in comparison to separate and distributed spectrum sensors. The simulation results also show an improved performance of cooperative detector. Additionally, the emulation results of Raspberry Pi are also presented.

ACKNOWLEDGEMENTS

The authors are highly thankful to the NED University of Engineering & Technology that provided all the required resources that were necessary for the successful completion of this paper.

REFERENCES

[1] M. J. Chang, et al., "WiMAX or LTE: Who will lead the broadband mobile Internet?," *IT professional*, pp. 26-32, 2010.

[2] M. S. Obaidat, et al., *Pervasive Computing and Networking*: Wiley, 2011.

[3] B. A. Fette, *Cognitive radio technology*: Academic Press, 2009.

[4] Y. Xiao and F. Hu, *Cognitive radio networks*: CRC press, 2008.

[5] S. Haykin, "Cognitive radio: brain-empowered wireless communications," *Selected Areas in Communications, IEEE Journal on*, vol. 23, pp. 201-220, 2005.

[6] D. Cabric, et al., "Implementation issues in spectrum sensing for cognitive radios," in *Signals, systems and computers, 2004. Conference record of the thirty-eighth Asilomar conference on*, 2004, pp. 772-776.

[7] F. Akyildiz, et al., "Cooperative spectrum sensing in cognitive radio networks: A survey," *Physical communication*, vol. 4, pp. 40-62, 2011.

[8] Z. Shaikh and T. Altaf, "Collaborative Spectrum Sensing under Suburban Environments," *International Journal of Advanced Computer Science & Applications*, vol. 4, 2013.

[9] Singh, et al., "Cooperative spectrum sensing in multiple antenna based cognitive radio network using an improved energy detector," *IEEE Communications Letters*, vol. 16, pp. 64-67, 2012.

[10] Z. Shaikh and T. Altaf, "Performance Analysis of Correlated Multiple Antenna Spectrum Sensing Cognitive Radio," *International Journal of Computer Applications*, vol. 50, 2012.

[11] E. Biglieri, et al., *Principles of cognitive radio*: Cambridge University Press, 2012.

[12] V. R. S. Banjade, et al., "Performance analysis of energy detection with multiple correlated antenna cognitive radio in Nakagami-m fading," *IEEE Communications Letters*, vol. 16, pp. 502-505, 2012.

[13] E. Visotsky, et al., "On collaborative detection of TV transmissions in support of dynamic spectrum sharing," in *New Frontiers in Dynamic Spectrum Access Networks, 2005. DySPAN 2005. 2005 First IEEE International Symposium on*, 2005, pp. 338-345.

[14] Ghasemi and E. S. Sousa, "Collaborative spectrum sensing for opportunistic access in fading environments," in *New Frontiers in Dynamic Spectrum Access Networks, 2005. DySPAN 2005. 2005 First IEEE International Symposium on*, 2005, pp. 131-136.

[15] R. Viswanathan and P. K. Varshney, "Distributed detection with multiple sensors I. Fundamentals," *Proceedings of the IEEE*, vol. 85, pp. 54-63, 1997.

[16] Z. Li, et al., "A cooperative spectrum sensing consensus scheme in cognitive radios," in *INFOCOM 2009, IEEE, 2009*, pp. 2546-2550.

[17] Sun, et al., "Cluster-based cooperative spectrum sensing in cognitive radio systems," in *Communications, 2007. ICC'07. IEEE International Conference on*, 2007, pp. 2511-2515.

[18] G. Ganesan and Y. Li, "Cooperative spectrum sensing in cognitive radio, part I: Two user networks," *Wireless Communications, IEEE Transactions on*, vol. 6, pp. 2204-2213, 2007.

[19] G. Ganesan and L. Ye, "Cooperative spectrum sensing in cognitive radio, part II: Multiuser networks," *Wireless Communications, IEEE Transactions on*, vol. 6, pp. 2214-2222, 2007.

[20] W. Zhang and K. B. Letaief, "Cooperative spectrum sensing with transmit and relay diversity in cognitive radio networks-[transaction letters]," *Wireless Communications, IEEE Transactions on*, vol. 7, pp. 4761-4766, 2008.

[21] S. A. Astaneh and S. Gazor, "Relay-assisted spectrum sensing," *IET Communications*, vol. 8, pp. 11-18, 2014.

[22] J. Ma, et al., "Soft combination and detection for cooperative spectrum sensing in cognitive radio networks," *Wireless Communications, IEEE Transactions on*, vol. 7, pp. 4502-4507, 2008.

[23] E. Upton and G. Halfacree, *Raspberry Pi user guide*: John Wiley & Sons, 2014.

[24] M. Richardson and S. Wallace, *Getting started with raspberry PI*: "O'Reilly Media, Inc.", 2012.

[25] Mehrotra, *GSM system engineering*: Artech House, Inc., 1997.

[26] E. Axell, et al., "Spectrum sensing for cognitive radio: State-of-the-art and recent advances," *Signal Processing Magazine, IEEE*, vol. 29, pp. 101-116, 2012.

[27] M. D. Srinath, et al., *Introduction to statistical signal processing with applications*: Prentice-Hall, Inc., 1995.

A Centralized Reputation Management Scheme for Isolating Malicious Controller(s) in Distributed Software-Defined Networks

Bilal Karim Mughal

Department of Computer Science
Bahria University
Karachi, Pakistan

Sufian Hameed

Department of Computer Science
National University of Computer and Emerging Sciences
Karachi, Pakistan

Ghulam Muhammad Shaikh

Department of Computer Science
Bahria University
Karachi, Pakistan

Abstract—Software-Defined Networks have seen an increasing in their deployment because they offer better network manageability compared to traditional networks. Despite their immense success and popularity, various security issues in SDN remain open problems for research. Particularly, the problem of securing the controllers in distributed environment is still short of any solutions. This paper proposes a scheme to identify any rogue/malicious controller(s) in a distributed environment. Our scheme is based on trust and reputation system which is centrally managed. As such, our scheme identifies any controllers acting maliciously by comparing the state of installed flows/policies with policies that should be installed. Controllers rate each other on this basis and report the results to a central entity, which reports it to the network administrator.

Keywords—SDN; controller security; malicious controllers; trust; reputation

I. INTRODUCTION

Software-defined networks (SDN) separate the data plane and control plane from each other, contrary to traditional networks in which both are embedded in the same hardware piece [1]. In SDN, a network administrator has to implement a policy only in the controller, which is then replicated across the network's forwarding devices [2]. Despite immense popularity and ever increasing growth in deployment of SDNs, much research is needed as to whether SDN can be deployed on a large scale, that too with all the security [3].

Various researchers including [4, 5] acknowledge control layer as a highly vulnerable section of the SDN, which, if compromised, can result in losing entire network to a malicious entity. However, the models proposed for deploying SDNs so far do not answer one basic question: how to identify malicious or rogue controllers within a network, and how to prevent them from causing damage [6].

In this paper, we propose a scheme to enhance controller security in a multi-controller environment. Our framework identifies malicious/rogue controllers by finding out if a mismatch exists between the flows which should be installed in the switches by the controllers and those which are actually installed. We make use of a centralized trust and reputation scheme inspired by [7], in which controllers are rated positive or negative by other controllers according to their performance. The results are then reported to a central entity called the Trust Collector which aggregates the results and passes them

on to the network administrator. Earliest detection of rogue controllers through such reputation management will ensure the isolation of rogue controllers before they can damage the network.

For enabling controllers to rate each other, we modified the Ryu controller code [8]. We also introduced two novel components, Policy Distributor and Trust Collector for managing trust and reputation, and for providing a benchmark to controllers against which they can compare the installed flows. The scheme was implemented in Emulab Network Emulation Testbed [9]. Initial evaluations show that our scheme is successful in identifying rogue controllers.

The rest of the paper is organized as follows. In Section 2, we briefly review the security threats to SDN controllers, and state-of-the-art. Section 3 discusses our architecture, components and the scheme flow. Section 4 talks about the implementation and evaluation. Section 5 sheds light on the need of introducing the central components. Section 6 concludes this paper after discussing the direction of our future work.

II. LITERATURE REVIEW

In SDN, the controllers are an easy target and are open to exploitation through unauthorized access. If the controller platform is not secure, an active adversary can hijack the network by deceiving the network devices. DNS servers are prone to these kind of attacks, shown by [10]. An entire network can be brought down if an adversary gains control of the network by hijacking the controller in this way [11].

Several threat vectors exist when it comes to security of the control plane. These include attacks on control plane communications, i.e. controller-controller or controller-switch communications. Apart from this, one should also be vigilant about certain higher-level applications which have access to network information through controller APIs because such applications can reprogram a network without causing much of a suspicion [11]. A major challenge here is to differentiate between the legit and malicious applications to allow/deny access. The authors in [5] argue that commonly used intrusion detection systems (IDS) might not prove to be completely useful in securing the controllers from misuse, as it may be difficult to ascertain which events resulted in the malicious behavior, and whether it should be labeled as malicious at all.

There are several studies which have tried to resolve controller security problems in SDN. For example, the Security-Enhanced Floodlight (SE-Floodlight) controller provides a mechanism for authentication of applications, role-based authorization for avoiding conflicts in flow-rule insertion, and conflict detection and resolution [12]. It does not, however, address one core problem, that is, isolating a compromised controller in a distributed environment.

SDNs are logically centralized networks in which a single controller maintains multiple switches and other network devices, but in case of a man-made or technical mishap, this proves to be a single point of failure too [13]. To overcome this, distributed architectures like DISCO [14] have been proposed in which multiple controllers manage the network for better resilience and faster network management. Some network architectures such as HyperFlow [15] and Onix [16] distribute the control plane physically, but keep it logically centralized.

The distributed systems described above, however, do not take into account the security aspects. For example, they do not provide a comprehensive framework for identifying and isolating a malicious controller out of several others. On the other hand, so-far proposed schemes for securing the control layer do not discuss the feasibility of their solutions in the distributed environments. To the best of our knowledge, no concrete work has been done to resolve this problem, and therefore this is an open challenge for research.

III. ARCHITECTURE

The objective of our work is to develop a framework for singling out a malicious controller in distributed SDN. We achieve this by employing a trust and reputation scheme among controllers. We are working on a distributed controller environment in which the secondary controllers are deployed not as a dormant backup but as active load-balancers. However, for either use case, the controllers need to have access to all switches, so that in case one controller goes down due to an act of sabotage or for any other reason, the other controllers can prevent disruptions in network environment.

In our architecture, controllers rate each other after verifying the policies installed by them in switches against the policies that are dictated by a central entity called the Policy Distributor. The Policy Distributor is a component introduced by us for consistent policy enforcement throughout the distributed SDN. The second component specific to our scheme is the Trust Collector, which asks controllers to rate their peer controllers and takes ratings from them. The code for both the components was written in Python and they were deployed as separate components. We describe the working of individual components below.

A. Components

1) *Policy Distributor*: It contains all of the policies that are to be installed by the controllers. Conventionally, a network administrator defines the policies directly into the controller, but in our scheme, a network administrator defines the policies in the Policy Distributor. These policies are then periodically pushed to all of the controllers in the network. This ensures network-wide consistency as there is only one place where

the policies need to be defined, thereby centralizing the administration of a distributed SDN. We used a HashMap for policy assignments which takes arguments (Controller, Policy). Copy of this HashMap can be retrieved by all controllers when needed, but every controller installs it in only the switches directly under its control.

This helps them later in verifying whether other controllers have installed correct policies or not, and is also good for fault tolerance; in case a controller goes down, other controllers will automatically know which flow rules were in effect in the affected controller. It is assumed that the Policy Distributor is secure and protected from hijacking, and any changes made to it are purely intentional.

2) *Trust Collector*: It is another central entity which is responsible for trust management. After the Policy Distributor has pushed the policies to the controllers, the Trust Collector after a specific duration, asks all the controllers of the network for their opinion about their peer controllers. Specifically, it asks other controllers to check whether their peer controllers have installed the policies in switches as dictated by the Policy Distributor, or they have (maliciously) installed different policies. The controllers then initiate their respective Policy Checkers (discussed in next section) and fetch the flow tables from the switches. If a controller finds any discrepancy between the flow tables fetched from switches and the policies sent by the Policy Distributor, it reports the results to the Trust Collector. We use the flow tuple format to specify and compare policies, e.g. policy1: {srcIP='8.8.8.8', action='drop'}.

3) *Policy Checker*: We introduce another simple component called the Policy Checker, integrated in the Ryu controller. The primary purpose of Policy Checker is to simply probe the switches to fetch the installed policies, so that they can be compared with the policies sent out by the Policy Distributor.

B. Trust Calculation

The mechanism of trust collection in our scheme is based on PET Model [7], however, we have made necessary changes to their method to suit our environment. The PET model is designed for strict P2P environments where there is no central entity, and the nodes are dependent on ratings obtained from each other to calculate trustworthiness. In our scheme, however, we have a central entity called the Trust Collector, which collects individually calculated trustworthiness values from all controllers and presents it to the operator for review.

When the Trust Collector asks controllers to find out any mismatch between policies installed and policies that had to be installed, the controllers start probing the switches. At this point, all the controllers simultaneously act as recommender and recommendee. A recommender who finds out a mismatch flags the recommendee based on following function.

$$h(x) = \begin{cases} S_1, x = G, S_1 > 0 \\ S_2, x = B, S_2 < 0 \end{cases} \quad \text{and} \quad |S_2| > S_1$$

Where G and B are the constants used for match and mismatch, respectively. In case of a match, a score of S1 is output, whereas in case of mismatch, S2 is given as output. The rating output by the hash function is then used in calculating the recommendation Er. Note that we use G to represent good

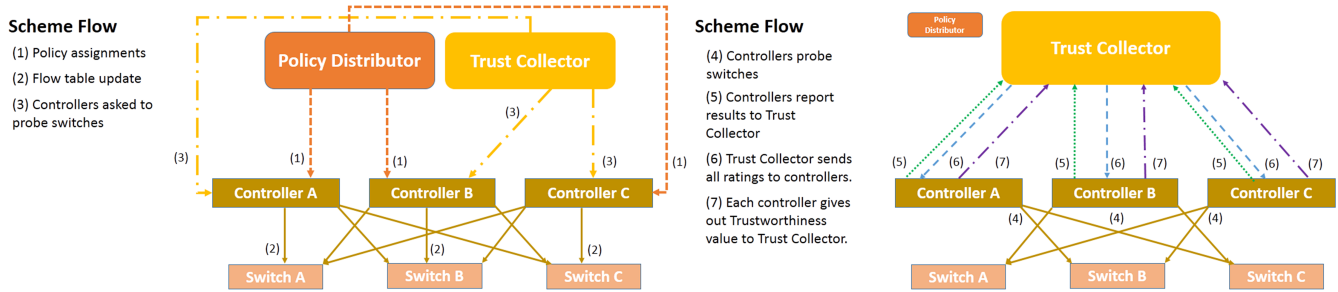


Fig. 1. Flow diagram for the entire scheme. Shows message exchange flow between switches, controllers, trust collector, and policy distributor.

behavior, similar to PET model [7], but we use B to represent bad behavior while PET model uses it to represent byzantine behavior.

Figure 2 shows the different parameters that go in to calculation of the trustworthiness value. The recommendation value E_r for a controller A is the average value of recommendations that other controller have given to A. Therefore, in order to calculate E_r for, let's say, controller A, controller B will need access to recommendations that other peers have given to A. The Trust Collector helps here by allowing all controllers to send their calculated recommendations about other controllers to itself. Once all recommendations are at the Trust Collector, each controller can then retrieve the (global) accumulation of all recommendations about any given controller from the Trust Collector.

The second thing the controllers need to calculate is the interaction-derived information I_r . In the PET model, I_r is a special recommendation given by a peer A to other peers based on how good or bad of a service those other peers have provided to only peer A, that is, unlike E_r , I_r does not take into account the recommendations from other peers.

Our controller environment is slightly different from the pure P2P environment assumed by the PET model, since in our environment no controllers directly provide any services to other controllers as in a P2P system, so we changed the meaning of I_r such that I_r is now each controller's individual recommendation about its peer controllers based on whether they have installed policies in the switches correctly or not. Thus I_r is an individual controller's own opinion about a given controller A and it does not take into account what other controllers say about A. This saves I_r from getting overwhelmed if a majority of controllers (maliciously) rate controller A as negative.

The E_r and I_r values are finally used to calculate the reputation Re in a weighted fashion such that,

$$W(E_r) = 0.2$$

$$W(I_r) = 0.8$$

The values are based on suggestions from the PET model. A higher value for $W(E_r)$ would mean that we put a lot of trust in the environment but since we consider our environment risky, therefore we have not set a very high value.

The purpose of reputation Re is to accumulate the past and current values of a controller's performance. That is, the

reputation value is the historical accumulation for a recommender's past behavior from the recommender's viewpoint. It will reflect the overall quality of the recommender for a long time period. For example, if a controller which is being rated has installed 99 correct policies but 1 incorrect policy due to, let's say, a software bug, then that controller's reputation doesn't immediately become completely negative. Rather, the final reputation value is calculated through a combination of current and past recommendations from both individual and collective group of controllers.

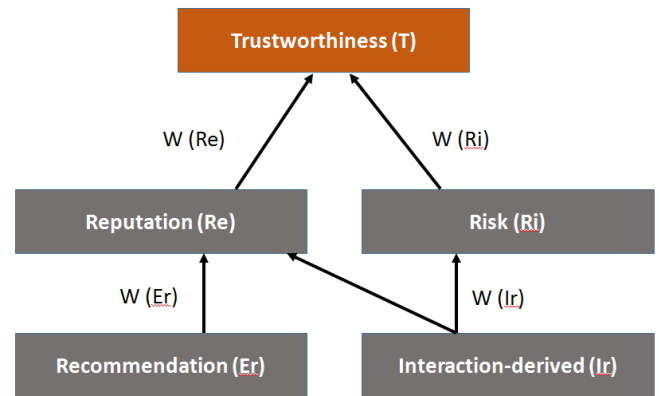


Fig. 2. Trust calculation model based on [7]. Nodes collect final trustworthiness value based upon number of factors.

Since I_r gives us the personalized view of a node for its peers, therefore the PET model uses only I_r to calculate the risk value R_i for the network. This results in each controller having its own R_i value that represents its own view of the risk in the network.

The reputation Re and risk R_i values are used by the controllers to calculate trustworthiness T values. Each controller thus generates one trustworthiness value that gets collected by the Trust Collector. On PET model's suggestions, we set the weight of reputation and weight of risk to 0.5 in all controllers for calculating the T value such that:

$$W(Re) = 0.5$$

$$W(R_i) = 0.5$$

The Trust Collector accumulates all these trust values it receives from controllers. It then averages all the trustworthiness values, and notifies the network administrator as to

which controllers are malicious since their trustworthiness value was very low or which controllers are good since their trustworthiness value was high.

C. Scheme Overview

In presence of the Policy Distributor, Trust Collector, and Policy Checker integrated within the controllers, our scheme progresses as follows:

We have a network with three controllers and three switches, such that each controller directly administers two switches. The network is in a full mesh setting, so that all the controllers have access to all switches for backup. Assuming that the network has just booted, and the switches do not have any flow rules as of now. A network administrator defines a policy in the Policy Distributor that all traffic originating from IP address 8.8.8.8 is to be dropped.

After some time, the Trust Collector asks controllers to probe all the switches to find out if there is a mismatch between installed policies, and those dictated by the Policy Distributor. The controllers then run their respective Policy Checkers over the network. As shown in Figure 1, each controller probes switches managed by other controllers too.

When the probe has finished and matches/mismatches have been found, each controller gives out a ratings map for every other controller, which contains good or bad scores for them. Three controllers will generate three such maps, such that in case of three controllers A, B and C, controller A will report about B and C, controller B will do it for A and C, and controller C will do it for A and B. All of these ratings are sent to the Trust Collector.

Once the Trust Collector has received the reports from all of the controllers, it combines all of them and sends back to all of the controllers, so that A will receive reports of B and C about each other, B will receive reports of A and C, and C will receive reports of A and B. Each of the controllers now has information about what its peer controllers think about other controllers. This information helps a controller in calculating average value of recommendation (E_r) for other controllers.

E_r combined with I_r are used to calculate reputation R_e . Combined with risk R_i , the R_e is used to calculate final trustworthiness as:

$$T = \text{Reputation } (R_e) * \text{Weight of Reputation } [W (R_e)] + \text{Risk } (R_i) * \text{Weight of Risk } [W (R_i)]$$

Each controller outputs trustworthiness values for other controllers. The results are fed to the Trust Collector, which aggregates the results from all the controllers and shows it to the network administrator for review.

IV. EVALUATIONS

We built a prototype implementation in Python for Trust Collector, Policy Distributor, Policy Checker and ratings mechanism of our controllers. The Policy Checker and ratings mechanism were integrated in Ryu controller, whereas the Policy Distributor and Trust Collector were deployed as separate modules. Small number of controllers and OpenFlow switches were also deployed. We used the Emulab network evaluation testbed.

In the topology, we used one Policy Distributor, one Trust Collector, and varying number of controllers and switches were deployed for different evaluations. For the scalability tests, we used simulated switches and increased the number of controllers to up to 15, and the number of switches to up to 30. The configurations used are shown in Table 1 and the results are shown in Figure 3.

TABLE I. SHOWS THE DIFFERENT NETWORK CONFIGURATIONS WE CREATED OF CONTROLLERS AND SWITCHES

Configuration	Controllers	Switches	Malicious controllers
Config 1	5	10	2
Config 2	10	20	4
Config 3	15	30	6

For our correctness evaluations, we deliberately triggered one or more of the controllers to randomly install a malicious policy and then ran the rating mechanism in the controllers. All other controllers were able to detect the controller which installed wrong policy, and rated it negative. The Trust Collector aggregated the ratings from all these controllers. For all the tests we conducted, the scheme was always able to find the malicious controller(s) with zero false positives or false negatives.

Figure 3 shows the time taken to perform the entire process of rating and trust collection as the number of controllers involved in the process is increased. As seen from the graph, the time shows a linear pattern of increase and our scheme is able to work fast in finding out malicious controller.

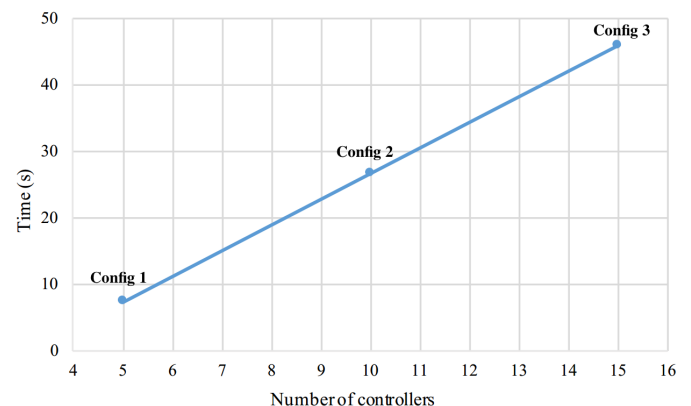


Fig. 3. Scalability of the scheme: Shows the time taken in seconds for our entire rating and trust collection scheme to finish as the number of controller is increased.

The scheme defines a specific number of message exchanges (as shown in Figure 4) between the different components in the system, i.e. the controllers, switches, Trust Collector, and Policy Distributor. We use a centralized graph database, Neo4j [17], which serves as a 'noticeboard' for communication using the publish-subscribe mechanism. This saves network bandwidth since the Policy Distributor or Trust Collector do not have to broadcast messages containing commands such as 'startTrustCalculation', a command meant to be sent to all controllers to start the trust calculation process, to all controllers. Instead, the Trust Collector can publish this command by writing it in the centralized database and the controllers can read it from there. Thus only one message

exchange has to be used instead of a broadcast of messages to all controllers.

Neo4j has a Python library that handles the lower level network communication code and provides a RESTful web API which we invoke from our code to perform publish or subscribe functions. Note that each node in our evaluation setup has an IP address, this includes the node running Neo4j, and so the REST API can be invoked on the Neo4j database from any of the controllers and Trust Collector or Policy Distributor components by using the IP of the Neo4j node.

The number of messages that need to be used for one complete process of our trust calculation is $O(N*M)$ where N is the number of controllers involved in calculating the trust and M is the number of switches in the network, and there exists one instance of the Policy Distributor component and one instance of the Trust Collector component. While the Neo4j database based communication scheme described earlier helps get rid of broadcast messages, each controller (from N number of controllers) has to communicate with each of the switches (from the M number of total switches).

TABLE II. DIFFERENT NETWORK CONFIGURATIONS WE CREATED OF CONTROLLERS AND SWITCHES FOR SCALABILITY EVALUATION OF NUMBER OF MESSAGES. IN EACH CONFIGURATION, NUMBER OF SWITCHES CONTROLLED BY ONE CONTROLLER IS EQUAL TO (NO. OF SWITCHES / NO. OF CONTROLLERS).

Configuration	Controllers	Switches	Malicious controllers
Config 1	1	3	0
Config 2	3	6	1
Config 3	6	12	2
Config 4	9	27	3

Table 2 shows the various configurations of controllers and switches which we created in our evaluation setup. Note that this set of configurations created are different than those created for the earlier evaluation and were shown in Table 1. Figure 4 shows the number of messages that were used to perform one complete process of trust collections for the various configurations mentioned in Table 2. Note that here a message from a component A to component B is defined as one write of a message from a component A and its corresponding read by a component B. As can be seen from the graph, our scheme scales smoothly as the number of controllers and switches involved in the process is increased. For the highest configuration, Config 4, with 9 controllers and 24 switches, the scheme uses less than 250 messages to finish the entire process of trust calculation.

V. DISCUSSION

Our test results presented earlier show that our scheme works correctly and efficiently in weeding out malicious controllers. Since the Trust Collector decides whether a controller is malicious based on aggregate of recommendations from all other controllers, therefore our scheme provides defense against bad mouthing attacks [18, 19].

In bad mouthing attacks, a malicious party provides dishonest recommendations for another good party to malign the name of the good party. But since our scheme does not make a decision of whether a controller is malicious based on recommendation from just one other controller, therefore

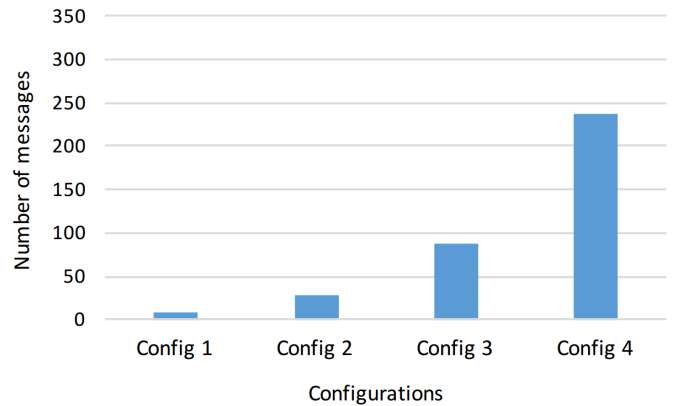


Fig. 4. Shows the number of message exchanges that take place for different network configurations of controllers and switches, the names of the configurations on the X-axis (e.g. Config1, Config2, ..) refer to the configurations in Table 1.

we can provide defense against bad mouthing as long as malicious controllers are not the majority in the total number of deployed controllers. This assumption is reasonable since we can guarantee the number of controllers which would need to become malicious before the network collapses. That is, in a network with N controllers, our scheme is guaranteed to work correctly and identify malicious controllers as long as $(N/2)+1$ controllers stay uncompromised. This assumption is realistic since majority of controllers is unlikely to become malicious in an instant and if they become malicious one by one over time, then our scheme will identify the malicious controllers at all times when $(N/2)+1$ controllers are still uncompromised.

Our scheme of collecting ratings and aggregating trust and reputation using a Trust Collector component works more robustly and accurately than delegating trust and reputation management entirely to individual controllers in a distributed environment. This is because we always need a central entity that can aggregate the ratings generated by all the controllers that are part of the distributed environment, and the central entity can then make a decision of whether a given controller is malicious by looking at what the majority of ratings say about that controller. Alternatively, the central entity can also output the result of the ratings to a human operator who can decide whether a given controller is malicious based on both their domain knowledge about the network and also based on the majority of ratings that were received for that controller.

Introducing a central trust managing entity also helps in solving an important dilemma, which is, what happens if majority of rogue controllers vote against a controller which otherwise has installed correct policies? Let us examine a case of distributed trust management, in which controllers find the policy mismatches themselves, and there is no central entity for managing the trust and reputation. There are three controllers in a network, A, B, and C, each managing one switch under them, and connected to other switches too. A network administrator defines one flow rule, i.e. block any traffic originating from IP address 200.0.0.1. The controllers install the flow rules in their respective switches. After sometime, controllers probe the switches to find out whether other controllers installed correct policies in their respective switches. A finds out that

TABLE III. DIFFERENT NETWORK CONFIGURATIONS WE CREATED OF CONTROLLERS AND SWITCHES FOR BAD MOUTHING EVALUATION. IN EACH CONFIGURATION, NUMBER OF SWITCHES CONTROLLED BY ONE CONTROLLER IS EQUAL TO (NO. OF SWITCHES / NO. OF CONTROLLERS). AND CX REFERS TO THE CONTROLLER NUMBER, E.G. C1, C2, ETC. THE BAD MOUTHING COLUMN SHOWS THE DETAILS OF WHICH CONTROLLER(S) BAD MOUTHED WHICH OTHER CONTROLLER(S). THE RESULT COLUMN SHOWS THE FINAL RESULT AFTER THE TRUST CALCULATION ROUND WHICH AGGREGATES TRUST VALUES FROM ALL CONTROLLERS IN THE NETWORK. AS SEE FROM RESULTS, THE POSITIVE OR NEGATIVE MAJORITY RATINGS AFFECT THE RESULT OF WHETHER A GIVEN CONTROLLER IS DEEMED TRUSTED OR UNTRUSTED.

Configuration	Controllers	Switches	#Malicious controllers	Bad mouthing	Result
Config 1	3	6	1	C1 bad mouthed C2	C2 found trusted
Config 2	3	6	2	C1, C2 bad mouthed C3	C3 found untrusted
Config 3	6	12	1	C1 bad mouthed C2 and C3	C2 and C3 found trusted
Config 4	6	12	2	C1, C2 bad mouthed C3 and C4	C3 and C4 found trusted

B and C have (maliciously) installed flow rules in their switches which allow traffic originating from 200.0.0.1. It rates B and C negative. B and C on the other hand rate A as negative. In presence of an automated solution of shutting down or restricting a malicious controller, this will prove to be disastrous. If, however, a human operator has to approve the shutting down or restricting of a malicious controller, then it will be a burden for him to sort through the conflicting ratings of controllers against each other.

Using the Trust Collector for aggregating the opinions about other controllers from each controller not only helps us in ascertaining the validity of recommendations with surety, but it also helps in eliminating broadcasts. If, for example, there are three controllers A, B, and C, then all of the nodes will have to send their reports to each other so that they can perform final trust calculation (since the final step in the trust calculation process inside a controller needs input from other controllers too).

However, by introducing the Trust Collector in between, all controllers send their reports to this central entity, which simply forwards it to individual controllers. While it is true that our scheme introduces this one central point of compromise, the Trust Collector, but we emphasize that it is much easier to guard and protect one component if it can help us have a safe distributed environment of controllers where each controller does not have to guarded very well. As long as majority of controllers are not compromised, our scheme guarantees that the network will keep functioning correctly.

VI. CONCLUSION AND FUTURE WORK

Securing the controllers in SDN is an open problem for research. Researches carried so far do not address the problem of identifying malicious controllers, especially in multi-controller environment. We tackle this problem by employing a trust management scheme in which controllers rate each other on the basis correctness of flow rules installed by them in switches. We do this by introducing a centralized entity which keeps record of policies to be installed, so that controllers can compare them with installed policies for rating purpose. We coded the scheme and implemented it in Ryu controller as prototype and found that the scheme is able to successfully flag a malicious controller. Our next step will be to extensively evaluate our scheme in different network topologies and number of nodes, and also by launching various kinds of attacks on our trust management system.

REFERENCES

[1] H. Kim, N. Feamster, Improving network management with software defined networking, Communications Magazine, IEEE 51 (2) (2013) 114-119.

[2] Hakiri, Akram, et al. "Software-defined networking: challenges and research opportunities for future internet." Computer Networks 75 (2014): 453-471.

[3] Sezer, Sakir, et al. "Are we ready for SDN? Implementation challenges for software-defined networks." Communications Magazine, IEEE 51.7 (2013): 36-43.

[4] Kreutz, Diego, et al. "Software-defined networking: A comprehensive survey." Proceedings of the IEEE 103.1 (2015): 14-76

[5] Kreutz, Diego, Fernando Ramos, and Paulo Verissimo. "Towards secure and dependable software-defined networks." Proceedings of the second ACM SIGCOMM workshop on Hot topics in software defined networking. ACM, 2013.

[6] Prasad, Abhinandan S., David Koll, and Xiaoming Fu. "On the Security of Software-Defined Networks." 2015 Fourth European Workshop on Software Defined Networks. IEEE, 2015.

[7] Liang, Zhengqiang, and Weisong Shi. "PET: A personalized trust model with reputation and risk evaluation for P2P resource sharing." Proceedings of the 38th annual Hawaii international conference on system sciences. IEEE, 2005.

[8] "Ryu SDN framework," <https://osrg.github.io/ryu/>

[9] "Emulab - Network Emulation Testbed," <http://emulab.net/>

[10] "Kaminsky DNS Attack," <http://dankaminsky.com>

[11] Shu, Zhaogang, et al. "Security in Software-Defined Networking: Threats and Countermeasures." Mobile Networks and Applications: 1-13.

[12] Porras, Phillip A., et al. "Securing the Software Defined Network Control Layer." NDSS. 2015.

[13] Nunes, Bruno, et al. "A survey of software-defined networking: Past, present, and future of programmable networks." Communications Surveys and Tutorials, IEEE 16.3 (2014): 1617-1634.

[14] Phemius, Kvin, Mathieu Bouet, and Jrmie Leguay. "Disco: Distributed multi-domain sdn controllers." 2014 IEEE Network Operations and Management Symposium (NOMS). IEEE, 2014.

[15] Tootoonchian, Amin, and Yashar Ganjali. "HyperFlow: A distributed control plane for OpenFlow." Proceedings of the 2010 internet network management conference on Research on enterprise networking. 2010.

[16] Koponen, Teemu, et al. "Onix: A Distributed Control Platform for Large-scale Production Networks." OSDI. Vol. 10. 2010.

[17] "Neo4j Graph Database," <http://neo4j.com>

[18] S. Buchegger and J. L. Boudec. "Coping with False Accusations in Misbehavior Reputation Systems for Mobile Ad-Hoc Networks." EPFL tech. rep. IC/2003/31, EPFL-DI-ICA, 2003.

[19] Sun, Yan, Zhu Han, and KJ Ray Liu. "Defense of trust management vulnerabilities in distributed networks." IEEE Communications Magazine 46.2 (2008): 112-119.

Crowd Mobility Analysis using WiFi Sniffers

Anas Basalamah
Computer Engineering Department
Umm Al-Qura University
Makkah, Saudi Arabia 21955

Abstract—Wi-fi enabled devices such as today’s smart-phones are regularly in-search for connectivity. They continuously send management frames called Probe Requests searching for previously accessed networks. These frames contain the sender’s MAC addresses in clear text, which can be used as an identifier for that sender. Being able to sniff that MAC address at several locations allows us to understand the mobility behavior of that device. In this paper, we present a solar-powered, beagle-bone based standalone system that continuously sniffs the air for probes and extract their MAC addresses. We deployed the system in the world’s largest gathering (The Hajj) and tested it at scale. Our objective was to build an infrastructure for non-invasive mass crowd analysis. Our deployment had a total of 8 sniffers covering a population of 185,000 people. We detected 37.5% of the population, analysed their arrival and departure behaviours, identified their smartphone manufacturers and extracted their transition patterns from one sub-location to another. By presenting valuable insights on the mobility of our target crowd, we validated the potential of our platform for crowd mobility analysis.

Keywords—WiFi Probes; Crowd Monitoring; Crowd Mobility Analysis

I. INTRODUCTION

Monitoring and understanding peoples behavior in public and private spaces like streets, parks, hospitals, malls is a big challenge for cities. Systems with information about mobility behavior of people are able to support the control and management process of pedestrians and vehicles and are able to reduce the management costs and travel times. Citizens can be informed about dense areas, traffic and travel times. Cities can better design public spaces to enrich the happiness of citizens.

Cameras and image processing technique have been used for years to detect crowd mobility [1][2]. However these techniques suffer from high implementation costs and accuracy limitations specially when tracking crowds across multiple feeds. Moreover, cameras raise major privacy concerns [3]. Therefore, cheaper, less invasive, more accurate techniques are encouraged to achieve crowd mobility monitoring.

The air around us is packed with WiFi packets transmitted from one device to another carrying massive amount of information. These packets originate from personal computers, laptop computers, ipads, TVs, and most importantly, the smartphones that we carry with us almost everywhere we go. The increasing usage of WiFi in smartphones offers new possibilities to monitor crowd mobility without the need for expensive additional hardware installations. This paper tries to leverage this unbreakable association between people and their smartphones to capture mobility patterns and understands people’s mobility behaviors.

Wifi-enabled devices periodically broadcast management frames called probes in search for nearby access points. These probes are sent in clear text and carry useful data such as device MAC address, which acts as a unique identifier for this particular device. Reading these over-the-air packets using low cost sniffers enables us to identify the presence of people at the 50-100 meter range of the Wi-Fi sniffer. Placing several sniffers around the city (or monitored spaces) allows us to understand the mobility of crowds by the observing the density of probes, dwell times, and mobility traces across multiple sniffers.

However, and to the best of our knowledge, a crowd mobility system based on Wi-Fi probes has not been realized in a scenario where hundred thousands of crowds mobilize in a controlled environment. We leveraged the worlds largest annual pilgrimage where 2-3 million people gather to perform the Hajj pilgrimage in the city of Makkah, Saudi Arabia. We deploy our system in a subset of a camp area called Arafat, where pilgrims occupy for only one day. The camp is infrastructure-less; no WiFi connectivity. This guarantees that there are no possible biases in the data from existing networks that could invalidate our findings. We installed 8 solar-powered WiFi sniffers at an isolated island inside Arafat where a population of 185,000 pilgrims gather, and collected data two days before and three days after the Arafat day.

Our results show that we were able to detect 69,467 devices leading to a detection rate of 37.5% of total population. 33.26% of which are iOS devices and remainder is Android and Windows phones. The data showed expected increase in arrival and decrease in departure as pilgrims arrived and departed the site. The data also showed expected mobility pattern between sniffer locations reflecting true mobility of pilgrims.

The contribution of this paper is of three folds:

- The paper presents an system architecture for wifi sniffing that is used to log all WiFi probe packets for mobility analysis. The system was built on Beagle-bone and is powered by solar energy. Data was sent to servers using 3G in real-time.
- We deployed our system in a real-world massive scenario where more than 185,000 people mobilize. The deployment was in the worlds largest pilgrim event (The Hajj).
- By analyzing our collected dataset we demonstrate a set of valuable insights on the mobility of our target crowd validating the potential of our platform for crowd mobility analysis.

The system presented in this paper can be generalized to

any public, private, indoor or outdoor space, and allows cities and businesses properly manage crowds and optimize their mobility.

II. RELATED WORKS

We have seen many explorations in the literature that address crowd mobility using passive sniffing of WiFi packets. In [4], Musa et al. deploy a real-world test bed for WiFi probe sniffing for traffic management in the city of Chicago. They present an approach for detecting wifi probes and estimating the spatio-temporal trajectories of smart phones. In [5], by only looking at WiFi probes, Barbera et al. was able to infer significant information on the social structure of a large crowd and its socioeconomic status. In [6], Chon et al. use smart phones as sniffers to demystify the potential and the threat that exist in sniffing wifi probes. They were able to showcase the effectiveness of estimating urban mobility via only a small number of participants. They also analyzed many issues related to sniffing WiFi probes such as feasibility, coverage, scalability, and threats to privacy. In [7], Bonn et al. deploy a WiFi sniffing experiment at a university campus and at a music festival. Their intention was to study the density estimates of crowds at those locations.

The limitation of previous works lies in the missing ground truth for real-world data and the lack of scalability of their deployments. Also not enough analysis was provided to demonstrate the validity of the WiFi probes for mass crowd analysis.

III. METHODOLOGY

In this section we explain the concept of sniffing WiFi probes and present the platform we built specifically for this purpose.

A. WiFi Probes

Smartphone manufacturers are keen in enabling users to connect to the internet as seamless as possible. As such, smartphones are designed to aggressively search for nearby Access Points (AP) and automatically re-connect to previously accessed networks that are saved on the smartphone. To achieve seamless auto-connectivity, a low-latency service discovery is required. A smartphone can discover nearby WiFi APs using a passive or an active discovery process [8]. In the passive mode, AP broadcast periodic beacon messages to advertise its presence within its coverage range. If the mobile device happens to be listening at that moment on that exact channel, it will receive this broadcast, otherwise it will be missed. After some time, the frame will be received and mobile devices will respond accordingly. Unfortunately, this approach leads to high discovery delays. In contrast, the active discovery mode requires mobile devices to continuously broadcast Probe Request messages at every channel consecutively to discover the nearby APs. This method is much faster in service discovery, and is the only way to find hidden networks. As such, mobile phones implement active mode and constantly send probe request messages. Empirical results with a variety of mobile devices show that an active scan is performed at least once within two minutes [7].

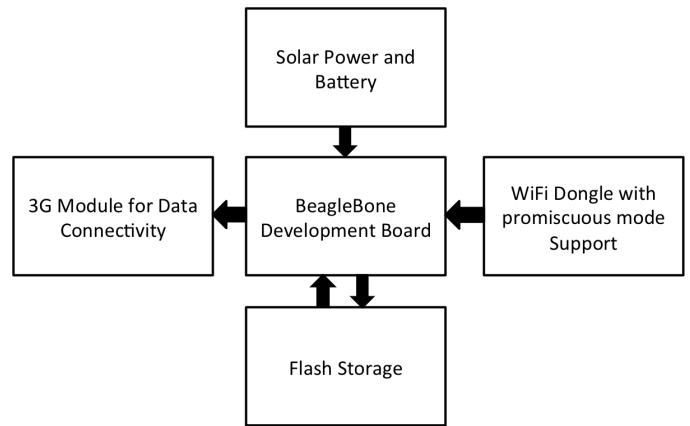


Fig. 1. Architecture for the sniffing platform

Probe requests frames carry the senders MAC address in clear text, which can be used as an identifier for the specific mobile phone. As a result, the more mobile devices with active WiFi are present in one area, the more corresponding WiFi probe frames are present, each with a unique identifier. Being able to capture those frames gives an indication of crowd density in that area. The ability to redetect the IDs at other locations can enable the measure of mobility between areas.

B. Sniffing WiFi Frames

There are several ways to sniff WiFi traffic and filter probe requests. There are some specialized products available for network professionals [9], and packages for mobile devices [10]. However, since we built our platform for a more stable setup, we decided to capture probes can using a type of wireless network interface cards (NIC) that operate on monitor mode, along with a linux-based packet capturing software (Wireshark[11]). Once monitor mode is enabled, the NIC is fixed on one frequency out of the Eleven frequencies defined in the IEEE802.11 standard. Since a probe is usually sent by each mobile device once on every channel, fixing one channel will increase the probability of capturing the probe frame.

C. WiFi Sniffing Platform

Fig. 1 shows the architecture of the platform we developed to capture WiFi probe requests and the components needed to operate it. The platform uses the beaglebone development board to run our linux based sniffing scripts, manage the data handling and communicate with the 3G module. We use a solar panel to charge a battery to run the platform 24h a day. A 3G dongle is used to communicate the data using a 3G network with unlimited data plan to the database. Flash storage was used to log the probe data temporarily before sending it to the 3G module. Fig. 2 shows the view of an installed system.

D. Deployment Design

Hajj is a unique annual event that happens only in Makkah, Saudi Arabia. Two to Three Million Muslims from all over the world gather to perform a pilgrimage referred to as Hajj. Hajj is a sequence of rituals performed within specific times and places. The Spatio-Temporal restrictions make the management of Hajj a very challenging task. It is only



Fig. 2. Deployed Sniffing Platform



Fig. 3. Selected Location in Arafat

by understanding how pilgrims behave, their patterns, their interactions, their needs and demands, that we can reach to a satisfying level of providing services and experiences. Considering the importance and the unique nature of the Hajj event, and enormous amount of data that can be collected for understanding crowd mobility, we decided to implement our system on a sub-location of Hajj, in a site called Arafat.

Arafat is located 12km southeast the Holy City of Makkah. It covers an area of 13m² of desert camp. No infrastructure exists as people stay in temporary tents. The camp is deserted throughout the year, except for the day of Arafat where all pilgrims spend their day before mobilizing to Muzdalifa (a neighboring camp) on that evening. Few management staff arrive few days before and leave few days after. Also some pilgrims arrive a day before to avoid traffic congestion.

We have chosen a contained island inside Arafat allocated for pilgrims coming from Turkey, Europe and the Americas. For management purposes, this area is sieged such that no other pilgrims can come in. The estimated size of population from those countries is estimated to be 185,000 pilgrims from other data sources. We placed 8 sniffing platforms in Arafat as shown in Fig. 3. The locations have been chosen carefully to capture all possible traffic in and out of the camp. Arafat day was on Oct 3rd which would exhibit the maximum number of detections in our data-set.

E. Data Analysis

In this section, we show the data analysis of the data collected on this deployment.

1) *Basic Summery Statistics*: The data we collected started Oct 1st and ended Oct 6th. The number of Wi-Fi probe records captured thought-out these days was 4,517,687. These probes resulted from 69,467 unique devices. Since we know the estimated ground truth for the number of pilgims in this subarafat area is 185,000 pilgrims, we were able to detect 37.5% of the population. This number is very significant. It tells us that 37.5% of pilgrims in that location carry smartphones with Wi-Fi enabled and can be tracked. While it is obvious that we cannot generalize this number with all pilgrims from all nationalities

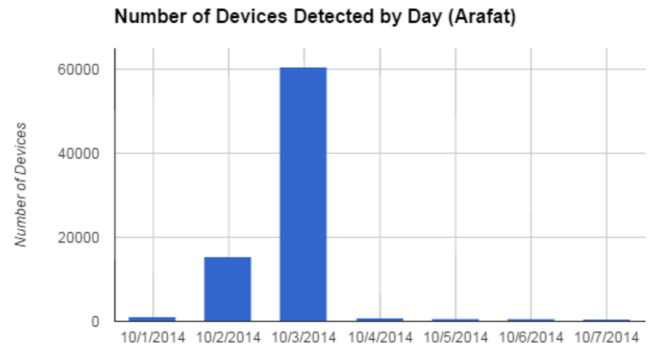


Fig. 4. Total unique Devices per day

due to economical differences, it does indicate the potential of our system in capturing detailed traces of pilgrims non-invasively.

It is also worth nothing that the average number of probes per device was 65.03.

2) *Unique Detections per day*: Fig. 4 shows the total number of detections per day considering all the sites combined. It is obvious that most of the detections happen on Arafat day (3rd of October) reaching up to 60,000 unique devices. The data also shows a large number of devices detected on the 2nd of October. This number is due to the arrivals of many pilgrims the day before Arafat day to avoid traffic. Although ground truth data for 2nd of October is not available to compare with this number, we found this result very insightful and would benefit the Hajj administration.

Fig. 5 shows the average of Unique number of devices shown per site per day. From the figure we notice that inner located sites such as 5, 8 and 16 show high detections compared to outer located sites such as 1 and 12. Generally, the reason is that outer sites are located at entry and exit points we pilgrims pass through quickly, leading to less detection opportunity compared to inner located sites were pilgrims spend most of their day increasing the likelihood of detection.

3) *Unique Detections per Hour*: Fig. 6 shows the number of total unique detections per hour on Arafat day. The figure

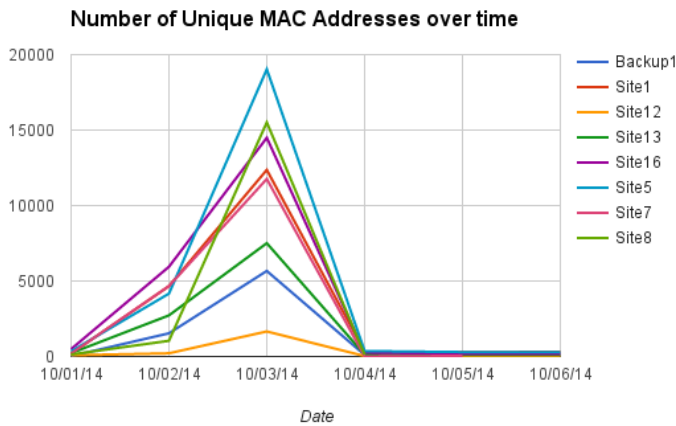


Fig. 5. Unique devices per pay per site

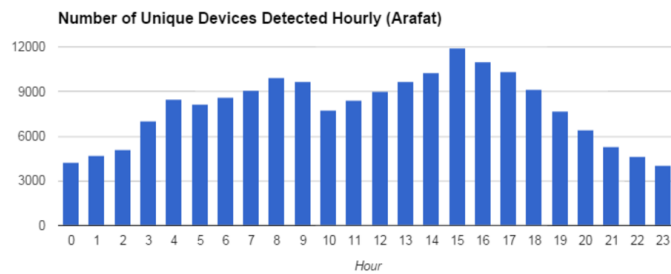


Fig. 6. Unique devices per Hour on Arafat Day

shows a peak at 6-9AM and another peak at 3-5PM. Those peaks successfully detect largest mobility activities of the day. In the morning peak, people come to Arafat, in the Afternoon peak, people leave to Muzdalifa. The pattens successfully show the overall activity at Arafat.

4) *Device Manufacturers:* The MAC addresses captured in the data-set allows us to map them to their manufacturers. Table I shows the list of mobile phone manufacturers. The numbers shown are really interesting because they can indicate the economic distribution of this population. 33.36% are Apple users compared to 26.98% Samsung users. 12.7 device manufacturers were un-known due to lack of information. Only around 13.79% of devices were from low cost unfamiliar manufacturers.

5) *Time between detections:* The time between detections is presented in Table II. This data shows that the majority of detections occur in sequence of less than a second (2,634,117 detections). This indicates the frequency of probe detections and the efficiency of using it as a tool for crowd analysis.

6) *Transition from one sub-location to another:* Table III shows the percentages of mobile devices that are detected at one sniffer then detected at another sniffer. As an example,

TABLE I. THE TYPES OF DEVICE MANUFACTURERS

Manufacturer	Number of Records	Percentage
Apple	23104	33.26
Samsung Electronics Co.	18742	26.98
Unknown	8823	12.7
Murata Manufacturing Co.	6723	9.68
Nokia	2494	3.59
Total for Top 5	59886	86.21

TABLE II. TIME BETWEEN DETECTIONS

Time between detections(sec)	Number of Detections
0	2,634,117
1	181,820
2	56,810
3	39,738
4	41,967
5	32,977
6	31,875
7	23,582
8	19,280
9	21,535
10	27,698
11-60	676,542
61-300	418,268
301-600	84,945
600-3600	102,286
3600-7200	19,903
7200+	34,877

TABLE III. TRANSITION MATRIX

	BK1	S1	S12	S13	S16	S5	S7	S8
BK1		4.24	2.25	1.82	33.72	1.92	1.07	25.18
S1	1.69		69.23	8.37	3.91	3.15	1.54	15.97
S12	0.38	2.08		0.96	1.01	0.43	0.57	8.23
S13	1.86	25.56	8.17		50.35	0.67	0.39	4.38
S16	86.19	25.2	9.59	85.78		3.91	2.63	22.72
S5	4.86	31.71	5.21	2.1	4.6		89.32	13.64
S7	2.16	7.15	1.66	0.55	2.17	86.21		9.48
S8	2.79	4.02	3.79	0.4	1.86	3.66	4.48	

85.78% devices being detected at 13 are detected next at 16. The opposite is only 50.35% which indicate that the majority of people mobilize from coverage location 13 to 16.

IV. CONCLUSION

This paper presented a system for crowd behaviour analysis using non-invasive WiFi probes. We presented a system architecture for wifi sniffing that is used to log all WiFi probe packets for mobility analysis. The system was built on Beaglebone and is powered by solar energy. Data was sent to servers using 3G in real-time. We deploy our system in a real-world massive scenario where more than 185,000 people mobilize. The deployment was in the worlds largest pilgrim event (The Hajj). By analyzing our collected dataset we demonstrate a set of valuable insights on the mobility of our target crowd validating the potential of our platform for crowd mobility analysis. The system presented in this paper can be generalized to any public, private, indoor or outdoor space, and allows cities and businesses properly manage crowds and optimize their mobility.

REFERENCES

- [1] A. Marana, S. Velastin, L. Costa, and R. Lotufo, "Automatic estimation of crowd density using texture," *Safety Science*, vol. 28, no. 3, pp. 165 – 175, 1998. [Online]. Available: <http://www.sciencedirect.com/science/article/pii/S0925753597000817>
- [2] H. Rahmalan, M. S. Nixon, and J. N. Carter, "On crowd density estimation for surveillance," in *2006 IET Conference on Crime and Security*, June 2006, pp. 540–545.
- [3] D. Gavrilu, "The visual analysis of human movement," *Comput. Vis. Image Underst.*, vol. 73, no. 1, pp. 82–98, Jan. 1999. [Online]. Available: <http://dx.doi.org/10.1006/cviu.1998.0716>
- [4] A. B. M. Musa and J. Eriksson, "Tracking unmodified smartphones using wi-fi monitors." in *SenSys*, M. R. Eskicioglu, A. Campbell, and K. Langendoen, Eds. ACM, 2012, pp. 281–294.

- [5] M. V. Barbera, A. Epasto, A. Mei, V. C. Perta, and J. Stefa, "Signals from the crowd: Uncovering social relationships through smartphone probes," in *Proceedings of the 2013 Conference on Internet Measurement Conference*, ser. IMC '13. New York, NY, USA: ACM, 2013, pp. 265–276. [Online]. Available: <http://doi.acm.org/10.1145/2504730.2504742>
- [6] Y. Chon, S. Kim, S. Lee, D. Kim, Y. Kim, and H. Cha, "Sensing wifi packets in the air: Practicality and implications in urban mobility monitoring," in *Proceedings of the 2014 ACM International Joint Conference on Pervasive and Ubiquitous Computing*, ser. UbiComp '14. New York, NY, USA: ACM, 2014, pp. 189–200. [Online]. Available: <http://doi.acm.org/10.1145/2632048.2636066>
- [7] B. Bonn, A. Barzan, P. Quax, and W. Lamotte, "Wifipi: Involuntary tracking of visitors at mass events," in *2013 IEEE 14th International Symposium on "A World of Wireless, Mobile and Multimedia Networks" (WoWMoM)*, June 2013, pp. 1–6.
- [8] S. Seneviratne, A. Seneviratne, P. Mohapatra, and P.-U. Tournoux, "Characterizing wifi connection and its impact on mobile users: Practical insights," in *Proceedings of the 8th ACM International Workshop on Wireless Network Testbeds, Experimental Evaluation & Characterization*, ser. WiNTECH '13. New York, NY, USA: ACM, 2013, pp. 81–88. [Online]. Available: <http://doi.acm.org/10.1145/2505469.2505480>
- [9] "WIFI PINEAPPLE MARK V STANDARD (Last Accessed November 23, 2015)," <https://hakshop.myshopify.com/products/wifi-pineapple>.
- [10] "Android PCAP Capture - Utility for capturing raw 802.11 frames. (Last Accessed November 23, 2015)," <https://www.kismetwireless.net/android-pcap/>.
- [11] "WLAN (IEEE 802.11) Capture Setup using WireShark (Last Accessed November 23, 2015)," <https://wiki.wireshark.org/CaptureSetup/WLAN>.

Fault-Tolerant Resource Provisioning with Deadline-Driven Optimization in Hybrid Clouds

Emmanuel Ahene

School of Computer Science
and Engineering

University of Electronic Science
and Technology of China

Chengdu, Sichuan 611731, P. R. China

Kingsley Nketia Acheampong

School of Software Engineering
University of Electronic Science

and Technology of China
Chengdu, Sichuan 611731, P. R. China

Heyang Xu

School of Computer Science
and Engineering

University of Electronic Science
and Technology of China

Chengdu, Sichuan 611731, P. R. China

Abstract—Resource provisioning remains as one of the challenging research problems in cloud computing, more importantly when considered together with service reliability. Fault-tolerance techniques such as fault-recovery is one of the techniques that can be employed to improve on service reliability. Technically, fault-recovery has obvious impact on service performance. Such impact requires detailed studies. Only few works on hybrid cloud resource provisioning address fault recovery and its impact. In this paper, we investigate the problem of resource provisioning in hybrid Clouds, considering the probability of hybrid cloud resource failure during job execution. We formulate this problem as an optimization model with operational cost as an objective function subject to the deadline constraint of jobs. Based on our proposed optimization model, we design a heuristic-based algorithm called dynamic resource provisioning algorithm (DRPA). We then perform extensive experiments to evaluate performance of the proposed algorithm based on a real world set of data. The results confirm the obvious impact of fault recovery on the performance metrics (operational cost and deadline violation rate) and also confirms that DRPA can be useful in minimizing operational cost.

Keywords—Deadline; fault recovery; hybrid Clouds; resource provisioning; software-as-a-service

I. INTRODUCTION

Cloud computing is a promising computing paradigm which has attracted more research attention in both the academia and the industry [1]. Among its benefit, the Cloud enables its users to have access to a pool of configurable computing resources across the internet independently without reference to its underlying hosting infrastructure.

The resource pool in the Cloud are often deployed in any of the four well known models, namely: public, private, community and hybrid deployment models. In the hybrid Cloud model, the Cloud infrastructure is made up of a combination of the private and public Cloud infrastructure. Provisioning of configurable resources with a private Cloud is known for its main advantage of being more secured than its alternatives. This is because, data is controlled on servers that no other company has access to except its users. However, since the resources in private Clouds are limited, organizations (such as SaaS providers) are faced with the challenge of capacity limitation when there is a high demand for resource by users. Compared to purchasing additional physical servers or building a new datacenter, many of such organizations prefer to rather

scale up their service capacity to the public Cloud so as to meet their users' need. The process where an organization would leverage both its private Cloud resource and the resource in the public Cloud to process its user's workload is called the hybrid Cloud resource provisioning. Currently, Open Text, a leading software provider in enterprise information management, employs the hybrid Cloud model to demonstrate their enterprise content management software. Moreover, one of the world's leading game companies, SEGA, has adopted hybrid Cloud to improve its development process [2].

Its worth noting that, Cloud applications tend to be inevitably useful in major business operations and so most users are always bent on having assurance from providers with respect to service delivery. These assurances are realized through Service Level Agreements (SLAs) established between the providers and users. In this way, providers express their commitment to deliver services to satisfy the user's requirement. To users, it is a warranty. However, to SaaS providers, it is a challenge to ensure efficient resource provisioning policies. Moreover, how to optimize the operational cost involved in the efficient provisioning of resources remains an important and challenging problem to SaaS providers especially, when there is a high workload of job requests with QoS constraints.

A. Our Contribution

Over the years, many researchers have done relevant studies on the problem of resource provisioning in both hybrid and public Cloud. However, one relevant facet of the problem that is rarely addressed is on the probability of resource failures. The tendency of resource failures during the execution of jobs cannot be overlooked because it has obvious impact on service performance. Such impact requires detailed studies. Our previous work [3] in addition to other works such as [4] [5] [6] happens to be part of the few works that address this issue. Fault-tolerance techniques such as fault recovery is one of the techniques that can be employed to improve reliability. It employs checkpoint and rollback/roll-forward scheme, that enables a resource to recover from an error and resume execution [14]. In this paper, we investigate the problem of resource provisioning in hybrid Clouds considering the probability of resource failure during job execution. We employ fault-recovery to address the problem of resource failure. Our contributions are as follows:

We present a hybrid Cloud model that enables the scalability of the resource-base of a software-as-a-service SaaS provider who intends to leverage resources in both private and public Cloud for job execution. We propose DRPA to address the problem of operational cost minimization associated with the leveraging of hybrid Cloud resources, considering the probability that resources (i.e. Virtual machines (VM) and communication links) may fail and recover. In addition, we take into account some practical issues such as communication cost, cost incurred at local (private cloud) and jobs that are dynamic in nature. Finally, we perform extensive experiments to evaluate the performance of the proposed algorithm in terms of operational cost and deadline violation rate.

The rest of the paper is organized into six sections. Section 2 presents related works while section 3 presents the system model and problem formulation. Section 4, presents the proposed DRPA, and its provisioning policies. In section 5, we discuss the experiments and their results against existing works. The paper is finally concluded in section 6.

II. RELATED WORKS

The optimal provisioning of the Cloud's configurable compute resources to meet certain predefined performance criteria is a complex problem. It has attracted much research attention [7], [8]. This problem comprises the steps involved in allocating suitable compute resources to tasks with the aim of optimizing certain objectives. Some widely known objective functions are; minimizing cost, minimizing the time of task completion and maximizing the utilization of resources.

To address the problem of operational cost minimization in Cloud resource provisioning context, authors in [9], proposed a new MapReduce Cloud service model called Cura, which automatically creates the best configuration of clusters for tasks so as to approach a global resource optimization. Specifically, the system employs a deadline-awareness method, which defers the execution of certain tasks, and necessitates global optimization with reduced cost. Wu et al. [10] proposed an SLA based resource allocation method, which is compatible to the heterogeneity of infrastructure and adaptable to the dynamic change of customer jobs. Their approach seeks to maximize the profit of the SaaS provider by minimizing the number of SLA violations and the cost by reusing VMs. Other related works [9], [11], [12], [13] and [14] also focused on cost-optimization strategies for resource provisioning. This paper is also focused on cost optimization and also considers workloads that are dynamic in nature. However, it is considered in the hybrid Clouds.

Unlike hybrid Clouds, extensive research work on resource provisioning has been conducted in public Clouds. Nevertheless, many industries have started using Hybrid Cloud for Cloud businesses [2]. In 2011, Tak et al. [15] did investigate the economic issues of the application deployment choice in the hybrid Cloud. The output of their research indicated the need to research on the solutions for various optimization problems associated with the hybrid SaaS concept. Subsequently, related works such as [16] and [17] focused on the design of cost efficient VM migration algorithms which enables the scale up of local data center resources to the public Cloud in the context of Cloud bursting. However, their works considers

workload characteristics as static. In [18], a model that extends the physical site cluster with Cloud resources elastically was proposed to adapt to the dynamic demands of applications. The central component of this model is an elastic site manager that handles resource provisioning. In [19] Li et al. implements Lyapunov optimization techniques to develop an online dynamic provisioning algorithm in the hybrid Cloud setting. Their algorithm seeks to minimize the operational cost of a hybrid SaaS provider with a delay-aware optimization. In their work, they focus on how the SaaS provider can leverage three types of VMs from the public in addition to the VMs at local for job execution. However, their work does not consider the probability of VM and communication link failure.

In contrast, other works such as [5] [6] [3] and [4] do not overlook the probability of VM or communication link failure. In [4], Javadi et al. studied on a problem that is comparatively similar to ours, however, they consider the probability of failure in the private Cloud only. In addition, they do not consider failure in communication links as well. Although we address a similar problem in this paper, we focus on some practical issues such as communication cost, the cost incurred at local (private Cloud), jobs that are dynamic in nature, and the probability that a VM (in both private and public) and a communication link between the public and private Cloud may fail. Specifically, this work considers how the SaaS provider can leverage VM instances at local and the On-demand VM instances in the public Cloud to process the job request of its users. Unlike [4] and [19], this paper proposes a resource provisioning algorithm which relies on the job runtime estimate, the prices of VM instances, and the availability-state of rented/local resource to decide what are the best types of VM instances to run each job and when jobs should run in the hybrid Cloud setting.

III. SYSTEM MODEL AND PROBLEM FORMULATION

A. System Model

In this paper, we assume that there is a SaaS provider who owns a private data center which comprise a finite number of local servers that implements virtualization concepts to run user jobs. The SaaS provider is assumed to have the ability to seamlessly scale up the capacity of its services by renting for On-demand VM instances from the public Cloud when there is a spike in resource demand. The provider can as well scale down the rented VM instances once they are not needed. Since the rendering of service with VMs at local (private cloud) and the renting of the public Cloud VMs is associated with much monetary cost, it is imperative for the SaaS provider to reduce such cost. The SaaS provider is therefore faced with the challenge of minimizing total operational cost without violating the deadline for job completion considering the probability of VM and communication link failure.

To address the challenge, the SaaS provider needs to decide on the number of VMs to rent and when to rent them. Emphatically, a job is first directed to the private Cloud but once the private VMs are busy, they are directed to a waiting queue. The SaaS provider decides on the number of VMs to rent when the waiting time of the job has exceeded a threshold delay value W_k . The decision of the SaaS provider is based on the runtime estimate of the job, the availability-state of

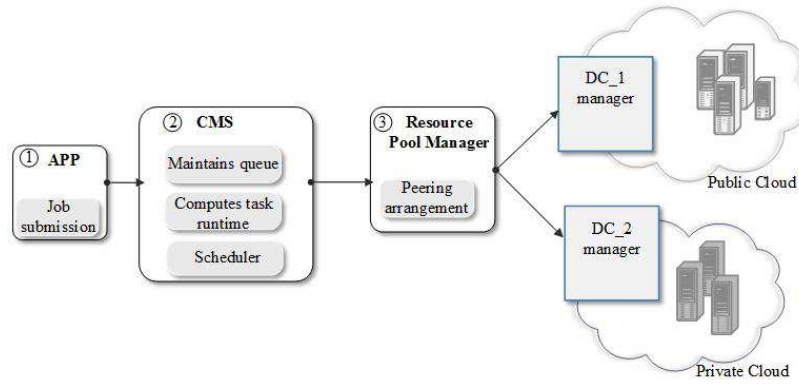


Fig. 1. Hybrid Cloud Architecture

the VMs and their associated prices. Technically, there is the probability of VM or communication link failure, however, since we adopt the fault recovery mechanism, it is assumed that all failures are recoverable. Given that all failures are recoverable, it is obvious that after some time (recovery time) VMs and communication links resumes execution [3]. The occurrence of failures, failure times, and recovery times are assumed to be mutually s -independent [5]. Table I shows a list of notations and their descriptions as used in this paper.

VM instances are assumed to be equivalent to the instance types available at Amazon EC2. Since there are diverse VM types in the public Clouds, we assume that the VM instances on public Cloud have similar capacity in terms of memory size and EC2 compute units (ECUs) as in the private Cloud [20]. However, for each type of similar instance, there exist an infinite number of them on the public Cloud while that of the private is limited. One ECU provides a processing capacity which is equivalent to a CPU capacity of 1.0 to 1.2 GHz 2007 AMD Opteron or 2007 Intel Xeon processor. In this paper, we consider VM instances with possible ECU values of $\{1, 8, 13, 16, \text{ and } 26\}$ [21]. The EC2 types which are of exact ECU characteristics are m1.small (1 ECU), c4.large (8 ECUs), m4.large (13 ECUs), c4.xlarge (16 ECUs), and m4.2xlarge (26 ECUs). Let R_{priv} represent the pool of VM instances in private Cloud and R_{pub} the pool of public Cloud VM instances. The total pool of VM instances $R_p = R_{priv} \cup R_{pub}$. Thus the union(\cup) of the set of private and public VMs. Emphatically, the number of VMs in R_{pub} is assumed to be infinite while that of R_{priv} is finite. For the purposes of clarity in representation, we represent the j^{th} VM in either the public or private Cloud by R_j respectively, where $1 \leq j \leq n$. Each R_j has the following parameters, number of ECUs U_j , availability a_j , bandwidth bw_j , memory Me_j , processor speed ps_j and price P_j . $R_j = \{U_j, a_j, bw_j, Me_j, ps_j, P_j\}$. The availability a_j of an instance refers to the state where that VM instance is not in use by other jobs. It is considered as an indicator value $\{0, 1\}$, which determines whether or not a VM can be provisioned. If a VM is in use regardless of the number of free compute units, the value of $a_j = 0$. However, as soon as a VM has finished processing the current job, $a_j = 1$ which indicates that VM is now idle for provisioning.

User jobs are assumed to contain parallel tasks with average parallelism (A_k) and a coefficient of the variance of parallelism as σ_k [22]. Each job can run on several virtual

TABLE I. NOTATIONS

Symbols	Description
t_i	The i^{th} Task which is a subset of a job
S	Scheduler
μ_r	Service rate of task
T_k^W	The waiting time of job
N	The maximum number of jobs allowed to be in queue
D_k	The deadline for the completion of job
T	The overall execution time with fault recovery
α_{kj}	the runtime estimate of the k^{th} on the j^{th} VM
W_k	Threshold waiting time of a job
b_w	Bandwidth
a_j	The availability-state of the j^{th} VM instance
R_p	The total pool of VM instances (public and private)
R_{priv}	The set of VM instances in the private Cloud
R_{pub}	The set of VM instances in the public Cloud
R_j	The j^{th} VM instance (public or private)
ps_j	Processing speed of a VM instance j
j	Failure rate
μ_j	Recovery rate
β	The fraction of the maximum power in idle state
ω_{max}	Maximum power consumed in active state
G	The communication cost
C	Overall cost considering fault recovery
ϵ	Constant price for power consumption in private Cloud
A_k	average parallelism of a job
σ_k	coefficient of the variance of parallelism
S_{kj}	Speedup of the K^{th} job on the j^{th} VM

processors(ECU) but restricted to one VM instance. There are l dynamic jobs that can be submitted to the SaaS provider for provisioning. Let the k^{th} job in l number of jobs be represented as j_k . Each job J_k , where $1 \leq k \leq l$ has t_i number of tasks, number of required processors rc_k , job length l_k and deadline for job completion D_k .

B. Overall Execution Time

For the processing of each job, a real life situation is considered, where the VM running tasks has the probability of failing and recovering. Jobs are made up of parallel tasks and each k^{th} job has i number of tasks where $1 \leq i \leq k$. The time for the execution of a job on VM j without considering the possibility of VM failure is denoted by $T_{kj}^{(e)}$. Mathematically,

$T_{kj}^{(e)}$ can be computed as shown in (1) ;

$$\begin{aligned} \tau_{ij} &= \frac{\text{length}(t_i)}{ps_j} \\ T_{kj}^{(e)} &= \max\{\tau_{ij}\} \end{aligned} \quad (1)$$

Where ps_j is the processing speed of VM j , $\text{length}(t_i)$ is the length of task i and $\max\{\tau_{ij}\}$ is the maximum finish time of the i^{th} task on j (i.e. the time the last task is completed on j). Assuming all failures are recoverable, then after some time (recovery time), the VM resumes execution. The failure rate on j follows a Poisson process with rate λ_j . Hence, the total number of failures $N_j(t)$ during a time interval of $(0, t]$ can be computed as shown in (2) [6];

$$Pr\{N_j(t) = b\} = \frac{(\lambda_j t)^b}{b!} e^{-\lambda_j t}, b = 0, 1, \dots \quad (2)$$

Given that b is the instance for an occurrence of failure. Moreover, let $RT_j^{(b)}$ represent the b^{th} recovery time on j , where $b = 0, 1, \dots$. Emphatically, all $RT_j^{(b)}$ are exponential random variables with parameter μ_j , given that μ_j is the rate of recovery on j . Let the total recovery time during a time interval of $(0, t]$ on j be denoted as $RT_j(t)$. $RT_j(t)$, can be computed as in (3) [3].

$$RT_j(t) = \sum_{b=1}^{N_j(t)} RT_j^b \quad (3)$$

it is obvious that $RT_j(t)$ is a compound Poisson process, whose mean value is;

$$E[RT_j(t)] = \frac{\lambda_j(t)}{\mu_j} \quad (4)$$

Hence, the actual execution time of a job denoted by $AT_{kj}^{(e)}$, with fault recovery, is the sum of $T_{kj}^{(e)}$ and the recovery time of job k on j .

$$AT_{kj}^{(e)} = T_{kj}^{(e)} + RT_{kj} \quad (5)$$

With an expectation of

$$E[AT_{kj}^{(e)}] = E[T_{kj}^{(e)} + RT_{kj}] \quad (6)$$

The value RT_{kj} is the recovery time of job k on j . Moreover, based on our scenario jobs can be transmitted from the private cloud to the public cloud. Hence, there exist a time for communication. Let $\Theta(j_k)$ be the set of links that can be used to transfer jobs. Let the communication time without considering the possibility of a link failure be denoted by T_c . T_c , can be computed as shown in (7). Mathematically, T_c is dependent on the amount of data transferred through link c to its destination and the bandwidth b_w such that $c \in \Theta(j_k)$ [5].

$$T_c = \frac{\text{data}_c(j_k)}{b_w} \quad (7)$$

Assuming all failures are recoverable, then after some time (recovery time), the communication link gets connected and allows for data transfer. Let γ_c be the failure rate on link c [3].

The failure rate follows a Poisson process with rate γ_c . Hence, the total number of failures $X_c(t)$ during a time interval of $(0, t]$ can be computed as;

$$Pr\{X_c(t) = b\} = \frac{(\gamma_c t)^b}{b!} e^{-\gamma_c t}, b = 0, 1, \dots \quad (8)$$

Here, b is the instance for an occurrence of failure. Moreover, let the b^{th} recovery time on link c , where $b=0,1,\dots$ be denoted as $RT_c^{(b)}$. All $RT_c^{(b)}$ are exponential random variables with parameter (δ_c) . Given that δ_c is the rate of recovery on link c . Let the total recovery time on link c be denoted as $RT_c(t)$, the total recovery time during a time interval of $(0, t]$ can be computed as [5];

$$RT_c(t) = \sum_{b=1}^{X_c(t)} RT_c^b \quad (9)$$

It can be seen that $RT_c(t)$, is a compound Poisson process, whose mean value is

$$E[RT_c(t)] = \frac{\gamma_c(t)}{\delta_c} \quad (10)$$

If RT_c is the recovery time for communication failure, then the communication time considering fault and recovery denoted as T^{ce} can be computed as;

$$T^{ce} = T_c + RT_c \quad (11)$$

with an expectation of

$$E[T^{ce}] = E[T_c + RT_c] \quad (12)$$

Finally, there is the probability that an incoming job may find other jobs in the system on its arrival. At the arrival of a job, if the queuing system currently has sufficient vacancies, then the job will enter the queue, else it will be blocked and the job request fails. Details for computing the blocking probability can be found in [5]. All jobs that enter the queue successfully will possibly reach the scheduler S (S refers to homogeneous schedulers, $S > 1$) after some waiting time. For k jobs, the expected waiting time of jobs of size l in a queue for $l \leq S$ is given by:

$$E[T_k^W] = \begin{cases} 0 & 0 \leq k \leq S - l \\ \frac{k-S+l}{\mu_r S} & S - l \leq k \leq N - l \end{cases} \quad (13)$$

Moreover, the expected waiting time of a job of size l in a queue given that $l > S$ is given by:

$$E[T_k^W] = \frac{k - S + l}{\mu_r S}, 0 \leq k \leq N - l \quad (14)$$

where N , μ_r is the maximum number of jobs allowed to be in a queue and the service rate respectively. Details of this model have been well studied in [5] [23].

Let the overall execution time for each job k on j be denoted by T_{kj} . T_{kj} is therefore the sum of the actual execution time AT_{kj} , the actual communication time $T^{(ce)}$ and the waiting time T_k^W . Moreover, let T denote the overall execution time

for processing all user jobs considering fault recovery. T and T_{kj} can be computed as follows:

$$T_{kj} = AT_{kj}^{(e)} + T^{(ce)} + T_k^W$$

$$T = \sum_{k=1}^l \sum_{j=1}^n T_{kj} \quad (15)$$

with an expectation of

$$E[T] = E\left[\sum_{k=1}^l \sum_{j=1}^n T_{kj}\right] \quad (16)$$

C. Total Operational Cost

1) *Cost for Private VMs:* The total operational cost refers to the overall expense the SaaS provider realizes for provisioning resources to execute client request. It is worth noting that, some related works such as [4] and [20], which focused on a similar problem to that of this paper, do not factor into account the cost incurred at private Cloud. Similar to [19], we argue that there is a cost for running local or private datacenters and such cost has an effect on the total expenditure of the SaaS provider. The cost incurred at local is therefore modeled as an energy cost. In the computation of the energy cost, private servers are assumed to be in two states, namely; idle and active state. A CPU of a server in its idle state is assumed to consume averagely 70% of the power consumed by a fully active CPU [24]. The energy cost is therefore modeled as follows: the power consumption rate P_u of servers is given by;

$$P_u(U) = \beta \cdot \omega_{max} + (1 - \beta) \cdot \omega_{max} \cdot U \quad (17)$$

β , refers to a fraction of the maximum power used in an idle state while ω_{max} refers to the maximum power consumed by server in an active state and U is the utilization factor of the servers. If $U=0$ then it means the server is in an ideal state. Hence, the fraction of the maximum power will be the value of the energy consumed. The utilization of the servers varies with respect to time due to the workload variability. Accordingly, the utilization is a function of time and it is represented as $U(t)$. The total energy consumption on a compute node is given by [24];

$$P_U^T = \int_0^1 P_u U(t) \quad (18)$$

Given that the price for the power consumption of a compute node is a constant ε , as extensively studied in [70]. The price P_j^{priv} of a private VM is simply considered as the product of the constant ε and the number of compute units of that VM instance. That is $P_j^{priv} = \varepsilon \cdot U_j$ where U_j is the number of ECU in that VM instance. However, if a compute node is in idle state it is reasonable to consider the price of its VM as 70% of the active VMs price. That is although it is not in use but it consumes 70% of the power consumed by a fully active compute node as studied in [24]. Since in this paper all idle VMs are released immediately for allocation, the cost of running jobs on private VMs is considered only for active state VMs. Hence, the cost C_{kj}^{priv} for running the k^{th} job on private VM j where $1 \leq k \leq l$ and $1 \leq j \leq n$ can be computed as:

$$C_{kj}^{priv} = P_j^{priv} \cdot T_{kj} \quad (19)$$

Here P_j^{priv} is the price of the j^{th} VM instance in the private Cloud, and T_{kj} is the overall time for the completing job k on that j^{th} VM instance.

2) *Cost for Public VMs:* The cost of using public VMs is modeled to follow the Amazon EC2 billing model. Each instance runs for a minimum of one hour, hence the cost is computed per the execution time for job completion. Given that the price of a VM instance is represented as P_j^{pub} , let the cost for renting a VM at public be denoted as C_{kj}^{pub} . The cost for renting a public VM can be computed as:

$$C_{kj}^{pub} = P_j^{pub} \cdot T_{kj} \quad (20)$$

where $1 \leq k \leq l$ and $1 \leq j \leq n$. Therefore the cost for running VMs at local and renting On-demand VMs can be computed as shown in (21), where G is the communication cost between the VMs across the public and private Cloud. G is considered to be a constant.

$$Cost_{kj} = C_{kj}^{pub} + C_{kj}^{priv} + G \quad (21)$$

Furthermore, the total operational cost for running all jobs on available VM instances can be computed as:

$$C = \sum_k^l \sum_j^n Cost_{kj} \quad (22)$$

Here $1 \leq k \leq l$ and $1 \leq j \leq n$. With an expectation of;

$$E[C] = E\left[\sum_k^l \sum_j^n Cost_{kj}\right] \quad (23)$$

D. Problem Formulation

First, it is expected that a VM or a communication link may fail during the execution of jobs. The SaaS provider is challenged to make decisions on the number of VM instances to rent or instantiate at local such that total operational cost is reduced. Technically, clients have an estimated time (deadline) by which they expect their jobs to be completed. That means although there is the need to reduce total operational cost, the execution time of a job must not be greater than the deadline for the job. In this section, we present the optimization model for this problem. The problem is to minimize the total operational cost while ensuring that jobs are completed within its deadline. Formally:

$$\min E[C] \quad (24)$$

s.t.

$$\forall k \in \{1 \dots l\}, \forall j \in \{1 \dots n\} \quad (25)$$

$$E[T_{kj}] \leq D_k \quad (26)$$

(24): This is the optimization objective. It refers to the decision to minimize the total or overall operational cost. For instance, assuming there are five instance types of ECU values $\{1, 8, 13, 16, \text{ and } 26\}$, and the runtime in seconds for running **job 1** on a standard VM instance of 1 ECU is 2, then the runtime in seconds for running **job 1** on all the other VM

instances are {16, 26, 32, and 52} respectively. To achieve (24), the choice of VM instance chosen to run **job 1** should satisfy the constraint (25) and (26).

(25): This constraint indicates that a job is restricted to one VM during execution.

(26): An SLA contract is signed between the SaaS provider and users specifying the deadline for each job. The provider must therefore ensure that the overall execution time for each job does not exceed the clients' estimated deadline.

IV. DYNAMIC RESOURCE PROVISIONING ALGORITHM

The VMs and communication links across the hybrid Cloud is considered to be failure prone. Therefore, the problem of minimizing operational cost without deadline violation is non-trivial. Based on our optimization model we are able to address this problem with two provisioning policies, namely: the private and public provisioning policies. These policies are implemented by an efficient algorithm (DRPA). Fig.1 gives an overview of the framework of DRPA. First, jobs arrive at the Cloud management system (CMS). The CMS maintains queue and computes the runtime estimate of jobs based on the information provided by the resource pool manager (RPM). The RPM handles the peering arrangement between Datacenter 1 (DC_1) manager and Datacenter 2 (DC_2) manager. It verifies whether or not a job must be transferred to the public Cloud for execution based on the runtime estimate of the incoming jobs, the availability state of the VMs and their associated prices. Once verified, the scheduler then schedules the job on the VM of choice. The VM of choice refers to the VM which satisfies the objective in (24) with respect to its constraint in (25) and (26).

A. Runtime Estimation

Studies have shown that Cloud provisioning strategies based on user supplied runtime estimate of job sometimes leads to overestimation or overprovisioning of resources [25], [26]. Several works have proposed approaches to predict job runtime [25], [27], [28], where the system computes the estimated runtime of a job and uses it rather than the users' only. Moreover, as indicated by [26], no single method of runtime estimation has proven to work well in all scenarios. The runtime estimation technique is popularly used in backfilling service techniques. However, we employ it to aid the decision making involved in efficiently leveraging VM instances across the hybrid Cloud. Without loss of generality, four approaches for computing runtime of jobs are considered in this paper. The four approaches are generated by adjusting the *user supplied runtime estimate*. The models are namely: *user supplied*, *fraction of user supplied*, *user runtime with error* and *recent average runtime estimation models*. Based on each VM instance comprising a number of compute units, we compute the runtime estimate of each job. We employ the speedup model of Downey [29] which was also used by [27] and [30]. Downey's model [29] depends on two important factors, namely; the degree of parallelism of a job (A_k) and the coefficient of the variance of parallelism σ_k . The values of A_k and σ_k are modeled based on the job characteristics provided by users using the model of Cirne & Berman [31]. This model [31] was also adopted in [27]. Given the speedup

of k^{th} job on the j^{th} VM as S_{kj} , the runtime estimate α_{kj} of a job k on VM j is computed as shown in (27). U_j refers to the number of ECUs in the j^{th} VM.

$$\alpha_{kj} = \frac{U_j}{S_{kj}} \quad (27)$$

In the computation of the *user supplied runtime*, the job length used is assumed to be the job length given by the user at job submission. Since studies have shown that the user-supplied values leads to overestimation, an alternate approach have been proposed. Thus the *fraction of user supplied runtime* estimation. This approach uses a value equal to 1/3 of original value of the job length as used in the user supplied approach. In computing the *user runtime with error*, the estimate is obtained by using a slightly modified value of the job length as used in the user supplied runtime estimate. The modification is done by adding up a uniformly distributed random percentage between 0 and ten percent (10%) to the job length. Finally, in computing the *recent average runtime*, the average runtime of at least two completed jobs are used to generate the runtime of the next incoming job. At the extent of decision-making, if there exists less than two completed jobs, then the estimated value is assumed to be given by the user supplied approach [27], [32].

B. Provisioning Policies

1) *Private Provisioning Policy*: In our scenario, the SaaS provider intends to first run the incoming jobs on the private VMs. However, the provider can scale up for more VMs from the public Cloud when the need arises, i.e. public Cloud VMs are rented only when the waiting time of a job has exceeded its' threshold delay value W_k such that no other VM instance at local is available (i.e. $a_j=0$). The threshold delay value W_k of a job k is the maximum estimated time the job can wait for a VM to be provisioned such that its due deadline is still met. Incoming jobs may eventually be redirected to the public Cloud once its waiting time for the VM of Choice exceeds the threshold delay value and all other VMs at local are busy (i.e. $a_j=0$). W_k is computed as shown in (28), where D_k is the deadline of the waiting job, T_k^{ar} is the arrival time of the job, α_{kj} is the runtime estimate of the job on its VM of Choice and ρ is the modifying factor. That means, $D_k - T_k^{ar}$ refers to the time until the deadline of the job.

$$W_k = \max(0, D_k - T_k^{ar} - \alpha_{kj} \cdot \rho) \quad (28)$$

The modifying factor introduced in the computation of W_k supports the decision making for renting VM resources from the public Cloud. Algorithm 1 becomes more conventional when the value of the modifying factor ρ is greater. Specifically, W_k approaches 0 with higher values of ρ . A value of $W_k=0$ indicates that a resource must be provisioned immediately from the public Cloud to complete the job within the given deadline. On the other hand, lower values of ρ indicates that the value of W_k would be greater than 0, leading to postponement of provisioning actions and a high probability of running jobs on private VMs which are comparatively cheaper than VMs in the public Cloud but associated with deadline violations. The provisioning of VM for incoming job k at local must satisfy (29), such that (25) and (26) holds. Thus the minimum resulting value that is yielded when the price of

each VM in the private Cloud is multiplied by the runtime estimate α_k of the k^{th} job.

$$\mathbf{P1} = \min(P_j^{priv} \cdot \alpha_{kj}) \quad (29)$$

Let the private provisioning policy problem be called **P1**

2) *Public Provisioning Policy*: Public Cloud VMs are rented only when the waiting time of a job has exceeded the threshold delay value W_k . A job may wait to be assigned to a VM of choice if the VM is expected to be free soon. However, if the waiting time of the job exceeds its threshold delay value W_k , then the SaaS provider must decide on the VM to rent from the public Cloud. The VM to rent from the public Cloud can be determined by solving (30). The VM of choice, with respect to the public provisioning policy, refers to the VM which satisfies the objective in (30) while constraint in (25) and (26) holds.

$$\mathbf{P1} = \min(P_j^{pub} \cdot \alpha_{kj}) \quad (30)$$

P_j^{pub} , is the price of the j^{th} VM instance in the public Cloud and α_{kj} is the runtime estimate of the job k on that instance. Let the public Cloud provisioning be called **P2**.

To achieve the optimization objective, we designed a heuristic-based dynamic resource provisioning algorithm DRPA as shown in Algorithm 1 to solve **P1** and **P2**. Each job is considered to have a number of parallel tasks. Jobs are either transferred to the public Cloud or run on the private Cloud based on its runtime estimate, deadline, waiting time as against the threshold value, the availability state and the prices of the VMs. Initially, no VM is rented from the public Cloud. For each job k that arrives at the CMS, its runtime estimate α_{kj} is computed. Given that the pool of VM instance is R_p , the job is first directed to the private Cloud on the condition that the available VMs in the private Cloud are free and satisfies **P1** (Step 1-8). The determination of the VM of choice in the private cloud is initiated by solving **P1**. The result of **P1** is simply the minimum resulting value that is yielded when the price of each VM in the private Cloud is multiplied by the runtime estimate α_{kj} of the k^{th} job. The VM of choice is then scheduled to run the k^{th} job. (step 9). Next, the availability-state of the VMs in the private cloud are updated (step 10). If the VM of choice is not available (i.e $a_j=0$) then the job j_k must wait provided that its' waiting time does not exceed the delay threshold factor W_k . If the job can wait, then it is added to the waiting list **W** and scheduled (added to the waiting list **W**) to run on the VM expected to be free or idle soon (Steps 12-14). As indicated in (steps 25-30), for each job found in **W**, the algorithm will first search for other VMs in the private Cloud which may be free and satisfies **P1** to complete the job. Otherwise, the VM instance in the public Cloud which satisfies **P2** will be rented On-demand to run the job (steps 16-18). The solution of **P2** is simply the minimum resulting value that is yielded when the price of each VM rented from the public Cloud is multiplied by the runtime estimate α_k of the k^{th} job. After the job is completed, the VM is shut down to avoid extra billing (step 19). The queue is updated and the next job follows (Step 34). The application of methods such as job runtime estimation, job postponing, and idle VM instance termination assures that the provisioning policy keeps an all encompassing view of the incoming jobs which are dynamic in nature.

Algorithm 1 Dynamic Resource Provisioning

Input: set of jobs, VM prices, VM instances

Output: Dynamic provisioning of VM resources with minimum cost

```
1: for each job  $j_k$  do
2:    $\alpha_{kj} \leftarrow$  compute runtime estimate on all instances;
3:    $R_p \leftarrow$  resource pool ( $R_{priv} \cup R_{pub}$ );
4:    $R_{pub} \leftarrow \emptyset$ ;
5:   decision  $\leftarrow$  select $R_{priv}$ ;
6:   compute  $W_k$ ;
7:   for each VM resource  $R_j$  in private Cloud do
8:     if ( $a_j = 1$ ) then
9:       solve P1;
10:      Update VMs  $a_j$  state;
11:    else
12:      if ( $W_k > 0$ ) then
13:        Delay job until  $W_k$ ;
14:        Add job to waiting list W;
15:      else
16:        decision  $\leftarrow$  select  $R_{pub}$ ;
17:        for each VM resource  $R_j$  in public Cloud do
18:          Solve P2;
19:          VMIdle.Shutdown;
20:        end for
21:      end if
22:    end if
23:  end for
24: end for
25: for each job  $J_k \in W$  do
26:   decision  $\leftarrow$  select  $R_{priv}$ ;
27:   for each VM resource  $R_j$  in private Cloud do
28:     if ( $a_j=1$ ) then
29:       Solve P1;
30:       Remove job  $J_k$  from W;
31:     end if
32:   end for
33: end for
34: Update queue;
```

V. PERFORMANCE EVALUATION

In this section, we study the performance of the proposed DRPA. We run a set of experiments using a real world workload log obtained from the Distributed ASCI Supercomputer 2 (DAS2 fs4) available at the Parallel Workloads Archive [33]. The original workload is composed of a total of 33,795 with parallel tasks submitted over a period of 11 months by a total of 40 users. This workload is suitable for the simulation in this work because of its property of parallelism and varied job lengths. It contains an information about the user supplied runtime estimate. However, as stated earlier, we shall conduct a further evaluation of the DRPA using other runtime estimation methods namely: *user runtime estimate with error*, *fraction of user supplied runtime estimate* and the *recent average runtime estimate*. The objective of our experimental study is to evaluate the performance of DRPA based on two metrics; cost and deadline violation rate in the presence of VM and communication link failure. In order to capture the performance of the proposed algorithm, our results are averaged on 50 simulation runs with varying number of jobs between 3,000 and 33,000.

In the first part of our experiments, we study the effects of the four runtime estimation approaches on the DRPA in two cases: first, considering fault and recovery; second, without considering fault and recovery. The objective is to determine the kind of runtime approach which works better as against our performance metrics. In the second part of our experiment, we conduct a comparative study with two benchmark approaches namely: the best and worse case approaches [19] [27] and also with a recent algorithm called Size-based Selective-backfilling hybrid Cloud provisioning policy [4]. The objective of such comparison is to demonstrate the efficiency of the proposed algorithm.

A. Experimental Setup

We performed all our experiments on a Pentium(R) Dual-Core processor with a processor speed of 2.8GHz and a memory of 4GB. The CloudSim toolkit [34] was used to simulate a Cloud system consisting of two datacenters, namely *datacenter1* and *datacenter2*. *datacenter1* is the datacenter for the public Cloud and *datacenter2* is the datacenter for the private Cloud. The NetworkTopology component of the CloudSim was modified to represent the communication between the Datacenters. Five instance types were simulated in the experiments. They were modeled after the characteristics of Amazon EC2 types [21]. The set of possible values of ECU is U_j : 1, 8, 13, 16, and 26. The EC2 types which are of the exact ECU characteristics are m1.small (1 ECU), c4.large (8 ECUs), m4.large (13 ECUs), c4.xlarge (16 ECUs), and m4.2xlarge (26 ECUs). The five VM instance types are hosted on each datacenter with distinguishing properties with respect to their ECUs. Since the public Cloud is perceived to have unlimited resources, five times of the VM instance type in the *datacenter1* are hosted on *datacenter2*. However, this number increases as may be required for renting. Moreover, to obtain the values of the processor speeds and prices in the public Cloud, we adopt a similar method as applied in [35], because their approach was modeled after Amazon EC2 services. The processor speed of each host is uniformly distributed within the range [100, 1000] with the average speed of 550 MIPS. Without loss of generality, the price of a VM have roughly linear relationship with its processor speed, so as to generally ensure that a faster host yields more execution cost than a slower host in executing the same job. The method to derive the processor speed in the private Cloud is generated in the same way as in the public. However, its prices are generated according the energy cost model. The value of the constant ε as used in the experiment is 0.04 (ε is the constant price assumed for energy consumption). The failure rates of the VMs and communication links are randomly generated from the interval of [0.01, 0.1] [5] [6]. All recovery rates are randomly generated from the interval of [0.05, 0.15]. The average bandwidth between the compute nodes is set to 10 Mbps as used in [4], and finally, the modifying factor ρ is a uniformly distributed random values between 0 and 2.

B. Effects of the Four Runtime Estimation Approaches

First, we evaluated DRPA using each of the runtime estimation approach against the performance metrics considering fault and recovery. The results in Fig. 2a and Fig.2b, shows the behavior of DRPA after job execution. It can be seen

that, the Total operational cost increases slowly when the workload is relatively small. This is attributed to the fact that at such point most of the jobs are run on the private Cloud. However, when the workload shoots up there is a relative increase in total operational cost due to the cost for renting resources from the public Cloud. Moreover, the peak cost for each of the approach varies. The fraction of user supplied runtime approach yields the cheapest cost with comparatively, the worst deadline violation as can be shown in Fig.2b. This is due to the underestimation of the user job length. This underestimation resulted in the acquisition of relatively minimum runtime estimate which led to the deployment of VMs with cheap cost, hence causing its total operational cost to be the cheapest. However, this caused much deadline violation, hence causing its deadline violation rate to be 25.46%. According to Fig.2a and Fig.2b, it is obvious that the user runtime with error approach achieved the best results with respect to the two performance metrics; Total operational cost and deadline violation rate. It comparatively achieved a total operational cost of \$3,749.00 which is about 14.4% better than the total operational cost of the user supplied runtime approach. Moreover, it yielded a deadline violation rate of 5.34% which is approximately 13% greater than the deadline violation rate of the user supplied runtime approach. The user runtime with error approach of the proposed ODPa performed consistently better.

Secondly, we evaluate DRPA using the four runtime approaches as against the performance metrics without considering fault and recovery. Fig.3a and Fig. 3b, shows the comparative results of the four approaches as against Total cost and deadline violation with and without fault recovery respectively. First, it is obvious to point out that without considering fault and recovery the various runtime approaches performs relatively better against cost and deadline violation than the case where fault and recovery is considered. In essence, this demonstrates the impact of fault recovery on service performance. It can be deduced that, it is relevant to develop a Cloud system that factors into account fault recovery, since it has relative impact on the cost and the execution time for job completion.

In summary, it can be observed that, for a given workload, having a perfect runtime estimate does not actually translate into a more efficient provisioning, especially in terms of cost. This is due to the fact that all of the approaches had a relatively low or high deadline violation. This can be attributed to moderate over or under estimations, which caused cheaper or relatively expensive instances to be requested. Analytically, the user runtime with error approach in this work appears to be comparatively better than the rest of the approaches against the two performance metrics (cost and deadline violation).

C. Comparative Analysis

In this experiment, we simulated three other algorithms namely: Size-based selective-backfilling algorithm [4], Best case algorithm [19], and worst case [27] algorithm. In the worst case, it is assumed that all jobs are processed with VMs rented from the public Cloud in an On-demand fashion. However, the information for each job is known. Jobs are run on the most efficient VMs. Similar to [19], in the best case scenario, it is assumed that there is an oracle that knows all the future

TABLE II. COMPARATIVE ANALYSIS OF DRPA WITH OTHER ALGORITHMS

Algorithms	Number of Jobs	Cost for Renting(\$)	Private Cost(\$)	Total Operational Cost(\$)	Deadline Violation Rate (%)
Best Case [19]	33,000	0	2,937.00	2,937.00	0
Worst Case [27]	33,000	7,764.00	0	7,764.00	0
SBSB [4]	33,000	3892.00	NC	3892.00	9.938
DRPA(USRWE)	33,000	3,531.00	218.00	3,749.00	5.34

DRPA(USRWE)- Dynamic resource provisioning algorithm with User runtime with error approach, NC- not considered

information and can use the most efficient VM instance for each job to achieve an ideal solution. It is worth noting that, the best case scenario is not real. However, it is hypothetically considered as a lower bound implemented to evaluate the cost-effectiveness of the proposed policy. The Size-based selective-backfilling algorithm (SBSB) [4] was proposed by Javadi et al. They considered a similar hybrid Cloud resource provisioning problem to ours. However, they do not consider the cost incurred at the private Cloud as well as the probability of failure in both the private and public Cloud. They assumed that only the VMs in the private Cloud are failure prone.

To evaluate our proposed algorithm, we adopt the user runtime with error approach (USRWE) as the base policy of DRPA and compare its result to the simulation results of the Best Case, Worst Case and the SBSB algorithms. The result in Fig. 4a, Fig. 4b and in Table II shows the behavior of the four algorithms after running 33,000 jobs. Comparing the results obtained in Table II for the cost of renting VMs in the case of each algorithm, the proposed DRPA(USRWE) outperforms the size-based selective backfilling (SBSB) and the Worst Case algorithms by a percentage of approximately 9.3% and 54.52% respectively. However, the Best Case algorithm yields a result that outperforms all the other three algorithms including our algorithm. It yielded no cost all (\$0.00), because in the Best Case scenario all jobs are run on the private Cloud.

On the other hand, our proposed DRPA(USRWE) outperforms the Best Case algorithm in terms of the operational cost at the private Cloud. The Worst Case yielded no cost at all (\$0.00) since in this scenario all jobs are run with VMs in the public Cloud. Hence, it outperformed both our DRPA(USRWE) which yielded a cost of \$218.00 and the Best Case which yielded a cost of \$2,937.00. In contrast, the SBSB algorithm does not factor into account the operational cost at the private Cloud. It must be noted that the cost of the Best case is high because in this scenario all the 33,000 jobs were run on the private Cloud. Moreover, considering the results of our proposed DRPA(USRWE) in terms of the cost for renting and the cost at the private Cloud, it can be observed that the cost for renting is fairly larger than the cost at private. This can be attributed to two factors: first, the assigned price for a VM at the private Cloud was fairly lower than that of the cost in the public Cloud. Second, about 55% of the jobs were run with VMs on the public Cloud due to the need to satisfy the deadline constraint of jobs.

Considering the total operational cost of all the algorithms, the proposed DRPA(USRWE) yielded \$3,749.00 which is approximately 51.71% better than the Worst Case. However, when compared with the Best Case, it is approximately 28% worse. Also it is 3.71% better than the SBSB algorithm. There was no deadline violation in the Best and Worst Case comparatively. Unlike Best and the Worst Case, the deadline

violation rate of the proposed DRPA(USRWE) is 5.34% which is 46.27% better than the SBSB algorithm.

In summary, the obtained results show that, by the adoption of the proposed DRPA(USRWE), SaaS providers can save 51.71% of total cost compared to the Worst Case scenario, even in the presence of VM and communication link failures, with a relatively low deadline violation rate of 5.34%. Moreover, the proposed DRPA(USRWE) performs better than SBSB by a percentage of 9.3% with respect to the cost for renting VM instances.

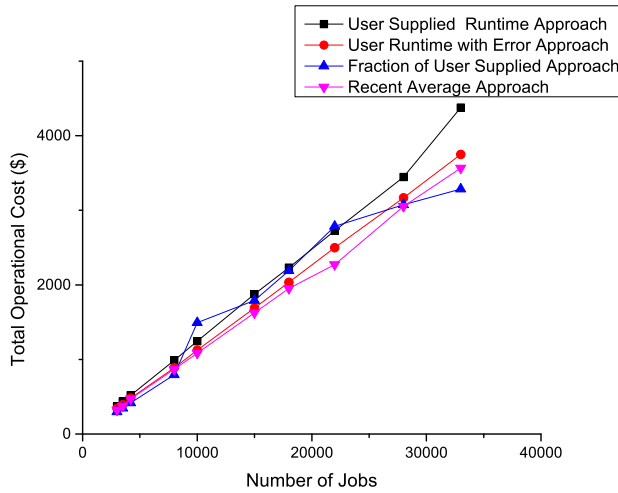
VI. CONCLUSION

In the hybrid Cloud paradigm, SaaS providers are faced with the challenge of minimizing cost without sacrificing resource provisioning service performance. The probability of VM and communication link failure is a real life factor which has an effect on service performance. This paper focuses on the problem of minimizing total operational cost involved in hybrid Cloud resource provisioning considering fault recovery. Specifically, we propose a heuristic-based algorithm which applies methods such as job runtime estimation, job postponing, and idle VM instance termination to assure that the provisioning policy keeps an all encompassing view of the incoming jobs which are dynamic in nature. The results obtained from our experimental study show that, by the adoption of the proposed DRPA(USRWE), SaaS providers can save 51.71% of total cost compared to the Worst Case scenario, even in the presence of VM and communication link failures, with a relatively low deadline violation rate of 5.34%. Moreover, the proposed DRPA(USRWE) outperforms the recently proposed SBSB by a percentage of 9.3% with respect to the cost for renting VM instances.

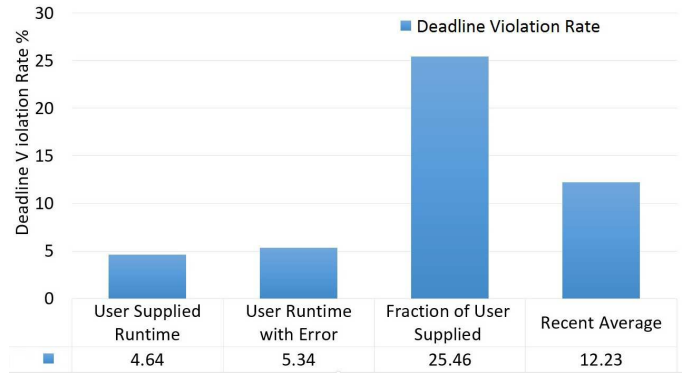
REFERENCES

- [1] R. Buyya, C. S. Yeo, S. Venugopal, J. Broberg, and I. Brandic, "Cloud computing and emerging {IT} platforms: Vision, hype, and reality for delivering computing as the 5th utility," *Future Generation Computer Systems*, vol. 25, no. 6, pp. 599 – 616, 2009.
- [2] D. Davis, *Companies Enjoying Big Success with Hybrid Cloud*. Skytap blog, 2013. [Online]. Available: <https://www.skytap.com/blog/companies-enjoying-big-success-with-hybrid-cloud/>
- [3] W. Q. Heyang Xu, Bo Yang and E. Ahene, "A multi-objective optimization approach to workflow scheduling in clouds considering fault recovery," *KSII Transactions on Internet and Information Systems*, vol. 10, no. 3, pp. 976–995, March 2016.
- [4] B. Javadi, J. Abawajy, and R. Buyya, "Failure-aware resource provisioning for hybrid cloud infrastructure," *Journal of Parallel and Distributed Computing*, vol. 72, no. 10, pp. 1318 – 1331, 2012.
- [5] B. Yang, F. Tan, and Y.-S. Dai, "Performance evaluation of cloud service considering fault recovery," *The Journal of Supercomputing*, vol. 65, no. 1, pp. 426–444, 2013.

- [6] B. Yang, H. Hu, and S. Guo, "Cost-oriented task allocation and hardware redundancy policies in heterogeneous distributed computing systems considering software reliability," *Comput. Ind. Eng.*, vol. 56, no. 4, pp. 1687–1696, May 2009.
- [7] R. Raman, M. Livny, and M. Solomon, "Matchmaking: An extensible framework for distributed resource management," *Cluster Computing*, vol. 2, no. 2, pp. 129–138, 1999.
- [8] K. Krauter, R. Buyya, and M. Maheswaran, "A taxonomy and survey of grid resource management systems for distributed computing," 2001.
- [9] B. Palanisamy, A. Singh, L. Liu, and B. Langston, "Cura: A cost-optimized model for mapreduce in a cloud," in *Parallel Distributed Processing (IPDPS), 2013 IEEE 27th International Symposium on*, May 2013, pp. 1275–1286.
- [10] L. Wu, S. K. Garg, and R. Buyya, "Sla-based resource allocation for software as a service provider (saas) in cloud computing environments," in *Cluster, Cloud and Grid Computing (CCGrid), 2011 11th IEEE/ACM International Symposium on*, May 2011, pp. 195–204.
- [11] S. Chaisiri, R. Kaewpuang, B. S. Lee, and D. Niyato, "Cost minimization for provisioning virtual servers in amazon elastic compute cloud," in *2011 IEEE 19th Annual International Symposium on Modelling, Analysis, and Simulation of Computer and Telecommunication Systems*, July 2011, pp. 85–95.
- [12] Q. Li, Q. Hao, L. Xiao, and Z. Li, "Adaptive management of virtualized resources in cloud computing using feedback control," in *2009 First International Conference on Information Science and Engineering*, Dec 2009, pp. 99–102.
- [13] M. Mishra, A. Das, P. Kulkarni, and A. Sahoo, "Dynamic resource management using virtual machine migrations," *IEEE Communications Magazine*, vol. 50, no. 9, pp. 34–40, September 2012.
- [14] T. R. G. Nair and M. Vaidehi, "Efficient resource arbitration and allocation strategies in cloud computing through virtualization," in *2011 IEEE International Conference on Cloud Computing and Intelligence Systems*, Sept 2011, pp. 397–401.
- [15] B. C. Tak, B. Urgaonkar, and A. Sivasubramaniam, "To move or not to move: The economics of cloud computing," in *Proceedings of the 3rd USENIX Conference on Hot Topics in Cloud Computing*, ser. HotCloud'11. Berkeley, CA, USA: USENIX Association, 2011, pp. 5–5.
- [16] M. Hajjat, X. Sun, Y.-W. E. Sung, D. Maltz, S. Rao, K. Sripanidkulchai, and M. Tawarmalani, "Cloudward bound: Planning for beneficial migration of enterprise applications to the cloud," *SIGCOMM Comput. Commun. Rev.*, vol. 40, no. 4, pp. 243–254, Aug. 2010.
- [17] T. Guo, U. Sharma, T. Wood, S. Sahu, and P. Shenoy, "Seagull: Intelligent cloud bursting for enterprise applications," in *Proceedings of the 2012 USENIX Conference on Annual Technical Conference*, ser. USENIX ATC'12. Berkeley, CA, USA: USENIX Association, 2012, pp. 33–33.
- [18] P. Marshall, K. Keahey, and T. Freeman, "Elastic site: Using clouds to elastically extend site resources," in *Cluster, Cloud and Grid Computing (CCGrid), 2010 10th IEEE/ACM International Conference on*, May 2010, pp. 43–52.
- [19] S. Li, Y. Zhou, L. Jiao, X. Yan, X. Wang, and M. R. Lyu, "Delay-aware cost optimization for dynamic resource provisioning in hybrid clouds," in *Web Services (ICWS), 2014 IEEE International Conference on*, June 2014, pp. 169–176.
- [20] B. Javadi, J. Abawajy, and R. O. Sinnott, "Hybrid cloud resource provisioning policy in the presence of resource failures," in *Cloud Computing Technology and Science (CloudCom), 2012 IEEE 4th International Conference on*, Dec 2012, pp. 10–17.
- [21] A. Inc, "Ec2 instances," pp. 1136 – 1142, 2007. [Online]. Available: <https://aws.amazon.com/ec2/instance-types/>
- [22] A. B. Downey, "A model for speedup of parallel programs," Berkeley, CA, USA, Tech. Rep., 1997.
- [23] P. Vijaya Laxmi and U. Gupta, "Analysis of finite-buffer multi-server queues with group arrivals: Gix/m/c/n," *Queueing Systems*, vol. 36, no. 1, pp. 125–140, 2000.
- [24] A. Beloglazov, J. Abawajy, and R. Buyya, "Energy-aware resource allocation heuristics for efficient management of data centers for cloud computing," *Future Generation Computer Systems*, vol. 28, no. 5, pp. 755 – 768, 2012, special Section: Energy efficiency in large-scale distributed systems.
- [25] D. Tsafirir, Y. Etsion, and D. G. Feitelson, "Backfilling using system-generated predictions rather than user runtime estimates," *IEEE Transactions on Parallel and Distributed Systems*, vol. 18, no. 6, pp. 789–803, June 2007.
- [26] D. Tsafirir, *Using Inaccurate Estimates Accurately*, E. Frachtenberg and U. Schwiegelshohn, Eds. Berlin, Heidelberg: Springer Berlin Heidelberg, 2010.
- [27] W. Voorsluys, S. K. Garg, and R. Buyya, "Provisioning spot market cloud resources to create cost-effective virtual clusters," in *Proceedings of the 11th International Conference on Algorithms and Architectures for Parallel Processing - Volume Part I*, ser. ICA3PP'11. Berlin, Heidelberg: Springer-Verlag, 2011, pp. 395–408. [Online]. Available: <http://dl.acm.org/citation.cfm?id=2075416.2075453>
- [28] W. Tang, N. Desai, D. Buettner, and Z. Lan, "Analyzing and adjusting user runtime estimates to improve job scheduling on the blue gene/p," in *Parallel Distributed Processing (IPDPS), 2010 IEEE International Symposium on*, April 2010, pp. 1–11.
- [29] A. B. Downey, "A model for speedup of parallel programs," Berkeley, CA, USA, Tech. Rep., 1997.
- [30] A. W. Mu'alem and D. G. Feitelson, "Utilization, predictability, workloads, and user runtime estimates in scheduling the ibm sp2 with backfilling," *IEEE Transactions on Parallel and Distributed Systems*, vol. 12, no. 6, pp. 529–543, Jun 2001.
- [31] W. Cirne and F. Berman, "Using moldability to improve the performance of supercomputer jobs," *Journal of Parallel and Distributed Computing*, vol. 62, no. 10, pp. 1571 – 1601, 2002.
- [32] D. Tsafirir, Y. Etsion, and D. G. Feitelson, "Modeling user runtime estimates," in *In 11th Workshop on Job Scheduling Strategies for Parallel Processing (JSSPP 2005)*. Springer-Verlag, 2005, pp. 1–35.
- [33] W. Archive, "Logs of real parallel workloads from production systems," 2003. [Online]. Available: <http://www.cs.huji.ac.il/labs/parallel/workload/>
- [34] R. N. Calheiros, R. Ranjan, A. Beloglazov, C. A. F. De Rose, and R. Buyya, "Cloudsim: A toolkit for modeling and simulation of cloud computing environments and evaluation of resource provisioning algorithms," *Softw. Pract. Exper.*, vol. 41, no. 1, pp. 23–50, Jan. 2011.
- [35] S. Abrishami, M. Naghibzadeh, and D. H. Epema, "Deadline-constrained workflow scheduling algorithms for infrastructure as a service clouds," *Future Generation Computer Systems*, vol. 29, no. 1, pp. 158 – 169, 2013, including Special section: AIRCC-NetCoM 2009 and Special section: Clouds and Service-Oriented Architectures.

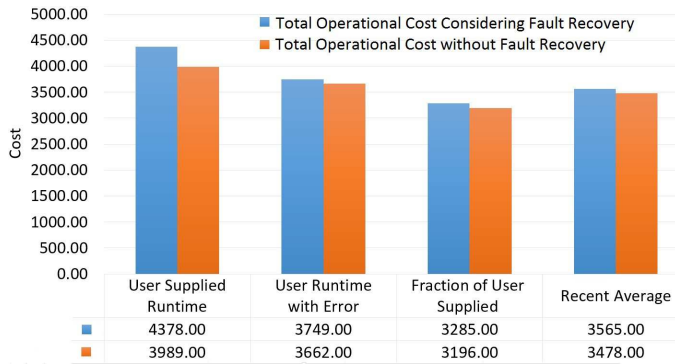


(a) Total Operational Cost of the four Runtime Approaches

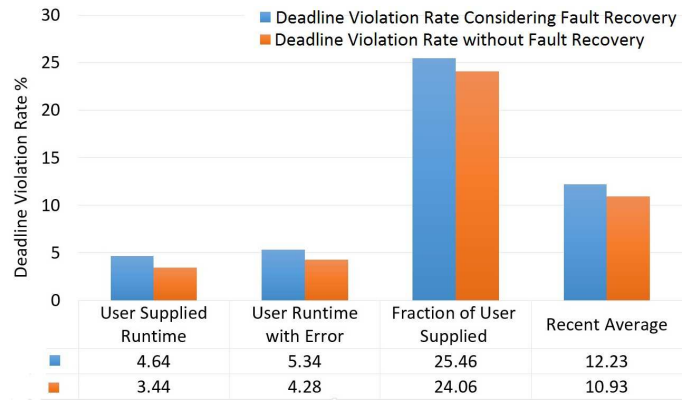


(b) Deadline Violation rate of the four Runtime Approaches

Fig. 2. Simulation results using the four approaches

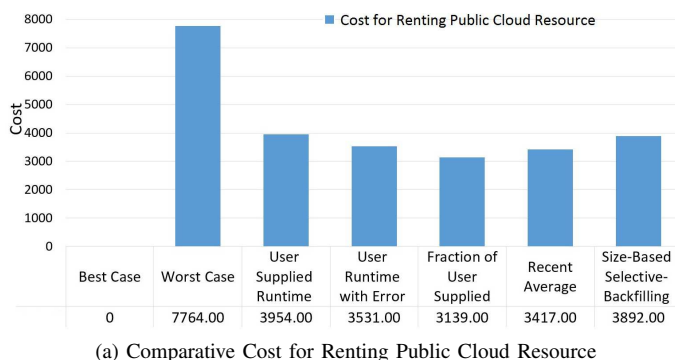


(a) Impact of Fault Recovery on Total Operational Cost

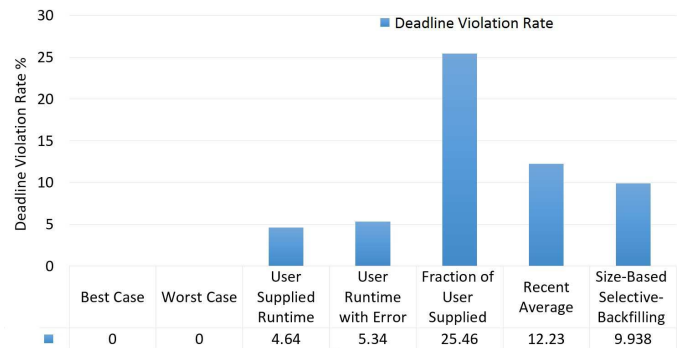


(b) Impact of Fault Recovery on Deadline Violation Rate

Fig. 3. Simulation results depicting the impact of Fault Recovery on DRPA



(a) Comparative Cost for Renting Public Cloud Resource



(b) Comparative Analysis of Deadline Violation Rate

Fig. 4. Simulation results depicting the performance of DRPA against other Algorithms

Using Real-World Car Traffic Dataset in Vehicular Ad Hoc Network Performance Evaluation

Lucas Rivoirard
Univ Lille Nord de France,
IFSTTAR, COSYS, LEOST
F-59650 Villeneuve d'Ascq, France

Martine Wahl
Univ Lille Nord de France,
IFSTTAR, COSYS, LEOST
F-59650 Villeneuve d'Ascq, France

Patrick Sondi
Univ. Littoral Côte d'Opale,
LISIC - EA 4491
F-62228 Calais, France

Marion Berbineau
Univ Lille Nord de France,
IFSTTAR, COSYS
F-59650 Villeneuve d'Ascq, France

Dominique Gruyer
IFSTTAR, COSYS, LIVIC
F-78000 Versailles, France

Abstract—Vehicular ad hoc networking is an emerging paradigm which is gaining much interest with the development of new topics such as the connected vehicle, the autonomous vehicle, and also new high-speed mobile communication technologies such as 802.11p and LTE-D. This paper presents a brief review of different mobility models used for evaluating performance of routing protocols and applications designed for vehicular ad hoc networks. Particularly, it describes how accurate mobility traces can be built from a real-world car traffic dataset that embeds the main characteristics affecting vehicle-to-vehicle communications. An effective use of the proposed mobility models is illustrated in various road traffic conditions involving communicating vehicles equipped with 802.11p. This study shows that such dataset actually contains additional information that cannot completely be obtained with other analytical or simulated mobility models, while impacting the results of performance evaluation in vehicular ad hoc networks.

Keywords—MOCOPO dataset; mobility models; vehicular ad hoc networks; simulation; performance evaluation

I. INTRODUCTION

VANET (Vehicular Ad Hoc Network) is a promising application of MANET (Mobile Ad Hoc Networks) where nodes consist of vehicles which organize themselves in order to communicate efficiently. Using ad hoc communications allow fast and direct vehicle-to-vehicle (V2V) exchanges, besides the telecommunication services that can be offered by an infrastructure, when it exists, through vehicle-to-infrastructure communications (V2I). For instance, vehicles can exchange contextual or traffic management information. Safety and security applications can also rely on V2V communications in order to avoid a collision or send post-crash warnings.

With the wide deployment of 3G and 4G infrastructures, many new mobile services are proposed to drivers through their smartphones or built-in car devices. Both the network service providers and the designers of these applications can make use of the information collected over thousands of users in order to evaluate and to improve the performance. Such opportunity is not yet accessible to vehicular ad hoc networks due to nonexistence of large-scale experimentation. Also, V2V applications will not be widely adopted unless serious studies

and evaluations prove their efficiency in realistic car traffic contexts. Consequently, building accurate testing environments for VANET performance evaluation is a crucial issue for the future of V2V communications. The performance of VANETs can be evaluated by means of real-world testings on the ground or through modelling and simulation. For the aforementioned reasons, the first solution may be costly and will not carry out the whole field situations: it is difficult to equip a significant number of vehicles and to experiment the performance of network communication in every different traffic conditions. The second solution, namely modelling, is easier to realize by means of computers and may include many complex models. However, the accuracy depends notably on the availability of realistic mobility models.

The authors of [1] and [2] show that, depending on the mobility model, the results of performance evaluation are different for the same routing protocol. An example is developed in [1] based on the DSR protocol. Generally in the literature, the modelling of vehicle mobility are made thanks to random patterns, microscopic traffic simulators, or real traces of vehicles. In this paper, the authors discuss the benefit of using real traces of vehicles extracted from car traffic dataset in simulation-based evaluation of vehicular ad hoc network performance. This study uses the real traces processed by [3] based on road videos filmed by helicopter within the context of the French research project named MOCOPO (Measuring and Modelling Congestion and Pollution).

The paper is organized as follows. First, some work related to mobility models in vehicular ad hoc network are presented. The MOCOPO dataset traces are described, and then discussed in comparison with other mobility models. A simulation system is configured in order to realize performance evaluation of a VANET using the proposed dataset. Finally, the simulation results are discussed, before the conclusion.

II. RELATED WORK

The works in [4]–[7] present the evolution of the mobility models used in VANET evaluation. This paper focuses on a brief review of the most representative models used during this

evolution, notably the historical Random Waypoint, the Manhattan model, the microscopic traffic simulators, and finally the real traces from car traffic dataset.

A. Random Waypoint model

The first mobility model used in VANET studies was the Random Waypoint model (RW). In this model, each node randomly chooses an origin and a destination in the simulation representation of the space, and also a speed value between zero and a given maximum limit. The speed remains fixed along the journey. Once the destination is reached, a timer is triggered, and the node selects a new destination and a new speed value.

This model, very simple to set up, is still used in many studies such as [8]–[11]. It is often used for VANET because it allows to define high speed nodes. In fact in most European countries, under normal conditions, a vehicle in a VANET can travel up to 130 km/h on the highway. Therefore, the relative speed between two vehicles can vary from 0 to 260 km/h.

However, the path followed by the nodes in RW model is always a straight line. Moreover, it does not take into account the restricted vehicle motion degrees imposed by the road layout. Last, the significant dispersion of the speed values over the time and space is also another important feature of mobility that cannot be taken into account with this model. Indeed, during its journey, vehicle speed on highway can be either 130 km/h in a fluid traffic or 5 km/h in case of congestion [12]–[14].

B. Manhattan model

The Manhattan model improves the Random Waypoint model by introducing a representation of the vehicle motion degrees. The nodes move on a road represented by a grid that limits the vehicle movement. Origins and destinations of the vehicle trajectories are randomly chosen. The trajectories are calculated either by algorithms such as the Dijkstra shortest path or by using a probability to select a direction when vehicles arrived at a cross-road. The Manhattan model is used for instance in [15] or [16].

However, in real life, road users must respect the traffic rules and sign regulations; vehicles are constantly reacting according to each other. This cannot be observed in the Manhattan model where vehicles can move across each other.

C. Microscopic traffic simulator

Various studies, related to traffic theories [12]–[14], [17], [18], strive to model driver behaviour. The models are realized through microscopic simulators which implement one of the following models : stochastic models, traffic flow models, car following models, queue models, or behaviour models. They simulate every car in detail, with breaks, accelerations and lane changing. Such simulators bring a road representation that the random mobility model does not, and they implement the significant dispersion of speed values over time and space. They easily allow researchers to schedule a mobility scenario such as a congested highway. Among them, SUMO [19] and VanetMobiSim [20] are the most referenced in the literature (for instance [21], [22]). They take into account multi-lane

roads, vehicles changing lane, speed limits, and intersection priorities (stop signs and traffic lights) [7].

Nevertheless, the choice of the origin and destination for a vehicle is randomly selected whatever the road reality. Another drawback is that microscopic simulators use probability profiles like acceleration or deceleration profiles which add a difference between the model and the reality. This is especially true for extreme driving behaviours which are not considered.

D. Real traces of vehicles

Mobility traces of vehicles through GPS data can be easily found nowadays. As an example, the Community Resource for Archiving Wireless Data At Dartmouth (CRAWDAD, [23]) provides trajectory datasets for VANET studies. GPS traces are obtained with map-matching algorithms. They come from specific vehicle fleets, such as bus or taxi fleets, which sometimes travel with dedicated work constraints. They do not come from common car users which are the first user class of road.

Real traces based on GPS can be used to study the connection time between vehicles. In this way, [24] uses GPS traces from taxis and shows that the high mobility of VANETs induces time-limited connections between vehicles. Indeed, two vehicles, travelling from opposite directions on the highway at 130 km/h and having a maximum communication range of 500-meter long, will only communicate for up to 15 s [25]. In fact, a difficulty of using GPS real traces is that, currently, either vehicles are not close together (dispersed within a wide area) or they include very few vehicles. Consequently, such traces do not allow an accurate study of V2V ad hoc communications with various vehicle density. However, the traces provided by CRAWDAD could be relevant to study the protocols and applications relying on vehicle-to-infrastructure communications.

It is possible to obtain real traces of vehicle trajectories with aerial road traffic recordings. Studies had been achieved in the past by mounting a camera on a fixed position or on-board aerial platform [26]. [3] notes that two main groups of datasets were constructed since the beginning of this century: series of datasets resulting from the experiments conducted in the Netherlands by the TU Delft [27] and the datasets of the NGSim project, conducted with the funding and supervision of FHWA [28]. Only the NGSim datasets are made publicly available on the web. But there is noise in the longitudinal and lateral positional information of vehicles, and data need to be filtered in order to determine their positions, velocities, and accelerations [29].

III. A CAR TRAFFIC DATASET FOR VANET EVALUATION

A. Presentation of the MOCOPo data

The MOCOPo research project (Measuring and Modelling Congestion and Pollution) was a French project aiming to improve the modelling of congestion and pollutant in urban highways (January 2011 - December 2013). The data collection was performed at the RN 87 (in the southern suburbs of Grenoble) in September 2011. A helicopter equipped with three high-definition cameras filmed the highway for several hours. In addition, pollutant measurement and loop detector

data were collected. The site of the project [30] provides maps and access to the data.



Fig. 1. The 500-meter-long RN87 section filmed in Grenoble southern suburb. The insertion lane is in green, the right lane in red, and the fast lane in blue.

Collected data are from a 500-meter-long express road with a speed limit of 70 km/h. For this area, data collection periods were chosen to cover the congestion occurring in morning rush hours.

In order to be transformed into trajectories, the MOCOPO videos were processed. Firstly, as the helicopter was not perfectly fixed, the MOCOPO research teams corrected the curvature of the image and stabilized the image. They also reframed the images to focus on a region of interest containing only the road. Secondly, a reference image was used to extract moving objects from all images of the video on the region of interest. This image was a photography of the infrastructure without any vehicle. They connected the different objects in order to build the trajectory of each vehicle. Thirdly, [3] implemented a new filtering approach based on polynomial fitting and the polar coordinates. The method was developed in two versions: piece-wise constant accelerations or piece-wise linear accelerations. [3] shows that their process provides values of acceleration fully compatible with the physical limits of vehicles found in the literature. Thus, there is no need to add extra constraints to the data such as a limitation for acceleration or deceleration.

As a result, [3] supplies a set of trajectory data from video recording of 16th September 2011 (between 7:58 and 8:58 am). This set is composed of a sample of 619 vehicles distributed in a 60-minute time window. Each trajectory consists of a sequence of location data provided every 0.1 s.

B. MOCOPO trajectory interest for VANETs

Getting real-world traces usable for VANETs studies is not obvious. GPS-trace databases concern vehicles geographically dispersed or few vehicles; NGSIM datasets need to be processed in order to obtain the final usable trajectories.

The MOCOPO database consists of vehicles close to each other recorded during rush hours. Its data contain the information on the driver behaviours (speed, acceleration, lane changing...). Moreover, the data show periods of congestion where vehicles stop and restart after a few moments (so-called stop and go wave) and where vehicle speeds are highly variable. It is therefore interesting to find time periods in the database where vehicles have high speed or respectively low speed.

C. Mobility profiles in MOCOPO data

The authors split the trajectory database of MOCOPO into groups corresponding to different congestion scenarios characterised by the speed of the vehicles. The result is shown

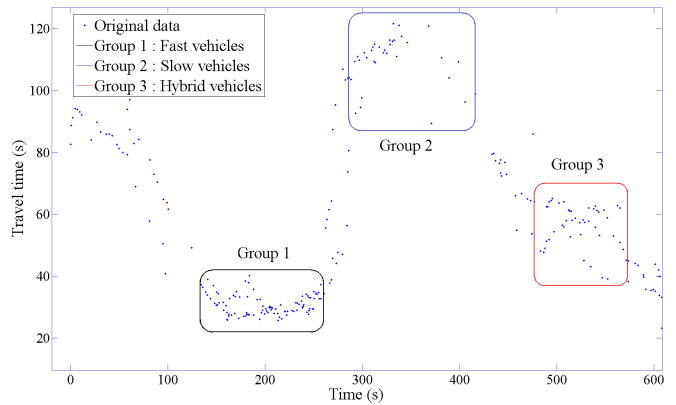


Fig. 2. Travel time of vehicles versus time. Travel times range from 30 to 120 s. Three groups are defined with fast, slow and hybrid vehicle speed.

in figure 2. A significant variation in travel time is observed over time. Some vehicles pass through the area in less than 30 s, i.e. with an average speed of 60 km/h, others in more than 120 s, i.e. with an average speed below 15 km/h.

In light of these results, it is relevant to define three groups of vehicles with different mobility features presented in table I. Figure 3 shows the travel distance versus the time for each three mobility groups. The slope of the curve representing each vehicle corresponds to their instantaneous speed. As it can be seen in the figure, the vehicles of group 1 maintain a high speed while the vehicles of group 2 suffer a period of stop and go wave (the slopes of the travel distance curve is horizontal, which means a zero speed). Vehicles of group 3 that are located on the right lane experiment a stop and go wave while those located on the left lane have higher speed. Figure 4 represents the speed distribution experienced by the vehicles in each group.

The three groups are built as follows.

Group 1: 83 vehicles have a short travel time ranging from 26.3 s to 40.2 s. Their date of entry into the area is between 133 s and 263 s. The average speed of this group is 51.3 km/h with a standard deviation of 8.5 km/h. This group is not constrained by stop and wave events. The traffic is dense, but it remains fluid.

Group 2: 31 vehicles have a longer travel time ranging from 89.4 s to 121.5 s. Their date of entry into the area is between 286 s and 399 s. The average speed is 14.28 km/h with a standard deviation of 16 km/h. All vehicles have both stop and wave effects. The traffic is congested.

Group 3: 47 vehicles have a hybrid travel time ranging from 38.3 s to 65.1 s. Their date of entry into the area is between 477 s and 580.5 s. The average speed is 29.1 km/h with a standard deviation of 16.7 km/h. Vehicles in the right lane have a low speed or even zero speed with stop and go wave. This slowing down has an impact on the vehicles in the left lane, but to a lower extent (traffic remains fluid).

TABLE I. CHARACTERISTICS OF THE THREE MOBILITY FEATURE GROUPS

Specifications	G1	G2	G3
Number of vehicles	83	31	47
Entry date of first vehicle (s)	133	286	477
Entry date of last vehicle (s)	263	399	580.5
Minimal travel time (s)	26.3	89.4	38.3
Maximal travel time (s)	40.2	121.5	65.1
Average speed (m/s)	14.3	3.9	8.1
Standard deviation (m/s)	2.4	4.4	4.6

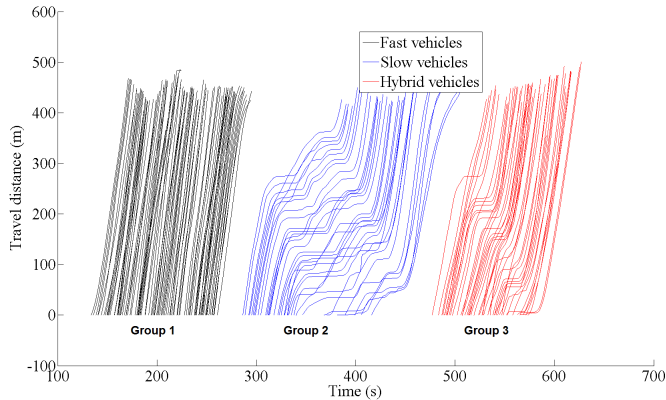


Fig. 3. Travel Distance versus time for each vehicle group. Vehicle travel times of Group 1 are below 40 s; the ones of Group 2 are greater than 90 s; Group 3 is an hybrid group with slow and speed vehicles. Stop and go wave occurs in Group 2 and 3 and spreads out from one vehicle to another.

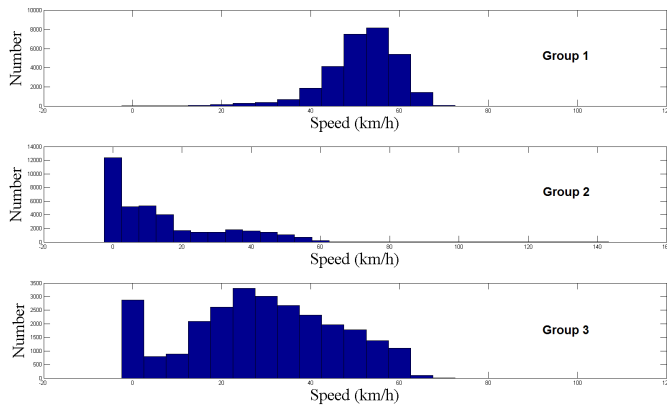


Fig. 4. Speed distribution of vehicles in each group. Distributions correspond to the experienced speed by the group vehicles at each time step (0.1 seconds)

IV. BUILDING MOBILITY MODELS USING MOCOPO DATA

In this paper, MOCOPO datasets are taken as a reference. Different mobility models were built by degrading the knowledge of the road traffic from the MOCOPO data (figure 5). The resulting models and trajectories are explained in this section.

A. MOCOPO data

The MOCOPO data consist of the positions of the vehicles provided every 0.1 second (see section III-B).

B. GPS-based model - Fixed speed

The GPS-based model, called fixed speed, is based on the knowledge of vehicle positions in the MOCOPO data, but by

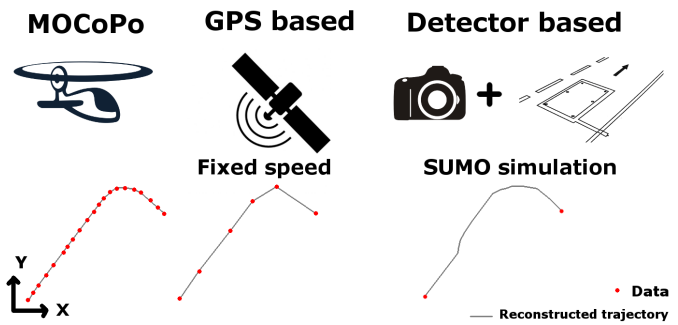


Fig. 5. Different mobility models according to the knowledge of the road traffic. (left) Real data extracted from MOCOPO data, (center) Fixed speed model with a position extracted every δ second from MOCOPO data, (right) SUMO simulation calibrated with travel times of vehicle as if coming from the knowledge of the departure and arrival time measured with electromagnetic loop detectors and merged with an identification system.

keeping a weaker refresh rate than 0.1 second. These data are built as if they were provided by vehicle GPS systems. The positions that each vehicle has every δ seconds are extracted from the MOCOPO data. Nodes are then forced to have these intermediate collected positions. Since the construction of this model assumes only the position of the vehicles at δ -second interval, fixed speeds are taken between two positions. Therefore, the node speed is given by the ratio between the travel distance and the δ -second interval. The chosen δ are : 0.5, 1, 3, 5 and 10. Each δ -second fixed speed trajectory is therefore designed as a set of segments meeting the original MOCOPO trajectory curve every five positions for $\delta = 0.5$, ten positions for $\delta = 1$, thirty positions for $\delta = 3$, fifty positions for $\delta = 5$, and hundred positions for $\delta = 10$. The highest refresh rate has been set at $\delta = 10$ seconds since some vehicles have a travel time inferior to 30 seconds.

C. Detector-based model - SUMO simulation

The detector-based model only keeps the knowledge of the departure and arrival times of the vehicles extracted from the MOCOPO data. The data used are then similar to the outputs of a system composed of two electromagnetic loop detectors and a vehicle identification system (such as an automatic number plate recognition, a camera, or a bluetooth system). The trajectories of vehicles are still to be built from these departure and arrival times. The SUMO microscopic traffic simulator software has been chosen to simulate the behaviour of the vehicles and create the trajectories.

A 500-meter-long two-lane road is represented under SUMO with a RN87-like curvature. The parameters of vehicle length is set to 5 meters and the speed limit is set to 70 km/h which corresponds to the legal speed limit on this road.

The default car following models included in SUMO simulator is a modification of Krauß model [31]. The model is simple : each vehicle drives up to its “desired speed”, while maintaining a perfect distance safety with the leader vehicle (*i.e.* the vehicle in front of it).

To calibrate the model according to the MOCOPO traffic groups, a set of parameters have to be defined for each one.

The sets of parameters are computed by the method of the root mean squared error (RMSE).

At the initialisation, a first random set of parameters is chosen and the simulation is launched using the real departure dates of vehicles in the MOCoPo data. The SUMO computed arrival dates of vehicles (called $Tsim_i$ for vehicle i) are then compared with the MOCoPo arrival dates of vehicles (called $Treal_i$). Another random set of parameters is drawn for a new simulation run. This method is carried out 500 times for each group of vehicles. Figure 6 sketches the method. The formula used to calculate the gap between the simulation and MOCoPo travel time is :

$$RMSE = \sqrt{\frac{\sum_{i=1}^n (Tsim_i - Treal_i)^2}{n}}$$

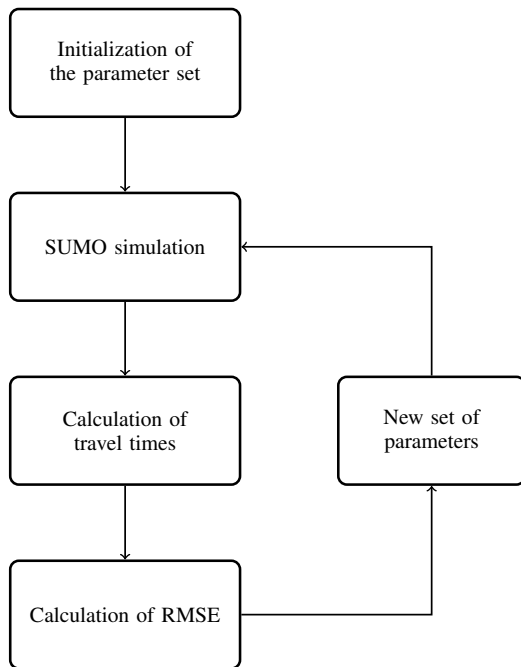


Fig. 6. Method for calibrating MOCoPo data according to travel times

The different parameters to calibrate the car following model are :

- Accel: the acceleration ability of vehicles $[m/s^2]$
- Decel: the deceleration ability of vehicles $[m/s^2]$
- Sigma: the driver imperfection (between 0 and 1)
- Tau: the driver's desired minimum time headway $[s]$
- MinGap: the offset to the leading vehicle when standing in a jam $[m]$.

Moreover, to achieve realistic car following behaviour, it is necessary to use speed distributions for the desired speed. Otherwise, if all vehicles have the same desired speed, they will not be able to catch up with their leader vehicle causing unrealistic situation. Therefore, two other parameters have to be calibrated to use speed distributions in SUMO: speedFactor and speedDev. For instance, using $speedFactor = 1$ and $speedDev = 0.1$ will result in a speed distribution where 95% of the vehicles drive at a speed ranging from 80% to 120% of the legal speed limit. The results of the calibration for each

group of mobility are presented in table II. The parameters inherent to car following model are relatively close to each other for the three mobility groups. However, the speedFactor parameter is specific to a mobility group.

TABLE II. MODEL MOBILITY PARAMETERS WITHIN THE SUMO FRAMEWORK

Parameters	Interval	Group 1	Group 2	Group 3
Accel $[m/s^2]$	[1:3]	2.28	2.19	1.2
Decel $[m/s^2]$	[1:3]	1.98	1.99	2.62
SpeedFactor	[0:1]	0.87	0.256	0.61
SpeedDev	[0.05:0.15]	0.058	0.065	0.054
Sigma	[0:1]	0.22	0.14	0.8
Tau $[s]$	[1:3]	1.8	1.47	1.87
MinGap $[m]$	[5:30]	7.7	7.27	7.5
RMSE $[s]$	-	3.8	8.23	8.72

D. Resulting trajectories

Figure 7 shows positions (graph a) and speeds (graph b) of node 40, taken as an example among the vehicles of group 1. Each curve represents the position (respectively the speed) of node 40 for each one of the mobility models presented. According to the positions, it can be observed that both the 0.5-second and 1-second fixed speed trajectories follow the MOCoPo curve, while the 3-second, 5-second and 10-second ones make the vehicle move away from the lane (near the arrival date). The trajectory simulated by SUMO leads to lane changing: node 40 starts on the left lane, then changes at coordinate $X=330$ m. The speed values presented in the curves (b) have been computed from the successive positions from the curves (a). The speed curves are piece-wise constant as a function of the sample time related to the positions.

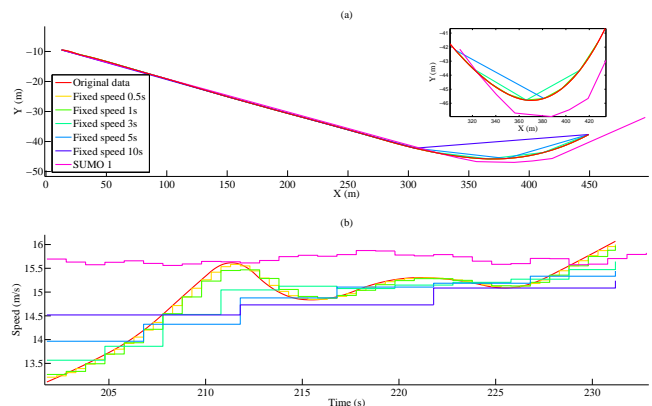


Fig. 7. (a) Position and (b) speed of node 40 group 1, over time for the different models of mobility

Figure 8 shows positions (graph a) and speeds (graph b) of node 10, taken as an example for the group 2, for the different mobility models.

Figure 9 shows positions (graph a) and speeds (graph b) of node 3, taken as an example for the group 3, for the different mobility models.

E. Comparison of the resulting trajectories

From the figures 7, 8, 9, it can be seen that despite the convergence of the positions, the speed profiles vary considerably according to the mobility model used. Especially,

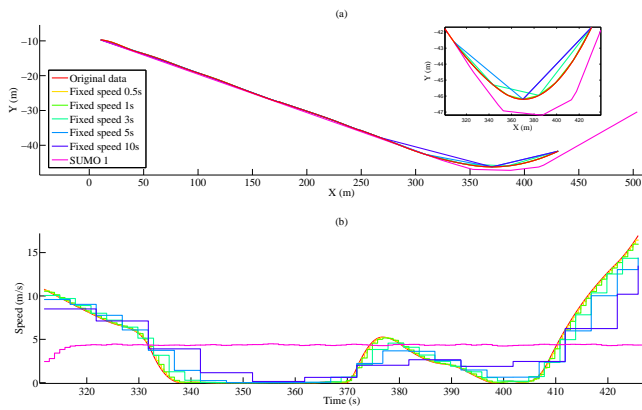


Fig. 8. (a) Position and (b) speed of node 10 group 2, over time for different models of mobility

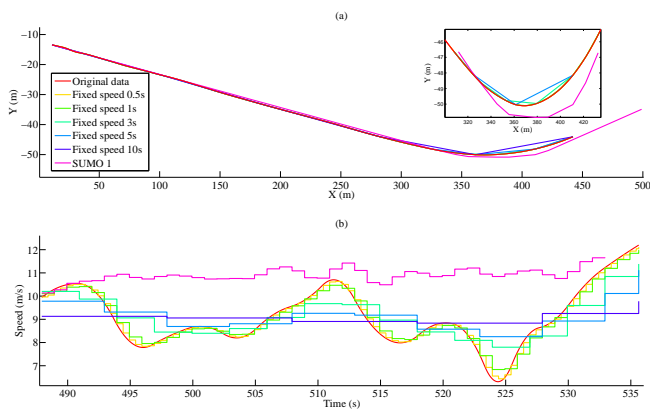


Fig. 9. (a) Position and (b) speed of node 3 group 3, over time for the different models of mobility

the speed profile obtained through SUMO simulation tends to be very smooth when compared to the original MOCOPo data. When considering the different approximations of this latter, namely the Fixed speed 0.5, 1, 3, 5 and 10, the curves show that they tend to get closer to SUMO curves as they are less precise in comparison with the original MOCOPo. This means that the simulated trajectory obtained through SUMO using the parameters that reproduce a specific traffic condition may result in a faithful trajectory in terms of positions while not offering any guarantee on the speed profile of the vehicles. Consequently, though simulated trajectories from SUMO could be useful for global simulation requiring realistic vehicle trajectories on the roads, the specific studies that investigate the performance in realistic traffic conditions, especially when the speed profile is important, should better rely on real-world traces such as car traffic dataset. Even when considering only few points of the original trajectory, in order to reduce the amount of data necessary to reproduce the trajectory in the simulation, one can observe that the resulting approximative curves (Fixed speed 0.5, 1, 3, 5 and 10) remain closer to the original traces when compared to SUMO trajectory. This is particularly clear when considering group 2 and group 3 which are the most concerned with speed variations due to congestion in their traffic.

Figure 10 shows the average speed of the vehicles for the

three mobility groups. As for the individual vehicles presented in figures 7, 8, 9, the average values on every vehicles in each group confirm that the speed profile obtained with SUMO is too smooth in comparison with the real traces, especially in group 2 and group 3.

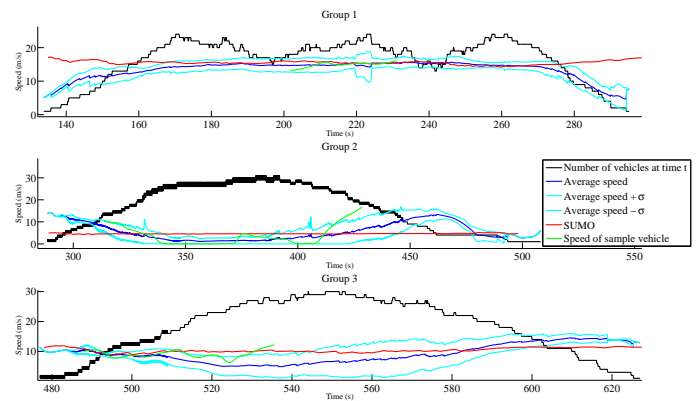


Fig. 10. Average speed of the vehicles in the network over time for group 1, 2 and 3 in the case of the MOCOPo (blue curves) and SUMO (red curves) models. The speed of MOCOPo vehicles number 40, 10 and 3 respectively taken as an example in group 1, 2 and 3 (green curves). Number of vehicles present in the network over time (black curves)

V. SIMULATION DESCRIPTION AND RESULTS

The purpose is to evaluate the impact of the differences in the speed profiles of the mobility models (the position traces are almost the same for all) on network performance through simulation results. The results obtained with original MOCOPo dataset traces are compared with those obtained using two other mobility models (fixed speed and SUMO) regarding the three groups of mobility (group 1, group 2, and group 3).

These simulations rely on the ability of Riverbed OPNET Modeler software to assign a trajectory to each node of a communication network by means of external TRJ files in the OPNET format. The following paragraphs present the simulation system configuration and the application. Then, the results are discussed.

A. Simulation system configuration

The simulated system is an ad hoc network formed with IEEE 802.11p nodes that use the proactive OLSR protocol as the routing protocol (Optimized Link State Routing Protocol [32]). IEEE 802.11p is an amendment of the IEEE 802.11 standard of 2012. Created to answer the challenges imposed by ad hoc vehicular networks [14], it applies in the frequency band of 5.9 GHz for wireless access in a vehicular environment (WAVE - Wireless Access in Vehicular Environment). IEEE 802.11p considers dedicated short range communication (DSCR). The implementation of IEEE 802.11p used is the one proposed with the OPNET modeler suite, and the chosen node configuration is summarized in table III.

The optimized link state routing protocol (OLSR) is one of the standardized proactive routing protocols for mobile ad hoc networks. Inspired from the open shortest path first (OSPF) protocol, OLSR maintains topology information and periodically computes the shortest path route (hop count) to

TABLE III. NODE CONFIGURATION

Attribute	Value
Physical Characteristics	5.0 GHz
Data Rate	13 Mb/s
Transmit power	0.001 W
Receiver sensitivity	-95 dBm
Transmission range	225 m
Packet length	75 bytes
Frequency of sending	40 Hz
Transport protocol	UDP
Response packets	0 byte

TABLE IV. ROUTING PROTOCOL CONFIGURATION

Routing protocols	Value
Hello interval	2 s
TC interval	2 s
Neighbour hold time	6 s
Topology hold time	15 s
Duplicate message hold time	30 s

each known destination. Moreover, OLSR tries to reduce the impact of flooding due to broadcast traffic by selecting a subset of special nodes called the multipoint relays (MPR) which are the only allowed to retransmit broadcast traffic in the entire ad hoc network. This latter reason makes it a good choice as the routing protocol for the evaluations performed in this paper since the dataset contains dense VANETs [33] in addition to the fact that a built-in implementation of OLSR is proposed in the OPNET modeler suite.

B. Application

A data traffic model for VANET studies is defined in [34]. The IEEE settings correspond to a 300-byte packet length sent with a 10-Hertz update rate. The authors are especially interested in future real-time VANET applications such as for autonomous cars. In such safety applications, on-board functions (sensor functions, geo-localization, extended perception, etc.) will have to share variables periodically (speed, acceleration, positioning information, etc.) for their inner process.

The deployed application in this paper consists in a transmission of a message from a source vehicle to all other vehicles in the network. This application may represent, for example, a safety alert in case of an accident. However, to operate really like a real-time application, a higher exchange frequency than the IEEE setting is needed. Keeping the same total amount of exchanged data, so the same throughput than the IEEE setting, a node will send 75-byte packets every 25 ms. The sender node is selected for each mobility group, respectively the nodes 40, 10 and 3 for the group 1, 2 and 3. The trajectories of these particular vehicles are shown in figure 7, 8, 9.

C. Performance metrics

The three following performance metrics are considered:

- The “load” metric represents the total number of bits forwarded from the wireless layer to higher layers. This metric measures the traffic received in all the network at a given time.
- The “throughput” metric represents the total number of bits submitted to the wireless layer by all higher layers. Its upper value is restricted by the bandwidth, so it

may give an idea of the local bandwidth obtained by each node with each mobility profile.

- The “end-to-end delay” metric concerns the time taken by a packet to reach the wireless layer of the receivers. It is measured as the difference between the arrival time of a packet at its destination and the creation time of this packet. This metric will help to evaluate the network performance in relation to the application requirements.

D. Scenarios and results

Each scenario is run several times with different seed values for the random generator in order to avoid that the related sequence favors one of the scenarios.

Figures 11 to 13 present the average results for each performance metric.

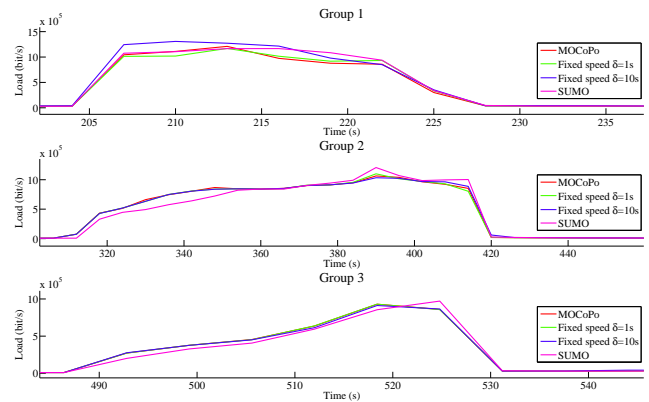


Fig. 11. Load for each mobility group with different mobility models

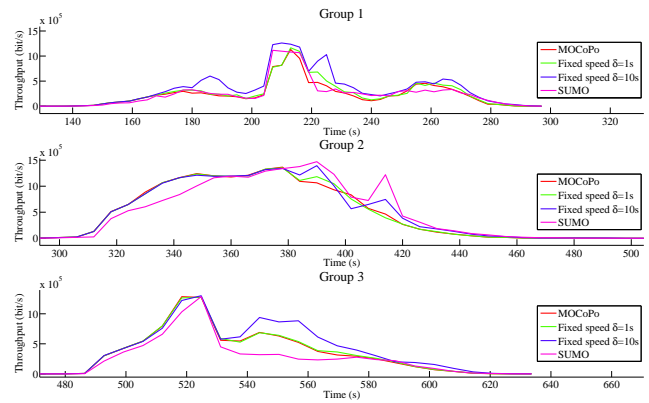


Fig. 12. Throughput for each mobility group with different mobility models

Figure 11 shows that the same amount of traffic is received through the entire network. However, when the vehicles start to meet congestion in group 2 and group 3, the throughput and more significantly the delay values become different. The main explanation is the difference in the speed profile which affects the communications. Particularly, it can be observed in table V that the SUMO traces produce similar results than fixed speed 5s in group 1 (no congestion), but they are clearly different in congested traffic conditions (group 2 and 3).

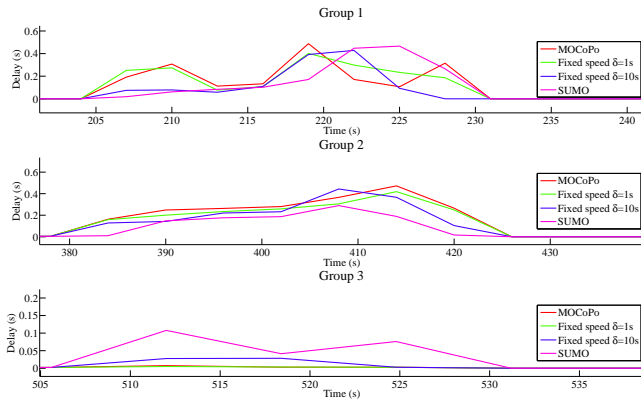


Fig. 13. Delay for each mobility group with different mobility models

TABLE V. MEAN OF GAP BETWEEN MOCOPo AND OTHER MOBILITY MODELS RESULTS

Mobility models	Group 1			Group2			Group 3		
	L	T	D	L	T	D	L	T	D
FS $\delta = 0.5$	8.3	3.3	11.7	4.6	16.0	4.2	1.8	9.8	0.2
FS $\delta = 1$	8.9	4.5	14.7	5	17.5	5.2	0.8	16	0.1
FS $\delta = 3$	9.2	4.2	13.7	9.4	23.3	6.7	2.3	21.2	0.1
FS $\delta = 5$	14.6	7.1	15.3	8.3	22.6	13	2.4	41.3	0.7
FS $\delta = 10$	20.6	12.8	20.8	5.4	46.3	16.5	5.6	81.2	1.9
SUMO	12.5	5.6	28.4	27.1	117.3	30.7	17.2	92.6	9.2

FS : fixed speed, L : load (kbit/s), T : throughput (kit/s), D : delay (s)

VI. CONCLUSION

The development of big data announces the availability of many datasets including vehicle trajectories in smart city. Targeting a future generalization of such data in the evaluation of vehicular networks, this paper demonstrates the use of the MoCoPo dataset which includes the real-world traces of the cars in a road section.

Though they were early acquired for studies in the domain of road traffic theory, one of the goals of this paper was to show that the MOCOPo data particularly fit to the evaluation of vehicular ad hoc networks in comparison with other mobility models such as those coming traffic simulators. After they have been split into three groups corresponding to different mobility profiles namely fluid (group 1) hybrid (group 2) and congested (group 3) traffics, the MOCOPo dataset traces have been used to simulate the scenarios of a group of communicating vehicles. Other mobility models have been used for the same scenarios in order to compare the behaviour of the system in both cases. The results demonstrate the importance of the granularity of the traces which affects the topology of the road traffic and therefore the communications.

Moreover, the real speed variations embedded in the MoCoPo trajectories cannot be reproduced using traffic simulator through basic parameters. The analyzed figures show that even if the position traces, average speed and acceleration threshold are the same, the instantaneous speed of the vehicles in real-world traces are never reproduced by traffic simulators which tend to smooth the speed profile according to the average speed. Therefore, the difference in the speed profiles has an impact on the results obtained through simulation for several performance metrics such as the load, the throughput and significantly the delay.

This work suggests that it is crucial to get real-world trajectory data with refined granularity in order to obtain, through simulation, a performance of vehicule-to-vehicule communication that reflects better the reality in comparison with other mobility models.

ACKNOWLEDGMENT

The authors gratefully thank Dr. Christine BUISSON, researcher in traffic theory at IFSTTAR, for her crucial role in the acquisition of the MOCOPo dataset and for allowing to use it. They acknowledge the support of the CPER ELSAT 2020, the Hauts-de-France region, and the European Community.

REFERENCES

- [1] T. Camp, J. Boleng, and V. Davies, "A survey of mobility models for ad hoc network research," *Wireless Communications and Mobile Computing*, vol. 2, no. 5, pp. 483–502, 2002.
- [2] A. Mahajan, *Urban mobility models for vehicular ad hoc networks*. phdthesis, Florida State University, 2006. <http://diginole.lib.fsu.edu/islandora/object/fsu%3A181041>.
- [3] C. Buisson, D. Villegas, and L. Rivoirard, "Using Polar Coordinates to Filter Trajectories Data without Adding Extra Physical Constraints," in *Transportation Research Board 95th Annual Meeting*, vol. 16, Transportation Research Board, 2016.
- [4] P. Manzoni, M. Fiore, S. Uppoor, F. J. M. Domínguez, C. T. Calafate, and J. C. C. Escriba, "Mobility Models for Vehicular Communications," in *Vehicular ad hoc Networks*, pp. 309–333, Springer International Publishing, 2015.
- [5] J. Harri, F. Filali, and C. Bonnet, "Mobility models for vehicular ad hoc networks: a survey and taxonomy," *IEEE Communications Surveys Tutorials*, vol. 11, no. 4, pp. 19–41, 2009.
- [6] C. Sommer and F. Dressler, "Progressing toward realistic mobility models in VANET simulations," *IEEE Communications Magazine*, vol. 46, pp. 132–137, Nov. 2008.
- [7] H. Hartenstein and K. Laberteaux, *VANET: vehicular applications and inter-networking technologies*, vol. 1. Wiley Online Library, 2010.
- [8] N. Garg and P. Rani, "An improved AODV routing protocol for VANET (Vehicular Ad-hoc Network)," *International Journal of Science, Engineering and Technology Research (IJSETR)*, vol. 4, no. 16, p. 1024, 2015.
- [9] A. Roy, B. Paul, and S. K. Paul, "VANET topology based routing protocols & performance of AODV, DSR routing protocols in random waypoint scenarios," pp. 50–53, 2015.
- [10] S. Mohapatra and P. Kanungo, "Performance analysis of AODV, DSR, OLSR and DSDV Routing Protocols using NS2 Simulator," *Procedia Engineering*, vol. 30, pp. 69 – 76, 2012.
- [11] D. Tian, Y. Wang, G. Lu, and G. Yu, "A vanets routing algorithm based on euclidean distance clustering," *2nd International Conference on Future Computer and Communication (ICFCC)*, vol. 1, pp. V1–183, 2010.
- [12] F. D. d. Cunha, A. Boukerche, L. Villas, A. C. Viana, and A. A. F. Loureiro, "Data Communication in VANETs: A Survey, Challenges and Applications," report RR-8498, INRIA Saclay ; INRIA, Mar. 2014.
- [13] J. Jakubiak and Y. Koucheryavy, "State of the Art and Research Challenges for VANETs," in *the 5th Conference IEEE Consumer Communications and Networking (CCNC '08)*, pp. 912–916, Jan. 2008.
- [14] S. Al-Sultan, M. M. Al-Doori, A. H. Al-Bayatti, and H. Zedan, "A comprehensive survey on vehicular Ad Hoc network," *Journal of Network and Computer Applications*, vol. 37, pp. 380–392, 2014.
- [15] G. He, "Destination-sequenced distance vector (DSDV) protocol," technical report, 2002. Networking Laboratory, Helsinki University of Technology.
- [16] P. Sondí, D. Gantsou, and S. Lecomte, "Design guidelines for quality of service support in optimized link state routing-based mobile ad hoc networks," *Journal on Ad Hoc Networks*, vol. 11, no. 1, pp. 298 – 323, 2013.

- [17] S. Xi and X.-M. Li, "Study of the Feasibility of VANET and its Routing Protocols," in *4th International Conference on Wireless Communications, Networking and Mobile Computing, 2008. WiCOM '08*, pp. 1–4, Oct. 2008.
- [18] I. B. Jemaa, *Multicast Communications for Cooperative Vehicular Systems*. phdthesis, Mines ParisTech, 2014. <https://hal.inria.fr/tel-01101679/document>.
- [19] SUMO, "Simulation of Urban MObility." http://sumo.dlr.de/wiki/Main_Page. [Online; accessed on November 28, 2016].
- [20] VanetMobiSim, "Vanet Mobility Simulation Environment." <http://vanet.eurecom.fr/>. [Online; accessed on November 28, 2016].
- [21] R. S. Shukla, N. Tyagi, A. Gupta, and K. K. Dubey, "A new position based routing algorithm for vehicular ad hoc networks," *Telecommunication Systems*, Dec. 2015.
- [22] K. C. Lee, P.-C. Cheng, and M. Gerla, "GeoCross: A geographic routing protocol in the presence of loops in urban scenarios," *Journal on Ad Hoc Networks*, vol. 8, pp. 474–488, July 2010.
- [23] CRAWDAD, "A Community Resource for Archiving Wireless Data At Dartmouth." <http://www.crowdad.org/>. [Online; accessed on November 28, 2016].
- [24] Y. Li, D. Jin, Z. Wang, L. Zeng, and S. Chen, "Exponential and Power Law Distribution of Contact Duration in Urban Vehicular Ad Hoc Networks," *IEEE Signal Processing Letters*, vol. 20, pp. 110–113, Jan. 2013.
- [25] S. Demmel, A. Lambert, D. Gruyer, A. Rakotonirainy, and E. Monacelli, "Empirical IEEE 802.11 p performance evaluation on test tracks," *Intelligent Vehicles Symposium (IV), '12 IEEE*, pp. 837–842, 2012.
- [26] M. Rafati Fard, A. Shariat Mohaymany, and M. Shahri, "A new methodology for vehicle trajectory reconstruction based on wavelet analysis," *Transportation Research Part C: Emerging Technologies*, vol. 74, pp. 150–167, Jan. 2017.
- [27] S. P. V. Z. Hoogendoorn, H. J. , M. Schreuder, B. Gorte, and G. Vosselman, "Microscopic traffic data collection by remote sensing," *Transportation Research Record: Journal of the Transportation Research Board*, no. 1855, 2003.
- [28] FHWA, "Traffic Analysis Tools: Next Generation Simulation (NGSIM)." <http://ops.fhwa.dot.gov/trafficanalysistools/ngsim.htm>. [Online; accessed on November 28, 2016].
- [29] C. Thiemann, M. Treiber, and A. Kesting, "Estimating acceleration and lane-changing dynamics from next generation simulation trajectory data," *Transportation Research Record: Journal of the Transportation Research Board*, no. 2088, 2008.
- [30] MOCOPO, "Measuring and modelling traffic congestion and pollution." <http://mocopo.ifsttar.fr/>. [Online; accessed on November 28, 2016].
- [31] S. Krau, *Microscopic modeling of traffic flow: Investigation of collision free vehicle dynamics*. PhD thesis, Institute of Transport Research, DLR-Forschungsbericht., 1998.
- [32] T. Clausen, P. Jacquet, C. Adjih, A. Laouiti, P. Minet, P. Muhlethaler, A. Qayyum, and L. Viennot, "Optimized link state routing protocol (OLSR)," *IETF, RFC 3626*, 2003.
- [33] P. Sondi, M. Wahl, L. Rivoirard, and O. Cohin, "Performance evaluation of 802.11p-based Ad Hoc Vehicle-to-Vehicle Communications for Usual Applications under Realistic Urban Mobility," *International Journal of Advanced Computer Science and Applications (IJACSA)*, vol. 7, May 2016.
- [34] European Telecommunications Standards Institute, "Intelligent Transport Systems (ITS); STDMA recommended parameters and settings for cooperative ITS; Access Layer Part," Tech. Rep. ETSI TR 102 861 V1.1.1 (2012-01), 2012. p. 12.

Modeling and Solving the Open-End Bin Packing Problem

Maiza Mohamed and Tebbal Mohamed and Rabia Billal
Laboratoire de Mathématiques Appliquées
Ecole Militaire Polytechnique
B.P. 17 Bordj-El-Bahri
Alger, 16111 Algérie

Abstract—In the Open-End Bin Packing Problem a set of items with varying weights must be packed into bins of uniform weight limit such that the capacity of the bin can be exceeded only by the last packed item, known as the *overflow item*. The objective is to minimize the number of used bins. In this paper, we present our Integer Linear Program model based on a modification of Cesili and Righini model [1]. Also, we propose two greedy heuristics to solve a problem. The first one is an adaptation of the *Minimum Bin Slack* heuristic where we have reduced to one unit capacity, the weight of the largest item in the current bin. While, the second heuristic is based on the well-known *First Fit Decreasing* heuristic. Computational results based on benchmark instances taken from the literature as well as generated instances show the effectiveness of the proposed heuristics in both solution quality and time requirement.

Keywords—Open-End Bin-packing; heuristics; discrete optimization; combinatorial problem

I. INTRODUCTION

The one dimensional open-end bin packing problem (OEBPP) is a variant of the classical bin packing problem. In the OEBPP, items with varying weights are packed into identical bins such that in each bin, the total items weight content before packing the last item is strictly less than the bin capacity. The aim of the OEBPP is to minimize the number of bins used to pack all items.

This problem was introduced by Leung et al. [2], where the authors proved that the OEBPP is NP-hard. Various application of this problem can be found in a wide variety of industries such as manufacturing, transportation, affectation tasks, etc. For example, in the fare payment system in the Hong Kong and Taipei subway stations, the passengers can buy a ticket of a fixed value. A machine at the entrance gateway records the ticket's value, while another machine deducts the fare from the ticket's value at the exit gateway. The machine at the exit gateway returns the ticket if the remaining balances of the ticket is positive; otherwise, it keeps the ticket. The objective from a passenger's point of view is to minimize the number of tickets they need to purchase as to minimize the number of bins generated by an algorithm. Another application can be found in job scheduling in the manufacturing environment that operates one shift per day. A worker loads jobs to a machine that can operate automatically. The objective is to schedule jobs to minimize the total time (days) to complete all the jobs. Intuitively, the job with the longest processing time is scheduled to the last to fully utilize

the automated machine when the worker leaves from work, and the worker can unload the finished job next day.

Whilst, a few work carried out on this problem, we present a modification of the 0-1 linear programming formulation proposed by Ceselli and Righini [1] in which the authors studied a variant of the open-end bin packing called Ordered Open-End Bin Packing Problem (OOEBBP). Then we present our contributions based on the proposition of two greedy heuristics for solving the problem in an offline mode while ensuring high quality solutions in very short computational time compared to solving the problem in optimal way.

The remainder of this paper is organized as follows. In the next Section, we present a few existing lower and upper bounds on which we based to develop our propositions. Suitable way to formulate the problem with an Integer Linear Program formulation without considering the order between items is presented in Section III. In Section IV, we describe and develop our proposed heuristics which are tested and compared by means of computational tests on benchmark instances in Section V. The last Section provides some final conclusions and directions for future work.

In the next, we assume the following notations:

- C : Bin capacity;
- I : Set of item;
- i, j : Index of items and bins respectively;
- w_i : Weight or size of item i ;
- r_j : Residual capacity of bin j ;
- \hat{S} : Set of candidate items;
- O : Set of overflow items;
- R : Overall residual capacity of used bins;

II. LITERATURE REVIEW

While there exists abundant research for the classical bin packing problem (interested reader can referred to the chapter of Coffman et al. [3] for an excellent survey of this topic), there is much less research on the OEBPP. Initially, Leung et al. [2] proposed this variant of bin packing, in which the authors modelled the ticketing system at the subway station in Hong Kong. The authors was showed that any online algorithm for the discussed problem have an asymptotic worst-case ratio of at least 2. Thereafter, Yang and Leng [4] studied the Ordered Open Bin Packing Problem which extends

the requirement corresponding to the order of passenger's itinerary in subway station problem. The same problem, which is the Ordered Open-End Bin Packing Problem, have been also studied by Cesili and Righini [1] where authors present branch and price algorithm for its exact optimization.

A. Lower bounds

In this section we briefly describe two existing lower bounds from the OEBPP literature.

Ongkunaruk's lower bound: Ongkunaruk [5] presented a simple idea used to compute a lower bound for the OEBPP, it consists in determining the number of needed overflow items firstly in order to apply the continuous lower bound for the rest of items. The overflow items are those selected to be packed as the last item which exceed the capacity of bin. Generally, overflow items have a large weight.

The main target in the OEBPP is to maximize the overflow items in order to minimize the capacity of items inside bins, so minimize the number of bins used.

For do, the author order items in the non-increasing size firstly, then determine the smallest integer K which indicate the number of overflow item, using the following formula:

$$\sum_{j=K+1}^n w_j \leq K\hat{C} \quad (1)$$

So the lower bound of Ongkunaruk L_{OEBPP}^0 can be expressed by:

$$L_{OEBPP}^0 = K \quad (2)$$

Ceselli's lower bound: Ceselli and Righini [1] proposed a combinatorial lower bound algorithm called in what follows *CBA*. This lower bound computes a set of *overflow items* iteratively in an optimal fractional packing by the following way; the authors define R to be the overall residual capacity of all the bins already initialized, whenever an item j is found, whose size is greater than R , a new bin is initialized and the overflow item of this bin is selected as the largest item among those already packed but not yet used as overflow items, then insert item j into the set O of overflow items in order to yield the maximum residual capacity for the next iteration. So this lower bound can be expressed by:

$$L_{CLB} = |O| \quad (3)$$

B. Upper bounds

Well known algorithms for the classical BPP: *First Fit Decreasing(FFD)* is one of the well-known algorithm often used to solve the classical BPP. Developed by Coffman et al. [3], FFD guarantees asymptotic worst case performance bounds of $11/9$ [6]. Let all items are sorted in the non-increasing weight order, the FFD algorithm consist on packing

the current item in the first opened bin, else, a new bin is opened.

Other effective algorithm for solving the classical BPP called *Minimum Bin Slack (MBS)*. This algorithm was proposed by Gupta and Ho [7]. At each step, an attempt is made to find a set of items that fits the bin capacity as much as possible. At each stage, a list of items not assigned yet is sorted in the decreasing order of their weights. Each time a packing is determined, the items involved are placed in a bin and removed from a set of unpacked items. Thereafter Fleszar et al. [8] proposed a variant of MBS called MBS', in which the item of maximum size is not unstuck. MBS has been used in several variants of bin packing problem, such as the bin packing problem with conflicts [9], and the variable sized bin packing problem [10].

Ongkunaruk's heuristic for the OEBPP: Ongkunaruk [5] proposed a modification of the well-known first fit decreasing algorithm for the OEBPP called *Modified First Fit Decreasing (MFFD)*, this modification consists of determining the overflow items firstly, then apply the first fit decreasing for the rest of items not yet packed.

In MFFD, the author computes the lower bound K defined above (equation (2)) and considered as overflow items, the K -first large items, then apply the first fit decreasing algorithm for the remaining items i not yet packed, where $i = k + 1$ to n . Finally, assign the overflow items into the bins using FFD algorithm.

III. PROBLEM FORMULATION

In this section, we propose a modification of the integer linear program initially proposed by Cesili and Righini [1]. The authors studied a variant of the open bin packing problem called the Ordered Open-End Bin Packing Problem (OOEBPP) in which items to be packed are sorted in a given order. For this formulation, the authors used the binary variable y_i to indicate whether item i is the overflow item in its bin, and the binary variable x_{ij} to indicate whether item i is assigned to the bin in which the overflow item is the item j . Because of the constraints on the order of the items, there is only x_{ij} variables with $i < j$. Instead, for the general OEBPP (without order), we have therefore x_{ij} decision variables with $i \neq j$.

$$\text{Minimize } \sum_{i \in N} y_i \quad (4)$$

s.t.

$$y_i + \sum_{i \neq j} x_{ij} = 1 \quad \forall i \in N \quad (5)$$

$$\sum_{i \neq j} w_i x_{ij} \leq (C - 1)y_j \quad \forall j \in N \quad (6)$$

$$x_{ij} \in \{0, 1\} \quad (7)$$

$$y_i \in \{0, 1\} \quad (8)$$

Each binary variable y_i indicates whether item i is the overflow item in its bin. Each binary variable x_{ij} indicates whether item i is assigned to the bin in which the overflow item is item j . Constraints (5) impose that each item must be assigned to a bin, while constraints (6) impose that the overall weight of the items assigned to a bin, excluding the overflow item, must fit into the bin and must leave at least one capacity unit available for accommodating the overflow item. The number of bins used is indicated in the objective function (4) by the number of binary variables y_i set to 1.

IV. PROPOSED HEURISTICS

A. Adapted First Fit Decreasing AFFD

In this section, we will describe our heuristic algorithm, called in the following *Adapted First Fit Decreasing (AFFD)*.

1) *Main idea*: In the open-end bin packing problem the capacity of any bin can be exceeded by only the last packed item, called the *overflow item*. Then, it is wise to consider the weightiest items as overflow items in order to minimize the number of used bins. In this way, Ongkunaruk [5] proposed MFFD algorithm which is a modification of the FFD runway. The author determines overflow items firstly before packing, then apply first fit decreasing with bins capacity equal to $C-1$.

Our Proposition is an adaptation of the well-known first fit decreasing where each selected overflow item can occupy at least one unit of bin capacity. Sorted items in decreasing order of their weight, the AFFD algorithm consist on assignment of the current item i into the lowest indexed opened bin which accommodate it, else, a new bin is opened. An opened bin can receive an item i if and only if the residual capacity -without take into account the overflow item- is sufficient to contain it. In other words, an item i can be placed into an opened bin if the weight w_i is less than or equal to $C-1-\sum_{j \in \hat{I}} w_j$ where \hat{I} is the set of items assigned to the opened bin, except the overflow item.

When a new bin is opened, a selection of an overflow item j is to be made. The overflow item j is selected as the weighted item among those already packed into all previous opened bins, but not yet used as overflow items. Once the overflow item is selected, a permutation of the placement between the selected item j and the current item i is performed.

2) *AFFD Pseudo code*: Let \hat{I}_j a set of items assigned to bin j , except the overflow item o_j . The AFFD heuristic can be summarized in the following steps:

- Step 0: Sort the items into a list I in decreasing order of their weight, set $i = 1$, $S = \emptyset$, $O = \emptyset$.
- Step 1: Until there are no items in a list I do
 - $S = S \cup i$;
 - Pack the current item i into the lowest indexed opened bin j^* in which the total weight of items \hat{I}_{j^*} already assigned to it -except, the over flow item- is strictly less than the bin

capacity. Open a new bin if it cannot be assigned to any existing bin;

- if a bin k is opened,
 - select the overflow item o_k such that $w_{o_k} = \text{argmax}_{i \in \hat{I}} \{w_i\}$ we pack firstly the overflow item;
 - Permute placement of the current item i and selected overflow item o_k
 - Set $O = O \cup o_k$ and update \hat{I} .
- Set $I = I \setminus i$
- Update the residual capacity of opened bins (We assume that the residual capacity of bin is the remaining of the capacity where we consider that the over flow item require only one unit)

3) *Algorithm*: Algorithm 1 details the AFFD procedure.

Algorithm 1: Adapted First Fit Decreasing AFFD

Data: I Set of items ordered in decreasing order of weights, w_i weight of item i , C Bins capacity.

Result: The number of used bins $|O|$

initialization

$O := \emptyset$

$S := \emptyset$

for $i = 1$ **to** n **do**

$S = S \cup \{i\}$

if (i can be assigned in one of opened bins) **then**

assign item i with bin capacity $C-1$ using FFD procedure

else

$j = \text{argmax}_{j \in S} \{S\}$

$S = S \setminus \{j\}$

$O = O \cup \{j\}$

Permute assignment between items i and j

AFFD procedure can be implemented on $O(n \log n)$ time, where n is the number of concerning items.

B. Adapted Minimum Bin Slack AMBS

We describe in the follow the second proposed heuristic which consists in a simple adaptation of MBS heuristic of Gupta and Ho [7]. We call this proposition, Adapted Minimum Bin Slack heuristic (AMBS). In this heuristic, we execute the MBS procedure, in which we consider that the weight of the largest item in the current bin is equal to one capacity unit. Otherwise, this item is considered as the overflow item of its bin, and this bin must leave at least one capacity unit available for the requirement of the overflow item. The AMBS heuristic is summarized in the following:

Until there are no items in the unpacked items set I :

- Select the largest item in I and assign this item as an overflow item in the current bin j . The residual capacity of bin j becomes $r_j = r_j - 1$. Then, remove the selected overflow item from the set I ;

- Apply the MBS-one search procedure on I with a capacity of bin equal to $C - 1$, in which we obtain the best subset of unpacked yet items.
- Remove the founded subset from I .

The complexity of MBS procedure is $O(2^n)$, but the computational experience shows that it is quite efficient in solving practical problem instances with various parameters [8][9]. This is due to the fact that in practical problem instances, the number of items involved in each packing is much smaller than n . If the maximum number of items that can be placed in one bin is u , then the complexity of MBS-one-packing procedure is reduced to $O(n^u)$ and thus packings for all bins are built in $O(n^{u+1})$.

V. COMPUTATIONAL RESULTS

Heuristics and lower bounds have been coded in java and run on an Intel i5 @ 2Go of RAM. The solver CPLEX 12.5 was used to solve the linear programming to the optimality.

We tested our heuristics algorithm on three data-sets called *uniform*, *triplet* and *random* instances. The two first data-sets contain eight instances classes were initially proposed by Falkenauer [11] and they were excessively used to test the performances of several bin packing problem variants. Each class contains 10 different instances. The uniform data-set includes four instances classes of bins capacities $C = 150$ and items with integer weights uniformly distributed in the interval of $[20 - 100]$. The number of items n for each class is respectively, 120,250,500 and 1000. The second data-set was called the triplet bin-packing instances because in the classical bin-packing problem, each bin can be filled with at most three items. This data-set includes also four instances classes of bin capacities $C = 1000$ and items with integer weights uniformly distributed over the interval $[25 - 50]$ with one decimal digit. The number of items n for each class is respectively, 60, 120, 249 and 501.

If for the triplet instances in the classical bin-packing problem (closed bin), each bin cannot contains more than three items, so for the open bin cases we can add no more than one item as an overflow item. Therefore, a valid lower bound (lower number of used bins) can be expressed by $L_{OBP}^T = \lceil \frac{n}{4} \rceil$ where n is the problem size or the number of items.

The last data-set was generated randomly and contains five classes of instances with different problem size, $n = 50, 100, 200, 500$ and 1000. For each class, items weight was generated using uniform distribution over four different intervals $[20 - 140]$, $[20 - 160]$, $[40 - 140]$ and $[40 - 160]$. The capacity of bins is fixed to 200. Ten different instances was generated for a given problem size and weight interval distribution.

The performance and average run time of tested heuristics on data-sets described above are shown in Table I, Table II and Table III respectively. Each line contains average results over ten OEBPP instances and the best results are shown in bold faced characters.

Table headings are as follows:

Dev. : Deviation of solution obtained by the corresponding heuristic(H) from the best lower bound provided by Ongkunaruk [5] LB_{OBP}^0 and the lower bound provided by Cesili and Righini [1] LB_{CBA} , computed as :

$$Dev(\%) = 100 * \frac{H - \max(LB_{OBP}^0, LB_{CBA})}{\max(LB_{OBP}^0, LB_{CBA})}$$

sec. : Computational time in seconds.

TABLE I. COMPUTATIONAL RESULTS FOR THE UNIFORM INSTANCES

Problem size	MFFD		AFFD		AMBS	
	<i>Dev.</i>	<i>sec.</i>	<i>Dev.</i>	<i>sec.</i>	<i>Dev.</i>	<i>sec.</i>
$u120$	2.99	<i>0</i>	2.99	<i>0</i>	3.65	<i>0.0031</i>
$u250$	1.41	<i>0.0085</i>	0.94	<i>0.0063</i>	2.50	<i>0.0031</i>
$u500$	1.33	<i>0.0266</i>	1.02	<i>0.014</i>	2.27	<i>0.0078</i>
$u1000$	1.42	<i>0.0312</i>	0.95	<i>0.0078</i>	2.10	<i>0.0328</i>
Average	1.78	<i>0.016</i>	1.47	<i>0.0070</i>	2.63	<i>0.0117</i>

TABLE II. COMPUTATIONAL RESULTS FOR THE TRIPLET INSTANCES

Problem size	MFFD		AFFD		AMBS	
	<i>Dev.</i>	<i>sec.</i>	<i>Dev.</i>	<i>sec.</i>	<i>Dev.</i>	<i>sec.</i>
$t60$	4.66	<i>0</i>	2.01	<i>0</i>	0	<i>0.0032</i>
$t120$	2.66	<i>0</i>	2.33	<i>0</i>	0	<i>0.0249</i>
$t249$	1.26	<i>0.0030</i>	1.26	<i>0</i>	0	<i>0.3557</i>
$t501$	1.34	<i>0.0157</i>	1.19	<i>0.0030</i>	0	<i>1.6488</i>
Average	2.48	<i>0.0047</i>	1.69	<i>0.0007</i>	0	<i>0.5081</i>

Table I shows computational results for the Falkenauer uniform instances, from these results we note that the average deviation decreases when the problem size increases, this is due to the convergence of the upper bounds and lower bounds from the optimal solution. In average, our heuristic AFFD performs better than heuristic provided by Ongkunaruk, more particularly when the problem size increase, this is due to the way on which MFFD algorithm extract the set of overflow items. In fact, the lower bound provided by Ongkunaruk performs worse when the problem size increase. Ongkunaruk's upper bound MFFD gives a further solution.

Concerning AMBS, this heuristic gives an important deviation from the optimal solution, this is due to the fact that from the MBS adaptation, some items with a large weight will be packed inside the bin. While, the optimal solution requires that all largest weight items must be packed as *overflow items* in order to minimize the number of used bins.

In Table II, we present the computational results of MFFD and proposed heuristic for the Falkenauer triplet instances. From these results, the overall attracting remarks that our heuristic AMBS give the optimal solution for this instances, because it is enough to find three items in each subset to be packed inside the bin, and one as *overflow item*. So the solution given by AMBS coincides with the lower bound value $L_{OBP}^T = \lceil \frac{n}{4} \rceil$. Moreover, from this table we note that both proposed heuristics AMBS and AFFD perform better

than MFFD.

For a given problem size, the results given by both AFFD and MFFD are better on the uniform instances comparing to the triplet instances. These remarks can be explained by the fact that the Falkenauer triplet instances are particularly difficult because in the optimal solution all constructed bins should have maximally three items as no overflow item plus one overflow item, therefore it is difficult to find an optimal subset of four items to each bin using first fit decreasing.

In overall, all the results present reasonable average computation time which confirms the good performances of our proposed heuristics. The time required by MFFD and AMBS are negligible. Furthermore, it is obvious to note that the time requirements increase with the problem size, but reasonable in order of some millisecond until problem size of 500 items.

Table III shows computational results for the random instances. In addition to both average deviation and execution time columns, we show the column *Diff* which represent the average difference of number of bins obtained by the proposed heuristics and the lower bound. From these results we remark that the average deviation decreases when the problem size increases, this is due to the convergence of the upper bounds and lower bounds from the optimal solution. The results also show that MFFD and AFFD methods performs better in quality of solution and computational time. An average deviation of 0% to 2.58% is given for the small problem size and 0.47% to 2.75% for the problems beyond to 200 items. Also, for such an interval of weight distribution, the average deviations decreases when the problem size increases which ensures the good performances of proposed methods. In overall proposed AFFD performs better with an overall average deviation of 1.29%. However, *MFFD* and *AMBS* show good performances and the same behaviour in the variation of deviation with an overall average deviation of 1.36% and 6.33% respectively. Although we have positive values of deviation, the average difference between the lower bound and the upper bounds is usually just two bins for MFFD and AFFD, while this difference is in order to average seven bins for AMBS. Obviously, this value of the difference increases with the problem size.

Generally, obtained results are given with reasonable average computation time, in order to some milliseconds for MFFD and AFFD heuristics and few large running time for AMBS, but always in order to milliseconds. The execution time increase with the problem size. For 1000 items, the solutions are obtained after average 28, 10 and 149 milliseconds for MFFD, AFFD and AMBS respectively. These results confirm the excellent performances of proposed heuristics.

VI. CONCLUSION

The open end bin-packing problem is an NP-hard combinatorial problem often encountered in the practical field. Few works are carried out to solve the problem in polynomial or pseudo-polynomial time. Through the present

paper, we have proposed and described two newly heuristics for the OEBPP problem, these heuristics are an adaptation of the well-known first fit decreasing algorithm and minimum bin slack algorithm.

Computational results based on a benchmark test bed show the good performance of proposed heuristics both on quality of solution, and on required execution time.

ACKNOWLEDGEMENT

This work was supported by Algerian state and performed jointly at LMA/EMP (Laboratoire de mathématiques appliquées de l'Ecole Militaire Polytechnique - Alger, Algérie) and CRIL (Centre de Recherche en Informatique de Lens CNRS - UMR 8188, France). This support is gratefully acknowledged.

REFERENCES

- [1] A. Ceselli and G. Righini, "An optimization algorithm for the ordered open-end bin-packing problem," *Operations Research*, vol. 56, no. 2, pp. 425–436, 2008.
- [2] J. Y. T. Leung, M. Dror, and G. H. Young, "A note on an open-end bin packing problem," *Journal of Scheduling*, vol. 4, no. 4, pp. 201–207, 2001.
- [3] J. E. G. Coffmann, M. R. Garey, and D. S. Johnson, *Approximation algorithms for NP-hard problems: Approximation algorithms for bin-packing-a survey*. Boston: PWS Publishing, 1997, ch. 2, pp. 46–96.
- [4] J. Yang and J. Y. T. Leung, "The ordered open-end bin-packing problem," *Operations Research*, vol. 51, no. 5, pp. 759–770, 2003.
- [5] P. Ongkunaruk, "Asymptotic worst-case analyses for the open bin packing problem," Ph.D. dissertation, Virginia Polytechnic Institute and State University, 2005.
- [6] D. S. Johnson, A. Demers, J. D. Ullman, M. R. Garey, and R. L. Graham, "Worst-case performance bound for simple one dimensional packing algorithms," *SIAM Journal on computing*, vol. 3, no. 4, pp. 299–325, 1974.
- [7] J. N. D. Gupta and J. C. Ho, "A new heuristic algorithm for the one-dimensional bin-packing problem," *Production Planning & Control*, vol. 10, no. 6, pp. 598–603, 1999.
- [8] K. Fleszar and K. S. Hindi, "New heuristics for one-dimensional bin-packing," *Computers & Operations Research*, vol. 29, pp. 821–839, 2002.
- [9] M. Maiza and M. S. Radjef, "Heuristics for solving the bin-packing problem with conflicts," *Applied Mathematical Sciences*, vol. 5, no. 35, pp. 1739 – 1752, 2011.
- [10] M. Maiza, A. Labed, and M. S. Radjef, "Efficient algorithms for the offline variable sized bin-packing problem," *Journal of Global Optimization*, vol. 57, no. 3, pp. 1025–1038, 2013.
- [11] E. Falkenauer, "A hybrid grouping genetic algorithm," *Journal of heuristics*, vol. 2, pp. 5–30, 1996.

TABLE III. COMPUTATIONAL RESULTS FOR THE RANDOM INSTANCES

		MFFD			AFFD			AMBS		
		% Dev	Diff	Sec.	% Dev	Diff	Sec.	% Dev	Diff	Sec.
R-50	[20-140]	1.66	0.2	0.0000	0.83	0.1	0.0000	3.21	0.4	0.0000
	[20-160]	0.00	0.0	0.0000	0.00	0.0	0.0000	5.07	0.7	0.0000
	[40-140]	1.42	0.2	0.0000	1.42	0.2	0.0000	2.14	0.3	0.0000
	[40-160]	1.91	0.3	0.0000	2.58	0.4	0.0000	3.83	0.6	0.0000
	Avg.	1.24	0.2	0.0000	1.20	0.2	0.0000	3.56	0.4	0.0000
R-100	[20-140]	1.16	0.3	0.0016	1.16	0.3	0.0000	5.84	1.5	0.0000
	[20-160]	0.35	0.1	0.0000	0.35	0.1	0.0000	5.09	1.4	0.0000
	[40-140]	2.50	0.7	0.0000	2.15	0.6	0.0015	5.36	1.5	0.0000
	[40-160]	2.07	0.6	0.0016	2.40	0.7	0.0000	5.79	1.7	0.0000
	Avg.	1.52	0.4	0.0008	1.51	0.4	0.0003	5.52	1.5	0.0000
R-200	[20-140]	0.79	0.4	0.0000	1.18	0.6	0.0000	6.94	3.5	0.0000
	[20-160]	0.75	0.4	0.0000	0.94	0.5	0.0000	7.72	4.1	0.0000
	[40-140]	2.34	1.3	0.0016	1.44	0.8	0.0000	6.29	3.5	0.0015
	[40-160]	1.71	1.0	0.0000	1.71	1.0	0.0016	7.00	4.1	0.0016
	Avg.	1.39	0.8	0.0004	1.31	0.7	0.0004	6.98	3.8	0.0007
R-500	[20-140]	0.47	0.6	0.0046	0.72	0.9	0.0031	8.14	10.1	0.0031
	[20-160]	0.82	1.1	0.0000	0.89	1.2	0.0000	7.85	10.5	0.0016
	[40-140]	2.68	3.7	0.0061	1.74	2.4	0.0032	6.97	9.6	0.0093
	[40-160]	1.56	2.3	0.0031	1.97	2.9	0.0047	7.55	11.1	0.0032
	Avg.	1.38	1.9	0.0034	1.33	1.9	0.0027	7.62	10.3	0.0043
R-1000	[20-140]	0.73	1.8	0.0265	0.77	1.9	0.0110	8.65	21.3	0.2511
	[20-160]	0.53	1.4	0.0173	0.68	1.8	0.0094	8.61	22.6	0.0764
	[40-140]	2.75	7.6	0.0407	1.48	4.1	0.0111	7.35	20.3	0.2683
	[40-160]	1.22	3.6	0.0264	1.63	4.8	0.0092	7.39	21.7	0.0014
	Avg.	1.30	3.6	0.0277	1.14	3.1	0.0101	8.00	21.5	0.1493
Total Avg.		1.36	1.4	0.0064	1.29	1.3	0.0027	6.33	7.5	0.0308

Performance Comparison between MAI and Noise Constrained LMS Algorithm for MIMO CDMA DFE and Linear Equalizers

Khalid Mahmood

Member Institute of Electrical and Electronic Engineers (IEEE)

Abstract—This paper presents a performance comparison between a constrained least mean squared algorithm for MIMO CDMA decision feedback equalizer and linear equalizer. Both algorithms are constrained on the length of spreading sequence, number of users, variance of multiple access interference as well as additive white Gaussian noise (new constraint). An important feature of both algorithms is that multiple access interference together with noise variance is used as a constraint in MIMO CDMA linear and decision feedback equalization systems. Convergence analysis is performed for algorithm in both cases. From the simulation results shown at the end show that algorithm developed for decision feedback equalizer has outperformed the algorithm developed for linear equalizer in MIMO CDMA case

Keywords—Least mean squared algorithm (LMS); linear equalizer (LE); multiple input; multiple output (MIMO); decision feedback equalizer (DFE); multiple access interference (MAI); Variance; adaptive algorithm

I. INTRODUCTION

It is shown in literature that performance of an adaptive algorithm may be enhanced if partial knowledge of the channel is included in algorithm design [1], [2], [3]. By using this idea, [1] developed an algorithm called noise-constrained least mean squared (LMS) for tracing of finite impulse response (FIR) channels by utilizing the statistics of the additive noise. An important feature of this algorithm is its superiority over traditional LMS algorithm in convergence while having almost same computational complexity. A complementary pair LMS (CP-LMS) [4], [5] was introduced later on using a constrained optimization technique named augmented Lagrangian. This technique could be used to resolve the problem of selecting an appropriate update step-size in LMS algorithm. Augmented technique was used in [6], incorporating the knowledge of the statistics (variance) of multiple access interference (MAI) and additive white noise and was named constrained LMS algorithm (MNCLMS) for single input, single output (SISO) CDMA system.

Since the MAI together with the white Gaussian noise (AWGN) badly effects the MIMO-CDMA systems, it is required to design a receiver design that would negate the damaging effect of MAI and additive AWGN. This necessitates an enactment of the MNCLMS algorithm derived in [7], [8] for the decision feedback equalizer (DFE) case. The said algorithm is developed by including statistics such as MAI and noise variances and is named MIMO-MAI plus noise constrained LMS (MIMO-MNCLMS) adaptive algorithm. A MIMO implementation of the MAI and noise constrained algorithm for linear equalizer (LE) was developed in [9]. In

this paper, we have presented the performance comparison of the MNCLS algorithm in decision feedback equalizer (DFE) and linear equalizer (LE).

Our paper is presented as,

Introductory remarks are given in section I, Section II discusses system model. Algorithm motivation for LE and DFE are presented in section III, whereas section V deals with computational complexity of the algorithm. Section VI presents the performance comparison between the DFE and LE for MNCLS algorithm. Conclusion is provided in section VII.

II. SYSTEM MODEL

In this paper, a typical CDMA transmitter model for a downlink of a mobile radio network is considered as shown in Fig. 1. It comprises of N transmitters and M receivers.

In this paper, we are using a fast Rayleigh fading channel. The impulse response between the n th transmitter and m th receiver for an l th symbol is [9]

$$H_{mn}^l(t) = h_{mn}^l e^{j\phi_l} \delta(t) \quad (1)$$

where

h_{mn}^l is the impulse response

ϕ_l is the phase of Rayleigh channel.

The sensor in the m th receiver sees the following,

$$r_m(t) = \sum_{n=1}^N \sum_{l=-\infty}^{\infty} \sum_{k=1}^K A^k b_n^{l,k} s_n^{l,k}(t) h_{mn}^l + \nu_m(t), \quad m = 1, 2, \dots, M \quad (2)$$

where

K = represents number of users,

$s_n^{l,k}(t)$ = represents rectangular signature waveform

$\{b_n^{l,k}\}$ = input bit stream of the k th user,

h_{mn}^l = channel tap between the m th transmitting antenna and the n th receiving antenna,

A^k = k th user amplitude,

ϖ_m = additive AWGN. It has zero mean

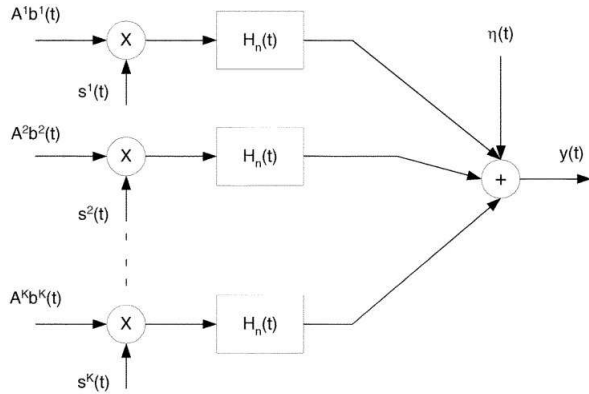


Fig. 1. Synchronous downlink CDMA system model

The receiving side is comprised of a matched filter. It is matched to the signature waveform of user 1 (desired user).

Output of the matched filter at the m th receiver is set up as:

$$\begin{aligned}
 y_m^l &= \int_{(l-1)T_b}^{lT_b} r_m(t) s_m^{l,1}(t) dt \\
 &= \sum_{n=1}^N A^1 b_n^{l,1} h_{mn}^l + \sum_{n=1}^N \sum_{k=2}^K A^k b_n^{l,k} \rho_n^{k,1}(t) h_{mn}^l \\
 &\quad + \varpi_m, \quad m = 1, 2, \dots, M
 \end{aligned} \quad (3)$$

MAI is represented by the Second term in equation 3. Mathematically, it is defined as:

$$\begin{aligned}
 z_m^l &= \sum_{n=1}^N \sum_{k=2}^K A^k b_n^{l,k} \rho_n^{k,1} h_{mn}^l, \quad m \\
 &= 1, 2, \dots, M
 \end{aligned} \quad (4)$$

MAI may also be set up as

$$\begin{aligned}
 z_m^l &\leq \sum_{n=1}^N \sum_{k=2}^K A^k b_n^{l,k} \rho_n^{k,1} \sum_{n=1}^N h_{mn}^l \\
 &\leq U_m \sum_{n=1}^N h_{mn}^l, \quad m = 1, 2, \dots, M
 \end{aligned} \quad (5)$$

where,

$$U_m^l = \sum_{n=1}^N \sum_{k=2}^K A^k b_n^{l,k} \rho_n^{k,1}.$$

III. ALGORITHM MOTIVATION

Certain adaptive algorithms (LMS and recursive least square (RLS)) don't use models for channel coefficients and additive noise, on the other hand, model based algorithms (random walk, auto-regressive etc) use models for estimating channel coefficients and AWGN [10].

Performance of an adaptive algorithm may be enhanced if even fractional knowledge of a channel statistics is available. According to the noise constrained LMS algorithm [3], weight update equation of an algorithm can be set up as

$$\mathbf{w}_{n+1} = \mathbf{w}_n + \mu_n^l e_n \mathbf{X}_n^l \quad (6)$$

where

\mathbf{X}_n^l = the input data

μ_n^l = positive step size

e_n^l = error between the output of the matched filter and an adaptive filter

$$\mu_{n+1} = 2\mu_n^l (1 + \gamma \lambda_n) \quad (7)$$

$$\lambda_{n+1} = \lambda_n + \beta \left[\left(\frac{1}{2} e_n^2 - \sigma_{v_m}^2 \right) - \lambda_n \right] \quad (8)$$

Where λ , α and β are positive step sizes (parameters). Computational cost of above mentioned algorithm is same as LMS but the convergence rate of the algorithm is much better than the LMS.

As MAI is a major factor in the system performance of a multiuser environment, it becomes important to come up with a receiver scheme which would reduce the damaging effects introduced by MAI and AWGN. In the previous research work, MAI was assumed to be a part of AWGN which is not valid. But using MAI alone as a constraint is not a viable choice since noise is an undeniable physical constraint and may not be ignored while developing such algorithms.

As NCLMS algorithm is noise constrained only, a new constrained algorithm is established for LE and DFE in [9] and [8] respectively. Variance of MAI and AWGN was used as new constraints in these algorithms.

IV. MIMO-CDMA MAI AND NOISE CONSTRAINED LMS ALGORITHM

A. MIMO-CDMA MNCLMS Constrained Algorithm for Linear Equalizer (LE)

LE algorithm was developed in [9] and is given as

$$\mathbf{s}_n^{l+1} = \mathbf{s}_n^l + \zeta_n^l e_n^l \mathbf{E}_n^l \quad (9)$$

where

ζ_n^l = positive step size and is the positive step size,

e_n^l = error of output of a matched filter and an adaptive filter. It is mathematically defined as:

$$e_n^l = \hat{x}_n - \mathbf{s}_n^l \mathbf{E}_n^l \quad (10)$$

\mathbf{E}_n^l in equation 10 is a joint input to the LE and is:

$$\mathbf{E}_n^l = \left[(\mathbf{y}_n^l)^T \right] \quad (11)$$

Order of $\mathbf{E}_n^l = (ML \times 1)$.

$\mathbf{z}_n^l = \left[(\mathbf{z}_1^l)^T \ (\mathbf{z}_2^l)^T \ \dots \ (\mathbf{z}_M^l)^T \right]^T$ is input to feed forward filter (FFF) having dimension $ML \times 1$. It is a collection of vectors consisting of z_m^l given by $\mathbf{z}_m^l = [z_m^l \ z_m^{l-1} \ \dots \ z_m^{l-L+1}]^T$.

and

$$\begin{aligned} \hat{\mathbf{x}}_n &= \mathbf{w}_o^T E_n^l \\ &= \mathbf{x}_n^l + \bar{\varphi}_n^l \end{aligned} \quad (12)$$

or

$$\mathbf{x}_n^l = \mathbf{w}_o^T E_n^l - \bar{\varphi}_n^l \quad (13)$$

$\bar{\varphi}_n^l$ is a filtered noise passing through (FFF). It is comprised of MAI and AWGN.

ς_n^l , is shown to be

$$\begin{aligned} \varsigma_n^l &= \varsigma_n (1 + \gamma_n \lambda_n^l) \quad m \\ &= 1, 2, \dots, M \end{aligned} \quad (14)$$

$$\begin{aligned} \lambda_n^{l+1} &= \lambda_n + \beta_n \left[\frac{1}{2} (e_n^{l2} - \sigma_{\bar{\varphi}_n^l}^2) - \lambda_n^l \right] \quad m \\ &= 1, 2, \dots, M \end{aligned} \quad (15)$$

where,

$\sigma_{\bar{\varphi}_n^l}^2$ is variance of the filtered noise.

B. MIMO-CDMA MNCLMS Constrained Algorithm for Decision Feedback Equalizer (DFE)

MIMO-CDMA MNCLMS algorithm was developed in [11] and is given as

$$\mathbf{w}_n^{l+1} = \mathbf{w}_n^l + \mu_n^l e_n^l E_n^l \quad (16)$$

where,

E_n^l is the combined input to the DFE and is given by

$$E_n^l = \left[(\mathbf{y}_n^l)^T \ (\mathbf{x}_n^l)^T \right]^T \quad (17)$$

and is of the order of $(MK + NQ) \times 1$

μ_n^l is a positive step size and is

$$\begin{aligned} \mu_n^l &= \mu_n (1 + \gamma_n \lambda_n^l) \quad m \\ &= 1, 2, \dots, M \end{aligned} \quad (18)$$

$$\begin{aligned} \lambda_n^{l+1} &= \lambda_n + \beta_n \left[\frac{1}{2} (e_n^{l2} - \sigma_{v_n^l}^2) - \lambda_n^l \right] \quad m \\ &= 1, 2, \dots, M \end{aligned} \quad (19)$$

V. COMPUTATIONAL COST OF LE AND DFE ALGORITHMS

Computational cost of any algorithm is an important aspect of that algorithm. Increased complexity can reduce the effectiveness of an algorithm. A tradeoff between performance and computational complexity is possible if increased complexity results in substantial performance gains. In this section, we are comparing computational costs of few algorithms. As shown in tables I and II, computational cost of the algorithm in case of DFE is more than the LE but cost is much lower than the RLS. Computational cost of the DFE and the LE algorithms is more than [6] but that is for SISO CDMA case, whereas, algorithms developed in [9] and [11] are for MIMO CDMA case.

VI. SIMULATION RESULTS

Following independent assumptions are used while performing the comparison analysis [13], [14].

- 1) Input random process $\{\mathbf{x}_n^l\}$ is an independent and identically distributed (i.i.d) random process.
- 2) AWGN is a zero mean i.i.d, Gaussian random process and is independent of input process.
- 3) MAI in AWGN environment is zero mean Gaussian random process. It is independent of the input process as well as AWGN.

A. Interference Elimination in an AWGN Channel for LE and DFE cases

In order to analyze the performance of the proposed algorithm for MIMO CDMA LE case, simulation results are presented in this section. Performance of MNCLMS algorithm is compared to standard LMS, MCLMS noise constrained LMS and zero noise algorithms and then later on performance of the algorithms in LE and DFE cases is compared to each other.

The following simulation setup is used to judge the performance.

- The average MSE is the performance parameter through which all the algorithms are analyzed.
- A 2×2 MIMO system is considered in this section
- SNR is kept at 20 dB for 10 and 20 users
- AWGN channel environment
- BPSK and QPSK modulations

Simulation results for comparison of the convergence speed of all algorithms for 10 and 20 users, in an AWGN channel, are shown, in figures.2 and 3 respectively. As evident from both figures, this algorithm is converging faster than its competitors. It is also noted that MSE degenerates as the number of users is increased from 10 to 20. When number of users is 10, MNCLMS algorithm for LE case achieved MSE at -6 dB in 120 iterations whereas the very first of other algorithms converged at MSE at -6dB in 140 symbols, MNCLMS algorithm achieved MSE at -2.6 dB and in 140 symbols when number of users is doubled.

The MNCLMS algorithm's performance is evaluated in the AWGN environment using. The result in figure 6 shows the

TABLE I. LE COMPUTATIONAL COST PER ITERATION FOR DIFFERENT ALGORITHMS

Algorithm	No. of Multiplications	No. of Additions
LMS	$2K + 1$	K
RLS	$K^2 + 5K + 1$	$K^2 + 3K$
MNCLMS[12]	$2K + 1$	$2K + 6$
MIMO-MNCLMS(LE)[9]	$2MK + 8$	$2MK + 4$

TABLE II. DFE COMPUTATIONAL COST PER ITERATION FOR DIFFERENT ALGORITHMS

Algorithm	No. of Multiplications	No. of Additions
LMS	$2K + 1$	$2K$
RLS	$K^2 + 5K + 1$	$K^2 + 3K$
MNCLMS[12]	$2K + 1$	$2K + 6$
MIMO-MNCLMS(DFE)[7]	$2(MK + NQ) + 8$	$MK + NQ + 4$

In both tables K shows length of the filter.

performance using BPSK modulation. As evident, MNCLMS algorithm for LE case, is much superior than the LMS and the NLMS algorithms as MNCLMS converges faster. The MNCLMS algorithm converges on MSE of -16 dB in 2000 symbols. A similar performance gain for MNCLMS can be seen using QPSK modulation as shown in figure 7. It is also evident that although there is a little deterioration in convergence rate but MNCLMS algorithm outclassed LMS and NLMS algorithms.

From simulation results, it is evident that although both have better performance than other constrained algorithms but when LE and DFE cases are compared with each other, it is evident that DFE is converging faster than the LE algorithm in the AWGN channel environment as in DFE case, the algorithm achieved MSE at -16 dB as compared to LE which achieved MSE at -6 dB.

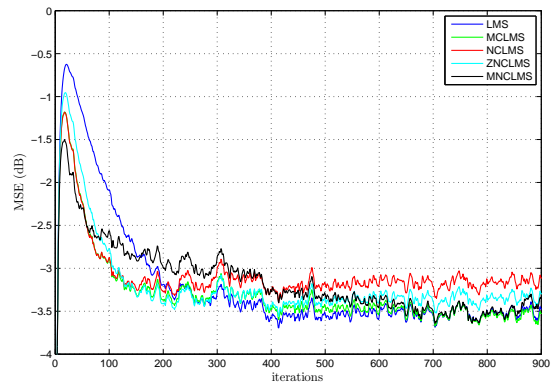


Fig. 3. Mean squared error (MSE) behavior of comparing algorithms in AWGN environment for 10 users at 20dB SNR

Behavior of step size of MNCLMS algorithm in LE case is shown in figure 4 for 10 users. In the transient state algorithm in LE case is having the biggest step size value as compared to other algorithms and, thus, converges faster. In the steady state condition, step size parameter of this algorithm is minimized as compared to LMS, NCLMS and ZNCLMS algorithms. Same behavior is achieved for 20 users as shown in figure 5.

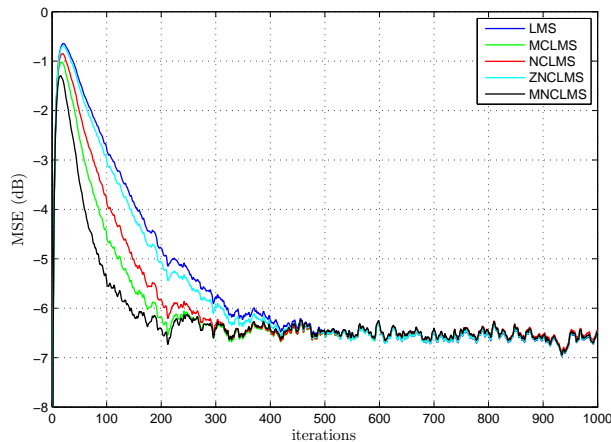


Fig. 2. Mean squared error (MSE) behavior of comparing algorithms in an AWGN channel environment for 10 users at 20dB SNR

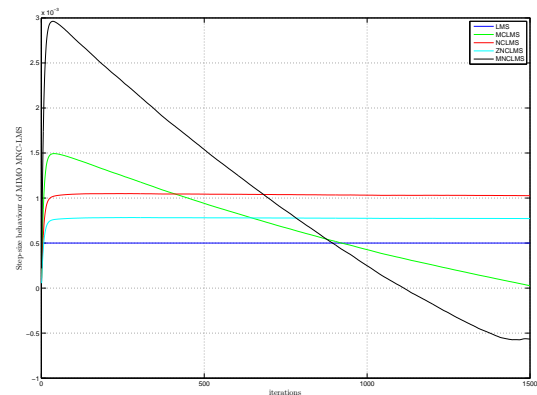


Fig. 4. Behavior of the step size of the LE algorithm for 10 users at 20 dB SNR

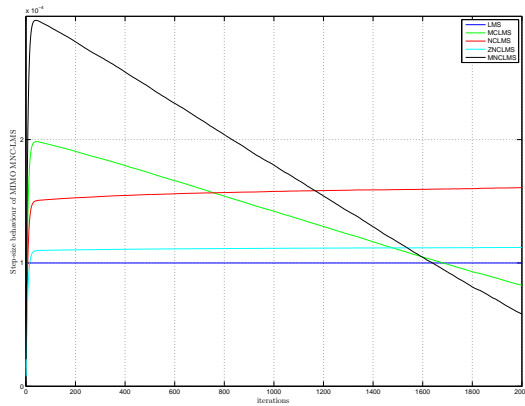


Fig. 5. Behavior of the step size of the MNCLMS algorithm for 25 users at 20 dB SNR

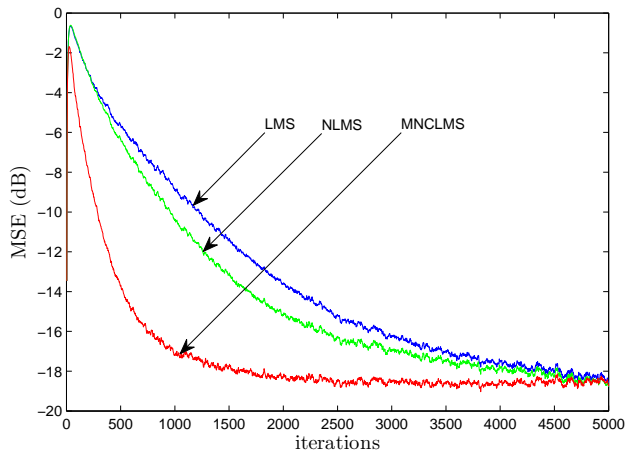


Fig. 6. Mean squared error (MSE) performance in AWGN channel environment at SNR=20 dB

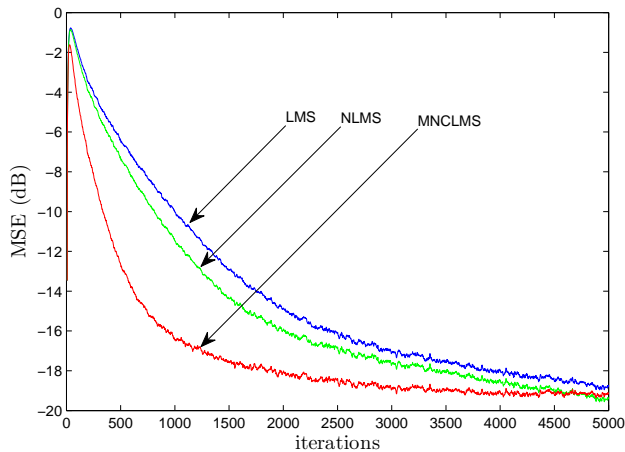


Fig. 7. Mean squared error (MSE) performance in AWGN environment at SNR=20 dB using QPSK signaling.

B. Interference Elimination in Rayleigh Fading Channel for LE and DFE Cases

Performance of the MNCLMS in the LE and DFE is compared to the standard LMS, MCLMS noise constrained LMS and ZNCLMS algorithms in this section.

The following simulation setup is used to judge the performance of algorithms

- 2×2 MIMO system
- Random signature sequence having a length of 31 and a rectangular chip waveforms
- The SNR is kept at 10 dB and 20 dB for 10 and 20 users respectively
- Rayleigh fading channel environment
- BPSK and QPSK modulations
- Doppler frequency of $f_d = 250\text{Hz}$

Simulation results for convergence of the above mentioned algorithms for 10 and 20 users, in the Rayleigh fading channel are presented in figures 8 and 9. It can be seen that MIMO CDMA MNCLMS algorithm converged faster than its competitor algorithms. For 10 users, the algorithm achieved MSE at -4.8 dB in 200 iterations. It is also observed that when number of users is enhanced to 20, the MNCLMS algorithm achieved MSE at -5.2 dB in 240 iterations.

In second case, a flat fast Rayleigh fading channel is considered. As evident, from figure 11, MNCLMS in DFE case converged much earlier than its competitors. Figure 10 shows performance of the MNCLMS algorithm using QPSK modulation and as evident again, this algorithm converged much earlier than the LMS, NLMS etc.

It is also evident from the simulation results that MNCLMS algorithm in DFE case is converging much faster than the algorithm in LE case. As shown in figures 10 and 11, the algorithm for DFE case achieved MSE in -16 dB, which is much smaller than the algorithm in LE equalizer case.

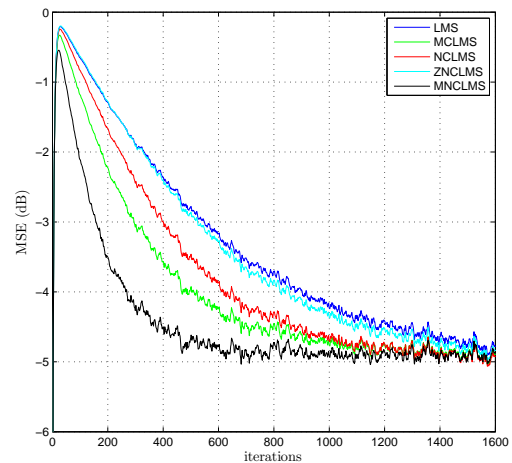


Fig. 8. Mean squared error (MSE) behavior for comparing algorithms in the Rayleigh fading environment for 10 users at 10 dB SNR

VII. CONCLUSION

A performance comparison between a MNCLMS algorithm for MIMO CDMA, DFE and LE cases is performed in this paper. Both algorithms are constrained on the length of spreading sequence, number of users, statistics (variances) of AWGN, MAI and additive noise. Simulation results are presented to compare the performance of the MNCLMS constrained algorithms in both cases and it is found that while both algorithms outperformed other constrained algorithms but when compared to each other, DFE has outperformed the LE.

REFERENCES

- [1] Yongbin Wei, Saul B Gelfand, and James V Krogmeier. Noise constrained lms algorithm. In *Acoustics, Speech, and Signal Processing, 1997. ICASSP-97., 1997 IEEE International Conference on*, volume 3, pages 2353–2356. IEEE, 1997.
- [2] RADU CIPRIAN Bilcu, Pauli Kuosmanen, and Corneliu Rusu. A noise constrained vs-lms algorithm. In *EUROCOMM 2000. Information Systems for Enhanced Public Safety and Security. IEEE/AFCEA*, pages 29–33. IEEE, 2000.
- [3] Yongbin Wei, Saul B Gelfand, and James V Krogmeier. Noise-constrained least mean squares algorithm. *Signal Processing, IEEE Transactions on*, 49(9):1961–1970, 2001.
- [4] SONG Woo-Jin. A complementary pair lms algorithm for adaptive filtering. *IEICE TRANSACTIONS on Fundamentals of Electronics, Communications and Computer Sciences*, 81(7):1493–1497, 1998.
- [5] SONG Woo-Jin. A complementary pair lms algorithm for adaptive filtering. *IEICE TRANSACTIONS on Fundamentals of Electronics, Communications and Computer Sciences*, 81(7):1493–1497, 1998.
- [6] M Moinuddin, A Zerguine, and Asrar U. H. Sheikh. Multiple-Access Interference Plus Noise-Constrained Least Mean Square (MNCLMS) Algorithm for CDMA Systems. *IEEE Transactions on Circuits and Systems I: Regular Papers*, 55(9):2870–2883, October 2008.
- [7] Khalid Mahmood, Syed Muhammad Asad, and Muhammad Moinuddin. Design of MAI Constrained Decision Feedback Equalizer for MIMO CDMA System. *Technology*.
- [8] Khalid Mahmood, Syed Muhammad Asad, Muhammad Moinuddin, and Shashi Paul. Design of MAI Constrained Decision Feedback Equalizer for MIMO CDMA System. 2011.
- [9] Khalid Mahmood, Syed Muhammad Asad, Muhammad Moinuddin, and Waqas Imtiaz. Mai and noise constrained lms algorithm for mimo cdma linear equalizer. *International Journal of Advanced Computer Science & Applications*, 1(7):702–711, Jan 2016.
- [10] A.H. Sayed and T. Kailath. A state-space approach to adaptive rls filtering. *Signal Processing Magazine, IEEE*, 11(3):18–60, 1994.
- [11] Khalid Mahmood, Syed Muhammad Asad, Muhammad Moinuddin, and Shashi Paul. Design of MAI constrained decision feedback equalizer for MIMO CDMA system. *2011 International Conference on Wireless Communications and Signal Processing (WCSP)*, pages 1–5, November 2011.
- [12] Muhammad Moinuddin, Azzedine Zerguine, and A Sheikh. Multiple-access interference plus noise-constrained least mean square (mnclms) algorithm for cdma systems. *Circuits and Systems I: Regular Papers, IEEE Transactions on*, 55(9):2870–2883, 2008.
- [13] Ali H Sayed. *Adaptive filters*. Wiley. com, 2008.
- [14] a.H. Sayed and H.V. Poor. Optimal Multiband Joint Detection for Spectrum Sensing in Cognitive Radio Networks. *IEEE Transactions on Signal Processing*, 57(3):1128–1140, March 2009.

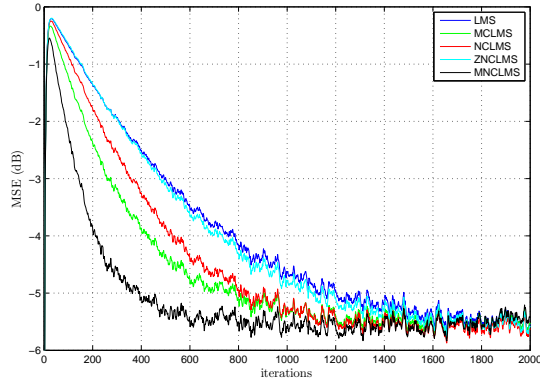


Fig. 9. Mean squared error (MSE) behavior for comparing algorithms in the Rayleigh fading environment for 20 users at 20 dB SNR

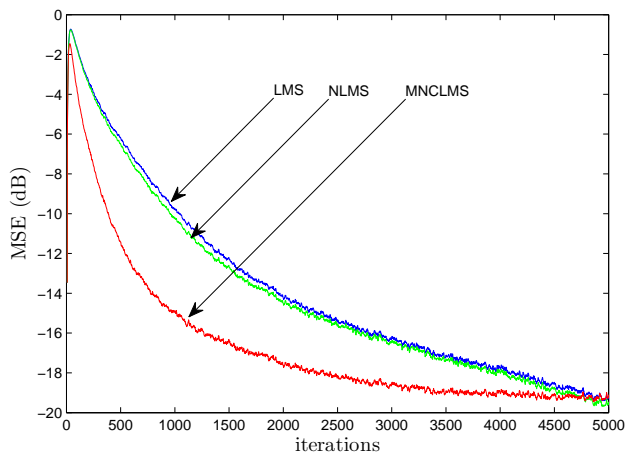


Fig. 10. Mean squared error (MSE) performance in Rayleigh fading environment with $f_d = 250\text{Hz}$ at $\text{SNR}=20\text{ dB}$

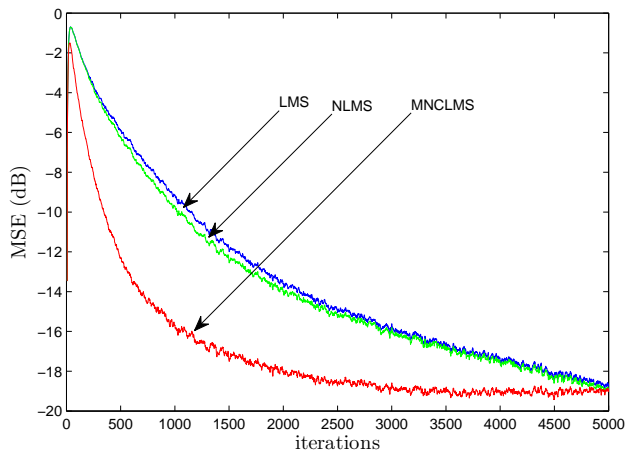


Fig. 11. Mean squared error (MSE) performance in Rayleigh fading environment with $f_d = 250\text{Hz}$ at $\text{SNR}=20\text{ dB}$

Software Defined Security Service Provisioning Framework for Internet of Things

Faraz Idris Khan, Sufian Hameed

IT Security Labs, National University of Computer and Emerging Sciences (FAST-NUCES), Pakistan

Abstract—Programmable management framework have paved the way for managing devices in the network. Lately, emerging paradigm of Software Defined Networking (SDN) have revolutionized programmable networks. Designers of networking applications i.e. Internet of things (IoT) have started investigating potentials of SDN paradigm in improving network management. IoT envision interconnecting various embedded devices surrounding our environment with IP to enable internet connectivity. Unlike traditional network architectures, IoT are characterized by constraint in resources and heterogeneous inter connectivity of wireless and wired medium. Therefore, unique challenges for managing IoT are raised which are discussed in this paper. Ubiquity of IoT have raised unique security challenges in IoT which is one of the aspect of management framework for IoT. In this paper, security threats and requirements are summarized in IoT extracted from the state of the art efforts in investigating security challenges of IoT. Also, SDN based security service provisioning framework for IoT is proposed.

Keywords—IoT; Software Defined Security; Security in IoT; Software Defined Networking; Software Defined based IoT (SDIoT)

I. INTRODUCTION

Recent revolution in embedded technologies and Internet have made it possible for the things surrounding us to be interconnected with each other [1]. It is expected in the coming era IoT devices will be part of the environment around us which will generate enormous amount of data. Processing is required on the generated data which is then presented in an understandable form to the requester.

Mobile operators, software developers, integrators and alternative access technology are involved in the IoT ecosystem [2]. There are many different application domains where IoT plays crucial role like manufacturing, health-care, transport, administration, insurance, public safety, local community, metering, road safety, traffic management, tracking, etc. IoT enables interconnection with people's devices exchanging information and performing actions with out humans involved. This is possible by amalgamating heterogeneous communication infrastructure. This has motivated the researcher to design smart gateways which connects IoT devices with traditional internet. Most recently, enabling *Everything as a Service model* by merging IoT and Cloud Computing is the focus of attention in the research community [3] (see figure 1).

In order to tackle management problems in IoT, resource management frameworks have received considerable attention. SDN paradigm offers an attractive solution to manage IoT resources which is been lately under focus. Proposal of a framework for managing traffic and network resources in an

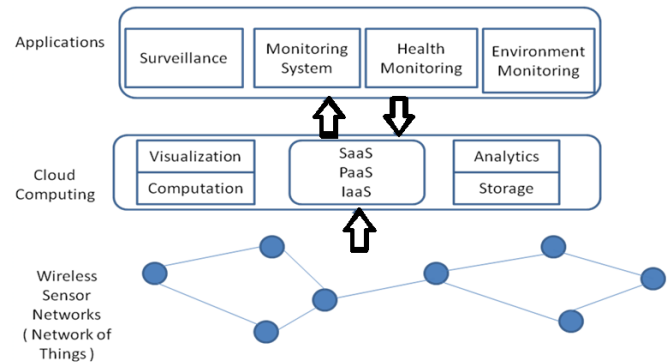


Fig. 1. IoT and Cloud Convergence

IoT environment is given in [4]. Other efforts which have adopted SDN based approach to solve management issues in IoT can be found in [5][6][7][8][9][10].

Numerous security challenges are illuminated with the increasing complexity of IoT networks. There is a desire for a complete framework which manages data generated from the IoT devices. Up till now there is no SDN based comprehensive security framework for IoT network. For managing security of IoT networks the promise of SDN to manage IoT resources makes it a prime candidate for management framework. Contribution in this paper is twofold which are as follows.

- 1) Identified and discussed management challenges of IoT. Furthermore in this paper security management of IoT is dealt with and security issues, threats, attacks and requirements in IoT are identified.
- 2) Proposed SDN based framework for provisioning security services over IoT network.

The paper is organized as follows. Section 2 gives a brief introduction on software defined networking paradigm. Management challenges of IoT are discussed in section 3. Section 4 gives detail insight into security issues and requirements of IoT. Section 5 discusses security threats and attacks in IoT. In section 6, general introduction to software defined networking framework for IoT (SDIoT) is given. Section 7, presents the proposal of SDN based IoT framework for security service provisioning. In the end, conclusion and future work is discussed.

II. INTRODUCTION TO SDN

Developments in programmable networks by Martin Casado, Nick Mckeown and Scott Shenker at Stanford Univer-

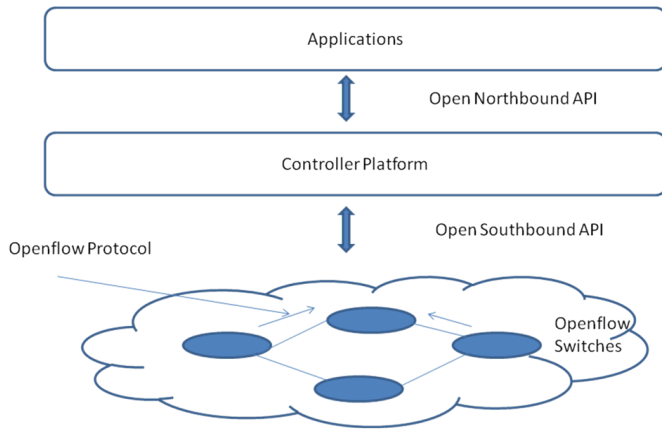


Fig. 2. SDN Architecture

sity resulted in a novel paradigm of SDN. Road to SDN with a brief discussion on the history of programmable networks can be found in [11]. SDN enables network administrators to manage network services by abstracting high level functionalities. Such abstraction is provided by separating control plane from the data plane. With such separation network management is simplified.

Appropriate forwarding decisions for the end network devices which are SDN enabled are given by a special central node called SDN controller. Openflow is the most widely used protocol used by the end devices to communicate with the SDN controller. Openflow supported devices are often called Openflow switches. An OpenFlow switch separates the data plane and control plane functions. High level routing decisions are moved to the controller. Switch have the data plane portion. Figure 2. illustrates a typical SDN architecture.

Secure connection with the network devices and SDN controller is established by Openflow control message exchanges. Furthermore, the message exchange result in installing forwarding instructions. Flow tables in the switches are maintained by the data plane. In flow tables, each flow table entry contains a set of packet fields to match an action (such as send-out-port, modify-field, or drop). Upon receiving a packet which is never seen by the Openflow switch and no matching flow entries is found. The switch sends such packet to the controller for making decision. Decision taken by the SDN controller can be of dropping the packet or adding flow entry in the Openflow switch for forwarding in future. Flow tables have flow entries which are defined by flow rules defined in Openflow. Heterogeneous network changes result in dynamic modification of flow rules.

III. MANAGEMENT CHALLENGES OF IOT

Conventional network management techniques are inapplicable in IoT due to distinctive challenges. IoT devices connected to the internet via gateway is shown in figure 3. CoAP (Constrained Application) protocol running over 6LowPAN is used for communication between gateway and IoT nodes. IoT network devices are not sufficient in resources. Usually in IoT network high fault rates are experienced due to shortfall in energy and connectivity interruptions. To improve the efficiency of the network main concerns are of monitoring

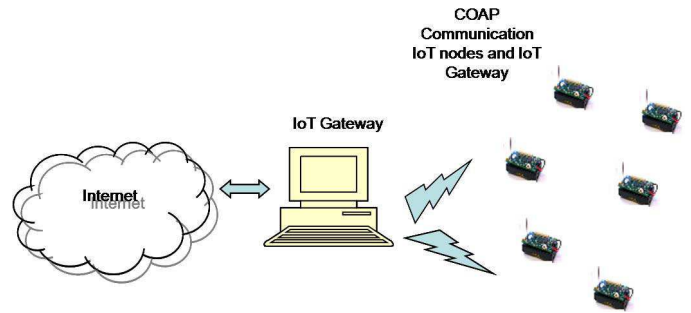


Fig. 3. IoT devices connected with Internet via IoT Gateway.

and administration of node communication. A typical management solution should provide various management functions integrating configuration, security operation, administration of devices and services of IoT. Following set of functions should be provided by management solution for IoT.

A. Fault Tolerance

Failures are encountered in the IoT network for various reasons. Depletion of batteries is one possibility. Effects on the sensing components results in inaccurate readings disseminated by the devices. Vigorous changes in network topology and partitions in the network is created due to inherent nature of adhoc wireless network links tendency of failures. Due to erroneous nature of communication, delivered packets get corrupted. Packet losses are not experienced due to failures of link but are also caused by congestion. Multihop communication nature of IoT worsen all the fault scenarios discussed. Efforts in this direction is summarized in [12].

B. Energy Management

IoT network are deployed in distant region. Due to scarcity of energy resource in IoT and its deployment in distant region depletion of available energy happens frequently. Substitute of energy is impossible. Balanced energy management among supply and load is required to avoid energy scarcity. Data traffic from devices can be controlled to balance energy in the network which is possible by techniques such as duty cycling, scheduling sleep and wake-up modes of devices studied in [13]. Management solution for IoT should address the energy issue by having essential function of energy management for smooth operation of IoT network.

C. Load balancing

Load balancing can be used for extending lifetime of IoT which results in lessening energy utilization. Load balancing is possible by techniques such as clustering. In clustering technique IoT network is organized into cluster which is coordinated by a cluster head. With such configuration there are numerous benefits, such as reduction in routing table size, conservation of network bandwidth, lengthening network lifetime, reduction in redundant data packets and decreasing energy consumption. This makes load balancing an essential component of management solution for IoT. Efforts in this direction can be found in [14].

D. Security Management

Security, privacy and trust are essential requirements in IoT. Due to resource constraint nature of IoT devices the provisioning of security has become more challenging. Novel techniques for provisioning of security is required as conventional security schemes are inapplicable. This poses unique challenges for management framework designer of IoT. Research on security management can be found in [15].

In this paper, security management issues of IoT network are dealt with. In addition, major security issues and requirements put forth by IoT are identified. In order to address these issues and requirements SDN based framework to provision security services over IoT is proposed.

IV. SECURITY ISSUES AND REQUIREMENTS IN IOT

In this section, major security issues and requirements are identified which are imposed by resource constrained IoT network. Traditional solutions are inapplicable in the domain of IoT due to resource constraint nature of IoT devices. In this section latest research efforts in each of the issues and requirements are outlined.

A. Privacy in IoT

IoT finds its uses in various heterogeneous fields which include remote monitoring of patients, control of energy consumption, traffic control, production chain, smart shopping etc. Hence, privacy in IoT is a prime security issue which needs full attention from researchers in academia and industry. There is a desire need to propose protocols and management framework for handling privacy in IoT. Latest attempts to address the issue can be found in literature such as [16], [17], [18].

B. Lightweight Cryptographic Framework for IoT

IoT is usually scarce in resources and faces number of challenges such as limitation in power and bandwidth, etc. Hence traditional heavy weight algorithms cannot be opted for IoT. There is a desire need to investigate how to make symmetric and asymmetric algorithms lightweight for IoT. Most recently, various efforts for lightweight solution for IoT can be found in [19], [20], [19], [21]. Some of the existing lightweight cryptographic solutions includes HIGHT, RC5 and PRESENT.

C. Secure Routing and Forwarding in IoT

IoT not only require provisioning of security services but often experience problems in routing and forwarding the data. Hence, there is a desire need to secure the routing algorithm for IoT. IoT routing usually experiences selective forwarding attacks, sink hole attack, Hello flood attack, Wormhole attack, clone ID and sybil attacks. Efforts have been putforward by the researchers to address routing attacks in IoT. A comprehensive state of the art in securing routing for WSN can be found in [22]. Latest efforts in proposing secure routing for IoT can be found in [23], [24], [25].

D. Robustness and Resilient Management in IoT

IoT applications require robustness as failures due to security attacks may not be affordable for low power devices. Hence, an ideal IoT management framework should have mechanisms to prevent such situations and ensure fault tolerance against security failures. Efforts in this direction can be found in [26], [27], [28], [29].

E. Management Framework for IoT

SDN offers tremendous amount of opportunities to manage future Internet. The conventional network protocols and equipment is not able to support huge traffic amount, mobility and elevated level of scalability. In literature, authors have proposed architecture for IoT [30]. Most of the researchers who have realized the potential of SDN for managing IoT network have proposed architecture which apply SDN and network virtualization for managing IoT networks [30]. Interestingly, authors uptill now have discussed at a very primitive level to provide security for IoT using SDN. Some of the latest work in this direction can be found in [31], [6], [8], [32]. A complete security framework to provide security in industrial IoT has received very little attention.

F. Access Control in IoT

Access control allows only authorized users to access the resources. In any typical IoT scenario like Smart Home, lack of proper access control mechanisms could result in disclosing sensitive and privileged information. It is very important that the user data is only disclosed to authorized parties.

G. Trust in IoT

In safety critical IoT applications (like health care), the trustworthiness of sensors and sensor's data is important. Any malicious sensor node or malicious sensor data can lead to a disaster. It is important to calculate trust and reputation of different entities involved in the IoT ecosystem.

H. Audit Control for IoT

IoT environment needs to know when their services are accessed and by whom. This will ensure in maintaining higher level of security. Maintaining an audit trail in IoT services is a challenging task. Having a centralized view of IoT network with SDN managed framework can help in logging activities across IoT network.

I. Secure Network Access

IoT devices when joining the network need to be authorized in order to avail services from the network. In case, a malicious node becomes part of the network it can perform malicious actions which either cause disruption in IoT services or modify the critical data with in the IoT network. There is a desire need to authorize IoT nodes entering the network with authentication algorithms and enforce security policies in order to inhibit IoT nodes to perform unauthorized actions. Such issues have been looked upon and discussed in literature such as in [33].

J. Secure Storage

Recent advances in flash memory storage technology have enabled IoT devices such as smart objects to have enormous amount of storage space. Most recently, IoT applications store data in IoT devices for improved performance [34]. Protecting sensitive data information have received attention from the research community. Stored data in IoT devices can be tampered and modified by malicious nodes or applications with in the network. Efforts in this domain can be found in [35] and [36].

K. Tamper Resistance

Malicious entities within the network can take hold of the IoT device or devices which can be tampered. Hence, an IoT device should be resistant to such tampering and fulfills all the security requirements. In literature, need for resistance against tampering is an issue that need to be addressed [37]. Hence, robust security management solution is desired which ensures resilience against such tampering.

L. User Identification and Identity Management

A node joining the network have to be authenticated. Along with authentication it is to be made sure that joining node is validated with the policies applicable to the particular joining node. It is desire to maintain ID of all the nodes in the network. Identity management is required for IoT and effort in this direction can be found in [38].

M. Availability

IoT devices usually sense data which is collected, aggregated and used by IoT application. IoT applications apply data analytics to infer from the collected data which is then used for making decisions. It is possible that attacks can be launch on IoT devices which hinders their proper operation and availability leading to unnecessary delays and errors in analyzing data. Availability can be targeted by (Denial of Service) DoS or (Distributed Denial of Service) DDoS attacks on IoT nodes or network. DoS and DDoS have received considerable attention from the research community and notable efforts can be found in [39].

V. SECURITY THREATS AND ATTACKS IN IOT

This section lists the security threats and attacks, which are applicable to IoT ecosystem. Efforts in summarizing challenges of security in IoT can be found in [40] [41] [42] [43] [44] [45]. Detail taxonomy of security challenges can be found in [41]. On the other hand, comprehensive identification of security challenges and requirements in IoT architecture is also carried out by various researchers most notable of them can be found in [43] [44] [45] [40]. Challenges from all the above efforts are summarized which are required to be addressed by a comprehensive security management solution for IoT. These threats and challenges are given below.

A. Eavesdropping

Because IoT involves wireless communication interface it is obviously vulnerable to eavesdropping. IoT services are expected to contain sensitive data, therefore it is important to protect the data of IoT connected objects against an eavesdropper for possible data leakages. Consider a Smart home environment where IoT objects control and monitor different activities. It is of major importance that the personal information of the smart home owner is kept private and the attacker/eavesdropper is not able to tap the communication between IoT devices.

B. Data Corruption

Instead of eavesdropping or listening to the data, an attacker can also try to modify the data which is transmitted over the air between the IoT devices. A simple motivation here would be to disturb the communication such that the receiving device is not able to understand and process the data sent by the other device. This attack is a simple form of DoS attack where the devices are not been able to perform the required operation over the data. Other than that this attack does not allow the attacker to manipulate the actual data.

C. Data Modification

IoT nodes are expected to exchange critical data with other services and some time also with intermediate entities i.e. authorities, service providers and control centers. This put stringent requirement that the sensed, stored and transmitted data must not be tampered either maliciously or accidentally. In data modification the attacker is capable of manipulating/modifying the data in such a way that the receiving device is unable to detect modification and treats the input to be valid. This is very different and sophisticated from just data corruption attack. It is crucial to design reliable and dependable IoT applications secure against active modification.

D. Identity Spoofing Attack

IoT device's identity can be compromised through which malicious traffic is sent to victim nodes in the network. This is a devastating attack which can disrupt the normal operation of IoT network. This can also be used to launch DoS and DDoS attacks in the network. There is a strong desire for a robust and resilient techniques for validating IoT devices in the network to prevent spoofing.

E. Injection Attack

IoT devices run lightweight code to assist IoT applications in sensing, data collection or performing some activity in a particular region in a field. There is a possibility a malicious code can be injected by the attacker on IoT devices which then perform malicious actions with the intention of disrupting normal operation of IoT network or application. Malicious code can also sabotage IoT device in the network.

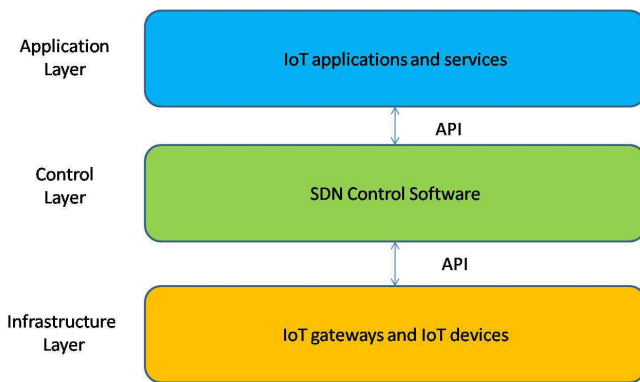


Fig. 4. SDN Architecture for IoT

F. Denial of Service and Insider Detection in IoT

Emerging technology of IoT experiences severe attacks in IoT. Insider attack is one of the devastating attacks that has received attention from researchers [46]. It is desired to address the issue by incorporating a mechanism in security management framework for IoT.

G. Attacks on Availability

Availability is extremely important for IoT services which enable access from anywhere at any time in order to provide information continuously. Existing security protocols fails to effectively prevent attacks on availability of IoT services. Lets consider an example of Smart Home application, where the sensor nodes are incapable of handling huge number of requests due to resource limitations. Attacker can leverage this limitation to launch DoS attack by sending huge volume of false service requests. Since the wireless transmissions are also battery hungry operation, unnecessary handling of service request will also drain the battery of IoT devices. Security management framework for IoT should be able to mitigate DoS attacks in IoT. Efforts in dealing with DoS attacks in IoT can be found in [47], [48].

H. Impersonation Attacks

In an IoT ecosystem, both the service provider and service consumer need to make sure that the service is accessed by the authenticated users and it is also offered by an authentic source. It is very crucial to have strong authentication mechanisms deployed to prevent any form of impersonation.

VI. SOFTWARE DEFINED NETWORK BASED FRAMEWORK FOR IOT

The heterogeneity of IoT multi-networks and its complexity is a challenge to organize and to make effective the use of heterogeneous resources with the objective of managing and securing as numerous jobs as possible. The researchers have considered SDN a hot candidate for solving resource management needs of IoT environment. This is due to inherent nature of SDN paradigm which is managed by a centralized controlling agent i.e. controller. Current practical implementation of SDN technologies are long way dealing with diversified and vigorous demands of IoT multi-network. Although, there are various differing SDN based solution for IoT a generic

architecture can be constructed from the existing solutions in the literature as shown in Figure 4. In this architecture, IoT applications and services are implemented at application layer. SDN controller related functionalities is implemented at control layer. While IoT devices and gateway exists at infrastructure layer. The control software interacts with the IoT application services at application layer and IoT devices at infrastructure layer using APIs. Various efforts in SDN based solutions for IoT can be found in literature some of the important ones are [49], [6], [8], [50] and [7].

1) *Sensor Openflow Switch(es)*: The IoT nodes are usually laid out in clusters with cluster head, which is a resource sufficient device that communicates with the IoT gateway. In order to implement SDN techniques the IoT nodes acting as relays or switching device play the role of sensor openflow switches. In contrast to traditional network components over the Internet, the IoT nodes are constrained in resources and require a lightweight openflow protocol for communication with the low power devices. The detailed design for the lightweight Openflow in IoT nodes requires resource efficient approach.

VII. SDN BASED IOT FRAMEWORK FOR SECURITY SERVICE PROVISIONING

Current architecture of IoT contains sensor nodes (IoT devices) connected to the conventional Internet via the IoT gateway. This architecture (IP connected IoT) is increasingly becoming popular today, where smart devices also referred to as the things are integrated with the Internet to form IoT. Low power Wireless Personal Area Network running with IPv6 (6LoWPAN) is the popular technology used as a communication technology.

SDN makes network services agile and flexible such that they can be automatically deployed and programmed. It further simplifies network management by separating the control plane (network intelligence that make data forwarding decisions) from data plane (forwarding elements). The control plane functions are moved into central Controller which acts as the brain regulating the whole paradigm.

In order to address the issues discussed in this paper SDN based framework for providing security services to IoT network is proposed. The framework consists of an IoT controller and SDN based security controller (see figure. 5). Both of these controllers are located in IoT gateway, which communicates with the IoT devices. Most commonly used topology by IoT network is cluster based topology. Where cluster head manages a cluster of IoT devices.

The proposed SDN based IoT framework essentially comprise of three main components.

- 1) IoT Controller.
- 2) SDN based Security Controller.
- 3) Sensor Openflow Switch(es) (briefly discussed above).

A. IoT Controller

The IoT controller act as a middle tier collecting information from IoT devices and transmitting it to application services for data analytics. It is responsible for data collection,

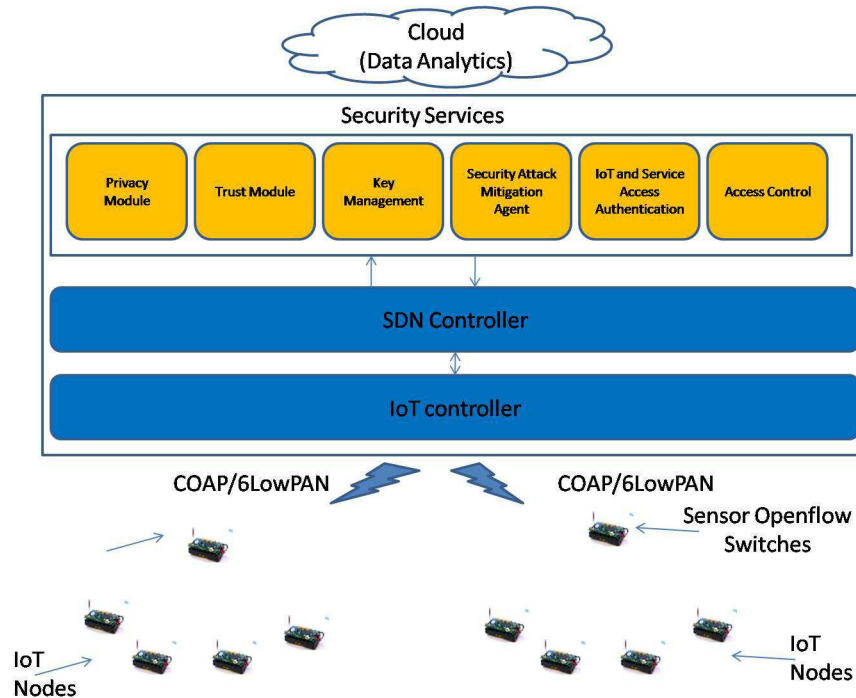


Fig. 5. Proposed SDN based Management and Security Framework for IoT

aggregation and transmission of data to the back end. This is realized through a monitoring agent that collects data across the IoT network as shown in figure 5.

B. SDN based Security Controller

The SDN based security controller is also placed in the IoT gateway and run on top of the IoT controller. In order to realize security provisioning with the IoT network the SDN based security controller interacts with the IoT controller to monitor the flows. The security controller utilize SDN techniques to provide different security services across IoT network. The SDN based controller interacts with security applications at the application plane to provision i) Privacy ii) Trust iii) Key Management iv) Access Control v) Service Access Authentication across IoT network and vi) Security Attack Mitigation. Figure 5. shows the SDN based framework for provisioning security where the security services are implemented at application plane of the SDN architecture. The network administrator will enforce security policies through the security applications by using custom API.

Security services at application plane will require status of the network nodes in IoT. Flow samples required by the network application is given by SDN based controller at the control plane which has the whole global view of the network. SDN based IoT controller have services which are implemented as modules to provision security services across IoT network. These modules are as follows.

C. Privacy Module

This component will preserve privacy in the IoT network. Privacy means that the data generated by the devices need to be transmitted anonymously without revealing any information

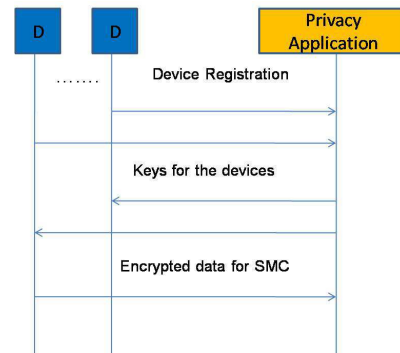


Fig. 6. Privacy process

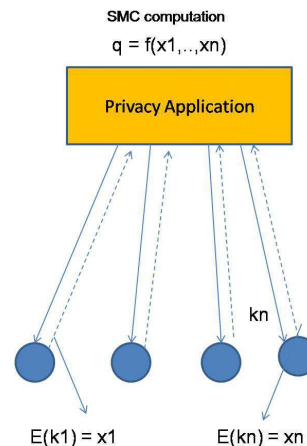


Fig. 7. SMC Computations

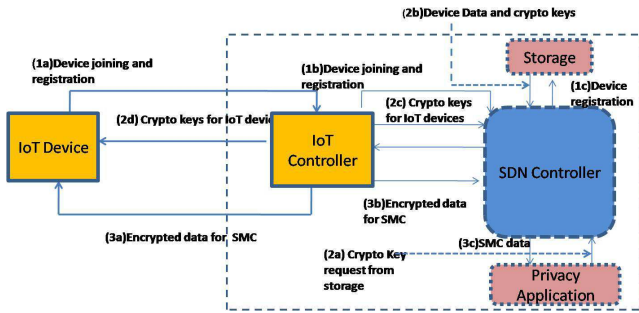


Fig. 8. Privacy Module

this to the intermediate or unauthorized nodes attempting to eaves drop on data. Generated data from IoT devices are collected and aggregated at the IoT controller. Privacy in the process of data collection and aggregation has to be ensured in IoT network which can be compromised by adversary either at collection or aggregation. SDN controller enables flows from each device on the IoT controller to centrally verify the authenticity of data originated from a device. This is possible by public key infrastructure (PKI) when the device is joined and registered the cryptographic credential valid during the lifetime of device is given.

Feasibility of PKI in low power devices has been studied a lot by the research community. It is often argued to be computationally intensive and practically not possible in IoT. Lately, making PKI feasible for IoT is under focus by the research community [51][52] and ECC (Elliptic Curve Cryptography) is being employed to adopt PKI in IoT [53]. Originated data from each device is encrypted by public key of the gateway which is then signed by the private key of the device. Encrypted packets in the flows from devices in the IoT network are then verified through SDN controller by the privacy application. In order to preserve privacy of the aggregated data Secure Multiparty Computation (SMC) [54] is incorporated which originated from the work of generating and exchanging secrets among two parties [55]. SMC is used in preserving privacy [56]. The principle of SMC works in a manner in which computation is secure when no party have the knowledge of anything except for the input and the result. Mathematically, given inputs

$$(n^1, n^2, \dots, n^n)$$

from the sources

$$(1, 2, 3, \dots, n)$$

which are to be processed by a trusted intermediate component as

$$f(n^1, n^2, \dots, n^n) = y$$

and then announce the results. Intermediate trusted component is a trusted third party (TTP) which keep the process anonymous by aggregating inputs from the devices. In our model, SDN controller along with privacy preserving application acts as a TTP to perform SMC and preserve privacy of the whole data collection process. Figure 8. shows the outline of the privacy module.

Privacy preserving process as shown in figure 6 and 7. is as follows

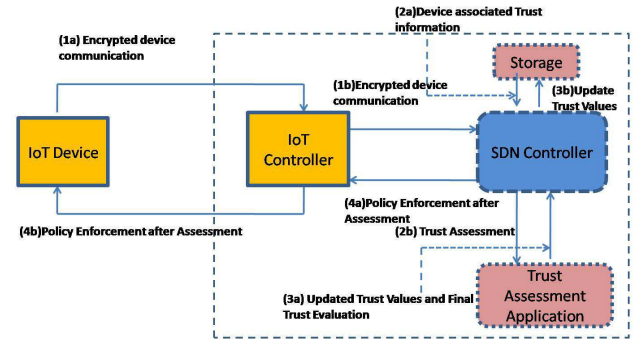


Fig. 9. Trust Module

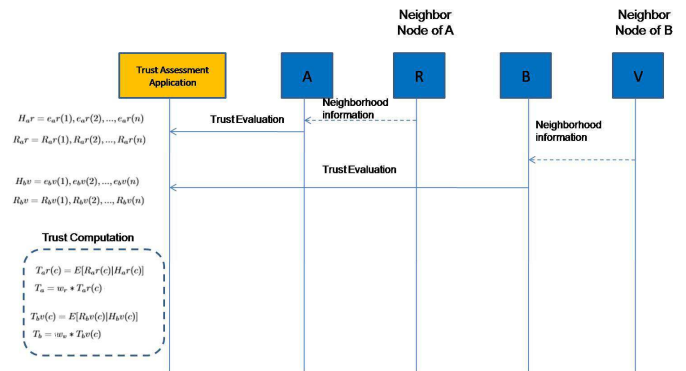


Fig. 10. Trust Evaluation Process

Step 1: IoT devices join the network by sending their request to the gateway which is collected by the IoT controller and passed on to the SDN controller which registers the device.

Step 2: Cryptographic credentials for confidentiality, integrity and SMC is generated by the privacy application which is stored for a registering device.

Step 3: Encrypted packets are sent from a device as a flow which is accounted by the SDN controller and along with privacy application verifies it and runs SMC algorithm. The computed result over inputs from IoT device is then provided to the back end application or data analytics possibly hosted in a cloud or if needed to the IoT devices for further processing.

D. Trust Module

Statistics of the IoT flows will be used to generate trust values across the IoT network. These trust values will be maintained by keeping a moving average over the historical statistics of IoT flows. An untrusted IoT node or flow attempting to manipulate the network will fail the trust evaluation test. In an IoT network there will be service requester and service provider. Service requester can be a thing or a user requesting a certain service. Service provider will first calculate the trust values of the nodes in collaboration with neighboring nodes. Trust values are computed on the basis of history maintained by keeping account of previous interactions of a device who's trust is to be computed with the neighboring device. Trust assessment application is inspired by [57] and [58]. For simplicity let us define history, if a binary random variable

$$(e_a b(i))$$

indicates an i th encounter between node a and b .

$$(e_{ab}(i))$$

can assume value of 1 if b 's action is cooperate and 0 otherwise. Then history H defined for a set of n encounters between a and b is represented by:

$$H_{ab} = e_{ab}(1), e_{ab}(2), \dots, e_{ab}(n)$$

Lets represent reputation of node between a and b for an i th encounter as follows:

$$R_{ab}(i) \in [0, 1]$$

As node a interacts with b the quantity

$$R_{ab}(i)$$

is updated with time as a 's perception with b changes

Trust value is then given as

$$T(i) = E[R(i)|H(i)]$$

Higher the trust value for a particular node in the network higher the expectation that particular node will reciprocate with the other entity involved in the communication.

Lets assume that a particular node E who's trust is to be computed have neighboring nodes A, B, C and D who's weights are given as

$$[w_a, w_b, w_c, w_d]$$

. Then the trust of E is given as:

$$T(E) = w_a * T(A) + w_b * T(B) + w_c * T(C) + w * dT(D)$$

Hence, trust is computed by taking into account the interactions of the node who's trust is to be computed with the neighboring nodes in the network.

Figure 9. shows the outline of trust module. Trust Module process is as follows.

Step 1: The request from each node is sent as encrypted to the gateway. Request is collected by the IoT controller which is then relayed to SDN controller. SDN controller accounts flows in the network.

Step 2: Trust assessment for each request from either the thing or service is carried out by trust application. At this step historical data of trust evaluation is taken as an input to assess new trust values.

Step 3: Updated trust values are used to make decision about the policies to be enforced based on new trust computation. These policies apply to both devices and service.

Step 4: Based on trust assessment on updated values computed by the trust application the policies generated for the device may be sent to the device via IoT controller. Policy ensures that no device in future can perform illegal operations or access.

Trust assessment application process is as follows. Figure 10. shows how the process works.

Step 1: Upon receiving the request for trust evaluation, nodes involve in servicing the request are assessed in case an IoT service application interacts with the devices. For node to node communication historical interaction between the two nodes are assessed for trust evaluation.

Step 2: Lets say group of nodes A, B are involved for servicing request from the IoT service i then historical interactions and reputations of the neighboring nodes with A, B are evaluated. For simplicity it is assumed A have neighbor node R , B have neighbor node V . Historical interactions for $1, \dots, n$ and reputation are given as

$$H_{ar} = e_{ar}(1), e_{ar}(2), \dots, e_{ar}(n)$$

$$H_{bv} = e_{bv}(1), e_{bv}(2), \dots, e_{bv}(n)$$

$$R_{ar} = R_{ar}(1), R_{ar}(2), \dots, R_{ar}(n)$$

$$R_{bv} = R_{bv}(1), R_{bv}(2), \dots, R_{bv}(n)$$

Step 3: Trust value for neighboring nodes with the nodes involved in communication A, B (at an instance x lying somewhere between $1, \dots, n$ historical interactions) is then given as

$$T_{ar}(x) = E[R_{ar}(x)|H_{ar}(x)]$$

$$T_{bv}(x) = E[R_{bv}(x)|H_{bv}(x)]$$

. Trust for nodes A and B with given weights of neighboring nodes R and V

$$w_r, w_v$$

is given as

$$T_a = w_r * T_{ar}(x)$$

$$T_b = w_v * T_{bv}(x)$$

Step 4: Service i then assess the trust values of nodes A, B and proceed with its communication.

E. Key Management

Considering the IoT resource requirements, key management module will implement lightweight key distribution scheme. Recently, efforts in light weight key distribution schemes have received considerable attention from the research community [59], [60], [61] and [62]. Elliptic Curve Cryptography based Diffie Hellman (ECDH) is a hot candidate for a lightweight key distribution scheme in IoT. Apart from key distribution scheme the module will implement lightweight key generation algorithm and revocation. Lightweight revocation have received attention from the community such as in [63]. The Keys generated by the module will be used by the IoT nodes and security modules to implement security services in the IoT network. When a device join a network crypto

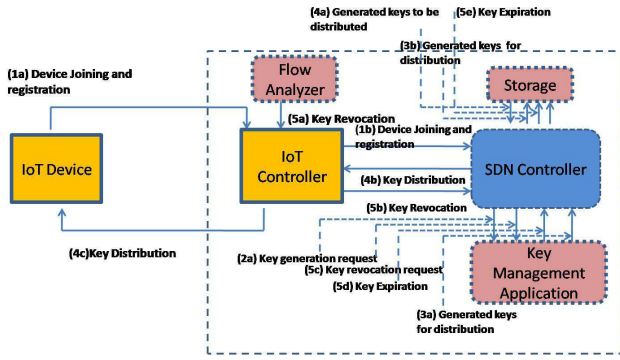


Fig. 11. Key Management Module

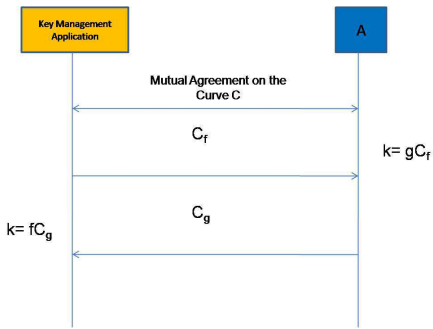


Fig. 12. Key Distribution using ECDH

keys for a device are generated and stored in storage. Upon revocation update takes place replacing the keys in the storage. Figure 11. shows the outline of key management module. Key management module process is as follows.

Step 1: Device joins the network and get registered.

Step 2: Key generation request is then initiated via SDN controller for a device from key management application.

Step 3: Crypto keys are generated and stored in the storage for a device.

Step 4: Generated keys are distributed to the devices using a key distribution algorithm.

Step 5: Key renewal and revocation process is carried out on the recommendations of flow analyzer to revoke list of nodes. Keys stored in the storage are expired and any data encrypted with the expired keys will not be considered valid.

Step 6: Keys generated are stored in the storage and distributed to the devices using a distribution algorithm.

Key generation process is as follows.

Step 1: Key management module and nodes for ECDH in the network agree on curve C. For each exchange between node (A) and node (B), node (A) generates a secret number f. This secret number f is used to compute corresponding public point which is computed as

$$U = (q_f, w_f) = C_f$$

B generate a secret number g with the use of which a

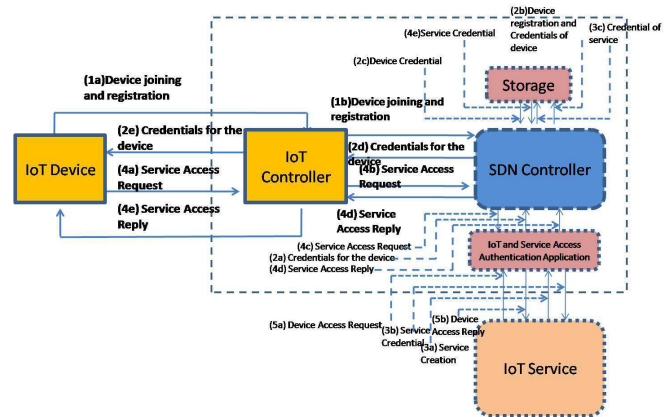


Fig. 13. IoT and Service Access Authentication Module

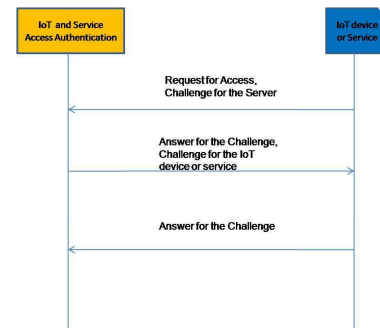


Fig. 14. Authentication Process

corresponding public point is computed

$$U = (q_g, w_g) = C_g$$

Key distribution scheme based on ECDH is as follows. Figure 12. shows how the process works.

Step 1: Compute the keys for nodes A and B,

$$U = (q_f, w_f) = C_f$$

and

$$U = (q_g, w_g) = C_g$$

by using elliptic curve cryptography.

Step 2:

$$C_f \text{ and } C_g$$

are exchanged over an insecure channel. Both the nodes can compute the shared secret as $k =$

$$fC_g = gC_f$$

F. IoT and Service Access Authentication

IoT nodes and services will use the associated service crypto keys to access. The authentication algorithm will use the keys to authenticate the IoT nodes during the join time and any network element accessing the IoT service. There are various authentication algorithms for WSN proposed in the literature

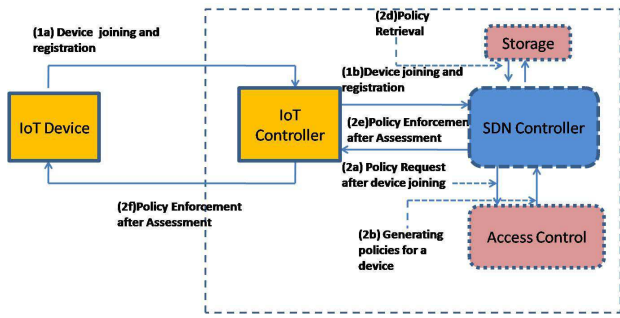


Fig. 15. Access Control Module

such as in [64], [65]. The keys to authenticate the access of the IoT services are called service access keys to ensure legitimate access of the IoT nodes by the service. A mutual authentication algorithm is used that authenticates the two parties at the same time using a challenge response authentication protocol. Figure 13. shows the outline of IoT and service access authentication module. The IoT and service access authentication process is as follows.

Step 1: Device upon joining get registered

Step 2: Crypto keys to access the service by the IoT nodes are distributed to the devices.

Step 3: IoT service wishing to access IoT nodes in future requests the IoT and service access authentication application to register and pass on the credentials to IoT services.

Step 4: When a service is requested by the IoT devices the authentication algorithm authenticates the devices.

Step 5: On the contrary if the device access is requested by the IoT services then the authentication algorithm authenticates the services based on the credential given to the service in step 3.

Authentication algorithm is shown in figure 14.

Step 1: When the network is deployed key distribution algorithm as described in the key management section will distribute the keys to the devices. Likewise, any IoT service wishing to gain access to IoT nodes will have the credentials by using key distribution algorithm.

Step 2: An IoT device or service wishing to gain access sends a challenge using credentials as given in step 1 to the IoT and service access authentication process. The process responds by answering the challenge using the credentials from step1 at the same time sending a challenge back to the IoT device.

Step 3: IoT device or service verifies the answer and at the same time responds to the challenge given by the IoT and service access authentication module using the credentials from step1.

Step 4: The IoT and service access authentication module verifies the answer from the IoT device or service, hence authenticating the device using the credentials from step1.

G. Access Control

The gateway will have a database of access control policies which are to be followed by the IoT nodes and the flows

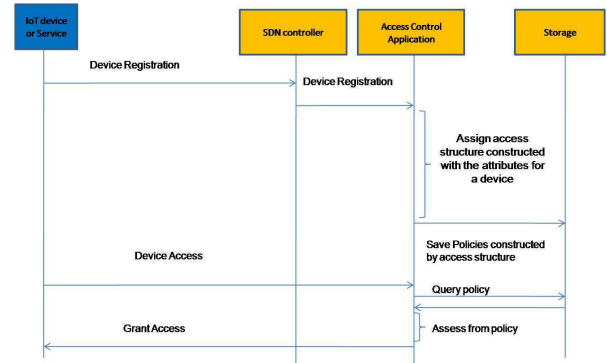


Fig. 16. Access Control Process

generated during the registration process. Access control algorithm will authorize, authenticate, approve access of the IoT resources based on access control policies. ABAC (Attribute based access control) is employed for IoT. ABAC is used in IoT for access control which can be seen in [66]. During the registration process access structure based on attributes is assigned to the device joining the network. SDN controller assists the access control module to implement the access control by constructing attribute access structure on the flows generated by the devices. Figure 15. shows the outline of access control module. Access control module process is as follows.

Step 1: When a device joins and registers, the policies are constructed on the basis of access structure assigned by the access control module

Step 2: Policies for a device are generated and stored in the storage.

Step 3: Based on the policies generated for a device, policies are enforced on the devices by the SDN controller via IoT controller. These policies influences the IoT devices access operations on IoT services.

Access control algorithm is shown in Figure 16. The process is as follows.

Step 1: Upon initiation of device registration request the access control application initiates policy creation process.

Step 2: Access structure is assigned to a device which is constructed by using access tree derived from attributes for a particular flow or user in the network.

Step 3: Policy on the basis of access structure is derived and stored in the storage.

Step 4: Flow initiated from a device accesses IoT network which is then regulated by the policies stored in the storage. The flow is granted access influenced by the policy.

H. Security Attack Mitigation Agent

The algorithm in the mitigation agent will use the current status of the IoT network and its flows to detect possible malicious activity in the network. Threshold based mechanism will be used for detecting attacks on the IoT nodes and services. Type of attacks detected by the agent will be network scan, spoofing, injection, impersonation, DoS and DDoS

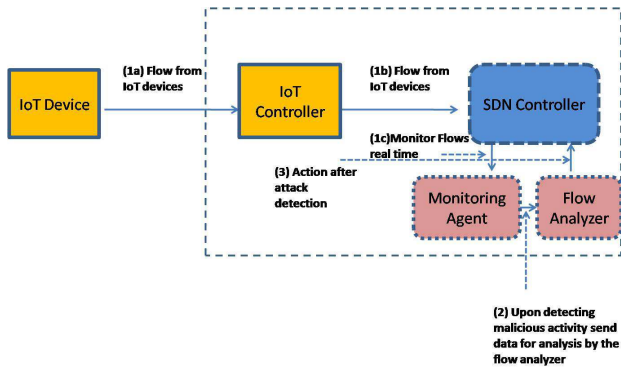


Fig. 17. Security Attack Mitigation Module

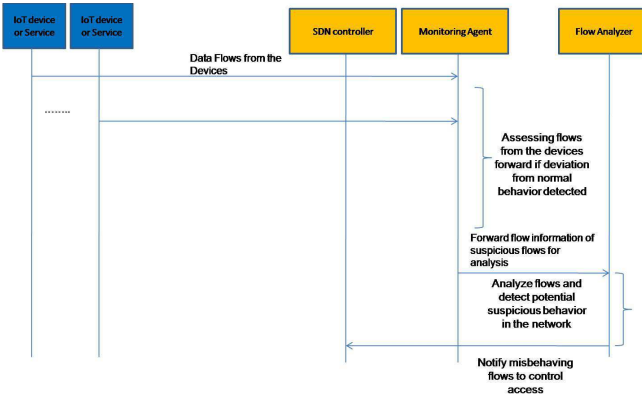


Fig. 18. Security Attack Mitigation Process

attacks. Besides a database of access control policies, there is a database for auditing the flows in the IoT network. This is maintained by monitoring agent with the assistance of SDN controller. The audit trails of the IoT flows will be used by the flow analyzer to detect malicious intrusion of the attackers in the network. It will also propose actions to be taken by the SDN controller with regards to the flows from IoT devices. Figure 17. shows the outline of security attack mitigation agent module. Security attack mitigation agent module works as follows.

Step 1: Flows from the IoT devices via IoT controller are accounted by the SDN controller which are monitored by the monitoring agent.

Step 2: Auditing of the flows is taken care of by the flow analyzer which proposes actions or defenses against a possible malicious operation by the devices. SDN controller then implements strategies to counter malicious activities by the flows in future.

Attack mitigation process is shown in Figure 18. The process is as follows

Step 1: Data flows from the devices are monitored in real time by the monitoring agent.

Step 2: Upon detection of deviation from normal behavior of any of the flow, Flow analyzer is notified about the deviated flows by the monitoring agent.

Step 3: After analysis by the flow analyzer, the SDN

controller is notified to limit access of the malicious devices.

VIII. SUMMARY OF IOT SECURITY REQUIREMENTS HANDLING BY PROPOSED MANAGEMENT FRAMEWORK

This section describes how the proposed management framework handles IoT security issues, requirements, threats and attacks. Table 1. summarizes what security services are fulfilled by the proposed framework. The modules are listed in the column of the table while security attacks, issues and threats in IoT are listed in the rows of the table. The table helps in assessing which modules in the proposed framework fulfills what security requirements, issues and threats of IoT in the network discussed earlier. Discussion on solutions and recommendations are as follows.

A. Confidentiality and Privacy

The SDN based security controller is responsible to facilitate confidentiality and privacy of data exchanged among the IoT devices. Privacy module together with key management module in the security framework is responsible for ensuring protection against eavesdropping, data corruption and modification across the IoT network. Key management module is responsible for managing cryptographic materials used by the privacy module.

B. Handling Security Attacks

The Security attack mitigation agent is responsible for regulating traffic within the IoT network. Constant monitoring of the traffic flows along with the analyzer helps in detecting DoS, DDoS, injection, spoofing and impersonation attacks.

C. Authentication in IoT

Authentication in IoT is ensured by IoT and service access authentication together with key management module in the security framework. The module ensures that the joining device accessing service from the IoT network is authenticated and authorized. Key management module is responsible for managing cryptographic materials used by the IoT and service access authentication module.

D. Access Control in IoT

Access control module in IoT implements security policies in the IoT network. Hence, the module ensures that IoT device perform authorized action while it is a part of the network. Illegitimate access should be denied by the access control module.

E. Trust in IoT

Trust module ensures trusted communication between IoT devices and IoT network. An IoT device or service reputation is downgraded if negative experiences are encountered over time. Hence, historical actions are taken into account to establish trusted linkage between the IoT devices and network.

TABLE I. SUMMARY OF SECURITY SERVICES PROVISIONED BY PROPOSED MANAGEMENT FRAMEWORK

Security Attacks, Issues and Threats in IoT	Privacy Module	Trust Module	Key Management Module	IoT and Service Access Authentication	Access Control	Security Attack Mitigation Agent
Confidentiality and Privacy	✓		✓			
Handling Security Attacks						✓
Authentication in IoT			✓	✓		
Identity Spoofing Attack						✓
Access Control in IoT					✓	
Trust in IoT		✓				
Attacks on Availability						
Impersonation Attacks						✓
Eavesdropping	✓		✓			✓
Data Corruption	✓		✓			
Data Modification	✓		✓			
Secure Routing and Forwarding in IoT				✓		✓
Robustness and resilience management in IoT						✓
Audit Control for IoT						✓
Secure Network Access			✓	✓		
Secure Storage					✓	
Tamper Resistance					✓	
User Identification and Identity Management				✓		

F. Eavesdropping

Privacy module together with key management module in the proposed framework ensures that the communication between IoT devices and the gateway takes place in a secure manner. This ensures that no malicious entity eavesdrop on the ongoing communication. Key management module manages cryptographic keys used for ensuring protection against eavesdropping.

G. Data Corruption

Corruption of data is prevented by the privacy module which work with key management module. The module implements cryptographic algorithm to ensure that no malicious entity can corrupt the data generated from the IoT devices. Cryptographic keys used are managed by key management module.

H. Data Modification

Illegal modification of the data is ensured by privacy module which works with key management module. Cryptographic algorithm enables secure communication which disallows any malicious nodes to modify the data originated from IoT devices. Key management module is responsible for managing cryptographic keys used by privacy module to ensure protection against illegal modification.

I. Secure Routing and Forwarding in IoT

IoT and service access authentication module and security attack mitigation agent ensures that the data is routed and forwarded in the IoT network in a secure manner. Any routing attacks are detected by the security attack mitigation agent hence ensuring secure data forwarding. IoT and service access authentication module filters legitimate nodes to become of the IoT network.

J. Robustness and Resilient Management in IoT

Security attack mitigation agent detects any kind of malicious attacks which halts the services offered by IoT network. Also, the agents takes appropriate actions to alleviate the situation hence ensuring that the IoT network runs in a normal manner.

K. Audit Control in IoT

Security attack mitigation agent monitors the flows in the IoT network which helps in auditing actions. If any inappropriate action is observed the agents reacts to the situation and ensures smooth operation of the network.

L. Secure Network Access

IoT and service access authentication module together with key management module authenticates all the joining nodes hence ensuring only validated ones become part of the network. Also, access control ensures only legitimate actions are carried out by the nodes in the IoT network. Key management module is responsible for managing cryptographic keys used by IoT and service access authentication module.

M. Secure Storage

Access control module ensures secure access of the storage as only legitimate nodes are able to access the data. Furthermore, these legitimate nodes perform only legal actions on the data stored in the node.

N. Tamper Resistance

Access control module ensures any illegal tampering of the IoT nodes in the network.

O. User identification and identity management

IoT and service access authentication module is responsible for validating the joining nodes hence verifying the identity of the nodes.

IX. CONCLUSION

Advancement in programmable networks have enabled novel paradigm of SDN which have opened opportunities of easing management of networks. Emerging interconnected embedded devices paradigm of IoT is different than conventional wired networks which are usually constrained in resources. Hence, managing such type of network raises challenges which are of unique nature. In this paper, management challenges of IoT are identified and discussed. One of the aspect of management solution for IoT is security provisioning. In this paper, security management of IoT is dealt with. Security threats, attacks, issues and requirements in IoT are discussed which need attention from the researchers. Lately, potentials of SDN to manage IoT is been investigated. It is no doubt that SDN paradigm offer an excellent opportunity to assure security in IoT as security control will be centralized.

Hence, in this paper, management framework based on SDN principles for provisioning security services in IoT is proposed. Proposed security controller consists of privacy, trust, key management, IoT and service access authentication and security attack mitigation agent module. Privacy module ensures privacy is preserved in IoT. Trust module makes sure that the communication in IoT network takes place in a trusted environment. Key management module handles key generation and revocation in IoT network. IoT and service access authentication authenticates nodes and services within IoT network. Security attack mitigation agent detects attacks in the network and takes countermeasure actions to prevent attacks. In the end, how the security attacks and threats in IoT are handled by the proposed SDN based framework is discussed. In the future, each module will be implemented and evaluated in the framework with respect to overall overheads and resource consumption.

REFERENCES

- [1] L. Atzori, A. Iera, and G. Morabito, "The Internet of Things: A survey," *Computer Networks*, vol. 54, no. 15, pp. 2787–2805, 2010. [Online]. Available: <http://linkinghub.elsevier.com/retrieve/pii/S1389128610001568>
- [2] A. Levakov and N. Sokolov, "Internet of Things, Smart Spaces, and Next Generation Networking," *Lecture Notes in Computer Science (including subseries Lecture Notes in Artificial Intelligence and Lecture Notes in Bioinformatics)*, vol. 7469, no. January, pp. 424–428, 2012. [Online]. Available: <http://www.scopus.com/inward/record.url?eid=2-s2.0-84866127166&partnerID=tZOTx3y1>
- [3] J. Gubbi, R. Buyya, S. Marusic, and M. Palaniswami, "Internet of things (iot): A vision, architectural elements, and future directions," *Future Generation Computer Systems*, vol. 29, no. 7, pp. 1645–1660, 2013.
- [4] Hai Huang, Jiping Zhu, and Lei Zhang, "An SDN_based management framework for IoT devices," *25th IET Irish Signals & Systems Conference 2014 and 2014 China-Ireland International Conference on Information and Communities Technologies (ISSC 2014/CICT 2014)*, pp. 175–179, 2014. [Online]. Available: <http://digital-library.theiet.org/content/conferences/10.1049/cp.2014.0680>
- [5] O. Flauzac, C. Gonzalez, A. Hachani, and F. Nolot, "SDN Based Architecture for IoT and Improvement of the Security," *2015 IEEE 29th International Conference on Advanced Information Networking and Applications Workshops*, pp. 688–693, 2015. [Online]. Available: <http://ieeexplore.ieee.org/lpdocs/epic03/wrapper.htm?arnumber=7096257>
- [6] N. Omnes, M. Bouillon, G. Fromentoux, and O. L. Grand, "A Programmable and Virtualized Network & IT Infrastructure for the Internet of Things," pp. 64–69, 2015.
- [7] Z. Qin, G. Denker, C. Giannelli, P. Bellavista, and N. Venkatasubramanian, "A software defined networking architecture for the internet-of-things," *IEEE/IFIP NOMS 2014 - IEEE/IFIP Network Operations and Management Symposium: Management in a Software Defined World*, pp. 1–9, 2014.
- [8] P. Hu, "A System Architecture for the Software-Defined Industrial Internet of Things," *Icuwb'15*, p. To appear, 2015.
- [9] Y. Jararweh, M. Al-Ayyoub, A. Darabseh, E. Benkhelifa, M. Vouk, and A. Rindos, "SDIoT: a software defined based internet of things framework," *Journal of Ambient Intelligence and Humanized Computing*, vol. 6, no. 4, pp. 453–461, 2015. [Online]. Available: <http://link.springer.com/10.1007/s12652-015-0290-y>
- [10] V. R. Tadinada, "Software Defined Networking: Redefining the Future of Internet in IoT and Cloud Era," *2014 International Conference on Future Internet of Things and Cloud*, pp. 296–301, 2014. [Online]. Available: <http://ieeexplore.ieee.org/lpdocs/epic03/wrapper.htm?arnumber=6984209>
- [11] N. Feamster, J. Rexford, and E. Zegura, "The Road to SDN: An Intellectual History of Programmable Networks," *ACM Sigcomm Computer Communication*, vol. 44, no. 2, pp. 87–98, 2014. [Online]. Available: <http://dl.acm.org/citation.cfm?id=2602204.2602219&coll=DL&dl=ACM&CFID=42>
- [12] L. Paradis and Q. Han, "A survey of fault management in wireless sensor networks," *Journal of Network and Systems Management*, 2007.
- [13] J. A. Khan, H. K. Qureshi, and A. Iqbal, "Energy Management in Wireless Sensor Networks : A Survey."
- [14] D. Wajgi and N. V. Thakur, "Load Balancing Algorithms in Wireless Sensor Network : A Survey," *IRACST International Journal of Computer Networks and Wireless Communications*, vol. 2, pp. 2250–3501, 2012.
- [15] S. T. Ali, V. Sivaraman, A. Radford, and S. Jha, "Securing Networks Using Software Defined Networking : A Survey," *IEEE Transactions on Reliability*, vol. 64, no. 3, pp. 1–12, 2013. [Online]. Available: <http://www2.ee.unsw.edu.au/~vijay/pubs/jrnl/15tor.pdf>
- [16] S. Sciancalepore, A. Caposelle, G. Piro, G. Boggia, and G. Bianchi, "Key Management Protocol with Implicit Certificates for IoT systems," *Workshop on IoT challenges in Mobile and Industrial Systems - IoT-Sys*, pp. 37–42, 2015. [Online]. Available: <http://dl.acm.org/citation.cfm?doi=2753476.2753477>
- [17] J. Liu, Y. Li, M. Chen, W. Dong, and D. Jin, "Software-defined internet of things for smart urban sensing," *IEEE Communications Magazine*, vol. 53, no. 9, pp. 55–63, 2015. [Online]. Available: <http://ieeexplore.ieee.org/lpdocs/epic03/wrapper.htm?arnumber=7263373>
- [18] I. Journal, O. F. Innovative, T. Volume, and I. No, "Madhura P M* et al." no. 3, pp. 2069–2074, 2015.
- [19] V. Lakkundit, "BlinkToSCoAP: An End-to-End Security Framework for the Internet of T hings," no. JANUARY, 2015.
- [20] J. L. Hernandez-Ramos, M. P. Pawlowski, A. J. Jara, A. F. Skarmeta, and L. Ladid, "Toward a Lightweight Authentication and Authorization Framework for Smart Objects," *IEEE Journal on Selected Areas in Communications*, vol. 33, no. 4, pp. 690–702, 2015. [Online]. Available: <http://ieeexplore.ieee.org/lpdocs/epic03/wrapper.htm?arnumber=7012039>
- [21] V. Lakkundit, "BlinkToSCoAP: An End-to-End Security Framework for the Internet of T hings," 2015.
- [22] S. Md Zin, N. Badrul Anuar, M. Laiha Mat Kiah, and A.-S. Khan Pathan, "Routing protocol design for secure WSN: Review and open research issues," *Journal of Network and Computer Applications*, vol. 41, pp. 517–530, 2014. [Online]. Available: <http://linkinghub.elsevier.com/retrieve/pii/S1084804514000460>
- [23] C. Cervantes, D. Poplade, M. Nogueira, and A. Santos, "Detection of Sinkhole Attacks for Supporting Secure Routing on 6LoWPAN for Internet of Things," 2015.
- [24] J. Duan, D. Yang, H. Zhu, S. Zhang, and J. Zhao, "TSRF: A Trust-Aware Secure Routing Framework in Wireless Sensor Networks," *International Journal of Distributed Sensor Networks*, vol. 2014, pp. 1–14, 2014. [Online]. Available: <http://www.hindawi.com/journals/ijdsn/2014/209436/>
- [25] D. Tang, T. Li, J. Ren, and J. Wu, "Cost-Aware SEcure Routing (CASER) Protocol Design for Wireless Sensor Networks," *IEEE Transactions on Parallel and Distributed*

- Systems, vol. 26, no. 4, pp. 960–973, 2015. [Online]. Available: <http://ieeexplore.ieee.org/lpdocs/epic03/wrapper.htm?arnumber=6800079>
- [26] T. N. Gia, A.-m. Rahmani, T. Westerlund, P. Liljeberg, and H. Tenhunen, "Fault Tolerant and Scalable IoT-based Architecture for Health Monitoring," 2015.
- [27] O. Garcia-Morchon, D. Kuptsov, A. Gurtov, and K. Wehrle, "Cooperative security in distributed networks," *Computer Communications*, vol. 36, no. 12, pp. 1284–1297, 2013. [Online]. Available: <http://dx.doi.org/10.1016/j.comcom.2013.04.007>
- [28] R. Kamal, C. S. Hong, and S. Member, "Autonomic Resilient Internet-of-Things (IoT) Management," vol. 13, no. 9, pp. 1–16, 2014.
- [29] C. Sommer, F. Hagenauer, and F. Dressler, "A networking perspective on self-organizing intersection management," *Internet of Things (WF-IoT), 2014 IEEE World Forum on*, pp. 230–234, 2014.
- [30] P. Diogo, L. P. Reis, and N. V. Lopes, "Internet of Things: A system's architecture proposal," *2014 9th Iberian Conference on Information Systems and Technologies (CISTI)*, pp. 1–6, 2014. [Online]. Available: <http://www.scopus.com/inward/record.url?eid=2-s2.0-84906658394&partnerID=ZOTx3y1>
- [31] F. Olivier, G. Carlos, and N. Florent, "New Security Architecture for IoT Network," *Procedia Computer Science*, vol. 52, no. BigD2M, pp. 1028–1033, 2015. [Online]. Available: <http://www.sciencedirect.com/science/article/pii/S1877050915008996>
- [32] S. Choi and J. Kwak, "Enhanced SDIoT Security Framework Models," vol. 2016, 2016.
- [33] A. Mordeno and B. Russell, "Identity and Access Management for the Internet of Things - Summary Guidance," *CSA Cloud Security Alliance*, 2015.
- [34] N. Tsiftes and A. Dunkels, "A Database in Every Sensor," *Technology*, p. 316, 2011. [Online]. Available: <http://dunkels.com/adam/tsiftes11database.pdf> \n<http://dl.acm.org/citation.cfm?doid=2070942.2070974>
- [35] I. Bagci, M. Pourmirza, S. Raza, U. Roedig, and T. Voigt, "Codo: confidential data storage for wireless sensor networks," *Proceedings of the 2012 IEEE 9th International Conference on Mobile Ad-Hoc and Sensor Systems (MASS 2012) - Supplement*, pp. 1–6, 2012.
- [36] N. Tsiftes, A. Dunkels, Zhitao He, T. Voigt, Z. He, and T. Voigt, "Enabling Large-Scale Storage in Sensor Networks with the Coffee File System," *Proceedings of the 2009 International Conference on Information Processing in Sensor Networks (IPSN 2009)*, no. 1, pp. 349–360, 2009. [Online]. Available: <http://dl.acm.org/citation.cfm?id=1602165.1602197>
- [37] S. Babar, A. Stango, N. Prasad, J. Sen, and R. Prasad, "Proposed embedded security framework for Internet of Things (IoT)," *2011 2nd International Conference on Wireless Communication, Vehicular Technology, Information Theory and Aerospace and Electronic Systems Technology, Wireless VITAE 2011*, pp. 1–5, 2011.
- [38] C. Chibelushi, A. Eardley, and A. Arabo, "Identity Management in the Internet of Things: the Role of MANETs for Healthcare Applications," *Computer Science and Information Technology*, vol. 1, no. 2, pp. 73–81, 2013.
- [39] P. Kasinathan, C. Pastrone, M. A. Spirito, and M. Vinkovits, "Denial-of-Service detection in 6LoWPAN based Internet of Things," *International Conference on Wireless and Mobile Computing, Networking and Communications*, no. October, pp. 600–607, 2013.
- [40] J. Singh, T. Pasquier, J. Bacon, H. Ko, and D. Evers, "Twenty Cloud Security Considerations for Supporting the Internet of Things," *IEEE Internet of Things Journal*, vol. 4662, no. c, pp. 1–1, 2015. [Online]. Available: <http://ieeexplore.ieee.org/lpdocs/epic03/wrapper.htm?arnumber=7165580>
- [41] S. Babar, P. Mahalle, A. Stango, N. Prasad, and R. Prasad, "Proposed security model and threat taxonomy for the Internet of Things (IoT)," *Communications in Computer and Information Science*, vol. 89 CCIS, pp. 420–429, 2010.
- [42] J. Pimentel, J. Castro, E. Santos, and A. Finkelstein, "Advanced Information Systems Engineering Workshops," *Lecture Notes in Business Information Processing*, vol. 112, pp. 159–170, 2012. [Online]. Available: <http://www.scopus.com/inward/record.url?eid=2-s2.0-84864687550&partnerID=ZOTx3y1>
- [43] H. Suo, J. Wan, C. Zou, and J. Liu, "Security in the internet of things: A review," *Proceedings - 2012 International Conference on Computer Science and Electronics Engineering, ICCSEE 2012*, vol. 3, pp. 648–651, 2012.
- [44] T. Heer, O. Garcia-Morchon, R. Hummen, S. L. Keoh, S. S. Kumar, and K. Wehrle, "Security challenges in the IP-based Internet of Things," *Wireless Personal Communications*, vol. 61, no. 3, pp. 527–542, 2011.
- [45] S. Li, T. Tryfonas, and H. Li, "The Internet of Things: a security point of view," *Internet Research*, vol. 26, no. 2, pp. 337–359, 2016. [Online]. Available: <http://www.scopus.com/inward/record.url?eid=2-s2.0-84961579337&partnerID=ZOTx3y1>
- [46] Y. Hu, Y. Wu, and H. Wang, "Detection of Insider Selective Forwarding Attack Based on Monitor Node and Trust Mechanism in WSN," no. November, pp. 237–248, 2014.
- [47] P. Kasinathan, C. Pastrone, M. a. Spirito, and M. Vinkovits, "Denial-of-Service detection in 6LoWPAN based Internet of Things," *International Conference on Wireless and Mobile Computing, Networking and Communications*, pp. 600–607, 2013.
- [48] V. Nigam, "Profile based Scheme against DDoS Attack in WSN," 2014.
- [49] Y. Jararweh, M. Al-Ayyoub, A. Darabseh, E. Benkhelifa, M. Vouk, and A. Rindos, "SDIoT: a software defined internet of things framework," *Journal of Ambient Intelligence and Humanized Computing*, vol. 6, no. 4, pp. 453–461, 2015. [Online]. Available: <http://link.springer.com/10.1007/s12652-015-0290-y>
- [50] J. Li, E. Altman, C. Touati, J. Li, E. Altman, C. Touati, and A. G. S.-b. Iot, "A General SDN-based IoT Framework with NVF Implementation To cite this version : A General SDN-based IoT Framework with NVF Implementation," 2015.
- [51] R. Roman and C. Alcaraz, "Applicability of Public Key Infrastructures in Wireless Sensor Networks," *EuroPKI*, vol. 4582, pp. 313–320, 2007. [Online]. Available: <http://www.springerlink.com/content/q4110ww348010131/>
- [52] E. Computing, "Revisiting Public-Key Cryptography for," no. November, pp. 85–87, 2005.
- [53] D. Malan, M. Welsh, and M. Smith, "A public-key infrastructure for key distribution in TinyOS based on elliptic curve cryptography," *Sensor and Ad Hoc Communications and Networks, 2004. IEEE SECON 2004. 2004 First Annual IEEE Communications Society Conference on. IEEE*, vol. 00, no. C, pp. 71–80, 2004.
- [54] C. Clifton, M. Kantarcioglu, J. Vaidya, X. Lin, and M. Y. Zhu, "Tools for privacy preserving distributed data mining," *ACM SIGKDD Explorations Newsletter*, vol. 4, no. 2, pp. 28–34, 2002.
- [55] A. C.-c. Yao, "How to Generate and Exchange Secrets," *Foundations of Computer Science*, no. 1, pp. 162–167, 1986.
- [56] Y. Lindell and B. Pinkas, "Secure multiparty computation for privacy-preserving data mining," *Journal of Privacy and Confidentiality*, no. 860, pp. 1–39, 2009. [Online]. Available: <http://repository.cmu.edu/cgi/viewcontent.cgi?article=1004&context=jpc>
- [57] L. Mui, M. Mohtashemi, and A. Halberstadt, "A computational model of trust and reputation," *System Sciences, 2002. ...*, vol. 00, no. c, pp. 1–9, 2002. [Online]. Available: http://ieeexplore.ieee.org/xpls/abs_all.jsp?arnumber=994181
- [58] Y. B. Reddy, "Agent-based Trust Calculation in Wireless Sensor Networks," no. c, pp. 334–339, 2011.
- [59] T. Chung and U. Roedig, "Efficient Key Establishment for Wireless Sensor Networks Using Elliptic Curve Diffie-Hellman," *Distribution*.
- [60] C. Lederer, R. Mader, M. Koschuch, J. Großschädl, A. Szekeley, and S. Tillich, "Energy-Efficient Implementation of ECDH Key Exchange for Wireless Sensor Networks," *Proc. of WISTP\,09*, pp. 112–127, 2009.
- [61] T. Chung and U. Roedig, "DHB-KEY: An efficient key distribution scheme for wireless sensor networks," *2008 5th IEEE International Conference on Mobile Ad Hoc and Sensor Systems*, no. October 2016, pp. 840–846, 2008. [Online]. Available: <http://ieeexplore.ieee.org/lpdocs/epic03/wrapper.htm?arnumber=4660127>
- [62] I. F. Akyildiz and M. C. Vuran, "Wireless Sensor Networks," no. October 2016, pp. 1–517, 2010. [Online]. Available: <file:///Users/dahuiluo/Documents/?????/Papers2/Articles/2010/Akyildiz/2010Akyildiz.pdf> \npapers2://publication/uuid/AF5D4F86-D9D5-4BC6-9539-EE0842672C55

- [63] I. Mansour, G. Chalhoub, P. Lafourcade, and F. Delobel, "Secure key renewal and revocation for Wireless Sensor Networks," *Proceedings - Conference on Local Computer Networks, LCN*, pp. 382–385, 2014.
- [64] O. Delgado-Mohatar, A. Fúster-Sabater, and J. M. Sierra, "A light-weight authentication scheme for wireless sensor networks," *Ad Hoc Networks*, vol. 9, no. 5, pp. 727–735, 2011.
- [65] S. R. Rajeswari and V. Seenivasagam, "Comparative Study on Various Authentication Protocols in Wireless Sensor Networks," vol. 2016, no. iii, 2016.
- [66] L. Lim, P. Marie, D. Conan, S. Chabridon, T. Desprats, and A. Manzoor, "Enhancing context data distribution for the internet of things using qoc-awareness and attribute-based access control," *Annales des Telecommunications/Annals of Telecommunications*, vol. 71, no. 3-4, pp. 121–132, 2016.

The Art of Crypto Currencies

A Comprehensive Analysis of Popular Crypto Currencies

Sufian Hameed, Sameet Farooq

IT Security Labs, National University of Computer and Emerging Sciences (FAST-NUCES), Pakistan

Abstract—Crypto Currencies have recently gained enormous popularity amongst the general public. With each passing day, more and more companies are radically accepting crypto currencies in their payment systems, paving way for an economic revolution. Currently more than 700 crypto-currencies are available at Coindesk alone for trade purposes. As of November 2016, the Crypto currencies hold a total market share of over 14 Billion USD¹ [5]. With no centralized institution to monitor the movement of funds, Crypto currencies and their users are susceptible to multiple threats. In this paper we present an effort to explain the functionality of some of the most popular crypto currencies available in the online market. We present an analysis of the mining methodologies employed by these currencies to induce new currency into the market and how they compete with each other to provide fast, decentralized transactions to the users. We also share, some of the most dangerous attacks that can be placed on these crypto currencies and how the overall model of the crypto currencies mitigates these attacks. Towards the end, we will present taxonomy of the five highly popular crypto currencies and compare their features.

Keywords—Crypto Currency; Bitcoin; Ripple; Litecoin; Dash coin; Stellar

I. INTRODUCTION

The need for crypto currency as laid down by Timothy May was to ensure the possibility of anonymous transactions of money and to create a society wherein secrecy and privacy are the prevailing features [25]. This initial idea was capitalized by many researchers and activists of Cypherpunk to make a practical application of cryptography in all spheres of life.

Wei Dai came up with the outlining protocol for "B-Money" in 1998 that was practical in nature and was introduced as a bi-product of Timothy May's Crypto-Anarchy [19]. The B-Money laid out the foundation on which Satoshi 10 years later constructed Bitcoin [27], the first decentralized crypto currency to be made publicly available.

The modern era is a digital era wherein the concept of fiat money has been challenged by crypto currencies. Crypto currencies are an alternative to fiat currencies with no central authority controlling the generation of money. The crypto currencies are different from conventional fiat system of currencies where no federal signatory governs the flow of currency. Unlike the fiat currency where the federal banks or governments are responsible for the generation and printing of money, the crypto currency is generated by a process called mining. Crypto currencies use complex hashing and time stamping methodologies to uniquely identify each coin within

that currency [15]. Crypto currency systems generally claim to provide anonymous, decentralized processing of transactions. This anonymity can be used as an additive preventive measure for user confidentiality and privacy.

The acceptance and demand of crypto currencies has increased a hundred fold over the past few years. Similarly, the industry around crypto currencies has evolved since its inception and a number of stake holders are now associated with the growing trade and acceptance of crypto currencies. Currently, crypto currencies are readily available at hundreds of exchanges around the world against fiat currency. Many large companies are now adopting crypto currencies into their payment systems. Bitcoins are easily accepted at Microsoft, Wordpress, Amazon, Apples App store, Wikipedia, Dell and other major brands in different sectors of life [18]. However, if a store is unwilling to accept crypto currencies in their online payment systems, coins can be converted to physical world goods via gift cards. Many gift card businesses accept major crypto currencies such as Bitcoin and provide the customers with gift cards to be availed at a physical store [16].

The increasing requirement of computational power to solve mining problems has resulted in the need of mining pools and many of these pools currently exist for a new miner to join and generate new currency. Similarly, cloud vendors provide mining resources on rental basis to miners, which has opened a new avenue of stake holders associated with mining of crypto currencies. Likewise, hardware companies have now built and configured special hardware components solely for the purpose of solving the mining problems and this has elevated the variety of the people associated with the rising industry of crypto currency itself.

As of now, hundreds of crypto currencies currently exist in the online market for trade purposes. These currencies are as expensive as Skidoo, one unit of which is equivalent to USD 2,350 dollars, to as cheap as GCoin, which is available for as low as few USD 0.000000001 [5]. Crypto Currencies can generally be classified as either Proof-of Work based currency or Consensus Based Currencies, depending on how they settle transactions within their devised protocols. Figure. 1 and Figure. 2 depict the overall architecture of the two genres of crypto currencies.

- **Proof-of-Work scheme:** This scheme add some work or difficulty to validate the transaction. In particular proof-of-work systems repeatedly run difficult hashing algorithms or other client puzzles to validate the electronic transactions.
- **Consensus scheme (Proof-of-Stake):** This scheme aims to achieve distributed consensus by asking users

¹The price and overall market capitalization might change at the time this article is being read.

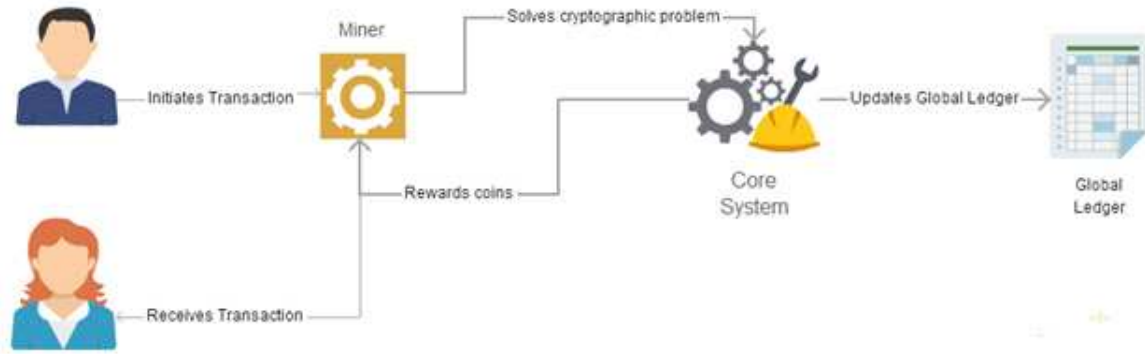


Fig. 1. Architecture of Proof-of Work based Currency

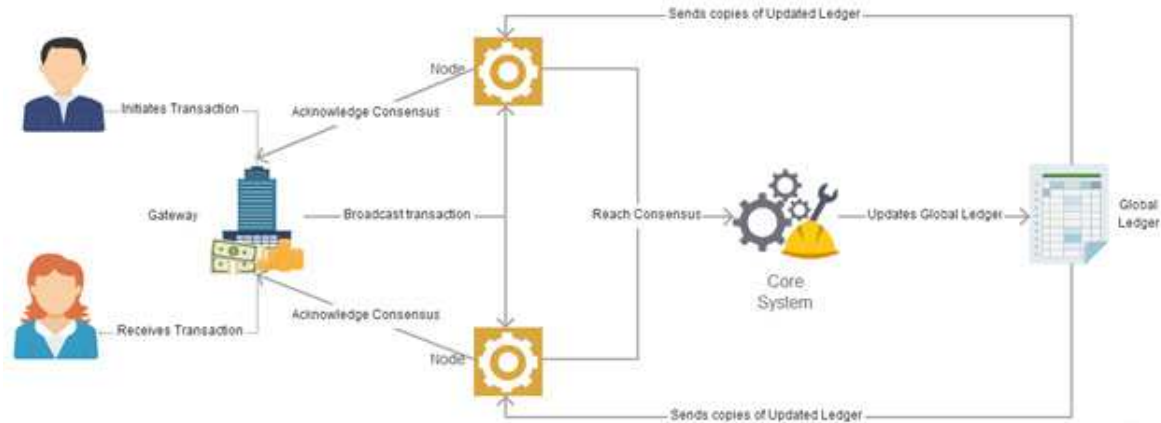


Fig. 2. Architecture of Consensus Based Currency

to prove ownership or their stake in the currency.

In this paper we carry out a survey of the five most popular crypto currencies on the basis of their market capitalization and compare their working and performance with each other. For each of the currency, we will explain the working model of the currency, the mining approach through which new currency is generated in the market. We will also explain some of the eminent limitations in the protocols and mitigation actions taken by each protocol to overcome these limitations.

II. BITCOIN

Bitcoin is the first decentralized crypto currency established in 2008 based on the work of a pseudonymous developer and researcher Satoshi Nakomoto [27]. It is a peer to peer network of nodes in which all nodes maintain a single copy of transactions known as Ledger. Bitcoin was proposed as a solution to double spending attack. Bitcoin has emerged as a widely acceptable medium of transaction over the past few years. As of November 2016, the price of one Bitcoin is above USD 700 and the Bitcoin has a market capitalization of over 11.9 billion dollars making it the most popular crypto currency to date (see fig. 3 for overall price and market capitalization of Bitcoin).

A. Design and Working

In order to understand the architecture presented in Bitcoin, one has to familiarize with the following keywords that formu-

late the entire architecture. A coin is a chain of digitally signed certificates. A transaction is the process in which a sender of a coin digitally signs the hash of the previous transaction with the public key of the receiver and adds it to the end of the coin (see fig. 4). A timestamp server contains the timestamp of each transaction initiated within the system. The block is a collection of transactions that need to be validated and broadcasted by the nodes running the Bitcoin core engine.

Each block is a Merkle Root of the transaction, meaning that each block contains the hash of previous block and a nonce to satisfy the requirements of hashing function which in case of Bitcoin is SHA-256 (see fig. 4). When a transaction takes place, it is broadcasted to all the nodes within the network. The nodes form a block of transactions and work on finding the difficult proof-of-work for its block. The proof-of-work is the validation step in which nodes spend computational resources to find the correct nonce that fulfills the requirement of the hashing algorithm thereby validating the transactions in the block. Once a proof-of-work has been computed, it is broadcasted to all the nodes in the network and the block gets added into the block chain.

B. Bitcoin Mining

Since Bitcoin is a decentralized crypto currency, it implies that no regulatory body is in control of producing new coins. However, Bitcoins are added in the online market via a process called mining. Similar to the conventional meaning of the



Fig. 3. Price and Market Capitalization of Bitcoin [2]

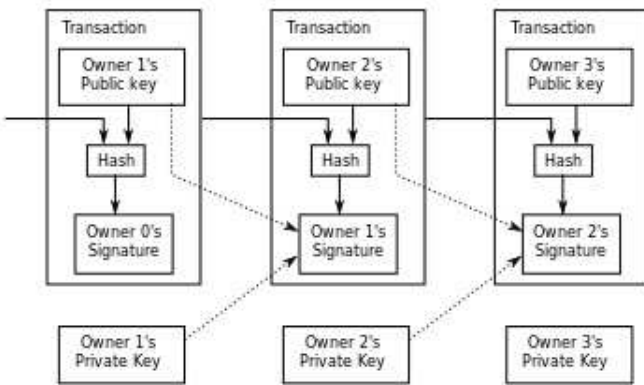


Fig. 4. Merkle Hashing Process in Block Generation [3]

word where the labor usually works to find precious metals within the ground, mining is a mechanism wherein the nodes labor their way to solving the proof-of-work problem of each block chain validation. As a result of successful validation, the nodes get rewarded a sum of 50 Bitcoins. This is how the new Bitcoins are added into the system. Bitcoin block mining reward halves every 210,000 blocks to match the effect of hyperinflation. Current block mining reward is 12.5 bitcoins which is expected to half in approx 3.5 years based on current projections [1].

C. Possible Attacks and Mitigation Actions

Over the years, the Bitcoin system has been under criticism due to its following vulnerabilities, many of which have been exploited so far.

1) *51 percent Attack*: This by far remains the greatest danger to the existence of Bitcoin and implies that a pool of dishonest nodes within the Bitcoin network gain 51 percent computational power of the entire network. If this scenario occurs, the security of the network is compromised since the

controlling pool can take decisions on how the consensus is to be reached for each subsequent block. This allows the controlling pool to spend money that was not theirs to spend thereby inducing the "double spending problem". Only recently, GashIO [7], a Bitcoin mining pool, reached the 51% computational mark thereby causing panic in the entire Bitcoin community [23].

The Bitcoin protocol was designed considering the fact that 51% of the nodes will remain honest to the network. However the protocol is setup to pick random nodes for mining thereby breaking the power of computation and disallowing attackers to gain 51% of attacking nodes in the system.

2) *Double Spending Problem*: A Bitcoin transaction usually takes 10 minutes before it is confirmed by the system. This waiting time is not acceptable to people who want transaction processing at a fast rate without waiting for confirmation. This gives rise to double spending problem without requiring 51% percent computational power. Researchers have been able to successfully carry out the double spending attack by broadcasting fraudulent transactions to a large number of nodes along with honest transactions. This allows the network to assume that fraudulent transactions should be accepted by the network as they get accepted in most of the nodes [17].

3) *Dust Transactions*: Another major limitation with Bitcoin was the increasing size of block chain. Previously the minimum amount for transaction was 1 Satoshi which caused block chain to reach upto 8GB in size [22]. However the protocol was redesigned to change the minimum transaction amount of 5430 Satoshis which resulted in a smaller block chain.

III. RIPPLE

Ripple is the third most popular crypto currency as of today and has a market capitalization of over USD 249 million. Ripple was formulated by the Ripple Labs to support the electronic cash payment system known as Ripple Consensus Protocol [29]. The Ripple consensus protocol was aimed at facilitating



Fig. 5. Price and Market Capitalization of Ripple [11]

high speed transaction processing to financial institutions and individuals at minimal fee. Ripple (XRP) works within the Ripple Network as a bridging currency between different fiat currencies and unlike the fiat currencies, it is only worth what the other person is willing to pay for it. Currently 1 Ripple is priced at 0.00695 USD (see fig. 5 for overall price and market capitalization of Ripple).

A. Design and Working

Ripple Consensus Protocol Algorithm (RPCA) was proposed keeping in view the three major challenges of decentralized payment networks i.e. Correctness, Agreement and Utility and works on the principal of Byzantine Agreement [29]. The RPCA consists of the following main components that we will be using throughout this section:

- **Server:** An entity running the Ripple Server software and participating in the consensus process.
- **Ledger:** A complete record of the account balances of every user in network. A ledger is updated with each transaction successfully completing the consensus process.
- **Last-Closed Ledger:** The state of the ledger after completion of last successful consensus process. It also determines the current state of the entire network.
- **Open- Ledger:** A current state of the ledger which has not yet been confirmed by the network via the consensus process.
- **Unique Node List (UNL):** A subset of the server nodes that a particular server trusts. It is a list maintained by each Server and can be updated at any time.
- **Proposer:** A server broadcasting a set of transactions to be considered in the next consensus round.

Consensus process in RPCA takes place every 3 seconds and a Server 'S' takes all the valid transactions it has encountered between the last closed ledger period and the new

consensus process and formulates a candidate set. This set is then broadcasted to all the UNLs of 'S'. All the UNLs are required to vote on the validity of the transactions based on the time stamp and balances that lay in their copy of the last closed ledger. If a minimum number of UNLs accept the transaction, the transaction is forwarded to the next round of consensus; else it is discarded to be taken into consideration in the next consensus process [29].

In the second round of consensus, the RPCA requires at least 80% of the UNLs to agree on a valid transaction from first round. The requirement of 80% of the UNLs is to ensure the correctness of the transaction and enforce that 80% of the nodes have to be honest within the network for a transaction to be validated. In order to ensure the utility of the protocol, the consensus takes place every 3 seconds, allowing the users to send and receive currency at a very high speed.

Based on the RPCA, the ripple network uses Gateways as an entry point into the network. A client can create an account with the trusted Gateway to send currency to other untrusted clients. Ripple Network allows different currencies to be maintained in its system, allowing the clients to leverage the transaction processing in whichever currency they required. With Ripple (XPR) as the native currency of the system, the clients can send and receive ripples without having to trust the Gateways.

B. Ripple Generation and Distribution

The Ripple System consists of 100 Billion Ripples generated and fed into the ledger at the time of initiation. The system cannot generate any further currency due to protocol restrictions. The creators gifted 80 Billion out of 100 Billion Ripples to Ripple Labs which are given away to the end consumers through one of the following programs [9]

- **Users:** Following the Paypals marketing strategy; new users are awarded free Ripples upon joining the Ripple Network.

- **Developers:** The developers are encouraged to catch bugs in the open source software and provide patches to the already reported bugs and rewarded with Ripples.
- **Merchants:** Ripples are distributed to the merchants for the amount of transactions they bring into the system.
- **Gateways:** The creators are trying to incentivize the running of system by creating strategic partners and granting Ripples as bounties to its partners.
- **Market Makers:** Financial institutions and Forex agents are compensated specially for bringing liquidity to the model.
- **Administrative Cost:** The administrative cost of running the network, creating new products is all waged using Ripples.

C. Possible Attacks and Mitigation Actions

Ripple network has a number of advantages as it was developed to improve on Bitcoin itself. In this section, we will determine some of the most popular attacks in the crypto currency domain and how Ripple leverages its consensus protocol to overcome these threats.

1) *51 percent Attack:* The highly feared attack in the crypto currencies, the 51 percent attack, is being repelled by the Ripple Consensus Protocol by introducing UNLs. A server trusts transaction only its UNL trusts thereby constraining the attacker to get hold of nodes already in the UNL. This is highly non trivial as the resulting double spending transaction would infinitely regard the node as distrustful by the server. Also latency checks are placed to make sure all nodes are running effectively and mechanisms are in place to make sure that UNL gets updated if nodes show suspicious behavior.

2) *Denial of Service Attack:* Ripple has mechanism in place for possible Denial of Service attack. For every transaction taking place in the system, 0.00001 XPR are destroyed by the system. Also a minimum of 20 XPR balance is to be maintained by a user in order to create a transaction in ledger [10]. The idea behind the two is to bankrupt the attacker in case of a DoS attack by burning out Ripples and making transactions expensive. However, they will continue to be deemed cheap for average users.

IV. LITECOIN

Created in 2011 by Charles Lee, a former Google engineer, the Litecoin was aimed at being "Silver to Bitcoin's Gold" [4]. Litecoin is the fourth largest currency with an overall market capitalization of more than USD 189 million. At the time of writing, 1 Litecoin is available in the online market for USD 3.90 (see fig. 6 for overall price and market capitalization of Litecoin). Litecoin was designed specifically to improve over the problems associated with Bitcoin and is the first crypto currency to have successfully deviated from the legacy proof-of-work of SHA-256 and implemented SCRYPT for block processing [28]. This deviation led to multiple advantages of Litecoin, the details of which will be presented in the next sections.

A. Design and Working

Litecoin uses the same code base of Bitcoin with minor deviations in the protocol to improve on the gaps identified in Bitcoin. The aim of Litecoin was to provide faster transactions and reduce the impact of 51 percent attack. Litecoin blocks are generated at 2.5 minutes as compared to traditional 10 minute mark of Bitcoin. The faster block creation in Litecoin allows faster confirmation of transactions as blocks gets accepted into the block chain 4 times faster than Bitcoin. The working of Litecoin is quite similar to the working of Bitcoin which is explained in the previous sections. The key difference between the working of two crypto currencies lies in the difference of Proof-of-work mechanism explained in the Litecoin Mining section.

B. Litecoin Mining

Litecoin mining traditionally follows the same trajectory as Bitcoin mining with one major difference in the Proof-of-work mechanism. Bitcoin uses SHA-256 as its hashing algorithm in the Merkle Tree of the block chain, whereas Litecoin uses SCRYPT [28] as its hashing algorithm. SCRYPT favors large amount of RAM memory and works in a serialized manner as compared to SHA-256 which is dependent on parallelization and computational power alone. This deviation of hashing algorithm led to the decentralization of Litecoin mining as it gives a chance to ordinary users with low computational power to participate in the mining process. Like Bitcoin, the Litecoin too rewards its mining nodes a sum 50 coins on solving a block. The sum is due to be halved every four years.

C. Advantages of Litecoin

Litecoin has a number of advantages over bitcoin which were highlighted in the previous sections but explained in this section:

- SCRYPT mining is more feasible than SHA-256 mining. The reason for this is that SCRYPT uses fast access to large amounts of memory rather than depending on fast amount of arithmetic operations as required by SHA-256. With the development of ASICs (Application-Specific Integrated Circuit) for bitcoin mining, the modern computers and GPUs cannot participate in the Bitcoin Mining. However, ASICs are more expensive to design for SCRYPT as the device would require large amount of expensive RAM. This would allow modern GPUs and CPUs to participate in the mining process and get rewarded.
- Since the ASICs are not feasible for SCRYPT, it would decentralize the mining power and consequently limiting the dreaded 51% attack. This would imply that no entity could be investing such a high amount of money to accumulate the mining power in order to carry out the double spending attack.
- Blocks are processed at 2.5 minutes rather than 10 minutes mark in Bitcoin. This allows faster confirmation of transaction. Also it allows more granularity in the network, e.g. a merchant can wait for two confirmations by the network and consume 5 minutes



Fig. 6. Price and Market Capitalization of Litecoin [8]

only as compared to one confirmation in Bitcoin that takes 10 minutes.

- The protocol implies that a total of 84 million Litecoins will be created in the life time, an amount four times greater than 21 million Bitcoins due to be created.
- The block retarget was 2016 in both Bitcoin and Litecoin. Since Litecoin blocks are generated 4 times faster, the difficulty mark needs to be adjusted every 3.5 days. The relatively quick adjustment in difficulty of the hashing function works fairly well in the event of a large number of miners suddenly dissipating from the network.

D. Limitations of Litecoin

The above advantages of Litecoin have some limitations associated with themselves, some of which are discussed below.

- In case of a Botnet attack, the owner could utilize the controlled bots for mining purposes and achieve a greater mining pool for itself. This would yield a higher benefit for the botnet owner as it would increase the probability of attacker solving the block chain problem. Where this attack is beneficial for the attacker, it also supplements the Litecoin network as the botnet controller brings with itself computational resources into the network. However the aim of crypto currency should be to put the greater good in front of individual benefits.
- The faster block generation results in bigger block chain. Accordingly, the block chain size would be 4x the block chain size of Bitcoin [4].

V. DASH COIN

Dash coin is another premier and one of the most popular crypto currencies, developed to add anonymity to Bitcoin [20].

Dashcoin differs from Bitcoin in a number of ways. Firstly it is based on the countermeasure of CoinJoin [24] to provide users of crypto currency with added security and anonymity over transactions. We will discuss the problem identified in CoinJoin in the following section. Secondly, it provides near instant transactions by employing a secondary network of Master Nodes. This implies that consensus must be reached within the quorums of Master Nodes on a transaction in order to accept the transactions. Currently, Dash coin is the seventh most popular currency in the list with a market capitalization of USD 62 Million. In the online market, Dash is available for trading at USD 9.10 per coin (see fig. 7 for overall price and market capitalization of Dash coin).

A. Design and Working

Dash coin employs an incentivized secondary network of nodes known as Master Nodes to cater the problem of reducing mining nodes in Bitcoin. Within Dash, Master nodes are engaged to enhance the functionality of the entire network. Maser nodes are utilized for message sending, consensus as well as providing anonymity to the users. For all these functionalities, the Master nodes are rewarded 45% of the total reward of block processing [20].

In order to deploy a Master Node, 1000 Dash must be reserved in the wallet as collateral. This amount is only reserved for a node to work as a Master node and receive its fair share of reward. If at any moment the limit for 1000 Dash is not fulfilled, the node gets ruled out of the Master Node list maintained by the client software. This puts an upper bound to the total number of Master Nodes running in the network. As the total available Dash is around 5.3 million, the total number of Master Nodes the system can accommodate is around 5300. Once a node has been categorized as Master Node, a ping message is sent every 15 minutes to check the liveness of the node.

Master Nodes help in reaching consensus by the use of validating transaction locks. Once a transaction has been initiated, a transaction lock is propagated to all the Master Nodes in



Fig. 7. Price and Market Capitalization of Dash coin [6]

the network. If a consensus is reached on the transaction lock by a quorum of nodes, it gives rise to the probability that the transaction will be accepted by the block chain. The transaction thus gets accepted by the system on achieving consensus and all the subsequent conflicting transactions are rejected. If however a consensus is failed to reach, the transaction gets validated via conventional block processing. This is how Dash preserves the integrity of the system against double spending attack. This module is called InstantX due to the fact that it allows near instant transactions in the system as the time to reach consensus is fairly low as compared to Bitcoin [21].

Dash also incorporates modules to preserve user's privacy. Although Bitcoin was developed to provide anonymous peer-to-peer transactions, academic research shows that it is possible for the observer to trace transactions back to the original user. This is done via forward linking or "through change linking" in which a user sends a proportion of total transaction amount to an identifiable source. The backward propagation from identifiable source results in losing anonymity of the transaction as described by Gregory Maxwell, one of the core developers of Bitcoin, in his concept of CoinJoin [24]. Dash overcomes these problems by Darksend, a module that uses the Master Nodes to merge/mix transactions of three different users into input and output sets so that at each round the input and the out values have equivalent sets with varying users. This reduces the probability of correctly observing a transaction to one-third. In order to complicate observation of transactions, a block chain approach is applied which elevates the complexity for the attacker.

B. Dash Mining

Dash uses X11 as its proof-of-work hashing instead of SHA-256 and SCRYPT, which are used by some of the other notable crypto currencies. The idea is to complicate the formation of ASICs and encourage traditional "hobbyist" mining. Dash is unique in the sense that it has a variable block reward that is based on difficulty. This means that while currently the block reward is 120, when difficulty rises the

block reward will fall. Eventually the block reward will be driven down to its lowest amount which is 15 Dash. After that, every 2 years the block reward is halved again. So in 2 years, 7.5 Dash, in 4 years, 3.75 Dash, etc.

C. Possible Attacks on Dash and Mitigation Actions

In this section we consider some of the probable attacks on Dash Consensus Network and in the event of these attack how the system will prevent itself from colossal damage.

D. Sybil Attack

A probable Sybil attack would require the attacker to gain control of at least two-third of the entire Master Node network. For a network of 1000 Master Nodes, the cost of adding 2000 further Master nodes to get 2/3 control of the network would require a demand of 2 million Dash. In a relatively small market of 5 million Dash, it would be difficult to get hold of 2 million Dash thereby thwarting the Sybil attack.

E. Finney Attacks

Finney Attacks implore that an attacker is mining a block normally. After the block has been processed, the attacker induces a transaction sending the payment back to him before another block has been attached to the block chain. This is prevented in the Dash by making sure locks are maintained by the Master Nodes until the transactions have been approved by consensus. The conflicting transactions are all rejected and discarded.

F. Transaction Lock Race

The protocol can also be tested by transaction lock race in which an attacker submits two racing locks, one with payment to the merchant and one with payment back to him. In this scenario the network would be split between correct and attacking locks. It is the responsibility of the master nodes to chip in their vote and remove confusion from the network.



Fig. 8. Price and Market Capitalization of Stellar [14]

In case of other attacks, the conventional block processing methodology is used to validate the blocks there by securing the block chain.

VI. STELLAR

With the aim to provide the access to a greater number of people across the globe by lowering boundaries of membership into the system, Stellar is also one of the most popular cryptographic currencies having already surpassed the market capitalization of USD 11.5 million. Stellar is backed by a non-profit organization Stellar Development Foundation [12] with an aim to spread financial literacy and access worldwide. Stellar, initially was based on Ripple however in May 2015, Stellar launched its unique consensus protocol, the Stellar Consensus Protocol [26], after limitations were identified in the former version. Most of the characteristics of the two currency exchange systems are the same. Currently, each Stellar is worth around USD 0.00169 (see fig. 8 for overall price and market capitalization of Stellar).

A. Design and Working

Stellar, like Ripple itself, acts as a bridging currency in the Stellar network. The difference between the two currency exchange networks is the consensus protocol each of them employs to validate a transaction. Stellar uses Federated Byzantine Agreement algorithm as a base around the Stellar Consensus Protocol (SCP). A transaction on a node in Stellar gets validated if a vast majority of the nodes it trusts validate the slot. The trusting nodes will in turn look to their own trusting nodes before calling any slot or transaction settled. The consensus is thus reached when a vast majority of the nodes in the network have called a transaction settled. This consensus is reached within a few seconds at most and results in fast processing of transactions. Stellar also claims to be the first protocol to provide decentralized control, flexible trust, low latency and asymptotic security all together.

An account on Stellar is identified by a unique "address", which is the (hashed) public key half of a public/private

key pair in public-key cryptography. To spend the balance or change a property of an account in the ledger, the account holder must sign a corresponding "transaction" using the private key half of the account's key pair, and submit it to a Stellar server for propagation to the network. The Stellar server will check the authenticity of the digital signature to confirm the transaction is signed with the correct private key. A Stellar transaction is a signed instruction broadcast to the entire network which modifies the state of one or more accounts in the ledger. A set of transactions is applied to the ledger after a consensus round, and a new ledger is created. There are many different types of transactions that an account can create, including: Payment, OfferCreate, TrustSet, AccountSet.

B. Stellar Generation and Distribution

Stellars cannot be mined like other crypto currencies. At the time of starting, 100 billion Stellars were deposited in the "root" account. These stellars are due to be utilized in the following manner [13].

- **Signup Program:** Signing up with Stellar gets you free Stellars. Stellar uses Facebook for identifying spam or duplicate accounts. 50 Billion Stellars are to be distributed via this method.
- **Non- Profit Organizations:** Since the idea behind Stellar is to promote financial reach to deserving people with limited connectivity or resources, Stellar plans to utilize 25% of its resources to be given away to non-profit organizations which plan to deliver these to remote areas.
- **Bitcoin Program:** Stellar has reserved 20% of the 100 billion stellars for the Bitcoin program. The idea behind this is to promote Bitcoin users to use stellar instead of Bitcoins with their wallets getting compensated in stellar.
- **Administrative Cost:** The remaining 5 percent of the Stellars will be used for administrative cost.

TABLE I. TAXONOMY OF CRYPTO CURRENCIES

Currency	Scheme	Decentralize Control	Low Latency	Flexible Trust	Asymptotic Security
Bitcoin	Proof-of-Work	Yes	No	No	No
Ripple	Byzantine Agreement	No	Yes	Yes	Yes
LiteCoin	Proof-of-Work	Yes	No	No	No
Dash Coin	Proof-of-Work	Yes	Yes	Yes	Maybe
Stellar	Federated Byzantine Agreement	Yes	Yes	Yes	Yes

Apart from the above distribution, SCP also has a mechanism for inducting new coins into market via inflation. Theoretically, 1% of the total Stellers are to be created every year. Every account can sign another account for getting new coins, the votes will be based on the number of Stellers in the account itself. Say, Alice has 120 Stellers in her account and she wants to vote for Bob to get the newly created Stellers. 120 Stellers in Alice's account will act as 120 votes for Bob. 50 contestants with most votes associated with their accounts will be rewarded the newly created Stellers.

C. Limitations of Stellar

Stellar by far claims to be the most secure consensus protocol but it has a few limitations associated with itself as pointed out by David Mazieres in his white paper for Stellar [26]. Firstly, the protocol has a mechanism for locking out blocking sets of nodes but it has no mechanism for unblocking them. Secondly, the quorum slices are configurable by the user which threatens the integrity of the system if being incorrectly configured. Thirdly, widely trusted nodes can leverage their position in the market to spoof transactions.

As the SCP protocol is relatively new, other limitations are yet to be explored.

VII. TAXONOMY

After having laid down the design details and limitations of the five most popular crypto currencies in the world today, we would like to provide taxonomy of these digital currencies by comparing them against one another in table I.

The matrix in table I amply scrutinizes some of the major archetypes for monitoring the effectiveness of these crypto currencies. This includes the scheme of device, transaction control system of the crypto currencies, latency of transactions within their system, robustness of the system to changing trust network and security measures in place to ensure smooth transaction processing. As it is evident from the matrix, not all high functioning crypto currencies provide asymptotic security to its consumers. The pioneering currencies including Bitcoin as well as LiteCoin which occupy over 85% of total market share are highly susceptible to the hazardous 51% attack. Stellar, being the latest amongst this lot ensure highly decentralized control of its general ledger, providing fast, anonymous transaction service, while Ripple compromised on Decentralization of the monetization of the currency. Dash, as per the analysis has the best Collateral based system in place when it comes to Proof-of-Concept solving schemes.

VIII. CONCLUSION

Having understood the finer details associated with each of the popular crypto currencies, we have come a long way from where Satoshi Nakomoto gave his idea of a peer-to-peer system but with an overall market capitalization of approximately 14 billion dollars, crypto currencies have miles to go before they can ultimately replace the fiat currency.

REFERENCES

- [1] Bitcoin block mining reward. https://en.bitcoin.it/wiki/Controlled_supply.
- [2] Bitcoin price and market capitalization. <http://coinmarketcap.com/currencies/bitcoin/>.
- [3] Bitcoin transaction visualization. https://github.com/graingert/bitcoin-IRP/blob/master/img/Bitcoin_Transaction_Visual.svg.
- [4] Comparison between litecoin and bitcoin. https://litecoin.info/User:Iddo/Comparison_between_Litecoin_and_Bitcoin.
- [5] Crypto currency market capitalization. <http://coinmarketcap.com>.
- [6] Dash coin price and market capitalization. <http://coinmarketcap.com/currencies/dash/>.
- [7] ghash: Bitcoin mining solutions. <http://ghash.io/>.
- [8] Litecoin price and market capitalization. <http://coinmarketcap.com/currencies/litecoin/>.
- [9] Ripple distribution strategy. <https://www.ripplelabs.com/xrp-distribution/>.
- [10] Ripple market makers. https://ripple.com/files/ripple_mm.pdf.
- [11] Ripple price and market capitalization. <http://coinmarketcap.com/currencies/ripple/>.
- [12] Stellar development foundation. <https://www.stellar.org/about/>.
- [13] Stellar distribution. <https://www.stellar.org/about/mandate/>.
- [14] Stellar price and market capitalization. <http://coinmarketcap.com/currencies/stellar/>.
- [15] What is cryptocurrency. <https://www.coinpursuit.com/pages/what-is-cryptocurrency/>.
- [16] What can you buy with bitcoin? <http://www.coindesk.com/information/what-can-you-buy-with-bitcoins/>, 2015.
- [17] Danny Bradbury. The problem with bitcoin. *Computer Fraud & Security*, 2013(11):5-8, 2013.
- [18] Jonas Chokun. Who accepts bitcoins as payment? list of companies, stores, shops. <https://99bitcoins.com/who-accepts-bitcoins-payment-companies-stores-take-bitcoins/>, 2016.
- [19] Wei Dei. B-money. <http://www.weidai.com/bmoney.txt>.
- [20] Evan Duffield and Daniel Diaz. Dash: A privacy-centric cryptocurrency, 2014.
- [21] Evan Duffield, Holger Schinzel, and Fernando Gutierrez. Transaction locking and masternode consensus: A mechanism for mitigating double spending attacks.
- [22] David Gilson. Bitcoin blockchain grows to 8gb. <http://www.coindesk.com/bitcoin-blockchain-grows-to-8gb/>, 2013.
- [23] Alec Liu. Bitcoin's fatal flaw was nearly exposed. <http://motherboard.vice.com/blog/bitcoins-fatal-flaw-was-nearly-exposed>, 2014.

- [24] Gregory Maxwell. Coinjoin: Bitcoin privacy for the real world. In *Post on Bitcoin Forum*. Available online: <https://bitcointalk.org/index.php>, 2013.
- [25] Timothy C. May. Cyphernomicon. <http://www.cypherpunks.to/faq/cyphernomicron/cyphernomicon.html>, 1994.
- [26] David Mazieres. The stellar consensus protocol: A federated model for internet-level consensus. *Draft, Stellar Development Foundation, 15th May*, available at: <https://www.stellar.org/papers/stellarconsensus-protocol.pdf>, 2015.
- [27] Satoshi Nakamoto. Bitcoin: A peer-to-peer electronic cash system, 2008.
- [28] Colin Percival. Stronger key derivation via sequential memory-hard functions. *Self-published*, pages 1–16, 2009.
- [29] David Schwartz, Noah Youngs, and Arthur Britto. The ripple protocol consensus algorithm. *Ripple Labs Inc White Paper*, page 5, 2014.

A New Approach of Graph Realization for Data Hiding using Huffman Encoding

Fatema Akhter, Member, IEEE
Jatiya Kabi Kazi Nazrul Islam University, Bangladesh

Md. Selim Al Mamun
Okayama University, Japan

Abstract—The rapid advancement of technology has changed the way of our living. Sharing information becomes inevitable in everyday life. However, it encounters many security issues when dealing with secret or private information. The transmission of such sophisticated information has become highly important and received much attention. Therefore, various techniques have been exercised for security of information. Graph steganography is a way of hiding information by translating it to plotted data in a graph. Because of numerous usages of graphs in everyday life, the transmission can take place without drawing any attention. In this paper, we propose a new graph realization technique for steganography that looks as if innocent and imperceptible to present day steganalytic attacks and the hidden message can only be read by its respective recipient. The secret message is first translated to prefix codes using Huffman encoding. Then the prefix code for separate word in the message is plotted in a graph. The proposed technique offers high embedding capacity and imperceptibility due to prefix presentation and word by word encoding of the message. The experimental outcomes show strong resistance towards steganalytic attacks in contrast to other approaches.

Keywords—Data hiding; Graph steganography; Huffman encoding; Steganalytic attack

I. INTRODUCTION

In recent years, electronic communication has become an integral part of everyday life. Be it email, audio or video, people exchange information mutually through electronic medium. The security of information has become essential as the transmission on public communication channel increases. This is mandatory to preserve the integrity and security of information that are being transmitted over public communication channel. Several methods and techniques have been studied in order to achieve the security of information. Unfortunately, they are still in research to enhance the security. Methods like Steganography [1]–[4] and cryptography [5]–[7] are commonly used for the security of information. However, in last two decades, steganography perhaps got much more attention than any other method. Steganography is the art of passing information in such a way that the existence of the message cannot be detected by intruders [8]. The cover can be any digital medium like image, audio or video.

Among numerous strategies of information security, steganography using graph has drawn a variety of interest of researchers as it can avoid noise within the cover [9]–[11]. The method avoids the noise in cover by plotting the information as facts in a graph for the secured transmission in contrast to other approaches. People use graph in daily life which makes it harmless and risk free to attract attention and preclude

numerous attacks. Any length of message can be translated to graph-data retaining the integrity of the information while transmission in public channel. Hiding message in graph is simple and straightforward. This does not require any special overhead. Consequently, it becomes a popular subject of studies in information security. The superiority of graph over other medium is tabulated in Table I. Hiding message in graph is an exceptionally new idea in the field of information security. The concept will shine with time due to interest of many researchers in this subject. In [12], the authors presented a technique for integration of message in graph that uses vertex-coloring method. In [13], the authors proposed a technique using integer wavelet transform (IWT) along with graceful graph to offer a secure and random image steganography with high imperceptibility. In [14], the authors presented a technique where the message is camouflaged as plotted data in graph. In [15], the authors presented a technique using Hamiltonian graph for the security of the message in public communication.

In this paper, we study popular strategies of information hiding in graph to grasp the ideas. Then, we propose a new graph realization technique from the message. In this work, we use Huffman encoding method to generate prefix code for every character in the message. The prefix codes are considered as the binary representation of the characters. Then, we classify the prefix code of character by the way of word within the message. The group of binary prefix code is then converted to its equivalent decimal value. We introduced two constants α and β that present the decimal value of a white space and scaling factor of decimal value of a word respectively. We add α to every word value to make it different from the white space. β is multiplied to the resultant value for diversion. Finally, we draw bar plot using these values in an excel file. To the best of our knowledge, similar technique for information hiding has not been addressed in any existing work. We investigated the proposed technique on various steganalytic attacks. Experimental outcomes show that the proposed technique is more secure as compared to other information hiding methods against various parameters such as embedding capacity, security and fidelity.

We prepare the remaining of the paper as follows: Section II presents the initial studies and provisions for the proposed technique. Section III presents the proposed technique for graph steganography. Section IV presents the experimental results and discussions. Finally, we conclude this paper in section V with some future works.

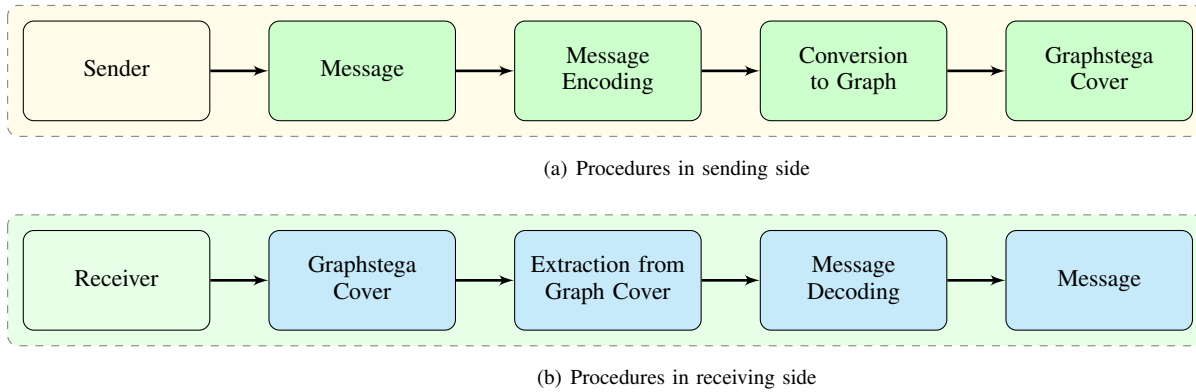


Fig. 1. General procedures in graph steganography: a) procedures in encoding in sender side and b) procedures in decoding in receiver side.

TABLE I. DIFFERENT STEGANOGRAPHY METHODS

Parameters	Steganography Methods		
	graph	image	audio
Noise	×	○	○
Distortion	×	○	○
Message size limit	×	○	○
Complexity	×	○	○
Less cost	○	×	×
Cover conversion	○	×	×
Traceable	×	○	○

II. PRELIMINARY STUDY

In this section, we present some preliminary studies for graph steganography. Specifically, we describe simple graph steganography and prefix code generation using huffman encoding algorithm.

A. Simple Graph Steganography

In graph steganography [16]–[18], messages are converted to facts or records to plot them in a graph. The generated graph looks simple that we frequently use in daily life. The presentation of message using graph can be carried out to a wide variety of domains of steganography where the cover needed to be noiseless. Unlike other steganography methods, graph steganography does not conceal facts in any digital medium like photograph, audio or video. This is referred to as noiseless steganography as it does not introduce noises within the cover while hiding information. A simple graph steganography interprets the message and converts to compatible data that can be plotted in a graph. Finally, the generated graph is transferred to the recipients of the message. Fig. 1 shows the procedures in a conventional graph steganography. The secret message to be transmitted is referred to as plaintext. In sending side, the plaintext is directly converted to facts in a graph. The titles and legends are given that look meaningful to facts in graph. The receiving side follows the methods in reverse order.

B. Huffman Encoding

Huffman encoding [19] is a method of generating an optimal prefix code for a string. The method assigns variable-length bit string to every character in the string that unambiguously represents that character. The variable-length bit string is called binary prefix codes throughout this paper. The method minimizes the number of bits required to represent

a standard string composed of these characters. The method counts the frequency of each character in a string and generates minimal prefix code for each character. The characters with higher frequency have fewer bits than the characters of lower frequency. An encoding tree is generated by utilizing a priority queue where nodes with lower frequency are assigned higher priority. The procedure of huffman encoding is given below:

- ① Create a leaf node for each symbol and add it to the priority queue.
- ② While there is more than one node in the queue:
 - a) Remove the node of highest priority (lowest probability) twice to get two nodes.
 - b) Create a new internal node with these two nodes as children and with the probability equal to the sum of the two probabilities of these two nodes.
 - c) Include the newly created node to the queue.
- ③ The node that remains in the queue, make it root of the tree. This completes the generation of tree.
- ④ Generate the prefix code by traversing the tree from root to leaves putting a zero (0) if every time a lefthand branch is taken and a one (1) if the right hand branch is taken.
- ⑤ The resultant 0 and 1 in the path from root to its leaf is the prefix code for the symbol at the leaf.

III. PROPOSED GRAPH STEGANOGRAPHY METHOD

The proposed graph steganography approach is composed of two methods:

- **Encoding:** In this method, the message is hidden into an excel graph.
- **Decoding:** In this method, the message is retrieved to its original form.

A. Proposed Encoding Method

Fig. 2 shows the steps of proposed encoding method for graph steganography. The method first interprets the message and converts every character in the message to its equivalent binary prefix code. Prefix code is generated using huffman encoding presented in II-B. The prefix codes are grouped by the word within the message. The prefix codes of characters are concatenated as they appear in the word and accumulated prefix code for each word is derived. The binary prefix code for

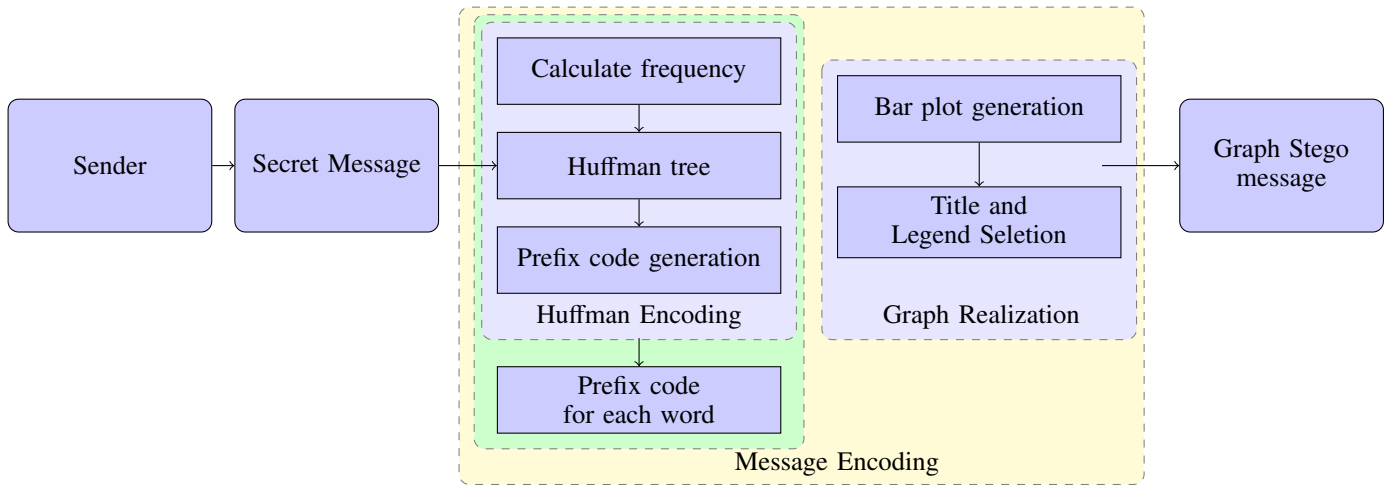


Fig. 2. Procedures of the proposed message encoding algorithm for the proposed graph steganography approach.

each word is then converted to its decimal value. The decimal value of white space is represented by a constant α . To avoid ambiguity, α is added to every decimal value of word. To avoid redundancy and to escape statistical attacks, a scaling factor β is introduced. β is multiplied to the resultant decimal value of each word. The resultant value becomes distinctive from the original prefix presentation of the message. These decimal values are then plotted as graph in an excel file. The steps of the proposed encoding method is given below:

Proposed Encoding Method

- ① Take the input message, M and read every character L_i within the message. Here L_i presents the i th character in message, M .
- ② Count the frequency $n(L_i)$ for character L_i and $n(SP)$ for white space. Here $n(L_i)$ and $n(SP)$ present the frequency of character L_i and white space respectively.
- ③ Call huffman encoding method on character set \mathcal{L} to assign prefix code P_i for the character L_i in the message M , where $\mathcal{L} = \{L_i : \forall i, L_i \in M\}$.
- ④ Concatenate the prefix code P_i of all characters within the message to generate the prefix code stream, P , where $P = P_1 \cdot P_2 \cdot P_3 \cdots P_m$.
- ⑤ The prefix code stream P is classified by the words W_i in the message M , where W_i presents the prefix code of the i th word in the message and $P = W_1 \cup W_2 \cup \dots$.
- ⑥ For each word, W_i within message M , do the following:
 - a) Obtain binary value B_i for each word W_i in the message. The binary B_i is converted to its equivalent decimal, D_i .
 - b) Add the white space value α to each decimal D_i to obtain $D_i + \alpha$.
 - c) Finally, multiply $D_i + \alpha$ by the scaling factor β to obtain $(D_i + \alpha) \times \beta$.
- ⑦ Multiply the white space value, α by the scaling factor, β to obtain $\alpha \times \beta$.
- ⑧ Plot each word $(D_i + \alpha) \times \beta$ and white space $\alpha \times \beta$ in a excel file to generate the graph..

B. Proposed Decoding Method

Fig. 3 shows the steps of proposed decoding method for graph steganography. The decoding method retrieves the original message from the received graph. The decoding method follows the reverse procedures of the encoding procedures. The received graph incorporates indices for word and space in x-axis where the corresponding decimal values in y-axis. The graph is first interpreted and the decimal values for word and spaces are extracted from the graph as they appear in the message. Then, every extracted decimal value is divided by β and the resultant value is compared to α to check whether it is a white space or character. The result is considered as a space if it equals to α , in any other case, the value is taken into consideration for a word within the message. The white space value α is deducted from the result to obtain the decimal presentation of every word in the message. The resultant decimal is converted to the prefix code using decimal-to-binary conversation. This is the prefix code of a word in the message. The prefix codes for all the characters in the message are derived from the huffman tree presentation Fig. 6. The steps of the proposed decoding method are given below:

Proposed Decoding Method

- ① Take the graph G as input and interpret all the decimal values, G_i in the graph. Here G_i is the y-axis value i th index in x-axis.
- ② For each decimal value, G_i in graph G , repeat the remaining steps.
- ③ Divide decimal value G_i by β to obtain R_i where β is the scaling factor and $R_i = \frac{G_i}{\beta}$.
- ④ Compare the resultant, R_i with α . Here α is the decimal value of white space. If $R_i = \alpha$, output R_i as the white space value.
- ⑤ Otherwise, if $R_i \geq \alpha$, do the following:
 - a) Output R_i as the decimal value of the i th word in the message.
 - b) Calculate $D_i = R_i - \alpha$. Here D_i is the decimal value of i th word in the message.

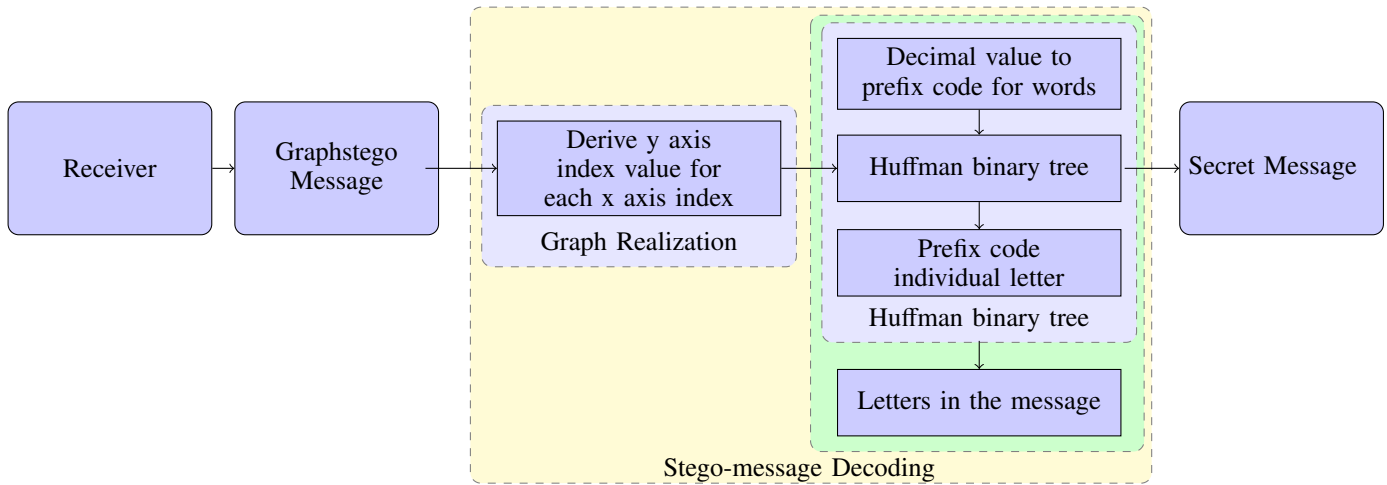


Fig. 3. Procedures of the proposed stego-message decoding algorithm for the proposed graph steganography approach.

- c) Calculate the binary value of the i th word, B_i from the decimal value D_i .
- d) Traverse the tree according to binary prefix code B_i to find the i th word W_i in the message.

⑥ Otherwise, show decoding error message.

C. Solution Example

To illustrate the proposed algorithm for graph steganography, an example of the proposed algorithm is described here. Let the message be “it is my war to win”. In the first step, the algorithm counts the frequency of individual letter in the message.

Letter	a	m	n	o	r	s	y	t	w	i
Frequency	1	1	1	1	1	1	1	2	2	3

In the second step, the list is sorted according to the frequency of the letter. For the tie break, the list is sorted alphabetically. In this phase *huffman encoding* is applied on the sorted list. This transforms two lowest elements to leaves and creates a parent node with a frequency that is the sum of frequencies of two lowest elements as shown in Fig. 4. The two-lowest frequency letters get replaced by their parent node with frequency 2 : * in the list. The list becomes as follows:

Letter	n	o	r	s	y	*	t	w	i
Frequency	1	1	1	1	1	2	2	2	3

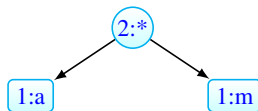


Fig. 4. Generation of prefix code using huffman encoding: step one.

Again, a parent node is created with the sum of the frequencies of two lowest elements in the list, as shown in Fig. 5. Two letters of lowest frequencies get replaced by their parent node with frequency 2 : * in the list and sorted as follows:



Fig. 5. Generation of prefix code using huffman encoding: step two.

Letter	r	s	y	*	*	t	w	i
Frequency	1	1	1	2	2	2	2	3

The process is repeated until there is only one element left in the list as shown in Fig. 6. This element becomes the root of the huffman binary tree. In the third step, the prefix code for each letter in the message is generated by traversing the huffman tree from the root to its leaves. A zero (0) and one (1) are embedded in the prefix code while traversing left branch and right branch respectively. This step ends with the generation of prefix code for every letter in the message. The generated prefix code for each letter is shown below:

Letter	i	y	a	m	n	o	r	s	t	w
Prefix code	00	010	0110	0111	1000	1001	1010	1011	110	111

In the fourth step, the prefix code for a word is constructed by concatenating the prefix codes of letters in the word. The generated prefix codes for the words in the message *it is my war to win*, are shown below:

Word	it	is	my	war	to	win
Prefix code	110	1011	111010	11101101010	1101001	111001000

In the fifth step, the prefix code of a word is considered as binary presentation and is converted to its equivalent decimal value. The resultant decimal value for each word in the message is shown below:

Word	it	is	my	war	to	win
Prefix code	110	1011	111010	11101101010	1101001	111001000
Decimal	6	11	58	1898	105	456

If the value for the white space is considered as $\alpha = 500$

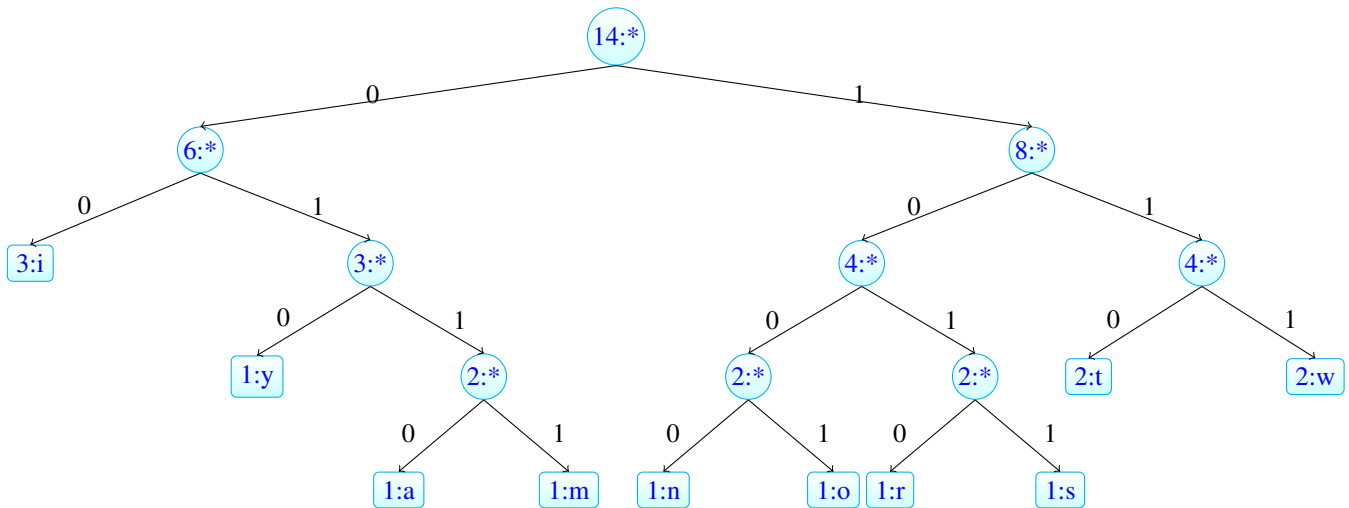


Fig. 6. Generation of prefix code using Huffman encoding for the given message *it is my war to win*.

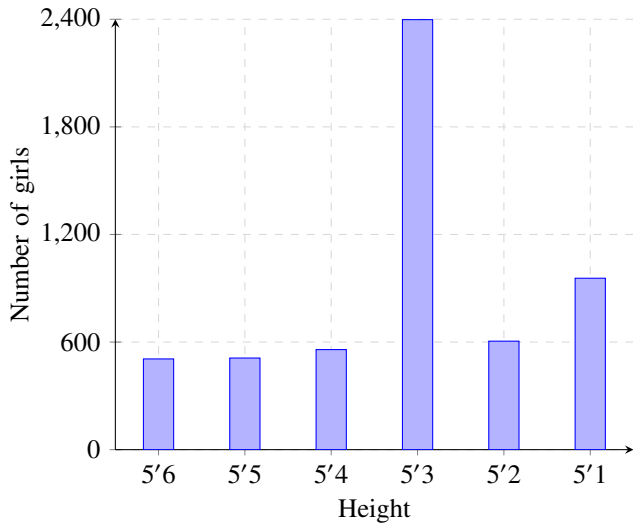


Fig. 7. A stego-graph for the message *it is my war to win* using proposed algorithm.

and the value for the scaling factor $\beta = 1$, then for every word, value of $(D_j + \alpha)\beta$ is computed which presents the plot data in the graph. The plot data for each word in the message becomes as below:

Word	<i>it</i>	<i>is</i>	<i>my</i>	<i>war</i>	<i>to</i>	<i>win</i>
Plot data	506	511	558	2398	605	956

Finally, the solution value for the message *it is my war to win* is plotted in a graph as shown in Fig. 7

IV. EXPERIMENTAL RESULTS AND DISCUSSIONS

In this section, we present experimental results of the proposed graph steganography technique and compare with existing works. We additionally describe the durability of the proposed technique against steganalytic attacks. The software and hardware configuration of this work are summarized in Table II.

TABLE II. HARDWARE AND SOFTWARE SUMMARY.

Graph Plot	Microsoft Excel 2007
IDE	Microsoft Visual Studio 2012
CPU	Intel Core i5
Memory	4 GB
Operating System	Windows 7

A. Resultant Graph

Fig. 7 shows the stego-graph encoded from the message *it is my war to win*. This graph displays some inconsistent peaks. Therefore, the cover *Girls with height above 5'* of an institution is chosen, because it suits well with the disparity of the number distribution. In an institution, it is more likely that girls with average height will be in majority than of others. And it matches perfectly with the graph-data.

B. Evaluation by Comparison

In this section, we evaluate the proposed graph steganography technique by comparing the results of the proposed technique with the existing method in [14]. The secret message that is considered for the purpose of comparison is:

- it is my war to win

Fig. 8 shows the comparison between the proposed algorithm and [14]. Both the graphs are generated from the message *it is my war to win*. Several points are worth noting from the comparison:

- Embedding Capacity
- Randomness of Data

The most eye-catching difference between the graphs is the number of bars. The graph generated using proposed algorithm has less bars than that of [14]. This clearly indicates the higher embedding capacity of the proposed algorithm than [14]. The proposed algorithm embeds word by word on contrary to the existing letter by letter approach [14]. Therefore, the proposed algorithm performs better in embedding long messages. Experimenting with long messages using [14] may produce disastrous results, because there will be numerous

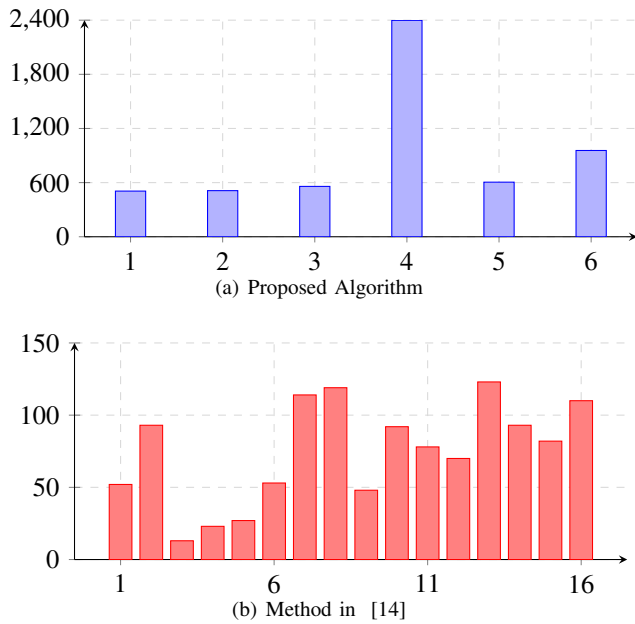


Fig. 8. Comparison of the proposed algorithm with [14] for the message **it is my war to win**

TABLE III. COMPARISON BETWEEN THE PROPOSED AND METHOD [14]

Parameters	Comparison	
	Proposed	[14]
Embedding unit	Word	Letter
Embedding value	Prefix	ASCII
Embedding capacity	High	Low
Security caution	α and β	Nothing special
Graph data	Word and space	Character
Letter based attack	Resistant	Vulnerable

data, difficult for handling. That is, difficult to represent as graph-data and choose a cover.

The next significant difference is the randomness of data. According to Fig. 8, the graph-data generated using proposed algorithm has a higher disparity than that of [14]. The difference is rooted in the methods chosen by each approach. Proposed algorithm uses prefix codes generated by Huffman encoding. Huffman encoding tries to eliminate redundancy by assigning less bits to the high frequent letters. While in the binary conversion of ASCII values, there is no such scope. So, the graph-data produced by [14] has less randomness than the proposed algorithm. The comparison results are summarized in Table III.

C. Effectiveness of Proposed Graph Steganography Technique

Effectiveness of the proposed approach may be evaluated considering the three basic aspects:

- **Payload:** Amount of information that can be hidden in a graph.
- **Security:** Impossibility of attack to detect hidden information in stego-graph.
- **Fidelity:** Inability of human eyes to distinguish between stego-graph and original graph.

Although there is no literal binding in the amount of information that can be embedded using graph steganography, proposed word by word message embedding approach outplays existing letter by letter graph steganography [14]. As the name suggests, proposed word by word embedding approach has significantly higher embedding capacity compared to [14]. Thus proposed approach serves better the first basic principle of steganography.

For ensuring security, proposed approach consults several experts. Firstly, it chooses graph as the cover that has an innocent look. Secondly, it consults the word by word embedding which is a very new technique in graph steganography. This can avert steganalytic attacks in contrast to character by character method. This is where the proposed technique makes the main difference from [14]. Thirdly, introduction of white space value α and scaling factor β increase the randomness to the produced graph-data and makes it strongly durable against attackers. Final two steps make the proposed approach far apart from [14]. Graph steganography can be imperceptible if it chooses appropriate cover or subject of graph relevant to graph-data. Otherwise, it may raise suspicion. From this respect, both proposed and existing [14] have same performance since both have the same advantage.

D. Resistance Against Traffic Analysis

Traffic analysis is a popular steganalytic attack. It works on the principle of analyzing any conversation sample between the sender and receiver that is publicly available or can be derived using any tool. That is, the intruder may intercept any publicly shared content from website or they may keep track of website visitors etc. The attack has three steps. First, interception of data. Second, checking if the data is meaningful or not. Third, verifying the meaning against the relation between communicating parties. Generally this attack performs best against cryptographic data. Because ciphers generally mean nothing and looks conspicuous, thus are easily distinguished by step two. Sometimes, it is also effective against image steganography, text steganography, audio steganography etc.

But when this attack is used against graph steganography, step three is checked before step two. That is, cover verification is the first priority, then comes data analysis. For example, if a customs officer sends data on prediction of tomorrow's temperature, it stinks of something fishy going on. But, if a meteorologist forecasts tomorrow's weather, then it is a normal phenomena. Still, the temperature has to be in the normal range, otherwise it will be subject to further analysis. Now, for proposed approach, we have used prefix codes which is almost next to impossible to find. To make it more difficult, we have taken advantage of space value α and scaling factor β . So, while implementing proposed method, cautions should be taken choosing the appropriate cover type. Thus, proposed method can play smoothly with traffic analysis attack as long as the cover is appropriate.

E. Resistance Against Statistical Analysis

Statistical analysis is another popular attack used both in cryptography and steganography. It benefits from the statistical behavior of a language in Cryptography. Against graph steganography, it is exercised only if found guilty in Traffic

analysis. Statistical analysis may take two forms against graph steganography. In one case, it may count occurrences of same decimals and try to interpret the frequency to something meaningful like any pattern in real life. Another approach may consult ASCII table and convert the decimals to letters if the decimals are in the range 0 – 255. There is no room for suspicion of word values. Because even if they do, there is no direct method of conversion for word values.

V. CONCLUSION AND FUTURE WORK

In this paper, we propose a new graph realization technique for information hiding by presenting information to facts in a graph. In the proposed graph steganography technique, we take a message as input and assign prefix code to every character within the message using Huffman encoding method. We concatenate all the prefix code in the message which are classified later according to the words in the message. Then we convert the prefix codes for all the words to obtain their equivalent decimal values. Finally, we plot these decimal values as a bar plot in an excel file. To verify the effectiveness of the proposed technique, we investigated the traffic analysis attack and the statistical analysis attack on the resultant graph. Finally, we compare the experimental outcomes with existing works. The results show the superiority of the proposed technique over existing techniques in terms of embedding capacity, security and strong resistance against steganalytic attacks such as traffic analysis attack and statistical analysis attack. In future, we want to further evaluate the proposed technique on various sizes of messages and investigate on other steganalytic attacks.

ACKNOWLEDGMENT

We are immensely grateful to all the anonymous referees for their constructive feedback and critical suggestions on an earlier version of the manuscript that helped us significantly to improve the quality of the work.

REFERENCES

- [1] F. Akhter, *A novel approach for image steganography in spatial domain*, Global Journal of Computer Science and Technology, vol. 13, no. 7-F, 2013.
- [2] A. Anees, A. M. Siddiqui, J. Ahmed and I. Hussain, *A technique for digital steganography using chaotic maps*, Nonlinear Dynamics, Springer Netherlands, vol. 75, no. 4, pp. 807-816, October 2013.
- [3] H. Tian, J. Liu and S. Li, *Improving security of quantization-index-modulation steganography in low bit-rate speech streams*, Multimedia systems, Springer Berlin Heidelberg, vol. 20, no. 2, pp. 143-154, February 2013.
- [4] Y. Y. Tsai, *An adaptive steganographic algorithm for 3D polygonal models using vertex decimation*, Multimedia Tools and Applications, Springer US, vol. 69, no. 3, pp. 859-876, June 2012.
- [5] B. Schneier, *Applied cryptography protocols, algorithm and source code in C*, Wiley India Edition, 2nd edition, 2007.
- [6] H. Delfs and K. Helmut, *Symmetric-Key Cryptography*, Introduction to Cryptography. Springer, Berlin Heidelberg, pp.11-48, 2015.
- [7] S. Garg, Y. Ishai, E. Kushilevitz, R. Ostrovsky, and A. Sahai *Cryptography with One-Way Communication*, In Annual Cryptology Conference, pp. 191-208, Springer, Berlin Heidelberg, Aug. 2015.
- [8] C. Cachin, *An information theoretic model for steganography*, Proc. 2nd Inform. Hiding Workshop, vol. 1525, pp. 306-318, 1998.
- [9] D. Martin and A. M. Barmawi, *List Steganography Based on Syllable Patterns*, PhD diss., Telkom University, 2015.
- [10] A. Desoky, *Noiseless Steganography: The Key to Covert Communications*, CRC Press LLC, 2012.

- [11] A. Desoky, *Nostega: A novel noiseless steganography paradigm*, J. of Digital Forensic Practice, vol. 2, no. 3, pp. 132-139, July 2008.
- [12] S. M. Douiri, O. Medeni and S. Elbernoussi, *New steganography scheme using graphs product*, in Interactive Collaborative Learning (ICL) IEEE Int. Conf., pp. 525-528, December 2014.
- [13] V. Thanikaiselvan, P. Arulmozhivarman, S. Subashanthini and R. Amirtharajan, *A graph theory practice on transformed image: A random image steganography*, The Scientific World J., October 2013, online available: <http://www.hindawi.com/journals/tswj/2013/464107/>
- [14] A. Desoky and M. Younis, *Graphstega: graph steganography methodology*, Journal of Digital Forensic Practice, vol. 2, no. 1, pp. 27-36, March 2008.
- [15] S. K. Muttoo and V. Kumar, *Hamiltonian graph approach to steganography*, Int. J. of Electronic Security and Digital Forensics, vol. 3, no. 4, pp. 311-332. February 2010.
- [16] F. Akhter, *A secured word by word Graph Steganography using Huffman encoding*, International Conference on Computer Communication and Informatics (ICCCI). IEEE, 2016.
- [17] H. Wu, H. Wang, H. Zhao and X. Yu, *Multi-layer assignment steganography using graph-theoretic approach*, Multimedia Tools and Applications, Springer US, vol. 74, no. 18, pp. 8171-8196, May 2014.
- [18] S. Hetzl and P. Mutzel, *A graph-theoretic approach to steganography*, In IFIP International Conference on Communications and Multimedia Security, pp. 119-128, Springer, Berlin Heidelberg, September 2005.
- [19] D. A. Huffman, *A method for the construction of minimum-redundancy codes*, Resonance, vol. 11, no. 2, pp. 91-99, February 2006.



Fatema Akhter received her B.Sc. (Engg.) degree in Computer Science and Engineering from Jatiya Kabi Kazi Nazrul University, Trishal, Mymensingh-2220, Bangladesh in 2016. She is currently working toward the MS degree in Computer science and Engineering. Her general research interests are in the area of Cryptography and Network Security, Public Key Cryptosystem, Image Steganography, Quantum Cryptography and Anonymous Credential System. Her current research focuses on Pseudo Random Sequence, Elliptic Curve Cryptography and Noiseless Steganography. She is a student member of IEEE, e-mail: fatema.kumu02@gmail.com.



Md. Selim Al Mamun received his B.Sc. and MS degree in Computer Science and Engineering from University of Dhaka, Dhaka-1000, Bangladesh in 2007 and 2009 respectively. He joined as a faculty member at the Department of Computer Science and Engineering, Jatiya Kabi Kazi Nazrul University, Trishal, Mymensingh-2223, Bangladesh in 2011. Since 2014, he has been working as a PhD student at the Graduate School of Natural Science and Technology, Okayama University, Japan. His research interests include Wireless Local Area Networks (WLANs), Cryptography and Network Security and Quantum Computing. He is a member of IEICE, e-mail: mamun0013@s.okayama-u.ac.jp.